BNL-98392-2012

RIKEN/RBRC Workshop
New Horizons for Lattice Computations with Chiral Fermions
May 14-16, 2012

Proceedings of RIKEN BNL Research Center Workshop

Volume 109

RBRC
RIKEN BNL Research Center

DISCLAIMER

This work was prepared as an account of work sponsored by an agency of the United States Government. Neither the United States Government nor any agency thereof, nor any of their employees, nor any of their contractors, subcontractors or their employees, makes any warranty, express or implied, or assumes any legal liability or responsibility for the accuracy, completeness, or any third party's use or the results of such use of any information, apparatus, product, or process disclosed, or represents that its use would not infringe privately owned rights. Reference herein to any specific commercial product, process, or service by trade name, trademark, manufacturer, or otherwise, does not necessarily constitute or imply its endorsement, recommendation, or favoring by the United States Government or any agency thereof or its contractors or subcontractors. The views and opinions of authors expressed herein do not necessarily state or reflect those of the United States Government or any agency thereof.

Notice: This manuscript has been authored by employees of Brookhaven Science Associates, LLC under Contract No. DE-AC02-98CH10886 with the U.S. Department of Energy. The publisher by accepting the manuscript for publication acknowledges that the United States Government retains a non-exclusive, paid-up, irrevocable, world-wide license to publish or reproduce the published form of this manuscript, or allow others to do so, for United States Government purposes.

Preface to the Series

The RIKEN BNL Research Center (RBRC) was established in April 1997 at Brookhaven National Laboratory. It is funded by the "Rikagaku Kenkyusho" (RIKEN, The Institute of Physical and Chemical Research) of Japan. The Memorandum of Understanding between RIKEN and BNL, initiated in 1997, has been renewed in 2002 and again in 2007. The Center is dedicated to the study of strong interactions, including spin physics, lattice QCD, and RHIC physics through the nurturing of a new generation of young physicists.

The RBRC has both a theory and experimental component. The RBRC Theory Group and the RBRC Experimental Group consists of a total of 25-30 researchers. Positions include the following: full time RBRC Fellow, half-time RHIC Physics Fellow, and full-time post-doctoral Research Associate. The RHIC Physics Fellows hold joint appointments with RBRC and other institutions and have tenure track positions at their respective universities or BNL. To date, RBRC has ~100 graduates of which 29 theorists and 15 experimenters have attained tenure positions at major institutions worldwide.

Beginning in 2001 a new RIKEN Spin Program (RSP) category was implemented at RBRC. These appointments are joint positions of RBRC and RIKEN and include the following positions in theory and experiment: RSP Researchers, RSP Research Associates, and Young Researchers, who are mentored by senior RBRC Scientists. A number of RIKEN Jr. Research Associates and Visiting Scientists also contribute to the physics program at the Center.

RBRC has an active workshop program on strong interaction physics with each workshop focused on a specific physics problem. In most cases all the talks are made available on the RBRC website. In addition, highlights to each speaker's presentation are collected to form proceedings which can therefore be made available within a short time after the workshop. To date there are over one hundred proceeding volumes available.

A 10 teraflops RBRC QCDOC computer funded by RIKEN, Japan, was unveiled at a dedication ceremony at BNL on May 26, 2005. This supercomputer was designed and built by individuals from Columbia University, IBM, BNL, RBRC, and the University of Edinburgh, with the U.S. D.O.E. Office of Science providing infrastructure support at BNL. Physics results were reported at the RBRC QCDOC Symposium following the dedication. QCDSP, a 0.6 teraflops parallel processor, dedicated to lattice QCD, was begun at the Center on February 19, 1998, was completed on August 28, 1998, and was decommissioned in 2006. It was awarded the Gordon Bell Prize for price performance in 1998. The next generation computer in this sequence, QCDCQ (600 Teraflops), is expected to be fully operational in June 2012.

N. P. Samios, Director
May 2012

***Work performed under the auspices of U.S.D.O.E. Contract No. DE-AC02-98CH10886.**

Contents

Presentations

AOKI, Sinya ..... Chiral Symmetry Restoration & Eigenvalue Density of Dirac Operator at Finite Temperature

AOKI, Yasumichi ..... Exploring for Technicolor from QCD

AUBIN, Christopher ..... An Approach to Non-leptonic B-decays on the Lattice

BERNARD, Claude ..... Status and Prospects for Some MILC and Fermilab/MILC Projects

BORICI, Artan ..... Chiral Fermions via Energy Level Splitting

BROWER, Richard ..... Prospects of Multi-grid and Domain Decomposition Dirac Solvers on GPU

CHIU, Ting-Wai ..... Optimal Domain-Wall Fermions

COHEN, Saul ..... Multigrid Acceleration for Domain-Wall Fermion Inversion

COSSU, Guido ..... The Axial Symmetry at Finite Temperature in Lattice QCD with Overlap Fermions

CREUTZ, Michael ..... On Quark Masses

DOI, Takumi ..... Exploring Three-Nucleon Forces in Lattice QCD

FENG, Xu ..... The Two-Photon Decay of Neutral Pion from Lattice QCD

FODOR, Zoltan ..... High-precision Scale Setting in Lattice QCD

GIUSTI, Leonardo ..... Thermodynamic Potentials from Shifted Boundary Conditions

GOLTERMAN, Maarten ..... On the Hadronic Vacuum Polarization Contribution to g-2

HASENFRATZ, Anna ..... A Novel Phase with Many Flavors of Staggered Fermions

JANSEN, Karl ..... Status of Four Flavor Simulations using Maximally Twisted Mass Fermions

JIN, Xiao-Yong ..... Exploring the Phases of QCD with Many Flavors

KANEKO, Takashi ..... Kaon Semileptonic Decays in QCD with Exact Chiral Symmetry

KELLY, Christopher ..... Progress Towards Delta I=1/2 K to pi pi Decays with G-parity Boundary Conditions

KIM, Hyung-Jin ..... Recent Progress in Multi GPU Conjugate Gradient Convertor with Staggered Fermion

KURAMASHI, Yoshinobu ..... 1+1+1 Flavor QCD+QED Simulation at the Physical Point

KUTI, Julius ..... The Composite Higgs Mechanism and the Conformal Window

LEE, Weonjong ..... Recent Progress in Calculating B_K using Staggered Fermions

LIN, C.-J. David ..... Lattice Study of the Phase Structure of the Strong-Yukawa Model

LIN, Huey-Wen ..... Medium-Modification Effects on Pion Structure

LIN, Meifeng ..... Many-flavor Domain Wall Fermions and Fixed Topology

LIU, Keh-Fei ..... Progress with Overlap Fermions

MAWHINNEY, Robert ..... Decaying Pseudoscalars from DWF LQCD

MEINEL, Stefan ..... Axial Couplings and Strong Decay Widths of Heavy Hadrons

MISUMI, Tatsuhiro .....New Fermion Discretizations and their Application
MUKHERJEE, Swagato.....Thermodynamics with Domain Wall Fermions and Anomaly in Hot QCD
NARAYANAN, Rajamani.....Large N Gauge Theories with Adjoint Fermions
NEUBERGER, Herbert.....Lattice Radial Quantization
ORGINOS, Kostas.....Lattice Gauge Theory and Applications to Nuclear Physics
PERIS, Santiago.....The Anomaly Triangle and g-2
ROBERTS, Lee .....The New Muon g-2 Experiment at Fermilab: A Challenge for Theorists and Experimentalists
SACHRAJDA, Christopher.....Prospects for the Computation of Rare Kaon Decay Amplitudes
SAKAI, Yoshihide.....Physics Prospects and Status of SuperKEKB/Belle II
SCHAEFER, Stefan.....Lattice QCD with Open Boundary Conditions
SEMERTZIDIS, Yannis.....Storage Ring Electric Dipole Moment Experiment for the Proton
SHAMIR, Yigal.....SU(N) Gauge Theories with Symmetric-representation Fermions
SHINTANI, Eigo.....Nucleon EDM from Lattice QCD
WITZEL, Oliver.....B-physics with Domain-wall Light and Relativistic Heavy Quarks
YAMADA, Norikazu.....Exploring Many Flavor QCD with Wilson Fermion
YAMAZAKI, Takeshi.....Light Nuclei from Quenched Lattice QCD
YU, Jianglei.....Computing the K_L – K_S Mass Difference in Lattice QCD
ZHOU, Ran.....B to Kll and B K\gamma Decay Form Factors from Three-flavor Lattice QCD

Agenda

Registered List of Participants

Additional RIKEN BNL Research Center Proceeding Volumes

Chiral Symmetry Restoration and Eigenvalue Density of Dirac Operator at Finite Temperature

Sinya AOKI

University of Tsukuba

with N. Fukaya and Y. Taniguchi for JLQCD Collaboration

“New Horizon for Lattice Gauge Theory Computations with Chiral Fermions ”,

2012.05.14-16, BNL, NY, USA

1. Introduction

Flavor-Chiral Symmetries of QCD at low T

$$U(N_f)_L \otimes U(N_f)_R \Rightarrow U(1)_B \otimes S(N_f)_L \otimes SU(N_f)_R \Rightarrow U(1)_B \otimes S(N_f)_V$$

flavor

chiral anomaly
(explicit breaking)

spontaneous breaking of
chiral symmetry

QCD at high T

deconfinement (QGP)

restoration of chiral symmetry

phase transition

low T $U(1)_B \otimes S(N_f)_V \Rightarrow$ high T $U(1)_B \otimes S(N_f)_L \otimes SU(N_f)_R$

Questions in this study

1. Constraints to eigenvalue density: $\rho(\lambda) = \lim_{V\to\infty} \frac{1}{V} \sum_n \delta(\lambda - \lambda_n)$

2. Constraint to singlet susceptibility: $\chi_{\rm singlet} = \int d^4x \, [\pi(x)\pi(0) - \eta(x)\eta(0)]$

Previous studies

$$\rho(\lambda) = \lim_{V\to\infty} \frac{1}{V} \sum_n \delta(\lambda - \lambda_n)$$

Lin (HotQCD11), DW

Cossu *et al.* (JLQCD11), Overlap

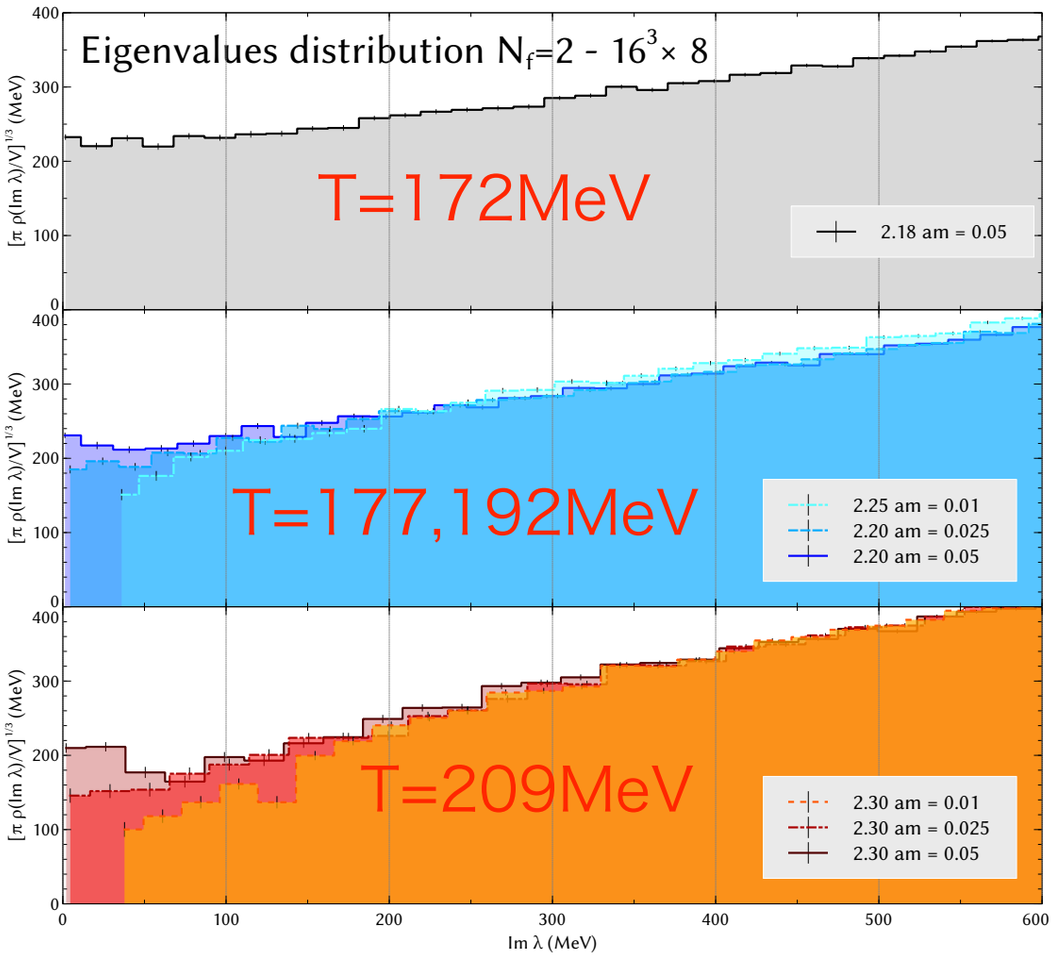

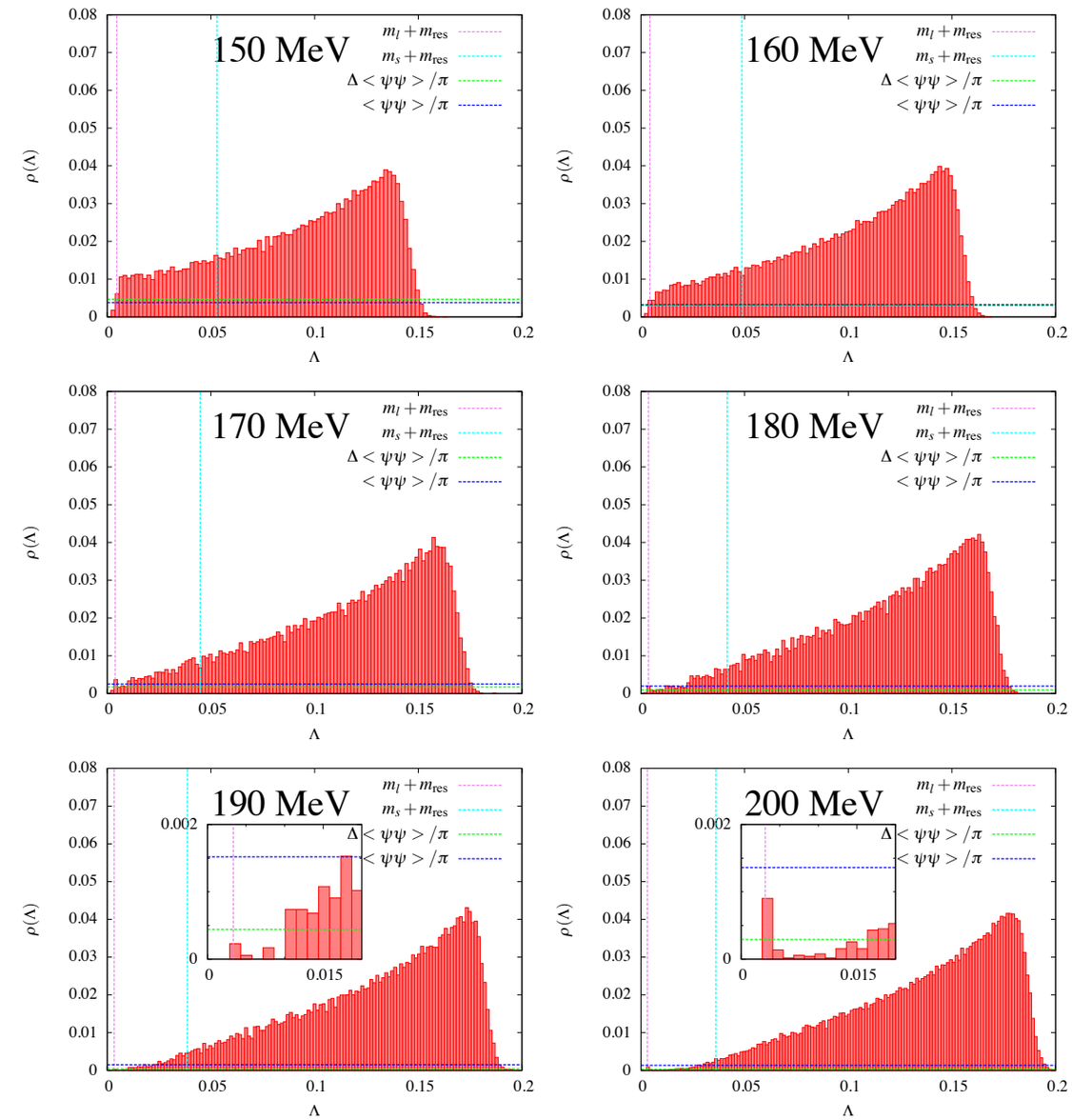

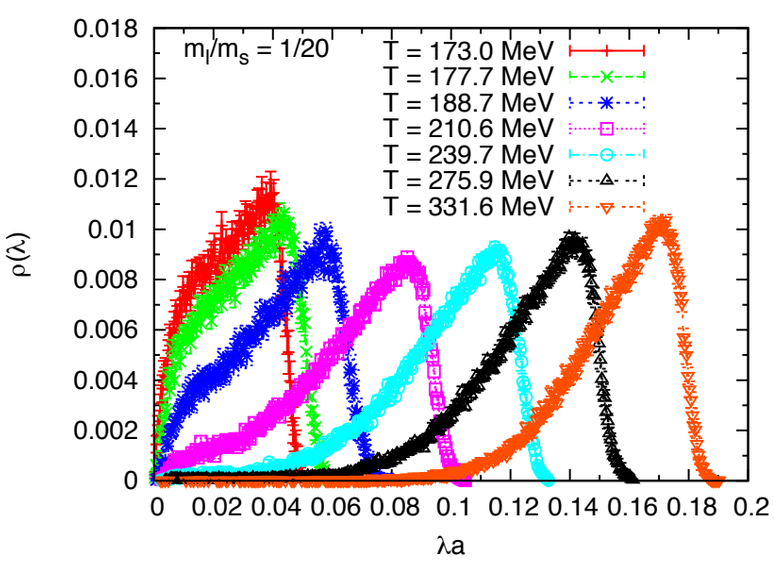

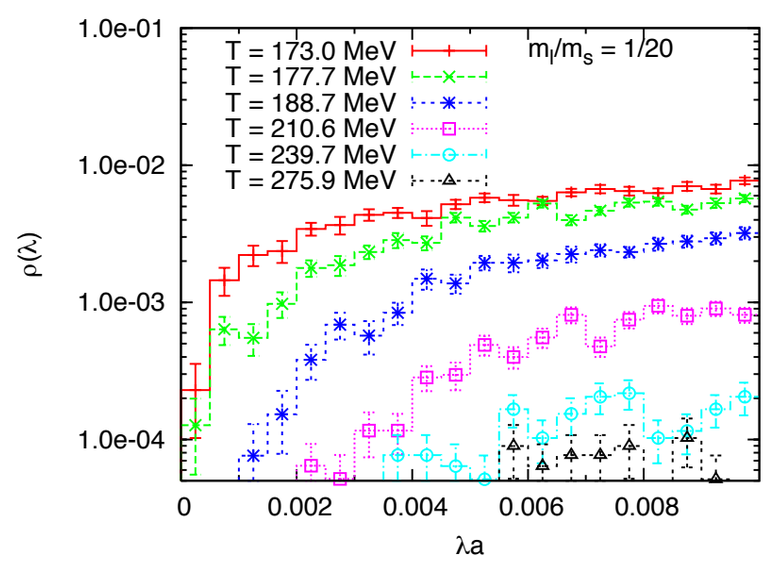

Ohno *et al.* (11), HISQ

Is a gap open at $\lambda = 0$?

Chandrasekharan-Christ(95), KS

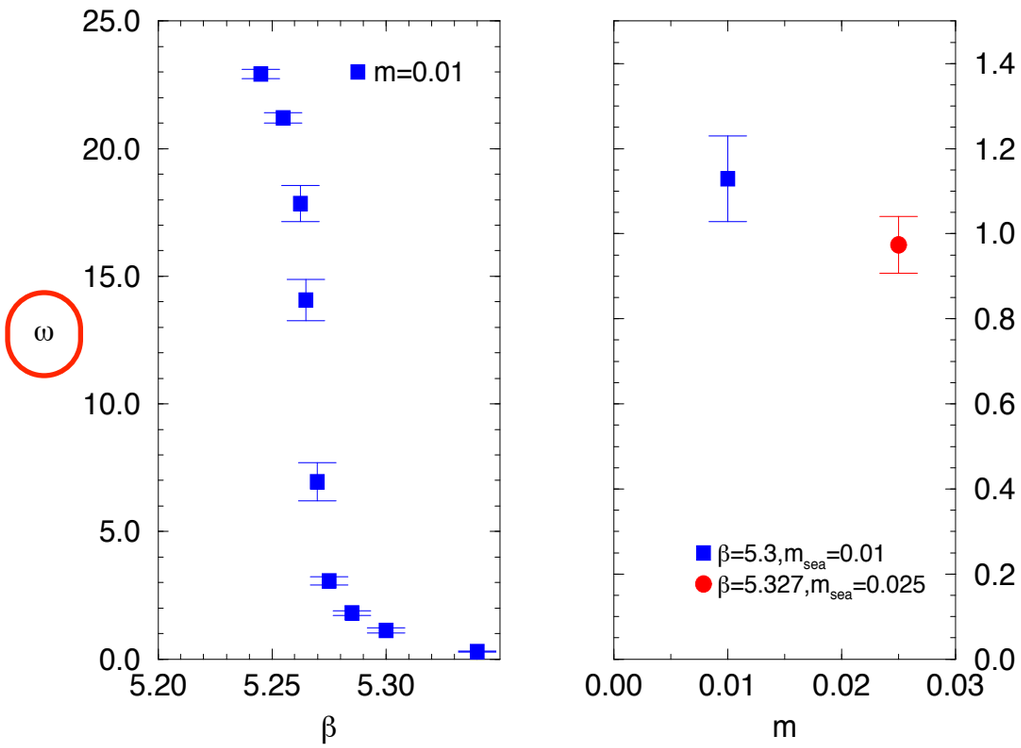

Bernald, *et al.* (96), KS

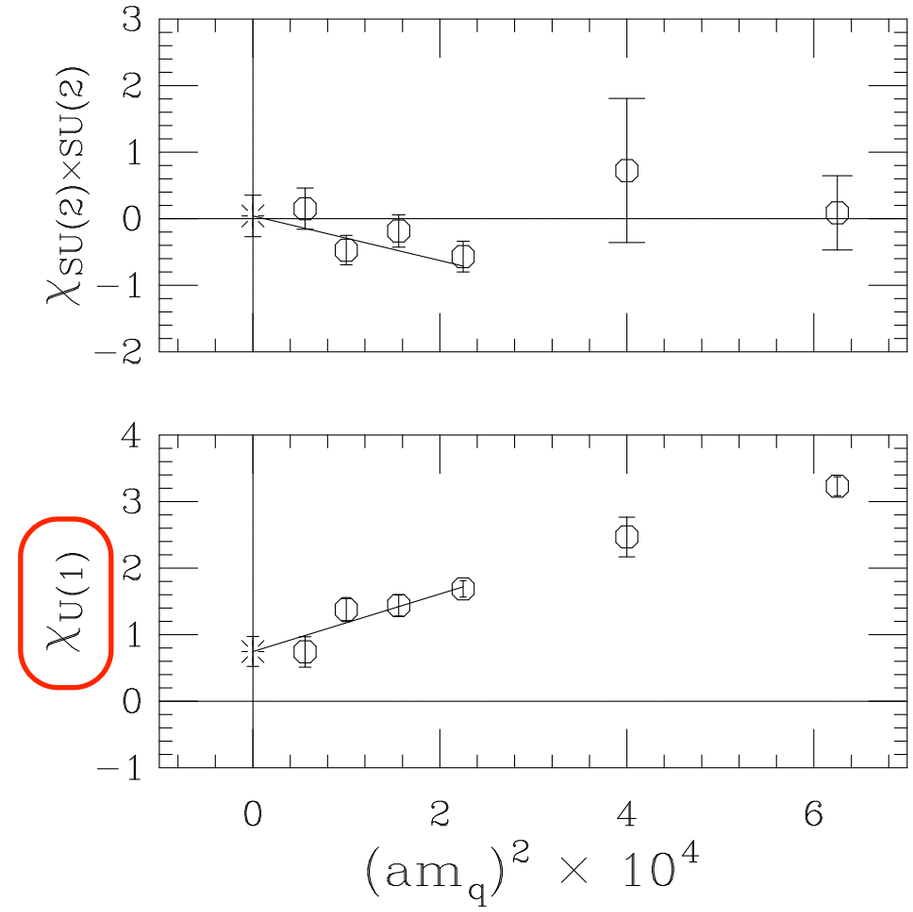

Chandrasekharan *et al.*, (98), KS

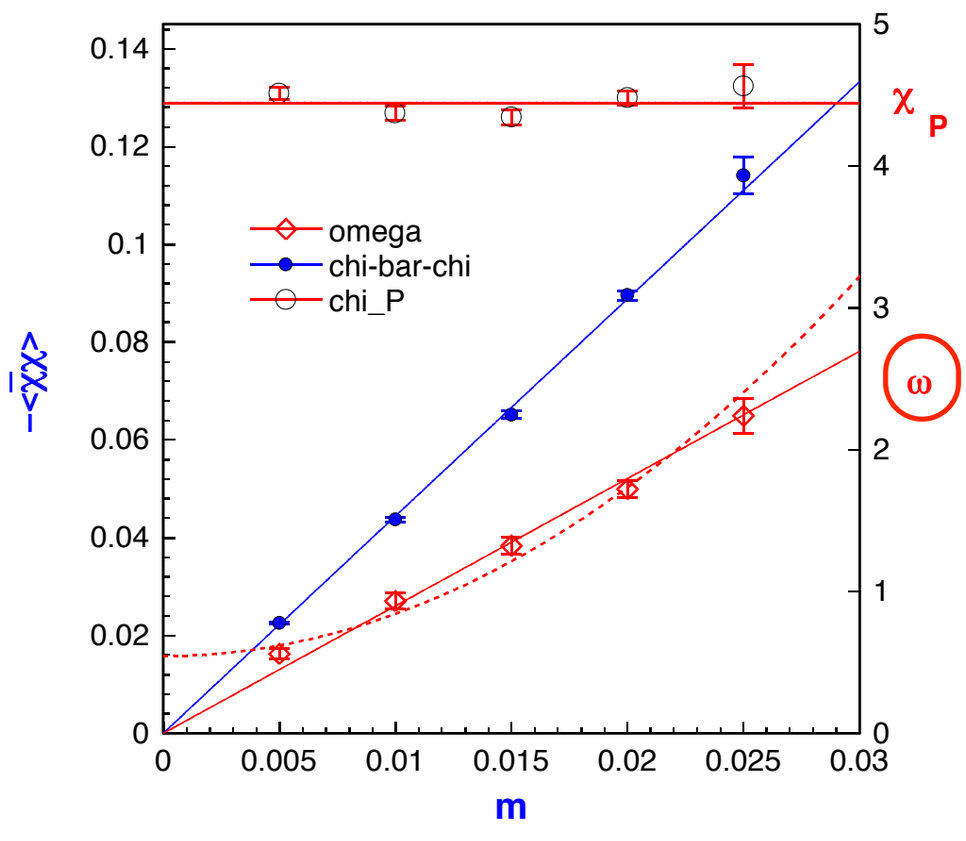

Hegde (HotQCD11), DW

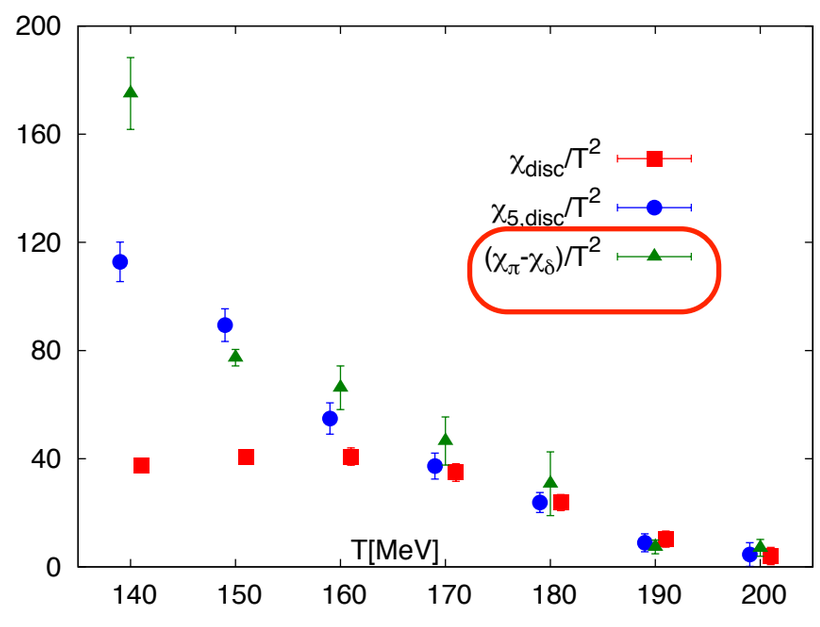

$$\chi_{\rm singlet} = 0\ ?$$

This talk

give constraints to eigenvalue densities of 2-flavor overlap fermions, if chiral symmetry in QCD is restored at finite temperature.
discuss a behavior of singlet susceptibility using the constraints.

Content

1. Introduction
2. Overlap fermions
3. Constraints to eigenvalue densities
4. Discussions: singlet susceptibility

2. Overlap fermions

Action $S = \bar{\psi}[D - mF(D)]\psi, \quad F(D) = 1 - \frac{Ra}{2}D$

Ginsparg-Wilson relation $D\gamma_5 + \gamma_5 D = aDR\gamma_5 D$

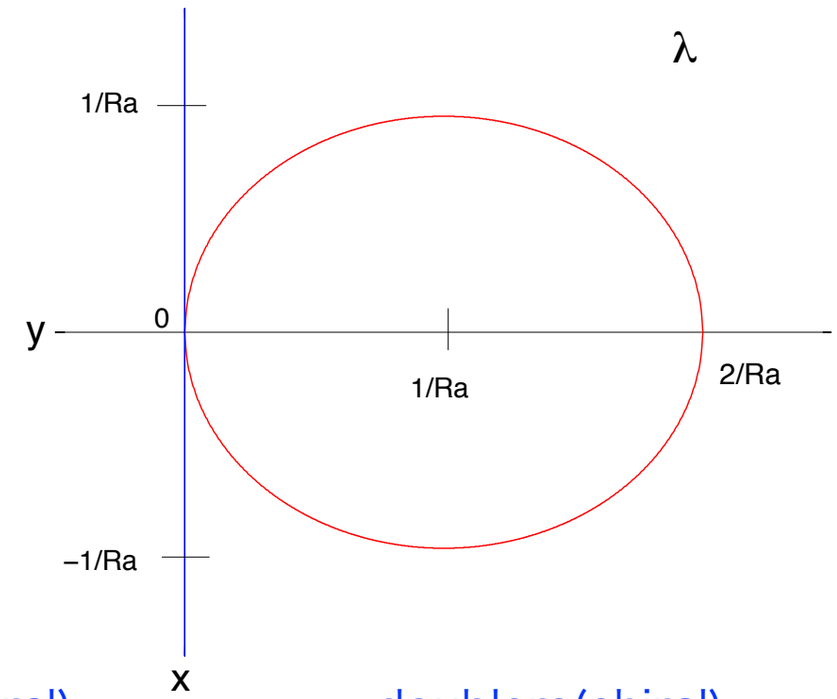

Eigenvalue spectrum

$$\lambda_n^A + \bar{\lambda}_n^A = aR\bar{\lambda}_n^A\lambda_n^A$$

$$D(A)\phi_n^A = \lambda_n^A\phi_n^A$$

$$D(A)\gamma_5\phi_n^A = \bar{\lambda}_n^A\gamma_5\phi_n^A$$

Propagator

bulk modes(non-chiral) zero modes(chiral) doublers(chiral)

$$S(x,y) = \sum_n \left[\frac{\phi_n(x)\phi_n^\dagger(y)}{f_m\lambda_n - m} + \frac{\gamma_5\phi_n(x)\phi_n^\dagger(y)\gamma_5}{f_m\bar{\lambda}_n - m}\right] - \sum_{k=1}^{N_{R+L}} \frac{1}{m}\phi_k(x)\phi_k^\dagger(y) + \sum_{K=1}^{N_D} \frac{Ra}{2}\phi_K(x)\phi_K^\dagger(y)$$

$$f_m = 1 + \frac{Rma}{2}$$

Measure $P_m(A) = e^{-S_{YM}(A)}(-m)^{N_f N_{R+L}^A}\left(\frac{2}{Ra}\right)^{N_f N_D^A} \prod_{\Im\lambda_n^A > 0}\left(Z_m^2\bar{\lambda}_n^A\lambda_n^A + m^2\right)$

$$Z_m^2 = 1 - (ma)^2\frac{R^2}{4}$$

positive definite and even function of $m \neq 0$ for even N_f

Ward-Takahashi identities under "chiral" rotation

$$\theta^a(x)\delta^a_x\psi(x) = i\theta^a(x)T^a\gamma_5(1-RaD)\psi(x),$$
$$\theta^a(x)\delta^a_x\bar{\psi}(x) = i\bar{\psi}(x)\theta^a(x)T^a\gamma_5,$$

$$\langle (J^a_x - \delta^a_x S)O + \delta^a_x \mathcal{O}\rangle = 0$$

$$\Rightarrow \quad \int d^4x \langle \{J^a_x + 2mP^a(x)\}\mathcal{O} + \delta^a_x\mathcal{O}\rangle = 0.$$

integrated WTI

"measure" term (anomaly)

$$J^a_x = -2i\mathrm{tr}\, T^a\gamma_5\left(1-\frac{R}{2}aD\right)(x,x) = -\delta^{a0}2iN_f\mathrm{tr}\,\gamma_5\left(1-\frac{R}{2}aD\right)(x,x)$$

Operators

$$S^a(x) = \bar{\psi}(x)T^aF(D)\psi(x),$$ scalar

$$P^a(x) = \bar{\psi}(x)T^a i\gamma_5 F(D)\psi(x),$$ pseudo-scalar

$$S^a = \int d^4x\, S^a(x), \quad P^a = \int d^4x\, P^a(x)$$

chiral rotation at N_f=2

$$\delta^b S^a = 2\delta^{ab}P^a, \quad \delta^b P^a = -2\delta^{ab}S^a$$
$$\delta^0 S^a = \delta^a S^0 = 2P^a, \quad \delta^0 P^a = \delta^a P^0 = -2S^a$$

$$\mathcal{O}_{n_1,n_2,n_3,n_4} = (P^a)^{n_1}(S^a)^{n_2}(P^0)^{n_3}(S^0)^{n_4} \qquad N = \sum_i n_i, \quad n_1+n_2 = \mathrm{odd},\ n_1+n_3 = \mathrm{odd}$$

$$\boxed{\lim_{m\to 0}\langle \delta^a \mathcal{O}_{n_1,n_2,n_3,n_4}\rangle_m = 0}$$

if the chiral symmetry is restored.

$$\frac{\delta^a}{2}\mathcal{O}_{n_1,n_2,n_3,n_4} = -n_1\mathcal{O}_{n_1-1,n_2,n_3,n_4+1} + n_2\mathcal{O}_{n_1,n_2-1,n_3+1,n_4} - n_3\mathcal{O}_{n_1,n_2+1,n_3-1,n_4} + n_4\mathcal{O}_{n_1+1,n_2,n_3,n_4-1}$$

3. Constraints to eigenvalue densities

N=1 $\quad \mathcal{O}_{1,0,0,0} = P^a, \ \delta^a \mathcal{O}_{1,0,0,0} = -2S^0$

$$\frac{1}{V}\langle S^0\rangle_m = \underbrace{\frac{N_f}{mV}\langle N^A_{R+L}\rangle_m}_{\to 0 \text{ as } V\to\infty} + N_f\langle I_1\rangle_m$$

$$\langle \mathcal{O}^A\rangle_m = \frac{1}{Z}\int \mathcal{D}A\, P_m(A)\mathcal{O}^A$$

$$I_1 \to \frac{1}{Z_m}\int_0^{\Lambda_R} d\lambda\, \underline{\rho^A(\lambda)}\frac{2m_R}{\lambda^2+m_R^2}g_0(\lambda)$$

$$m_R = \frac{m}{Z_m}, \ g(\lambda) = 1 - \frac{\lambda^2}{\Lambda_R^2}$$

$\Lambda_R = \frac{2}{Ra}$: cut-off

$$\rho^A(\lambda) \equiv \lim_{V\to\infty}\frac{1}{V}\sum_n \delta\left(\lambda - \sqrt{\bar{\lambda}^A_n\lambda^A_n}\right) = \sum_{k=0}^{\infty}\rho^A_k\frac{|\lambda|^k}{k!} = \rho^A_0 + \rho^A_1|\lambda| + \cdots,$$

$$\Rightarrow \quad I_1 = \pi\rho^A_0 + O(m)$$

$$\lim_{m\to 0}\lim_{V\to\infty}\frac{1}{V}\langle S^0\rangle_m = 0 \quad \Rightarrow \quad \lim_{m\to 0}\langle\rho^A_0\rangle_m = 0$$

$$\Rightarrow \quad \langle\rho^A_0\rangle_m = O(m^2)$$

1st constraint

N=2

$$\chi^{\sigma-\pi} = \frac{1}{V^2}\langle S_0^2 - P_a^2\rangle_m, \qquad \chi^{\eta-\delta} = \frac{1}{V}\langle P_0^2 - S_a^2\rangle_m$$

$$\chi^{\sigma-\pi} = \left\langle N_f^2 \left(\frac{1}{mV} N_{R+L} + I_1\right)^2 \right\rangle_m + O\left(\frac{1}{V}\right)$$

$$\Rightarrow \quad \lim_{m\to 0}\lim_{V\to\infty} \frac{1}{m^2V^2}\underbrace{\langle (N_{R+L}^A)^2\rangle_m}_{O(m^{N_f V})} = \lim_{m\to 0}\lim_{V\to\infty}\frac{1}{mV}\underbrace{\langle N_{R+L}^A\,\rho_0^A\rangle_m}_{O(m^{N_f V})} = \lim_{m\to 0}\underbrace{\langle (\rho_0^A)^2\rangle_m}_{O(m^2)} = 0$$

These conditions are automatically satisfied.

$$\chi^{\eta-\delta} = N_f \left\langle \frac{1}{m^2V}\{2N_{R+L} - N_f Q(A)^2\} + \frac{1}{Z_m}\left(\frac{I_1}{m_R} + I_2\right)\right\rangle_m \qquad Q(A) = N_R^A - N_L^A$$

$$\frac{I_1}{m_R} + I_2 = \rho_0^A\left(\frac{\pi_m}{m} + \frac{2}{\Lambda_R}\right) + 2\rho_1^A + O(m), \qquad I_2 = \frac{2}{Z_m}\int_0^{\Lambda_R} d\lambda\,\rho^A(\lambda)\,\frac{m_R^2 - \lambda^2 g_0(\lambda^2) g_m}{(\lambda^2 + m_R^2)^2}, \quad g_m = \frac{1}{Z_m^2}\left(1 + \frac{m^2}{2\Lambda_R^2}\right)$$

$$\lim_{m\to 0}\chi^{\eta-\delta} = 0 \quad \Rightarrow \quad \lim_{m\to 0}\underbrace{\frac{N_f^2\langle Q(A)^2\rangle_m}{m^2V}}_{O(m^{N_f\sqrt{V}-2})} = 2\lim_{m\to 0}\langle \rho_1^A\rangle_m$$

$$\Rightarrow \quad \langle \rho_1^A\rangle_m = O(m^2)$$

2nd constraint

N=3

$$\langle \mathcal{O}_{2001}\rangle_m \to 0, \quad \langle -\mathcal{O}_{0201} + 2\mathcal{O}_{1110}\rangle_m \to 0, \quad \langle \mathcal{O}_{0021} + 2\mathcal{O}_{1110}\rangle_m = 0$$

$$\langle -\mathcal{O}_{0003} + 2\mathcal{O}_{2001}\rangle_m \to 0, \quad \langle \mathcal{O}_{0021} - \mathcal{O}_{0201} + \mathcal{O}_{1110}\rangle_m \to 0,$$

$$\lim_{m\to 0}\lim_{V\to\infty}\frac{\chi_3}{V^4} = \pi N_f \lim_{m\to 0}\left[\frac{\langle \rho_0^A\rangle_m}{m^2} + \underbrace{\frac{2\bar{\rho}_1}{m\pi}}_{O(m)} + \frac{\langle \rho_2^A\rangle_m}{2}\right], = 0$$

+ positivity

$$\langle \rho_0^A\rangle_m = O(m^4), \ \langle \rho_2^A\rangle_m = O(m^2)$$

3rd constraints

N=4 No additional constraints

Final results

$$\lim_{m\to 0}\langle \rho^A(\lambda)\rangle_m = \lim_{m\to 0}\langle \rho_3^A\rangle_m \frac{|\lambda|^3}{3!} + O(\lambda^4)$$

4. Discussion:Singlet susceptbility

Singlet susceptibility

$$\chi^{\pi-\eta} = \lim_{V\to\infty} \frac{N_f^2}{m^2 V} \langle Q(A)^2 \rangle_m = (m^{N_f\sqrt{V}-2})$$

$$\Rightarrow \quad \lim_{m\to} \chi^{\pi-\eta} = 0$$

singlet susceptibility becomes zero if the chiral symmetry is recovered at hight T.

This, however, does not mean U(1)_A symmetry is recovered at high T.

$\lim_{m\to} \chi^{\pi-\eta} = 0$ is necessary but NOT sufficient for the recovery of U(1)_A .

Future

new constraints at N > 4 ?

eigenvalues of Dirac operator have a gap near zero ?

$$\rho(\lambda) = 0 \text{ at } |\lambda| \leq \lambda_c$$

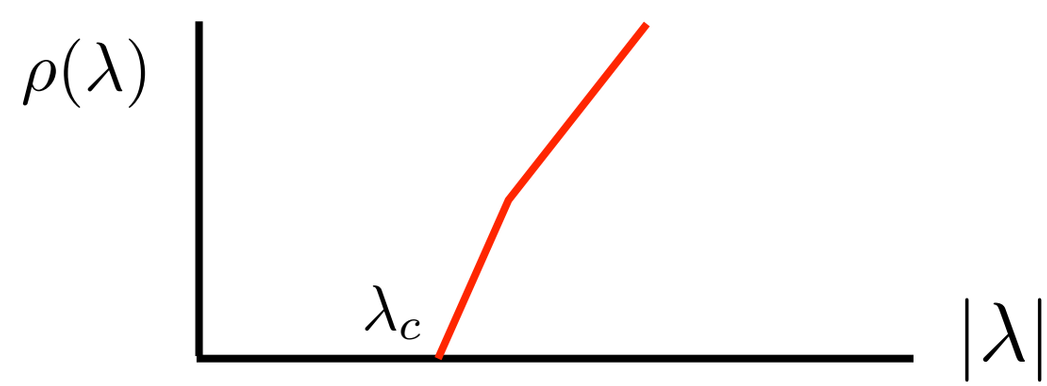

Exploring technicolor from QCD

Yasumichi Aoki [Koboyashi-Maskawa institute, Nagoya University]

for the LatKMI collaboration

- RBRC workshop: New Horizons for Lattice Gauge Theory Computations -

May 16, 2012

名古屋大学

LatKMI collaboration

- YA, T.Aoyama, M.Kurachi, T.Maskawa, K.Nagai, H.Ohki,

K.Yamawaki, T.Yamazaki

名古屋大学

- A.Shibata

KEK

conformal window and walking coupling

- non-Abelian gauge theory with N_f massless fermions -

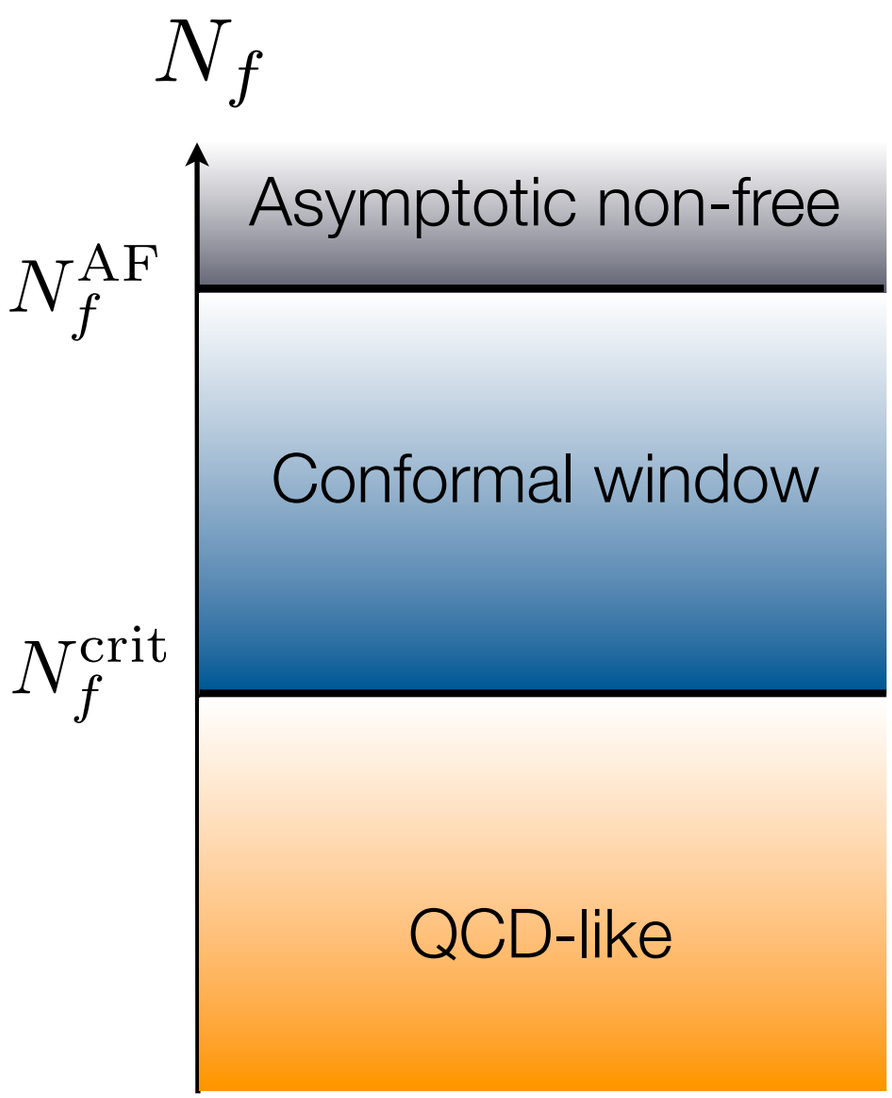

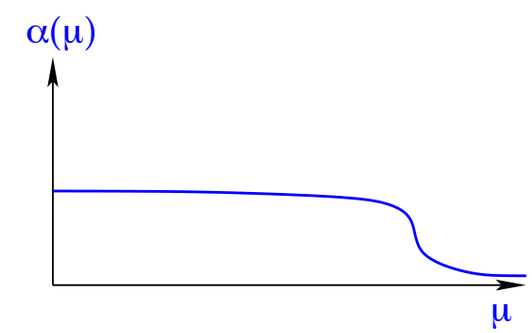

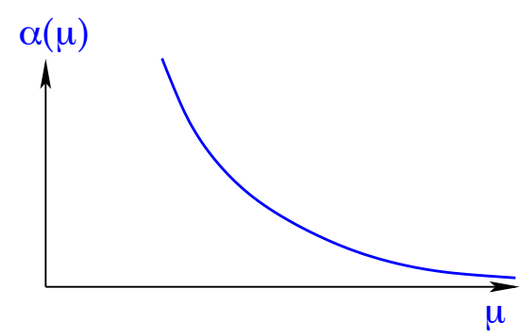

conformal window and walking coupling

- non-Abelian gauge theory with N_f massless fermions -

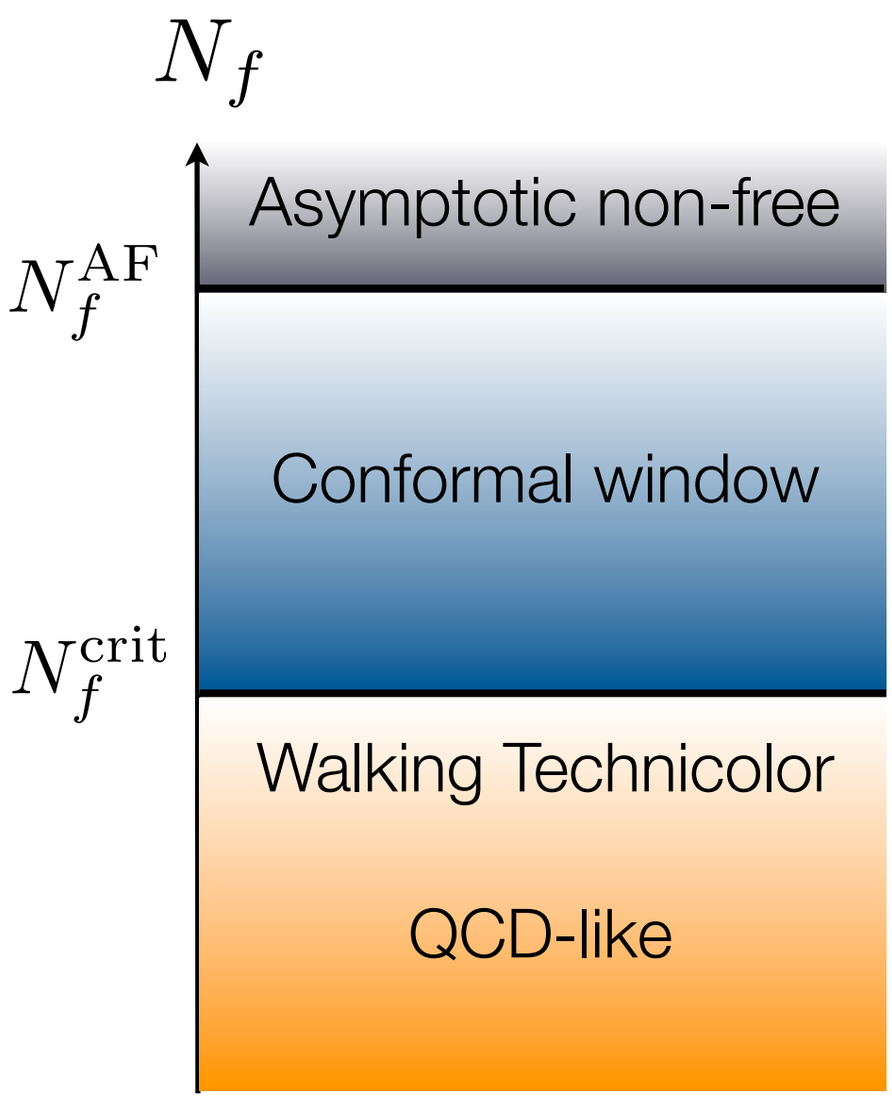

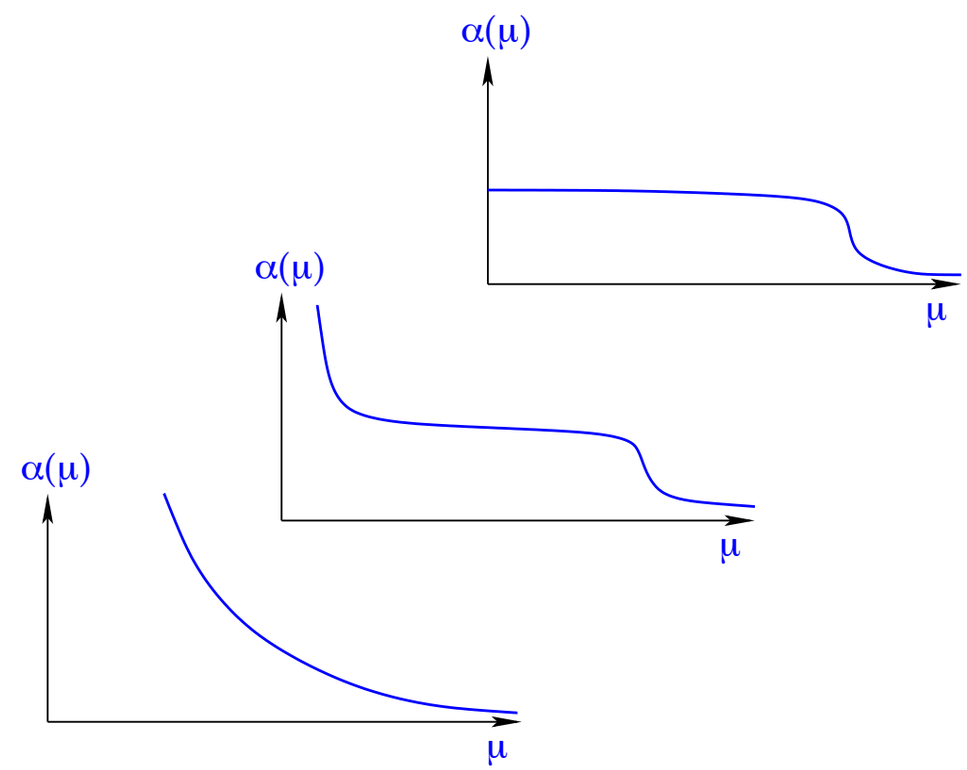

conformal window and walking coupling

- non-Abelian gauge theory with N_f massless fermions -

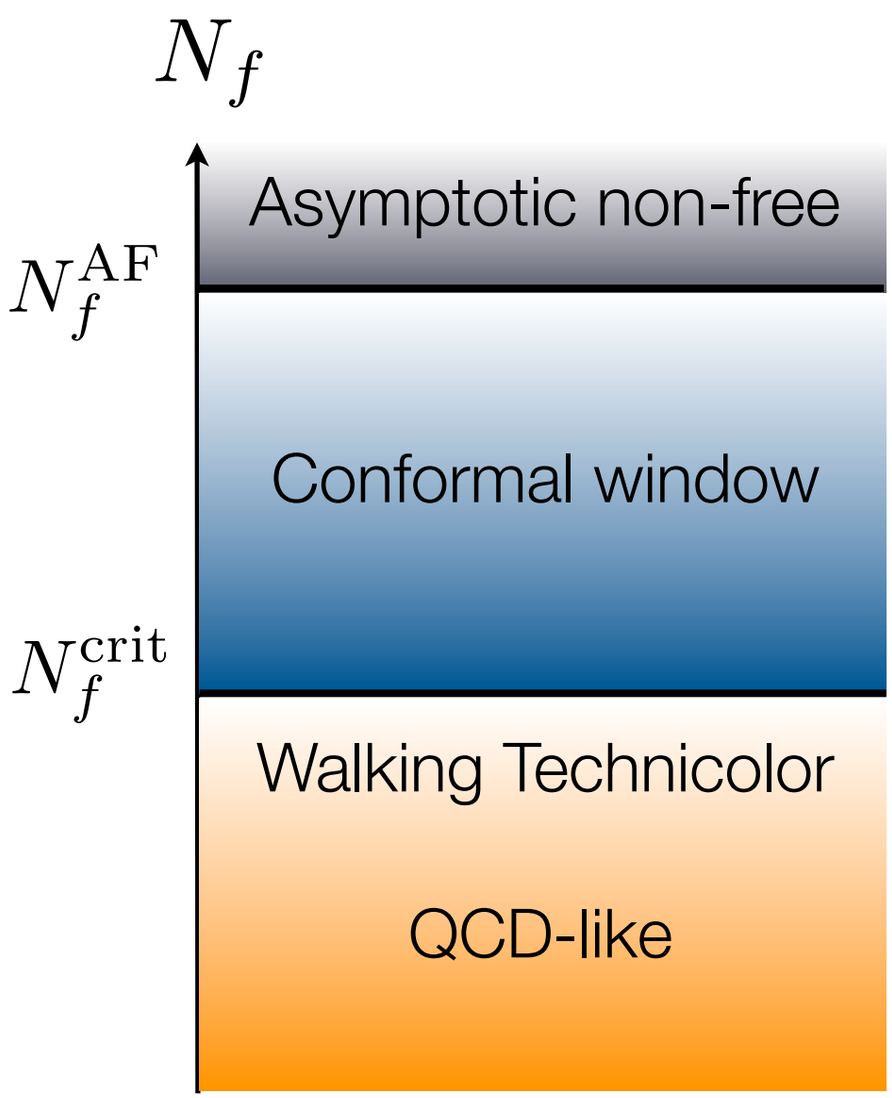

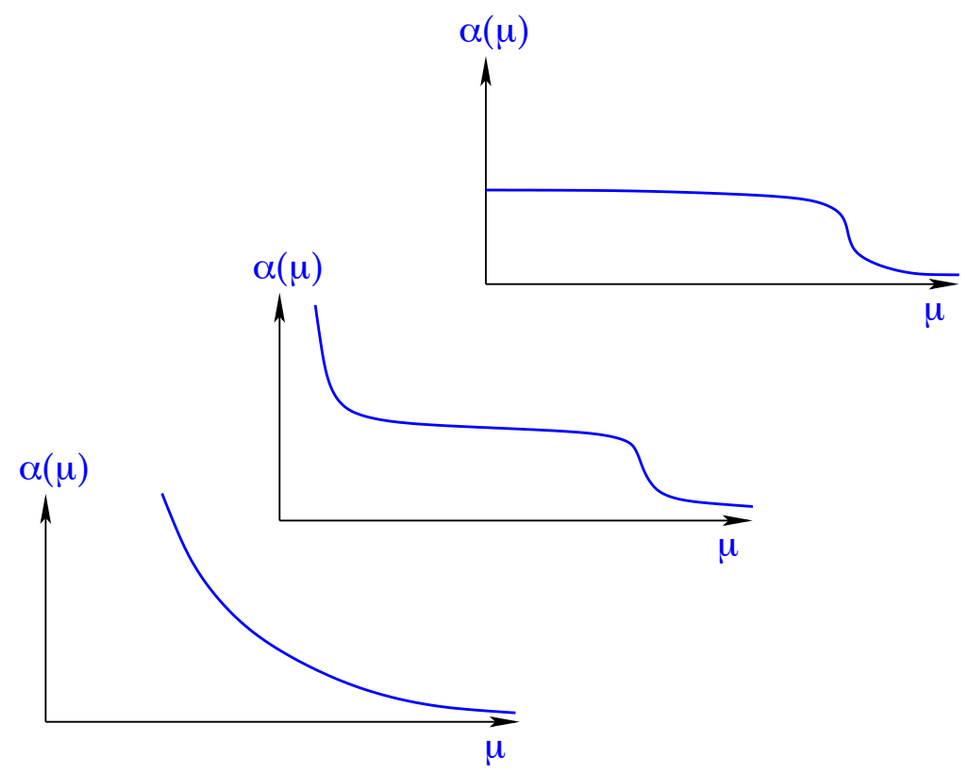

- Walking Techinicolor could be realized just below the conformal window

conformal window and walking coupling

- non-Abelian gauge theory with N_f massless fermions -

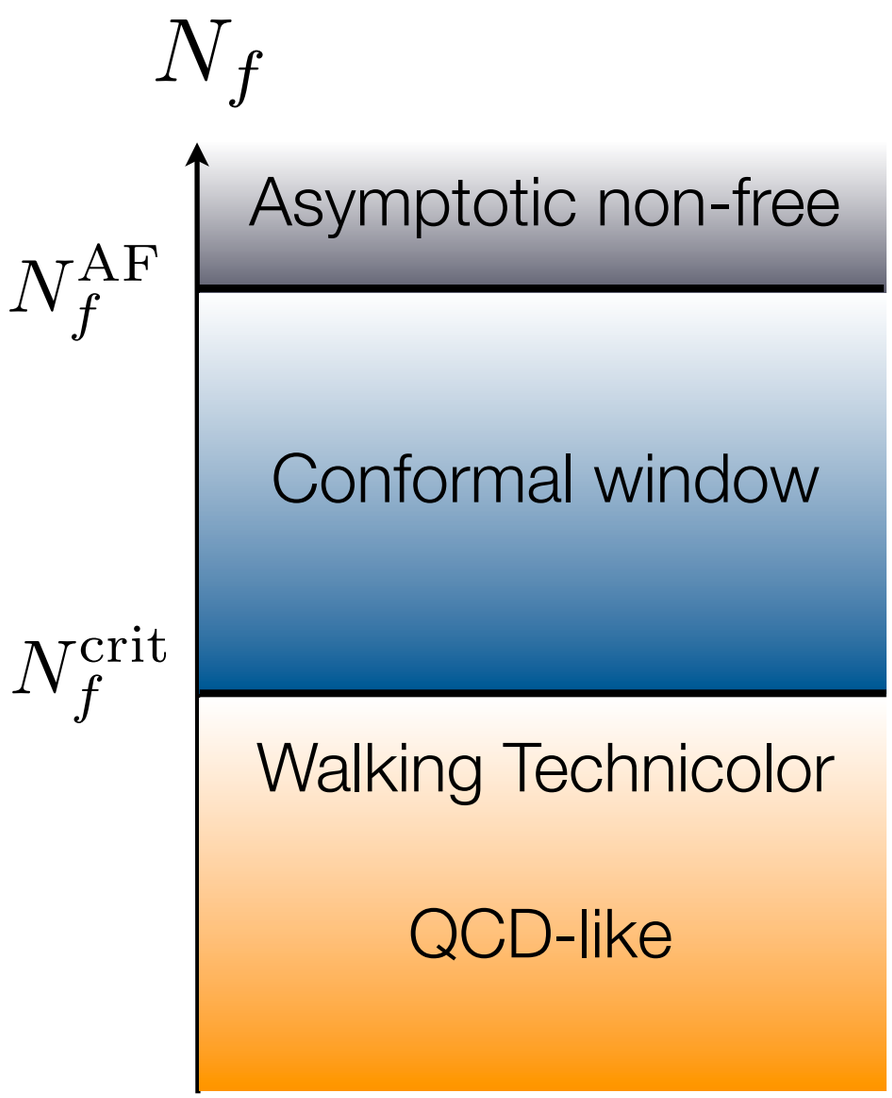

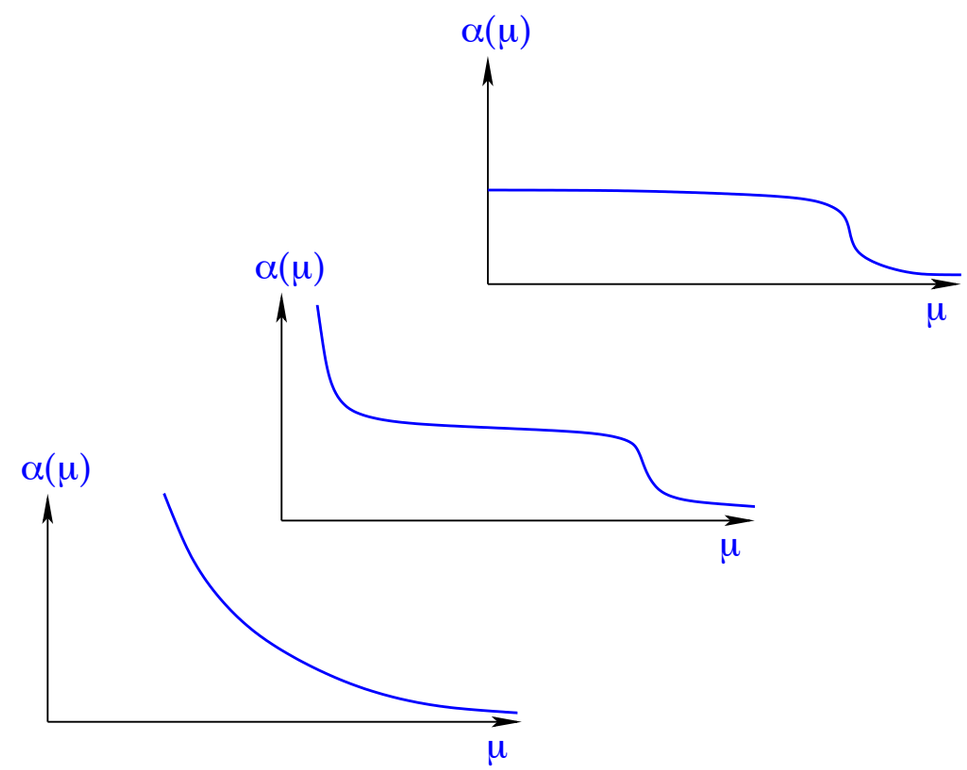

- Walking Techinicolor could be realized just below the conformal window
- crucial information: N_f^{crit} & mass anomalous dimension around N_f^{crit}

models being studied:

- SU(3)
  - fundamental: Nf=6, 8, 10, 12, 16
  - sextet: Nf=2
- SU(2)
  - adjoint: Nf=2
  - fundamental: Nf=8
- SU(4)
  - decuplet: Nf=2

SU(N) Phase Diagram

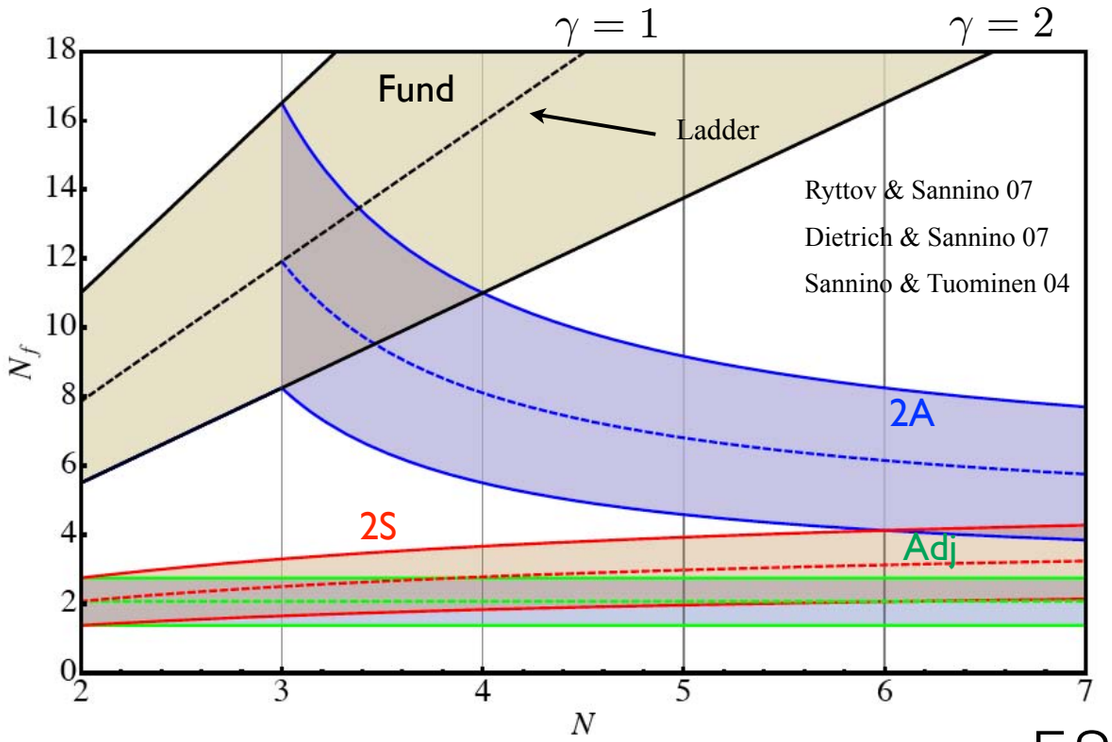

F.Sanino

models being studied:

- SU(3)
  - fundamental: Nf=6, 8, 10, 12, 16
  - sextet: Nf=2
- SU(2)
  - adjoint: Nf=2
  - fundamental: Nf=8
- SU(4)
  - decuplet: Nf=2

SU(N) Phase Diagram

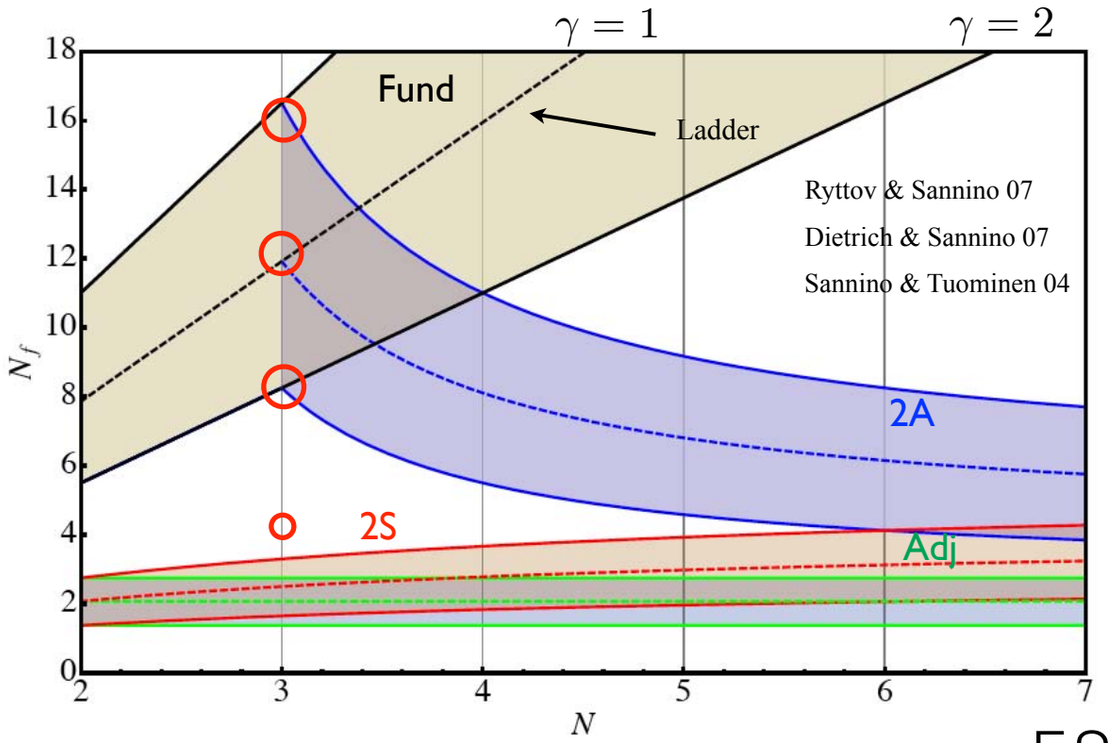

F.Sanino

models being studied:

- SU(3)
  - fundamental: Nf=6, 8, 10, 12, 16
  - sextet: Nf=2
- SU(2)
  - adjoint: Nf=2
  - fundamental: Nf=8
- SU(4)
  - decuplet: Nf=2

SU(N) Phase Diagram

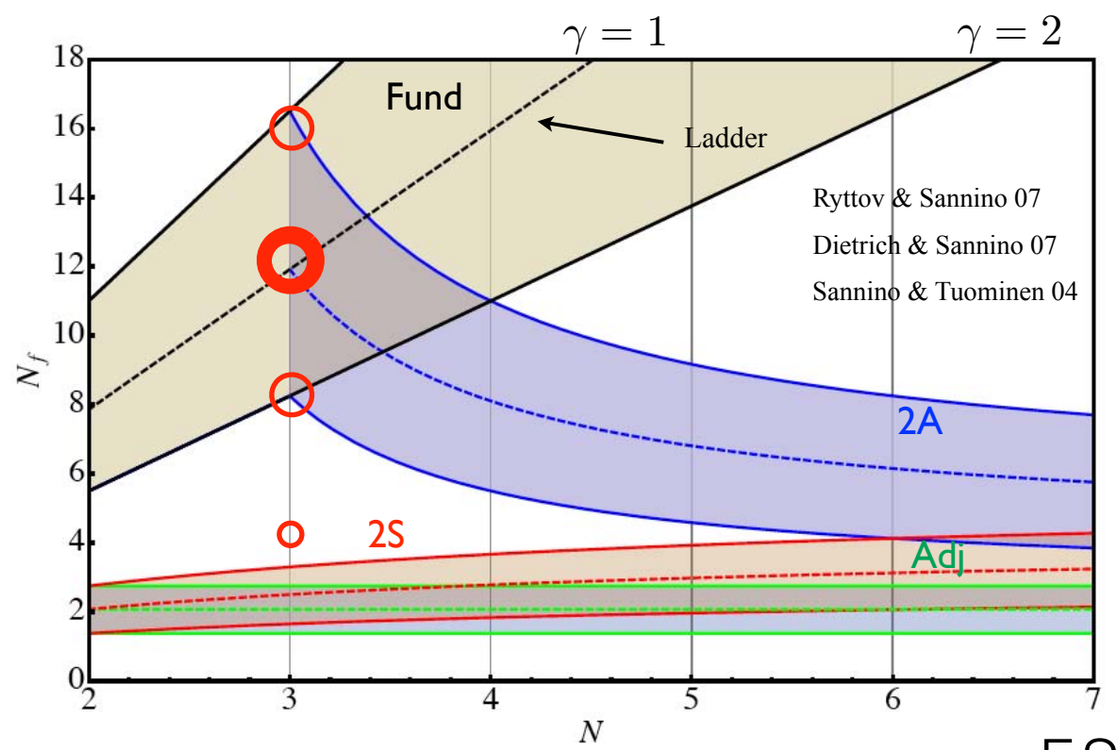

F.Sanino

SU(3) + N_f=12 [fundamental]

Hadron spectrum: m_f-response in mass deformed theory

- IR conformal phase:
  - coupling runs below $\mu = m_f$: like $n_f=0$ QCD with $\Lambda_{QCD} \sim m_f$
  - multi particle / glueball state : $M_H \propto m_f^{1/(1+\gamma_m^*)}$; $F_\pi \propto m_f^{1/(1+\gamma_m^*)}$
- S χ SB phase:
  - ChPT (but, large N_f, small F $\Leftrightarrow$ real QCD)
    - hard to get to the chiral regime
  - at leading: $M_\pi^2 \propto m_f$, ; $F_\pi = F + c\, m_f$
  - so far no chiral logs are observed $\rightarrow$ polynomial in m_f

Simulation

- N_f=12 HISQ (Highly Improved Staggered Quarks)
- tree level Symanzik gauge
- $\beta=6/g^2=3.7$, $V=L^3xT$: L/T=3/4; L=18, 24, 30, $0.04 \leqq m_f \leqq 0.2$
- $\beta=6/g^2=4.0$, $V=L^3xT$: L/T=3/4; L=18, 24, 30, $0.05 \leqq m_f \leqq 0.24$
- N_f=4 HISQ for the reference of S χ SB for comparison
- using MILC code v7 with some modifications

staggered flavor symmetry for N_f=12 HISQ

- comparing mesonic mass with local PS and V operators for β=3.7

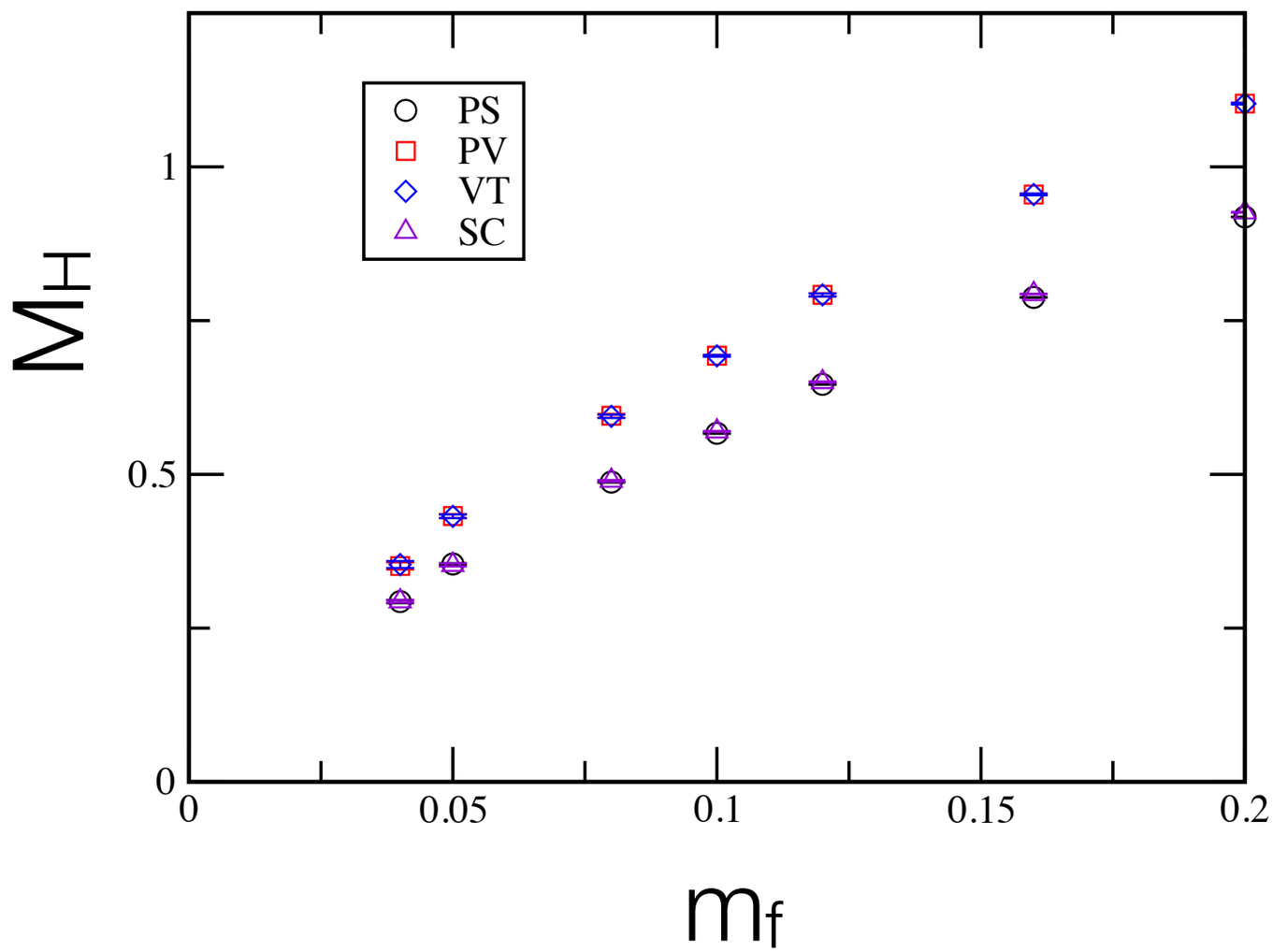

a crude analysis: F_π/M_π vs M_π

N_f=12: HISQ

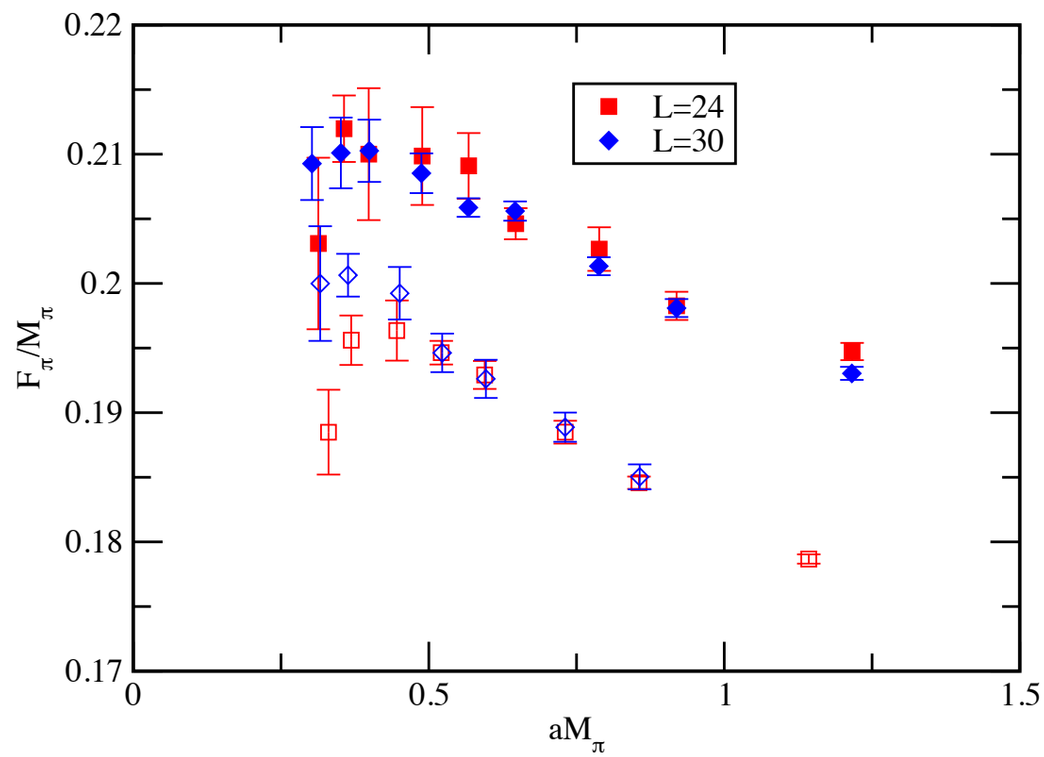

N_f=4: HISQ β=3.7

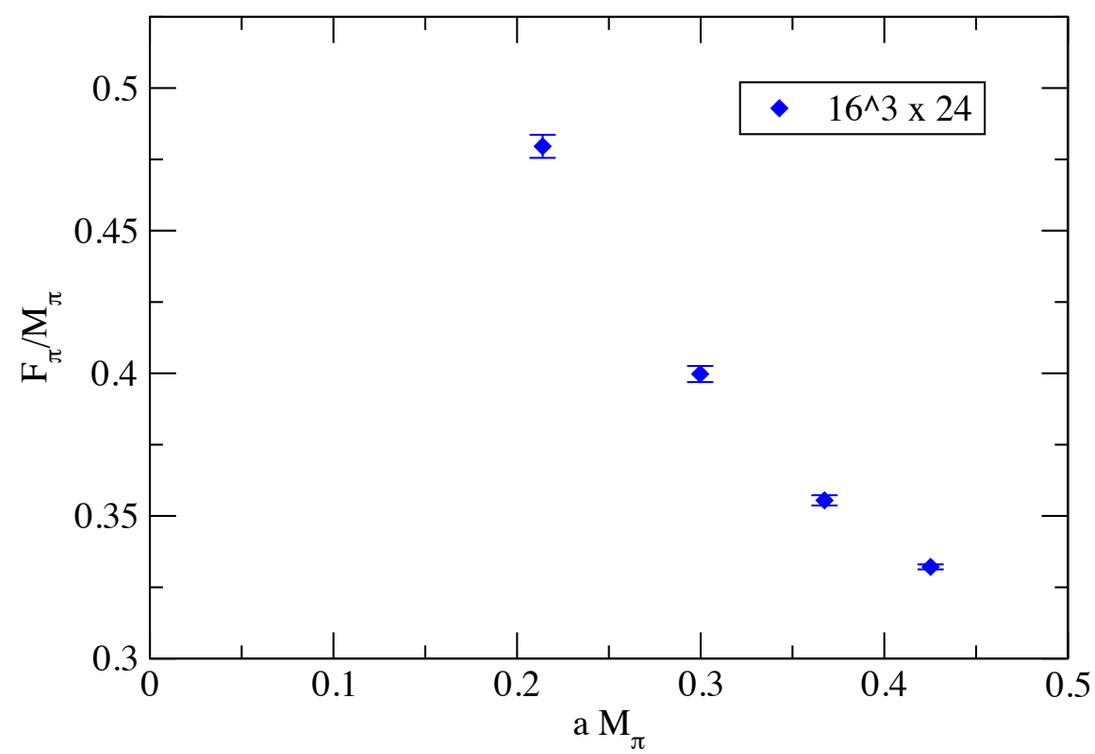

a crude analysis: F_π/M_π vs M_π

N_f=12: HISQ

flat: β=3.7

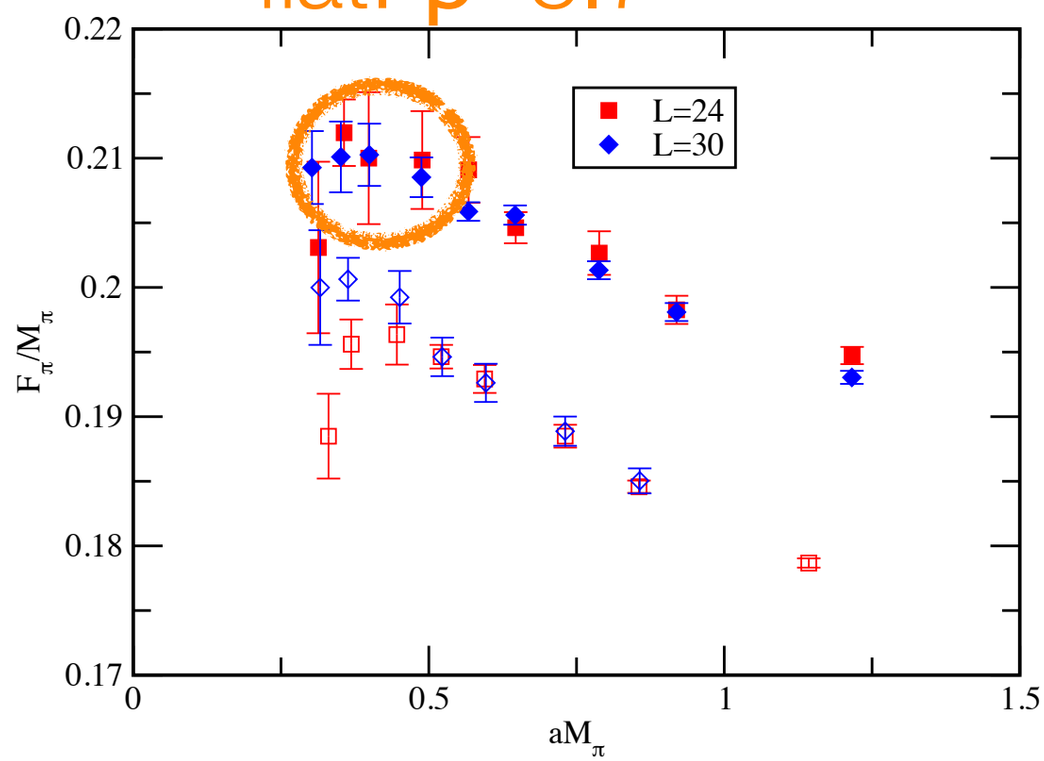

N_f=4: HISQ β=3.7

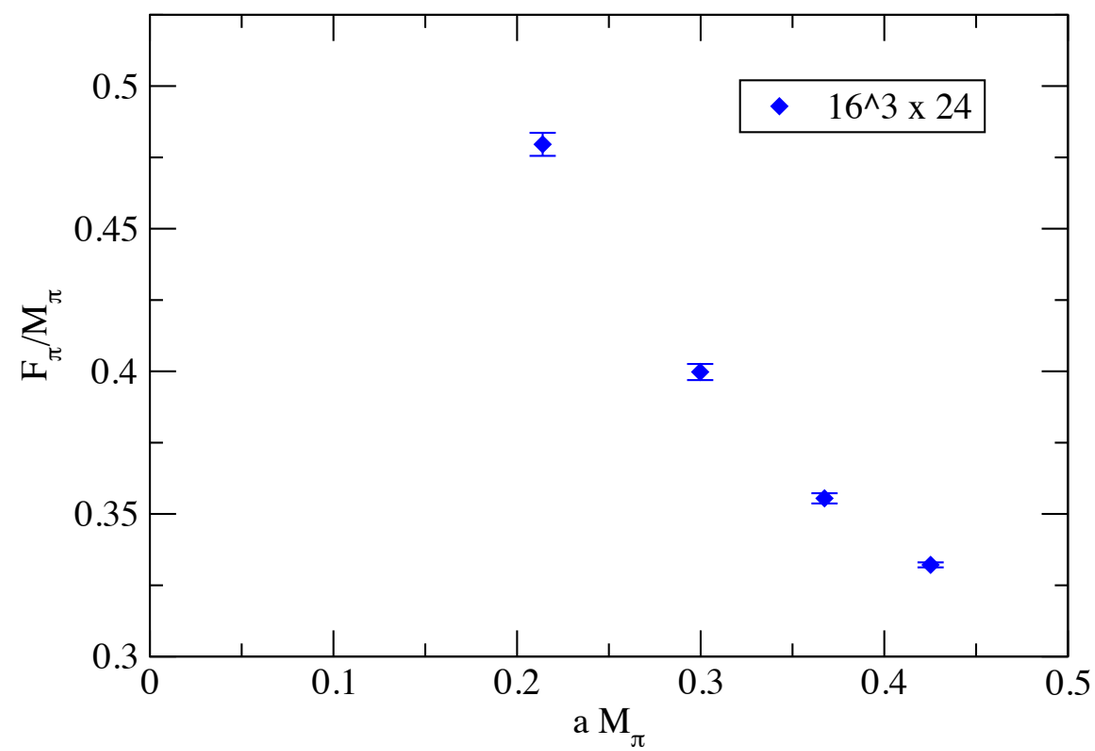

- β=3.7: small mass: consistent with hyper-scaling

a crude analysis: F_π/M_π vs M_π

N_f=12: HISQ

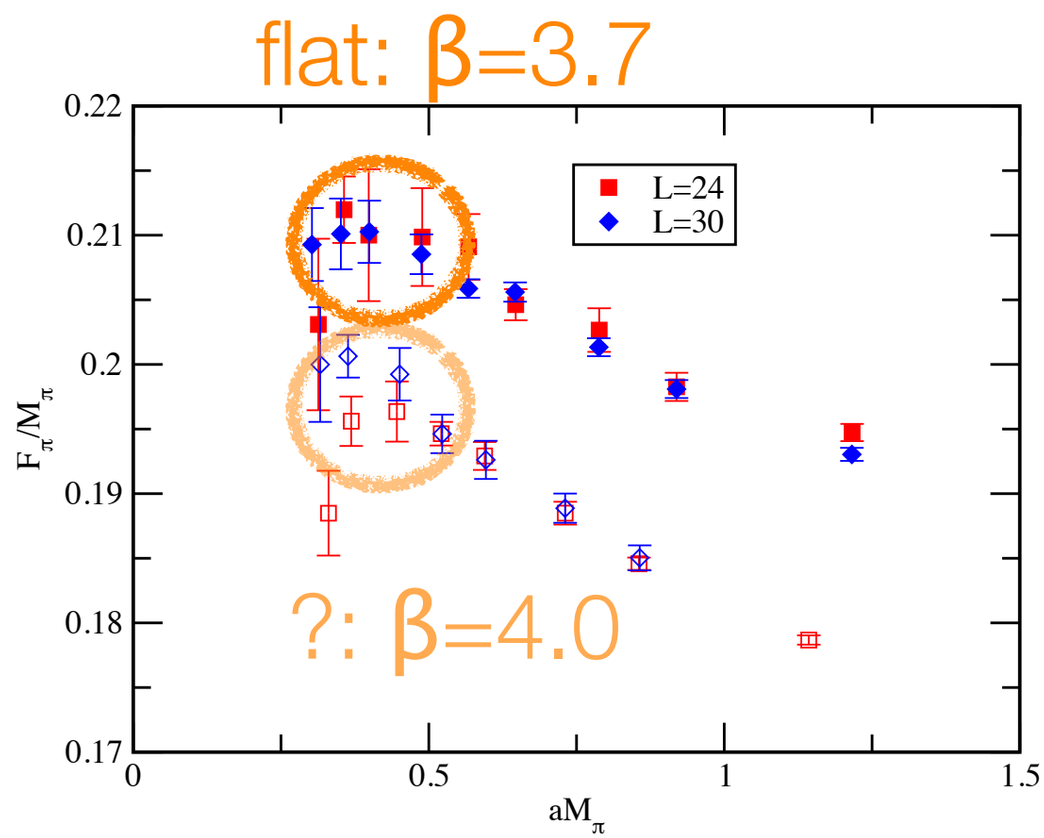

N_f=4: HISQ β=3.7

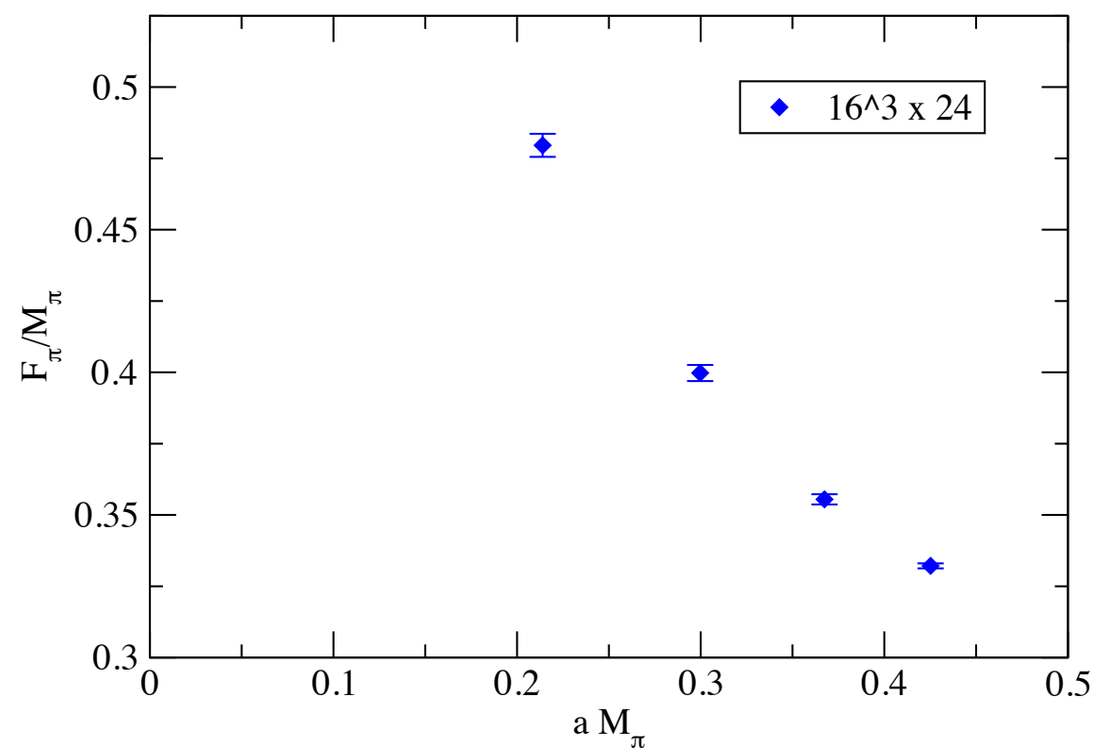

- β=3.7: small mass: consistent with hyper-scaling
- β=4.0: mass too heavy ? inconsistent with being in the hyper-scaling region

a crude analysis: M_ρ/M_π vs M_π

N_f=12: HISQ

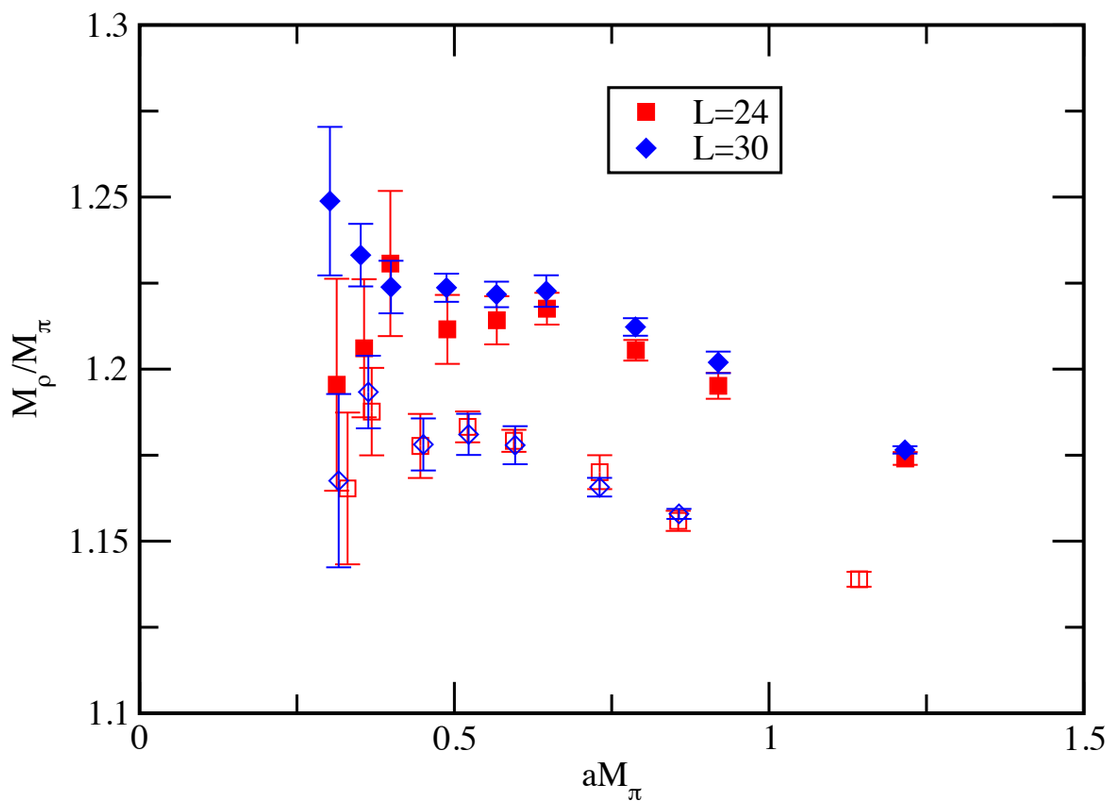

a crude analysis: M_ρ/M_π vs M_π

N_f=12: HISQ

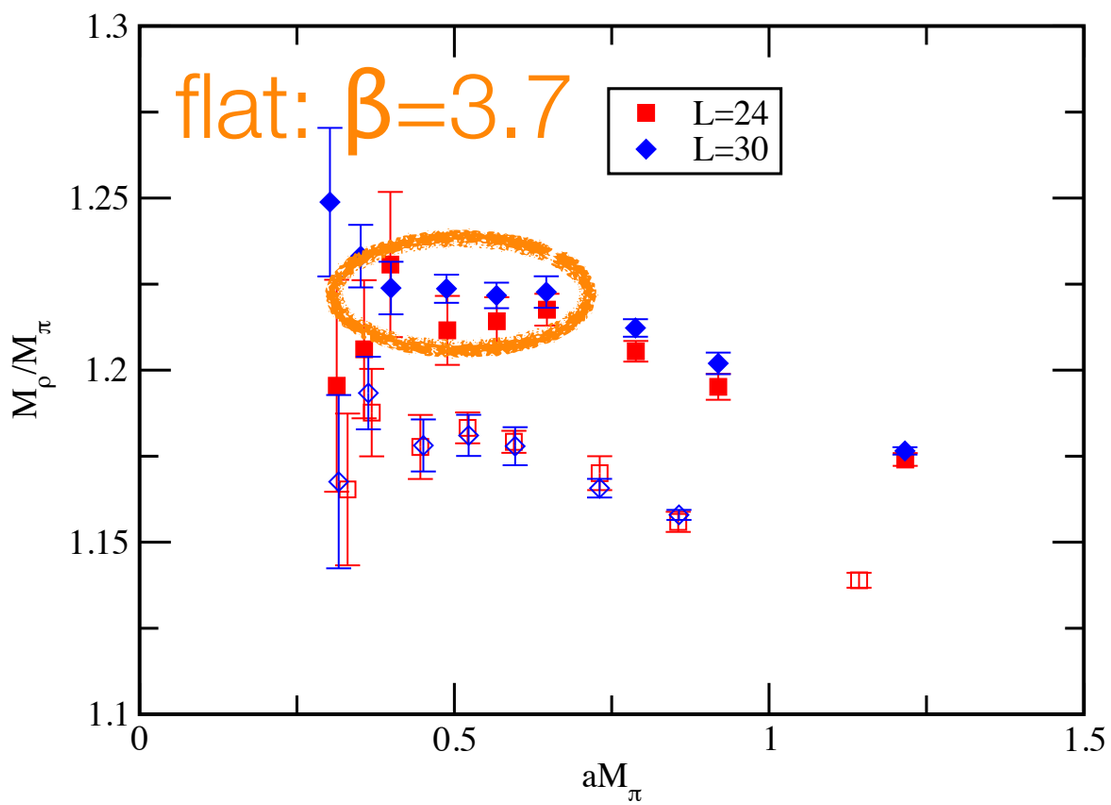

a crude analysis: M_ρ/M_π vs M_π

N_f=12: HISQ

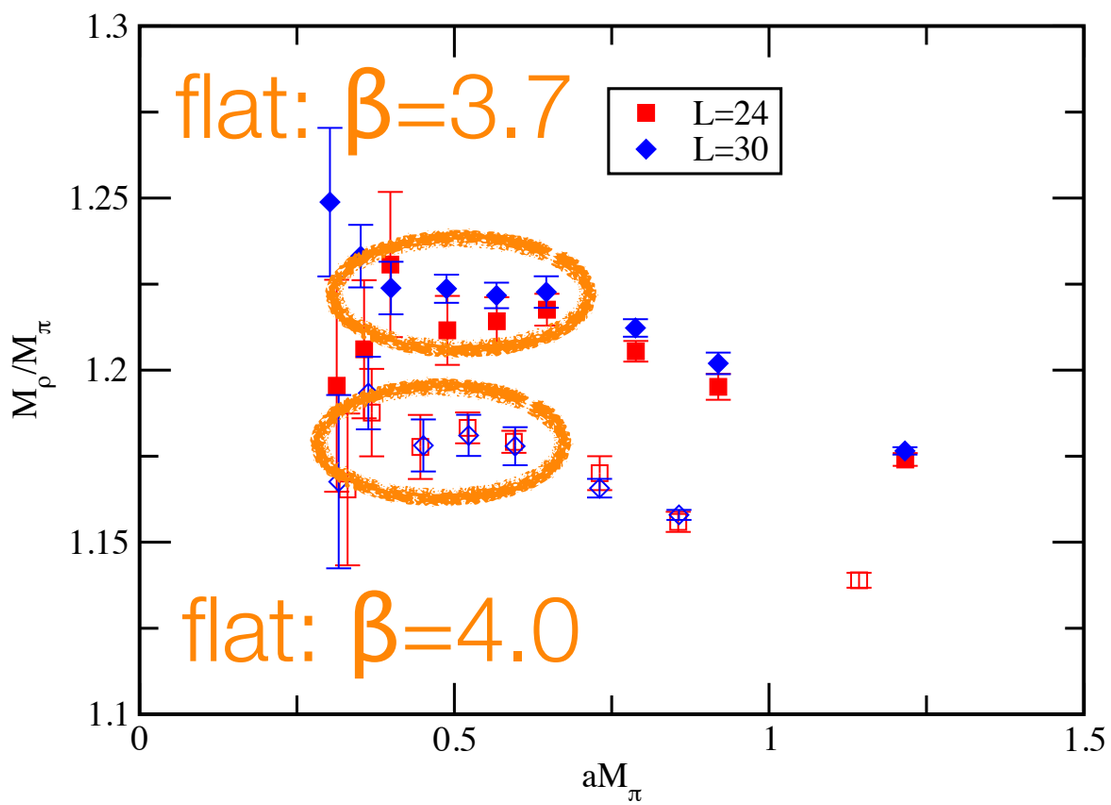

- β=3.7 & 4.0: small mass (wider than F_π): consistent with hyper scaling (HS)

a crude analysis: M_ρ/M_π vs M_π

N_f=12: HISQ

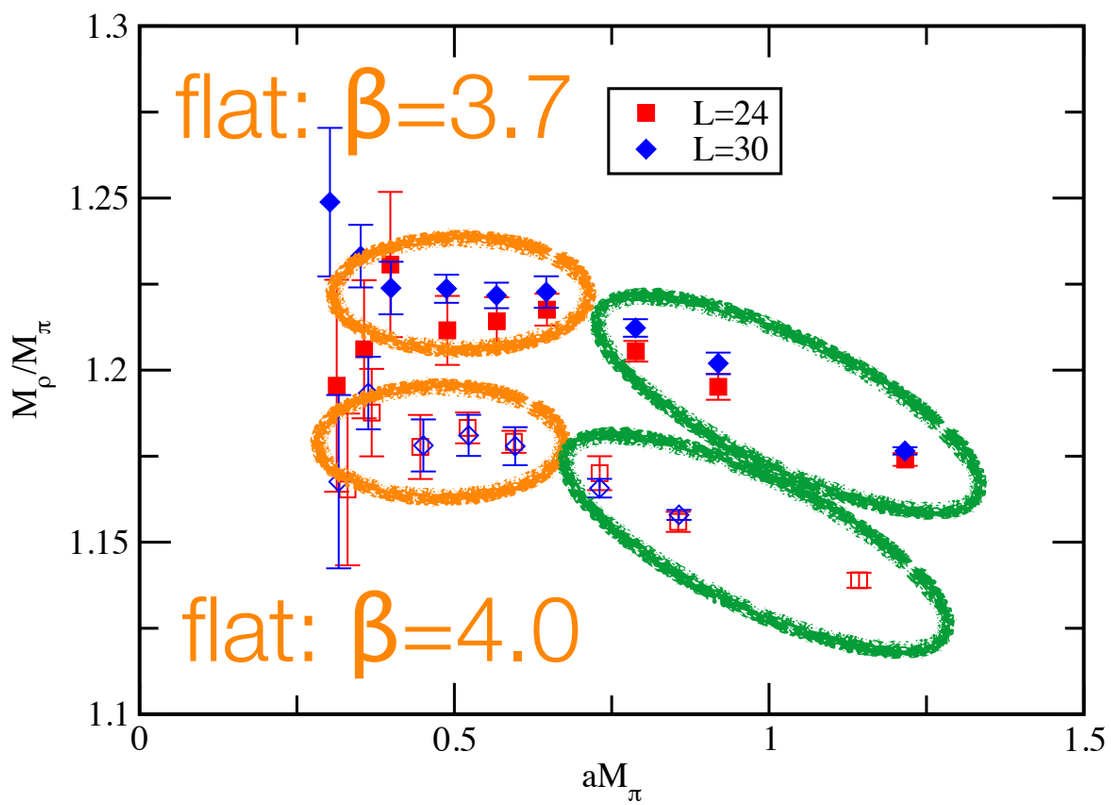

- β=3.7 & 4.0: small mass (wider than F_π): consistent with hyper scaling (HS)
- mass dependence at the tail is due to non-universal mass correction to HS

a crude analysis: M_ρ/M_π vs M_π

N_f=12: HISQ

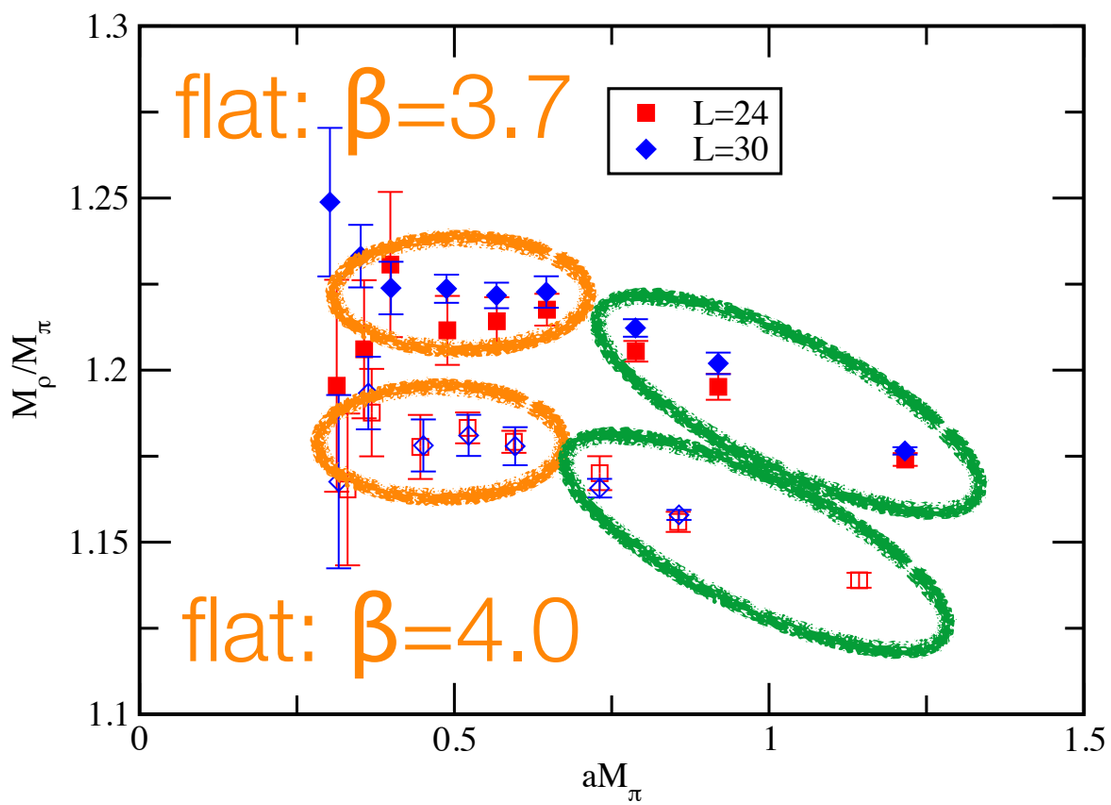

- one can attempt to perform a matching

- β=3.7 & 4.0: small mass (wider than F_π): consistent with hyper scaling (HS)
- mass dependence at the tail is due to non-universal mass correction to HS

a crude analysis: M_ρ/M_π vs M_π

N_f=12: HISQ

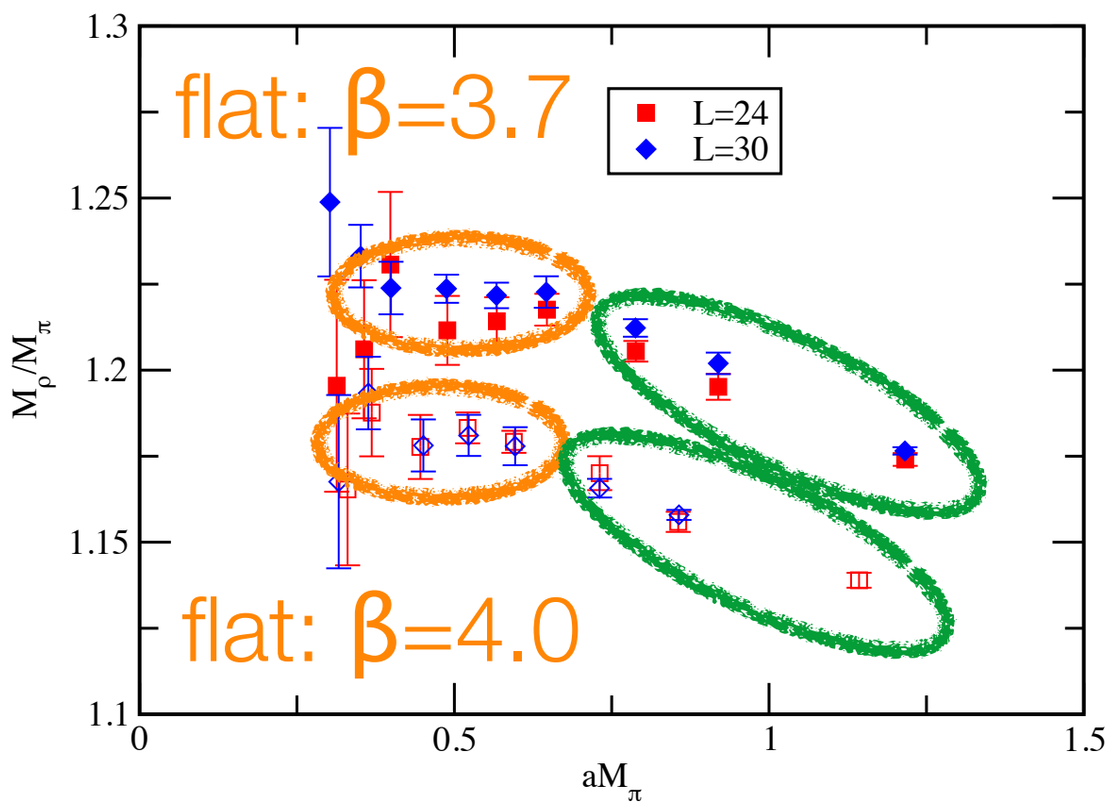

- one can attempt to perform a matching
- a(β=3.7) > a(β=4.0)

- β=3.7 & 4.0: small mass (wider than F_π): consistent with hyper scaling (HS)
- mass dependence at the tail is due to non-universal mass correction to HS

a crude analysis: M_ρ/M_π vs M_π

N_f=12: HISQ

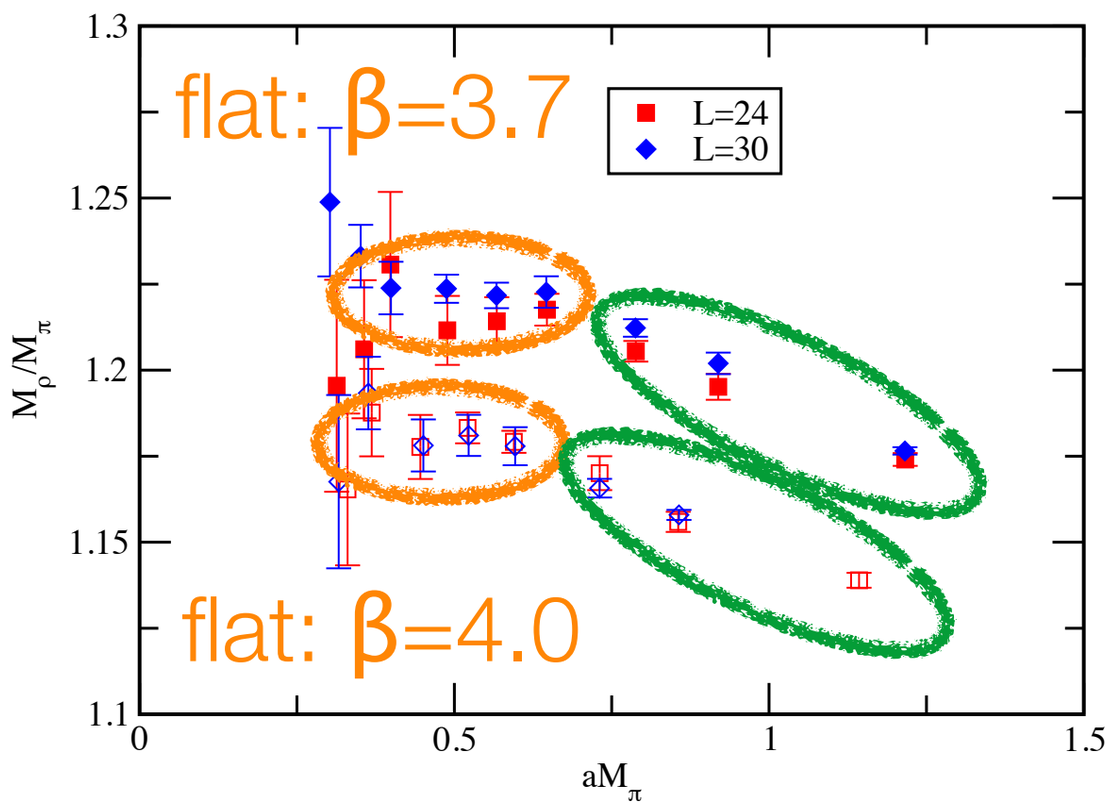

- one can attempt to perform a matching
- a(β=3.7) > a(β=4.0)
  - movement: correct direction in asymptotically free domain !

- β=3.7 & 4.0: small mass (wider than F_π): consistent with hyper scaling (HS)
- mass dependence at the tail is due to non-universal mass correction to HS

conformal (finite size) scaling

- Scaling dimension at IR fixed point [Wilson-Fisher]; Hyper Scaling [Miransky]
- mass dependence is described by anomalous dimensions at IRFP
  - quark mass anomalous dimension γ^*
  - operator anomalous dimension
- meson mass and pion decay constant obey same scaling

$$m_\pi = c_m m_f^{\frac{1}{1+\gamma^*}} \qquad f_\pi = c_f m_f^{\frac{1}{1+\gamma^*}}$$

- finite size scaling in a L^4 box (DeGrand; Del Debbio et al)
  - scaling variable: $x = L m_f^{\frac{1}{1+\gamma^*}}$

$$L f_\pi = F(x) \qquad L m_\pi = G(x)$$

N_f=4 see if data align at some γ

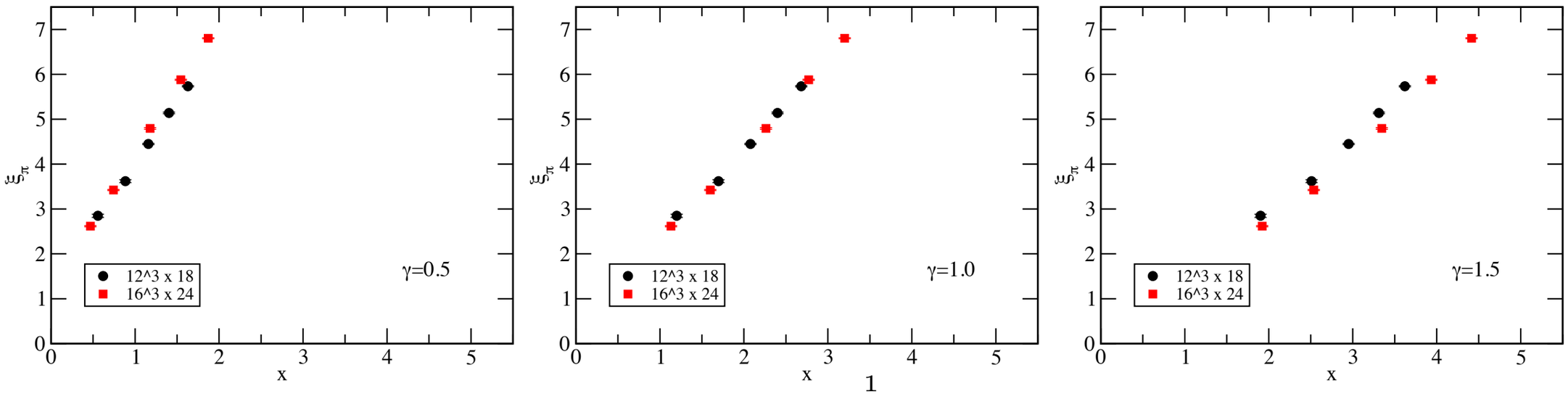

$$x = L m_f^{\frac{1}{1+\gamma}}$$

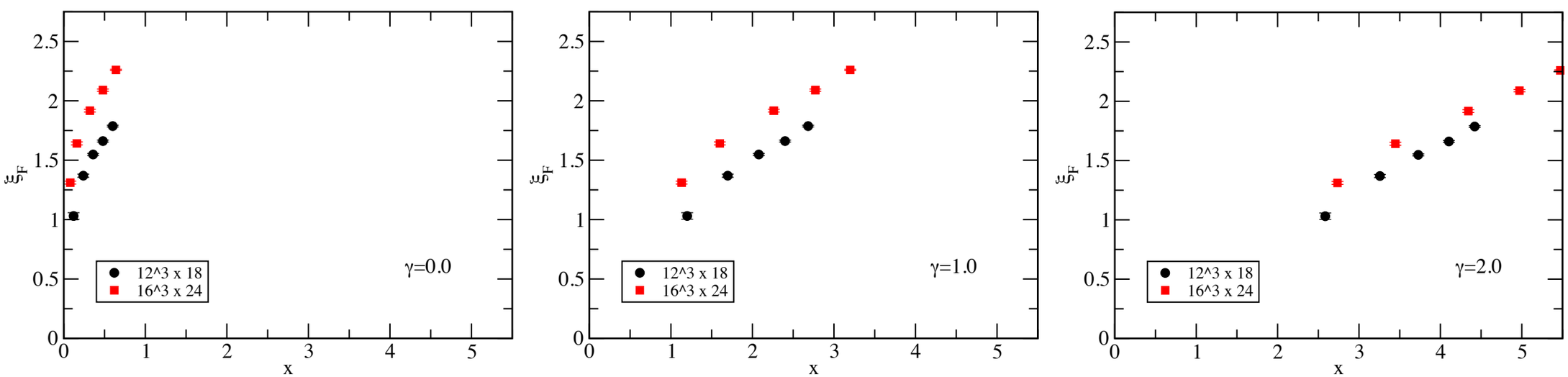

N_f=4 see if data align at some γ

$$M_\pi L \propto m_f^{1/2} L$$

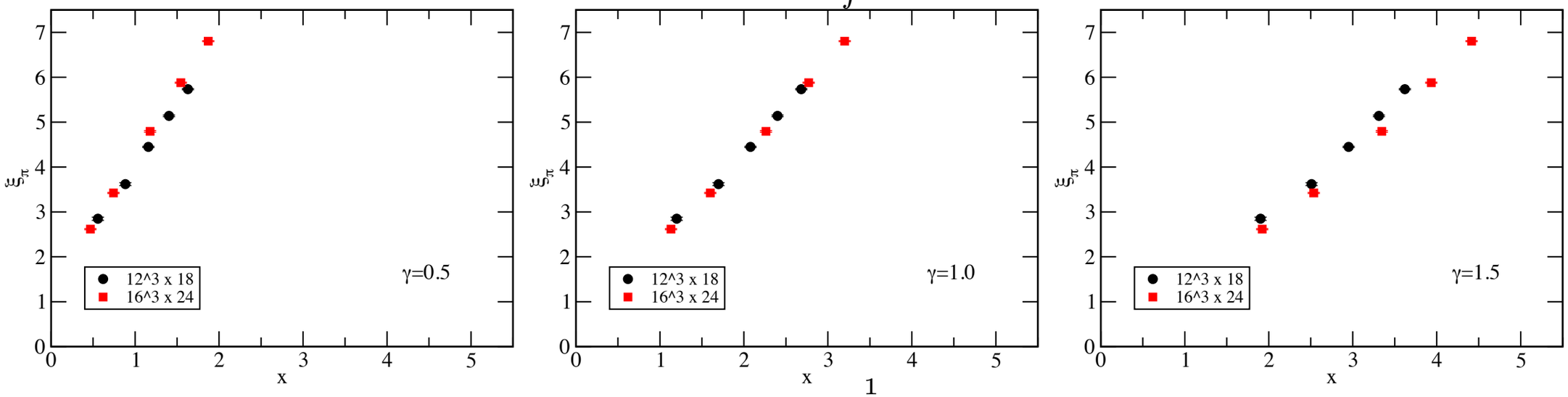

$$x = L m_f^{\frac{1}{1+\gamma}}$$

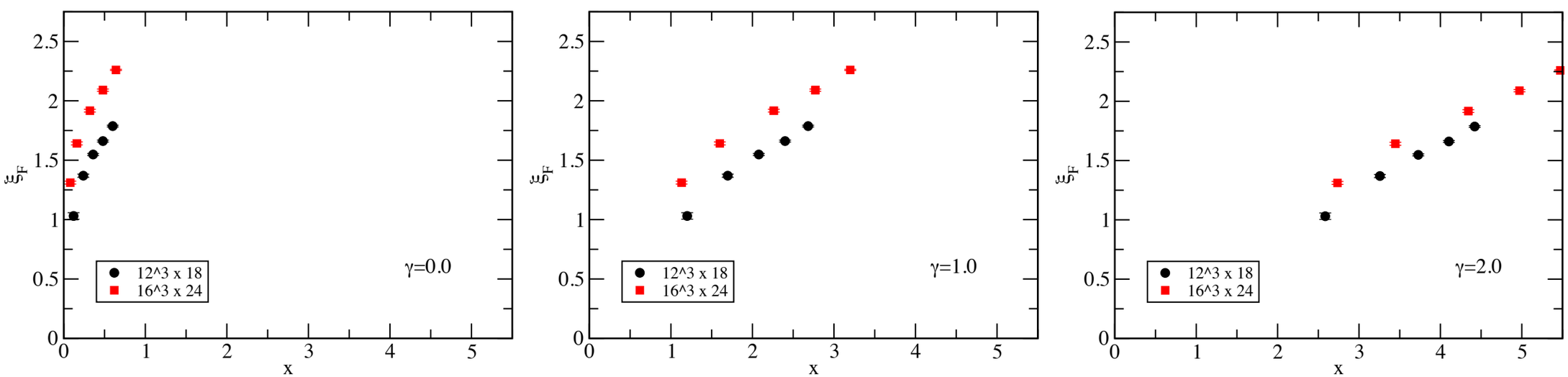

N_f=4 see if data align at some γ

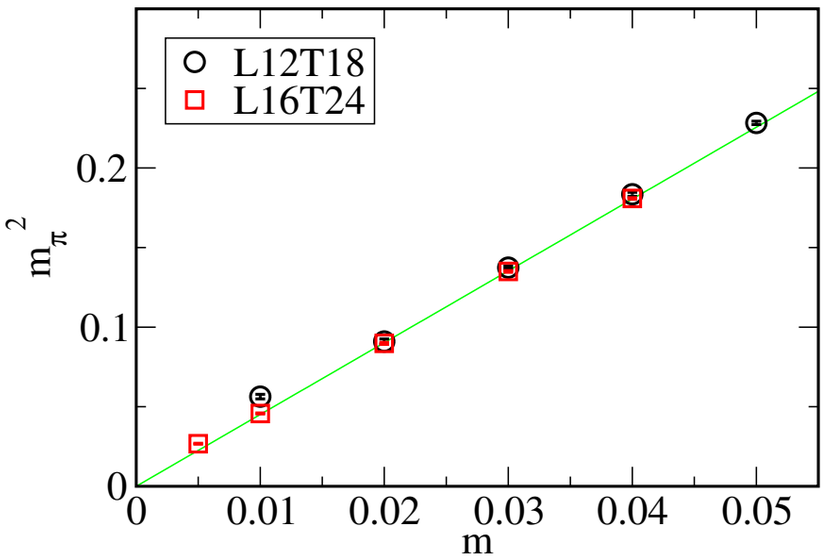

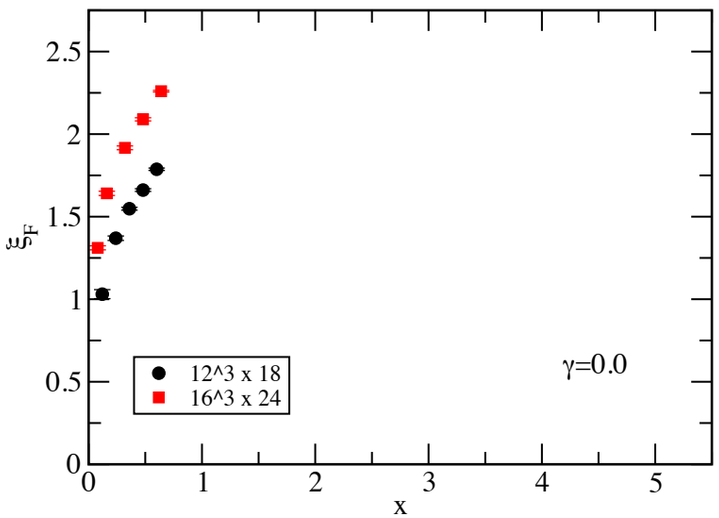

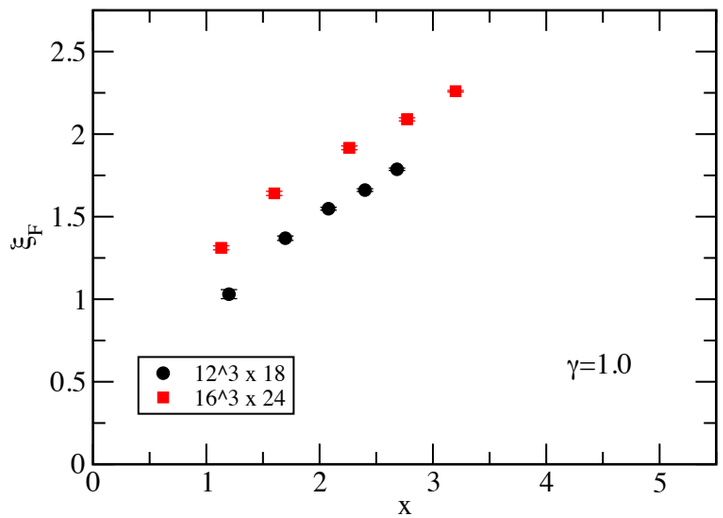

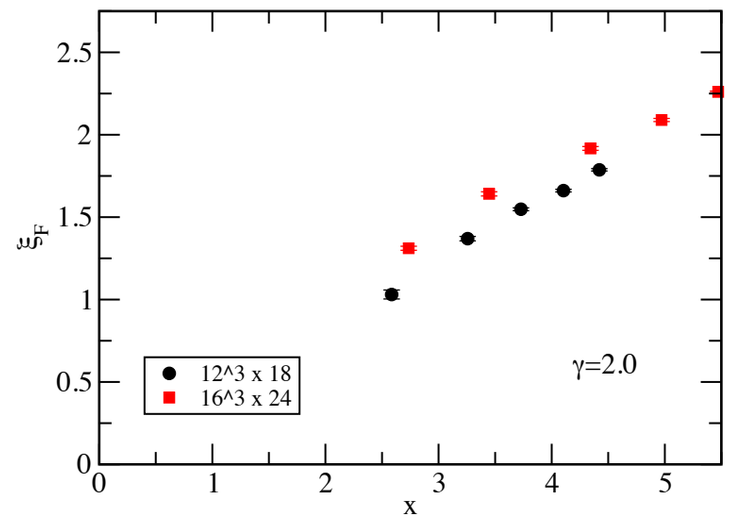

N_f=4 see if data align at some γ

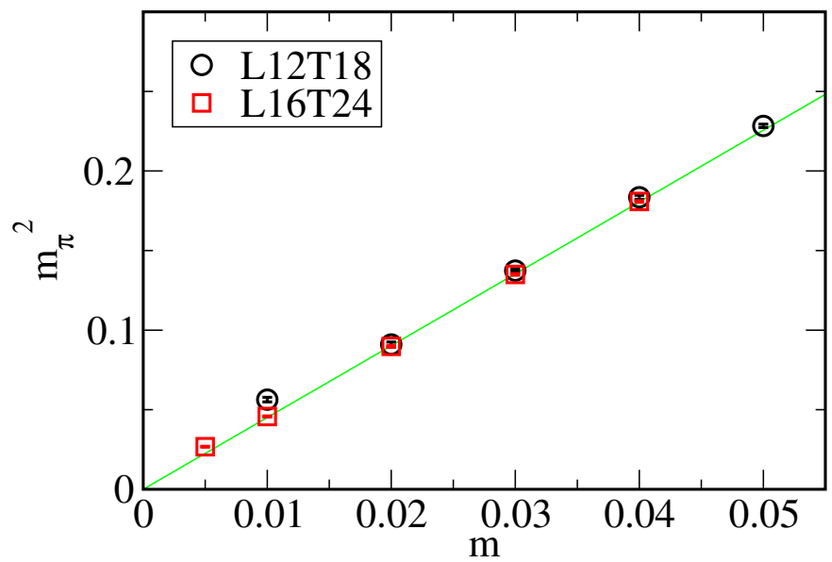

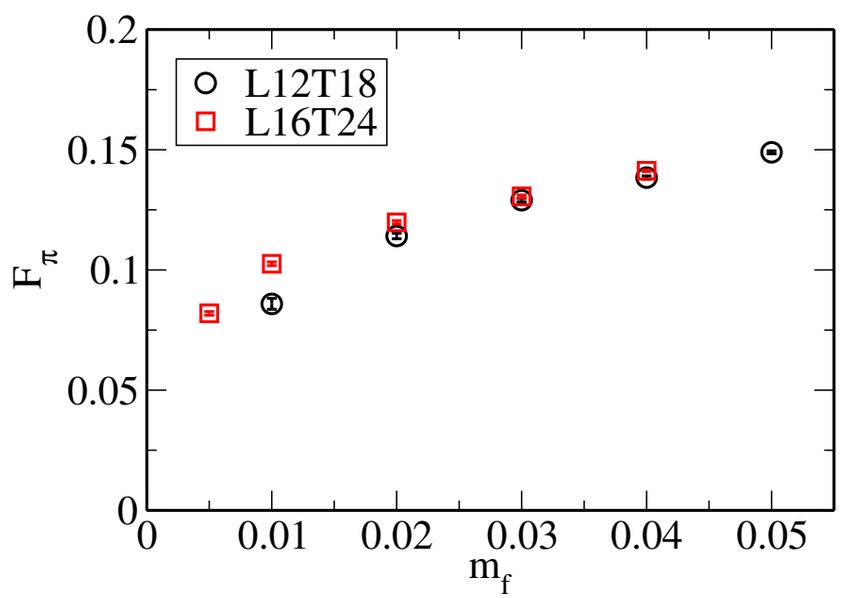

N_f=12 see if data align at some γ

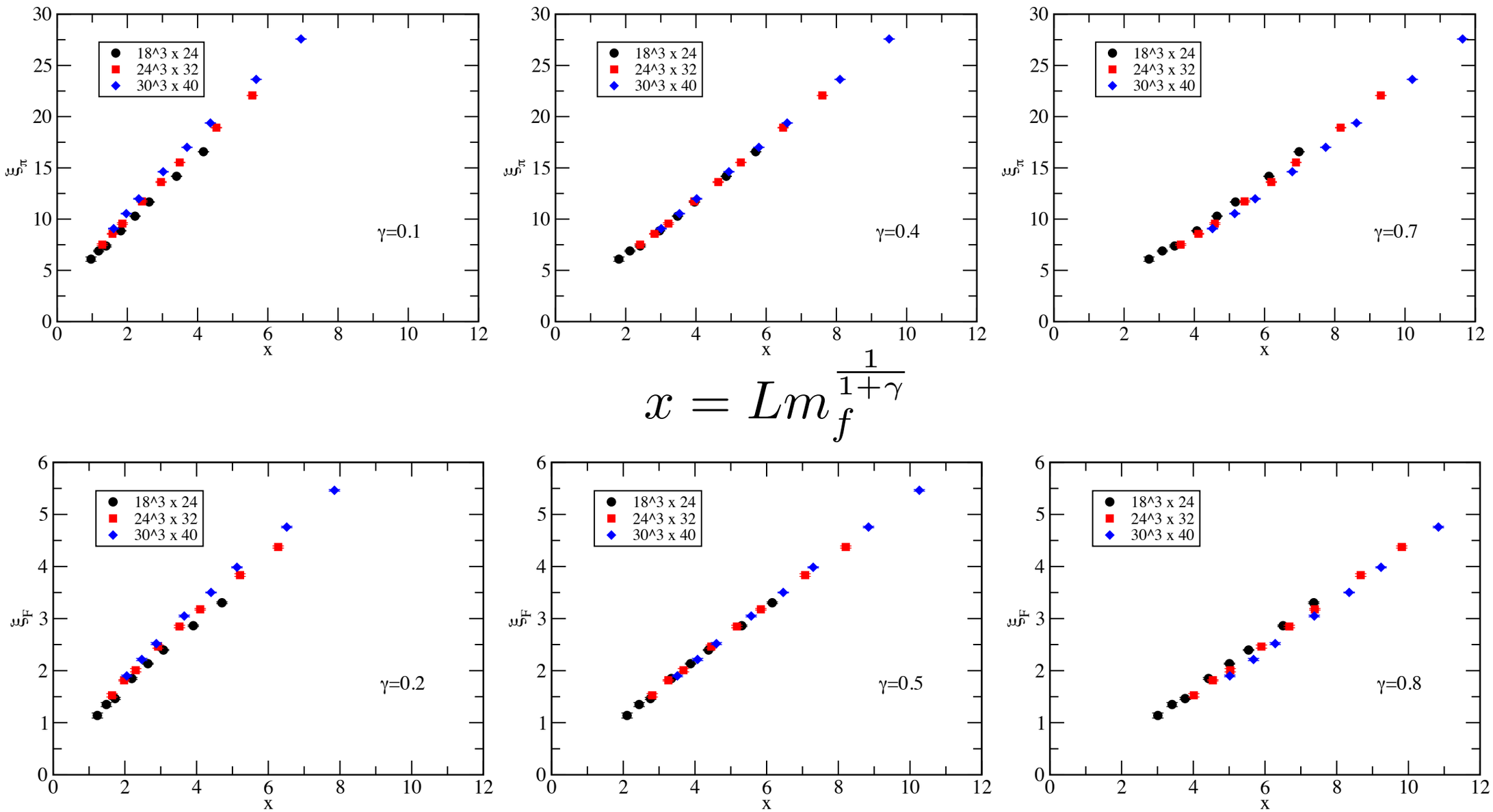

$$x = L m_f^{\frac{1}{1+\gamma}}$$

to quantify the “alignment” without resorting to a model

to quantify the “alignment” without resorting to a model

- γ of optimal alignment will minimize:

$$P_p(\gamma) = \frac{1}{\mathcal{N}} \sum_K \sum_{j \notin K} \frac{|\xi_p^j - f_p^{(K)}(x_j)|^2}{\delta^2 \xi_p^j}$$

to quantify the “alignment” without resorting to a model

- γ of optimal alignment will minimize:

$$P_p(\gamma) = \frac{1}{\mathcal{N}} \sum_K \sum_{j \notin K} \frac{|\xi_p^j - f_p^{(K)}(x_j)|^2}{\delta^2 \xi_p^j}$$

  - $\xi_p = LM_p$ for $p=\pi, \rho$; $\xi_F = LF_\pi$

to quantify the “alignment” without resorting to a model

- γ of optimal alignment will minimize:

$$P_p(\gamma) = \frac{1}{\mathcal{N}} \sum_K \sum_{j \notin K} \frac{|\xi_p^j - f_p^{(K)}(x_j)|^2}{\delta^2 \xi_p^j}$$

  - $\xi_p = LM_p$ for p=π, ρ; $\xi_F = LF_\pi$
  - $f_p(x)$: interpolation .... linear

to quantify the “alignment” without resorting to a model

- γ of optimal alignment will minimize:

$$P_p(\gamma) = \frac{1}{\mathcal{N}} \sum_K \sum_{j \notin K} \frac{|\xi_p^j - f_p^{(K)}(x_j)|^2}{\delta^2 \xi_p^j}$$

  - $\xi_p = LM_p$ for p=π, ρ; $\xi_F = LF_\pi$
  - $f_p(x)$: interpolation .... linear
    - (quadratic for a systematic error)

to quantify the “alignment” without resorting to a model

- γ of optimal alignment will minimize:

$$P_p(\gamma) = \frac{1}{\mathcal{N}} \sum_K \sum_{j \notin K} \frac{|\xi_p^j - f_p^{(K)}(x_j)|^2}{\delta^2 \xi_p^j}$$

  - $\xi_p = LM_p$ for p=π, ρ; $\xi_F = LF_\pi$
  - $f_p(x)$: interpolation .... linear
    - (quadratic for a systematic error)
- if ξ^j is away from $f(x_i)$ by $\delta\ \xi^j$ as average→P=1

to quantify the "alignment" without resorting to a model

- γ of optimal alignment will minimize:

$$P_p(\gamma) = \frac{1}{\mathcal{N}} \sum_K \sum_{j \notin K} \frac{|\xi_p^j - f_p^{(K)}(x_j)|^2}{\delta^2 \xi_p^j}$$

  - $\xi_p = LM_p$ for p=π, ρ; $\xi_F = LF_\pi$
  - $f_p(x)$: interpolation .... linear
    - (quadratic for a systematic error)
- if ξ^j is away from $f(x_i)$ by $\delta\ \xi^j$ as average→P=1

M_π at β=3.7

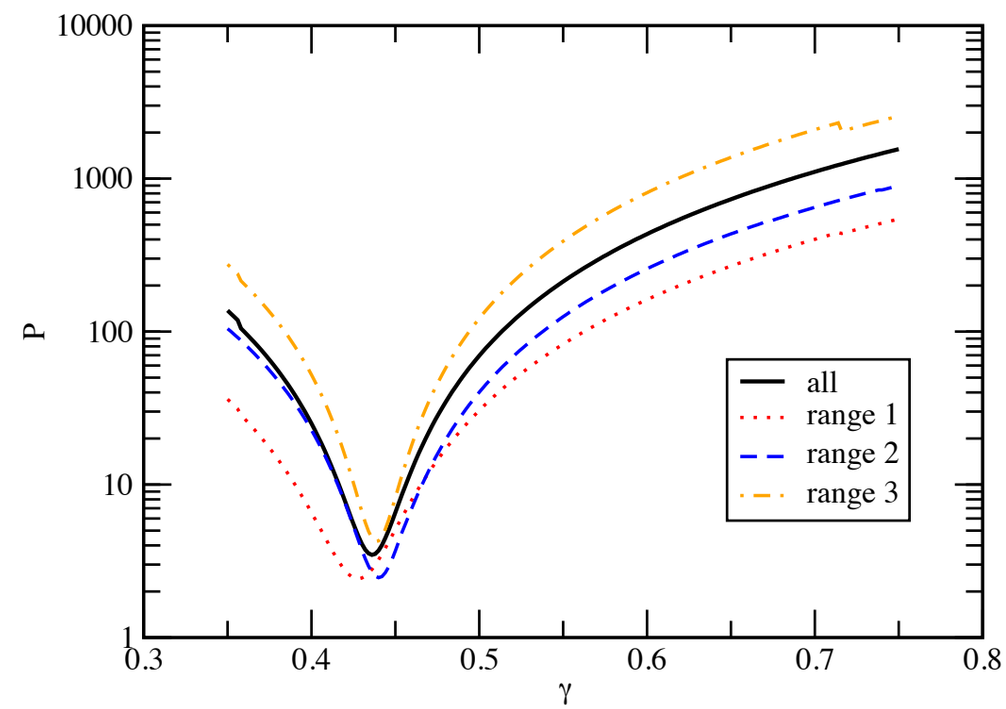

to quantify the "alignment" without resorting to a model

- γ of optimal alignment will minimize:

$$P_p(\gamma) = \frac{1}{\mathcal{N}} \sum_K \sum_{j \notin K} \frac{|\xi_p^j - f_p^{(K)}(x_j)|^2}{\delta^2 \xi_p^j}$$

  - $\xi_p = LM_p$ for p=π, ρ; $\xi_F = LF_\pi$
  - $f_p(x)$: interpolation .... linear
    - (quadratic for a systematic error)
- if ξ^j is away from $f(x_i)$ by $\delta\,\xi^j$ as average→P=1
- optimal γ from the minimum of P

M_π at β=3.7

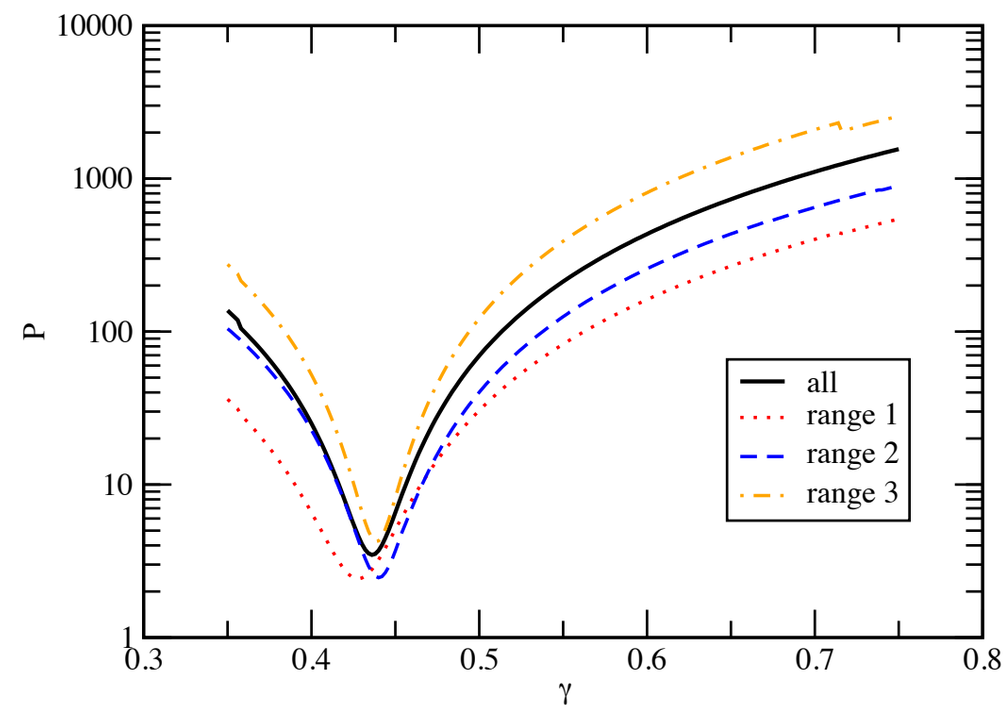

to quantify the "alignment" without resorting to a model

- γ of optimal alignment will minimize:

$$P_p(\gamma) = \frac{1}{\mathcal{N}} \sum_K \sum_{j \notin K} \frac{|\xi_p^j - f_p^{(K)}(x_j)|^2}{\delta^2 \xi_p^j}$$

  - $\xi_p = LM_p$ for p=π, ρ; $\xi_F = LF_\pi$
  - $f_p(x)$: interpolation .... linear
    - (quadratic for a systematic error)
- if ξ^j is away from $f(x_i)$ by $\delta\ \xi^j$ as average→P=1
- optimal γ from the minimum of P

M_π at β=3.7

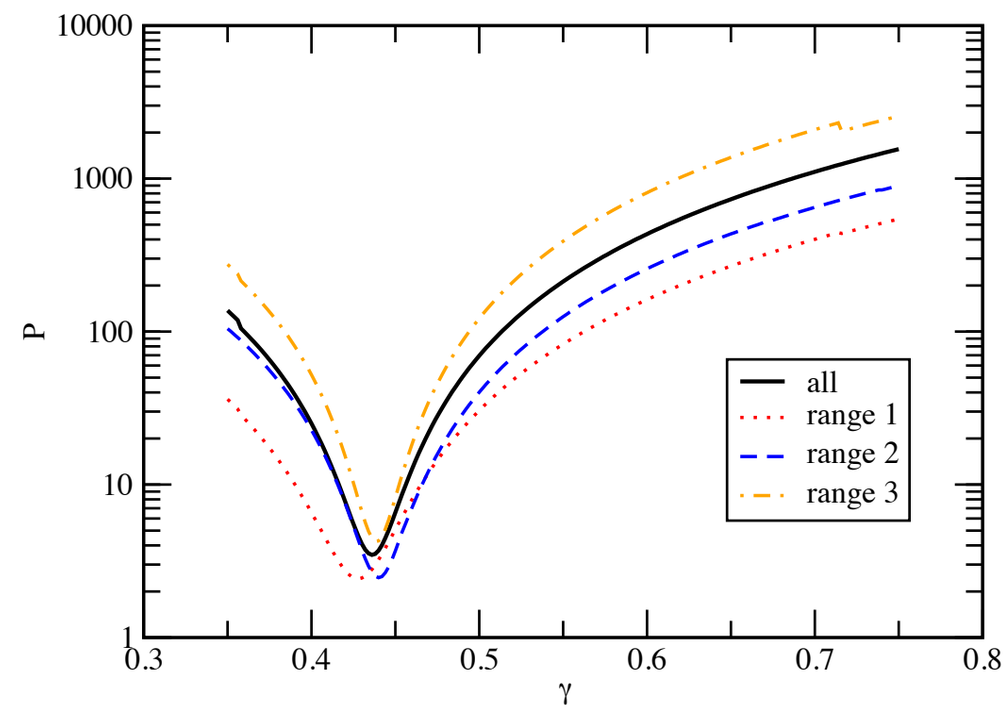

- systematic error due to small L, large m estimated by examining the x and L range dependence

summary of γ obtained by minimizing P(γ)

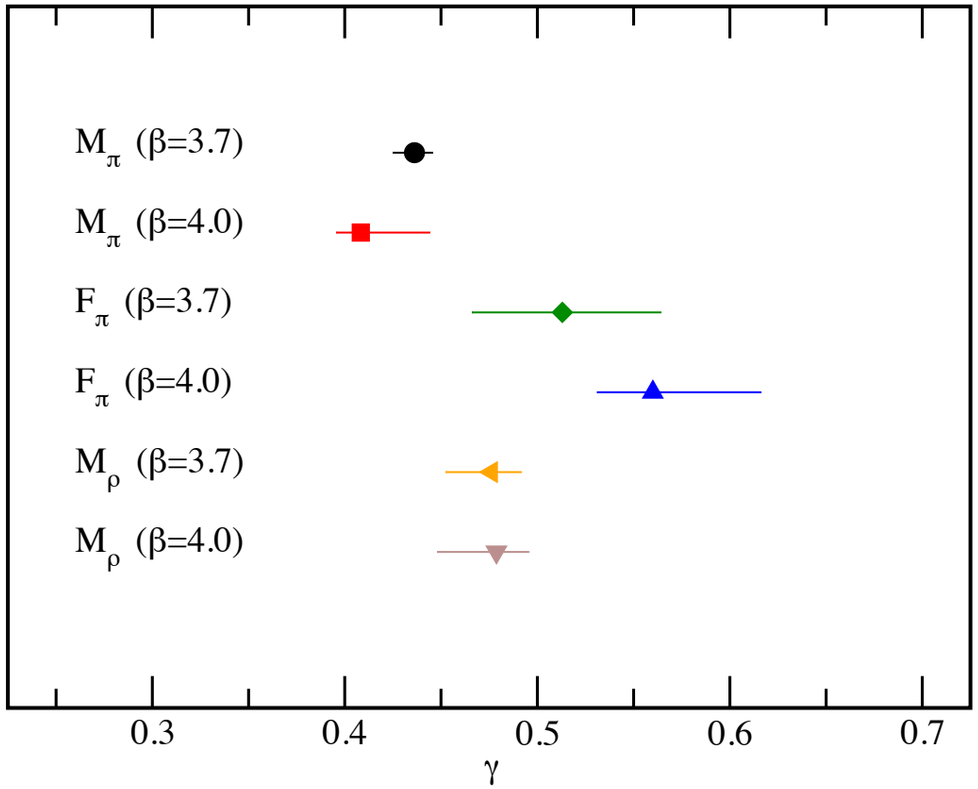

summary of γ obtained by minimizing P(γ)

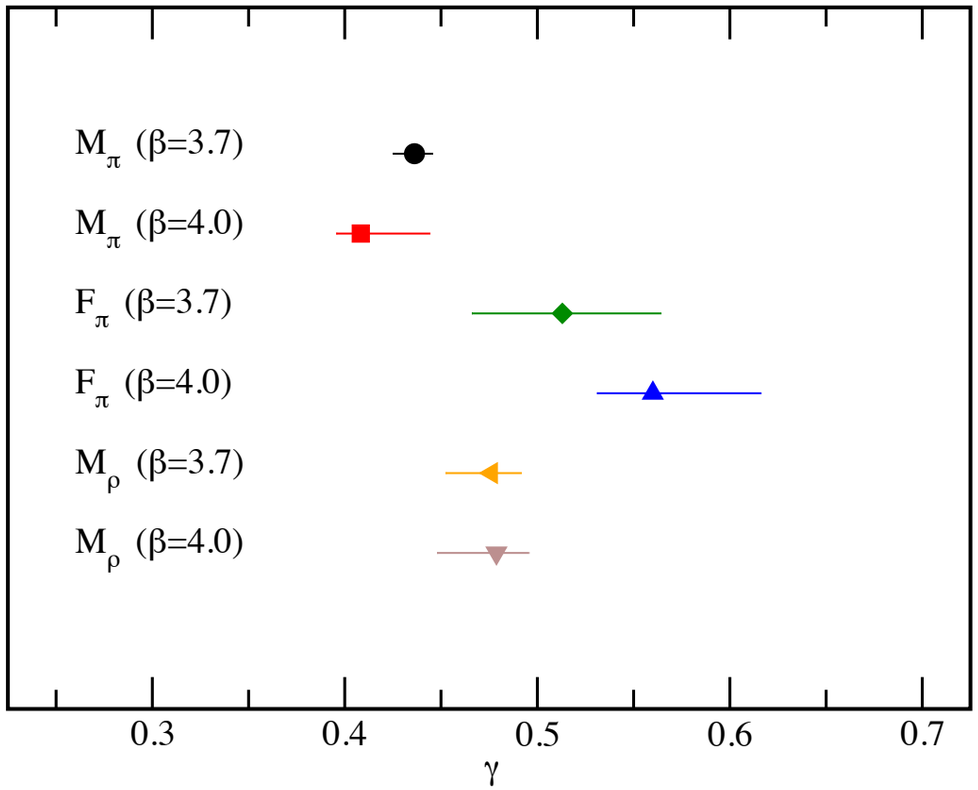

- consistent γ by 1.5 σ level except for F_π at β=4.0

summary of γ obtained by minimizing P(γ)

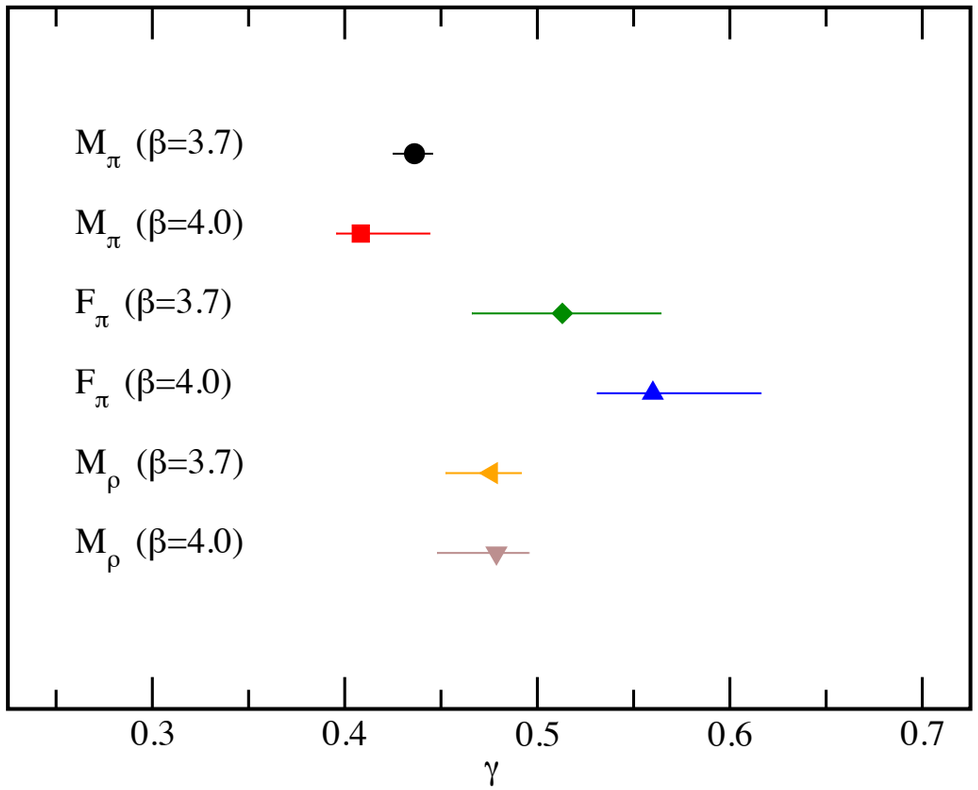

- consistent γ by 1.5 σ level except for F_π at β=4.0
- remember: F_π at β=4.0 speculated to be out of the scaling region

summary of γ obtained by minimizing P(γ)

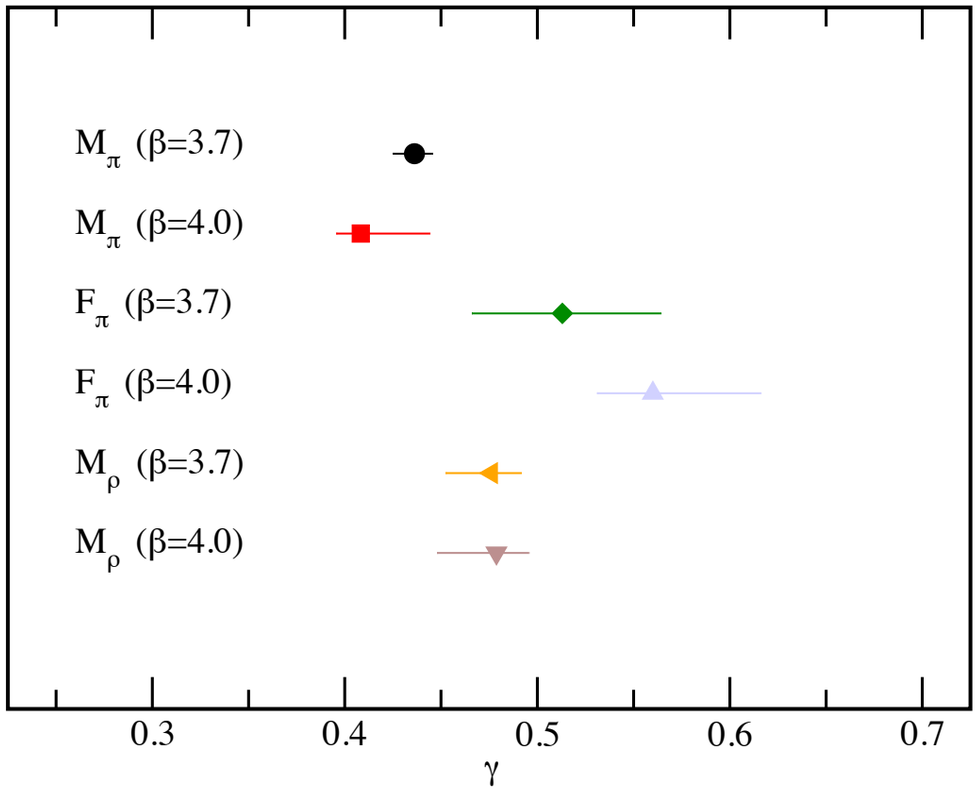

- consistent γ by 1.5 σ level except for F_π at β=4.0
- remember: F_π at β=4.0 speculated to be out of the scaling region
- universal low energy behavior: good with $0.4<\gamma_*<0.5$

Conformal type fit with finite volume correction

$$\xi = LM_\pi,\ LF_\pi,\ LM_\rho$$

$$\xi = c_0 + c_1 L m_f^{1/(1+\gamma)} \quad \cdots \text{fit a},$$

$$\xi = c_0 + c_1 L m_f^{1/(1+\gamma)} + c_2 L m_f^{\alpha} \quad \cdots \text{fit b}.$$

	γ	α	χ^2/dof
fit a	0.455(3)	-	5.43
fit b-1	0.417(10)	$\frac{(3-2\gamma)}{(1+\gamma)}$	1.88
fit b-2	0.431(8)	[2]	1.83

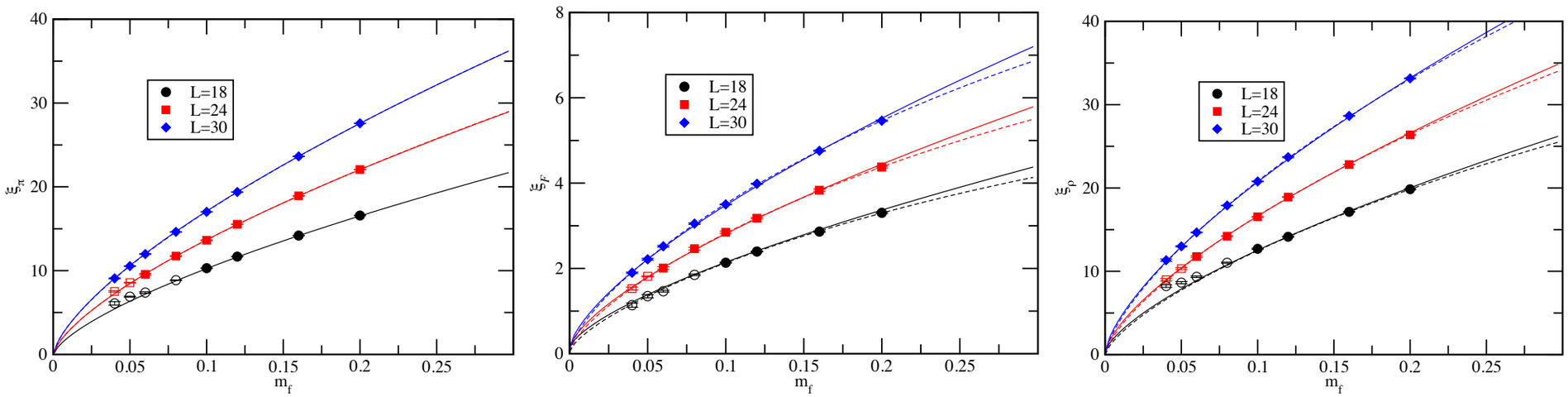

- simultaneous fit it with a leading mass dependent correction is not bad
  - b-1: Ladder Schwinger-Dyson, b-2: $(am)^2$ lattice artifact
- resulting γ is consistent with the model independent analysis

ChPT fit (after infinite volume extrapolation)

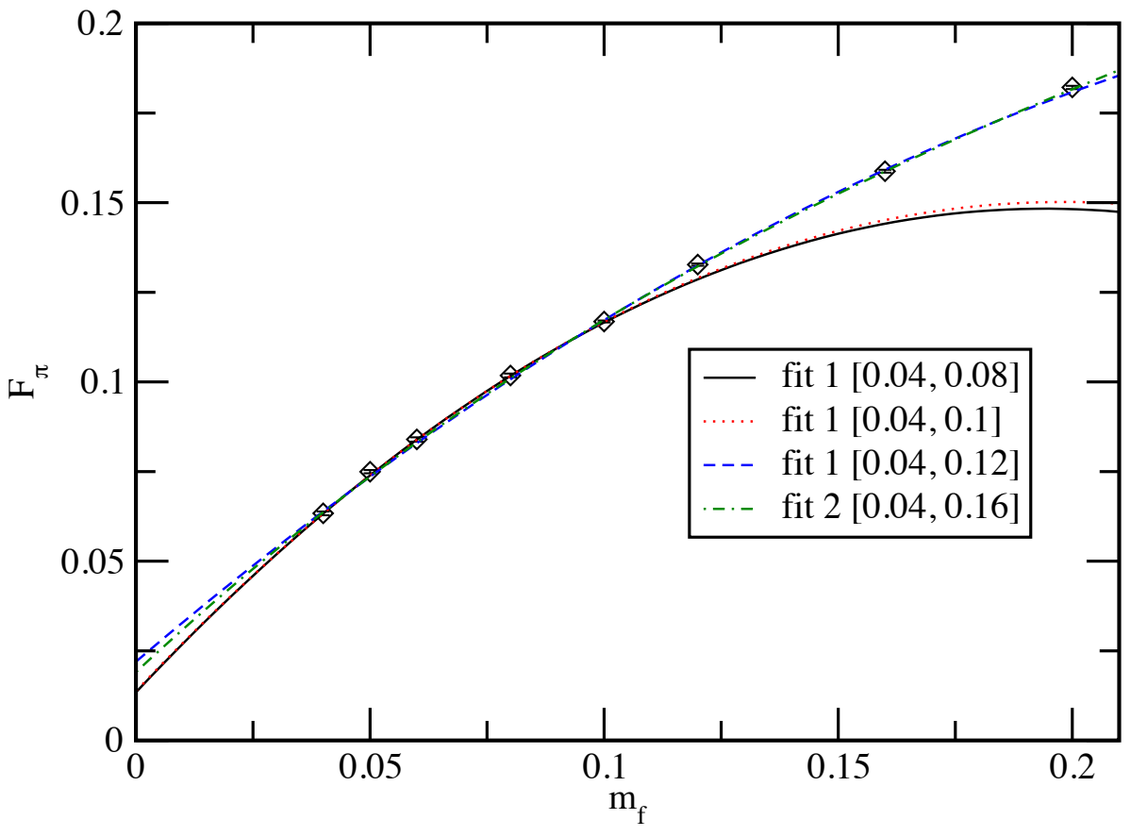

$$h(m_f) = \begin{cases} c_0 + c_1 m_f + c_2 m_f^2 & \cdots \text{fit1} \\ c_0 + c_1 m_f + c_2 m_f^2 + c_3 m_f^3 & \cdots \text{fit2} \end{cases}$$

fit range	c_0	c_1	c_2	c_3	χ^2/dof
fit 1 : $[0.04, 0.08]$	0.0101(54)	1.53(19)	-4.8(1.5)	-	2.09
fit 1 : $[0.04, 0.1]$	0.0138(29)	1.39(88)	-3.62(61)	-	1.39
fit 1 : $[0.04, 0.12]$	0.0226(17)	1.113(45)	-1.64(27)	-	5.42
fit 2 : $[0.04, 0.16]$	0.0182(34)	1.28(13)	-3.4(1.3)	6.0(4.2)	4.75

- 2nd order polynomial fit is reasonably good for small mass range & $c_0>0$

ChPT fit (after infinite volume extrapolation)

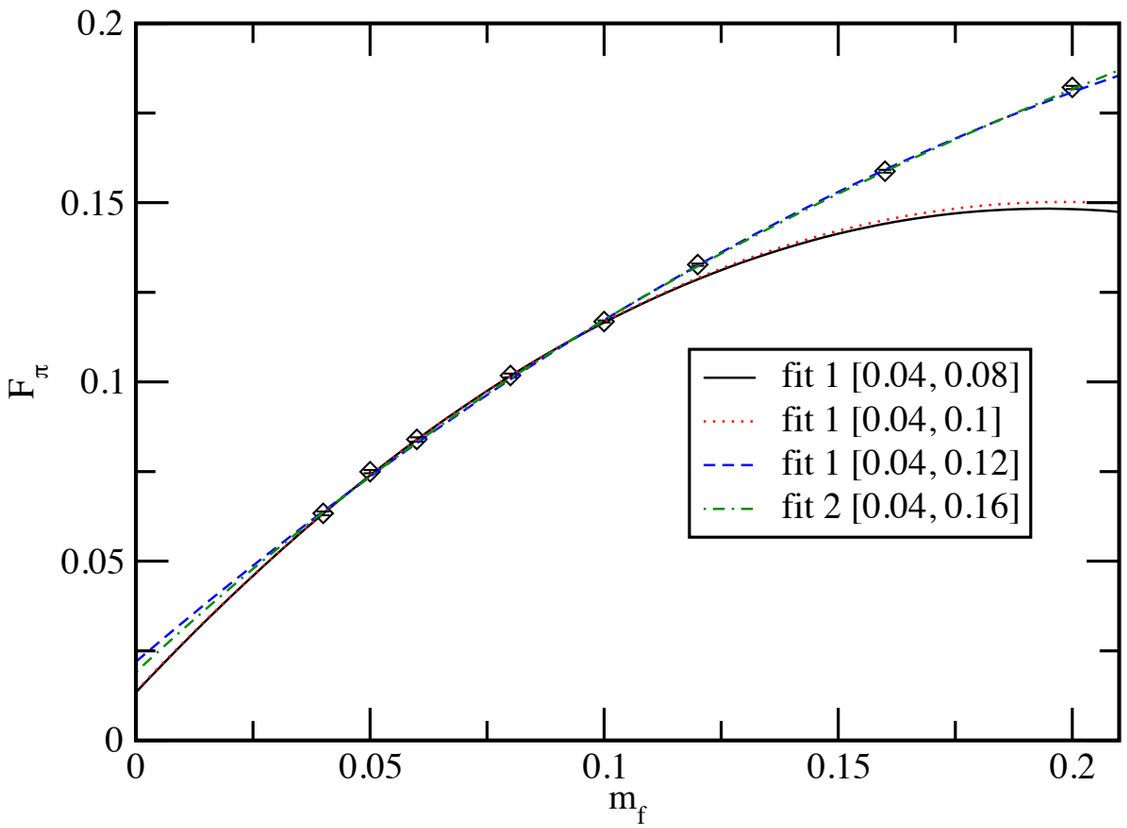

$$h(m_f) = \begin{cases} c_0 + c_1 m_f + c_2 m_f^2 & \cdots \text{fit1} \\ c_0 + c_1 m_f + c_2 m_f^2 + c_3 m_f^3 & \cdots \text{fit2} \end{cases}$$

fit range	c_0	c_1	c_2	c_3	χ^2/dof
fit 1 : $[0.04, 0.08]$	0.0101(54)	1.53(19)	-4.8(1.5)	-	2.09
fit 1 : $[0.04, 0.1]$	0.0138(29)	1.39(88)	-3.62(61)	-	1.39
fit 1 : $[0.04, 0.12]$	0.0226(17)	1.113(45)	-1.64(27)	-	5.42
fit 2 : $[0.04, 0.16]$	0.0182(34)	1.28(13)	-3.4(1.3)	6.0(4.2)	4.75

- 2nd order polynomial fit is reasonably good for small mass range & $c_0>0$

ChPT fit (after infinite volume extrapolation)

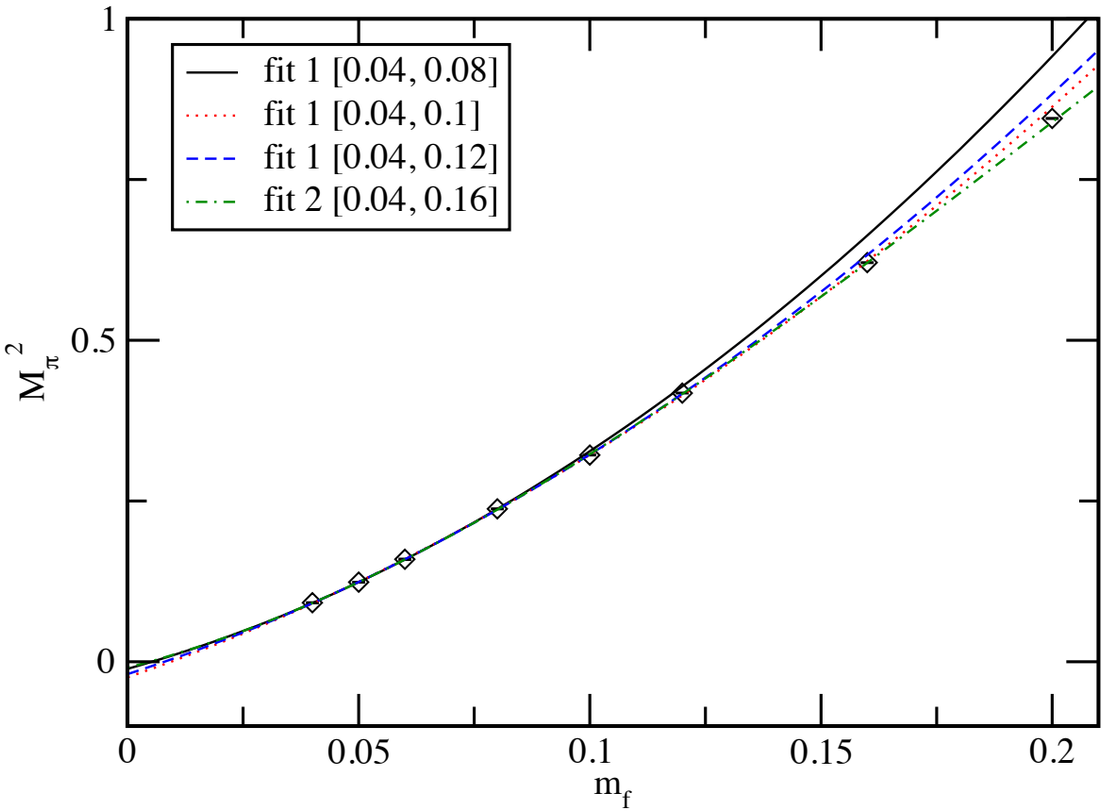

$$M_\pi^2 = h(m_f) = \begin{cases} c_0 + c_1 m_f + c_2 m_f^2 & \cdots \text{fit1} \\ c_0 + c_1 m_f + c_2 m_f^2 + c_3 m_f^3 & \cdots \text{fit2} \end{cases}$$

fit range	c_0	c_1	c_2	c_3	χ^2/dof
fit 1 : $[0.04, 0.08]$	-0.0090(93)	1.95(32)	14.2(2.6)	-	0.16
	[0]	1.640(31)	16.68(47)	-	0.56
fit 1 : $[0.04, 0.1]$	-0.0232(50)	2.46(16)	9.9(1.1)	-	1.75
	[0]	1.754(21)	14.73(25)	-	8.54
fit 1 : $[0.04, 0.12]$	-0.0174(31)	2.27(85)	11.32(52)	-	1.93
	[0]	1.801(16)	14.09(16)	-	9.36
fit 2 : $[0.04, 0.16]$	-0.0044(61)	1.69(22)	19.1(2.4)	-32.9(7.6)	3.28
	[0]	1.537(29)	20.76(53)	-38.2(2.3)	2.59

ChPT fit (after infinite volume extrapolation)

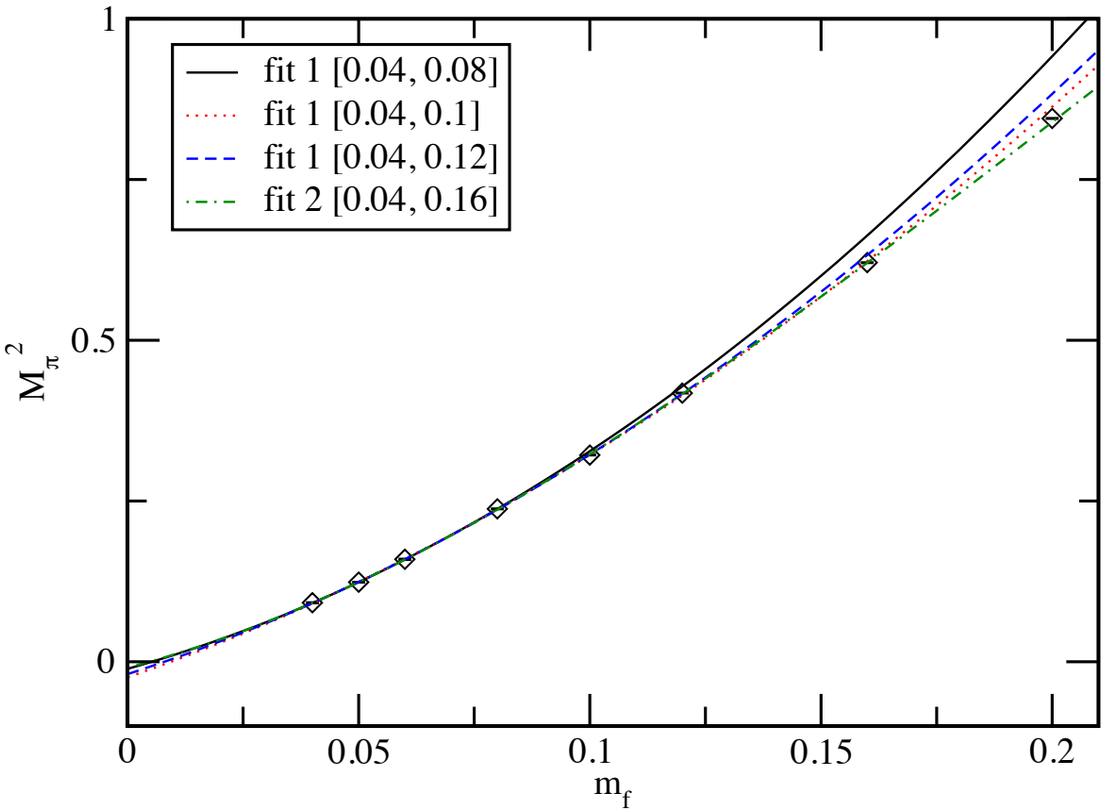

$$M_\pi^2 = h(m_f) = \begin{cases} c_0 + c_1 m_f + c_2 m_f^2 & \cdots \text{fit1} \\ c_0 + c_1 m_f + c_2 m_f^2 + c_3 m_f^3 & \cdots \text{fit2} \end{cases}$$

fit range	c_0	c_1	c_2	c_3	χ^2/dof
fit 1 : $[0.04, 0.08]$	-0.0090(93)	1.95(32)	14.2(2.6)	-	0.16
	[0]	1.640(31)	16.68(47)	-	0.56
fit 1 : $[0.04, 0.1]$	-0.0232(50)	2.46(16)	9.9(1.1)	-	1.75
	[0]	1.754(21)	14.73(25)	-	8.54
fit 1 : $[0.04, 0.12]$	-0.0174(31)	2.27(85)	11.32(52)	-	1.93
	[0]	1.801(16)	14.09(16)	-	9.36
fit 2 : $[0.04, 0.16]$	-0.0044(61)	1.69(22)	19.1(2.4)	-32.9(7.6)	3.28
	[0]	1.537(29)	20.76(53)	-38.2(2.3)	2.59

- wide range fit ends up $c_0<0$

ChPT fit (after infinite volume extrapolation)

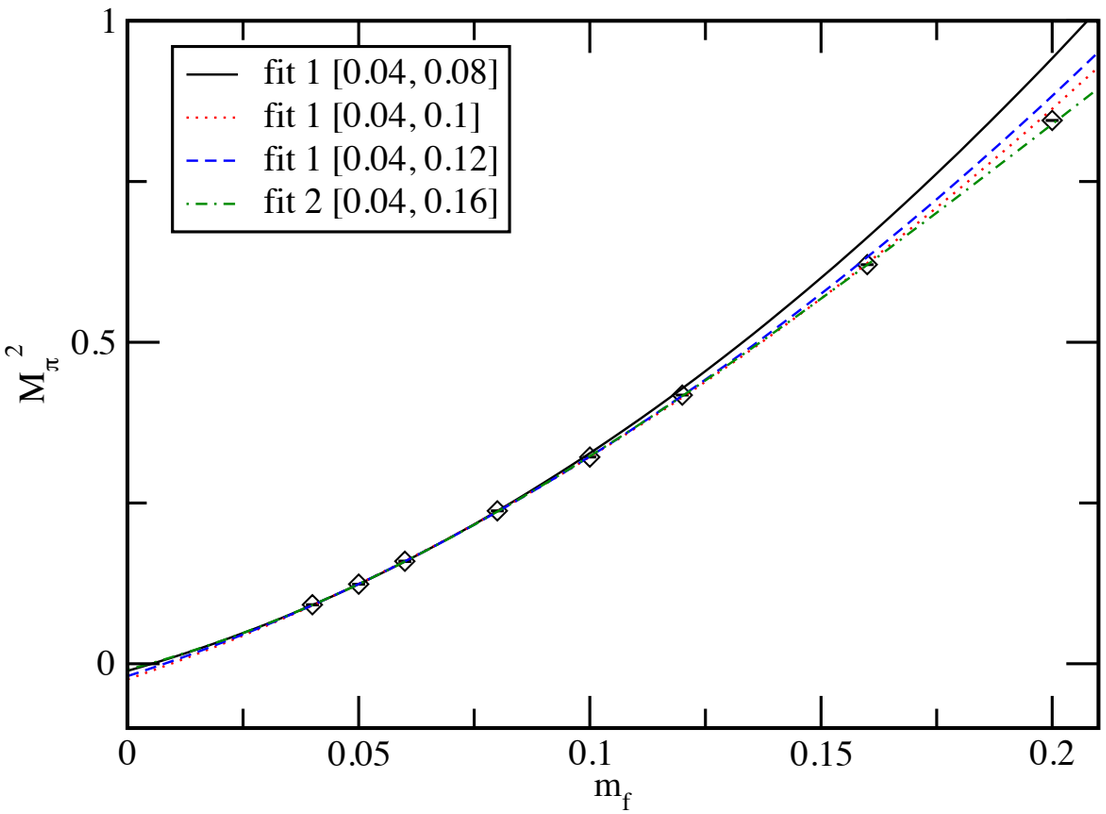

$$M_\pi^2 = h(m_f) = \begin{cases} c_0 + c_1 m_f + c_2 m_f^2 & \cdots \text{fit1} \\ c_0 + c_1 m_f + c_2 m_f^2 + c_3 m_f^3 & \cdots \text{fit2} \end{cases}$$

fit range	c_0	c_1	c_2	c_3	χ^2/dof
fit 1 : $[0.04, 0.08]$	-0.0090(93)	1.95(32)	14.2(2.6)	-	0.16
	[0]	1.640(31)	16.68(47)	-	0.56
fit 1 : $[0.04, 0.1]$	-0.0232(50)	2.46(16)	9.9(1.1)	-	1.75
	[0]	1.754(21)	14.73(25)	-	8.54
fit 1 : $[0.04, 0.12]$	-0.0174(31)	2.27(85)	11.32(52)	-	1.93
	[0]	1.801(16)	14.09(16)	-	9.36
fit 2 : $[0.04, 0.16]$	-0.0044(61)	1.69(22)	19.1(2.4)	-32.9(7.6)	3.28
	[0]	1.537(29)	20.76(53)	-38.2(2.3)	2.59

- wide range fit ends up $c_0<0$
- consistent with $c_0=0$ for small mass range

ChPT fit (after infinite volume extrapolation)

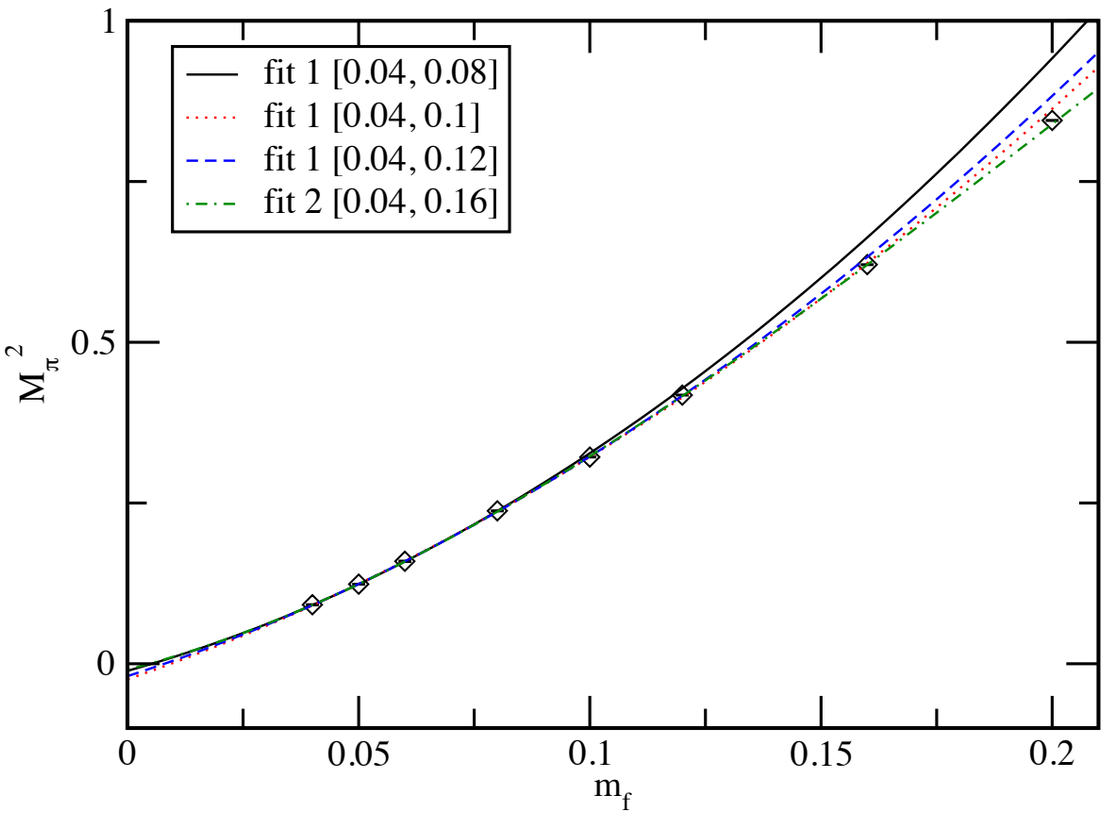

$$M_\pi^2 = h(m_f) = \begin{cases} c_0 + c_1 m_f + c_2 m_f^2 & \cdots \text{fit1} \\ c_0 + c_1 m_f + c_2 m_f^2 + c_3 m_f^3 & \cdots \text{fit2} \end{cases}$$

fit range	c_0	c_1	c_2	c_3	χ^2/dof
fit 1 : [0.04, 0.08]	-0.0090(93)	1.95(32)	14.2(2.6)	-	0.16
	[0]	1.640(31)	16.68(47)	-	0.56
fit 1 : [0.04, 0.1]	-0.0232(50)	2.46(16)	9.9(1.1)	-	1.75
	[0]	1.754(21)	14.73(25)	-	8.54
fit 1 : [0.04, 0.12]	-0.0174(31)	2.27(85)	11.32(52)	-	1.93
	[0]	1.801(16)	14.09(16)	-	9.36
fit 2 : [0.04, 0.16]	-0.0044(61)	1.69(22)	19.1(2.4)	-32.9(7.6)	3.28
	[0]	1.537(29)	20.76(53)	-38.2(2.3)	2.59

- wide range fit ends up $c_0<0$
- consistent with $c_0=0$ for small mass range
- But: $M_\pi/(4\pi F)\sim 2$ at lightest point → difficult to tell real chiral behavior

Summary:

SU(3) gauge theory with N_f=12 fundamental fermion simulation with HISQ

- β=3.7, 4.0: consistent with being in the asymptotically free regime
- M_π, F_π, M_ρ: consistent with the finite size hyper scaling for conformal theory
- resulting γ^* from different quantities, lattice spacings are consistent except
  - F_π at β=4.0 (m_f likely too heavy for universal mass dep. to dominate)
- need careful continuum scaling needed to get more accurate than $0.4<\gamma^*<0.5$
- real / remnant (approximate) conformal property is definitely there
- could not exclude S χ SB with very small breaking scale
- even if S χ SB, γ_m too small for walking theory of phenomenological interest
- N_f=8 theory is interesting & under investigation with same lattice set up

Thank you for your attention

ChPT inspired infinite volume limit (β=3.7)

$$M_\pi(L) - M_\pi = c_{M_\pi} \frac{e^{-LM_\pi}}{(LM_\pi)^{3/2}}$$

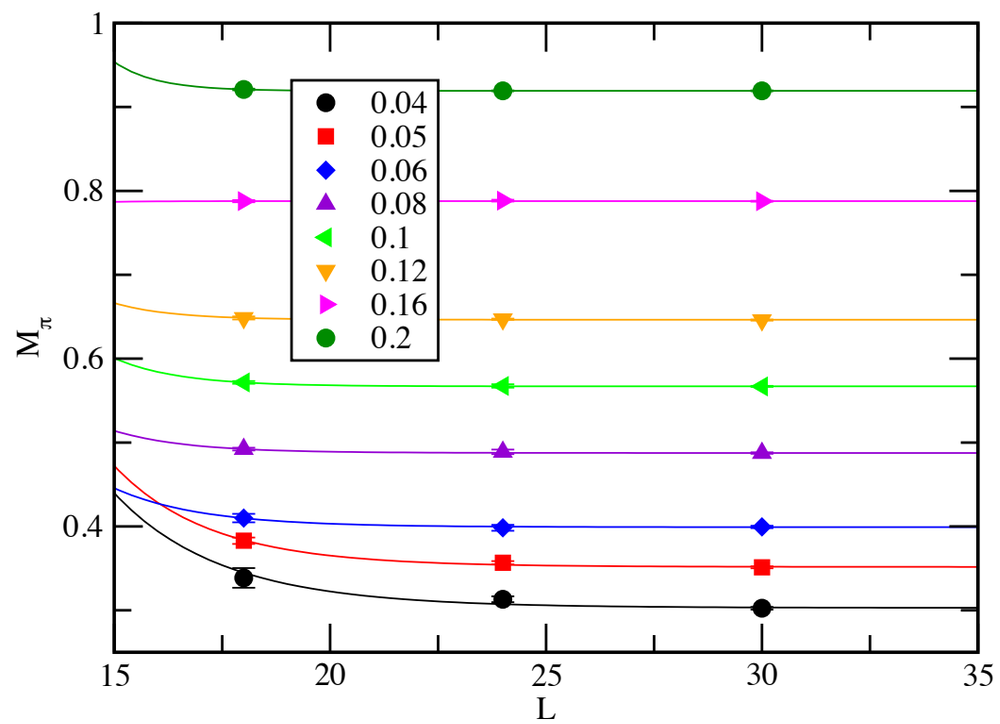

- ChPT type finite volume effect → chiral fit results not inconsistent with S χ SB

HISQ action

- proposed by HPQCD collaboration for
  - smaller taste violation than other approaches
  - better handling of heavy quarks
- being used in simulations
  - MILC: Nf=2+1+1 QCD
  - HOTQCD: QCD thermodynamics: Bazavov-Petreczky (Lat'10 proceedings)
    - HISQ/tree is **best** of [HISQ/tree, Asqtad, stout]

      for flavor (taste) symmetry, dispersion relation

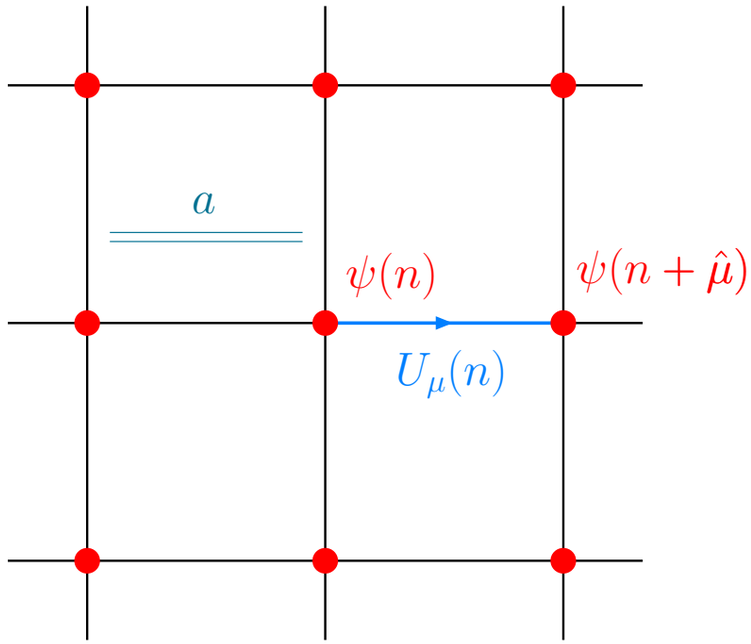

HISQ action

- proposed by HPQCD collaboration for
  - smaller taste violation than other approaches
  - better handling of heavy quarks
- being used in simulations
  - MILC: Nf=2+1+1 QCD
  - HOTQCD: QCD thermodynamics: Bazavov-Petreczky (Lat'10 proceedings)
    - HISQ/tree is **best** of [HISQ/tree, Asqtad, stout]

      for flavor (taste) symmetry, dispersion relation

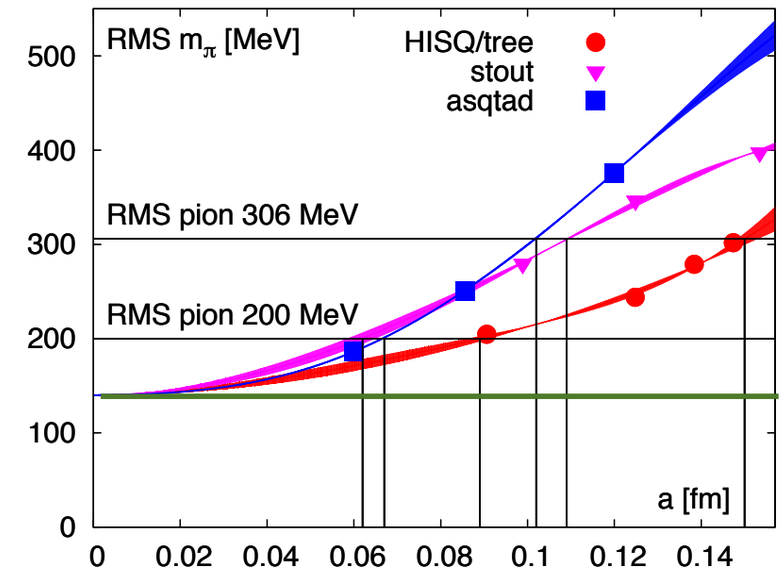

Figure 2: RMS pion mass when $m_{\gamma_5} = 140$ MeV. See details in the text.

LHC (Large Hadron Collider)

- excess @ ~125 GeV
  - 1 σ level (look elsewhere)
  - larger when ATLAS & CMS results are combined ?
  - $M_W = M_Z \cos\theta_W = gF_\pi/2$ ($F_\pi = v_{weak} = 246$ GeV)
  - $M_H \sim 500$ GeV: problem ?
- even if scalar is fund at ~125 GeV
  - possible techni-dilaton (Matsuzaki-Yamawaki,,)
  - 0++ glueball tends to be much lighter than techni-hadrons
    - Cf. SU(2) lattice work by Del Debbio et al
- important to investigate glueball for SU(3) as well !!!

An approach to non-leptonic B-decays on the lattice

Christopher Aubin

May 15, 2012

New Horizons for Lattice Computations with Chiral Fermions

with

David Lin & Amarjit Soni

Phys. Let. B710 164

FORDHAM UNIVERSITY

THE JESUIT UNIVERSITY OF NEW YORK

Outline

Nonleptonic *B* decays (CKM)
Weak operators
Four-point functions on the lattice

Starting points:
- Chiral Perturbation Theory
- Resonance contribution
- Hard pion ChPT

FORDHAM UNIVERSITY
THE JESUIT UNIVERSITY OF NEW YORK

$B^- \to D^0 P^-$ ← experimentally accessible

$B^- \to \overline{D}^0 P^-$

The ratio

$$r_{BP} = \frac{\mathrm{Br}[B^- \to \overline{D}^0 P^-]}{\mathrm{Br}[B^- \to D^0 P^-]}$$

can give insight into γ

(HFAG, arXiv:1010.1589)

On the lattice, define a reduced ratio:

$$r_{BP}^{\mathrm{red}} \equiv \frac{r_{BP}}{V_{CKM}^{\mathrm{combo}}} = r_{BP} \frac{|V_{cb}^* V_{uq}|^2}{|V_{ub}^* V_{cq}|^2}$$

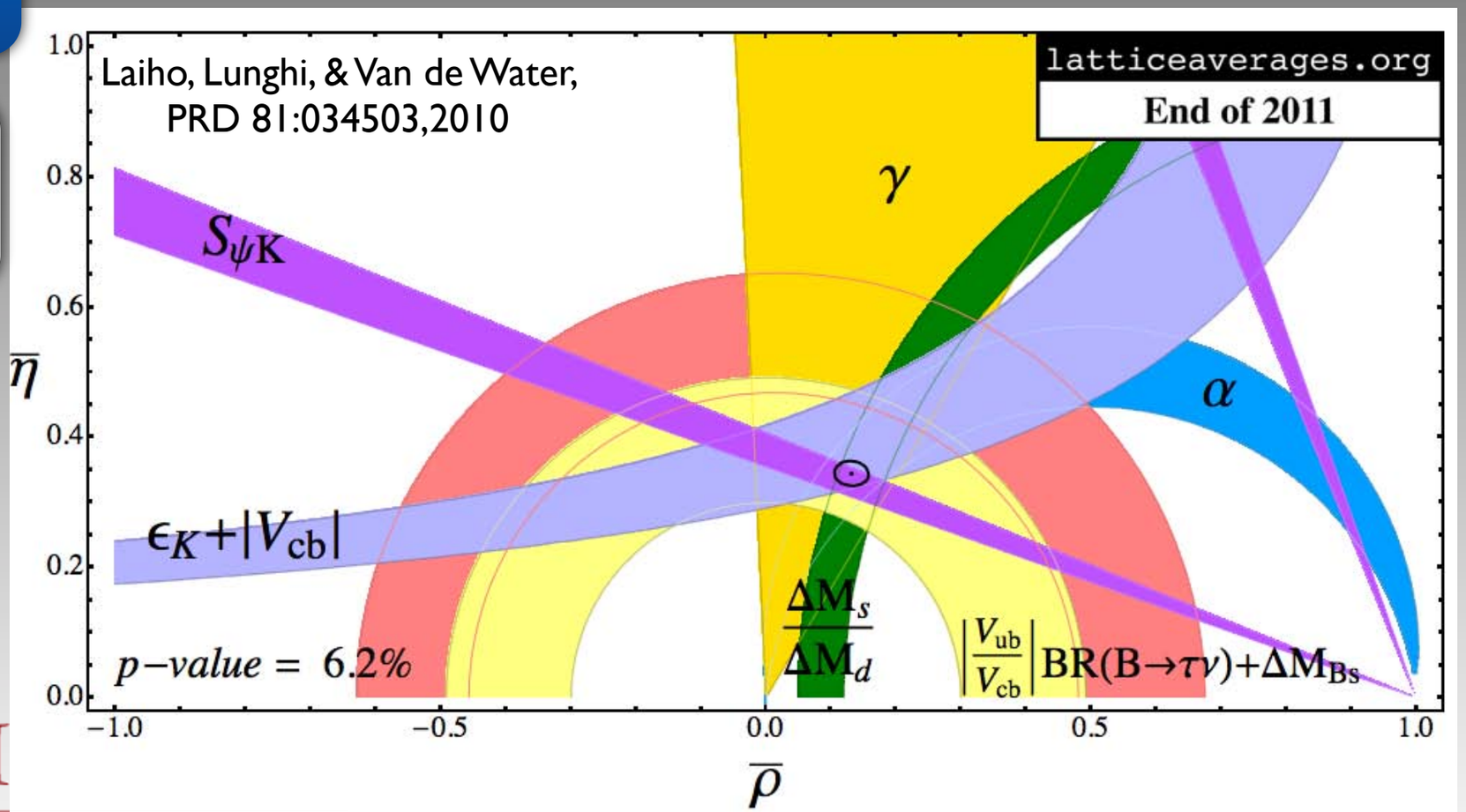

FORDHAM UNI

THE JESUIT UNIVERSITY OF NEW YORK

$B^- \to D^0 P^-$ $B^- \to \overline{D}^0 P^-$

γ	$O(25\%)$
α	$O(5\%)$
β	$O(3\%)$

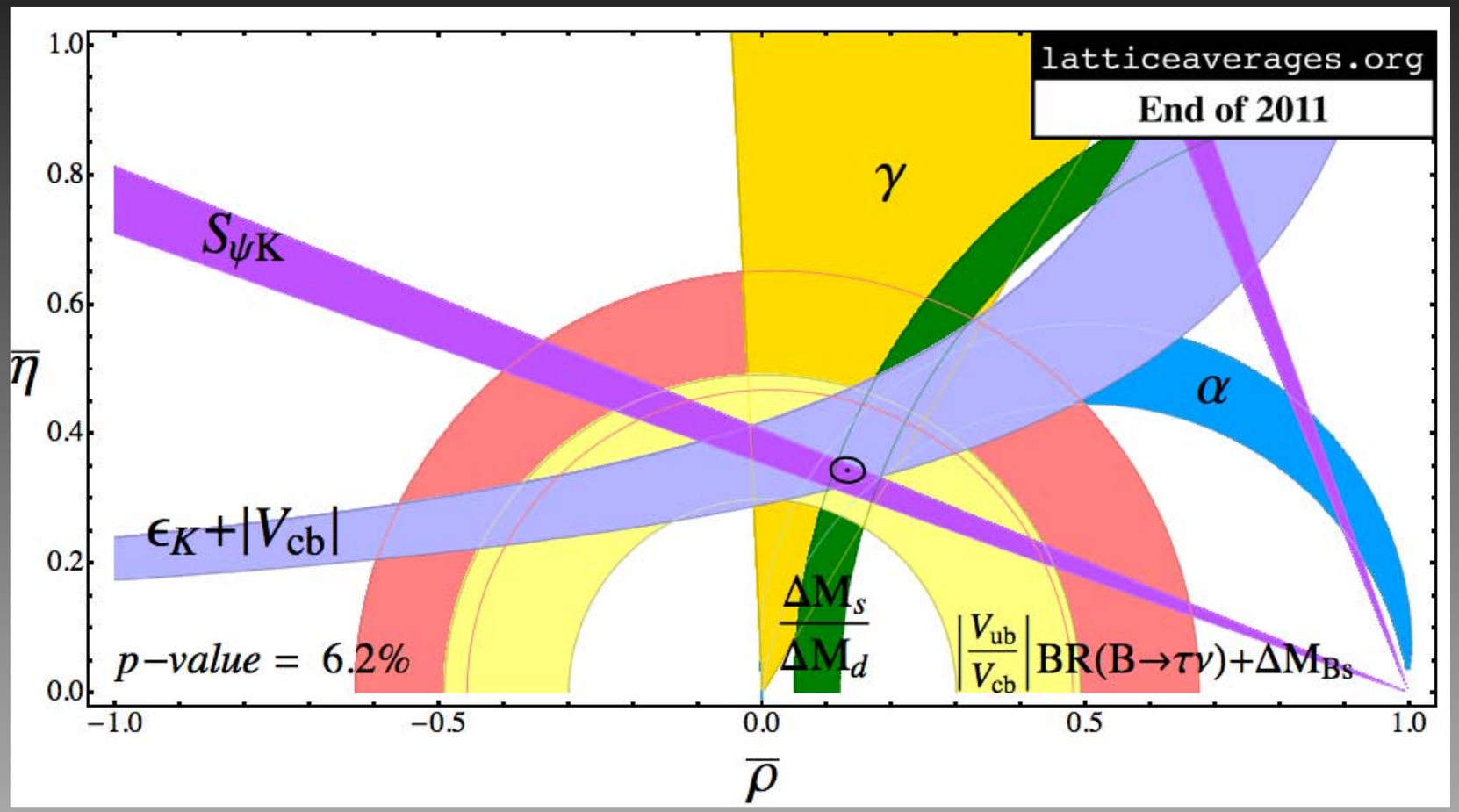

Hope:

Determination of the real part of these amplitudes to 15-20% [~5 years?]

$\Rightarrow \gamma \sim 10\%$

Weak operators

$$
\begin{aligned}
Q_1^{b\to c,i} &= (\overline{q}^i_\alpha \gamma^\mu (1-\gamma_5) b_\alpha)(\overline{c}_\beta \gamma_\mu (1-\gamma_5) u_\beta) \\
Q_2^{b\to c,i} &= (\overline{q}^i_\alpha \gamma^\mu (1-\gamma_5) b_\beta)(\overline{c}_\beta \gamma_\mu (1-\gamma_5) u_\alpha) \\
Q_1^{b\to \overline{c},i} &= (\overline{q}^i_\alpha \gamma^\mu (1-\gamma_5) b_\alpha)(\overline{u}_\beta \gamma_\mu (1-\gamma_5) c_\beta) \\
Q_2^{b\to \overline{c},i} &= (\overline{q}^i_\alpha \gamma^\mu (1-\gamma_5) b_\beta)(\overline{u}_\beta \gamma_\mu (1-\gamma_5) c_\alpha)
\end{aligned}
$$

Maiani-Testa theorem

$$\langle 0|\pi D \mathcal{O}_{\rm weak} B|0\rangle$$

4pt functions only yields real part (no strong phase)

Can be circumvented
(Lellouch-Lüscher, RBC/UKQCD)
e.g., $K \to 2\pi$

FORDHAM UNIVERSITY
THE JESUIT UNIVERSITY OF NEW YORK

Heavy-light meson ChPT

$$\mathcal{L}_{\rm G} = \frac{f^2}{8}{\rm Tr}\left(\partial_\mu\Sigma\partial^\mu\Sigma^\dagger\right) + \frac{1}{4}\mu f^2 {\rm Tr}\left(\mathcal{M}\Sigma + \mathcal{M}\Sigma^\dagger\right)$$

$$\Sigma \longrightarrow L\,\Sigma\,R^\dagger, \text{ where } L \in {\rm SU(3)_L}, \text{ and } R \in {\rm SU(3)_R}$$

$$H_{v,a}^{(\overline{Q})} = \left(\gamma^\mu \mathcal{V}_{\mu,a}^{*(\overline{Q})} - \gamma_5 \mathcal{P}_a^{(\overline{Q})}\right)\left(\frac{1-\not{v}}{2}\right)$$

HL fields with anti-quark

$$H_{v,a}^{(Q)} = \left(\frac{1+\not{v}}{2}\right)\left(\gamma^\mu \mathcal{V}_{\mu,a}^{*(Q)} - \gamma_5 \mathcal{P}_a^{(Q)}\right)$$

HL fields with quark

$$\mathbb{V}_\mu = \frac{i}{2}\left[\sigma^\dagger\partial_\mu\sigma + \sigma\partial_\mu\sigma^\dagger\right]$$

$$\mathbb{A}_\mu = \frac{i}{2}\left[\sigma^\dagger\partial_\mu\sigma - \sigma\partial_\mu\sigma^\dagger\right]$$

$$H_Q(x) \to S\,H_Q(x)\,\mathbb{U}^\dagger(x)\ ,\ \overline{H}_Q(x) \to \mathbb{U}(x)\,\overline{H}_Q(x)\,S^\dagger$$

$$H_{\overline{Q}}(x) \to \mathbb{U}(x)\,H_{\overline{Q}}(x)\,S^\dagger\ ,\ \overline{H}_{\overline{Q}}(x) \to S\,\overline{H}_{\overline{Q}}(x)\,\mathbb{U}^\dagger(x)$$

$$S \in U(4)$$

$$\sigma = \sqrt{\Sigma} = {\rm e}^{i\Phi/f}$$

$$\sigma(x) \to L\,\sigma(x)\,\mathbb{U}^\dagger(x) = \mathbb{U}(x)\,\sigma(x)\,R^\dagger$$

$$\mathcal{L}_{\rm HL,1} = -i\,{\rm Tr}(\overline{H}Hv\cdot\overleftarrow{D}) + g_\pi\,{\rm Tr}(\overline{H}H\gamma^\mu\gamma_5\mathbb{A}_\mu)$$

FORDHAM UNIVERSITY

THE JESUIT UNIVERSITY OF NEW YORK

Heavy-light meson ChPT

Chiral-level Weak operators:

$b \to c$ operators

$$\mathcal{O}_{\chi,i} = \sum_x \left\{ \alpha_{1,x} \mathrm{Tr_D} \left[\left(\sigma_{1k} \overline{H}^{(c)}_{v',k} \right) \Gamma_2 \Xi'_x \Xi_x \Gamma_1 \left(H^{(b)}_{v,l} \sigma^\dagger_{li} \right) \right] + \alpha_{2,x} \mathrm{Tr_D} \left[\left(\sigma_{1k} \overline{H}^{(c)}_{v',k} \right) \Gamma_2 \Xi'_x \right] \mathrm{Tr_D} \left[\Xi_x \Gamma_1 \left(H^{(b)}_{v,l} \sigma^\dagger_{li} \right) \right] \right\}$$

$b \to \bar{c}$ operators

$$\overline{\mathcal{O}}_{\chi,i} = \sum_x \left\{ \overline{\alpha}_{1,x} \mathrm{Tr_D} \left[\Xi'_x \Gamma_2 \left(\overline{H}^{(\bar{c})}_{v',k} \sigma^\dagger_{k1} \right) \Xi_x \Gamma_1 \left(H^{(b)}_{v,l} \sigma^\dagger_{li} \right) \right] + \overline{\alpha}_{2,x} \mathrm{Tr_D} \left[\Xi'_x \Gamma_2 \left(\overline{H}^{(c)}_{v',k} \sigma^\dagger_{k1} \right) \right] \mathrm{Tr_D} \left[\Xi_x \Gamma_1 \left(H^{(b)}_{v,l} \sigma^\dagger_{li} \right) \right] \right\}$$

$$\{\Xi'_x, \Xi_x\} = \Big\{ \{1,1\}, \{\gamma_\nu, \gamma^\mu\}, \{\not{v}', \not{v}\}, \{\not{v}', 1\}, \{1, \not{v}\}, \{\sigma_{\mu\nu}, \sigma^{\mu\nu}\},$$
$$\{\gamma_5, \gamma_5\}, \{\gamma_\mu \gamma_5, \gamma^\mu \gamma_5\}, \{\not{v}' \gamma_5, \not{v} \gamma_5\}, \{\not{v}' \gamma_5, \gamma_5\}, \{\gamma_5, \not{v} \gamma_5\} \Big\}$$

FORDHAM UNIVERSITY

THE JESUIT UNIVERSITY OF NEW YORK

Heavy-light meson ChPT

$$
\begin{aligned}
\mathcal{O}_{\chi,i} = \quad & [\beta_1 + (\beta_1+\beta_2)(v'\cdot v)]\left[\left(\sigma_{1k}\mathcal{P}_k^{(c)\dagger}\right)\left(\mathcal{P}_l^{(b)}\sigma_{li}^\dagger\right)\right] \\
+ \; & [(\beta_1-\beta_2)v'^\mu - \beta_1 v^\mu]\left[\left(\sigma_{1k}\mathcal{P}_k^{(c)\dagger}\right)\left(\mathcal{V}_{\mu,l}^{*(b)}\sigma_{li}^\dagger\right)\right] \\
+ \; & [\beta_1 v'^\mu - (\beta_1+\beta_2)v^\mu]\left[\left(\sigma_{1k}\mathcal{V}_{\mu,k}^{*(c)\dagger}\right)\left(\mathcal{P}_l^{(b)}\sigma_{li}^\dagger\right)\right] \\
- \; & 4\left[(\beta_1-\beta_2)+\beta_1(v'\cdot v)\right]\left[\left(\sigma_{1k}\mathcal{V}_{\mu,k}^{*(c)\dagger}\right)\left(\mathcal{V}_l^{*(b)\mu}\sigma_{li}^\dagger\right)\right],
\end{aligned}
$$

$$
\begin{aligned}
\overline{\mathcal{O}}_{\chi,i} = \quad & [\overline{\beta}_1 + \overline{\beta}_2(v'\cdot v)]\left[\left(\mathcal{P}_k^{(\bar{c})\dagger}\sigma_{k1}^\dagger\right)\left(\mathcal{P}_l^{(b)}\sigma_{li}^\dagger\right)\right] \\
- \; & [\overline{\beta}_2 v'^\mu - (\overline{\beta}_1+\overline{\beta}_5)v^\mu - \overline{\beta}_3(v'\cdot v)v^\mu]\left[\left(\mathcal{P}_k^{(\bar{c})\dagger}\sigma_{k1}^\dagger\right)\left(\mathcal{V}_{\mu,l}^{*(b)}\sigma_{li}^\dagger\right)\right] \\
+ \; & [\overline{\beta}_1 v'^\mu - \overline{\beta}_2 v^\mu]\left[\left(\mathcal{V}_{\mu,k}^{*(\bar{c})\dagger}\sigma_{k1}^\dagger\right)\left(\mathcal{P}_l^{(b)}\sigma_{li}^\dagger\right)\right] \\
+ \; & [4\overline{\beta}_2 - \overline{\beta}_3 - 2(\overline{\beta}_1+\overline{\beta}_4+\overline{\beta}_5)(v'\cdot v)]\left[\left(\mathcal{V}_{\mu,k}^{*(\bar{c})\dagger}\sigma_{k1}^\dagger\right)\left(\mathcal{V}_l^{*(b)\mu}\sigma_{li}^\dagger\right)\right],
\end{aligned}
$$

FORDHAM UNIVERSITY

THE JESUIT UNIVERSITY OF NEW YORK

Leading order

$$\langle D^0 K^- | \mathcal{O}_{\chi,s} | B^- \rangle = \langle D^0 \pi^- | \mathcal{O}_{\chi,d} | B^- \rangle = \frac{i}{f} \langle D^- | \mathcal{O}_{\chi,s} | B^- \rangle,$$

$$\langle \overline{D}^0 K^- | \overline{\mathcal{O}}_{\chi,s} | B^- \rangle = \langle \overline{D}^0 \pi^- | \overline{\mathcal{O}}_{\chi,d} | B^- \rangle = \frac{i}{f} \langle D^- | \overline{\mathcal{O}}_{\chi,s} | B^- \rangle \ .$$

similar expressions for $K \to 2\pi$
[Bernard et al, PRD32 2343]

Can also include resonances:

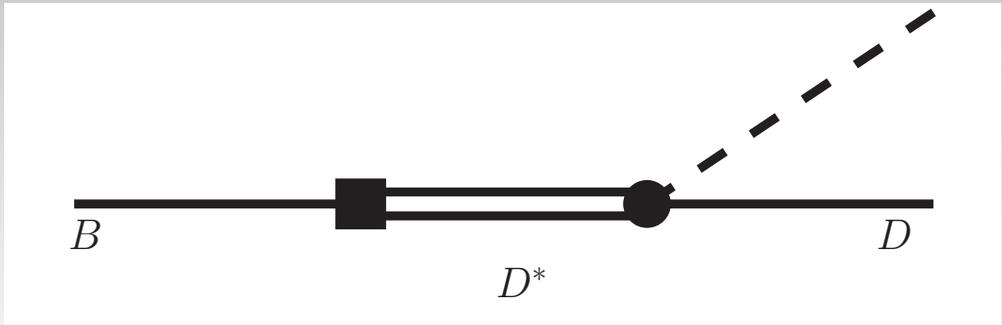

FORDHAM UNIVERSITY
THE JESUIT UNIVERSITY OF NEW YORK

Of course here the physical point has

$$\mathbf{p}_\pi = \mathbf{p}_D \approx 2 \text{ GeV}$$

Not appropriate for chiral expansion unless one takes the unphysical point

$$m_B \approx m_D$$

But then we're far from the point of interest.

How to go beyond tree-level?

FORDHAM UNIVERSITY

THE JESUIT UNIVERSITY OF NEW YORK

Beyond tree-level:

Hard-pion ChPT (HPChPT)

Exploit the fact that hard scales can be absorbed into LEC's

Flynn & Sachrajda, Nucl.Phys. B812, 64 $K_{\ell 3}$
Bijnens & Celis, Phys.Lett. B680, 466 $K \to 2\pi$
Bijnens & Jemos, Nucl.Phys. B840, 54 $B \to \pi$

FORDHAM UNIVERSITY
THE JESUIT UNIVERSITY OF NEW YORK

HPChPT

In the SU(2) chiral theory,
we have the generic one-loop form

tree-level amplitude

$$\mathcal{M} = \mathcal{M}^{\text{tree}} \left[1 + a \frac{m_\pi^2}{16\pi^2 f^2} \ln\left(\frac{m_\pi^2}{\Lambda^2}\right) + L m_\pi^2 \right]$$

a and *L* are LEC's that depend on the hard scales

FORDHAM UNIVERSITY
THE JESUIT UNIVERSITY OF NEW YORK

HPChPT example

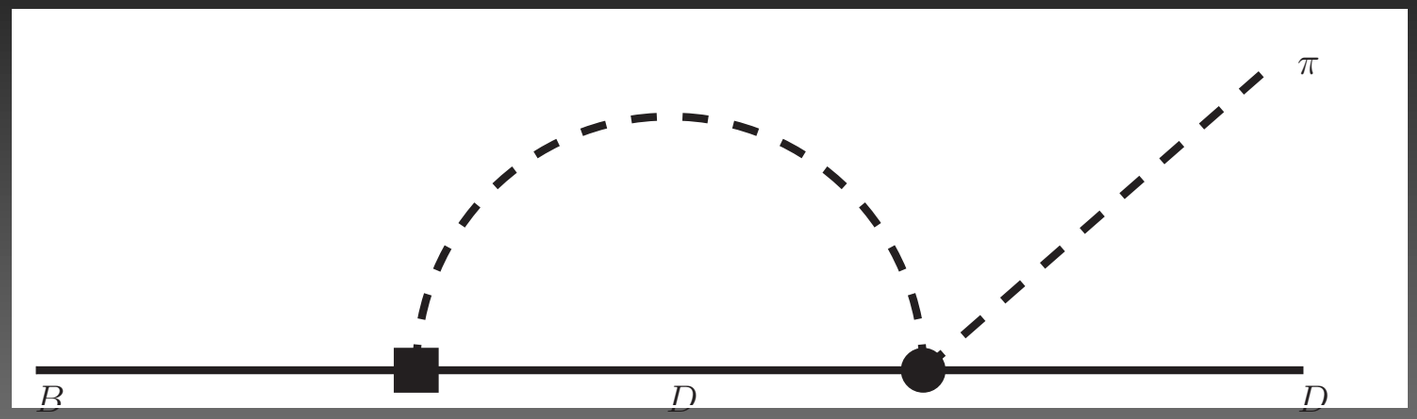

$$\frac{\langle D^0\pi^-|\mathcal{O}_{\chi,d}|B^-\rangle^{\rm tree}}{8f^2}\int\frac{d^d\ell}{(2\pi)^d}\frac{i}{\ell^2-m_\pi^2+i\epsilon}\frac{iv'\cdot(\ell-p_\pi)}{v'\cdot(\ell-k-p_\pi)-\Delta+i\epsilon}\,,$$

$$\frac{\langle D^0\pi^-|\mathcal{O}_{\chi,d}|B^-\rangle^{\rm tree}}{8}I\,,$$

$$I=\frac{1}{16\pi^2f^2}\left[\frac{v'\cdot k+\Delta}{v'\cdot(k+p_\pi)+\Delta+i\epsilon}I_2(m_\pi,v'\cdot(k+p_\pi)+\Delta+i\epsilon)-m_\pi^2\ln\left(\frac{m_\pi^2}{\Lambda^2}\right)\right]$$

FORDHAM UNIVERSITY

THE JESUIT UNIVERSITY OF NEW YORK

$$I = \frac{1}{16\pi^2 f^2}\left[\frac{v'\cdot k + \Delta}{v'\cdot(k+p_\pi) + \Delta + i\epsilon} I_2(m_\pi, v'\cdot(k+p_\pi) + \Delta + i\epsilon) - m_\pi^2 \ln\left(\frac{m_\pi^2}{\Lambda^2}\right)\right]$$

in the limit $v' \cdot k \gg m_\pi$

$$I_2(m_\pi, v'\cdot(k+p_\pi) + \Delta) \approx -m_\pi^2 \ln\left(\frac{m_\pi^2}{\Lambda^2}\right)$$

Inject momentum into weak vertex so that...

FORDHAM UNIVERSITY

THE JESUIT UNIVERSITY OF NEW YORK

$p_\pi \approx 0$

$$I(p_\pi \approx 0) \to -2\frac{m_\pi^2}{16\pi^2 f^2}\ln\left(\frac{m_\pi^2}{\Lambda^2}\right)$$

$p_\pi \approx k$

$$I(p_\pi \approx k) \to -\frac{3}{2}\frac{m_\pi^2}{16\pi^2 f^2}\ln\left(\frac{m_\pi^2}{\Lambda^2}\right)$$

Different contributions to *a*, *L* in above expression

Both *a* and *L* have unknown dependence on kinematics, but pion mass dependence is known.

FORDHAM UNIVERSITY

THE JESUIT UNIVERSITY OF NEW YORK

Conclusion

Problem is far from solved

Need full one-loop calculation

Need lattice calculations (takers?)

Key: Feasible problem for lattice to tackle

FORDHAM UNIVERSITY

THE JESUIT UNIVERSITY OF NEW YORK

Status and Prospects for some MILC and Fermilab/MILC Projects

Claude Bernard
Washington University
St. Louis
(MILC & Fermilab Lattice/MILC Collaborations)

New Horizons for Lattice Computations with Chiral Fermions
Brookhaven, May 14-16, 2012

Heavy-light Decay Constants

- Fermilab heavy quarks with MILC 2+1 Asqtad staggered light quarks
  - "Old data" project
    - 0.15 fm ≤ a ≤ 0.09 fm
    - 4 sources per configuration
    - renormalization mostly non-perturbative; 1-loop perturbation theory for remainder
    - to appear in PRD shortly
  - "New data" project: similar to above, but:
    - 0.15 fm ≤ a ≤ 0.045 fm
    - 2 to 5 times more configurations/ensemble
    - in progress
- For D system, ongoing HISQ project with MILC 2+1+1 HISQ quarks: more later.

Heavy-light Decay Constants

- Fermilab heavy quarks with MILC 2+1 Asqtad staggered light quarks
  - "Old data" project
    - 0.15 fm ≤ a ≤ 0.09 fm
    - 4 sources per configuration
    - renormalization mostly non-perturbative; 1-loop perturbation theory for remainder
    - to appear in PRD shortly
  - "New data" project: similar to above, but:
    - 0.15 fm ≤ a ≤ 0.045 fm
    - 2 to 5 times more configurations/ensemble
    - in progress

J. Simone, D. Toussaint, CB

- For D system, ongoing HISQ project with MILC 2+1+1 HISQ quarks: more later.

Asqtad Ensembles

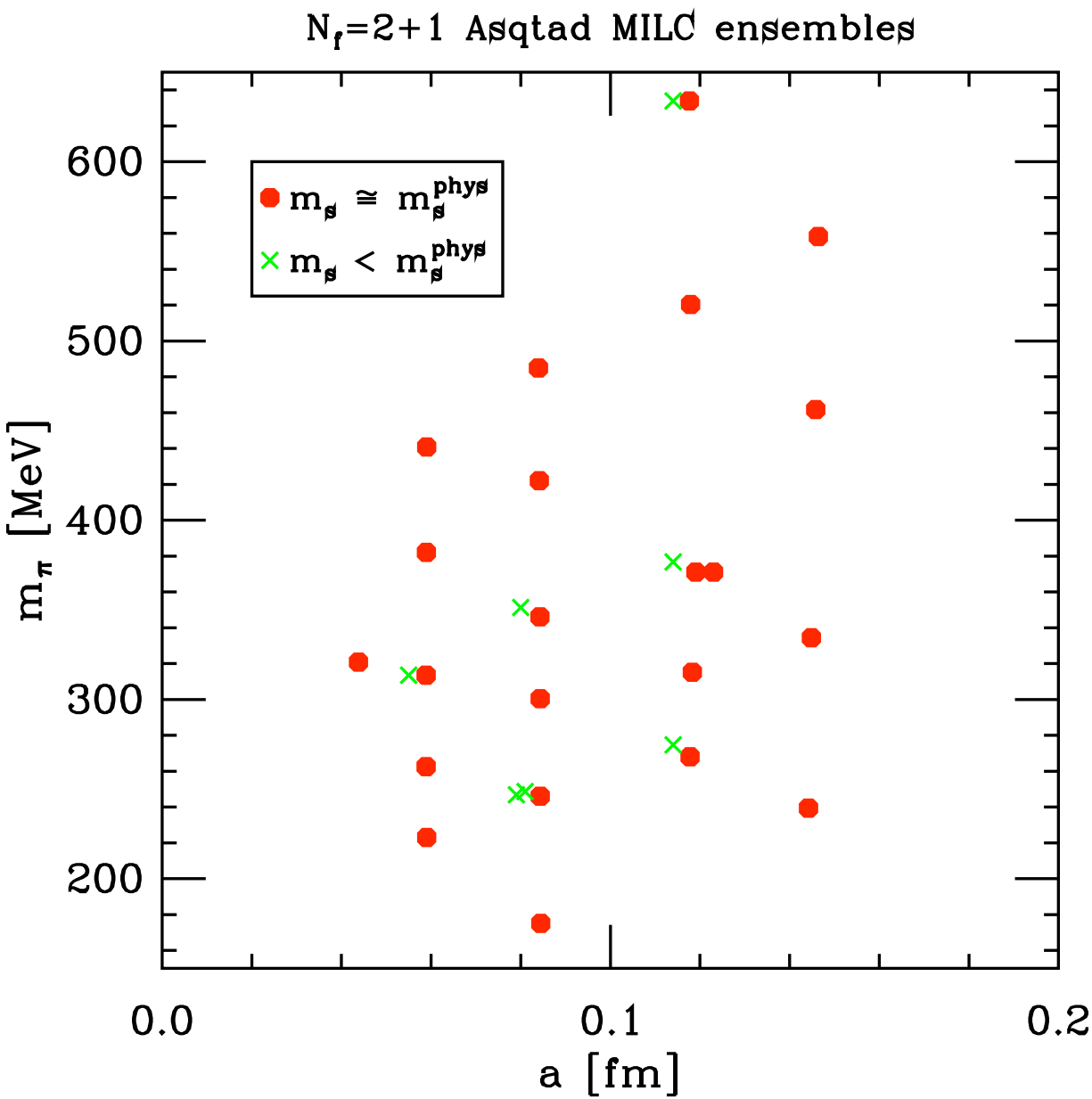

Asqtad Ensembles

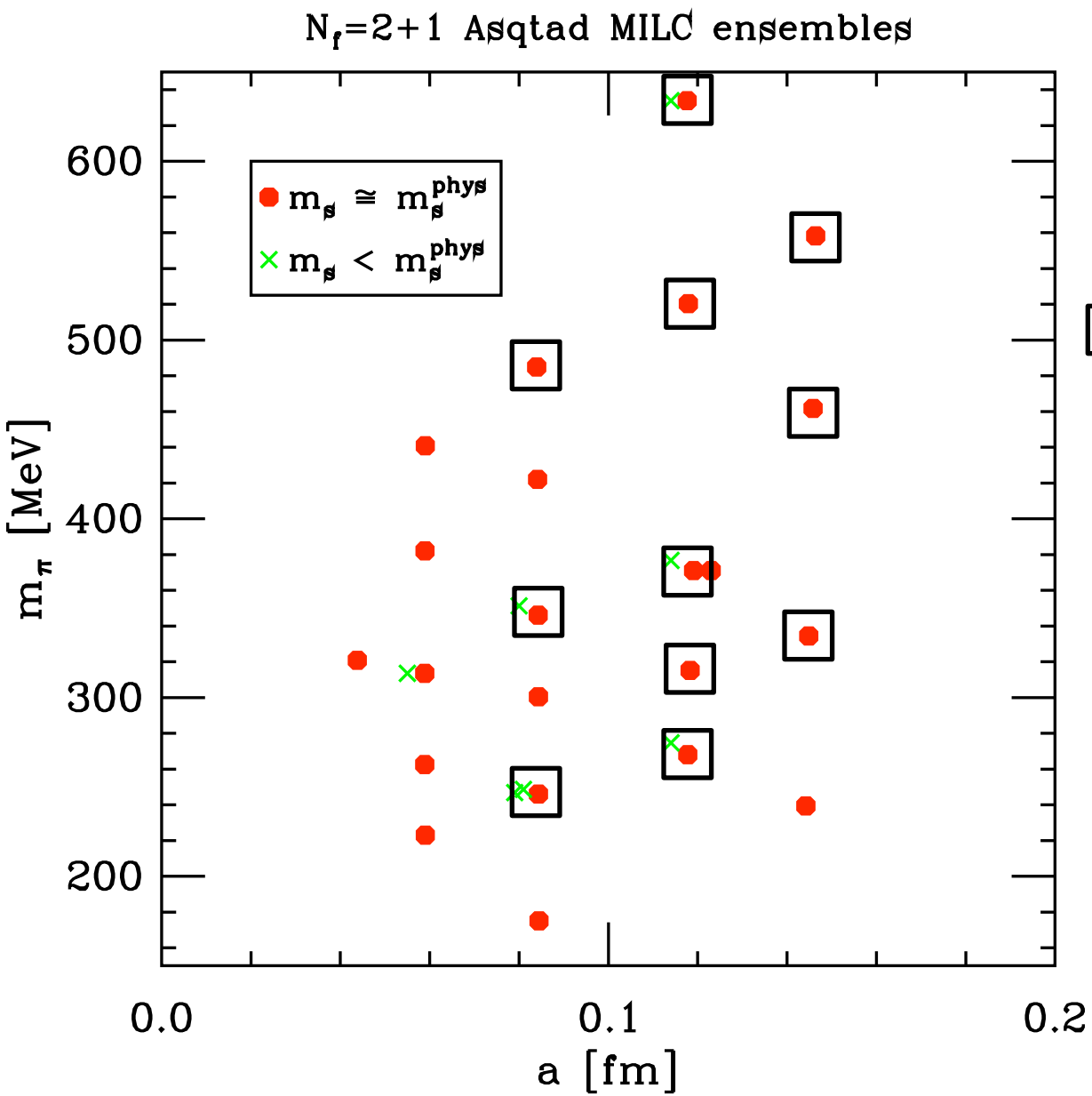

"old data" heavy-light decay const. analysis

Asqtad Ensembles

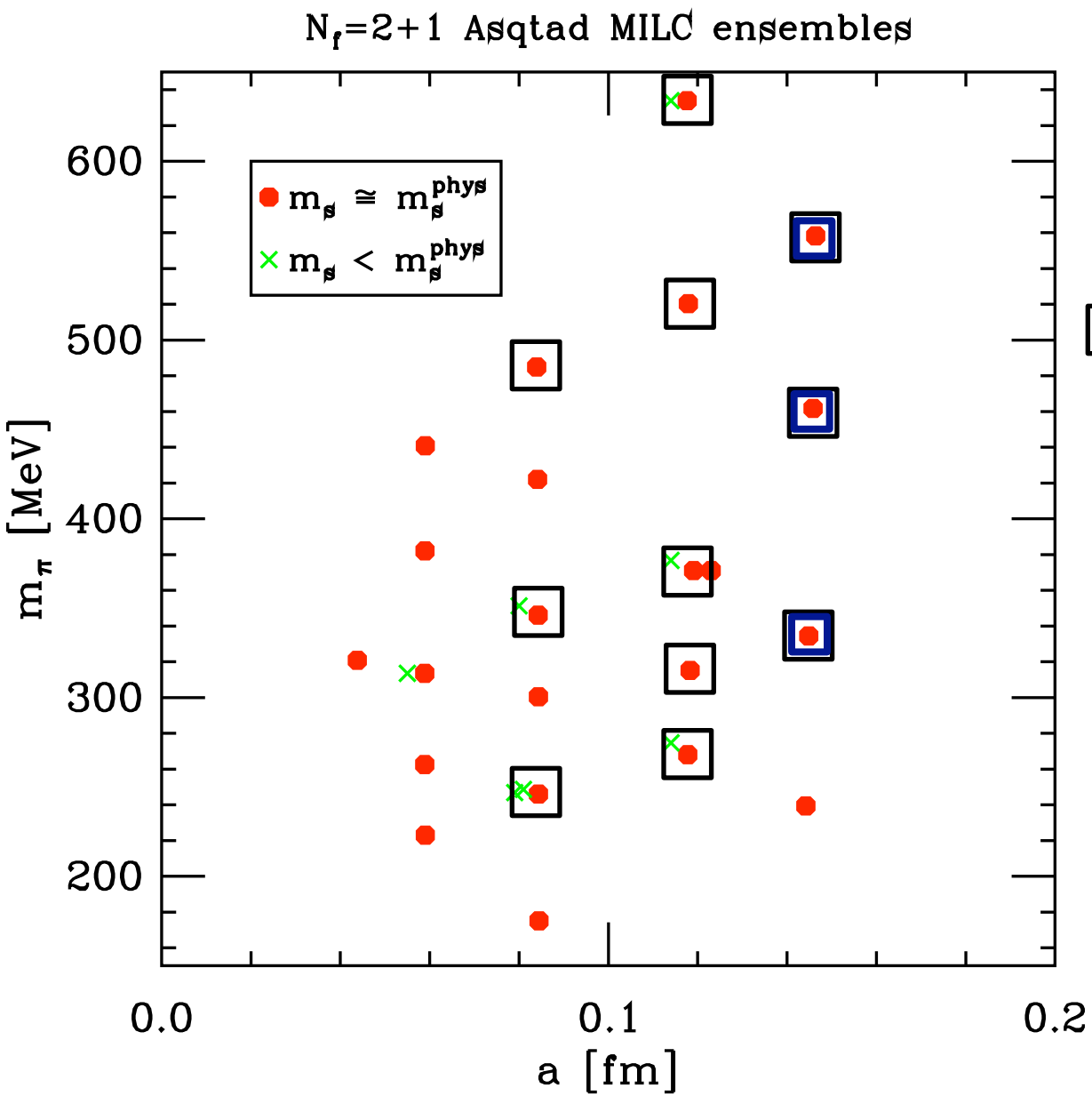

"old data" heavy-light decay const. analysis

not in central value but in error analysis

D system

- f_D as function of light valence mass m_q (= light sea mass m_l).
- f_{Ds} as function of light sea mass m_l.
  - valence mass held fixed ≈ m_s.
- a≅0.15 fm points not included in fit.
  - note qualitatively different behavior

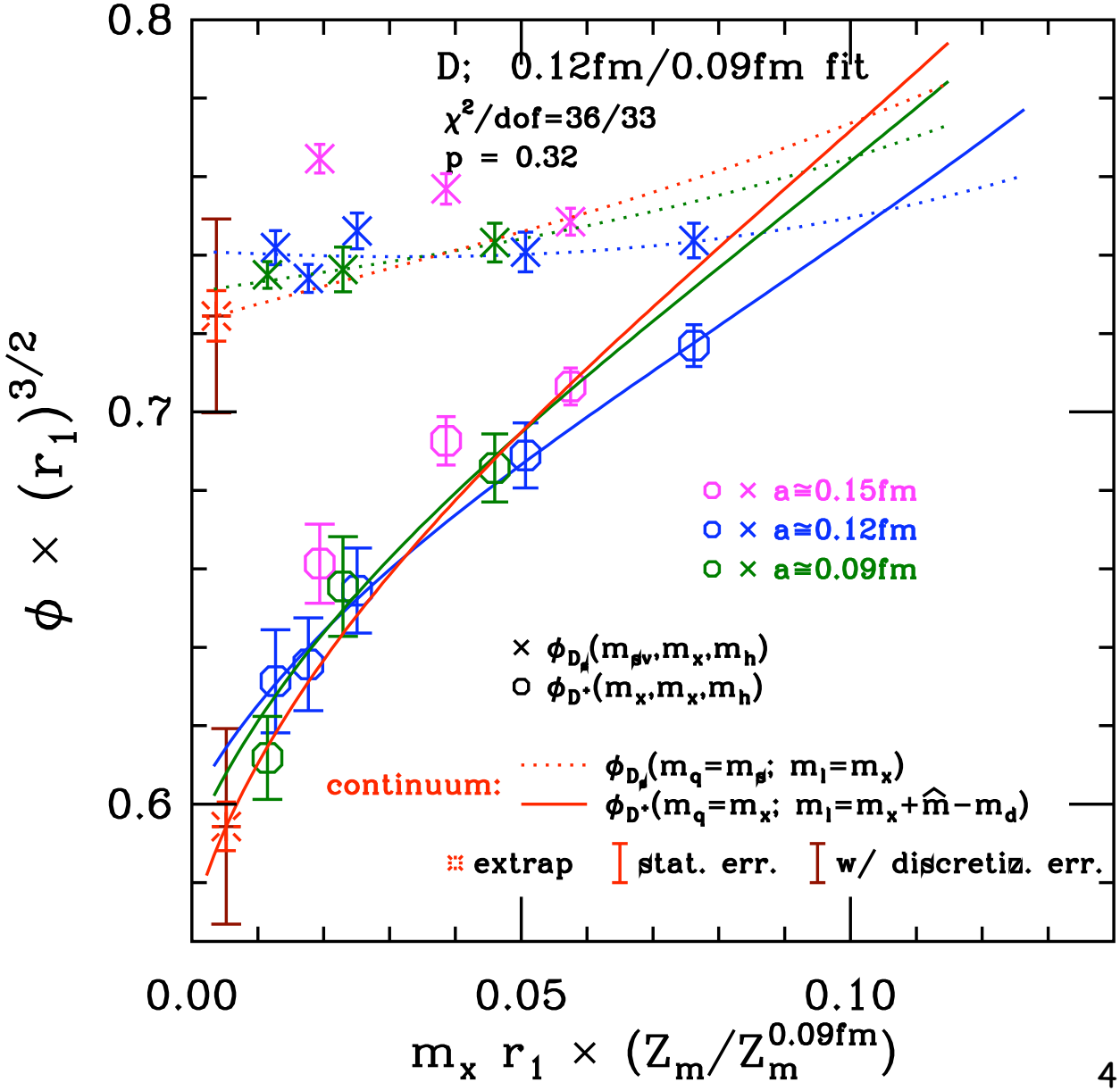

B system

- f_B as function of light valence mass m_q (= light sea mass m_l).
- f_{Bs} as function of light sea mass m_l.
  - valence mass held fixed ≈ m_s.
- a≅0.15 fm points not included in fit.
  - qual. different behavior + large stat. errors

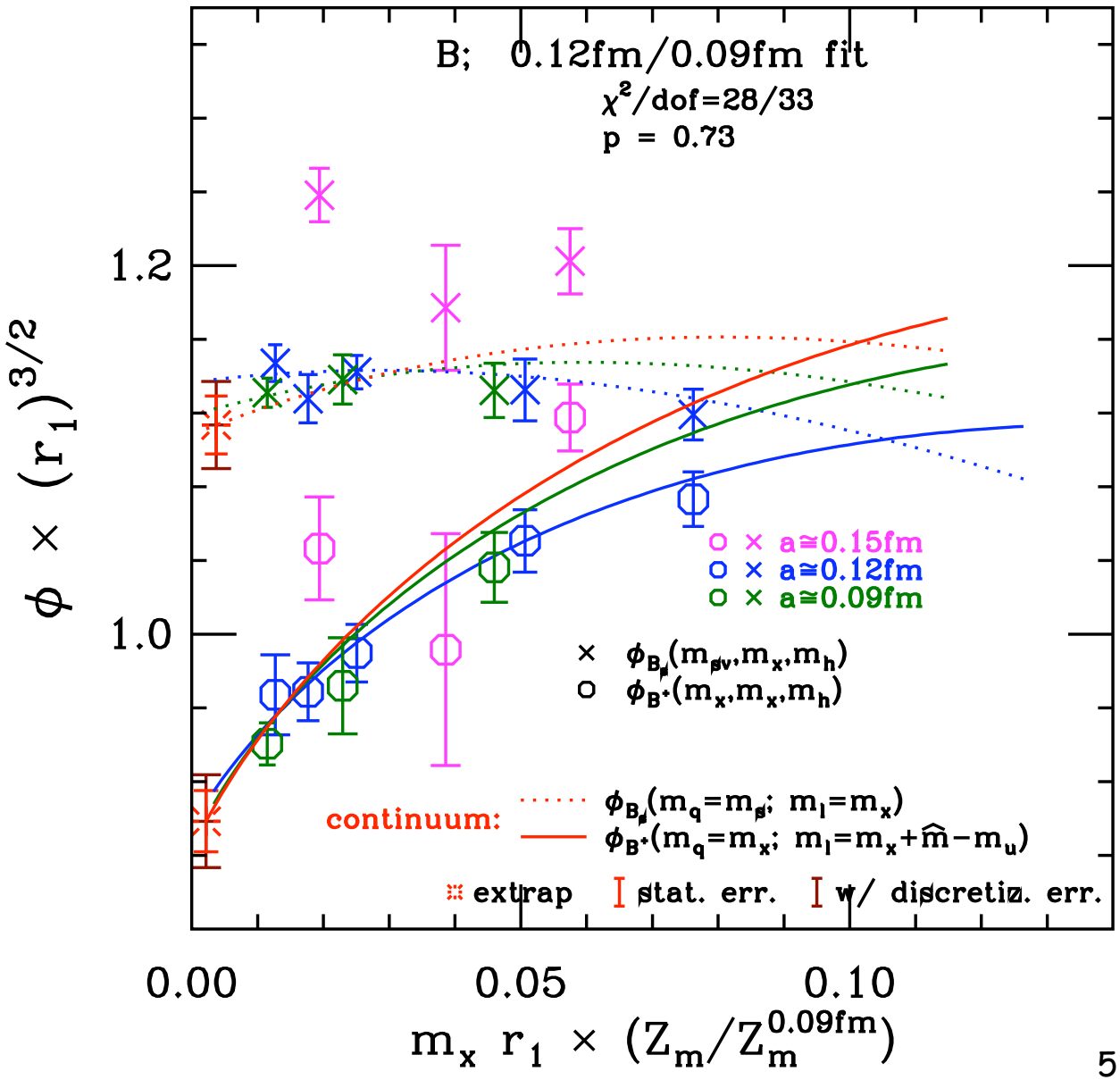

Fermilab/MILC Results

$$
\begin{aligned}
f_{D_s} &= 260.1 \pm 10.8 \text{ MeV} \\
f_{D^+} &= 218.9 \pm 11.3 \text{ MeV} \\
f_{D_s}/f_{D^+} &= 1.188 \pm 0.025 \\
f_{B_s} &= 242.0 \pm 9.5 \text{ MeV} \\
f_{B^+} &= 196.9 \pm 8.9 \text{ MeV} \\
f_{B_s}/f_{B^+} &= 1.229 \pm 0.026
\end{aligned}
$$

- errors include statistics and systematic errors
  - discretization errors for heavy & light quarks automatically included with statistics errors by our Bayesian procedure
  - have added on other systematics in quadrature

Comparison w/ other calculations & expt

D System

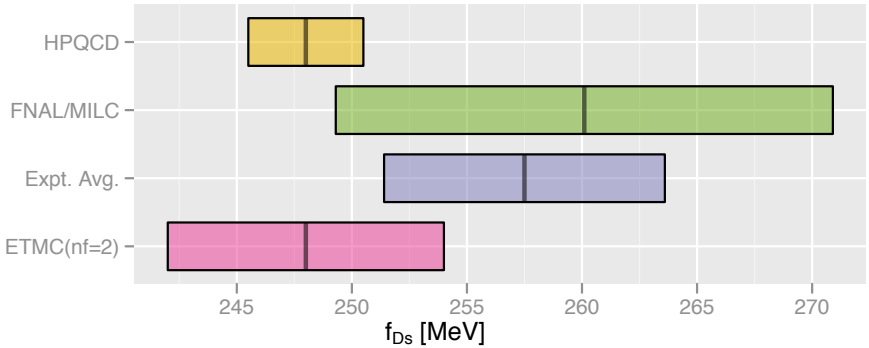

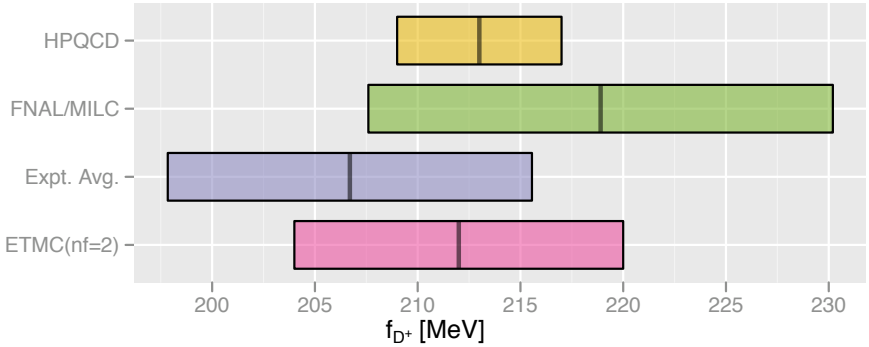

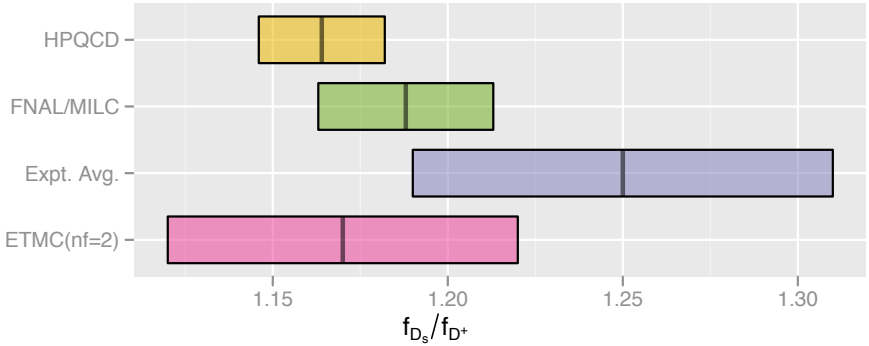

B System

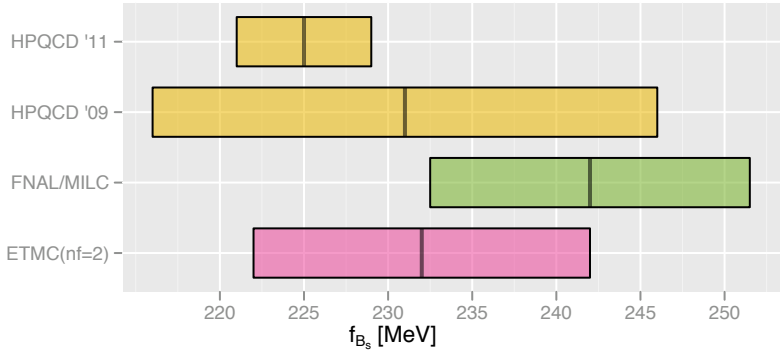

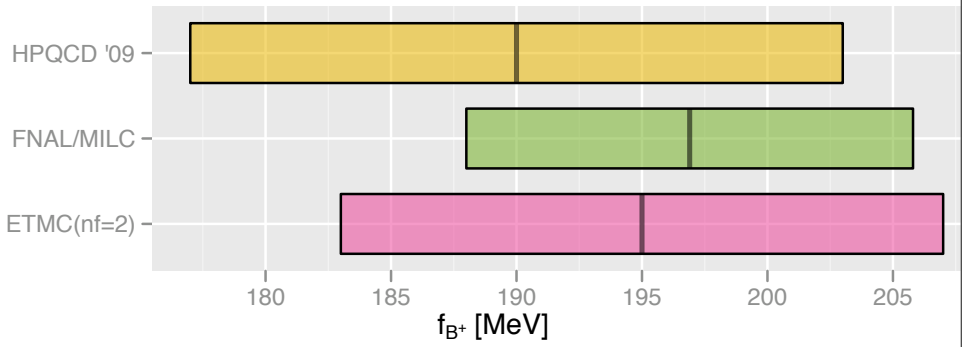

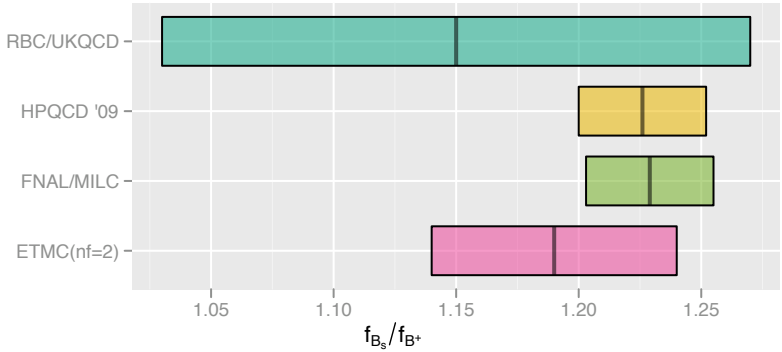

Heavy-light Decay Constants

- Fermilab heavy quarks with MILC 2+1 asqtad staggered light quarks
  - "Old data" project
    - 0.15 fm ≤ a ≤ 0.09 fm
    - 4 sources per configuration
    - renormalization mostly non-perturbative; 1-loop perturbation theory for remainder
    - to appear in PRD shortly
  - "New data" project: similar to above, but:
    - 0.15 fm ≤ a ≤ 0.045 fm
    - 2 to 5 times more configurations/ensemble
    - in progress

E. Neil

- For D system, ongoing HISQ project with MILC 2+1+1 HISQ quarks: more later.

Asqtad Ensembles

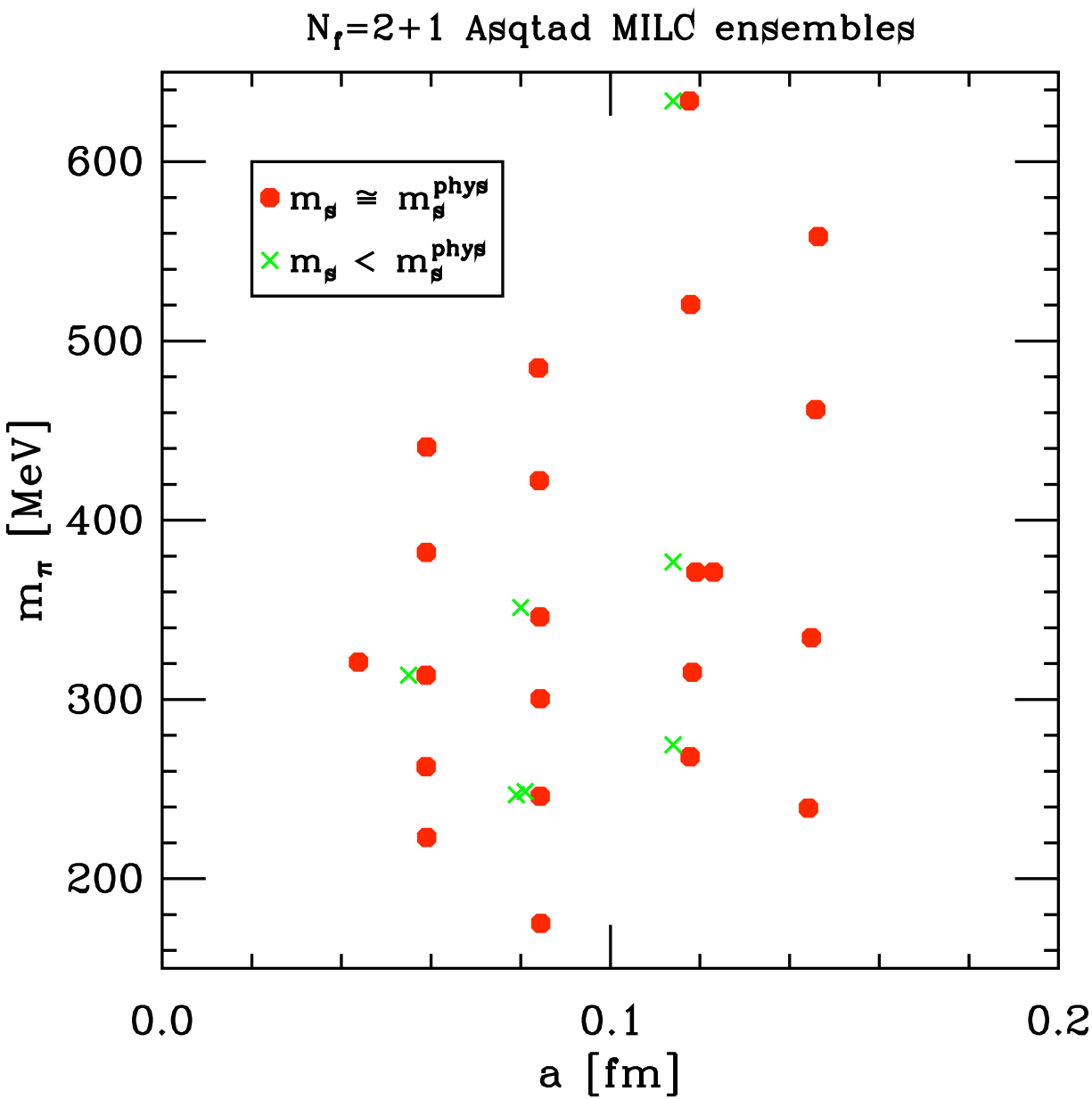

Asqtad Ensembles

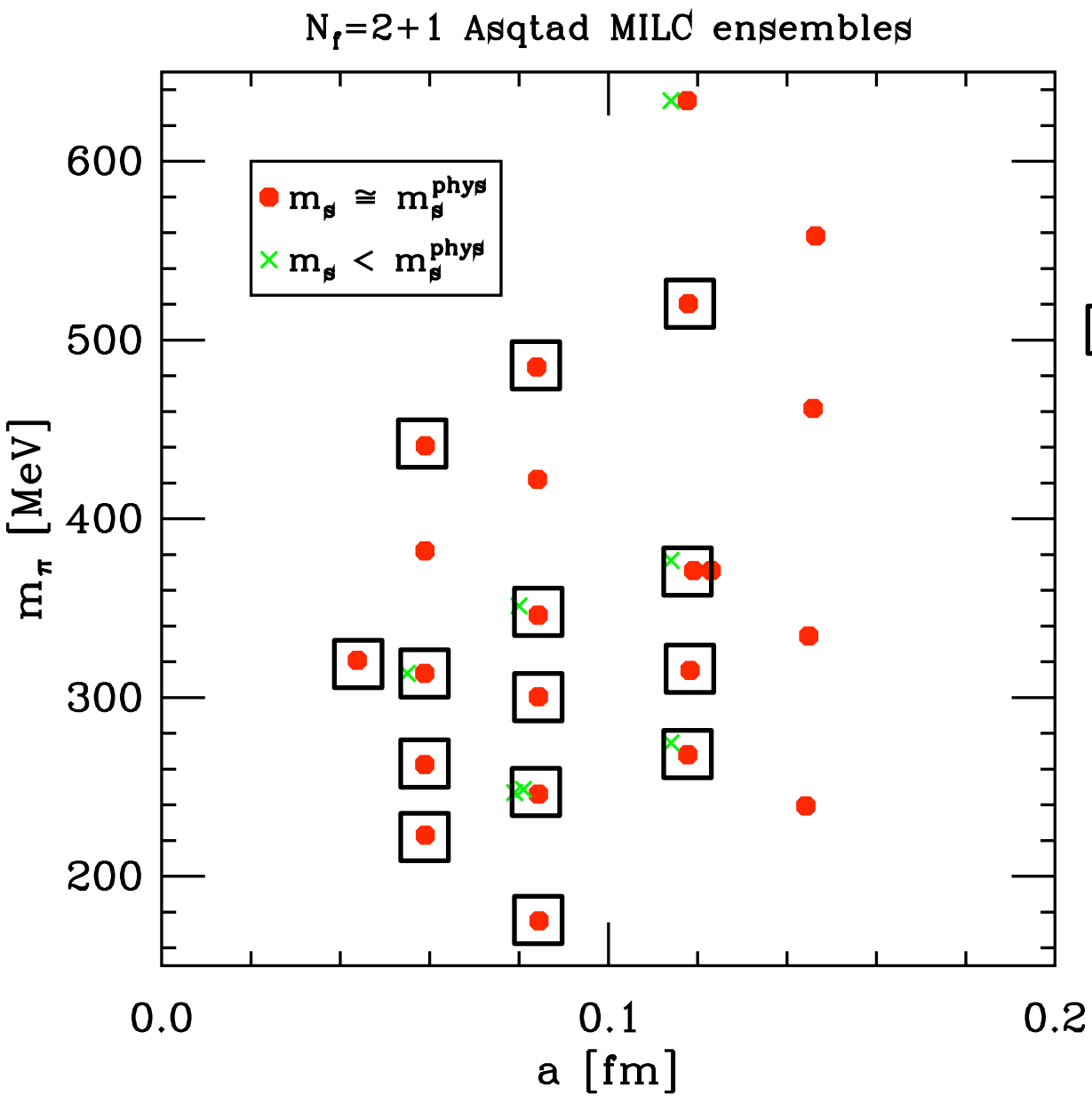

"new data" heavy-light decay const. analysis

Asqtad Ensembles

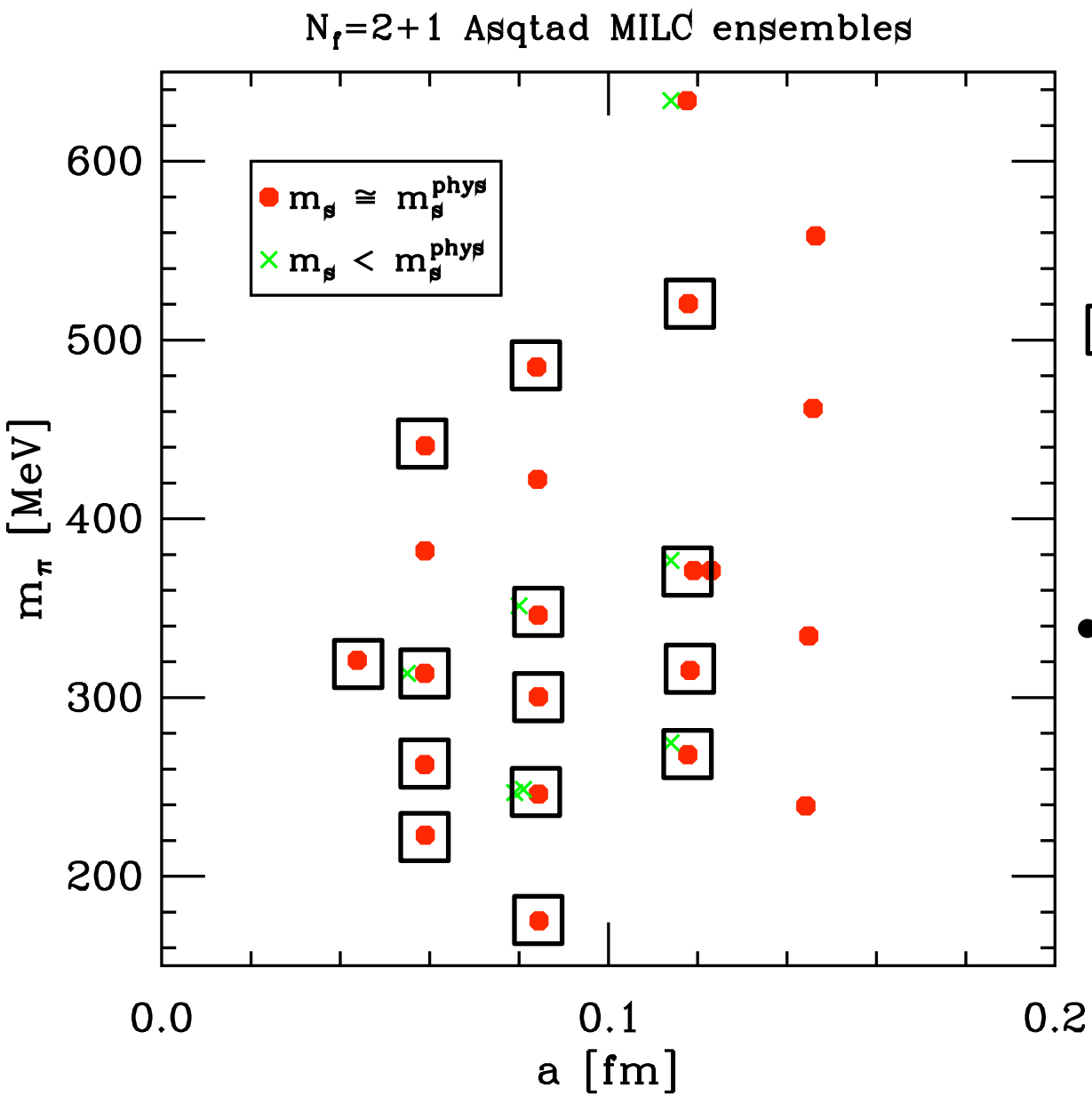

"new data" heavy-light decay const. analysis

- 0.06 fm and 0.045 ensembles added.

Asqtad Ensembles

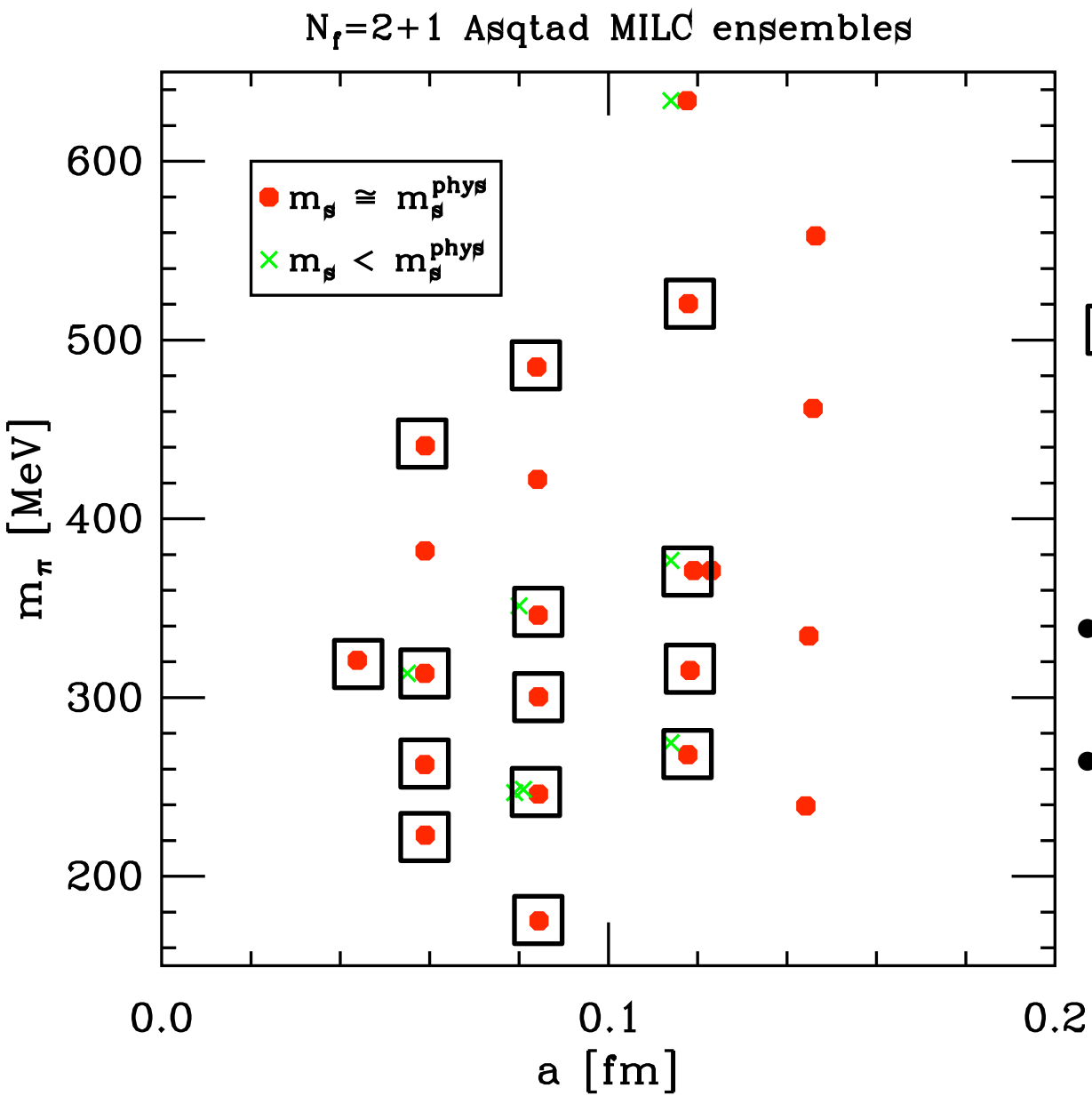

"new data" heavy-light decay const. analysis

- 0.06 fm and 0.045 ensembles added.
- runs lengthened by factor of ~2 to ~5.

“New Data” f_D

- statistical errors reduced as expected.
- correlator fits still need work; chiral fits are in progress.
- trend: f_D and f_{Ds} ↓ as a ↓

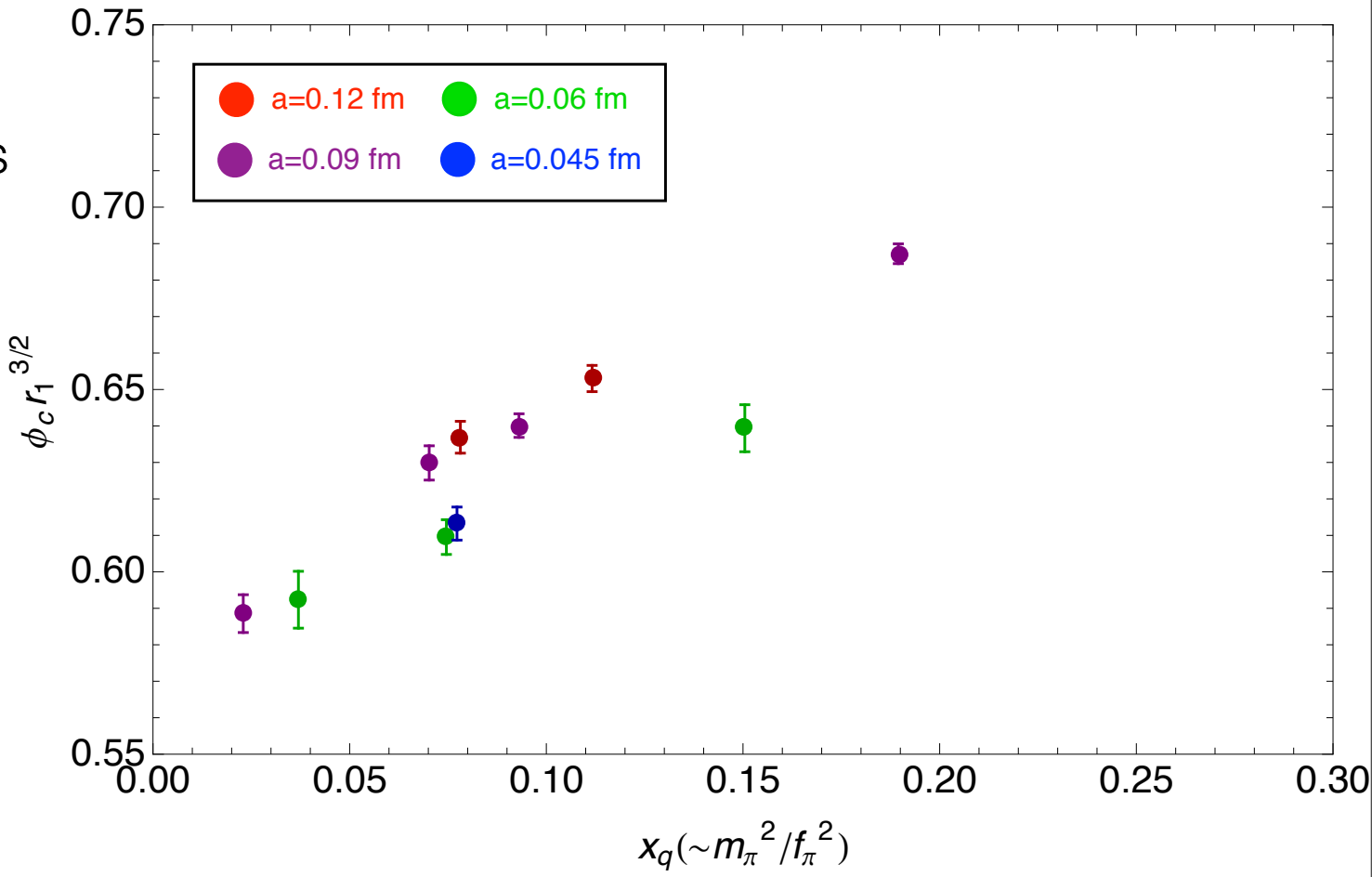

Outlook: Fermilab/MILC

Quantity	% Errors	
	"Old data" arXiv:1112.3051	"New data" (in progress)
f_{Ds}	4.2	2.2
f_D	5.2	2.8
f_{Ds}/f_D	2.1	1.1
f_{Bs}	3.9	2.6
f_B	4.5	2.8
f_{Bs}/f_B	2.1	1.2

B Mixing

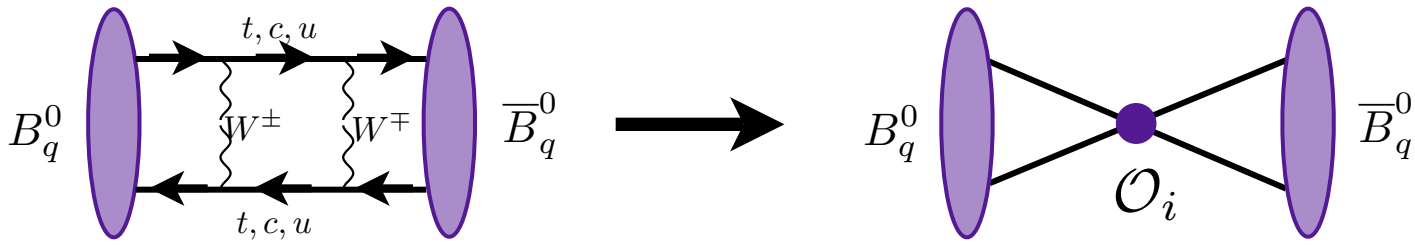

$$\mathcal{H}_{\rm eff} = \sum_{i=1}^{5} C_i \mathcal{O}_i$$

Operators are

SM

$$\mathcal{O}_1 = (\bar{b}^\alpha \gamma_\mu L q^\alpha)\,(\bar{b}^\beta \gamma_\mu L q^\beta)$$
$$\mathcal{O}_2 = (\bar{b}^\alpha L q^\alpha)\,(\bar{b}^\beta L q^\beta)$$
$$\mathcal{O}_3 = (\bar{b}^\alpha L q^\beta)\,(\bar{b}^\beta L q^\alpha)$$

BSM

$$\mathcal{O}_4 = (\bar{b}^\alpha L q^\alpha)\,(\bar{b}^\beta R q^\beta)$$
$$\mathcal{O}_5 = (\bar{b}^\alpha L q^\beta)\,(\bar{b}^\beta R q^\alpha)$$

Common parametrization

$$\langle \bar{B}_q^0 | \mathcal{O}_i(\mu) | B_q^0 \rangle \propto f_{B_q}^2 B_i(\mu)$$

B Mixing

- Fermilab heavy quarks with MILC 2+1 asqtad staggered light quarks
  - "Old data" project
    - 0.12 fm ≤ a ≤ 0.09 fm
    - focus on SM operators, and in particular on 0_1, which gives

$$\xi = f_{B_s}\sqrt{\hat{B}_{B_s}}/f_{B_d}\sqrt{\hat{B}_{B_d}}$$

    - construct operators from Fermilab quark + naive quark (made from staggered).
      - drop NLO "wrong spin" terms [⇒systematic error estimate].
    - 1-loop perturbation theory for mixing.
    - to be posted in next month or so.
  - "New data" project: similar to above, but:
    - 0.15 fm ≤ a ≤ 0.045 fm.
    - complete set of SM and BSM operators.
    - all wrong spin terms included correctly in ChPT.
    - in progress.

B Mixing

✦ Fermilab heavy quarks with MILC 2+1 asqtad staggered light quarks

- "Old data" project
  - 0.12 fm ≤ a ≤ 0.09 fm
  - focus on SM operators, and in particular on 0_1, which gives

$$\xi = f_{B_s}\sqrt{\hat{B}_{B_s}}/f_{B_d}\sqrt{\hat{B}_{B_d}}$$

  - construct operators from Fermilab quark + naive quark (made from staggered).
    - drop NLO "wrong spin" terms [⇒systematic error estimate].
  - 1-loop perturbation theory for mixing.
  - to be posted in next month or so.
- "New data" project: similar to above, but:
  - 0.15 fm ≤ a ≤ 0.045 fm.
  - complete set of SM and BSM operators.
  - all wrong spin terms included correctly in ChPT.
  - in progress.

R.T. Evans, E. Gámiz

Asqtad Ensembles

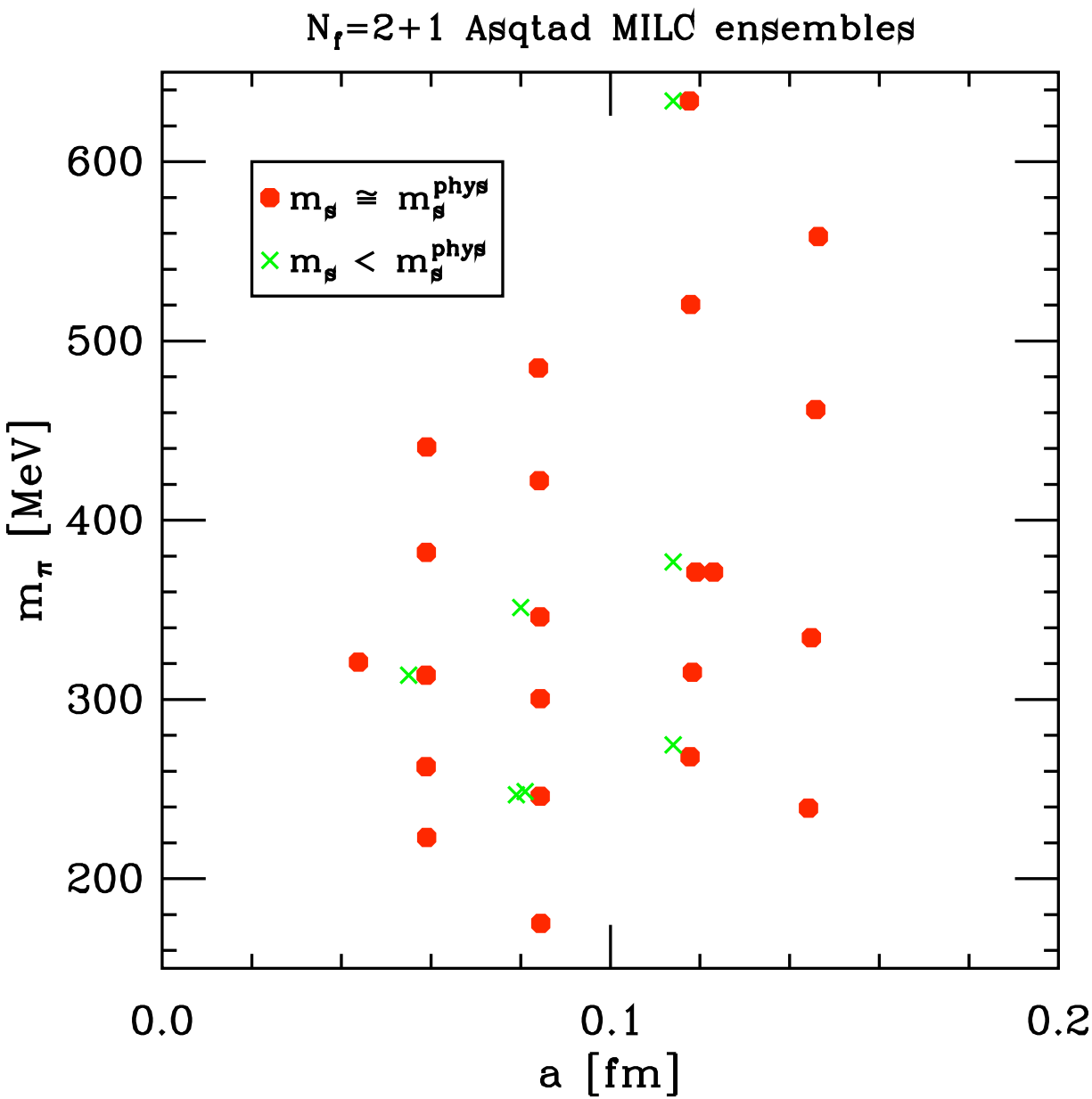

Asqtad Ensembles

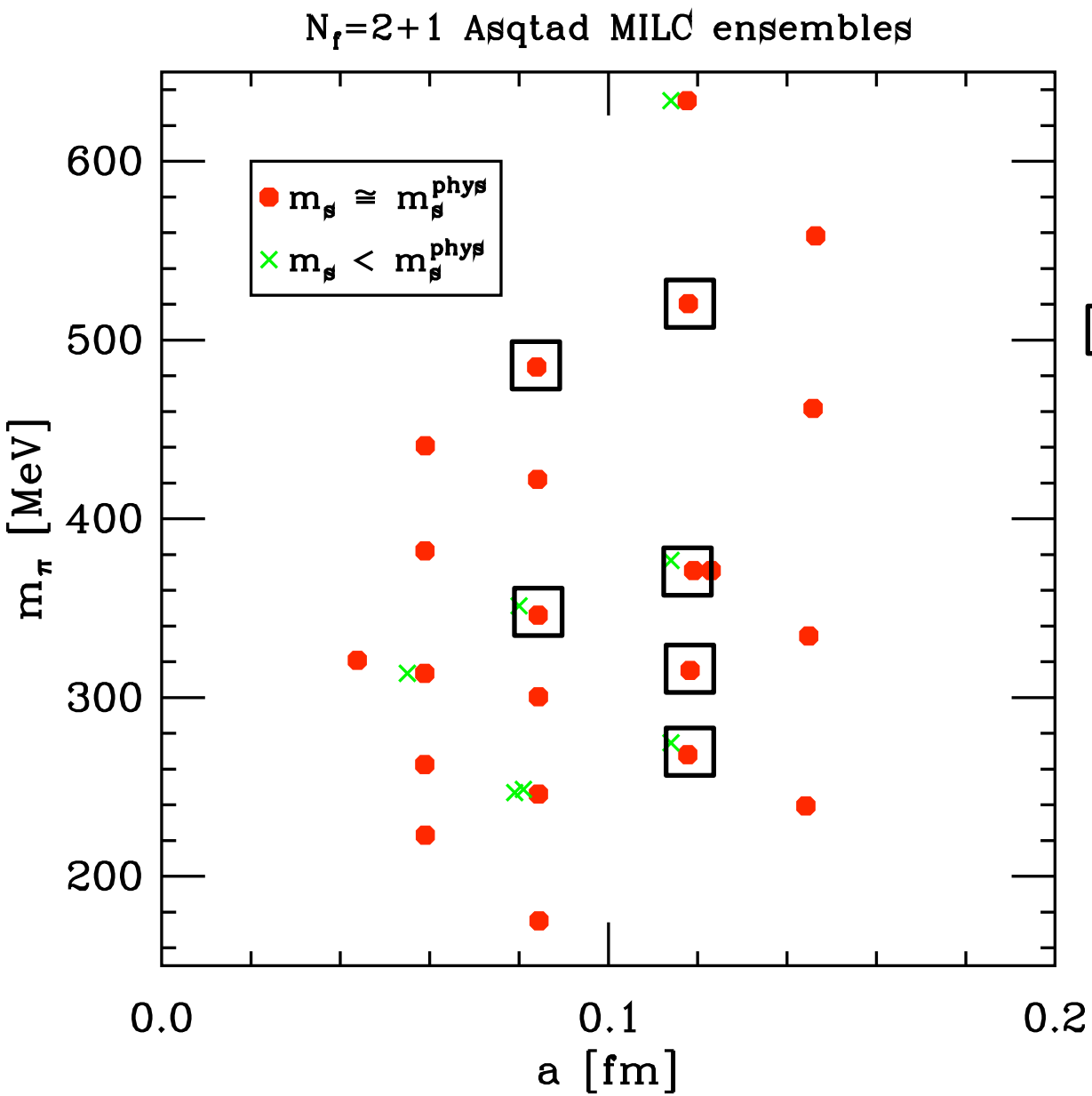

"old data" B-mixing analysis

“Wrong spin” Issue

- Four quark operators as in [HPQCD, PRD 80 (’09)014503].
  - local products of bilinears of heavy quark fields $\bar{Q}(x)$ and naive quarks $\Psi(x)$ (made from staggered):

$$\bar{Q}(x)\Gamma\Psi(x)\ \bar{Q}(x)\Gamma'\Psi(x)$$

- Desired spin-taste of staggered quarks not constructed by separately summing each bilinear over hypercube
  $\Rightarrow$ contributions from unwanted spin-tastes.
  - vanish in continuum limit by taste conservation.
  - but will appear in staggered ChPT at some order.
  - we had an argument (in a collaboration note) that chiral logs from wrong-spin taste first appear at NNLO. [Was used in HPQCD paper.]
  - in writing up our B mixing computation, found flaw in previous argument: such terms appear at NLO and need to be included.

"Wrong-spin" and Chiral/Continuum Errors

- Effects of wrong spin ops have now been calculated to 1-loop in staggered ChPT [CB].
  - don't have all needed matrix elements in old-data calc, but can estimate effect by sample new-data calc.

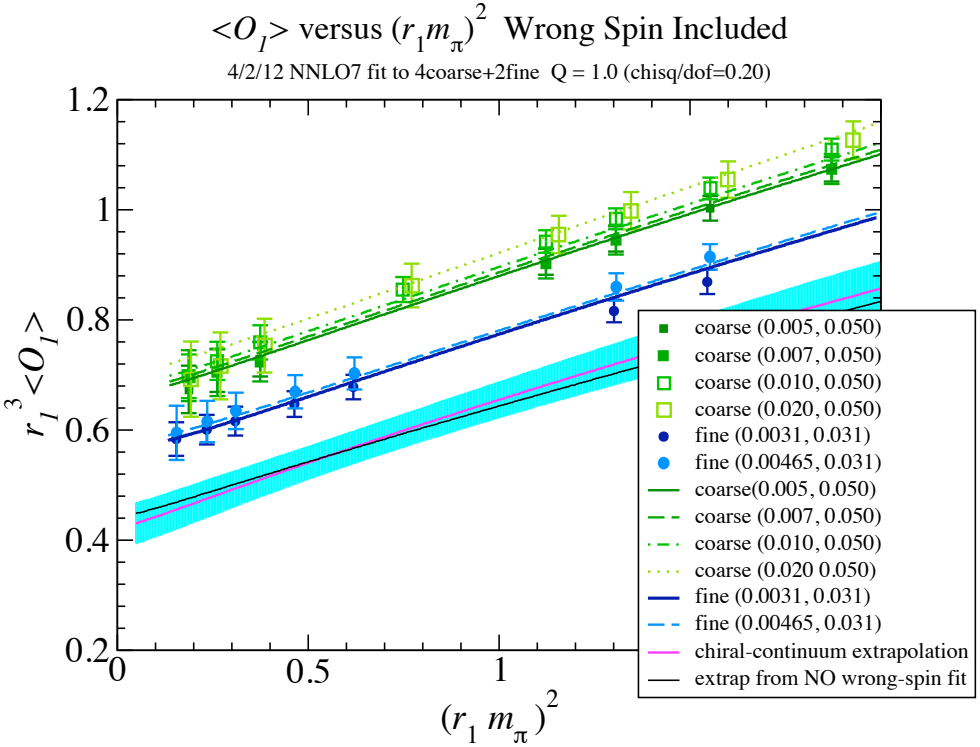

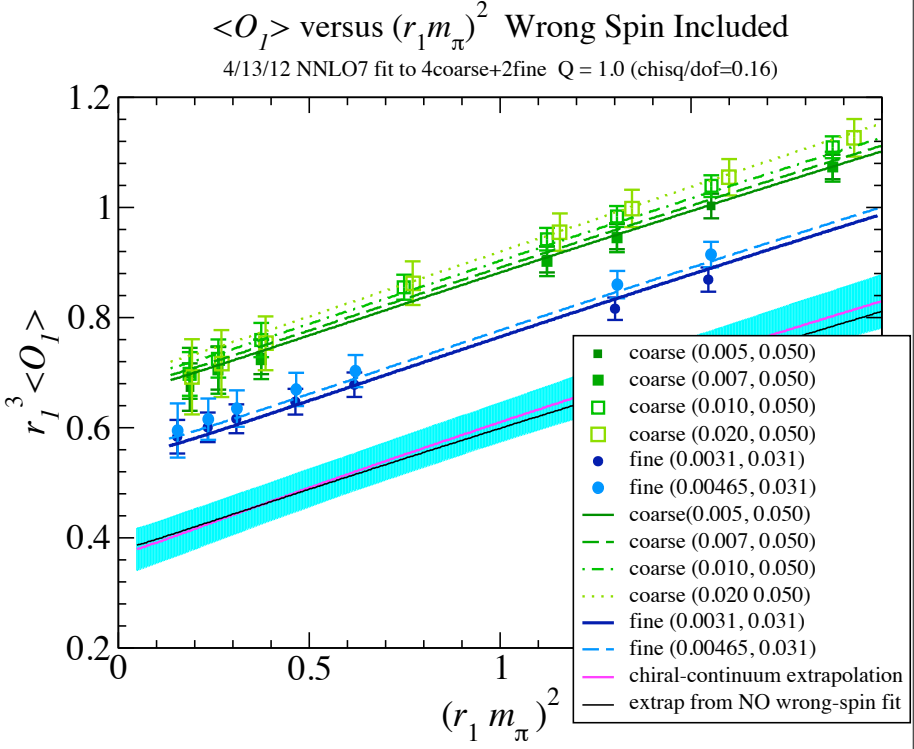

  - wrong-spin contrib < stat + other chiral/continuum errors, but effect on slope seems significant ⇒ tends to increase ξ .

Final "Old-Data" Results

TABLE IX. Complete error budget and total error for the B^0 mixing parameter ξ. All errors are given in %.

Source of uncertainty	Error (%)
Statistics $\oplus$ light-quark disc. $\oplus$ chiral extrapolation	3.7
Mixing with wrong-spin operators	3.2
Heavy-quark discretization	0.3
Scale uncertainty (r_1)	0.2
$g_{BB^*\pi}$	0.7
Light-quark masses	0.5
One-loop matching	0.5
Tuning κ_b	0.4
Finite volume	0.1
Mistuned coarse u_0	0.1
Total Error	5.0

Final "Old-Data" Results

TABLE IX. Complete error budget and total error for the B^0 mixing parameter ξ. All errors are given in %.

Source of uncertainty	Error (%)
Statistics $\oplus$ light-quark disc. $\oplus$ chiral extrapolation	3.7
Mixing with wrong-spin operators	3.2
Heavy-quark discretization	0.3
Scale uncertainty (r_1)	0.2
$g_{BB^*\pi}$	0.7
Light-quark masses	0.5
One-loop matching	0.5
Tuning κ_b	0.4
Finite volume	0.1
Mistuned coarse u_0	0.1
Total Error	5.0

small because ratio

Final "Old-Data" Results

TABLE IX. Complete error budget and total error for the B^0 mixing parameter ξ. All errors are given in %.

Source of uncertainty	Error (%)
Statistics $\oplus$ light-quark disc. $\oplus$ chiral extrapolation	3.7
Mixing with wrong-spin operators	3.2
Heavy-quark discretization	0.3
Scale uncertainty (r_1)	0.2
$g_{BB^*\pi}$	0.7
Light-quark masses	0.5
One-loop matching	0.5
Tuning κ_b	0.4
Finite volume	0.1
Mistuned coarse u_0	0.1
Total Error	5.0

Result: ξ = 1.268(63) (nearly final)

B Mixing

- Fermilab heavy quarks with MILC 2+1 asqtad staggered light quarks
  - "Old data" project
    - 0.12 fm ≤ a ≤ 0.09 fm
    - focus on SM operators, and in particular on 0_1, which gives

$$\xi = f_{B_s}\sqrt{\hat{B}_{B_s}}/f_{B_d}\sqrt{\hat{B}_{B_d}}$$

    - construct operators from Fermilab quark + naive quark (made from staggered).
      - drop NLO "wrong spin" terms [⇒systematic error estimate].
    - 1-loop perturbation theory for mixing.
    - to be posted in next month or so.
  - "New data" project: similar to above, but:
    - 0.15 fm ≤ a ≤ 0.045 fm.
    - complete set of SM and BSM operators.
    - all wrong spin terms included correctly in ChPT.
    - in progress.

C. Bouchard, E. Freeland

Asqtad Ensembles

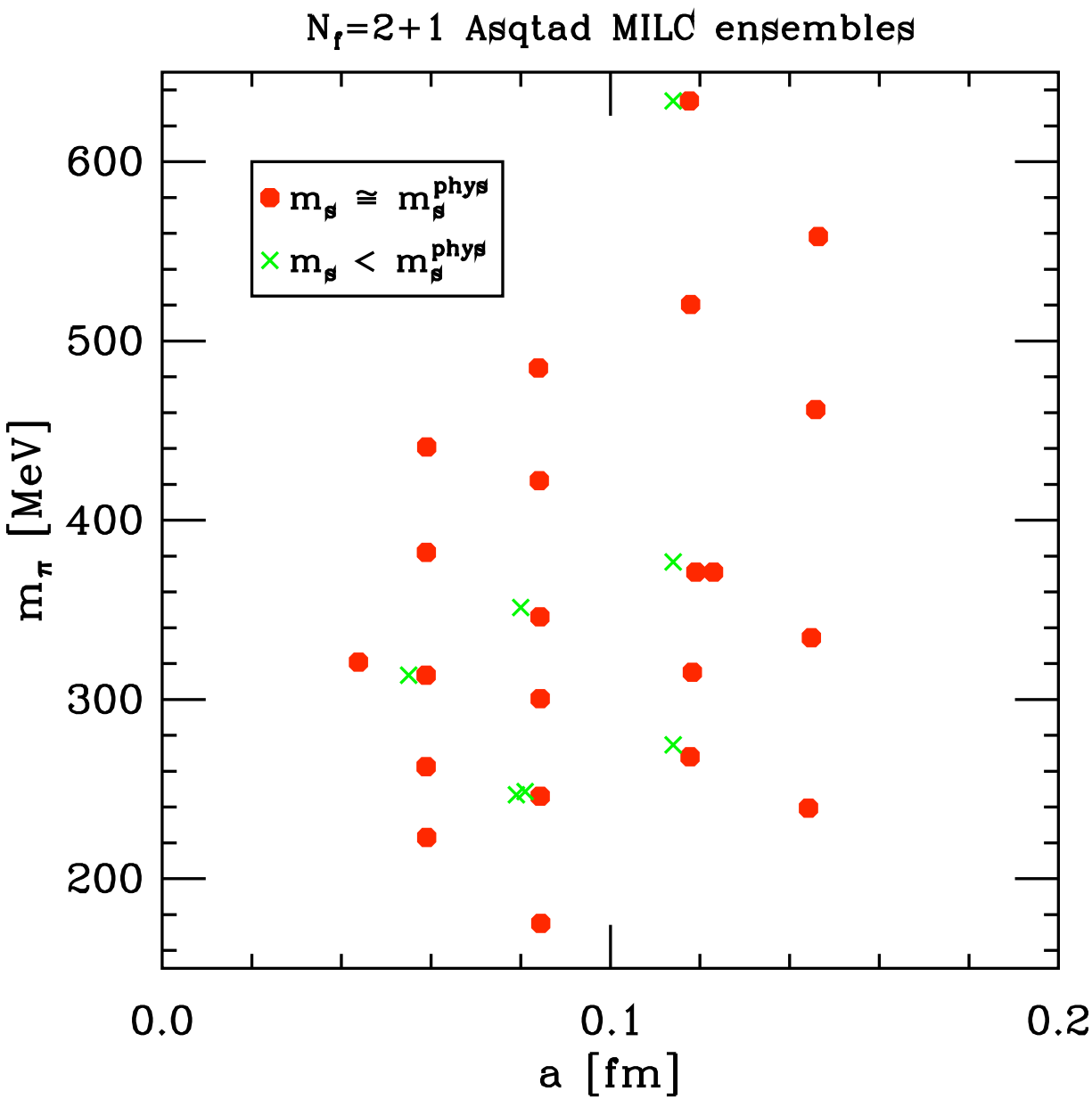

Asqtad Ensembles

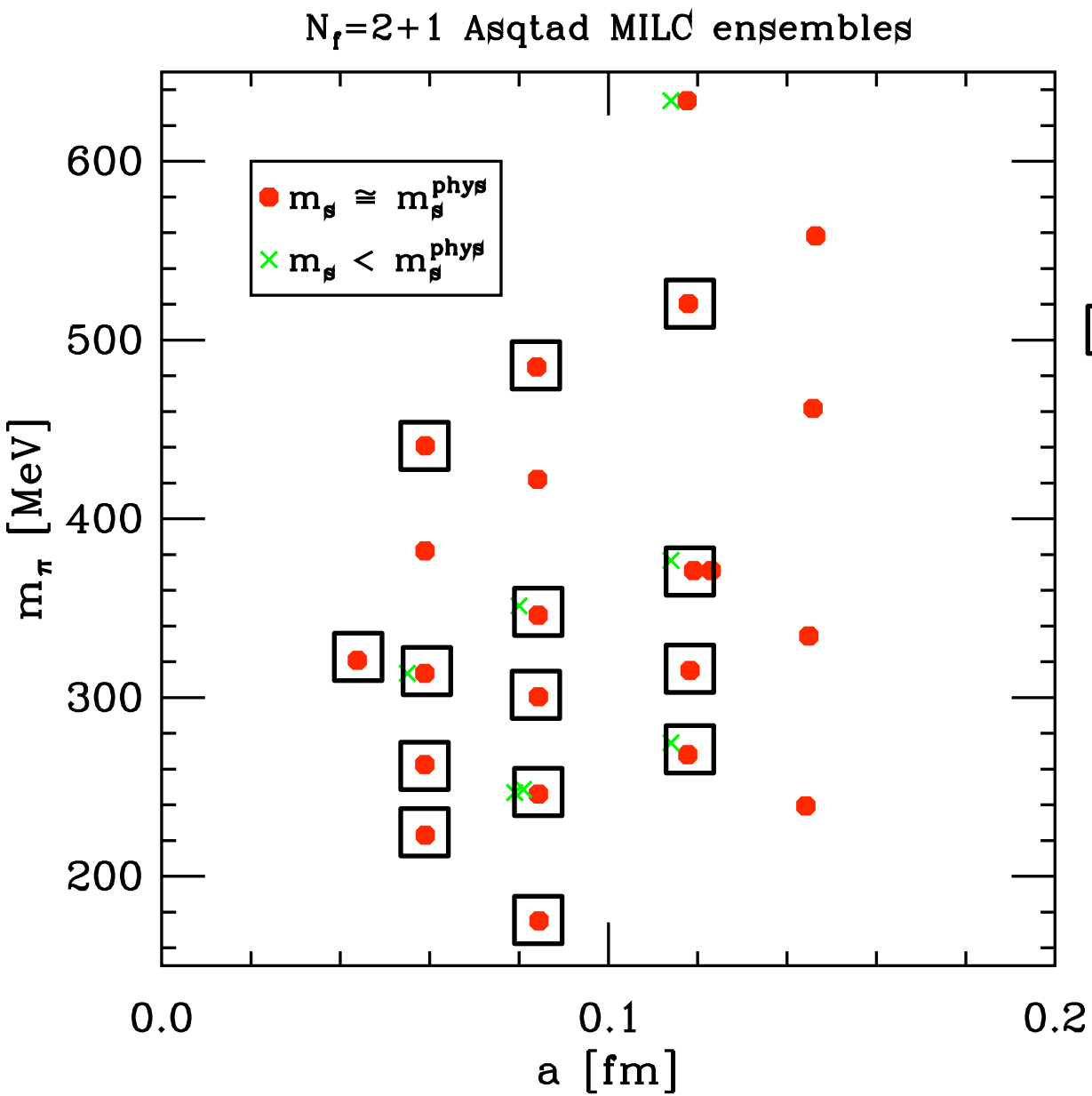

"new-data" B-mixing: plan

Asqtad Ensembles

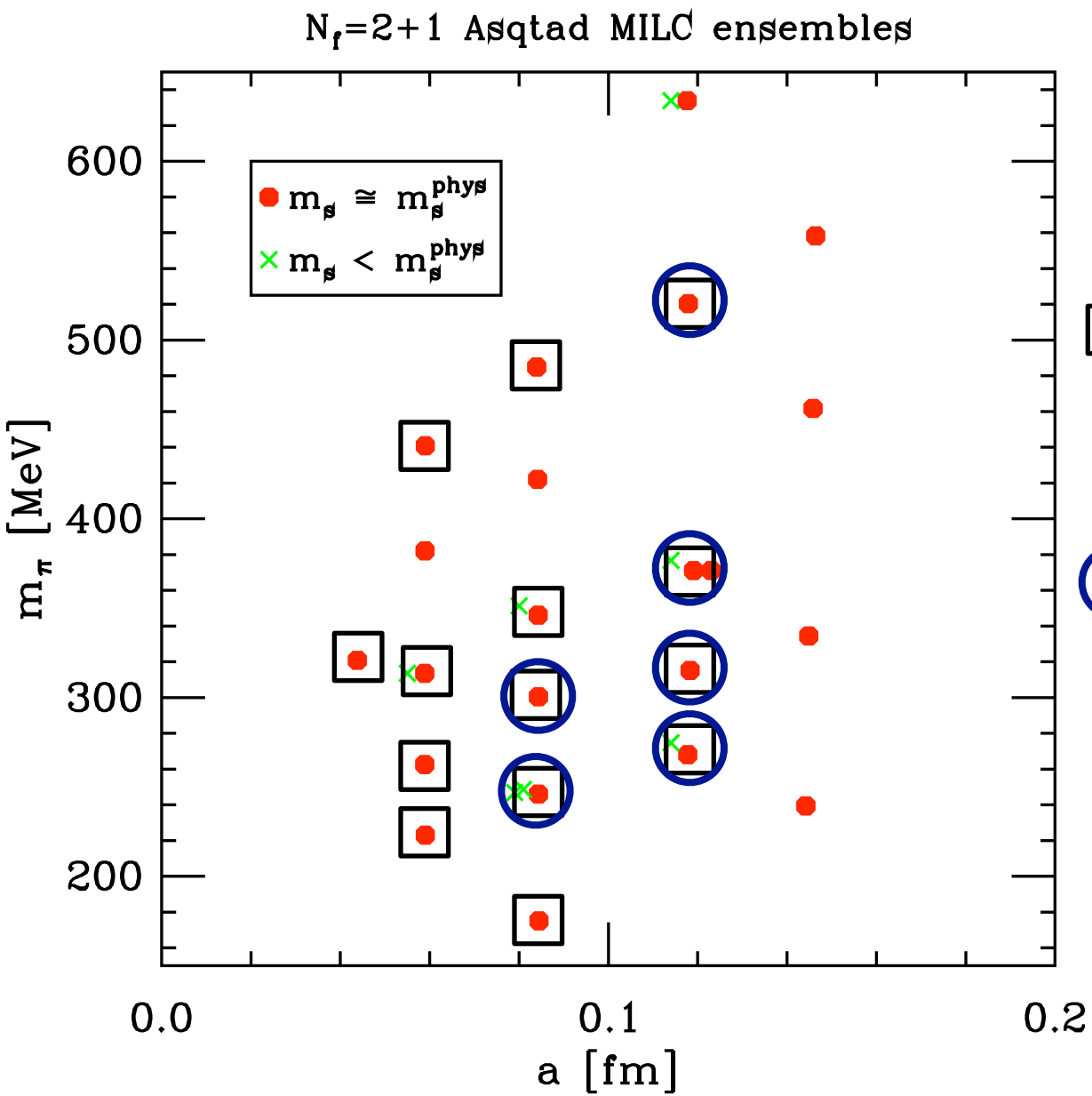

"new-data" B-mixing: plan

completed

Asqtad Ensembles

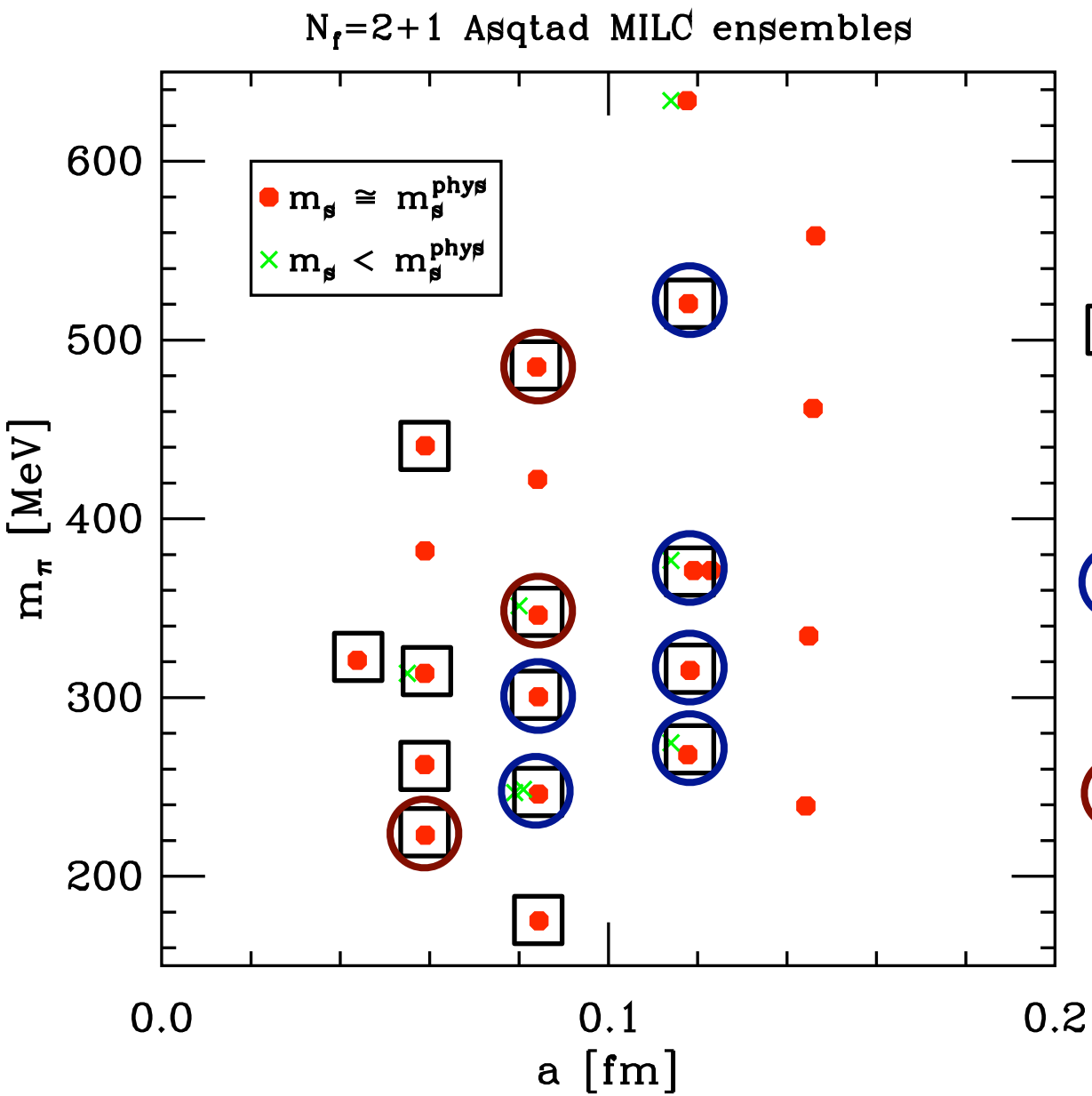

"new-data" B-mixing: plan

completed

subset of operators done

Matrix element of O_2

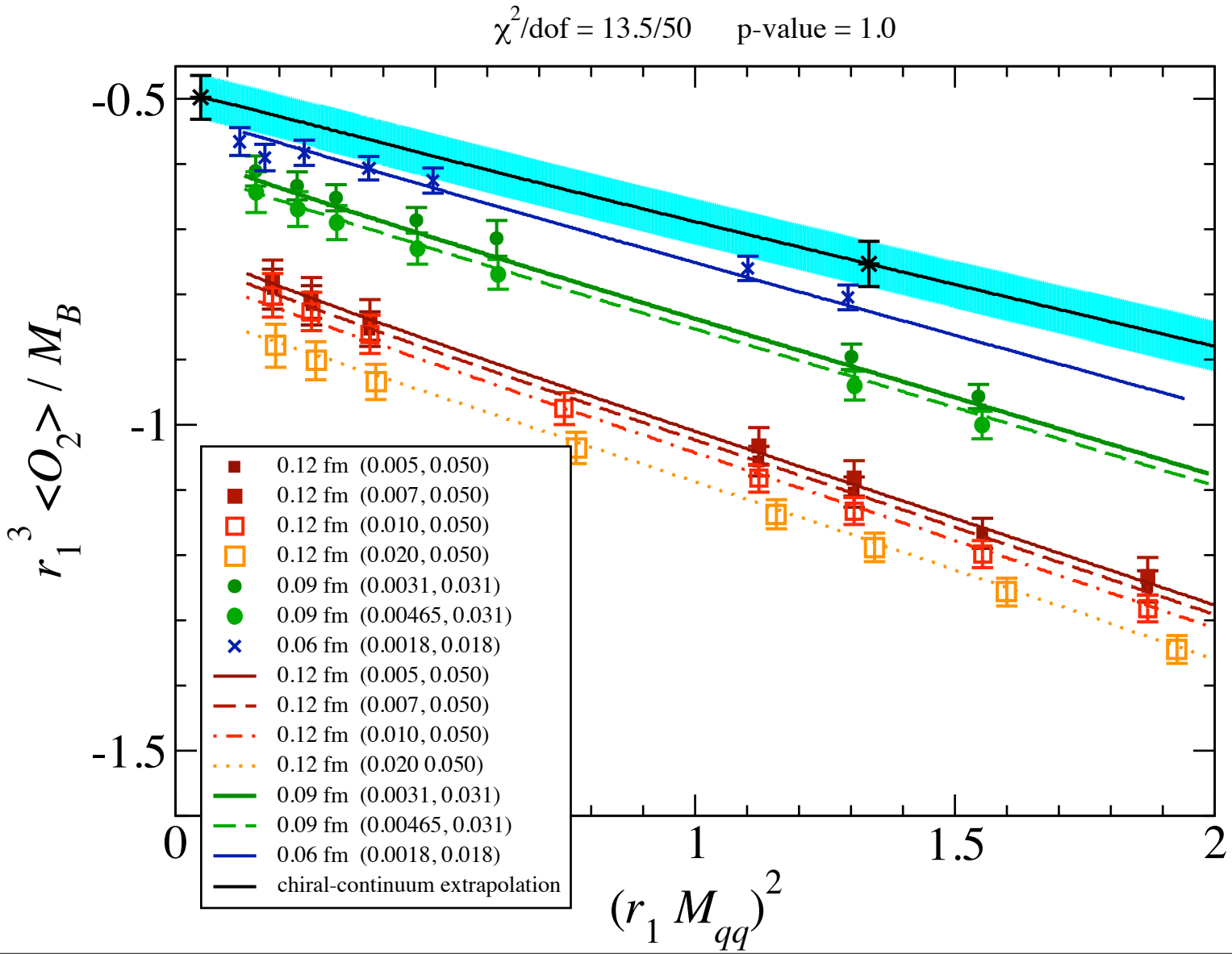

(needed in SM for ΔM and ΔΓ ; also BSM)

Anticipated Error Budget

Anticipated Error Budget

- Snapshot of statistical and chiral-continuum extrap errors at current state of running:

	Source of Error [%]	$\langle \mathcal{O}_1 \rangle$	$\langle \mathcal{O}_2 \rangle$	$\langle \mathcal{O}_3 \rangle$	$\langle \mathcal{O}_4 \rangle$	$\langle \mathcal{O}_5 \rangle$
B_d^0	statistical	8.6	6.8	16	4.3	5.5
	chiral-continuum systematic	12	11	3.3	0.2	4.4
B_s^0	statistical	6.7	4.6	10	2.5	3.4
	chiral-continuum systematic	1.8	6.6	4.5	1.6	3.7

Anticipated Error Budget

- Snapshot of statistical and chiral-continuum extrap errors at current state of running:

	Source of Error [%]	$\langle \mathcal{O}_1 \rangle$	$\langle \mathcal{O}_2 \rangle$	$\langle \mathcal{O}_3 \rangle$	$\langle \mathcal{O}_4 \rangle$	$\langle \mathcal{O}_5 \rangle$
B_d^0	statistical	8.6	6.8	16	4.3	5.5
	chiral-continuum systematic	12	11	3.3	0.2	4.4
B_s^0	statistical	6.7	4.6	10	2.5	3.4
	chiral-continuum systematic	1.8	6.6	4.5	1.6	3.7

  - Should decrease significantly as we add finer ensembles.

Anticipated Error Budget

- Snapshot of statistical and chiral-continuum extrap errors at current state of running:

	Source of Error [%]	$\langle \mathcal{O}_1 \rangle$	$\langle \mathcal{O}_2 \rangle$	$\langle \mathcal{O}_3 \rangle$	$\langle \mathcal{O}_4 \rangle$	$\langle \mathcal{O}_5 \rangle$
B_d^0	statistical	8.6	6.8	16	4.3	5.5
	chiral-continuum systematic	12	11	3.3	0.2	4.4
B_s^0	statistical	6.7	4.6	10	2.5	3.4
	chiral-continuum systematic	1.8	6.6	4.5	1.6	3.7

  - Should decrease significantly as we add finer ensembles.

- Some other expected errors:

Source of Error [%]	$\langle \mathcal{O}_i \rangle$
scale (r_1)	3
κ_b tuning	4
light-quark masses	1
heavy-quark discretization	4
one-loop matching	8
finite-volume effects	1
subtotal	10

Anticipated Error Budget

- Snapshot of statistical and chiral-continuum extrap errors at current state of running:

	Source of Error [%]	$\langle \mathcal{O}_1 \rangle$	$\langle \mathcal{O}_2 \rangle$	$\langle \mathcal{O}_3 \rangle$	$\langle \mathcal{O}_4 \rangle$	$\langle \mathcal{O}_5 \rangle$
B_d^0	statistical	8.6	6.8	16	4.3	5.5
	chiral-continuum systematic	12	11	3.3	0.2	4.4
B_s^0	statistical	6.7	4.6	10	2.5	3.4
	chiral-continuum systematic	1.8	6.6	4.5	1.6	3.7

  - Should decrease significantly as we add finer ensembles.

- Some other expected errors:

  - limit to precision.

Source of Error [%]	$\langle \mathcal{O}_i \rangle$
scale (r_1)	3
κ_b tuning	4
light-quark masses	1
heavy-quark discretization	4
one-loop matching	8
finite-volume effects	1
subtotal	10

Anticipated Error Budget

- Snapshot of statistical and chiral-continuum extrap errors at current state of running:

	Source of Error [%]	$\langle \mathcal{O}_1 \rangle$	$\langle \mathcal{O}_2 \rangle$	$\langle \mathcal{O}_3 \rangle$	$\langle \mathcal{O}_4 \rangle$	$\langle \mathcal{O}_5 \rangle$
B_d^0	statistical	8.6	6.8	16	4.3	5.5
	chiral-continuum systematic	12	11	3.3	0.2	4.4
B_s^0	statistical	6.7	4.6	10	2.5	3.4
	chiral-continuum systematic	1.8	6.6	4.5	1.6	3.7

  - Should decrease significantly as we add finer ensembles.

- Some other expected errors:

Source of Error [%]	$\langle \mathcal{O}_i \rangle$
scale (r_1)	3
κ_b tuning	4
light-quark masses	1
heavy-quark discretization	4
one-loop matching	8
finite-volume effects	1
subtotal	10

  - limit to precision.
  - may be able to reduce a bit (to ~6%?) with finer spacings.

MILC HISQ 2+1+1 Ensembles

- Asqtad ensembles are complete; though there is more physics still to extract.
- For higher precision, have moved to HISQ [Follana et al. [HPQCD], PRD 75 (2007) 054502].
  - Reduced $O(\alpha_S a^2)$ and $O(\alpha_S^2 a^2)$ errors with respect to Asqtad.
  - $(am_c)^4$ errors reduced ⇒ treat charm with same relativistic action as light quarks.
  - Ensembles include charm sea quarks
    - (although error of quenching charm is probably negligible in most cases, it doesn't cost much to include it in sea.)

[A. Bazavov, D. Toussaint]

HISQ Ensembles

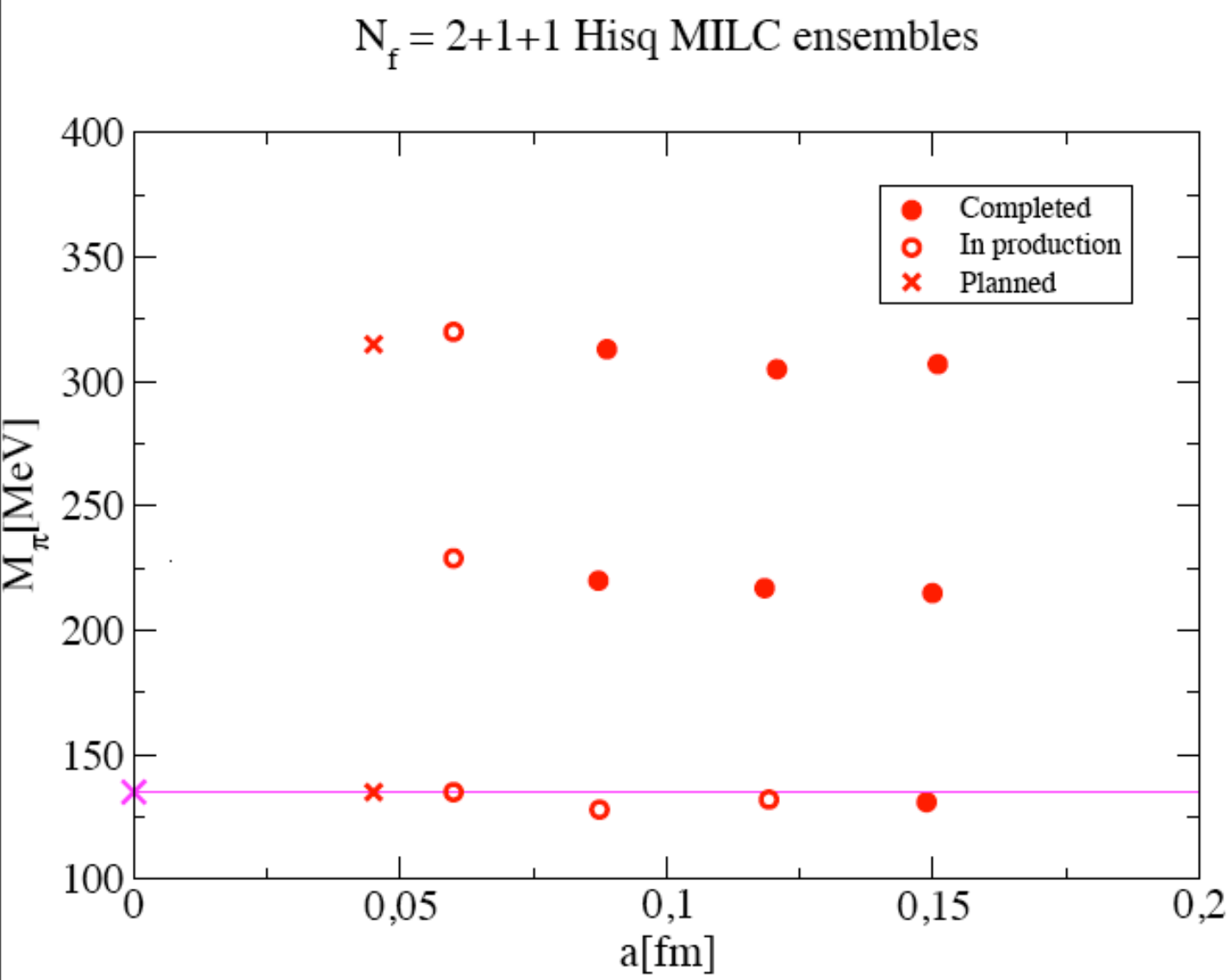

HISQ Ensembles

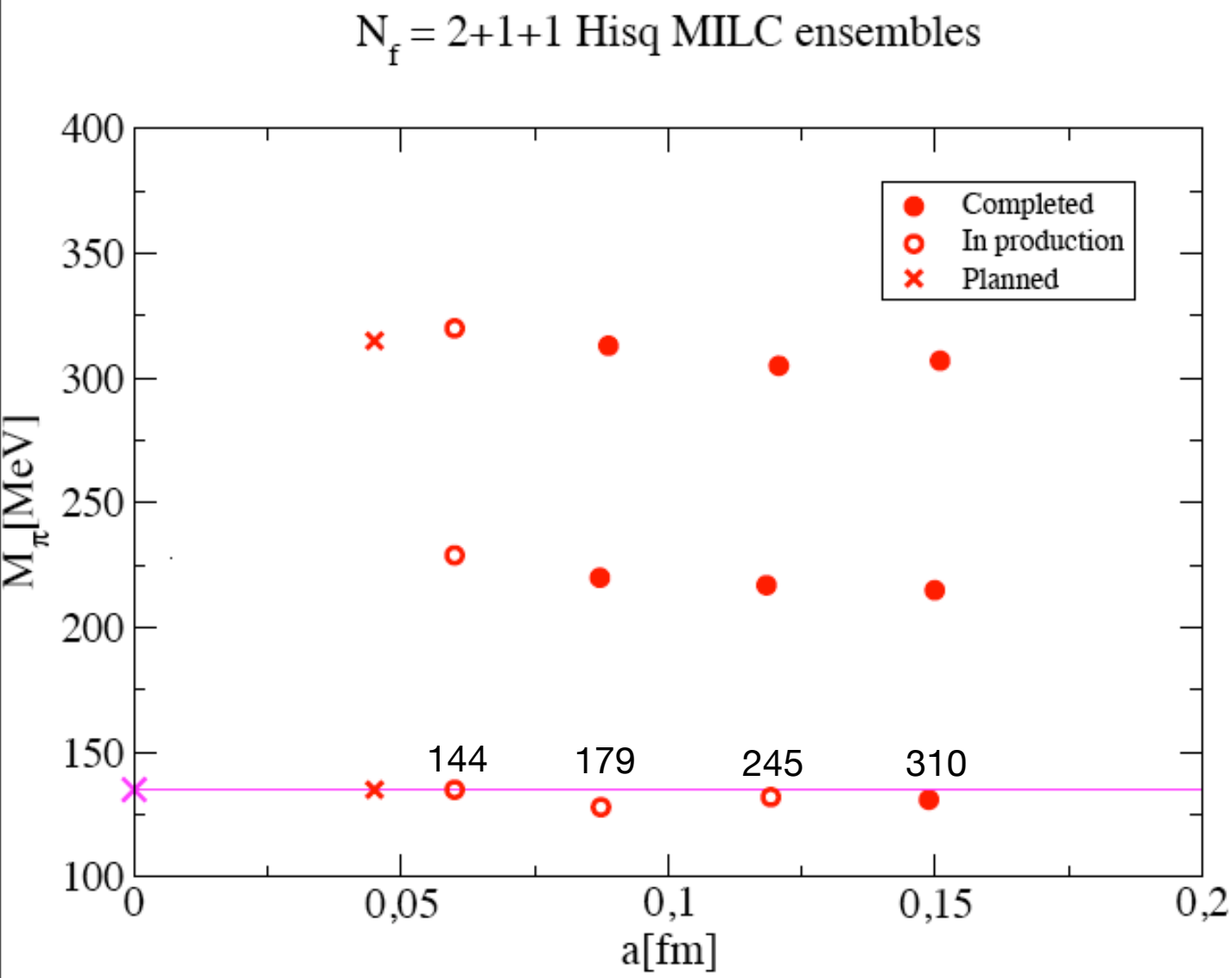

m_π^{RMS} [MeV]

HISQ Ensembles

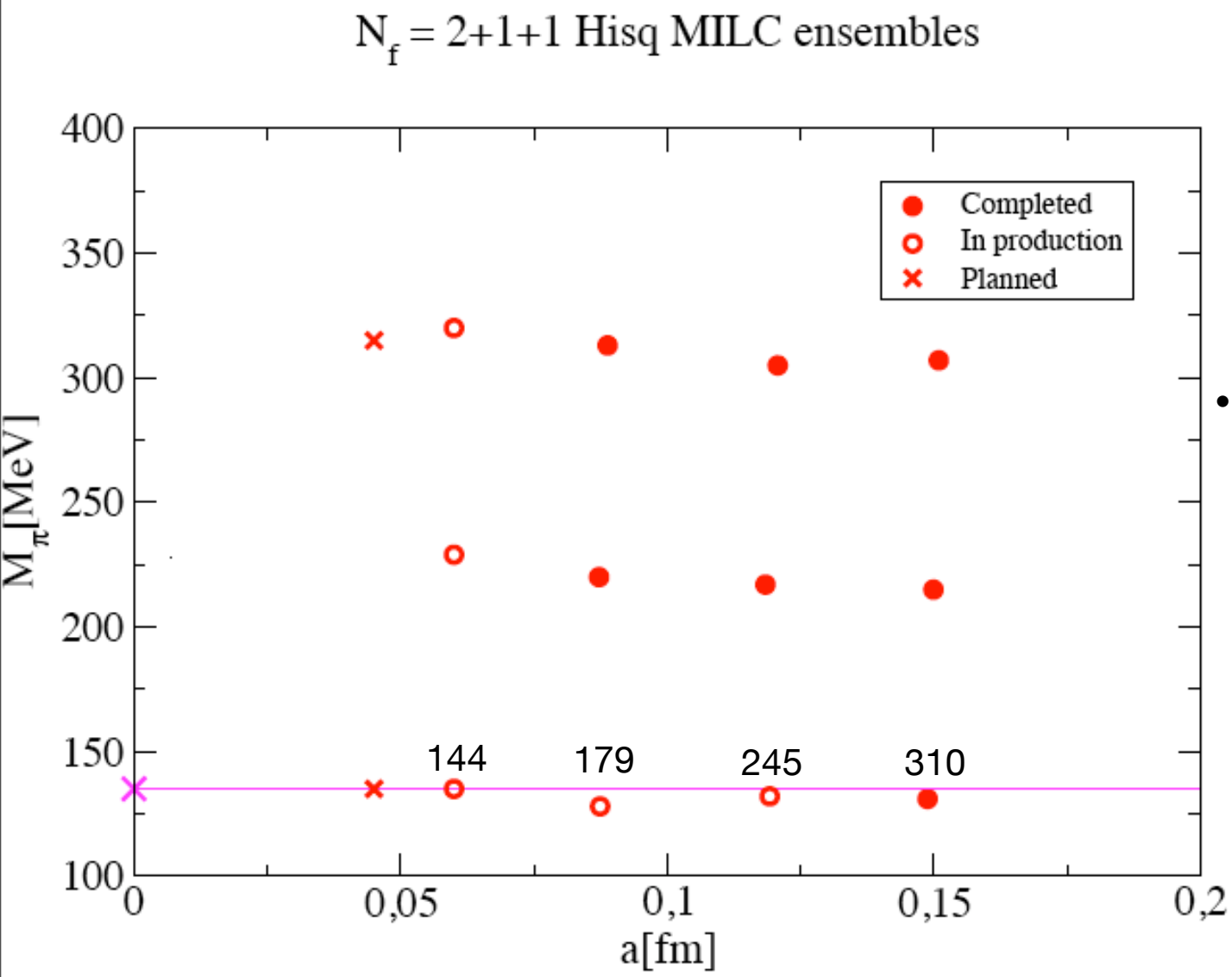

m_π^{RMS} [MeV]

- recall that coupling of these sea pions to valence pions is NLO in ChPT.

HISQ Ensembles

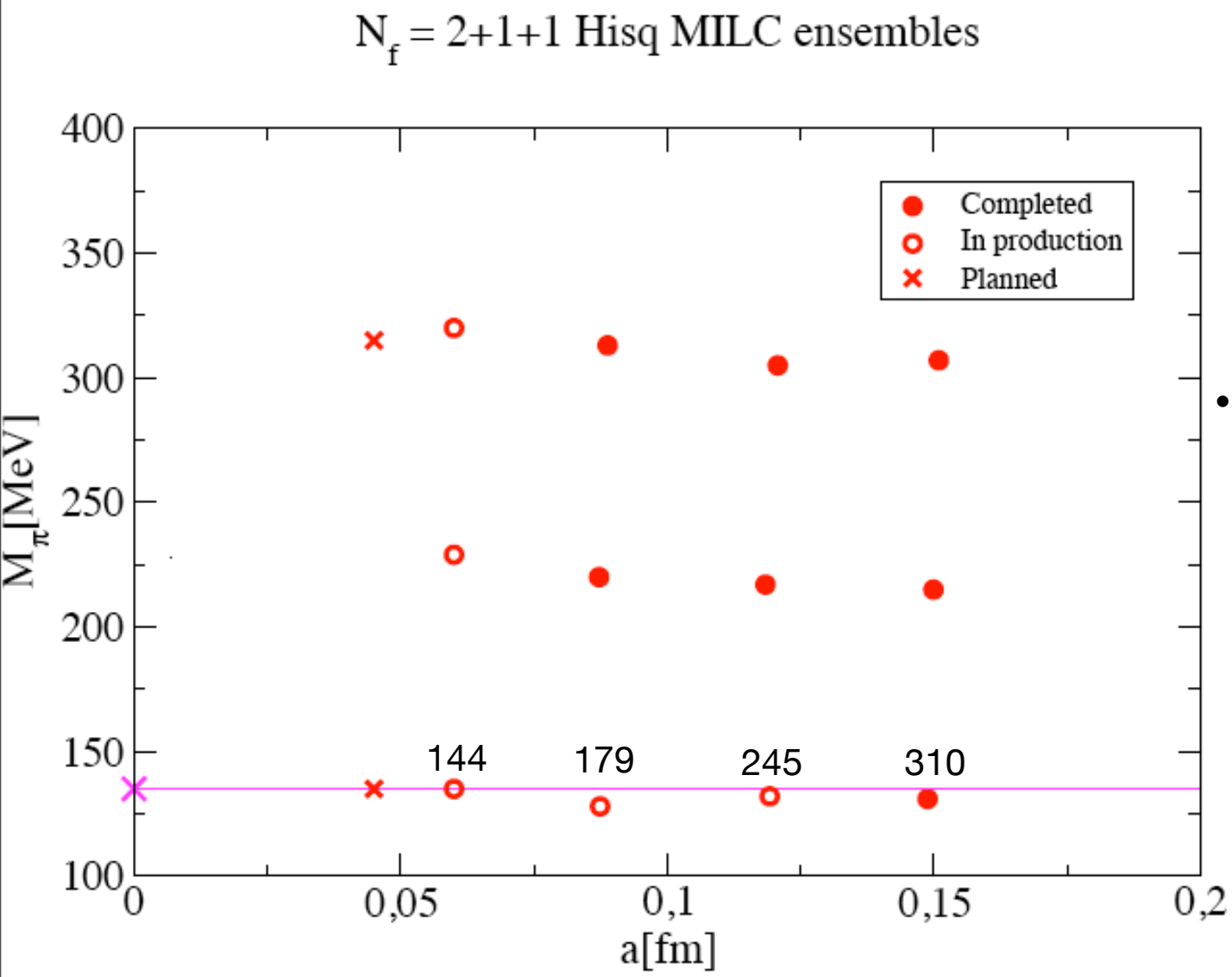

m_π^{RMS} [MeV]

- recall that coupling of these sea pions to valence pions is NLO in ChPT.

$\Rightarrow$ suppressed by $\frac{(m_\pi^{\mathrm{RMS}})^2}{16\pi^2 f_\pi^2}$

Light decay constants w/ 2+1+1 HISQ

- In Asqtad case, needed ensembles with m_s lighter than physical to control SU(3) chiral extrapolation.
- In HISQ case, such ensembles have not been available (but are coming on line now...), so SU(3) fits have not yet been very successful.
- "Heavy kaon" SU(2) chiral perturbation theory [*à la* RBC/UKQCD and PACS-CS], has been recently worked out for staggered case [CB, Du, and Lightman], but not yet tried.
- So focus for now on physical-mass HISQ ensembles, where ChPT not needed.

[M. Lightman]

HISQ f_π , f_K

✦ On each ensemble:

- for valence masses m_x, $m_y \lesssim m_s$, meson mass squared $(m_{xy})^2$ is very linear in $m_x + m_y$.
- decay const f_{xy} appears linear for $m_x + m_y \lesssim 0.5\ m_s$, but there is separate dependence on m_x and m_y for heavier masses.

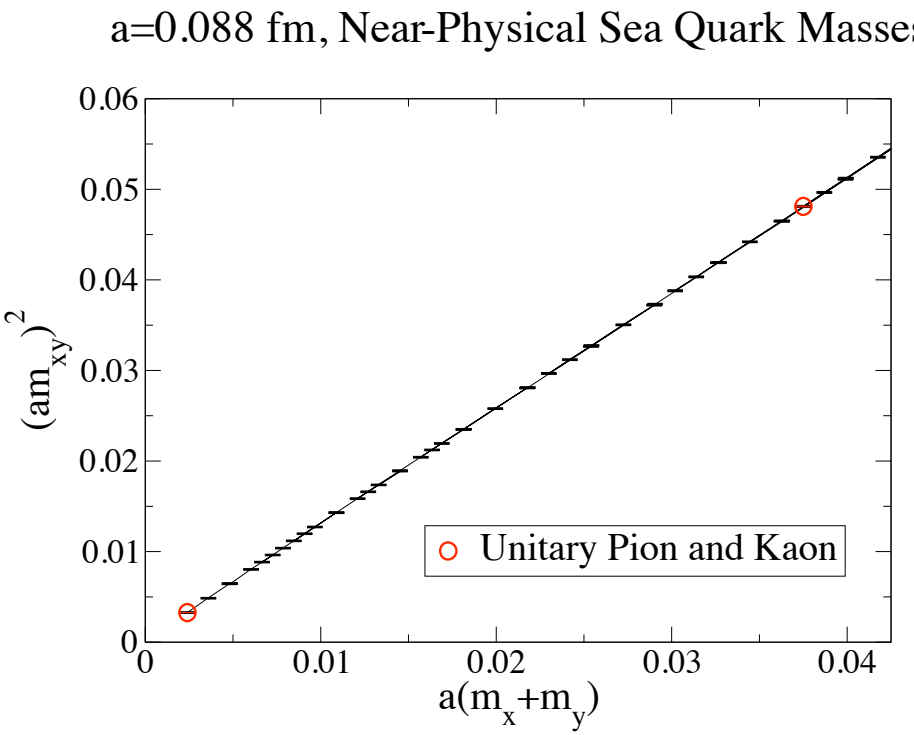

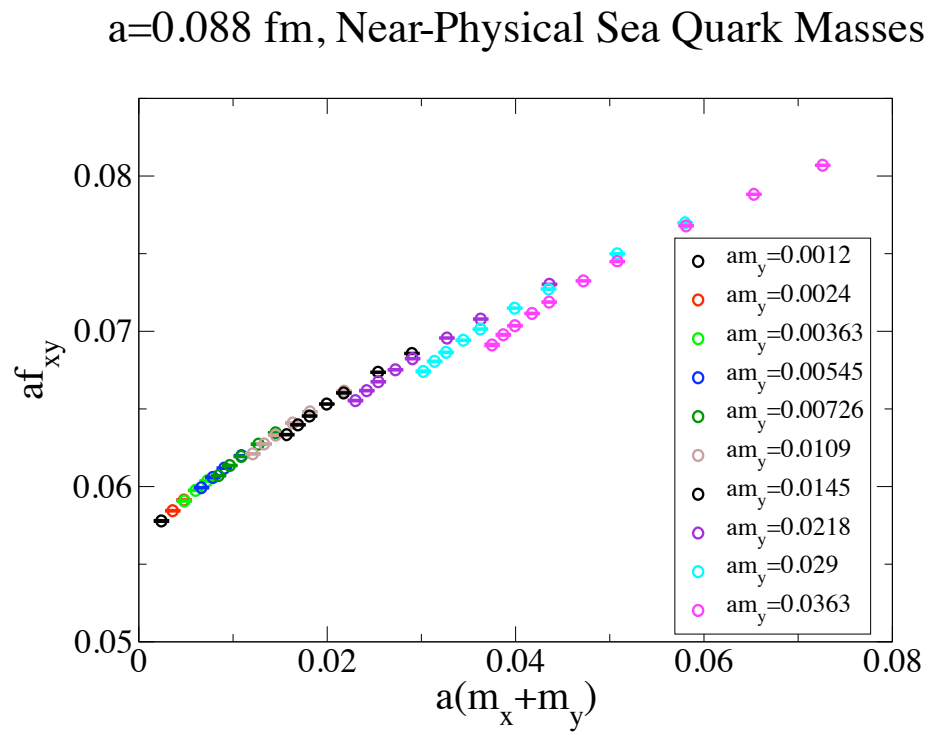

HISQ f_π , f_K

- Suggests following interpolating forms:

$$(am_{xy})^2 = A_1 + B_1(am_x + am_y)$$

$$af_{xy} = \begin{cases} A_2 + B_2(am_x + am_y), & \text{for } m_x \sim m_l \text{ and } m_y \sim m_l \\ A_3 + B_3 am_x + C_3 am_y, & \text{for } m_x \sim m_l \text{ and } m_y \sim m_s \end{cases}$$

- On each ensemble, do linear interpolations of this form between $(m_x, m_y) = (m_l, m_l)$ and its nearest neighbor, and between $(m_x, m_y) = (m_l, m_s)$ and its nearest neighbors.
- Require that $(f_{xx}/m_{xx})^2 = (f_\pi/m_\pi)^2$, solve for m_x to determine physical light mass m_l^{phys}
  - (Checked that quadratic interpolation with 3 points makes little difference)
- Require that $(m_{xy}/m_{xx})^2 = (m_K/m_\pi)^2$, solve for m_y to determine physical strange mass m_s^{phys}
  - (Checked that interpolating $2(m_{xy})^2-(m_{xx})^2$ to find m_s^{phys} with makes little difference)

HISQ f_π , f_K

✦ Then linearly interpolate f and f to physical masses.

- for the moment focus on f_K/f_π ; compute it for each ensemble.
- then fit it as function of a^2.

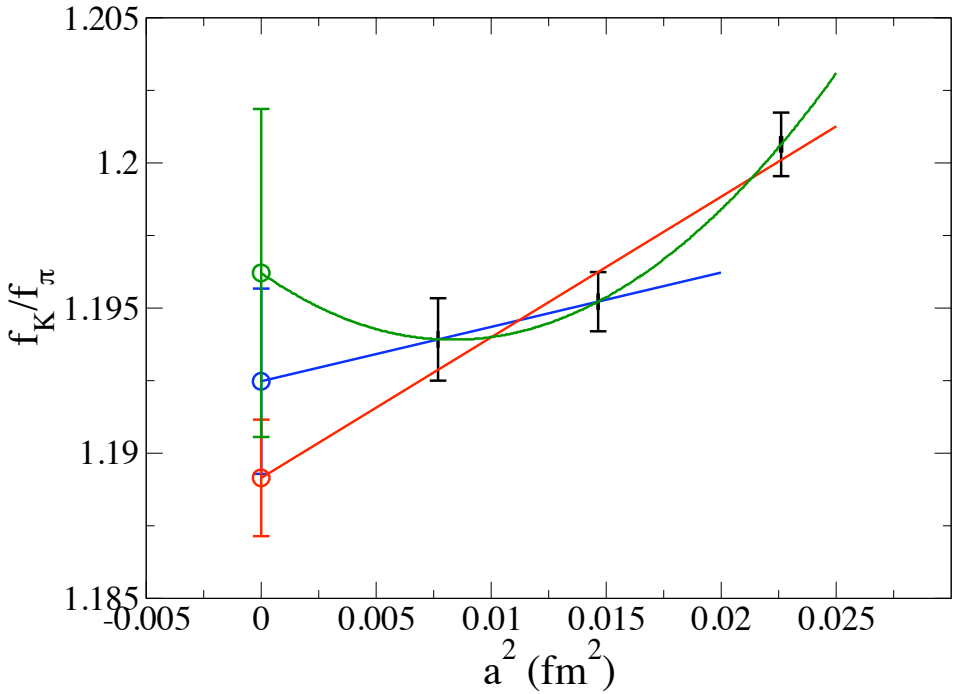

- two finest points in linear fit: $(f_K/f_\pi)_{continuum}$ = 1.1925(32)
- all 3 points in linear fit: $(f_K/f_\pi)_{continuum}$ = 1.1892(20)
- parabola through all 3 points: $(f_K/f_\pi)_{continuum}$ = 1.1962(56)

HISQ f_π , f_K: systematic errors

- Half the largest difference between continuum extraps to estimate that error.
- Finite volume effects from ensembles with L=24, 32, and 40 with a=0.12 fm and m_l = 0.1 m_s.

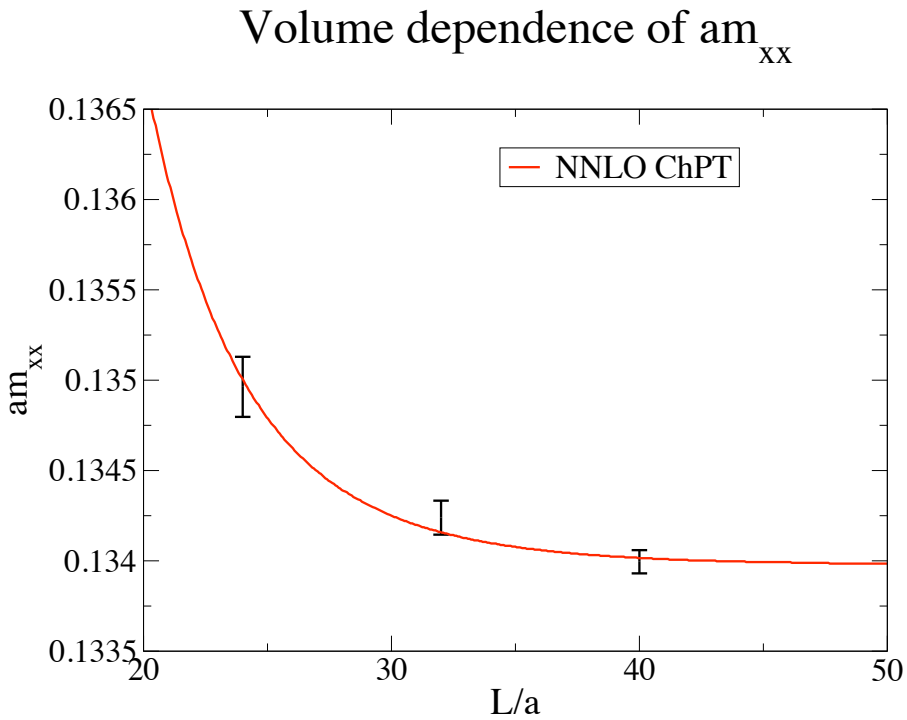

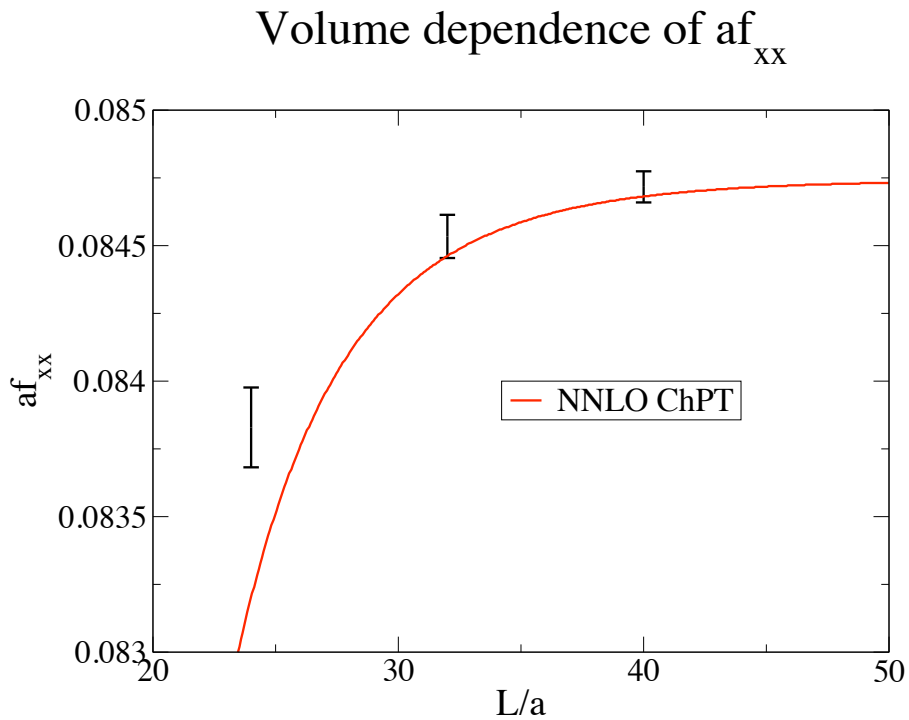

- "NNLO ChPT" means using Colangelo, Dürr, Haefeli, NPB 721 ('05) 136] to terms of $\mathcal{O}([m_\pi^2/16\pi^2 f^2]^2)$.

HISQ f_π , f_K: preliminary result

- Find: $f_K/f_\pi = 1.1925(32)_{stat}(36)_{continuum}(32)_{finite\ volume}$
- Effect still to investigate: tuning error in sea quark masses.
- More study of interpolating fits also needed.
  - A systematic way will be to use the SU(2) staggered ChPT; will also allow us to get information out of the ensembles with u,d mass heavier than physical, and find LECs.
  - Some ensembles with m_s lighter than physical have recently been completed; SU(3) fits should now also be possible.

D decay constants w/ 2+1+1 HISQ

- advantage of HISQ: discretization errors sufficiently reduced (both a^2 and $(ma)^4$) that charm may be treated with same action as light quarks.
  - avoid renormalization errors and many tuning issues.
  - shares to some degree the small statistical errors of staggered light pseudoscalars.

[D. Toussaint, J. Kim]

HISQ Ensembles

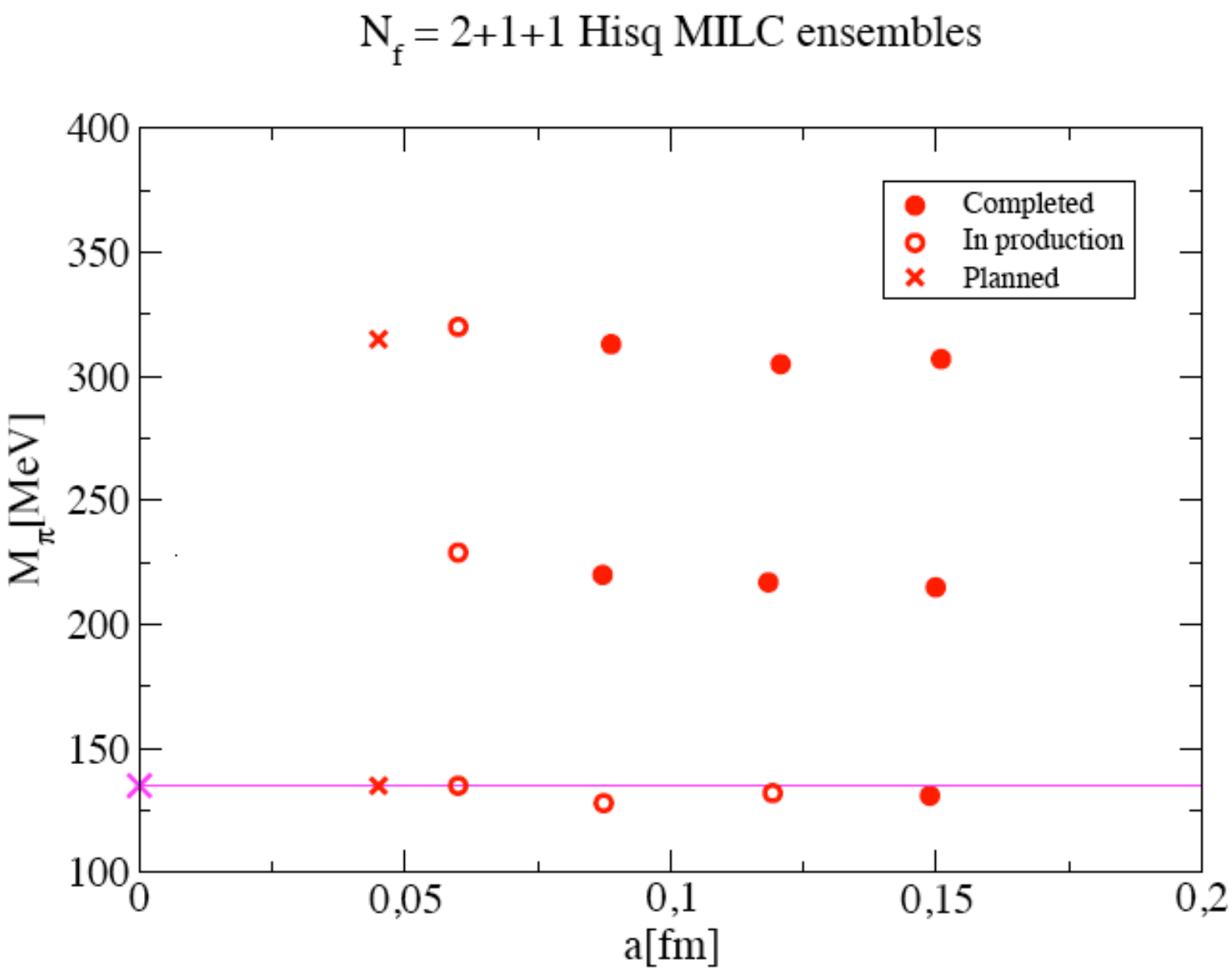

HISQ Ensembles

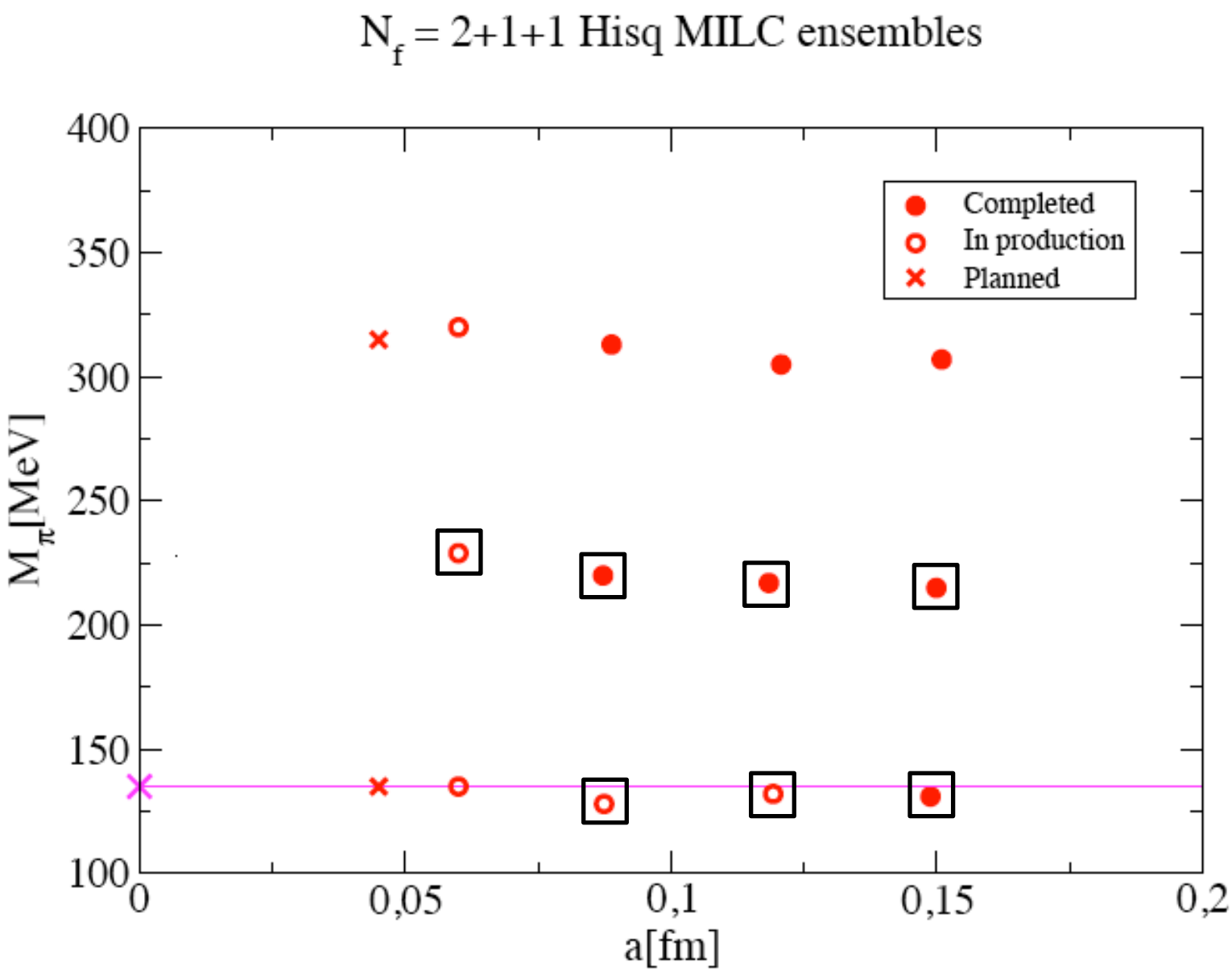

f_D project

HISQ Ensembles

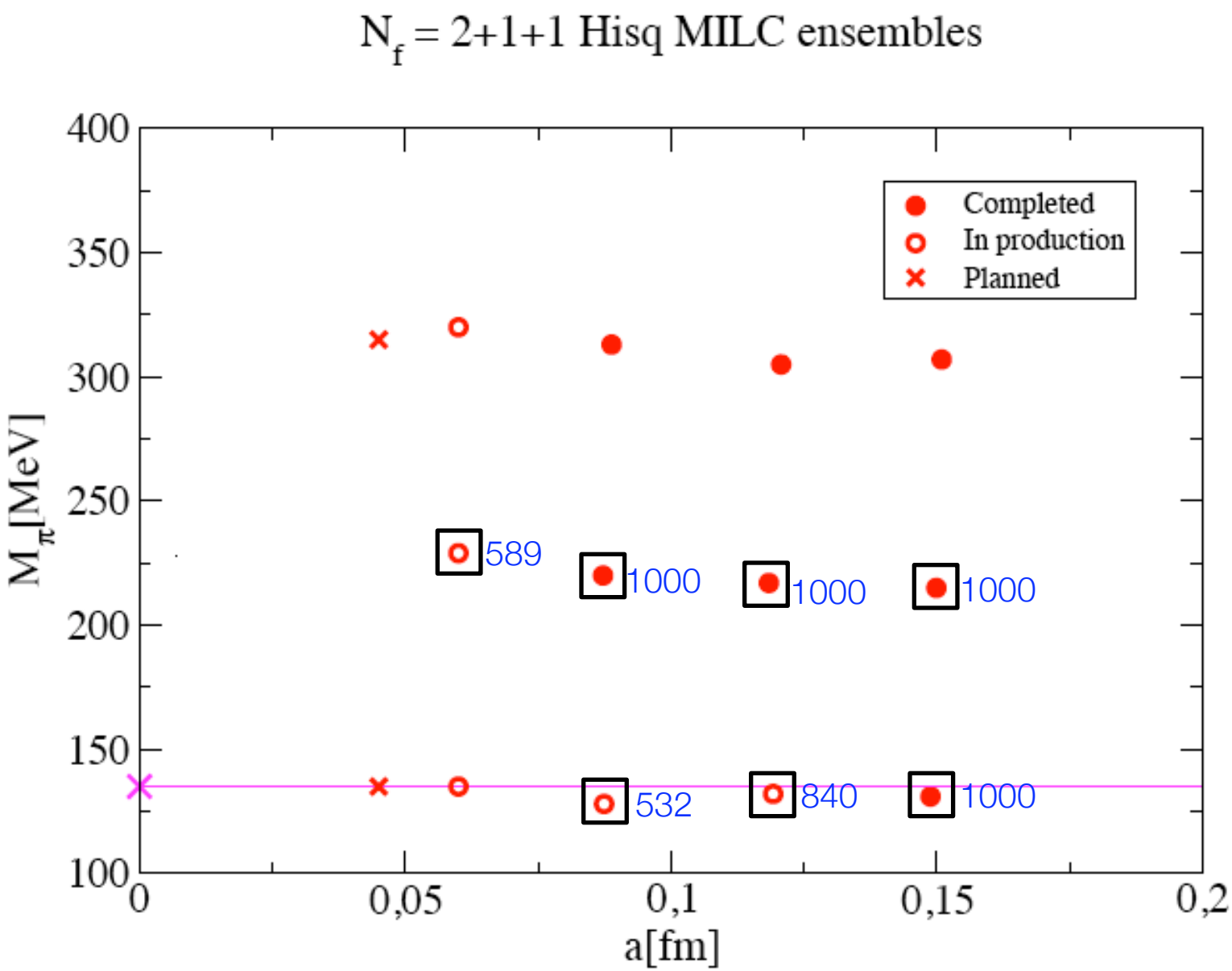

f_D project

configs.

f_D , f_{Ds} procedure

✦ On each ensemble:

- $(M_\pi/f_\pi)^2 \to am_{u,d}^{\rm phys}$, and then $\longrightarrow a$
  (cubic interpolation through 3 light valence masses)

- $2M_K^2 - M_\pi \to am_s^{\rm phys}$
  (linear interpolation/extrapolation through 2 strange valence masses)

- $M_{D_s} \to am_c^{\rm phys}$
  (linear interpolation/extrapolation through 2 charm valence masses)

- $f \to f_D$, $f \to f_{D_s}$ at proper adjusted masses
  (linear interpolation in light, strange and charm masses)

HISQ f_D , f_{Ds}

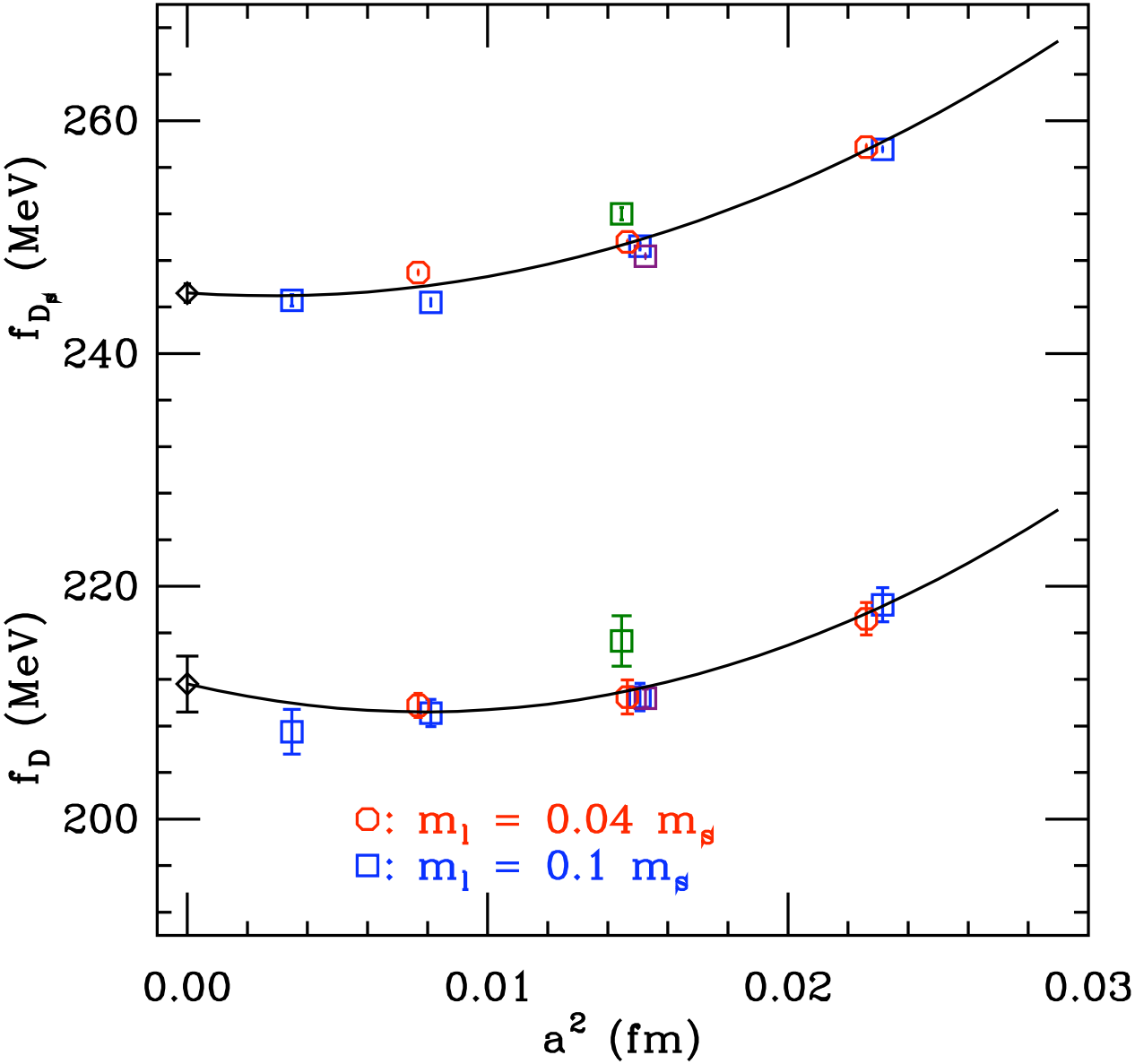
260
240
220
200
f_{D_s} (MeV)
f_D (MeV)
○: m_l = 0.04 m_s
□: m_l = 0.1 m_s
0.00
0.01
0.02
0.03
a^2 (fm)

HISQ f_D , f_{Ds}

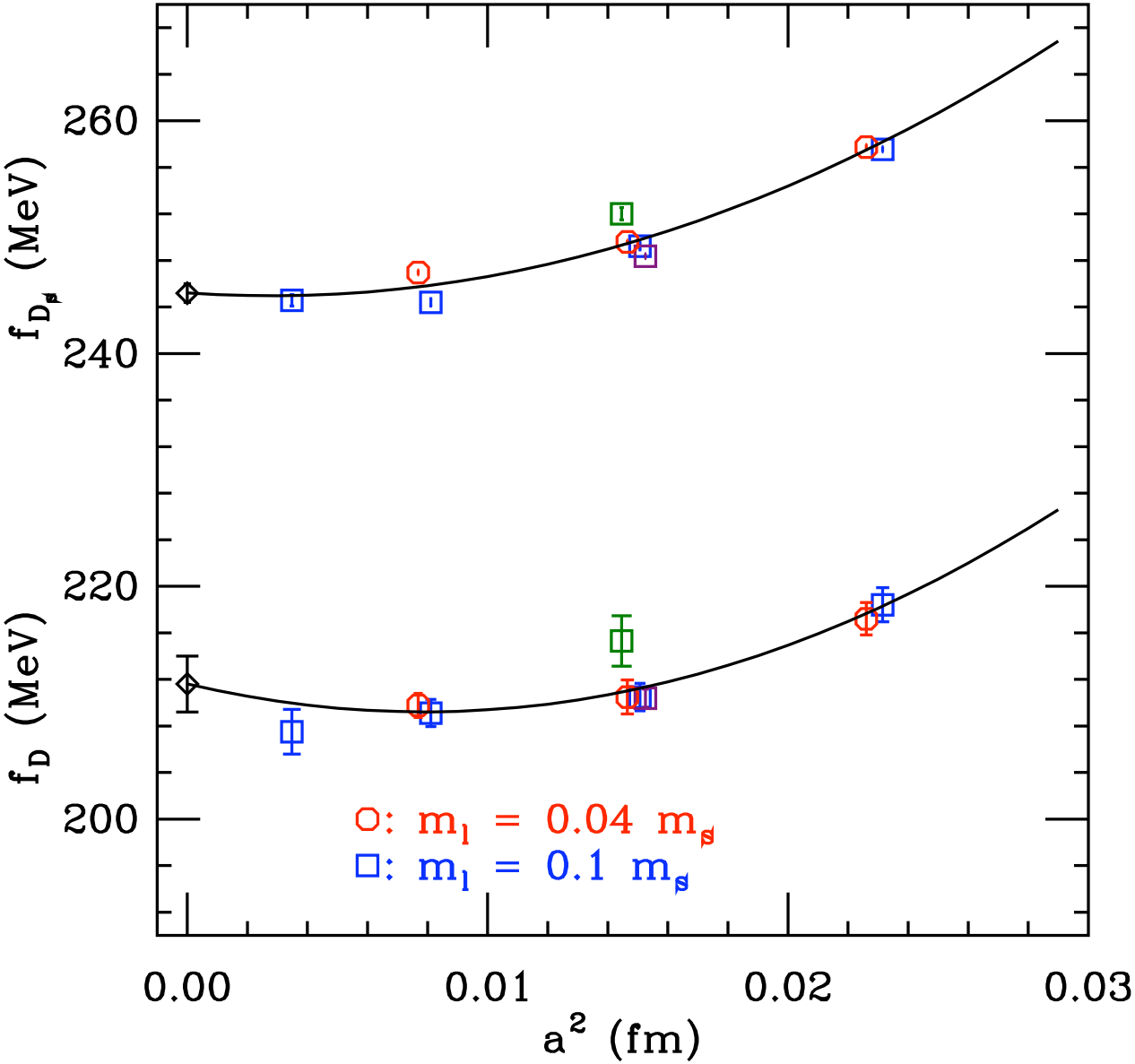

quadratic continuum extrapolation and sea-mass chiral interpolation(!)

HISQ f_D , f_{Ds}

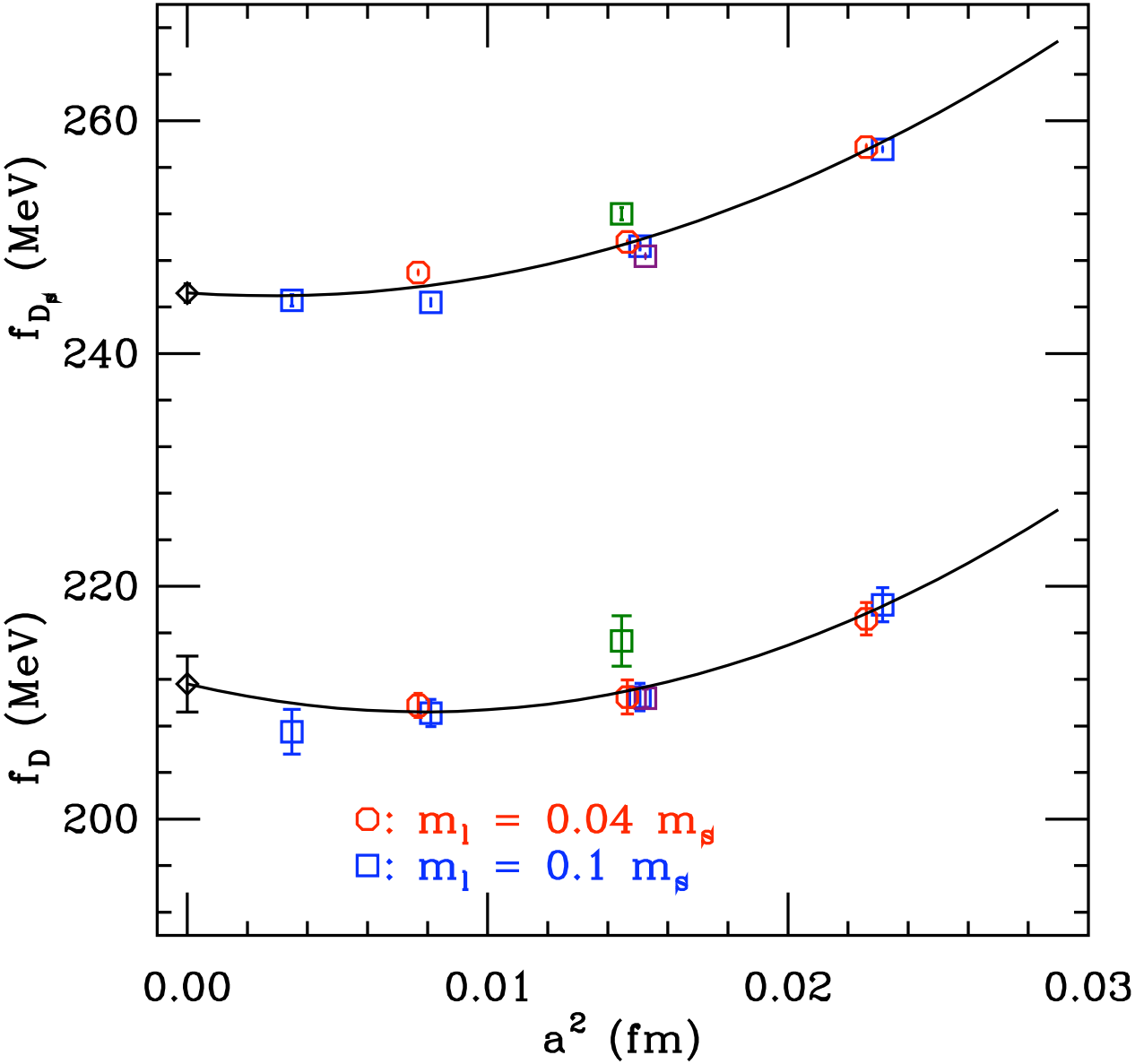

quadratic continuum extrapolation and sea-mass chiral interpolation(!)

finite volume effects:

HISQ f_D , f_{Ds}

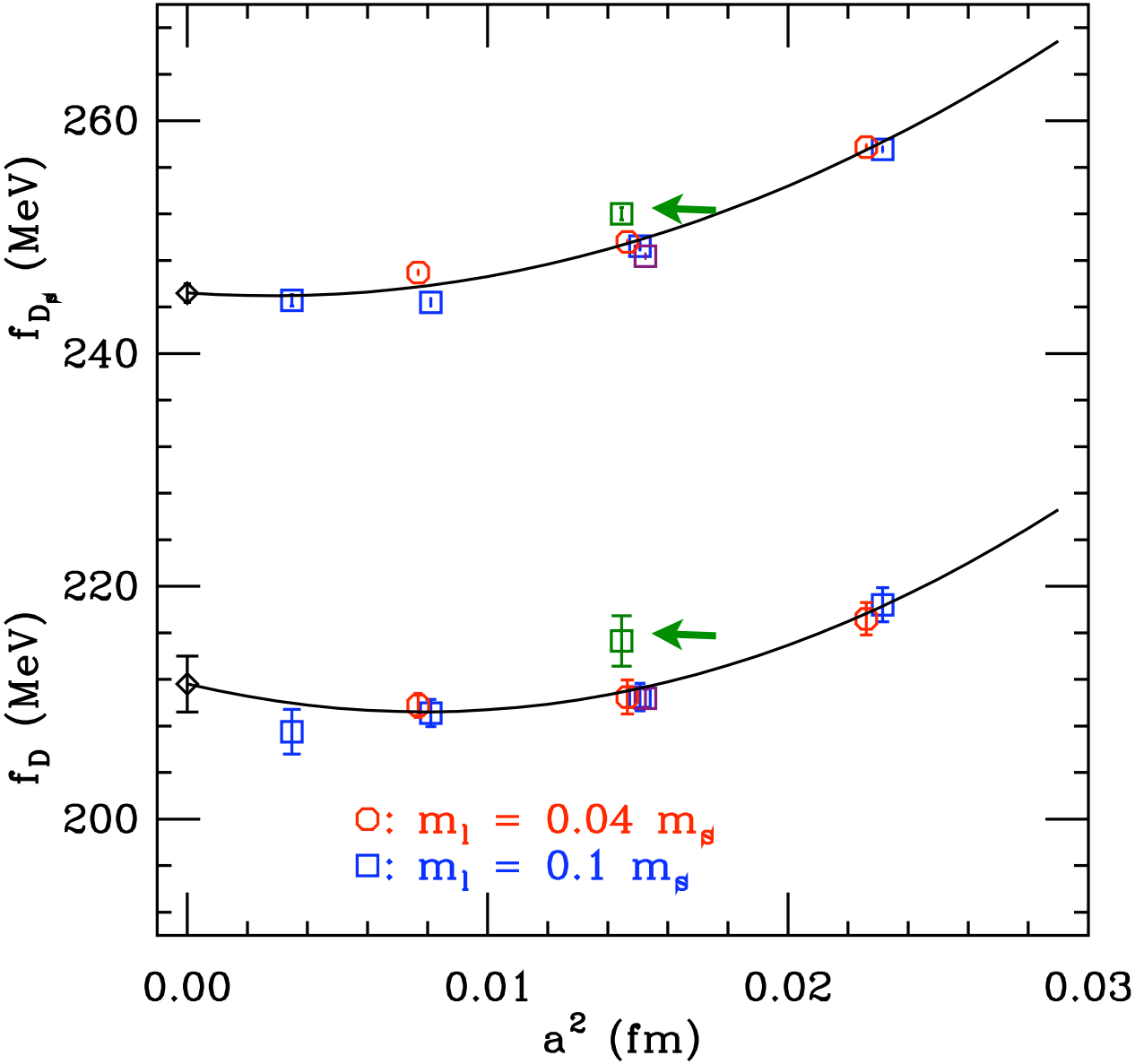

quadratic continuum extrapolation and sea-mass chiral interpolation(!)

finite volume effects:
smaller volume

HISQ f_D , f_{Ds}

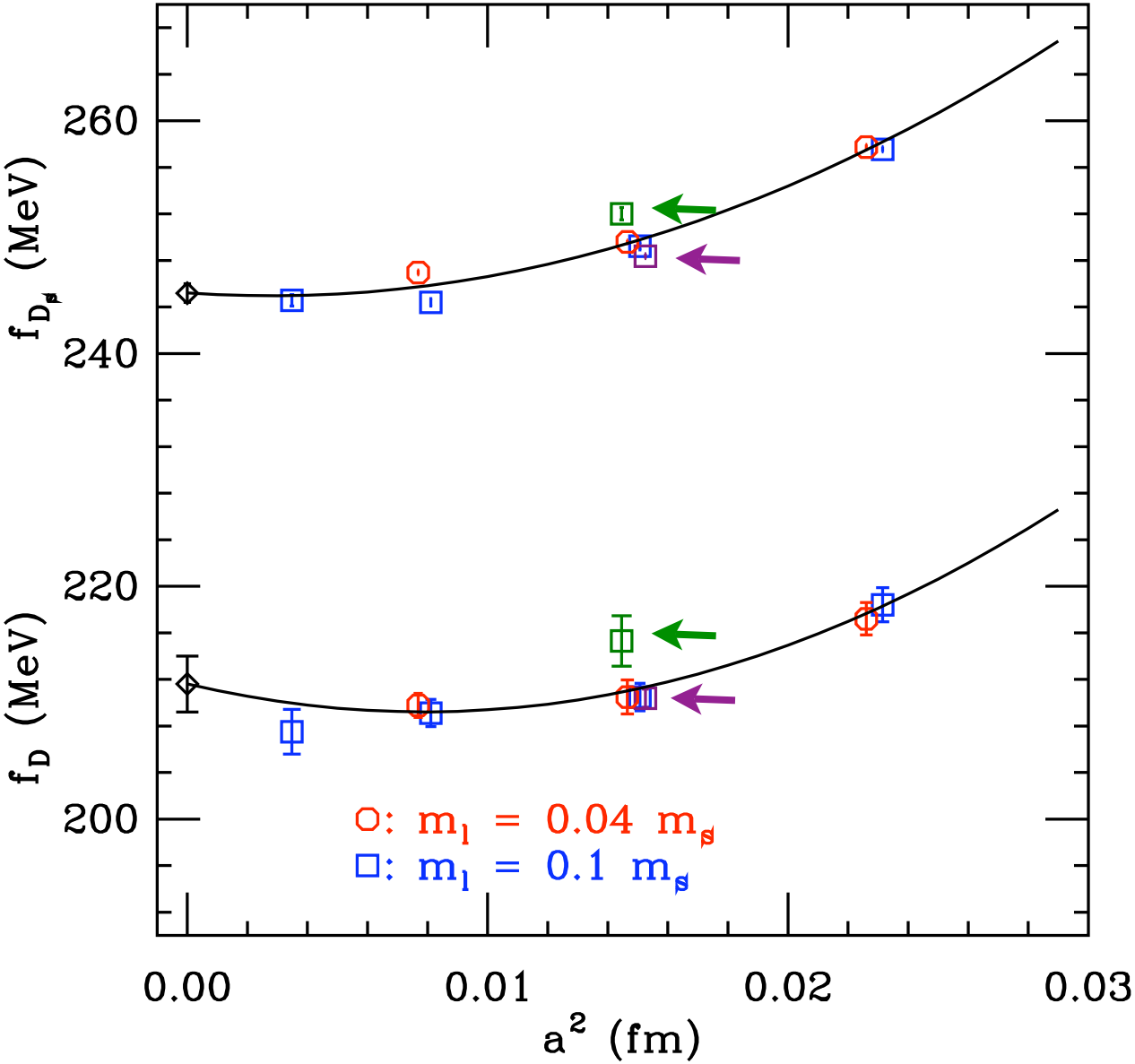

quadratic continuum extrapolation and sea-mass chiral interpolation(!)

finite volume effects:
smaller volume
larger volume

HISQ f_D , f_{Ds}

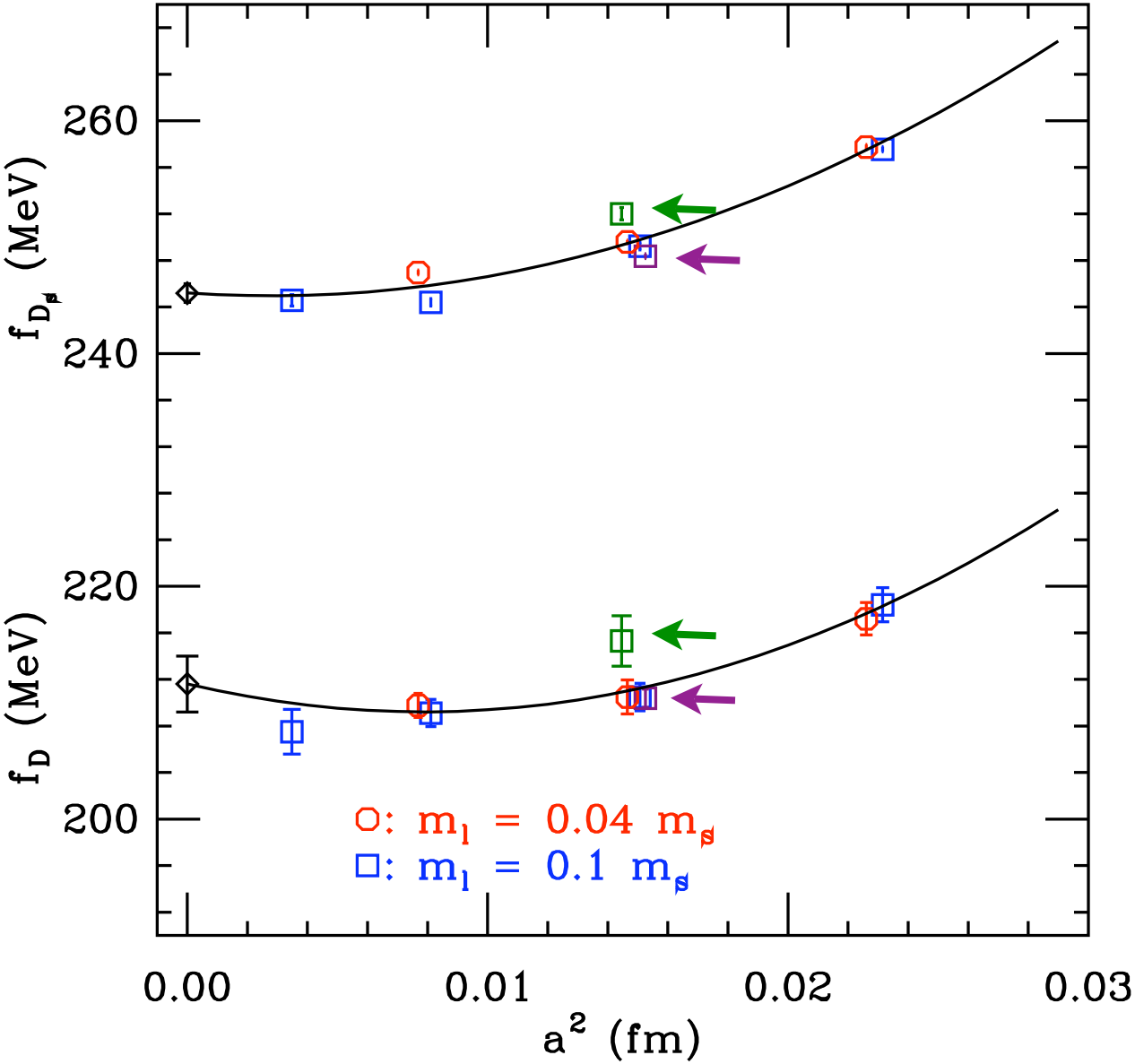

quadratic continuum extrapolation and sea-mass chiral interpolation(!)

finite volume effects:
smaller volume
larger volume

(primarily from f_π scale setting)

Finite size effects

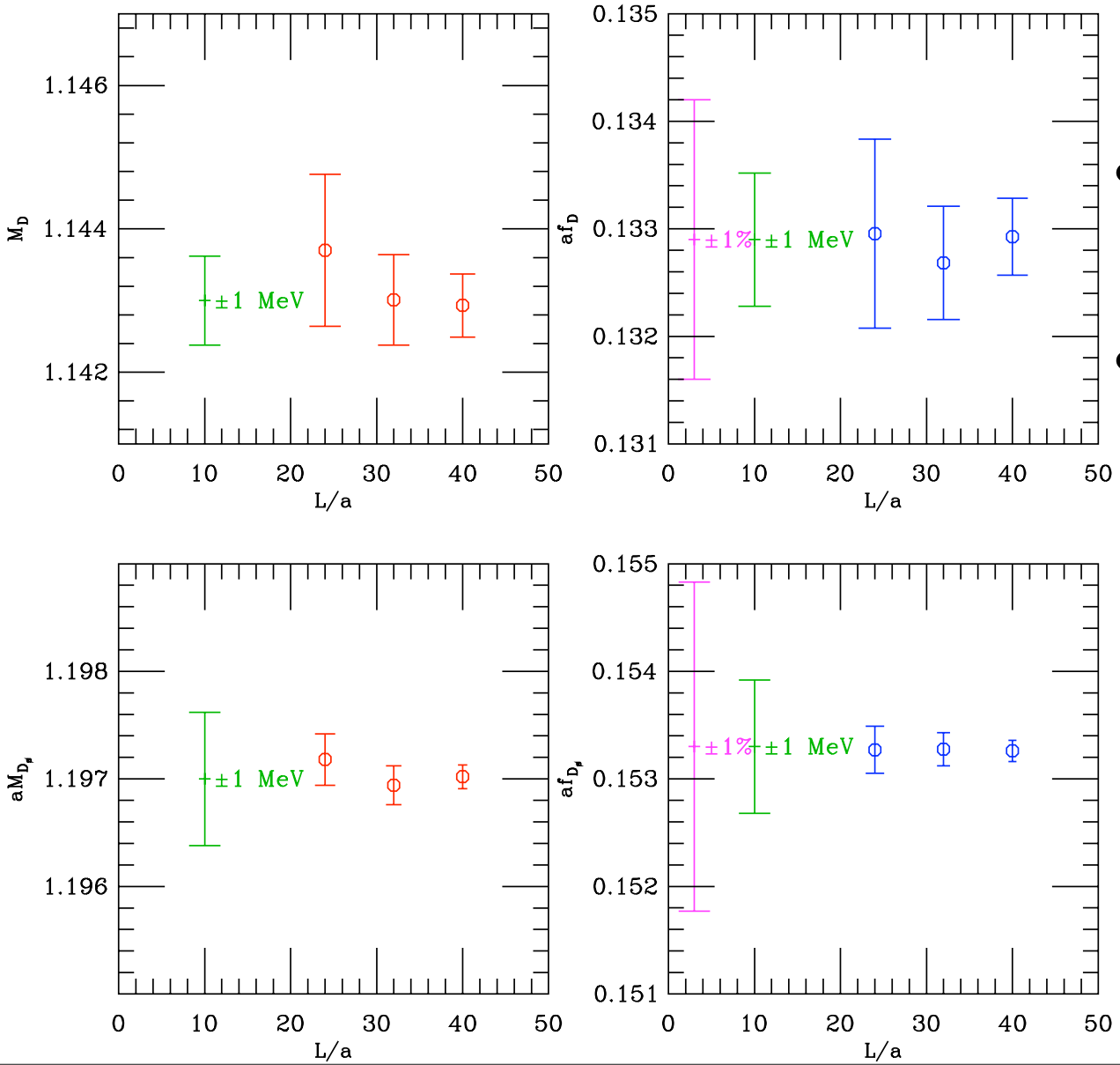

- Not much evidence for finite size effects.
- Here, results are in lattice units.
  - Finite-volume effects can enter if scale is set in finite-volume-dependent way, e.g. f_π.

HISQ f_D , f_{Ds}

✦ Very preliminary results:

$$f_D = 211.6 \pm 2.4 \pm ??? \text{ MeV}$$
$$f_{D_s} = 245.2 \pm 0.8 \pm ??? \text{ MeV}$$

- ??? are systematic errors, including:
  - continuum extrapolation/chiral interpolation
    - staggered ChPT has been worked out [CB and J. Komijani] and may help to control continuum extrapolation.
  - finite volume.
  - isospin: easy to determine valence isospin breaking, *e.g.*, f_{D^+} vs. generic f_D .
  - EM effects: from Gläßle and Bali, arXiv:1111.3958 and Davies, et al., PRD 82 (2010) 114504, expect < 0.5%
    - ultimately plan to check with our EM code....

Outlook: Fermilab/MILC

Quantity	% Errors		
	"Old data" Fermilab (c,b) arXiv:1112.3051	"New data" Fermilab (c,b) (in progress)	HISQ (c) / Fermilab (b) (in progress)
f_{Ds}	4.2	2.2	1.0
f_D	5.2	2.8	1.5
f_{Ds}/f_D	2.1	1.1	0.5
f_{Bs}	3.9	2.6	~1.5?
f_B	4.5	2.8	~2.0?
f_{Bs}/f_B	2.1	1.2	~0.8?

Outlook: Fermilab/MILC

Quantity	% Errors		
	"Old data" Fermilab (c,b) arXiv:1112.3051	"New data" Fermilab (c,b) (in progress)	HISQ (c) / Fermilab (b) (in progress)
f_{D_s}	4.2	2.2	1.0
f_D	5.2	2.8	1.5
f_{D_s}/f_D	2.1	1.1	0.5
f_{B_s}	3.9	2.6	~1.5?
f_B	4.5	2.8	~2.0?
f_{B_s}/f_B	2.1	1.2	~0.8?

HISQ valence & sea

Outlook: Fermilab/MILC

Quantity	% Errors		
	"Old data" Fermilab (c,b) arXiv:1112.3051	"New data" Fermilab (c,b) (in progress)	HISQ (c) / Fermilab (b) (in progress)
f_{D_s}	4.2	2.2	1.0
f_D	5.2	2.8	1.5
f_{D_s}/f_D	2.1	1.1	0.5
f_{B_s}	3.9	2.6	~1.5?
f_B	4.5	2.8	~2.0?
f_{B_s}/f_B	2.1	1.2	~0.8?

HISQ valence & sea

Fermilab B to D ratios + HISQ D (valence & sea)

Comment

✦ Best direction for us for B physics not obvious.

- Use Fermilab or Oktay-Kronfeld (improved Fermilab) b quarks?
- Push/extrapolate HISQ up to the b [HPQCD]?
- Leverage HISQ data for D (or heavier D) by using Fermilab quarks for B/D ratios?
- In any case, will eventually need non-perturbative or 2-loop matching for many quantities to match other systematic improvements.

$K \to \pi$ semileptonic decay

- Focus at $q^2=0$, where we can use the method HPQCD proposed for semileptonic D decay:
  - Full matrix element of vector current V_μ is hard because conserved current is complicated and local current needs renormalization.
  - Instead use $\partial^\mu V_\mu = (m_b - m_a) S$
    - S is local, and product $(m_b - m_a)S$ not renormalized.
  - This is sufficient for $f_+(q^2=0) = f_0(q^2=0)$.
- Two-part program:
  - HISQ valence on 2+1 Asqtad ensembles (close to completion).
  - HISQ valence on 2+1+1 HISQ ensembles (early stage).
    - ultimately to include $D \to K$, and $q^2 \neq 0$

$K \to \pi$ semileptonic decay

- Focus at $q^2=0$, where we can use the method HPQCD proposed for semileptonic D decay:
  - Full matrix element of vector current V_μ is hard because conserved current is complicated and local current needs renormalization.
  - Instead use $\partial^\mu V_\mu = (m_b - m_a) S$
    - S is local, and product $(m_b - m_a)S$ not renormalized.
  - This is sufficient for $f_+(q^2=0) = f_0(q^2=0)$.
- Two-part program:
  - HISQ valence on 2+1 Asqtad ensembles (close to completion). [E. Gámiz]
  - HISQ valence on 2+1+1 HISQ ensembles (early stage).
    - ultimately to include $D \to K$, and $q^2 \neq 0$

Asqtad Ensembles

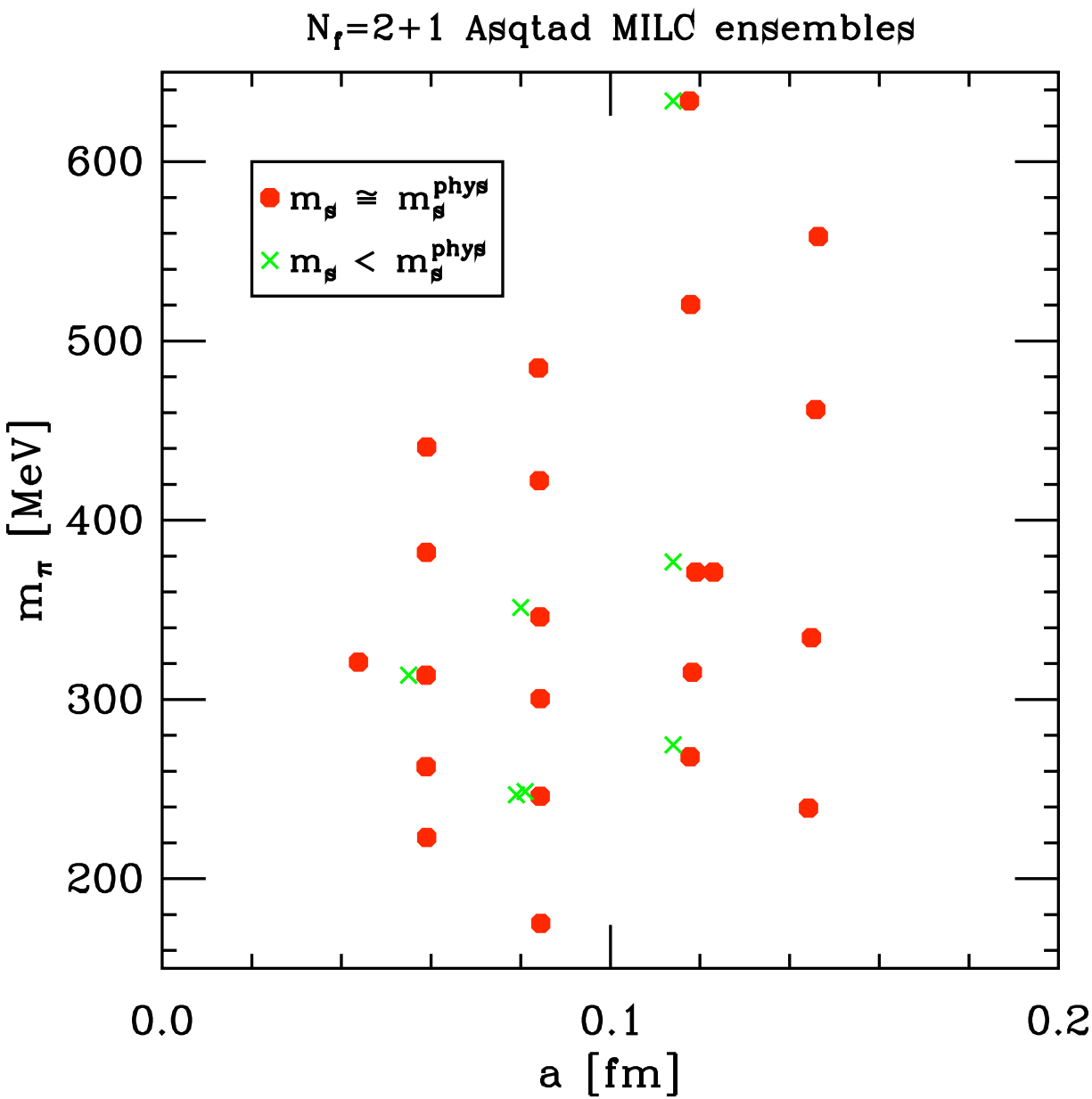

Asqtad Ensembles

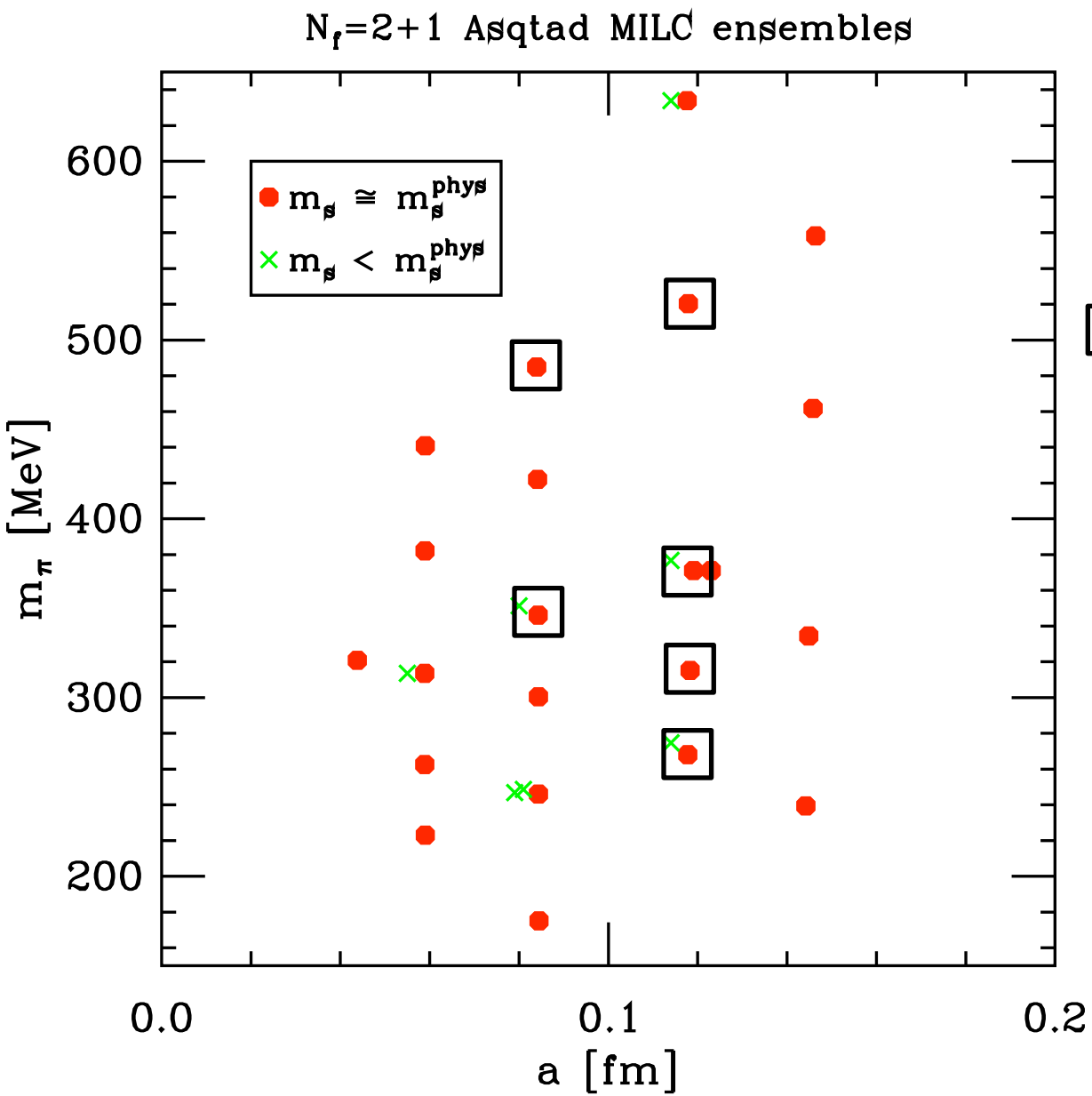

K→π project
(HISQ on Asqtad)

K→π ; HISQ on Asqtad

- Strange HISQ valence mass tuned to its physical value [from Davies, et al, PRD 81 (2010) 034506, using the "η_s"].
- Light HISQ valence mass tuned to Asqtad sea by:

$$\frac{m_l^{\rm val}({\rm Hisq})}{m_s^{\rm phys}({\rm Hisq})} = \frac{m_l^{\rm sea}({\rm Asqtad})}{m_s^{\rm phys}({\rm Asqtad})}$$

- So as close to "unitary" as possible for m_l in this mixed-action theory.

- Mixed-action SChPT at 1-loop has been calculated [E. Gámiz and CB], but still needs checking.

K→π ; HISQ on Asqtad

Sample Chiral Fit

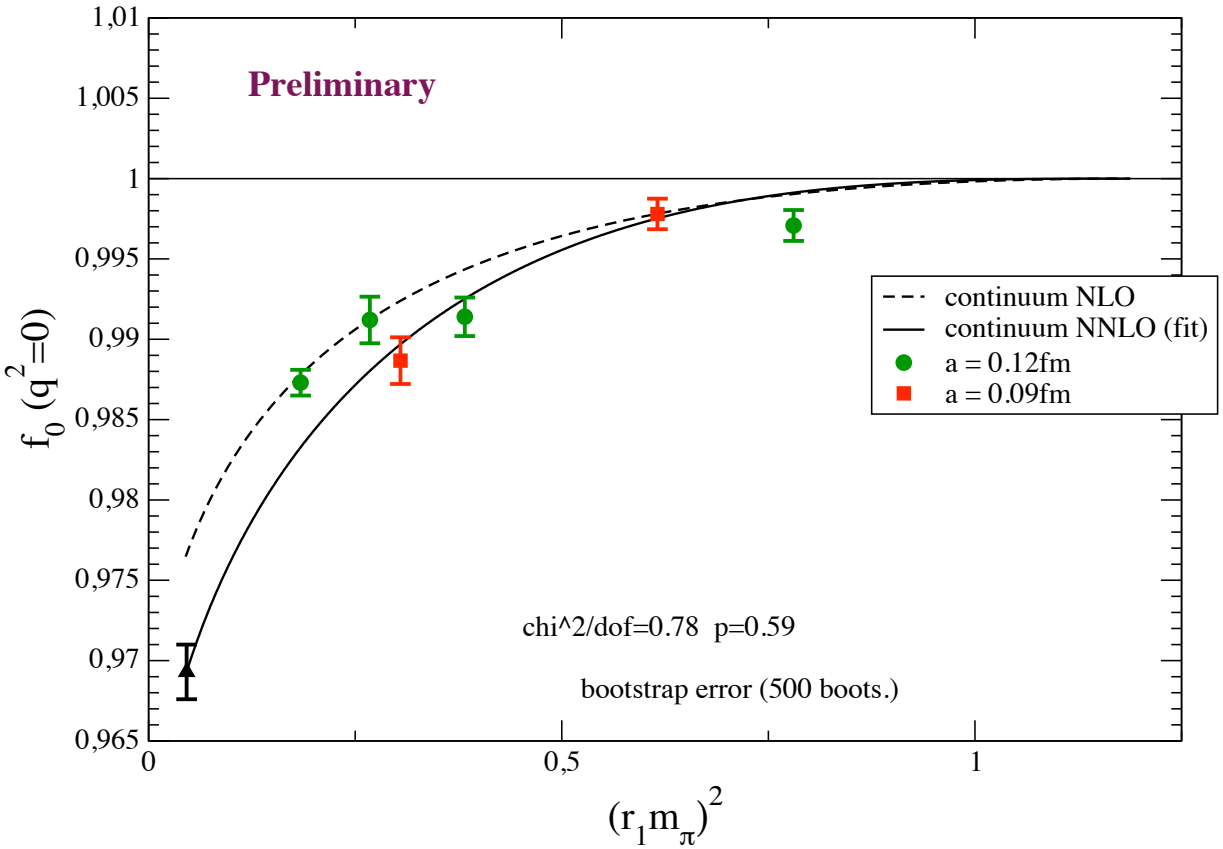

- Statistical errors: ~0.2% -- 0.3%
- Different chiral fits tried so far agree within 1 stat. σ. E.g.:
  - 1-loop SChPT + 2-loop continuum ChPT.
  - 1-loop SChPT + higher order analytic.

- Need to understand the size of a^2 effects better; check SChPT.

$K \to \pi$; HISQ on Asqtad

- Expected error budget:
  - Statistical: 0.2--0.3%
  - Chiral extrapolation, fitting function: 0.1%
  - Discretization: 0.15%
  - Mistuning of m_s in the sea: 0.2%
- Total: 0.35%--0.5%, should be competitive with state of the art: RBC/UKQCD.

K→ π semileptonic decay

- Focus at $q^2=0$, where we can use the method HPQCD proposed for semileptonic D decay:
  - Full matrix element of vector current V_μ is hard because conserved current is complicated and local current needs renormalization.
  - Instead use $\partial^\mu V_\mu = (m_b - m_a) S$
    - S is local, and product $(m_b-m_a)S$ not renormalized.
  - This is sufficient for $f_+(q^2=0) = f_0(q^2=0)$.
- Two-part program:
  - HISQ valence on 2+1 Asqtad ensembles (close to completion).
  - HISQ valence on 2+1+1 HISQ ensembles (early stage).
    - ultimately to include D → K, and $q^2 \neq 0$

[E. Gámiz]

HISQ Ensembles

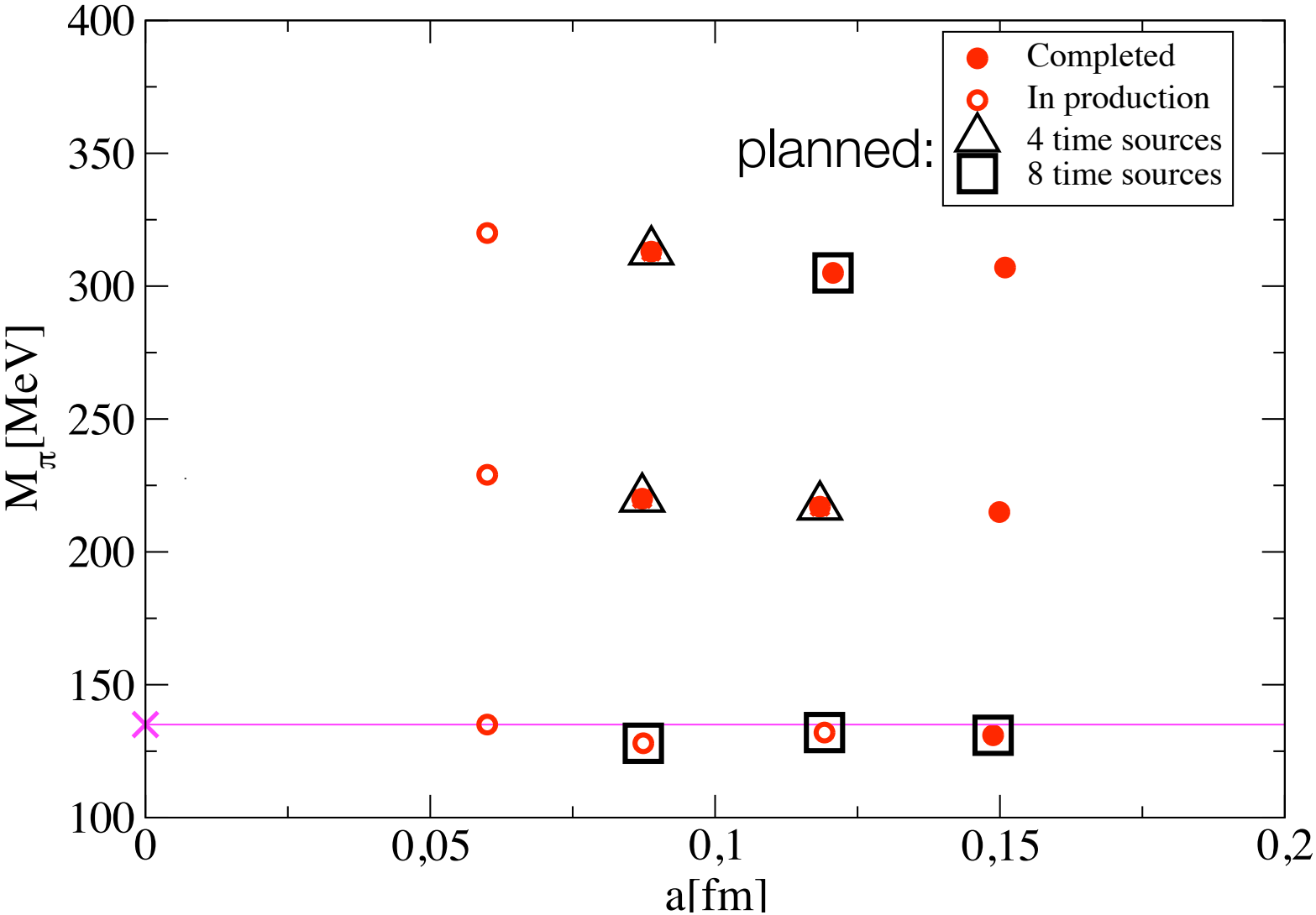

HISQ Ensembles

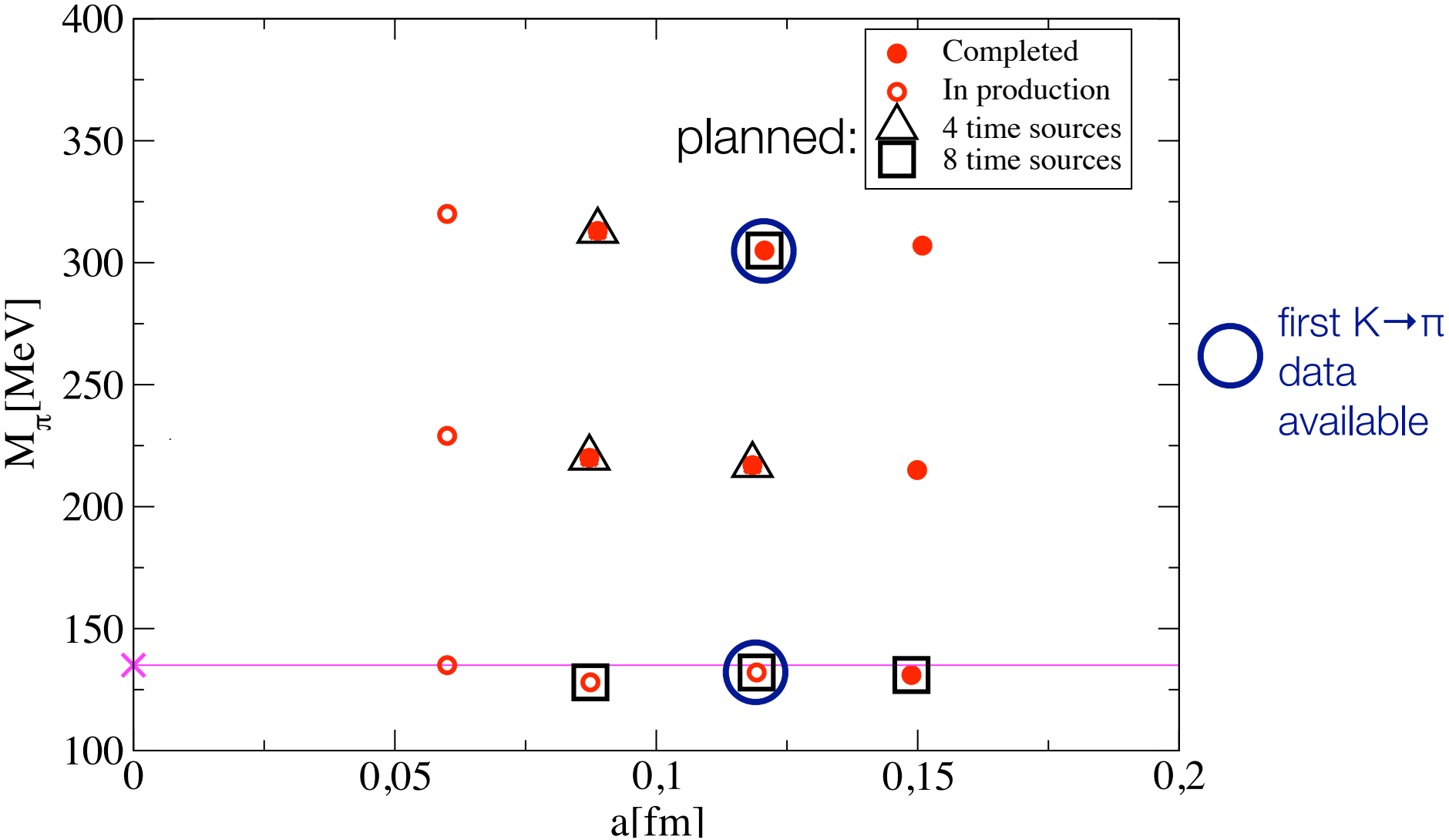

K→π : including HISQ on HISQ

Sample Chiral Fit

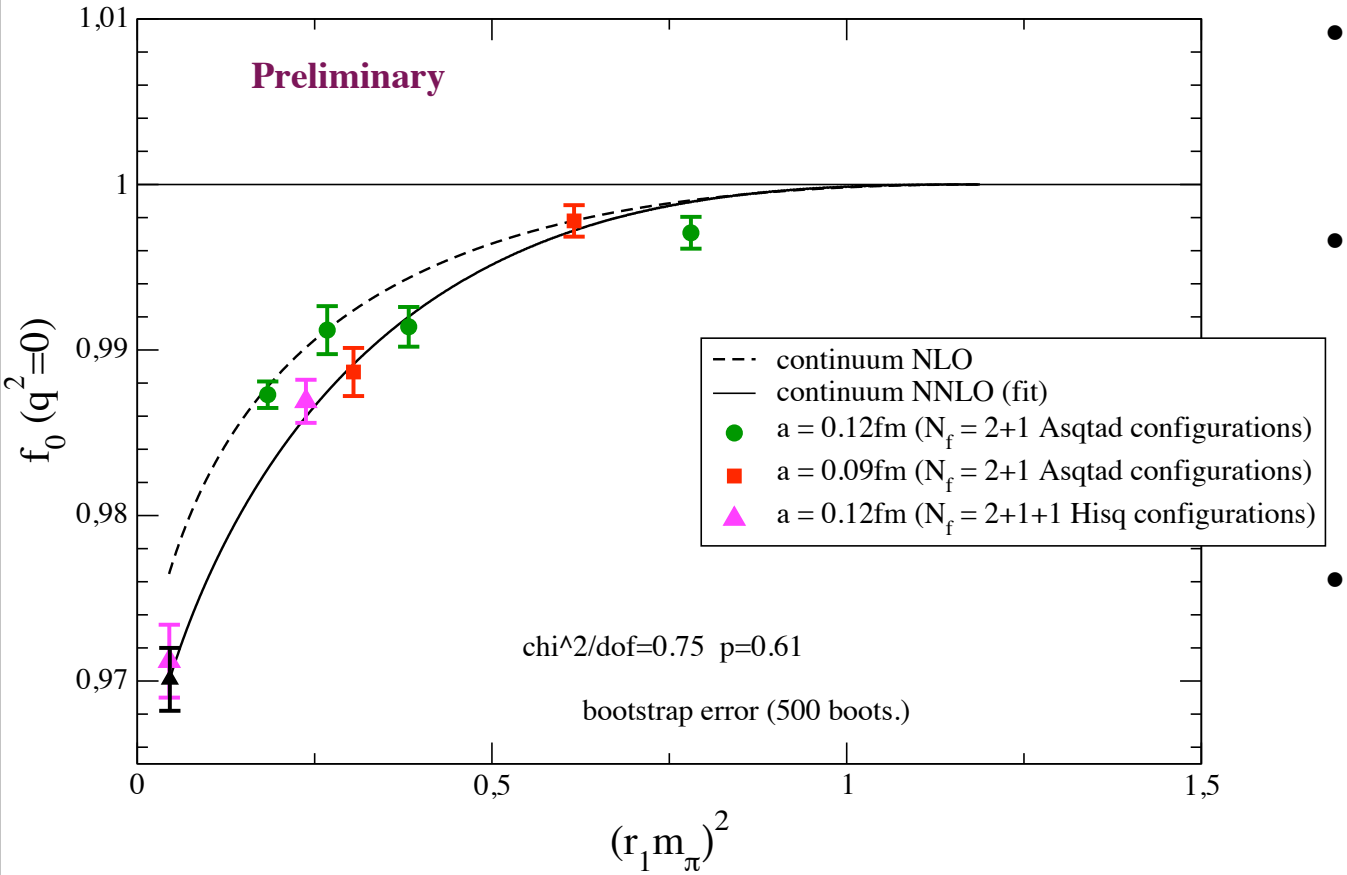

- Consistency with extrapolated HISQ on Asqtad results.
- Stat. errors larger on physical mass ensemble; momentum needed for q=0 is larger.
- Ensembles with heavier-than-physical u,d mass important for reducing final error.

- D→K being done in parallel, but fits not analyzed yet...

Some projects I didn't talk about:

Heavy-Quark Semileptonic Decays [Fermilab/MILC]

- ✦ $B \to D^* \ell \nu$ [arXiv:0808.2519, arXiv:1011.2166] (J. Laiho)
- ✦ $B \to D \ell \nu$ [arXiv:1111.0677] (S. Qiu)
- ✦ $B \to K \ell \ell$; $B \to K^* \gamma$ [arXiv:1111.0677] [R. Zhou; see his talk]
- ✦ $B \to \pi \ell \nu$ [arXiv:0811.3640] (R. Van de Water)
- ✦ $B_s \to \mu^+ \mu^-$ [using f for $(B_s \to D_s)/(B \to D)$; arXiv:1202.6346] (D. Du)
- ✦ $D \to \pi\ l\ \nu$, $D \to K\ l\ \nu$ [arXiv:0811.3640] (J. Bailey)

Quarkonia [Fermilab/MILC]

- ✦ [arXiv, 0912.2701, arXiv:1012.1837] (L. Levkova, C. DeTar, A. El-Khadra, E. Freeland,S. Gottlieb, A. Kronfeld,...)

Some projects I didn't talk about:

Electromagnetic Effects [MILC]

- ✦ Pseudoscalar mesons [arXiv:0812.4486, arXiv: 1011.3994, PoS(Lat10) 127] (S. Basak, A. Torok, S. Gottlieb, L. Levkova, E. Freeland, CB)
- ✦ Baryons (S. Gottlieb & students)

Strangeness content of the nucleon, *etc.* [MILC]

- ✦ Nucleon strangeness [arXiv:0905.2432, arXiv:1011.5271] (D. Toussaint, W. Freeman)
- ✦ Nucleon charm [arXiv:1204.3866] (D. Toussaint, W. Freeman)
- ✦ $\sigma_{\pi N}$ (D. Toussaint, W. Freeman)

Fermilab Lattice/MILC Collaboration

J. Bailey	Seule U.
A. Bazavov	U. of Arizona
C. Bernard	Washington U.
C. Bouchard	Ohio State
C. DeTar	U. of Utah
A.X. El-Khadra	U. of Illinois
R.T. Evans	U. of Illinois, North Carolina State U.
E.D. Freeland	U. of Illinois, Benedictine U.
W. Freeman	George Washington U.
E. Gamiz	Fermilab, U. de Granada
S. Gottlieb	Indiana U.
J. Komijani	Washington U.
U.M. Heller	APS
J.E. Hetrick	U. of the Pacific
J. Kim	U. of Arizona
A.S. Kronfeld	Fermilab
J. Laiho	U. of Glasgow
L. Levkova	U. of Utah
M. Lightman	Washington U.
P.B. Mackenzie	Fermilab
E. Neil	Fermilab
M.B. Oktay	U. of Utah
J. Simone	Fermilab
R. Sugar	U.C. Santa Barbara
D. Toussaint	U. of Arizona
R.S. Van de Water	BNL

Chiral Fermions via Energy Level Splitting

Artan Boriçi

University of Tirana

borici@fshn.edu.al

Outline of the talk

- Overlap/Domain Wall and Minimally Doubled fermions
- Crank-Nicolson discretisation scheme
- Applications: I. Crank-Nicolson-Wilson operator
- Applications: II. Crank-Nicolson chiral operator

Chiral Fermions and the Lattice

- Lorentz invariance broken to hypercubic symmetry:
  - there is no such a thing like spin on the lattice;
    - at least in the sense of SU(2) representations;
    - Dirac field does not fit the lattice.
- $\Rightarrow$ Requiring emerging spin on the lattice brings undesirable results;
- **Theorem** (Nielsen-Ninomiya). *There are no local chiral fermions on the lattice.*
- Broken Lorentz invariance + emerging spin makes a "choose-only-one-item" menu:
  - Many chirality pairs of flavours (naive, minimally doubled,...);
  - One flavour of explicitely broken chirality (Wilson,...).

Overlap/Domain Wall Fermions

Adding a new item in the menu:

On shell chirality but an extra dimension.

- Satisfy Ginsparg-Wilson relation: on shell chiral symmetry;
- Expensive to compute: involves nested Krylov subspaces;
- Large density of near zero modes of the kernel;
- Topology stalling simulation algorithms; Solution:
  - Fixed topology overlap: unitarity violations
  - Fat links: lattice spacing of smoothed configuration?

Minimally Doubled Fermions

- Reduce the number of doubler to two: 25 years old idea revived 5 years ago with new actions;
- That is nice but in expense of hypercubic symmetry:
  - Symmetry restoration requires fine tuning i.e. non-perturbative renormalization;
  - Simulation of one flavour needs rooting.

Lesson: lose symmetry in favour of less doublers.

Question: How far can one push it?

One can isolate a single flavour compensated by ghost particles, i.e. no Dirac/Weyl content:

Weyl and ghost fermions on the lattice, A.B. ArXiv:1010.5156

Nielsen-Ninomiya theorem can be genralized, but the result is essentially the same: the ghosts remain in the continuum limit.

Wilson strategy: distribute doublers in the real axis, revived recently by Creutz and collaborators.

Crank-Nicolson discretization

- Example: Schrödinger equation in Euclidean space:

$$\partial_t \psi(t,x) = H\psi(t,x) \ , \qquad \psi(0,x) = \psi_o(x) \ .$$

- Solution $\psi(t,x) = e^{tH}\psi(0,x)$.
- Numerical problem: exp approximation.
  - Problem: non-local grid in t;
  - Requirement: stay with nearest neighbours, i.e. Euler scheme: $\Rightarrow$ order $O(a)$ errors.
- Crank-Nicholson scheme:

$$\partial\psi(t,x) \to \frac{1}{a}\left[\psi(t+a,x) - \psi(t,x)\right] \ , \quad H\psi(t,x) \to \frac{H}{2}\left[\psi(t,x) + \psi(t+a,x)\right] \ .$$

$$\Rightarrow \ \psi(t+a,x) = \frac{\mathbb{1}+\frac{a}{2}H}{\mathbb{1}-\frac{a}{2}H}\psi(t,x) = \left(\mathbb{1} + aH + \frac{a^2}{2}H^2 + O(a^3)\right)\psi(t,x) \ ;$$

$\Rightarrow$ order $O(a^2)$ errors in expense of solving linear systems.

Crank-Nicolson and Dirac operator

- Momentum space spin-1/2 Hamiltonian on the lattice: $H = \vec{\sigma} \sin \vec{p}$;
- $\Rightarrow$ Crank-Nicolson time discretised operator:

$$D(p) = e^{ip_4} - 1 + \frac{1}{2}\vec{\sigma} \sin \vec{p} \, (e^{ip_4} + 1) \ .$$

- Particle content:

$$D(p) = 0 \ \Leftrightarrow \ 4 \sin^2 \frac{p_4}{2} + \sin^2 \vec{p} \ \cos^2 \frac{p_4}{2} = 0 \ .$$

- $\Rightarrow$ 8 particles located at the edges of the 3d Brillouin zone.
- Result:

The number of doublers is reduced by a factor of two!

Crank-Nicolson-Wilson operator

- Reduce the number of doublers using the Wilson approach:

$$D_{CNW}(p) = \gamma_4(e^{ip_4} - 1) + \frac{1}{2}\left[i\vec{\gamma}\sin\vec{p} + \sum_k (1 - \cos p_k)\right](e^{ip_4} + 1) \ .$$

- $D_{CNW}(p) = 0 \ \Leftrightarrow$

$$4\sin^2\frac{p_4}{2} + \left\{\sin^2\vec{p} + \left[\sum_k (1 - \cos p_k)\right]^2\right\}\cos^2\frac{p_4}{2} = 0 \ .$$

- Result:
  - Second order accurate in time;
  - Smaller additive mass renormalisation;
  - Hypercubic symmetry broken to cubic symmetry.

Degenerate doublet of Crank-Nicolson-Wilson fermions

Restore hybercubic symmetry defining a doublet of Crank-Nicolson-Wilson fermions:

$$\mathcal{D}_{CNW} = \begin{pmatrix} D^{(+)}_{CNW}(m) & 0 \\ 0 & D^{(-)}_{CNW}(m) \end{pmatrix}$$

where:

$$D^{(+)}_{CNW}(m) = m\mathbb{1} + \gamma_4(e^{ip_4} - 1) + \frac{1}{2}\left[i\vec{\gamma}\sin\vec{p} + \sum_k (1 - \cos p_k)\right](e^{ip_4} + 1)$$

$$D^{(-)}_{CNW}(m) = m\mathbb{1} + \gamma_4(1 - e^{-ip_4}) + \frac{1}{2}\left[i\vec{\gamma}\sin\vec{p} + \sum_k (1 - \cos p_k)\right](e^{-ip_4} + 1)$$

- Hypercubic symmetry restored under flavour exchanging operation;
- Result: $O(a_t^2)$ errors theory without fine tuning + 3-space Wilson.

A chiral theory with doublers

- Start with a general theory of many chirality pairs flavours:

$$E_n(\vec{p}) = \alpha_n \vec{\sigma}\vec{p} \ , \quad n = 1, 2, \ldots, m \ ,$$

- For example naive fermions have this continuum limit with $\alpha_n = \pm 1$;
- We are seeking a theory with a singlet chirality ground state:
  - the opposite chirality counterpart should occupy a different level;
  - the theory has a energy gap $\Delta(\vec{p}) = E_1(\vec{p}) - E_0(\vec{p})$.
- Energy gap increases with momenta:
  - A non-uniform gap;
  - Maximal gap at cuttoff.
- $\Rightarrow$ A chiral theory of free fermions with doublers.

Lattice implementation

- Start from Crank-Nicolson discretisation in time and naive discretisation in 3-space:

$$D(p)' = e^{ip_4} - 1 + \frac{1}{2}\vec{\sigma}\sin\vec{p}\,(e^{ip_4} + 1)\ ;$$

- Add a pure imaginary operator of the Wilson type:

$$D(p) = e^{ip_4} - 1 + \frac{1}{2}\left[\vec{\sigma}\sin\vec{p} + ir\sum_k(1-\cos p_k)\right](e^{ip_4} + 1)\ .$$

- $D(p) = 0 \ \Leftrightarrow$

$$\left\{2\sin\frac{p_4}{2} + \left[r\sum_k(1-\cos p_k)\right]\cos\frac{p_4}{2}\right\}^2 + \sin^2\vec{p}\,\cos^2\frac{p_4}{2} = 0\ .$$

Particle spectra

- 8 zeros in the edges of 3d Brillouin zone:

  $\vec{p}^{\,*} \in \{(0,0,0),(0,0,\pi),(0,\pi,0),(\pi,0,0),(0,\pi,\pi),(\pi,0,\pi),(\pi,\pi,0),(\pi,\pi,\pi)\}$

- Define $n(\vec{p}^{\,*}) = \frac{1}{2}\sum_k (1-\cos p_k^*)$

- $\Rightarrow\ D(p) = 0 \ \Leftrightarrow \tan\frac{p_4^*}{2} = -rn(\vec{p}^{\,*})$.

- Define chirality $\chi(\vec{p}^{\,*}) = \cos p_1^* \cos p_2^* \cos p_3^* \quad \Rightarrow$

$\vec{p}^{\,*}$	$n(\vec{p}^{\,*})$	$\chi(\vec{p}^{\,*})$	Degeneracy
$(0,0,0)$	0	1	1
$(0,0,\pi),(0,\pi,0),(\pi,0,0)$	1	-1	3
$(0,\pi,\pi),(\pi,0,\pi),(\pi,\pi,0)$	2	1	3
(π,π,π)	3	-1	1

- Continuum limit dispersion relation: $E_n(\vec{p}) \to \frac{\vec{\sigma}\vec{p}}{1+r^2n^2}\ , \quad n = 0,1,2,3.$

Broken hypercubic symmetry

- Restore hypercubic symmetry defining a quartet of such fermions:

$$\mathcal{D} = \begin{pmatrix} 0 & 0 & 0 & D_r^{(+)} \\ 0 & 0 & D_{-r}^{(+)} & 0 \\ 0 & D_r^{(-)} & 0 & 0 \\ D_{-r}^{(-)} & 0 & 0 & 0 \end{pmatrix}$$

- $\Rightarrow$ symmetry is restored under $(+)$ and $(-)$ flavour exchange as well as under r and $-r$ flovour exchange.
- Result: a free theory of four flavours with definity chirality.
- Interacting theory: close to continumm theory should be Ok;
- Strong coupling: doubler mixing.

Conclusions

- Crank-Nicolson discretisation scheme offers new definitions of fermions on the lattice:

  I. Crank-Nicolson-Wilson operator is a one flavour theory with broken chiral symmetry and second order discretisation errors in a_t.

  II. A free fermion chiral theory via doubler level splitting.

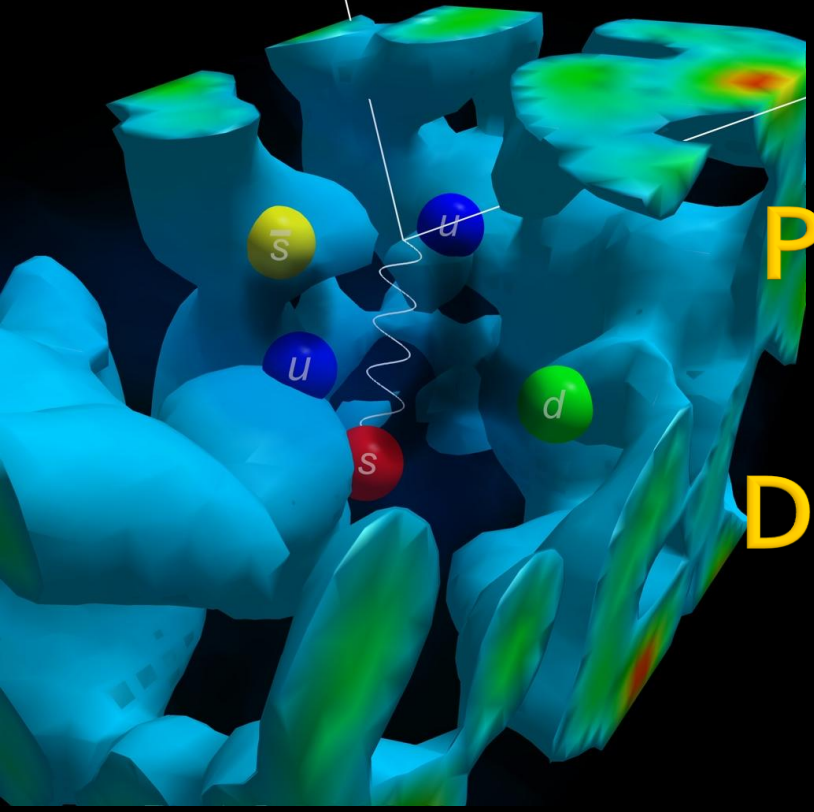

Prospects of Multi-grid and Domain Decomposition Dirac Solvers on GPU

Richard C. Brower (with SciDAC collaborators Ron Babich, Mike Clark, James Osborn et al!)

New Horizons for Lattice Computations with Chiral Fermions

BNL May 15, 2012

Algorithms are increasingly Essential and increasingly Complex.

- Causes:
  - Higher resolution physics.
  - Hierarchical Petascale hardware.

- Long multi-year cycle:
  1. Physical Insight
  2. Mathematics of Complexity (flops & comms)
  3. Coding prototype on New Hardware
  4. Testing and Integration into Applications

Outline:
A few future (spectacular?) examples.

I. Moebius DW Fermions (retrospective!)

II. Multigrid Wilson-clover Dirac Solver (at last!)

III. GPUs with Domain Decomposition

IV. The Future: MG/GPU/DD for HMC

- (MG for Domain Wall: next talk by Saul Cohen)

I. Moebius as Scaled Shamir DW

Moebius Retrospective

Why: *Shamir: mres = O(1/Ls)* → *Moebius: mres = O(1/(Ls*Ls))*

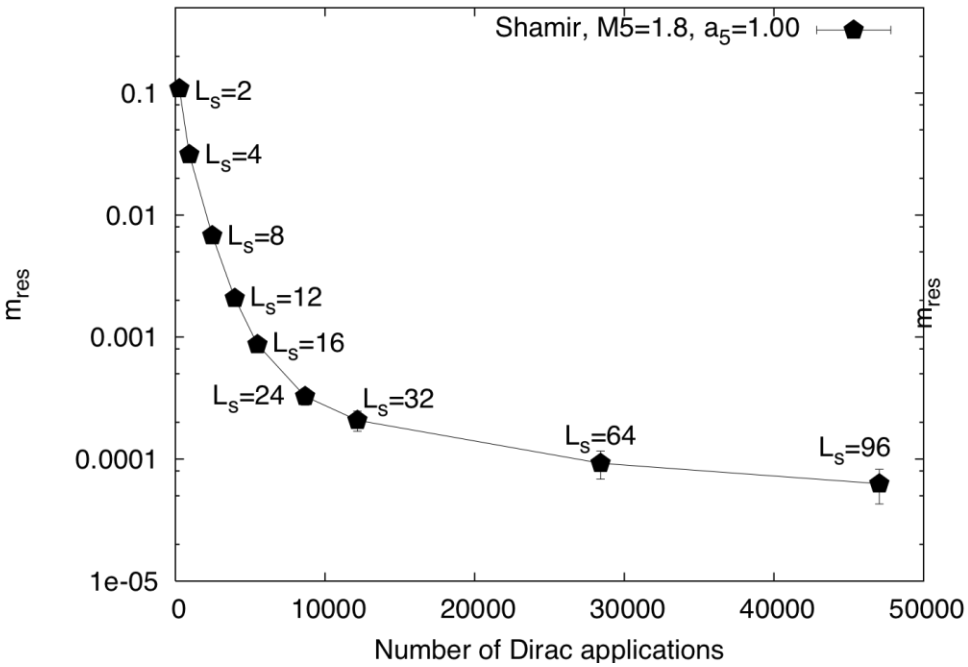

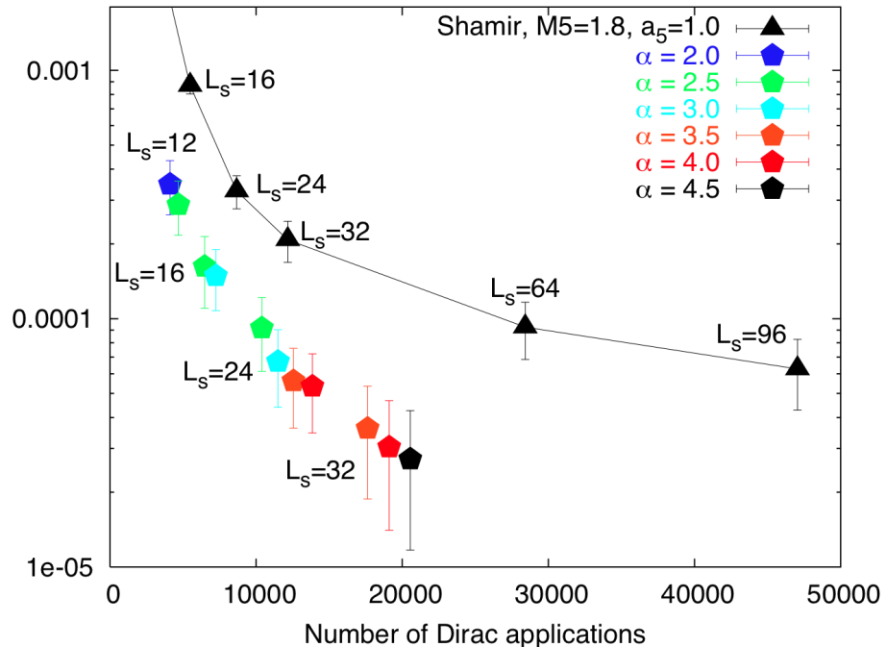

$$\epsilon_{L_s}[\alpha H_5] = \frac{(1+\alpha H_5)^{L_s} - (1-\alpha H_5)^{L_s}}{(1+\alpha H_5)^{L_s} + (1-\alpha H_5)^{L_s}}$$

$\epsilon_{L_s}[\lambda]$ for $1/L_s < |\lambda| < L_s$

Good to $O(L_s)$

$O(1/L_s)$

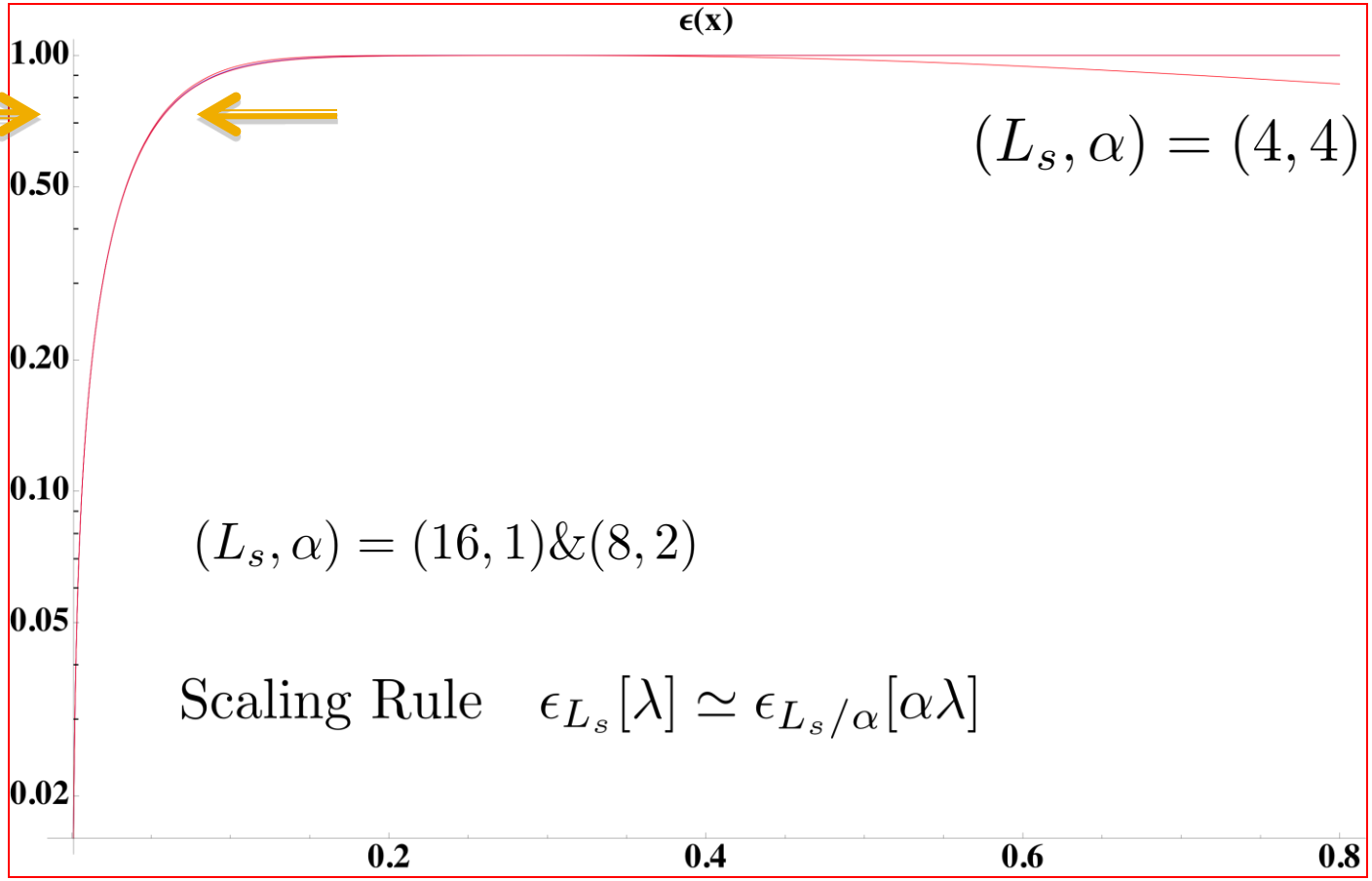

Scaling Rule $\epsilon_{L_s}[\lambda] \simeq \epsilon_{L_s/\alpha}[\alpha\lambda]$

$\lambda_{max} < 3/4$

Estimate of Mres

$$\overline{m}_{res} = \frac{Tr[D_{ov}^{\dagger -1} \Delta_{L_s}(H_5) D_{ov}^{-1}]}{Tr\left[D_{ov}^{-1} D_{ov}^{\dagger -1}\right]} = \sum_{\lambda} w_{\pi}(\lambda)\, \Delta_{L_s}(\lambda)$$

$$\Delta_{L_s}(\alpha\lambda) = \frac{1}{4}(1 - \epsilon_L^2[\alpha\lambda])$$

$$\rightarrow e^{-L_s|\log(1+\alpha\lambda) - \log(1-\alpha\lambda)|} \simeq e^{-2L_s\alpha\lambda}$$

Error from $|\lambda| < 1/2\alpha Ls \sim 1/L_s^2$

Small density of "topological defects"

Thus Moebius for Ls = 32 ➔ Shamir at Ls = 1000 !!!!!

II. Multigrid for Wilson clover Solver

Multigrid Premier: Classic example - PDE with NO scale!

No change when $x \to \lambda x, y \to \lambda y, z \to \lambda z$

- Laplace: $\phi \to \lambda^{-1}\phi$

$$-\nabla^2\phi(x,y,z) = -[\frac{\partial^2}{\partial x^2} + \frac{\partial^2}{\partial y^2} + \frac{\partial^2}{\partial z^2}]\phi = e^2\delta(x)\delta(y)\delta(z)$$

- Solution (Green's function)

$$\phi = \frac{1}{4\pi}\frac{e^2}{\sqrt{x^2+y^2+z^2}} = \frac{e^2}{4\pi r}$$

Precondition operator on a = h by "renormalized" operator on a = 2h

$$A\phi = b \implies \phi(x+h) - 2\phi(x) + \phi(x-h) + h^2 m^2 \phi(x) = b(x)$$

h ➔ 2h Restriction R = $P^\dagger$

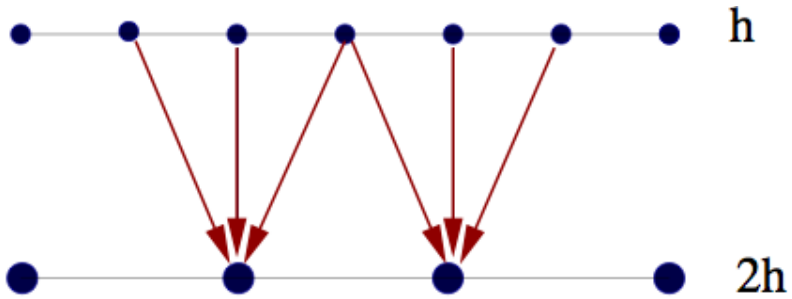

2 h ➔ h Prologation P

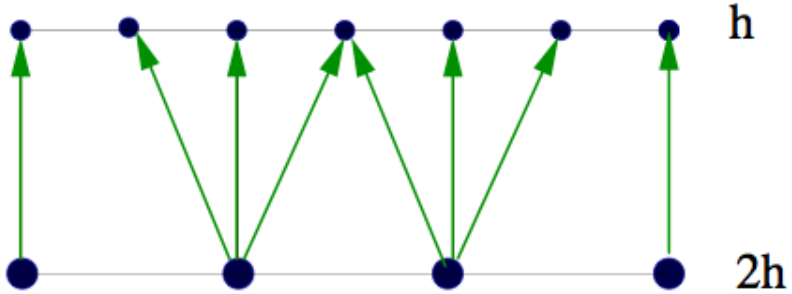

(1) Restriction must preserves the scale invariant solutions

(2) Coarse operator is renormalized: m ➔ 2 m (in units h = 1)

Multi-grid V-Cycle

- Restrict until exact solve possible
- Interpolate back to fine grid
- *O(N) to O(N log N)* scaling
- Memory O(N)
- Extra Work: 1 + w + w*w + .. < 1/(1-w)

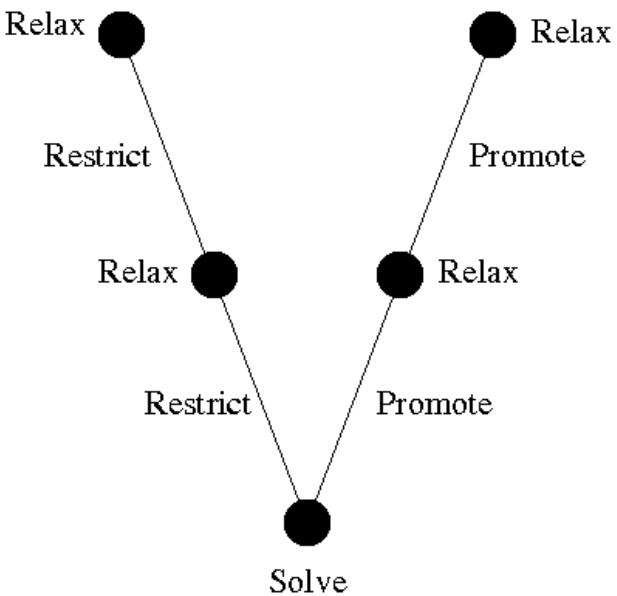

Ren Group motivated attempts in 1990's:

See Thomas Kalkretuer hep-lat/9409008 review on "MG Methods for Propagators in LGT".

Israel: Ben-Av, M. Harmatz, P.G. Lauwers & S.Solomon

Boston: Brower, Edwards, Rebbi & Vicari

Amsterdam: A. Hulsebos, J Smit J. C. Vick

Hamburg: T. Kalkreuter, G. Mack & M. Speh

group	operator to be inverted	gauge field	lattice sizes
"Israel	$\not{D} + m$	2-d $U(1)$	$\leq 256^2$
[3, 13, and references therein]	staggered fermions	2-d $SU(2)$	$\leq 256^2$
1989–ongoing		2-d $SU(3)$	$\leq 128^2$
"Amsterdam"	$-\not{D}^2 + m^2$	2-d $SU(2)$	$\leq 128^2$
[14, and references therein]	staggered fermions		
1990–1992	staggered fermions	2-d $SU(2)$	$\leq 128^2$
	and Wilson fermions		
"Boston"	$-\Delta + m^2$	2-d $U(1)$	$\leq 64^2$
[7, and references therein]		4-d $U(1)$	$\leq 16^4$
1990–1991		2-d $SU(2)$	$\leq 32^2$
	$(\gamma_\mu + 1)D_\mu + m$	2-d $U(1)$	64^2
	Wilson fermions		
[29]	$(\gamma_\mu + 1)D_\mu + m$	2-d $U(1)$	64^2
1990–1992	Wilson fermions	4-d $SU(3)$	16^4
"Hamburg"	$-\Delta + m^2$	2-d $SU(2)$	$\leq 128^2$
[21, 18, 22, 23, 1, 17, 19, 20, 2, 24]		4-d $SU(2)$	$\leq 18^4$
1990–ongoing	$-\not{D}^2 + m^2$	2-d $SU(2)$	$\leq 162^2$
	staggered fermions	4-d $SU(2)$	$\leq 18^4$

Table 1: *Overview of works on MG methods for propagators in lattice gauge theories.*

受入
91-5-116
高工研図書室

SUPERCOMPUTER
COMPUTATIONS
RESEARCH INSTITUTE

PROJECTIVE MULTIGRID FOR WILSON FERMIONS

by

Richard C. Brower, Robert G. Edwards,
Claudio Rebbi, and Ettore Vicari

FSU-SCRI-91-54

2x2 Blocks for 2-d U(1) Dirac (Naive scaling of free problem)

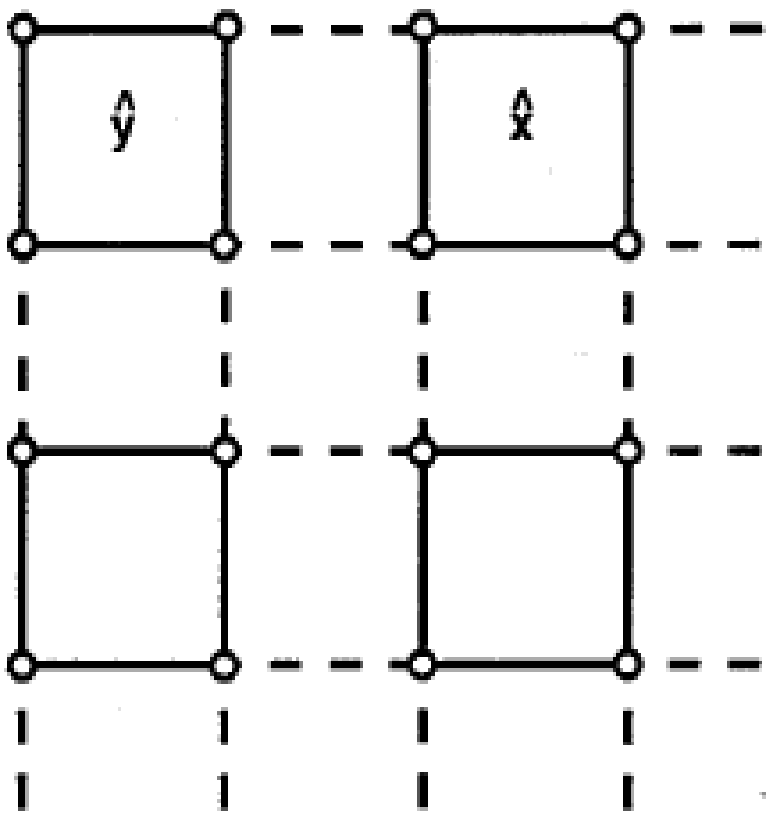

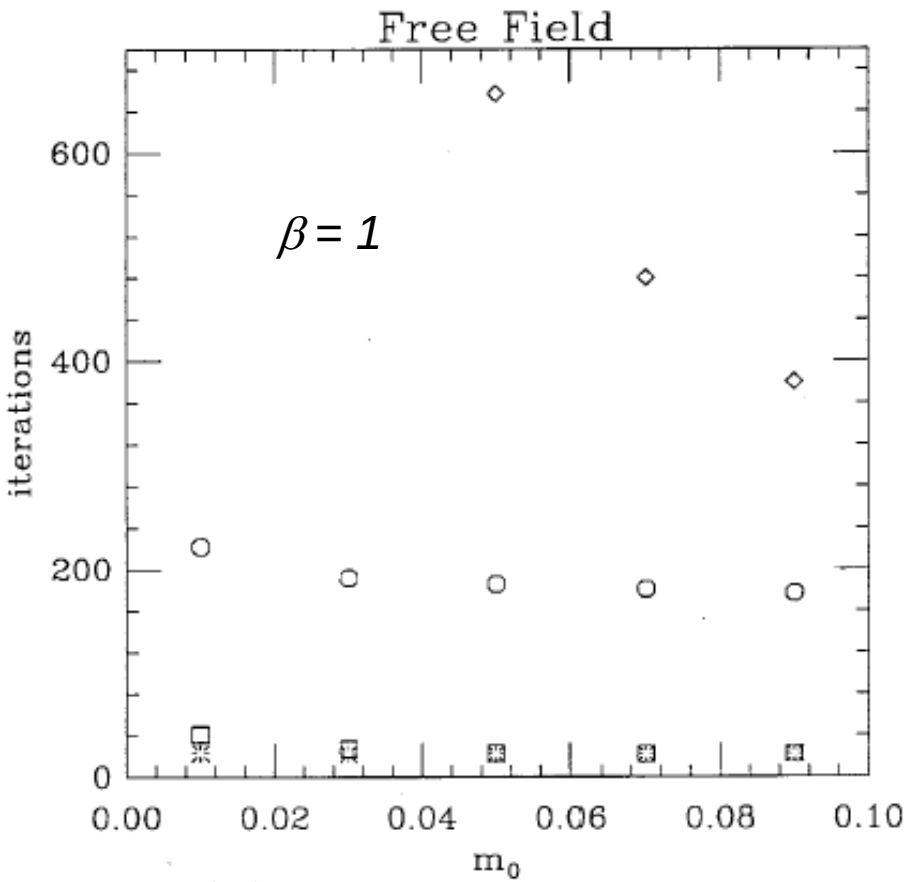

$$U_\mu(x) = 1$$

2-d Lattice, $U_\mu(x)$ on links $\Psi(x)$ on sites

Gauss-Jacobi (Diamond), CG (circle), V cycle (square), W cycle (star)

Universal critical slowing: $\tau = F(m\, l_\sigma)$

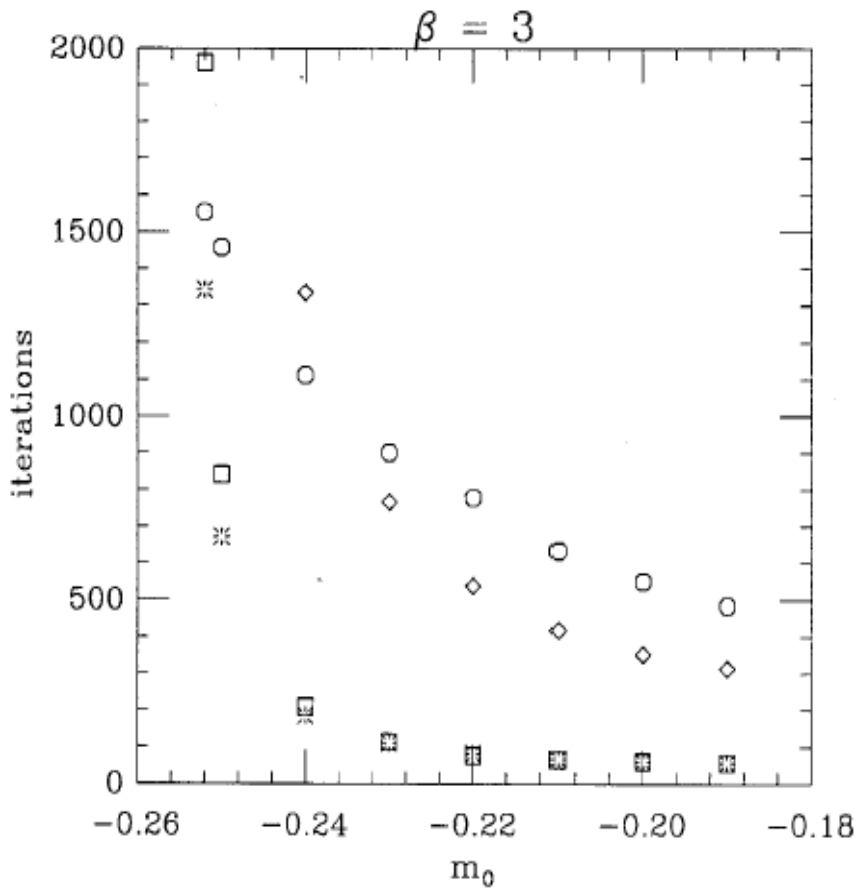

Gauss-Jacobi (Diamond), CG(circle), 3 level (square & star)

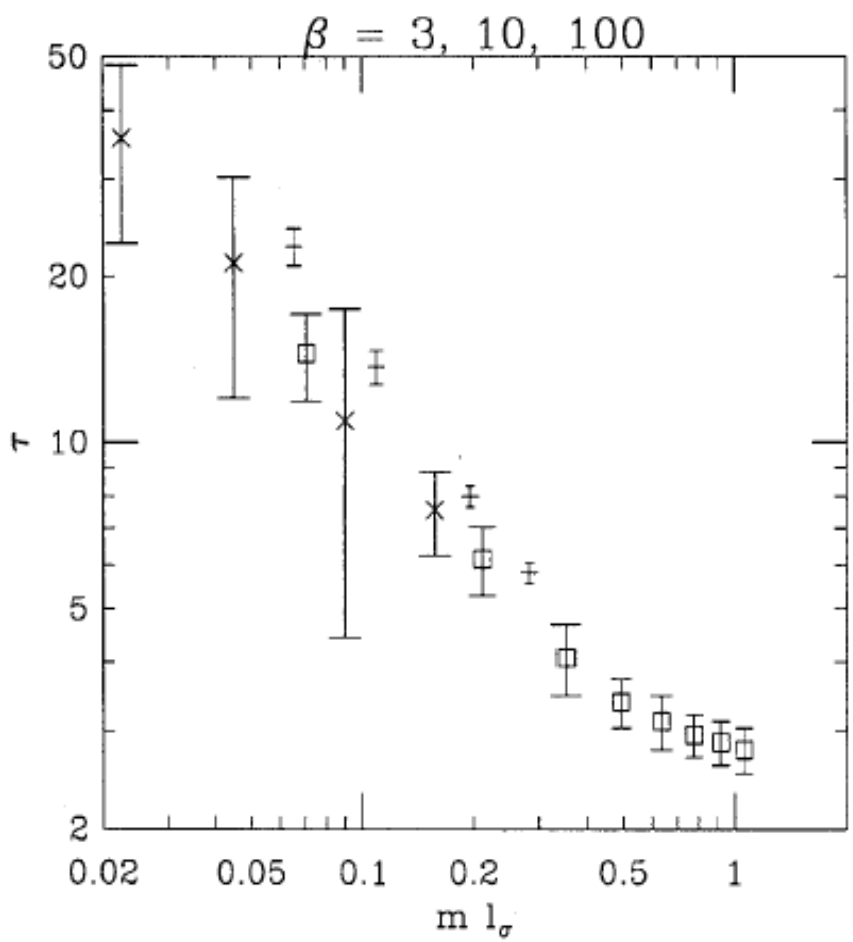

β = 3 (cross) 10(plus) 100(square)

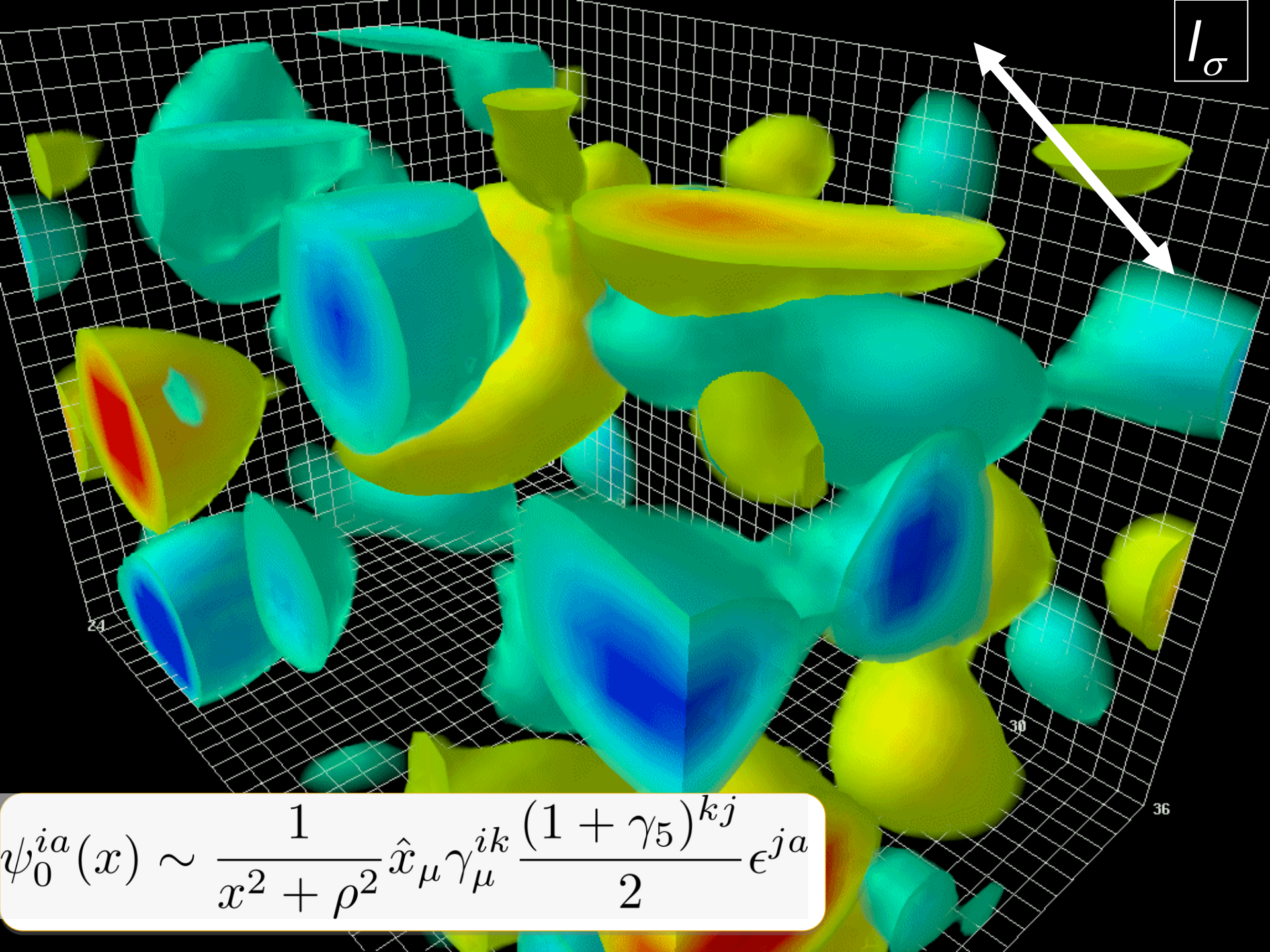

$$\psi_0^{ia}(x) \sim \frac{1}{x^2+\rho^2}\hat{x}_\mu \gamma_\mu^{ik} \frac{(1+\gamma_5)^{kj}}{2}\epsilon^{ja}$$

QCD Multigrid Applied Math/Physics Collaboration

Many different people (TOPS, QCD) and institutions involved in the collaboration

- CU Boulder
  - Tom Manteuffel
  - Steve McCormick
  - Marian Brezina
  - John Ruge
  - James Brannick
  - Christian Ketelsen
  - Scott MacLachlan
- Lawrence Livermore
  - Rob Falgout
- Columbia
  - David Keyes

- Boston University
  - Rich Brower
  - Claudio Rebbi
  - Mike Clark
  - James Osborn
  - *Saul Cohen*
- Penn State
  - James Brannick
  - Ludmil Zikatanov
- Tufts
  - Scott MacLachlan
- Argonne
  - James Osborn

Harvard U

Mike Clark

- *Ron Babich*

•*INT Seattle*

- *Saul Cohen*

Adaptive Smooth Aggregation Algebraic Multigrid

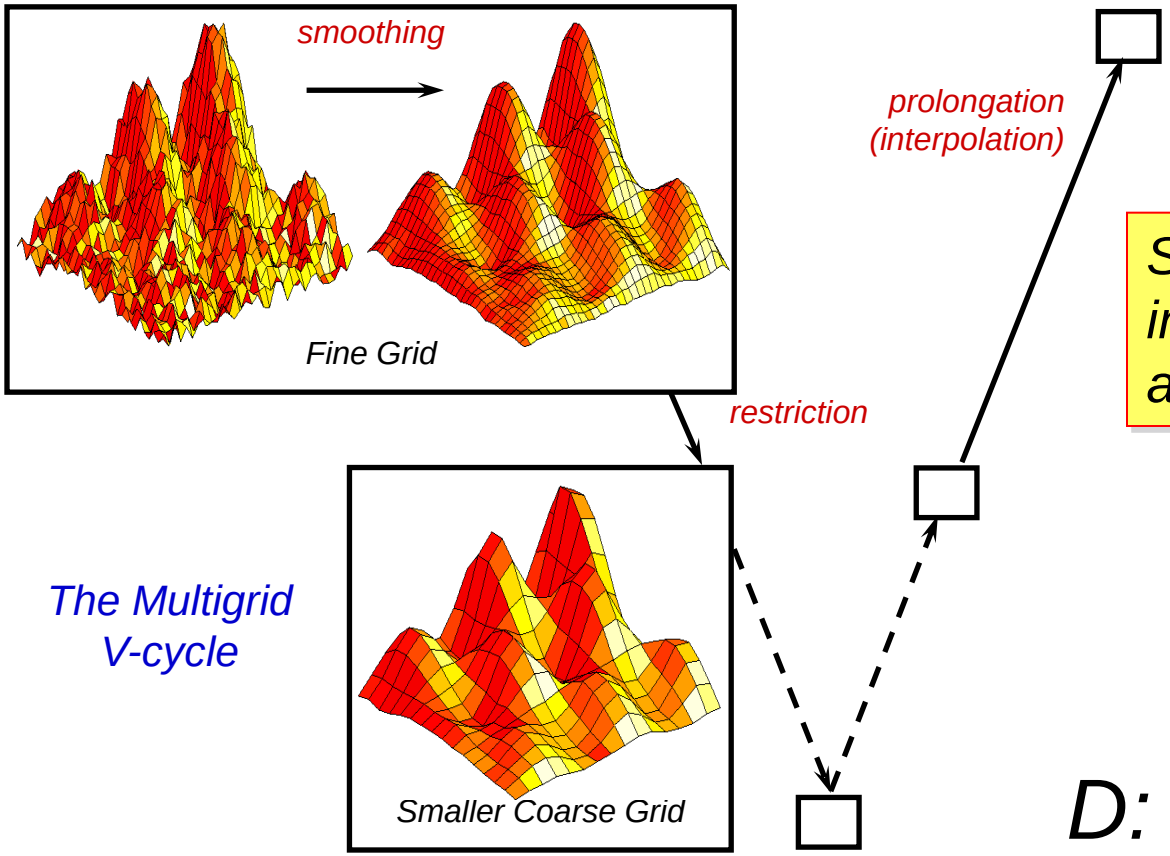

The Multigrid
V-cycle

Spilt the vector space into near null space S and the complement $S_?$

D: S ' 0

Slow convergence of Dirac solver is due to small eigenvalues for vectors in near null subspace: S .

Physical Requirements

- Partial success (RG) weak coupling
- Maintain Gauge invariance
- Maintain γ_5 Hermiticity
- Local adaptive blocking: Projective MG
- Chiral Symmetry (density of small e.v.)
- Null vector: Atya- Singer Index Theorem

$$H = \gamma_5 D = D^\dagger \gamma_5$$

$$\text{Prolongator} \quad P \implies \text{Restrictor} \quad R = P^\dagger \gamma_5$$

P^y:fine ! coarse (non-square matrix^y)

(fine lattice vector space) *(coarse lattice vector space)*

But $PyP = 1_{cc}$ so $Ker(P) = 0$

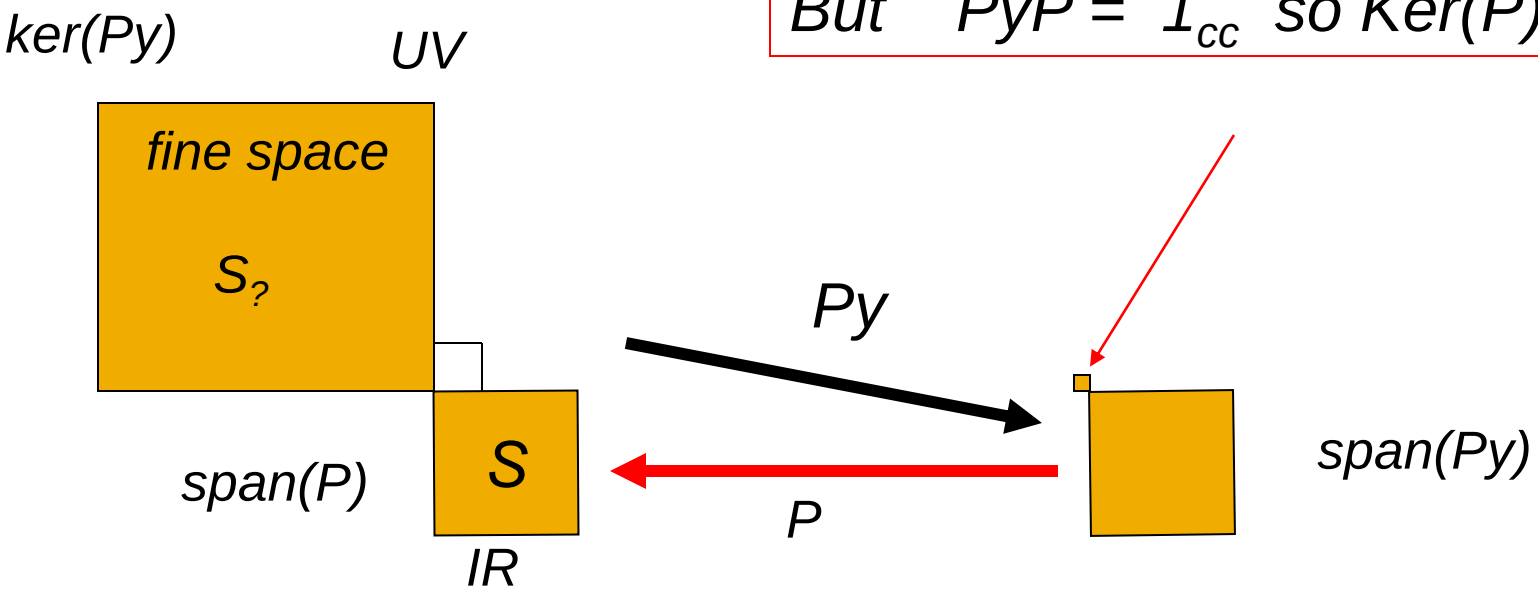

$S = span(P) = Image(Py)$

$rank(P) = rank(Py) = dim(S) = N_o N_B = 2N_o L4/44$

y See Front cover of Gilbert Strang's undergraduate text !

General Problem: D Ã = b

- *"split" vector space into:*
  - *near null* $D\,S'o$ & *Complement* $S_?$
- *Schur decomposition (of course) does this!*
  - *Coarse = near null (IR) , Fine = complement (UV)*

Splitting is essential the idea of the Schur complement:

$$\begin{bmatrix} D_{cc} & D_{cf} \\ D_{fc} & D_{ff} \end{bmatrix} = \begin{bmatrix} 1 & 0 \\ D_{fc}D_{cc}^{-1} & 1 \end{bmatrix} \begin{bmatrix} D_{cc} & 0 \\ 0 & D_{ff} - D_{fc}D_{cc}^{-1}D_{cf} \end{bmatrix} \begin{bmatrix} 1 & D_{cc}^{-1}D_{cf} \\ 0 & 1 \end{bmatrix}$$

Implies

$$D^{-1} = \begin{bmatrix} 1 & -D_{fc}D_{cc}^{-1} \\ 0 & 1 \end{bmatrix} \begin{bmatrix} D_{cc}^{-1} & 0 \\ 0 & D_{Schur}^{-1} \end{bmatrix} \begin{bmatrix} 1 & 0 \\ -D_{cc}^{-1}D_{cf} & 1 \end{bmatrix}$$

with $D_{Schur} \equiv D_{fc}D_{cc}^{-1}D_{cf}$

Petrov-Galerkin oblique projection

$$D_{Schur} = [D - DP\frac{1}{P^\dagger DP}PD] = [1 - DP\frac{1}{P^\dagger DP}P]D$$

$$P^\dagger D_{Schur} = D_{Schur}P = 0$$

The coarse operator : $\hat{D} = D_{cc} = P^\dagger DP$

The projection op to coarse space : $PP^\dagger$

But the Schur complement use "oblique projects:

$$\Pi_L^\dagger = DP\frac{1}{P^\dagger DP}P^\dagger \quad , \quad \Pi_R = P\frac{1}{P^\dagger DP}P^\dagger D$$

$$D_{Schur} = D - \Pi_L^\dagger D\Pi_R = (1 - \Pi_L^\dagger)D(1 - \Pi_R)$$

2-level Multigrid Cycle (simplified)

- Smooth $x = (1 - D)x^0 + b \quad \Longrightarrow \quad r = (1 - D)r^0$
- Coarsen $D_c = P^\dagger D P \quad \& \quad r_c = P^\dagger r$
- Solver $A_c e_c = r_c \quad \Longrightarrow \quad e_c = A_c^{-1} P^\dagger r$
- Interpolate $e = P e_c$
- Update $x' = x + e \quad \Longrightarrow \quad r' = b - D(x + e)$
- Hence $r' = [1 - DP \frac{1}{P^\dagger D P} P^\dagger] r \quad \Longrightarrow \quad P^\dagger r' \equiv 0$

Exact null space "deflation" by right "preconditioner:

$$M^{-1} = P \frac{1}{P^\dagger D P} P^\dagger$$

AMG on Wilson-clover Dirac Operator

- Devil is in the details!
  - Rigorous MG proofs for normal equation ($D^y D \tilde{A} = b$)
  - But would like to project D to avoid higher complexity.
  - Multigrid is recursive to multi-levels.
  - Must preserves Gauge invariance and $°_5$ ($[°_5, P] = 0$)
- First benchmarks for Wilson-Dirac Operator:
  - Asym $V=16^3 \times 64$, $24^3 \times 64$, $32^3 \times 96$ ($N_f = 2$, 400MeV pion)
  - $N_o = 20$ null vectors $\tilde{A}^s_x$ with 4th order MR with subset refinement.
  - MG Blocks = $4^4 \times N_c \times 2$ and 3 level V MG cycle
  - pre and post-smoothing is done by 4 iteration GCR (later GMRES)
  - Extend to Red/Black preconditioning

(James Osborn implement on BG/P in SciDAC-2 API

Future SciDAC-3 develop in HYPER framework/GPUs etc).

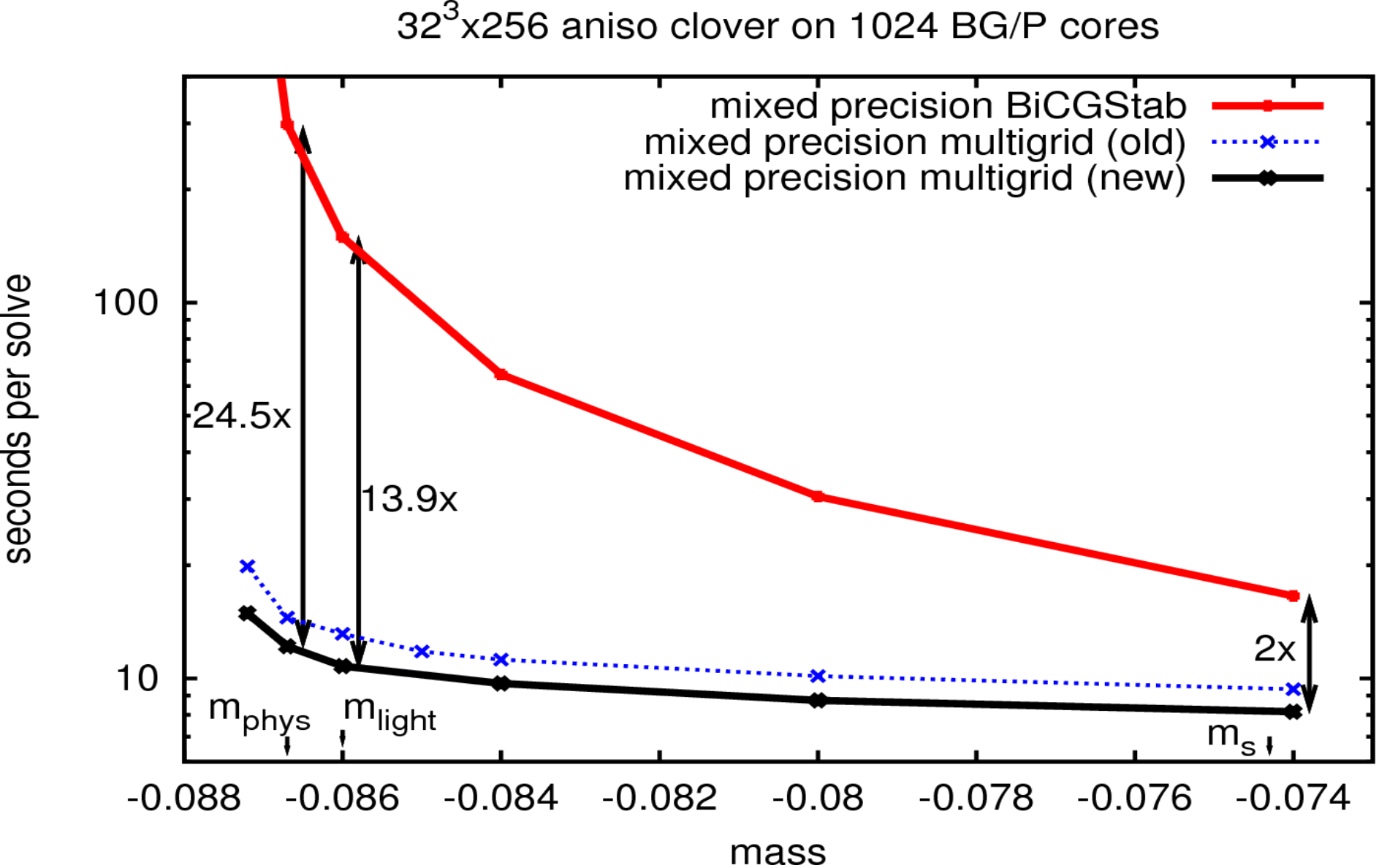

"Adaptive multigrid algorithm for the lattice Wilson-Dirac operator" R. Babich, J. Brannick, R. C. Brower, M. A. Clark, T. Manteuffel, S. McCormick, J. C. Osborn, and C. Rebbi, Phys. Rev. Lett. 105, 201602 (2010).

(Latest Result: Finite T lattice 128^3x96 ➔ 32 x speed up! James Osborn.)

Total cost 32^3x256

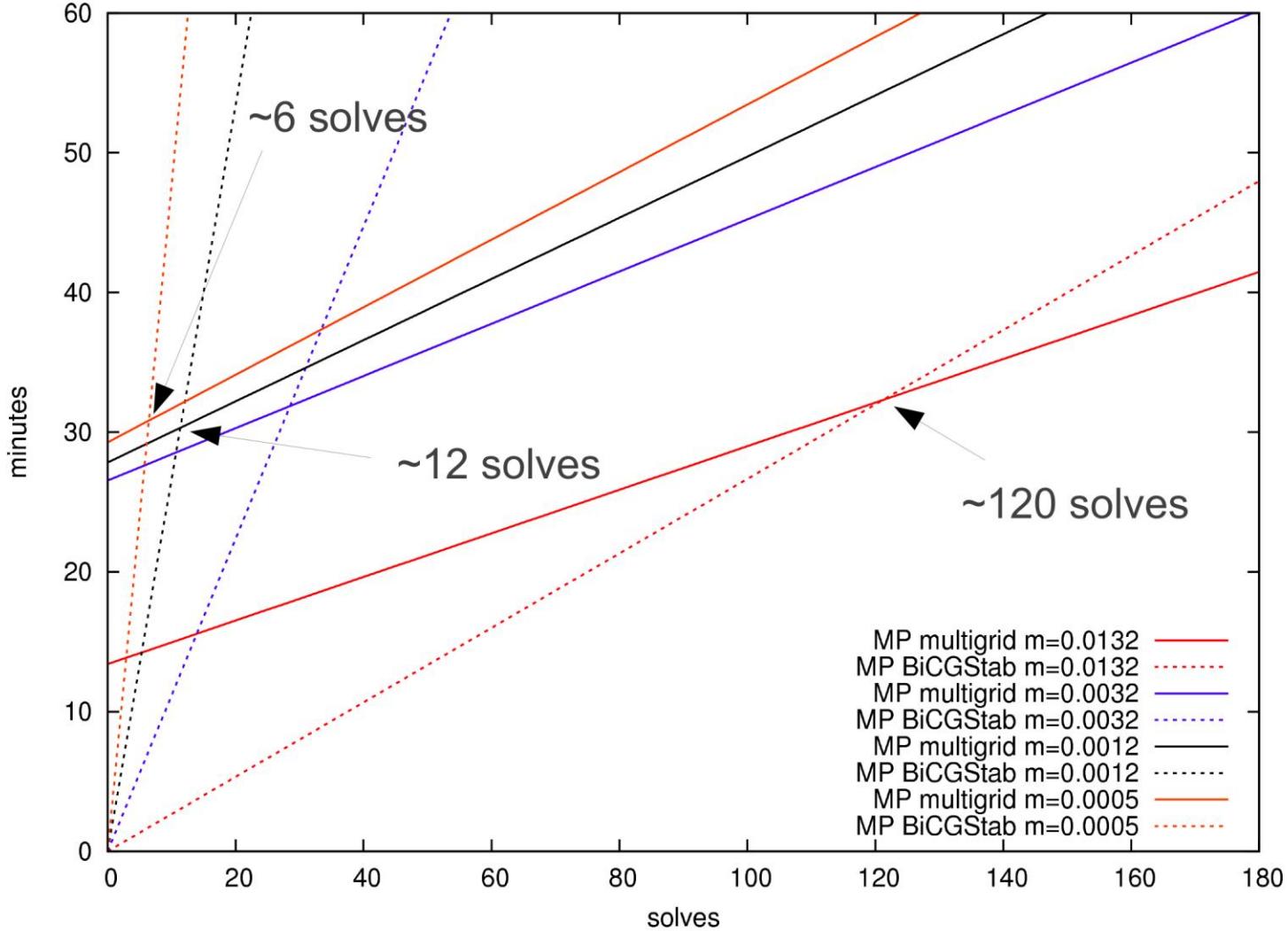

Error vs residual

- Error:
  $e = x^* - x$
- Residual:
  $r = b - A x$
  $= A e$
- Residual not as sensitive to low modes

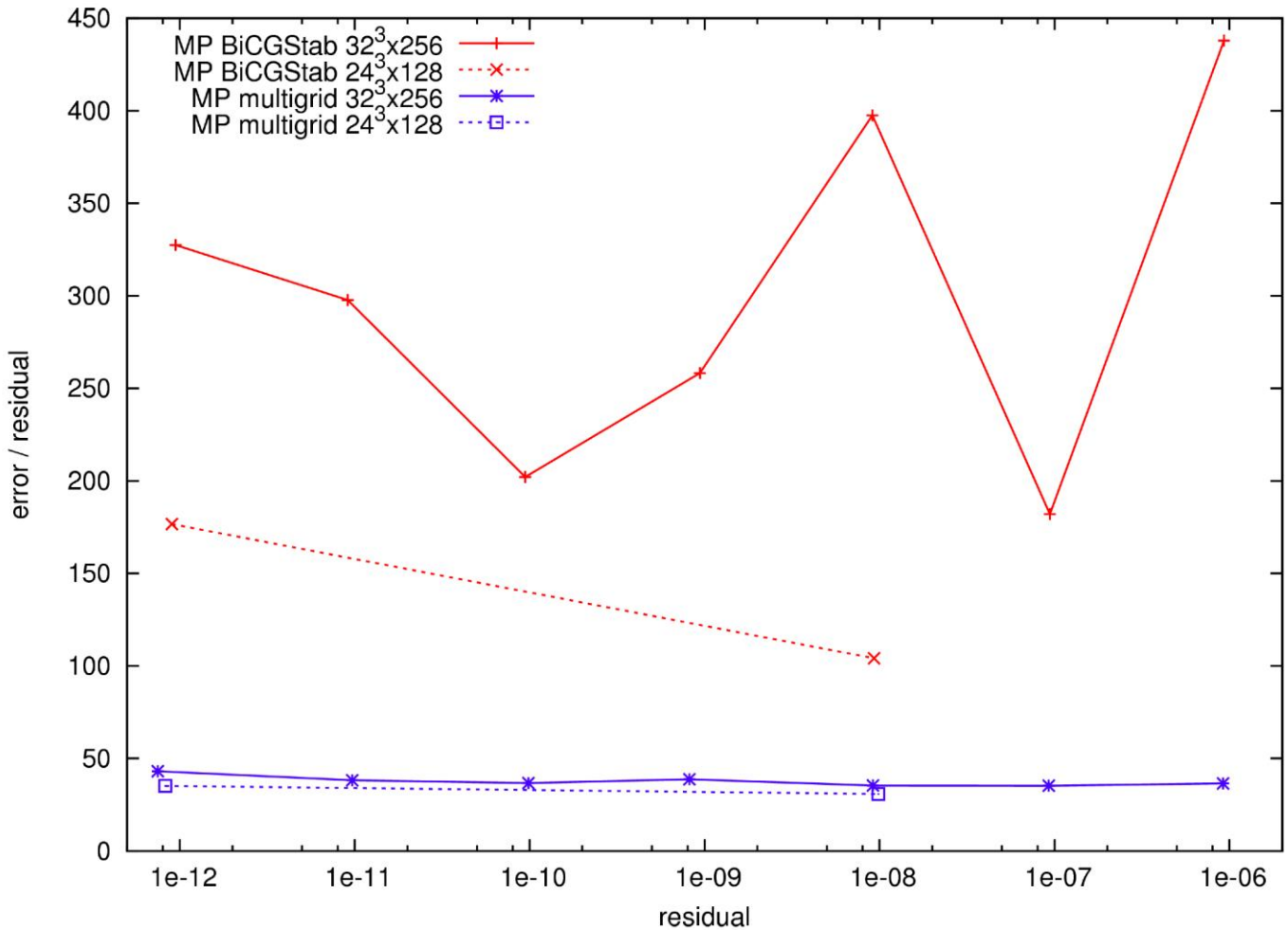

Speed up is even better at fixed error.

III. QUDA: QCD in CUDA for GPUs

Disruptive many-core Architectures

- 1/4 CM-2

Nvidia FERMI chip

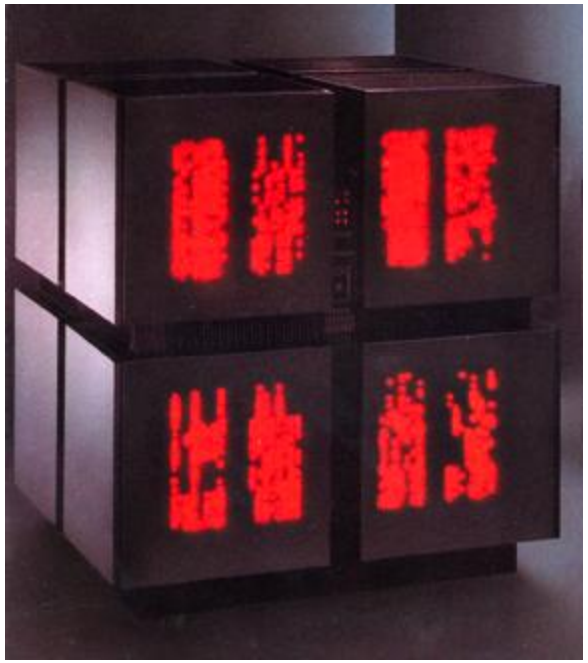

)

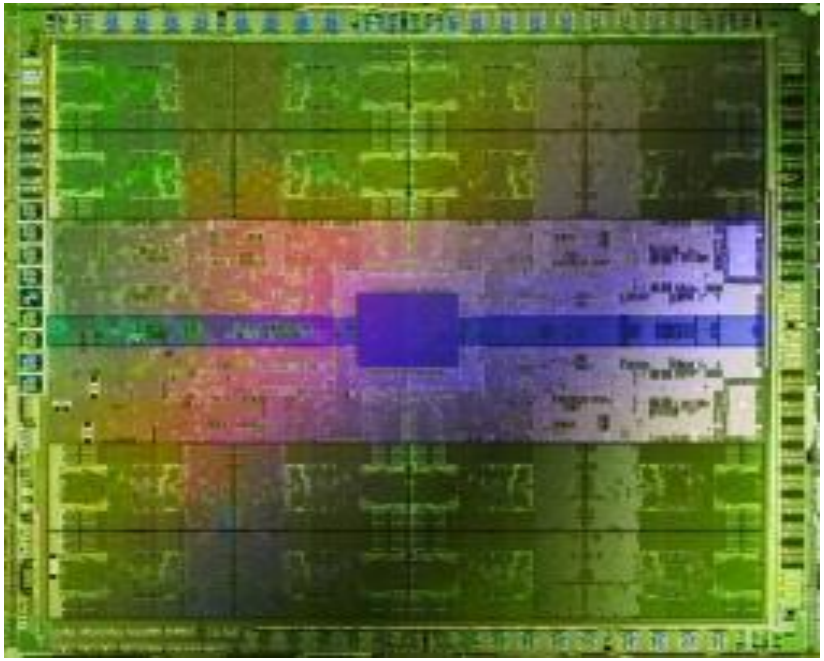

16 K bit serial PE.)

512 x 32 bit PE = 16 K bits

Nvidia Kepler has 1536 Floating point cores! Maxwell ??? Next ???

The pioneers of GPU computing in lattice QCD

2005-2006

ELSEVIER

Available online at www.sciencedirect.com

ScienceDirect

Computer Physics Communications 177 (2007) 631–639

Computer Physics Communications

www.elsevier.com/locate/cpc

Lattice QCD as a video game

Győző I. Egri [a], Zoltán Fodor [a,b,c,*], Christian Hoelbling [b], Sándor D. Katz [a,b], Dániel Nógrádi [b], Kálmán K. Szabó [b]

[a] *Institute for Theoretical Physics, Eötvös University, Budapest, Hungary*
[b] *Department of Physics, University of Wuppertal, Germany*
[c] *Department of Physics, University of California, San Diego, USA*

Received 2 February 2007; received in revised form 29 May 2007; accepted 7 June 2007

Available online 15 June 2007

Abstract

The speed, bandwidth and cost characteristics of today's PC graphics cards make them an attractive target as general purpose computational platforms. High performance can be achieved also for lattice simulations but the actual implementation can be cumbersome. This paper outlines the architecture and programming model of modern graphics cards for the lattice practitioner with the goal of exploiting these chips for Monte Carlo simulations. Sample code is also given.

© 2007 Elsevier B.V. All rights reserved.

QUDA (QCD/CUDA) collaborators

- Ronald Babich (BU → PSC → NVIDIA)*
- Kipton Barros (BU → LANL)
- Michael Clark (BU→ Harvard → NVIDIA)*
- Justin Foley (Utah)
- Joel Giedt (Rensselear)
- Steven Gottlieb (Indiana)
- Balint Joo (Jefferson Lab)
- James Osbone (Utah → BU → Argonne)
- Claudio Rebbi (BU)
- Gouchin Shi (NCSA)
- et al

How to get QUDA & join the Fun

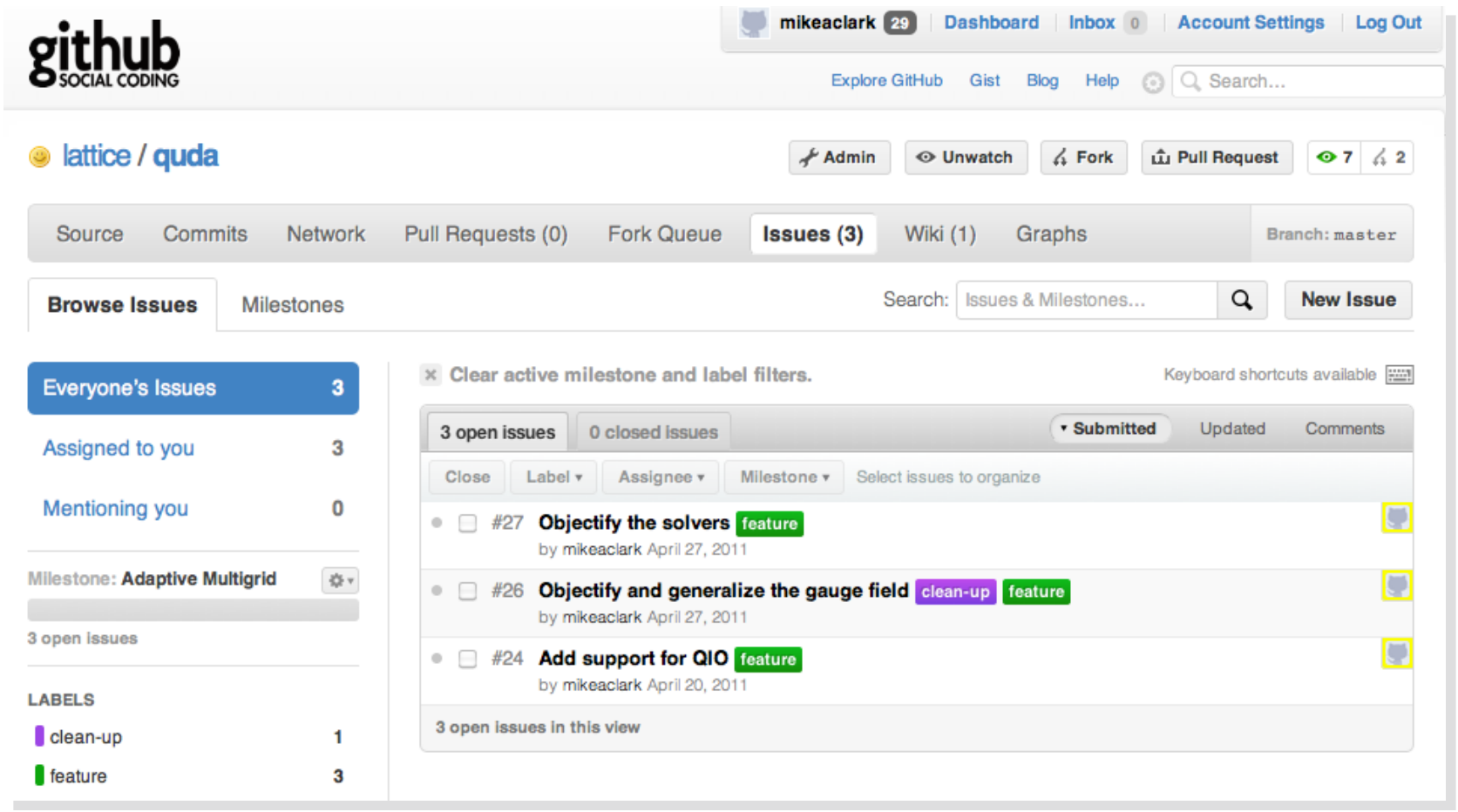

https://github.com/lattice/quda

GPU memory hierarchy

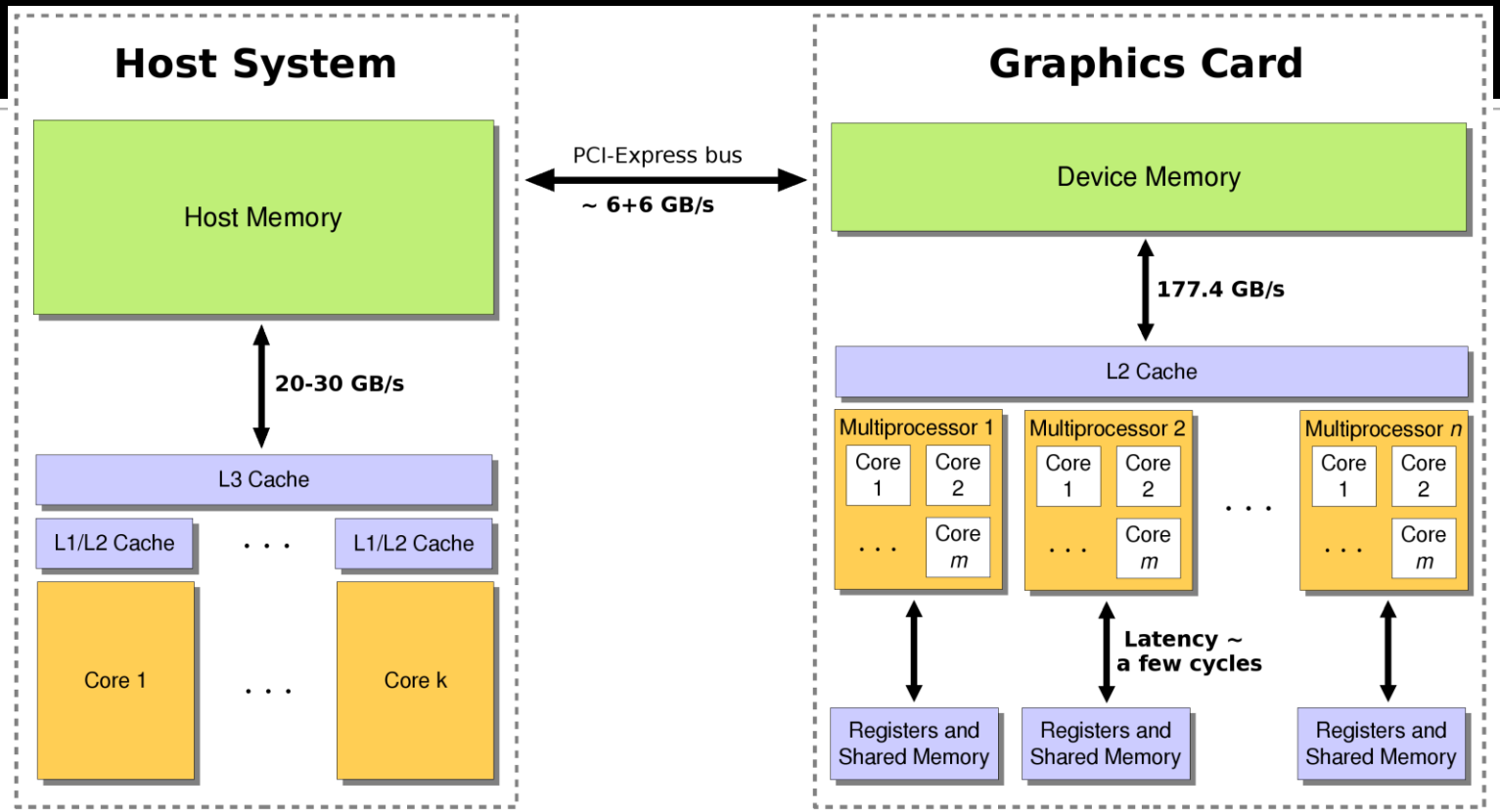

(GeForce GTX 480)

Tricks to reduce memory traffic

- Reconstruct SU(3) matrices from 8 or 12 real numbers on the fly, e.g.,

$$\begin{pmatrix} \mathbf{a} \\ \mathbf{b} \\ \mathbf{c} \end{pmatrix} = \begin{pmatrix} a_1 & a_2 & a_3 \\ b_1 & b_2 & b_3 \\ c_1 & c_2 & c_3 \end{pmatrix}$$

$$\mathbf{c} = (\mathbf{a} \times \mathbf{b})^*$$

$$SU(2) : U = a_0\sigma_0 + \vec{a} \cdot \sigma$$

$$a_0^2 + \vec{a} \cdot \vec{a} = 1 \implies S_3 \text{ sphere}$$

Better still SU(3) has 8 parameters on $S_3 \times S_5$

- Choose a gamma basis with $\square_4$ diagonal.

$$P^{\pm 4} = \begin{pmatrix} 1 & 0 & \pm 1 & 0 \\ 0 & 1 & 0 & \pm 1 \\ \pm 1 & 0 & 1 & 0 \\ 0 & \pm 1 & 0 & 1 \end{pmatrix} \Rightarrow \left\{ \begin{array}{l} P^{+4} = \begin{pmatrix} 2 & 0 & 0 & 0 \\ 0 & 2 & 0 & 0 \\ 0 & 0 & 0 & 0 \\ 0 & 0 & 0 & 0 \end{pmatrix} \\ P^{-4} = \begin{pmatrix} 0 & 0 & 0 & 0 \\ 0 & 0 & 0 & 0 \\ 0 & 0 & 2 & 0 \\ 0 & 0 & 0 & 2 \end{pmatrix} \end{array} \right\}$$

similarity transforms on D

- Fix to the temporal gauge (setting gauge links in the *t*-direction to the identity).

Mixed precision with reliable updates

- Using a mixed-precision solver incorporating “reliable updates” (Clark et al., arXiv:0911.3191) with half precision greatly reduces time-to-solution while maintaining double precision accuracy.

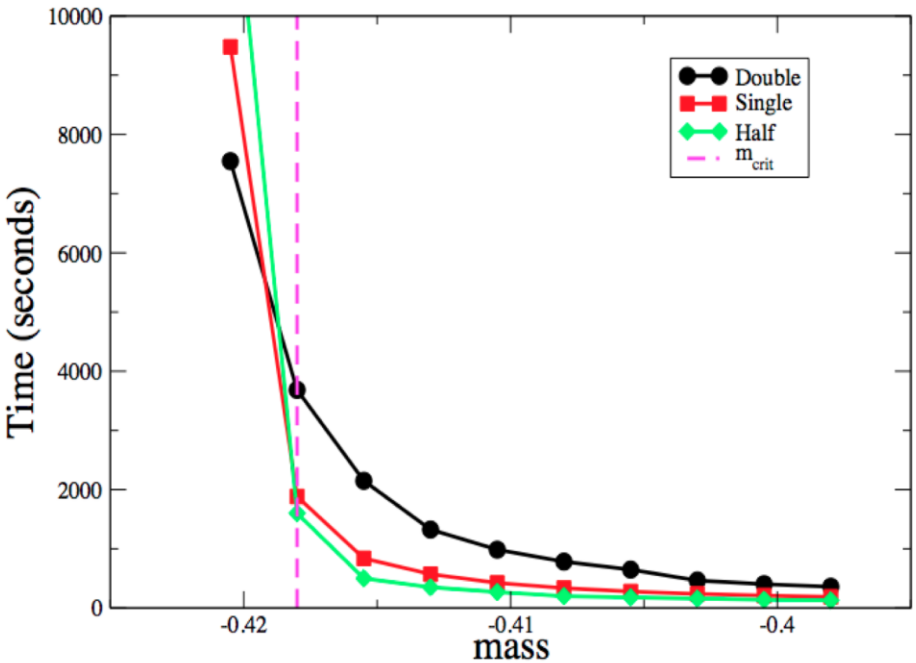

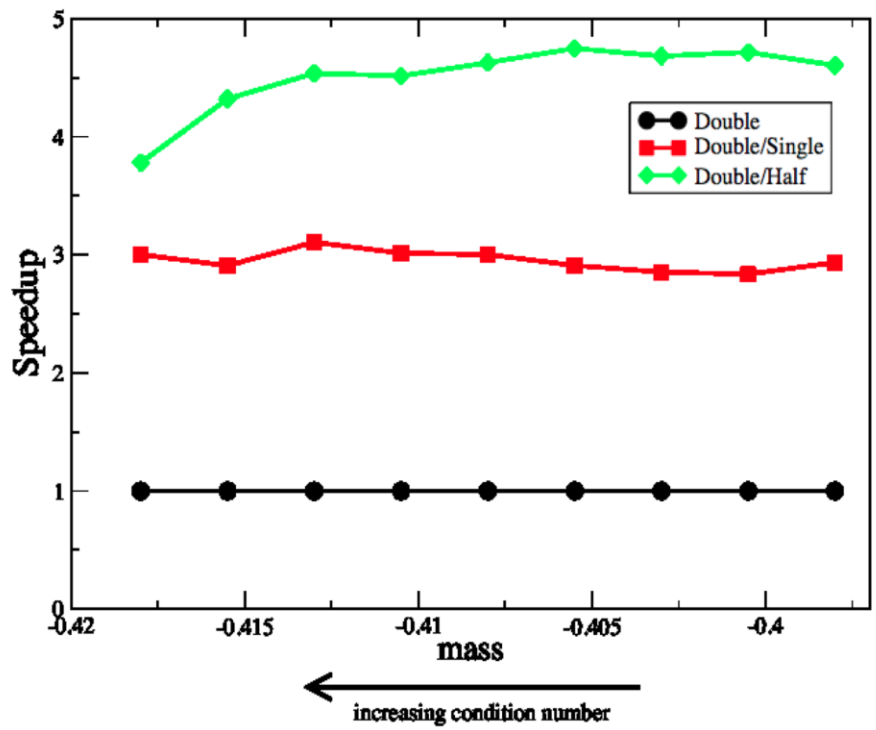

Big Cray/GPU machines are coming.

Cray XK6 Compute Node

CRAY THE SUPERCOMPUTER COMPANY

XK6 Compute Node Characteristics
AMD Opteron 6200 Interlagos 16 core processor
Tesla X2090 @ 665 GF
Host memory 16 or 32GB 1600 MHz DDR3
Tesla X090 memory 6GB GDDR5 capacity
Gemini high speed Interconnect
Upgradeable to NVIDIA's Kepler many-core processor

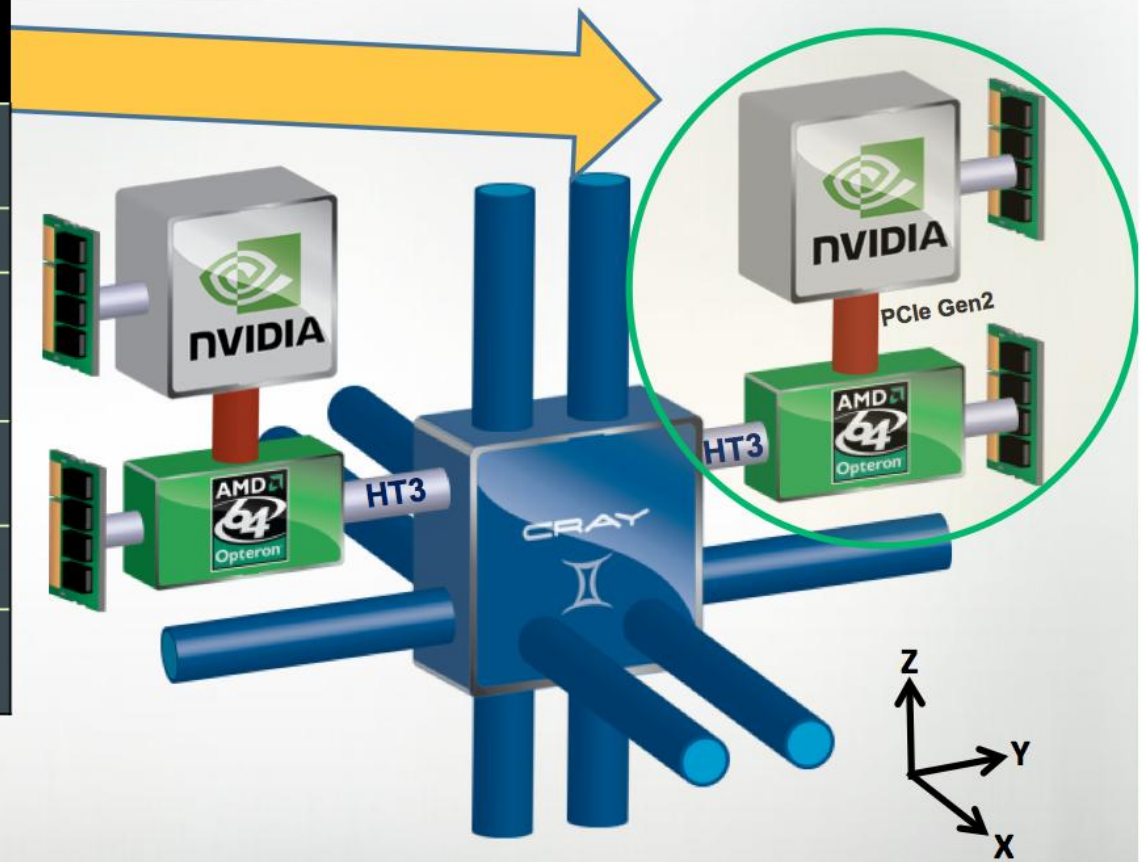

Slide courtesy of Cray, Inc.

Disclaimer: No contract with vendor is in place

LOCATION
LOCATION
LOCATION!

TO GET STRONG SCALING NEED TO MANAGE A MULTILEVEL MEMORY HEIRARCHY

THIS IS THE CHALLENGE OF HETEROGENOUS ARCHITECTURE OF THE PRESENT AND THE FUTURE!

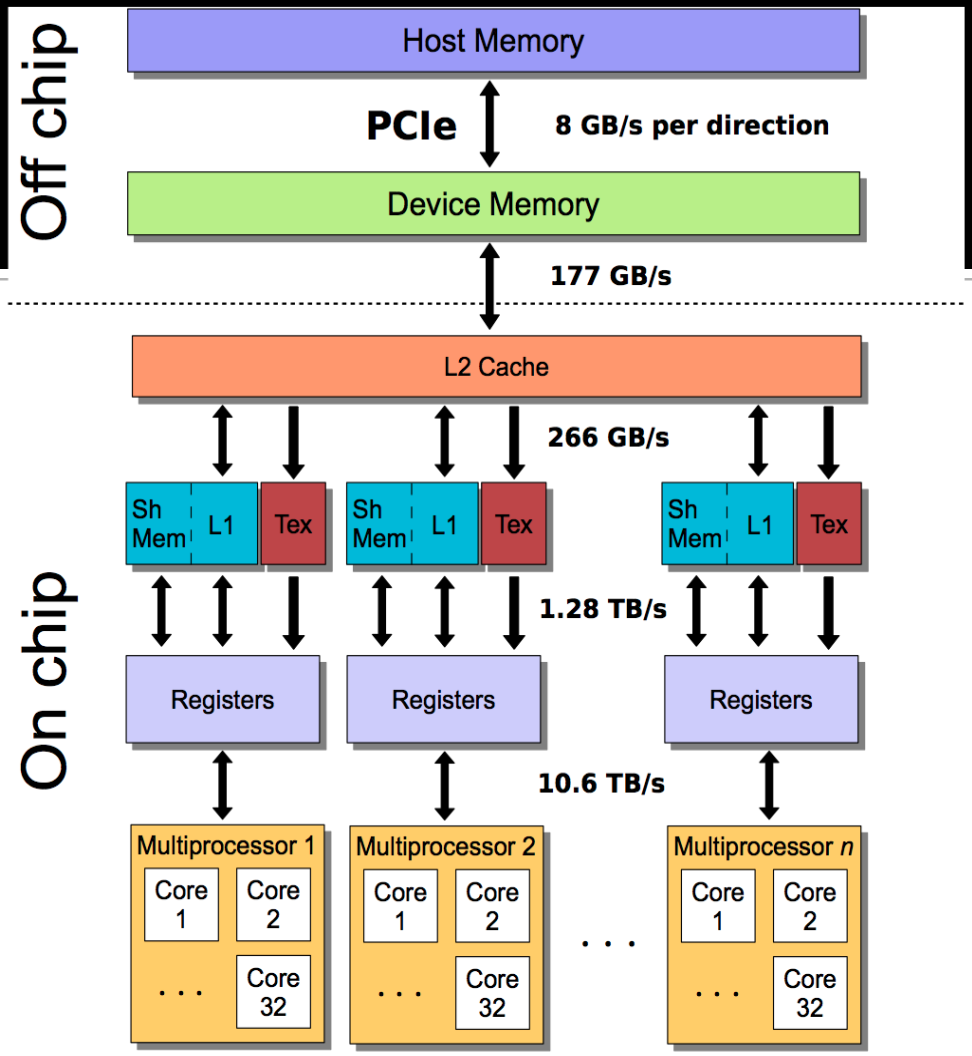

Figure 1: Peak bi-directional bandwidth between various levels of the memory hierarchy on a Tesla M2090.

Additive Schwarz

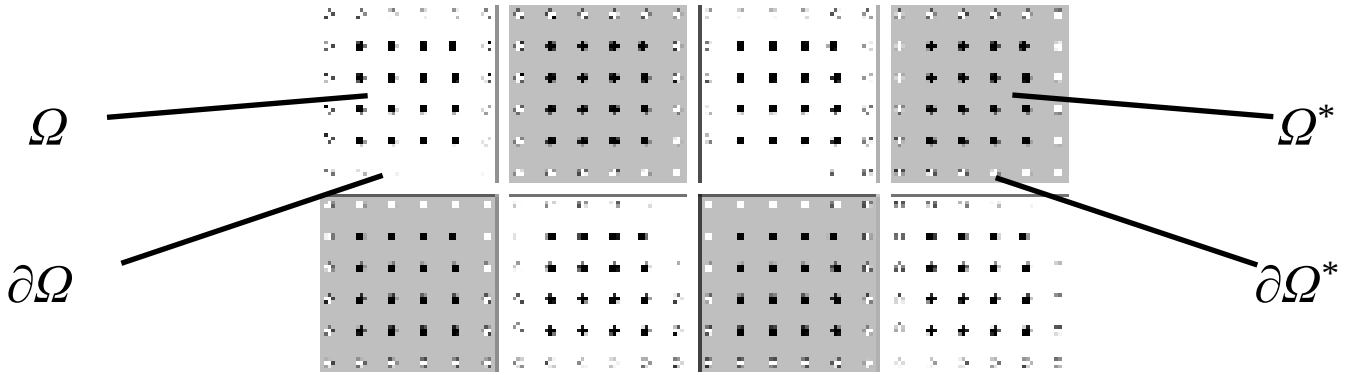

- Update domains simultaneously Block Jacobi
- Expect higher iteration count than multiplicative
- Algorithm is trivially parallel
  - Well suited to GPU architecture

Block Jacobi "DD" on LLNL Edge

Flops versus speedup

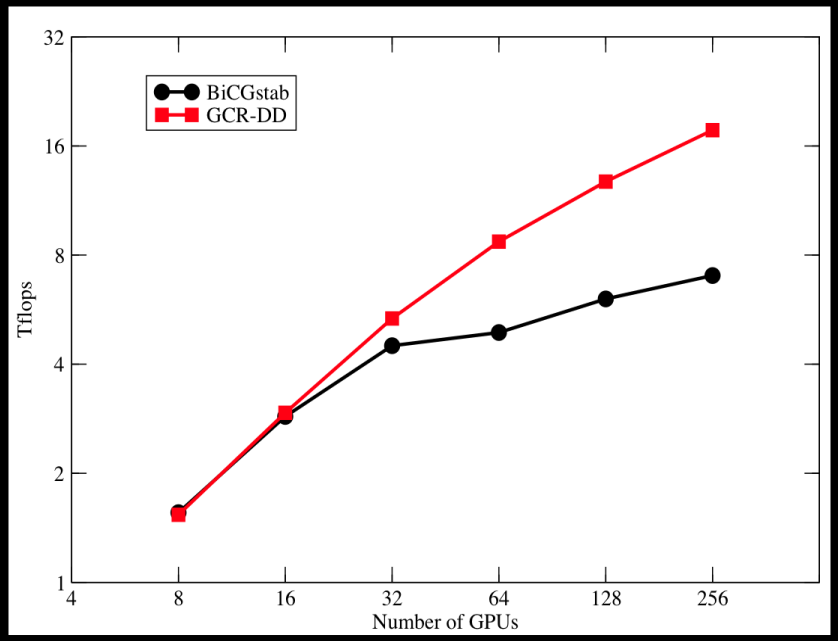

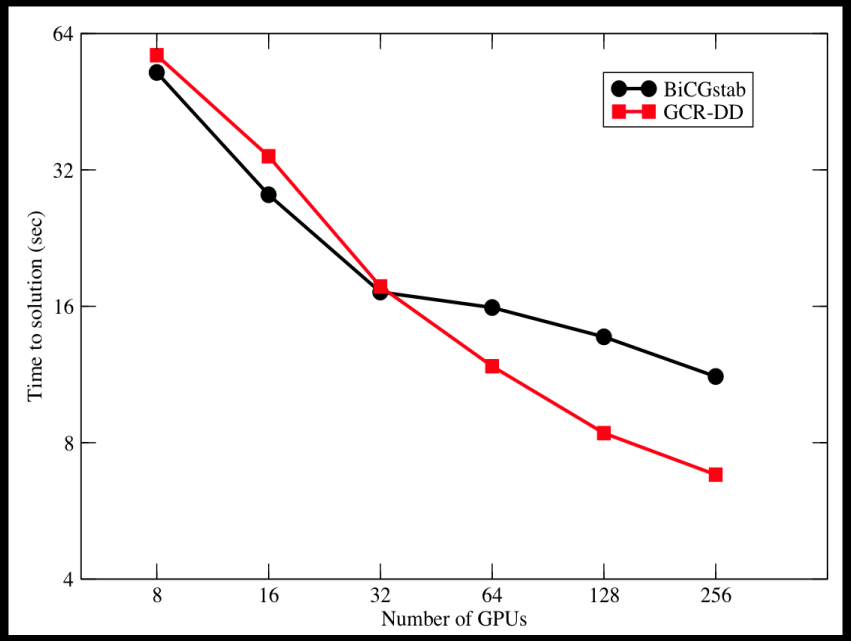

Babich, Clark, Joo, Shi, Brower, Gottlieb, "Scaling Lattice QCD beyond 100 GPUs," SC'11

Compare with Cray: 32K = 64 GPUs

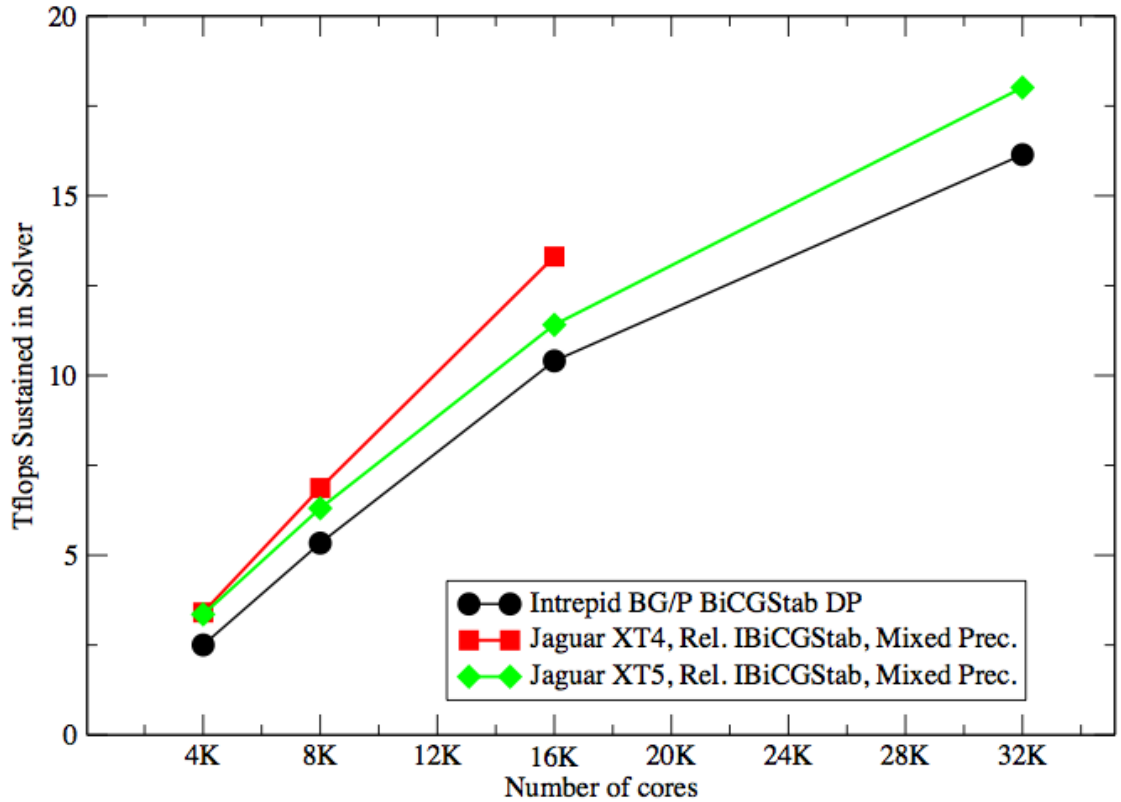

Mike Clark and Balint Joo's Mixed DD GCR Algorithm

Mixed-Precision GCR-DD solver

(Re)Start

$$r_0 = b - Mx$$
$$\hat{r}_0 = r_0$$
$$\hat{x}_0 = 0$$
$$k = 0$$

Generate Subspace

Apply Preconditioner: reduced precision inner solve

$$\hat{p}_k = \hat{K}^{-1}\hat{r}_k$$

Reduced Precision M v

$$\hat{z}_k = \hat{M}\hat{p}_k$$
$$\beta_{i,k} = (\hat{z}_i, \hat{z}_k)$$

Orthogonalize $\hat{z}$-s

$$\gamma_k = ||\hat{z}_k||$$

normalize $\hat{z}_k$

$$\alpha_k = (\hat{z}_k, \hat{r}_k)$$
$$\hat{r}_{k+1} = \hat{r}_k - \alpha_k \hat{z}_k$$
$$k = k + 1$$

repeat for all k or until residuum drops enough or convergence

Update Solution

Solve for χ_l l=k,k-1,...,0:

$$\gamma_l \chi_l \sum_{i=l+1}^{k} \beta_{l,i}\chi_l = \alpha_l$$

Compute correction for x:

$$\hat{x} = \sum_{i=0}^{k-1} \chi_i p_i$$
$$x = x + \hat{x}$$

Full precision restart if not converged

Quantities with ^ are in reduced precision

TitanDev (Balint and Clark)

Benchmarks: + GPU (DD+GCR)

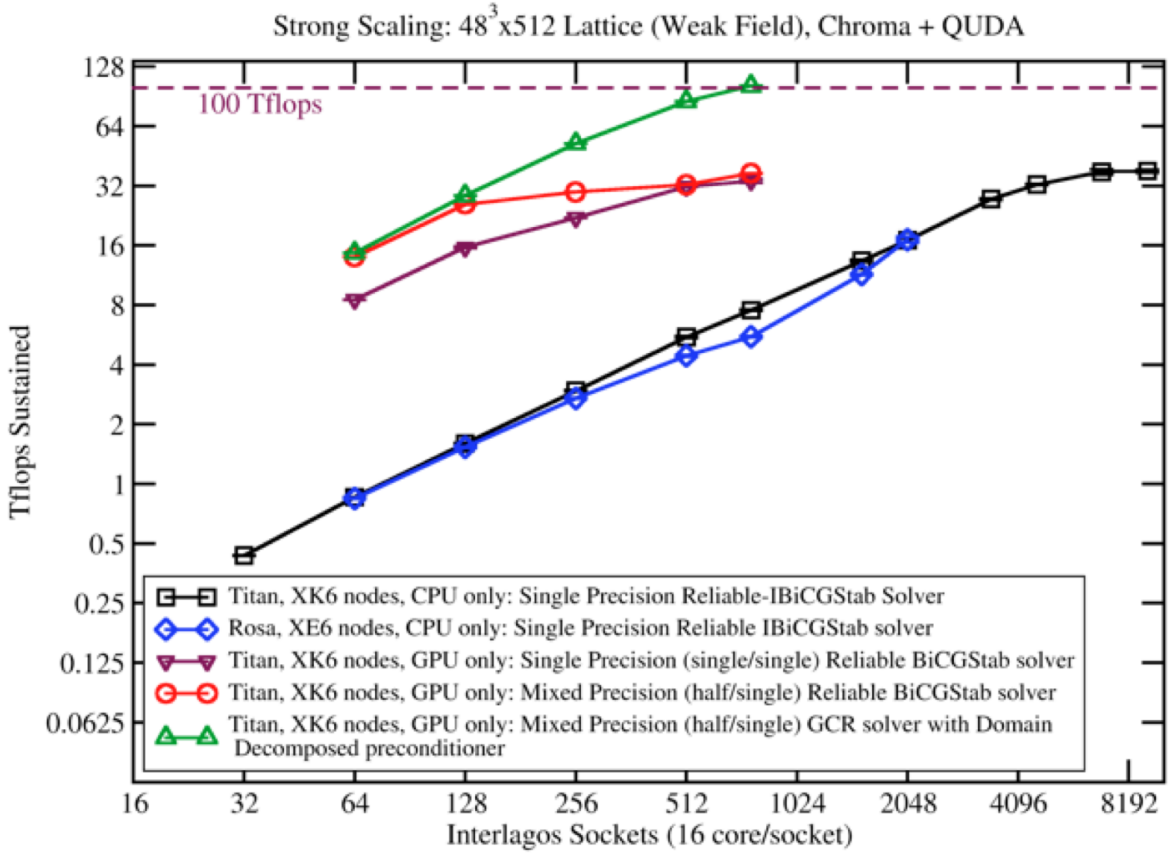

Next Project: MG on GPU

Cost in $s reduced by a at least factor of

100X

GPU O(10x)

MG O(10x)

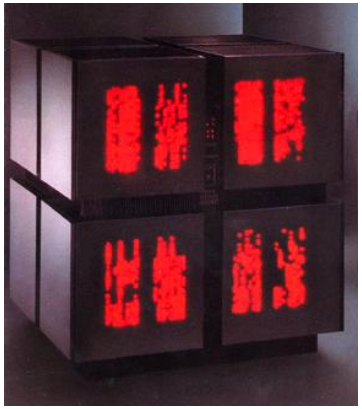

IV. The Future: MG/GPU/DD for HMC

Multigrid for HMC?

- Parallel MG works: When size is too small the common practice is to copy lower levels to all nodes and solver with zero comm.

- Set up can be amortized by refining near null vectors from past or intermittent refresh

- Good for BSM Technicolor HMC! Faster solver encourage optimization with more solves.

Monte Carlo Evolution: Lüscher's intermittently update of S subspace(0710.6417v1)

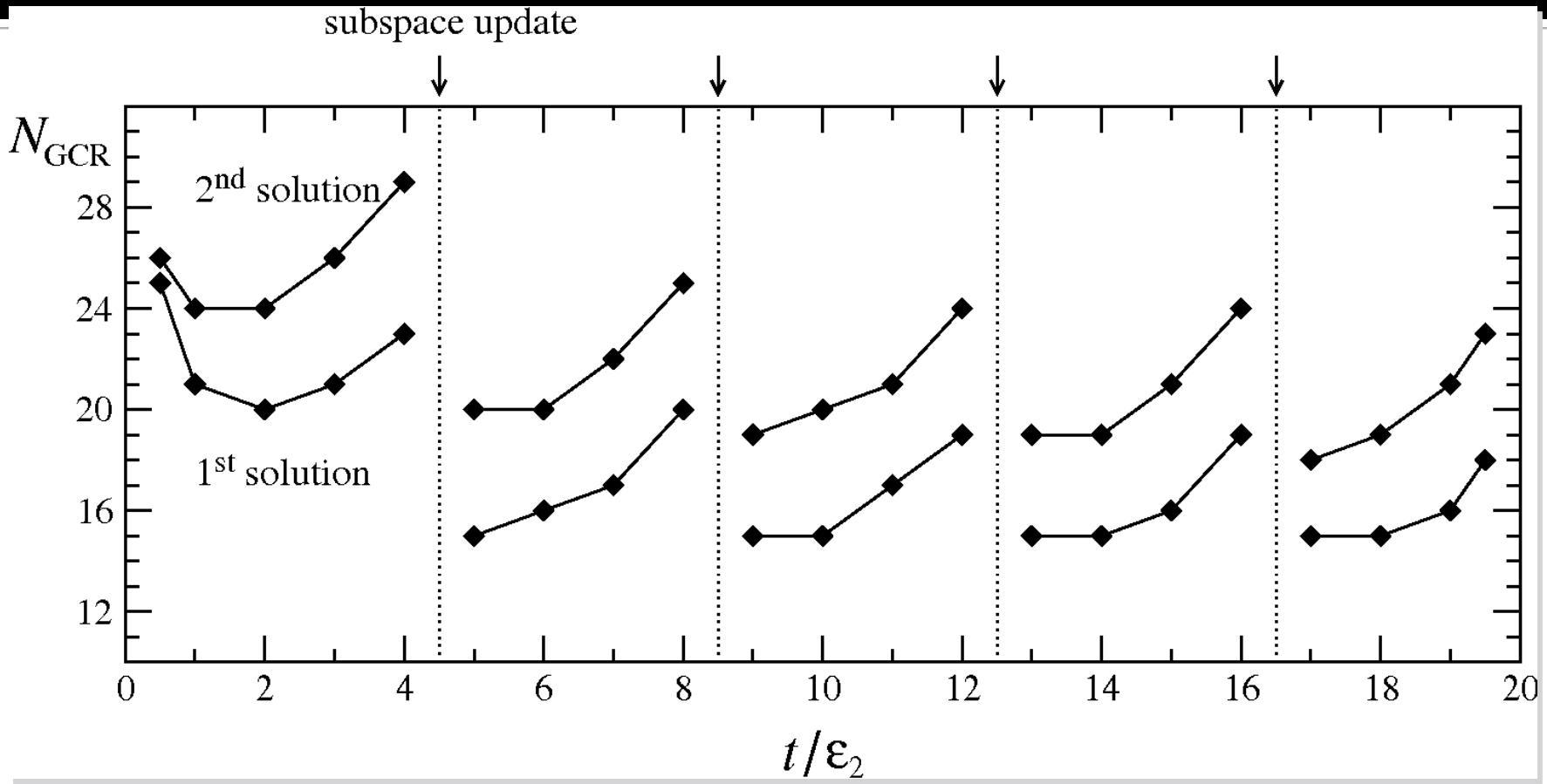

y *Combined with "Chronological Inverter" Brower, Ivaneko, Levi, Orginos*

At Conformal FT: Radial Quantization CFT

- Exact:

$$G(x-y) = \frac{c}{|x-y|^{2\Delta}}$$

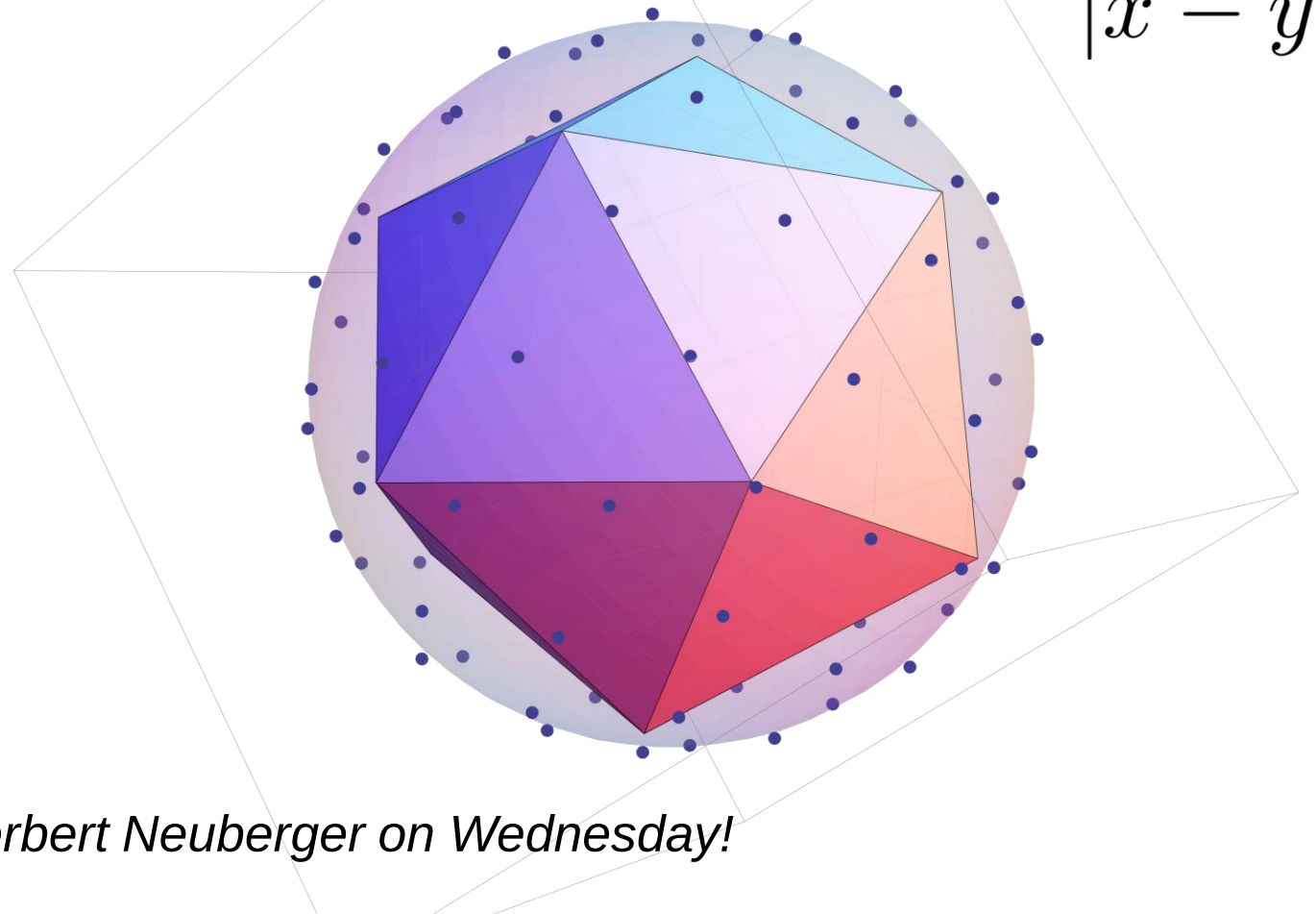

See Herbert Neuberger on Wednesday!

Summary: Multiscale Narrative for Lattice Field Theories

- Past: 1990-2010

  The good olde days of "MPI Data Parallel code" for SPMD algorithms "easily" mapped on to uniform architecture of Beowulf clusters.

- Present 2010-2012

  Transition to high resolution multi-scale QCD and MPI network of threaded multi-core micros

- Future: 2012-2018

  Profound challenges to adapt efficient multi-scale algorithm to a complex heterogeneous architecture with deep memory hierarchies.

FINI

Extra Slide!

NEXT TALK: Domain Wall Multigrid

- 5-d Wilson with "negative mass" and Dirichlet B.C. in 5th "time" interval [o,Ls]
- New Gamma 5: $$\Gamma_5 = \gamma_5 \mathcal{R}(s \leftrightarrow L_s - s)$$
- D is now violently not normal: $$D^\dagger D \neq D D^\dagger$$
- Physical long wavelength mode are low singular (eigen)vectors NOT eigenvectors of D!

A Chiral Fermion

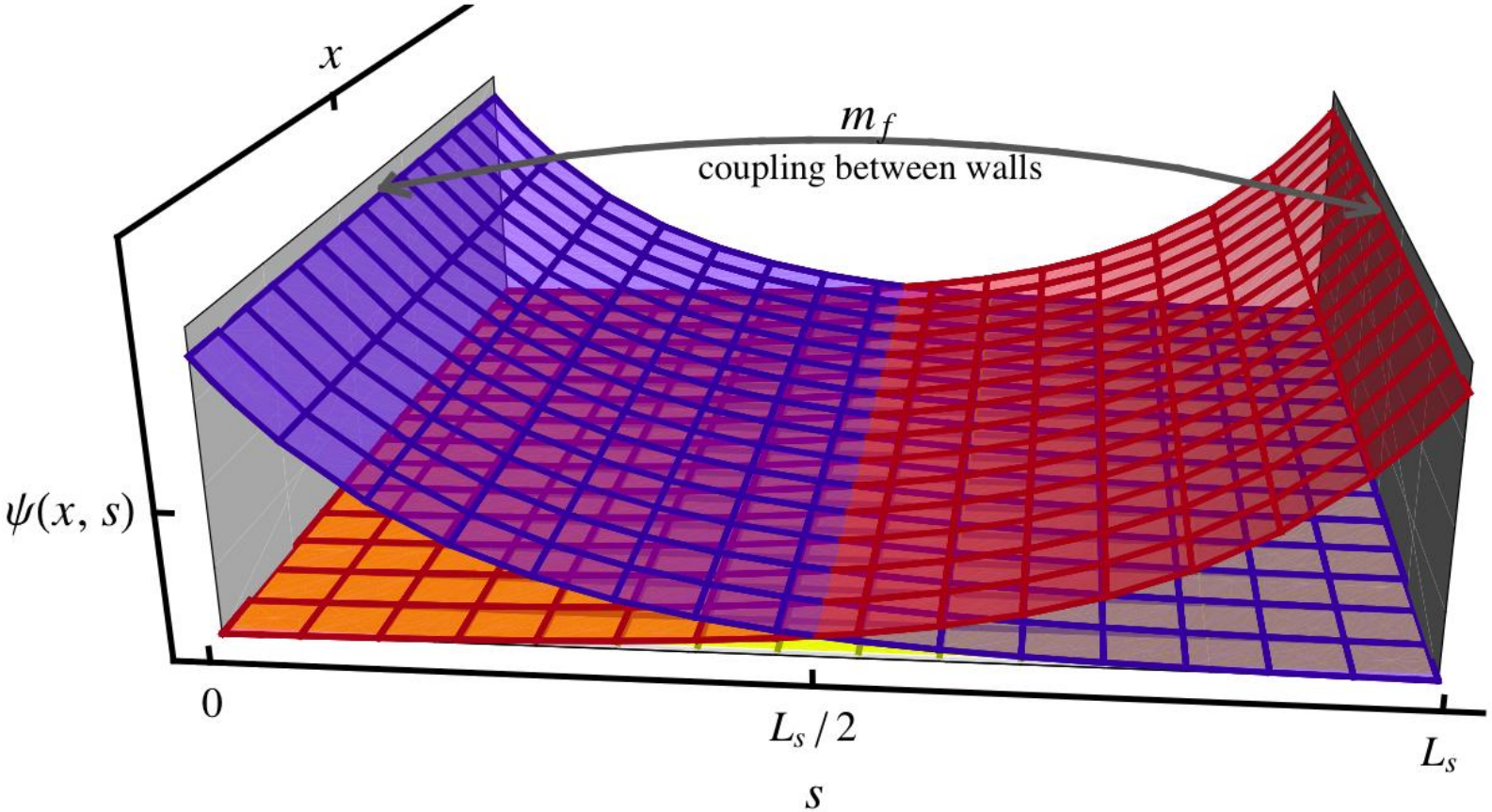

Domain-Wall Operator

Spectrum

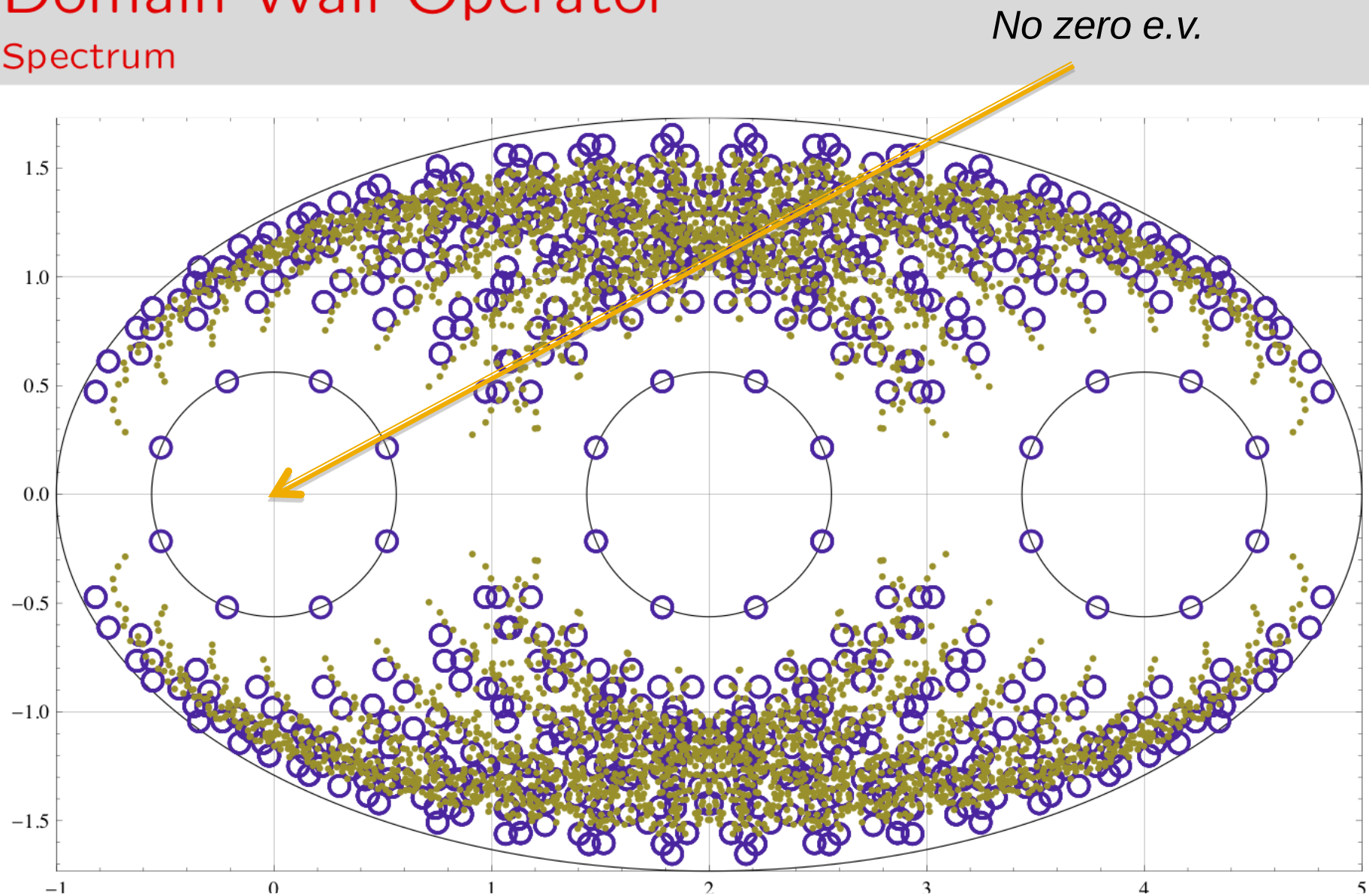

2 + 1 d but 4 + 1 d would have 5 eyes

Some References

- "Adaptive multigrid algorithm for the lattice Wilson-Dirac operator" R. Babich, J. Brannick, R. C. Brower, M. A. Clark, T. Manteuffel, S. McCormick, J. C. Osborn, and C. Rebbi, arXiv:1005.3043v2 [hep-lat], Phys. Rev. Lett. 105, 201602 (2010).
- "Adaptive Multigrid Algorithm for Lattice QCD" J. Brannick, R. C. Brower, M. A. Clark, J. C. Osborn, C. Rebbi, arXiv:0707.4018 Phys. Rev. Lett. 100, 041601 (2008)
- "Multigrid solver for clover fermions", R. Babich, J. Brannick, R. Brower, M. Clark, S. Cohen, J. Os- born and C. Rebbi, Lattice 2010, Villasimius, Sardinia, Italy (2010).
- "The role of multigrid algorithms for LQCD", R. Babich, J. Brannick, R. C. Brower, M. A. Clark, S. D. Cohen, J. C. Osborn and C. Rebbi, PoS **LAT2009, 031 (2009) [arXiv:0912.2186 [hep-lat]].**
- "The removal of critical slowing down", J. Brannick, R. C. Brower, M. A. Clark, S. F. McCormick, T. A. Manteuffel, J. C. Osborn and C. Rebbi, PoS **LATTICE2008, 035 (2008) [arXiv:0811.4331 [hep-lat]].**

- "Algorithms for Lattice Field Theory at Extreme Scales", Richard C. Brower, Ronald , Anthony Kennedy, James Osborn and Claudio Rebbi, SciDAC 2010, Chattanooga, TN (2010).

- "Hadronic Physics using Lattice QCD and GPUs" B. Joo, R. Babich, R. C. Brower, M. A . Clark, J. Chen, J. Dudek, R. G. Edwards, M. J. Peardon, C. Rebbi, D. G. Richards, G. Shi, C. Thomas, W. Watson, USQCD Collaboration and Hadron Spectrum Collaboration, SciDAC 2010, Chattanooga, TN (2010).

- "Solving Lattice QCD systems of equations using mixed precision solvers on GPUs", M. A. Clark, R. Babich, K. Barros, R. C. Brower and C. Rebbi, Comput. Phys. Commun. **181, 1517-1528 (2010) [arXiv:0911.3191 [hep-lat]].**

- "Blasting through lattice calculations using CUDA", K. Barros, R. Babich, R. Brower, M. A. Clark and C. Rebbi, PoS **LATTICE2008, 045 (2008) [arXiv:0810.5365 [hep-lat].**

- "Moebius Algorithm for Domain Wall and GapDW Fermions", R. Brower, R. Babich, K. Orginos,C. Rebbi, D. Schaich and P. Vranas, PoS **LATTICE2008, 034 (2008) [arXiv:0906.2813 [hep-lat]].**

QUDA: QCD on CUDA

- QUDA library http://lattice.bu.edu/quda
- **CG** and **BiCGstab** solvers for Wilson and clover-improved Wilson, **mixed precision** .
- Release 0.3 staggered fermions, contributed by Steve Gottlieb, Guochun Shi, …
- Domain wall (Joel Giedt), twisted mass (contributed by Alexei Strelchenko), and **multi-GPU** …
- Interfaced to Chroma/QDP++, QDP/C, CPS, etc.

MG Dirac Solvers for fun and profit.

Lattice QCD/CFT

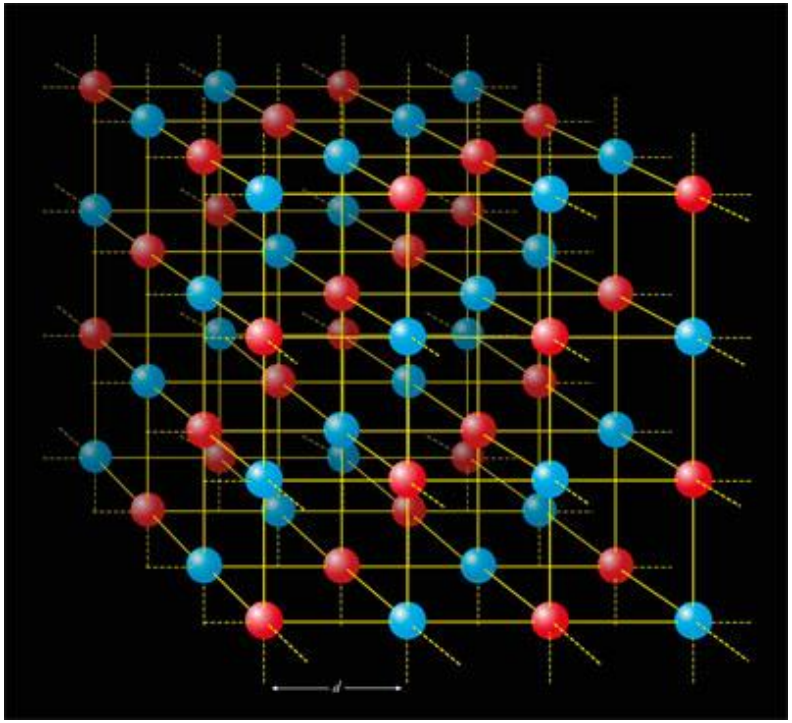

Graphene

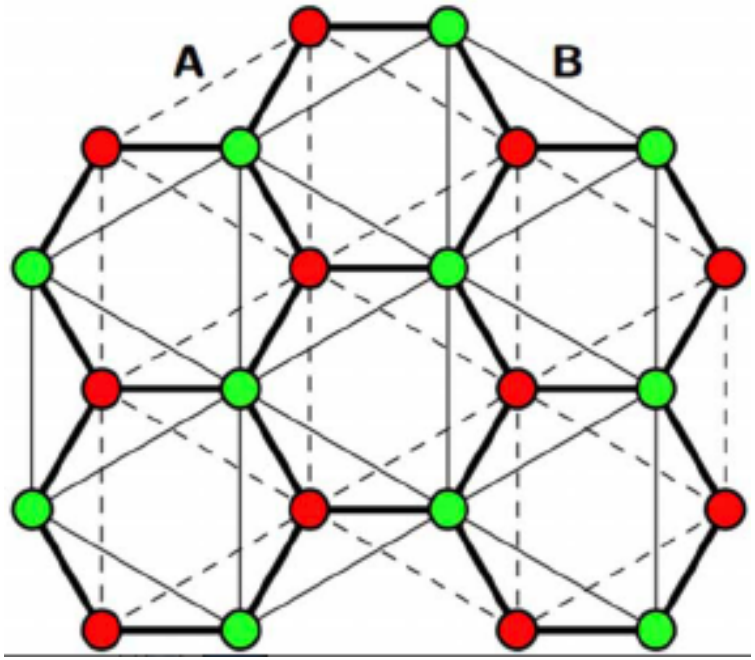

Lack of Critical slowing down:

CG iteration count is insensitive to quark mass and lattice volume!

Lattice volumes

Mass:	$16^3 \times 64$	$24^3 \times 64$	$32^3 \times 96$
-.3980	40	40	41
-.4005	41	41	42
-.4030	42	42	43
-.4055	42	43	43
-.4080	43	44	45
-.4105	44	46	49
-.4130	45	49	52
-.4155	47	54	57
-.4180	50	62	89

m_s (- 0.38922)

Small increase is probably not significant?

physical $m2_{¼}$

Chiral limit: $m2_{¼} = 0$

"Adaptive Multigrid Algorithm for Lattice QCD" J. Brannick, R. C. Brower, M. A. Clark, J. C. Osborn, C. Rebbi, Phys. Rev. Lett. 100, 041601 (2008)

Clover performance (singleprecision)

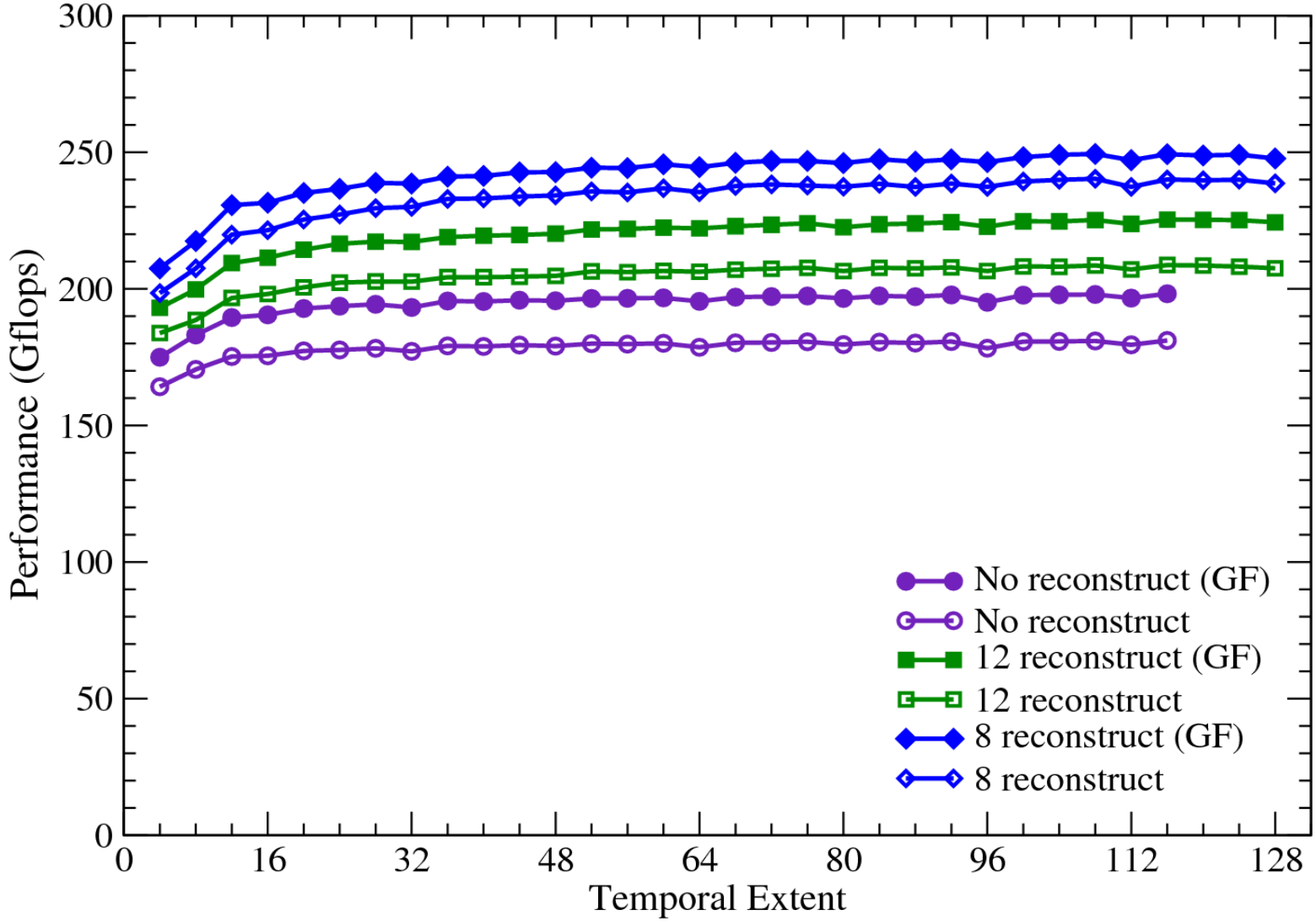

Dslash performance (half precision)

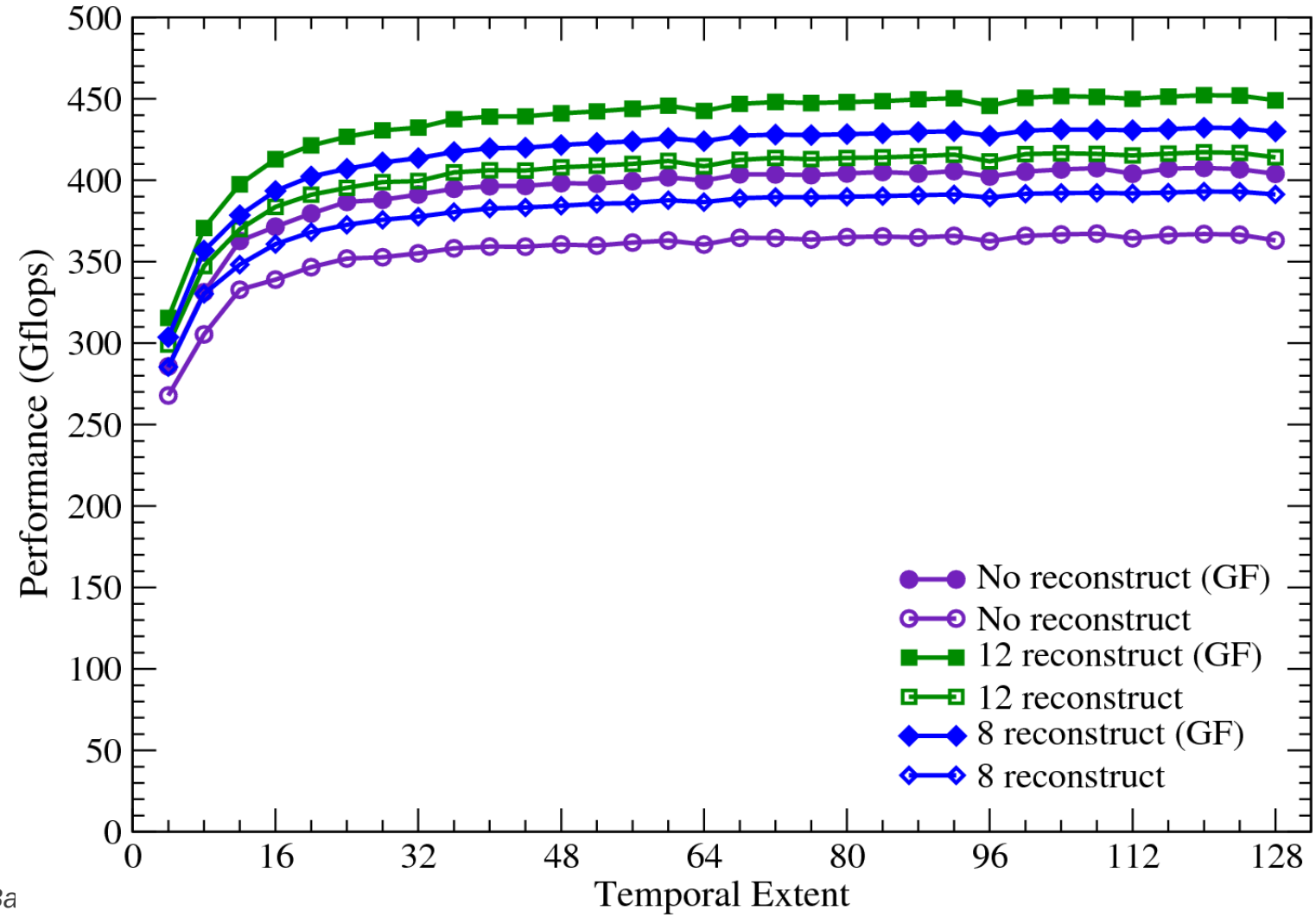

Dslash performance (double precision)

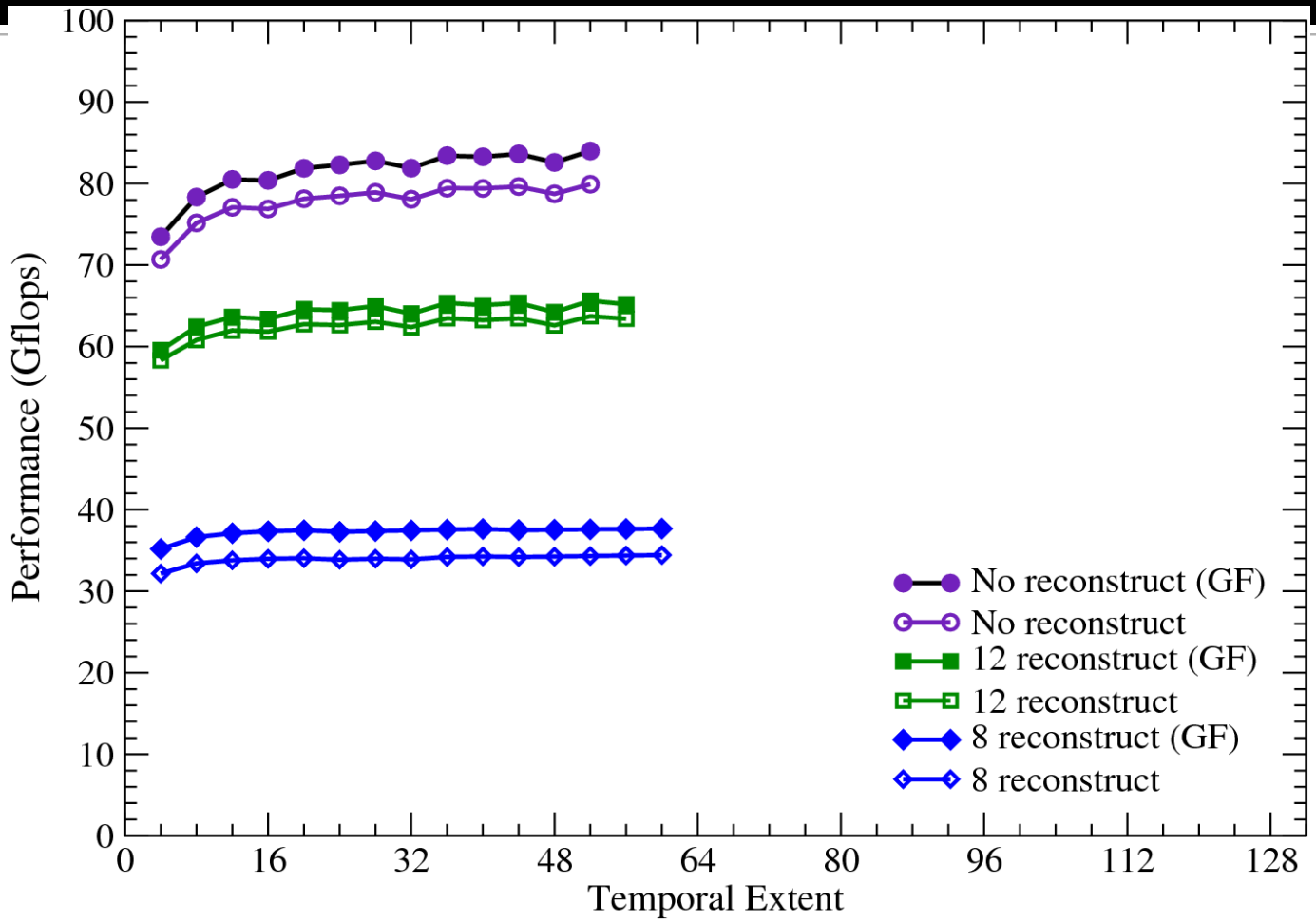

GPUs are in serious use for "analysis"

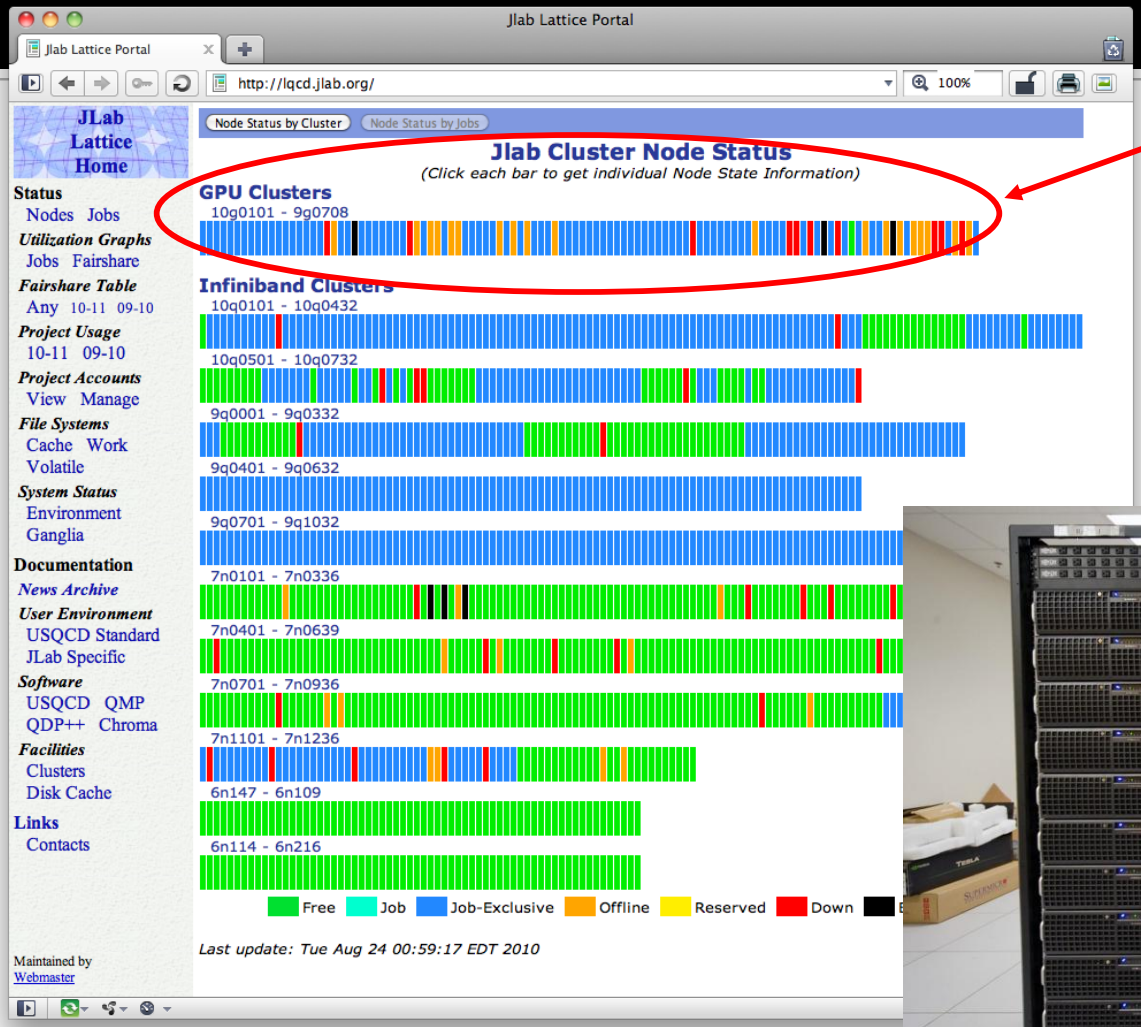

~ 500 GPUs dedicated to LQCD at Jefferson Lab

Can they also make a dent here?

"Intrepid" - Argonne Leadership Computing Facility

QPACE – NIC Juelich

"Jaguar" - Oak Ridge Leadership Computing Facility

ORNL's "Titan" 20 PF System Goals

- Initial 1 PF delivery in 2011, final 20 PF system in 2012
- Designed for science from the ground up
- Similar number of cabinets, cabinet design, and cooling as Jaguar
- Operating system upgrade of today's Linux Operating System
- Gemini interconnect
  - 3-D Torus
  - Globally addressable memory
  - Advanced synchronization features
- New accelerated node design using GPUs
- 20 PF peak performance
  - 9x performance of today's XT5
- Larger memory
- 3x larger and 4x faster file system

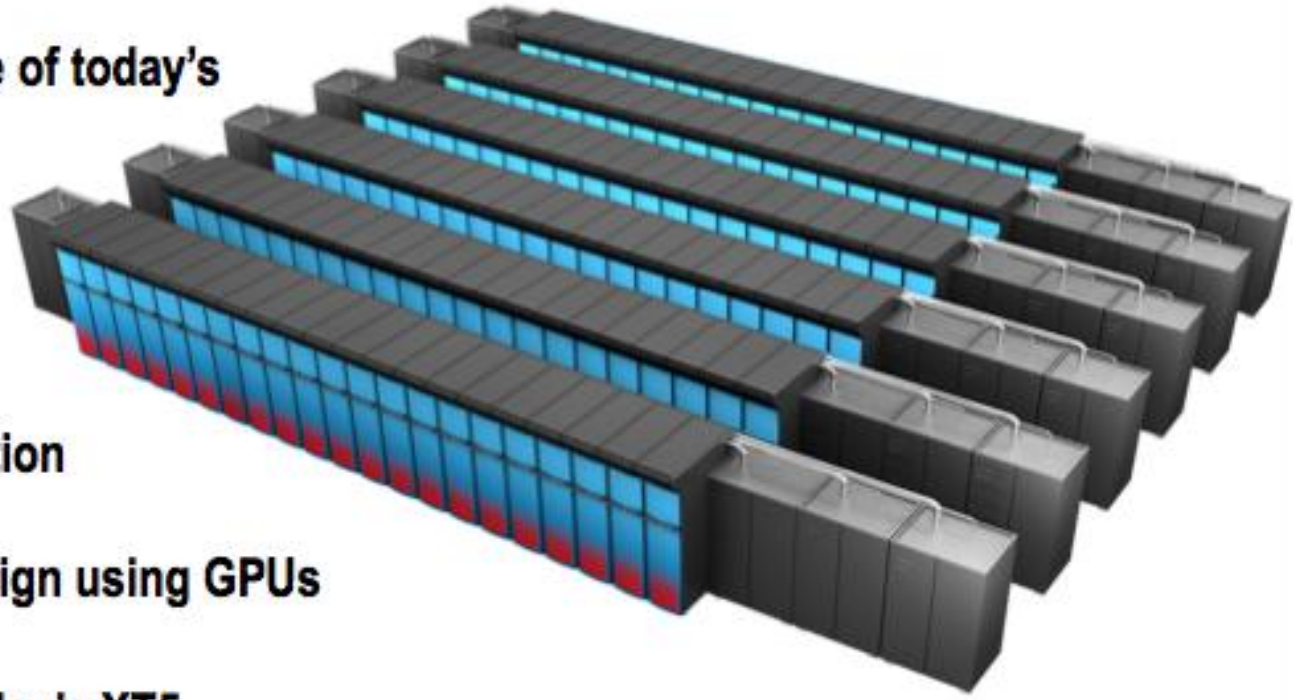

Part III: Future Challenges

- Fermions PDEs are ubiquitous in Quantum Field theories an Nano materials. Lattice geometries and boundary condition present new fun challenges.
  - Finite T lattice (e.g. 32 x speed up on $128^3 \times 96$ lattice*)
  - Old/New RG Geometric /Adaptive Hybrid MG
  - Monte Carlo Evolution of QCD: Sim implicit integrator
  - Conformal Theories for LHC Higgsless models
  - Radial lattices for conform/string duals
  - Domain Wall/Overlap 5-d fore EXACT chirality
  - Conformal Graphene Lagrangian
  - etc etc ...

* has 4.8 x10**9 d.o.f.

NCSA: Blue Waters_2 (post IBM)

- Blue Waters will be composed of more than 235 Cray XE6 cabinets based on the recently announced AMD Opteron™ 6200 Series processor (formerly code-named "Interlagos") and more than 30 cabinets of a future version of the recently announced Cray XK6 supercomputer with NVIDIA® Tesla™ GPU computing capability.

Potential Exascale Architecture Swimlanes

System attributes	2010	"2015"		"2018"	
System peak	2 Peta	200 Petaflop/sec		1 Exaflop/sec	
Power	6 MW	15 MW		20 MW	
System memory	0.3 PB	5 PB		32-64 PB	
Node performance	125 GF	0.5 TF	7 TF	1 TF	10 TF
Node memory BW	25 GB/s	0.1 TB/sec	1 TB/sec	0.4 TB/sec	4 TB/sec
Node concurrency	12	O(100)	O(1,000)	O(1,000)	O(10,000)
System size (nodes)	18,700	50,000	5,000	1,000,000	100,000
Total Node Interconnect BW	1.5 GB/s	20 GB/sec		200 GB/sec	
MTTI	days	O(1day)		O(1 day)	

Source: Andy White and Rick Stevens talk on "A decadal DOE plan for providing exascale applications and technologies for DOE mission needs," DOE ASCAC meeting, March 2010

IBM BG/Q++

CRAY Titan ++

exascale swimlanes

•Stronger scaling on the EDGE

Scaling Lattice QCD beyond 100 GPUs

Authors: R. Babich, M. A. Clark, B. Joó, G. Shi, R. C. Brower, S. Gottlieb

arXiv:1109.2935v1 [hep-lat] and SuperComputing 2011

Byte/flop ratios

- bandwidth to memory, rather than raw floating point throughput.
- We've seen that applying the Wilson Dirac operator (in single precision) requires that we move **1440 bytes** for every **1320 flops**.
- Clover-improved Wilson (Sheikholeslami-Wohlert) is a bit "better" (less memory-bound), at **1728 bytes** and **1824 flops**.
- Asqtad and HISQ are a bit worse, at **1560 bytes** and **1146 flops**.
- Other operations (beyond the matrix-vector product) are often much worse. For example, adding two vectors of length *N* involves reading/writing a total of **12*N* bytes** but consists of only ***N* flops.**

CUDA programming model

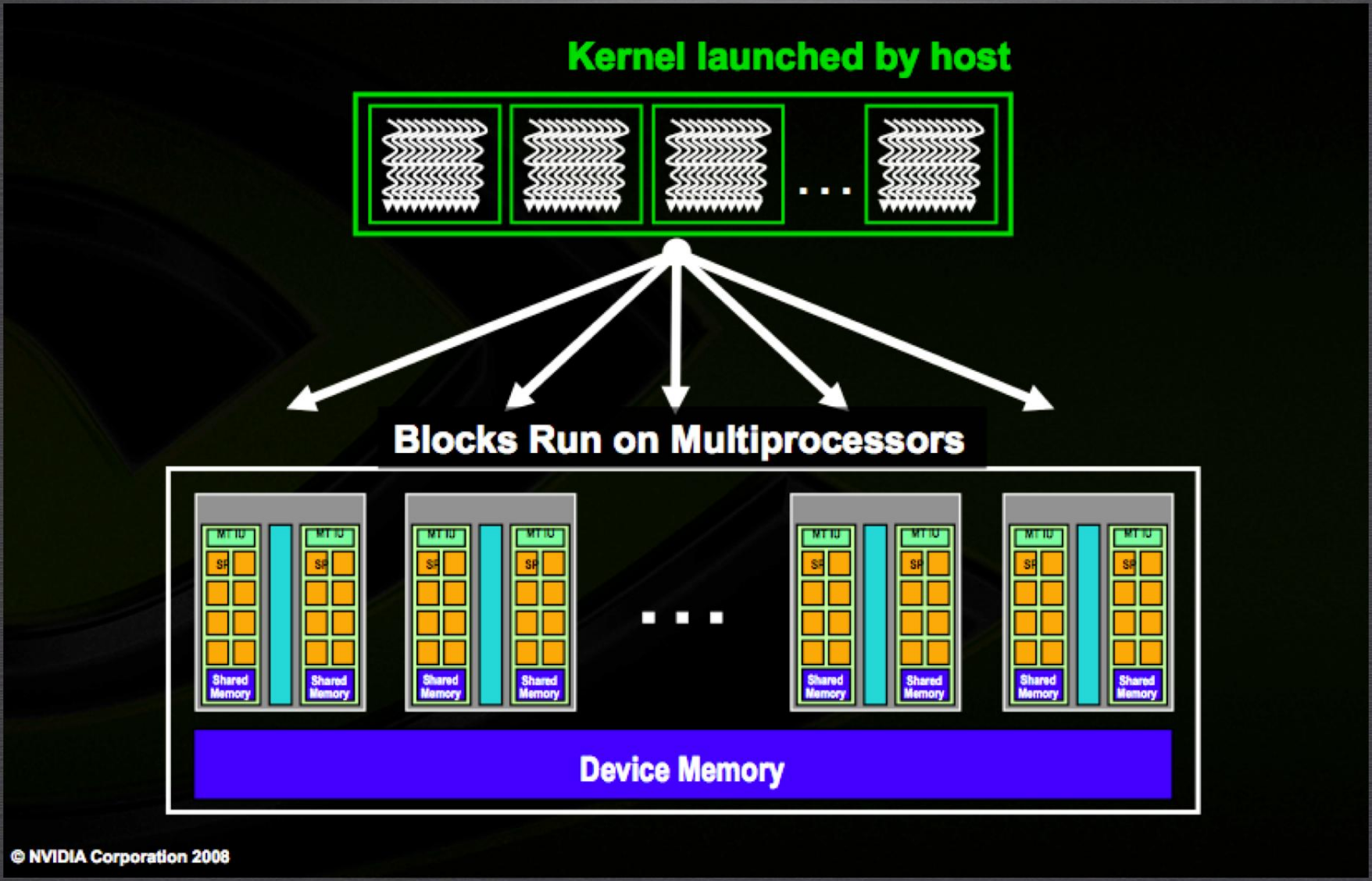

Serial on CPU and Data Parallel on GPU

CUDA Programming

```
void saxpy_serial(int n, float a, float *x, float *y)
{
    for (int i = 0; i < n; ++i)
        y[i] = a*x[i] + y[i];
}
// Invoke serial SAXPY kernel
saxpy_serial(n, 2.0, x, y);
```

Standard C Code

```
__global__ void saxpy_parallel(int n, float a, float *x, float *y)
{
    int i = blockIdx.x*blockDim.x + threadIdx.x;
    if (i < n)  y[i] = a*x[i] + y[i];
}
// Invoke parallel SAXPY kernel with 256 threads/block
int nblocks = (n + 255) / 256;
saxpy_parallel<<<nblocks, 256>>>(n, 2.0, x, y);
```

Parallel C Code

A tale of two processors

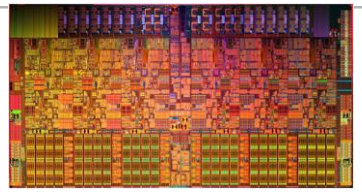

"Gulftown"

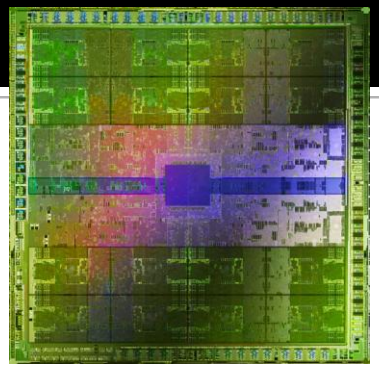

"Fermi"

- **Intel Xeon X5680**
- 6 cores (each with 4-wide SSE unit)
- 1.17 billion transistors
- Shared L3 Cache: 12 MB
- L1+L2: 6 x (320 KB) = 1920 KB
- **160 Gflops (SP)**
- **32 GB/s memory bandwidth**
- up to 288 GB (96 GB is realistic)

- **NVIDIA GeForce GTX 480**
- 480 cores
- 3.0 billion transistors
- Shared L2 Cache: 768 KB
- L1+SM+Reg: 15 x 192 KB = 2880 KB
- **1345 Gflops (SP)**
- **177 GB/s memory bandwidth**
- 1.5 GB (up to 6 GB in Tesla variant)

5:1

7.5:1

Mixed precision with reliable updates

- As discussed yesterday, in the usual method of *iterative refinement* (or "*defect correction*"), the Krylov subspace is thrown away at every restart:

$$
\begin{array}{l}
r_0 = b - Ax_0; \\
k = 0; \\
\textbf{while } ||r_k|| > \epsilon \textbf{ do} \\
\quad \text{Solve } Ap_{k+1} = r_k \text{ to precision } \epsilon^{in}; \\
\quad x_{k+1} = x_k + p_{k+1}; \\
\quad r_{k+1} = b - Ax_{k+1}\ ; \\
\quad k = k + 1; \\
\textbf{end}
\end{array}
$$

An alternative is "*reliable updates*," originally introduced to combat residual drift caused by the erratic convergence of BiCGstab: G. L. G. Sleijpen, and H. A. van der Vorst, "Reliable updated residuals in hybrid Bi-CG methods," Computing 56, 141-164 (1996).

Chiral Symmetry and Residual Mass in Lattice QCD with Domain-Wall Fermions

Ting-Wai Chiu (趙挺偉)
Physics Department
National Taiwan University

"New Horizons for Lattice Computations with Chiral Fermions"
Brookhaven National Laboratory, USA
May 14-18, 2012

Outline

- **Introduction**
- **Axial Ward Idenity in Lattice QCD with ODWF**
- **Generating Functional for n-point Green's Function**
- **A New Formula for the Residual Mass**
- **An Upper Bound for the Residual Mass**
- **Concluding Remarks**

Reference:

Yu-Chih Chen, TWC, "Chiral Symmetry and Residual Mass in Lattice QCD with Optimal Domain-Wall Fermion", in preparation

Domain-Wall Fermions [Kaplan, 1992]

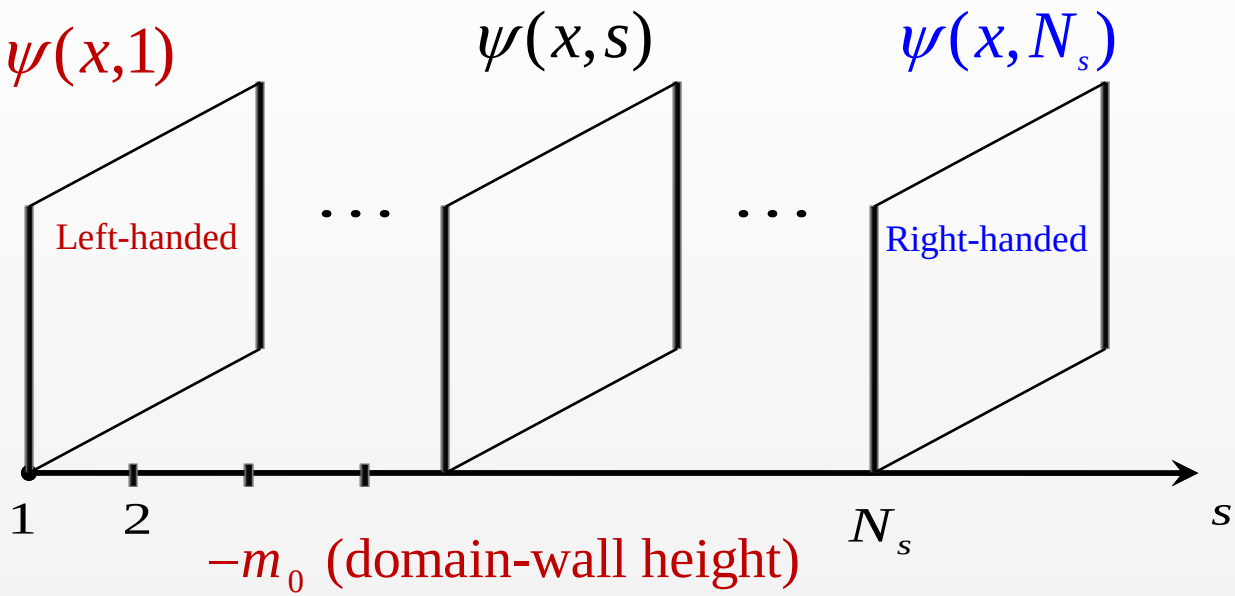

D_{dwf} is a local op. with the nearest neighbor coupling along $\hat{s}$

$$\int [d\bar{\psi}][d\psi]\exp\left(-\bar{\Psi}D_{\text{dwf}}\Psi\right) = \det D_c \qquad D_c = \frac{1+\gamma_5 S}{1-\gamma_5 S}$$

$$N_s \to \infty, \quad S \to \frac{H}{\sqrt{H^2}}, \qquad D_c\gamma_5 + \gamma_5 D_c = 0, \text{ Exact Chiral Sym.}$$

At finite N_s, S is not equal to the optimal rational approx.

Optimal Rational Approximation for Square Root

For the inverse square root function, the optimal rational approx. was obtained by Zolotarev in 1877.

$$\frac{1}{\sqrt{x}},\ x \in [1,b]$$

$$R_Z^{(n-1,n)}(x) = \frac{2\Lambda}{1+\Lambda}\frac{1}{M}\frac{\prod_{l=1}^{n-1}\left(1+x/C_{2l}\right)}{\prod_{l=1}^{n}\left(1+x/C_{2l-1}\right)}$$

$$R_Z^{(n,n)}(x) = \frac{2\lambda}{1+\lambda}\frac{1}{m}\frac{\prod_{l=1}^{n}\left(1+x/c_{2l}\right)}{\prod_{l=1}^{n}\left(1+x/c_{2l-1}\right)}$$

where $\lambda, \Lambda, m, M, C_{2l}, C_{2l-1}, c_{2l}, c_{2l-1}$ are expressed in terms of the Jacobian Elliptic functions.

Yegor **I**vanovich **Zolotarev** (1847 –1878)

Salient Feature of Optimal Rational Approximation

$$1-\sqrt{x}R_Z^{(n,m)}(x)$$

Has $(n+m+2)$ alternate change of sign in $[x_{\min}, x_{\max}]$, and attains its max. and min. (all with equal magnitude)

In the figure, $n = m = 6$ it has 14 alternate change of sign in [1,1000]

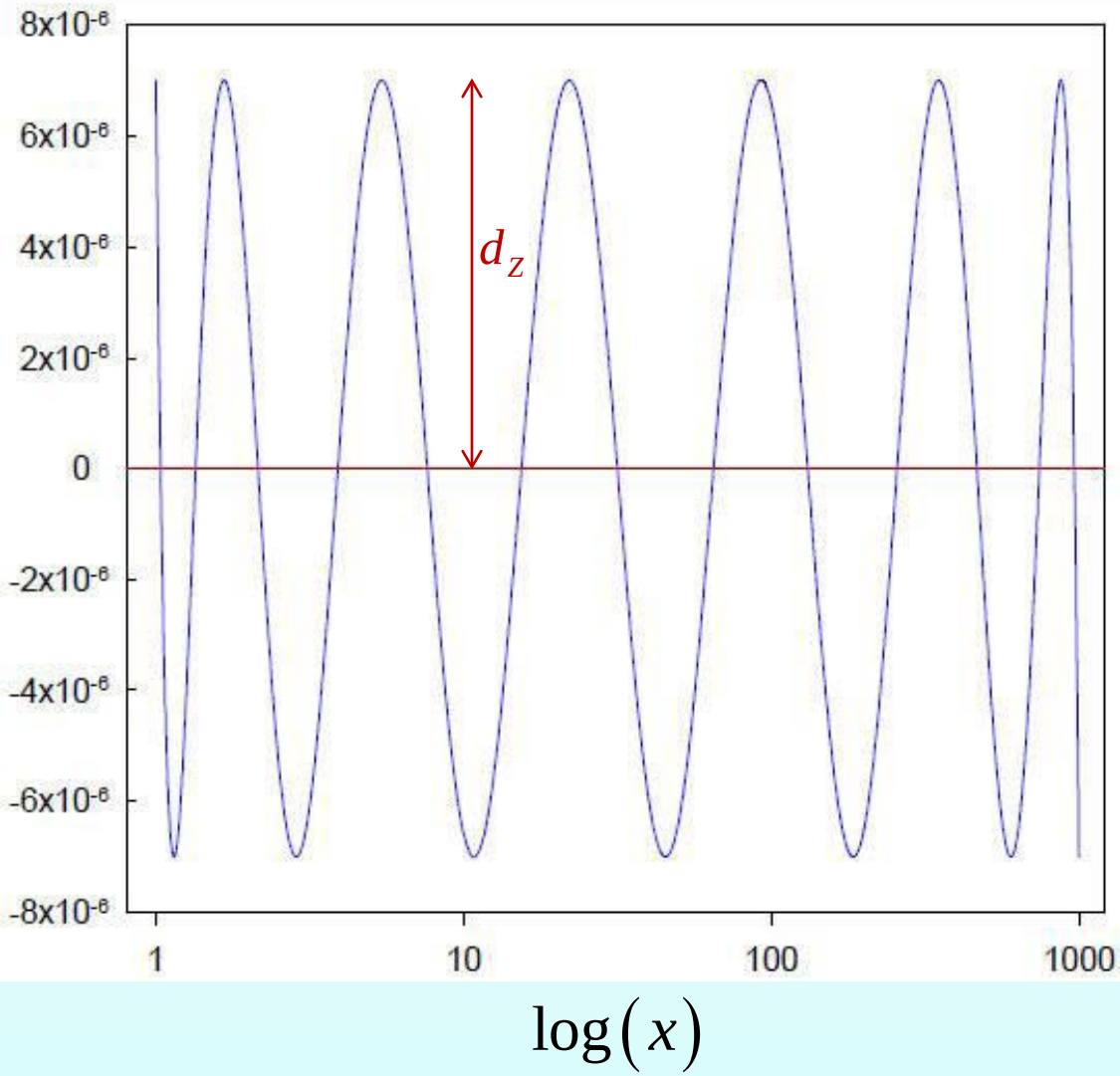

Optimal Domain-Wall Fermion

[TWC, Phys. Rev. Lett. 90 (2003) 071601]

$$A_{\text{odwf}} = \sum_{s,s'=1}^{N_s} \sum_{x,x'} \bar{\psi}_{x,s} \left[\left(I + \rho_s D_w \right)_{x,x'} \delta_{s,s'} - \left(I - \sigma_s D_w \right)_{x,x'} \left(P_- \delta_{s',s+1} + P_+ \delta_{s',s-1} \right) \right] \psi_{x',s'}$$

$$\equiv \bar{\Psi} D_{\text{odwf}} \Psi$$

$$D_w = \sum_{\mu=1}^{4} \gamma_\mu t_\mu + W - m_0, \qquad m_0 \in (0,2)$$

$$t_\mu(x,x') = \frac{1}{2}\left[U_\mu(x) \delta_{x',x+\mu} - U_\mu^\dagger(x') \delta_{x',x-\mu} \right]$$

$$W(x,x') = \sum_{\mu=1}^{4} \frac{1}{2}\left[2\delta_{x,x'} - U_\mu(x) \delta_{x',x+\mu} - U_\mu^\dagger(x') \delta_{x',x-\mu} \right]$$

with boundary conditions

$$P_+ \psi(x,0) = -r m_q P_+ \psi(x,N_s), \qquad m_q\text{: bare quark mass}$$

$$P_- \psi(x,N_s+1) = -r m_q P_- \psi(x,1), \qquad P_\pm = \frac{1}{2}(1 \pm \gamma_5)$$

Optimal Domain-Wall Fermion (cont.)

The action for Pauli-Villars fields is similar to A_{odwf}

$$A_{PV} = \sum_{s,s'=1}^{N_s} \sum_{x,x'} \bar{\phi}_{x,s} \left[\left(I + \rho_s D_w \right)_{x,x'} \delta_{s,s'} - \left(I - \sigma_s D_w \right)_{x,x'} \left(P_- \delta_{s',s+1} + P_+ \delta_{s',s-1} \right) \right] \phi_{x',s'}$$

but with boundary conditions: $P_+ \phi(x,0) = -P_+ \phi(x, N_s),$

$$P_- \phi(x, N_s + 1) = -P_- \phi(x,1)$$

- In the original formulation of ODWF, $\rho_s = \sigma_s = \omega_s$

$$\omega_s = \frac{1}{\lambda_{\min}} \sqrt{1 - \kappa'^2 sn^2(v_s; \kappa')}, \quad s = 1, \cdots, N_s$$

where $sn(v_s; \kappa')$ is the Jacobian elliptic function with argument v_s and modulus $\kappa' = \sqrt{1 - \lambda_{\min}^2 / \lambda_{\max}^2}$,
$\lambda_{\min}^2$ and $\lambda_{\max}^2$ are lower and upper bounds of the eigenvalues of H_w^2

Optimal Domain-Wall Fermion (cont.)

$$\int [d\bar{\psi}][d\psi]\left[d\bar{\phi}\right][d\phi]\exp\left(-A_{\text{odwf}} - A_{\text{PV}}\right) = \det D(m_q)$$

The effective 4D Dirac operator

$$D(m_q) = m_q + \left(m_0 - m_q/2\right)\left[1 + \gamma_5 S_{opt}\left(H_w\right)\right]$$

$$S_{opt}\left(H_w\right) = \frac{1 - \prod_{s=1}^{N_s} T_s}{1 + \prod_{s=1}^{N_s} T_s}, \quad T_s = \frac{1 - \omega_s H_w}{1 + \omega_s H_w}$$

$$= \begin{cases} H_w R_Z^{(n-1,n)}\left(H_w^2\right), & N_s = 2n \\ H_w R_Z^{(n,n)}\left(H_w^2\right), & N_s = 2n+1 \end{cases}$$

Zolotarev optimal rational approximation for $\dfrac{1}{\sqrt{H_w^2}}$

Optimal Domain-Wall Fermion (cont.)

- For $\rho_s = c\omega_s + d,\ \sigma_s = c\omega_s - d,\quad c, d$ (constants)

The effective 4D Dirac operator becomes

$$D(m_q) = m_q + \left(m_0(1 - dm_0) - \frac{m_q}{2} \right)\left[1 + \gamma_5 S_{opt}(H)\right],\quad H = \frac{cH_w}{1 + d\gamma_5 H_w}$$

$$S_{opt}(H) = \frac{1 - \prod_{s=1}^{N_s} T_s}{1 + \prod_{s=1}^{N_s} T_s},\quad T_s = \frac{1 - \omega_s H}{1 + \omega_s H}$$

$$= \begin{cases} HR_Z^{(n-1,n)}(H^2), & N_s = 2n \\ HR_Z^{(n,n)}(H^2), & N_s = 2n+1 \end{cases}$$

only $d = 0$ is good for the projection of low-modes of $D(0)$

Optimal Domain-Wall Fermion (cont.)

- For the special case $\rho_s = 1,\ \sigma_s = 0$

It reduces to the conventional DWF which does not have the optimal chiral symmetry.

$$D(m_q) = m_q + \left(\frac{m_0}{2}(2 - m_0) - \frac{m_q}{2} \right) \left[1 + \gamma_5 S_{\text{polar}}(H) \right], \quad H = \frac{H_w}{2 + \gamma_5 H_w}$$

$$S_{\text{polar}}(H) = \frac{1 - T^{N_s}}{1 + T^{N_s}}, \qquad T = \frac{1 - H}{1 + H}$$

$$b_l = \sec^2\left[\frac{\pi}{N_s}\left(l - \frac{1}{2} \right) \right]$$

$$d_l = \tan^2\left[\frac{\pi}{N_s}\left(l - \frac{1}{2} \right) \right]$$

$$= \begin{cases} H\left(\dfrac{2}{N_s} \displaystyle\sum_{l=1}^{n} \dfrac{b_l}{H^2 + d_l} \right), & N_s = 2n \\ H\left(\dfrac{1}{N_s} + \dfrac{2}{N_s} \displaystyle\sum_{l=1}^{n} \dfrac{b_l}{H^2 + d_l} \right), & N_s = 2n + 1 \end{cases}$$

Polar approximation

Axial Ward Idenity in Lattice QCD with ODWF

$$\mathcal{A}_f = \sum_{s,s'=0}^{N_s+3} \sum_{x,x'} \bar{\psi}_s(x)\{(\rho_s D_w + \mathbb{1})_{x,x'}\delta_{s,s'} + (\sigma_s D_w - \mathbb{1})_{x,x'}(P_-\delta_{s',s+1} + P_+\delta_{s',s-1})\}\psi_{s'}(x')$$

with boundary conditions

$$P_+\psi(x,-1) = -rm_q P_+\psi(x,N_s+3),$$

$$P_-\psi(x,N_s+4) = -rm_q P_-\psi(x,0),$$

Transparent layers:

[TWC, hep-lat/0303008]

$$\rho_0 = \rho_{N_s+3} = \sigma_0 = \sigma_{N_s+3} = 0$$

$$\rho_n = \rho_{n+1} = \sigma_n = \sigma_{n+1} = 0 \qquad n = [N_s/2]$$

The quark fields are defined in terms of the boundary modes

$$q(x) = \sqrt{r}\left[P_-\psi_0(x) + P_+\psi_{N_s+3}(x)\right],$$

$$\bar{q}(x) = \sqrt{r}\left[\bar{\psi}_0(x)P_+ + \bar{\psi}_{N_s+3}(x)P_-\right].$$

Axial Ward Idenity (cont.)

Now we consider N_f flavors of quarks with degenerate mass m_q, and the infinitesimal flavor non-singlet transformation

$$\delta\psi_s(x) = i\theta_s(x)\lambda^a\psi_s(x)$$

$$\delta\bar{\psi}_s(x) = -i\theta_s(x)\lambda^a\bar{\psi}_s(x)$$

$$\theta_s(x) = \begin{cases} \theta(x), & 0 \le s \le n, \;\; n \equiv \left[\frac{N_s}{2}\right], \\ -\theta(x), & n+1 \le s \le N_s + 3. \end{cases}$$

Here λ^a is one of the flavor group generators in the fundamental representation

$$\delta \sum_{s=0}^{N_s+3} \sum_{x,y} \rho_s \left[\bar{\psi}_s(x)\lambda^a D_w(x,y)\psi_s(y)\right] = \sum_x i\theta(x) \sum_\mu \Delta_\mu \hat{j}^a_\mu(x)$$

$$\delta \sum_{s=0}^{N_s+3} \left[-\bar{\psi}_s(x)\lambda^a P_-\psi_{s+1}(x) - \bar{\psi}_s(x)\lambda^a P_+\psi_{s-1}(x)\right] = -\sum_x 2i\theta(x)\left[J^a_5(x,n) + m_q\bar{q}(x)\lambda^a\gamma_5 q(x)\right]$$

$$\delta \sum_{s=0}^{N_s+3} \sum_{x,y} \sigma_s \{\bar{\psi}_s(x)\lambda^a D_w(x,y)[P_-\psi_{s+1}(y) + P_+\psi_{s-1}(y)]\} = \sum_x i\theta(x) \sum_\mu \Delta_\mu \hat{k}^a_\mu(x)$$

Axial Ward Idenity (cont.)

$$J_5^a(x,n) = -\bar{\psi}_n(x)\lambda^a P_- \psi_{n+1}(x) + \bar{\psi}_{n+1}(x)\lambda^a P_+ \psi_n(x)$$

$$\hat{j}_\mu^a(x) \equiv \sum_{s=1}^{N_s+2} \mathrm{sign}\left(n - s + \frac{1}{2}\right) j_\mu^a(x,s)$$

$$j_\mu^a(x,s) = \frac{\rho_s}{2}\left[\bar{\psi}_s(x)\lambda^a(1-\gamma_\mu)U_\mu(x)\psi_s(x+\mu) - \bar{\psi}_s(x+\mu)\lambda^a(1+\gamma_\mu)U_\mu^\dagger(x)\psi_s(x)\right]$$

$$\hat{k}_\mu^a(x) \equiv \hat{k}_\mu^{a+}(x) + \hat{k}_\mu^{a-}(x),$$

$$\hat{k}_\mu^{a\pm}(x) \equiv \sum_{s=1}^{N_s+2} \mathrm{sign}\left(n - s + \frac{1}{2}\right) k_\mu^{a\pm}(x,s)$$

$$k_\mu^{a\pm}(x,s) = \frac{\sigma_s}{2}\left[\bar{\psi}_s(x)\lambda^a(1-\gamma_\mu)U_\mu(x)P_\pm\psi_{s\mp1}(x+\mu) - \bar{\psi}_s(x+\mu)\lambda^a(1+\gamma_\mu)U_\mu^\dagger(x)P_\pm\psi_{s\mp1}(x)\right]$$

$$J_\mu^a(x) \equiv \hat{k}_\mu^a(x) + \hat{j}_\mu^a(x)$$

$$\Delta_\mu f(x,s) \equiv f(x,s) - f(x-\mu,s)$$

Axial Ward Idenity (cont.)

For any observable $\mathcal{O}$, $\delta^a \langle \mathcal{O} \rangle = 0$, which gives the axial Ward identity

$$\Delta_\mu \langle J^a_\mu(x)\mathcal{O}(y)\rangle = 2m_q \langle \bar{q}(x)\lambda^a\gamma_5 q(x)\mathcal{O}(y)\rangle + 2\langle J^a_5(x,n)\mathcal{O}(y)\rangle + i\langle \delta^a \mathcal{O}(y)\rangle$$

As $N_s \to \infty$, the anomalous term $\langle J^a_5(x,n)\mathcal{O}(y)\rangle$ vanishes if $\mathcal{O}(y)$ only involves the quark fields [Furman & Shamir, 1995]

After summing over all sites x

$$-i\sum_x \langle \delta^a \mathcal{O}(y)\rangle = 2m_q \sum_x \langle \bar{q}(x)\lambda^a\gamma_5 q(x)\mathcal{O}(y)\rangle + 2\sum_x \langle J^a_5(x,n)\mathcal{O}(y)\rangle$$

Thus, the effect of chiral symmetry breaking due to finite N_s can be regarded as an additive mass to the bare quark mass m_q, the so-called residual mass

$$m_{res}[\mathcal{O}(y)] = \frac{\sum_x \langle J^a_5(x,n)\mathcal{O}(y)\rangle}{\sum_x \langle \bar{q}(x)\lambda^a\gamma_5 q(x)\mathcal{O}(y)\rangle}$$

dependent on O, and y

Axial Ward Idenity (cont.)

Summing over all sites y in the AWI gives the global residual mass

$$M_{res}[\mathcal{O}] = \frac{\sum_{x,y}\langle J_5^a(x,n)\mathcal{O}(y)\rangle}{\sum_{x,y}\langle \bar{q}(x)\lambda^a\gamma_5 q(x)\mathcal{O}(y)\rangle}$$

For $\mathcal{O}(y) = \bar{q}(y)\lambda^b\gamma_5 q(y)$ pseudoscalar

$$m_{res}(y) = \frac{\sum_{x}\langle J_5^a(x,n)\bar{q}(y)\lambda^b\gamma_5 q(y)\rangle}{\sum_{x}\langle \bar{q}(x)\lambda^a\gamma_5 q(x)\bar{q}(y)\lambda^b\gamma_5 q(y)\rangle}$$ local

$$M_{res} = \frac{\sum_{x,y}\langle J_5^a(x,n)\bar{q}(y)\lambda^b\gamma_5 q(y)\rangle}{\sum_{x,y}\langle \bar{q}(x)\lambda^a\gamma_5 q(x)\bar{q}(y)\lambda^b\gamma_5 q(y)\rangle}$$ global

which are usually used as a measure of the chiral symmetry breaking due to finite N_s

Generating Functional for n-point Green's Function

Use the transformation

$$\eta_s = (P_-\delta_{s',s} + P_+\delta_{s',s-1})\psi_{s'} \Leftrightarrow \psi_s = (P_-\delta_{s',s} + P_+\delta_{s',s+1})\eta_{s'}$$

$$\bar{\eta}_s = \bar{\psi}_s\gamma_5 Q^s_- \Leftrightarrow \bar{\psi}_s = \bar{\eta}_s(Q^s_-)^{-1}\gamma_5$$

$$Q^s_\pm \equiv \rho_s H_w P_\pm + \sigma_s H_w P_\mp \pm 1$$

$$T_s = -(Q^s_+)^{-1}Q^s_- = \frac{1-H_s}{1+H_s}$$

$$H_s = (\rho_s + \sigma_s)H_w[2 + (\rho_s - \sigma_s)\gamma_5 H_w]^{-1}$$

$$\begin{aligned}\mathcal{A}_f &= \bar{\eta}_0(P_- - rm_q P_+)\eta_0 - \bar{\eta}_0\eta_0 + \sum_{s=1}^{N_s+2}[\bar{\eta}_s\eta_s - \bar{\eta}_s T_s^{-1}\eta_{s+1}] \\ &\quad + \bar{\eta}_{N_s+3}\eta_{N_s+3} - \bar{\eta}_{N_s+3}(P_+ - rm_q P_-)\eta_0,\end{aligned}$$

Generating Functional (cont.)

Including external sources

$$\bar{\eta}_n J_n + \bar{J}_{n+1}\eta_{n+1} + \bar{\eta}_{n+1} J_{n+1},$$

$$\bar{J}_q q + \bar{q} J_q = \bar{J}\eta_0 - \bar{\eta}_0 P_+ J + \bar{\eta}_{N_s+3} P_- J,$$

$$J \equiv \sqrt{r} J_q$$

$$\bar{J} \equiv \sqrt{r} \bar{J}_q$$

$$Z[J_q, \bar{J}_q, J_n, J_{n+1}, \bar{J}_{n+1}] = \mathcal{J} \int [d\bar{\eta}][d\eta] e^{-S_J}$$

$$S_J = \mathcal{A}_f - \bar{J}\eta_0 + \bar{\eta}_0 P_+ J - \bar{\eta}_n J_n - \bar{J}_{n+1}\eta_{n+1} - \bar{\eta}_{n+1} J_{n+1} - \bar{\eta}_{N_s+3} P_- J$$

$\mathcal{J}$ is the Jacobian of the transformation

$$\mathcal{J} = \prod_{s=0}^{N_s+3} \det[\gamma_5(\rho_s H_w P_- + \sigma_s H_w P_+ - 1)]$$

Generating Functional (cont.)

Integrating $(\eta_s, \bar{\eta}_s)$ successively from $s = N_s + 3$ to $s = 0$:

$$Z[J_q, \bar{J}_q, J_n, J_{n+1}, \bar{J}_{n+1}]$$

$$= K \det[r(D_c + m_q)] \exp\Big\{ \bar{J}_{n+1} T_U^{-1} P_- J + \bar{J}_{n+1} J_{n+1} + \\ + \left[\bar{J} + \bar{J}_{n+1} T_U^{-1}(P_+ - r m_q P_-)\right] (r D_c + r m_q)^{-1} \left[J + \widehat{T}^{-1} J_n + \widehat{T}^{-1} J_{n+1}\right] \Big\}$$

$$T_L^{-1} \equiv \prod_{s=1}^{n} T_s^{-1}$$

$$T_U^{-1} \equiv \prod_{s=n+1}^{N_s+2} T_s^{-1}$$

$$T^{-1} \equiv \prod_{s=1}^{N_s+2} T_s^{-1} = T_L^{-1} T_U^{-1}$$

$$\widehat{T}^{-1} \equiv \left(-P_+ + T^{-1} P_-\right)^{-1} T_L^{-1}$$

$$K \equiv \mathcal{J} \det\left[-P_+ + T^{-1} P_-\right]$$

$$D_c = \frac{1}{r} \frac{1 + \gamma_5 S}{1 - \gamma_5 S}$$

$$S = \frac{1 - \prod_{s=0}^{N_s+3} T_s}{1 + \prod_{s=0}^{N_s+3} T_s}$$

$$T_s = \frac{1 - H_s}{1 + H_s}$$

$$H_s = (\rho_s + \sigma_s) H_w [2 + (\rho_s - \sigma_s) \gamma_5 H_w]^{-1}$$

Generating Functional (cont.)

(I) The valence quark propagator

$$\langle q(x)\bar{q}(y)\rangle = -\frac{1}{Z}\frac{\delta^2 Z}{\delta\bar{J}_q(x)\delta J_q(y)}\bigg|_0 = (D_c + m_q)^{-1}(x,y)$$

(II) The mixed correlator of the first kind

$$\begin{aligned}\langle q(x)\bar{\eta}_n(y)\rangle &= -\frac{1}{Z}\frac{\delta^2 Z}{\delta\bar{J}_q(x)\delta J_n(y)}\bigg|_0 \\ &= \sqrt{r}(rD_c + rm_q)^{-1}\left(-P_+ + T^{-1}P_-\right)^{-1} T_L^{-1} \\ &= -\frac{1}{\sqrt{r}}D^{-1}(m_q)\gamma_5\frac{T_L^{-1}}{T^{-1}+1}\end{aligned}$$

$$D^{-1}(m_q) = (1 + rD_c)(D_c + m_q)^{-1} = r + (1 - rm_q)(D_c + m_q)^{-1}$$

the sea quark propagator.

Generating Functional (cont.)

(III) The mixed correlator of the second kind

$$\begin{aligned}\langle q(x)\bar{\eta}_{n+1}(y)\rangle &= -\frac{1}{Z}\frac{\delta^2 Z}{\delta\bar{J}_q(x)\delta J_{n+1}(y)}\bigg|_0 \\ &= \sqrt{r}(rD_c + rm_q)^{-1}\left(-P_+ + T^{-1}P_-\right)^{-1}T_L^{-1} \\ &= -\frac{1}{\sqrt{r}}D^{-1}(m_q)\gamma_5\frac{T_L^{-1}}{T^{-1}+1} = \langle q(x)\bar{\eta}_n(y)\rangle.\end{aligned}$$

(IV) The mixed correlator of the third kind

$$\begin{aligned}\langle \eta_{n+1}(x)\bar{q}(y)\rangle &= -\frac{1}{Z}\frac{\delta^2 Z}{\delta\bar{J}_{n+1}(x)\delta J_q(y)}\bigg|_0 \\ &= T_U^{-1}(-rm_qP_- + P_+)(rD_c + rm_q)^{-1}\sqrt{r} + T_U^{-1}P_-\sqrt{r} \\ &= T_U^{-1}\frac{1}{2\sqrt{r}}\left(1 + \frac{1+rm_q}{1-rm_q}\gamma_5\right)D^{-1}(m_q) - \frac{\sqrt{r}}{1-rm_q}T_U^{-1}\gamma_5\end{aligned}$$

A New Formula for the Residual Mass

$$m_{res}(y) = \frac{\sum_x \langle J_5^a(x,n)\bar{q}(y)\lambda^b\gamma_5 q(y)\rangle}{\sum_x \langle \bar{q}(x)\lambda^a\gamma_5 q(x)\bar{q}(y)\lambda^b\gamma_5 q(y)\rangle}$$

$$\sum_x \langle \bar{q}(x)\lambda^a\gamma_5 q(x)\bar{q}(y)\lambda^b\gamma_5 q(y)\rangle$$
$$= -\mathrm{tr}_F(\lambda^a\lambda^b)\mathrm{tr}_{DC}\{[(D_c+m_q)^{-1}]^\dagger(D_c+m_q)^{-1}\}(y,y)$$

$$\sum_x \langle J_5^a(x,n)\bar{q}(y)\lambda^b\gamma_5 q(y)\rangle$$

$$J_5^a(x,n) = -\bar{\psi}_n(x)\lambda^a P_-\psi_{n+1}(x) + \bar{\psi}_{n+1}(x)\lambda^a P_+\psi_n(x)$$

$$= \mathrm{tr}(\lambda^a\lambda^b)\left\{\sum_x \mathrm{tr}[\langle q(y)\bar{\psi}_n(x)\rangle P_-\langle\psi_{n+1}(x)\bar{q}(y)\rangle\gamma_5] - \sum_x \mathrm{tr}[\langle q(y)\bar{\psi}_{n+1}(x)\rangle P_+\langle\psi_n(x)\bar{q}(y)\rangle\gamma_5]\right\}$$
$$= \mathrm{tr}(\lambda^a\lambda^b)\sum_x \mathrm{tr}[\langle q(y)\bar{\eta}_n(x)\rangle\langle\eta_{n+1}(x)\bar{q}(y)\gamma_5\rangle]$$
$$= -\mathrm{tr}(\lambda^a\lambda^b)\frac{1}{4r}\mathrm{tr}\{[D^{-1}(m_q)]^\dagger(1-S^2)D^{-1}(m_q)](y,y)$$

A New Formula for the Residual Mass

$$m_{res}(y) = \frac{\sum_x \langle J_5^a(x,n)\bar{q}(y)\lambda^b\gamma_5 q(y)\rangle}{\sum_x \langle \bar{q}(x)\lambda^a\gamma_5 q(x)\bar{q}(y)\lambda^b\gamma_5 q(y)\rangle}$$

$$= \frac{1}{4r}\frac{\mathrm{tr}\{[D^{-1}(m_q)]^\dagger(1-S^2)D^{-1}(m_q)\}(y,y)}{\mathrm{tr}\{[(D_c+m_q)^{-1}]^\dagger(D_c+m_q)^{-1}\}(y,y)}$$

$D^{-1}(m_q) = r + (1 - rm_q)(D_c + m_q)^{-1}$: sea quark propagator

$(D_c + m_q)^{-1}$: valence quark propagator

$$M_{res} = \frac{1}{4r}\frac{\mathrm{Tr}\{[D^{-1}(m_q)]^\dagger(1-S^2)D^{-1}(m_q)\}}{\mathrm{Tr}\{[(D_c+m_q)^{-1}]^\dagger(D_c+m_q)^{-1}\}}$$

However, it is tedious to use these formulas to compute the residual mass since they involve the multiplication of

$$S = (1 - \prod_s T_s)(1 + \prod_s T_s)^{-1} = H\sum_{i=1}^n b_i(H^2 + d_i)^{-1}$$

to the columns of the sea-quark propagator, requiring multi-shift CG.

A New Formula for the Residual Mass (cont.)

$$\mathrm{tr}\{[D^{-1}(m_q)]^\dagger(1-S^2)D^{-1}(m_q)\}(y,y)$$

$$= \mathrm{tr}\left\{[D^{-1}(m_q)]^\dagger D^{-1}(m_q)\right\}(y,y) - \mathrm{tr}\left\{[SD^{-1}(m_q)]^\dagger(SD^{-1}(m_q))\right\}(y,y)$$

Using

$$S = \gamma_5\left[2r\frac{D(m_q)-m_q}{1-rm_q} - 1\right]$$

$$\begin{aligned} SD(m_q)^{-1} &= \gamma_5\left[\frac{2r}{1-rm_q} - \frac{1+rm_q}{1-rm_q}D(m_q)^{-1}\right] \\ &= \gamma_5\left[r-(1+rm_q)(D_c+m_q)^{-1}\right]. \end{aligned}$$

$$\begin{aligned} &\mathrm{tr}\left\{[SD^{-1}(m_q))]^\dagger(SD^{-1}(m_q)\right\}(y,y) \\ &= r^2\mathrm{tr}\,\mathbb{I} - 2r(1+rm_q)\mathrm{Re}\ \mathrm{tr}(D_c+m_q)^{-1}(y,y) \\ &\qquad +(1+rm_q)^2\mathrm{tr}\{[(D_c+m_q)^{-1}]^\dagger(D_c+m_q)^{-1}\}(y,y). \end{aligned}$$

A New Formula for the Residual Mass (cont.)

Using

$$D^{-1}(m_q) = (1 + rD_c)(D_c + m_q)^{-1} = r + (1 - rm_q)(D_c + m_q)^{-1}$$

$$\begin{aligned}
&\mathrm{tr}\left\{[D^{-1}(m_q)]^\dagger D^{-1}(m_q)\right\}(y,y) \\
&= r^2 \mathrm{tr}\,\mathbb{I} + 2r(1 - rm_q)\mathrm{Re}\ \mathrm{tr}(D_c + m_q)^{-1}(y,y) \\
&\qquad + (1 - rm_q)^2 \mathrm{tr}\left\{[(D_c + m_q)^{-1}]^\dagger (D_c + m_q)^{-1}\right\}(y,y)
\end{aligned}$$

Thus

$$\mathrm{tr}\{[D^{-1}(m_q)]^\dagger (1 - S^2) D^{-1}(m_q)\}(y,y)$$

$$= 4r\ \mathrm{Re}\ \mathrm{tr}\{(D_c + m_q)^{-1}(y,y)\} - 4rm_q \mathrm{tr}\{[(D_c + m_q)^{-1}]^\dagger (D_c + m_q)^{-1}\}(y,y)$$

$$\boxed{m_{res}(y) = \frac{\mathrm{Re}\ \mathrm{tr}\{(D_c + m_q)^{-1}(y,y)\}}{\mathrm{tr}\{[(D_c + m_q)^\dagger (D_c + m_q)]^{-1}(y,y)\}} - m_q}$$

which immediately gives the residual mass once the 12 columns of $(D_c + m_q)^{-1}(x,y)$ have been computed.

An Upper Bound for the Global Residual Mass

$$M_{res} = \frac{1}{4r}\frac{\mathrm{Tr}\{[D^{-1}(m_q)]^\dagger(1-S^2)D^{-1}(m_q)\}}{\mathrm{Tr}\{[(D_c+m_q)^{-1}]^\dagger(D_c+m_q)^{-1}\}}$$

$$= \frac{\mathrm{Re}\ \mathrm{Tr}\{(D_c+m_q)^{-1}\}}{\mathrm{Tr}\{[(D_c+m_q)^\dagger(D_c+m_q)]^{-1}\}} - m_q$$

$$\mathrm{Tr}\{[D(m_q)^{-1}]^\dagger(1-S^2)D^{-1}(m_q)\} = \mathrm{Tr}\{(1-S^2)(D^\dagger D)^{-1}(m_q)\} \leq \sum_j \alpha_j\beta_j$$

von Neumann's trace inequality

α_j and β_j are the eigenvalues of $(1-S^2)$ and $(D^\dagger D)^{-1}(m_q)$ respectively

For ODWF, $S = S_{opt}$, $|\alpha_j| \leq 2d_Z$. Thus

$$\mathrm{Tr}\{[D(m_q)^{-1}]^\dagger(1-S_{opt}^2)D^{-1}(m_q)\} \leq 2d_Z\mathrm{Tr}\{(D^\dagger D)^{-1}(m_q)\}.$$

An Upper Bound for the Residual Mass (cont.)

$$M_{res} \leq \frac{d_Z}{2r} \frac{\mathrm{Tr}\{[D(m_q)^{-1}]^\dagger D^{-1}(m_q)\}}{\mathrm{Tr}\{[(D_c+m_q)^{-1}]^\dagger (D_c+m_q)^{-1}\}}$$

$\because$ $$D^{-1}(m_q) = (1+rD_c)(D_c+m_q)^{-1} = r + (1-rm_q)(D_c+m_q)^{-1}$$

$\therefore$ $$\lambda_j = r + (1-rm_q)\xi_j$$

ξ_j is a singular value of $(D_c+m_q)^{-1}$

λ_j is the corresponding singular value of $D^{-1}(m_q)$

$\therefore$ $$\frac{\sum_j |\lambda_j|^2}{\sum_j |\xi_j|^2} = (1-rm_q)^2 + 2r(1-rm_q)\frac{\langle \mathrm{Re}(\xi)\rangle}{\langle |\xi|^2\rangle} + \frac{r^2}{\langle |\xi|^2\rangle}$$

$$\langle |\xi|^2\rangle = \frac{1}{N}\sum_{j=1}^{N} |\xi_j|^2, \quad \langle \mathrm{Re}(\xi)\rangle = \frac{1}{N}\sum_{j=1}^{N} \mathrm{Re}(\xi_j)$$

N is the total number of singular values of $(D_c+m_q)^{-1}$

An Upper Bound for the Residual Mass (cont.)

$$\therefore \quad \frac{\mathrm{Tr}\{[D(m_q)^{-1}]^\dagger D^{-1}(m_q)\}}{\mathrm{Tr}\{[(D_c+m_q)^{-1}]^\dagger (D_c+m_q)^{-1}\}} = (1-rm_q)^2 + 2r(1-rm_q)\frac{\langle \mathrm{Re}(\xi)\rangle}{\langle|\xi|^2\rangle} + \frac{r^2}{\langle|\xi|^2\rangle}$$

$$\Rightarrow \quad M_{res} \le \frac{d_Z}{2r}\left[(1-rm_q)^2 + 2r(1-rm_q)\frac{\langle \mathrm{Re}(\xi)\rangle}{\langle|\xi|^2\rangle} + \frac{r^2}{\langle|\xi|^2\rangle}\right]$$

Thus, to obtain the upper bound of M_{res} amounts to working out

(i) an upper bound for $\langle \mathrm{Re}(\xi)\rangle / \langle|\xi|^2\rangle$

(ii) a lower bound for $\langle|\xi|^2\rangle$

It can be shown that

$$\frac{\langle \mathrm{Re}(\xi)\rangle}{\langle|\xi|^2\rangle} \le m + \frac{(1+m)d_Z}{2-(3-m)d_Z}$$

$$\langle|\xi|^2\rangle \ge \frac{r^2}{1+m}\left[\frac{2-(3-m)d_Z}{2m+(1-m)^2 d_Z}\right]$$

An Upper Bound for the Residual Mass (cont.)

$$M_{res} \leq \frac{d_Z}{2r}\left\{(1-rm_q)^2 + 2r(1-rm_q)\left[rm_q + \frac{(1+rm_q)d_Z}{2-(3-rm_q)d_Z}\right] + (1+rm_q)\left[\frac{2rm_q + (1-rm_q)^2 d_Z}{2-(3-rm_q)d_Z}\right]\right\}$$

For light quarks, $rm_q \ll 1$

$$M_{res} \leq \frac{d_Z}{2r}$$

For ODWF, $d_Z \ll 1$ in most cases

$$M_{res} \leq \frac{d_Z}{2r}\left[(1+2r^2m_q)^2(1-rm_q) + 2r^2m_q^2\right] \equiv \frac{d_Z}{2r}F(r,m_q)$$

$$M_{res}[d_Z/(2r)]^{-1} = F(r,m_q)$$

An Upper Bound for the Residual Mass (cont.)

It is clear that the derivation also goes through for the conventional DWF with nonzero weights $\rho_s = c_1(\text{constant})$ and $\sigma_s = c_2(\text{constant})$

by replacing $||1 - S_{opt}|| \leq d_Z$ with $||1 - S_{polar}|| < \Delta_{max}$

Δ_{max} can be determined for given λ_{min} and λ_{max}

$$M_{res} \leq \frac{\Delta_{max}}{2r} \left\{ (1 - rm_q)^2 + 2r(1 - rm_q) \left[rm_q + \frac{(1 + rm_q)\Delta_{max}}{2 - (3 - rm_q)\Delta_{max}} \right] + (1 + rm_q) \left[\frac{2rm_q + (1 - rm_q)^2 \Delta_{max}}{2 - (3 - rm_q)\Delta_{max}} \right] \right\}$$

if Δ_{max} is sufficiently small

$$M_{res}[\Delta_{max}/(2r)]^{-1} \approx F(r, m_q)$$

universal for any DWF

An Upper Bound for the Residual Mass (cont.)

How does the residual mass depend on the quark mass ?

Consider $\rho_s = c\omega_s + d$, $\sigma_s = c\omega_s - d$, with

$$H = cH_w(1 + d\gamma_5 H_w)^{-1},\ r = [2m_0(1 - dm_0)]^{-1}$$

(i) $c = 1,\ d = 0,\ H = H_w,\ r = 1/(2m_0)$

(ii) $c = 1/2,\ d = 1/2,\ H = H_w(2 + \gamma_5 H_w)^{-1},\ r = [m_0(2 - m_0)]^{-1}$

An Upper Bound for the Residual Mass (cont.)

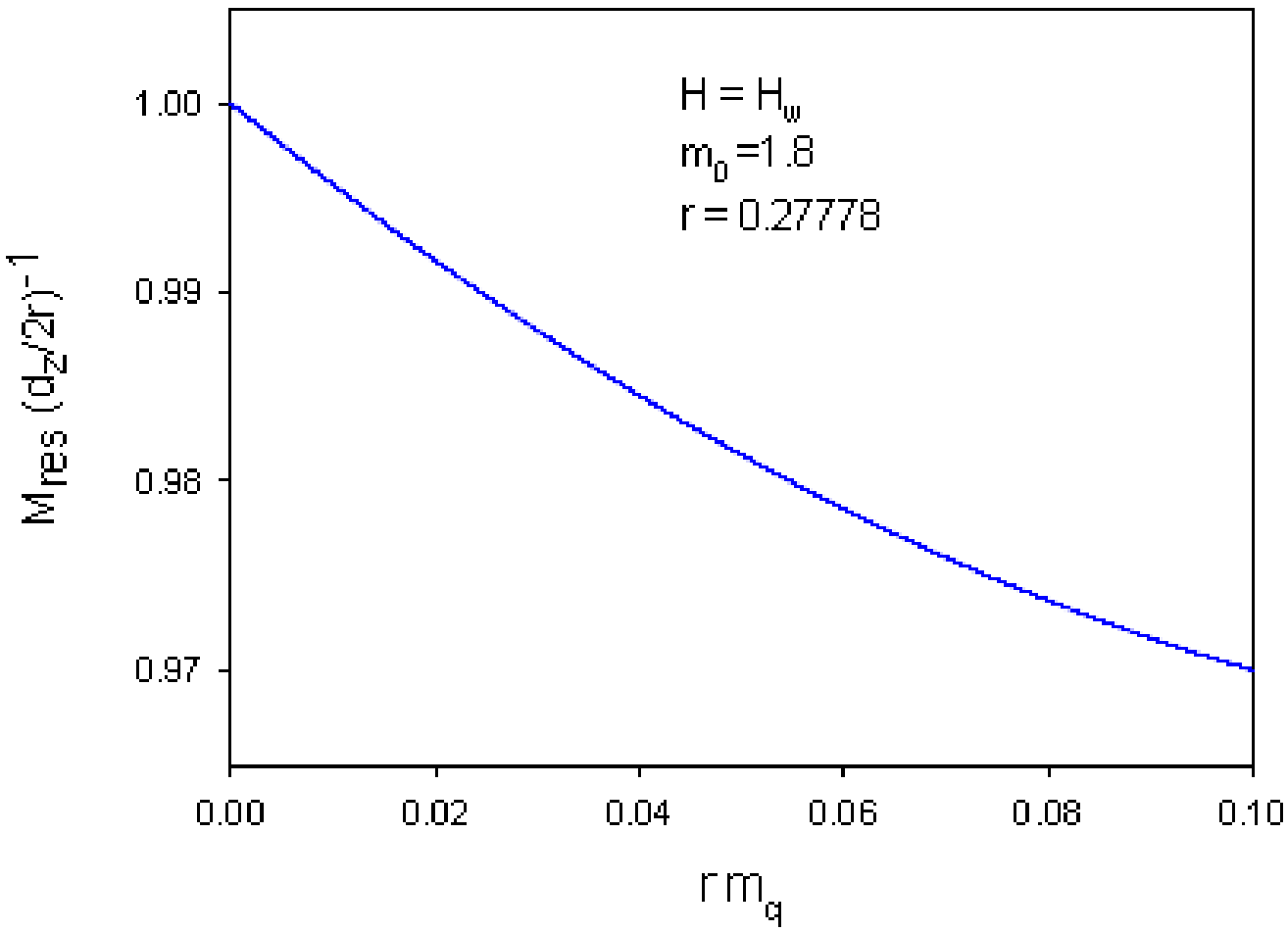

An Upper Bound for the Residual Mass (cont.)

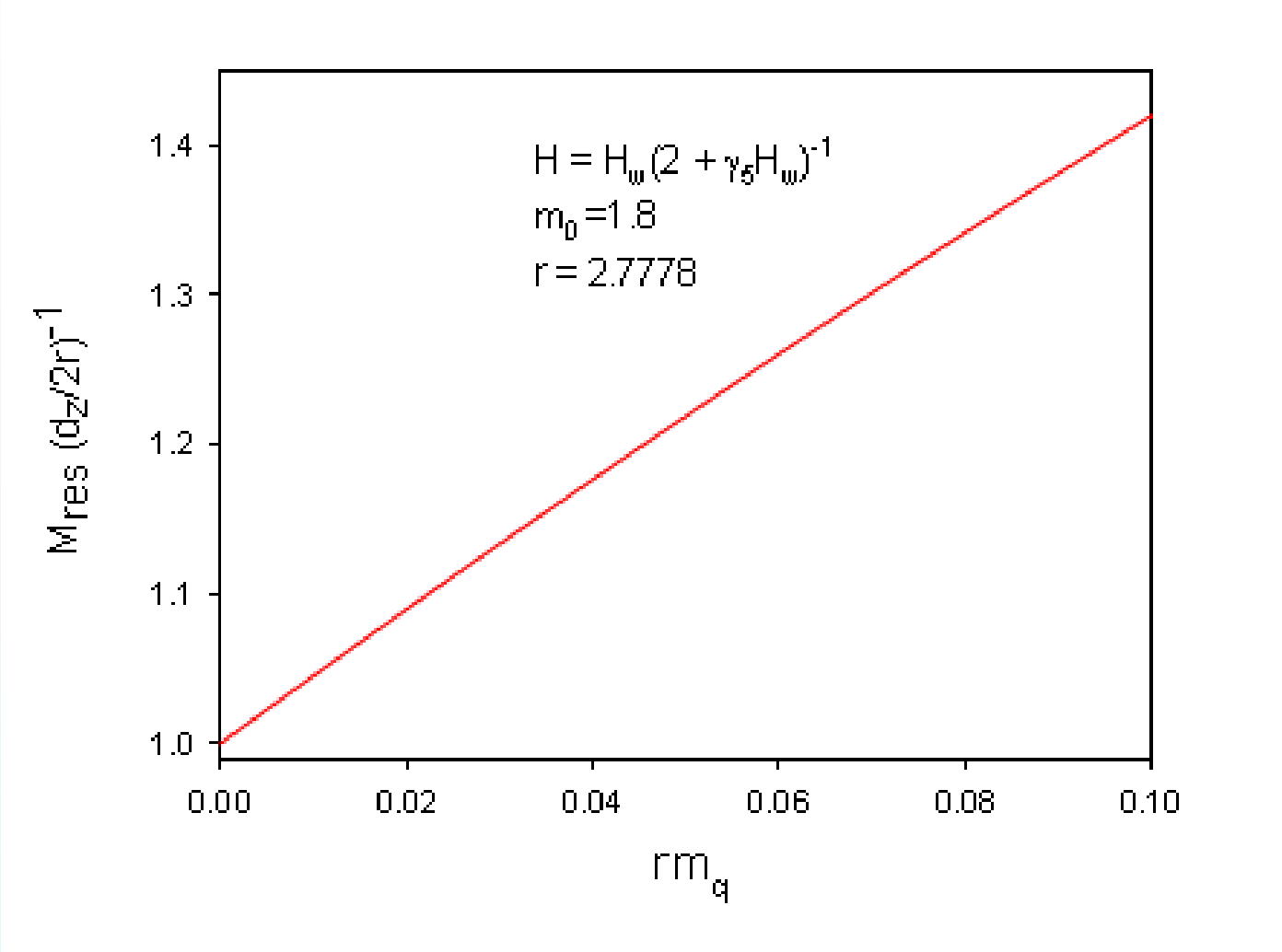

Concluding Remarks

- Axial Ward identity is derived for LQCD with ODWF
- Z[J] for n-point Green's function is obtained
- A practical formula for the residual mass is obtained
- An upper bound for the residual mass is obtained
  - It provides a guideline for designing simulations with DWF
  - The normalized residual mass is expressed as

$$F(r, m_q) = (1 + 2r^2 m_q)(1 - r m_q) + 2r^2 m_q^2$$

which is universal for any DWF with sufficiently small $\Delta_{\max}$

- The residual mass of quark for any observable O should be measured respectively.

Multigrid Acceleration for Domain-Wall Fermion Inversion

Saul D. Cohen

UNIVERSITY of WASHINGTON

New Horizons for Lattice Computations with Chiral Fermions
2012 May 15

Observables on the Lattice

...That Are Exceedingly Difficult

- Disconnected diagrams (strangeness of the proton, dark matter couplings)
- Zero-flavor physics (η', a_0 properties)
- Precision physics (nuclear binding energies, NPLQCD use 100s of sources)

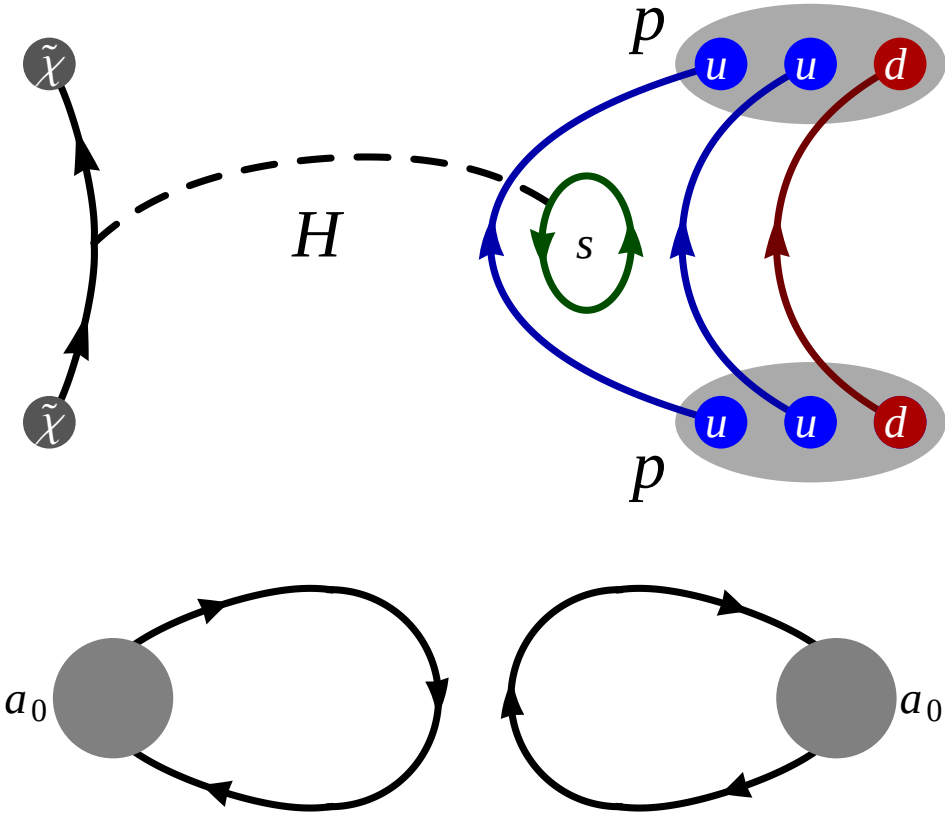

A Chiral Fermion

Domain-Wall Fermions

- Low-lying eigenstates: chiral modes bound to the edges of 5th dimension
- Very helpful for weak matrix elements (B_K), NPR, operator mixing

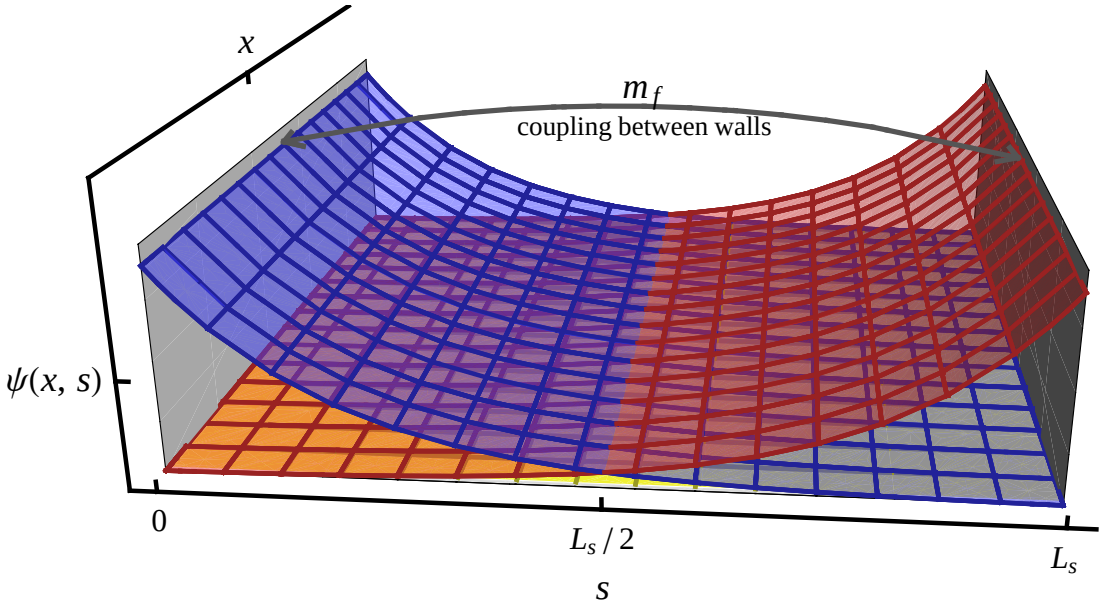

Domain-Wall Operator

Spectrum

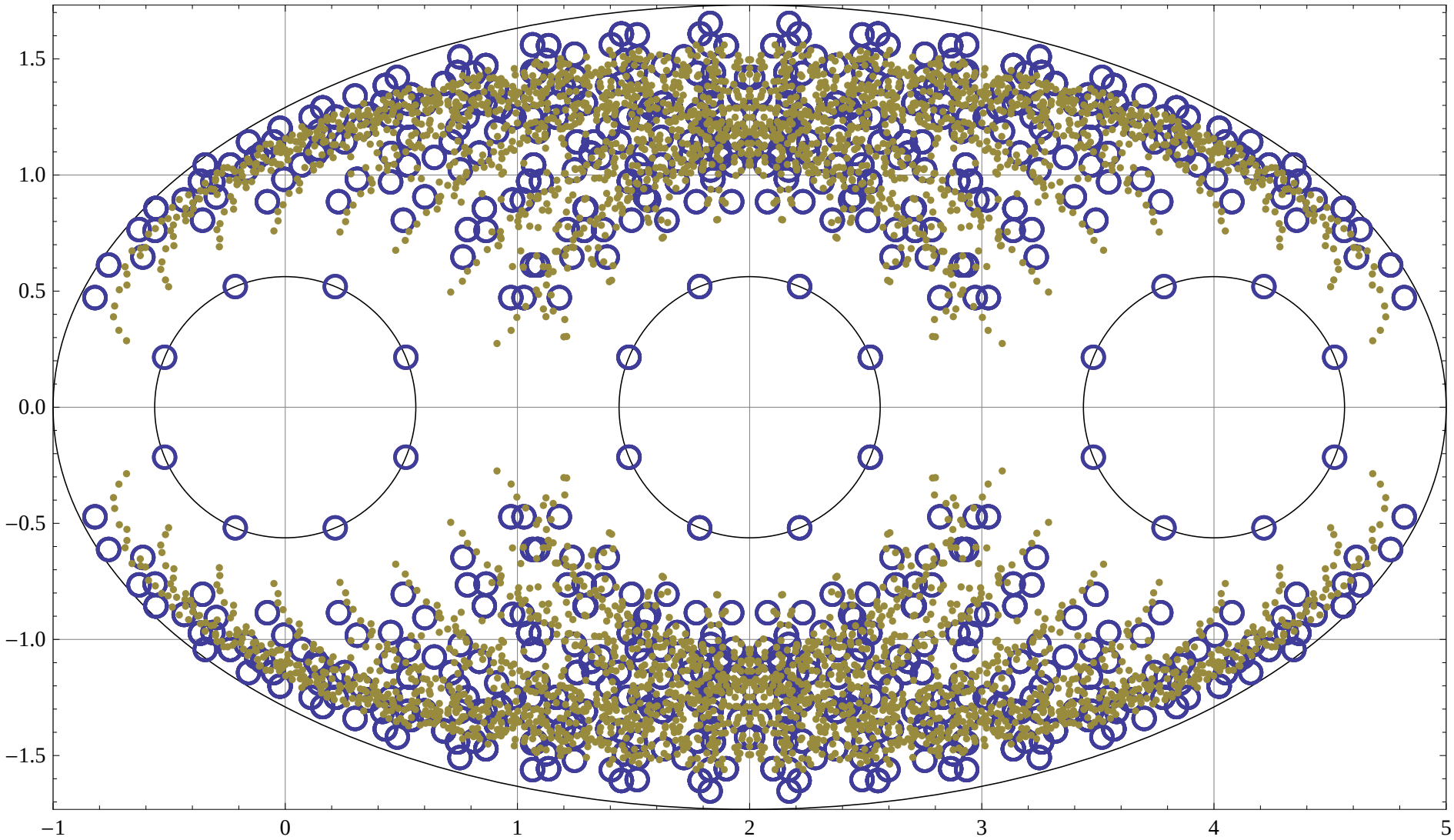

Krylov Subspace Solvers

Krylov solvers spend 50–90% of a lattice calculation's computer power

- Includes the very common conjugate-gradients (CG) algorithm
- Constructs the Krylov subspace $\mathcal{K}_n = \{r, Ar, A^2 r, \ldots, A^n r\}$
- Number of iterations scales like the square-root of the matrix's condition-number: $\sqrt{\kappa}$
- For the Dirac operator, $\kappa \propto 1/m =$ "critical slowing"
- Very efficient at eliminating modes with large eigenvalues

Algorithm Study

Due to the indefinite spectrum of the DWF operator, none of the standard Krylov solvers is guaranteed to work.

Most solvers, including BiCGStab, fail to converge.

TFQMR and QMR work, but very slowly.

CGNR is by far the fastest.

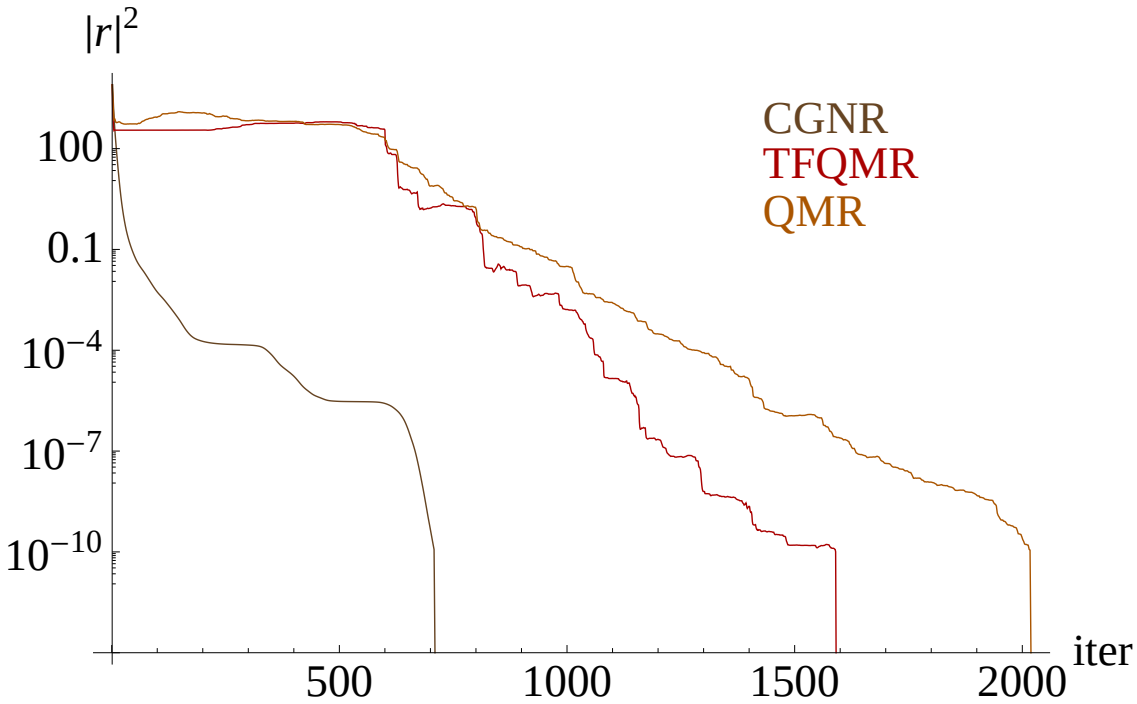

Normal-Equation Solvers

If we accept that we must use the normal equation, most Krylov solvers work.

CG remains fastest.

However, it cannot be preconditioned in a flexible way.

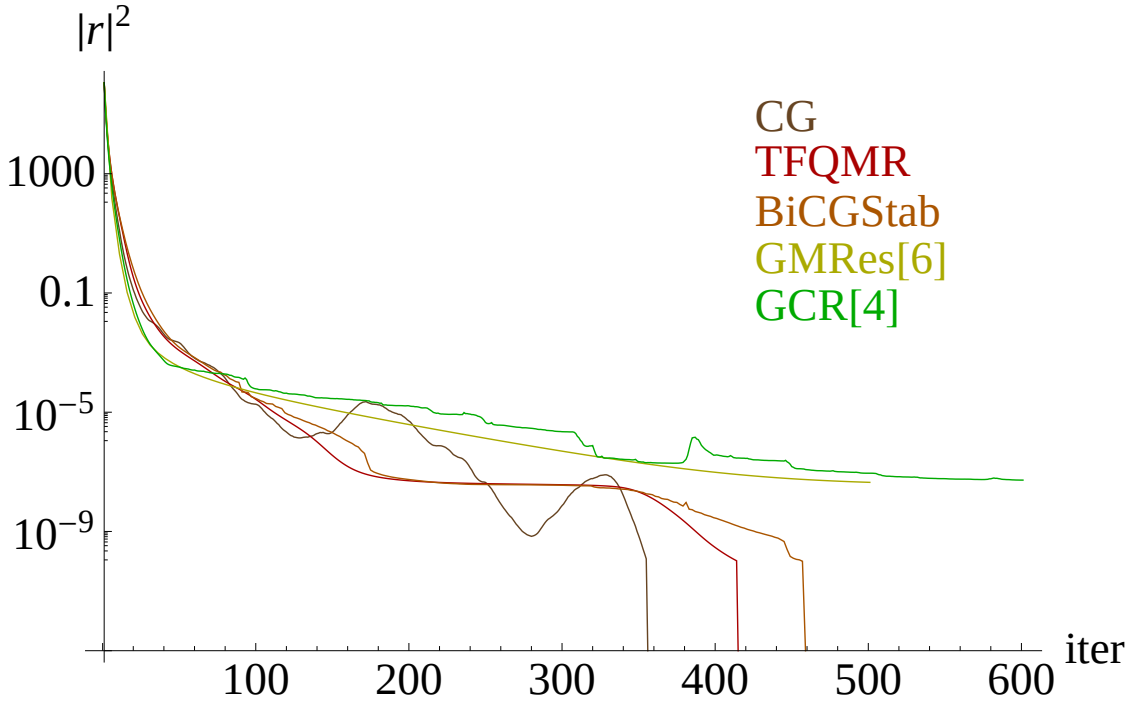

Sketch of Multigrid Algorithm

V-Cycling

$$D\,x = b$$

$$x_1 = S^{\nu_1}\left(D^\dagger D,\ D^\dagger b\right) \qquad x = x_1 + P\,x_2 + S^{\nu_3}\left(D^\dagger D,\ D^\dagger b_3\right.$$

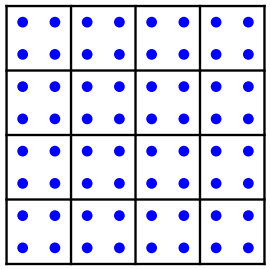

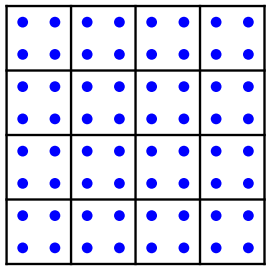

$$x_2 = S^{\nu_2}\left(P^\dagger\ D^\dagger D\ P,\ b_2\right)$$

$$b_2 = P^\dagger\left(D^\dagger b - D^\dagger D x_1\right)$$

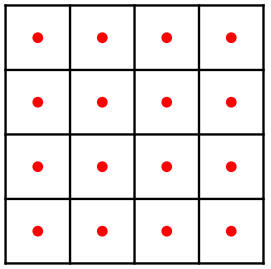

$$b_3 = b - D\,(P\,x_2 + x_1)$$

Sketch of Multigrid Algorithm

Constructing the Coarse Space

$$V = \left(\begin{array}{cccc|cccc|c} v_1^{(1)} & v_2^{(1)} & v_3^{(1)} & v_4^{(1)} & v_5^{(1)} & v_6^{(1)} & v_7^{(1)} & v_8^{(1)} & \cdots \\ v_1^{(2)} & v_2^{(2)} & v_3^{(2)} & v_4^{(2)} & v_5^{(2)} & v_6^{(2)} & v_7^{(2)} & v_8^{(2)} & \cdots \\ \vdots & \vdots & \vdots & \vdots & \vdots & \vdots & \vdots & \vdots & \ddots \end{array}\right)$$

$$P = \left(\begin{array}{cccc|cccc|c} v_1^{(1)} & v_2^{(1)} & v_3^{(1)} & v_4^{(1)} & 0 & 0 & 0 & 0 & \cdots \\ 0 & 0 & 0 & 0 & v_5^{(1)} & v_6^{(1)} & v_7^{(1)} & v_8^{(1)} & \cdots \\ \vdots & \vdots & \vdots & \vdots & \vdots & \vdots & \vdots & \vdots & \cdots \\ v_1^{(2)} & v_2^{(2)} & v_3^{(2)} & v_4^{(2)} & 0 & 0 & 0 & 0 & \cdots \\ 0 & 0 & 0 & 0 & v_5^{(2)} & v_6^{(2)} & v_7^{(2)} & v_8^{(2)} & \cdots \\ \vdots & \vdots & \vdots & \vdots & \vdots & \vdots & \vdots & \vdots & \ddots \end{array}\right)$$

Sketch of Multigrid Algorithm

Visualizing the Subspaces

$$r' = \left[1 - AP\frac{1}{P^\dagger AP}P^\dagger\right] r$$

Multigrid

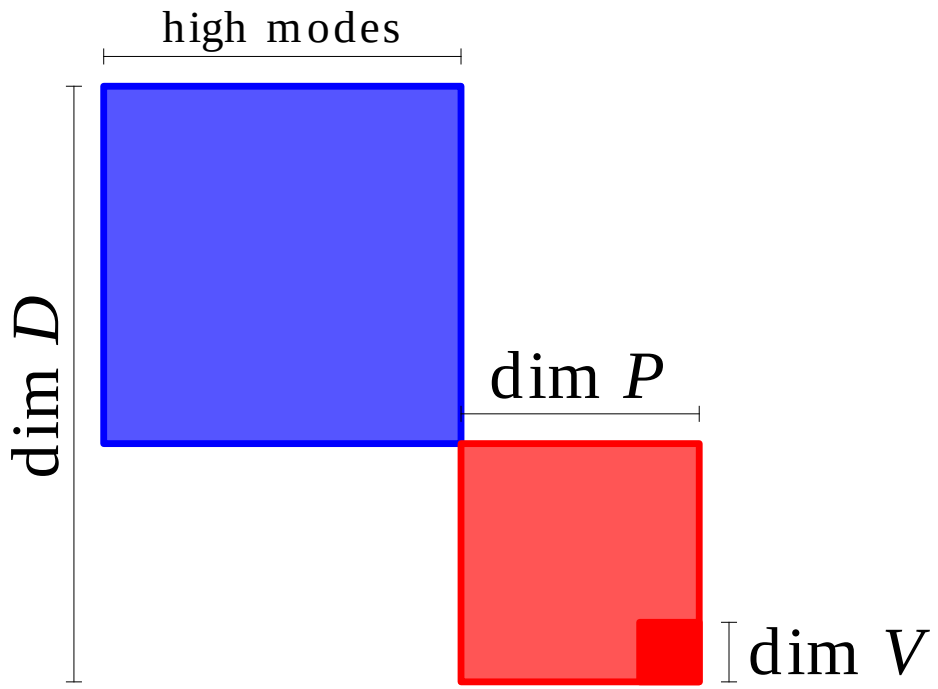

Deflation

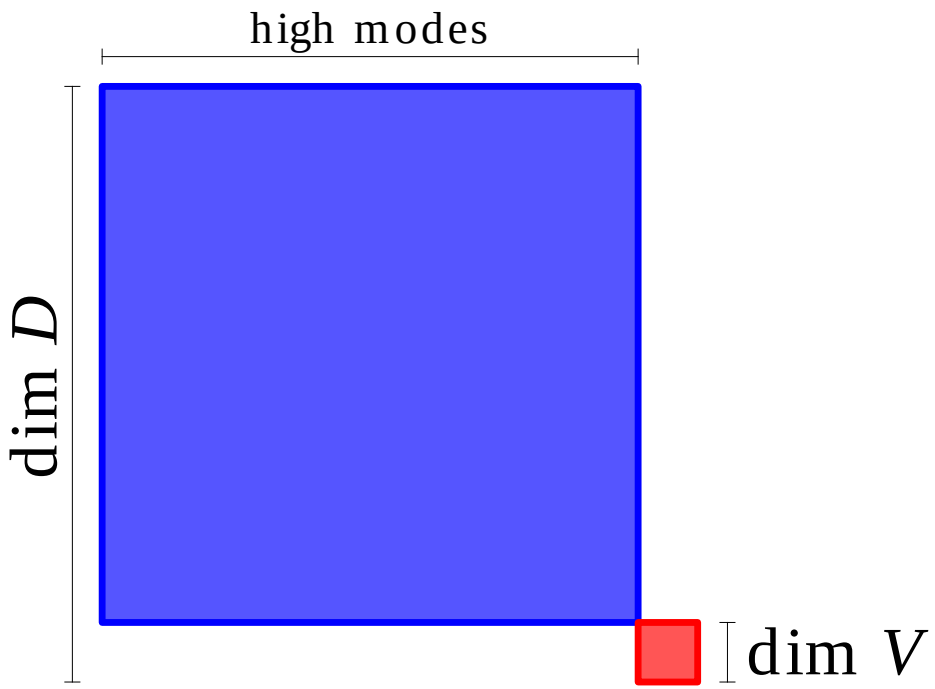

Sketch of Multigrid Algorithm

Visualizing the Subspaces

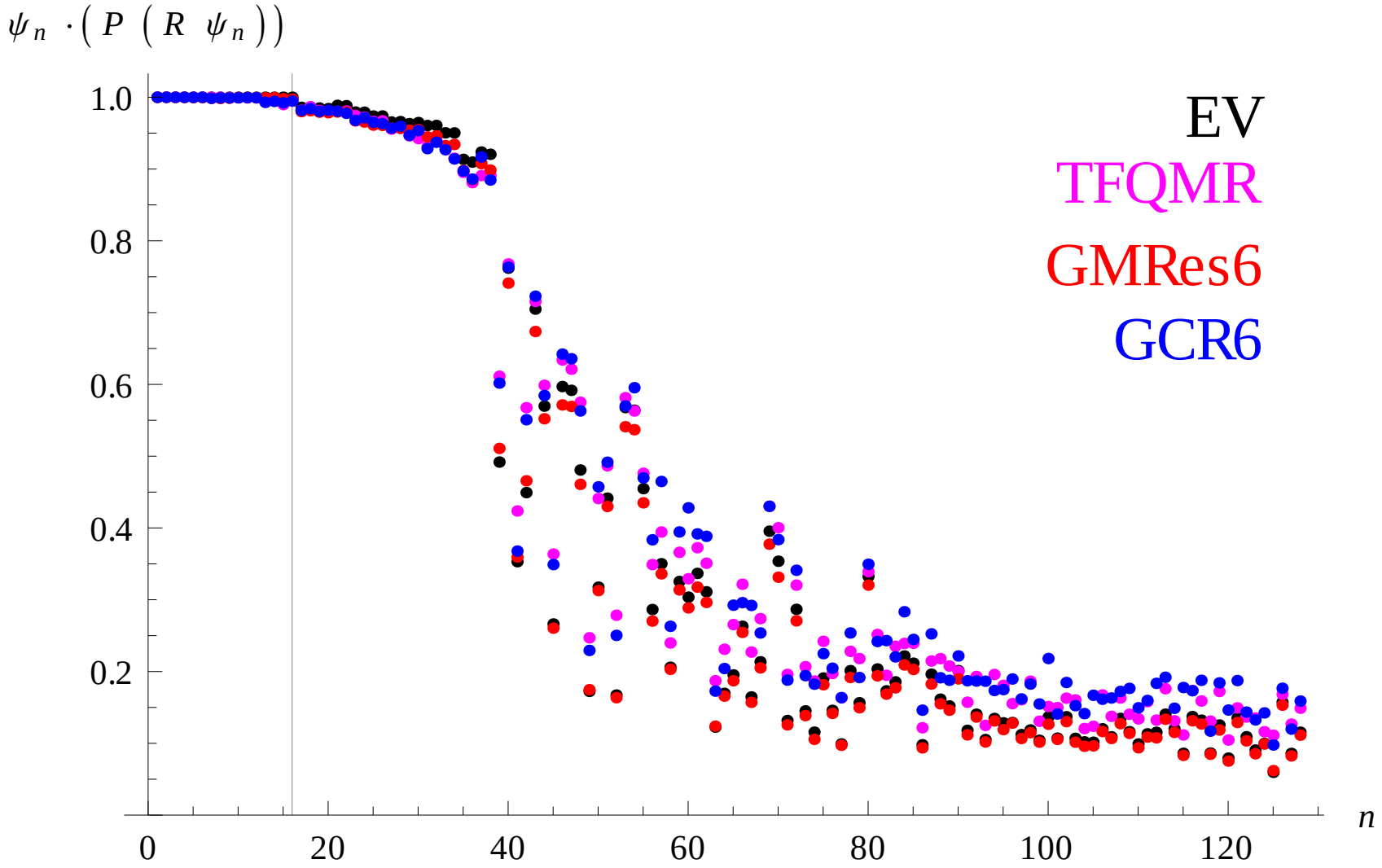

Adaptive Smoothed Algebraic Multigrid

1. Find a set of near-null vectors V for which $\psi^\dagger D^\dagger D\psi \approx 0$ for all $\psi \in V$.
2. Block the vectors to form the prolongator P. Let the unprolongator be $P^\dagger$.
3. Construct the coarse operator $P^\dagger D^\dagger DP$. Use a V-cycle with Krylov smoother and Krylov iteration on coarse operator as a preconditioner to an outer Krylov solver.

The method by which V is constructed does not matter much. Using a solver that will be reused later is convenient, but not necessary.

Adaptive Smoothed Algebraic Multigrid

1. Find a set of near-null vectors V for which $\psi^\dagger D^\dagger D\psi \approx 0$ for all $\psi \in V$.
2. Block the vectors to form the prolongator P. Let the unprolongator be $P^\dagger$.
3. Construct the coarse operator $P^\dagger D^\dagger DP$. Use a V-cycle with Krylov smoother and Krylov iteration on coarse operator as a preconditioner to an outer Krylov solver.

Since $D^\dagger D$ is normal, its left and right eigenvectors are the same. P and R can be constructed from the same set of near-null vectors.

Adaptive Smoothed Algebraic Multigrid

1. Find a set of near-null vectors V for which $\psi^\dagger D^\dagger D\psi \approx 0$ for all $\psi \in V$.
2. Block the vectors to form the prolongator P. Let the unprolongator be $P^\dagger$.
3. Construct the coarse operator $P^\dagger D^\dagger DP$. Use a V-cycle with Krylov smoother and Krylov iteration on coarse operator as a preconditioner to an outer Krylov solver.

The outer solver must be flexibly preconditioned. The selection of the smoother has some effect, but the coarse-level solver can be anything.

Adaptive Smoothed Algebraic Multigrid

1. Find a set of near-null vectors V using the previously described algorithm for which $\psi^\dagger D^\dagger D\psi \approx 0$ for all $\psi \in V$.
2. Block the vectors to form the prolongator P. Let the unprolongator be $P^\dagger$.
3. Construct the coarse operator $P^\dagger D^\dagger DP$. Use a V-cycle with Krylov smoother and Krylov iteration on coarse operator as a preconditioner to an outer Krylov solver.

How is this "adaptive"? We can select new near-null vectors from those that are poorly converged by our current algorithm. Repeat as necessary.

Applied ASAM on DWF Normal Equation

$20^2 \times 8$, U(1), quenched

This algorithm seems to work well on the 2d U(1) DWF normal equation, removing the slowing at small masses.

$20^2 \times 8$ U(1) lattice

$4^2 \times 8$ blocks
$N_v = 16$

Outer solver: CG
Smoother: GMRes(6)
Coarse solver: CG
Coarse r^2: 10^{-3}

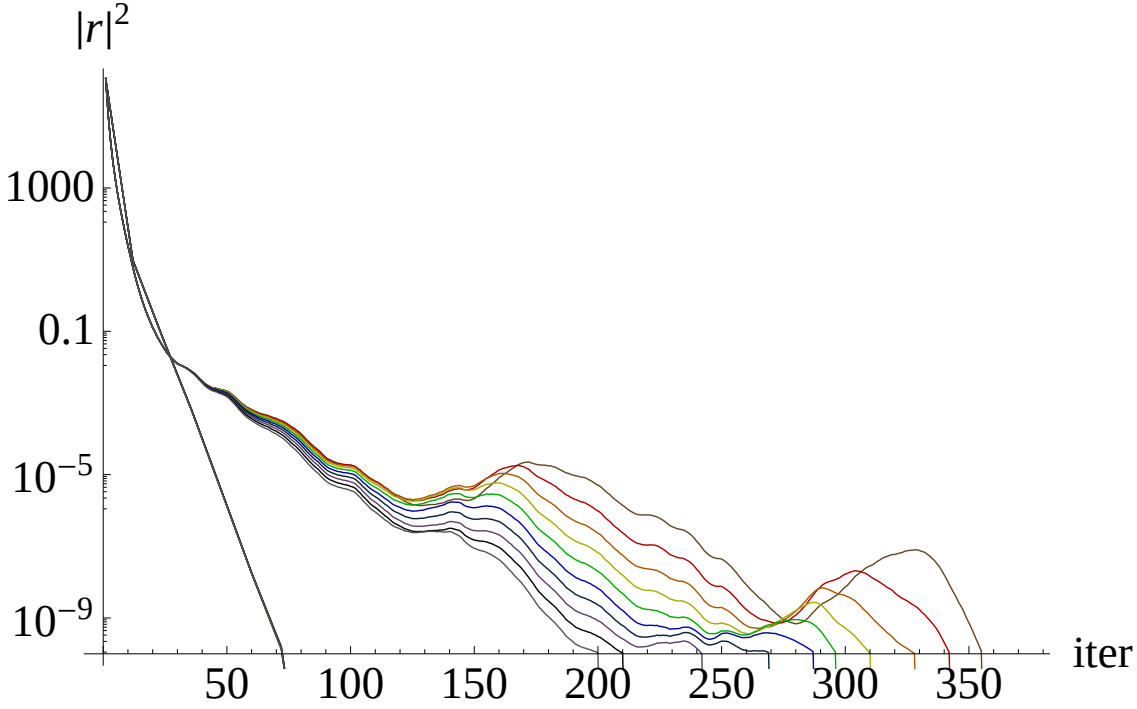

Applied ASAM on DWF Normal Equation

$20^2 \times 8$, U(1), quenched

This algorithm seems to work well on the 2d U(1) DWF normal equation, removing the slowing at small masses.

$20^2 \times 8$ U(1) lattice

$4^2 \times 8$ blocks
$N_v = 16$

Outer solver: CG
Smoother: GMRes(6)
Coarse solver: CG
Coarse r^2: 10^{-3}

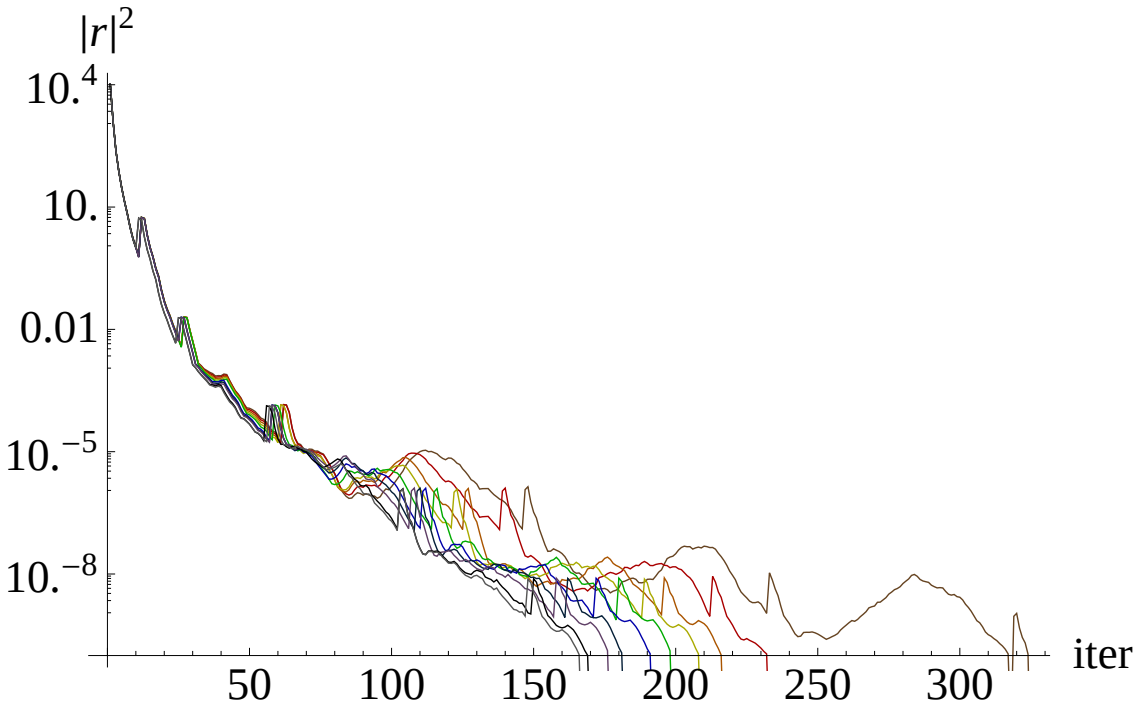

Applied ASAM on DWF Normal Equation

$16^3 \times 32 \times 16$, SU(3), 6-flavor

The effect is equally impressive on a moderately-sized production lattice.

$16^3 \times 32 \times 16$ Technicolor lattice

$4^4 \times 16$ blocks
$N_v = 24$

Outer solver: GCR(12)
Smoother: $12 \times$ GCR(12)
Coarse solver: CG
Coarse r^2: to 10^{-4} then 10^{-2}/cycle

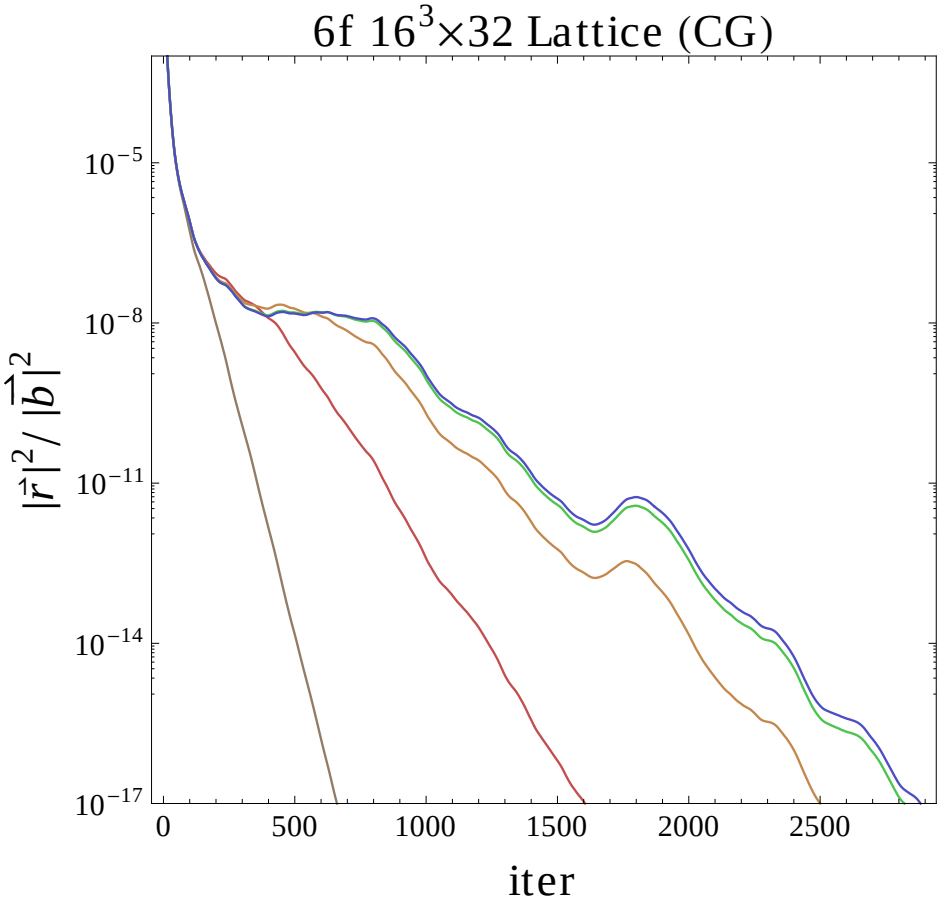

Applied ASAM on DWF Normal Equation

$16^3 \times 32 \times 16$, SU(3), 6-flavor

The effect is equally impressive on a moderately-sized production lattice.

$16^3 \times 32 \times 16$ Technicolor lattice

$4^4 \times 16$ blocks
$N_v = 24$

Outer solver: GCR(12)
Smoother: $12 \times$ GCR(12)
Coarse solver: CG
Coarse r^2: to 10^{-4} then 10^{-2}/cycle

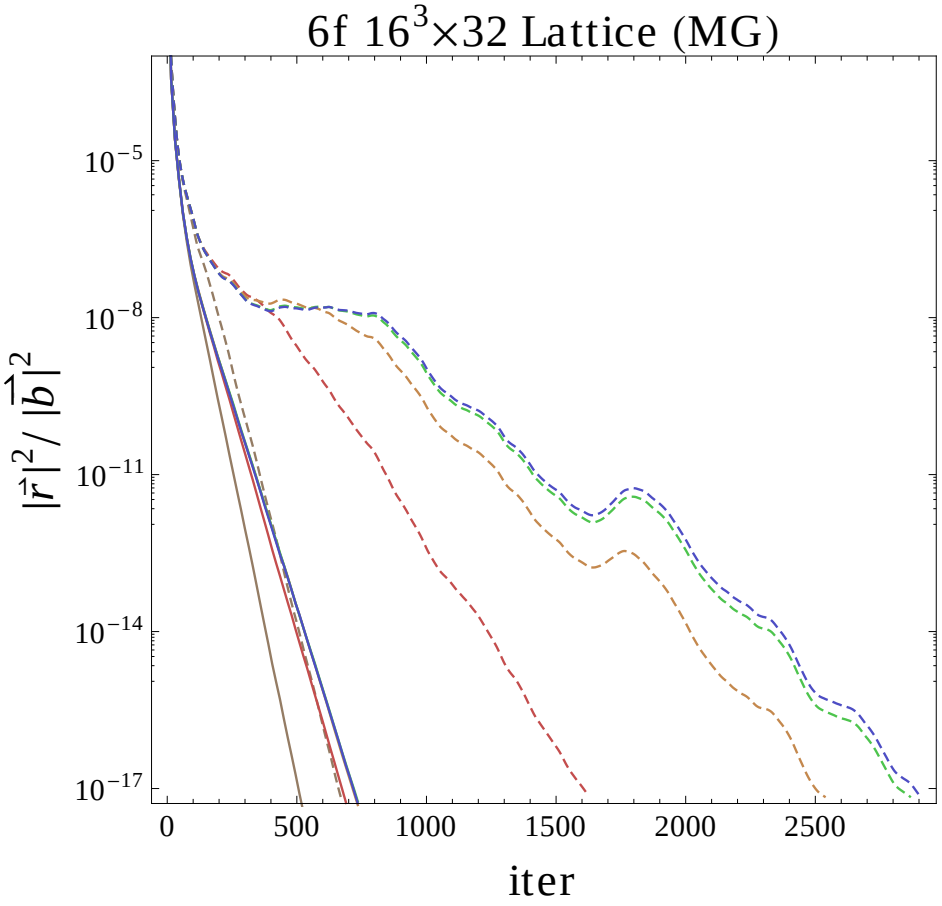

Applied ASAM on DWF Normal Equation

$16^3 \times 32 \times 16$, SU(3), 6-flavor

The effect is equally impressive on a moderately-sized production lattice.

$16^3 \times 32 \times 16$ Technicolor lattice

$4^4 \times 16$ blocks
$N_v = 24$

Outer solver: GCR(12)
Smoother: $12 \times$ GCR(12)
Coarse solver: CG
Coarse r^2: to 10^{-4} then 10^{-2}/cycle

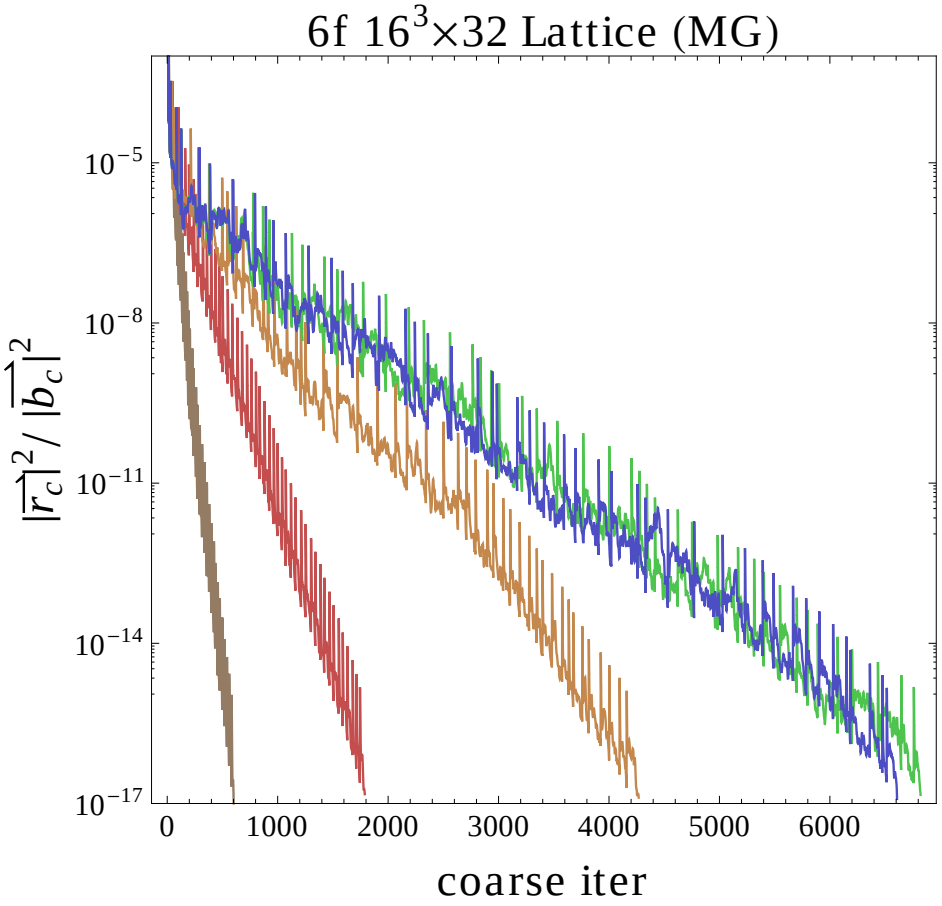

Applied ASAM on DWF Normal Equation

$16^3 \times 32 \times 16$, SU(3), 6-flavor

The effect is equally impressive on a moderately-sized production lattice.

$16^3 \times 32 \times 16$ Technicolor lattice

$4^4 \times 16$ blocks
$N_v = 24$

Outer solver: GCR(12)
Smoother: $12 \times$ GCR(12)
Coarse solver: CG
Coarse r^2: to 10^{-4} then 10^{-2}/cycle

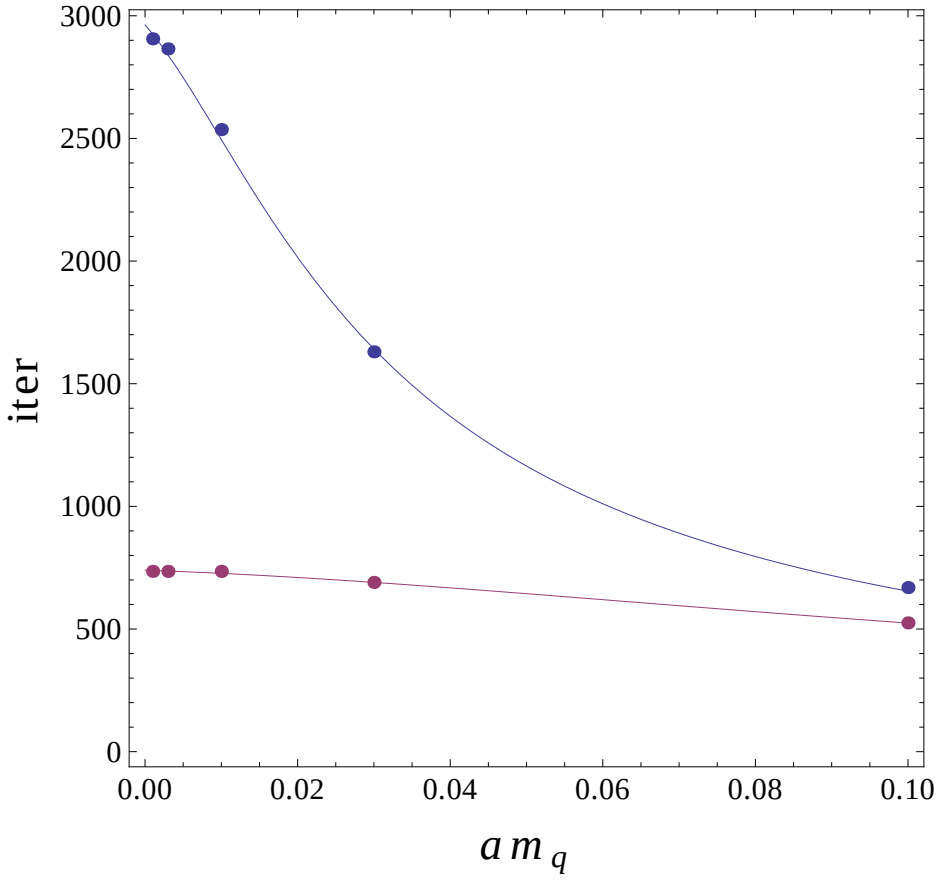

Applied ASAM on Clover-Wilson Fermions

Graphics courtesy of J. Osborn

Multigrid works even better on clover fermions.

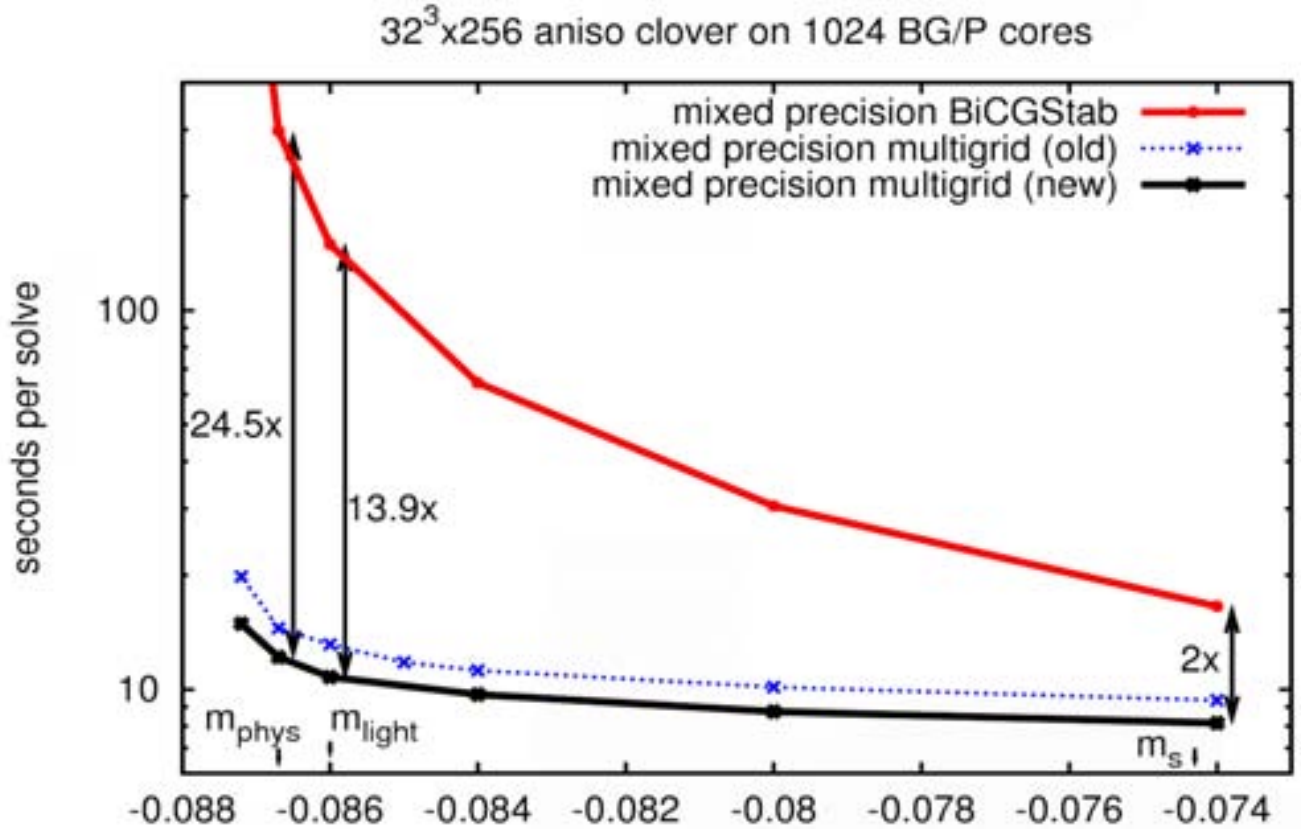

Applied ASAM on Clover-Wilson Fermions

Graphics courtesy of J. Osborn

If the 2-level multigrid starts to slow at very low mass, add more levels.

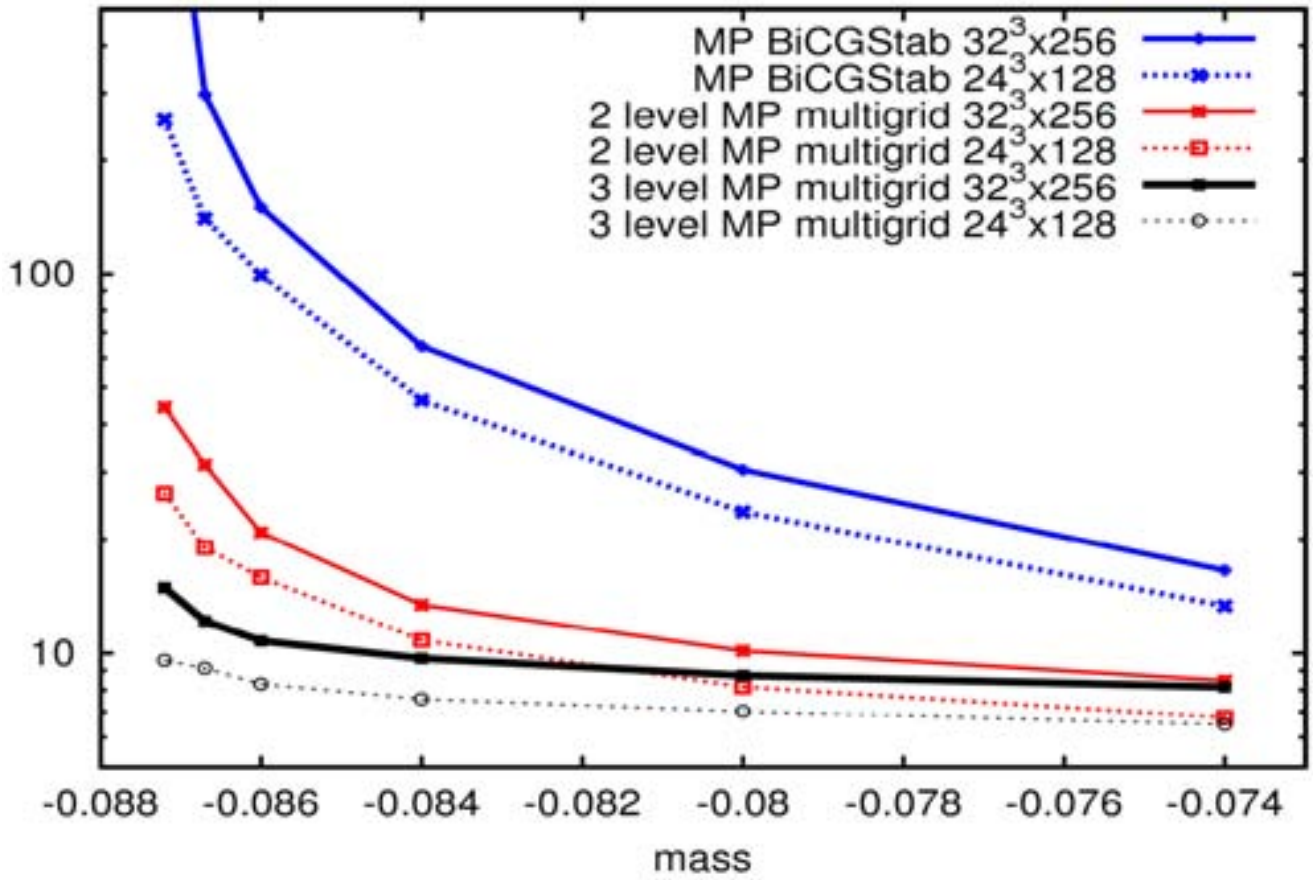

Improved Error for Fixed Residual

Graphics courtesy of J. Osborn

Since multigrid works efficiently on relevant eigenmodes, the quality of the solution is better than standard solvers.

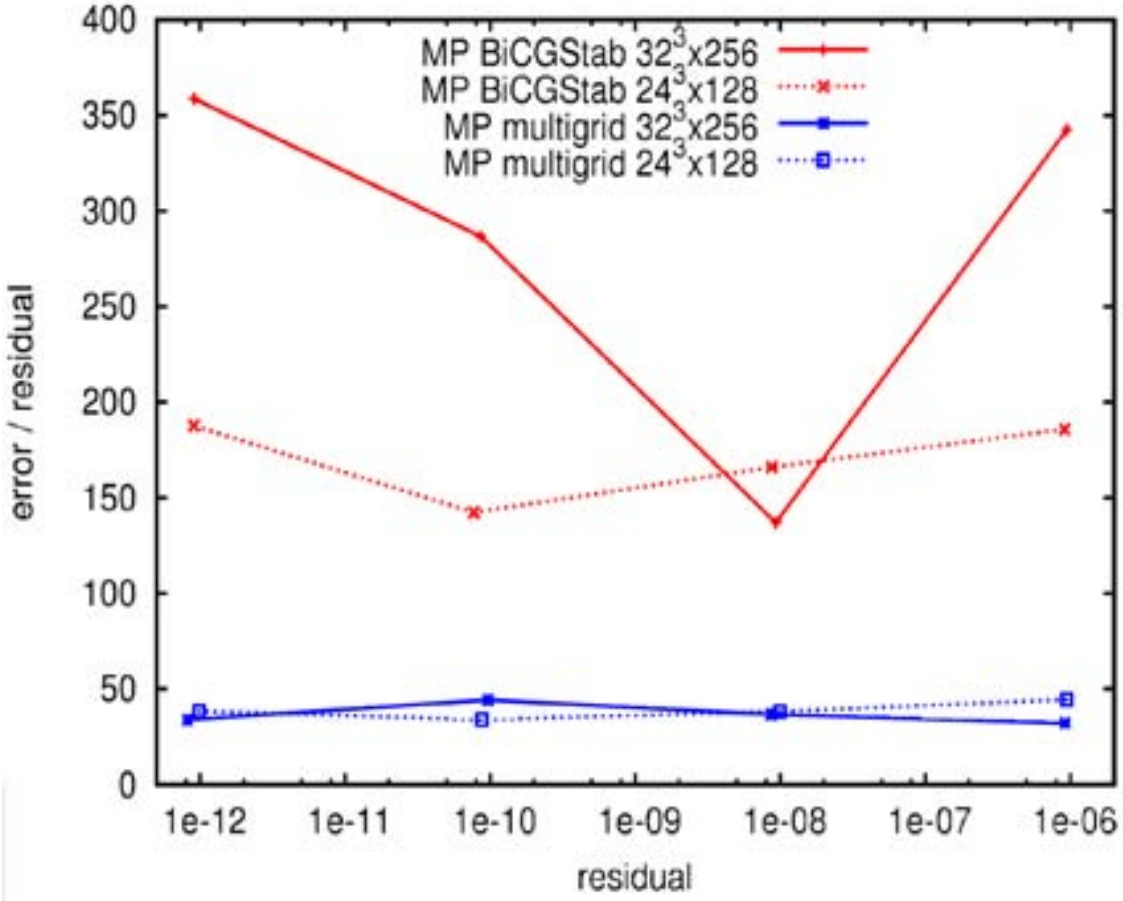

Summary

- Conclusions
  - Multigrid greatly speeds calculation of propagators
  - For clover fermions at the physical mass: $20\times$ faster
  - Works for DWF normal equation; improved by factor of 4–8
  - Multigrid works even better on larger lattices
- Recent advances
  - Integrated as a user-friendly module in Chroma
  - Scaling tests for DWF on large lattices (running on Kraken)
- Future Work
  - Port to GPUs

Is This Algorithm Good Enough?

- Advantages
  - Blocks away the entire 5th dimension.
  - Factor of 4–8 decrease in fine-operator applications.
  - Removes the critical slowing at small quark masses.
  - Should have excellent scaling with the lattice volume.
- Disadvantages
  - Not a nearest-neighbor operator; poor parallelization.
  - Are there more vectors in P (and R) than we need?

Constructing a 1-Hop Coarse Operator

Can we use $(P^\dagger D^\dagger P)(P^\dagger DP)$ as a coarse operator?

- No, the DWF operator is not normal:
  left-vectors are not right-vectors (conjugated).

Can we use $(P^\dagger \Gamma_5 DP)^2$ as a coarse operator?

- $\Gamma_5 = \gamma_5 \mathcal{R}$, where $\mathcal{R}$ reverses the 5th dimension
- Sounds promising, but empirical tests show no convergence

We know $(P^\dagger D^\dagger 1)(1DP)$ works; how do we get closer to that?

Constructing a 1-Hop Coarse Operator

Can we use $(P^\dagger D^\dagger P)(P^\dagger DP)$ as a coarse operator?

- No, the DWF operator is not normal:
  left-vectors are not right-vectors (conjugated).

Can we use $(P^\dagger \Gamma_5 DP)^2$ as a coarse operator?

- $\Gamma_5 = \gamma_5 \mathcal{R}$, where $\mathcal{R}$ reverses the 5th dimension
- Sounds promising, but empirical tests show no convergence

We know $(P^\dagger D^\dagger 1)(1DP)$ works; how do we get closer to that?

Constructing a 1-Hop Coarse Operator

Can we use $(P^\dagger D^\dagger P)(P^\dagger DP)$ as a coarse operator?

- No, the DWF operator is not normal:
  left-vectors are not right-vectors (conjugated).

Can we use $(P^\dagger \Gamma_5 DP)^2$ as a coarse operator?

- $\Gamma_5 = \gamma_5 \mathcal{R}$, where $\mathcal{R}$ reverses the 5th dimension
- Sounds promising, but empirical tests show no convergence

We know $(P^\dagger D^\dagger 1)(1DP)$ works; how do we get closer to that?

Constructing a 1-Hop Coarse Operator

Try $(P^\dagger D^\dagger R^\dagger)(RDP)$ where $\dim R > \dim P$.
In the limit where $\dim R \to \dim D$, this is the known-good algorithm.

$16^3 \times 32 \times 16$ Technicolor lattice

$4^4 \times 16$ blocks
$N_v(R) = 48$
$N_v(P) = 12$–48

$m_q = 0.01$

Requires fast implementation of rectangular-matrix linear algebra

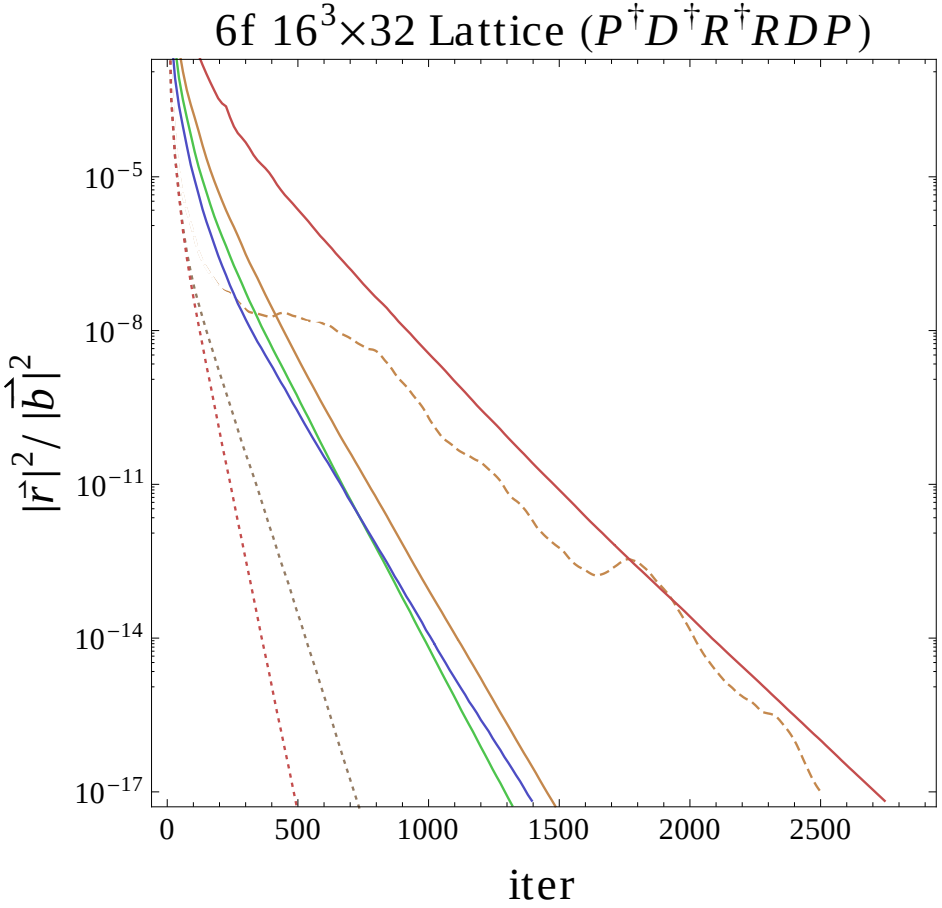

The axial symmetry at finite temperature in Lattice QCD with Overlap fermions

Guido Cossu, KEK

高エネルギー加速器研究機構

New Horizons for Lattice Computations with Chiral Fermions

RIKEN BNL Research center workshop – May 14, 2012

Summary:

- ✔ Motivation
- ✔ Chiral phase transition at finite temperature and axial symmetry
- ✔ Simulating dynamical (overlap) fermions
- ✔ Topology fixing and friends
- ✔ Methodology and results (quenched and $N_f=2$)
- ✔ Discussion and conclusions

People involved in this project

JLQCD group: S. Hashimoto, S. Aoki, T. Kaneko, H. Matsufuru, J. Noaki, E. Shintani

See for example POS(Lattice2010)174 (arXiv:1011.0257), PoS(Lattice 2011)188 (arXiv:1204.4519), article in prep.

Motivation

Pattern of chiral symmetry breaking at low temperature QCD

$$SU(N_f)_V \times SU(N_f)_A \times U(1)_V \times U(1)_A \rightarrow SU(N_f)_V \times U(1)_V$$

Well known facts about axial symmetry

- Axial anomaly – Non vanishing topological susceptibility
- Mass splitting of the η' (958 Mev) with respect to the lighter Goldsone bosons

What is the fate of the axial $U_A(1)$ symmetry at finite temperature($T \gtrsim T_c$)?

Dirac Overlap operator, retaining the maximal amount of chiral symmetry on the lattice is, theoretically, the best way to answer this question.

- Experimental data: PHENIX(BNL) Phys.Rev. C83 (2011) 054903

"*the mass of the eta' meson is reduced by Delta-m $>$ 200 MeV, at the 99.9% confidence level, in the considered model class*"

Goal of the current project

Check restoration of axial $U_A(1)$ symmetry by measuring (spatial) meson correlators at finite temperature in full QCD with overlap

Degeneracy of correlators is the signal that we are looking for

$$\begin{tikzcd}
\sigma(1_4 \otimes 1_2) \arrow[r, leftrightarrow, "\textit{Chiral sym.}"] \arrow[d, leftrightarrow, "U(1)_A"'] & \pi(i\gamma_5 \otimes \tau^a) \arrow[d, leftrightarrow, "U(1)_A"] \\
\eta(i\gamma_5 \otimes 1_2) \arrow[r, leftrightarrow, "\textit{Chiral sym.}"] & \delta(1_4 \otimes \tau^a)
\end{tikzcd}$$

As I will show in this talk,

there is one issue to solve before attacking the real problem...

Simulating dynamical overlap fermions

In order to avoid expensive tricks to handle the zero modes of the Hermitian Wilson operator JLQCD simulations use (JLQCD 2006):

- Iwasaki action (suppresses Wilson operator near zero modes)
- Extra Wilson fermions and twisted mass ghosts to rule out the zero modes

Topology is thus fixed throughout the HMC trajectory.

The effect of fixing topology is expected to be a Finite Size Effect (actually O(1/V)), next slides

Fixing topology: how to deal with it at T=0 (I)

Partition function at fixed topology

$$Z_Q = \frac{1}{2\pi}\int_{-\pi}^{\pi} d\theta \, \exp(-VF(\theta)) \qquad F(\theta) \equiv E(\theta) - i\theta Q/V$$

where the energy can be expanded $E(\theta) = \sum_{n=1}^{\infty} \frac{c_{2n}}{(2n)!}\theta^{2n} = \frac{\chi_t}{2}\theta^2 + O(\theta^4)$

Using saddle point expansion around $\theta_c = i\frac{Q}{\chi_t V}(1 + O(\delta^2))$

one obtains the Gaussian distribution

$$Z_Q = \frac{1}{\sqrt{2\pi\chi_t V}} \exp\left[-\frac{Q^2}{2\chi_t V}\right]\left[1 - \frac{c_4}{8V\chi_t^2} + O\left(\frac{1}{V^2}, \delta^2\right)\right].$$

Fixing topology: how to deal with it at T=0 (II)

From the previous partition function we can extract the relation between correlators at fixed θ and correlators at fixed Q

In particular for the topological susceptibility and using the Axial Ward Identity we obtain a relation involving fermionic quantities:

$$\lim_{|x|\to\text{large}} \langle mP(x)mP(0)\rangle_Q^{\text{disc}} \equiv \frac{1}{V}\left(\frac{Q^2}{V} - \chi_t - \frac{c_4}{2\chi_t V}\right) + O(e^{-m_\pi|x|})$$

P(x) is the flavor singlet pseudo scalar density operator

Aoki *et al.* PRD76,054508 (2007)

What is the effect of fixing Q at finite temperature?

Results

- ✔ Simulation details
- ✔ Eigenvalues distribution
- ✔ Finite temperature quenched SU(3) at fixed topology
- ✔ Meson correlators in two flavors QCD

BG/L
Hitachi SR16K

Simulation details

Pure gauge (16^3x6, 24^3x6):

Iwasaki action + top. fixing term

β	*a(fm)*	*T (MeV)*	*T/Tc*
2.35	0.132	249.1	0.86
2.40	0.123	268.1	0.93
2.43	0.117	280.9	0.97
2.44	0.115	285.7	0.992
2.445	0.114	288	1.0
2.45	0.1133	290.2	1.01
2.46	0.111	295.1	1.02
2.48	0.107	305.6	1.06
2.50	0.104	316.2	1.10
2.55	0.094	347.6	1.20

Two flavors QCD (16^3x8)

Iwasaki + Overlap + top. Fix

O(300) trajectories per T

am=0.05, 0.025, 0.01

β	*a(fm)*	*T (MeV)*	*T/Tc*
2.18	0.1438	171.5	0.95
2.20	0.1391	177.3	0.985
2.25	0.12818	192.2	1.06
2.30	0.1183	208.5	1.15
2.40	0.1013	243.5	1.35
2.45	0.0940	262.4	1.45

Eigenvalue distribution

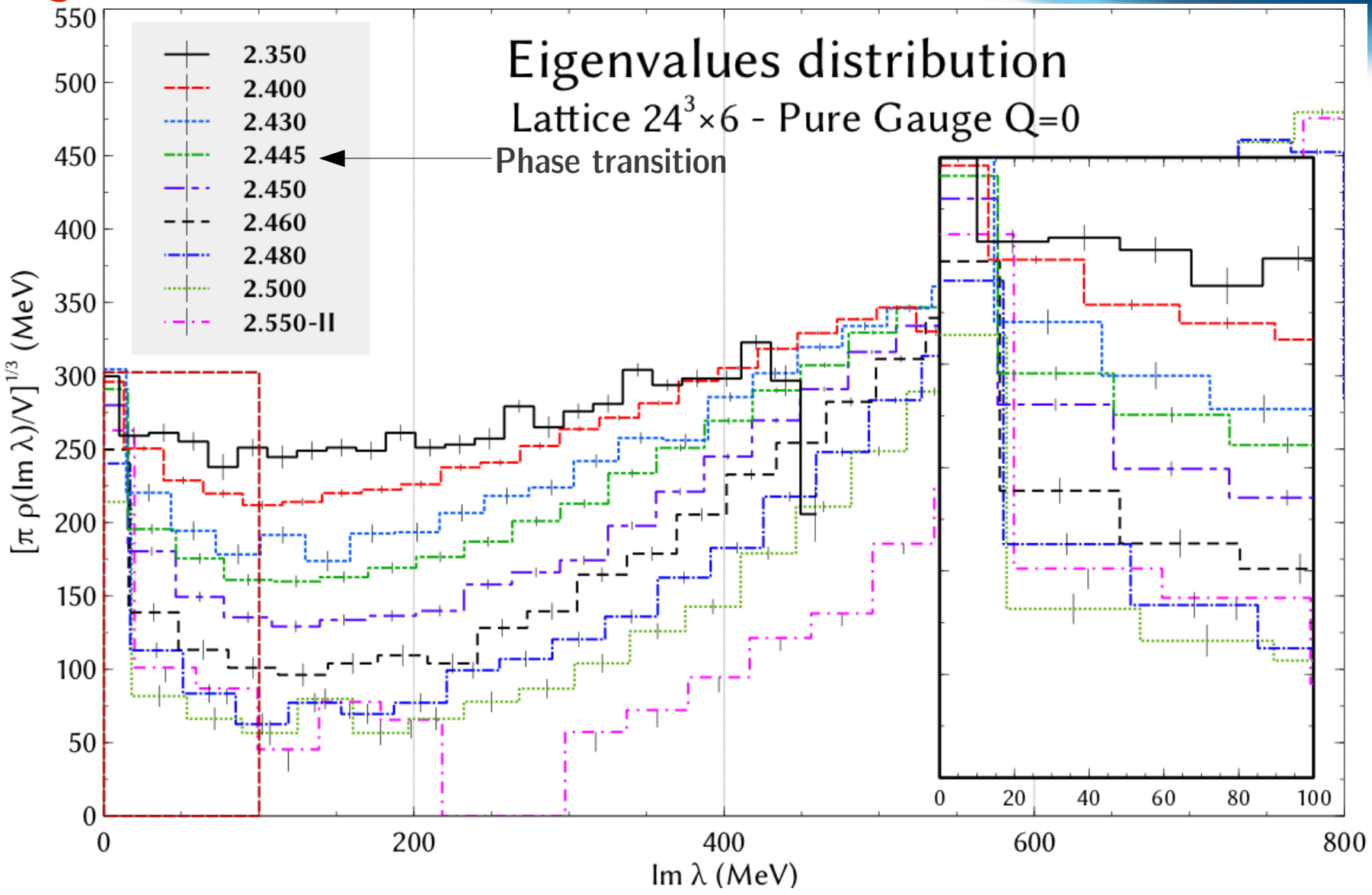

Topological susceptibility in pure gauge theory - I

$$\lim_{|x|\to\text{large}} \langle mP(x)mP(0)\rangle_Q^{\text{disc}} \equiv \frac{1}{V}\left(\frac{Q^2}{V} - \chi_t - \frac{c_4}{2\chi_t V}\right) + O(e^{-m_\pi|x|})$$

- (Spatial) Correlators are always approximated by the first 50 eigenvalues
- Pure gauge: double pole formula for disconnected diagram
- Topological susceptibility estimated by a joint fit of connected and disconnected contribution.

Topological susceptibility in pure gauge theory - II

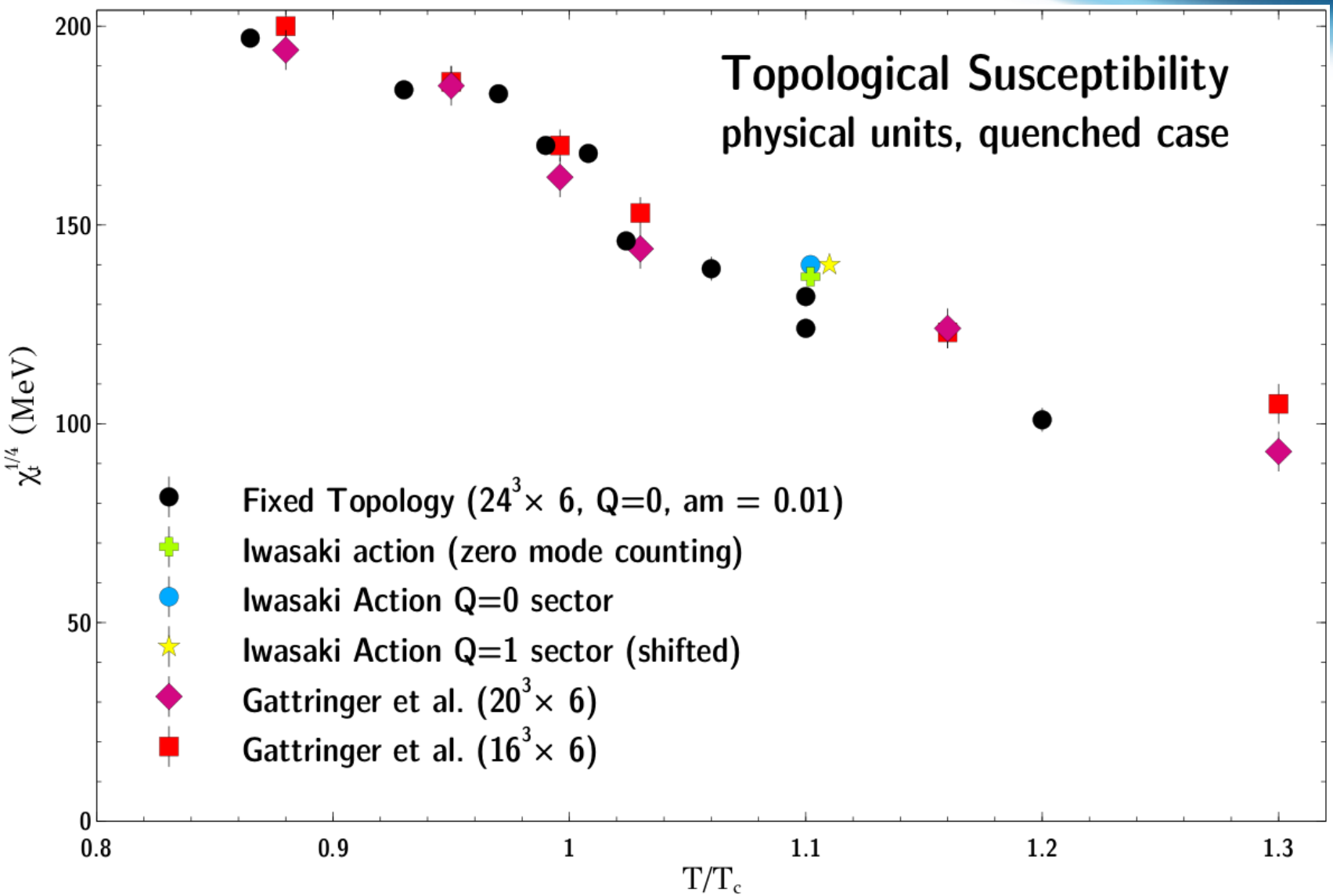

Full QCD – Eigenvalues

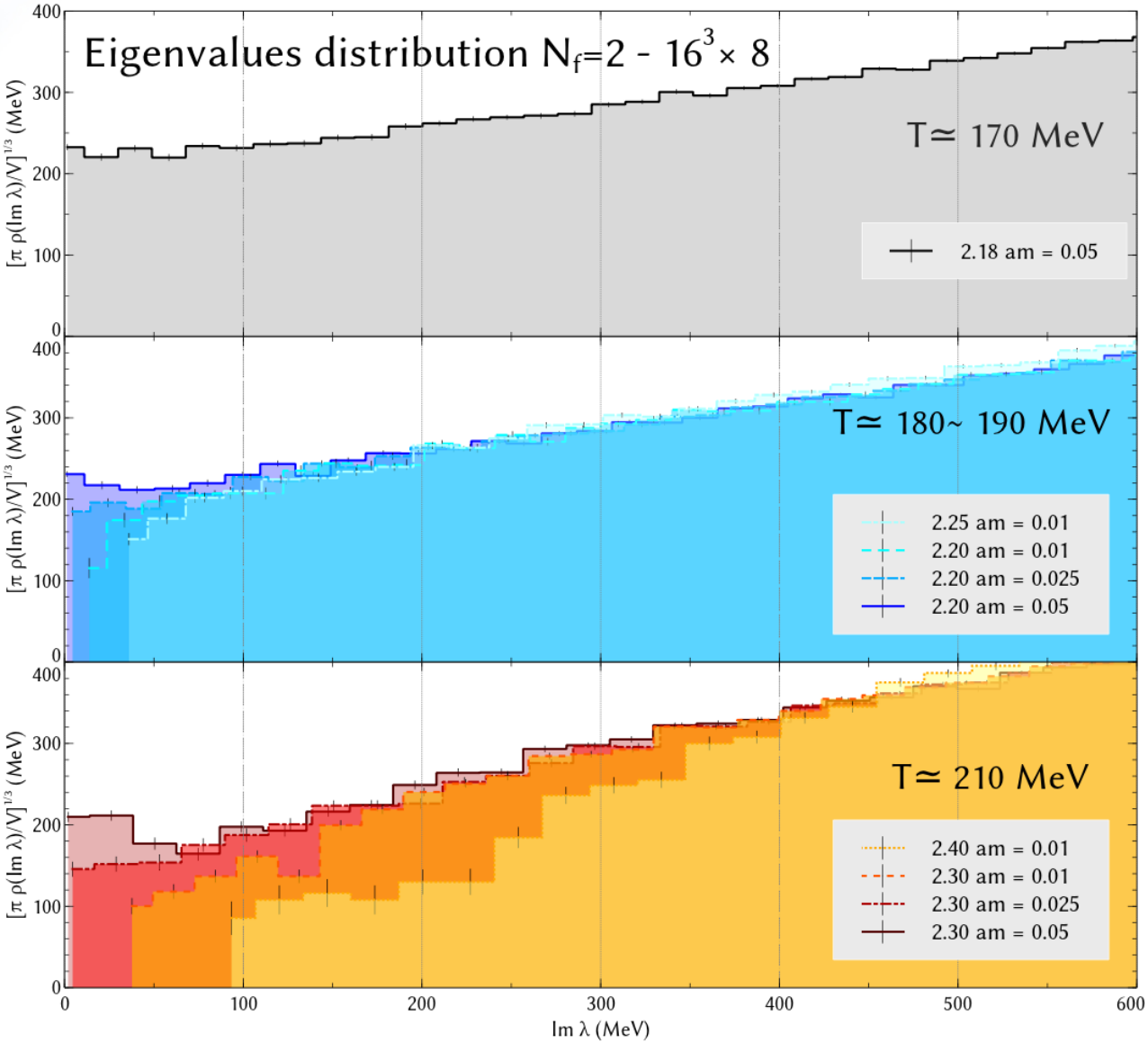

Effect of axial symmetry on the Dirac sperctrum

$$\chi^{\pi-\delta} = \int d\lambda \rho_m(\lambda) \frac{4m^2}{\lambda^2 + m^2}$$

If axial symmetry is restored we can conclude that

$$\lim_{\lambda\to 0} \lim_{m\to 0} \frac{\rho_m(\lambda)}{\lambda} = 0$$

Ref: S. Aoki, internal note

Full QCD – Meson correlators

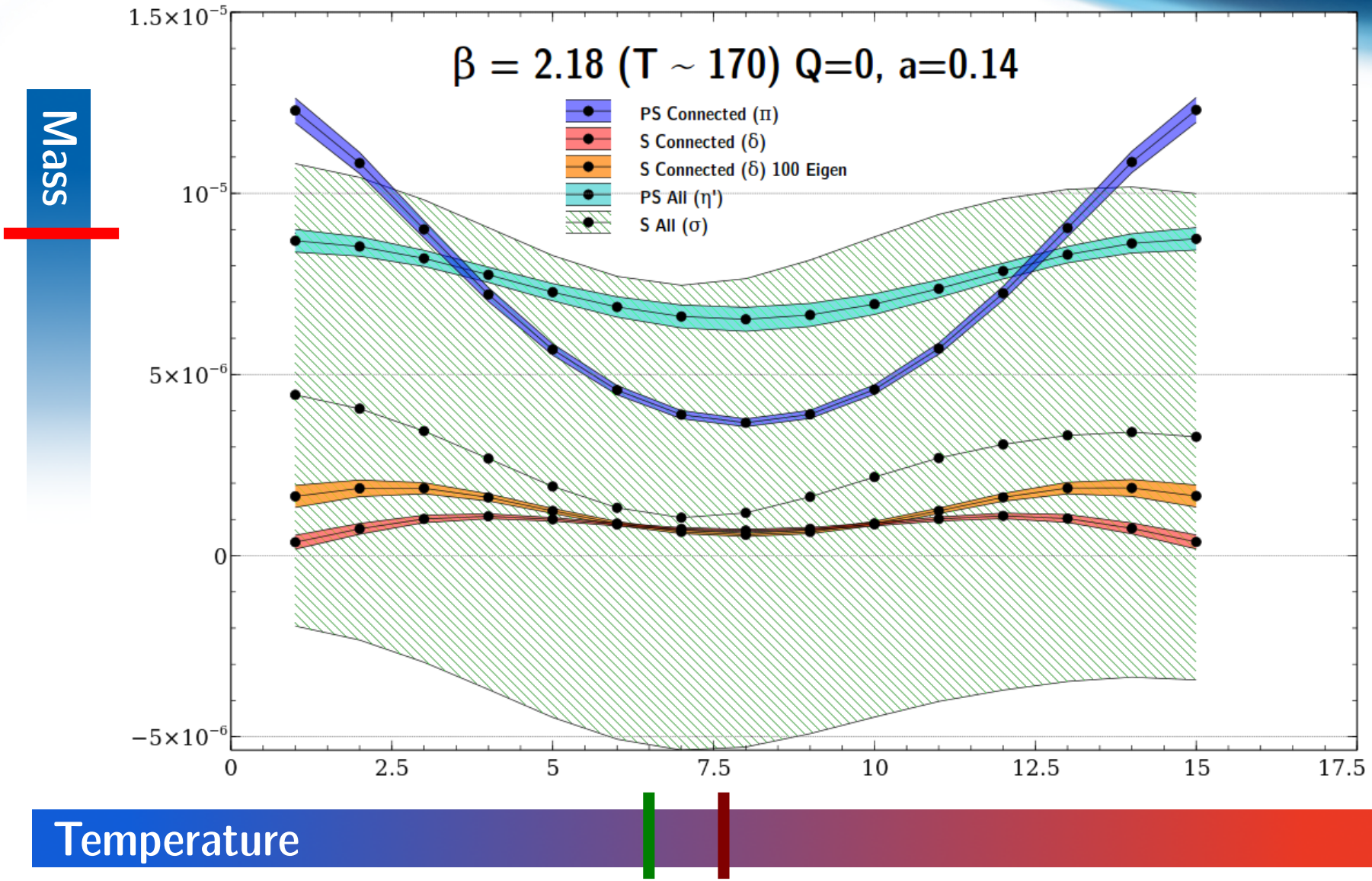

Full QCD – Meson correlators

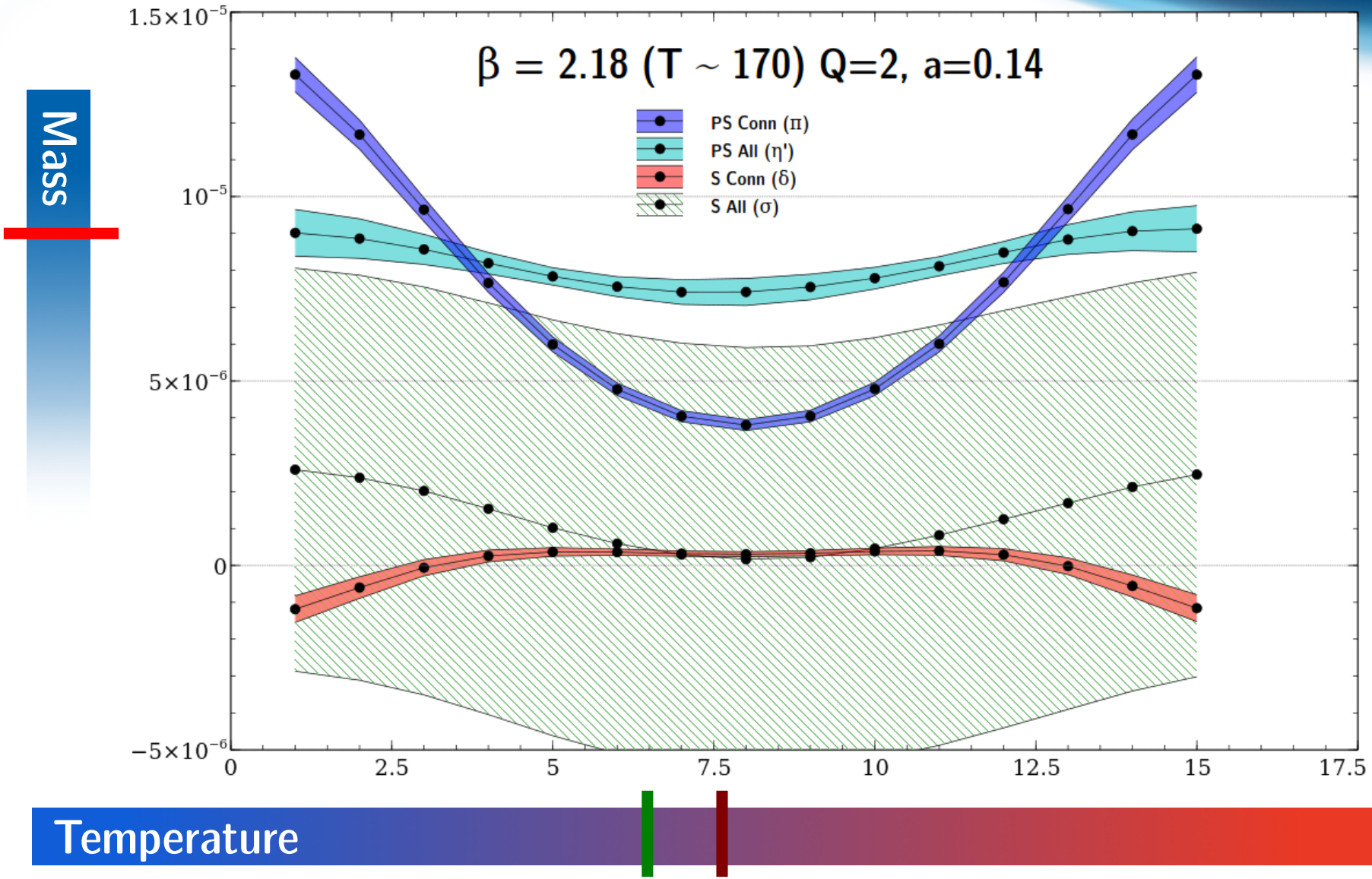

Full QCD – Meson correlators

Mass

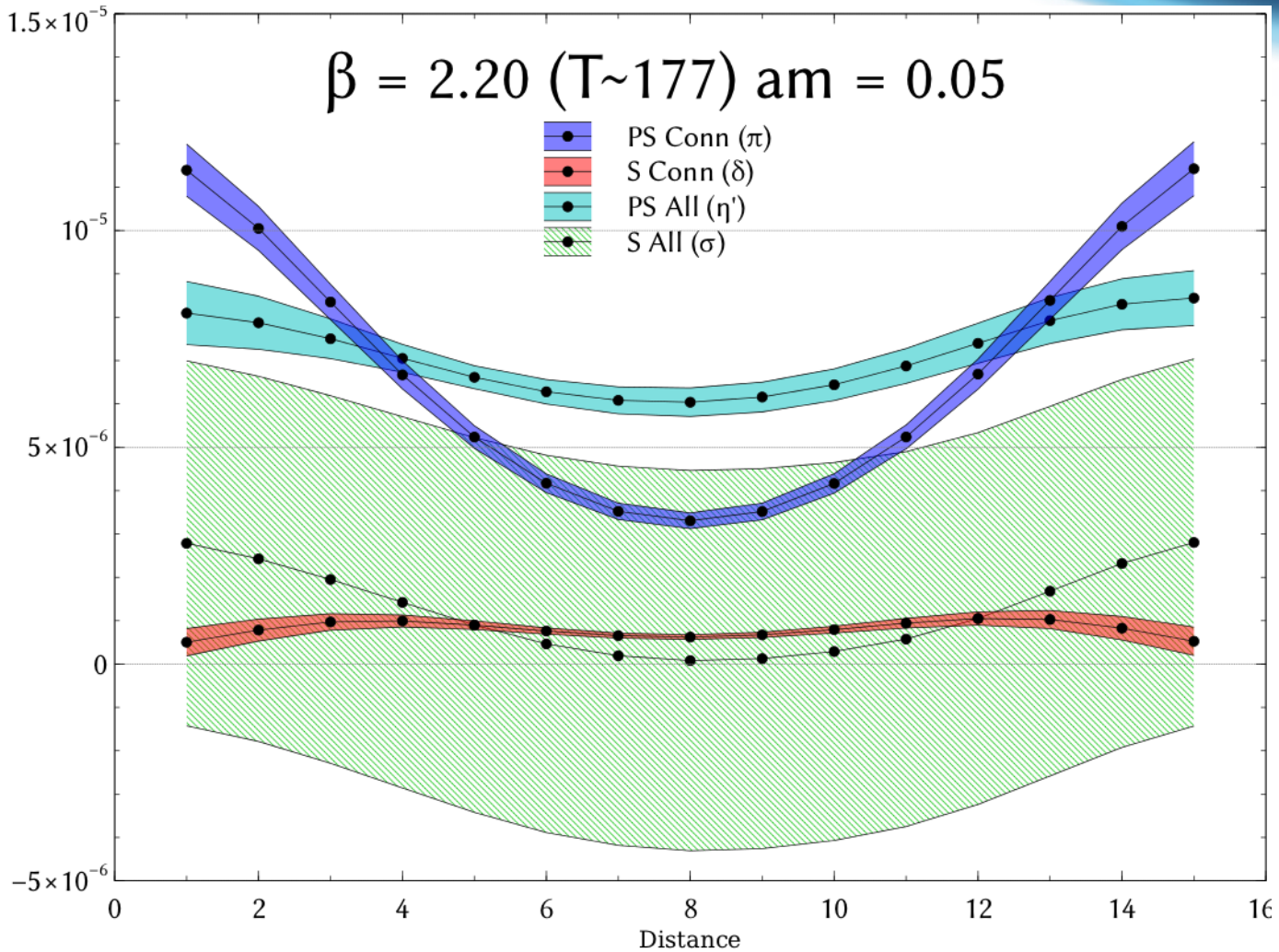

Temperature

Full QCD – Meson correlators

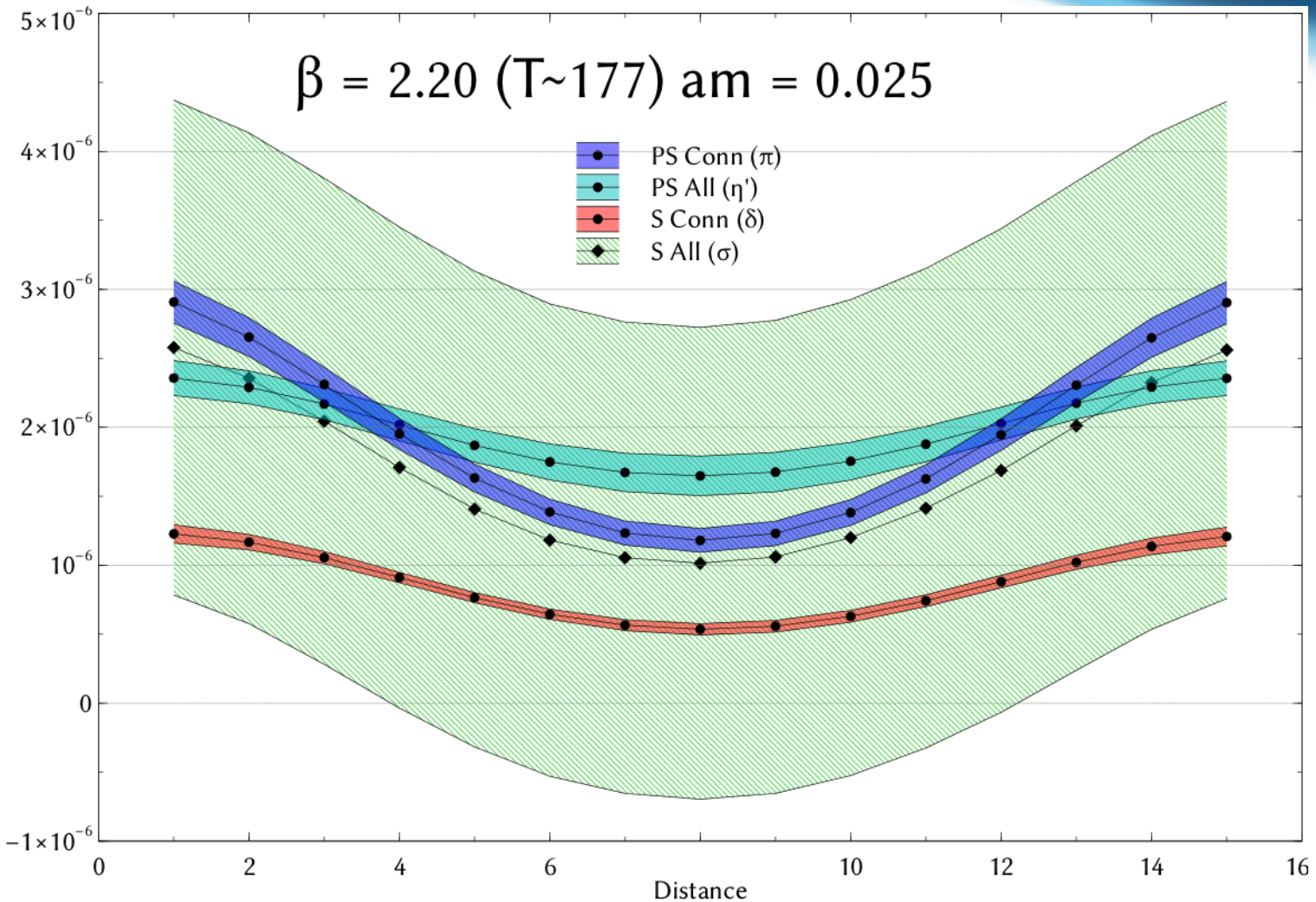

Mass

Temperature

Full QCD – Meson correlators

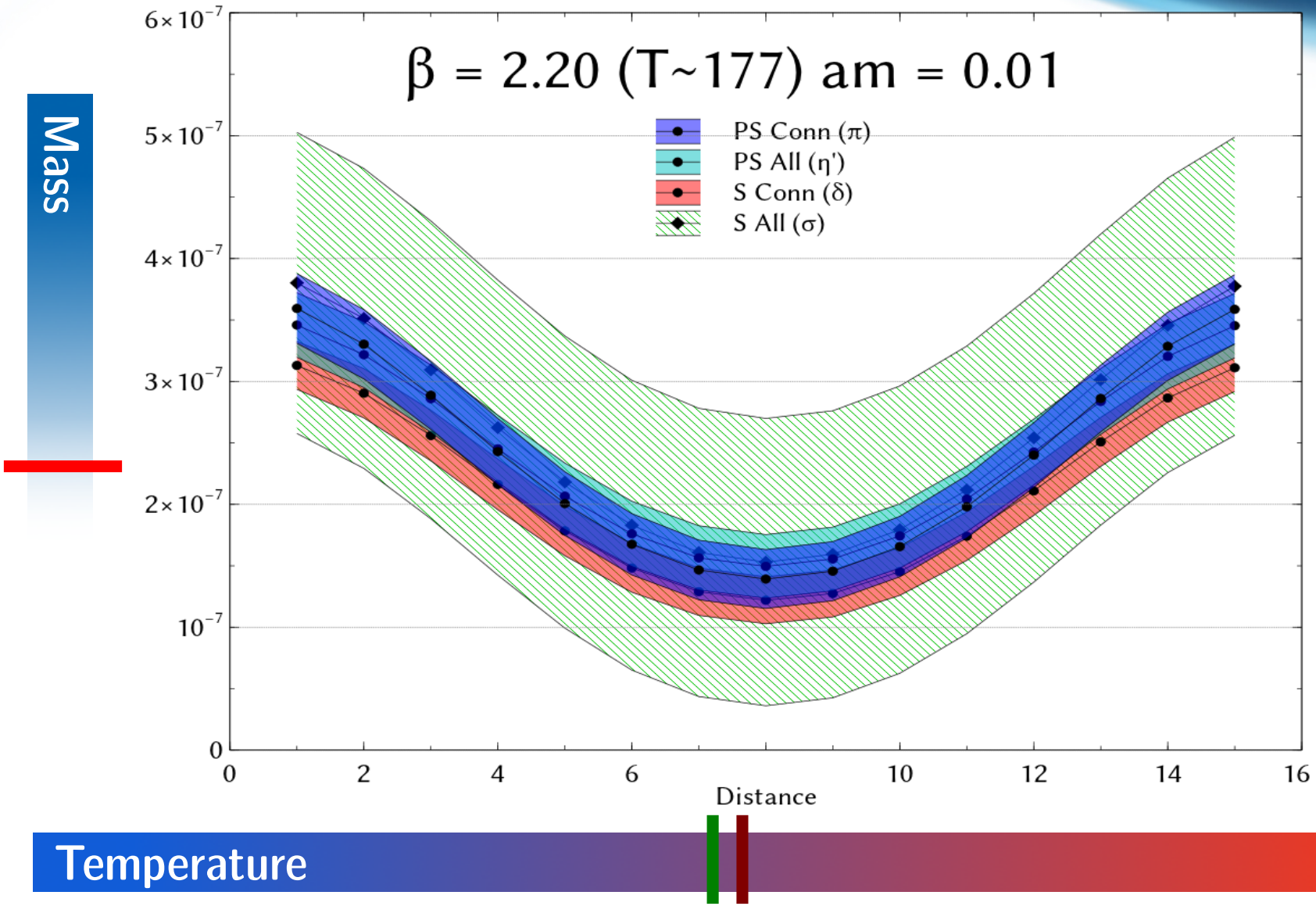

Full QCD – Meson correlators

Mass

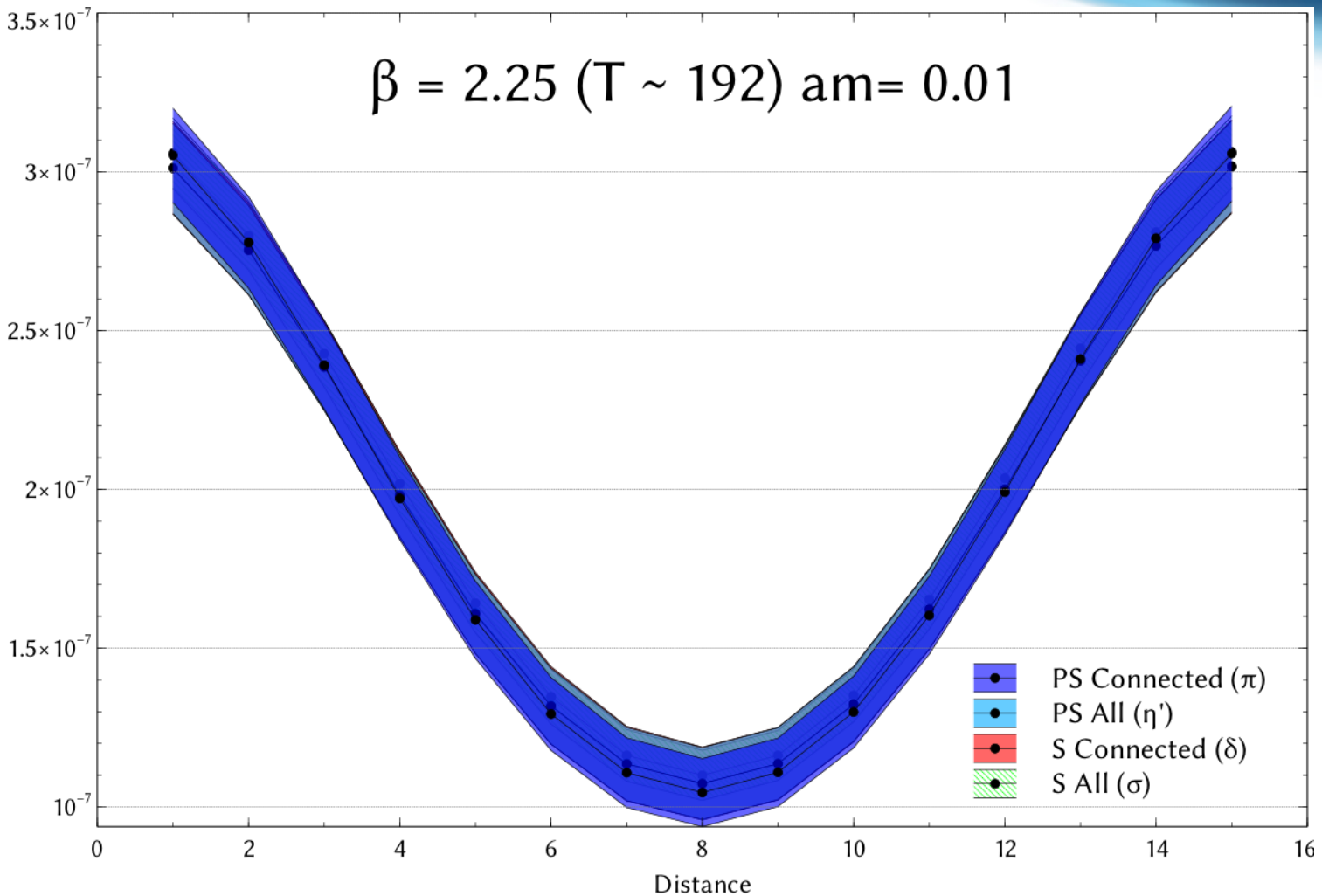

Temperature

Full QCD – Meson correlators

Mass

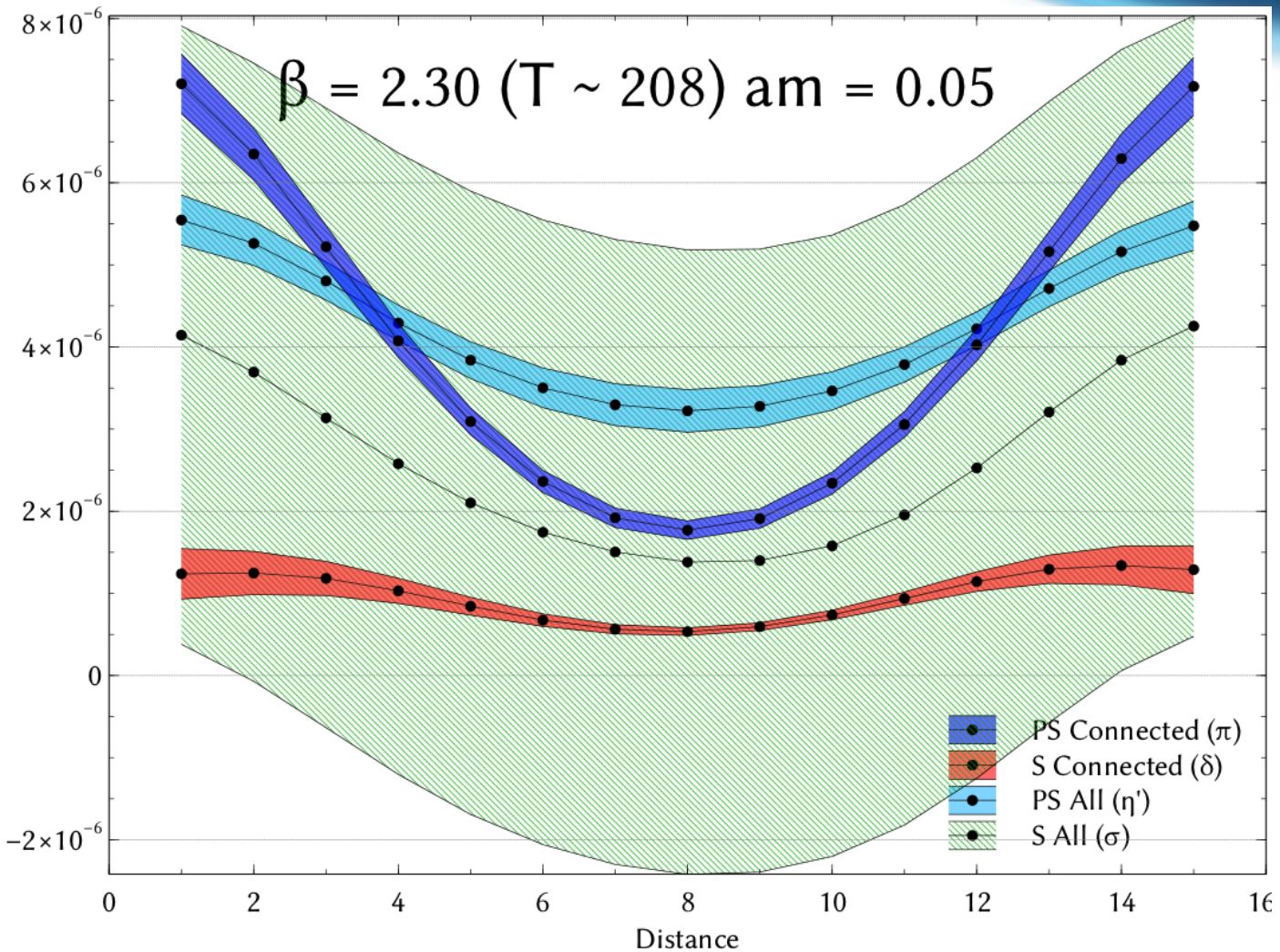

Temperature

Full QCD – Meson correlators

Mass

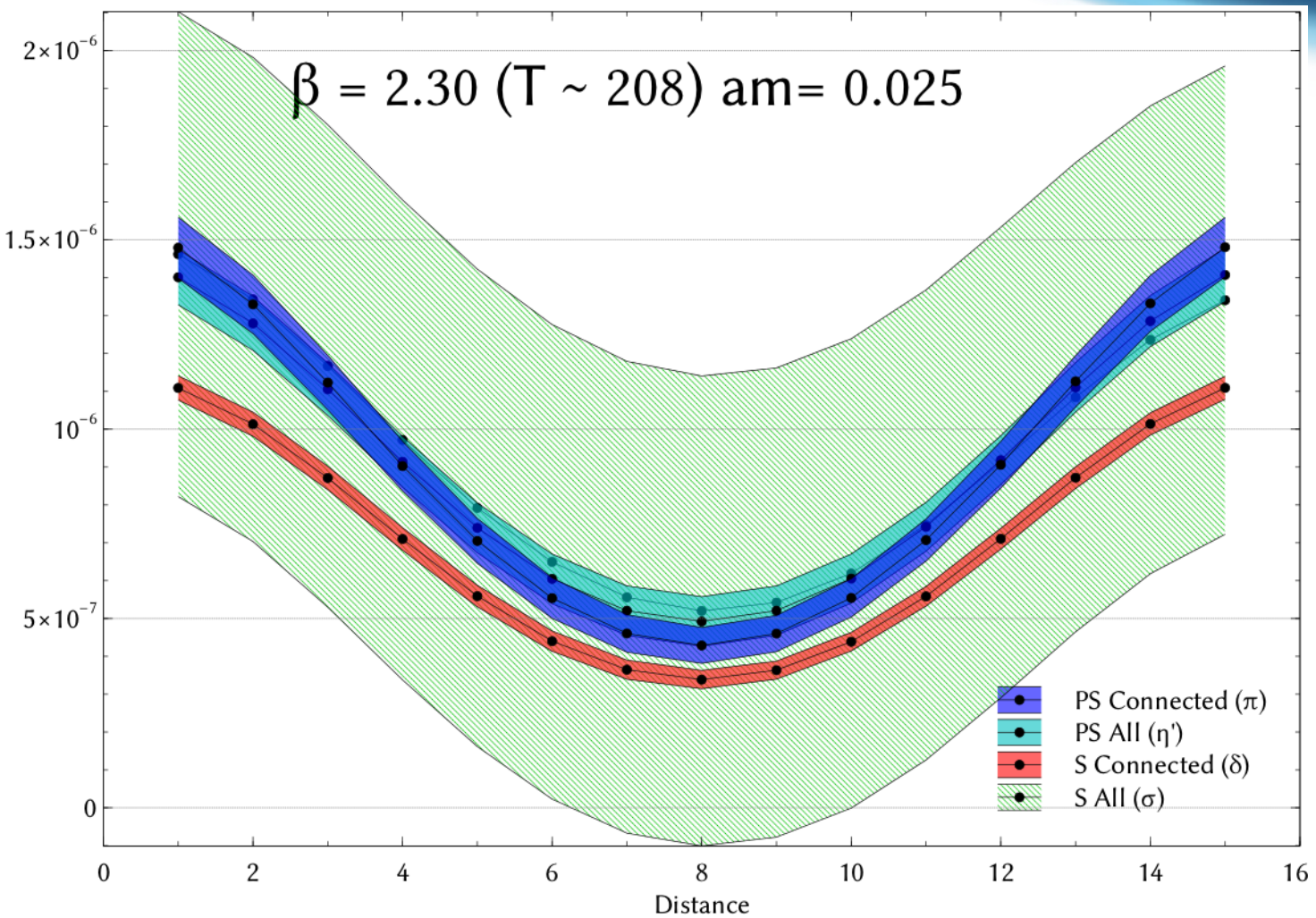

Temperature

Full QCD – Meson correlators

Mass

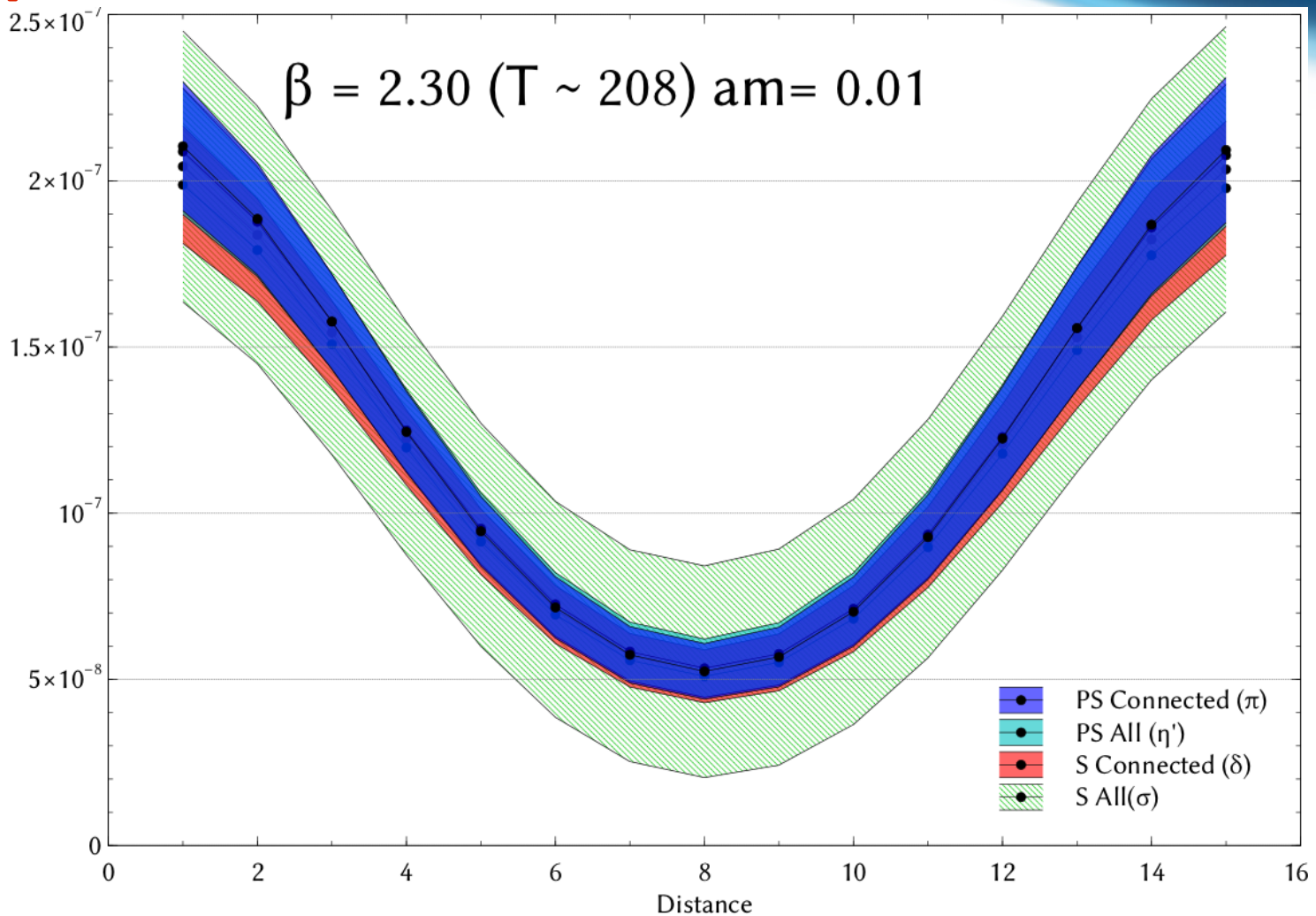

Temperature

Full QCD – Meson correlators

Mass

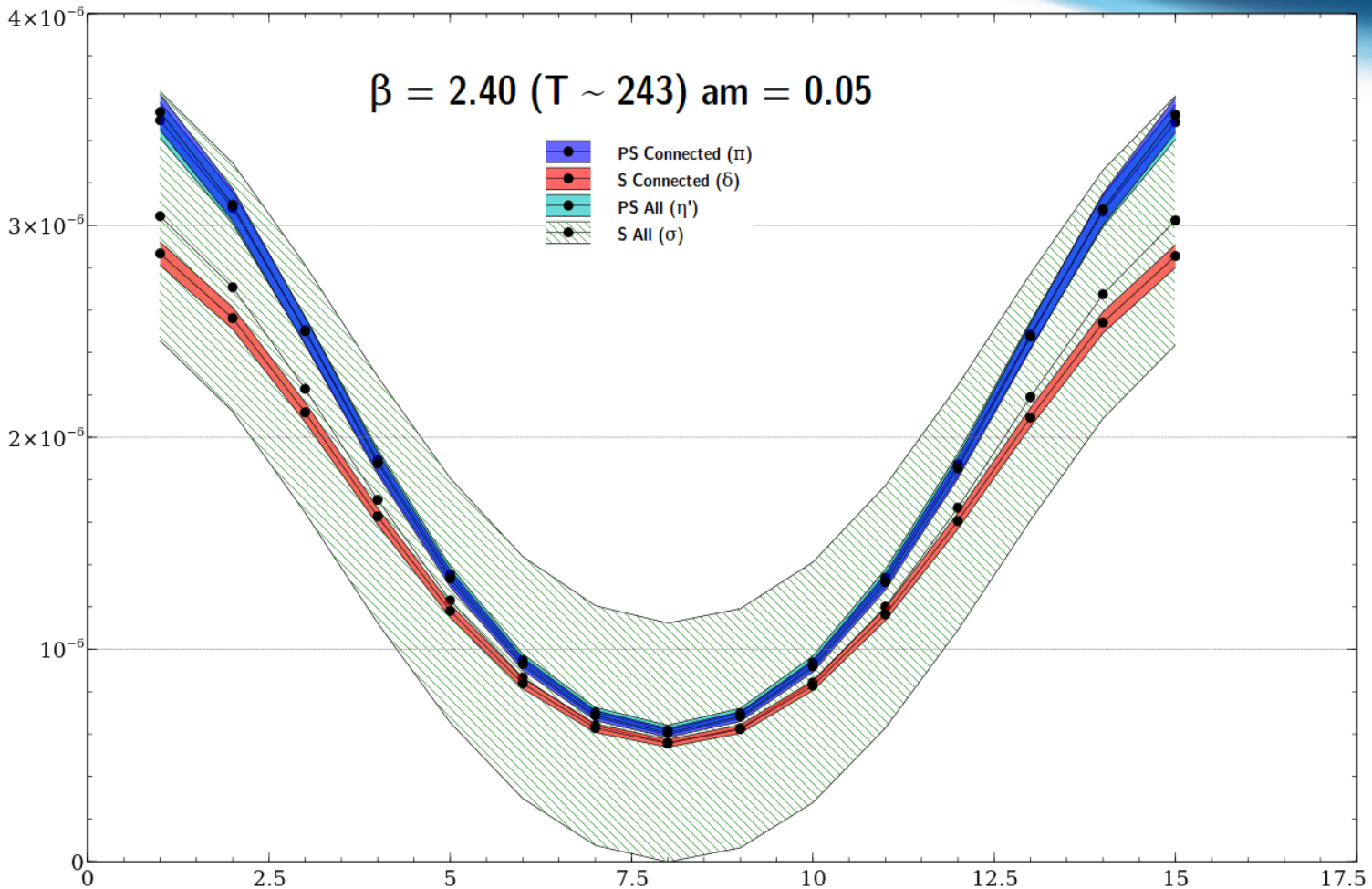

Temperature

Summary

- Overlap fermions are the best choice to check axial anomaly at finite temperature
- Current machine and algorithms permit now realistic simulations...
- ...at the cost of fixing topology
- We checked feasibility of finite t. sim. by test runs in pure gauge theory
- In pure gauge systematic errors are under control.

- Results in Full QCD show signal of restoration of axial $U_A(1)$ symmetry
- We need 1-2 points more in the chiral limit

ご清聴ありがとうございました

LuxRay Artistic Rendering of Lowest Eigenmode

Backup slides

Previous analyses

Vranas (Nucl.Phys.Proc.Suppl. 83 (2000) 414-416)
Measured the difference of susceptibilities χ of π and δ.

- Action: DWF, $L_s=24$
- Found a very small relative difference just above T_c in the chiral limit
- Residual mass effects?

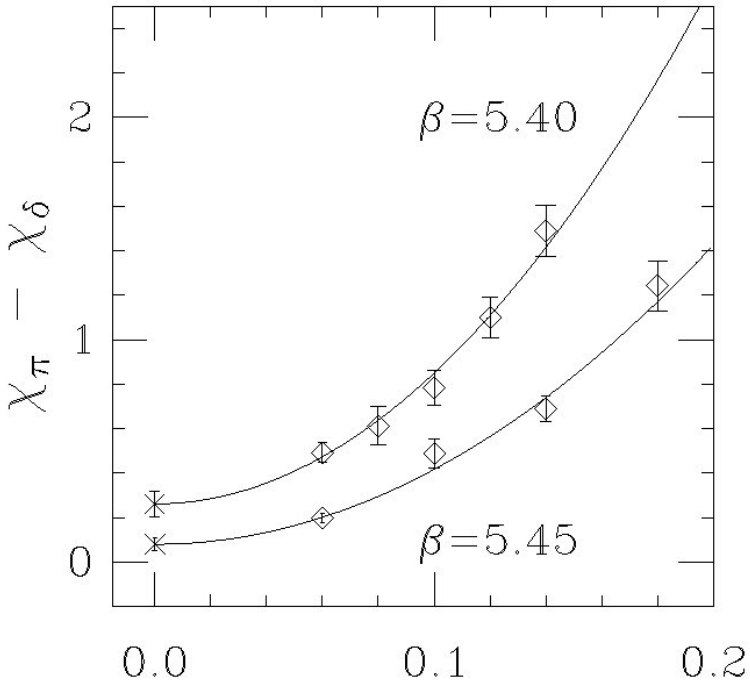

Other works with staggered fermions established a restoration at $T>T_c$
Even bigger problems due to breaking of $U_A(1)$ by staggered fermions.

Topological susceptibility in pure gauge theory - III

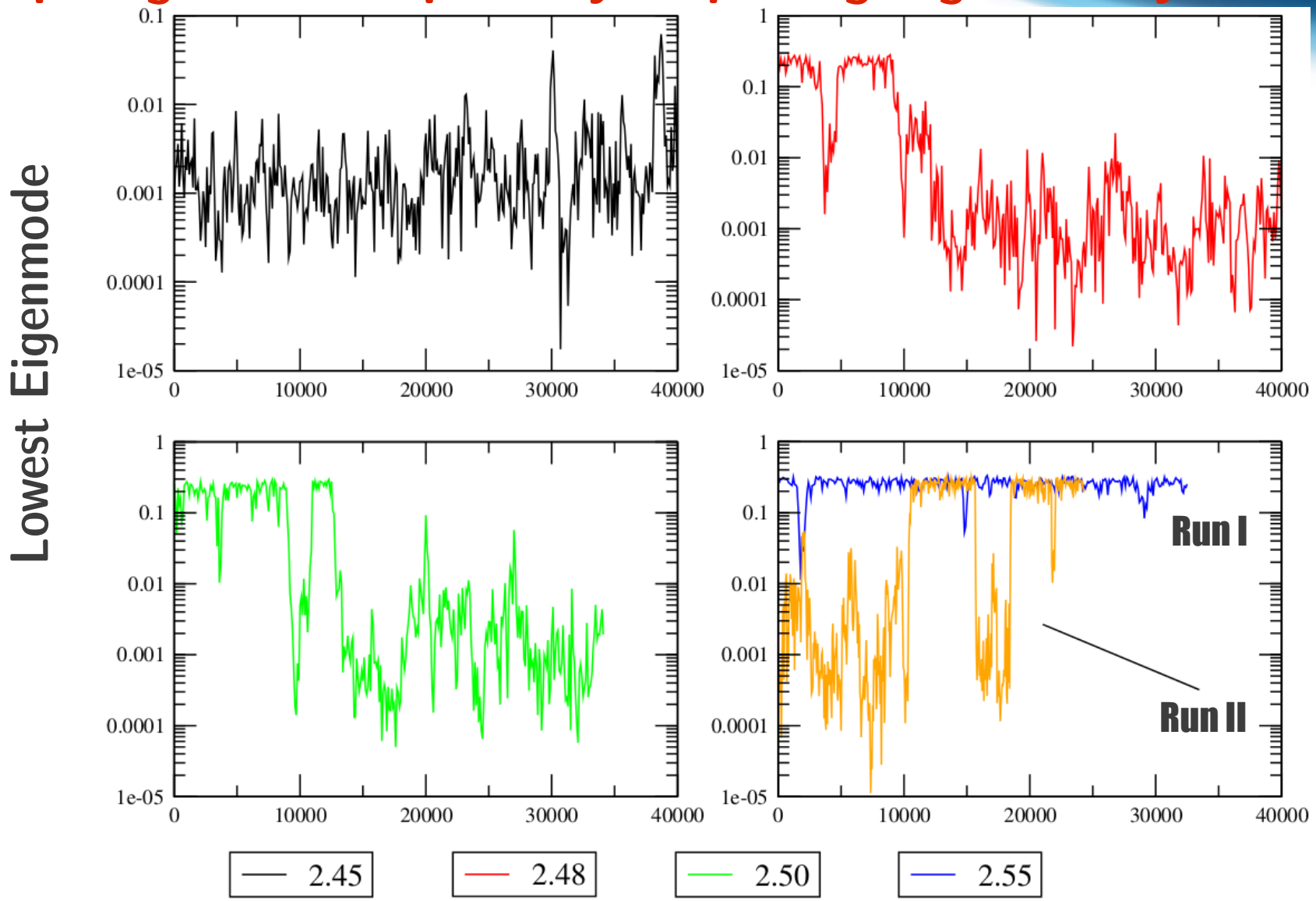

Topological susceptibility in pure gauge theory

$\beta = 2.50$

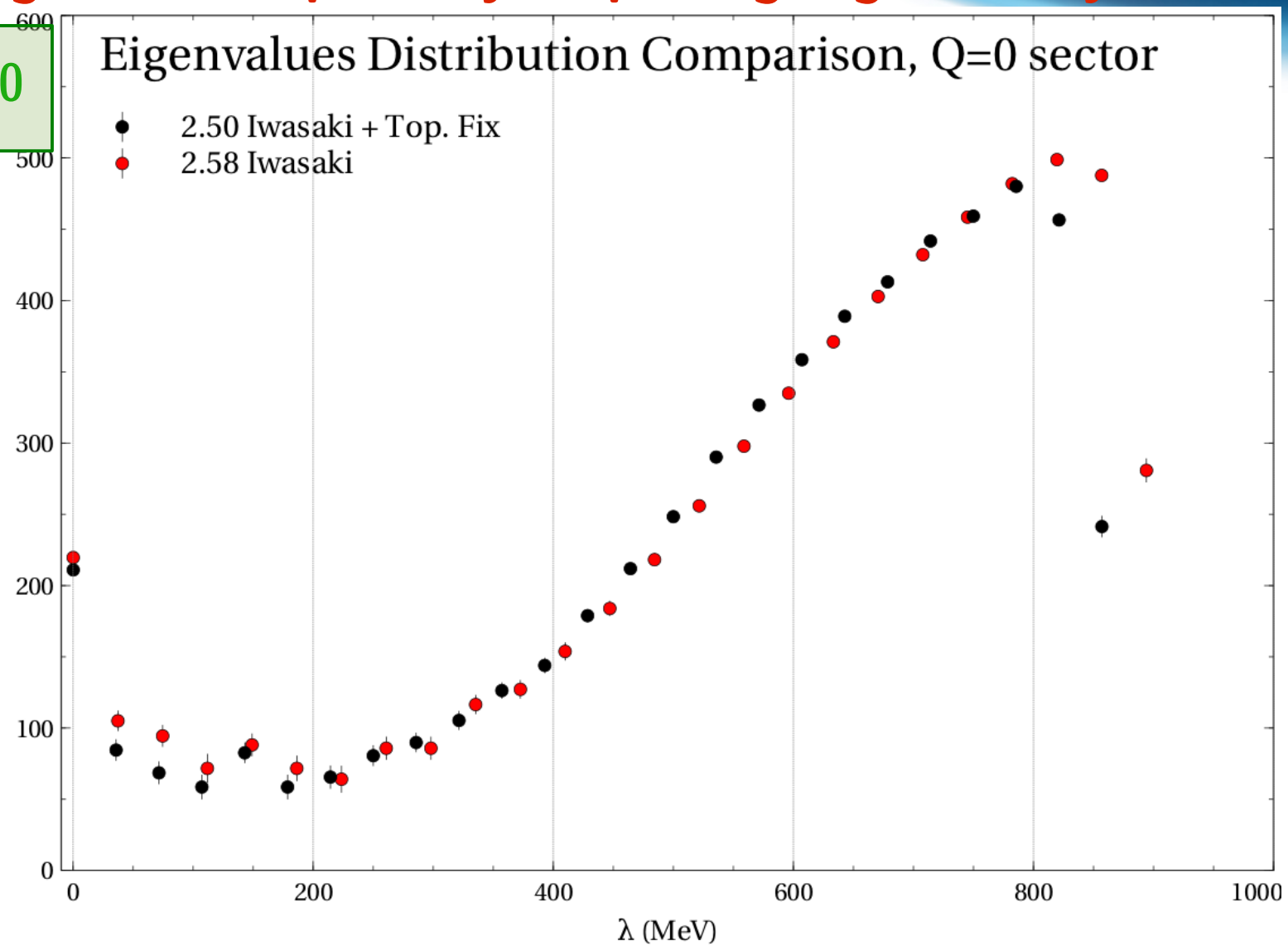

Topological susceptibility in pure gauge theory - VII

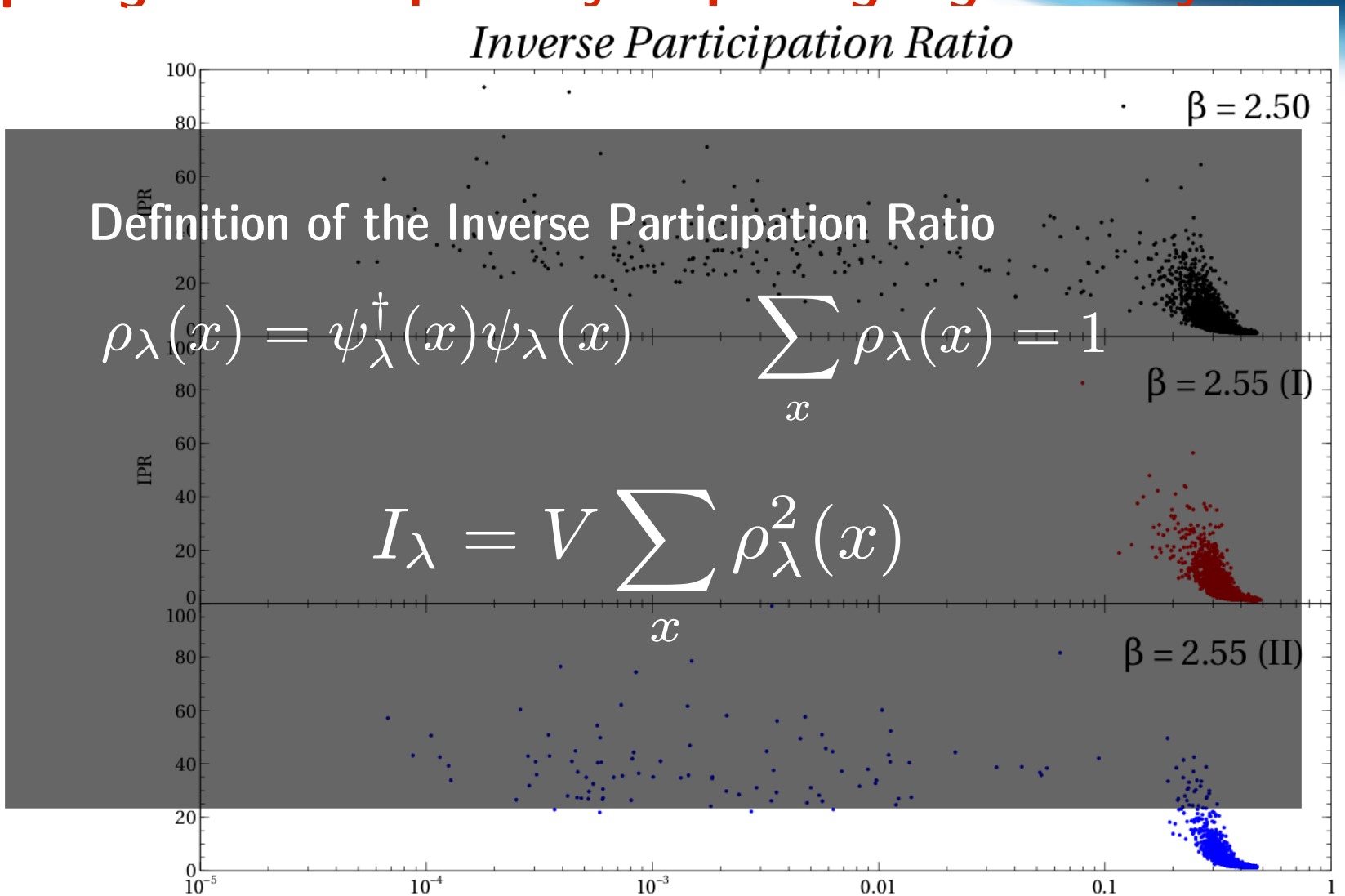

Definition of the Inverse Participation Ratio

$$\rho_\lambda(x) = \psi^\dagger_\lambda(x)\psi_\lambda(x) \qquad \sum_x \rho_\lambda(x) = 1$$

$$I_\lambda = V \sum_x \rho^2_\lambda(x)$$

Topological susceptibility in pure gauge theory - VII

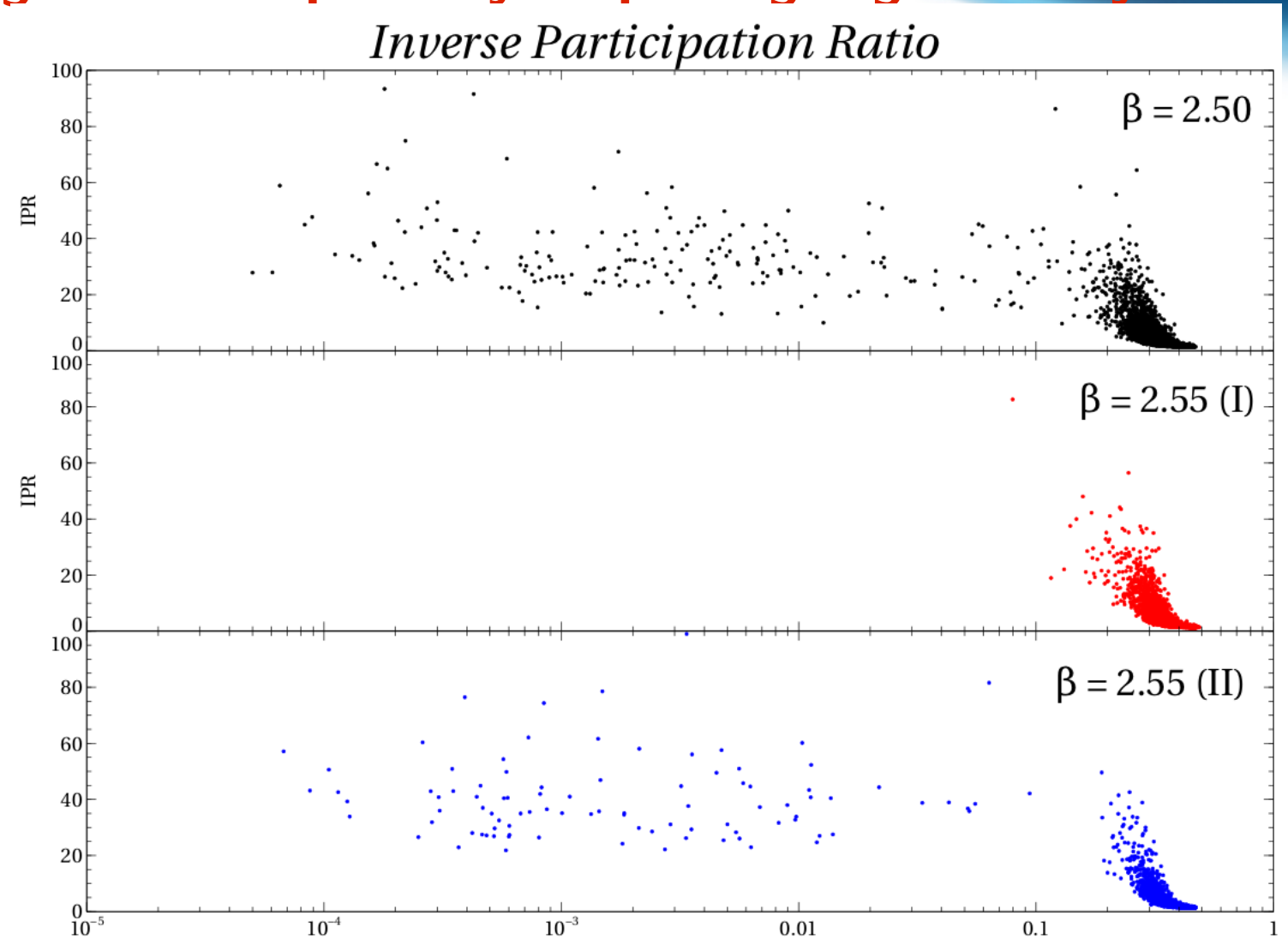

Axial symmetry at finite temp. with overlap fermions

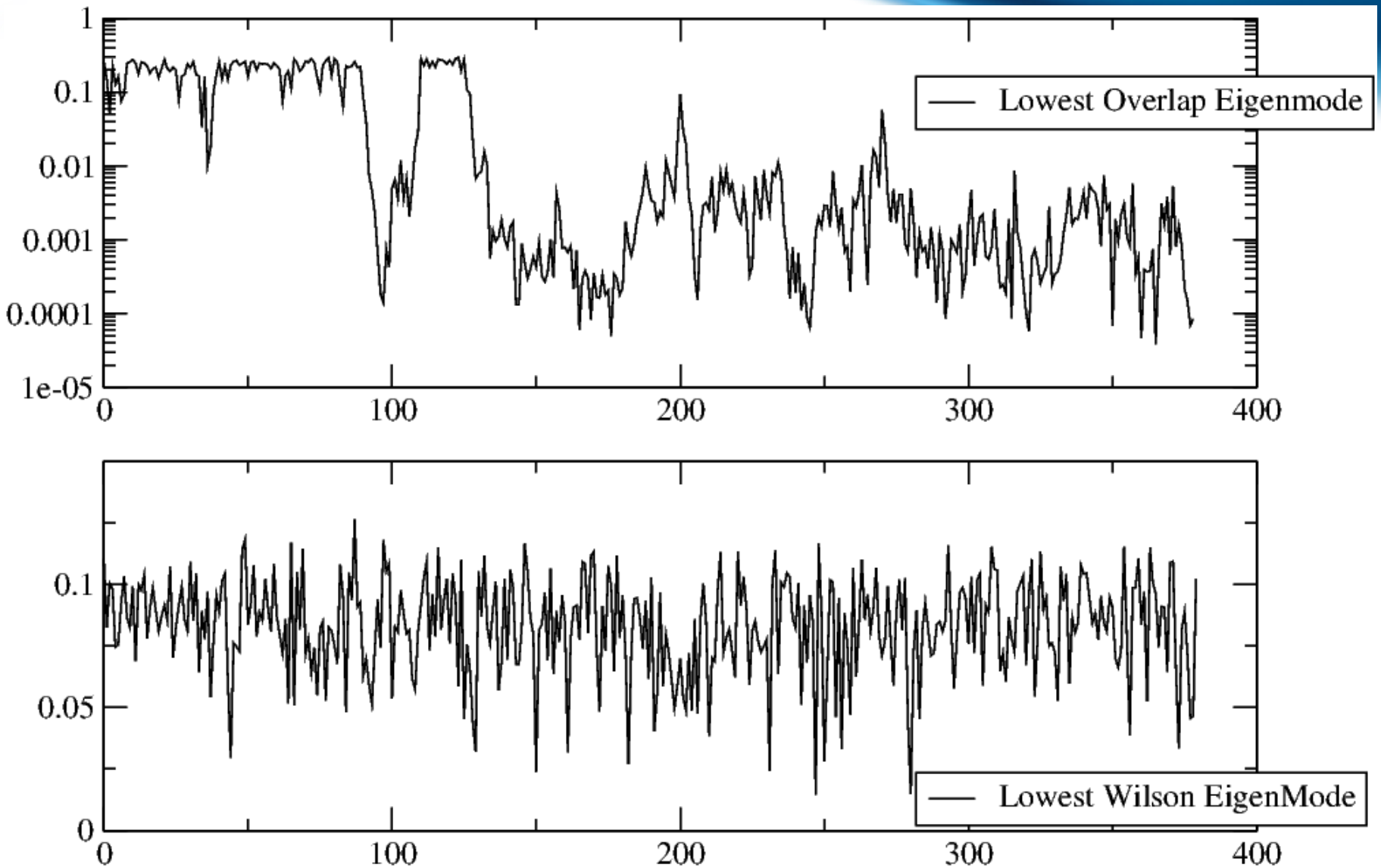

Axial symmetry at finite temp. with overlap fermions

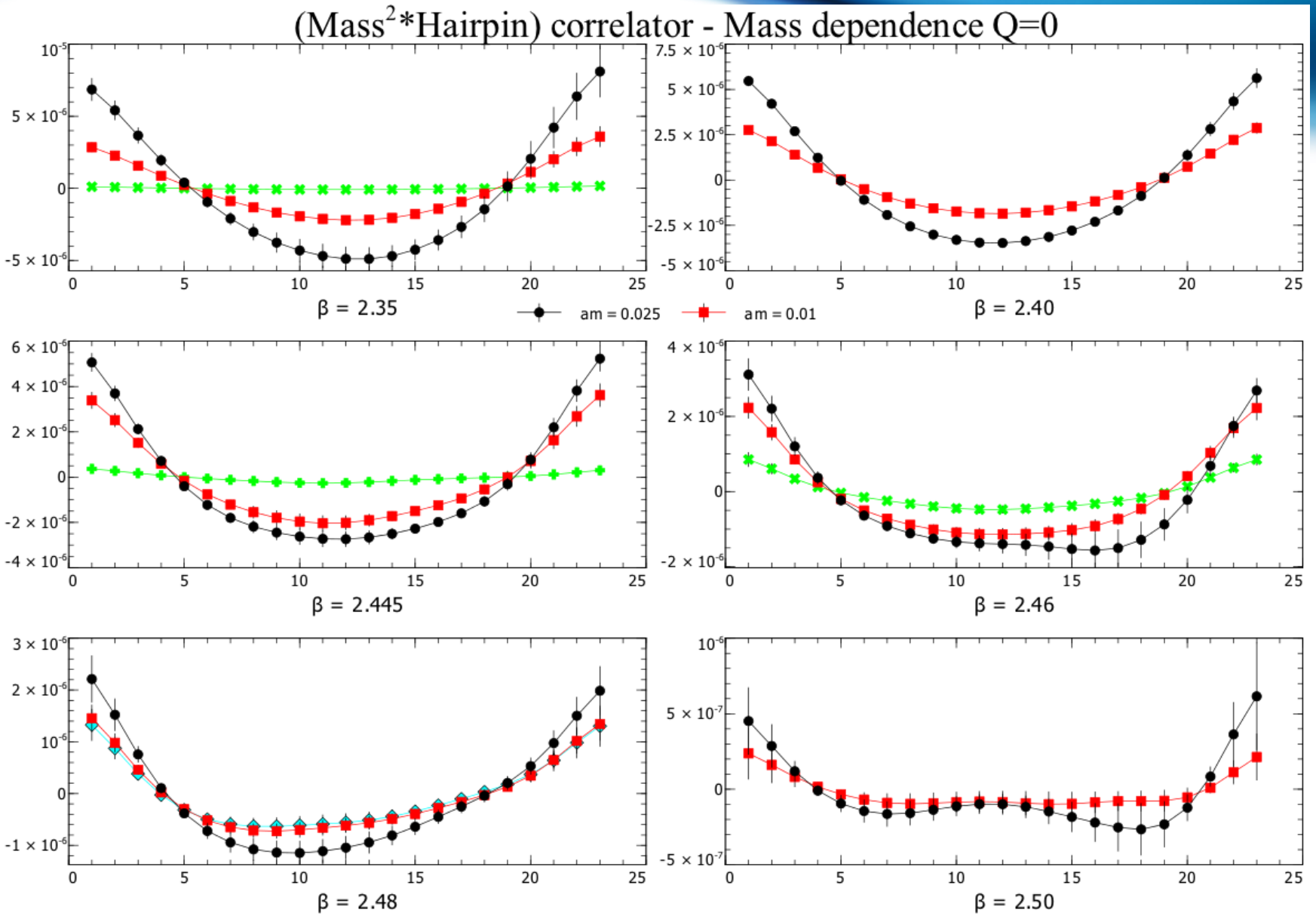

Axial symmetry at finite temp. with overlap fermions

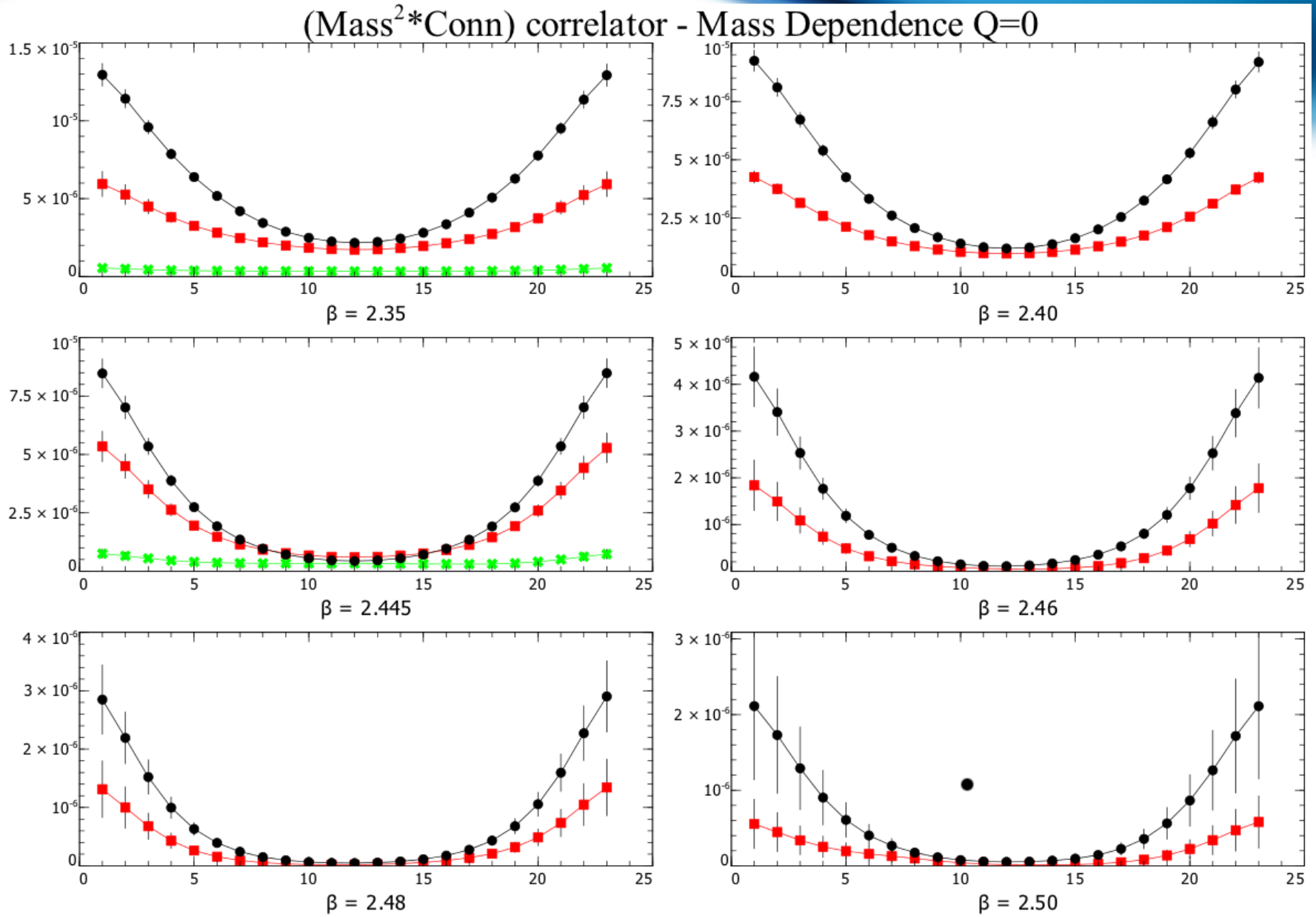

Axial symmetry at finite temp. with overlap fermions

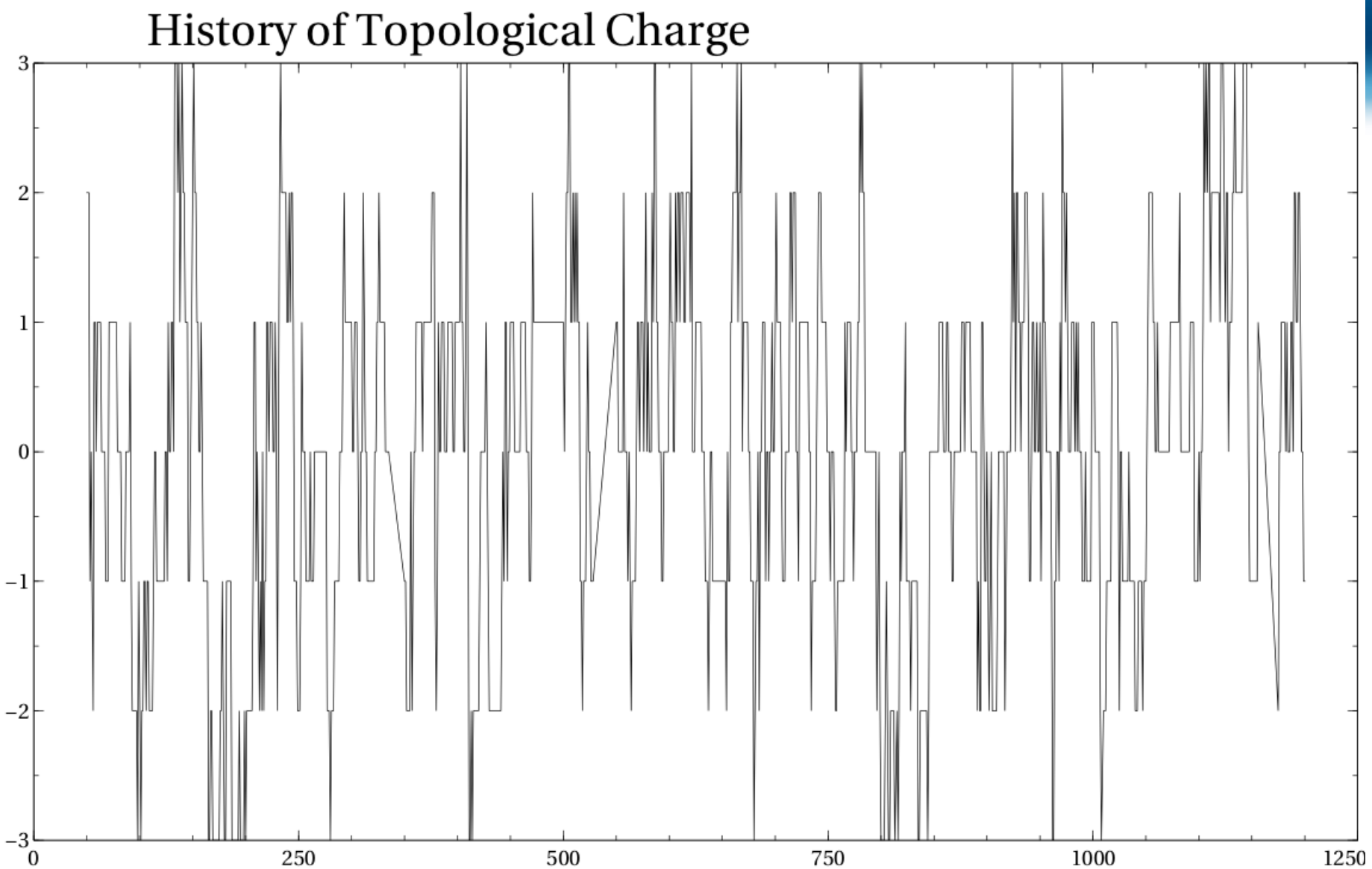

On quark masses

Michael Creutz

BNL

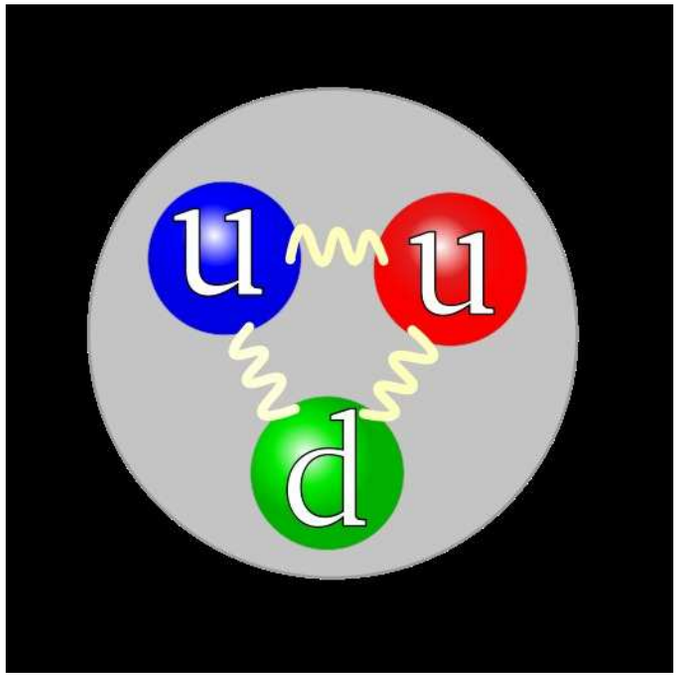

Pseudoscalars in two flavor QCD

- fix m_d , vary m_u
  - $M_\pi^2 \propto \frac{m_u+m_d}{2}$
  - $M_{\eta'} \sim \Lambda_{qcd}$
- with isospin broken
  - $M_{\pi_\pm}^2 - M_{\pi_0}^2 \propto (m_d - m_u)^2$
  - η', π_0, glueballs all mix

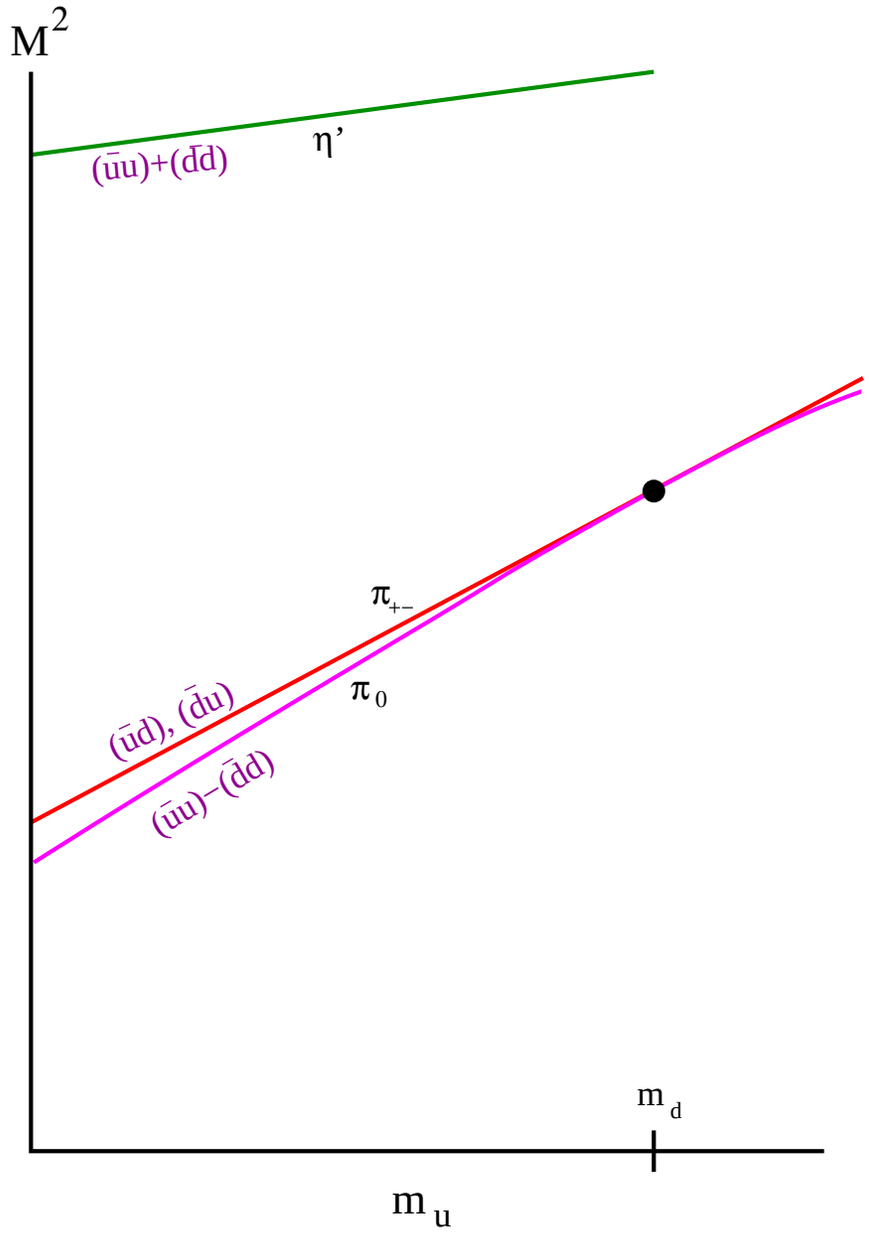

No singularity at $m_u = 0$

- extrapolate to negative m_u
- $M^2_{\pi_0}$ can go negative
- pion condensate forms
  - $\langle \pi_0 \rangle \neq 0$
  - CP broken
- occurs at $\Theta = \pi$
  - $\prod_q m_q < 0$

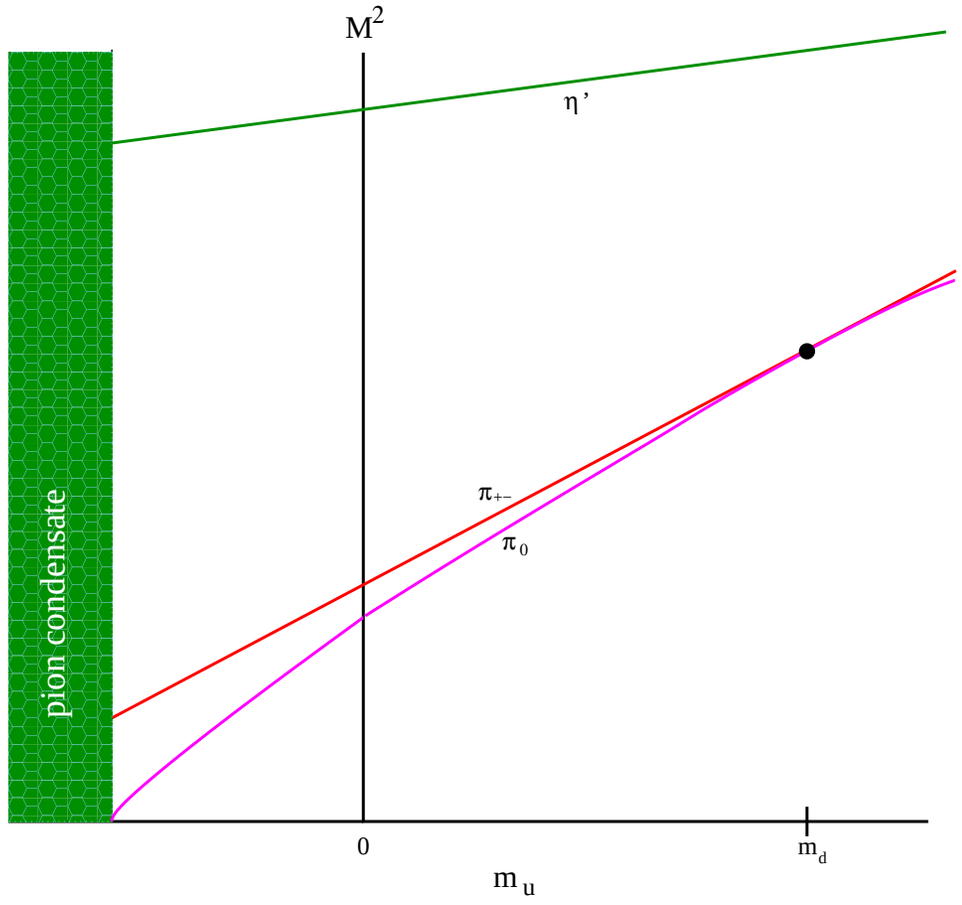

Dashen 1971

Manifested in both ‘‘linear’’ and ‘‘nonlinear’’ sigma models

Second order transition at non-vanishing m_u and m_d of opposite sign

- long distance physics without small Dirac eigenvalues

No structure at $m_u = 0$ when $m_d \neq 0$

- no long distance physics despite possible small Dirac eigenvalues

At the heart of several frustrating and bitter controversies

- Does $m_u = 0$ have any fundamental meaning?
- Do rooted staggered fermions make sense?
- Is topological susceptibility a physical observable?

Two flavors in the massless limit: $m_u = m_d = 0$

- massive proton, neutron, eta prime, glueballs
- 3 massless Goldstone pions

Eta prime and neutral pion: distinct mixtures of $\overline{u}u$, $\overline{d}d$, and glue

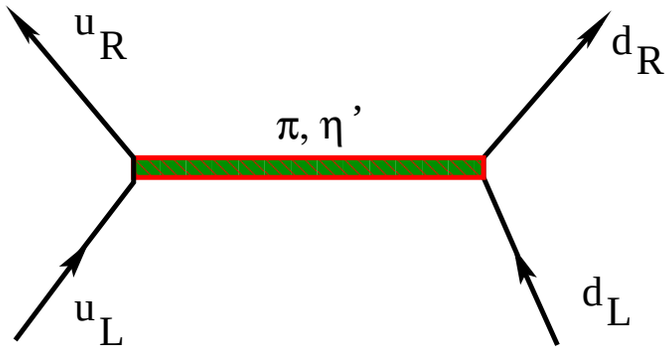

- anomaly: π_0 and η' not degenerate
- four point vertex $\langle \overline{u}_L u_R \, \overline{d}_L d_R \rangle$ does not vanish

Helicity-flip quark-quark scattering does not vanish in the chiral limit

Now turn on a small d quark mass

- closing d loop induces u_L u_R mixing

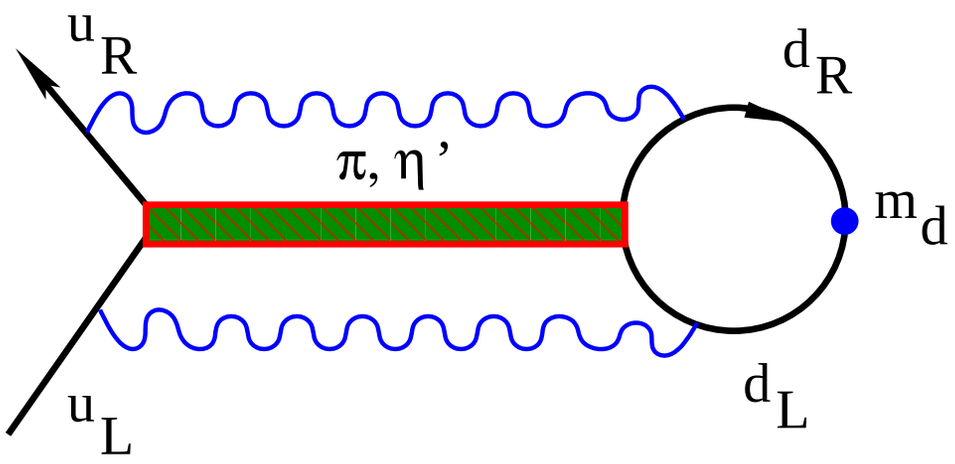

- gluons inserted to compensate for odd meson parity

Non-zero d quark mass induces an effective mass for the u quark

Non-perturbative effects

- renormalize $\frac{m_u}{m_d}$
- quark mass ratios not renormalization group invariant
  - (except in isospin limit)

Effect automatically included in lattice simulations

Old point

- Georgi, McArthur, 1981 (unpublished)
- Banks, Nir, Seiberg, 1994 (conference proceedings)
- MC, 2003 (unpublished)
- MC, 2004 (PRL)

Intense consternation from the perturbative community

- effect not seen perturbatively, i.e. in the $\overline{MS}$ scheme
- consequences
  - mass renormalization is not flavor blind
  - mass independent regularization problematic
  - inherent ambiguities defining $m_u = 0$

$\overline{MS}$ is only a perturbative regulator

- when $m_u \neq m_d$

Matching lattice masses to $\overline{MS}$ is not appropriate!

Specific critiques

Complaint 1:

- Use a mass independent regularization
  - $a\frac{dm_i}{da} = \gamma(g)m_i \;\Rightarrow\; \frac{m_i}{m_j} =$ constant

Response:

- allowed, but obscures above off-diagonal m_d effect on m_u
- no guarantee that $\frac{m_i}{m_j}$ universal between schemes
- lattice is not a mass independent scheme
  - unclear how to do matching

When $m_u \neq m_d$

- isospin broken
  - $\frac{M^2_{\pi^0}}{M^2_{\pi^\pm}} = 1 - O\left(\frac{(m_u - m_d)^2}{(m_u + m_d)\Lambda_{qcd}}\right)$

Holding quark mass ratios fixed

- hadronic mass ratios scale dependent

Holding hadronic mass ratios fixed

- quark mass ratios scale dependent

Complaint 2:

- Do matching at 100 GeV
- instantons exponentially suppressed and irrelevant

Response:

- the lattice simulations are not done at miniscule scales
  - instanton effects must be included
- $1/g^2 \sim \log(\mu) \sim \log(1/a)$
  - exponential suppression in $1/g^2$ $\rightarrow$ power in scale μ

Effect controlled by

- $M_{\eta'} - M_{\pi_0} \propto \mu\, g^{-\beta_1/\beta_0^2}\, e^{-1/(2\beta_0 g^2)} \not\to 0$
  - $\beta_0 = \frac{1}{16\pi^2}(11 - 2N_f/3)$
  - $\beta_1 = \left(\frac{1}{16\pi^2}\right)^2 (102 - 38N_f/3)$
- also proportional to $m_d - m_u$
- estimate at scale $\mu = 2$ GeV
  - $\Delta m_u(\mu) \sim \frac{(M_{\eta'} - M_{\pi_0})\,(m_d - m_u)}{\mu} = O(1\text{ MeV})$
  - same magnitude as quoted ‘‘results’’

Note

- $M_{\eta'} \propto \mu\, g^{-\beta_1/\beta_0^2}\, e^{-1/(2\beta_0 g^2)}$

- exponential behavior controlled by

  - $\frac{1}{2\beta_0 g^2} = \frac{8\pi^2}{(11-2n_f/3)g^2} << \frac{8\pi^2}{g^2} =$ classical instanton action

- topological excitations above quantum, not classical, vacuum

- classical instanton action strongly overestimates suppression

Rooted staggered quarks

- tastes: $(SU(4)_u, SU(4)_d)$
- well separated spurious states
- not only in chiral limit
- one massless at $m_u = 0$
  - required by symmetry

Can multiple artifacts cancel?

- requires unitarity violation

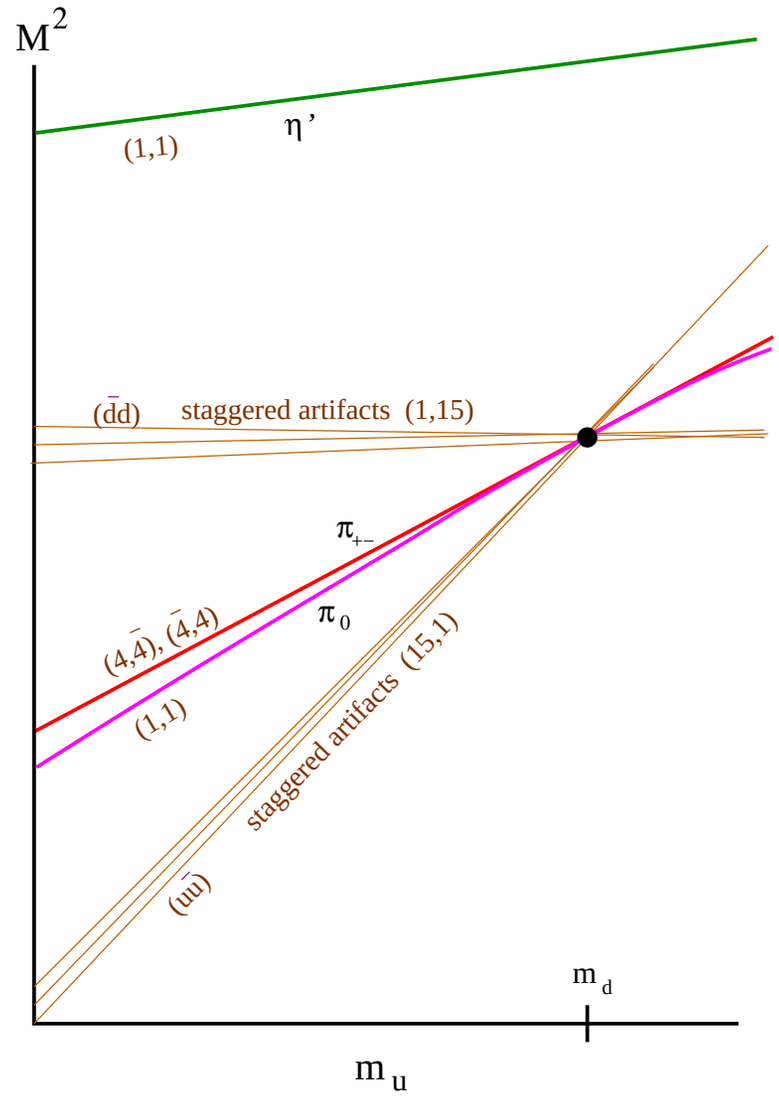

Plausible???

Summary

Non-perturbative effects mix mass terms for different species

- effect absent in perturbation theory
  - inappropriate to match lattice and perturbative masses

Interesting phase structure with negative mass quarks

- CP violating pion condensation
- no structure at $m_u = 0$ when $m_d \neq 0$

Crucial to resolving many controversies

  - $m_u = 0$, topological susceptibility, rooting

Review: Acta Physica Slovaca 61, 1 (2011), arXiv:1103.3304

free download at http://www.physics.sk/aps/

Extra Slides

Ising-like transition at $m_u < 0$

- order parameter $\langle \pi_0 \rangle \neq 0$
- breaks CP spontaneously

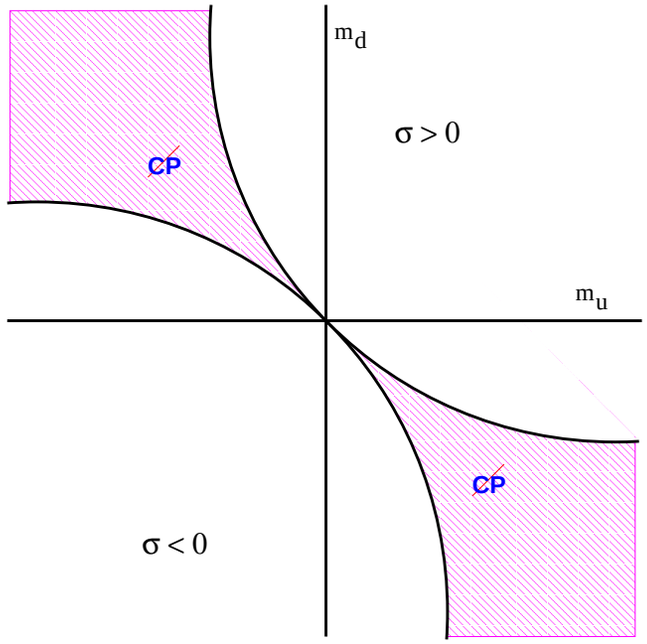

Connected with the anomaly and $M_{\eta'} \sim \Lambda_{qcd}$

- non-perturbative

General mass term $m_1\overline{\psi}\psi + m_2\overline{\psi}\tau_3\psi + im_3\overline{\psi}\gamma_5\psi$

- average quark mass, quark mass difference, CP violation from Theta

Two intersecting first order surfaces

- $(m_1 = 0, m_3 \neq 0)$ and $(m_1 < m_2, m_3 = 0)$

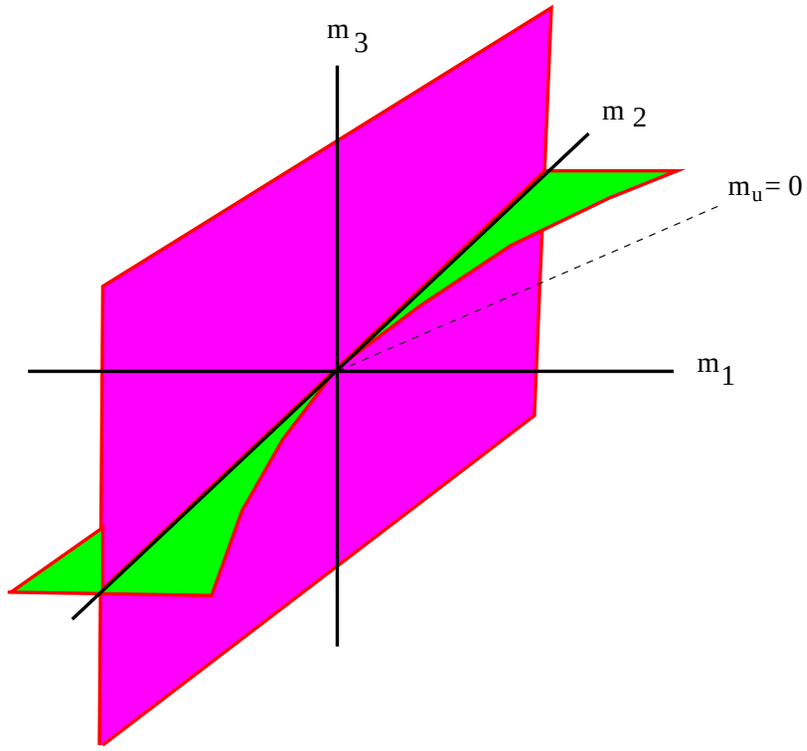

Second order edge at $m_3 = 0, 0 < |m_1| < |m_2|$

CP breaking related to the Aoki phase

- Wilson fermion lattice artifacts
- phase persists in isospin limit

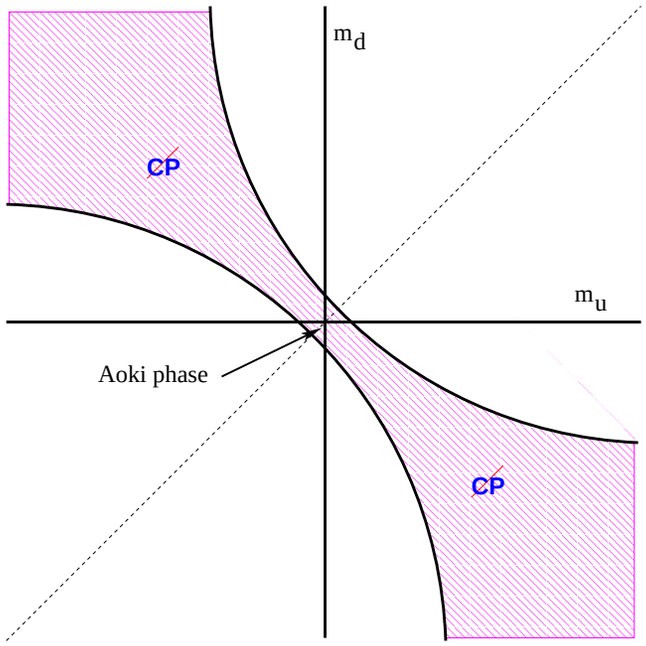

- First order alternative

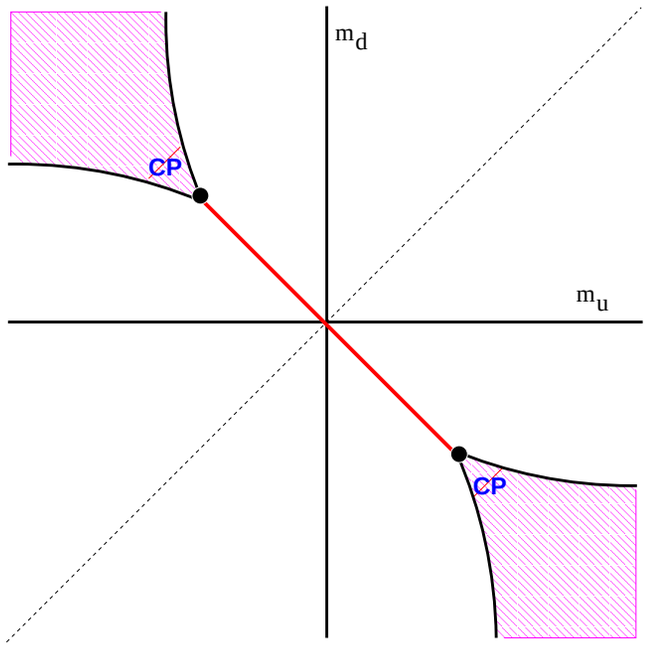

Which alternative remains controversial

- can depend on lattice action

Exploring Three-Nucleon Forces in Lattice QCD

Takumi Doi

(Nishina Center, RIKEN)

for HAL QCD Collaboration

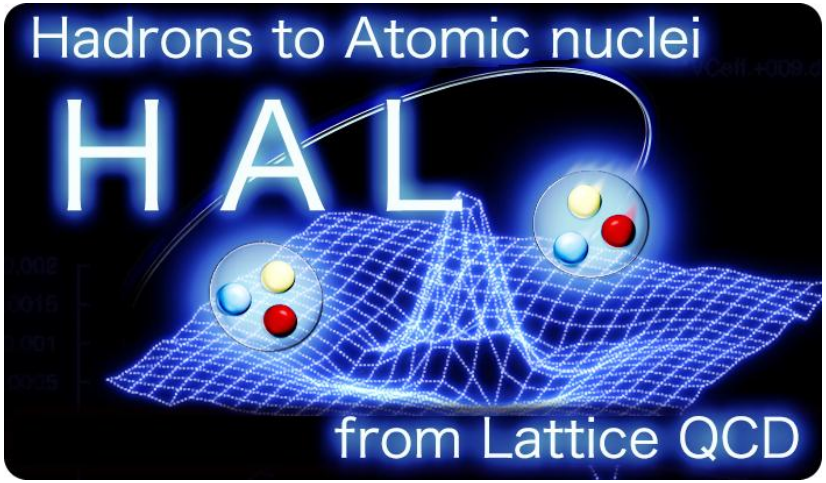

S. Aoki, N. Ishii, H. Nemura, K. Sasaki, M. Yamada (Univ. of Tsukuba)
B. Charron (Univ. of Tokyo)
T. Hatsuda (RIKEN)
Y. Ikeda (Tokyo Inst. Tech.)
T. Inoue (Nihon Univ.)
K. Murano (RIKEN)

Nuclear Physics on the Lattice

- Frontier in the (coming) physical point Lattice era
  - Nuclear Physics directly from Lattice QCD (+QED)
  - (Many other interesting topics in this workshop…)
- Traditional Nuclear Physics

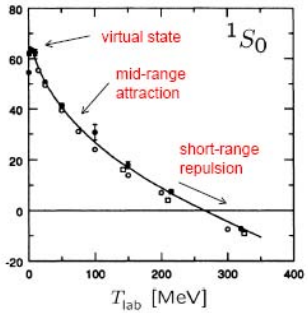

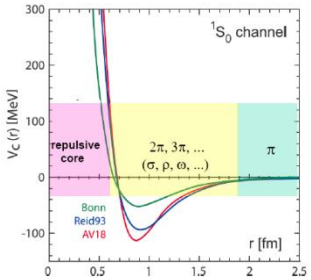

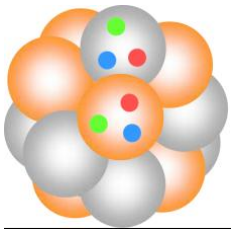

NN phase shifts from experiments → **Phenomenological Nuclear Forces** → **Various applications**

- No clear connection to QCD so far
- ➔ Lattice QCD can establish firm foundations for Nuclear Physics

Nuclear Forces *play* ***significant roles***

Nuclear Physics and Astrophysics from Lattice QCD

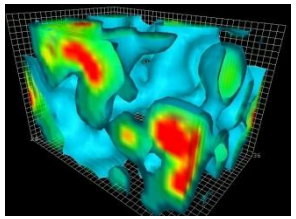

QCD Vacuum

Baryon

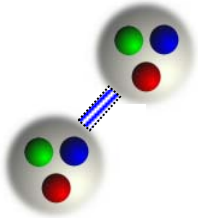

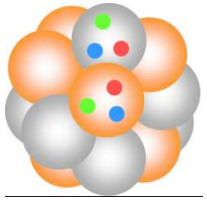

Few-Body / Light Nuclei

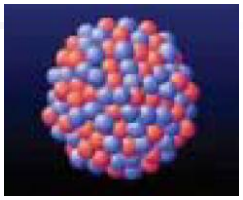

Heavy Nuclei

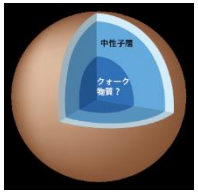

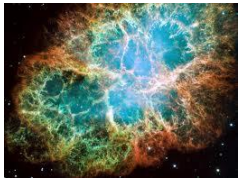

Neutron Star / Supernova

Standard Model

1st-principle lat calc.

Nuclear Forces

Ab-initio nuclear calc.

Nuclear and Astro Physicists thirst for Lattice QCD predictions !

1st-principle lat calc.

(Yamazaki's talk)

(Another talk by Orginos)

Frontier in Hadron-Hadron Interactions

⇒Three-Nucleon Forces (3NF)

What is 3NF ?

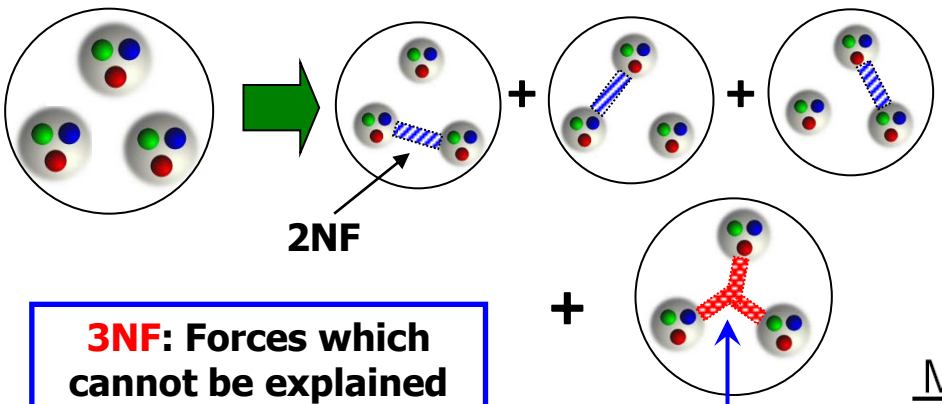

3NF: Forces which cannot be explained by pair-wise 2NF

Neutron Star

(Densest system in the Universe)

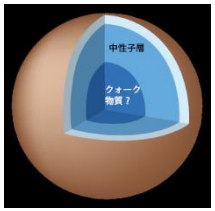

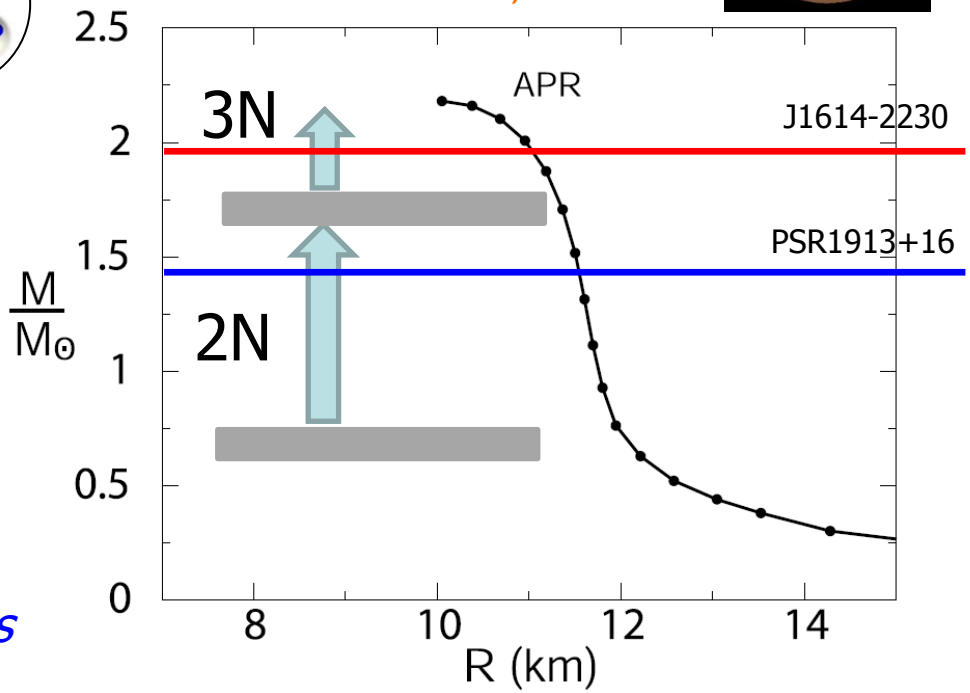

- *EoS of high density matter*
- *Neutron rich nuclei / Nucleosynthesis*
- *B.E. of light nuclei*

Short-range repulsive 3NF is required

Can we understand it from QCD ?

Nuclear Force from Lattice QCD [HAL QCD strategy]

- Potential is constructed so as to reproduce the NN phase shift (or, S-matrix)
- Nambu-Bethe-Salpeter(NBS) wave function

$$\psi(\vec{r}) = \langle 0|N(\vec{x}+\vec{r},t)N(\vec{x},t)|2N\rangle$$

  - Key concept: asymptotic region ←→ phase shift

$$(\nabla^2 + k_\delta^2)\psi(\vec{r}) = 0, \quad r > R$$

- Define the potential at interaction region

$$(\nabla^2 + k_\delta^2)\psi(\vec{r}) = \int d\vec{r}' U(\vec{r},\vec{r}')\psi(\vec{r}'), \quad r < R$$

  - Non-local, but E-independent potential
- The combination of (2NF, 3NF) → observables
  - ← systematic determination by Lat QCD

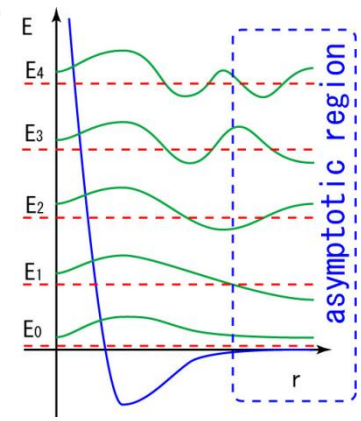

Luscher, NPB354(1991)531

C.-J.Lin et al., NPB619(2001)467
CP-PACS Coll., PRD71(2005)094504

Ishii-Aoki-Hatsuda PRL99(2007)
Aoki-Hatsuda-Ishii PTP123(2010)89

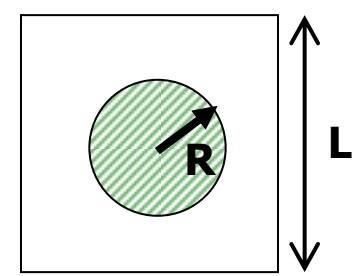

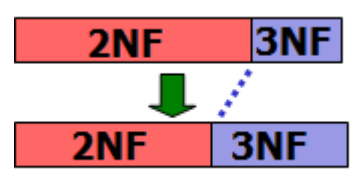

Challenges in multi-baryons on the lattice

- S/N issue in the system of #baryon = A

$$S/N \sim \exp[-A(m_N - 3m_\pi/2)t]$$ Lepage(1989)

  - small energy splitting by scatt. $\Delta E \simeq \frac{\vec{p}^2}{m_N} \simeq \frac{1}{m_N}\frac{(2\pi)^2}{L^2}$
    - ➔ requires larger t …

- Enormous computational cost for correlator
  - # of Wick contraction $\sim [\,(\frac{3}{2}A)!\,]^2$
  - # of color/spinor contractions $\sim 6^A \cdot 4^A$

    (color) (spinor)

See also T.Yamazaki et al., PRD81(2010)111504

S/N issue ➔ New algorithm (t-dep Schrodinger eq)

Elastic scatt states share the same potential

(E-indep of potential U(r,r') is the key)

$$\left(k^2/m_N - H_0\right)\psi_E(\vec{r}) = \int d\vec{r}' U(\vec{r},\vec{r}')\psi_E(\vec{r}')$$

$$\Downarrow$$

$$\left(-\frac{\partial}{\partial t} - H_0\right) R(\vec{r},t) = \int d\vec{r}' U(\vec{r},\vec{r}') R(\vec{r}',t)$$

Grand state saturation is NOT necessary !

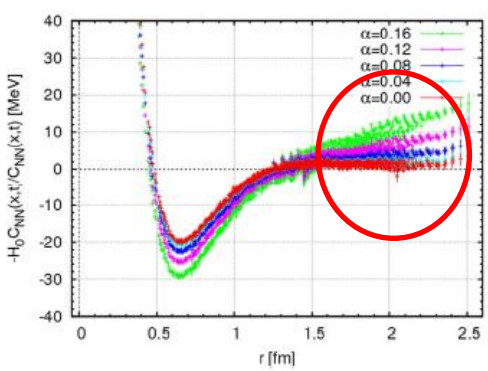

Poor Convergence

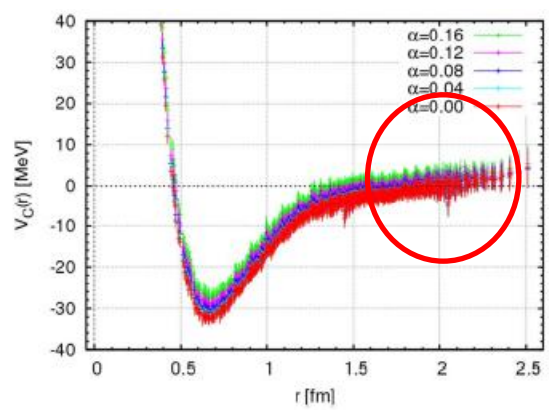

Good Convergence !

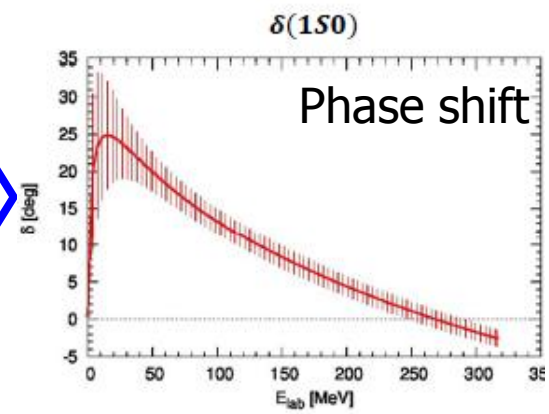

$$a_0(^1S_0) = 1.6(11)\ \text{fm}$$

Computational cost issue
➔Unified contraction algorithm

- Traditional algorithm

color/spinor contractions

$$\Pi^{2N} \simeq \langle qqqqqq(t)\bar{q}(\xi_1')\bar{q}(\xi_2')\bar{q}(\xi_3')\bar{q}(\xi_4')\bar{q}(\xi_5')\bar{q}(\xi_6')(t_0)\rangle \times \mathrm{Coeff}^{2N}(\xi_1', \cdots, \xi_6')$$

color ϵ_{abc}, spinor $(C\gamma_5)$, etc.

Permutations
(Wick contractions)

- New algorithm
  - For each flavor, we impose same spacial label at source quark
  - ➔ Permutation applies to color/spinor indices at "Coeff"

Permuted Sum

$$\Pi^{2N} \simeq \langle qqqqqq(t)\bar{q}(\xi_1')\bar{q}(\xi_2')\bar{q}(\xi_3')\bar{q}(\xi_4')\bar{q}(\xi_5')\bar{q}(\xi_6')(t_0)\rangle \times \mathrm{Coeff}^{2N}(\xi_1', \cdots, \xi_6')$$

Sum over color/spinor unified list

  - Construct a list for color/spinor sum
  - **🡐 Wick contraction and color/spinor contractions are unified**
  - Significant improvement

$\times 192$ for $^3\mathrm{H}/^3\mathrm{He}$, $\times 20736$ for $^4\mathrm{He}$ (x add'l. speedup)

TD, Endres, arXiv:1205.0585

Lattice QCD Calculations

Numerical
Setup & Results

BG/L@KEK

T2K@Tsukuba

SR16000
@YITP, KEK

「SR16000 モデル XM1」

Lattice calculation setup

- Nf=2 clover fermion + RG improved gauge action (CP-PACS)
  - 598 configs x 32 measurements
  - beta=1.95, (a^{-1}=1.27GeV, a=0.156fm)
  - 16^3 x 32 lattice, L=2.5fm
    - $M(\pi)$ = 1.13GeV
    - M(N) = 2.15GeV
    - $M(\Delta)$ = 2.31GeV

(κ(ud) =0.13750)

($M\pi$ L=14)

CP-PACS Coll. S. Aoki et al., Phys. Rev. D65 (2002) 054505

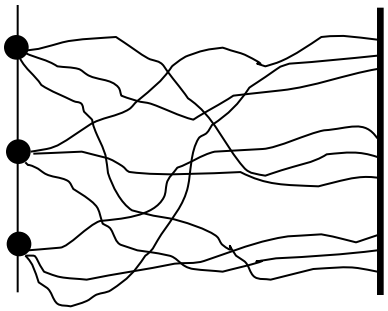

t=t(sink) t=t(src)

  - Correlators
    - **Standard nucleon op** to define the wave function / potential **at sink**

$$N = \epsilon_{abc}(q_a^T C\gamma_5 q_b)q_c$$

    - **Non-rela limit op** is used to create 3N state **at source**

$$G(\vec{r}_2, t-t_0) = \sum_{\vec{x}}\langle 0|\underbrace{N(\vec{x}+\vec{r}_2,t)N(\vec{x}-\vec{r}_2,t)N(\vec{x},t)}_{\textbf{sink}}\underbrace{\overline{NNN}(t_0)}_{\textbf{source}}|0\rangle$$

See also T.Yamazaki et al., PRD81(2010)111504

3NF calculation in Lat QCD

- We fix the geometry of 3N to extract the genuine 3NF
  - We study **linear setup** ➔ reduced to 3x3 coupled channel

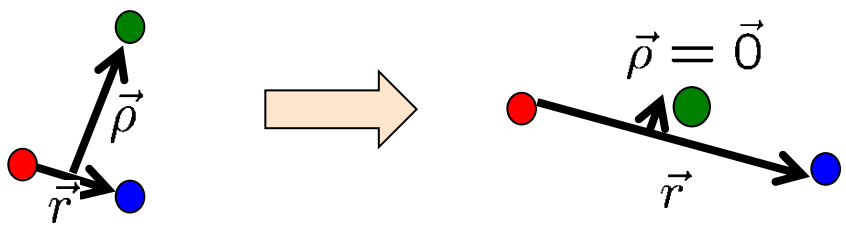

We consider Triton channel

$(\vec{r}_2 \equiv \vec{r}/2)$

  - **Linear setup** with various distance "**r_2**"

short "r_2" setup

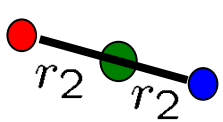

Study r_2-dependence of 3NF

long "r_2" setup

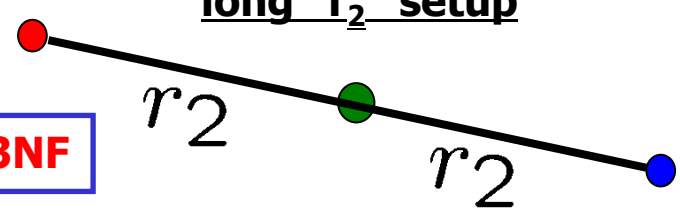

Results for wave functions

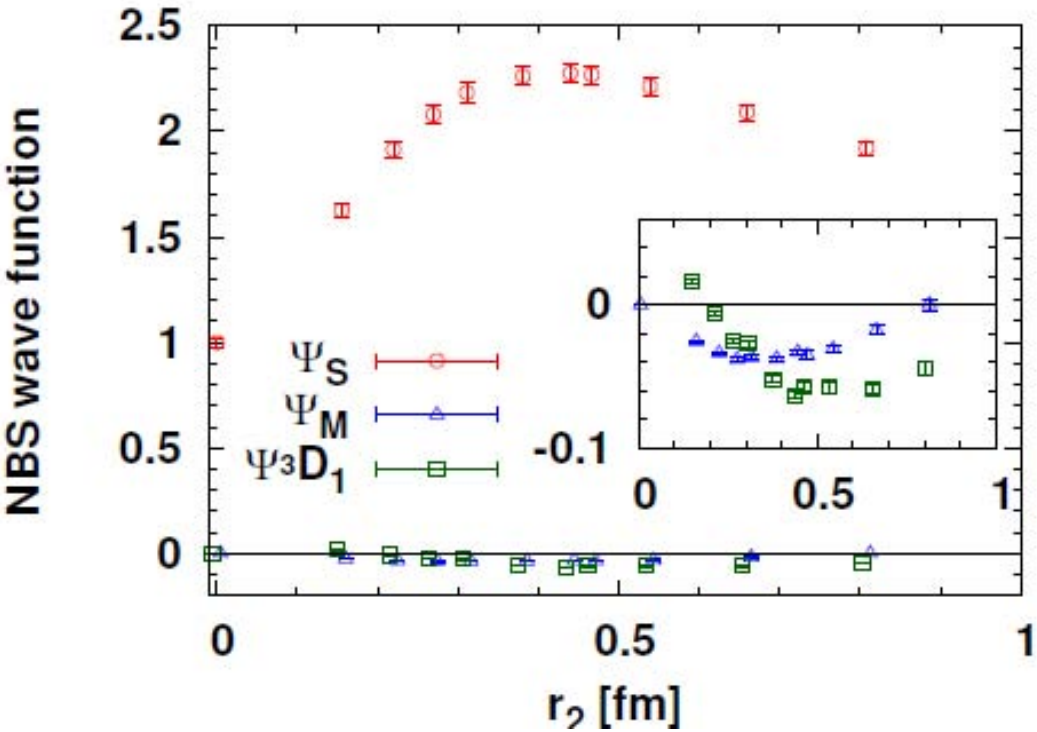

Red: Ψ_S
Blue: Ψ_M
Green: Ψ_{3D1}

Ψ_S overwhelms the wave function:

➔ Indication of the dominance of all S-wave component, higher waves suppressed

T.D. et al. (HAL QCD)
PTP127(2012)723

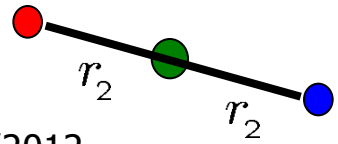

Genuine 3NF from Lat QCD

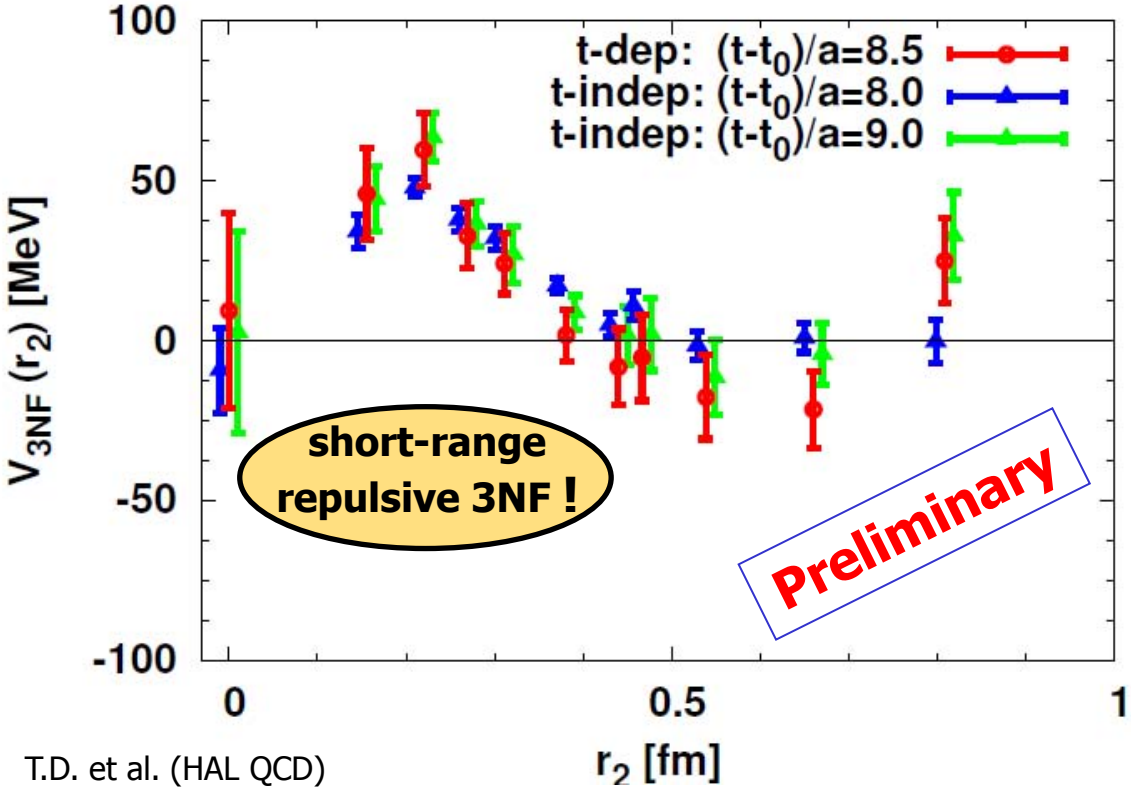

T.D. et al. (HAL QCD)
PTP127(2012)723

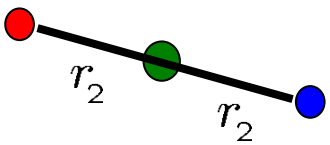

Huge Impact on physics of high density matters !

Results from t-dep method are consistent w/ t-indep method (but larger stat errors)

Summary/Outlook

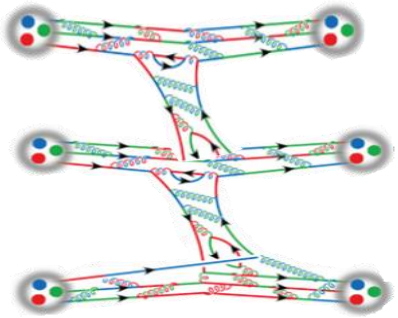

- Nuclear Physics on the Lattice
  - New Horizons for Lattice Computations
- Lattice Predictions are highly awaited
  - Huge impact on astrophysics as well
- **Three-Nucleon Force (3NF)** from Lattice QCD
  - **Repulsive 3NF at short distance** observed
- Outlook
  - Realistic potentials with physically light masses w/ large volumes

Ab-initio calculation using 2NF, 3NF as well as hyperon forces from Lat QCD

Backup Slides

Parity-even 2N potentials (input)

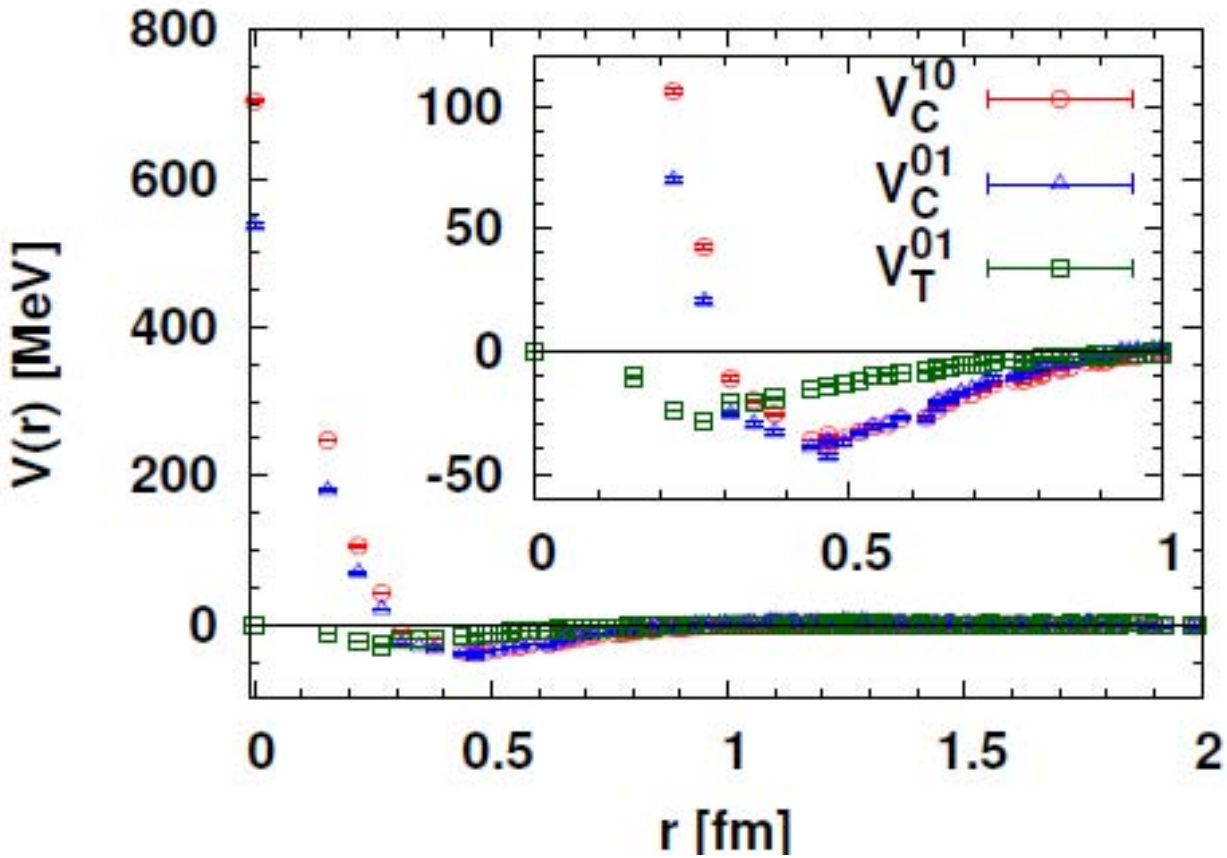

M(π)=1.13GeV

Extension to Three-Nucleon Systems

- We extend the HAL QCD Strategy to 3N system to directly determine 3NF

- c.f. Current status of 3N (3B, 4N) Lattice calc
  - T. Yamazaki et al. [PACS-CS Coll.] PRD81(2010)111504
    - Quenched clover, m(pi)=0.8GeV, L=3-12fm
    - B.E. : ^{3}He(=^{3}H)=18.2(3.5)(2.9)MeV, ^{4}He=27.7(7.8)(5.5)MeV
  - S. Beane et al. [NPLQCD Coll.] PRD80(2009)074501
    - Nf=2+1 clover, m(pi)=0.39GeV, L=2.5fm
    - ($\Xi^0\Xi^0$n) and (pnn) are explored, $E_{3B} - E_{th} \gtrsim 0$
  - Only (binding) energies have been calculated in these studies

How can we tackle 3NF in Lattice QCD ?

- **In the case of 2N system…**
  - Calc 4pt func ➔NBS amp.

$$\psi(\vec{r}) = \langle 0|N(\vec{x}+\vec{r};t)N(\vec{x};t)|2N\rangle$$

- **Extention to 3N system**
  - Calc 6pt func ➔NBS amp. of 3N

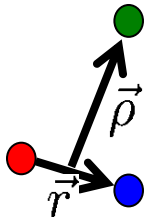

$$\psi(\vec{r},\vec{\rho}) = \langle 0|N(\vec{x}+\vec{r})N(\vec{x})N(\vec{x}+\vec{r}/2+\vec{\rho})|3N\rangle$$

  - Obtain 3NF through

$$(E-H_0^r-H_0^\rho)\psi(\vec{r},\vec{\rho}) = \left[\sum_{i<j} V_{ij}(\vec{r}_{ij}) + V_{3NF}(\vec{r},\vec{\rho})\right]\psi(\vec{r},\vec{\rho})$$

by 2N calc

  - Difficulty(1): volume factor
    - 2N: naïve $O(L^6)$ calc ➔ $O(L^3 \log L^3)$
    - 3N: naïve $O(L^9)$ calc ➔ $O(L^6 \log L^6)$

$O(10^4\text{-}10^5)$ factor

  - Difficulty(2): naïve calc of quark dof grows in factorial ($\sim N_u!\ N_d!$)
    - 2N: $O(L^3)$ X N_{wick} X color/spinor loops
    - 3N: $O(L^6)$ X N_{wick} X color/spinor loops

$O(L^3)$ X $O(4000)$ = $O(10^7\text{-}10^8)$ factor

3NF is exceptionally challenging problem !

Features of Linear setup for ^{3}H

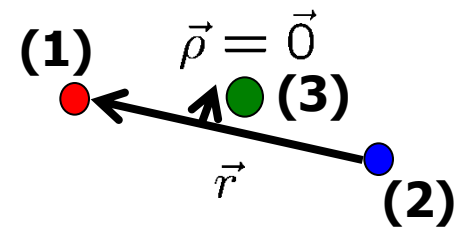

- Simplified coupled channel analysis possible
  - The vector to 3rd particle $\vec{\rho} = \vec{0}$
  - ➔ $L^{(1,2)\text{-pair}} = L^{\text{total}} = 0$ or 2 only
  - ➔ Possible **bases are only three**, which can be labeled by **$^1S_0$, $^3S_1$, $^3D_1$ for (1,2)-pair**

Schrodinger Eq.

$$\hat{H}_0 \begin{pmatrix} \psi_{(^1S_0)} \\ \psi_{(^3S_1)} \\ \psi_{(^3D_1)} \end{pmatrix} + \underbrace{\begin{pmatrix} & V & \\ & (V_{2N} + V_{3NF}) & \end{pmatrix}}_{\text{3x3 Matrix}} \begin{pmatrix} \psi_{(^1S_0)} \\ \psi_{(^3S_1)} \\ \psi_{(^3D_1)} \end{pmatrix} = E \begin{pmatrix} \psi_{(^1S_0)} \\ \psi_{(^3S_1)} \\ \psi_{(^3D_1)} \end{pmatrix}$$

Kinetic energy

Parity-odd potential Issue

- However, in order to determine 3NF in **3x3 coupled channel**, we need information of parity-odd potential
  - Although (1,2)-pair is L=even, (3,1),(2,3)-pair have L=odd components
- Parity-odd potential from lattice QCD is under R&D now (K.Murano et al.)
  - ➔3X3 channel, but unknown $V_C^{I,S=0,0}$,$V_C^{I,S=1,1}$,$V_T^{I,S=1,1}$,3NF(s)

$$\hat{H}_0 \begin{pmatrix} \psi_{(^1S_0)} \\ \psi_{(^3S_1)} \\ \psi_{(^3D_1)} \end{pmatrix} + \begin{pmatrix} & V & \\ & (V_{2N} + V_{3NF}) & \\ & & \end{pmatrix} \begin{pmatrix} \psi_{(^1S_0)} \\ \psi_{(^3S_1)} \\ \psi_{(^3D_1)} \end{pmatrix} = E \begin{pmatrix} \psi_{(^1S_0)} \\ \psi_{(^3S_1)} \\ \psi_{(^3D_1)} \end{pmatrix}$$

$V_C^{I,S=1,0}, V_C^{I,S=0,1}, V_T^{I,S=0,1}$: (P = even)

$V_C^{I,S=0,0}, V_C^{I,S=1,1}, V_T^{I,S=1,1}$: (P = odd)

unknown

Target to be determined

Solution using "symmetric" wave function

- We can construct the wave function in which <u>any 2N pair</u> is spin/isospin anti-symmetric

$\psi_S =$ 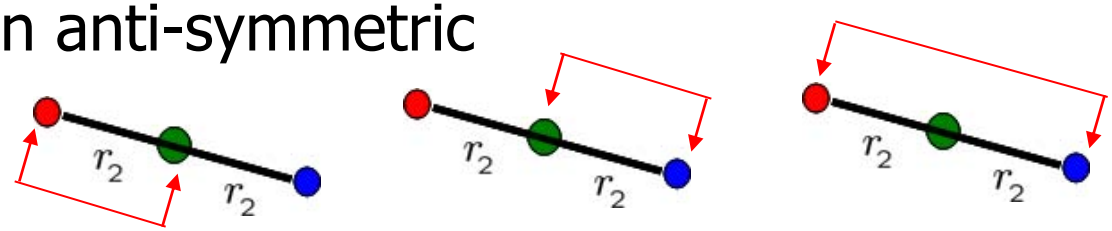

  - ➔ **<u>L=even for any 2N pair</u>** automatically guaranteed
  - Bases are rotated as $|\psi_{^1S_0}\rangle, |\psi_{^3S_1}\rangle, |\psi_{^3D_1}\rangle \longrightarrow |\psi_S\rangle, |\psi_M\rangle, |\psi_{^3D_1}\rangle$

$$|\psi_S\rangle = 1/\sqrt{2}\left(-|\psi_{^1S_0}\rangle + |\psi_{^3S_1}\rangle\right) \qquad |\psi_M\rangle = 1/\sqrt{2}\left(+|\psi_{^1S_0}\rangle + |\psi_{^3S_1}\rangle\right)$$

All pair P=even

$$\hat{H}_0 \begin{pmatrix} \psi_S \\ \psi_M \\ \psi_{^3D_1} \end{pmatrix} + \begin{pmatrix} & & \\ & V_{2N} & \\ & & \end{pmatrix} \begin{pmatrix} \psi_S \\ \psi_M \\ \psi_{^3D_1} \end{pmatrix} + \hat{V}_{3NF} \begin{pmatrix} \psi_S \\ \psi_M \\ \psi_{^3D_1} \end{pmatrix} = E \begin{pmatrix} \psi_S \\ \psi_M \\ \psi_{^3D_1} \end{pmatrix}$$

No V(P=odd)

Solution using "symmetric" wave function

- We can construct the wave function in which <u>any 2N pair</u> is spin/isospin anti-symmetric
  - ➔ **<u>L=even for any 2N pair</u>** automatically guaranteed
- 3x3 coupled channel is reduced to
  - **<u>one channel with only 3NF unknown</u>**
  - two channels with $V_C^{I,S=0,0}$, $V_C^{I,S=1,1}$, $V_T^{I,S=1,1}$,(3NF) unknown

$$\begin{pmatrix} H_0 \end{pmatrix}\begin{pmatrix} \psi_S \\ \psi_M \\ \psi_{^3D_1} \end{pmatrix} + \begin{pmatrix} V_{2N} \end{pmatrix}\begin{pmatrix} \psi_S \\ \psi_M \\ \psi_{^3D_1} \end{pmatrix} + \begin{pmatrix} V_{3NF} \end{pmatrix}\begin{pmatrix} \psi_S \\ \psi_M \\ \psi_{^3D_1} \end{pmatrix} = E\begin{pmatrix} \psi_S \\ \psi_M \\ \psi_{^3D_1} \end{pmatrix}$$

No V(P=odd)

Target to be determined

(L^2-dep ignored)

- ➔ Even without parity-odd V, we can determine one 3NF
  - This method works for any fixed 3D-geometry other than linear

Short-Range 3NF

- We determine 3NF effectively represented by a scalar/isoscalar functional form
  - c.f. phenomenological 3NF to reproduce saturation point of nuclear matter, etc.

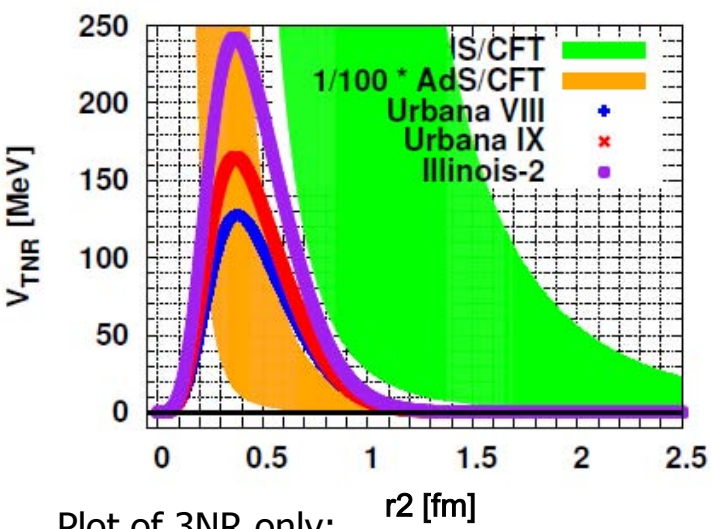

Plot of 3NR only:
there is cancellation from 3NA

$$V_{3NF} = V_{2\pi E} + (V_{3\pi R}) + V_{3NR}$$

Urbana/Illinois

$$V_{3NR} = U_0 \sum_{cyc} T^2(r_{12}) T^2(r_{13})$$

$$T(r) = \left(1 + \frac{3}{\mu r} + \frac{3}{\mu^2 r^2}\right) \frac{e^{-\mu r}}{\mu r} T_{cut}(r)$$

AdS/CFT: $V_{3NF} = +\text{const.} \cdot \frac{1}{r^4}$

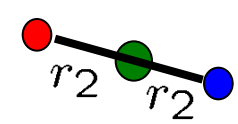

K.Hashimoto, N.Iizuka
JHEP 1011 (2010) 058

Effective Schrodinger equation with E-independent potential

$$K(\vec{x};E) \equiv \vec{\nabla}^2 + k^2 \quad \psi(\vec{x};E)$$

[START] local but E-dep pot. (L^3xL^3 dof)

(1) We assume ψ(x; E) for different E is linearly independent with each other.

(2) ψ(x; E) has a "left inverse" as an integration operator as

$$E \equiv 2\sqrt{m_N^2 + k^2}$$

$$\int d^3x \tilde{\psi}(\vec{x};E')\psi(\vec{x};E) = 2\pi\delta(E-E')$$

(3) K(x; E) can be factorized as

$$\equiv m_N U(\vec{x},\vec{y})$$

$$\begin{aligned} K(\vec{x};E) &= \int \frac{dE'}{2\pi} K(\vec{x};E') \times \int d^3y \tilde{\psi}(\vec{y};E')\psi(\vec{y};E) \\ &= \int d^3y \left\{ \sum_\alpha \int \frac{dE'}{2\pi} K(\vec{x};E')\tilde{\psi}(\vec{y};E') \right\} \psi(\vec{y};E) \end{aligned}$$

(4) We are left with an effective Schrodinger equation with an E-independent potential U.

$$\vec{\nabla}^2 + k^2 \quad \psi(\vec{x};E) = m_N \int d^3y \boxed{U(\vec{x},\vec{y})} \psi(\vec{y};E)$$

Intuitive understanding

[GOAL] non-local but E-indep pot. (L^3xL^3 dof)

Two-Photon Decay of Neutral Pion from Lattice QCD

Xu Feng (KEK)

work with S. Aoki, H. Fukaya, S. Hashimoto, T. Kaneko, J. Noaki and E. Shintani on behalf of JLQCD collaboration

BNL, New York, 2012/05/14

Motivation

- PrimEx@JLab: $\Gamma_{\pi^0\gamma\gamma} = 7.82(22)$ eV [PrimEx, PRL106, 2011]
- Precision: 2.8% $\rightarrow$ 1.4% (projected goal)
- Benchmark test in the chiral anomaly sector of QCD
- $\Gamma_{\pi^0\gamma\gamma} = (\pi/4)\alpha_e^2 m_\pi^3 \mathcal{F}^2_{\pi^0\gamma\gamma}(m_\pi^2, 0, 0)$
  - $\mathcal{F}_{\pi^0\gamma\gamma}(m_\pi^2, p_1^2, p_2^2)$: $\pi^0 \rightarrow \gamma^*\gamma^*$ transition form factor
  - m_π: π^0 mass; p_1, p_2: photon 4-momentum

Lattice setup

- overlap fermion: exact chiral symmetry $\Rightarrow$ test chiral anomaly
- all-to-all propagators $\Rightarrow$ $C(t_1, t_2, t_3)$
  - low mode: low-lying eigenvalues and eigenvectors
  - high mode: stochastic propagators
  - calculate correlator at any time slice of t_1, t_2, t_3
  - disconnected diagram

Ensemble information

- four $m_{u,d}$: $m_\pi = 540 \to 290$ MeV $\Rightarrow$ chiral exapolation
- m_s fixed to be close to its physical value $\Rightarrow$ dynamical s-quark effects
- $L/a = 16$ and 24 $\Rightarrow$ finite-size effects
- $Q = 0$ and 1 $\Rightarrow$ fixing-topology effects
- $a = 0.11$ fm $\Rightarrow$ study possible lattice artifacts

Theoretical setup

- starting point: S-matrix

$$\langle \gamma(p_1, \lambda_1)\gamma(p_2, \lambda_2)|\pi^0(q)\rangle$$

- transition form factor is defined by matrix element

$$\underbrace{\int d^4x e^{ip_1 x}\langle \Omega| T\{J_\mu(x)J_\nu(0)\}|\pi^0(q)\rangle}_{\mathcal{M}_{\mu\nu}} = \epsilon_{\mu\nu\alpha\beta}p_1^\alpha p_2^\beta F_{\pi^0\gamma\gamma}(m_\pi^2, p_1^2, p_2^2)$$

  - $\epsilon_{\mu\nu\alpha\beta}p_1^\alpha p_2^\beta$: induced by the negative parity of the π^0
  - chiral limit, photon on-shell, ABJ anmoaly:

$$\mathcal{F}_{\pi^0\gamma\gamma}(0,0,0) = \mathcal{F}^{\mathrm{ABJ}}_{\pi^0\gamma\gamma} = \frac{1}{4\pi^2 F_\pi}$$

Method

- matrix element in the Minkowski space-time

$$\mathcal{M}_{\mu\nu} = \int d^4x e^{ip_1 x} \langle \Omega | T\{J_\mu(x) J_\nu(0)\} | \pi^0(q) \rangle$$

- analytical continuation from Minkowski to Euclidean space-time [Ji, Jung, 2001; Dudek, Edwards, 2006]

$$\mathcal{M}_{\mu\nu} = \int dt e^{\omega t} \int d^3\vec{x} e^{-i\vec{p}_1 \cdot \vec{x}} \langle \Omega | T\{J_\mu(x) J_\nu(0)\} | \pi^0(q) \rangle$$

- pion is on-shell: $q = (E_\pi, \vec{q}) \Rightarrow q^2 = m_\pi^2$
- photon 4-momentum: $p_1 = (\omega, \vec{p}_1)$ and $p_2 = (E_\pi - \omega, \vec{q} - \vec{p}_1)$
- requirement: $p_{1,2}^2 < m_\rho^2$ or $E_{\pi\pi}^2$ (hadron production threshold)

Amplitude $A_\pi(\tau)$

- observable:

$$\mathcal{M}_{\mu\nu} = \int dt e^{\omega t} \int d^3\vec{x} e^{-i\vec{p}_1\cdot\vec{x}} \langle\Omega| T\{J_\mu(x) J_\nu(0)\} |\pi^0(q)\rangle$$

- correlation function:

$$C_{\mu\nu} = \langle\Omega| J_\mu(\vec{p}_1, t_1) J_\nu(\vec{p}_2, t_2) \pi^0(-\vec{q}, t_\pi) |\Omega\rangle$$

- set $\tau = t_1 - t_2$ and $t = \min\{t_1, t_2\}$

$$A_\pi(\tau) \equiv \lim_{t - t_\pi \to \infty} C_{\mu\nu}(t_1, t_2, t_\pi) / e^{-E_\pi (t - t_\pi)}$$

- matrix element $\mathcal{M}_{\mu\nu}$ is given by

$$\mathcal{M}_{\mu\nu} = \frac{2E_\pi}{\phi_\pi} \left(\int_0^\infty d\tau \; e^{\omega\tau} A_\pi(\tau) + \int_{-\infty}^0 d\tau \; e^{(\omega - E_{\pi,\vec{q}})\tau} A_\pi(\tau) \right)$$

Distribution of $A_\pi(\tau)$

- $\langle J_\mu(\vec{p}_1, t_1) J_\nu(\vec{p}_2, t_2) \pi^0(\vec{q}, t_\pi)\rangle$: $\mu = 1$, $\nu = 2$

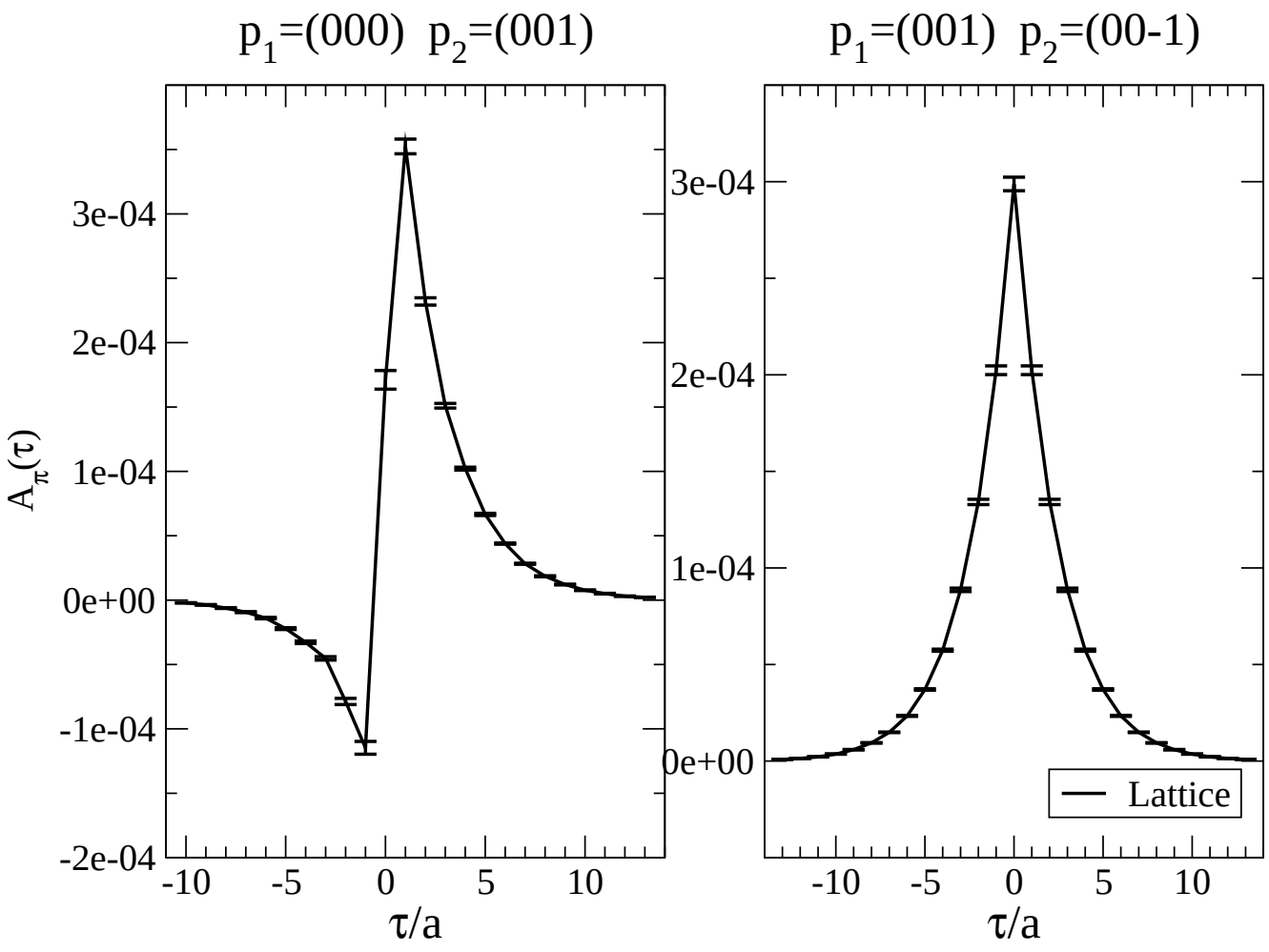

Time dependence of $A_{\pi,1,2}$

- VMD model: $\mathcal{F}^{\rm VMD}_{\pi^0\gamma\gamma}(m_\pi^2, p_1^2, p_2^2) = c_V G_V(p_1^2) G_V(p_2^2)$
- $G_V(p^2) = M_V^2/(M_V^2 - p^2)$ is the vector meson propagator, $M_V = m_\rho$

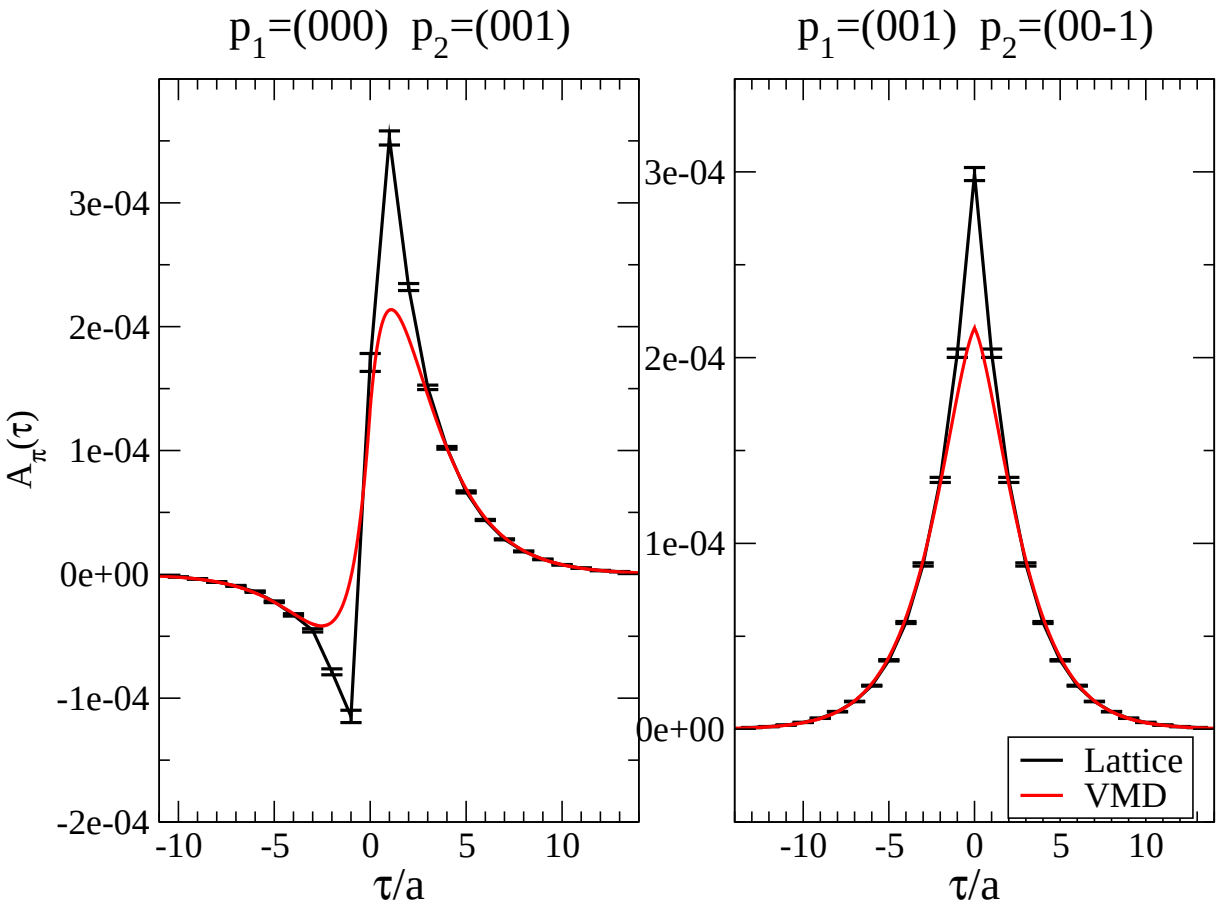

Fit ansatz

- lowest vector meson effects should be accounted for first
- corrected by including excited-state effects

$$\begin{aligned}\mathcal{F}_{\pi^0\gamma\gamma}(m_\pi^2, p_1^2, p_2^2) &= c_V G_V(p_1^2) G_V(p_2^2) \\ &+ \sum_{V'} c_{V'} \left(G_V(p_1^2) G_{V'}(p_2^2) + G_{V'}(p_1^2) G_V(p_2^2) \right) \\ &+ \sum_{V',V''} c_{V'V''} G_{V'}(p_1^2) G_{V''}(p_2^2)\end{aligned}$$

- replace $G_{V'}(p^2)$ by a basis of polynomial function

$$\begin{aligned}\mathcal{F}_{\pi^0\gamma\gamma}(m_\pi^2, p_1^2, p_2^2) &= c_V G_V(p_1^2) G_V(p_2^2) \\ &+ \sum_{m} c_m \left((p_2^2)^m G_V(p_1^2) + (p_1^2)^m G_V(p_2^2) \right) \\ &+ \sum_{m,n} c_{m,n} (p_1^2)^m (p_2^2)^n\end{aligned}$$

Form factor

- $\mathcal{F}_{\pi^0\gamma\gamma} = \int dt\ e^{\omega t} \langle \Omega | T\{J_\mu(\vec{p}_1, t) J_\nu(\vec{p}_2, 0)\} | \pi^0(q) \rangle / \epsilon_{\mu\nu\alpha\beta} p_1^\alpha p_2^\beta$
- tunning ω: $p_1^2 = \omega^2 - \vec{p}_1^2 \quad p_2^2 = (E_\pi - \omega)^2 - \vec{p}_2^2$

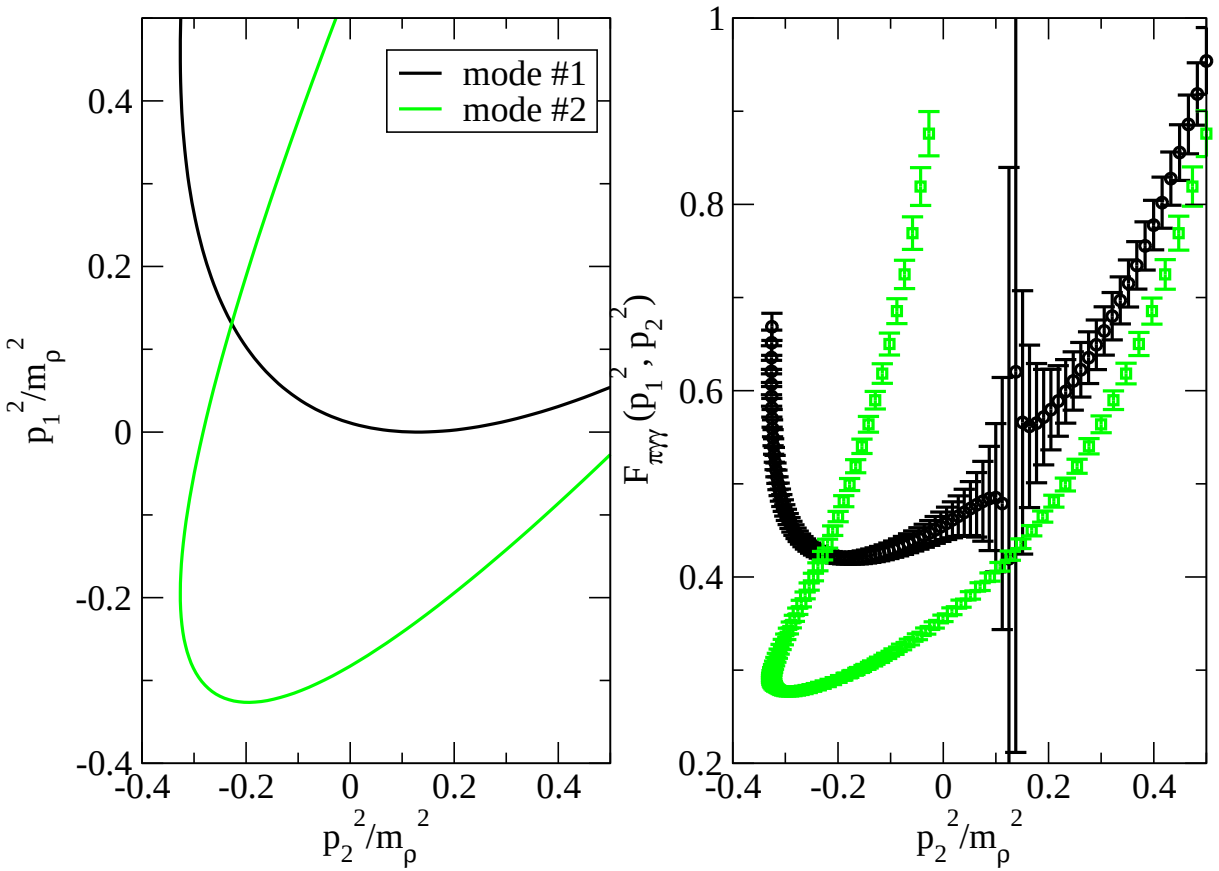

Combined fit

- fit ansatz $\mathcal{F}_{\pi^0\gamma\gamma}(m_\pi^2, p_1^2, p_2^2) = c_V G_V(p_1^2) G_V(p_2^2) +$

$$\sum_m c_m \left((p_2^2)^m G_V(p_1^2) + (p_1^2)^m G_V(p_2^2) \right) + \sum_{m,n} c_{m,n} (p_1^2)^m (p_2^2)^n$$

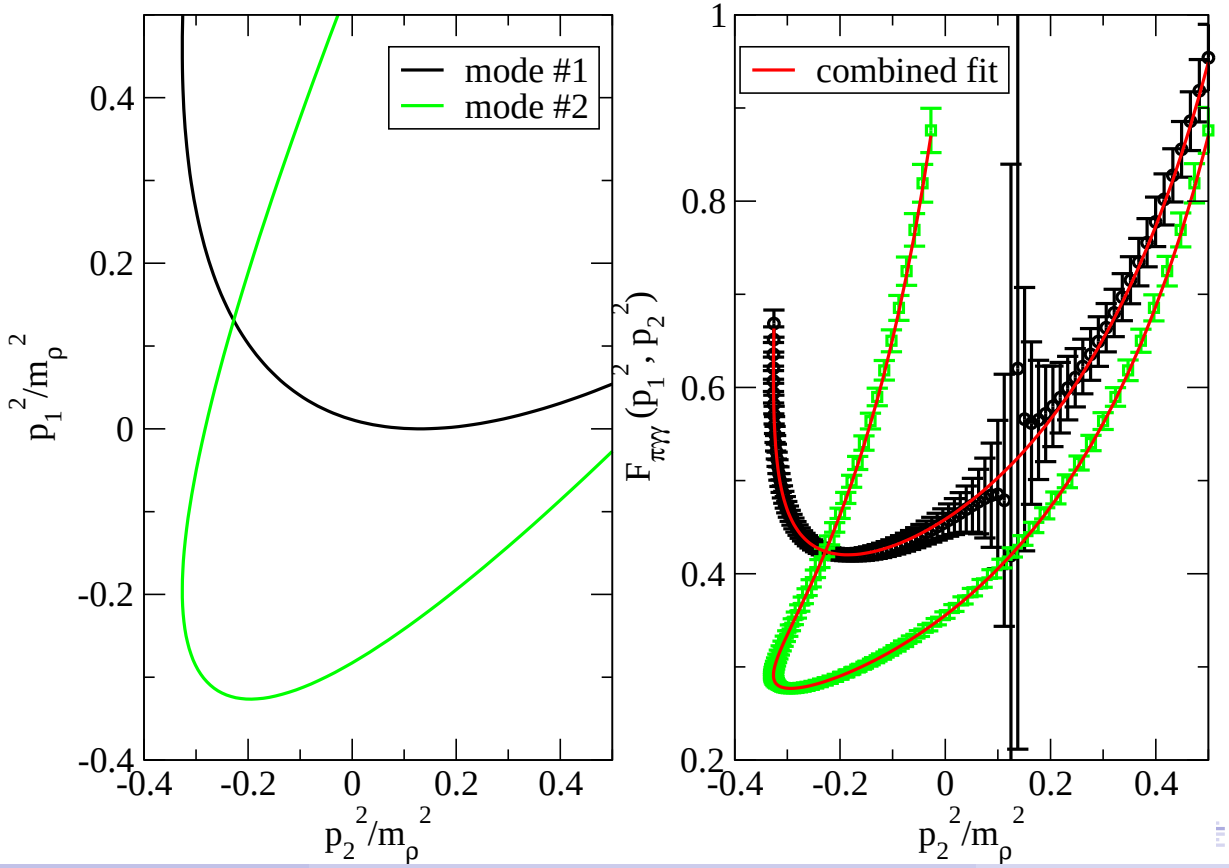

On-shell photon limit

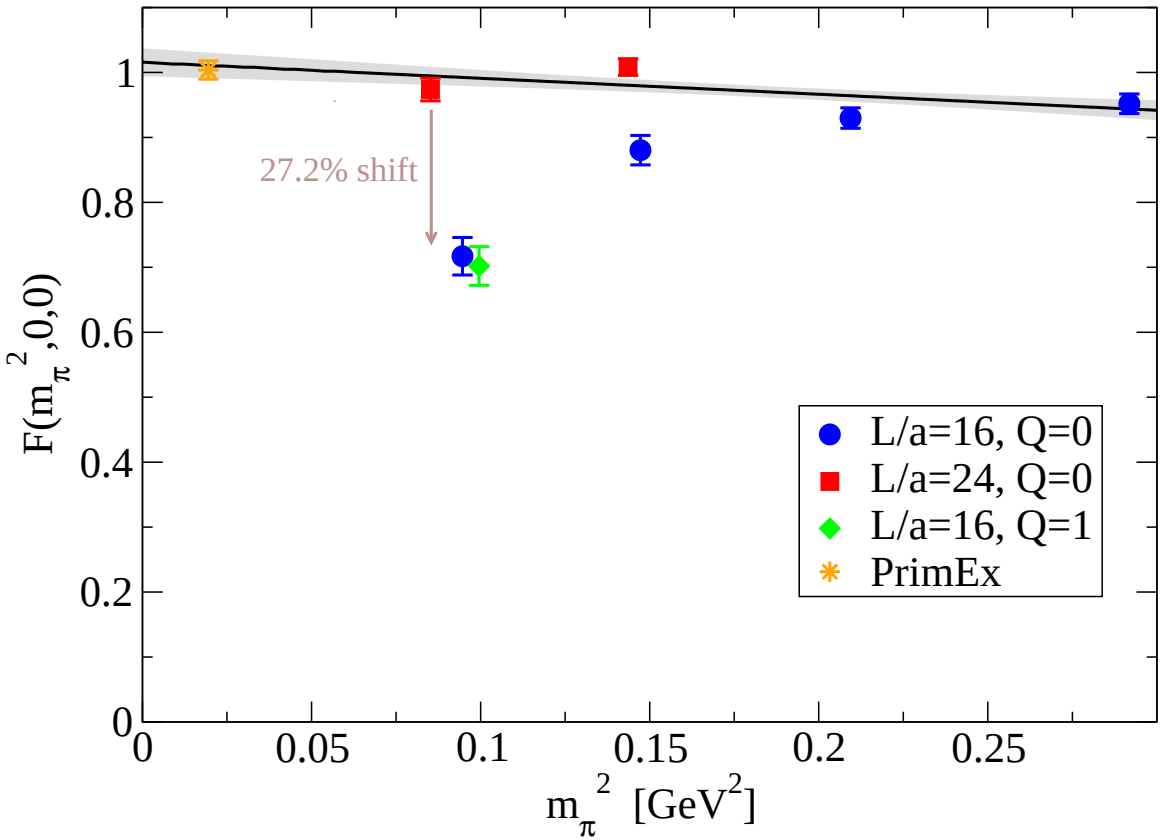

- $F(m_\pi^2, 0, 0) \equiv \mathcal{F}_{\pi^0\gamma\gamma}(m_\pi^2, 0, 0)/\mathcal{F}^{\rm ABJ}_{\pi^0\gamma\gamma}$
- data with $m_\pi L \geq 4$: consistent with ABJ and PrimEx
- $L = 16$: smallest two quark mass, $m_\pi L < 4$, big FS effects
- FS effects checked at topological sector $Q = 0$ and 1

Expansion of matrix element

- expand the correlator into three hadronic matrix elements:

$$\langle J_\mu J_\nu \pi^0 \rangle \to \langle \Omega | J_\mu | V \rangle \langle V | J_\nu | \pi^0 \rangle \langle \pi^0 | \pi^0 | \Omega \rangle$$

- vector-meson electromagnetic coupling g_V

$$\langle \Omega | J_\mu | V, p, \varepsilon \rangle = M_V F_V \varepsilon_\mu(p) = M_V^2 g_V \varepsilon_\mu(p)$$

- $V\pi\gamma$ coupling $g_{V\pi\gamma}$, $V \to \pi\gamma$ decay

$$\langle V, \varepsilon_\mu(p_1) | j_\nu(0) | \pi^0(q) \rangle = \frac{g_{V\pi\gamma}}{M_V} \varepsilon_{\mu\nu\alpha\beta} p_{1\alpha} p_{2\beta} K_V(p_2^2) \ , \quad p_2 = q - p_1$$

- pion decay constant F_π

$$\langle \pi^0 | \pi^0 | \Omega \rangle = \frac{m_\pi^2}{2 m_{u,d}} F_\pi$$

Finite-size effects

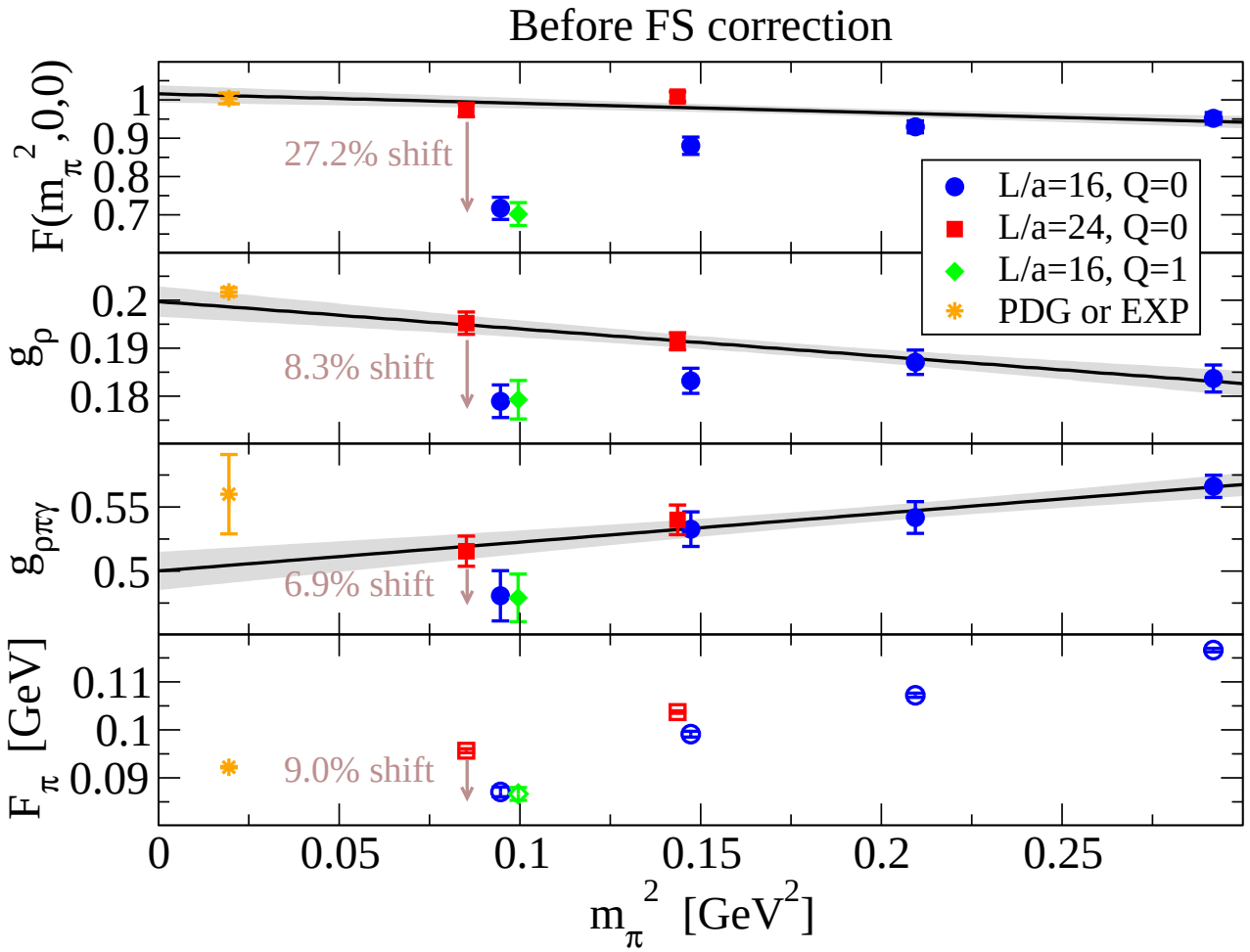

- FS effects accumulate and add up to a large effect

Finite-size corrections

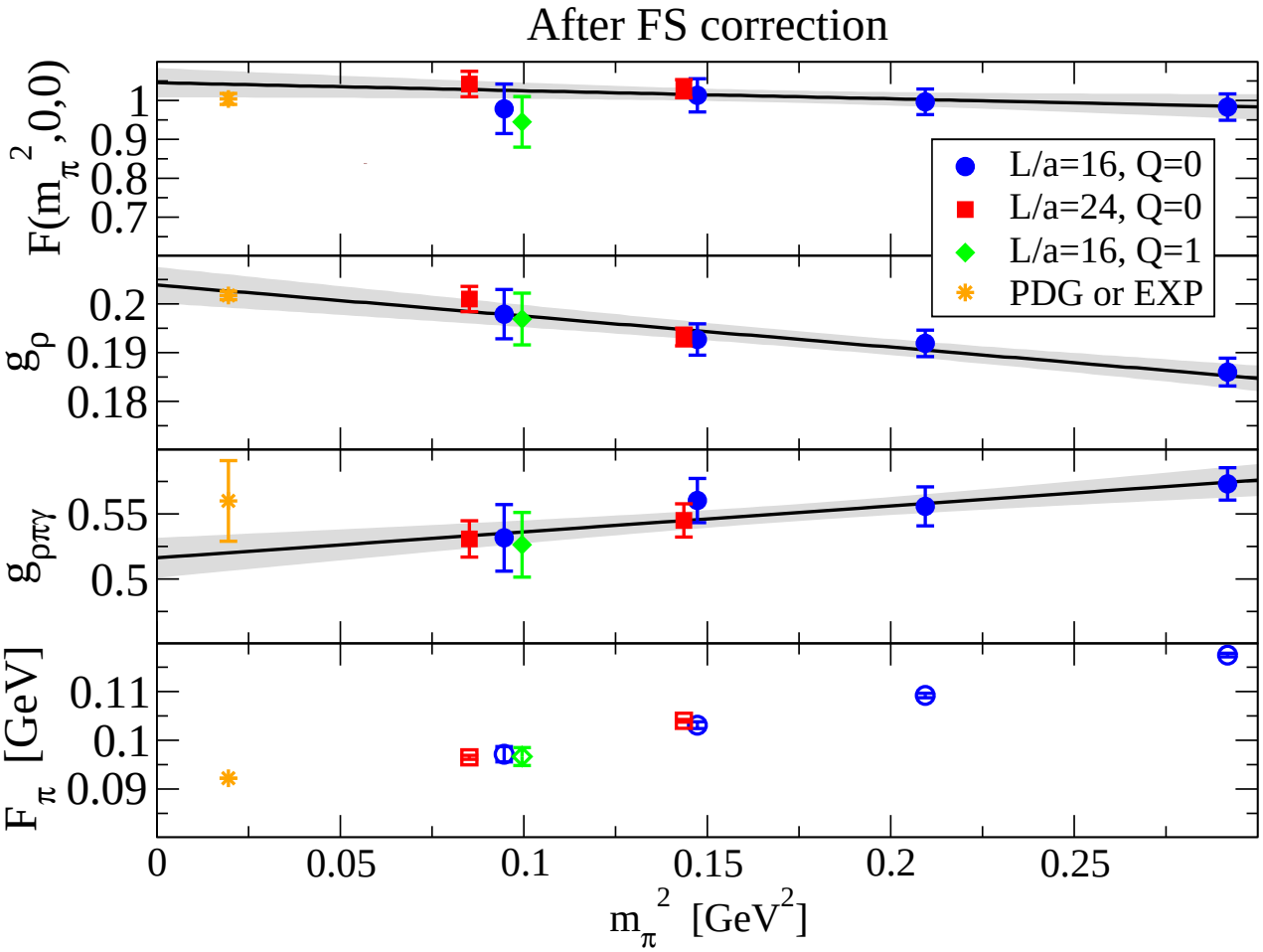

- FS corrections $R_{\mathcal{O}} \equiv \mathcal{O}(\infty)/\mathcal{O}(L)$ with $\mathcal{O} = g_\rho$, $g_{\rho\pi\gamma}$ and F_π
- assume that $R_{F(m_\pi^2,0,0)} = R_{g_\rho} R_{g_{\rho\pi\gamma}} R_{F_\pi}$

Disconnected-diagram effects

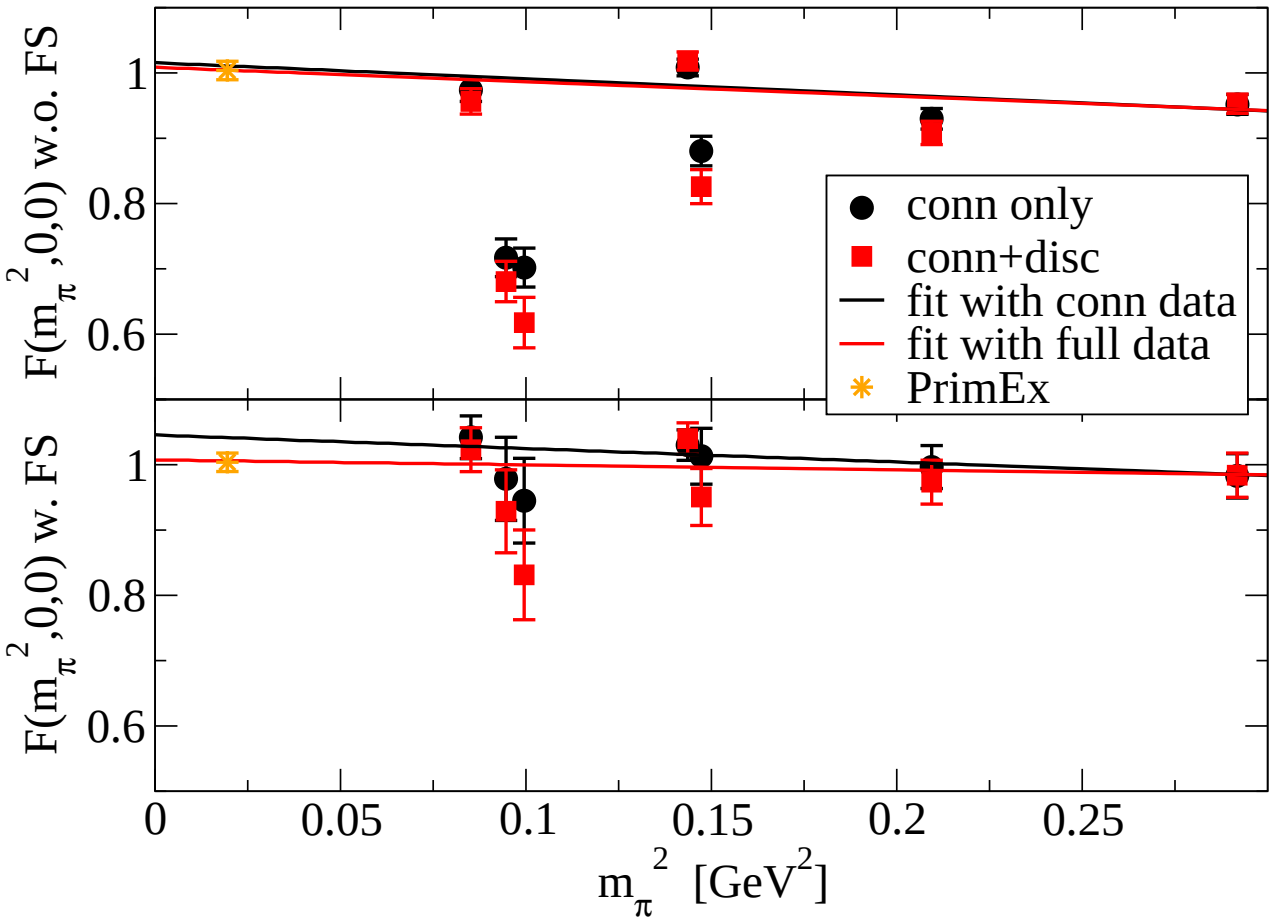

- all-to-all propagator: control error of disc. contribution
- although not significant, conn+disc systematically shift down
- precision level (2% for form factor): disc. diagram should be included

Lattice artifacts

- discrete data v.s. continuum case?
- right fig: turnover obtained; left fig: not obtained?

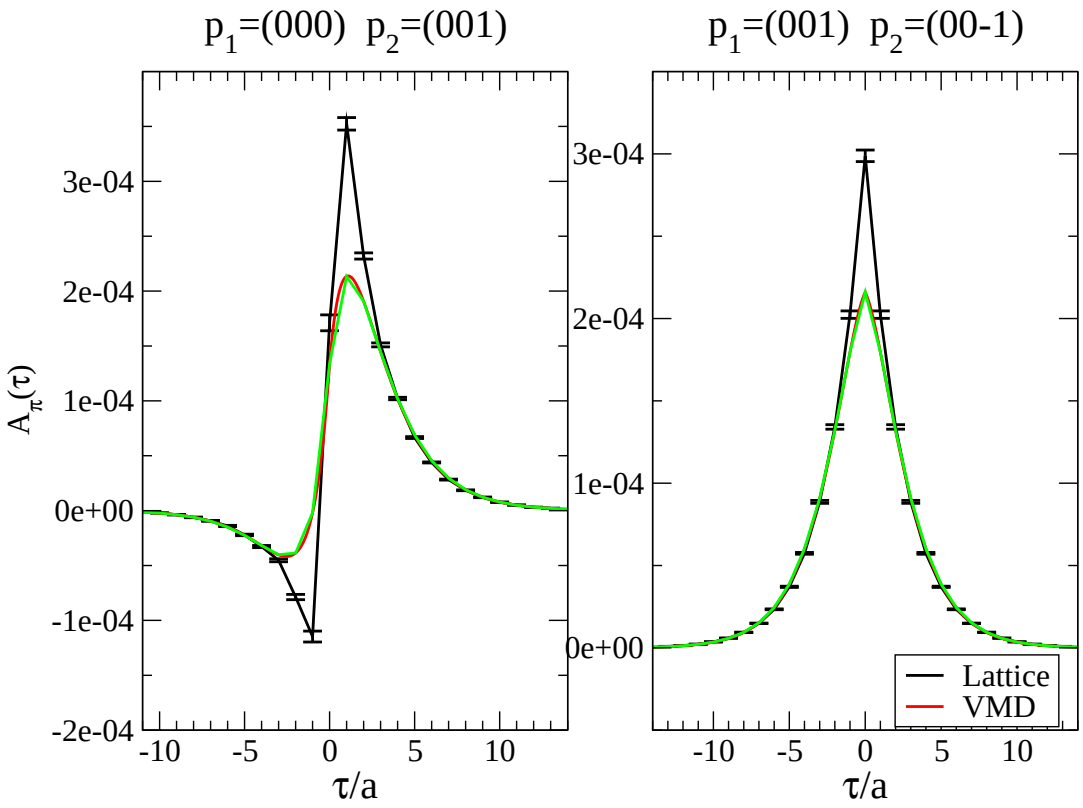

- disc. effects in VMD model: less than 5×10^{-4}, neglegiable
- turnover contributed by ground and excited states, not very large

Conclusion

- after examining possible systematic effects

$$
\begin{aligned}
F(0,0,0) &= 1.009(22)(29) \\
F(m^2_{\pi,\mathrm{phy}},0,0) &= 1.005(20)(30) \\
\Gamma_{\pi^0\gamma\gamma} &= 7.93(29)(43)\ \mathrm{eV}
\end{aligned}
$$

- ABJ anomaly and PrimEx measurement

$$
\begin{aligned}
F(0,0,0) &= 1 \\
F(m^2_{\pi,\mathrm{phy}},0,0) &= 1.004(14) \\
\Gamma_{\pi^0\gamma\gamma} &= 7.82(22)\ \mathrm{eV}
\end{aligned}
$$

- $m_u \neq m_d$, effects mixing of m_π with η and η' are not yet studied

Motivated by muon $g_\mu - 2$

- Exp. determination of $g_\mu - 2$ to 0.54 ppm [E821@BNL, PRD73, 2006]
- S.M. prediction of $g_\mu - 2$ to 0.51 ppm [Jegerlehner, EPJC71, 2011]
- Discrepancy: $3.3\sigma \Rightarrow$ New Physics ??
- HLbL is predicted to be dominant error in the next round

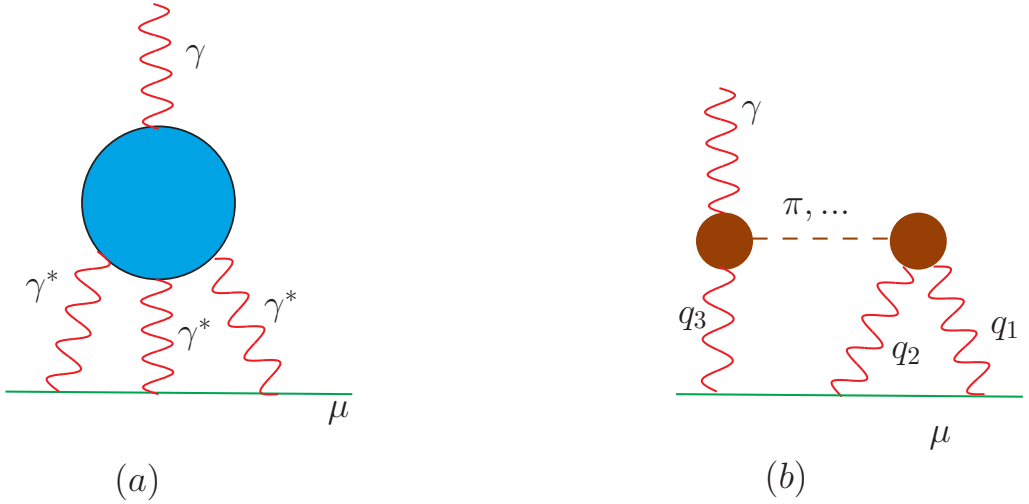

- Difficult: HLbL involves $\langle J_\mu J_\nu J_\rho J_\sigma \rangle$
- Better to start with $\pi^0(\eta,\ \eta') \to \gamma^*\gamma^*$

π^0 contribution

Contribution	BPP	HKS	KN	MV	BP	PdRV	N/JN
π^0, η, η'	85±13	82.7±6.4	83±12	114±10	–	114±13	99±16
π, K loops	−19±13	−4.5±8.1	–	–	–	−19±19	−19±13
π, K loops + other subleading in N_c	–	–	–	0±10	–	–	–
axial vectors	2.5±1.0	1.7±1.7	–	22± 5	–	15±10	22± 5
scalars	−6.8±2.0	–	–	–	–	−7± 7	−7± 2
quark loops	21± 3	9.7±11.1	–	–	–	2.3	21± 3
total	83±32	89.6±15.4	80±40	136±25	110±40	105±26	116±39

- summary table [Jegerlehner, Nyffeler, Phys.Rept.477:1-110,2009]
  - $\pi^0(\eta,\ \eta') \to \gamma^*\gamma^*$ are consistent to total contributions
  - Among three PS mesons, π^0 takes about $\tilde{7}0\%$
  - calulation on the $\pi^0 \to \gamma^*\gamma^*$ can be duplicated to the η, η' sector

Non-perturbative nature

- Invariant mass spectrum for two-photon

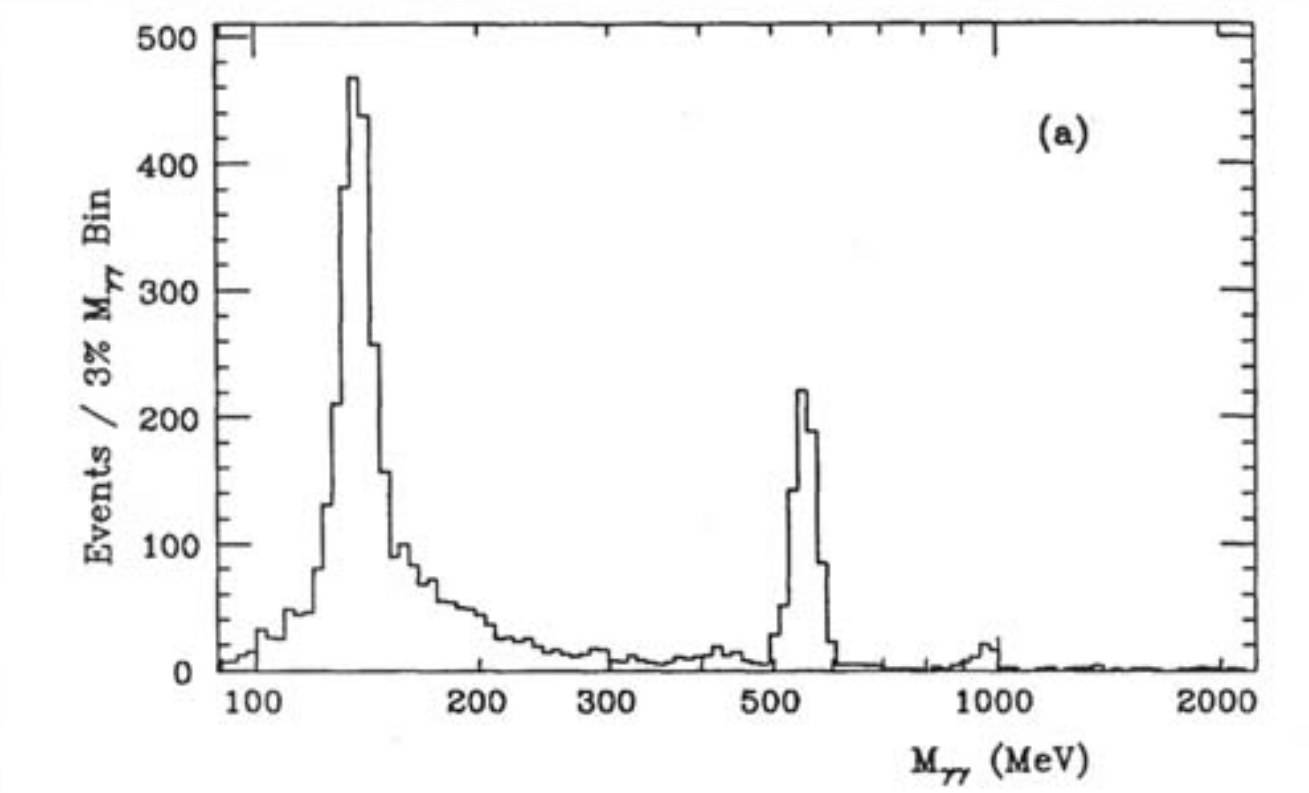

- Three spikes presents three bound states: π^0, η, η'
- Bound states $\rightarrow$ confinement $\rightarrow$ LQCD

Rho mass

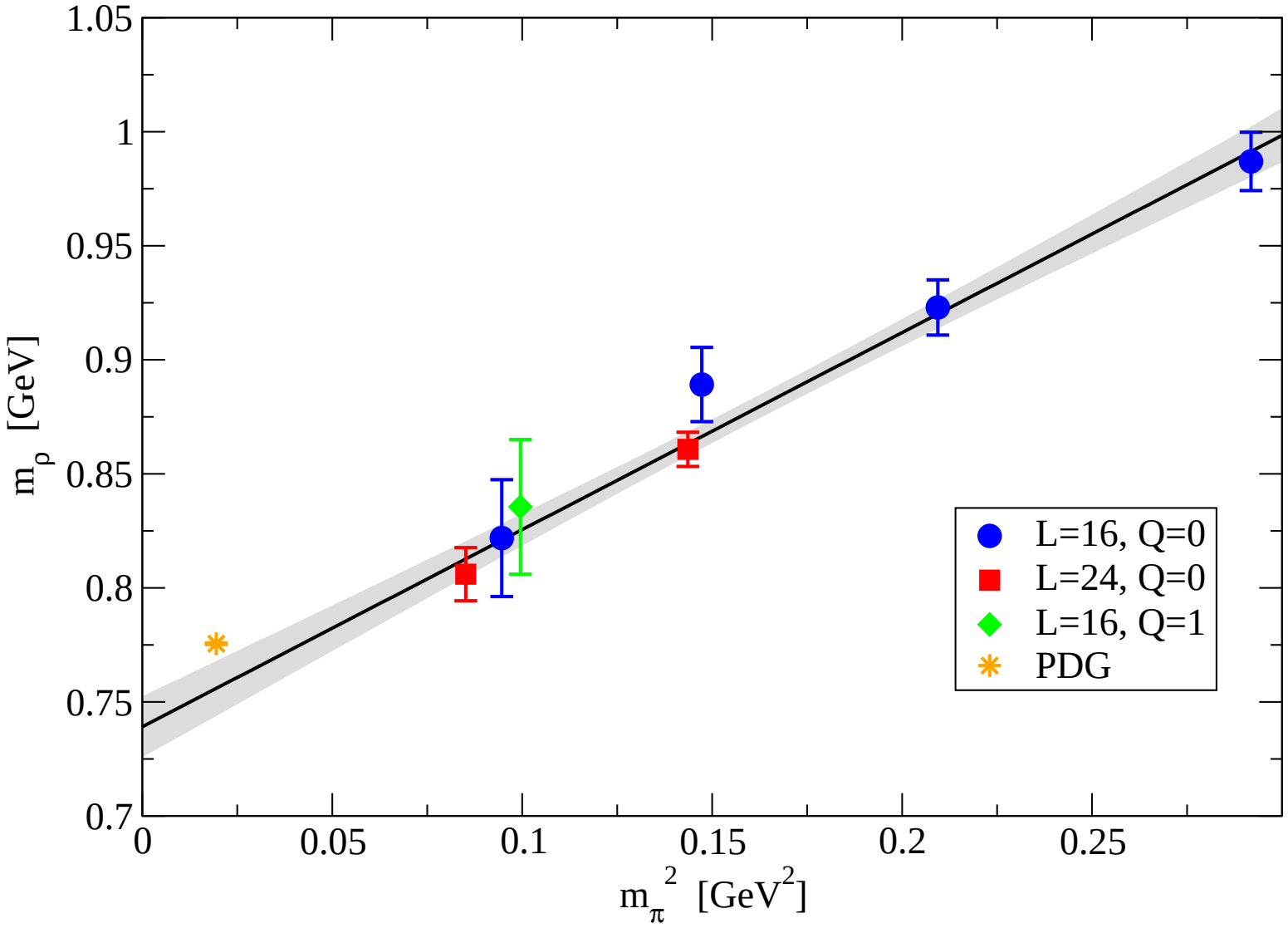
1.05
1
0.95
0.9
0.85
0.8
0.75
0.7
0
0.05
0.1
0.15
0.2
0.25
m_ρ [GeV]
m_π^2 [GeV^2]
L=16, Q=0
L=24, Q=0
L=16, Q=1
PDG

High precision scale setting

Z. Fodor

University of Wuppertal & Budapest, UCSD, FZJ

Budapest-Marseille-Wuppertal Collaboration, 1203.4469*

BNL, May 14, 2012

Outline

1. Scale setting
2. Flow of the gauge field
3. Pure gauge
4. Full QCD

Scale settings and the static potential

raw output of lattice QCD: physical quantities in lattice unit
$\Rightarrow$ measure a dimensionful quantity Q (M_Ω or f_K)
the lattice spacing is given by a=$(aQ^{lat})/Q^{exp}$

today erros below 2% for several lattice predictions
it depends crucially on the error of the lattice spacing
need for a controlled/small error lattice spacing determination

not necessarily directly accesable for experiments e.g. potential
popular choices are:
string tension (strictly speaking doesn't exist: string breaking)
the Sommer-scale $r_x^2 \cdot dV/dr = C_x$
originally r_0 with $C_0 = 1.65$ or MILC choice r_1 with C_1=1

Sommer-scale, Omega mass, f_π and f_K

unfortunately, the calculations of r_0 & r_1 are quite involved
far more complicated than fitting the masses of particles

complications are reflected in the literature
MILC: r_1=0.3117(22) fm (less than 1% accuracy)
RBC/UKQCD: r_1=0.3333(93)(1)(2) fm
7% difference and 2.3σ tension between them

another popular way is to use the Omega baryon mass
the experimental value of M_Ω is well known
more CPU demanding & sensititve to the strange quark mass
mismatched strange quark mass leads to a mismatched scale

difficulties with f_π (chiral extrapolation) & f_K (mismatched m_s)

suggestion of M. Luscher: use the Wilson flow to set the scale

Definition of the flow of the gauge field

Morningstar, Peardon PRD 69 (2004) 054501; Narayan, Neuberger, JHEP 0603 (2006) 064; Luscher JHEP 1008 (2010) 071

consider the flow: $B_\mu(t,x)$ for $t>0$ with $B_\mu(0,x)=A_\mu(x)$
flow equation: $\partial_t B_\mu = D_\nu G_{\mu\nu}$ with $G_{\mu\nu}=\partial_\mu B_\nu - \partial_\nu B_\mu + [B_\mu, B_\nu]$

the evolution in t has a smoothing effect:

$\partial_t B_\mu = \Delta B_\mu - \partial_\mu \partial_\nu B_\nu$ + non-linear terms

the first term is the same as in the heat-equation

$B_\mu(t,x) = \int d^4x K_t(x-y) A_\mu(y) + ...$

K_t four dimensional heat kernel $K_t(r) = \exp(-r^2/4t)/(4\pi t)^2$
smoothing effect with $\sqrt{8t}$ smoothing range

on the lattice regularize it: $V_t(x,\mu)$ for $t>0$ with $V_0(x,\mu)=U(x,\mu)$
flow equation with (Z) staples: $\partial_t V_t(x,\mu) = Z(V_t(x,\mu)) \cdot V_t(x,\mu)$

Wilson flow: technical realization

flow equation: $\dot{V}_t = Z(V_t)V_t$, where Z is the staple equivalent to a series of infinitesimal stout smearing steps

in our case it is integrated with 4th-order Runge-Kutta scheme

M. Luscher, JHEP 1008 (2010) 071

evolution from time t to time $t+\epsilon$ is given by $Z_i = \epsilon Z(W_i)$

$$
\begin{aligned}
W_0 &= V_t, \\
W_1 &= \exp\left(\frac{1}{4}Z_0\right) W_0, \\
W_2 &= \exp\left(\frac{8}{9}Z_1 - \frac{17}{36}Z_0\right) W_1, \\
V_{t+\epsilon} &= \exp\left(\frac{3}{4}Z_2 - \frac{8}{9}Z_1 + \frac{17}{36}Z_0\right) W_2
\end{aligned}
$$

Wilson flow and the coupling

M. Luscher, JHEP 1008 (2010) 071

as a representative example $E = G^a_{\mu\nu} G^a_{\mu\nu}/4$ is considered
lattice: E(t) can be defined by the (1-plaquette) or clover terms
they only differ by discretization effects
lattice: we expect $\langle E \rangle \propto$(1-plaquette)$\cdot t^2$ behavior

very important results about the renormalization of the Wilson flow

calculation of $\langle E \rangle$ up to $\alpha_s^2(q)$ with $q = (8t)^{-1/2}$
(result has been obtained in the continuum $\overline{MS}$ scheme)

$$\langle E \rangle = \frac{3}{4\pi t^2} \alpha(q) \{1 + k_1 \alpha(q) + \mathcal{O}(\alpha^2)\}, \quad k_1 = 1.0978 + 0.0075 N_f$$

above the cut-off (small t): lattice and continuum quite different

Lattice study of the Wilson flow (pure gauge)

the perturbation QCD expansion works for small t ($\ll$1 fm)
for large t one uses numerical lattice simulations
SU(3) pure gauge theory with lattice spacing a=0.05 fm

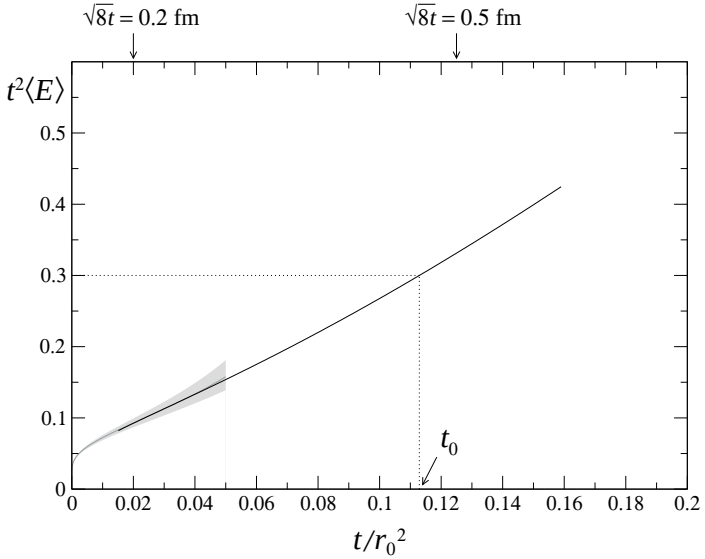

statistical error: smaller than the thickness of the (linear) line
lattice: expect (1-plaquette)$\cdot t^2$ behavior for small t
perturbation theory is given by the band (uncertainty on Λ)

Wilson flow for scale setting: quenched

$\langle E \rangle$ is physical: approaches its continuum limit with a^2
test it with the reference scale t_0 given by

$$\left\{ t^2 \langle E \rangle \right\}_{t=t_0} = 0.3$$

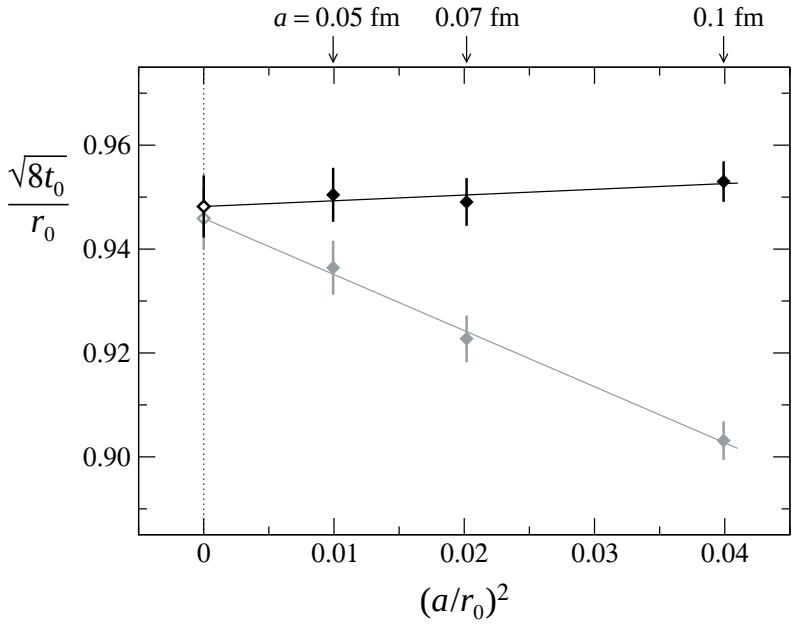

scaling violation increases toward smaller reference scales
for which the smoothing range is only 2-3 times the lattice spacing

Gauge flow for dynamical fermions & w_0

one can determine the gauge flow also for the dynamical case
use the Wilson flow or the gauge flow defined by the action

$t^2\langle E(t)\rangle$ incorporates informations from all $t>\mathcal{O}(1/\sqrt{t})$
its derivative (almost constant) mostly from scales around $\mathcal{O}(1/\sqrt{t})$
advantage: flow at small $t \sim a^2$ is a subject of cutoff effects

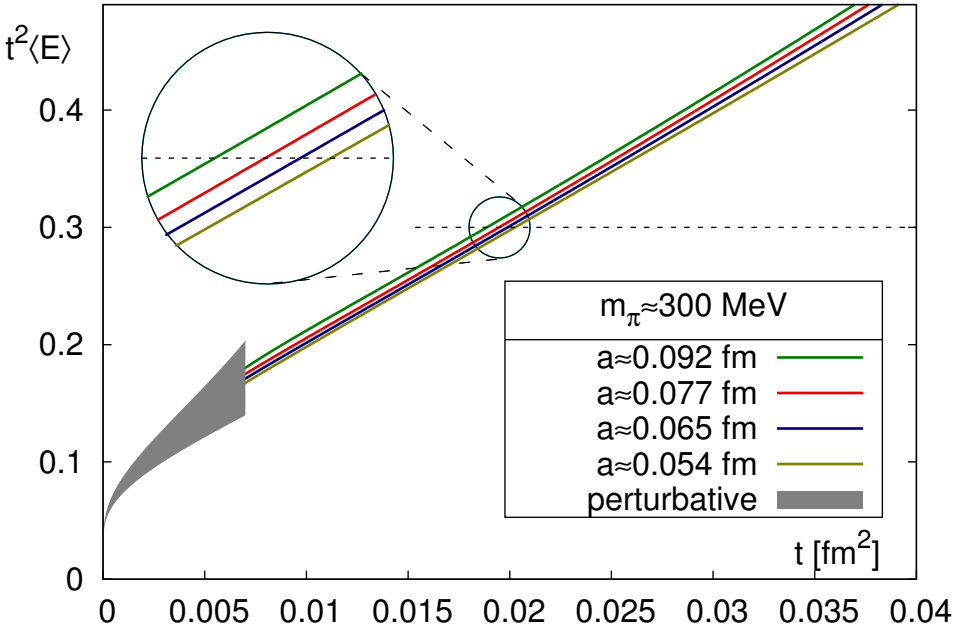

observed "linearity" for $t^2\langle E\rangle$
one can extract it by $t \cdot dt^2\langle E\rangle/dt$
instead $t^2\langle E\rangle$=0.3 (M. Luscher)
$t \cdot dt^2\langle E\rangle/dt$=0.3 ($w_0$ scale)

a→0: non-universal part shrinks
w_0 has less cutoff effects than t_0

Continuum limit is the same

different definitions should have the same continuum limit
one can use the Wilson flow or the Symanzik flow: M_π=135 MeV

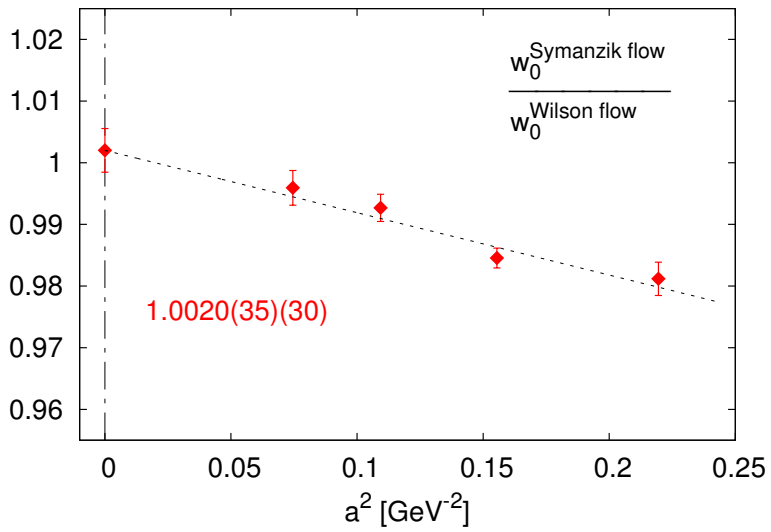

original definition of Luscher has the largest cut-off effect
various definitions of w_0 have tiny ones (a few % or less)
(statistical errors are neglible, good for scale setting)

Finite volume effects

how sensitive is w_0 to the size of the system
only for boxes <2 fm: $M_\pi L \approx 1.35$ instead of 4
$\Longrightarrow$ finite volume effects are tiny, far below the 1% level

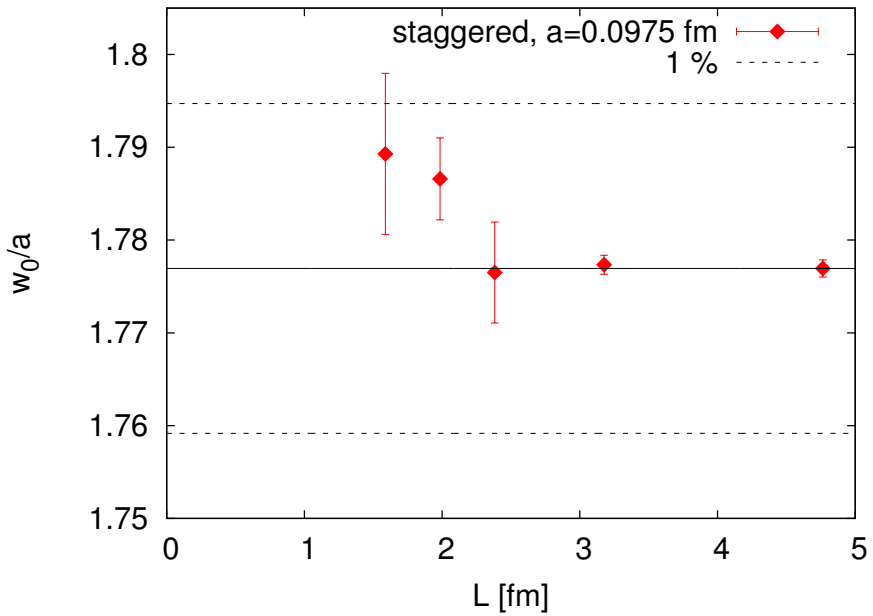

robust and stable method for determining the scale

a→ 0: Wilson & staggered w_0 Budapest-Marseille-Wuppertal Collaboration, 1203.4469*

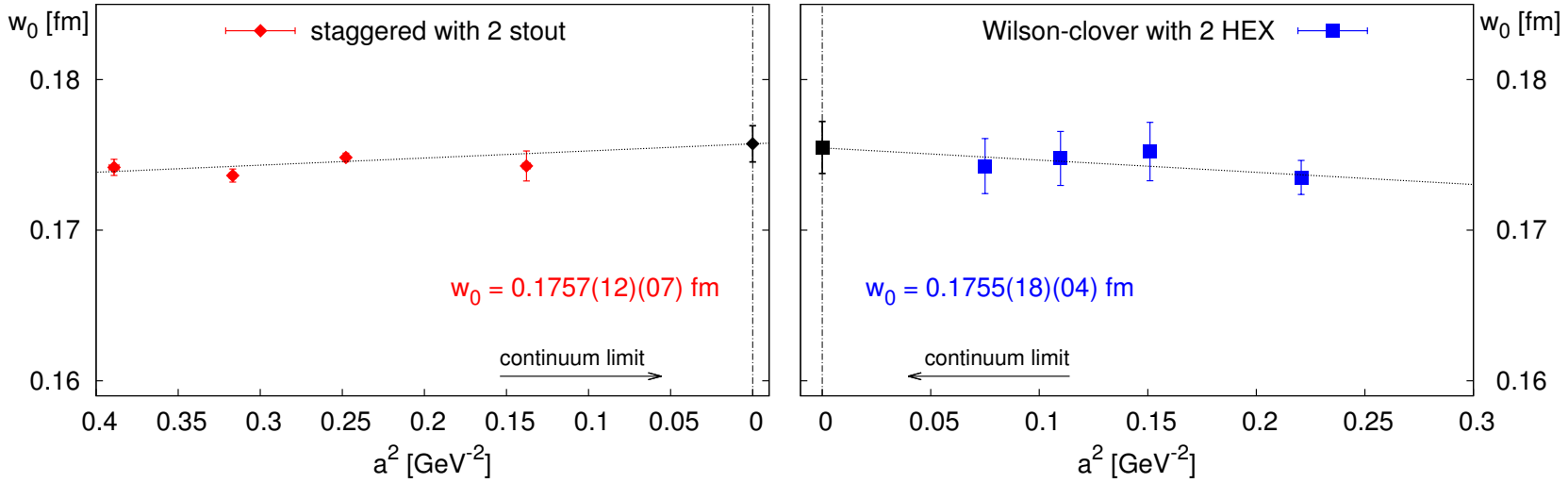

the physical scale was obtained by the Omega baryon mass

our final result is the Wilson result (staggered is a cross check)
(no rooting $\Longrightarrow$ theoretically cleaner)

$$w_0 = 0.1755(18)(04) \text{ fm}$$

error (dominantly statistical) is 1%
(and comes not from the gauge flow itself, but from M_Ω)

a→ 0: Wilson & staggered w_0 Budapest-Marseille-Wuppertal Collaboration, 1203.4469*

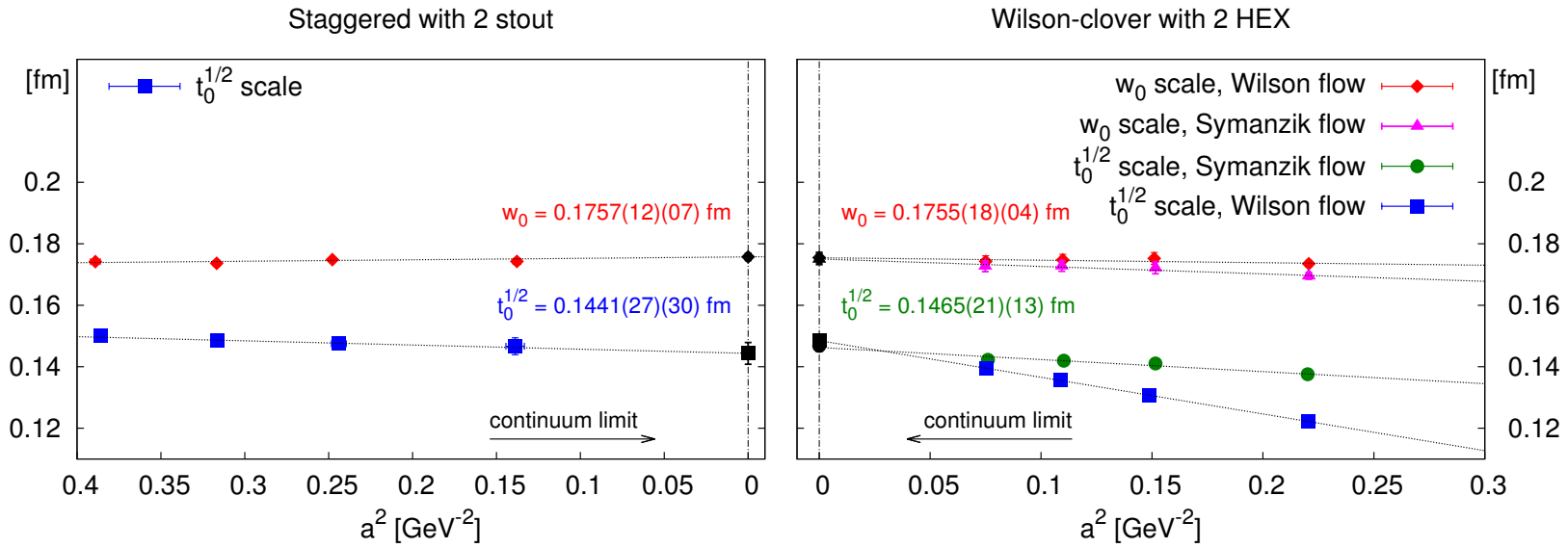

the physical scale was obtained by the Omega baryon mass

our final result is the Wilson result (staggered is a cross check)
(no rooting $\Longrightarrow$ theoretically cleaner)

$$w_0 = 0.1755(18)(04) \text{ fm}$$

error (dominantly statistical) is 1%
(and comes not from the gauge flow itself, but from M_Ω)

Scale off the physical point

usually runs aren't at physical masses: what is the scale there
measure M_π, M_K and w_0: $x = w_0^2 M_\pi^2$ and $y = w_0^2(M_K^2 - M_\pi^2/2)$

w_0=0.18515-0.5885x^2-0.0497y-0.11xy-1.476x^3$\pm 18\cdot 10^{-3} \pm 4\cdot 10^{-3}$[fm]

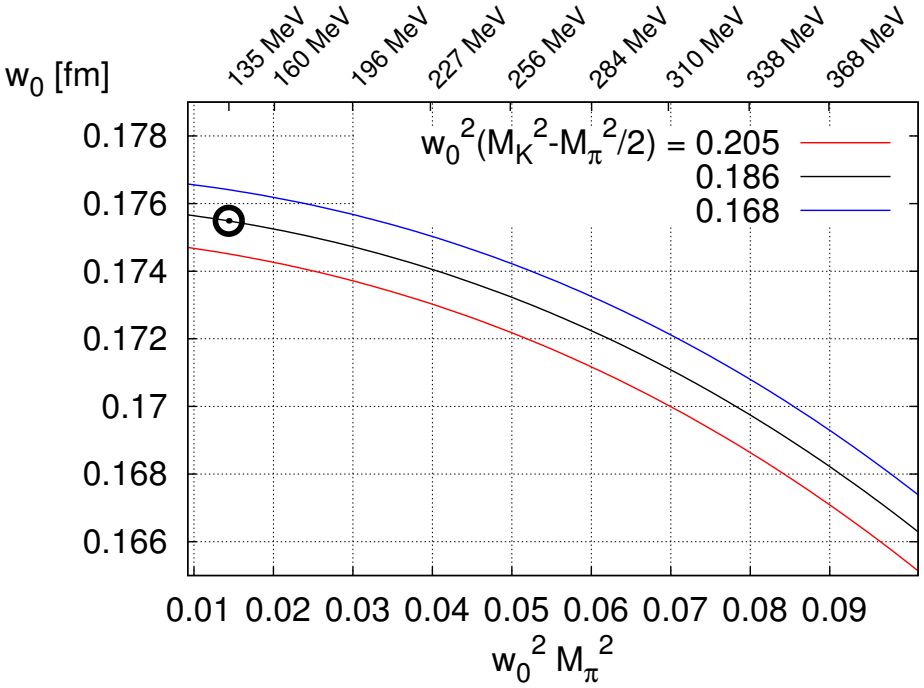

change M_π from 135 to 350 MeV

4% change in the lattice spacing
(same size as cutoff effects)

change m_s by 10%
0.5% change in the lattice spacing

error is 1% in the continuum limit

Error analysis: 2HEX data set

histogram method to give statistical and systematic errors
64 possible results (m_q interpolation, M_π cut, a→0, fit range, scale)

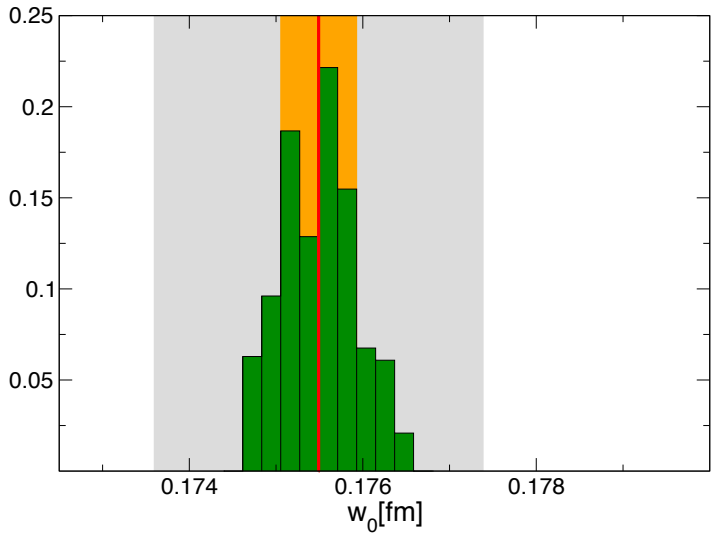

orange/gray bands: systematic/full error; red line: result

interpolation	M_π-cut	a→0	fit range	scale
15%	40%	55%	55%	45%

Outline

1. Scale setting
2. Flow of the gauge field
3. Pure gauge
4. Full QCD

Thermodynamic potentials from shifted boundary conditions

Leonardo Giusti

University of Milano-Bicocca

Based on: L. G. and H. B. Meyer PRL 106 (2011) 131601, arXiv:1110.3136 and in preparation

Outline

- Relation between the entropy density and the response of the system to the shift

$$s = -\frac{1}{T^2} \lim_{V\to\infty} \frac{1}{V} \frac{d^2}{dz^2} \ln Z(\{0,0,z\})\Big|_{z=0}$$

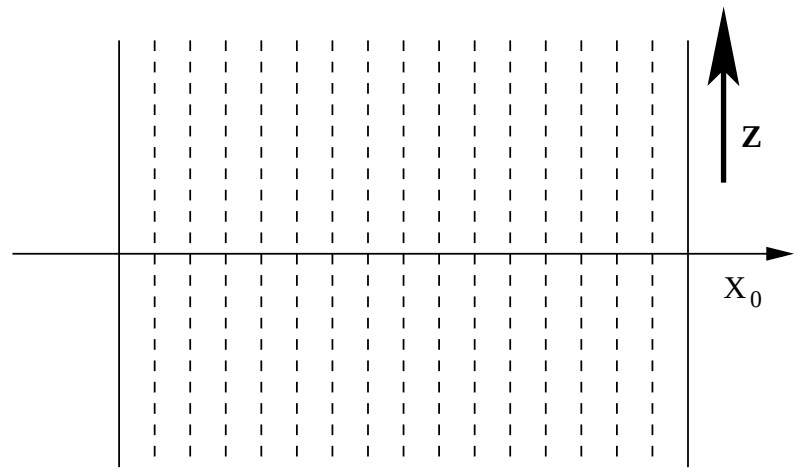

- Generalization to the specific heat
- Finite-size effects
- Extension to the lattice (and exploratory numerical study for $SU(3)$ Yang–Mills)
- Conclusions and outlook

Momentum distribution from shifted boundary conditions

- The relative contribution to the partition function of states with momentum $\mathbf{p}$ is $[T = 1/L_0]$

$$\frac{R(\mathbf{p})}{V} = \frac{\mathrm{Tr}\{e^{-L_0 \hat{\mathrm{H}}}\, \hat{\mathrm{P}}^{(\mathbf{p})}\}}{\mathrm{Tr}\{e^{-L_0 \hat{\mathrm{H}}}\}}$$

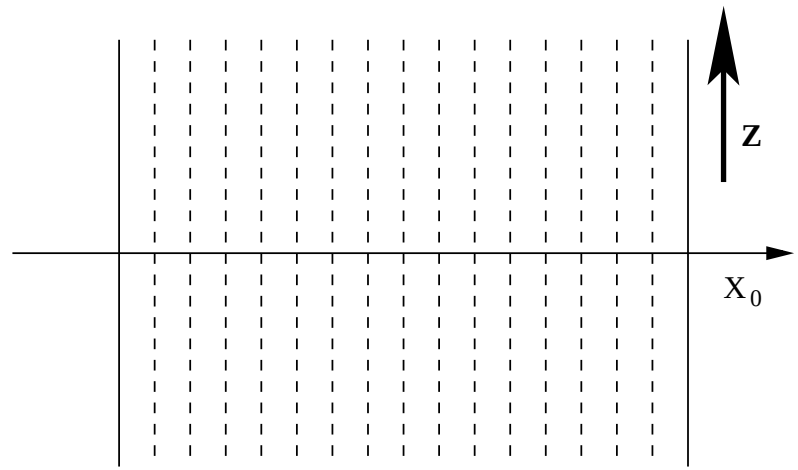

where

$$\hat{\mathrm{P}}^{(\mathbf{p})} = \frac{1}{V} \int d^3\mathbf{z}\, e^{-i\mathbf{p}\cdot\mathbf{z}}\, e^{i\hat{\mathbf{p}}\cdot\mathbf{z}}\,, \qquad e^{i\hat{\mathbf{p}}\mathbf{z}}|\phi\rangle = |\phi^{\mathbf{z}}\rangle$$

- The momentum distribution can then be written as

$$\frac{R(\mathbf{p})}{V} = \frac{1}{V} \int d^3\mathbf{z}\, e^{-i\mathbf{p}\cdot\mathbf{z}}\, \frac{Z(\mathbf{z})}{Z}\,, \qquad \phi(L_0, \mathbf{x}) = \phi(0, \mathbf{x} + \mathbf{z})$$

where $Z(\mathbf{z})$ is the usual path integral but with shifted boundary conditions in time direction

Cumulant generator

- As usual the generator of its cumulants is defined as

$$e^{-K(\mathbf{z})} = \frac{1}{V}\sum_{\mathbf{p}} e^{i\mathbf{p}\cdot z}\, R(\mathbf{p}) \qquad \Longrightarrow \qquad e^{-K(\mathbf{z})} = \frac{Z(\mathbf{z})}{Z}$$

- The momentum cumulants can then be written as

$$\frac{\langle \hat{p}_1^{2n_1}\, \hat{p}_2^{2n_2}\, \hat{p}_3^{2n_3} \rangle_c}{V} = \frac{(-1)^{n_1+n_2+n_3}}{V} \frac{\partial^{2n_1}}{\partial z_1^{2n_1}} \frac{\partial^{2n_2}}{\partial z_2^{2n_2}} \frac{\partial^{2n_3}}{\partial z_3^{2n_3}} \ln\left[\frac{Z(\mathbf{z})}{Z}\right]_{\mathbf{z}=\mathbf{0}}$$

- In the continuum they equal the standard definition

$$\langle \hat{p}^{2n_1}\, \hat{p}^{2n_2}\, \hat{p}^{2n_3} \rangle_c = (-1)^{n_1+n_2+n_3} \langle \overline{T}_{01} \cdots \overline{T}_{03} \rangle_c \,, \qquad \overline{T}_{0k}(x_0) = \int d^3x\, T_{0k}(x)$$

and, being conn. corr. functions of the momentum charge, they are finite as they stand.
The generator $K(\mathbf{z})$ and the distribution $R(\mathbf{p})$ are thus expected to be finite as well

Momentum distribution from shifted boundaries on the lattice [Della Morte, LG 10; LG, Meyer 10]

- On the lattice a theory is invariant under a discrete group of translations only. It is still possible, however, to factorize the Hilbert space in sectors with definite conserved total momentum

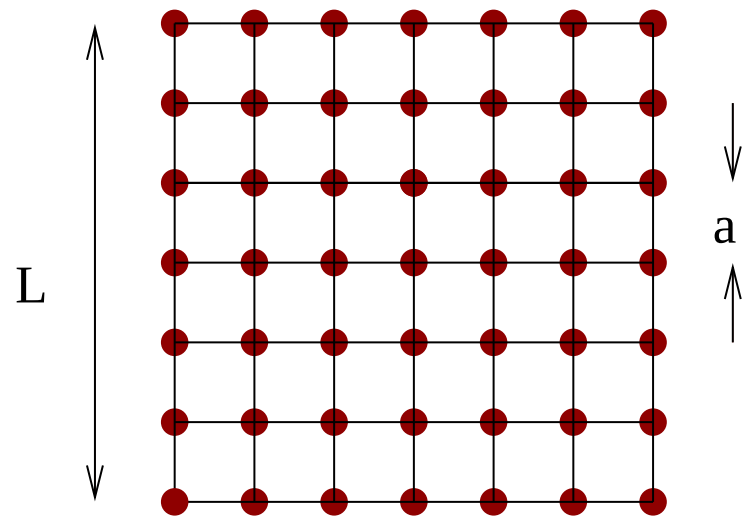

- The momentum distribution is given by

$$\frac{\mathcal{R}(\mathbf{p})}{V} = \frac{a^3}{V} \sum_{\mathbf{z}} e^{-i\mathbf{p}\cdot\mathbf{z}} \frac{\mathcal{Z}(\mathbf{z})}{\mathcal{Z}}$$

where $\mathcal{Z}(\mathbf{z})$ is the usual PI but with (discrete) shifted boundary conditions.

- Since only physical states contribuite to it, $\mathcal{R}(\mathbf{p})$ is expected to converge to the continuum universal value without need for UV renormalization

- The shifted boundary conditions allow us to define connected correlation functions of the momentum which do not require any UV renormalization

- Their continuum limit satisfies the standard EMT WIs, which can be used to interpret the cumulants in terms of basic thermodynamic potentials

Ward identities for two-point correlators of $\overline{T}_{0k}$ (I)

- In the continuum a judicious combination of WIs associated with translational invariance

$$\partial_\mu \langle T_{\mu\nu}(x)\, O_1 \ldots O_n \rangle = -\sum_{i=1}^{n} \langle O_1 \ldots \delta_x O_i \ldots O_n \rangle \ ,$$

leads to $(x_0 \neq y_0\ ,\ w_k \neq z_k)$

$$L_0\, \langle \overline{T}_{0k}(x_0)\, T_{0k}(y) \rangle - L_k\, \langle \widetilde{T}_{0k}(w_k)\, T_{0k}(z) \rangle = \langle T_{00} \rangle - \langle T_{kk} \rangle$$

where

$$\overline{T}_{0k}(x_0) = \int d^3x\, T_{0k}(x)\ , \qquad \widetilde{T}_{0k}(x_k) = \int \Big[\prod_{\nu \neq k} dx_\nu \Big]\, T_{0k}(x)$$

- Note that:

  * All operators at non-zero distance
  * Number of EMT on the two sides different
  * Trace component of EMT does not contribute
  * On the lattice it can be imposed to fix the renormalization of T_{0k}

Ward identities for two-point correlators of $\overline{T}_{0k}$ (II)

- The commutator of boost with momentum

$$[\hat{K}_k, \hat{p}_k] = i\hat{H}$$

is expressed in the Euclidean by the WIs

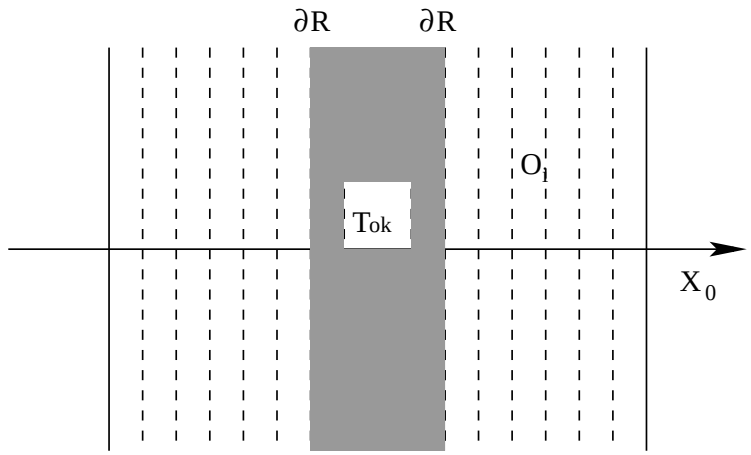

$$\int_{\partial R} d\sigma_\mu(x)\, \langle K_{\mu;0k}(x)\, \overline{T}_{0k}(y_0)\, O_1 \ldots O_n \rangle_c = \langle \overline{T}_{00}(y_0)\, O_1 \ldots O_n \rangle_c$$

when the O_i are localized external fields.

- In a 4D box boost transformations are incompatible with (periodic) boundary conditions. WIs associated with $SO(4)$ rotations must be modified by finite-size contributions

- The finite-volume theory is translational invariant, and it has a conserved $T_{\mu\nu}$. Modified WIs associated to boosts constructed from those associated to translational invariance

$$L_0\, \langle \overline{T}_{0k}(x_0)\, T_{0k}(y) \rangle - L_k\, \langle \widetilde{T}_{0k}(w_k)\, T_{0k}(z) \rangle = \langle T_{00} \rangle - \langle T_{kk} \rangle$$

Ward identities for two-point correlators of $\overline{T}_{0k}$ (III)

- In the thermodynamic limit the WI reads ($y_0 \neq x_0$)

$$L_0 \, \langle \overline{T}_{0k}(x_0) \, T_{0k}(y) \rangle = \langle T_{00} \rangle - \langle T_{kk} \rangle$$

- By remembering that in the Euclidean

$$\hat{p}_k \leftrightarrow -i \, \overline{T}_{0k} \, , \quad e = -\langle T_{00} \rangle \, , \quad p = \langle T_{kk} \rangle \qquad \Longrightarrow \qquad \frac{\langle \hat{p}_k^2 \rangle}{V} = T \, \{e + p\} = T^2 s$$

- In a finite box and for $M \neq 0$ (M lightest screening mass)

$$\langle \overline{T}_{0k}(x_0) \, T_{0k}(y) \rangle = -T \, \{e + p\} + \frac{\nu M T^2}{2\pi L} \left[M + 3T \frac{\partial M}{\partial T} \right] e^{-ML} + \ldots$$

i.e. leading finite-size effects are known functions of M, and are exponentially small in ML

Entropy density from shifted boundary conditions

- By putting together the two formulas

$$s = -\frac{1}{T^2} \lim_{V\to\infty} \frac{1}{V} \frac{d^2}{dz^2} \ln Z(\{0,0,z\})\Big|_{z=0}$$

- On the lattice the only difference is the discrete derivative

$$s = -\frac{1}{T^2} \lim_{V\to\infty} \lim_{a\to 0} \frac{2}{n_z^2 a^2 V} \ln\left[\frac{\mathcal{Z}(\{0,0,n_z a\})}{\mathcal{Z}}\right]$$

  with n_z being kept fixed when $a \to 0$

- Note that:
  - $*$ No ultraviolet renormalization
  - $*$ Finite volume effects exponentially small
  - $*$ Discretization effects $\mathcal{O}(a^2)$ once action improved

Recursive relation for higher order cumulants

- There is more information in $K(\mathbf{z})$. Again a judicious combination of WIs leads to

$$\langle \overline{T}_{0k}(x_0^1)\,\overline{T}_{0k}(x_0^2)\ldots\overline{T}_{0k}(x_0^{2n})\rangle_c = \langle \overline{T}_{00}(x_0^1)\,\overline{T}_{kk}(x_0^2)\ldots\overline{T}_{0k}(x_0^{2n})\rangle_c + \text{f.s.c.}$$

- At finite temperature and volume

$$L_0\,\langle \overline{T}_{00}(y_0)\,\overline{T}_{0k}(x_0^1)\ldots\overline{T}_{0k}(x_0^{2n})\rangle_c \quad = \quad L_0\frac{\partial}{\partial L_0}\,\langle \overline{T}_{0k}(x_0^1)\ldots\overline{T}_{0k}(x_0^{2n})\rangle_c$$

$$L_0\,\langle \overline{T}_{kk}(y_0)\,\overline{T}_{0k}(x_0^1)\ldots\overline{T}_{0k}(x_0^{2n})\rangle_c \quad = \quad \left\{L_k\frac{\partial}{\partial L_k}+2n\right\}\langle \overline{T}_{0k}(x_0^1)\ldots\overline{T}_{0k}(x_0^{2n})\rangle_c$$

- By combining these relations, and by taking the infinite volume limit

$$\langle \overline{T}_{0k}(x_0^1)\ldots\overline{T}_{0k}(x_0^{2n})\rangle_c = (2n-1)\,\frac{\partial}{\partial L_0}\left\{\frac{1}{L_0}\,\langle \overline{T}_{0k}(x_0^1)\ldots\overline{T}_{0k}(x_0^{2n-2})\rangle_c\right\}$$

- Expression of finite-size corrections similar to the one of two-point corr. functions

Specific heat

- Written for cumulants the recursive relation reads

$$\langle \hat{p}_z^{2n} \rangle_c = (2n-1)\, T^2 \, \frac{\partial}{\partial T} \left\{ T \, \langle \hat{p}_z^{2n-2} \rangle_c \right\}$$

  and analogously for mixed ones

- The definition of the specific heat implies

$$c_v = T \frac{\partial}{\partial T} s \qquad \Longrightarrow \qquad c_v = \frac{1}{V} \left[\frac{\langle \hat{p}_z^4 \rangle_c}{3T^4} - 3 \, \frac{\langle \hat{p}_z^2 \rangle_c}{T^2} \right]$$

  and therefore

$$c_v = \lim_{V \to \infty} \frac{1}{V} \left[\frac{1}{3T^4} \frac{d^4}{dz^4} + \frac{3}{T^2} \frac{d^2}{dz^2} \right] \ln Z(\{0,0,z\}) \Big|_{z=0}$$

- On the lattice the only difference are the discrete derivatives. Finite-size corrections are again known, and are exponentially suppressed

Scale-invariant case

- If T is the only dimensionful parameter in the problem, the recursive relation implies

$$\frac{\langle \hat{p}_z^{2n} \rangle_c}{V} = c_{2n}\, T^{2n+3} \qquad \Longrightarrow \qquad c_{2n} = \frac{(n+1)}{4}\,(2n!)\, c_2$$

- By using the moment-cumulant transformation, the generator of the cumulants reads

$$K(\{0,0,z\}) = \sum_{n=1}^{\infty} (-1)^{n+1}\, \frac{\langle \hat{p}_z^{2n} \rangle_c}{2n!}\, z^{2n}$$

- The series can be re-summed to obtain

$$\frac{K(\{0,0,z\})}{V} = \frac{s}{4}\left\{1 - \frac{1}{(1+z^2T^2)^2}\right\}$$

i.e. the entropy determines all the cumulants. The combination of scale and relativistic invariance fixes the functional form to be the one of the free case.

Numerical algorithm for the cumulant generator (I)

- The most straightforward way for computing the cumulant generator is to rewrite it as

$$\frac{\mathcal{Z}(\mathbf{z})}{\mathcal{Z}} = \prod_{i=0}^{n-1} \frac{\mathcal{Z}(\mathbf{z}, r_i)}{\mathcal{Z}(\mathbf{z}, r_{i+1})}$$

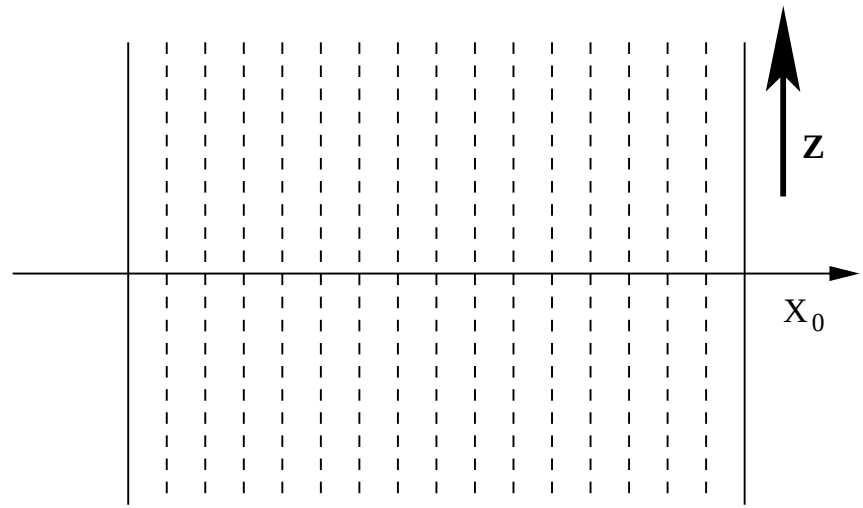

where a set of $(n+1)$ systems is designed so that the relevant phase spaces of successive path integrals overlap and that $\mathcal{Z}(\mathbf{z}, r_0) = \mathcal{Z}(\mathbf{z})$ and $\mathcal{Z}(\mathbf{z}, r_n) = \mathcal{Z}$

- The path integrals of the interpolating systems are defined as

$$\mathcal{Z}(\mathbf{z}, r) = \int DU \, DU_{4,L_0/a-1} \; e^{-\overline{S}_G[U,U_4,r]}$$

where $U_{4,L_0/a-1}$ is an extra (5th) temporal link assigned to each point of last time-slice

Numerical algorithm for the cumulant generator (II)

- The action of the interpolating systems is

$$\overline{S}_G[U,U_4,r] = S_G[U] + \frac{\beta}{3}(1-r)\sum_{\mathbf{x},k}\mathrm{ReTr}\Big\{U_{0k}(L_0/a-1,\mathbf{x}) - U_{4k}(L_0/a-1,\mathbf{x})\Big\}$$

with the extra space-time plaquette given by

$$U_{4k}(L_0/a-1,\mathbf{x}) = U_4(L_0/a-1,\mathbf{x})\,U_k(0,\mathbf{x}+\mathbf{z})\,U_4^\dagger(L_0/a-1,\mathbf{x}+\hat{k})\,U_k^\dagger(L_0/a-1,\mathbf{x})$$

- If we define the "reweighting" observable as

$$O[U,r_{i+1}] = e^{\overline{S}_G[U,U_4,r_{i+1}]-\overline{S}_G[U,U_4,r_i]}$$

then

$$\frac{\mathcal{Z}(\mathbf{z},r_i)}{\mathcal{Z}(\mathbf{z},r_{i+1})} = \langle\, O[U,r_{i+1}]\,\rangle_{r_{i+1}}$$

Numerical algorithm for the cumulant generator (II)

- The action of the interpolating systems is

$$\overline{S}_G[U,U_4,r] = S_G[U] + \frac{\beta}{3}(1-r)\sum_{\mathbf{x},k}\mathrm{ReTr}\Big\{U_{0k}(L_0/a-1,\mathbf{x}) - U_{4k}(L_0/a-1,\mathbf{x})\Big\}$$

with the extra space-time plaquette given by

$$U_{4k}(L_0/a-1,\mathbf{x}) = U_4(L_0/a-1,\mathbf{x})\,U_k(0,\mathbf{x}+\mathbf{z})\,U_4^\dagger(L_0/a-1,\mathbf{x}+\hat{k})\,U_k^\dagger(L_0/a-1,\mathbf{x})$$

- On each lattice the entropy is finally given by

$$s = -\frac{2}{\mathbf{z}^2T^2V}\sum_{i=0}^{n-1}\ln\left[\frac{\mathcal{Z}(\mathbf{z},r_i)}{\mathcal{Z}(\mathbf{z},r_{i+1})}\right]$$

Numerical results for the entropy

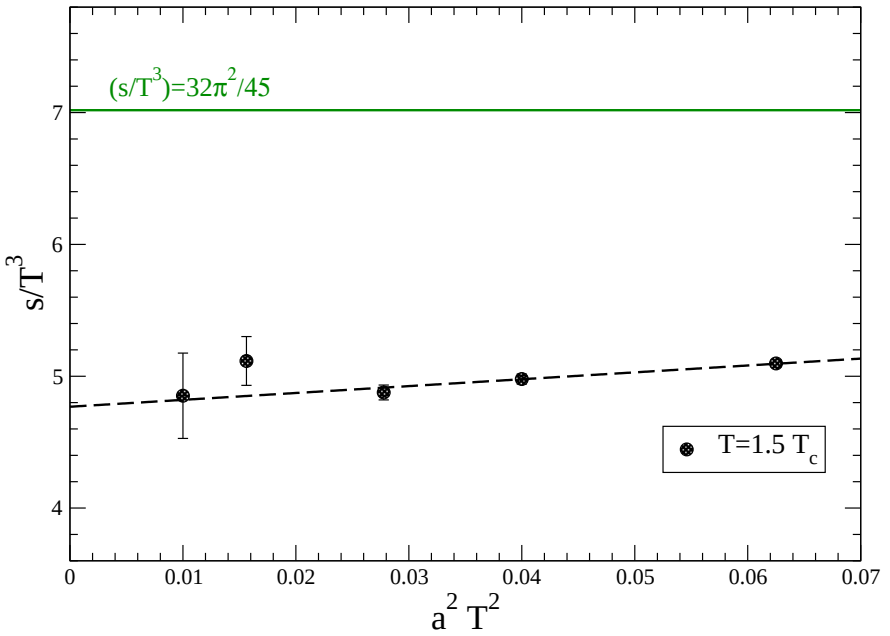

Lat	$6/g_0^2$	L_0/a	L/a	$K(\mathbf{z},a)$	$\frac{2K(\mathbf{z},a)}{\lvert\mathbf{z}\rvert^2 T^5 V}$
A_1	5.9	4	12	17.20(11)	5.10(3)
A_{1a}	5.9	4	16	40.71(15)	5.089(19)
A_2	6.024	5	16	13.05(10)	4.98(4)
A_3	6.137	6	18	7.32(8)	4.88(6)
A_4	6.337	8	24	4.32(16)	5.12(19)
A_5	6.507	10	30	2.62(17)	4.9(3)

Numerical results for the entropy

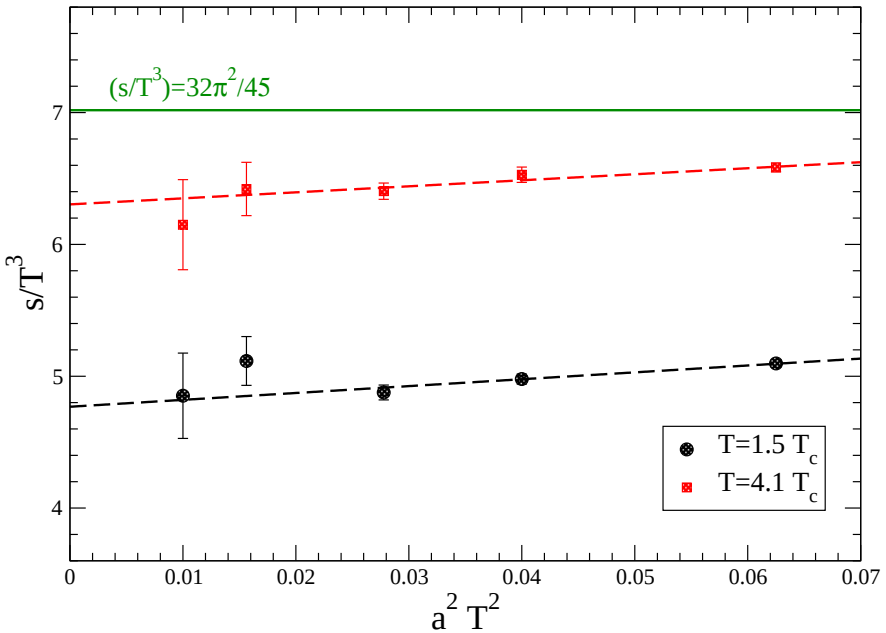

- A linear extrapolation in a^2 gives

$$\frac{s}{T^3} = 4.77 \pm 0.08 \pm ?? \qquad T = 1.5\,T_c$$

$$\frac{s}{T^3} = 6.30 \pm 0.09 \pm ?? \qquad T = 4.1\,T_c$$

- Compatible with previous computations, but continuum extrapolation must be improved

  [Boyd et al. 96; Namekawa et al. 01]

Lat	$6/g_0^2$	L_0/a	L/a	$K(\mathbf{z},a)$	$\frac{2K(\mathbf{z},a)}{\lvert\mathbf{z}\rvert^2 T^5 V}$
A_1	5.9	4	12	17.20(11)	5.10(3)
A_{1a}	5.9	4	16	40.71(15)	5.089(19)
A_2	6.024	5	16	13.05(10)	4.98(4)
A_3	6.137	6	18	7.32(8)	4.88(6)
A_4	6.337	8	24	4.32(16)	5.12(19)
A_5	6.507	10	30	2.62(17)	4.9(3)

Lat	$6/g_0^2$	L_0/a	L/a	$K(\mathbf{z},a)$	$\frac{2K(\mathbf{z},a)}{\lvert\mathbf{z}\rvert^2 T^5 V}$
B_1	6.572	4	12	22.22(11)	6.58(3)
B_{1a}	6.572	4	16	53.47(16)	6.684(20)
B_2	6.747	5	16	17.11(15)	6.53(6)
B_3	6.883	6	18	9.61(9)	6.40(6)
B_4	7.135	8	24	5.42(17)	6.42(20)
B_5	7.325	10	30	3.32(18)	6.1(3)

Numerical results for the entropy

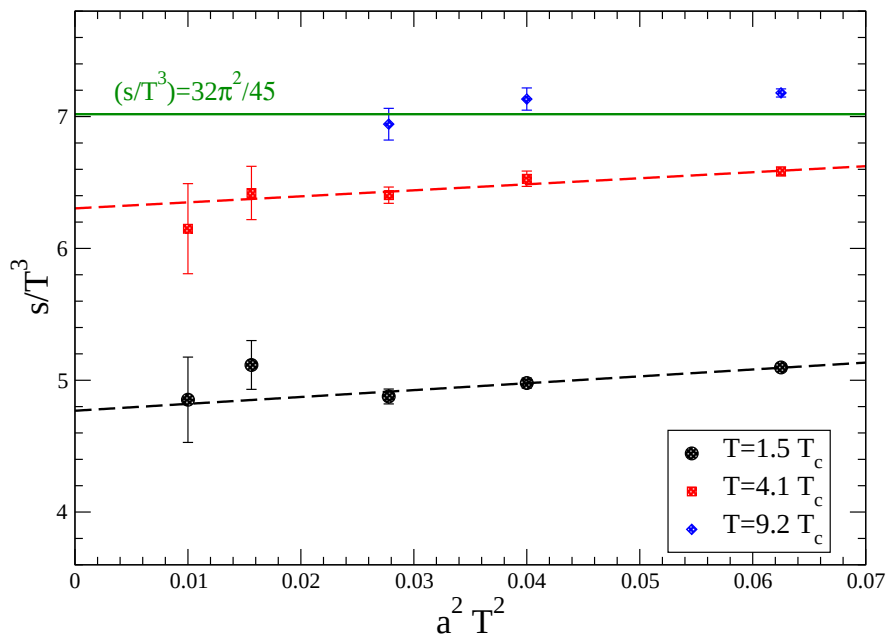

Lat	$6/g_0^2$	L_0/a	L/a	$K(\mathbf{z},a)$	$\frac{2K(\mathbf{z},a)}{\lvert\mathbf{z}\rvert^2 T^5 V}$
A_1	5.9	4	12	17.20(11)	5.10(3)
A_{1a}	5.9	4	16	40.71(15)	5.089(19)
A_2	6.024	5	16	13.05(10)	4.98(4)
A_3	6.137	6	18	7.32(8)	4.88(6)
A_4	6.337	8	24	4.32(16)	5.12(19)
A_5	6.507	10	30	2.62(17)	4.9(3)

- A linear extrapolation in a^2 gives

$$\frac{s}{T^3} = 4.77 \pm 0.08 \pm ?? \qquad T = 1.5\,T_c$$

$$\frac{s}{T^3} = 6.30 \pm 0.09 \pm ?? \qquad T = 4.1\,T_c$$

- Compatible with previous computations, but continuum extrapolation must be improved

[Boyd et al. 96; Namekawa et al. 01]

Lat	$6/g_0^2$	L_0/a	L/a	$K(\mathbf{z},a)$	$\frac{2K(\mathbf{z},a)}{\lvert\mathbf{z}\rvert^2 T^5 V^3}$
C_1	7.234	4	16	57.44(25)	7.18(3)
C_2	7.426	5	20	36.5(4)	7.13(8)
C_3	7.584	6	24	24.7(4)	6.94(12)

Conclusions and outlook

- Correlation functions of total momentum fields can be related to derivatives of path integrals with shifted boundary conditions

- One of the applications is the computation of thermodynamic potentials, which can be connected to the cumulants via Ward identities of EMT. The entropy, for instance, is

$$s = -\frac{1}{T^2} \lim_{V\to\infty} \frac{1}{V} \frac{d^2}{dz^2} \ln Z(\{0,0,z\})\Big|_{z=0}$$

- If lightest screening mass $M \neq 0$, leading finite-size corrections exponentially small in ML

- On the lattice these formulas apply once the derivative is discretized and the continuum limit is taken. No additive (vac. subtraction) or multiplicative UV renormalization is needed

- Same WIs allow for a non-perturbative renormalization of T_{0k}

- Feasibility study very promising even with a very simple-minded (expensive) algorithm

Padé approximants and g-2 for the muon

Christopher Aubin, Tom Blum, Maarten Golterman, Santi Peris

New Horizons for Lattice
Computations with Chiral Fermions
BNL, May 14-16, 2012

Contribution from lowest-order hadronic vacuum polarization (HLO)

$$a_\mu^{\rm HLO} = 4\alpha^2 \int_0^\infty dQ^2\, f(Q^2)\left(\Pi(0) - \Pi(Q^2)\right)$$

(Lautrup, Peterman, de Rafael 1971, Blum 2002)

$f(Q^2) =$

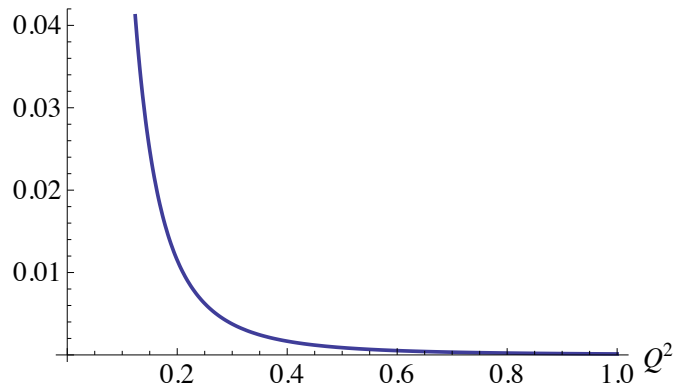

Data for $\Pi(Q^2)$:

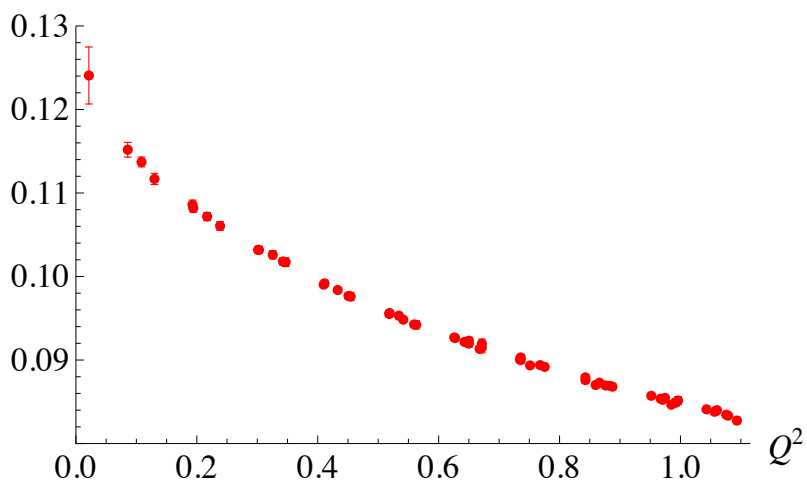

Need to fit data to compute integral; VMD introduces model dependence

Multi-point Padé approximants:

Write $\left(\Pi(0) - \Pi(Q^2)\right)/Q^2 = \int_{4m_\pi^2}^{\infty} dt \, \frac{\rho(t)}{t(t+Q^2)} \equiv \Phi(Q^2) \ , \quad \rho(t) \geq 0$

This integral is a Stieltjes function, analytic everywhere except cut $(-\infty, -4m_\pi^2]$.

Theorem: Given P points $(Q_i^2, \Phi(Q_i^2))$ a sequence of PAs can be constructed which converge to $\Phi(Q^2)$ on any closed, bounded region of the complex place excluding the cut, in the limit $P \to \infty$. (Baker 1969, Barnsley 1973)

Construction: $$\Phi(Q^2) = \cfrac{\Psi_0}{1 + \cfrac{(Q^2 - Q_1^2)\Psi_1}{1 + \ddots \, \cfrac{(Q^2 - Q_{P-2}^2)\Psi_{P-2}}{1 + (Q^2 - Q_{P-1}^2)\Psi_{P-1}}}}$$

with Ψ_i related to $\Phi(Q^2_{j \leq i+1})$ ($\Psi_0 = \Phi(Q_1^2)$, etc.), yields a $[[(P-1)/2], [P/2]]$ PA.

Parametrization and strategy

Furthermore, can prove that (Baker, Barnsley)

$$\Pi(Q^2) = \Pi(0) - Q^2 \left(a_0 + \sum_{n=1}^{[P/2]} \frac{a_n}{b_n + Q^2} \right)$$

with $a_n > 0$ (positive residues) and $b_{[P/2]} > \cdots > b_1 > 4m_\pi^2$ (all poles on cut), $a_0 = 0$ for P even .

Fit this form for $P = 2, 3, 4, 5$; yields $[0,1],\ [1,1],\ [1,2],\ [2,2]$ PAs.

Compute $a_\mu^{\mathrm{HLO},Q^2 \leq 1} = 4\alpha^2 \int_0^{1\ \mathrm{GeV}^2} dQ^2\, f(Q^2)\, \left(\Pi(0) - \Pi(Q^2)\right)$

Note: VMD is same as $[0,1]$ PA with $b_1 = m_\rho^2$ fixed; NOT a (valid) PA!

Test on MILC lattices with $a = 0.09$ fm , $m_\pi = 480$ MeV

		correlated interval $0 < Q^2 \leq 0.6$ GeV^2		**uncorrelated** interval $0 < Q^2 \leq 1$ GeV^2	
PA	# parameters	χ^2/dof	$10^{10} a_\mu^{\mathrm{HLO},Q^2\leq 1}$	χ^2/dof	$10^{10} a_\mu^{\mathrm{HLO},Q^2\leq 1}$
VMD	2	5.86/3*	363(7)	4.37/18	413(8)
[0, 1]	3	11.4/8	338(6)	3.58/17	373(37)
[1, 1]	4	7.49/7	350(8)	3.36/16	424(116)
[1, 2]	5	7.49/6	350(8)	3.35/15	443(293)
[2, 2]	6	7.49/5	350(7)	3.35/14	445(432)

* interval $0 < Q^2 \leq 0.35$ GeV^2
uncorrelated VMD fit agrees with Aubin and Blum, 2007

- Correlated: VMD bad, clear improvement with addition of parameters
- Difficult to determine 2nd pole, but a_μ insensitive to higher poles
- Internal consistency, except uncorr. VMD (unknown systematic error!) and correlated PAs

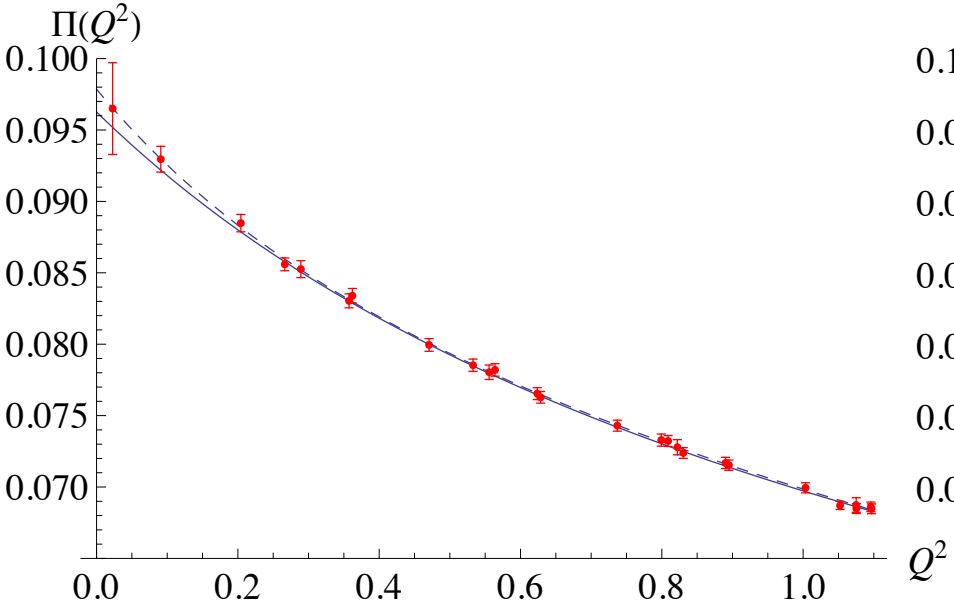

[1,1] corr. (solid) and uncorr. (dashed)

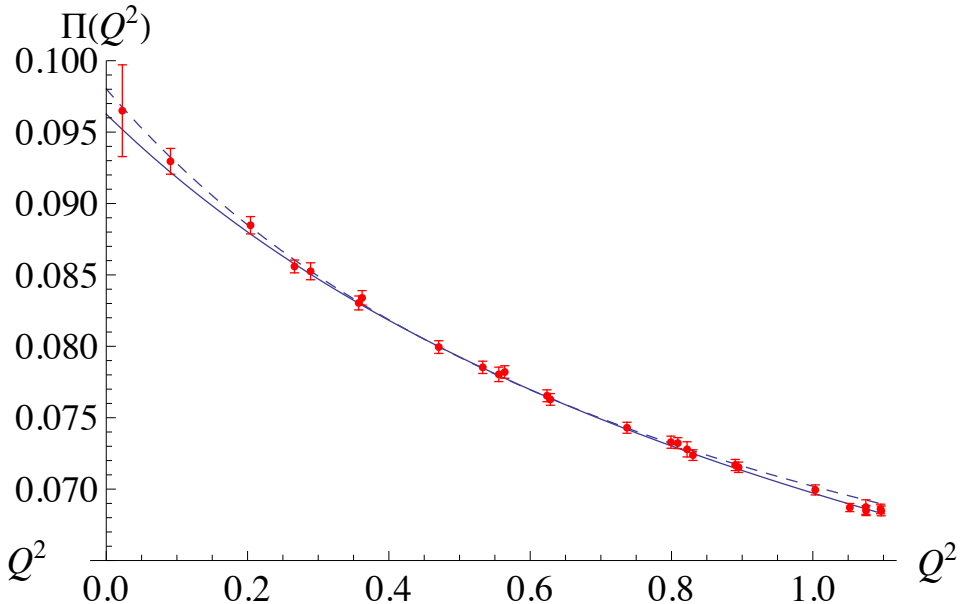

[1,1] corr. (solid) and VMD uncorr. (dashed)

- uncorrelated fits look better at small Q^2
- also considered MILC lattices with $a = 0.06 \text{ fm}$, $m_\pi = 220 \text{ MeV}$ – similar

$a_\mu^{\text{HLO},Q^2\leq 1} = 572(41) \times 10^{10}$ [1,1] corr. , $a_\mu^{\text{HLO},Q^2\leq 1} = 646(8) \times 10^{10}$ VMD uncorr.

- not possible to decide which fit is best, based on current data

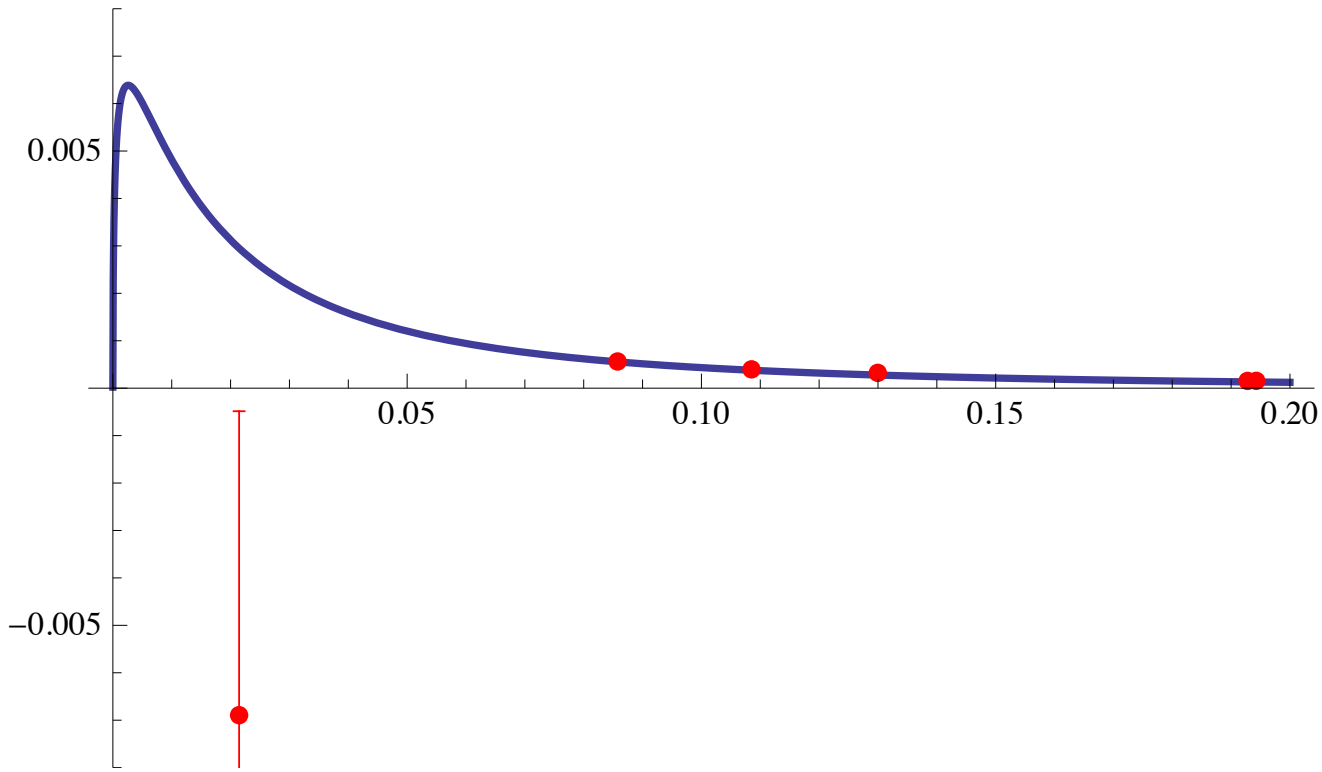

Integrand of $a_\mu^{\rm HLO}/(4\alpha^2)$ compared with data
(MILC, $a = 0.06$ fm , $m_\pi = 220$ MeV)

⇒ need more data at low Q^2 with smaller errors! In progress…

Conclusions

- New method to parametrize hadronic vacuum polarization;
  avoid model dependence of vector meson dominance.
  Based on representation of vacuum polarization in terms of Stieltjes function.

- Tested on two examples of numerical data for vacuum polarization.
  Padé approximant fits can lead to larger statistical errors, but avoid unknown systematic error associated with VMD.

- Method looks promising, but data at lower momenta and smaller errors are indispensible (difference between $a_\mu(VMD)$ and $a_\mu([1,1])$ is about 17%).

- Note: long chiral extrapolation – also need data with small pion mass!

Backup slide 1: comparison with polynomial fits

	Poly 3		Poly 4		PA [1,1]		PA [1,2]	
# points	χ^2/dof	$a_\mu^{(1)}$	χ^2/dof	$a_\mu^{(1)}$	χ^2/dof	$a_\mu^{(1)}$	χ^2/dof	$a_\mu^{(1)}$
16	9.6/12	543	9.5/11	483	9.7/12	564	9.7/11	565
18	11.4/14	526	10.5/13	596	11.2/14	541	11.5/13	561
20	13.1/16	536	13.1/15	535	13.9/16	572	13.9/15	572
22	16.5/18	541	15.9/17	513	18.5/18	566	18.5/17	566
24	16.6/20	537	16.4/19	521	19.4/20	583	19.4/19	583
26	30.7/22	505	23.6/21	580	26.8/22	557	26.7/21	560

- Poly 3, PA [1,1] and PA [1,2] correlated fits all good, not so Poly 4.
- Stability from PA [1,1] to PA [1,2], not from Poly 3 to Poly 4.

Backup slide 2: chiral extrapolation

Assume VMD, and approximate $\Pi(Q^2)_{subtr} = g_\rho^2 Q^2/m_\rho^2$ (continuum)

$\Pi(Q^2)_{subtr} = g_V^2 Q^2/m_V^2$ (lattice)

Define $I_H = \alpha^2 \int_0^\infty \frac{dQ^2}{Q^2}\, w\left((Q^2/m_\mu^2)(H_{phys}^2/H_{latt}^2)\right) \Pi(Q^2)_{subtr}$

(Feng et al. 2011)

Then $I_H = \left(\frac{H_{latt}}{H_{phys}}\right)^2 \frac{g_V^2}{g_\rho^2}\frac{m_\rho^2}{m_V^2}\, I_{model}$ hence choose $H_{latt} = m_V/g_V$

Whatever choice: model dependent! 1st PA pole not equal to m_V^2
Cannot avoid small pion masses (much smaller than 300 MeV)

A novel phase in SU(3) gauge theory with many light fermions

Anna Hasenfratz
University of Colorado

New Horizons for Lattice Computations Workshop
BNL
May 16 2012

In collaboration with A. Cheng, D. Schaich and G. Petropoulos
ArXiv:1111:2317

The many faces of gauge-fermion systems

Renormalization group β function at 2 loops

$$\beta(g^2) = \frac{dg^2}{d\log(\mu^2)} = \frac{b_1}{16\pi^2}g^4 + \frac{b_2}{(16\pi^2)^2}g^6 + \dots$$

$$b_1 = -11 + \frac{2}{3}N_f\,,$$

$$b_2 = -102 + \frac{38}{3}N_f$$

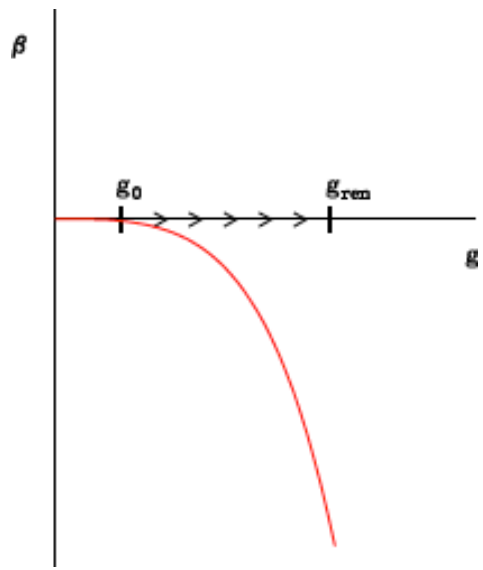

$N_f < 8.05$

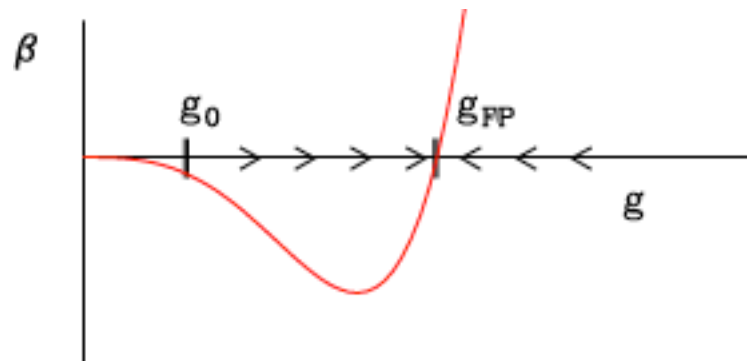

$8 < N_f < 16.5$

The many faces of gauge-fermion systems

Renormalization group β function at 2 loops

$$\beta(g^2) = \frac{dg^2}{d\log(\mu^2)} = \frac{b_1}{16\pi^2}g^4 + \frac{b_2}{(16\pi^2)^2}g^6 + \ldots$$

$$b_1 = -11 + \frac{2}{3}N_f\,,$$
$$b_2 = -102 + \frac{38}{3}N_f$$

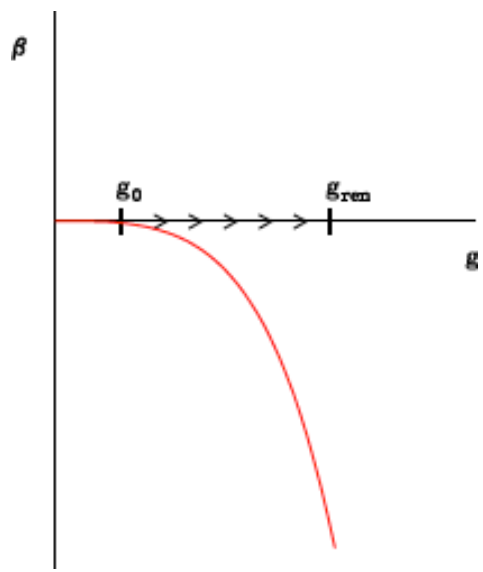

$N_f < 8.05$

Chirally broken & confining

- QCD with 2+1 (+1) flavors
- Original technicolor candidates

The many faces of gauge-fermion systems

Renormalization group β function at 2 loops

$$\beta(g^2) = \frac{dg^2}{d\log(\mu^2)} = \frac{b_1}{16\pi^2}g^4 + \frac{b_2}{(16\pi^2)^2}g^6 + \dots$$

$$b_1 = -11 + \frac{2}{3}N_f\,,$$
$$b_2 = -102 + \frac{38}{3}N_f$$

Conformal

- IRFP where g_0 is irrelevant
- universal anomalous dimension

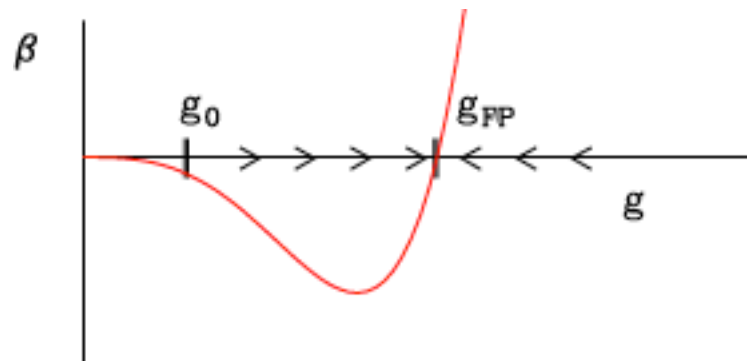

$8 < N_f < 16.5$

The many faces of gauge-fermion systems

Renormalization group β function at 2 loops

$$\beta(g^2) = \frac{dg^2}{d\log(\mu^2)} = \frac{b_1}{16\pi^2}g^4 + \frac{b_2}{(16\pi^2)^2}g^6 + \ldots$$

$$b_1 = -11 + \frac{2}{3}N_f\,,$$

$$b_2 = -102 + \frac{38}{3}N_f$$

What we really want is walking

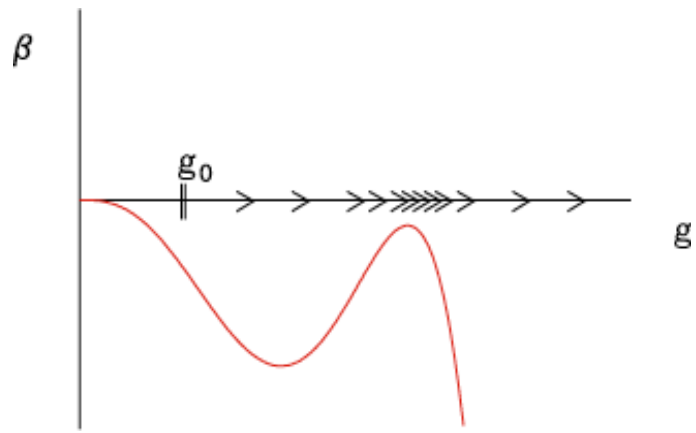

The gauge coupling changes slowly and the anomalous mass dimension remains large across an extended energy scale

Roadmap for the conformal window

S-D type calculations

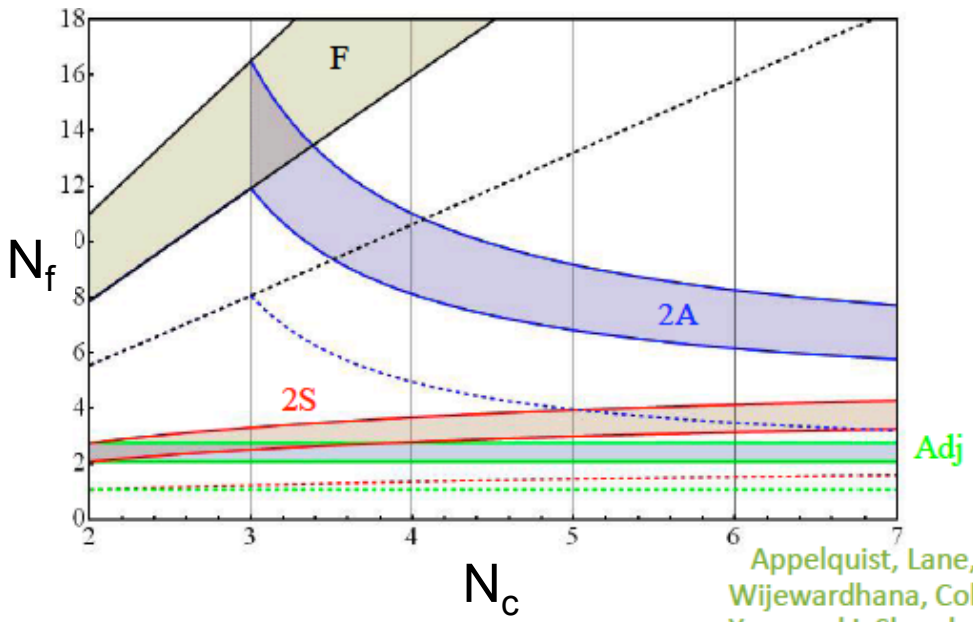

Appelquist, Lane, Mahanta, Wijewardhana, Cohen, Georgi, Yamawaki, Shrock, Dietrich, Sannino, Tuominen

- Which models are conformal?
- Which – if any - is walking?
- What is the anomalous mass ?
- S parameter?

Roadmap for the conformal window

S-D type calculations

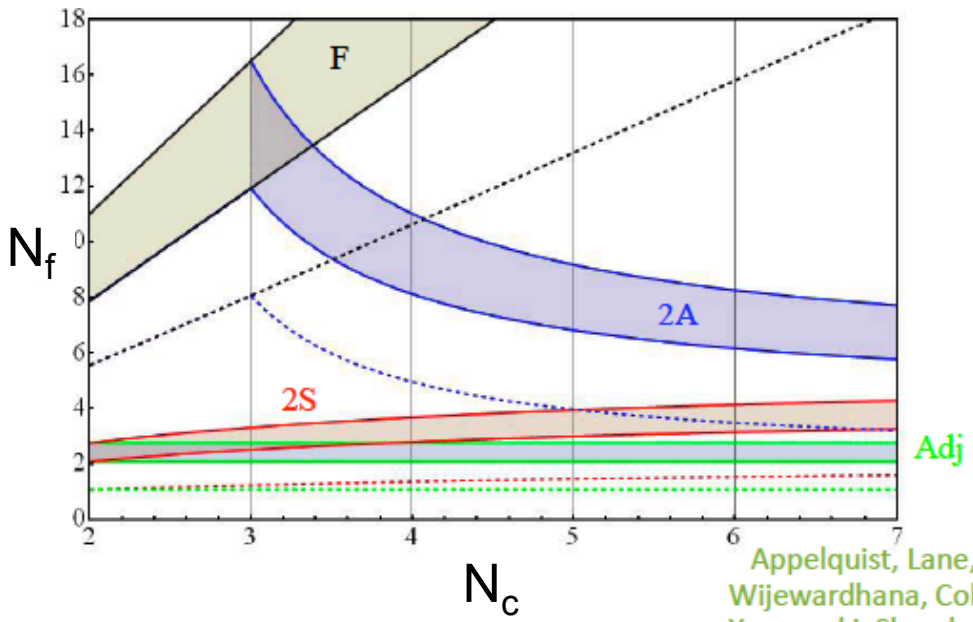

Appelquist, Lane, Mahanta, Wijewardhana, Cohen, Georgi, Yamawaki, Shrock, Dietrich, Sannino, Tuominen

- What is the best approach to study these systems?
- Do we understand the systematics?

Don't be unpatient : QCD has a 25 year head start

A phase with novel symmetry breaking pattern

Strongly coupled systems can lead to unexpected phenomena:

N_f=12 and 8 flavors SU(3) with staggered fermions

- 8 flavors: most likely chirally broken
- 12 flavors: still controversial

Goal: study the phase diagram both at zero and at finite temperature and contrast the two systems

(Lattice action: it's a good one)

Why Finite temperature ?

QCD like

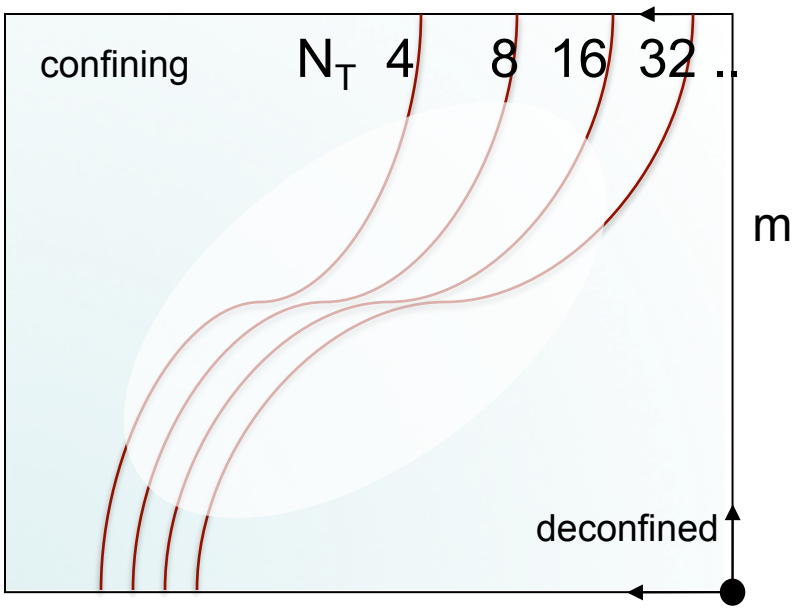

$\beta_c \rightarrow \infty$ as $N_T \rightarrow \infty$

Conformal

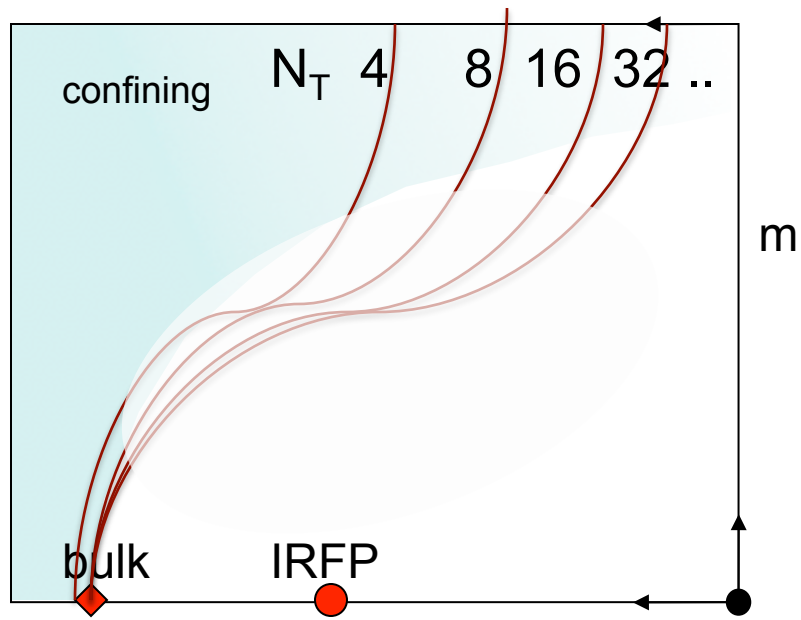

$\beta_c \rightarrow \beta_{bulk}$ as $N_T \rightarrow \infty$

The scaling of β_c is a good test of conformality (possibly)

The phase stucture of N_f=12

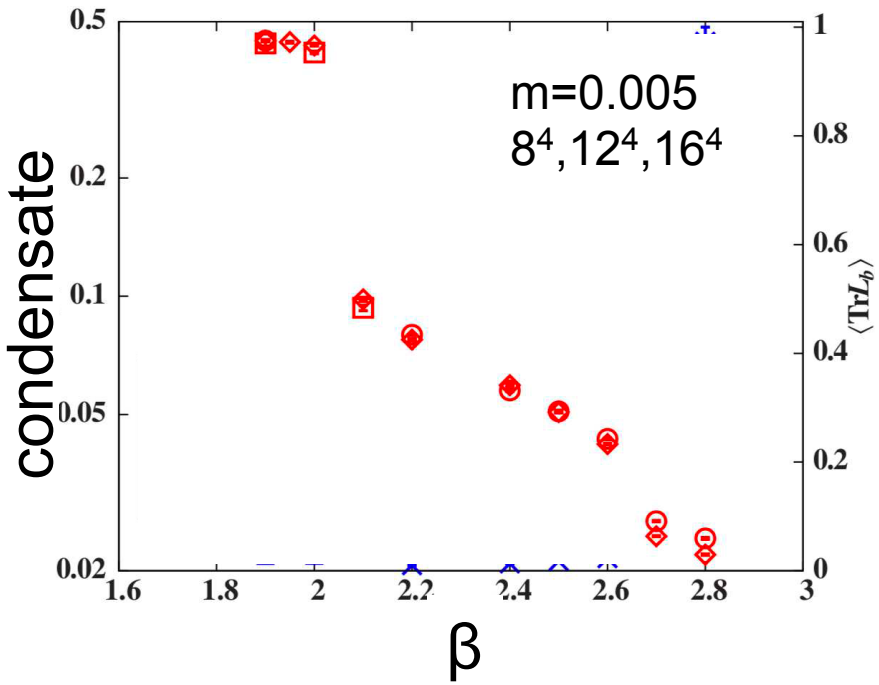

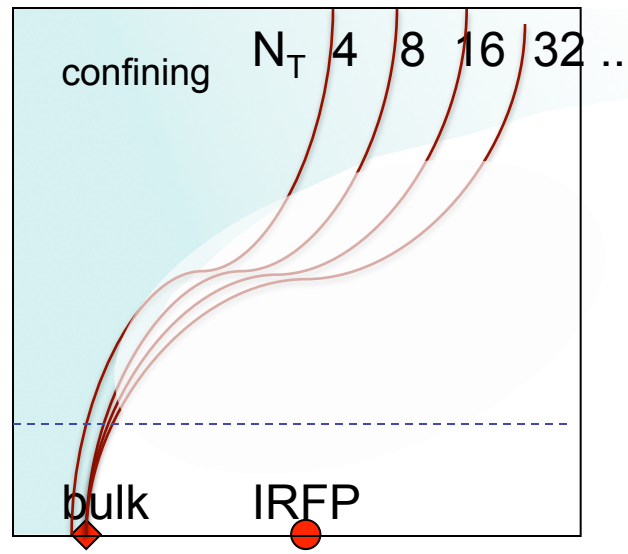

$\beta_c \rightarrow \beta_{bulk}$ as $N_T \rightarrow \infty$

The phase stucture of N_f=12

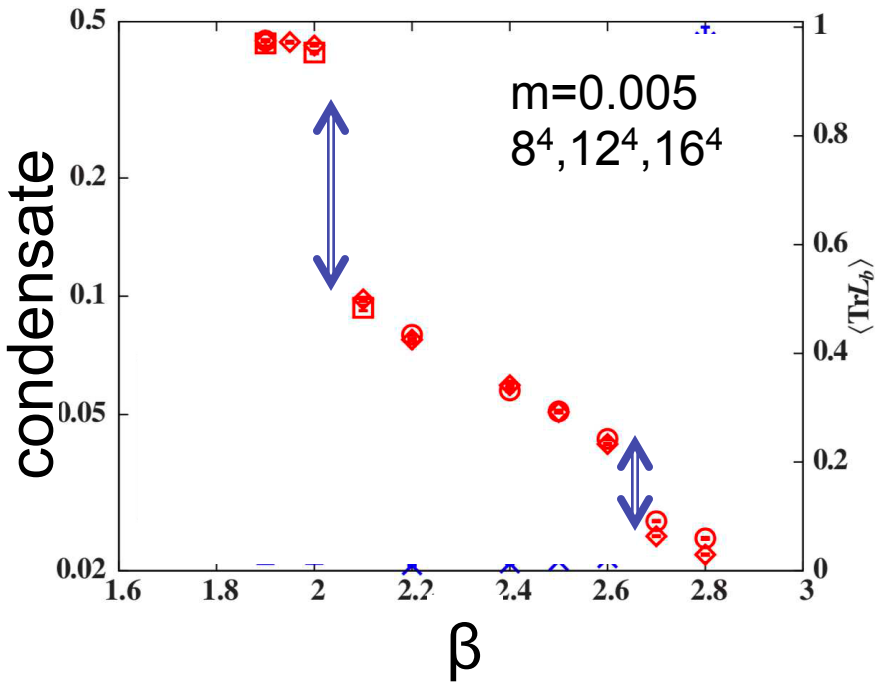

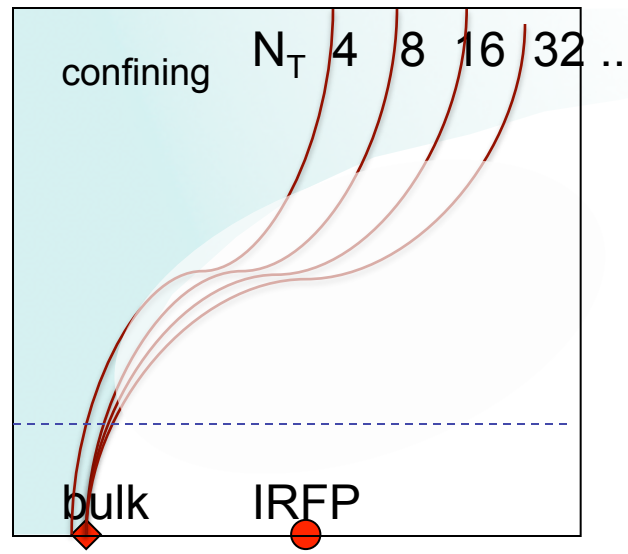

$\beta_c \rightarrow \beta_{bulk}$ as $N_T \rightarrow \infty$

Similar transitions were observed previously by INFN/Groeningen group and LHC collaboration

Phase diagram β-m plane N_f=12

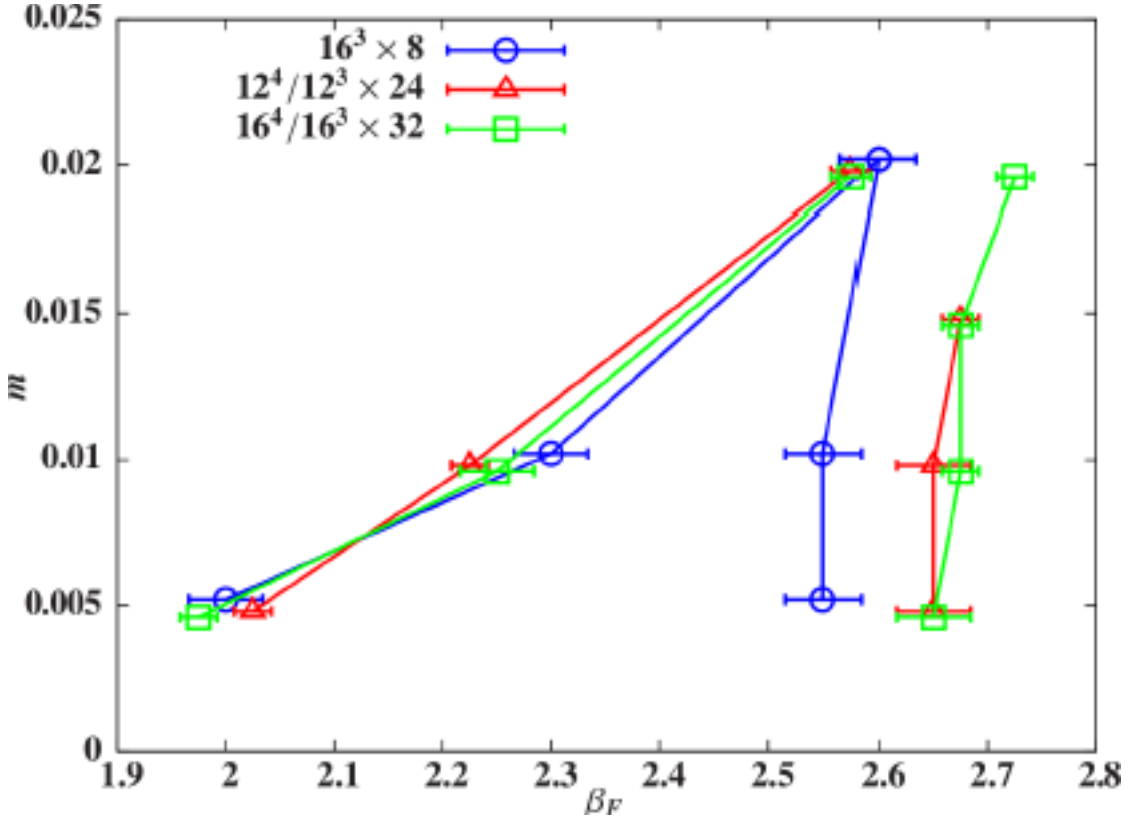

Intermediate phase bordered by bulk 1st order transitions

Phase diagram β-m plane N_f=12

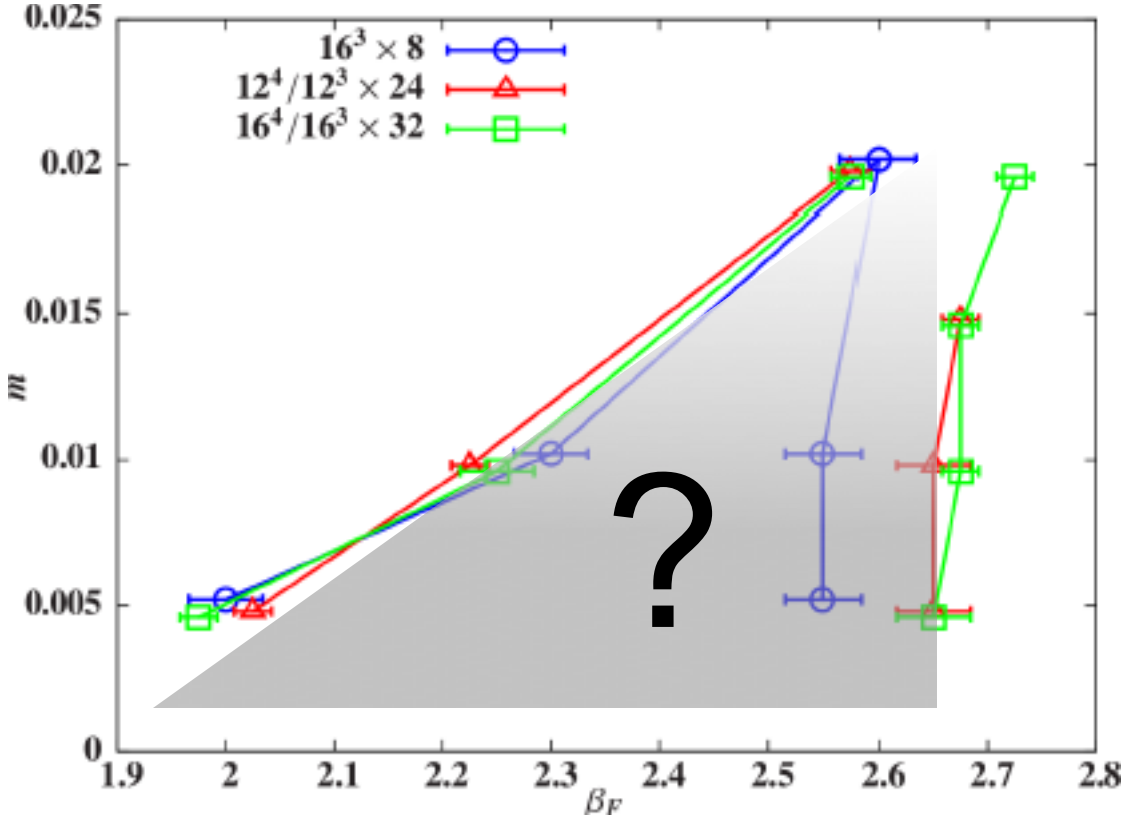

Intermediate phase bordered by bulk 1st order transitions

New symmetry breaking pattern in the IM phase

Single-site shift symmetry (S^4) of the staggered action

$$\chi(n) \to \xi_\mu(n)\chi(n+\mu), \qquad \xi_\mu(n) = (-1)^{\sum_{\nu>\mu} n_\nu}$$
$$U_\mu(n) \to U_\mu(n+\mu),$$

is broken → plaquette expectation value is “striped”

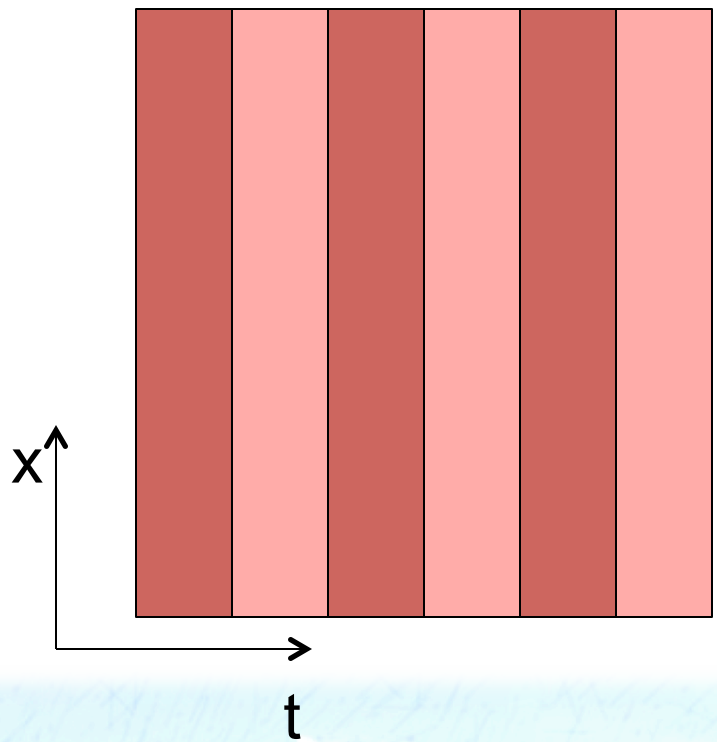

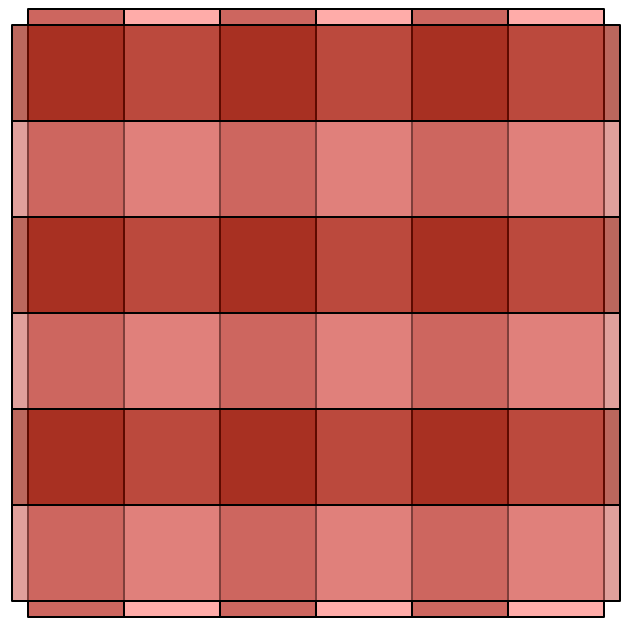

New symmetry breaking pattern

Order parameter I:

$$\Delta P_\mu = \langle \mathrm{Re}\,\mathrm{Tr}\,\Box_n - \mathrm{Re}\,\mathrm{Tr}\,\Box_{n+\mu} \rangle_{n_\mu \mathrm{even}}$$

Plaquette on even & odd time slices are different – this is on the background gauge configuration!

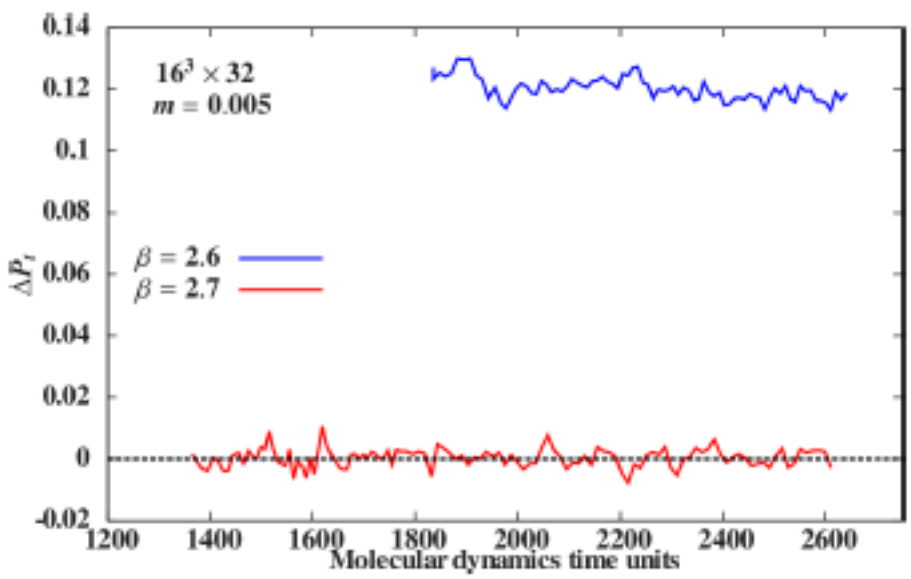

β = 2.6 IM phase

β=2.7 weak coupling phase

New symmetry breaking pattern

S^4 breaking occurs at the fermionic level:

Order parameter –II: link difference

$$\Delta L_\mu = \langle \alpha_\mu(n)\overline{\chi}(n)U_\mu(n)\chi(n+\mu) - \alpha_\mu(n+\mu)\overline{\chi}(n+\mu)U_\mu(n+\mu)\chi(n+2\mu)\rangle_{n_\mu \mathrm{ev}}$$

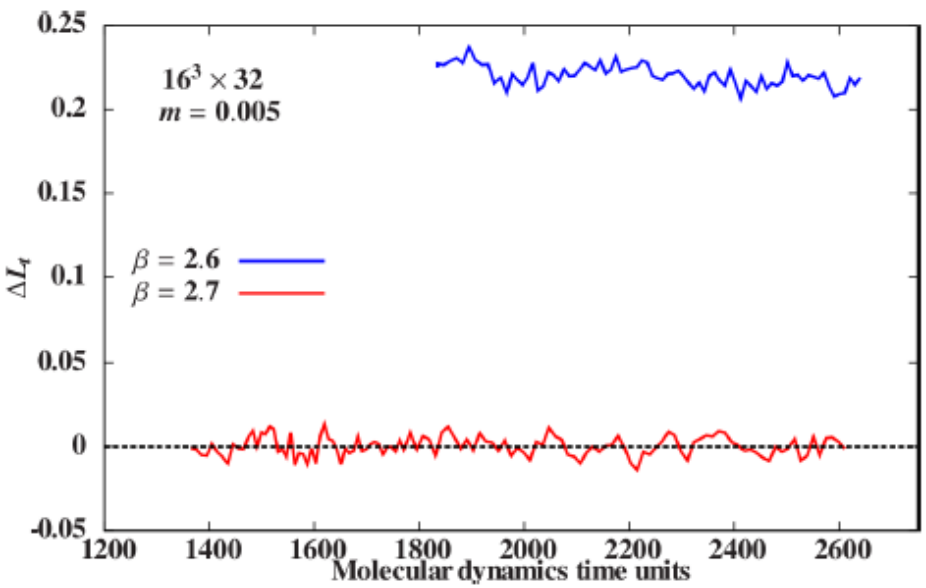

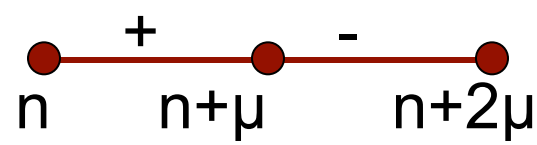

β=2.6 IM phase

β=2.7 weak phase

New symmetry breaking pattern

- Single-site shift symmetry is exact in the action.
- Both ΔP and ΔL are order parameters of S^4
- When S^4 is broken, the phase has to be separated by a “real” phase transition
- The S^4 broken ($\not{S}^4$) phase cannot go away with the volume
- S^4 is related to taste so this could be a special taste breaking

What are the physical properties of the S^4b phase?

The Polyakov line

Is it deconfining? Polyakov line is very noisy but the blocked Poly line is sensitive:

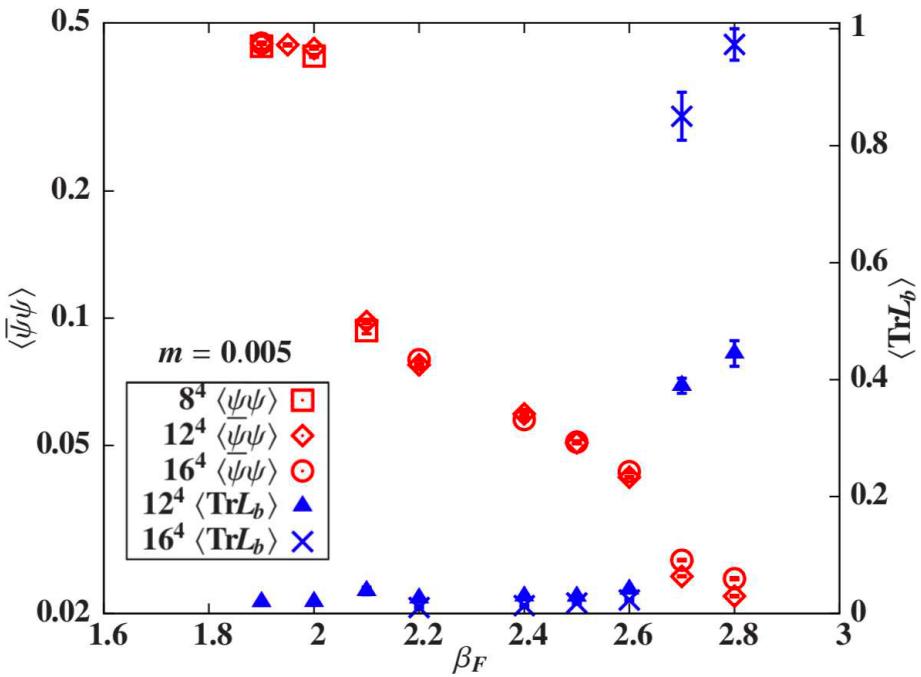

Blocked Poly line is measured on RG blocked lattices:

- improved Poly line

or

- Poly line on renormalized trajectory, after removing UV fluctuations

The static potential → Confinement!

Static potential on 12^3,16^3 volumes (no volume dependence!)
shows a linear term: r_0=2.1 – 2.7, $\sqrt{\sigma}$ =0.40 -- 0.48

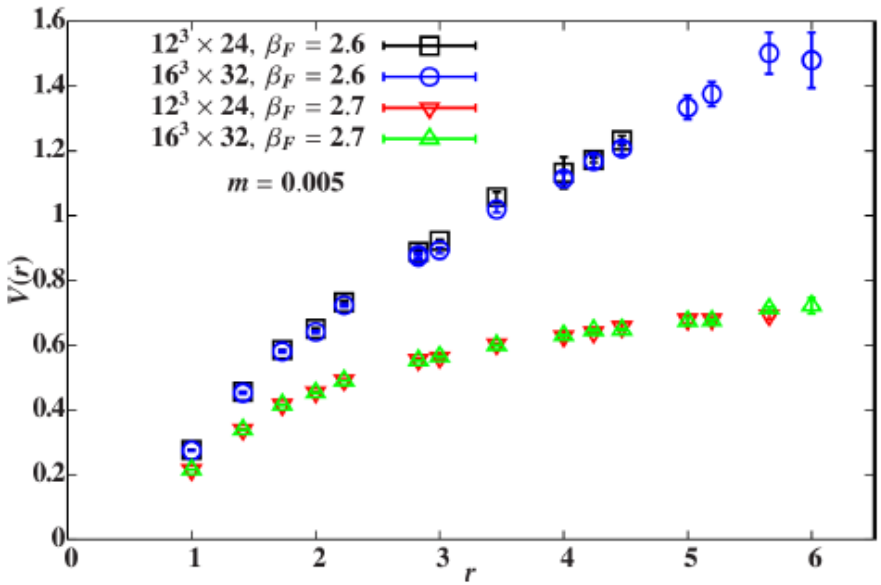

β=2.6 – IM phase

β=2.7 – weak coupling

No comment about the weak coupling side
from the potential – too small volume

Chiral properties : Dirac eigenvalue spectrum

4 different volumes, 12 eigenvalues each:

β=2.6 – IM phase

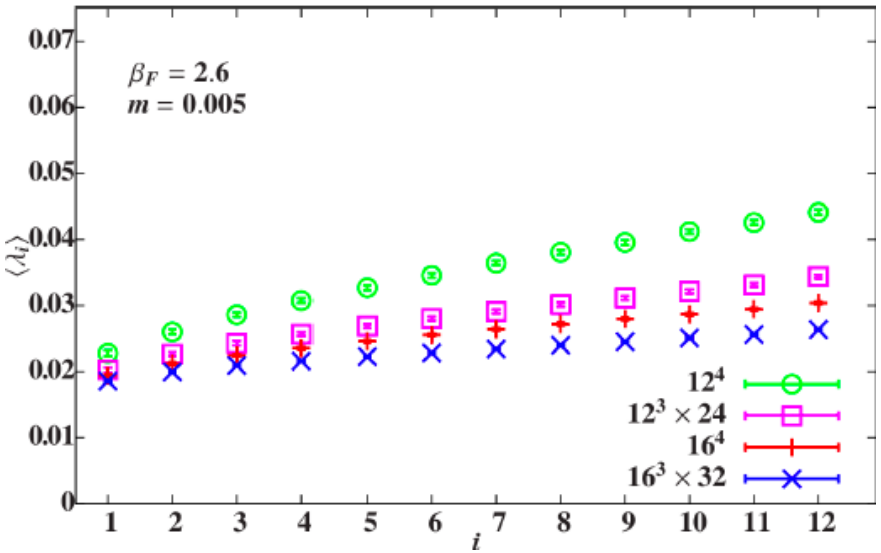

β=2.7 – weak coupling phase

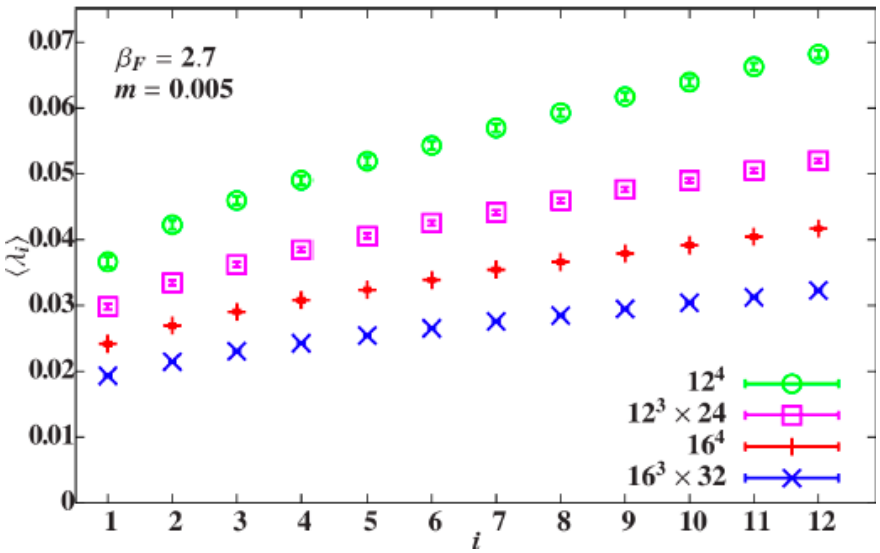

Qualitatively different – quantitative description?

Dirac eigenvalue spectrum

- RMT predictions require knowledge of the dynamics
- Simple volume scaling is more general. In the chiral limit

$$\rho(\lambda) \sim (\lambda - \lambda_0)^{\alpha}$$

λ_0 : soft edge

$$\int_m^n \rho(\lambda) d\lambda = \frac{n-m}{V} + \mathrm{O}(1/V^2)$$

$$\lambda_n - \lambda_0 \sim \left(\frac{n - x_0}{V} \right)^{1/(\alpha+1)}, \qquad \frac{D}{\alpha+1} = y_m$$

- Conformal IRFP : $y_m = 1 + \gamma^*$, : independent of V, β
- Confining system : $y_m = 1 + \gamma(L)$: in volumes smaller than the confinement scale

Dirac eigenvalue spectrum

Fit in S^4b phase (β=2.6):

Needs soft edge λ_0=0.0175 with α=0.6(1) (RMT prediction: α=1/2)

Very chiral symmetric! (Even $U(1)_A$ restoring)

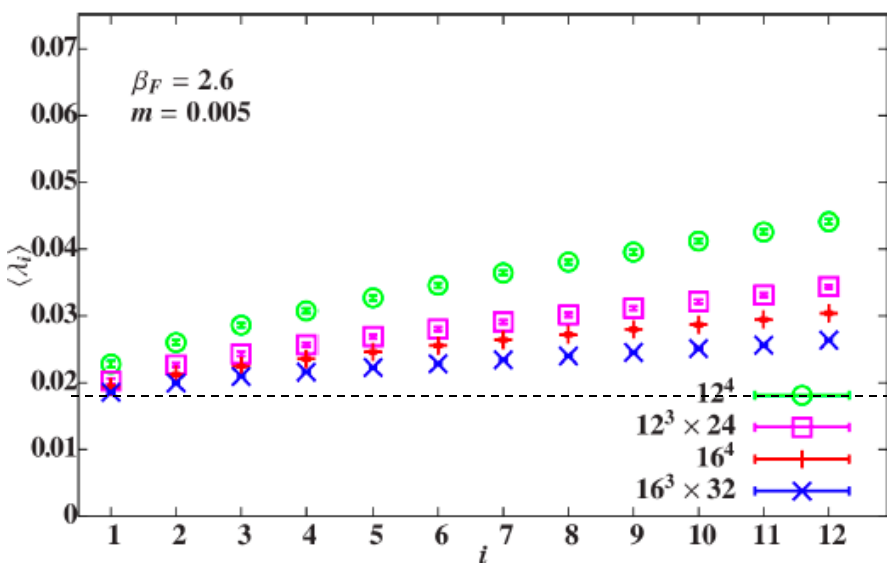

$\log(\lambda_n - \lambda_0)$ vs $\log(n/V)$

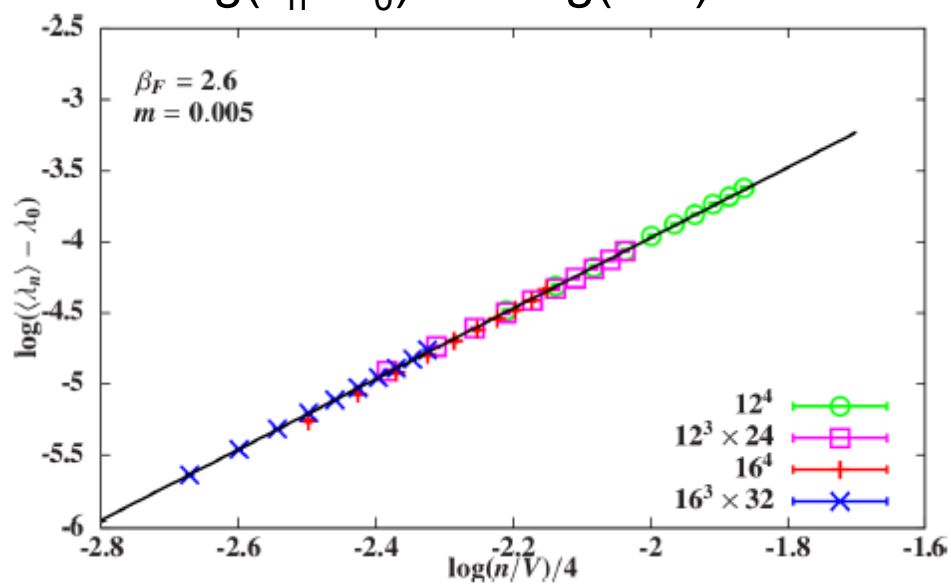

Scaling of Dirac eigenmodes, $N_f = 12$, weak coupling side

$$\lambda_n \sim \left(\frac{n - x_0}{V}\right)^{y_m/4}$$

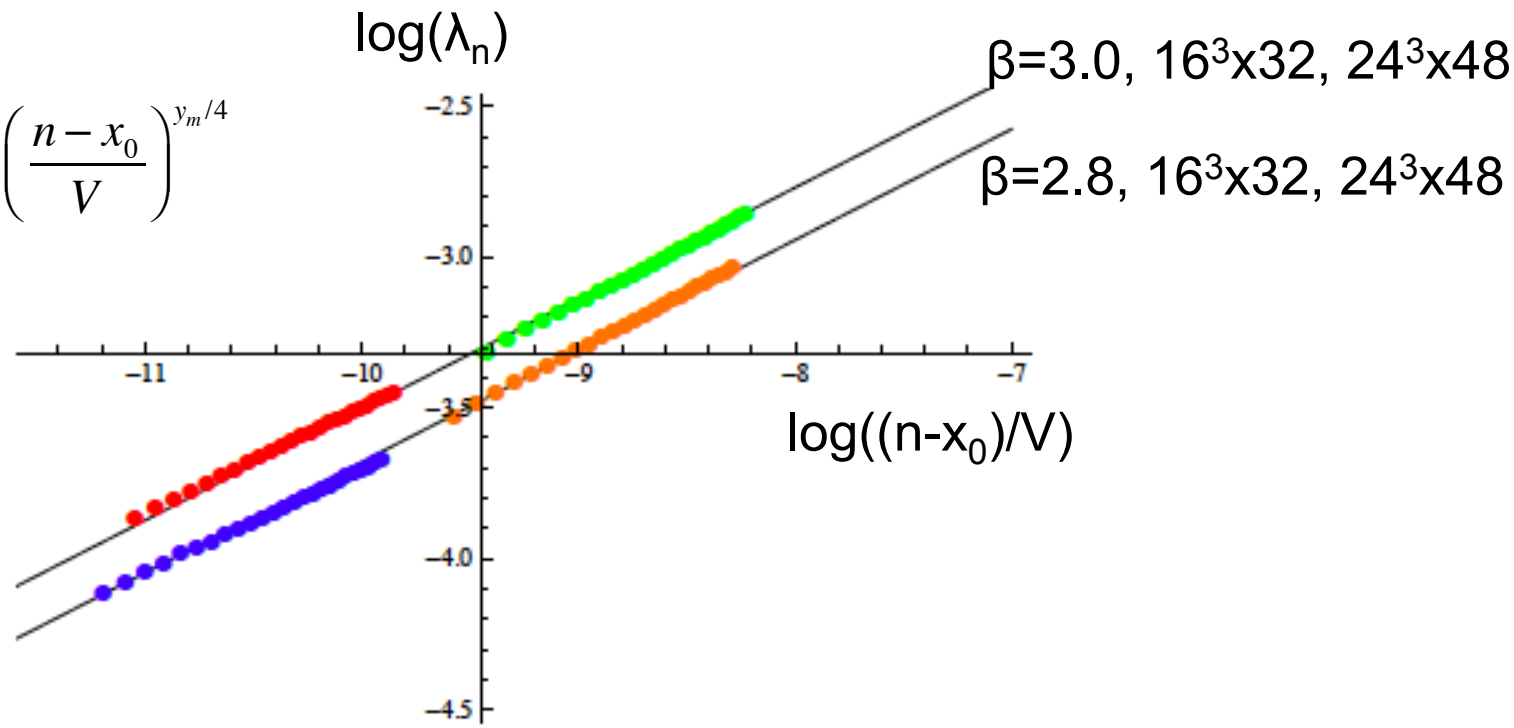

Two coupling values, four volumes with 30 eigenmodes each are consistent, predict γ_m=0.47(2)

Very efficient method to determine the anomalous dimension

(we need larger volumes, other β, more eigenmodes to reduce error)

The S^4b phase

Is most likely a lattice artifact

- Breaks single-site translational symmetry
- It is confining with small correlation length
- It is chirally symmetric
- (yes, it would violate the ‘t Hooft anomaly matching in the continuum)

What happens at finite temperature?

Phase structure at finite T, N_f=12

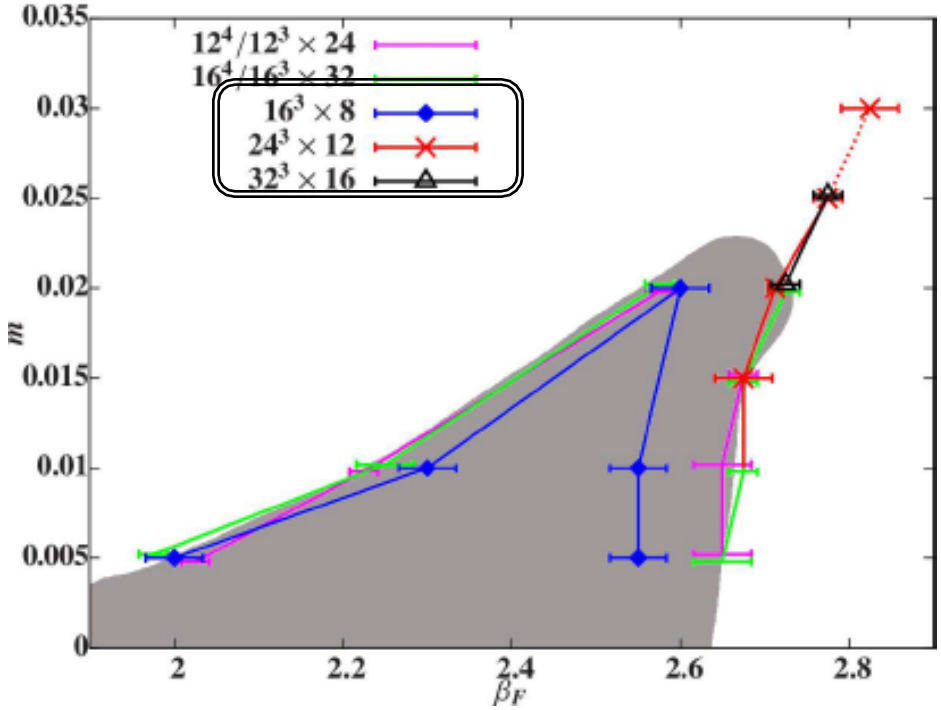

N_T=12, 16 transitions

- indistinguishable
- run into the S^4b phase

The weak coupling, m<0.03 region is either

- conformal or
- has N_T >16

Preliminary; more data in progress

Improved Polyakov line

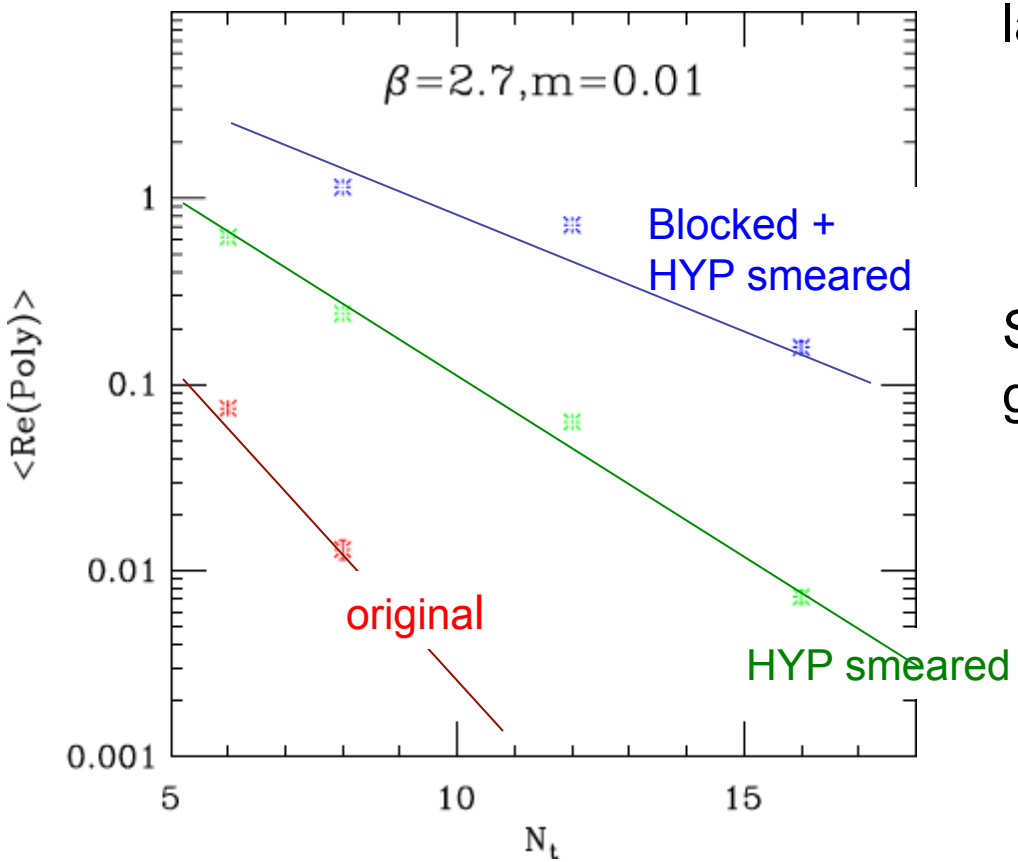

Poly line is difficult to measure at large N_t as it decays exponentially

$$\langle P \rangle \sim \exp(-f * N_t)$$

Smeared (HYP) or blocked Poly gives a better signal

S^4b phase in other systems

There are signs of the intermediate phase with other N_f=12 actions

Is it unique to N_f=12?

No.

Phase structure with N_f=8

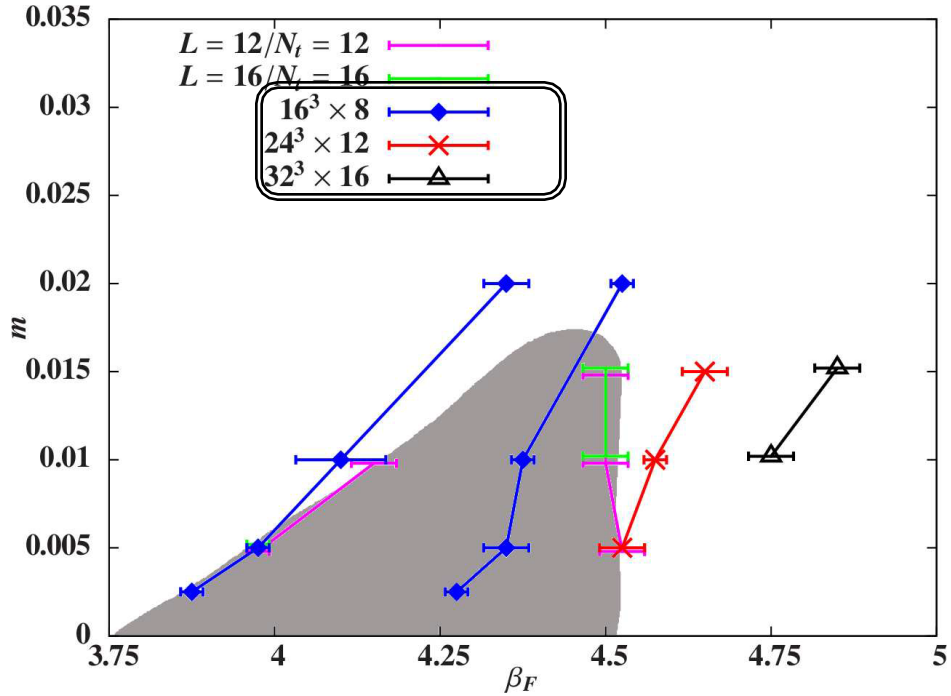

The S^4b phase, bordered by bulk transitions, is present
→ S^4b does not imply conformality

But N_T=12, 16 transitions behave differently: move toward $g^2 = 0$ as N_T increases

This is consistent with confinement

Preliminary; more data in progress

Summary & Outlook

These systems are complicated and have strange (strong coupling) lattice artifacts

Progress is steady but we need better understanding

The S^4b phase is present with 2 sets of staggered fermions. Could it show up in 2+1 flavor simulations?

Four flavour simulations with maximally twisted mass QCD

Karl Jansen

for the **European Twisted Mass Collaboration**

- **Twisted mass fermions**
- **Selected results for $N_f = 2 + 1 + 1$ flavours**
- **A glimpse at our next plans**

- Cyprus (Nicosia)
- France (Orsay, Grenoble)
- Italy (Rome I,II,III, Trento)
- Netherlands (Groningen)
- Poland (Poznan)
- Spain (Huelva, Madrid, Valencia)
- Switzerland (Bern)
- United Kingdom (Glasgow, Liverpool)
- Germany (Berlin/Zeuthen, Bonn, Frankfurt, Hamburg)

Collaboration performed very successful $N_f = 2$ research programme

Simulation results versus PDG

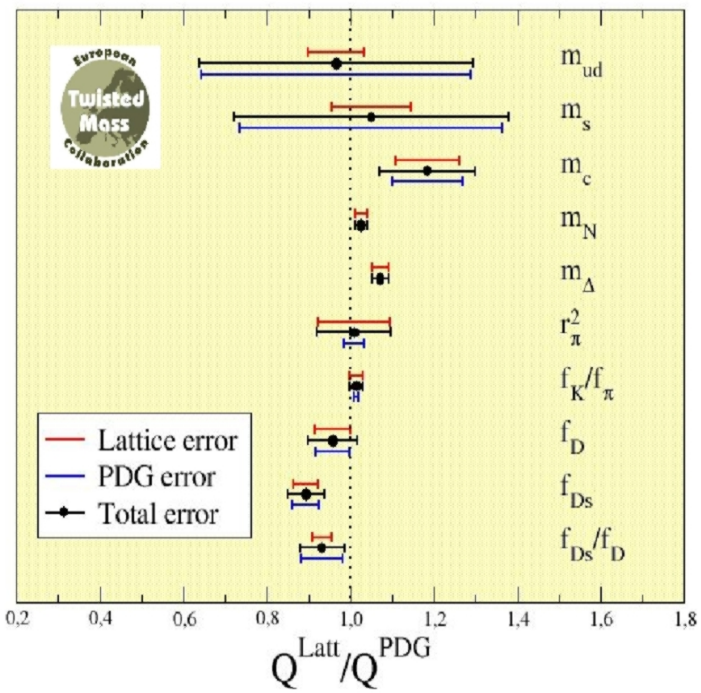

Low energy constants

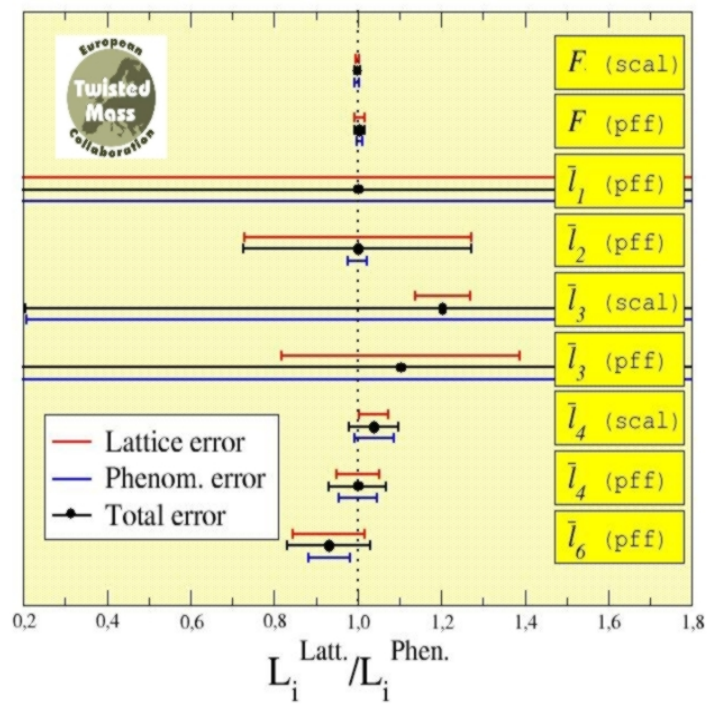

The ρ-meson resonance: dynamical quarks at work

(X. Feng, D. Renner, K.J.)

- usage of three Lorentz frames

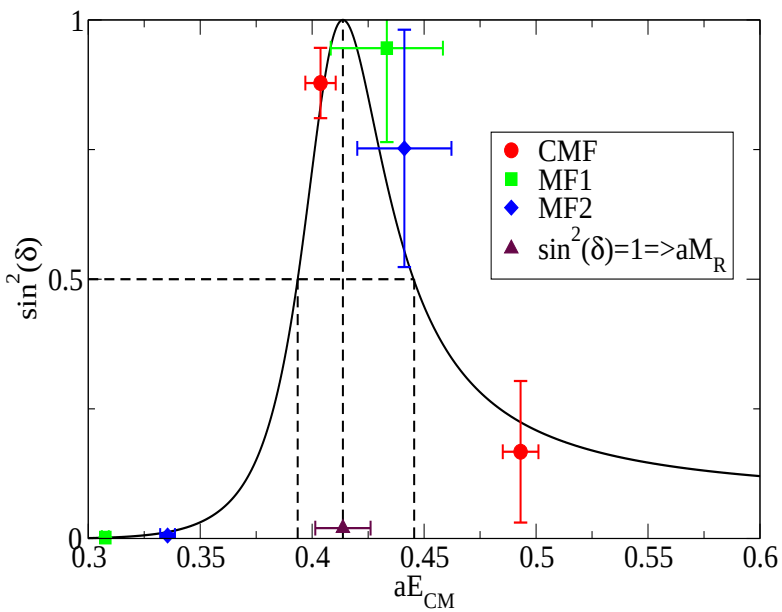

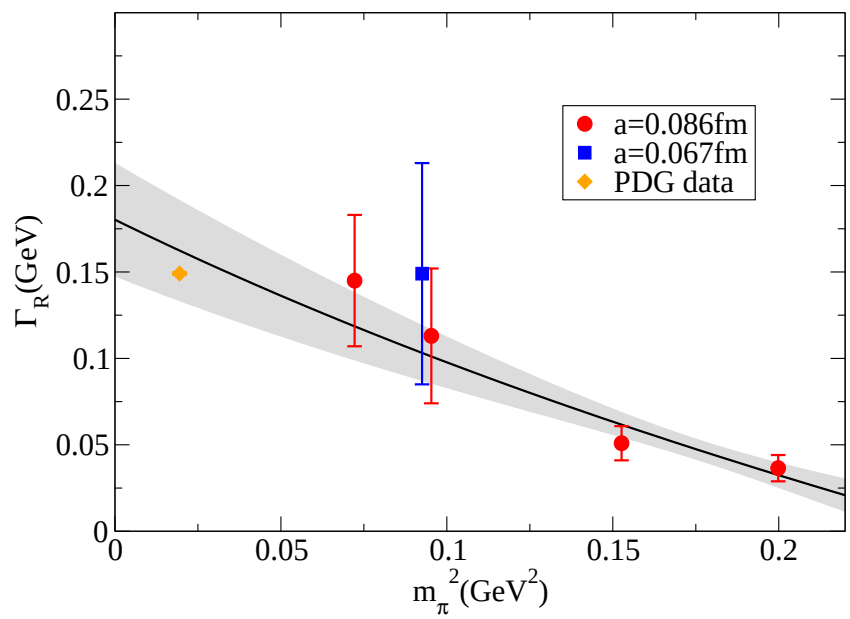

$m_{\pi^+} = 330$ MeV, $a = 0.079$ fm, $L/a = 32$

fitting $z = (M_\rho + i\frac{1}{2}\Gamma_\rho)^2$

$m_\rho = 1033(31)$ MeV, $\Gamma_\rho = 123(43)$ MeV

Natural^2 next step: move to four flavours

- twisted mass: works with quark doublets
  - maximal twist: automatic $O(a)-$improvement
  - infrared cut-off due to twisted quark mass
  - simplification in renormalization $(f_\pi,\ \langle N|\bar{q}q|N\rangle)$

$\star\ \star\ \star$ need to control isospin splitting effects

- strange and charm quarks needed for physical quantities
  - mesons: $m_{\rm strange}$, $m_{\rm charm}$, f_D, f_{D_s}, η', η_c
  - baryons: spectrum, $\langle N|\bar{q}q|N\rangle$
  - $g_\mu - 2 \leftarrow$ can unambiguously compare to experimental value
  - running of $\alpha_{\rm strong}(\mu)$ with four flavours

Wilson (Frezzotti, Rossi) twisted mass QCD (Frezzotti, Grassi, Sint, Weisz)

Fermion action of twisted mass fermions

$$S_l = \sum_x \bar{\chi}^l_x \left[m_q + \tfrac{1}{2}\gamma_\mu \left[\nabla_\mu + \nabla^*_\mu \right] - ar\tfrac{1}{2}\nabla^*_\mu \nabla_\mu + i\mu_{\rm tm}\tau_3\gamma_5 \right] \chi^l_x$$

$$S_h = \sum_x \bar{\chi}^h_x \left[m_q + \tfrac{1}{2}\gamma_\mu \left[\nabla_\mu + \nabla^*_\mu \right] - ar\tfrac{1}{2}\nabla^*_\mu \nabla_\mu i\gamma_5\tau_1\mu_\sigma + \tau_3\mu_\delta \right] \chi^h_x$$

- quark mass parameter m_q , twisted mass parameter $\mu_{\rm tm}$
- strange and charm quark masses

$$m_s = Z_P^{-1}\mu_\sigma - Z_S^{-1}\mu_\delta$$

$$m_c = Z_P^{-1}\mu_\sigma + Z_S^{-1}\mu_\delta$$

- note, m_q the same in S_l and S_h

A word on flavour breaking

- isospin (flavour symmetry) violation at any $a \neq 0$: $m_\pi^\pm - m_\pi^0 \neq 0$
- observe large $O(a^2)$ effect in neutral pion mass
- effect visible both for $N_f = 2$ and $N_f = 2+1+1$
- theoretical understanding (Dimopoulos et.al., Phys. Rev. **D81**, 034509 (2010))
- χPT analysis of meson sector including pion mass splitting a^2 effect (O. Bär, Phys.Rev. D82 (2010) 094505)

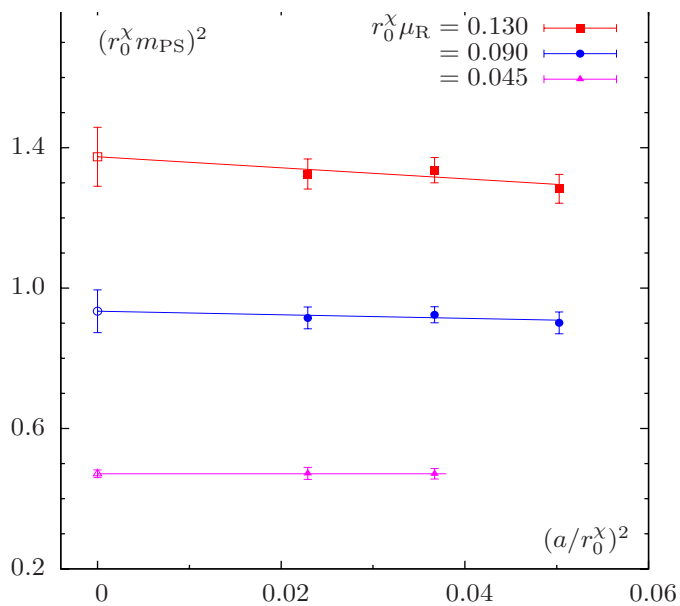

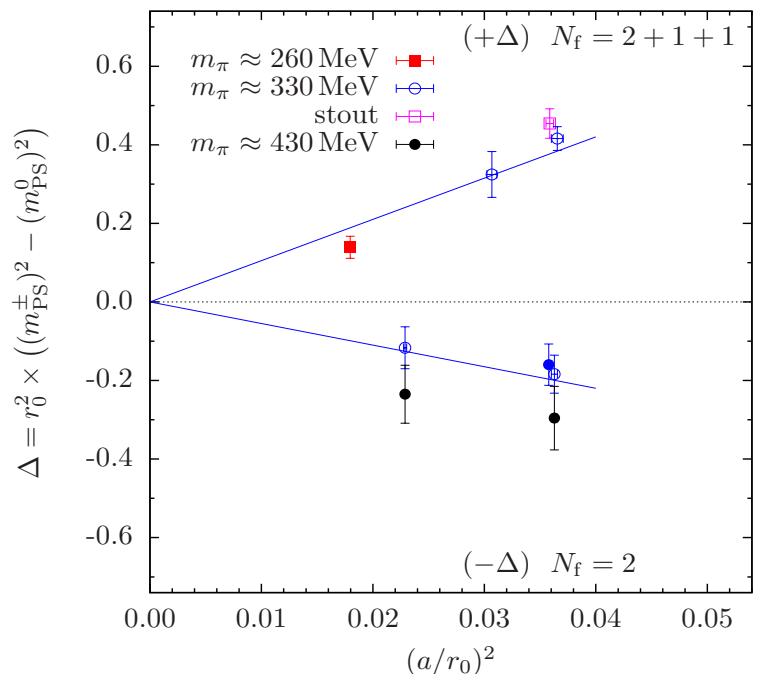

Tuning to maximal twist

Maximal twist: tune m_q such that

$$m_{\rm PCAC} = \frac{\sum_{\rm x}\langle \partial_0 A_0^a(x) P^a(0)\rangle}{2\sum_{\rm x}\langle P^a(x) P^a(0)\rangle} = 0$$

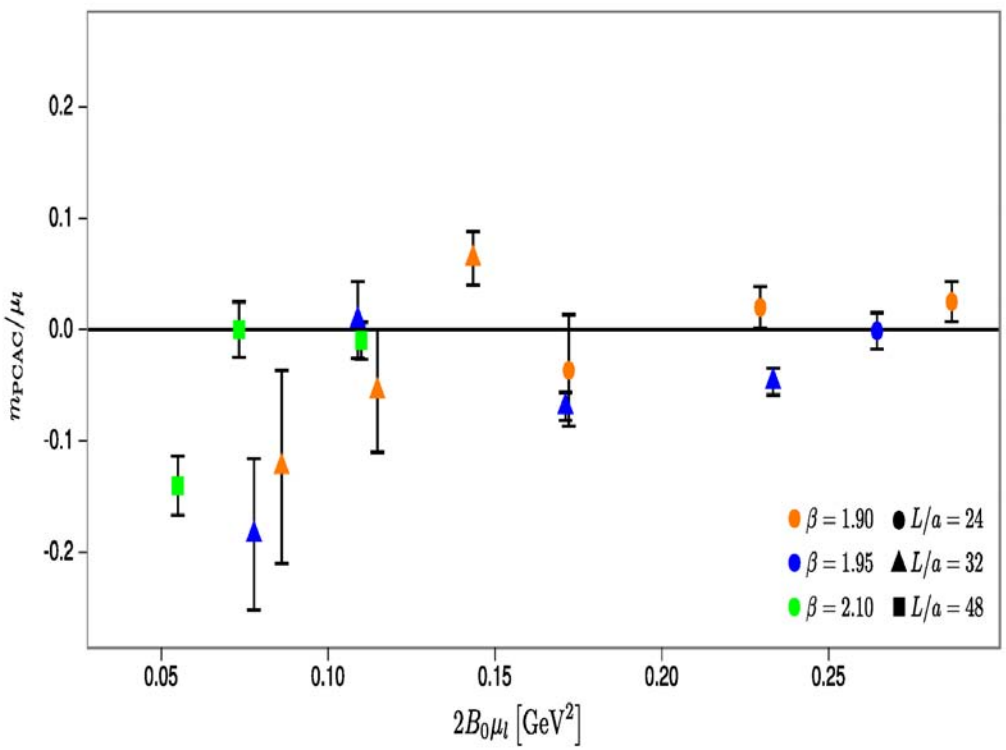

- tuning of m_q at *each* $\mu_{\rm tm}$ used
- demand $m_{\rm PCAC} \lesssim 0.1\mu_{\rm tm}$
- demand $\Delta(m_{\rm PCAC}) \lesssim 0.1\mu_{\rm tm}$

Autocorrelations from gradient flow

(Deuzemann, Wenger) see also talk by Z. Fodor

- flow of the gauge field $U(x,\mu)$ according to the flow equation

$$\frac{\partial}{\partial t} V_t(x,\mu) = -g_0^2 \{\partial_{x,\mu} S_{\rm latt} W(V_t)\}\, V_t(x,\mu)$$

$$V_{t=0}(x,\mu) = U(x,\mu)$$

- lattice: discrete integration scheme with *finite step size* ϵ for integration

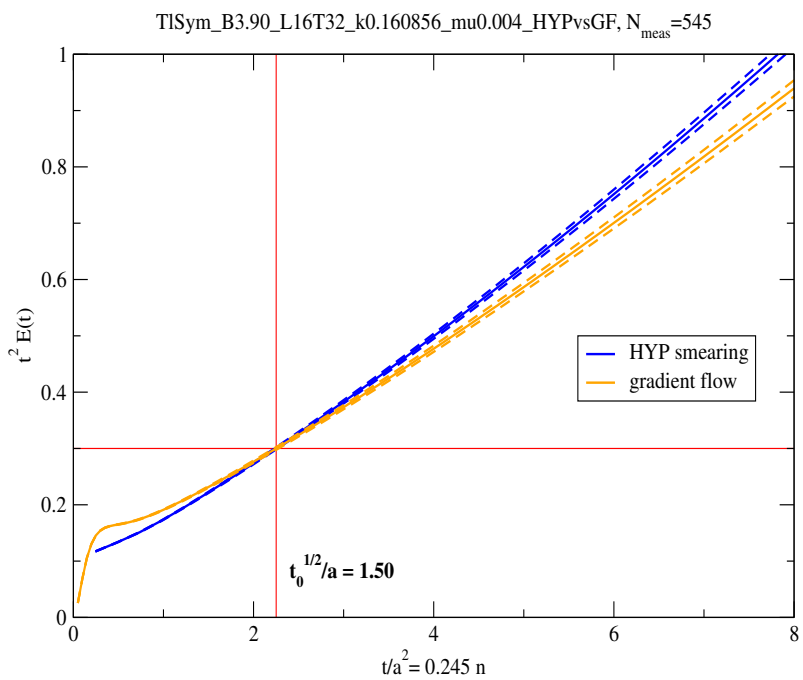

$a \approx 0.08$fm $m_\pi \approx 300$MeV

energy density:

$$E(t) = 2 \sum_{\rm plaq} {\rm Retr}[1 - V_t({\rm plaq})]$$

Topology and autocorrelations

- topological charge well defined on smooth configurations V_t
- use standard field theoretic definition $F_{\mu\nu}\tilde{F}_{\mu\nu}(V_t)$

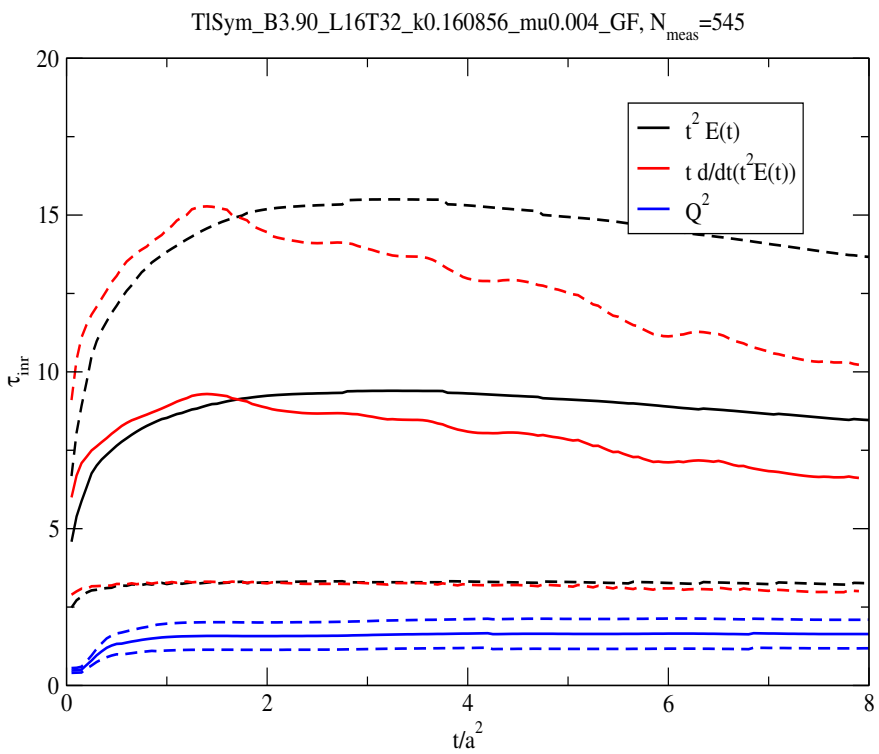

gradient flow gives largest autocorrelation

autocorrelation from topological susceptibility significantly smaller

★ ★ ★ warning

$N_f = 2+1+1$ light quark sector: scaling

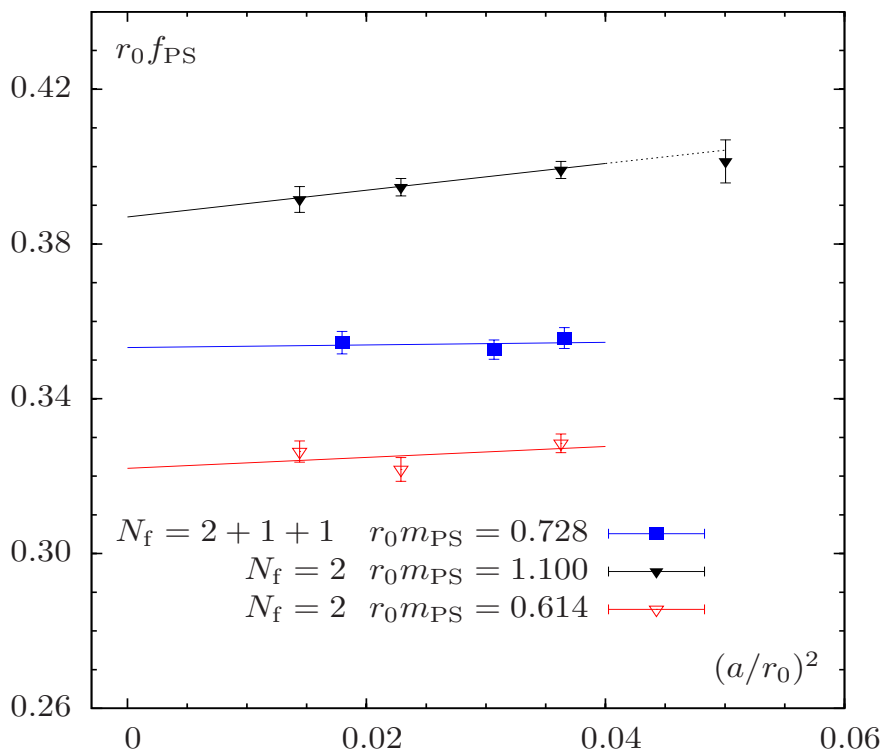

pseudoscalar decay constant $f_{\rm PS}$

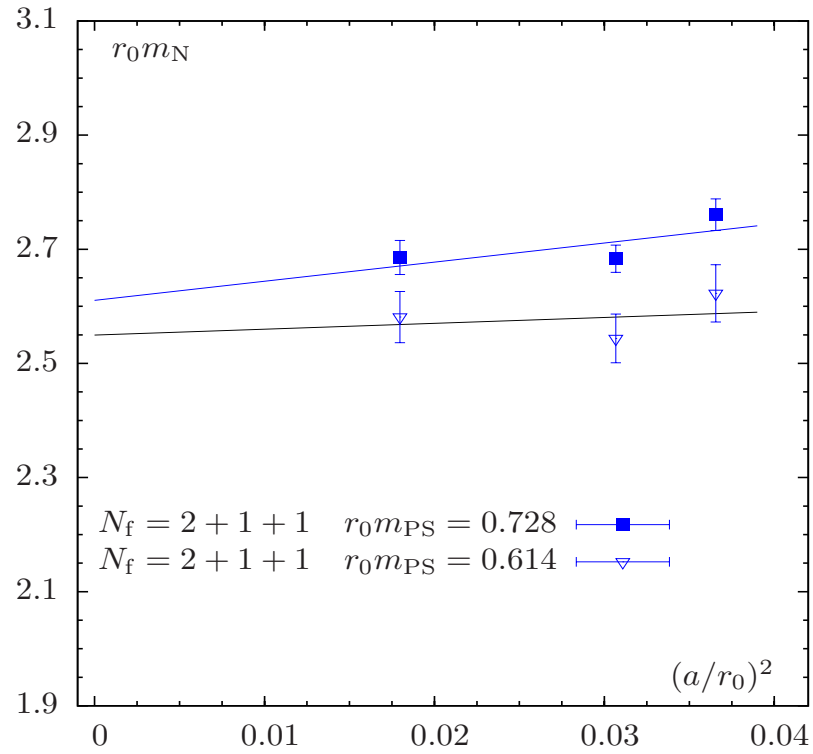

nucleon mass

$N_f = 2+1+1$ light quark sector: χPT fit

- basic formulae: $N_f = 2$ continuum χPT at NLO

$$
\begin{aligned}
m_{\rm PS}^2 &= \chi_\mu \left[1 + \xi \log(\chi_\mu/\Lambda_3^2)\right] \quad K_m^2(L) \\
f_{\rm PS} &= f_0 \quad \left[1 - 2\xi \log(\chi_\mu/\Lambda_4^2)\right] \; K_f(L)
\end{aligned}
$$

$\chi_\mu = 2\hat{B}_0 Z_\mu \mu_q \,, \quad \xi = \chi_\mu/(2\pi f_0)^2$

- finite size corrections $K_m(L), K_f(L)$
  (Gasser, Leutwyler, 1987, 1988; Colangelo, Dürr, Haefeli, 2005)
  in preparation: analysis a la Colangelo, Wenger, Wu; Bär; Ueda, Aoki

- fit simultaneously to our data at all β-values

- fit includes renormalisation constant $Z_\mu = 1/Z_P$

$N_f = 2+1+1$ light quark sector: χPT fit

- estimate systematic effects : lattice artifacts, FSE

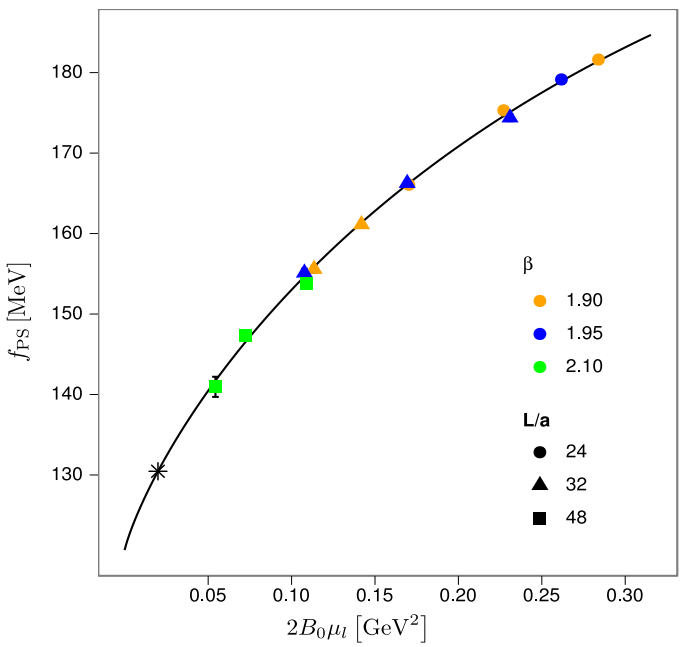

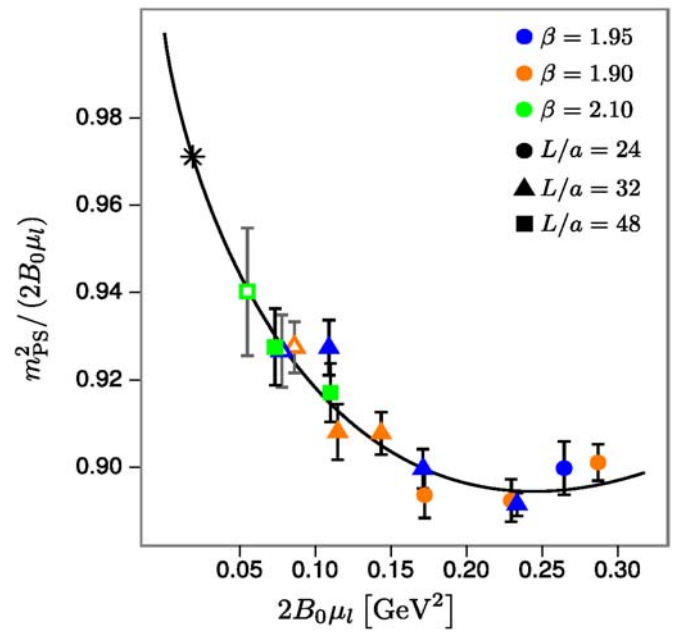

Comparison of low energy constants

	$N_f = 2$	$N_f = 2+1+1$
$\bar{\ell}_3$	3.70(27)	3.50(31)
$\bar{\ell}_4$	4.67(10)	4.66(33)
f_π/f_0	1.076(3)	1.076(9)
B_0 [MeV]	2437(120)	2638(200)
$\langle r^2 \rangle_s^{\mathrm{NLO}}$ [fm^2]	0.710(28)	0.715(77)

$N_f = 2+1+1$ adding strange quark: fit formulae

- $SU(2)$ χPT Fit Formulae for f_K and f_π:

$$f_{\rm PS}(\mu_\ell,\mu_\ell,\mu_\ell) = f_0 \cdot (1 - 2\,\xi_{\ell\ell}\ln\xi_{\ell\ell} + b\,\xi_{\ell\ell})$$

$$f_{\rm PS}(\mu_\ell,\mu_\ell,\mu_s) = (f_0^{(K)} + f_m^{(K)}\,\xi_{ss}) \cdot \left[1 - \tfrac{3}{4}\xi_{\ell\ell}\ln\xi_{\ell\ell} + (b_0^{(K)} + b_m^{(K)}\,\xi_{ss})\,\xi_{\ell\ell}\right]$$

$$\xi_{XY} = \frac{m_{\rm PS}^2(\mu_\ell,\mu_X,\mu_Y)}{(4\pi f_0)^2}$$

(Gasser, Leutwyler (1984); Allton et al (2008); ETMC, Blossier et al. (2010))

- correct for finite size effects using NLO χPT
(Gasser, Leutwyler (1987); Becirevic, Villadoro (2004))

$N_f = 2+1+1$ light quark sector: fit results

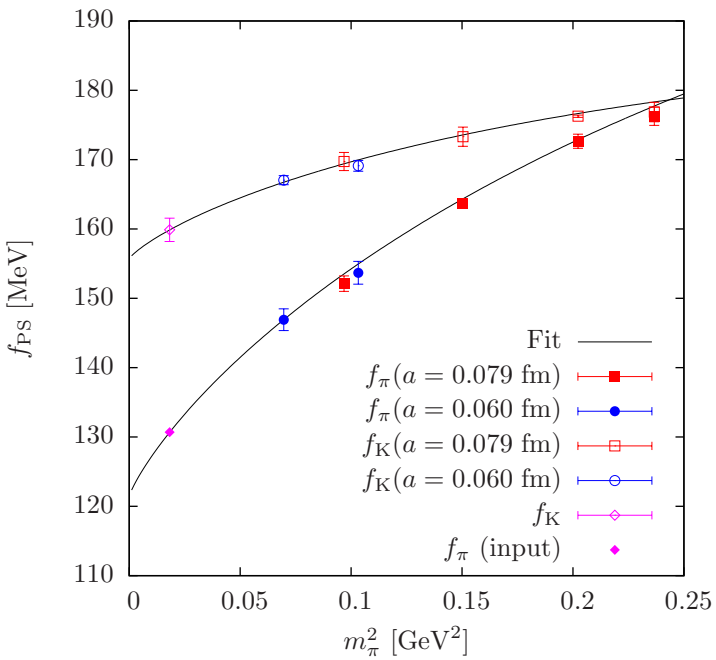

- fit $\beta = 1.95$ $(a = 0.079\text{fm})$ and $\beta = 2.10$ $(a = 0.06\text{fm})$ simultaneously
- from setting $m_{\rm PS}^2(\mu_\ell, \mu_s, \mu_s) = 2m_K^2 - m_\pi^2$
- $m_\pi = 135$ MeV, $f_\pi = 130.7$ MeV, $m_K = 497.7$ MeV

preliminary fit results:

- $f_K/f_\pi = 1.224(13)$, $f_K = 160(2)$ MeV, $\bar{\ell}_4 = 4.78(2)$, $|V_{\rm us}| = 0.220(2)$
- errors statistical only

$N_f = 2+1+1$ heavy quark sector

Wilson twisted mass Dirac operator for (c, s) pair:

$$D_h = \begin{pmatrix} \gamma_\mu \tilde{\nabla}_\mu + \mu_\sigma + \mu_\delta & i\gamma_5 \left(\frac{a}{2}\nabla^*_\mu \nabla_\mu - m_q\right) \\ i\gamma_5 \left(\frac{a}{2}\nabla^*_\mu \nabla_\mu - m_q\right) & \gamma_\mu \tilde{\nabla}_\mu + \mu_\sigma - \mu_\delta \end{pmatrix}$$

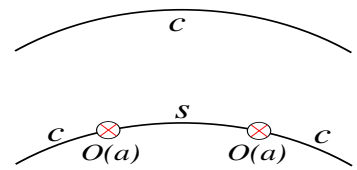

- mixing of c and s flavour and of parity
- Kaon is the ground state : good precision
- D meson appears as an excited state
- three independent methods:
  - generalised eigenvalue problem
  - multi-exponential fits
  - imposing parity and flavour restoration at finite a
- they provide consistent results for m_D
- overcome mixing of flavour $\rightsquigarrow$ mixed action

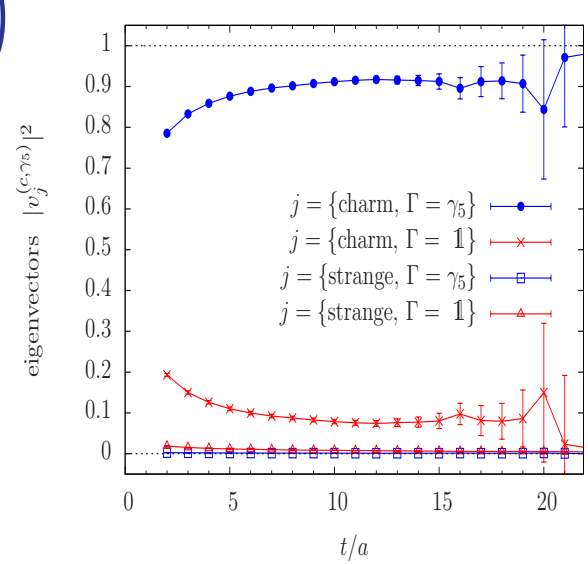

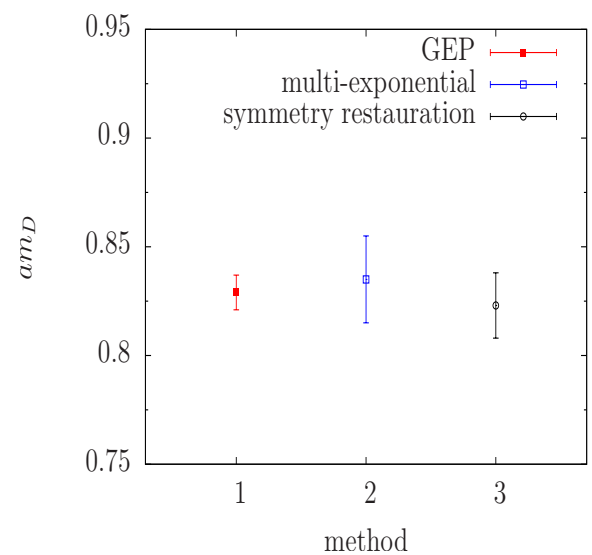

$N_f = 2 + 1 + 1$ approaching the charm quark

- introduce Wilson twisted mass doublets in the valence sector

$$D_{tm}(\mu_{val}) = D + m_{\rm crit} + i\ \mu_{val}\gamma_5\tau^3$$

(Osterwalder, Seiler (1990), Pena et al. (2004); Frezzotti, Rossi (2004))

- $m_{\rm crit}$ from unitary set-up
- $4 - 6$ values for μ_{val} in the strange μ_s and the charm μ_c region inversions with multi-mass solver
- matching to unitary set-up using m_K and m_D
- $\Rightarrow$ avoid flavour breaking

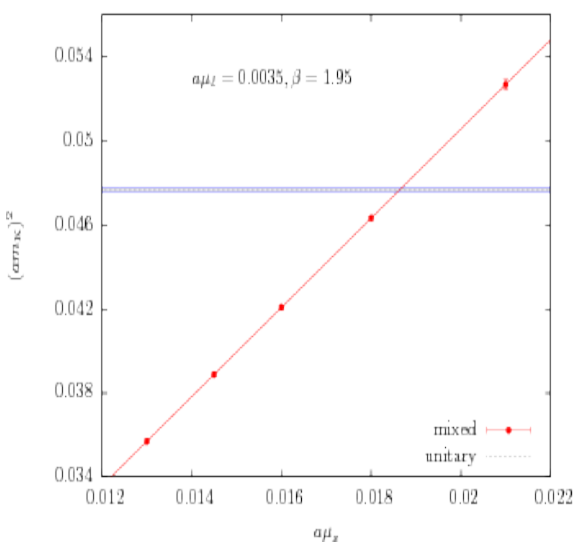

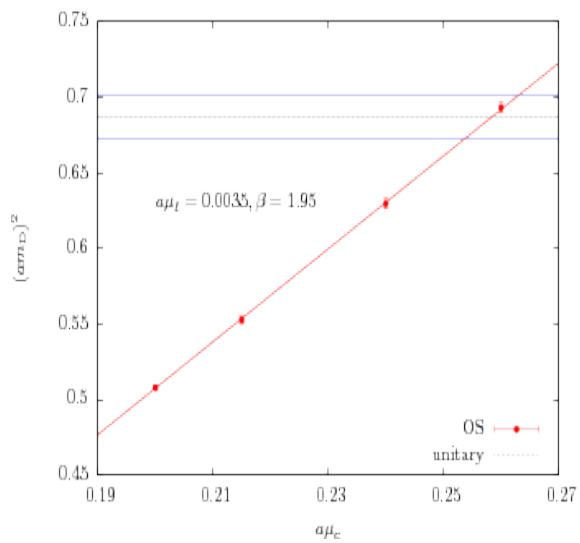

Unitary versus Osterwalder-Seiler: f_K

- the unitary f_K can be computed from: $f_K = (m_\ell + m_s)\frac{\langle 0|P_K|K\rangle}{m_K^2}$
  with $m_s = \mu_\sigma - (Z_{\rm P}/Z_{\rm S})\mu_\delta$
- similar formula for f_D
- P_K is the physical Kaon projecting operator
- the mixed action f_K computed from: $f_{\rm PS} = \left(\mu_{val}^{(1)} + \mu_{val}^{(2)}\right) \frac{|\langle 0|P|PS\rangle|}{m_{\rm PS}\,\sinh m_{\rm PS}}$,

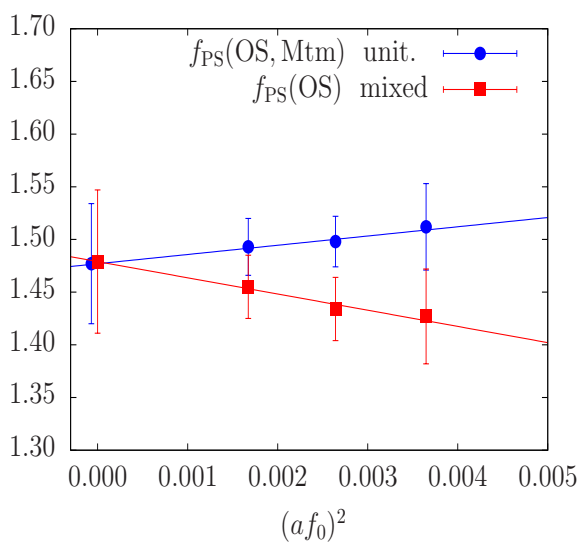

Test for $N_f = 2$

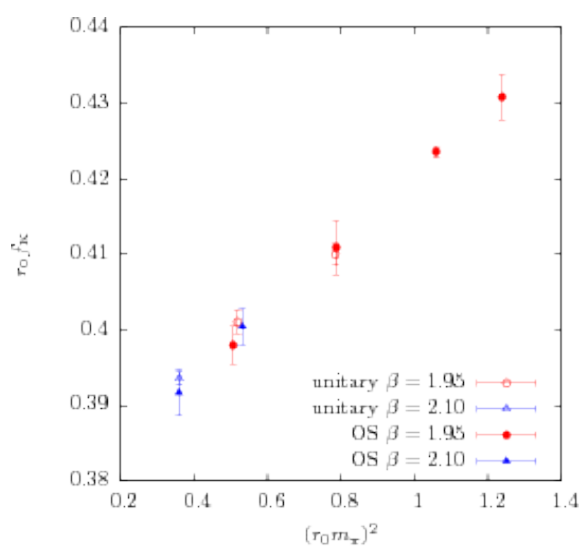

situation for $N_f = 2 + 1 + 1$

Decay constants, F_D, F_{D_s}

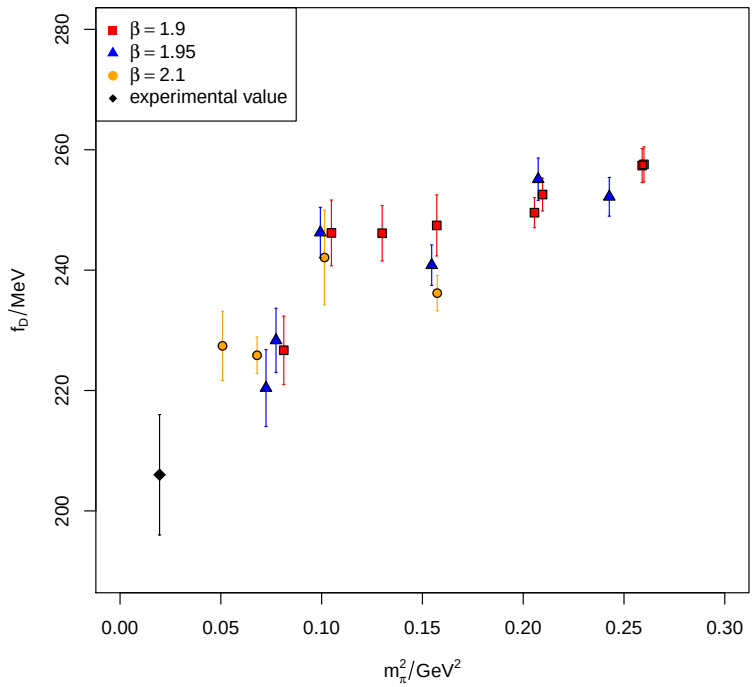

- quark mass dependence of f_D
- input: $m_\pi = 135$ MeV, $f_\pi = 130.7$ MeV, $m_K = 497.7$ MeV
- all results preliminary

- results very encouraging
  $f_{D_s} = 250(3)$ MeV, $f_D = 204(3)$ MeV, $f_{D_s}/f_D = 1.230(6)$
- very preliminary but very first results from $N_f = 2+1+1$!

The strange quark content of the nucleon

(Drach, Dinter, Frezzotti, Herdoiza, Rossi, K.J.)

- neutralino in supersymmetric models candidate for dark matter
- interaction with nucleon most strongly through the strange quark content via the Higgs boson exchange diagram

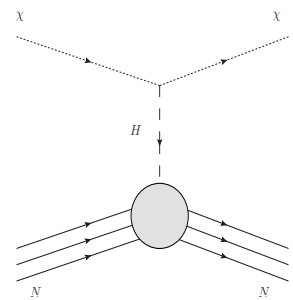

spin independend cross section:

$$\sigma_{\rm SI} \propto \sum_q \frac{f_{T_q}}{m_q} \quad ; q = u, d, s, c$$

$$f_{T_q} = \frac{\langle N | m_q \bar{q} q | N \rangle}{m_N} \equiv m_q B_q$$

$\Rightarrow$ cross section proportional to quark content; independent from quark mass

Study here: $\langle N | \bar{s} s | N \rangle = m_N B_s$; $\langle N | \bar{c} c | N \rangle = m_N B_c$

The problem

spin independent cross section strongly dependend on pion-nucleon sigma term $\Sigma_{\pi N}$

Varying $48\mathrm{MeV} < \Sigma_{\pi N} < 80\mathrm{MeV}$

$\Rightarrow$ cross section changes by an order of magnitude

$\Sigma_{\pi N}$ connected to y_N parameter

$$y_N = \frac{2B_s}{B_u+B_d} \quad ; B_q = \frac{\langle N|\bar{q}q|N\rangle}{m_N}$$

relation: $y_N = 1 - \sigma_0/\Sigma_{\pi N}$

$$\sigma_0 = m_q\langle N|\bar{u}u + \bar{d}d - 2\bar{s}s|N\rangle \ , \quad m_q = (m_u + m_d)/2$$

from χPT: $y_N = 0.44(13) \rightarrow$ quite large

want: a first principle, non-perturbative computation of f_{T_s}, f_{T_c} and y_N

Twisted mass fermions: special noise reduction technique

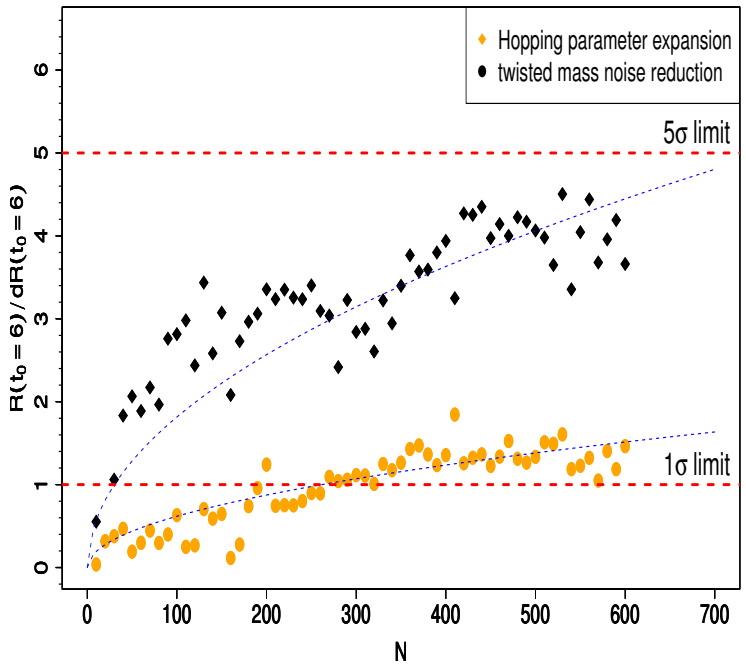

- standard calculation very (too?) difficult
- using techniques for twisted mass fermions
  $\rightarrow$ can obtain a signal with reasonable statistics
- remark: calculation of dis-connected contribution to neutral pion mass much easier

Twisted mass fermions: strange and charm: $\langle N|\bar{s}s|N\rangle$, $\langle N|\bar{c}c|N\rangle$,

- charm quark content

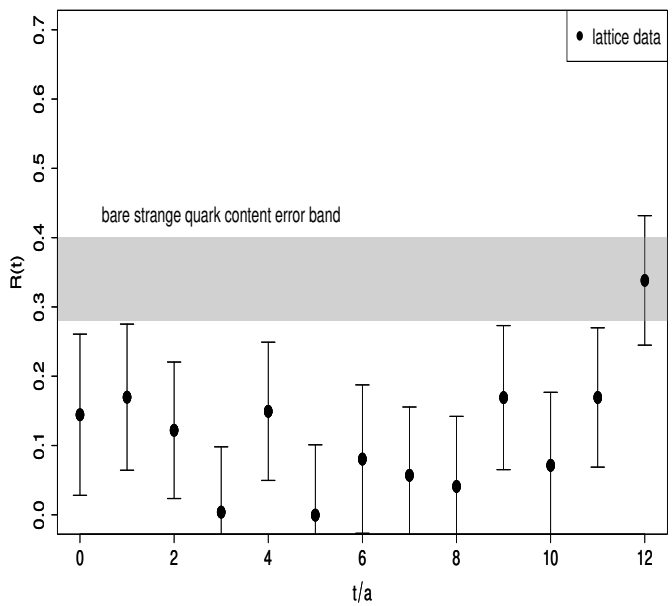

band: plateau value for strange quark content

- $\langle N|\bar{c}c|N\rangle < \langle N|\bar{s}s|N\rangle$ (note: still need mulitplication with quark mass)
- $f_{T_s} = 0.011(2)(1),\ \sigma_0 = 0.137(2)(3)\ \mathrm{MeV},\ y_N = 0.065(12)(2)$
  (note: all results still need extrapolation to physical point)
- still $y_N^{\mathrm{latt}} \ll y_N^{\mathrm{XPT}} \rightarrow$ bad news for experiments if value persists in chiral limit
- for twisted mass: no mixing effects in renormalization

Spectral projectors: Σ and $\chi_{\rm topo}$

(Giusti, Lüscher; Lüscher, Palombi; Giusti, Rossi, Testa)

- In the continum:

$$\frac{\Sigma}{\pi} = \lim_{\lambda\to 0}\lim_{m\to 0}\lim_{V\to\infty}\rho(\lambda,m)$$

$$\rho(\lambda,m) = \frac{1}{V}\sum_{k=1}^{\infty}\langle\delta(\lambda-\lambda_k)\rangle\,, \qquad \Sigma = -\lim_{m\to 0}\lim_{V\to\infty}\langle\bar{u}u\rangle$$

- mode number $\nu \rightsquigarrow$ average number of eigenmodes of $D_m^\dagger D_m$ with $\lambda \le M^2$

$$\nu(M,m) = V\int_{-\Lambda}^{\Lambda} d\lambda\rho(\lambda,m), \qquad \Lambda = \sqrt{M^2-m^2}$$

$\nu(M,m) = \nu_R(M_R,m_R) \quad \rightsquigarrow$ renormalization-group invariant

- $\Sigma_R \propto \frac{\partial}{\partial M_R}\nu_R$

Condensate

- Spectral Projector $\mathbb{P}_M$ to compute $\nu(M, m)$

$$\nu(M, m_q) = \langle \mathrm{Tr}\{\mathbb{P}_M\} \rangle$$

- Approximation of $\mathbb{P}_M$:

$$\mathbb{P}_M \approx h(\mathbb{X})^4,$$
$$\mathbb{X} = \frac{2M^2}{D_m^\dagger D_m + M^2} - 1$$

- $h(x)$ is an approximation to the step function $\theta(x)$ in the interval $[-1, 1]$

$$h(x) = \tfrac{1}{2}\{1 - xP(x^2)\}$$

where $P(x)$ is the polynomial which minimizes $\delta = \max_{\epsilon \leq y \leq 1} \|1 - \sqrt{y}P(y)\|$

- $\nu(M, m_q) = \langle \mathcal{O}_N \rangle, \quad \mathcal{O}_N = \frac{1}{N}\sum_{k=1}^{N}(\eta_k, \mathbb{P}_M \eta_k)$
  η_k sources generated randomly

Chiral limit of scalar condensate

(Cichy, Garcia Ramos, K.J.)

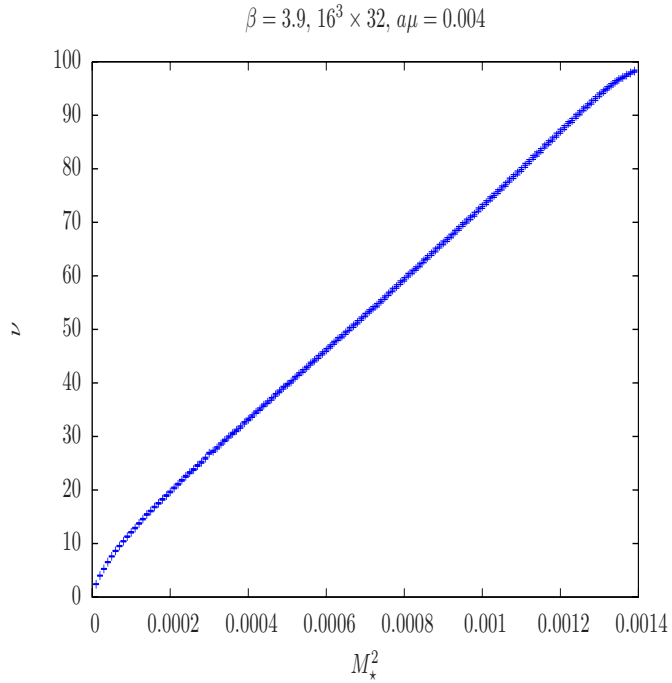

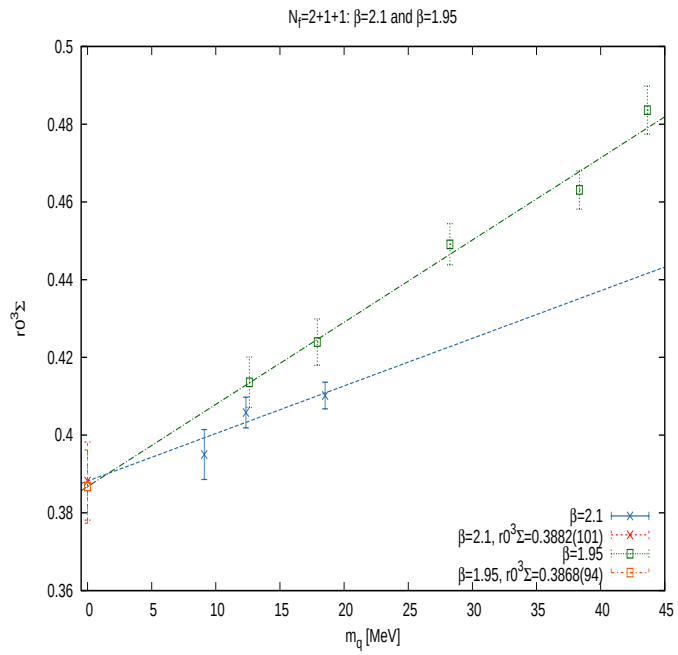

linear behaviour of mode number

slope: $\Sigma^{\rm ren}_{\rm spectral}$

chiral extrapolation of condensate

two lattice spacings

Non-perturbative renormalization for $N_f = 2+1+1$

renormalisation factors computed from dedicated $N_f = 4$ flavour simulations of Wilson fermions

- RI-MOM scheme at non zero values of both the standard and twisted mass parameters

$$M_R = \frac{1}{Z_{\rm P}} \sqrt{(Z_{\rm A} m_{\rm PCAC})^2 + \mu_q^2} \quad \rightarrow \quad 0$$

- $O(a)$ improvement via average of simulations with $+m_{\rm PCAC}$ and $-m_{\rm PCAC}$

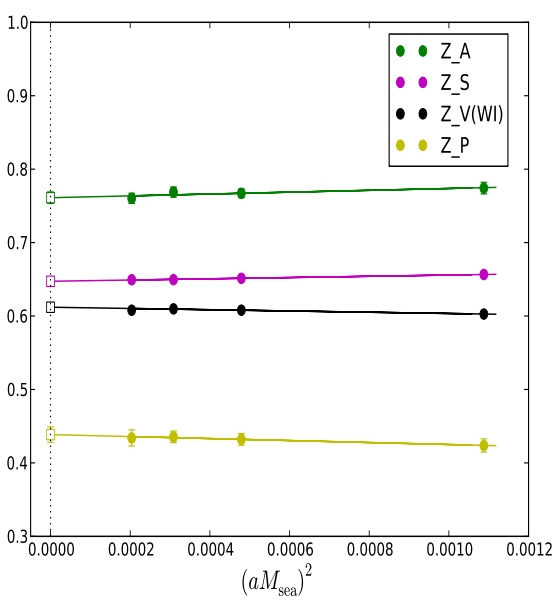

study at $\beta = 1.95$

$a = 0.08$ fm, $L = 1.9$ fm

- linear mass dependence
- allows for chiral extrapolation

Simulation setup for $N_f = 2+1+1$
Configurations available through ILDG

β	a[fm]	L^3T/a^4	m_π[MeV]	therm/production
1.9	≈ 0.085	$24^3 48$	300 – 500	1500/5000
1.95	≈ 0.075	$32^3 64$	300 –500	1500/5000
2.0	≈ 0.065	$32^3 64$	300	1500/5000
2.1	≈ 0.055	$48^3 96$	230 – 500	1500/5000

- can go down to $m_\pi \approx 230\mathrm{MeV}$
- see only small lattice spacing scaling
- can perform rich physics programme

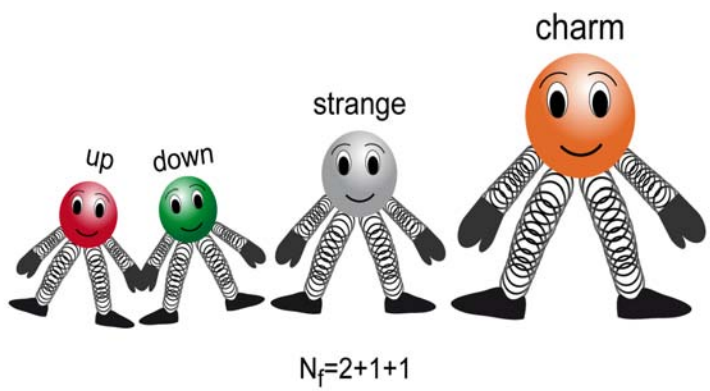

Size of cut-off effects: pion mass splitting

- question: how fast can we reach the physical point?

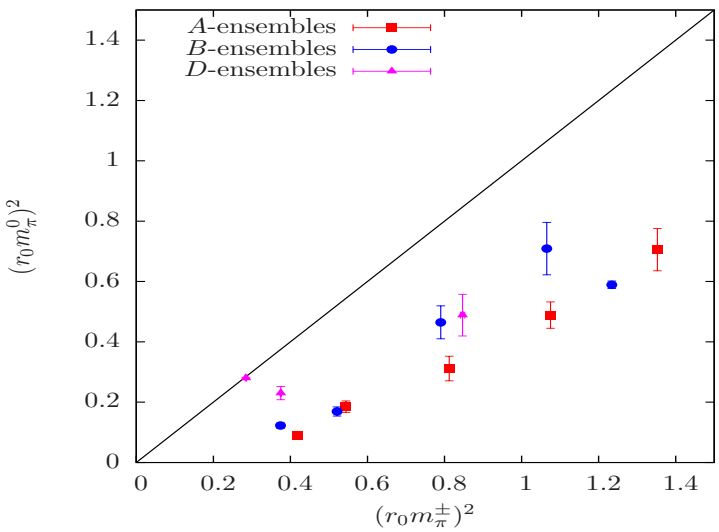

- Preliminary!
- $m_\pi^0 < m_\pi^\pm \rightarrow c_2 < 0$

significant flavour violations

- answer: not fast enough!

Effects of smearing for $N_f = 2+1+1$

action	$a\mu_\ell$	$\kappa_{\rm crit}$	$Z_V[\mathrm{WI}]$	Z_P/Z_S
0-stout	0.0060	0.163265	0.60	0.67
	0.0080	0.163260		
	0.0080	0.163204		
1-stout	0.0060	0.145511	0.73	0.77
	0.0080	0.145510		
4-stout	0.0015	0.136720	0.82	0.86

- $\kappa_{\rm crit} \rightarrow$ moves closer to $1/8$
- Z factors $\rightarrow$ move closer to 1
- plaquette behaves much smoother:

$$\left.\frac{\Delta[\langle P\rangle]}{\Delta[(2\kappa)^{-1}]}\right|_{\kappa_{\rm crit}} = 11.4(\text{no stout}) \rightarrow -3.4(\text{stout})$$

- proof-tested that simulations at $m_\pi/f_\pi = \text{physical}$ feasible at lattice spacing $a \approx 0.1\text{fm}$

Summary

- **ETMC** successful simulations with $N_f = 2$ and $N_f = 2 + 1 + 1$ quark flavour
  - found good scaling behaviour
  - could achieve accurate results for many quantities
  - performed dedicated renormalization programme
- simulation at physical point difficult with present action
- developed new (maximally) twisted mass action
  - reach $m_\pi / f_\pi = \mathrm{physical}$ at lattice spacing $a \approx 0.1\mathrm{fm}$
  - $m_\pi^0 \approx m_\pi^\pm$
- plan new simulations at physical point (+isospin + electromagnetism)

Exploring the phases of QCD with many flavors

Xiao-Yong Jin

RIKEN Advanced Institute for Computational Science

New Horizons for Lattice Computations with Chiral Fermions

with Robert Mawhinney (Columbia University)

Introduction

- Detailed data in:
  - My dissertation (2011):
    http://academiccommons.columbia.edu/catalog/ac:137844
  - Lattice conference proceedings (2008-2011).

- Goal: Identify the phase (walking or conformal or ...)
  - Hadronic observables from zero temperature simulations, including meson propagators and masses, π decay constant, Quark potential and string tension...
  - Zero temperature and finite temperature
  - DBW2 gauge with naïve staggered fermion action

To see the whole picture

The subject of this talk

- Understand the direct implication of our data
- Carefully speculate about our blind spots

Summary of data

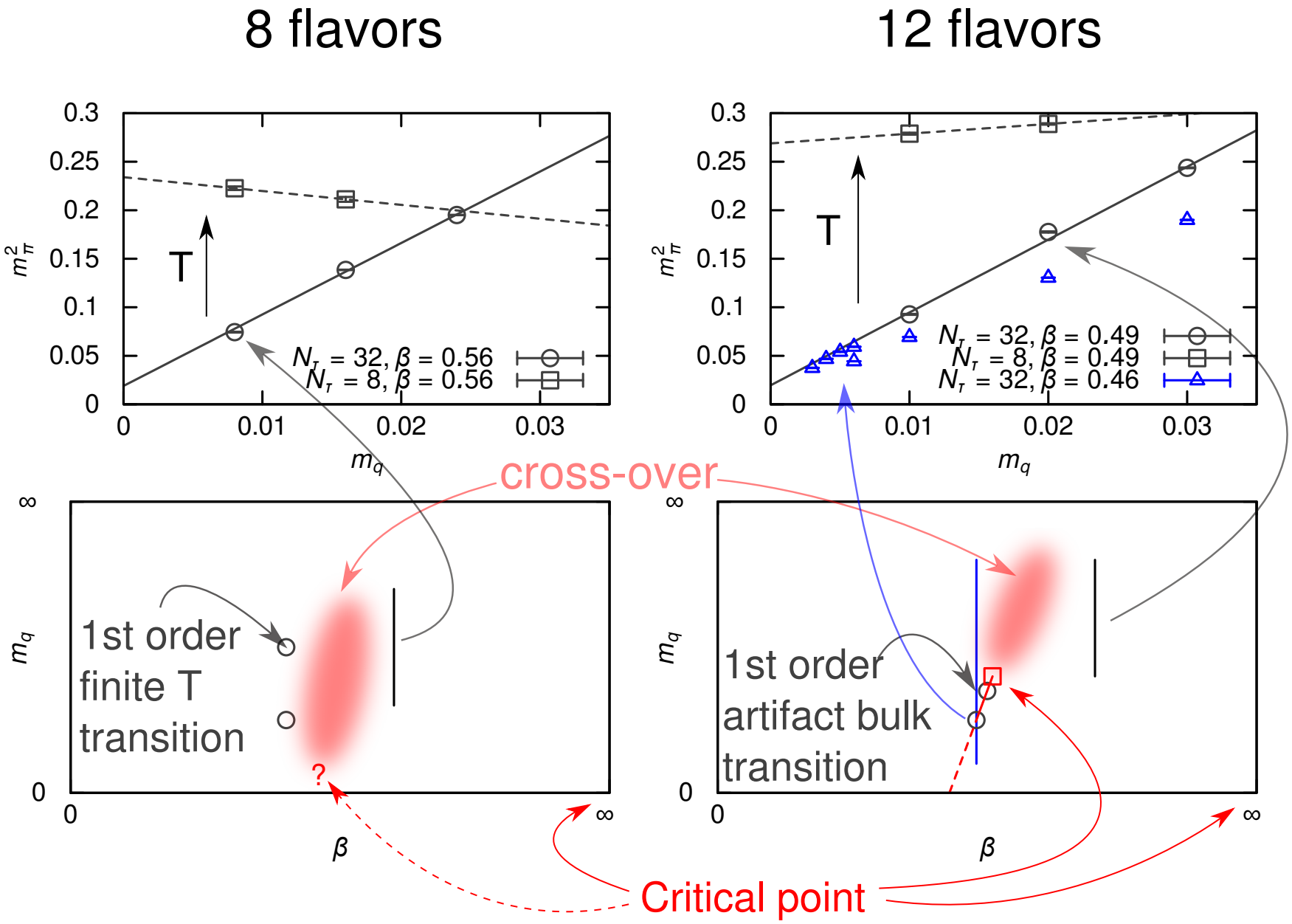

Zero temperature simulations

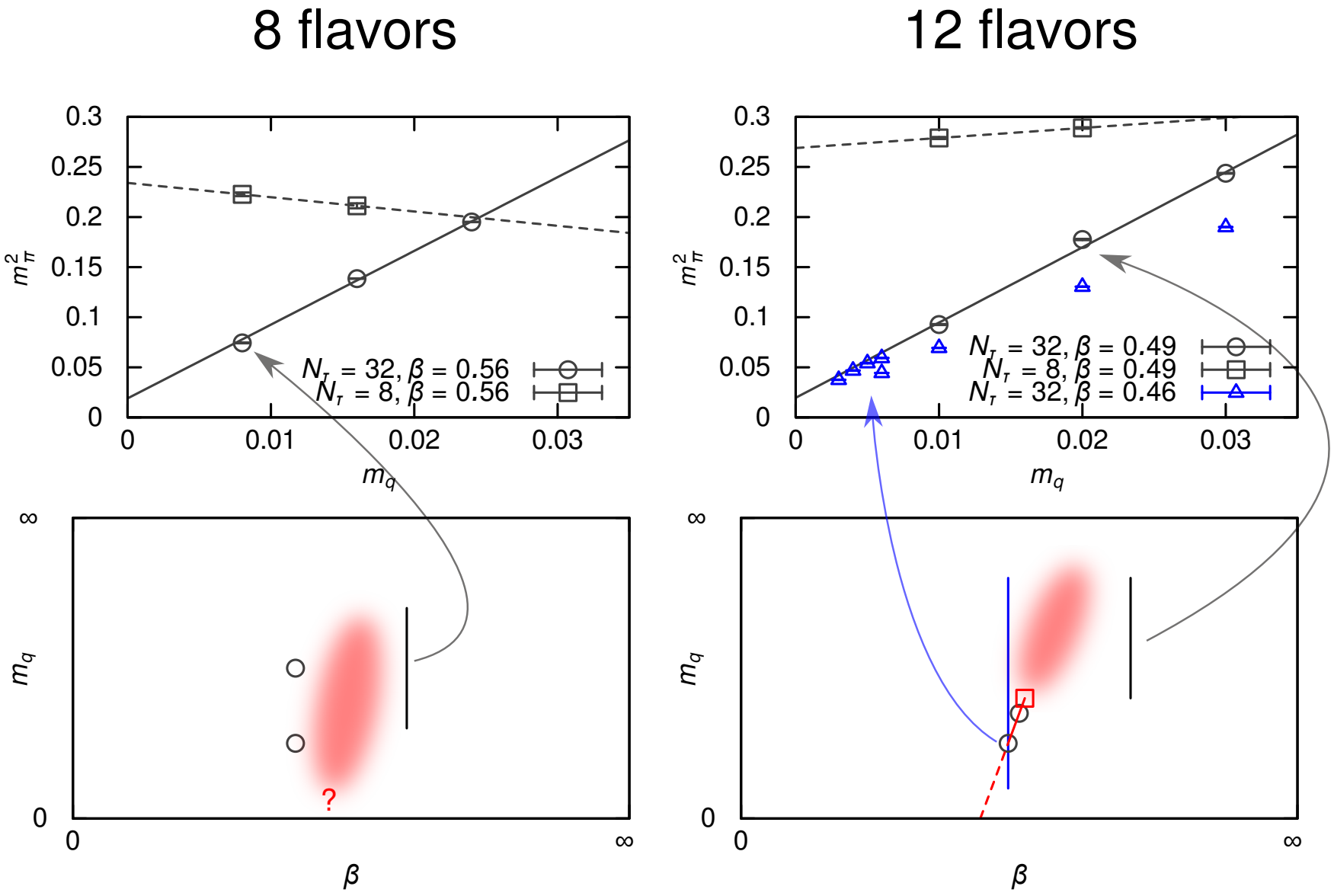

Finite temperature

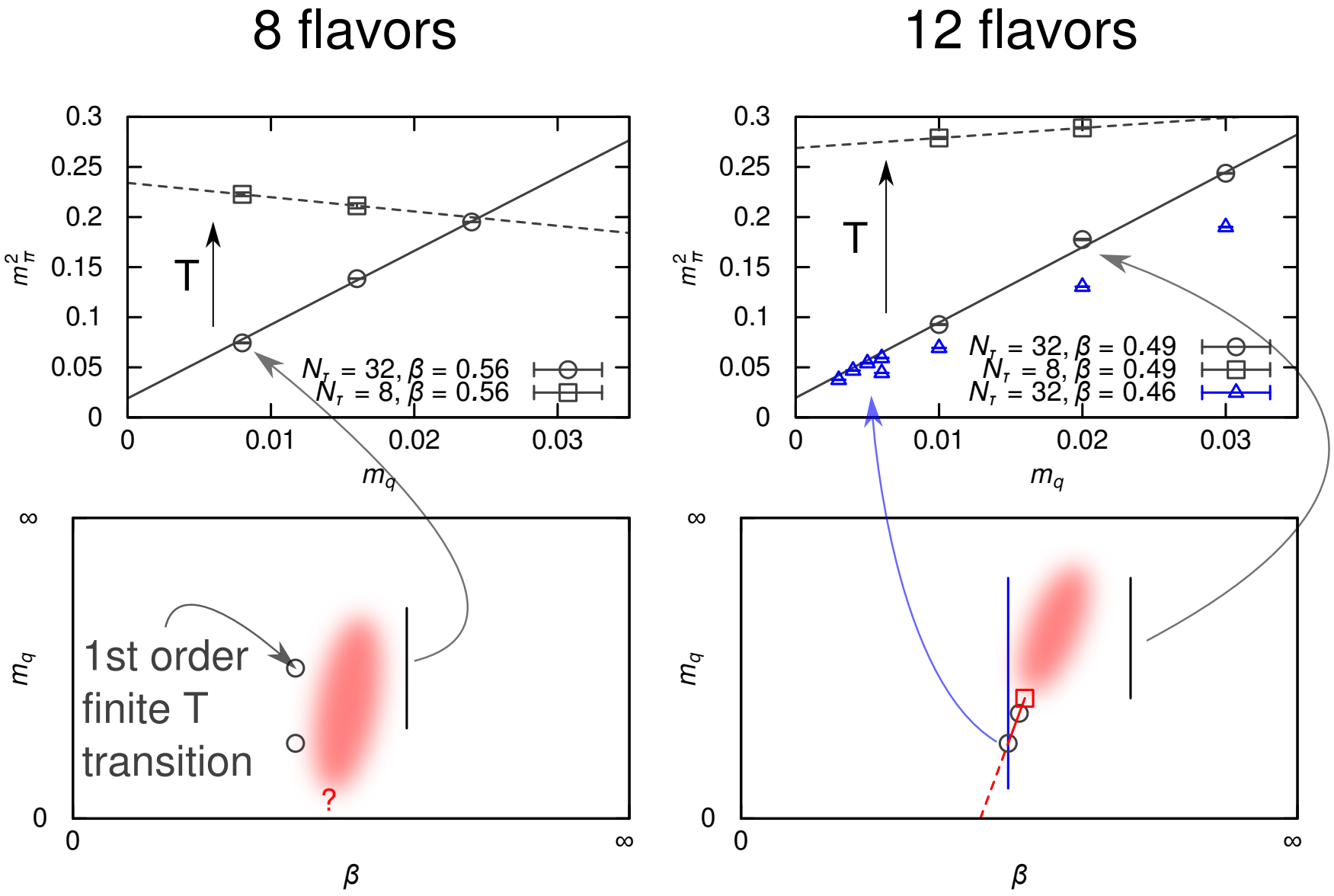

The bulk transition

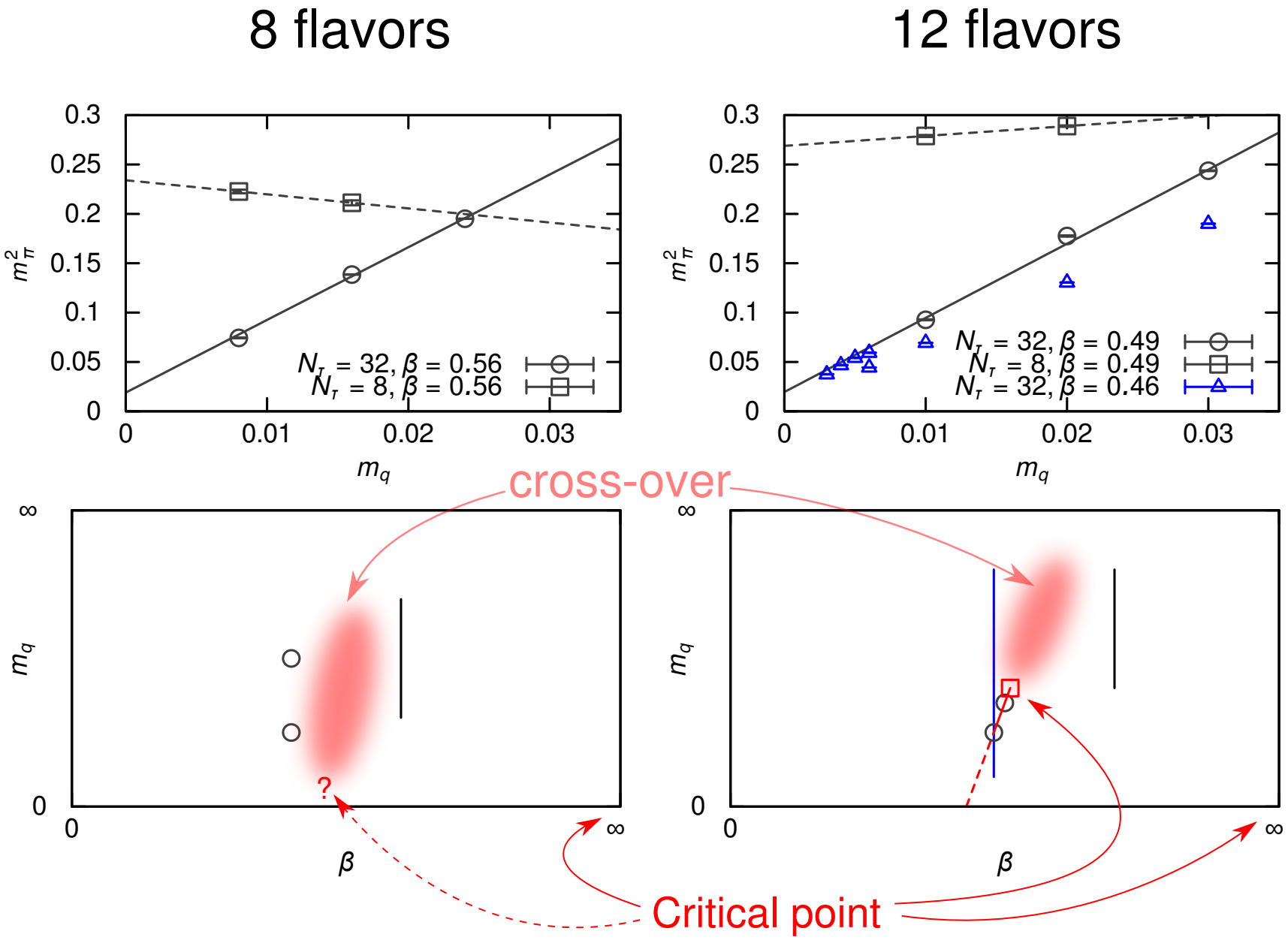

The bulk transition

- 8 flavors:
  - Bulk transition appears (strengthens) when simple plaquette action is used instead of DBW2.
- 12 flavors:
  - Volume independent $\longrightarrow$ finite temperature effect less likely.
  - For most channels, the difference in particle masses on the two sides of the bulk transition become smaller and vanish when quark mass is increased.
  - The scalar singlet is found to be special.

Scalar singlet meson

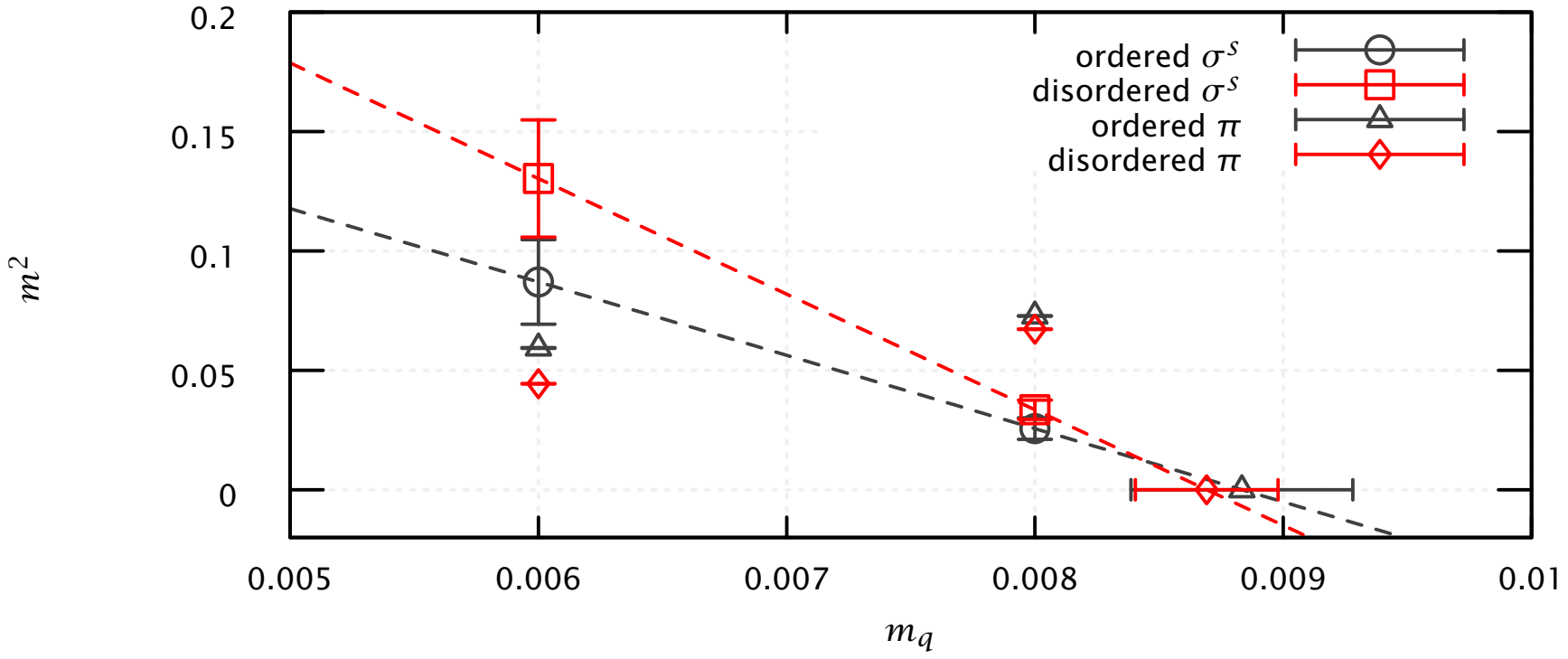

- The scalar singlet meson becomes lighter along the 1st order bulk transition line approaching the 2nd order critical end point.
- Critical exponent is consistent with Ginzburg-Landau theory.
- Continuum limit of the lattice theory at second order critical point is likely a free scalar field theory.

Consequences of a light scalar singlet meson

Chiral perturbation theory is not applicable.

Scaling of m_{ρ_2}/f_π versus quark mass

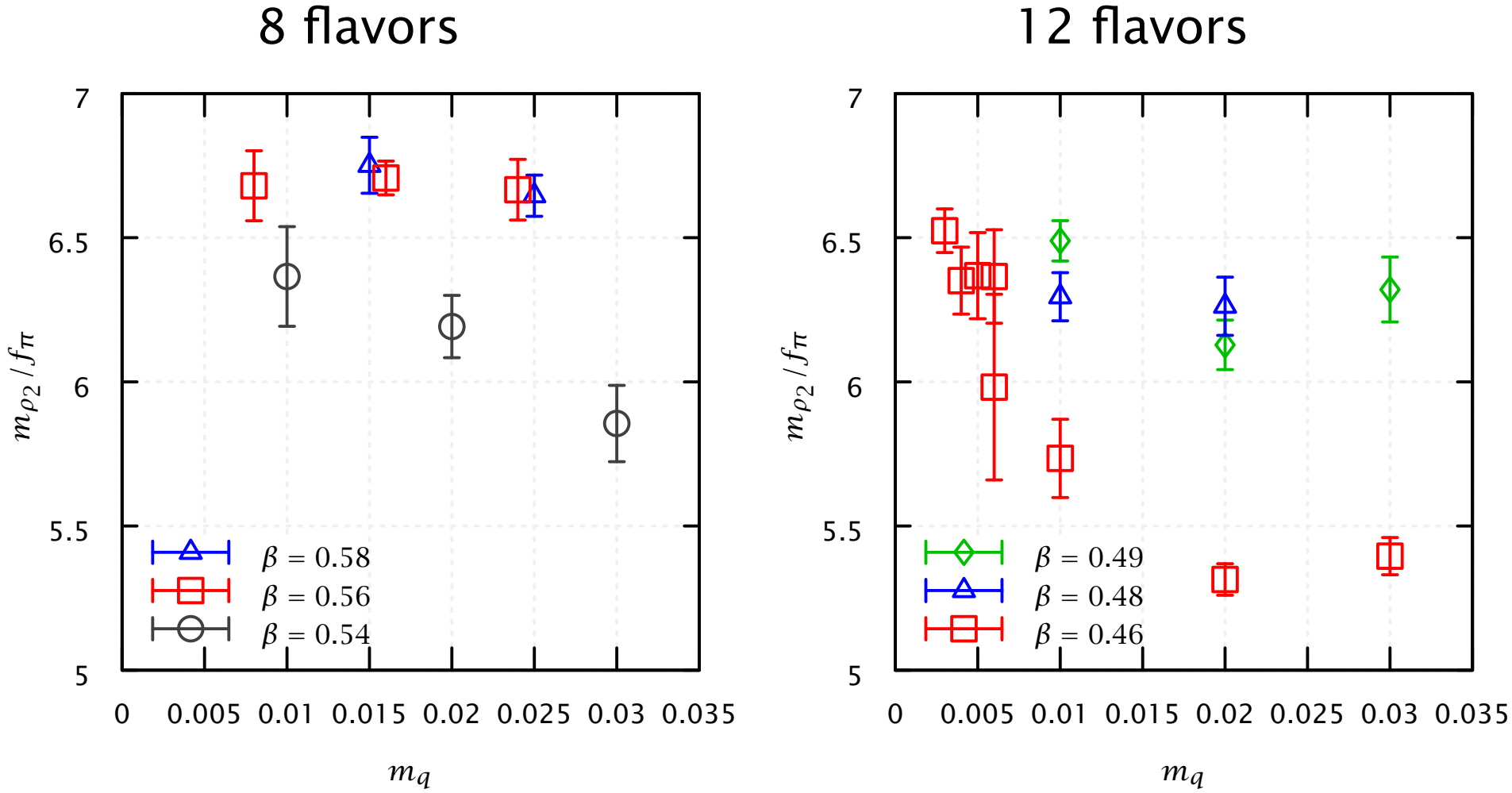

- Approaches to a constant at weak couplings
- Other ratios behave the same, except for pion masses

Scaling of m_π / f_π versus quark mass

8 flavors

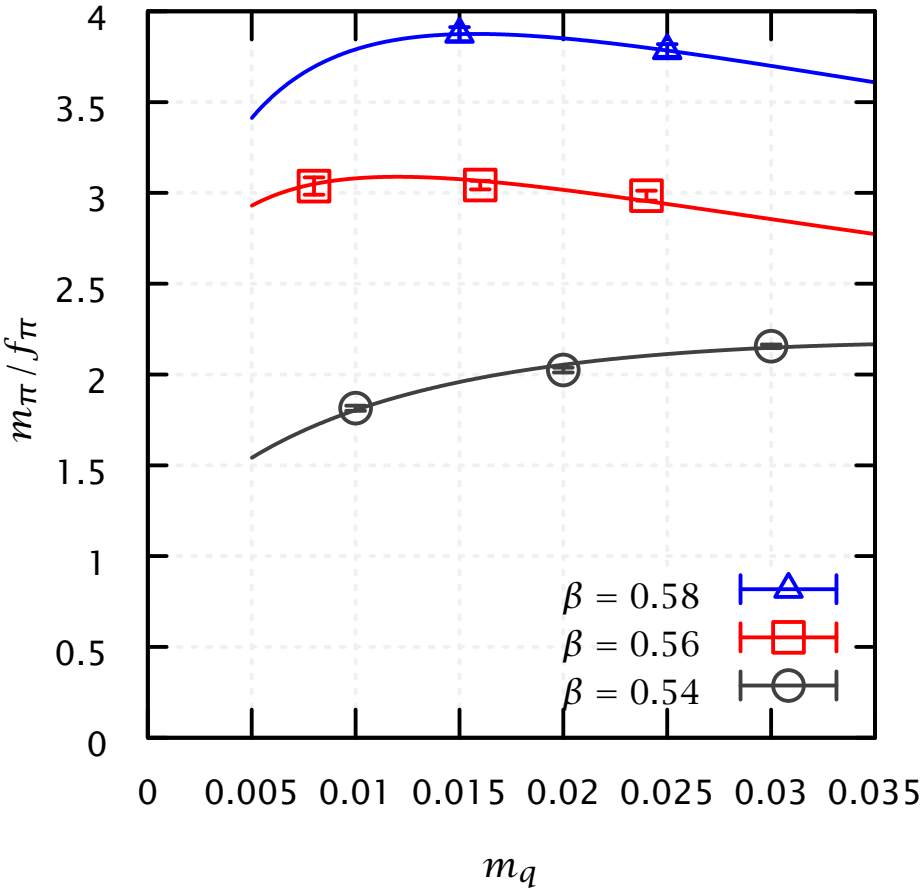

12 flavors

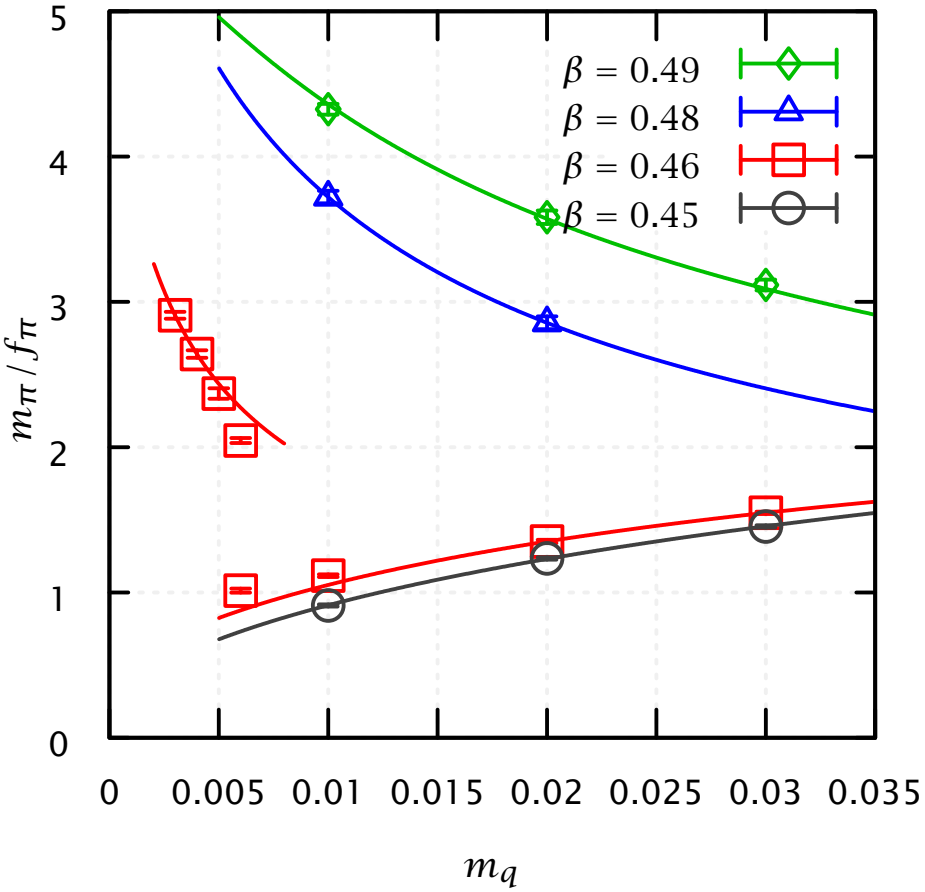

Warnings:

- Backward flow of constant m_π / f_π in weaker couplings.
- Misleading conclusions at large m_q.

The flow of constant physics (m_π / f_π)

A sketch of m_π / f_π surface parameterized by m and β.

Strong coupling side

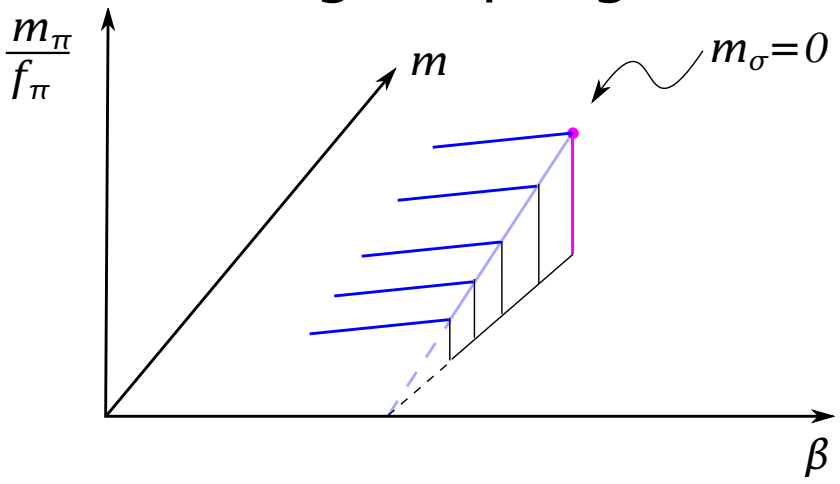

Same as QCD except the $\beta \to \infty$ cannot be reached, because the bulk transition blocks the way.

Weak coupling side

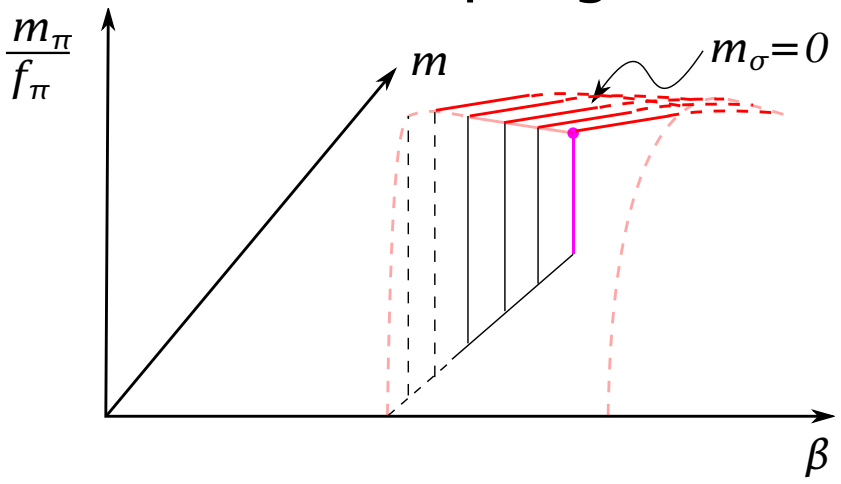

Comparing with 8-flavor data, we conjecture that only when m_q is much smaller and β is much larger than the bulk transition, can we recover QCD behavior.

Conjectured lines of constant physics (m_π / f_π)

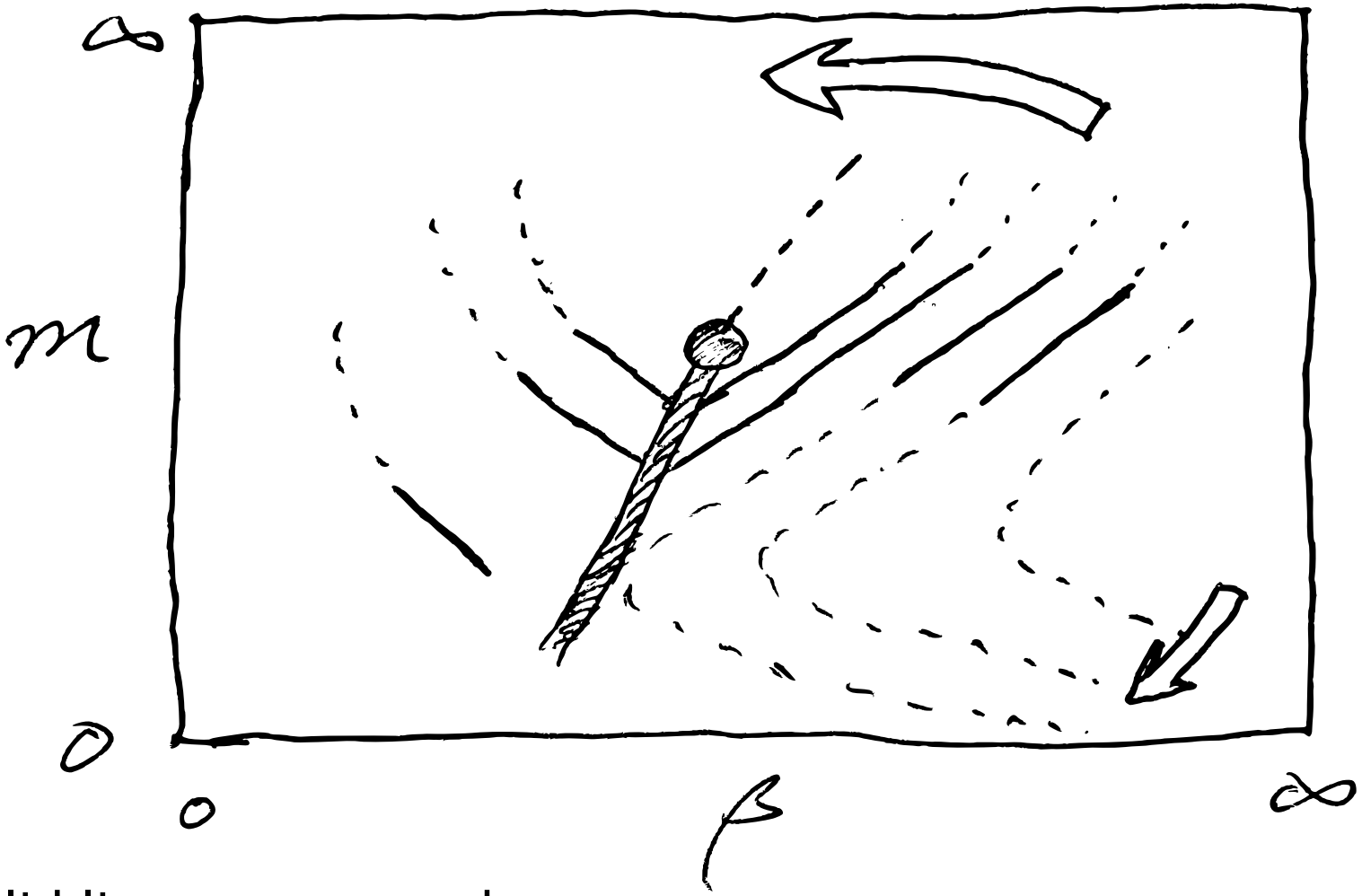

- Solid lines represent data.
- Dashed lines are our conjecture.
- Arrows denotes the direction of m_π / f_π going smaller.

Conclusion

- Our data show:
  - 12-flavor has an additional critical point where scalar correlation length diverges.
  - 12-flavor show the same behavior as 8-flavor at larger m_q.
- We conjecture:
  - Possible bulk transition with 8-flavor at smaller m_q.
  - For 12 flavors, much smaller m_q and/or much weaker coupling is required to move away from the additional critical point and recover the physics at $\beta \to \infty$.

Kaon semileptonic decays in lattice QCD with exact chiral symmetry

T. Kaneko for JLQCD collaboration

KEK Theory Center

RIKEN BNL Research Center Workshop, May 15, 2012

1. introduction

$K \to \pi$ decay form factors

$$\langle \pi^+(p')|V_\mu|K^0(p)\rangle = (p+p')_\mu\, f_+(q^2) + (p-p')_\mu\, f_-(q^2),$$

$$f_0(q^2) = f_+(q^2) + \frac{q^2}{M_K^2 - M_\pi^2} f_-(q^2), \qquad \xi(q^2) = \frac{f_-(q^2)}{f_+(q^2)}$$

- vector form factor at $q^2 = 0$: $f_+(0)$ $\Leftrightarrow$ determination of $|V_{us}|$
  - $M_{\pi,\mathrm{sim}} \lesssim M_K$: $N_f = 3$: *RBC/UKQCD, 2008,2010*, $N_f = 2$: *ETM, 2009*

    (see also MILC/FNAL/HPQCD, 2005; FNAL/MILC @ Lat'11)
  - $\Gamma \Rightarrow |V_{us}| f_+(0) = 0.2163(5)$ (*FlaviaNet, 2010*) $\Leftrightarrow$ $f_+(0)$ w/ $\lesssim 1$ % accuracy
- other information of ME : $f_-(0)$, $\lambda'^{,''}_{+,0}$ $\Leftrightarrow$ consistency with ChPT, exp't

1. introduction

this talk

report on JLQCD's calculation of $K \to \pi$ form factors in $N_f = 2+1$ QCD

- overlap quarks $\Rightarrow$ straightforward comparison w/ ChPT ($a = 0$)
- all-to-all quark prop. $\Rightarrow$ precise calculation of relevant meson correlators

outline

- simulation method
- extraction of form factors
- q^2 interpolation
- chiral extrapolation

2. simulation method

configurations

- $N_f = 2+1$ QCD
- Iwasaki gauge + overlap quarks + $\det[H_W^2]/\det[H_W^2+\mu^2]$ $\Rightarrow$ speed up, fix Q
- $a =$ 0.1120(5)(3) fm (M_Ω as input) $\Leftrightarrow$ $O((a\Lambda_{\rm QCD})^2) \approx$ 8 % error

2. simulation method

configurations

- $N_f = 2+1$ QCD
- Iwasaki gauge + overlap quarks + $\det[H_W^2]/\det[H_W^2+\mu^2]$ $\Rightarrow$ speed up, fix Q
- $a =$ 0.1120(5)(3) fm (M_Ω as input) $\Leftrightarrow$ $O((a\Lambda_{\rm QCD})^2) \approx$ 8 % error

measurements of meson correlators

- 4 m_{ud}'s $\Rightarrow$ $M_\pi \simeq$ 290 – 540 MeV; $m_s =$ 0.080 $\Leftrightarrow$ $m_{s,\rm phys} =$ 0.081
- $16^3 \times 48$ or $24^3 \times 48$ (depending on m_{ud}) $\Rightarrow$ $M_\pi L \gtrsim$ 4
- in $Q=0$ sector $\Rightarrow$ fixed Q effects $\propto V^{-1}$; sub-% for $M_{\{\pi,K\}}$, $f_{\{\pi,K\}}$
- 50 conf $\times$ 50 HMC traj. for each (m_{ud},m_s)

2. simulation method

configurations

- $N_f = 2+1$ QCD
- Iwasaki gauge + overlap quarks + $\det[H_W^2]/\det[H_W^2+\mu^2]$ $\Rightarrow$ speed up, fix Q
- $a =$ 0.1120(5)(3) fm (M_Ω as input) $\Leftrightarrow$ $O((a\Lambda_{\rm QCD})^2) \approx$ 8 % error

measurements of meson correlators

- 4 m_{ud}'s $\Rightarrow$ $M_\pi \simeq$ 290 – 540 MeV; $m_s =$ 0.080 $\Leftrightarrow$ $m_{s,\rm phys} =$ 0.081
- $16^3 \times 48$ or $24^3 \times 48$ (depending on m_{ud}) $\Rightarrow$ $M_\pi L \gtrsim$ 4
- in $Q=0$ sector $\Rightarrow$ fixed Q effects $\propto V^{-1}$; sub-% for $M_{\{\pi,K\}}$, $f_{\{\pi,K\}}$
- 50 conf $\times$ 50 HMC traj. for each (m_{ud},m_s)

- w/ all-to-all propagator $\Rightarrow$ 160 - 240 low-modes + noise method
- twisted boundary conditions (TBCs) $\Rightarrow$ $q^2 \in [-0.1\,\text{GeV}^2, q^2_{\rm max}]$
- reweighting $\Rightarrow$ additional $m_s =$ 0.060

3.1 ratio method

$$C^{PQ}_{V_\mu}(\mathbf{p},\mathbf{p}') = \langle \mathcal{O}_Q(\mathbf{p}') V_{\mu,\mathrm{lat}} \mathcal{O}^\dagger_P(\mathbf{p})\rangle \sim \frac{\sqrt{Z_Q(\mathbf{p}')Z_P(\mathbf{p})}}{4E_P E_Q\, Z_V} \langle Q(\mathbf{p}')|V_\mu|P(\mathbf{p})\rangle e^{-E_Q\Delta t' - E_P \Delta t}$$

$$C^P(\mathbf{p}) = \langle \mathcal{O}_P(\mathbf{p}')\mathcal{O}^\dagger_P(\mathbf{p})\rangle \sim \frac{Z_P}{2E_P} e^{-E_Q \Delta t'} \quad (P,Q = K \text{ or } \pi)$$

ratio method *(Hashimoto et al., 1999)*

(partially) cancel Z_V, $\exp[-E_{\pi(K)}\Delta t]$, fluctuation in $C^{PQ}_{V_\mu}(\mathbf{p},\mathbf{p}')$ and $C^P(\mathbf{p})$

$$R = \frac{C^{K\pi}_{V_4}(\mathbf{0},\mathbf{0})\, C^{\pi K}_{V_4}(\mathbf{0},\mathbf{0})}{C^{KK}_{V_4}(\mathbf{0},\mathbf{0})\, C^{\pi\pi}_{V_4}(\mathbf{0},\mathbf{0})} \rightarrow \frac{(M_K+M_\pi)^2}{4M_K M_\pi} f_0(q^2_{\max})^2 \quad (q^2_{\max} = (M_K - M_\pi)^2)$$

$$\tilde{R} = \frac{C^{K\pi}_{V_4}(\mathbf{p},\mathbf{p}')\, C^K(\mathbf{0})\, C^\pi(\mathbf{0})}{C^{K\pi}_{V_4}(\mathbf{0},\mathbf{0})\, C^K(\mathbf{p})\, C^\pi(\mathbf{p}')} \rightarrow \left\{1 + \frac{E_K(\mathbf{p}) - E_\pi(\mathbf{p}')}{E_K(\mathbf{p}) + E_\pi(\mathbf{p}')}\xi(q^2)\right\} \frac{f_+(q^2)}{f_0(q^2_{\max})}$$

$$R_k = \frac{C^{K\pi}_{V_k}(\mathbf{p},\mathbf{p}')\, C^{KK}_{V_4}(\mathbf{p},\mathbf{p}')}{C^{K\pi}_{V_4}(\mathbf{p},\mathbf{p}')\, C^{KK}_{V_k}(\mathbf{p},\mathbf{p}')} \rightarrow \text{a function of } \xi(q^2)$$

$\Rightarrow$ can construct $f_+(q^2)$, $f_0(q^2)$, $\xi(q^2)$

3.2 extraction of form factors : statistical accuracy

all-to-all propagator $\Rightarrow$ can improve stat. accuracy

$C_{V_\mu}^{K\pi}$ at each jackknife sample

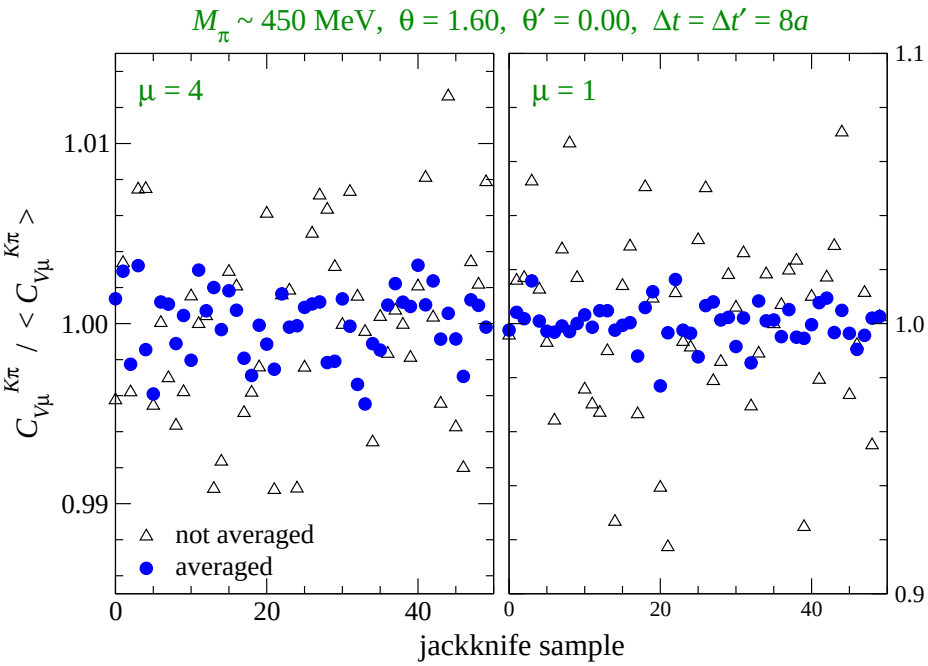

$\xi(q^2; \Delta t, \Delta t')$ vs Δt

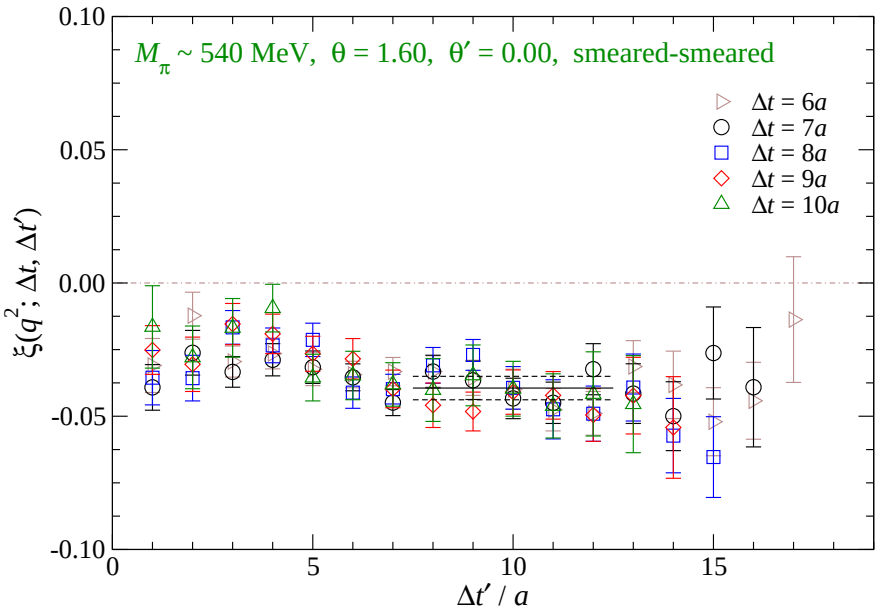

- all-to-all $\Rightarrow$ average over location of meson source op.
  $\Leftrightarrow$ a factor of 3 (4) improvement for $\mu = 4$ (1)
- clear signal for $\xi(q^2)$: 10 – 30% (comparison w/ exp't (later))
- $f_{\{+,0\}}(q^2)$: statistical accuracy sub-% level

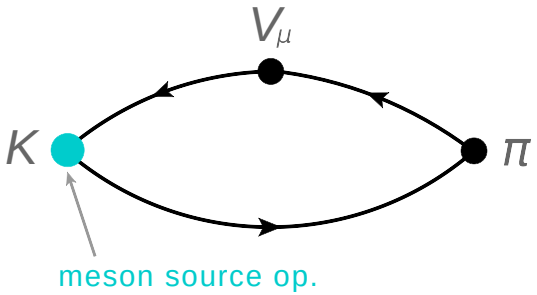

3.2 extraction of form factors : statistical accuracy

reweighting $\Rightarrow$ can impair stat. accuracy

$$\langle C^{PQ}_{V_\mu}\rangle_{m'_s} = \langle C^{PQ}_{V_\mu}\, \tilde{w}(m'_s, m_s)\rangle_{m_s}$$

$$\tilde{w}(m'_s, m_s) = \frac{w(m'_s, m_s)}{\langle w(m'_s, m_s)\rangle_{m_s}}$$

$$w(m'_s, m_s) = \det[D(m'_s)]/\det[D(m_s)]$$

$$= \frac{\prod_{k=1}^{N_e}\lambda_k(m'_s)}{\prod_{k=1}^{N_e}\lambda_k(m_s)} \times \frac{1}{N_r}\sum_{r=1}^{N_r} e^{-\frac{1}{2}\xi_r^\dagger \frac{D(m'_s)}{D(m_s)}\xi_r}$$

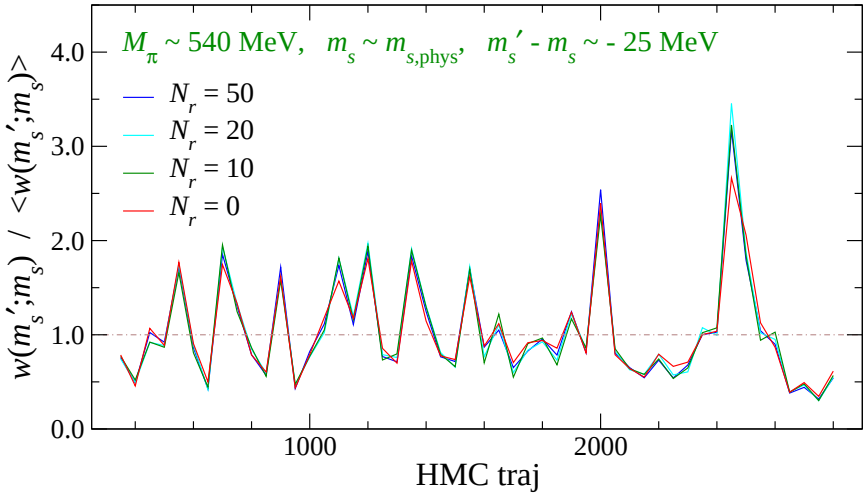

- $24^3(16^3)\times 48$, $\approx$ 200 low-modes
  - $\Rightarrow$ do not need large N_r
- largely increase $\Delta[C^{PQ}_{V_\mu}]$
- at most $\times$ 2 for ratios

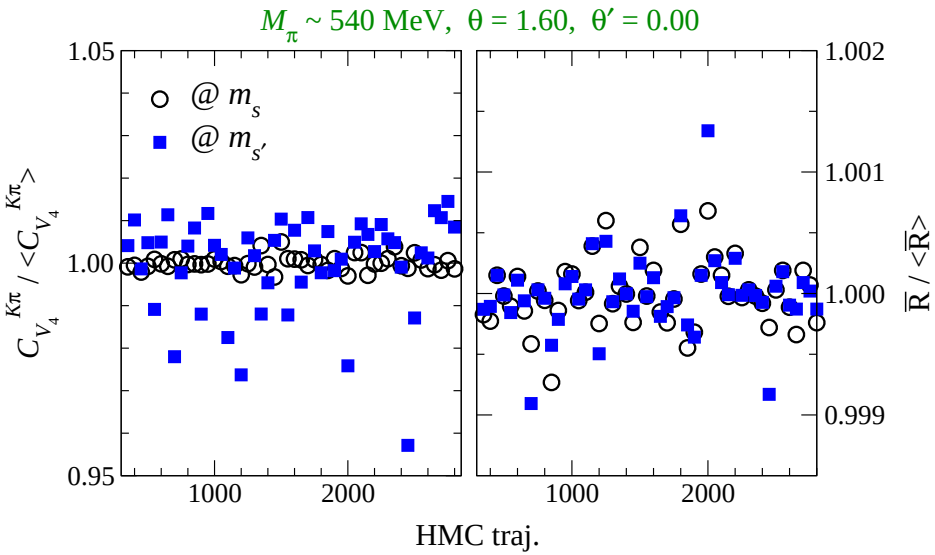

all-to-all + ratio + reweight $\Rightarrow$ $\Delta[f_{+,0}(q^2)] \lesssim 1.5\,\%$, $\Delta[\xi(q^2)] \sim 20-40\,\%$

4. q^2-dependence

$f_0(q^2)$ vs q^2

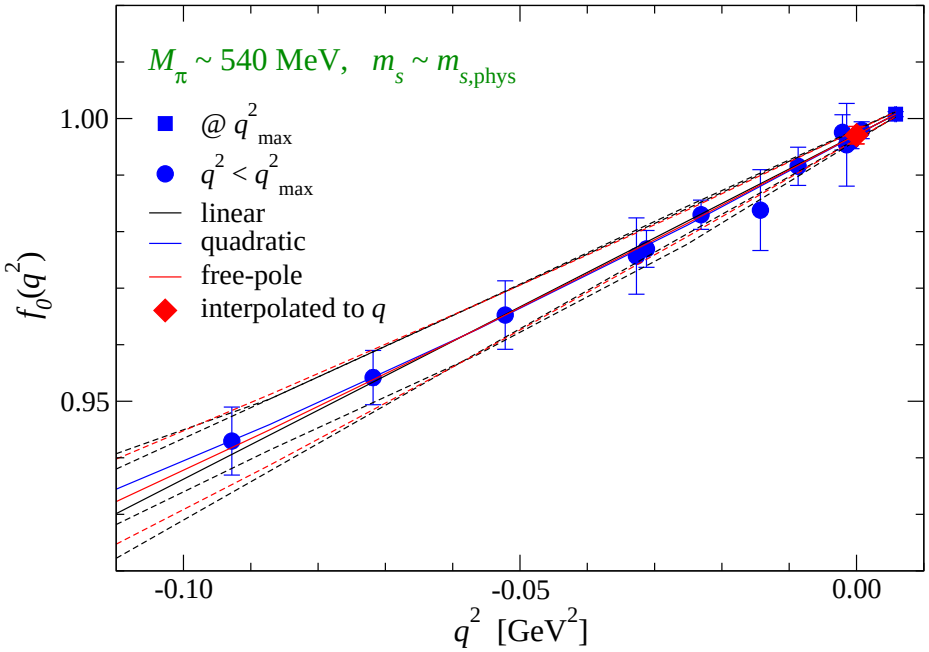

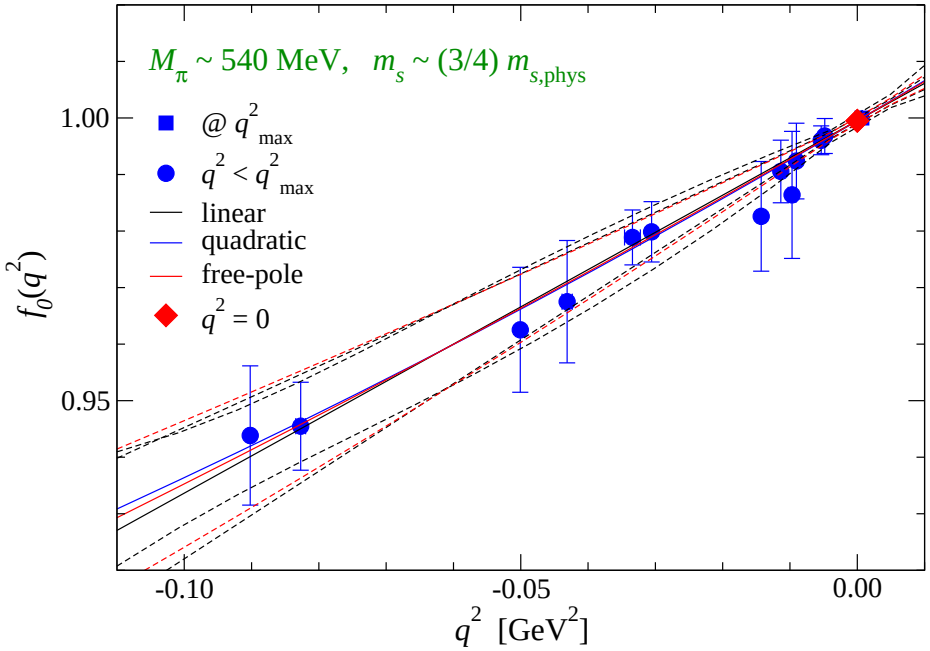

- reweighting $\Rightarrow$ slightly larger error
- small curvature in simulated region of q^2

  $\Leftrightarrow$ M_{pole}=1.2 – 1.3 GeV @ $m_{q,\mathrm{phys}}$ *(PDG, 2010)* $\Rightarrow$ $q^4/M^4_{\mathrm{pole}} \lesssim$ 0.6%
- well described by any of

$$f_0(q^2) = f_0(0)(1 + a_1 q^2), \quad f_0(0)(1 + a_1 q^2 + a_2 q^4), \quad \frac{f_0(0)}{1 - q^2/M^2_{\mathrm{pole}}}$$

4. q^2-dependence

$f_0(q^2)$ vs q^2

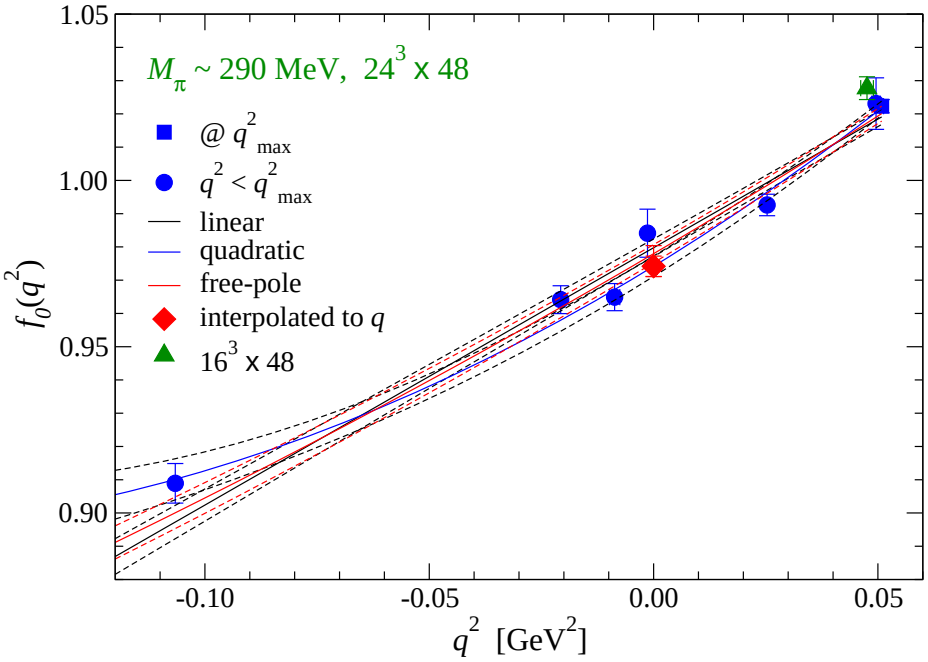

fit results for $f_+(0)$

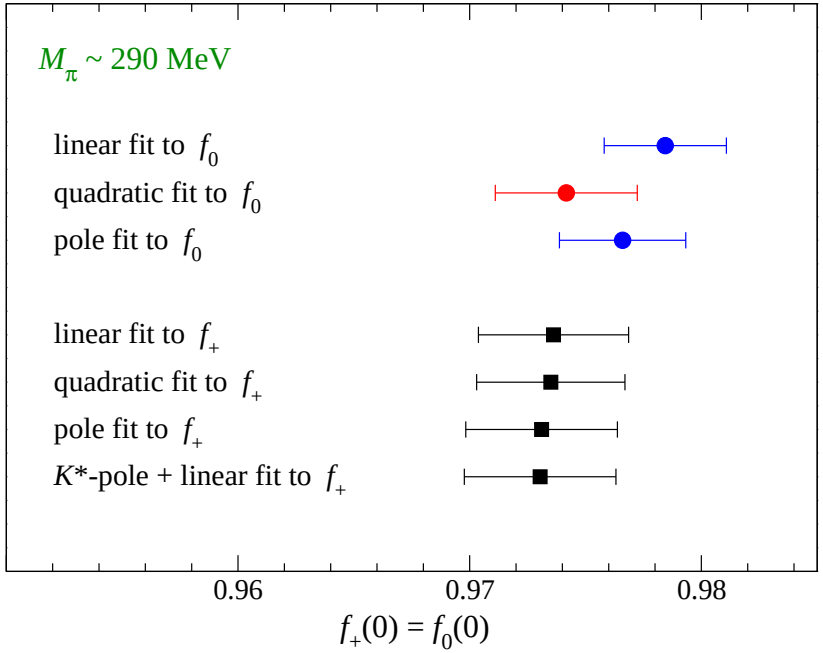

- $f_+(0)$ $(= f_0(0))$, $df_{+,0}(0)/dq^2|_{q^2=0}$: stable against choice of fit form
- small finite volume effects $\Leftrightarrow$ lattice boundaries + fixed Q

  $16^3 \times 48 \Leftrightarrow 24^3 \times 48$: 0.4 – 0.7% ($\lesssim$ 2.2-2.5σ) $\Rightarrow$ even smaller on $24^3 \times 48$ (?)
- this talk : quadratic fit $\Rightarrow$ $f_+(0)$, $df_+(q^2)/dq^2|_{q^2=0}$

5.1 chiral fit : $f_+(0)$

chiral expansions *(cf. JLQCD, 2008)*

$$f_+(0) = 1 + f_2 + f_4 + \cdots = 1 + f_2 + \Delta f$$

- $x_{\pi(K)} \equiv M^2_{\pi(K)}/(4\pi F_0)^2$ ("x-expansion")

  small $F_0 = 52.5(5.1)$ MeV $\ll F_\pi$ $\Rightarrow$ enhanced chiral corrections $\mathcal{O}_{2n} = (M_\pi/F_0)^{2n}$

- $\xi_{\pi(K)} \equiv M^2_{\pi(K)}/(4\pi F_\pi)^2$ ("ξ-expansion")

  better convergence for $M_{\{\pi,K\}}$, $F_{\{\pi,K\}}$ *(JLQCD, 2008 ($N_f = 2$) ; 2009 ($N_f = 2+1$))*

5.1 chiral fit : $f_+(0)$

chiral expansions *(cf. JLQCD, 2008)*

$$f_+(0) = 1 + f_2 + f_4 + \cdots = 1 + f_2 + \Delta f$$

- $x_{\pi(K)} \equiv M^2_{\pi(K)}/(4\pi F_0)^2$ ("x-expansion")

  small $F_0 = 52.5(5.1)$ MeV $\ll F_\pi$ $\Rightarrow$ enhanced chiral corrections $\mathcal{O}_{2n} = (M_\pi/F_0)^{2n}$

- $\xi_{\pi(K)} \equiv M^2_{\pi(K)}/(4\pi F_\pi)^2$ ("ξ-expansion")

  better convergence for $M_{\{\pi,K\}}$, $F_{\{\pi,K\}}$ *(JLQCD, 2008 ($N_f = 2$) ; 2009 ($N_f = 2+1$))*

fitting w/ ξ-expansion

- NLO *(Gasser-Leutwyler, 1985)*

  Ademollo-Gatto $\Rightarrow$ $f_2(F_\pi, M_{\{\pi,K,\eta\}})$

- NNLO and higher orders

  (Post-Schilcher, 2001; Bijnens-Talavera, 2003)

  $\Delta f(F_\pi, \{L_i\}, \{C_i\}, M_{\{\pi,K,\eta\}})$

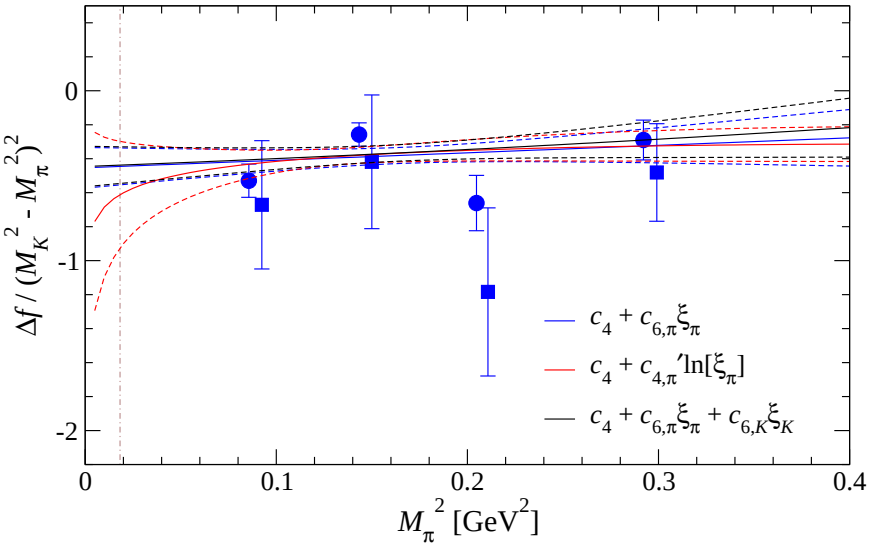

- modeling Δf (as in previous studies)

$$\Delta f = (M_K^2 - M_\pi^2)^2 (\, c_4 \quad + c_4' \ln[\xi_\pi], \quad c_4'' \ln^2[\xi_\pi], \quad c_{6,\pi}\xi_\pi, \quad c_{6,K}\xi_K)$$

5.1 chiral fit : $f_+(0)$

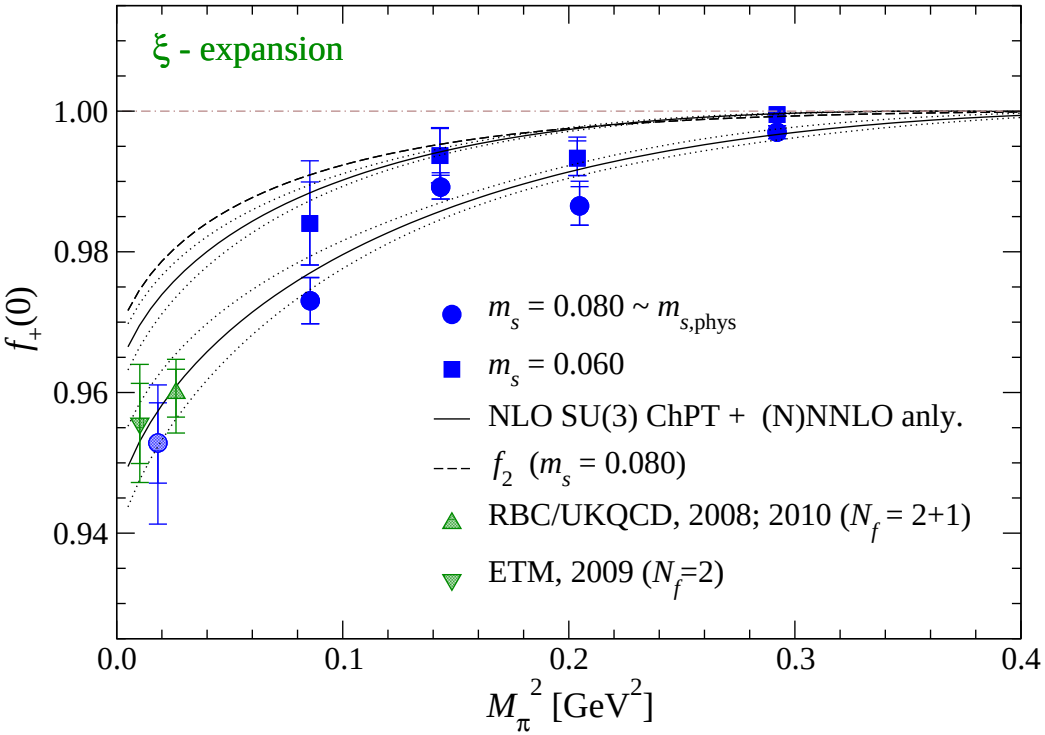

fit results

- test parameterizations of Δf
  - $c_4 + c_{6,\pi}\,\xi_\pi \;\Rightarrow$ central value
  - c_4
  - $c_4 + c_{6,\pi}\,\xi_\pi + c_{6,K}\,\xi_K$
  - $c_4 + c'_{4,\pi}\,\ln[\xi_\pi]$ (ill-determined c_X)
  - fit excluding largest m_{ud}
- assume $O((a\Lambda)^2)$ error in $f_2 + \Delta f$

$$f_+(0) = 0.953(6)_{\mathrm{stat}}\,\binom{+4}{-9}_{\mathrm{chiral}}\,(4)_{a\neq 0}$$

5.1 chiral fit : $f_+(0)$

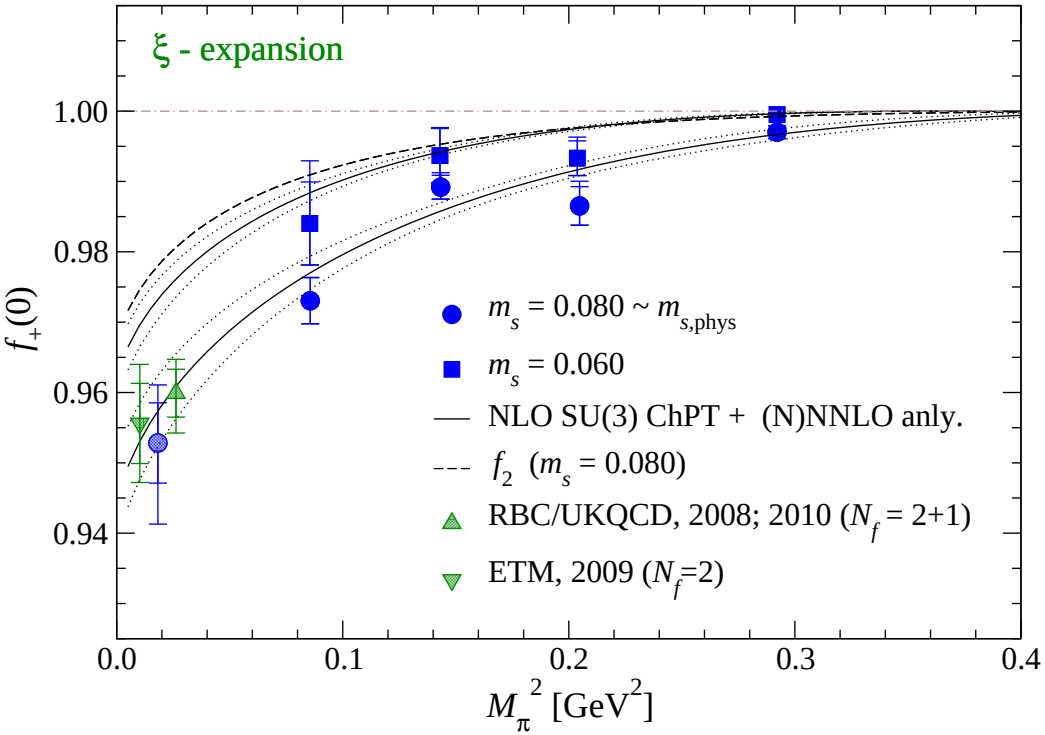

fit results

- test parameterizations of Δf
  - $c_4 + c_{6,\pi}\,\xi_\pi$ $\Rightarrow$ central value
  - c_4
  - $c_4 + c_{6,\pi}\,\xi_\pi + c_{6,K}\,\xi_K$
  - $c_4 + c'_{4,\pi}\,\ln[\xi_\pi]$ (ill-determined c_X)
  - fit excluding largest m_{ud}
- assume $O((a\Lambda)^2)$ error in $f_2 + \Delta f$

$$f_+(0) = 0.953(6)_{\rm stat}\,\binom{+4}{-9}_{\rm chiral}\,(4)_{a\neq 0}$$

CKM unitarity

$|V_{us}|f_+(0) = 0.2163(5)$ *(FlaviaNet, 2010)* $\Rightarrow$ $|V_{us}| = 0.2270(+20/-27)$

$|V_{ud}| = 0.9743(2)$, $|V_{ub}| \sim 10^{-3}$ (ICHEP'10)

$$\Delta_{\rm CKM} = |V_{ud}|^2 + |V_{us}|^2 + |V_{ub}|^2 - 1 = 0.0007(+9/-13)$$

5.2 chiral fit : $\langle r^2\rangle_V^{K\pi}$

slope of $f_+(q^2)$

- $f_+(q^2) \;=\; f_+(0)\left\{1 + (1/6)\langle r^2\rangle_V^{K\pi} q^2 + \cdots\right\}$
- SU(3) NLO ChPT *(Gasser-Leutwyler, 1985)* + NNLO analy., ξ-expansion,

  $\langle r^2\rangle_V^{K\pi} \;=\; 12L_9^r/F_\pi^2 - (1/F_\pi^2)$ "logs" $+\, c_\pi\xi_\pi \,+\, c_K\xi_K$

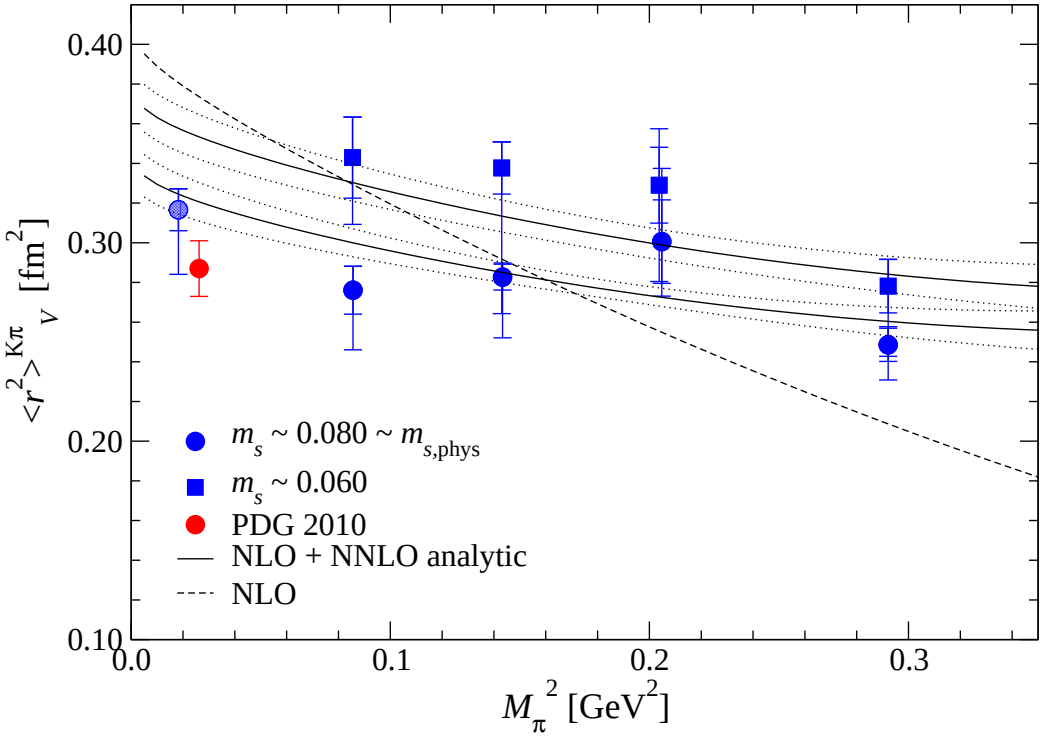

- significant NNLO @ $m_{ud(s),\mathrm{sim}}$

  $\Rightarrow$ milder m_{ud}-dependence

  $\Leftrightarrow$ $\langle r^2\rangle_V^{\pi}$, $\langle r^2\rangle_V^{K}$ *(JLQCD, $N_f = 2, 3$)*
- $L_9^r(M_\rho)$: consistent w/ pheno.
  - $L_9^r = 6.2(0.5)(2.7) \times 10^{-3}$
  - pheno. : $5.91(4) \times 10^{-3}$

    (Bijnens, 2007, ξ-expansion)
- $\langle r^2\rangle_V^{K\pi}$: consistent w/ exp't

5.3 chiral fit : $\xi(0) = f_-(0)/f_+(0)$

$\xi(q^2)$ vs q^2

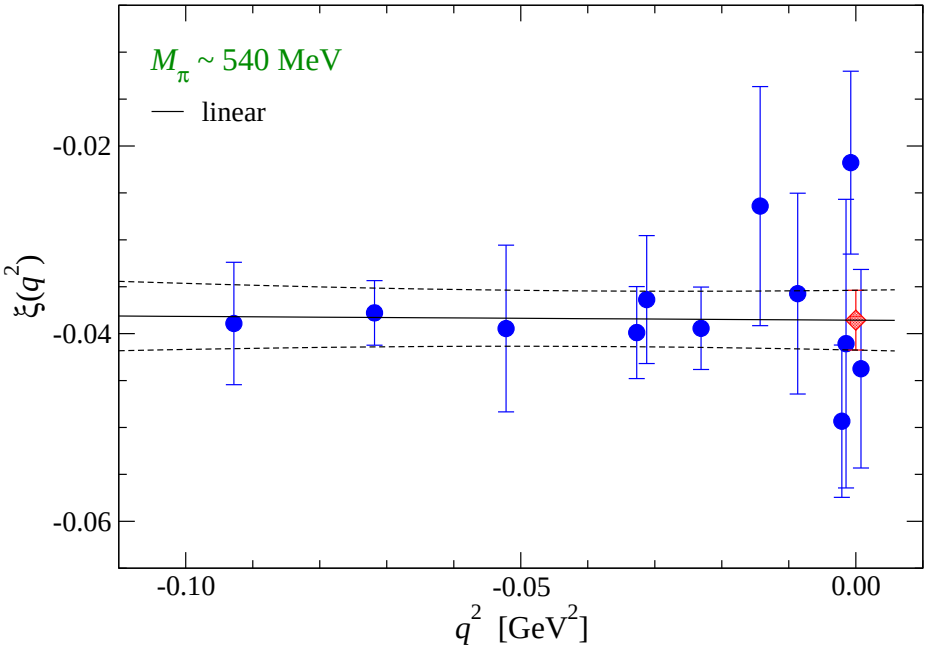

$\xi(0)$ vs $M_K^2 - M_\pi^2$

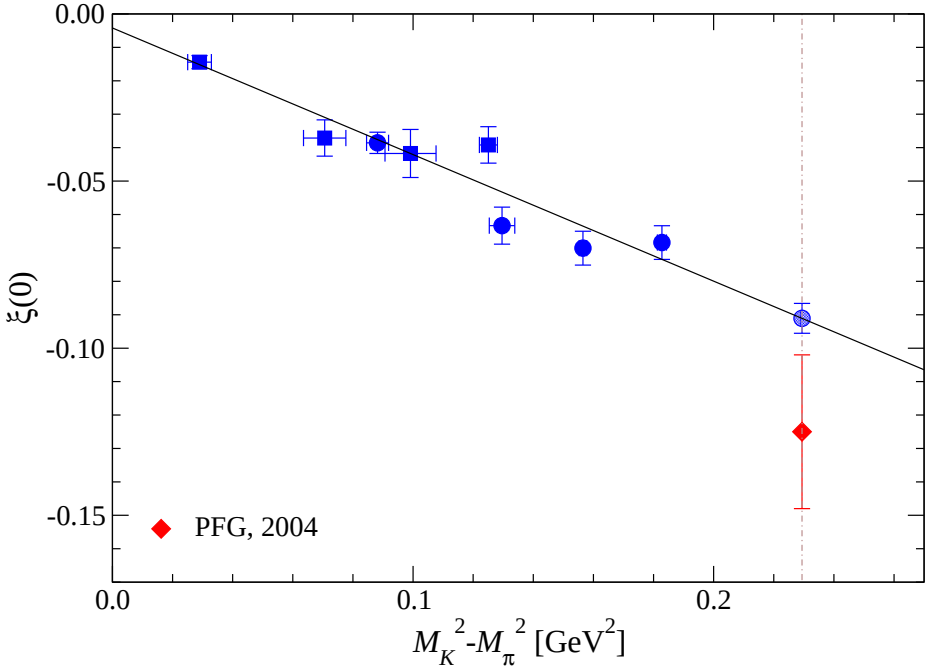

- mild q^2 dependence w/ our statistical accuracy

$$cf. \quad f_{-,\text{analy}}(q^2) \;=\; (M_K^2 - M_\pi^2)\,(4L_5^r/F_\pi^2 - 2L_9^r/F_\pi^2) \quad \textit{(Bijnens-Talavera 2003)}$$

- (for simplicity) fit form linear in $(M_K^2 - M_\pi^2)$: $\xi(0) = c_0 + c_1(M_K^2 - M_\pi^2)$
  - vanish in SU(3) limit as expected : $c_0 = -0.0017(9)$
  - consistent w/ experiment : $\xi(0) = -0.125(23)$ *(PDG 2004, K_{l3}^+)*
  - one-loop chiral log.s (and two-loops?) should be included *(Bijnens-Talavera 2003)*

6. summary

kaon semileptonic form factors in $N_f = 2 + 1$ QCD with overlap quarks

- techniques
  - all-to-all propagators $\Rightarrow$ precise determination of $f_{+,0}(q^2)$
  - TBCs $\Rightarrow$ precise determination of $f_+(0)$, $\xi(0)$, $\langle r^2 \rangle_{V,S}^{K\pi}$
  - reweighting $\Rightarrow$ additional m_s
- chiral fits
  - $f_+(0) = 0.953(6)_{\rm stat}\,(^{+4}_{-9})_{\rm chiral}(4)_{\rm a\neq 0}, \quad |V_{us}| = 0.2270(^{+17}_{-26}),$

    $\Delta_{\rm CKM} = |V_{ud}|^2 + |V_{us}|^2 + |V_{ub}|^2 - 1 = 7\,(^{+9}_{-13}) \times 10^{-4}$
  - $\langle r^2 \rangle_V^{K\pi}$, $\xi(0)$: reasonably consistent w/ exp't
- future directions
  - further refinements $\Leftrightarrow$ more rigorous treatment of NNLO $\Leftrightarrow$ overlap quarks
  - π, K EM form factors $\Leftrightarrow$ test of ChPT
  - D, B meson decays $\Leftrightarrow$ flavor physics

7.1 chiral fit : $f_+(0)$

F_0

- phenomenological estimates

  (Bijnens @ Lattice'07; $\mu = 0.77$ GeV)

$10^3 L_4^r$	$\equiv 0$	$\equiv 0.5$	$\equiv 0.2$
$10^3 L_6^r$	$\equiv 0$	$\equiv 0.1$	$\equiv 0$
F_0[MeV]	87.7	70.4	80.4

- JLQCD's analysis *(Noaki @ Lattice'10)*
  - NNLO fit to $M_{\{\pi,K\}}$, $F_{\{\pi,K\}}$
  - chiral expansion w/ M_π^2/F_π^2 instead of M_π^2/F_0
    $\Rightarrow$ better convergence
  - single lattice spacing $\sim$ 0.11 fm
  - $F_0 = 52.5(5.1)$ MeV

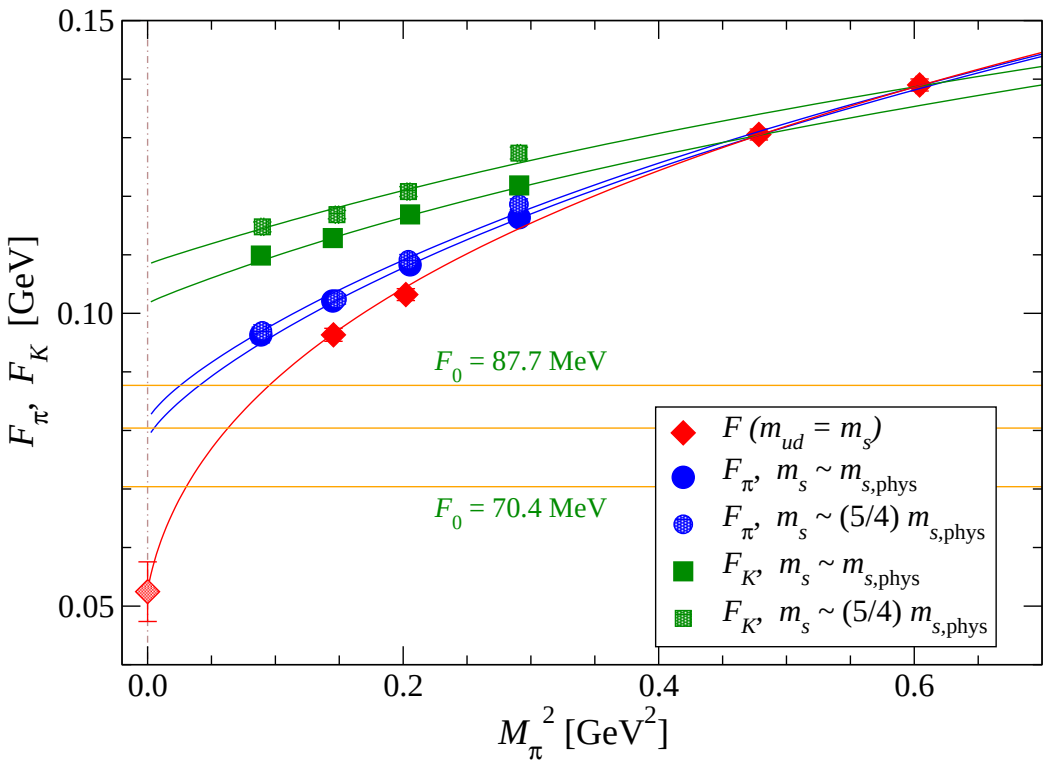

small F_0 $\Rightarrow$ enhance chiral corrections : NLO $\propto 1/F_0^2$; NNLO $\propto 1/F_0^4$

Progress Towards $\Delta \mathrm{I} = 1/2\ \mathrm{K} \to \pi\pi$ Decays with G-parity Boundary Conditions

Christopher Kelly
Columbia University

Outline

- Motivation
- Challenges
- G-Parity Implementation
- G-Parity Contractions
- The Strange Quark
- Conclusions and Outlook

Motivation

$\mathrm{K} \to \pi\pi$ Decays

- Direct CP-violation first observed in $K \to \pi\pi$ decays.
- Two types of decay:

$$\begin{aligned} \Delta I = 3/2 \ &: K^+ \to (\pi^+\pi^0)_{I=2} \quad \text{with amplitude } A_2 \\ \Delta I = 1/2 \ &: K^0 \to (\pi^+\pi^-)_{I=0} \\ & \quad K^0 \to (\pi^0\pi^0)_{I=0} \quad \text{with amplitude } A_0 \end{aligned}$$

- Direct CP-violation: $\epsilon' = \dfrac{i\omega e^{i(\delta_2-\delta_0)}}{\sqrt{2}}\left(\dfrac{\mathrm{Im}A_2}{\mathrm{Re}A_2} - \dfrac{\mathrm{Im}A_0}{\mathrm{Re}A_0}\right)$

  where

  $\omega = \mathrm{Re}A_2/\mathrm{Re}A_0$ and δ_I are strong rescattering phase shifts.

- Strong interactions very important – origin of the so-called $\Delta I = 1/2$ rule: preference to decay to $I = 0$ final state. Mechanism for this is not yet understood.

$\mathrm{K} \to \pi\pi$ Decays on the Lattice.

- Direct calculation of $K \to \pi\pi$ decays essential to understanding $\Delta I = 1/2$ rule and in the search for BSM physics.
- Lattice computation of realistic decays has only recently become possible.
- RBC & UKQCD recently published (arXiv:1111.1699) calculation of $\Delta I = 3/2$ decay using:
  - 2+1f domain wall fermions on a $32^3 \times 64 \times 32$ lattice with $a^{-1} = 1.37(1)\ \mathrm{GeV}$.
  - Near physical pions: $m_\pi^{PQ} \sim 140\ \mathrm{MeV}, m_\pi^{\mathrm{uni}} \sim 170\ \mathrm{MeV}$
  - Energy conserving decays
- Determined $\mathrm{Re}A_2$ and $\mathrm{Im}A_2$.

$\mathrm{K} \to \pi\pi$ Decays on the Lattice.

- Combining results of $\Delta I = 3/2$ calculation with experimental value for ϵ'/ϵ, we obtained first value for $\mathrm{Im}A_0$
- Calculation of A_0 from first principles is much more difficult.

Challenges

Forming the $\pi\pi$ Propagator

- $\pi\pi$ state has vacuum quantum numbers, hence there are disconnected diagrams:

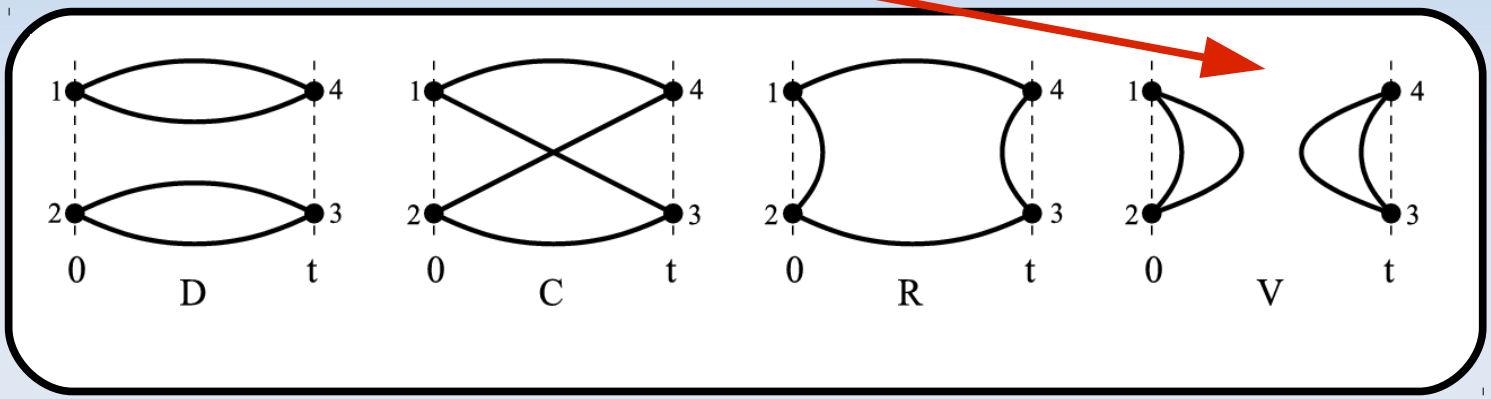

- Need large statistics and many source positions (or A2A/AMA propagators) to resolve.
- With Blue Gene/Q resources we can now perform such calculations with large enough physical volumes.

Physical Kinematics

- Best method is to use a stationary kaon and pions moving with equal momentum in opposite directions.
- This is an excited state of the $\pi\pi$ system – normally require very large statistics for decent signal.
- Instead impose antiperiodic BCs on d-quark propagator. $\pi^{\pm}$ gains momentum π/L, but for π^0 the p's cancel.
- This breaks isospin symmetry! However for $\Delta I = 3/2$ we can use Wigner-Eckart theorem and isospin to relate $\Delta I_z = 1/2\ K^+ \to \pi^+\pi^0$ to $\Delta I_z = 3/2\ K^+ \to \pi^+\pi^+$.
- As $\pi^+\pi^+$ is only charge-2 final state (q-conservation still true), isospin breaking becomes unimportant as this state cannot mix with $I = 0$ states.
- Note: In practise we needed APBC in 2 dirs for physical kinematics.

Physical Kinematics

- For $\Delta I = 1/2$ the Wigner-Eckart trick cannot be used.
- Isospin-breaking BCs would allow mixing between $I = 0$ and $I = 2$ final states. Separation would be difficult.
- Need to apply BCs that commute with isospin.
- Also, for $\Delta I = 1/2$ the vacuum plays a role, so the BCs must be applied to both the valence and sea quarks.

G-Parity Boundary Conditions

- G-parity is a charge conjugation followed by a 180 degree isospin rotation about the y-axis:

$$\hat{G} = \hat{C} e^{i\pi \hat{I}_y} \quad : \qquad \begin{aligned} \hat{G}|\pi^{\pm}\rangle &= -|\pi^{\pm}\rangle \\ \hat{G}|\pi^{0}\rangle &= -|\pi^{0}\rangle \end{aligned}$$

- At the quark level:

$$\hat{G}\begin{pmatrix} u \\ d \end{pmatrix} = \begin{pmatrix} -C\bar{d}^T \\ C\bar{u}^T \end{pmatrix} \text{ where } C = \gamma^2\gamma^4 .$$

- G-parity commutes with isospin.
- Pions are all eigenstates with e-val -1, hence G-parity BCs make pion wavefunctions antiperiodic, with minimum momentum π/L.

G-Parity Implementation

Gauge Field Boundary Conditions

- d-field becomes $C\bar{u}^T$ across the boundary. Consider a bilinear on the boundary under a gauge transformation V :

$$\bar{d}(L-1)U_y(L-1)C\bar{u}^T(0)$$
$$\longrightarrow \bar{d}(L-1)V^\dagger(L-1)U_y(L-1)V^*(0)C\bar{u}^T(0)\,.$$

- Link must transform as

$$U_y(L-1) \to V(L-1)U_y(L-1)V^T(0)$$

- Link parallel to boundary on on other side $(y \geq L)$ must then transform as:
- $U_x(x,y,..) \to V^*(x,y,..)U_x(x,y,..)V^T(x+1,y,..)$
- Gauge fields therefore obey complex-conjugate BCs.

The Two-Flavor Method

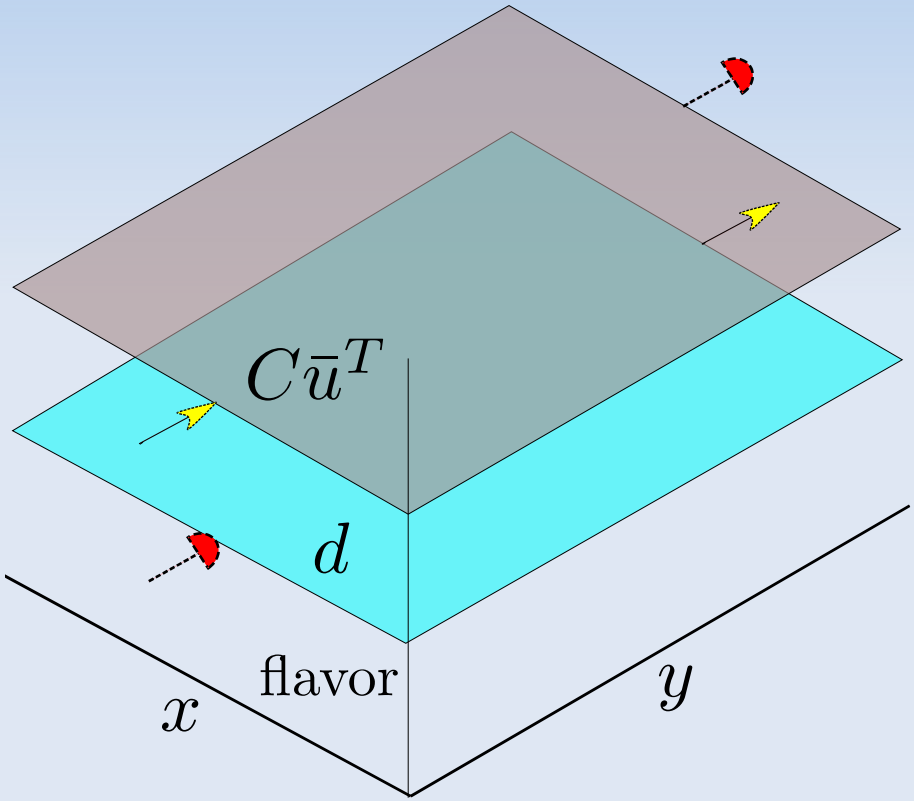

- Two fermion fields on each site indexed by flavor index:

$$\psi^{(1)}(x) = d(x),\ \psi^{(2)}(x) = C\bar{u}^T(x)$$

- BCs are:

$$\psi^{(1)}(x + L\hat{y}) = \psi^{(2)}(x),$$
$$\psi^{(2)}(x + L\hat{y}) = -\psi^{(1)}(x),$$

- Periodic BCs in other dirs.
- Single U-field shared by both flavors, with complex conj BCs.
- Dirac op for $\psi^{(2)}$ uses U_μ^*.

The One-Flavor Method

- Obtain equivalent formulation by unwrapping flavor indices onto two halves of doubled lattice:

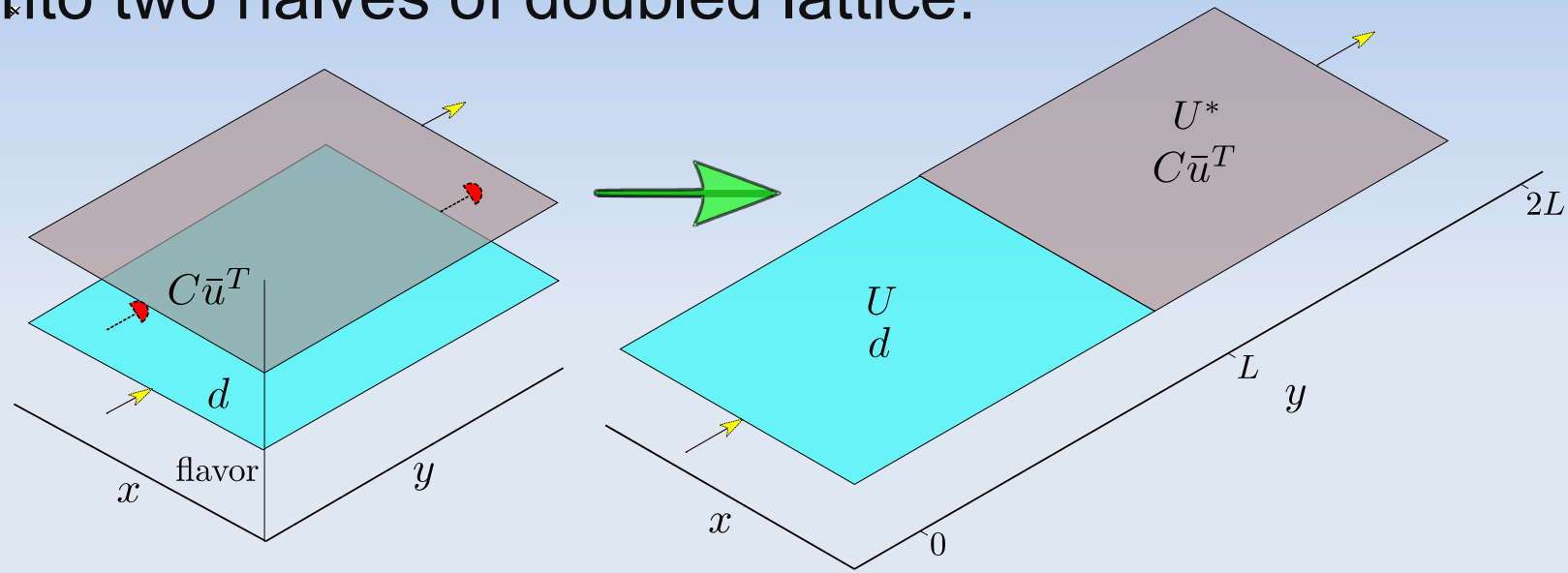

- Antiperiodic boundary conditions in G-parity direction.
- U-field on first half and U^*-field on second half.

Choosing an Approach

- One flavor setup is much easier to implement.
- However recall that we needed APBC in 2 directions for physical kinematics in $\Delta I = 3/2$ calculation.
- G-parity in >1 dir using one-flavor method requires doubling the lattice again, which is highly inefficient.
- A second approach requires non-nearest neighbour communication:

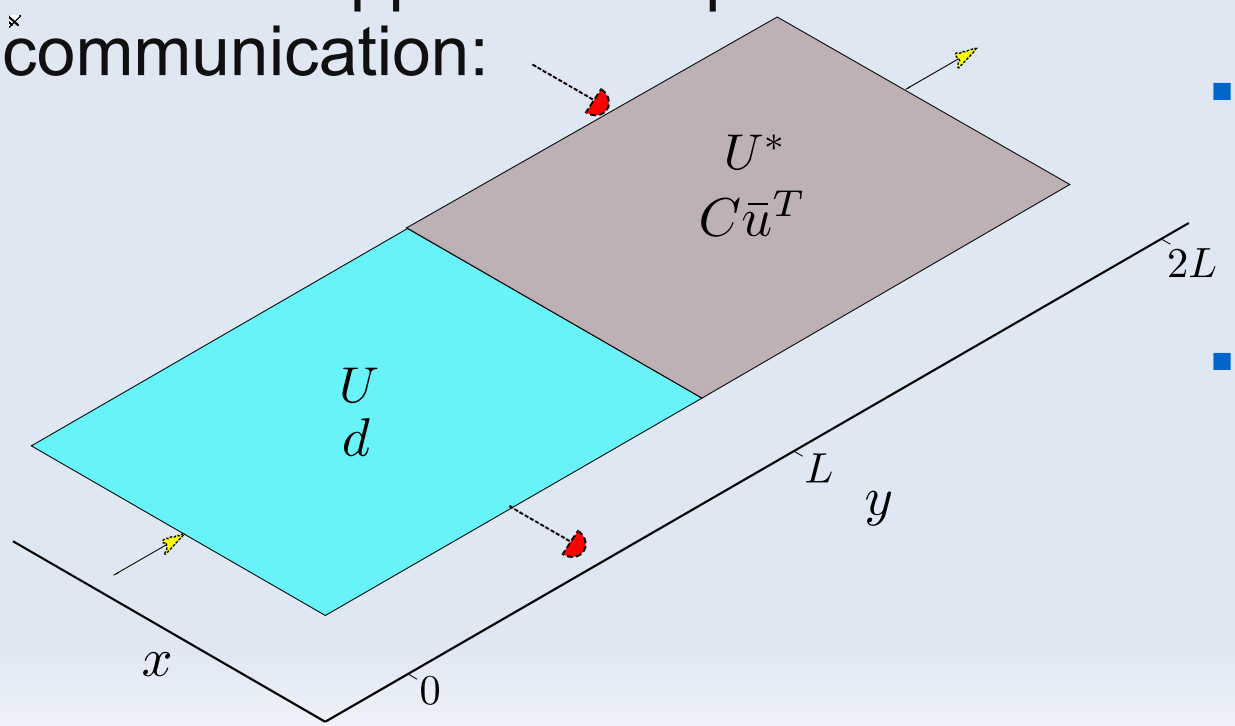

- Also inefficient depending on machine architecture.
- Choose to implement two-flavor method.

G-Parity Contractions

Unusual Contractions

- Flavor mixing at boundary allows contraction of up and down fields:

$$\overbracket{\psi_x^{(2)}\bar{\psi}_y^{(1)}} = \mathcal{G}_{x,y}^{(2,1)} = C\overbracket{\bar{u}_x^T\bar{d}_y}\,,$$
$$\overbracket{\psi_y^{(1)}\bar{\psi}_x^{(2)}} = \mathcal{G}_{y,x}^{(1,2)} = -\overbracket{d_y u_x^T}C^T$$

- Interpret as boundary creating/destroying flavor (violating baryon number):

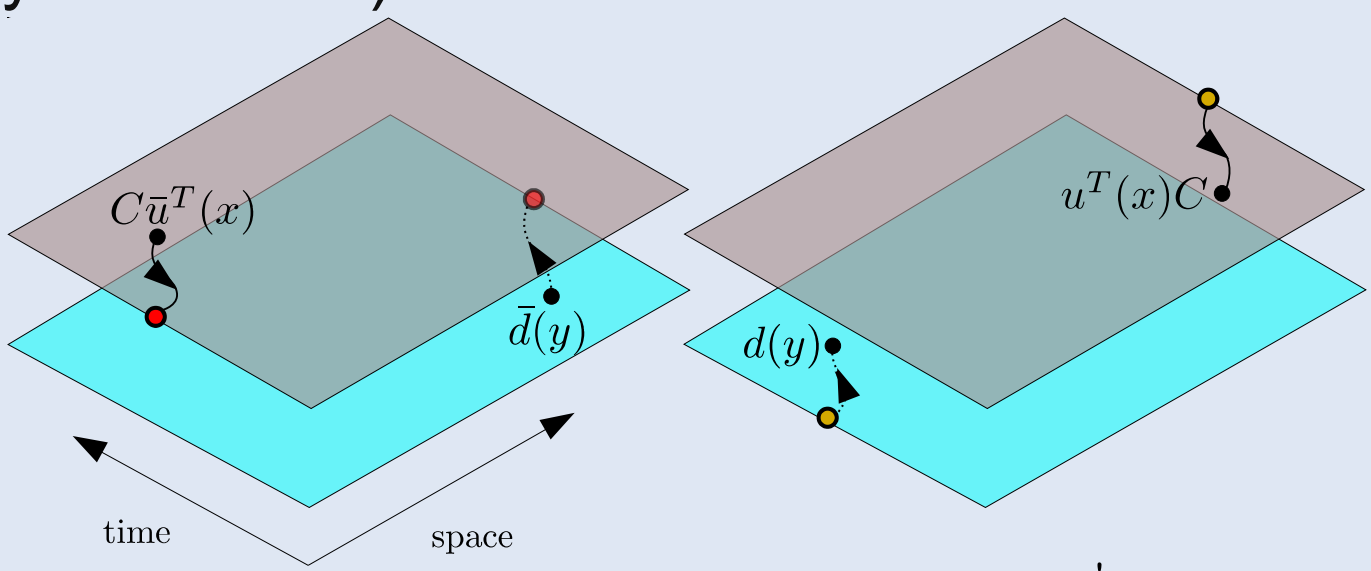

- Also have γ^5-hermiticity: $\left[\gamma^5\mathcal{G}_{x,y}^{(2,1)}\gamma^5\right]^\dagger = \mathcal{G}_{y,x}^{(1,2)}$

Pion Correlation Functions

- π^+ correlation function

$$\langle \bar{d}_x \gamma^5 u_x \bar{u}_y \gamma^5 d_y \rangle = \langle \bar{\psi}_x^{(1)} [\gamma^5 C] \bar{\psi}_x^{(2)\,T} \psi_y^{(2)\,T} [C\gamma^5] \psi_y^{(1)} \rangle$$

- Now has *two* contractions:

$$\mathrm{tr}\left\{ \mathcal{G}_{x,y}^{(1,1)\,T} C\gamma^5 \mathcal{G}_{x,y}^{(2,2)} \gamma^5 C \right\} + \mathrm{tr}\left\{ \mathcal{G}_{x,y}^{(1,2)\,T} C\gamma^5 \mathcal{G}_{x,y}^{(2,1)} \gamma^5 C \right\}$$

arrows point from source to sink

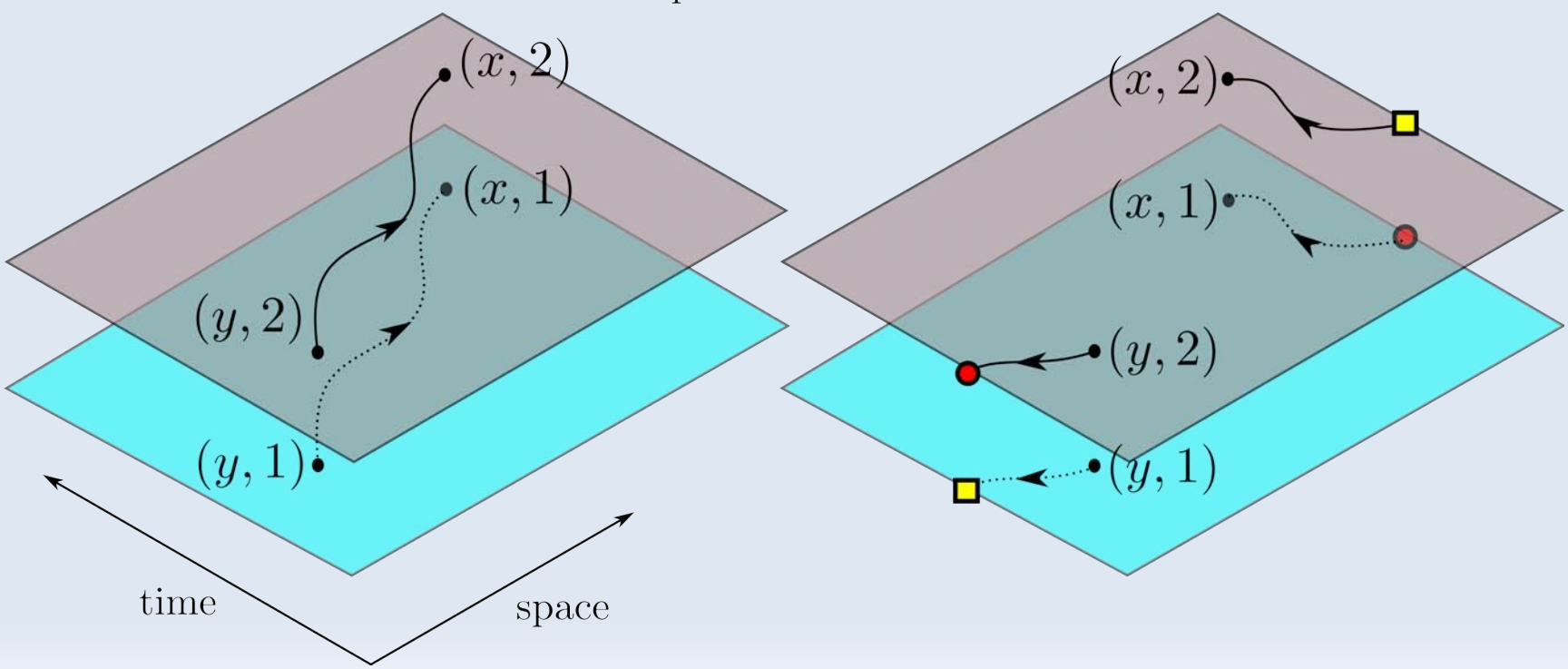

Results: Pion Correlator

- Generated an $8^3 \times 32 \times 10$ DWF quenched ensemble.
- ~150 configs (20 MD tu's sep) with G-parity in 0,1,2,3 dirs.
- Coulomb-gauge fixed wall source propagators.

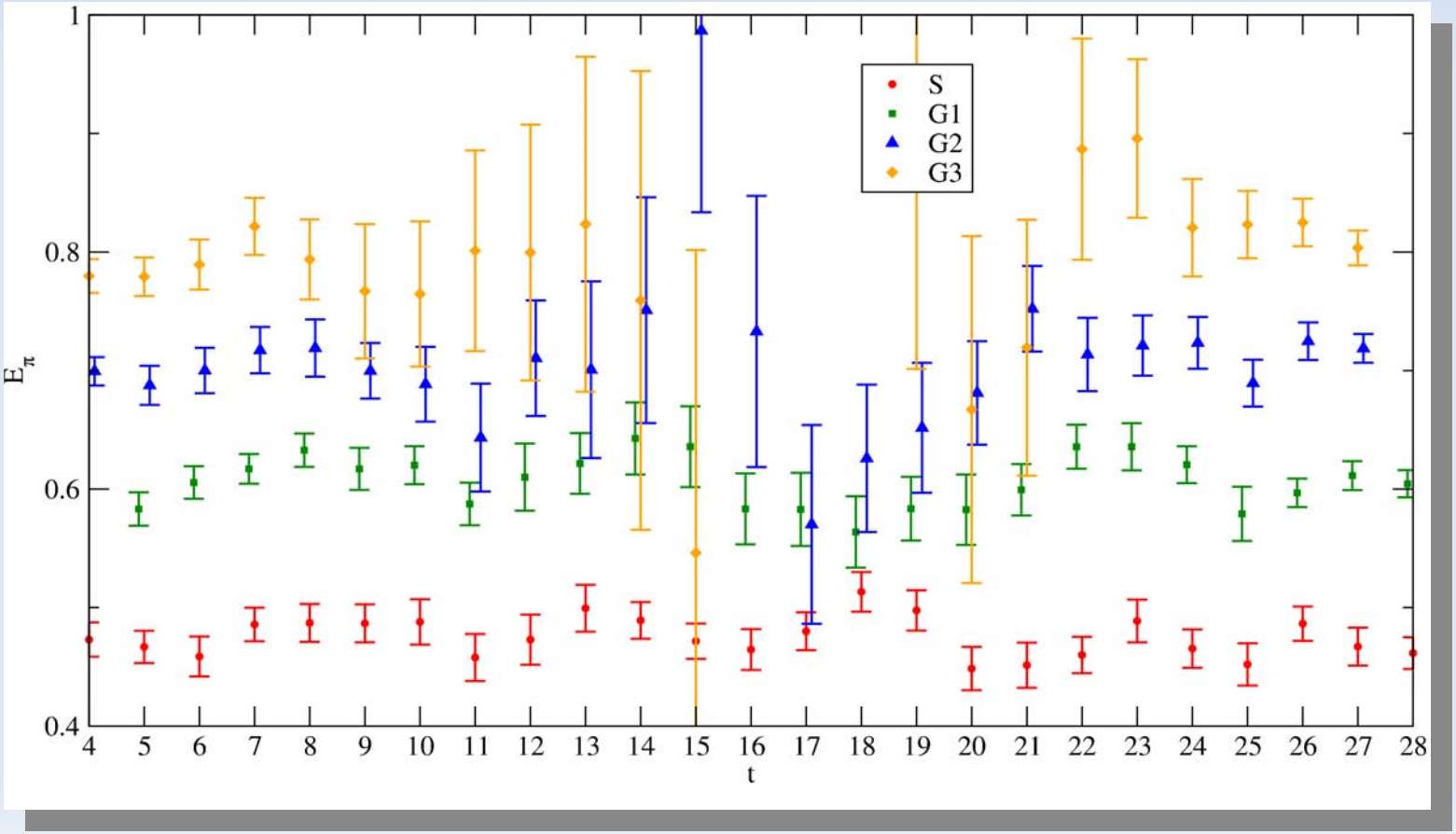

Results: Pion Dispersion Relation

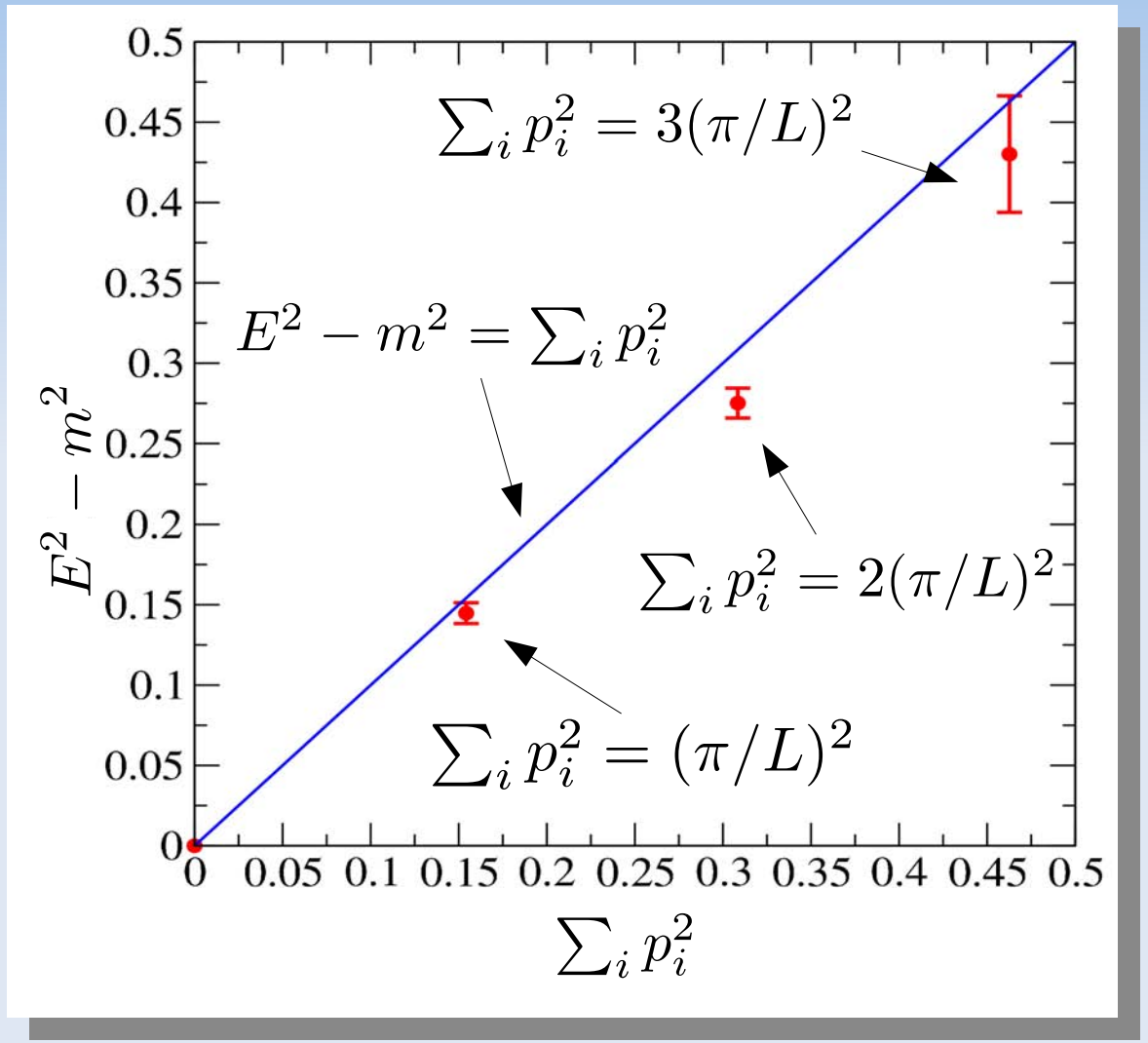

- Deviations from continuum disp. reln. expected on lattice. e.g. free-field: $E^2 - m^2 = \sum_i \sin^2(p_i)$

The Strange Quark

Kaons

- $K \to \pi\pi$ calculation needs stationary K^0.
- $\frac{1}{\sqrt{2}}(\bar{s}d + \bar{d}s)$ not a G-parity eigenstate.

- Need an eigenstate with e-val +1 for periodic BCs and hence $p_{\min} = 0$.
- Introduce 'strange isospin' (I'): s-quark in doublet $\begin{pmatrix} s' \\ s \end{pmatrix}$
- A neutral kaon-like state:

$$K_0' = \frac{1}{2}(\bar{s}d + \bar{d}s + \bar{s}'u + \bar{u}s')$$

  is an eigenstate of 'modified G-parity': $\hat{G} = \hat{C}e^{i\pi\hat{I}_y}e^{i\pi\hat{I}'_y}$ with e-val +1.

- Need factor of 2 in decay calc as only 1/2 of components of initial kaon couple to $\pi\pi$.

Locality

- Theory has one too many flavors. Must take square-root of s'/s determinant in evolution to revert to 3 flavors.
- Determinant becomes non-local.
- Non-locality is however only a boundary effect that vanishes as $L \to \infty$. With sufficiently large volumes the effect should be minimal.

Charged Kaon Correlator

- K^+ analogue: $|K^{+\prime}\rangle = (\bar{u}\gamma^5 s - \bar{s}'\gamma^5 d)|0\rangle$
- 2-point function has 4 contractions:

$$\mathrm{tr}\left\{\mathcal{G}^{(2,2)\,T}_{x,y}\gamma^5 C\mathcal{G}^{(3,3)}_{x,y}\gamma^5 C\right\} + \mathrm{tr}\left\{\mathcal{G}^{(4,4)\,T}_{x,y}\gamma^5 C\mathcal{G}^{(1,1)}_{x,y}\gamma^5 C\right\}$$
$$-\mathrm{tr}\left\{\mathcal{G}^{(1,2)\,T}_{x,y}\gamma^5 C\mathcal{G}^{(4,3)}_{x,y}\gamma^5 C\right\} - \mathrm{tr}\left\{\mathcal{G}^{(3,4)\,T}_{x,y}\gamma^5 C\mathcal{G}^{(2,1)}_{x,y}\gamma^5 C\right\}$$

- If we make the masses of the (s', s) and (u, d) doublets the same this reduces to:

$$2\mathrm{tr}\left\{\mathcal{G}^{(1,1)\,T}_{x,y}C\gamma^5\mathcal{G}^{(2,2)}_{x,y}\gamma^5 C\right\} - 2\mathrm{tr}\left\{\mathcal{G}^{(1,2)\,T}_{x,y}C\gamma^5\mathcal{G}^{(2,1)}_{x,y}\gamma^5 C\right\}$$

- This is just twice the π^+ correlation function but with the *opposite sign* between the 2 contractions.
- Periodicity of spatial dependence appears to arise due to some cancellation between the two contractions.

Results: Degenerate $K^{+\prime}$ Dispersion Relation

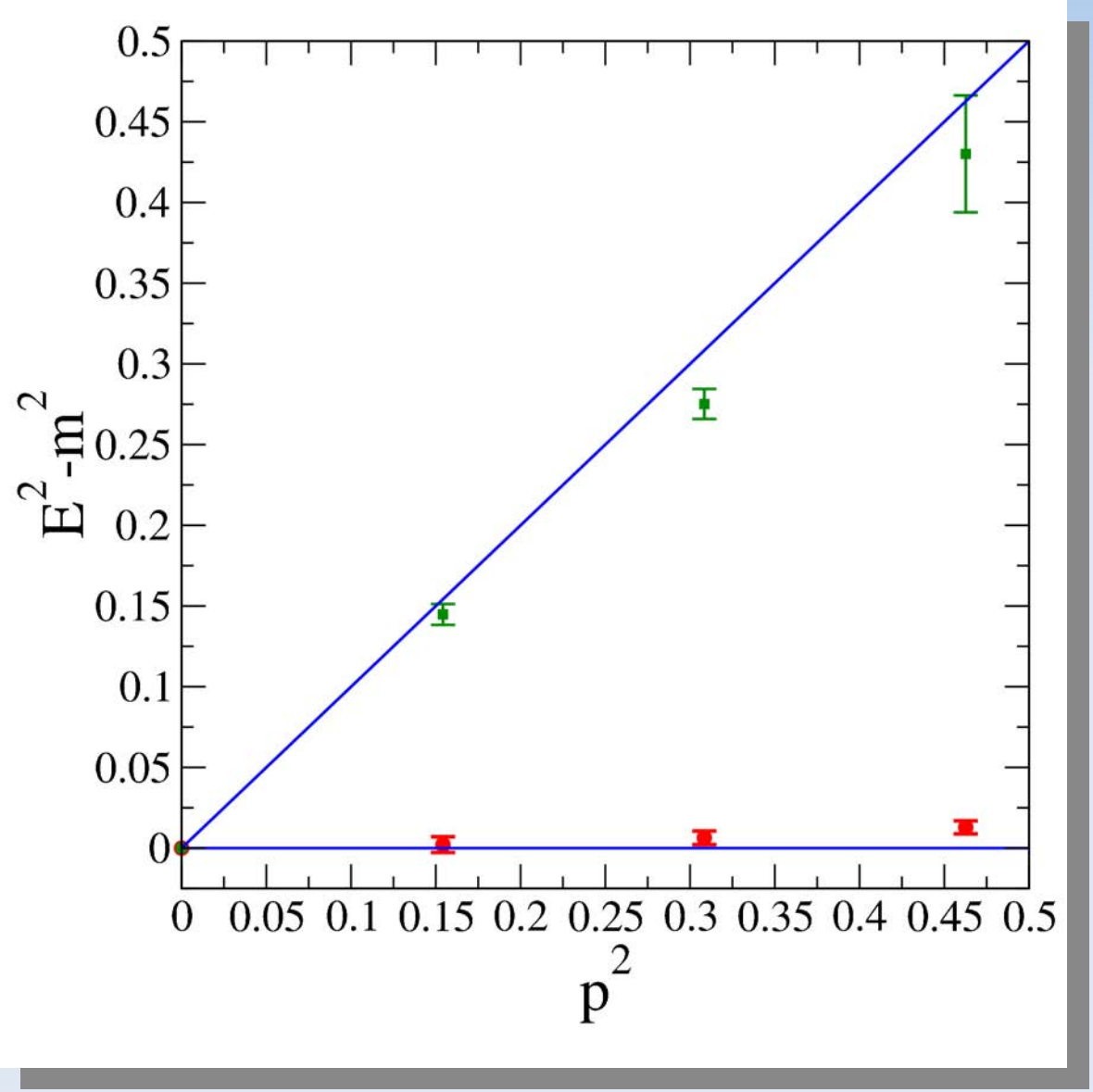

Conclusions and Outlook

Conclusions and Outlook

- G-parity boundary conditions look to be very promising for realising $\Delta I = 1/2 \; K \to \pi\pi$ decays with physical kinematics.
- Direct calculation of A_0 is essential for understanding $\Delta I = 1/2$ rule and in the search for BSM physics.
- Coding two-flavor method is challenging but significant progress has been made.
- Aim to dedicate significant BlueGene/Q resources towards generating $32^3 \times 64 \times 32$ DWF Iwasaki+DSDR ensembles with G-parity BCs and physical pions.

Recent progress in multi GPU conjugate gradient convertor with staggered fermion

New Horizons for Lattice Gauge Theory Computations at BNL 2012

Hyung-Jin Kim
Brookhaven National Laboratory

BROOKHAVEN NATIONAL LABORATORY

Introduction

1. GPU computation for HPC
   - GPGPU: General Purpose computation using GPU.
   - CUDA : C extension(API) for GPGPU by nVIDIA
   - Open CL : Standard C extension for GPGPU
2. Conjugate Gradient algorithm

   Iterative method for solving linear algebraic equations : $b = Ax$
3. CG implementation on CUDA

Why use the GPU ?

High performance computing

1. If money is not a problem~?

   - Just buy a good super computer

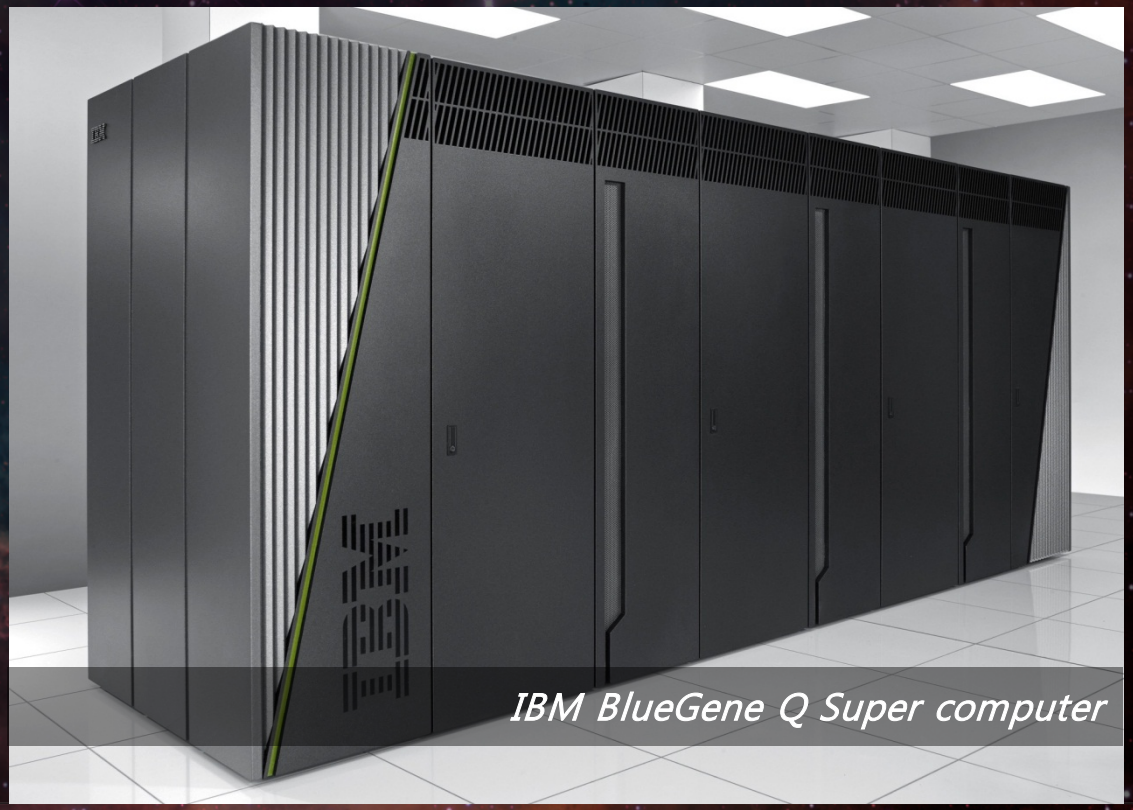

IBM BlueGene Q Super computer

Why use the GPU ?

High performance computing

2. Physicist in Korea?
   - No money.
   - Find alternative way
   - GPU Supercomputing !
     - Cost & energy effective
     - Hard to develop

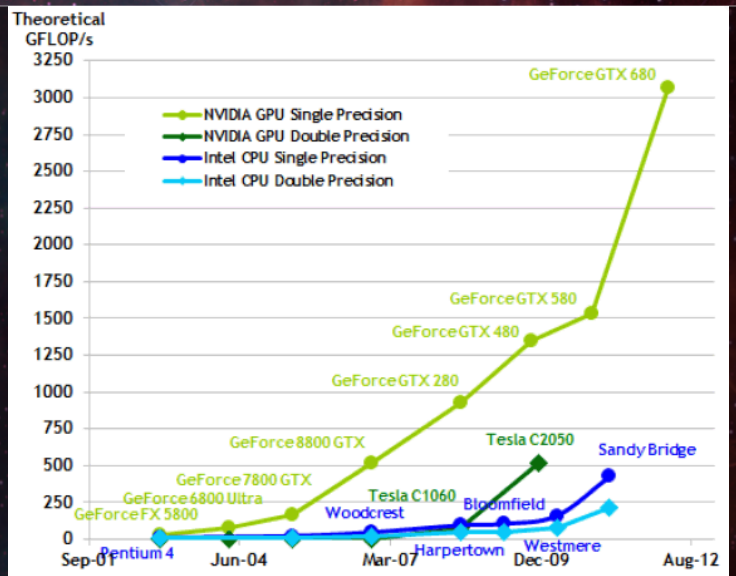

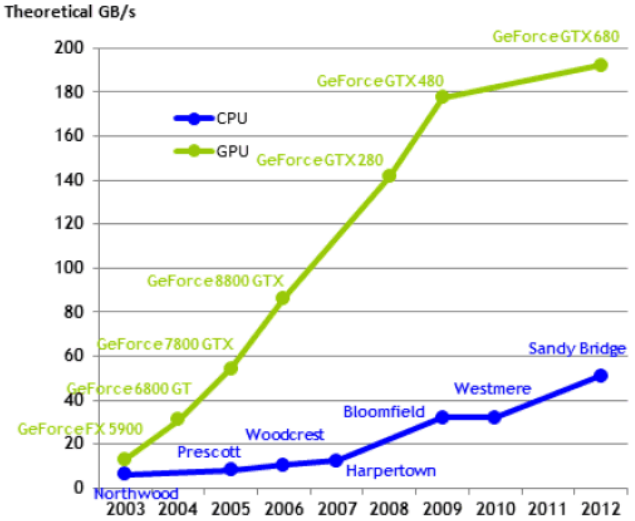

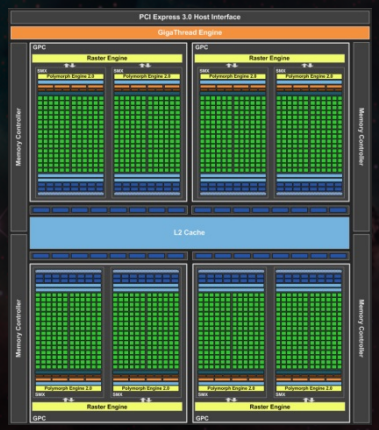

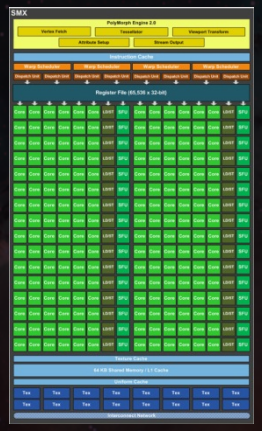

Machine Environment in SNU

David Cluster

64x GTX 480 GPUs + 16x GTX 590 GPUs
20Gb 32nodes + 40Gb 8 nodes Infiniband

- David 1, 2 GPU cluster
  - Intel core i7 920 , 32 node
  - 32 x 2 x GTX 480 GPUs
  - 20Gbps infiniband network
  - Theoretical performance

    SP : 1.34 TFLOPS / GPU

    DP : 168 GFLOPS / GPU

    Bandwidth : 177.4 GB / sec / GPU
- David 3 GPU cluster
  - Intel core i7 950 , 8 node
  - 8 x 2 x GTX 590 GPUs
  - 40Gbps infiniband network

CG Algorithm

- Conjugate gradient operation

$r = b - Ax$

$d = r$

$\delta_{new} = r\dagger r$

$\delta_0 = \delta_{new}$

Initial Condition

r : residual vector
d : directional vector
ε : tolerance
Ax(or Ad): Dirac operation

for ($i = 0$; $i < N_{dim}$ and $\delta_{new} > \varepsilon^2\delta_0$; i++){

$Tmp = Ad$

$\alpha = \delta_{new} / d\dagger Tmp$

$r = r - \alpha Tmp$

$\delta_{old} = \delta_{new}$, $\delta_{new} = r\dagger r$

$x = x + \alpha d$

$\beta = \delta_{new} / \delta_{old}$

$d = r + \beta d$

}

Update process

Staggered Dirac Operator

2. Dirac operation

- Dirac equation $h = A\chi$; $A \equiv -D^2 + m^2$

  $D_{x,y} = U_\mu(x)\delta_{y,x+\mu} - U_\mu(x-\mu)\delta_{y,x-\mu}$

  $\Rightarrow\ D\,\chi(x) = \Sigma\, U_\mu(x)\chi(x+\mu) - U_\mu(x-\mu)\chi(x-\mu)$

  $$\begin{pmatrix} x''1 \\ x''2 \\ x''3 \end{pmatrix} = \begin{pmatrix} a1 & a2 & a3 \\ b1 & b2 & b3 \\ c1 & c2 & c3 \end{pmatrix} \begin{pmatrix} x1 \\ x2 \\ x3 \end{pmatrix} - \begin{pmatrix} a'1 & a'2 & a'3 \\ b'1 & b'2 & b'3 \\ c'1 & c'2 & c'3 \end{pmatrix} \begin{pmatrix} x'1 \\ x'2 \\ x'3 \end{pmatrix}$$

- 6 $[\chi(x)]$ + 8 x 6 $[\chi(x\pm\mu)]$ + 8 x 18 $[U_\mu(x)]$ = 198 : 792 bytes(SP), 1584 bytes(DP)
- $U_\mu(x)X(x+\mu)$ part has 72 floating point calculations

  → 8 x 72 = 576 floating point calculations per site
- For 28^3 x 96 lattice, there are 10^6 of lattice even(or odd) sites

  → 0.61 Giga floating point calculations (Total 1 CG iteration = 0.624×10^9)

  → 1.55 Giga bytes(DP) of data transfer : Memory IO is major bottle neck !

C & CUDA Code Comparison

CPU code(CPS Lib.)

```
...
for(x = 0;x < Nx ;x++)
for(y = 0;y < Ny ;y++)
for(z = 0;z < Nz ;z++)
for(t = 0;t < Nt ;t++)
{
   for( μ = 0; μ < 4 ; μ++)
   {
      ...
      if( cur_l[mu] == nx[mu]-1 )
         ...
      else
         ...
      uDotXPlus(sol, U, src);
      ...
      uDagDotXMinus(sol, U, src);
      ...
   }
}
```

CUDA code

```
...
position = blockIdx.x*blockDim.x+
           threadIdx.x;
Get_location(cur_l, position);
...
for( μ= 0; μ < 4; μ++)
{
   ...
   if( cur_l[mu] == nx[mu]-1 )
      ...
   else
      ...
   uDotXPlus(sol, U, src);
   ...
   uDagDotXMinus(sol, U, src);
   ...
}
```

- Initial performance is 0.97 GFLOPS per 1 GPU(DP).
- GPU is only twice faster than CPU code (0.46GFLOPS, DP).

CUDA Optimization(1)

1. Coalesced memory access
2. Using fast on-chip memory(register & shared memory)
   - Increase data reusability
3. Adjust the code for CUDA architecture
   - Higher CUDA occupancy
   - Reduce the branch code
4. Data compression
   - SU(3) data reconstruction(8, 10, 12 parameter)
5. Using mixed precision
   - Load balancing between single precision and double precision calculation

CUDA Optimization(2)

- Coalesced Memory Access

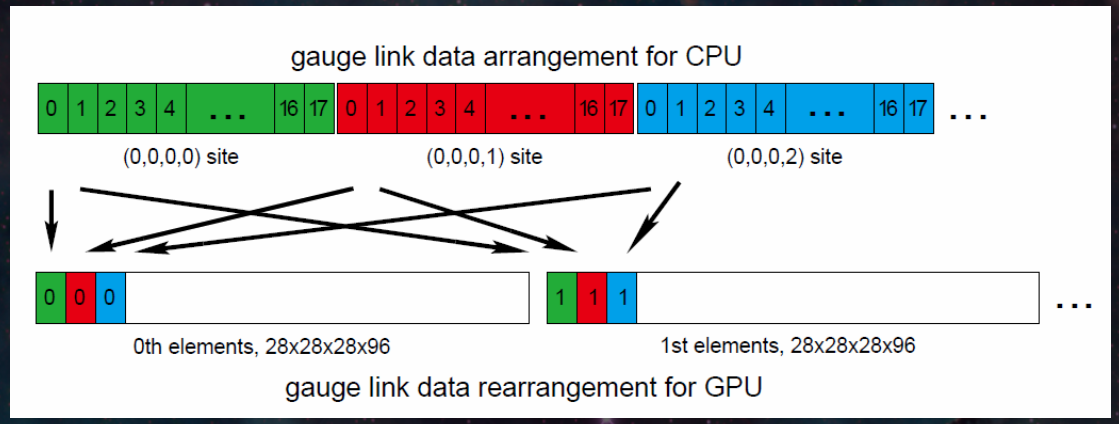

  - 64 bit memory access channel
  - Multiple data accesses by Warp(32 threads)

- Using Fast On-chip Memory (register & shared memory)

$$\begin{pmatrix} x''1 \\ x''2 \\ x''3 \end{pmatrix} = \begin{pmatrix} a1 & a2 & a3 \\ b1 & b2 & b3 \\ c1 & c2 & c3 \end{pmatrix} \begin{pmatrix} x1 \\ x2 \\ x3 \end{pmatrix} - \begin{pmatrix} a'1 & a'2 & a'3 \\ b'1 & b'2 & b'3 \\ c'1 & c'2 & c'3 \end{pmatrix} \begin{pmatrix} x'1 \\ x'2 \\ x'3 \end{pmatrix}$$

  - Output vector is accessed 6 times
  - Input vectors are accessed 2 times

CUDA Optimization(3)

- Data Reconstruction (Data Compression)
  - In most application, The performance of GPU application is bounded to memory bandwidth
  - Need to load balancing between calculation and data accessing
  - Data has SU(3) symmetry, so this property can be used for data compression
    - 8, 10, 12 parameter SU(3) reconstructions
    - Each method needs different optimization
    - 10 parameter method is chosen to production

CUDA Optimization(4)

- Using Mixed Precision
  - Performance gap between Single Precision and Double Precision in GPU
  - Tesla : DP / SP = 1/2, Geforce : DP / SP = 1/8, 1/12 or 1/24 !
  - To retrieve this performance discrepancy, mixed precision method can be used
  - The main idea of iterative refinement is using two types of iterative loops to get the true solution value.
    - At first, by using the single precision iteration, we can approach fast to the roughly estimated solution
    - Next, double precision or more precise iteration can be used to get the more accurate solution

MPI Communication

- Practical multi GPU performance
  - Network IO (include PCI-E bus IO) : bottle-neck
  - MPI(mvapich) is used for multi GPU implementing

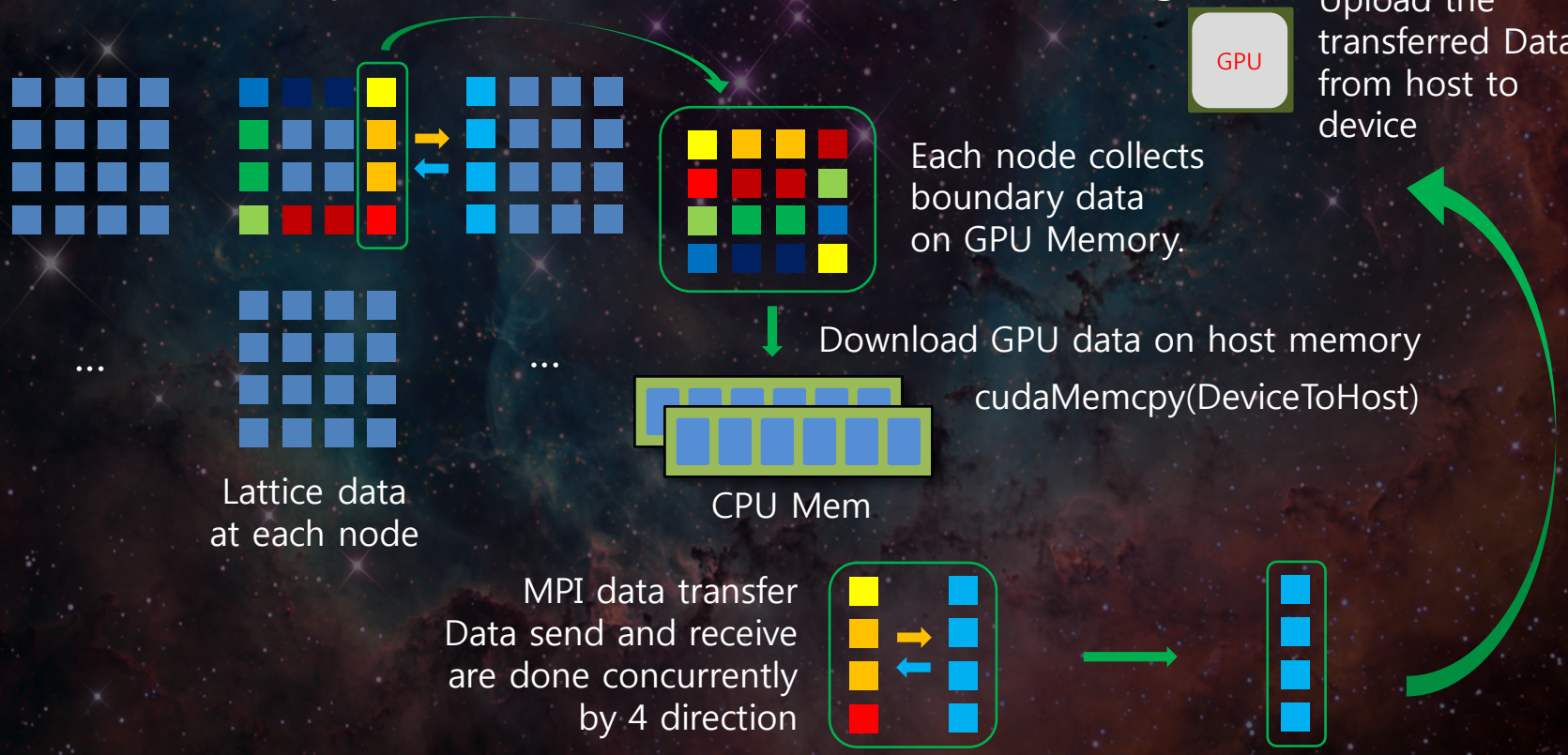

Communication Optimization(1)

1. Reduce the size of surface data

2. Reduce the unnecessary data transfer

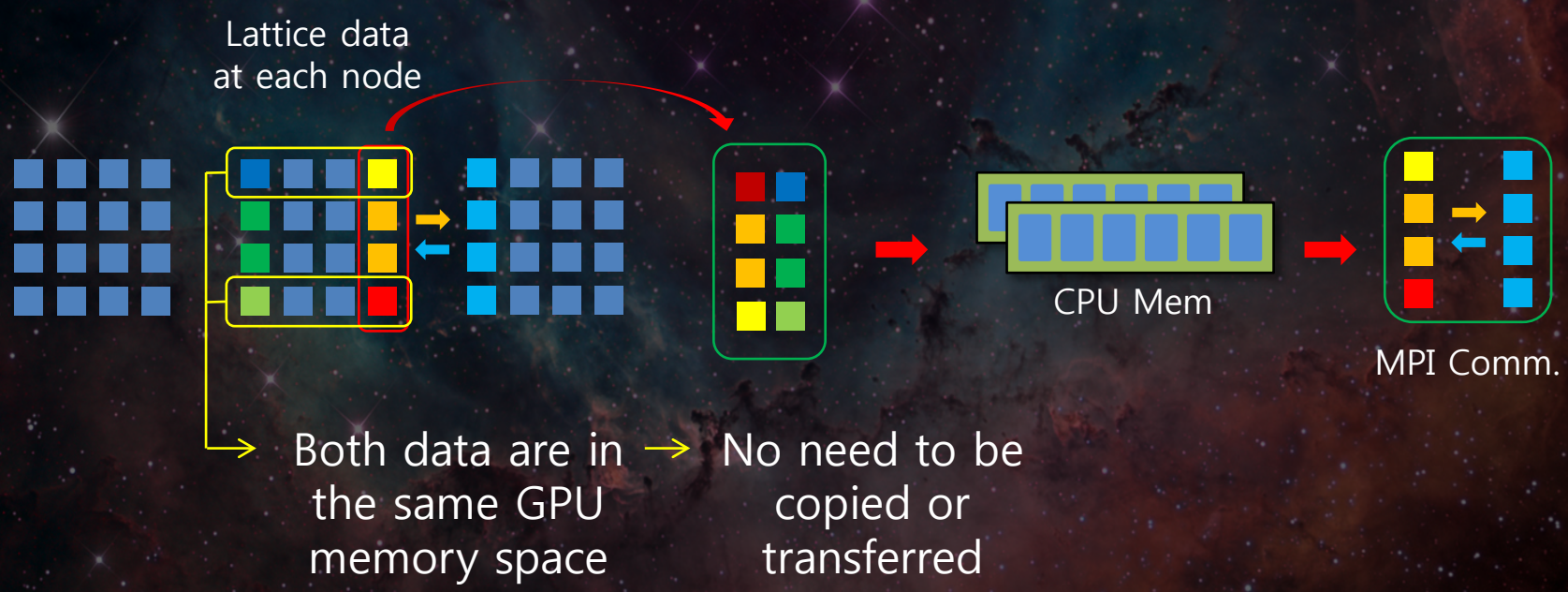

Communication Optimization(2)

3. Use GPU direct technology

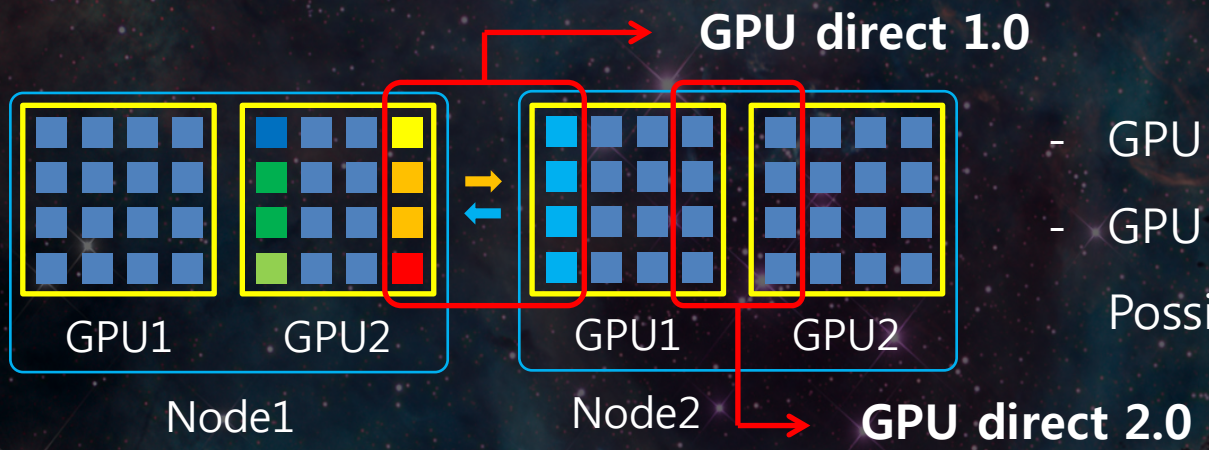

- GPU direct 1.0
- GPU direct Access

Possible only in Tesla GPU

GPU direct 2.0
Key features

- GPU direct Transfer is now implementing
- It may give ~20% enhancement on network

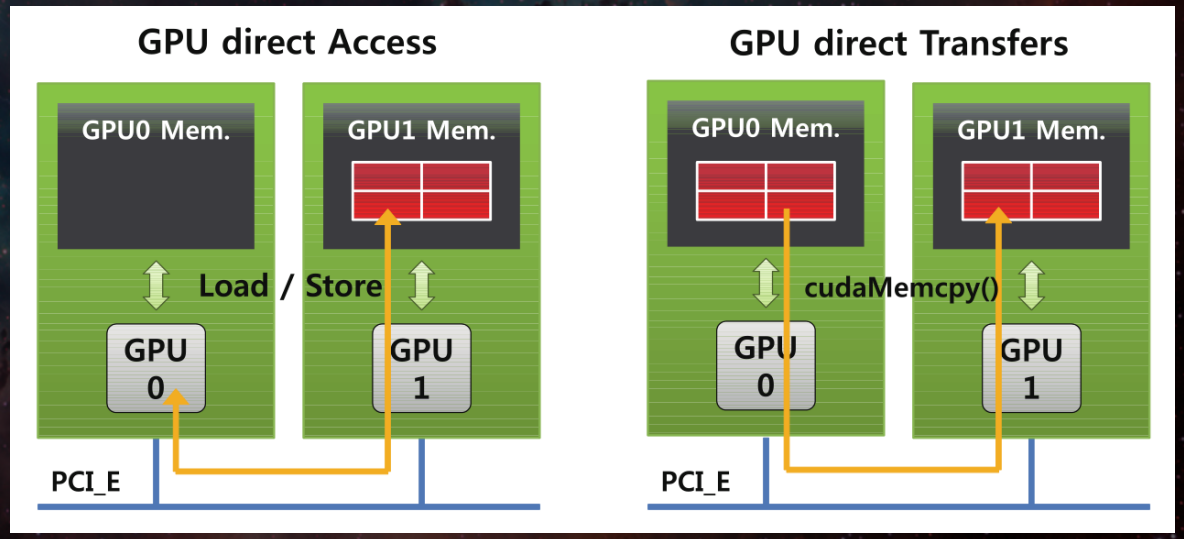

Performance (1)

- Total CG Performance(exclude network, used 4 GPU, 2896 lattice)
  - Used GTX 480 : bandwidth = 118GBytes/sec (measured), SP FLOPS = 1344 GF (ideal) , DP FLOPS = 168 GF (ideal)
  - For 1 Dirac operation,

    In double precision, it takes 2 x 2.77 ms

    → 576 x 28 x 28 x 28 x 96 /4 /2 / 0.00277

    = **55 GFLOPS**

    In single precision, it takes 2 x 1.04 ms

    → 576 x 28 x 28 x 28 x 96 /4 /2 / 0.00104

    = **145 GFLOPS**
  - Total mixed iteration = 30468(SP) + 52(DP)

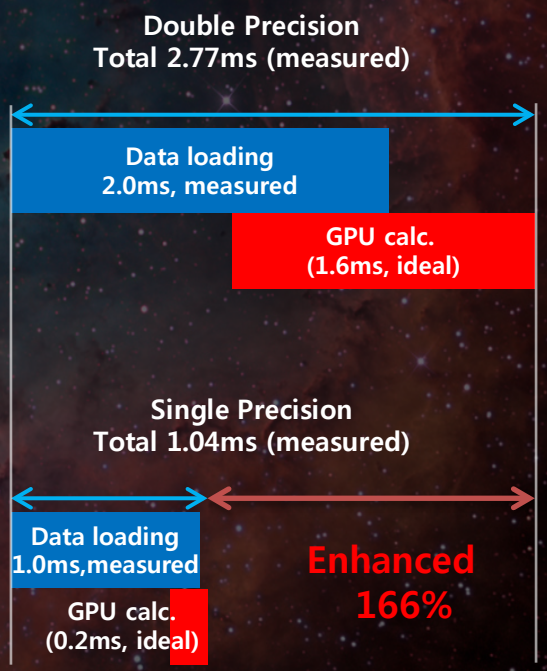

Performance (2)

- Time table of total sequence : For 1 $D\chi(x)$ operation,

GTX 480, 590 Optimized Result	Double Precision (ms)	Single Precision (ms)
GPU calculation time	2.77	1.04
boundary data collect	0.5	0.38
Memcpy GPU to CPU	1.3	0.25
MPI communication	2.1	0.6
Memcpy CPU to GPU	1.3	0.26
Total Comm. time	~5.5	~1.5
Total time	~8.3	2.6
GFLOPS(measured)	18.8	44

HISQ action

- We are also implemented HISQ action to our CG invertor
  - by Boram Yoon(in SNU)
- In single precision, for 1 Dirac operation, it takes 2 x 1.98 ms
  - 2 x 576 x 28 x 28 x 28 x 96 /6 /2 / 0.00198 = **102 GFLOPS**
  - Most of times are also used for data loading
- Include network comm., real performance is **18.2GFLOPS**
  - **Boundary data size is doubled!**
  - Optimization is still in progress

Summary

- CUDA version of CG invertor is successfully implemented on CPS library
- For better performance, many optimization method were applied
- Network communication can be optimized a little bit more
- In mixed precision, CUDA version of staggered CG invertor shows 44 GFLOPS / GPU of performance
- We are also preparing HISQ CG invertor

1+1+1 Flavor QCD+QED Simulation at the Physical Point

Y.Kuramashi (U. of Tsukuba/RIKEN AICS)
for PACS-CS Collaboration

May 16, 2012 @ BNL

Collaboration members

- Physicists:

S.Aoki, N.Ishizuka, K.Kanaya, Y.Kuramashi, Y.Namekawa, Y.Taniguchi, A.Ukawa, N.Ukita, T.Yamazaki, T.Yoshie	Tsukuba
K.-I.Ishikawa, M.Okawa	Hiroshima
D.Kadoh, Y.Nakamura, T.Izubuchi	RIKEN

- Computer scientists:

T.Boku, M.Sato, D.Takahashi, O.Tatebe T.Sakurai, H.Tadano	Tsukuba

Plan of talk

§1. Introduction

§2. Previous works

§3. Method

§4. Parameters and solver

§5. Results

§6. Summary

§1. Introduction

Isospin symmetry breaking

- Quark mass difference:
  $m_u \neq m_d$
- Electric charge difference
  $e_{ph}Q_u \neq e_{ph}Q_d$, $e_{ph}^2 = 4\pi/137$

→

Mass splittings among isospin multiplets

$m_{\pi 0} - m_{\pi\pm}$, $m_{K0} - m_{K\pm}$, $m_n - m_p$

1+1+1 flavor QCD+QED simulation is a straightforward way

isospin multiplets ⇔ u,d,s quark masses

§2. Previous works

Group	Ref	Action
Duncan et al.	PRL76(1996)3896	qQED+qQCD Wilson
Blum et al.	PRD76(2007)114508	qQED+Nf=2 QCD DW
Blum et al.	PRD82(2010)094508	qQED+Nf=2+1 QCD DW
MILC	Lat08,Lat10	qQED+Nf=2+1 QCD Stag
BMW	Lat10	qQED+Nf=2+1 QCD Clover
Duncan et al.	PRD71(2005)094509	Test of RW for fQED DW
Ishikawa et al.	arXiv:1202.6018	fQED+Nf=2+1 QCD DW RW for fQED

§3. Method

Reweighting from Nf=2+1 QCD to Nf=1+1+1 QCD+QED

$$\langle \mathcal{O}[U](\kappa_{\rm u}^*, \kappa_{\rm d}^*, \kappa_{\rm s}^*)\rangle_{(\kappa_{\rm u}^*,\kappa_{\rm d}^*,\kappa_{\rm s}^*),\rm fQED} = \frac{\langle \mathcal{O}[U](\kappa_{\rm u}^*, \kappa_{\rm d}^*, \kappa_{\rm s}^*)\det[W_{\rm uds}[U]]\rangle_{(\kappa_{\rm ud},\kappa_{\rm s}),\rm qQED}}{\langle \det[W_{\rm uds}[U]]\rangle_{(\kappa_{\rm ud},\kappa_{\rm s}),\rm qQED}}$$

with (κ_u*,κ_d*,κ_s*) hopping parameters at the physical point

$$W_{\rm uds}[U] = \prod_{q={\rm u,d,s}} \frac{D(e_{\rm ph}Q_q, \kappa_q^*)}{D(0, \kappa_q)}$$

Evaluation of det[W_{uds}[U]]

Introduce a complex bosonic field η

$$|\det[W_{\rm uds}]|^2 \;=\; \langle \mathrm{e}^{-|W_{\rm uds}^{-1}\eta|^2+|\eta|^2}\rangle_\eta$$

Given a set of η_i (i=1,…,N_η) with Gaussian distribution

$$\det[W_{\rm uds}[U]] \;=\; \left[\lim_{N_\eta\to\infty}\frac{1}{N_\eta}\sum_{i=1}^{N_\eta}\mathrm{e}^{-|W_{\rm uds}^{-1}[U]\eta_i|^2+|\eta_i|^2}\right]^{\frac{1}{2}}$$

Reduction of fluctuations in stochastic evaluation

- Determinant breakup Hasenfratz et al.,PRD78(2008)014515

  divide the reweighting path ($e=0$; κ_{ud}, κ_s) ⇒ ($e=e_{ph}$; $\kappa_u^*, \kappa_d^*, \kappa_s^*$)
  in the parameter space into N_B subintervals

$$\det[W_{\rm uds}] \;=\; \det[W_{\rm uds}^{(1)}] \times \det[W_{\rm uds}^{(2)}] \times \cdots \times \det[W_{\rm uds}^{(N_B)}]$$

- Combined reweighting factor

  explained in next slides

- Averaged photon field

Combined reweighting factor

Ishikawa et al., arXiv:1202.6018

・Combined reweighting factor for u,d,s quarks with a single set of noise

$$\det[W_{\rm uds}[U]] \;=\; \left[\lim_{N_\eta\to\infty}\frac{1}{N_\eta}\sum_{i=1}^{N_\eta} {\rm e}^{-|W_{\rm uds}^{-1}[U]\eta_i|^2+|\eta_i|^2}\right]^{\frac{1}{2}}$$

det[W_{uds}] rather than det[W_u]×det[W_d]×det[W_s]

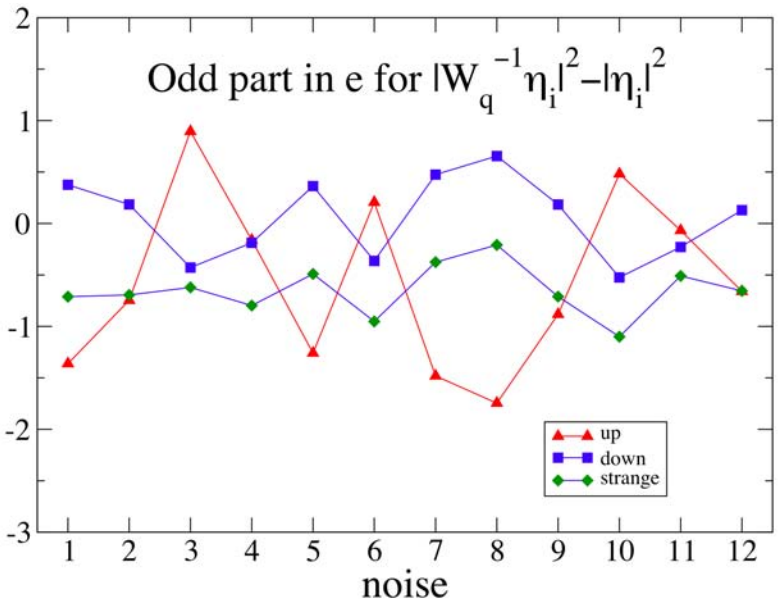

Odd part is extracted from ±e calculations

Leading contribution of O(e) is partially cancelled due to $Q_u+Q_d+Q_s=0$

Averaged photon field (1)

- generate photon field b_μ on $64^3\times128$ lattice ($\Leftrightarrow$ $32^3\times64$ QCD lattice) with non-compact pure gauge action

$$S_b = \sum_{n,\mu,\nu} \frac{1}{4}(\partial_\mu b_\nu(n) - \partial_\nu b_\mu(n))^2 + \sum_{n,\mu,\nu} c_1(\partial_\mu(\partial_\mu b_\nu(n) - \partial_\nu b_\mu(n)))^2$$

c_1=−0.646 is chosen such that

$$\left\langle \sum_{N,\mu,\nu} \frac{1}{4}(\nabla_\mu A_\nu(N) - \nabla_\nu A_\mu(N))^2 \right\rangle = \left\langle \sum_{N,\mu,\nu} \frac{1}{4}(\nabla_\mu B_\nu(N) - \nabla_\nu B_\mu(N))^2 \right\rangle$$

$A_\mu(N = n/2)$ $\Longleftrightarrow$ $B_\mu(N = n/2) = b_\mu(n) + b_\mu(n + \mu/2)$

$$S_A = \sum_{N,\mu,\nu} \frac{1}{4}(\partial_\mu A_\nu(N) - \partial_\nu A_\mu(N))^2$$

Averaged photon field (2)

- averaged photon fields over independent paths inside the 2^4 hypercube on the QED lattice

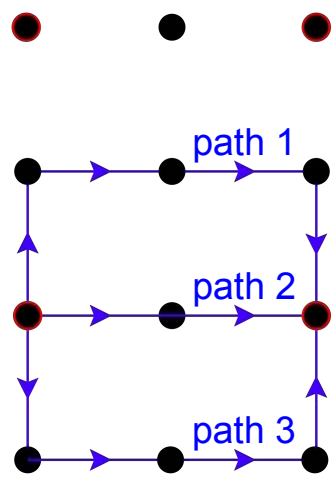

$$
\begin{aligned}
\bar{B}_\mu(N=n/2) \quad = \quad & \frac{1}{27}[(b_\mu(n)+b_\mu(n+\hat{\mu}/2)) \\
& +\sum_{\nu\neq\mu}\sum_{\nu_s=\pm\nu}(b_{\nu_s}(n)+b_\mu(n+\hat{\nu_s}/2)+b_\mu(n+\hat{\nu_s}/2+\hat{\mu}/2)-b_{\nu_s}(n+\hat{\mu})) \\
& +\frac{1}{2}\sum_{\rho\neq\nu\neq\mu}\sum_{\rho_s=\pm\rho}\sum_{\nu_s=\pm\nu}(b_{\rho_s}(n)+b_{\nu_s}(n+\hat{\rho}_s/2) \\
& \quad +b_\mu(n+\hat{\rho}_s/2+\hat{\nu}_s/2)+b_\mu(n+\hat{\rho}_s/2+\hat{\nu}_s/2+\hat{\mu}/2) \\
& \quad -b_{\rho_s}(n+\hat{\mu})-b_{\nu_s}(n+\hat{\rho}_s/2+\hat{\mu})) \\
& +\frac{1}{6}\sum_{\sigma\neq\rho\neq\nu\neq\mu}\sum_{\sigma_s=\pm\sigma}\sum_{\rho_s=\pm\rho}\sum_{\nu_s=\pm\nu}(b_{\sigma_s}(n)+b_{\rho_s}(n+\hat{\sigma}_s/2)+b_{\nu_s}(n+\hat{\sigma}_s/2+\hat{\rho}_s/2) \\
& \quad +b_\mu(n+\hat{\sigma}_s/2+\hat{\rho}_s/2+\hat{\nu}_s/2)+b_\mu(n+\hat{\sigma}_s/2+\hat{\rho}_s/2+\hat{\nu}_s/2+\hat{\mu}/2) \\
& \quad -b_{\sigma_s}(n+\hat{\mu})-b_{\rho_s}(n+\hat{\sigma}_s/2+\hat{\mu})-b_{\nu_s}(n+\hat{\sigma}_s/2+\hat{\rho}_s/2+\hat{\mu}))]
\end{aligned}
$$

- construct U(1) link variable in terms of the averaged photon field
- numerically checked that the averaged and conventional photon fields give consistent results for m_{PS0}-$m_{PS\pm}$

§4. Parameters and solver

・Configuration parameters PACS-CS,PRD81(2010)074503

Nf=2+1 flavor QCD near the physical point

NP O(a)-improved Wilson-clover quark and Iwasaki gauge action

β=1.9, $32^3\times64$, a～0.1fm, (κ_{ud},κ_s)=(0.137785,0.13660), 2000 MD time

・Reweighting parameters

physical point: $(\kappa_u^*,\kappa_d^*,\kappa_s^*)$=(0.13787014, 0.13779700,0.13669510)

determined from π^+,K^+,K^0,Ω^- masses

$e_{ph}^2=4\pi/137$

N_B=426, N_η=12 for each piece of divided determinant

・Modified block BiCGStab Nakamura et al.,CPC183(2012)34

quark matrix inversions for N_η=12 noises

a factor of 3～4 cost reduction compared with non-block solvers

Modified block BiCGStab (1)

A solver algorithm for linear eqs with multiple right-hand sides

$Dx^{(i)}=b^{(i)}$ (i=1,…,L) ⇒ DX=B

1 **initial guess** $X \in \mathbb{C}^{N\times L}$
2 $R = B - AX$
3 $P = R$
4 **choose** $\tilde{R} \in \mathbb{C}^{N\times L}$
while $\max_i(|\boldsymbol{r}^{(i)}|/|\boldsymbol{b}^{(i)}|) \leqslant \epsilon$
do
- 4.1 **QR decomposition** $P = Q\gamma,\ \ P \leftarrow Q$
- 4.2 $U = MP$
- 4.3 $V = AU$
- 4.4 **solve**$(\tilde{R}^H V)\alpha = \tilde{R}^H R$ **for** α
- 4.5 $T = R - V\alpha$
- 4.6 $S = MT$
- 4.7 $Z = AS$
- 4.8 $\zeta = \mathrm{Tr}(Z_k^H T_k)/\mathrm{Tr}(Z_k^H Z_k)$
- 4.9 $X \leftarrow X + U\alpha + \zeta S$
- 4.10 $R = T - \zeta Z$
- 4.11 **solve**$(\tilde{R}^H V)\beta = -\tilde{R}^H Z$ **for** β
- 4.12 $P \leftarrow R + (P - \zeta V)\beta$

5 **return** (X)

Basic idea: blocked version searches the solution vectors with the enlarged Krylov subspace

Modified block BiCGStab (2)

<u>a representative case</u>

Nf=2+1 QCD, $32^3 \times 64$, a∼0.1fm,
(κ_{ud},κ_s)=(0.137785,0.13660), point source

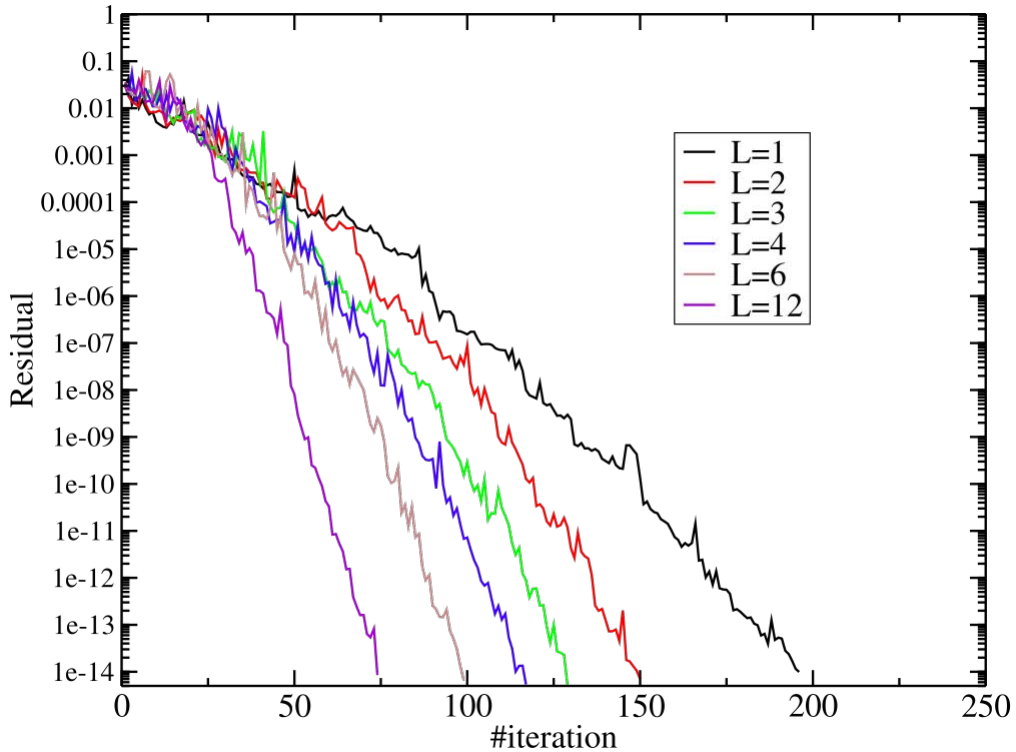

Modified block BiCGStab (3)

Performance test averaged over 10 configs

$Dx^{(i)}=b^{(i)}$ (i=1,…,12)

$L \times 12/L$	Time [s]	T (gain)	NMVM	NM (gain)
1×12	3827 (755)	1	17 146 (3326)	1
2×6	2066 (224)	1.9	12 942 (1379)	1.3
3×4	1619 (129)	2.4	10652 (832)	1.6
4×3	1145 (99)	3.3	9343 (835)	1.8
6×2	1040 (87)	3.7	7888 (663)	2.2
12×1	705 (70)	5.4	6106 (633)	2.8

T(gain) > NM(gain) is thanks to effective usage of cache

§5. Results

Configuration dependence of reweighting factor

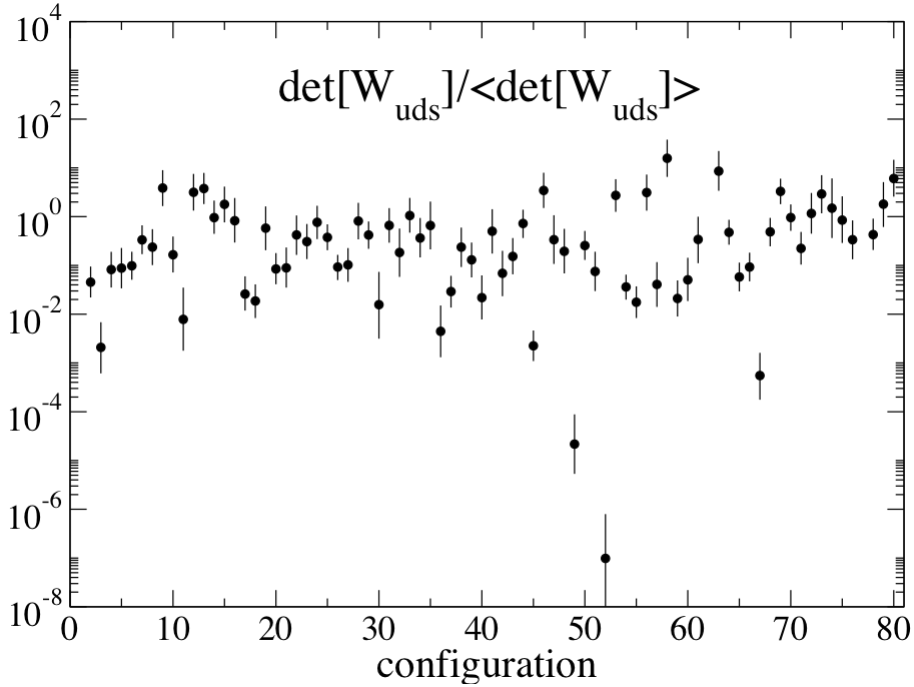

Normalized by <det[W_{uds}]>

$$\langle \mathcal{O}[U](\kappa_{\rm u}^*, \kappa_{\rm d}^*, \kappa_{\rm s}^*)\rangle_{(\kappa_{\rm u}^*,\kappa_{\rm d}^*,\kappa_{\rm s}^*),\rm fQED} = \frac{\langle \mathcal{O}[U](\kappa_{\rm u}^*, \kappa_{\rm d}^*, \kappa_{\rm s}^*)\det[W_{\rm uds}[U]]\rangle_{(\kappa_{\rm ud},\kappa_{\rm s}),\rm qQED}}{\langle \det[W_{\rm uds}[U]]\rangle_{(\kappa_{\rm ud},\kappa_{\rm s}),\rm qQED}}$$

Effective masses for $\pi^+, K^+, K^0, \Omega^-$

Smear-local propagators, N_η=12

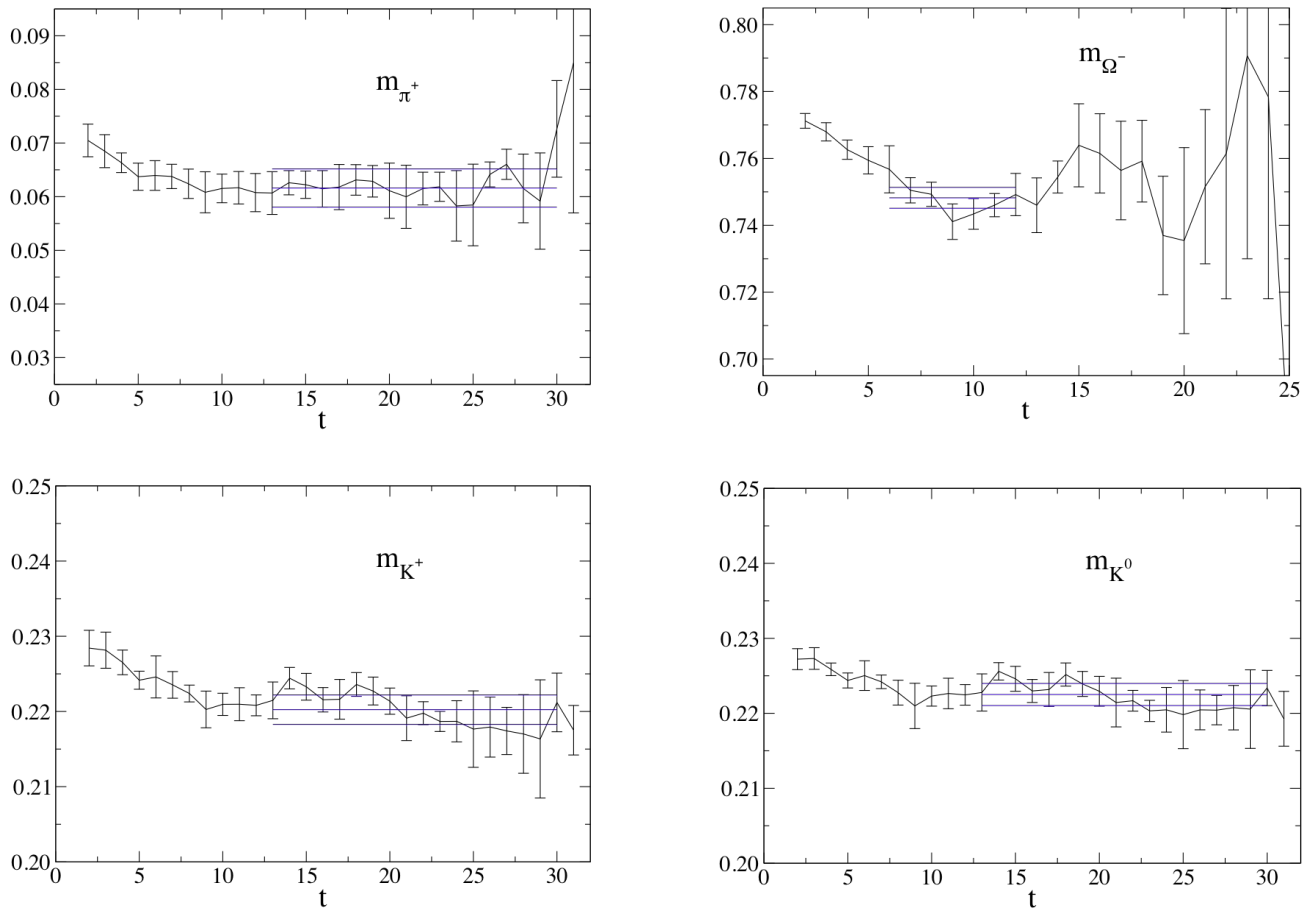

N_η dependence of hadron mass ratios

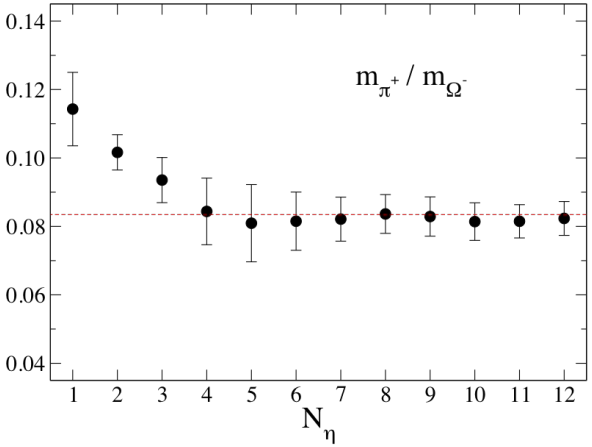

	Our results [MeV]	Experiment [MeV]
$m_{\pi+}$	137.7(8.0)	139.57018(35)
m_{K+}	492.3(4.7)	493.677(16)
m_{K^0}	497.4(3.7)	497.614(24)
$m_{\Omega-}$	input	1672.45(29)

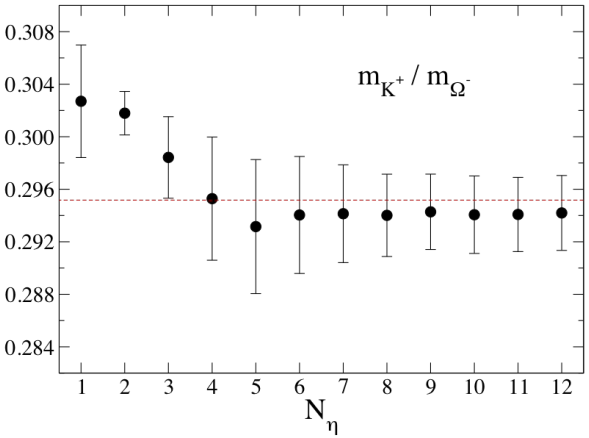

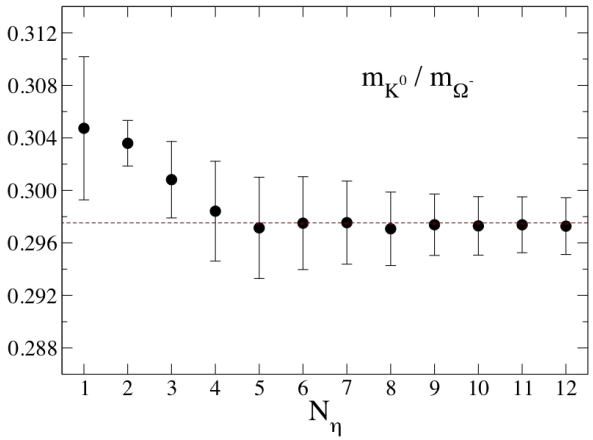

plateau close to the experimental value for $N_\eta \gtrsim 4$

Ratio of K^0 to K^+ propagators

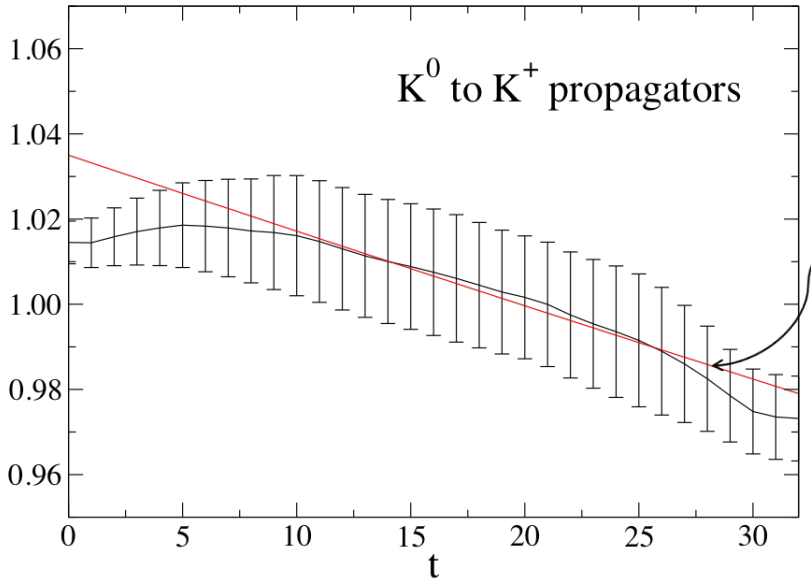

Exp value for K^0-K^+ mass diff

$$\frac{\langle K^0(t)K^0(0)\rangle}{\langle K^+(t)K^+(0)\rangle} \simeq Z\left(1-(m_{K^0}-m_{K^+})t\right)$$

much smaller than 1

Fit result 4.54(1.09) MeV is consistent with exp value 3.937(28) MeV

Quark masses with NP renormalization factor

- NP renormalization factor with Schrödinger functional scheme
  PACS-CS, JHEP1008(2010)101
  PRD81(2010)074503 [2+1f QCD (1)]
  PRD79(2009)034503 [2+1f QCD (2)]
- neglect QED corrections to the renormalization factor
- physical inputs: $m_{\pi+}$, m_{K0}, m_{K+}, $m_{\Omega-}$
- MS-bar scheme at μ=2GeV

	This work	2+1f QCD (1)	2+1f QCD (2)
m_u [MeV]	2.57(26)(07)		
m_d [MeV]	3.68(29)(10)		
m_s [MeV]	83.60(58)(2.23)	86.7(2.3)	87.7(3.1)
m_{ud} [MeV]	3.12(24)(08)	2.78(27)	3.05(12)
m_u/m_d	0.698(51)		
m_s/m_{ud}	26.8(2.0)	31.2(2.7)	28.78(40)

- possible QED finite size effects: −13.50% for u, +2.48% for d, −0.07% for s
  Blum et al., PRD82(2010)094508

§6. Summary

- 1+1+1 flavor QCD+QED simulation at the physical point
- Dynamical quark effects in QED and u-d quark mass difference are incorporated by reweighting technique
- u,d,s quark masses are determined with $m_{\pi+}$, m_{K0}, m_{K+}, $m_{\Omega-}$ as physical inputs
- Direct investigation of finite size effects due to QED is left as a future work

USQCD BSM

BNL workshop 2012

The Composite Higgs Mechanism and the Conformal Window

Lattice Higgs Collaboration (LHC)

with Zoltan Fodor, Kieran Holland, Daniel Nogradi, Chris Schroeder, Chik Him Wong

Julius Kuti

University of California, San Diego

New Horizons for Lattice Computations with Chiral Fermions
BNL May 14, 2012

Outline

- **LHC Higgs search and BSM implications**
  focus on SU(3) fermion representation with two flavors

- **Two RG based strategies**

- **New results on the Nf=2 sextet model in the SU(3) color rep**

- **Cosmology connection**
  (dark baryon matter and EW phase transition)

- **Conformal FSS method**

- **New results on FSS in the Nf=12 model in the fundamental SU(3) rep**

- **Outlook**

Atlas and CMS compared (from Vivek Sharma)

For low Higgs mass hypothesis both CMS & ATLAS see an excess in event yield over expected background

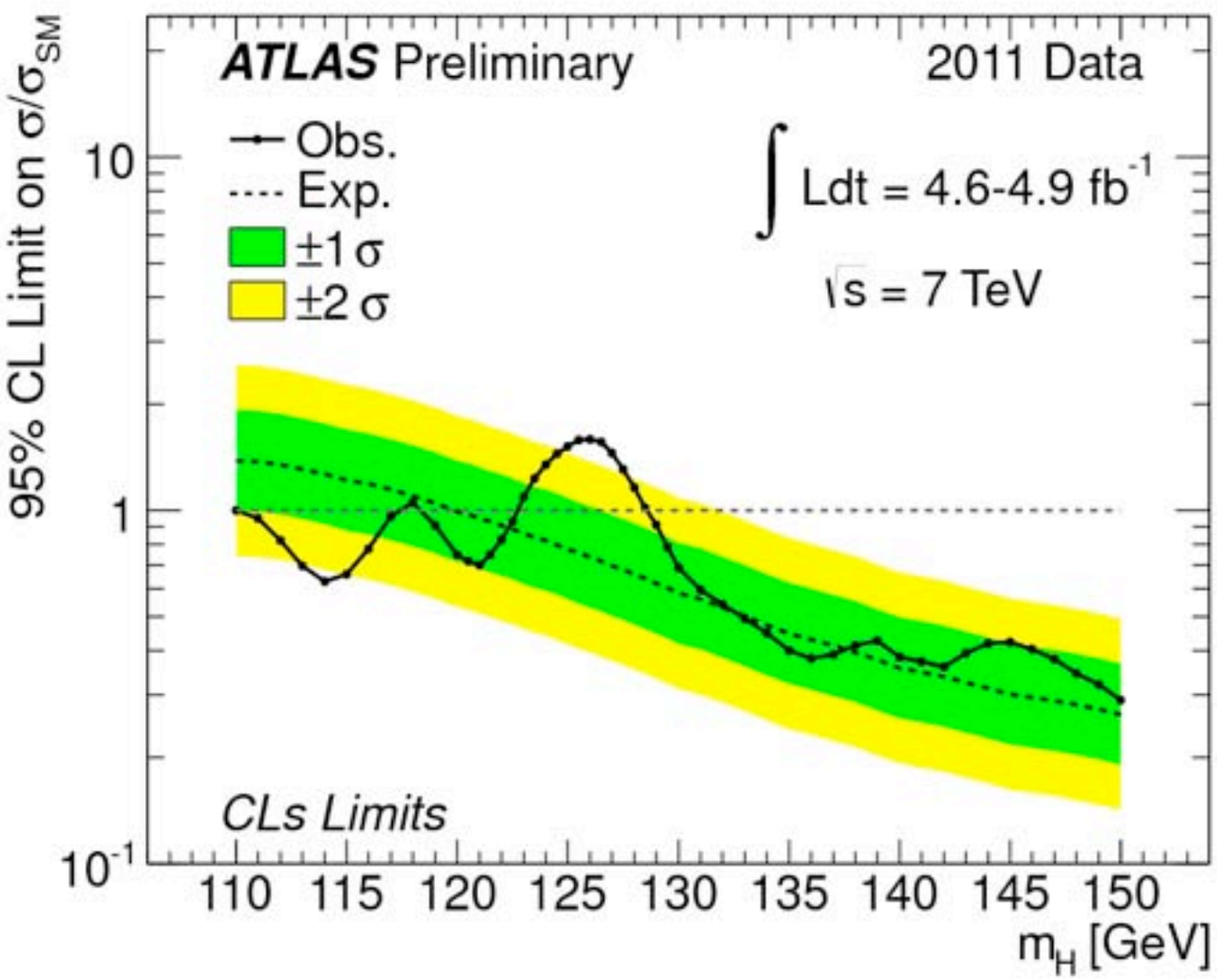

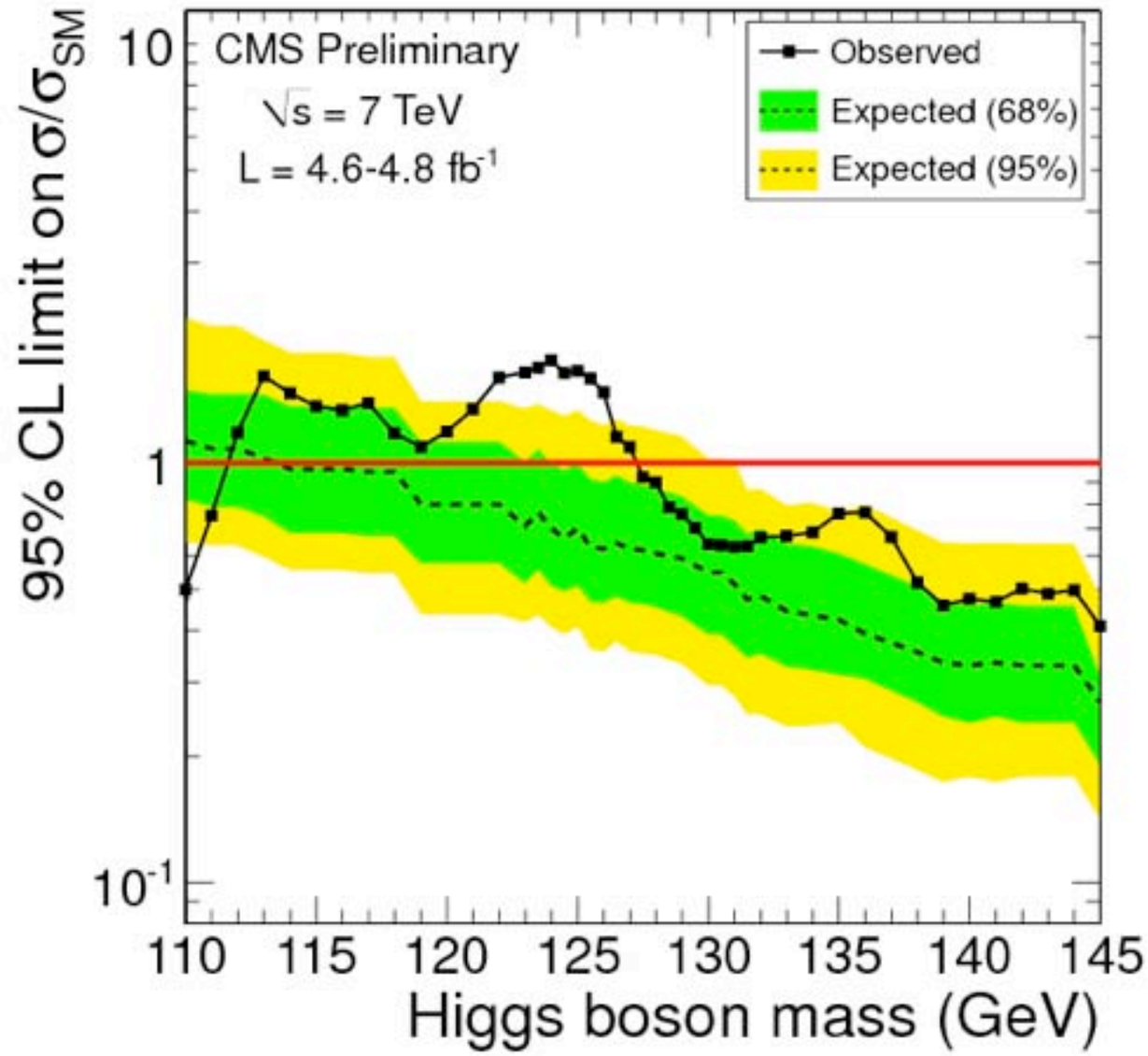

ATLAS excess at M ≈ 126 GeV

CMS excess at M ≈125 GeV

What comes at the end of the LHC run?

- light Higgs with non-SM couplings (dilaton?)

- Heavy Higgs, or Higgsless

- SM Higgs (SUSY symmetry breaking?)

- USQCD composite Higgs and SUSY - timely efforts

What comes at the end of the LHC run?

- light Higgs with non-SM couplings (dilaton?)

- Heavy Higgs, or Higgsless

- SM Higgs (SUSY symmetry breaking?)

- USQCD composite Higgs and SUSY - timely efforts

- Composite Higgs mechanism

- The paradigm is important again

- Higgsless QCD-like (cutoff Λ to 3 TeV)

- changes close to conformal windo

- non-perturbative lattice studies needed

- USQCD effort:

What comes at the end of the LHC run?

- light Higgs with non-SM couplings (dilaton?)

- Heavy Higgs, or Higgsless

- SM Higgs (SUSY symmetry breaking?)

- USQCD composite Higgs and SUSY - timely efforts

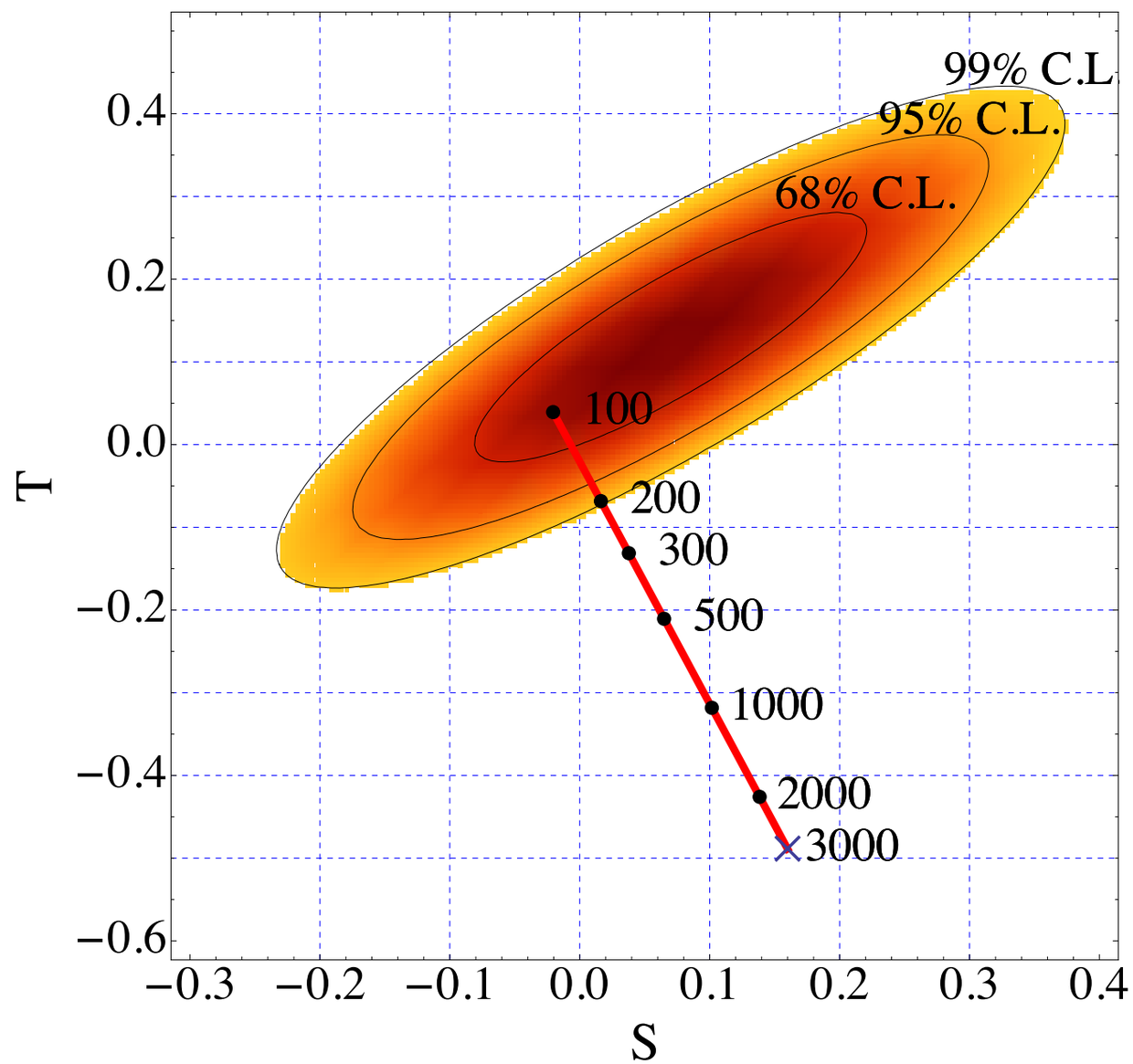

- Composite Higgs mechanism

- The paradigm is important again

- Higgsless QCD-like (cutoff Λ to 3 TeV)

- changes close to conformal windo

- non-perturbative lattice studies needed

- USQCD effort:

$$S = 4\pi N_D \lim_{Q^2 \to 0} \frac{d}{dQ^2} \Pi_{V-A}(Q^2) - \Delta S_{SM}$$

composite Higgs? example: Nf=2 SU(3) sextet rep TC (ETC) language used

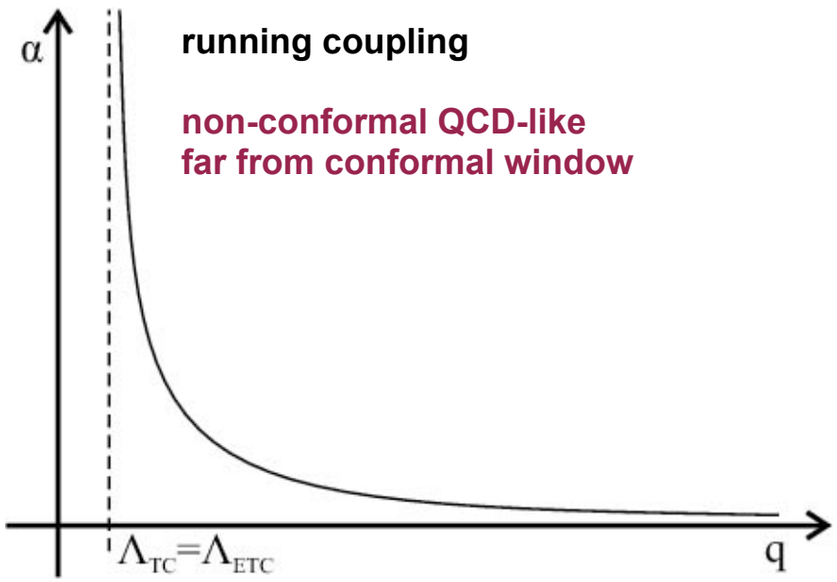

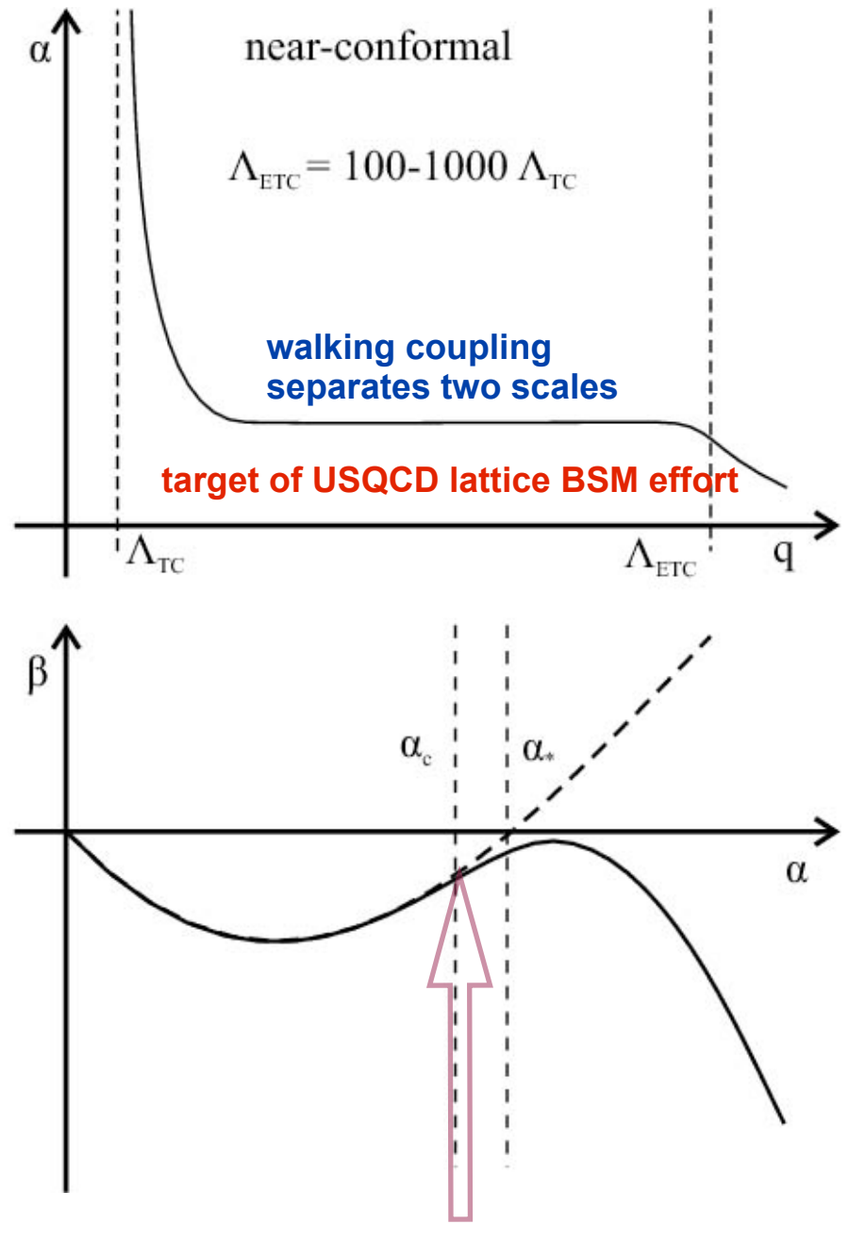

Chiral symmetry breaking turns conformal FP into walking

Extended Technicolor paradigm:

- requires walking gauge coupling chiral SB on $\Lambda_{TC} \sim TeV$ scale
- fermion mass generation from scale at $\Lambda_{ETC} \sim 100 - 1000 \Lambda_{TC}$
- can solve problem of flavor changing currents
- composite Higgs mechanism
- broken scale invariance (Dilaton) → light non-SM composite Higgs particle?
- can avoid conflict with EW precision constraints
- *candidate models require non-perturbative lattice studies*
- ***focus is on composite Higgs mechanism***

original Technicolor paradigm replaced with sextet SU(3) color rep:

$$\begin{bmatrix} u \\ d \end{bmatrix}$$

- one massless fermion doublet chiral SB
- three Goldstone pions
- become longitudinal components of weak bosons

$\Lambda_{TC} \sim TeV$

- composite Higgs mechanism scale of Higgs condensate ~ F=250 GeV
- flavor changing currents and fermion mass generation would be problems
- conflicts with EW precision constraints?

important for lattice studies in BSM theory space

theory space and conformal window critically important for composite Higgs

space of color, flavor, and massless fermion representation

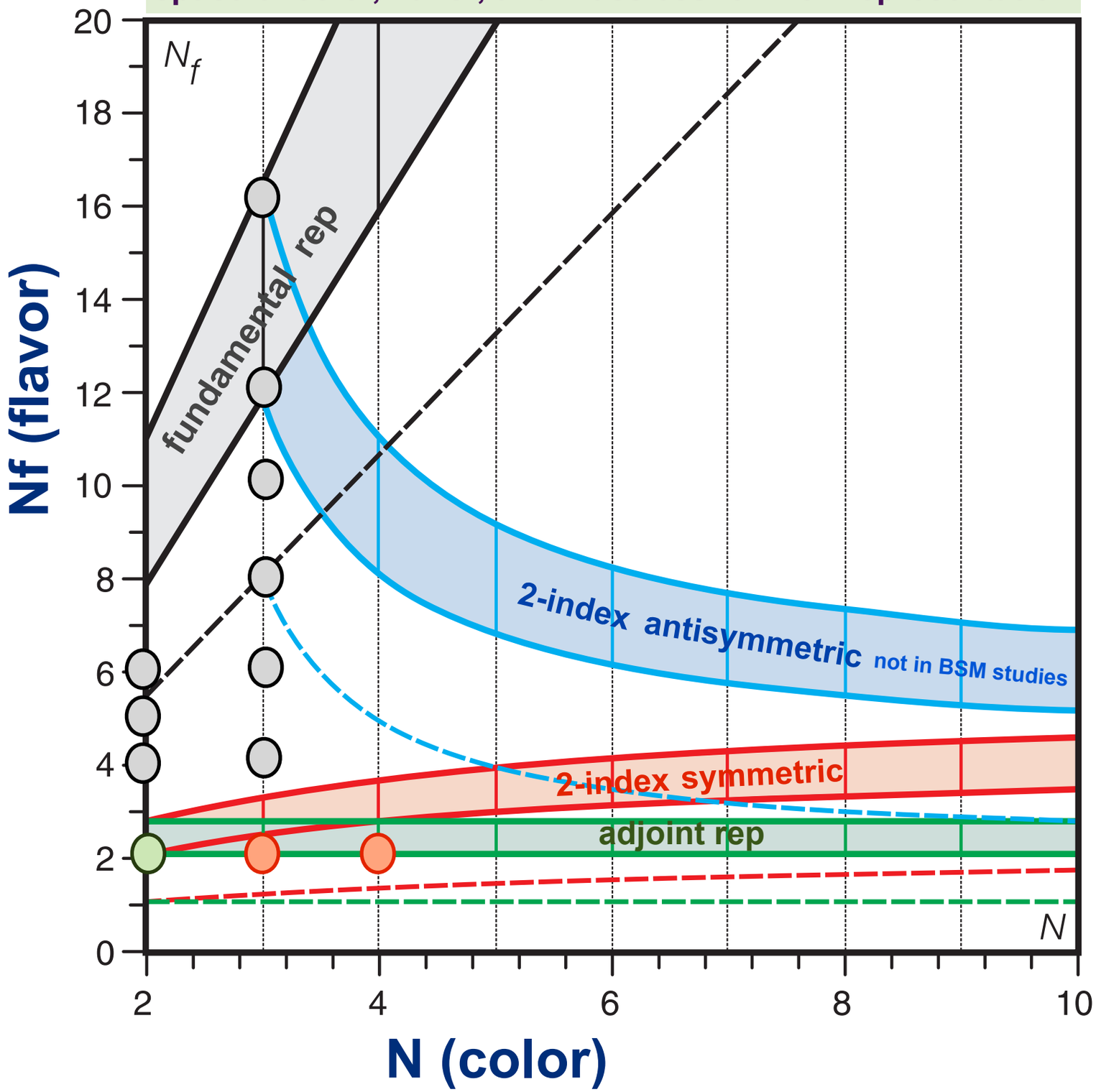

for each rep BSM interest is below conformal window but close to it:

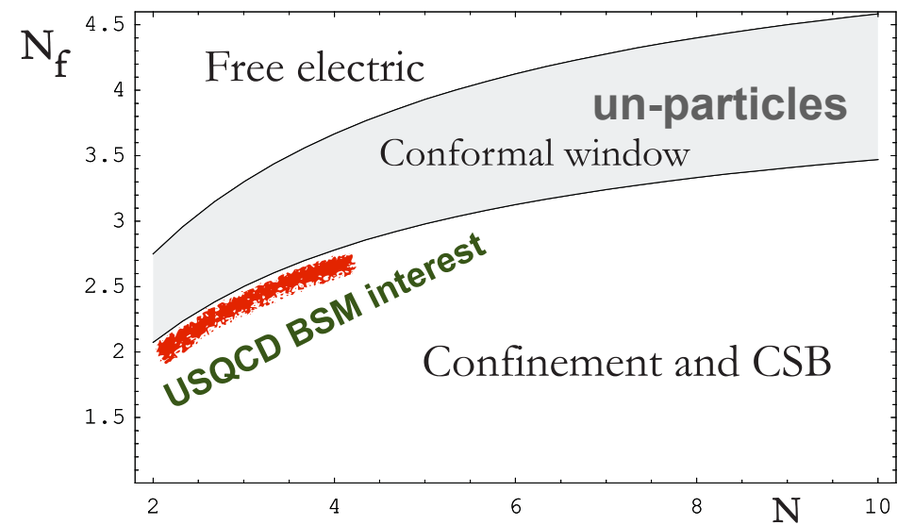

USQCD BSM results of last 12 months in 3 reps including new projects just starting

theory space and conformal window critically important for composite Higgs

space of color, flavor, and massless fermion representation

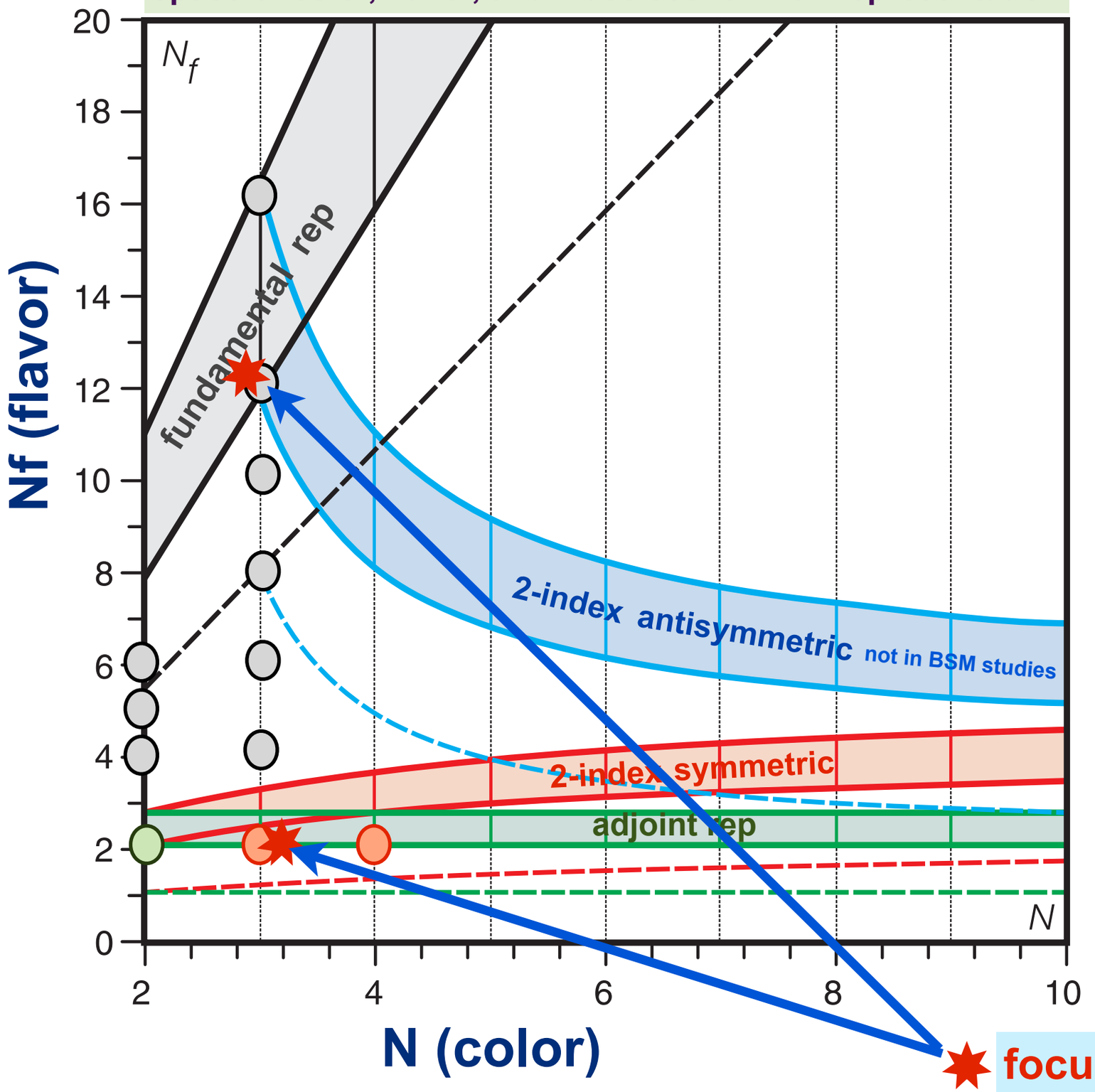

for each rep BSM interest is below conformal window but close to it:

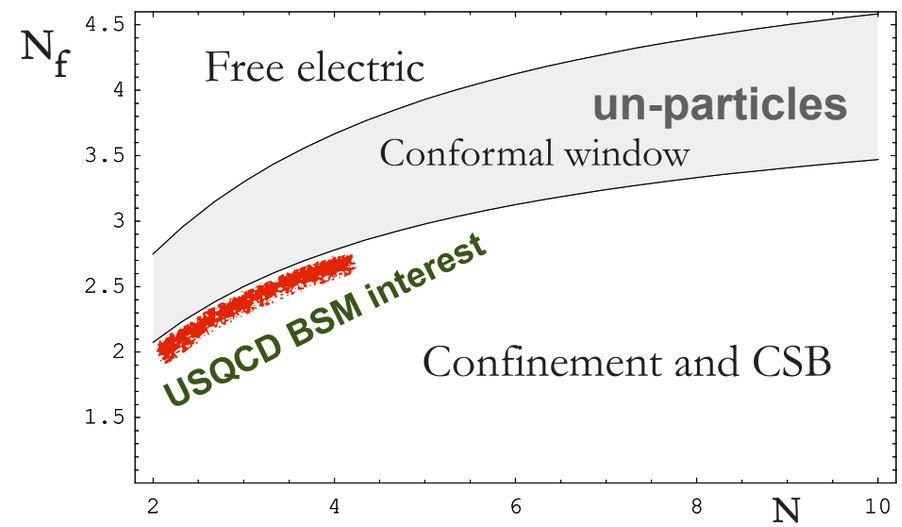

USQCD BSM results of last 12 months in 3 reps including new projects just starting

arXiv:1205.1878 [hep-lat]

New extended data set and analysis

Lattice navigation map

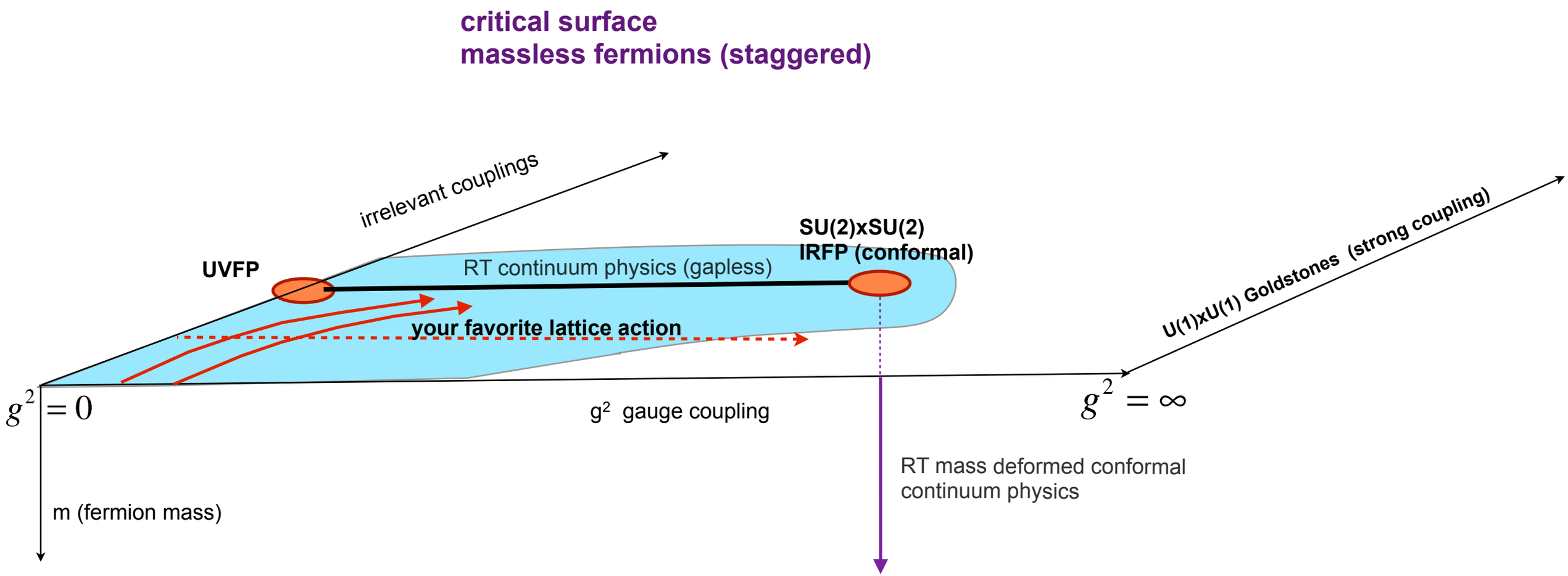

Lattice navigation map

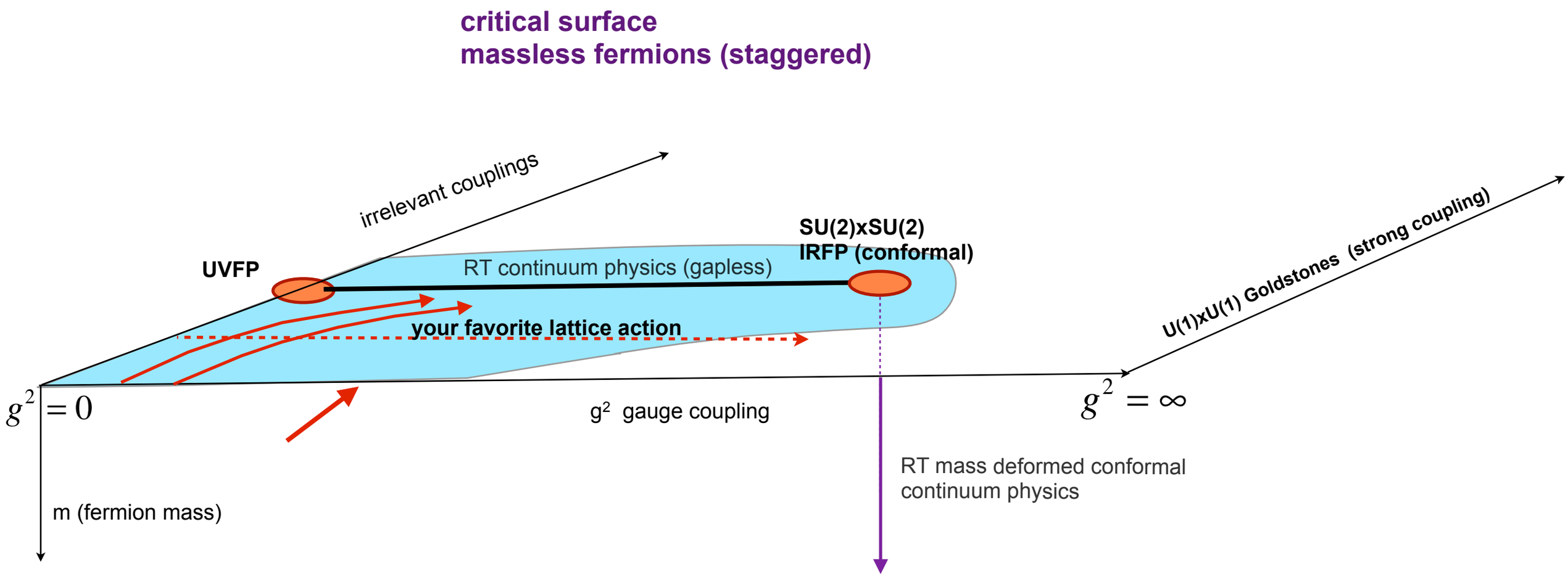

Lattice navigation map

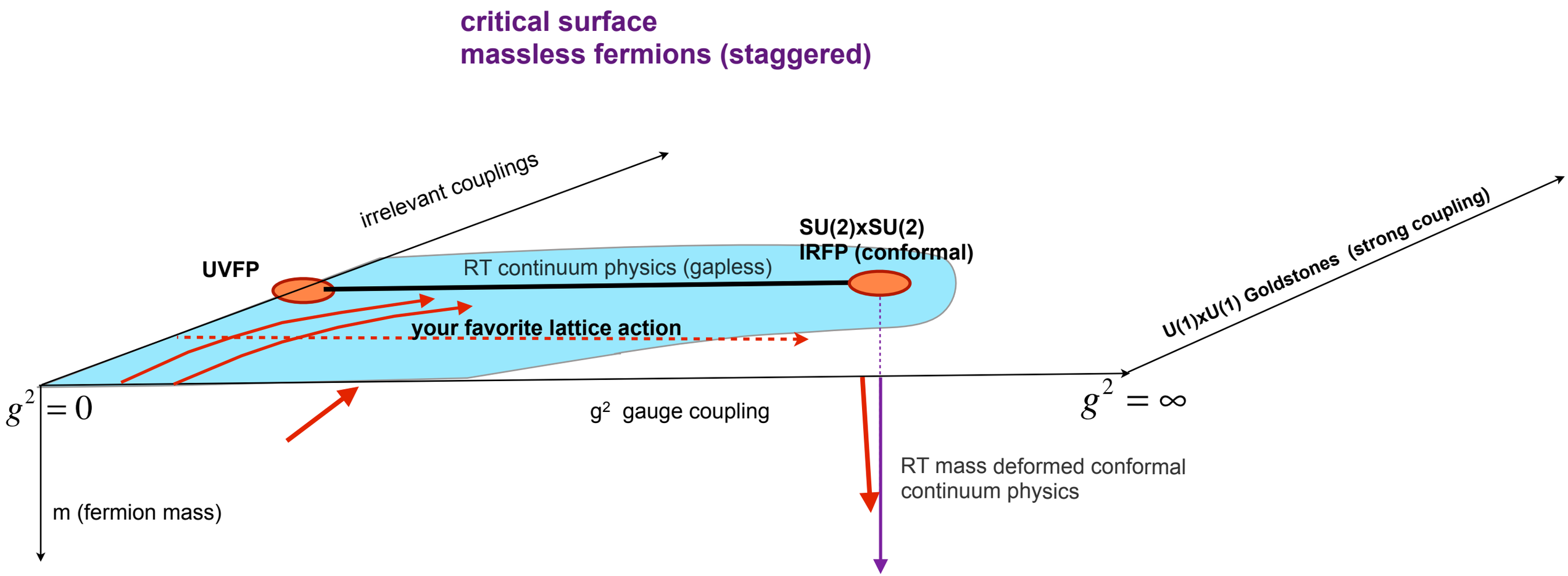

Lattice navigation map

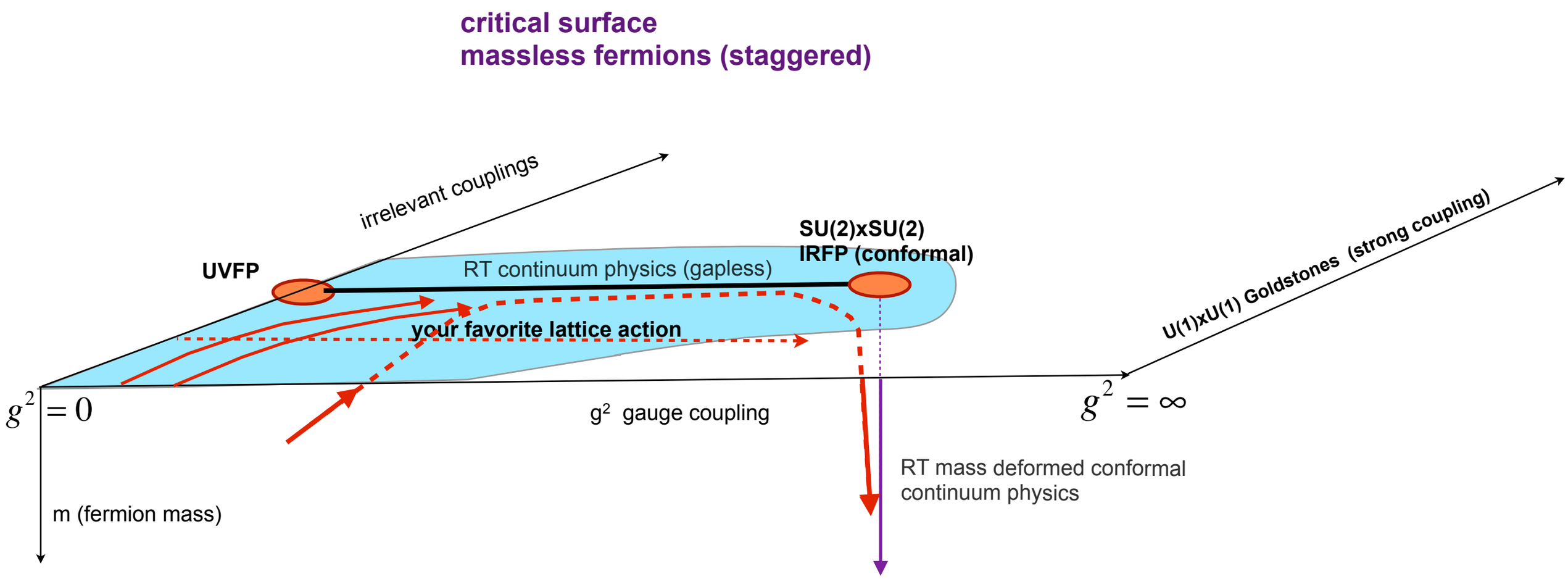

Lattice navigation map

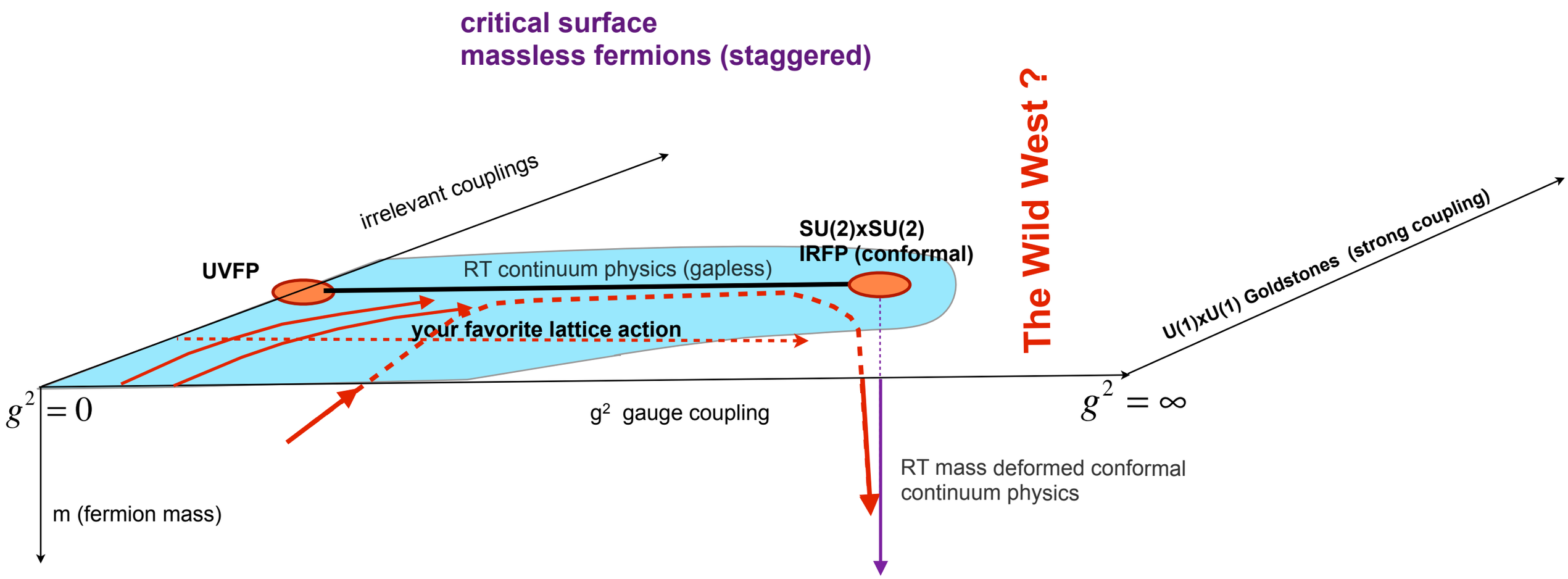

status of SU(3) Nf=2 sextet model
minimal composite Higgs model?

our group: mass-deformed theory close to m=0 critical surface and m->0 limit:

- two strategies complement: (1) inf volume conform scaling
  (2) mass-deformed FSS
  (1) is used in sextet model

- direct access to effective anomalous dimension γ

- similar to tests of RG scaling laws of moments of current correlator functions (in progress)

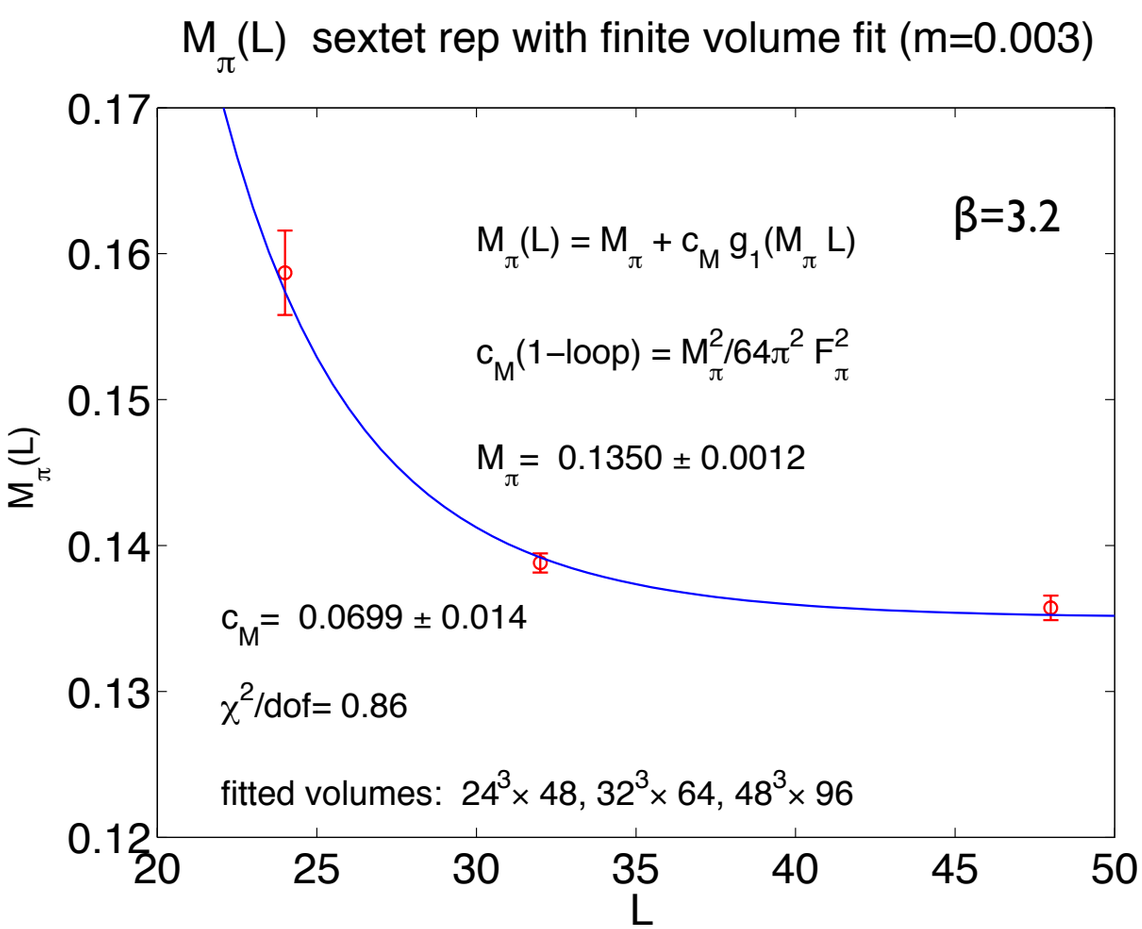

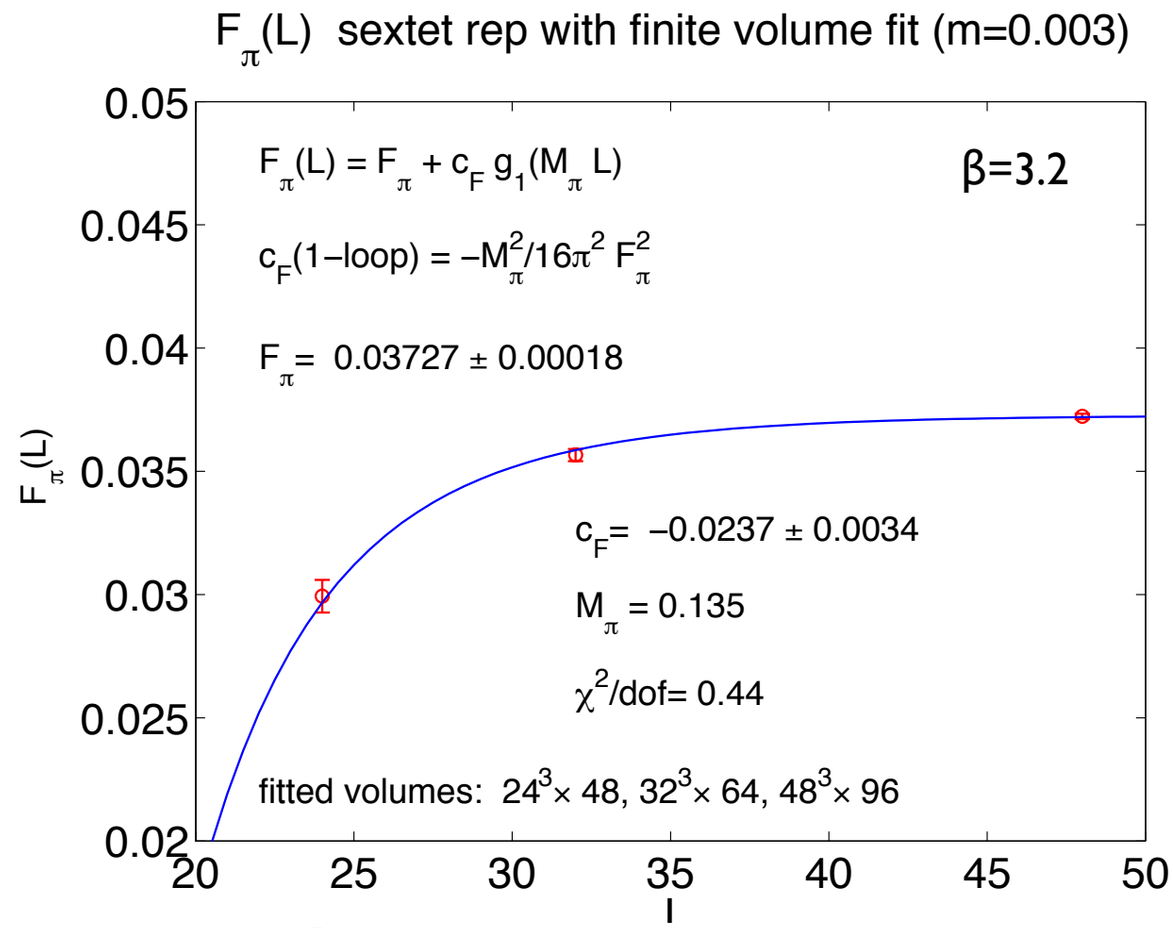

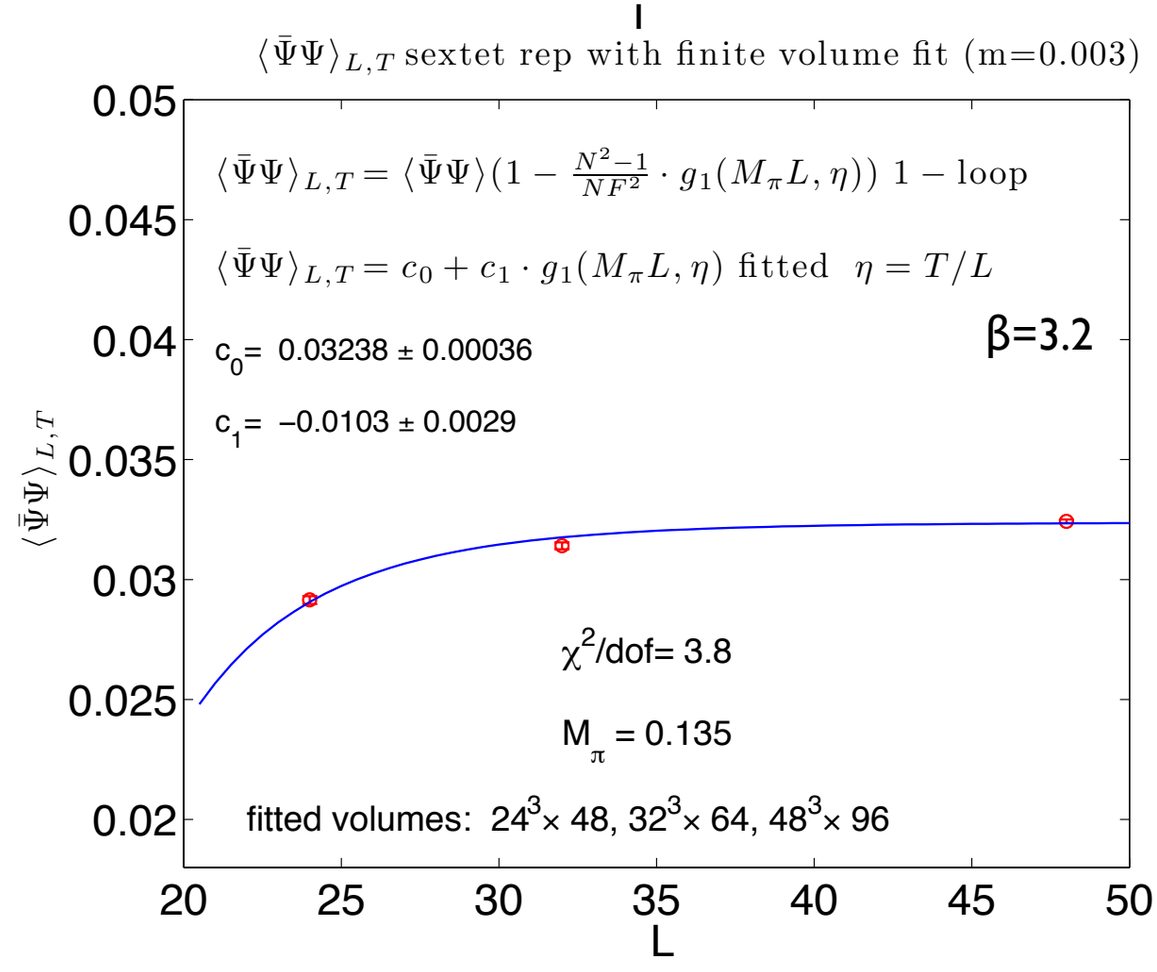

mass-deformed theory

close to m=0 critical surface

inf volume extrapolated chiral and conform scaling tests in sextet model

for L·Mπ > 5 one percent level reached

Nf=2 SU(3) sextet chiral condensate

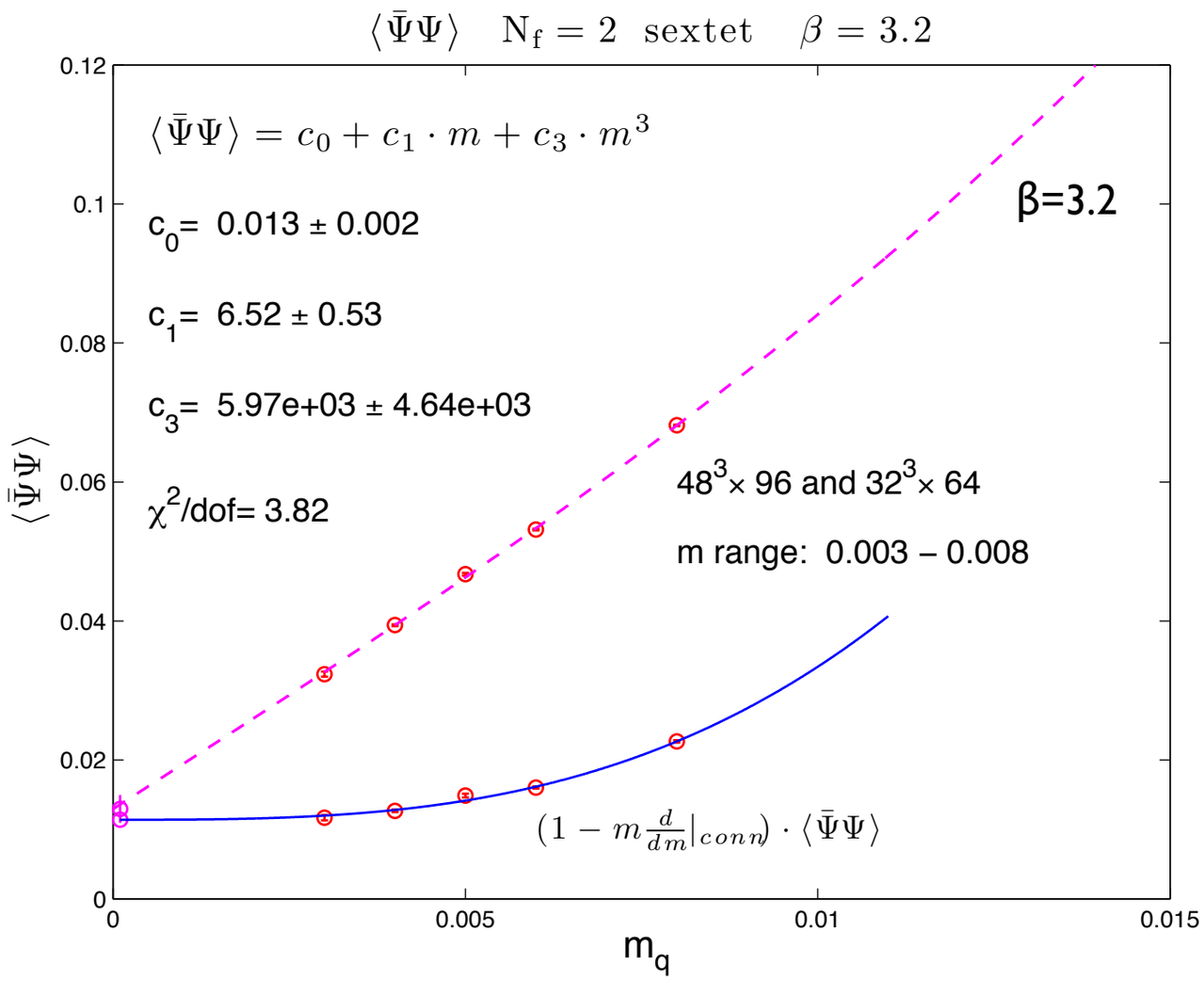

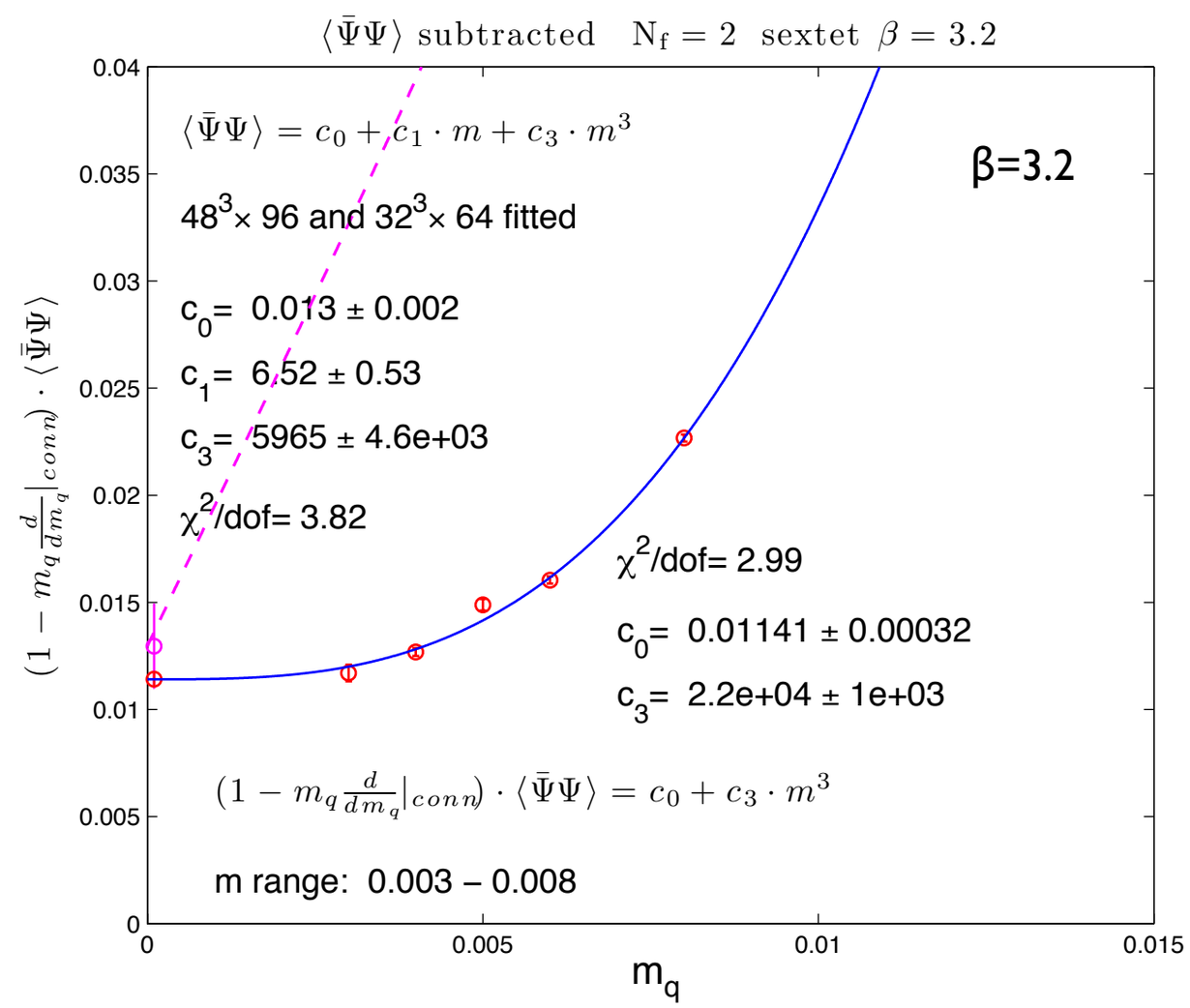

- two independent determinations of the chiral condensate
- consistently non-vanishing in chiral limit
- all sextet results are treated as inf volume (only m=0.003 is truly extrapolated)

Nf=2 SU(3) sextet chiral fits M_π and F_π

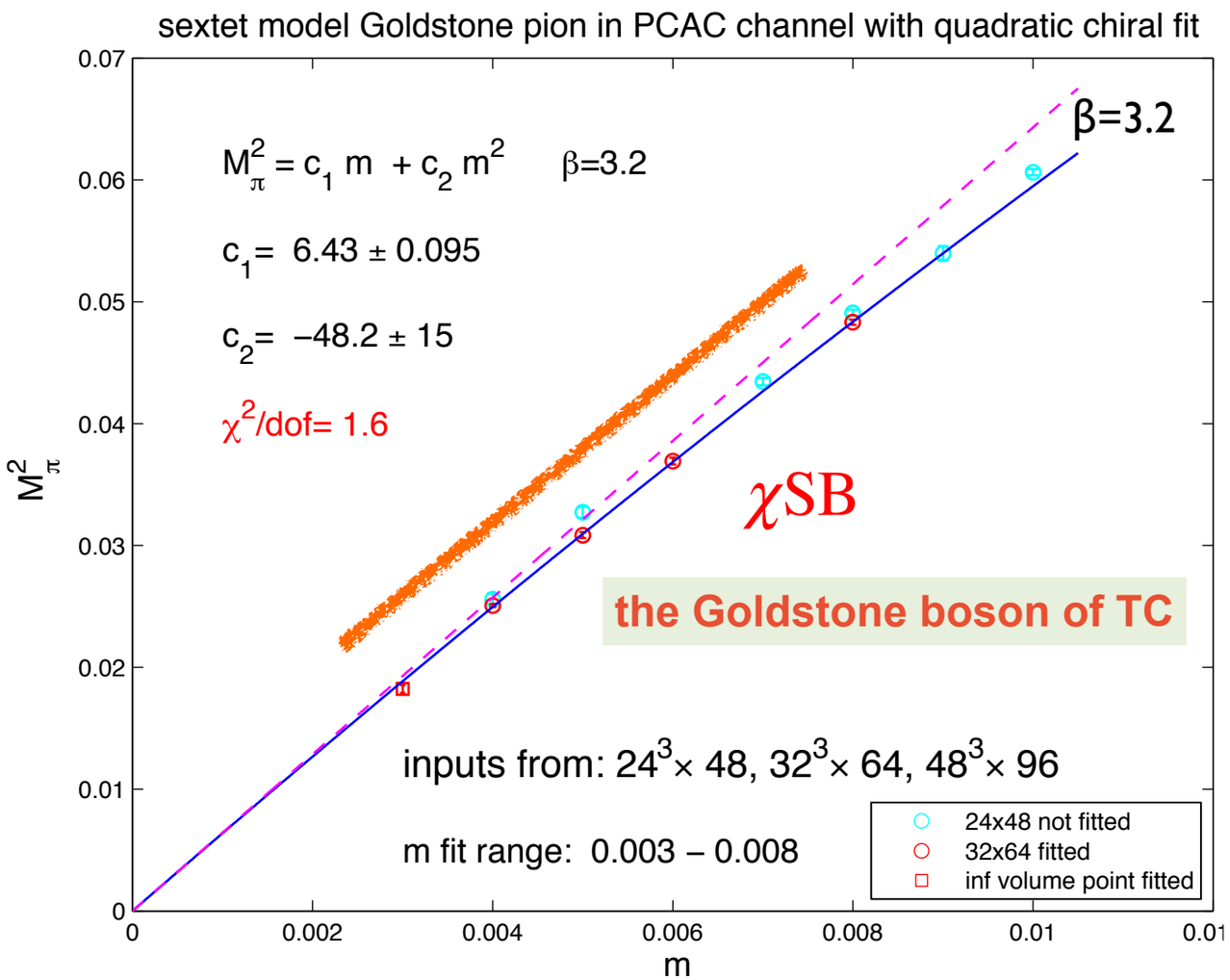

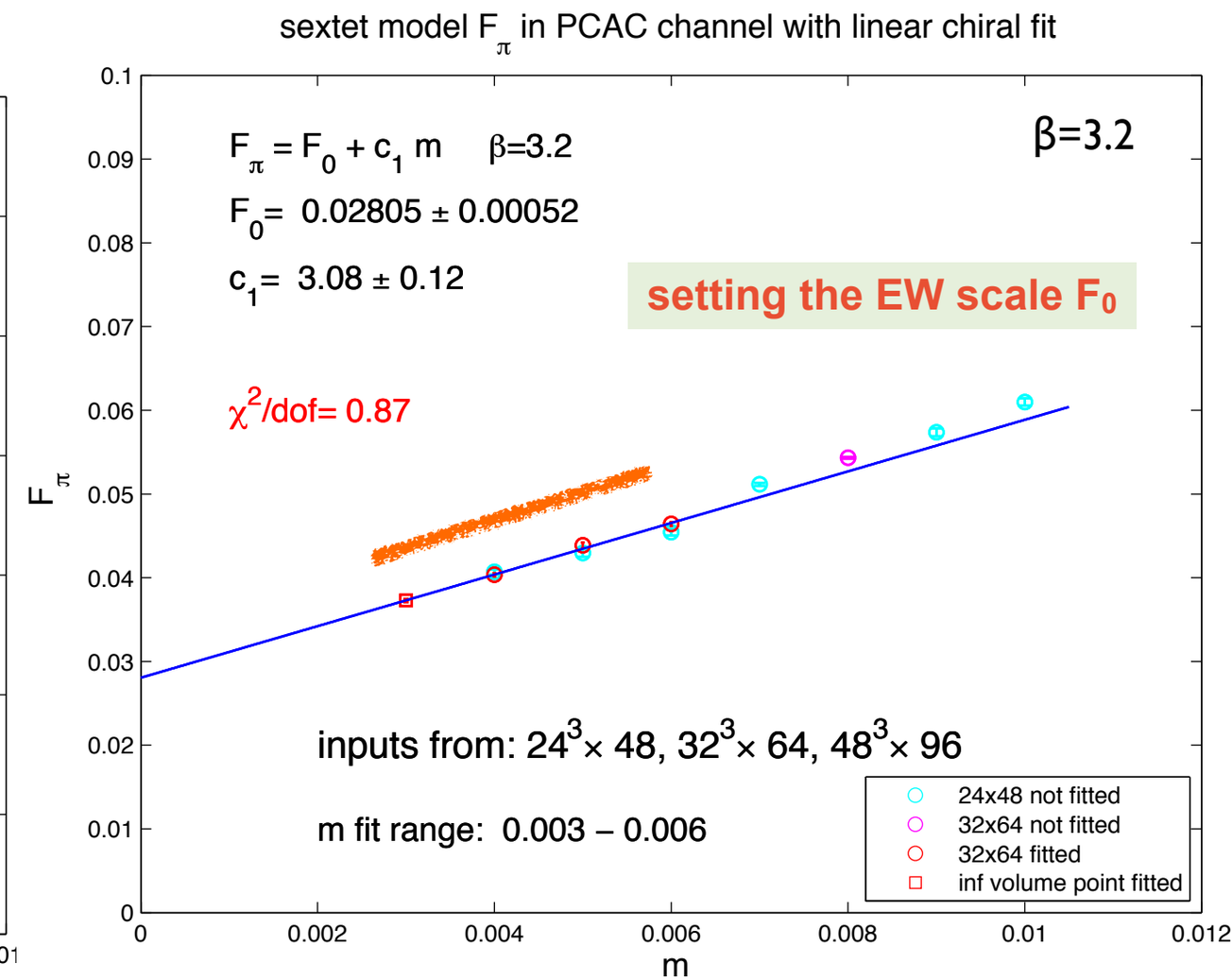

m=0.003-0.006 range close to chiral log regime? Nf=2 helps!

log detection will require even more precise data

Nf=2 SU(3) sextet chiral fits M_ρ and M_H

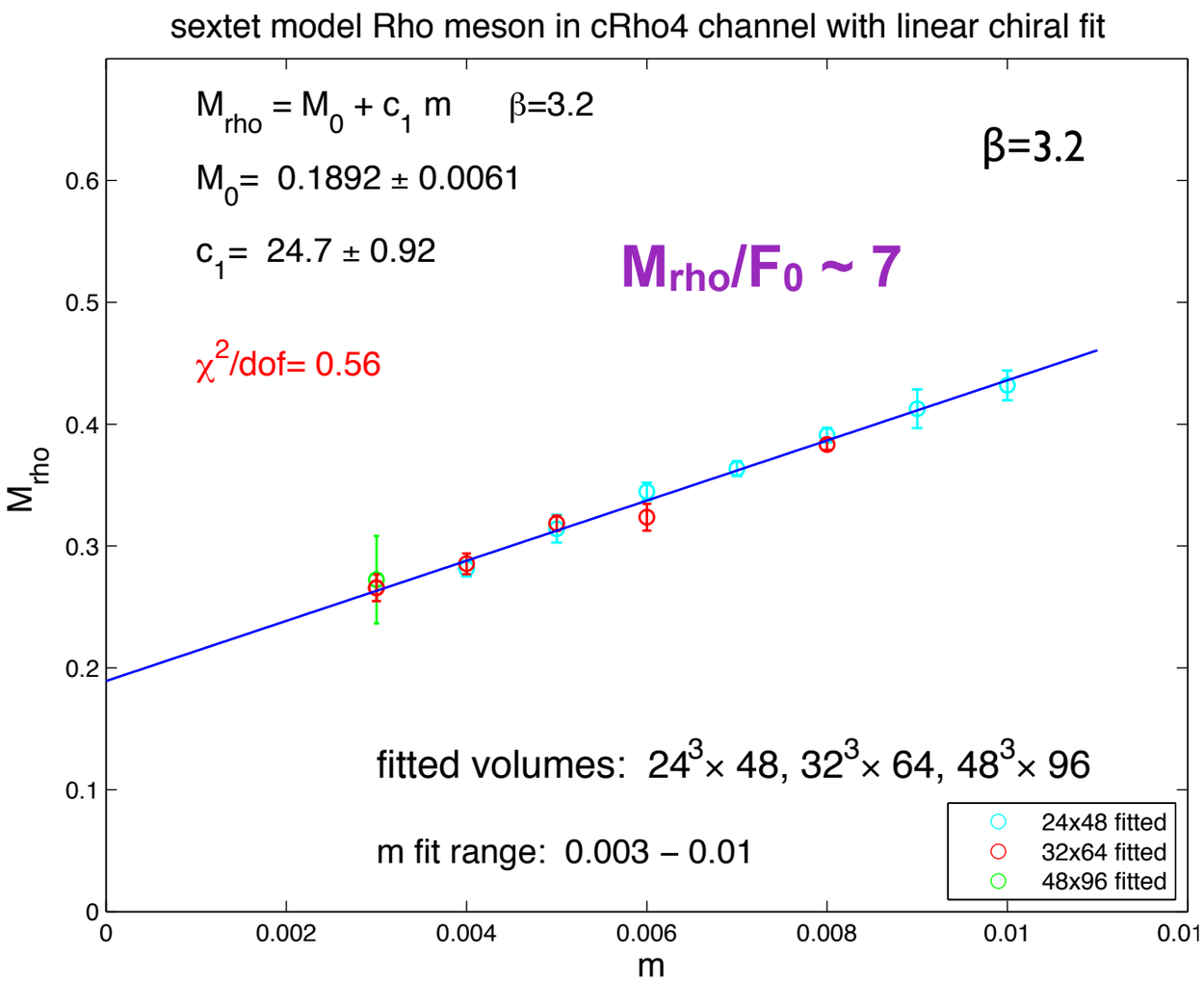

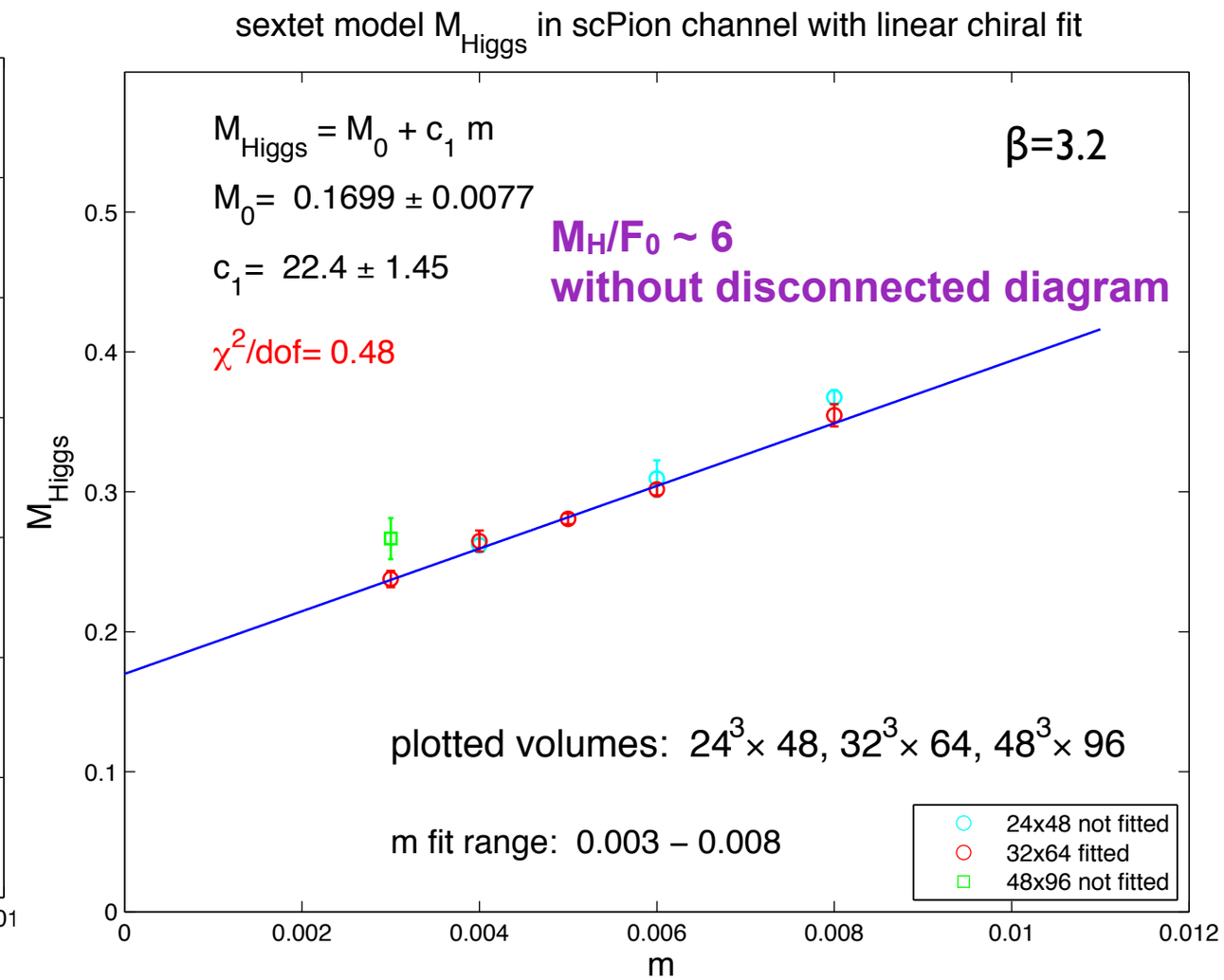

m=0.003-0.006 range close to chiral log regime? Nf=2 helps!

log detection will require even more precise data

conformal hypothesis breaks down in global fits:

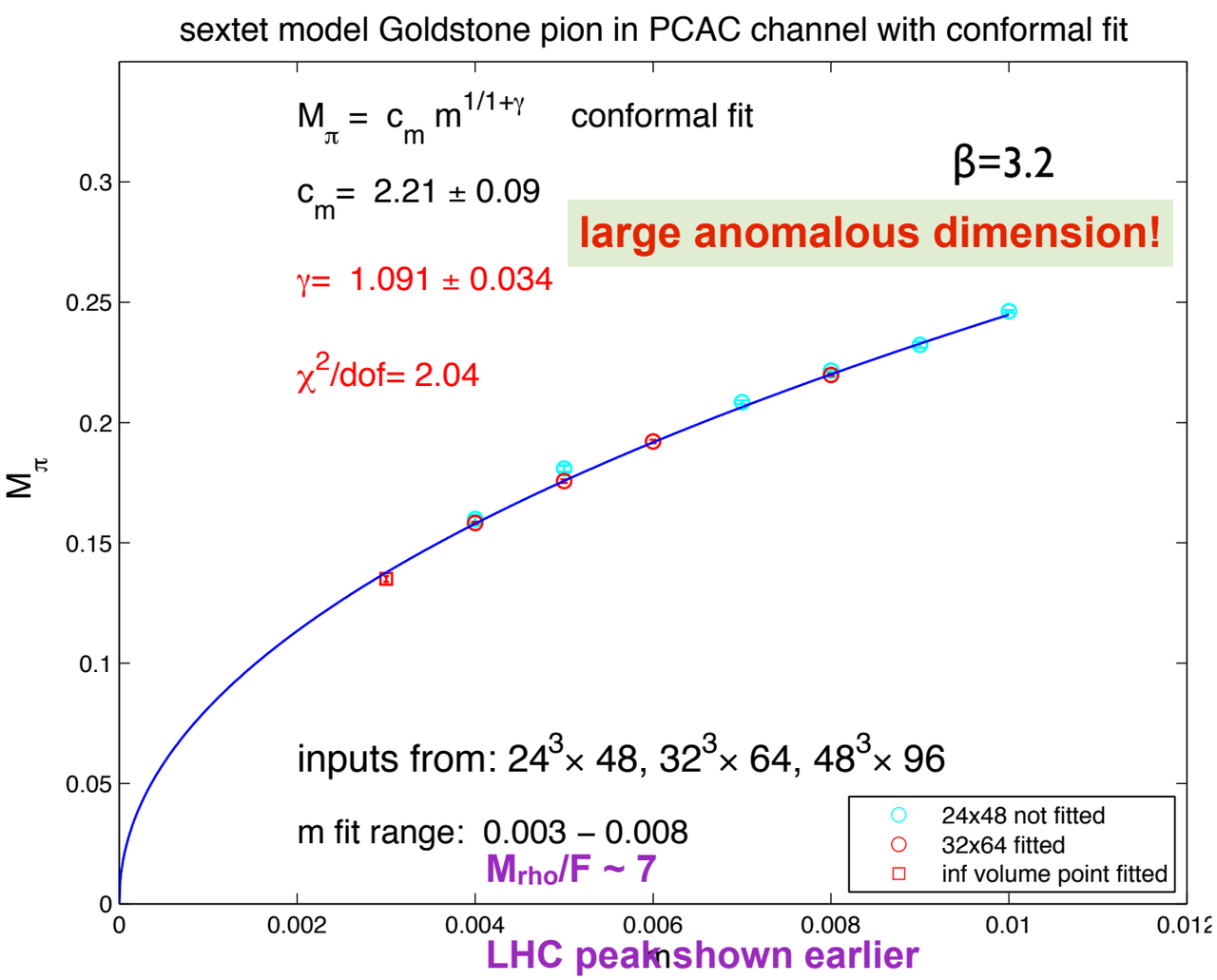

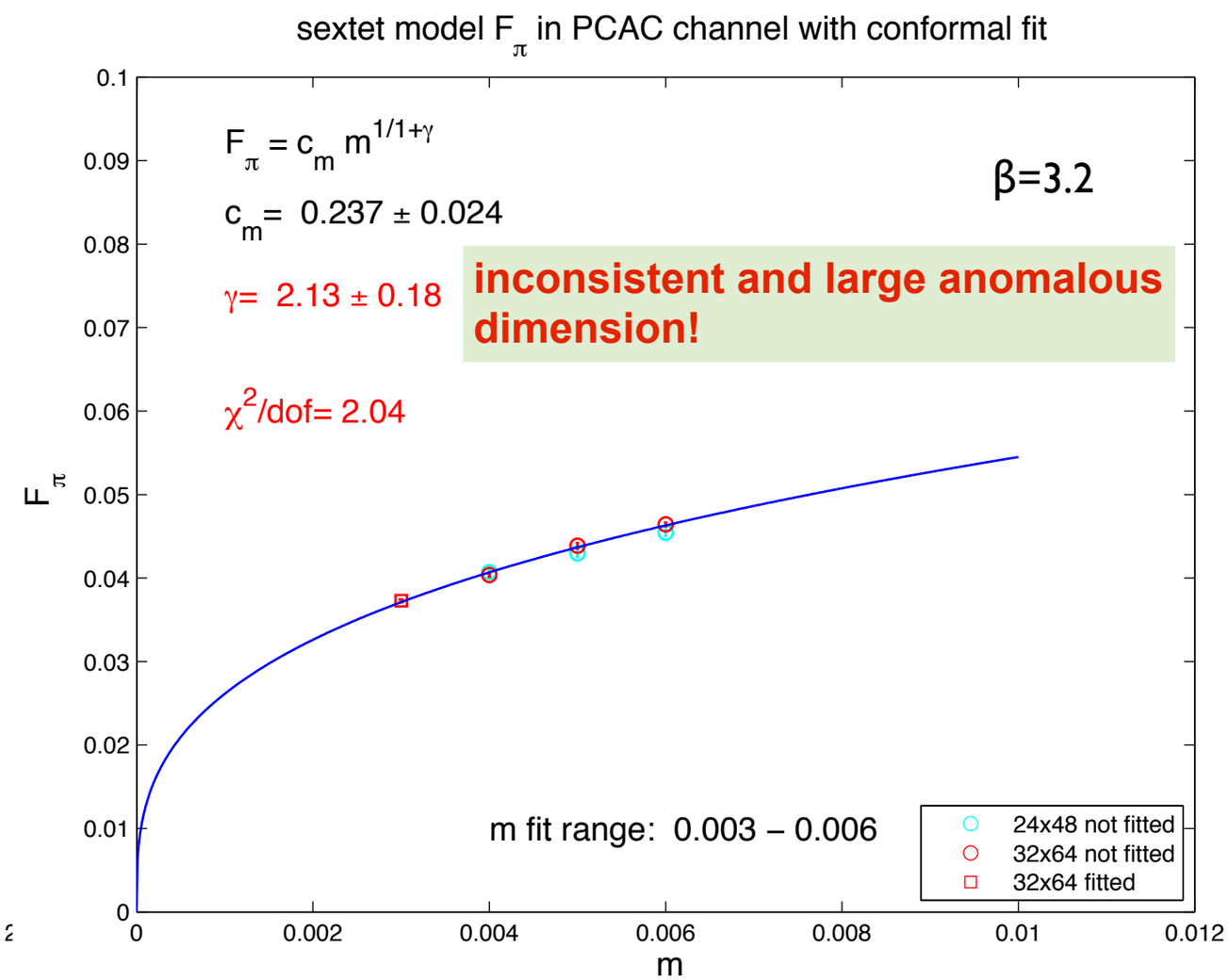

inconsistent large critical exponents γ

conformal hypothesis breaks down in global fits:

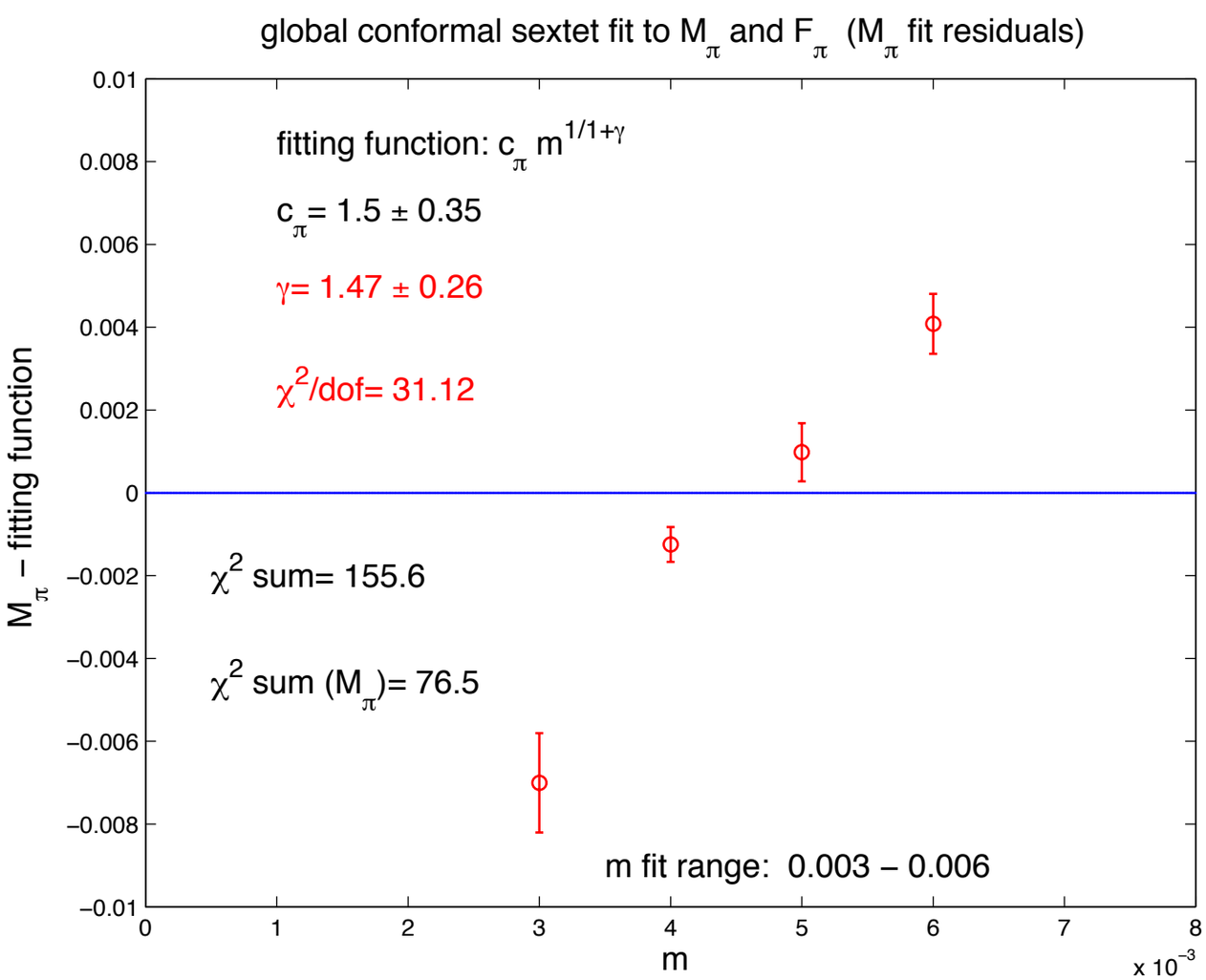

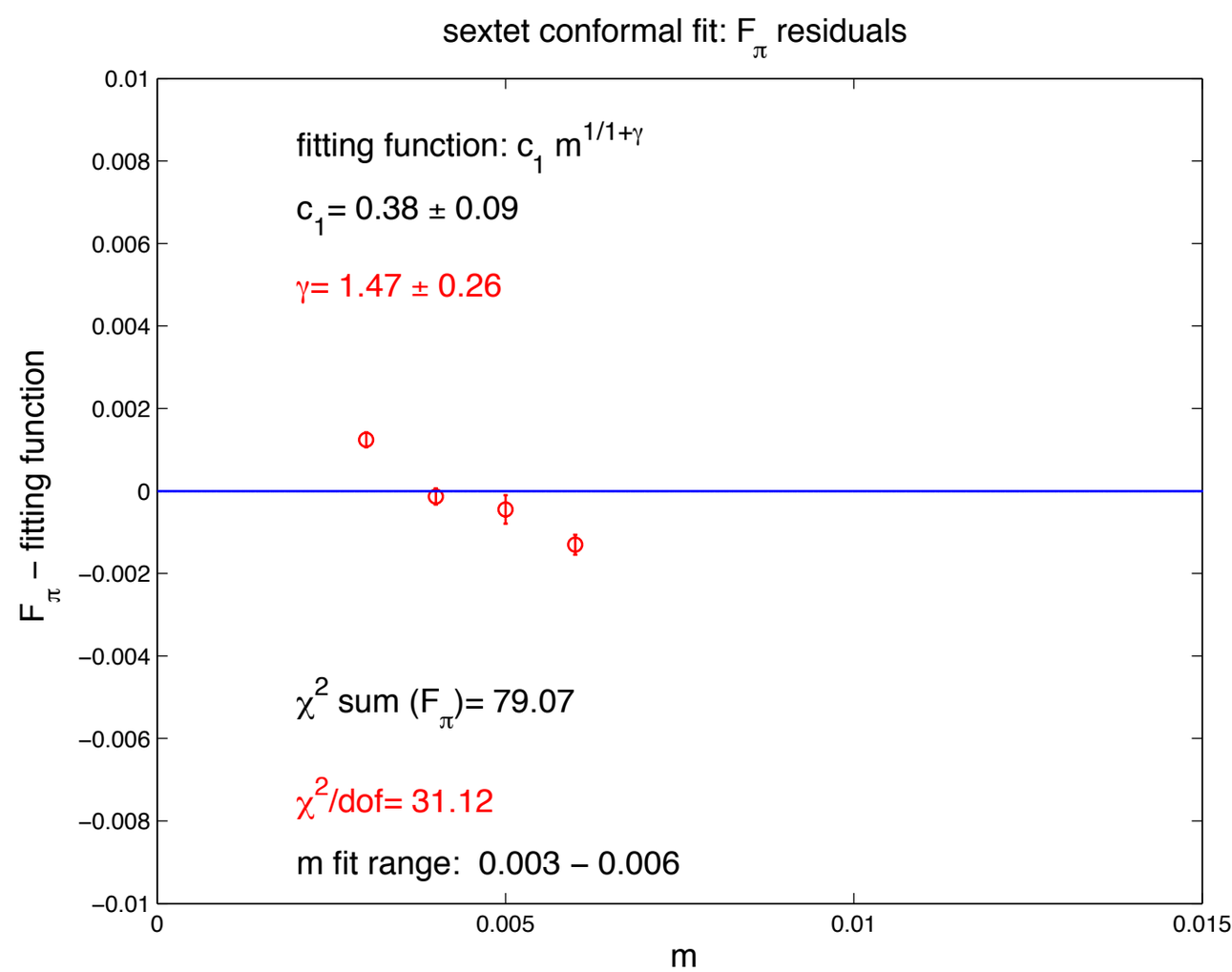

large and inconsistent critical exponents γ

are we close enough to the critical surface?

working on baryon spectrum

dark matter candidate

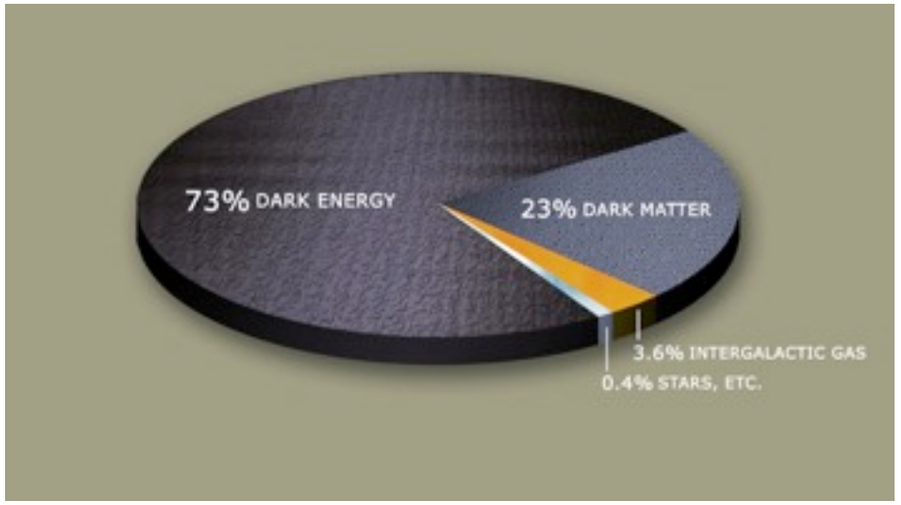

- lightest technibaryon can be stable by analog of $U(1)_B$

- an initial matter/anti-matter asymmetry gets shared among baryons, leptons, technibaryons via sphalerons

(Chivukula, Barr, Fahri, Nussinov)

- can get observed $\Omega_{DM}/\ \Omega_B$ easily for ~ TeV scale DM

must be electrically neutral, EW singlets to avoid direct detection

Then leading operators are charge radius and polarizability:

ex.) $$\frac{B^* B\, v_\mu\, \partial_\nu F^{\mu\nu}}{\Lambda_{TC}^2}\,,\ \frac{B^* B\, F_{\mu\nu} F^{\mu\nu}}{\Lambda_{TC}^3}$$

lattice input?

from Adam Martin

EW phase transition in sextet Higgs model - early universe

sextet model ***(Kogut-Sinclair)***

potential implications in early cosmology

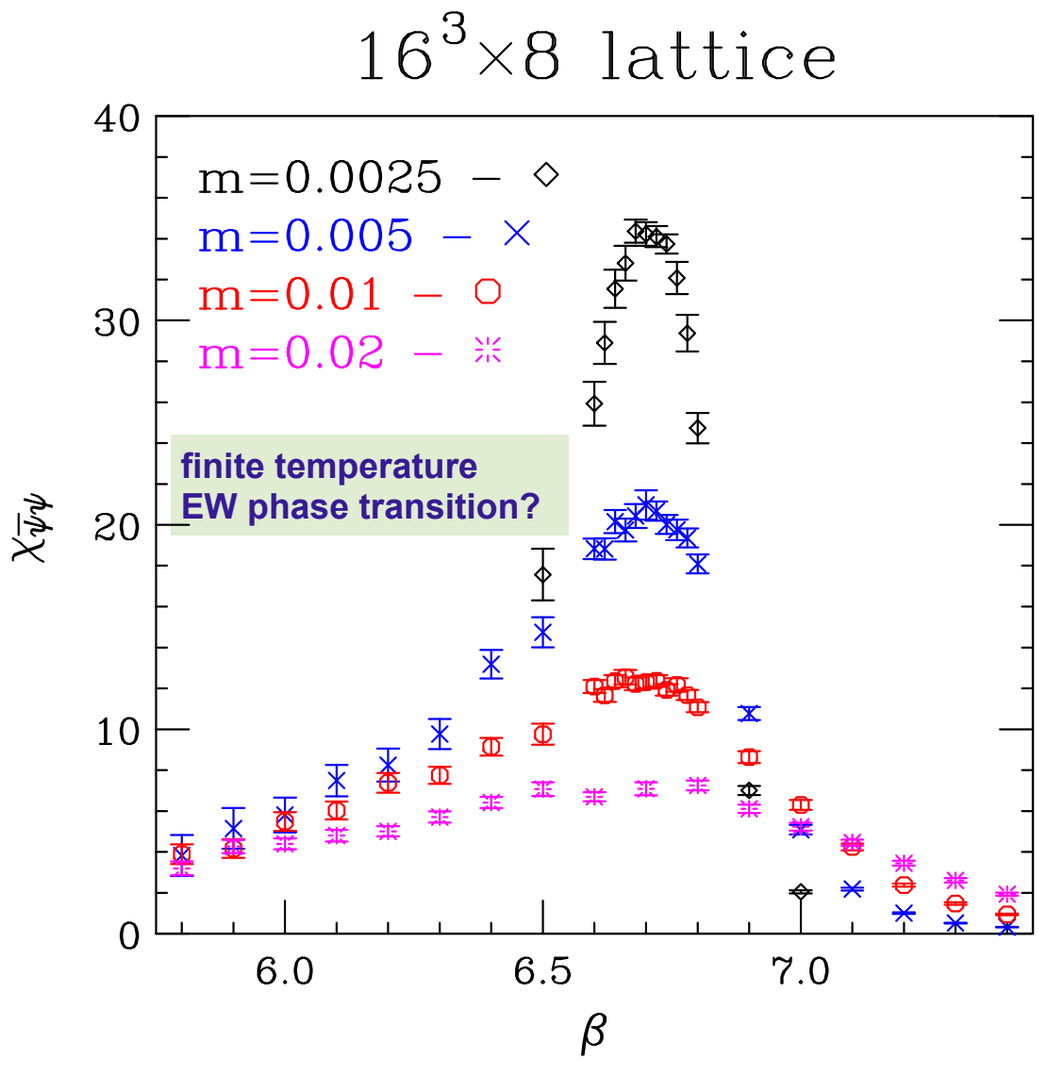

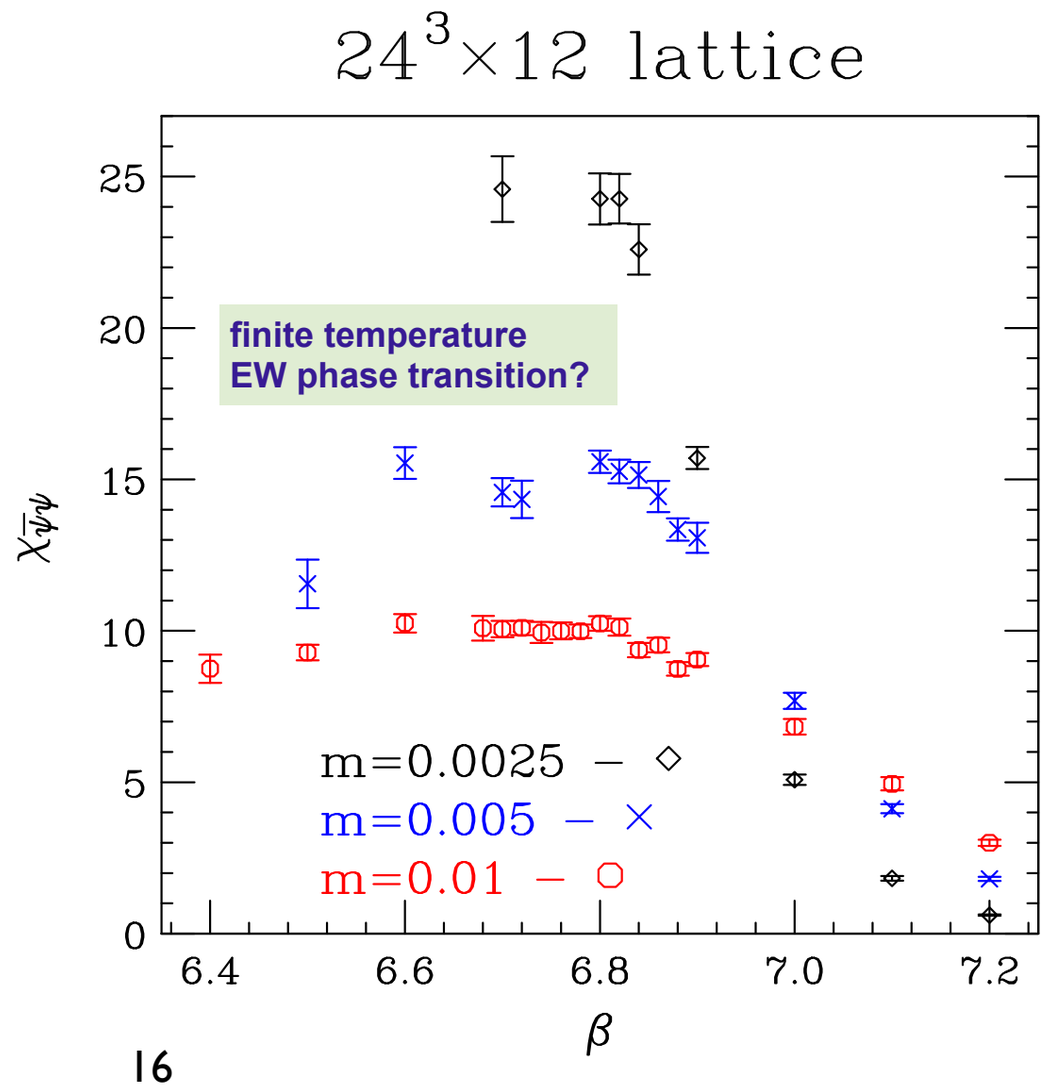

Nf=2 SU(3) sextet rep summary:

- No inconsistency with χSB in Nf=2 SU(3) sextet model

- We find inconsistency with conformal symmetry in all tests

- The effective anomalous dimension is inconsistent and large γ is in 1-2 range

- Kogut and Sinclair: looking for finite temperature χSB phase transition

- No inconsistency with χSB in Nf=2 SU(3) sextet model

- We find inconsistency with conformal symmetry in all tests

- The effective anomalous dimension is inconsistent and large γ is in 1-2 range

- Kogut and Sinclair: looking for finite temperature χSB phase transition

- DeGrand et al. find: Nf=2 sextet beta function might have an IRFP zero?
- uninteresting model with small anomalous dimension ?

$\gamma < 0.45$ controversy is not resolved

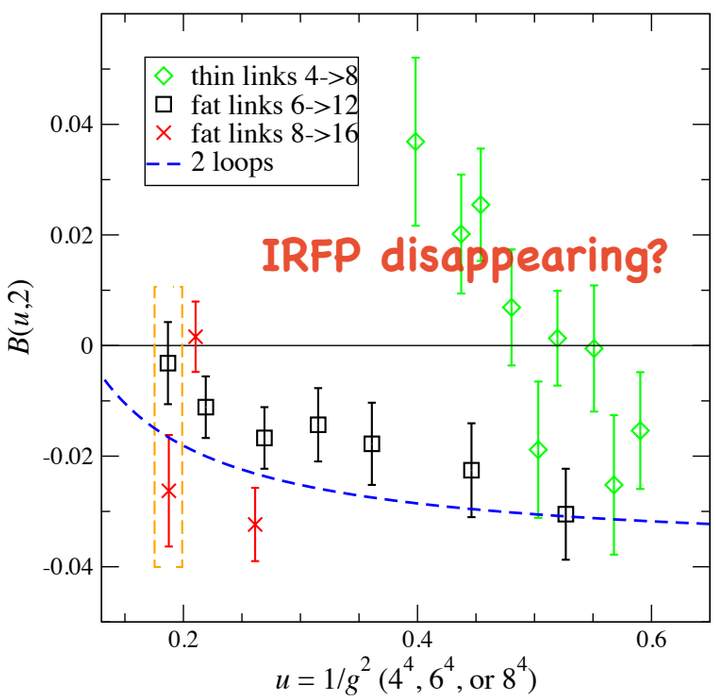

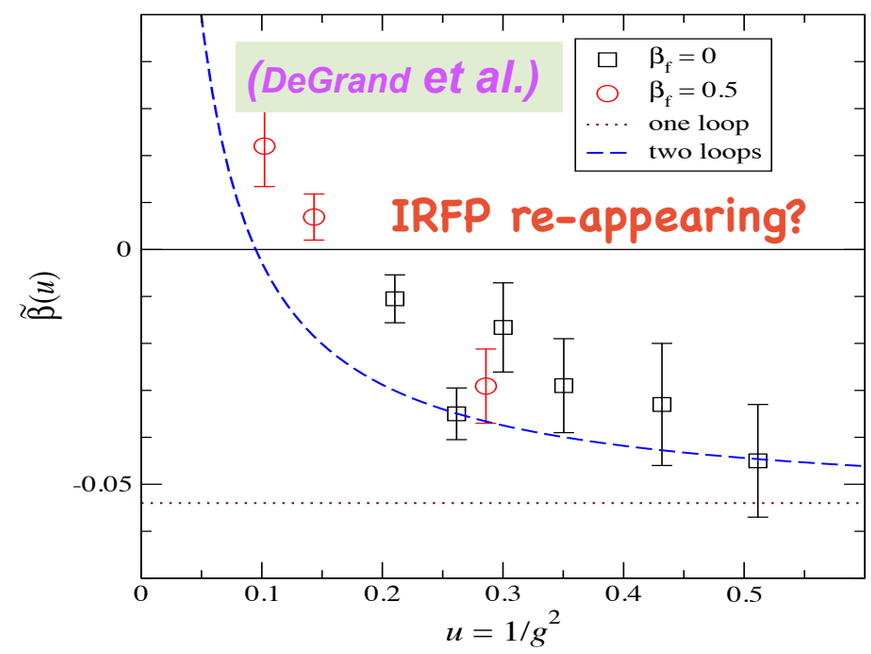

- No inconsistency with χSB in Nf=2 SU(3) sextet model

- We find inconsistency with conformal symmetry in all tests

- The effective anomalous dimension is inconsistent and large γ is in 1-2 range

- Kogut and Sinclair: looking for finite temperature χSB phase transition

- DeGrand et al. find: Nf=2 sextet beta function might have an IRFP zero?
- uninteresting model with small anomalous dimension ?

  $\gamma < 0.45$ controversy is not resolved

- We expect: the Nf=2 sextet model with SU(3) color is an interesting candidate for the composite Higgs mechanism

- But viability requires confirmation, studies of the running coupling, the S-parameter, and composite Higgs physics

status of SU(3) Nf=12 fundamental rep

our group: mass-deformed theory close to m=0 critical surface and m->0 limit:

- two strategies complement: (1) inf volume conform scaling
  (2) mass-deformed FSS
  (2) is used in Nf=12 fundamental SU(3) rep

- direct access to some effective anomalous dimension

- similar to tests of RG scaling laws of moments of correlator functions (in progress)

bulk transition? (Schroeder, Latt 2011)

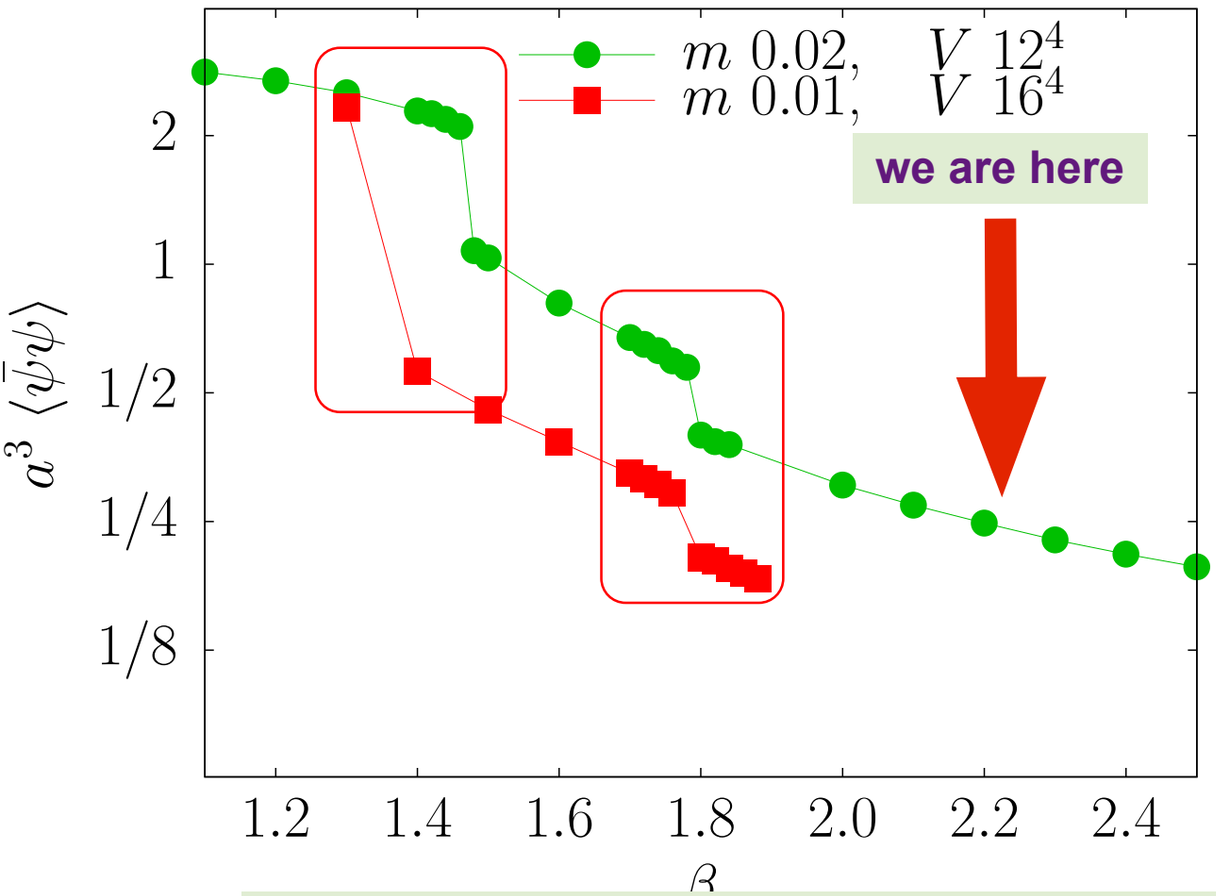

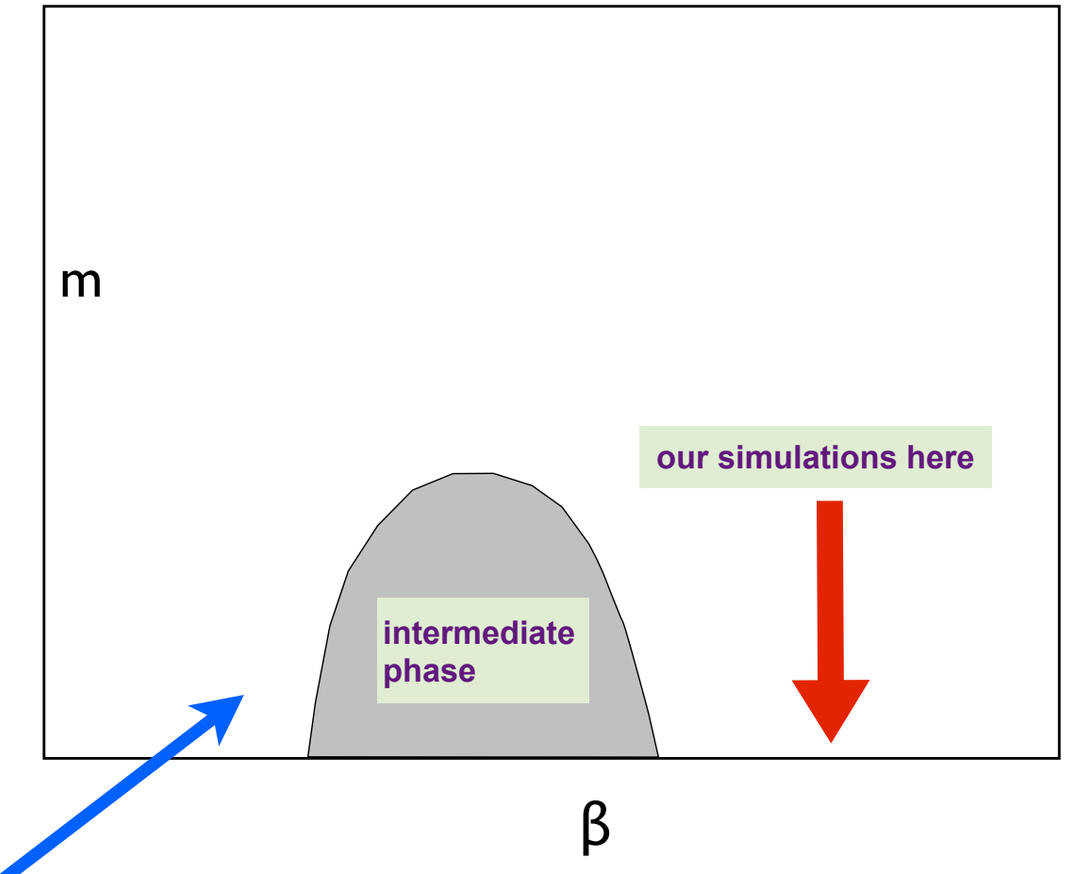

Deuzeman et al. new study

A. Hasenfratz et al. new study

Our simulation are not effected

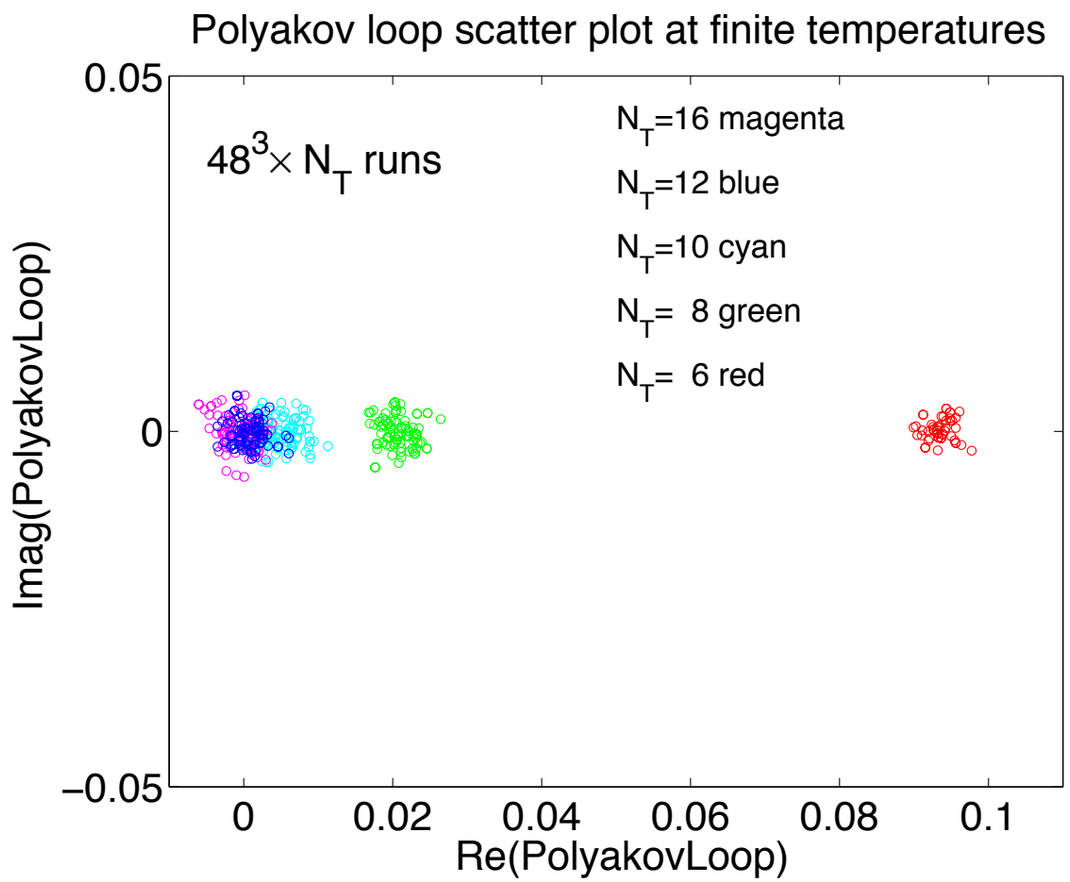

finite T transition at β=2.2?

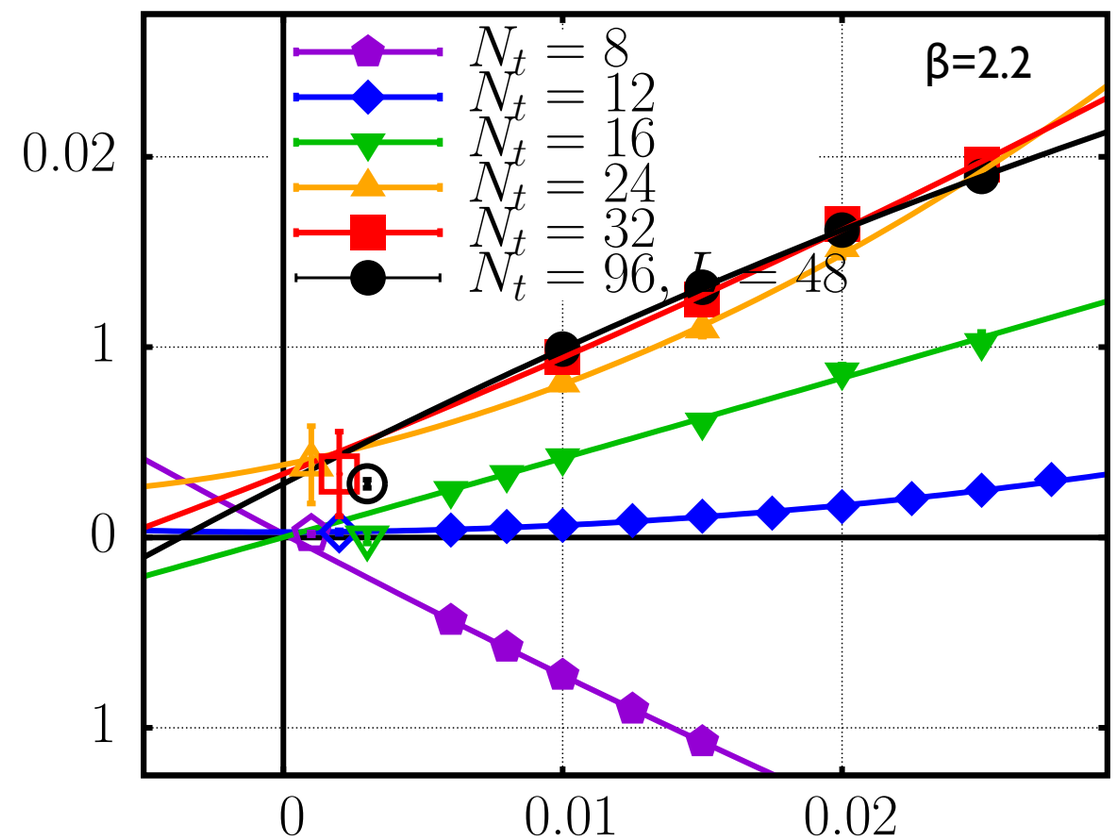

$48^3 \times N_t$ sequence
(Schroeder, Latt 2011)

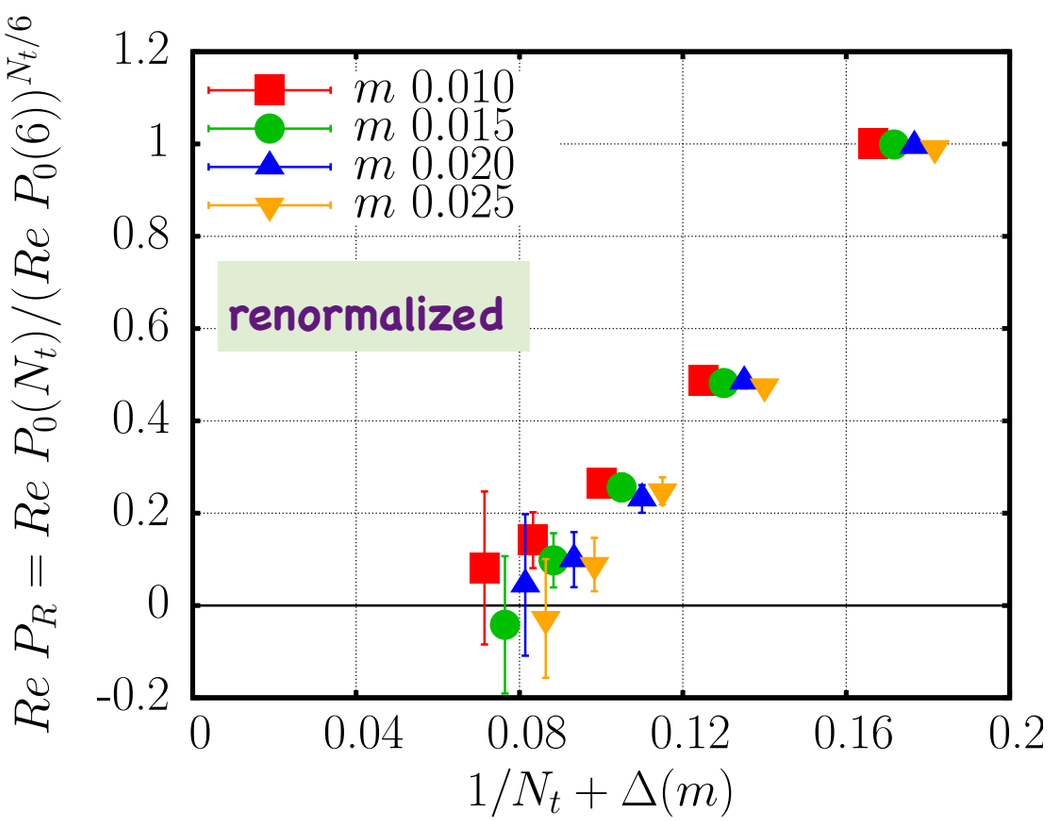

Re P approaches zero at low temperature

zero temp confinement - running coupling without IRFP ?

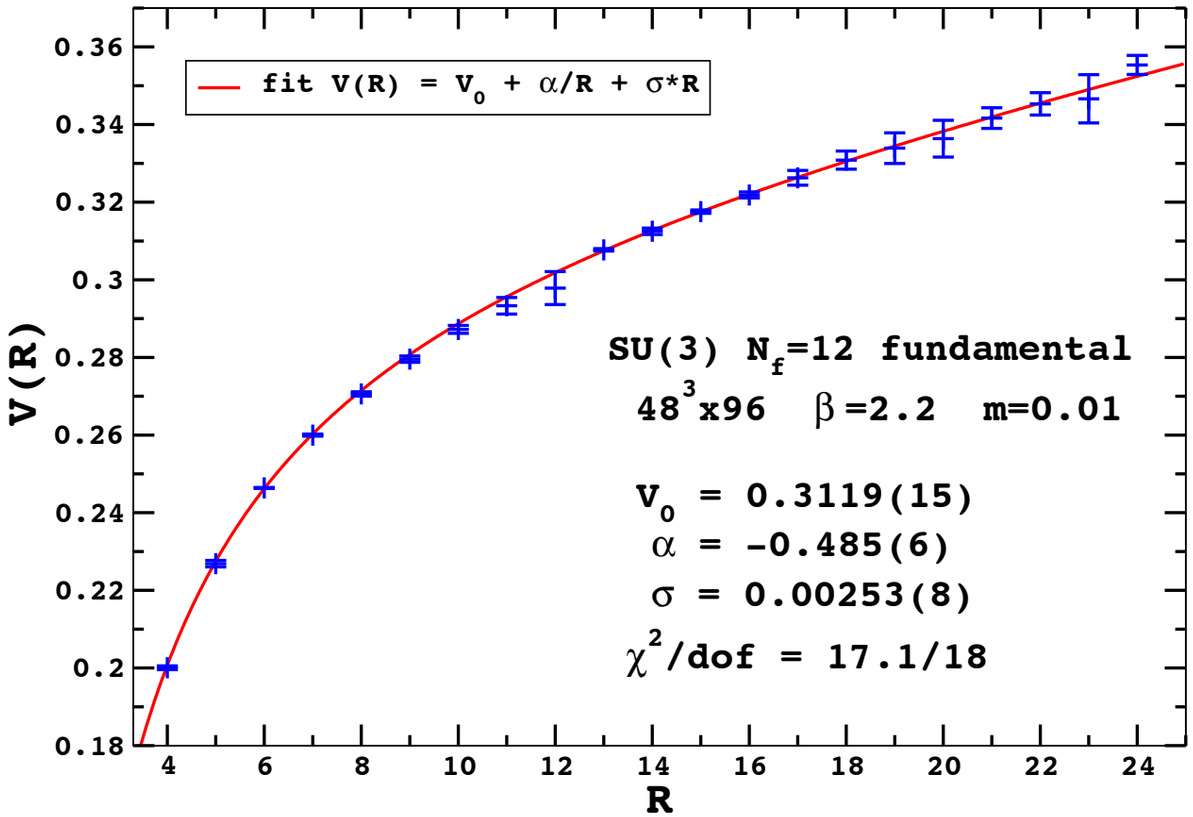

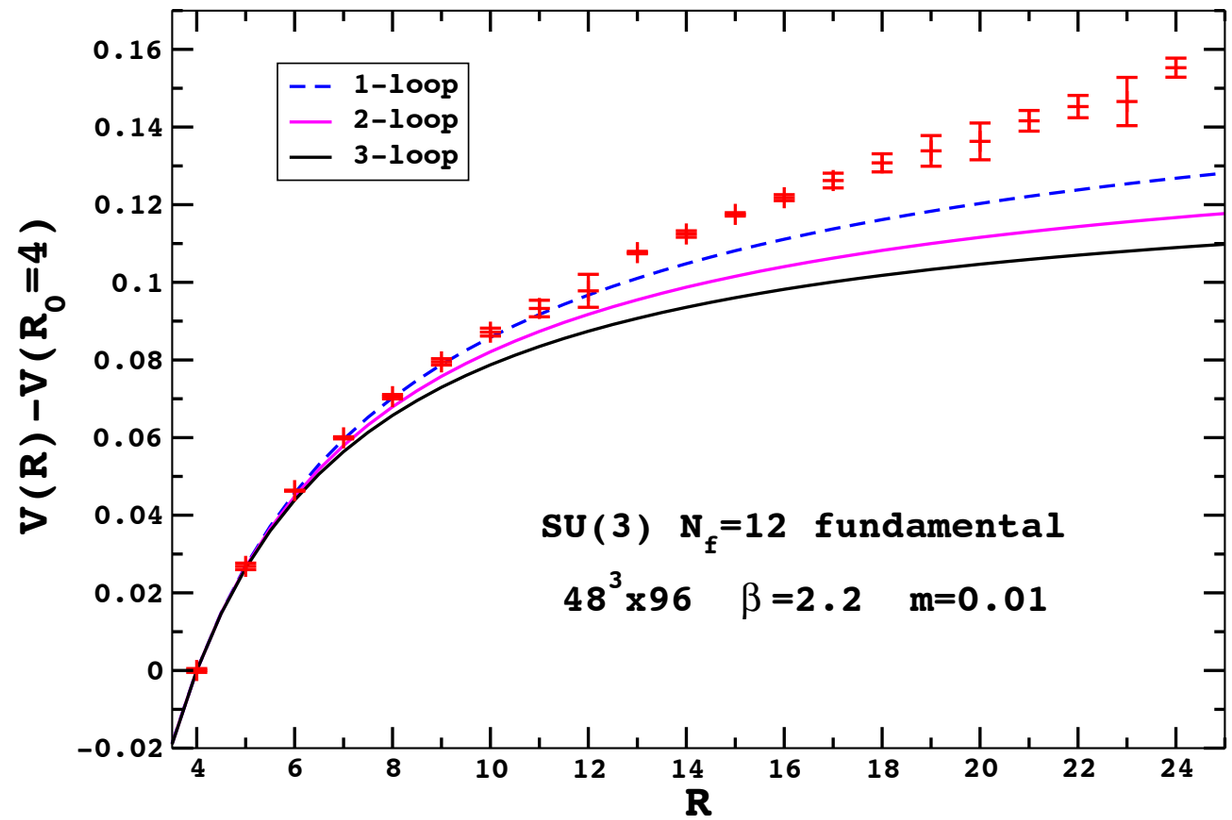

m --> 0 and a --> 0 limits? finite volume effects?

useful to compare with other methods:

- SF?
- MCRG?
- two new methods we are developing:
  current correlator moments and wilson flow

small chiral symmetry breaking condensate

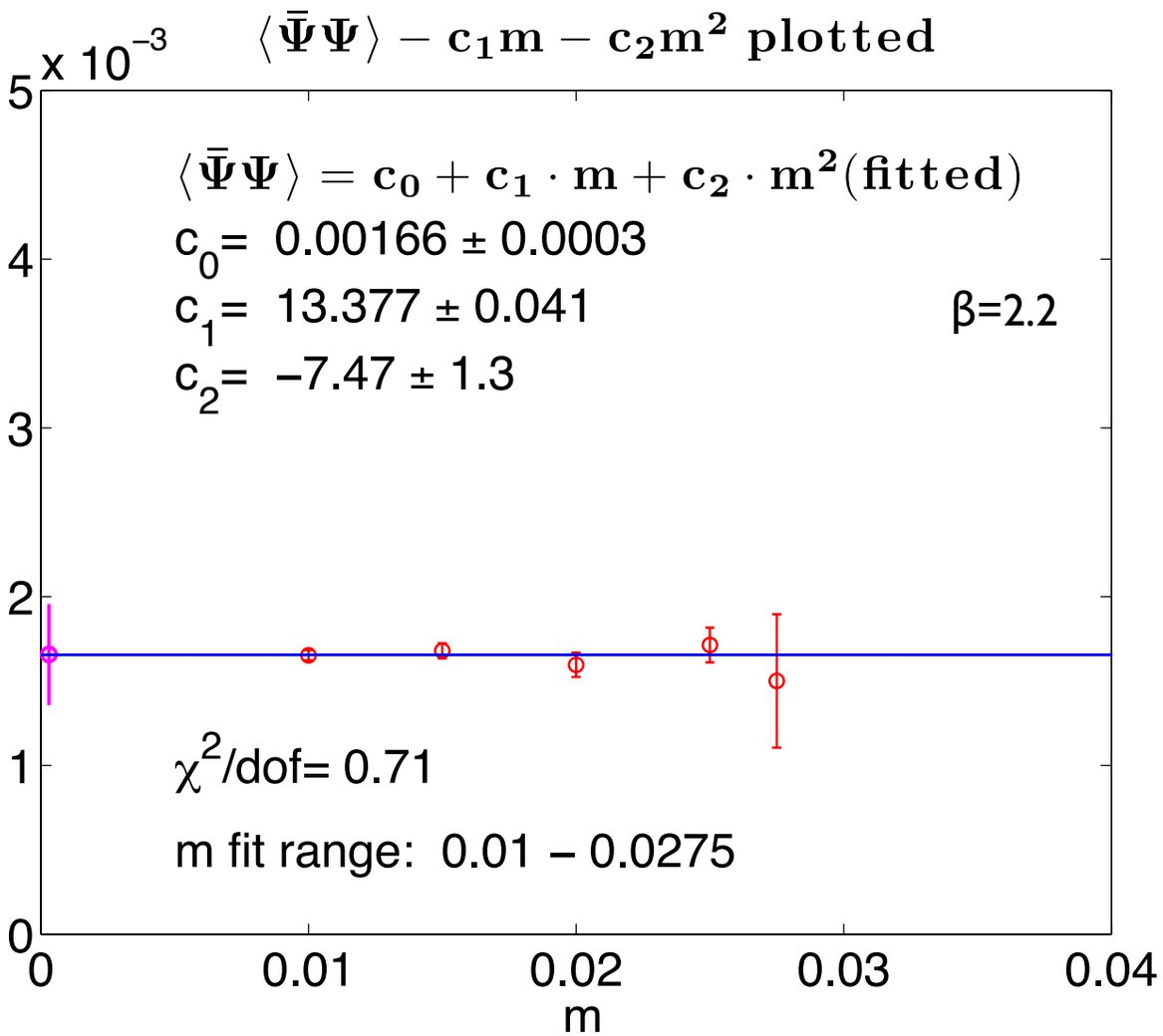

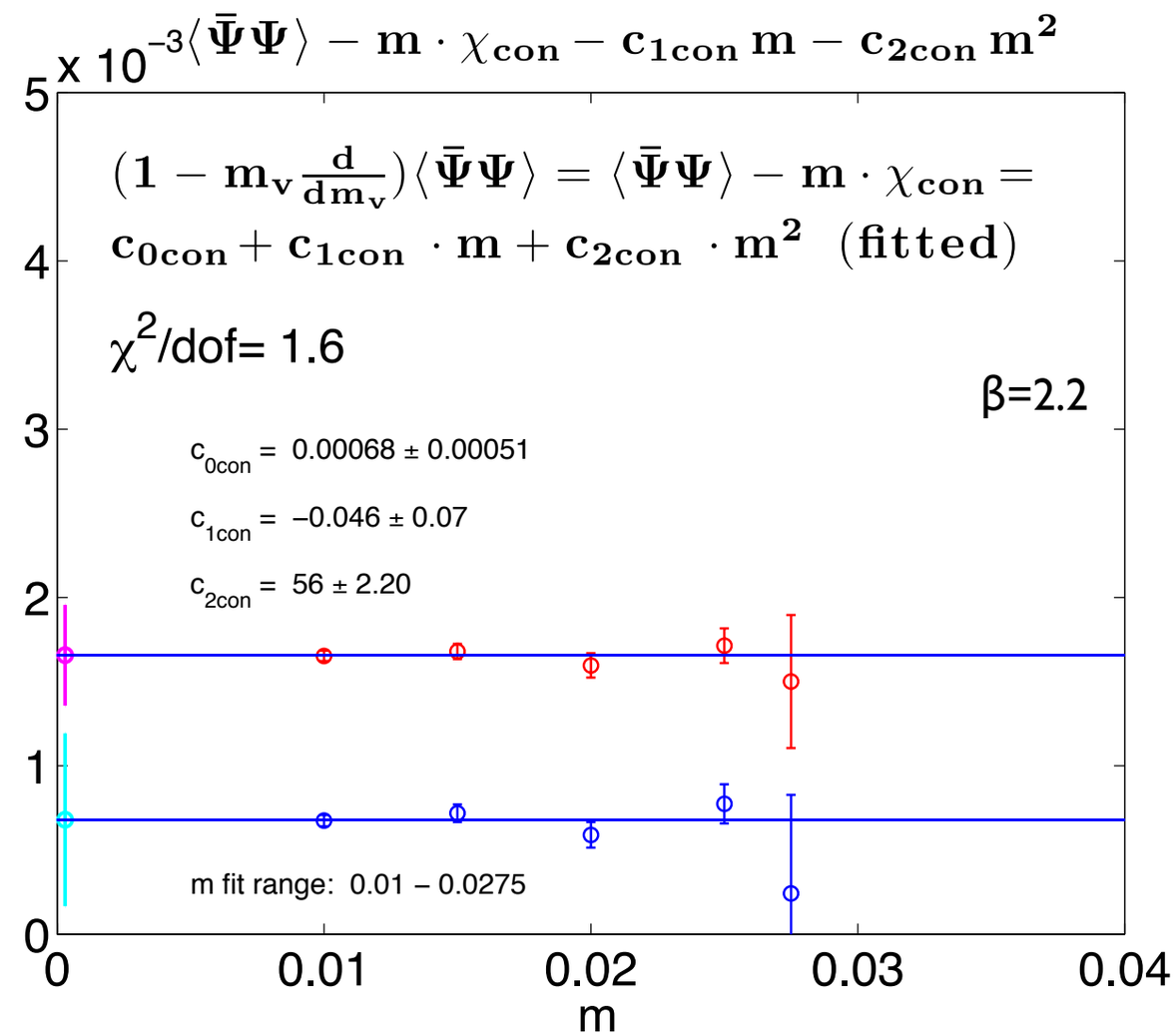

- two independent extrapolation
- condensate very small
- would not be decisive without other tests

conformal scaling test with FSS

heavy use of RG theory

$$LM = f(x) + L^{-\omega} g(x)$$

$$x = m^{1/1+\gamma} L$$

$$\omega = \beta'(g^*)$$

conformal scaling test with FSS - physical model fit

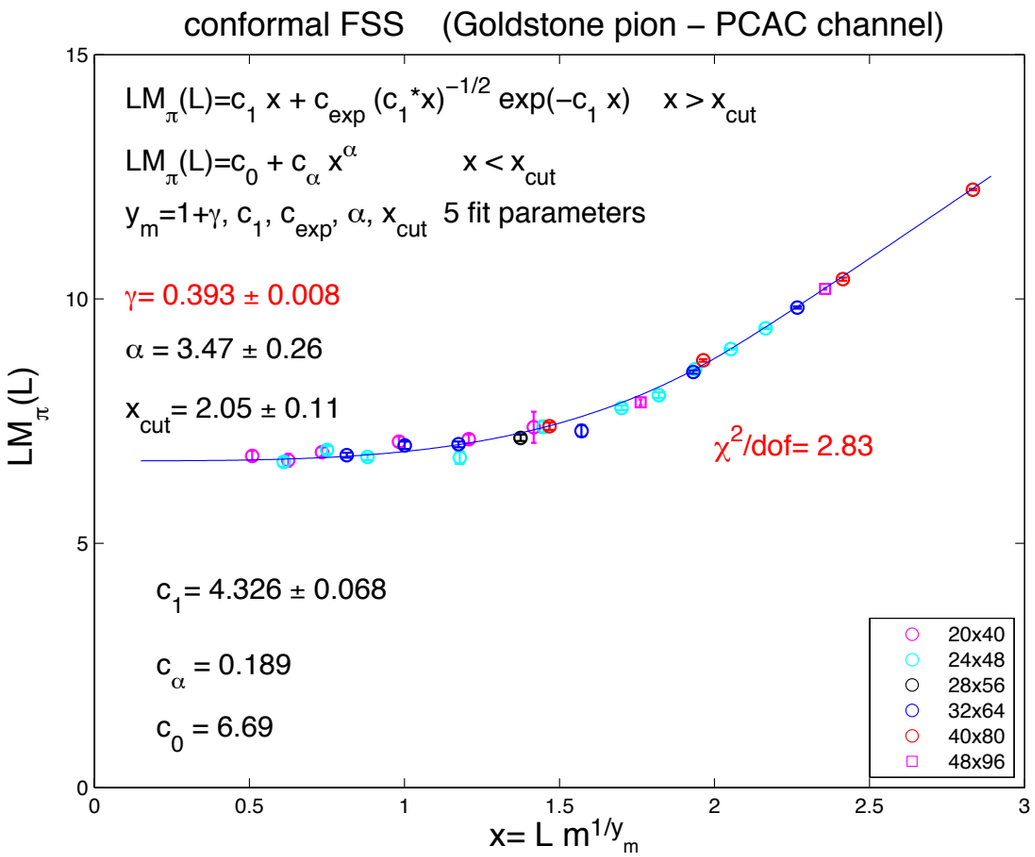

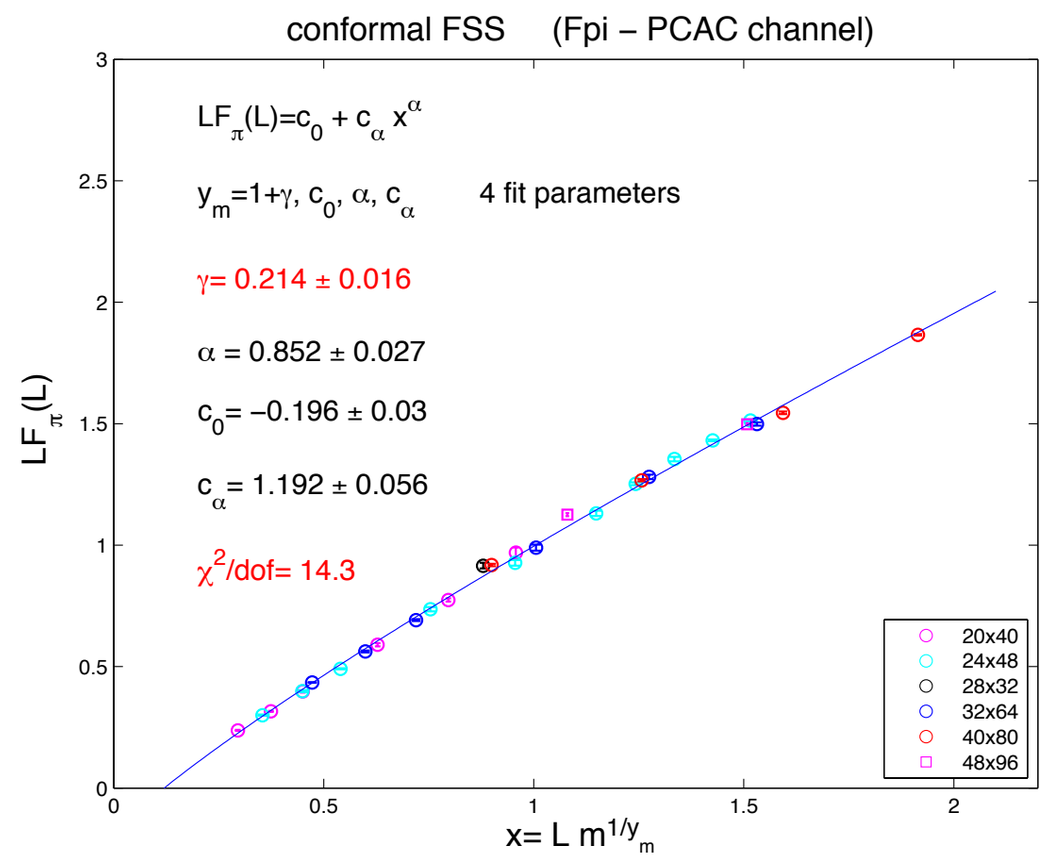

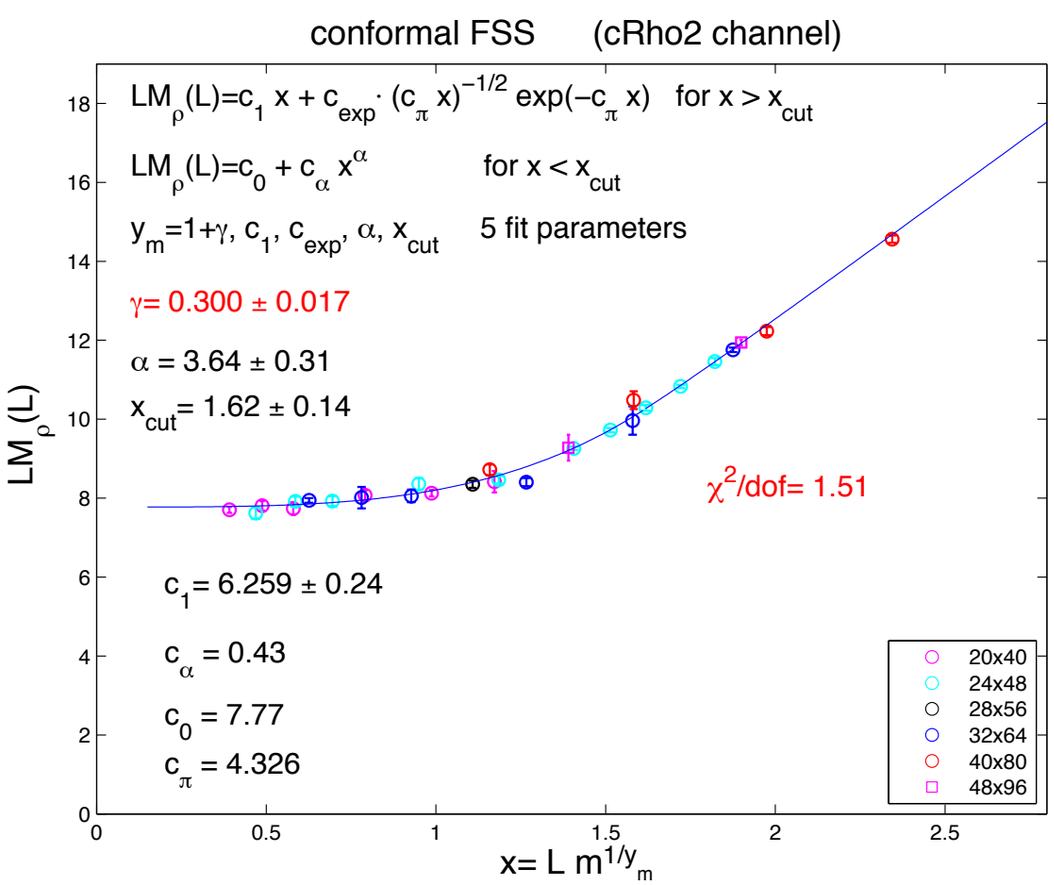

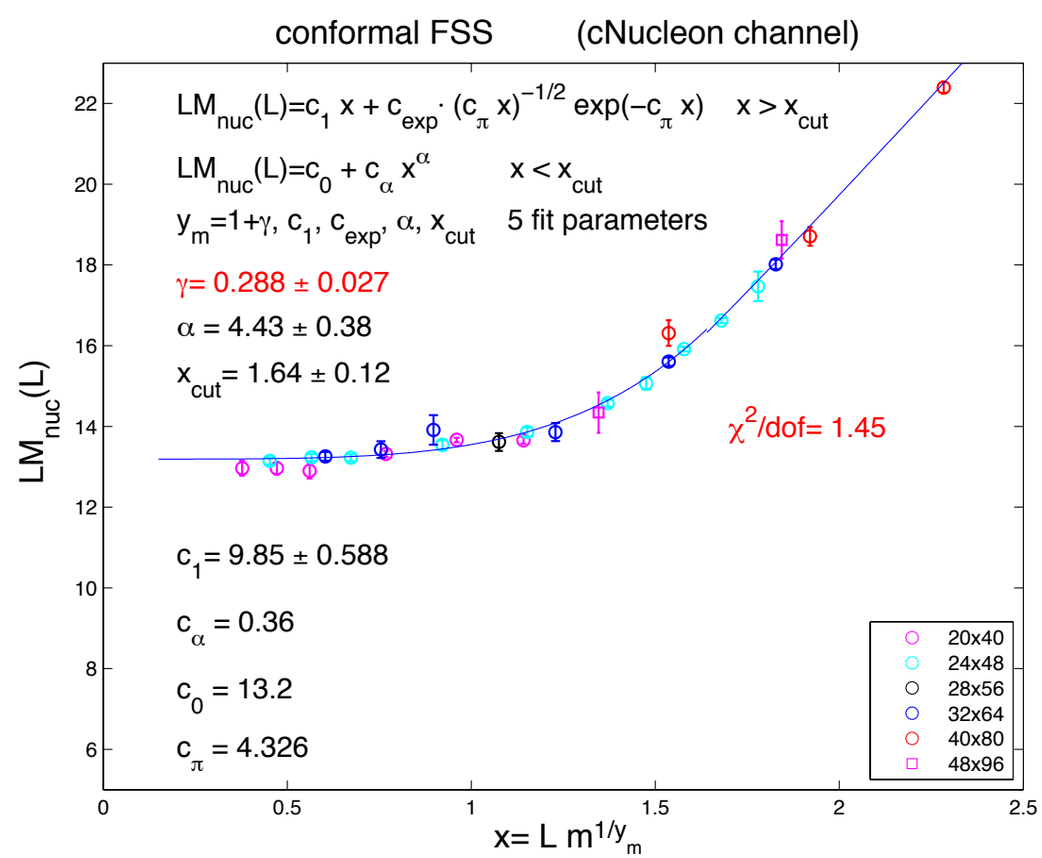

conformal scaling - spline B-form fits

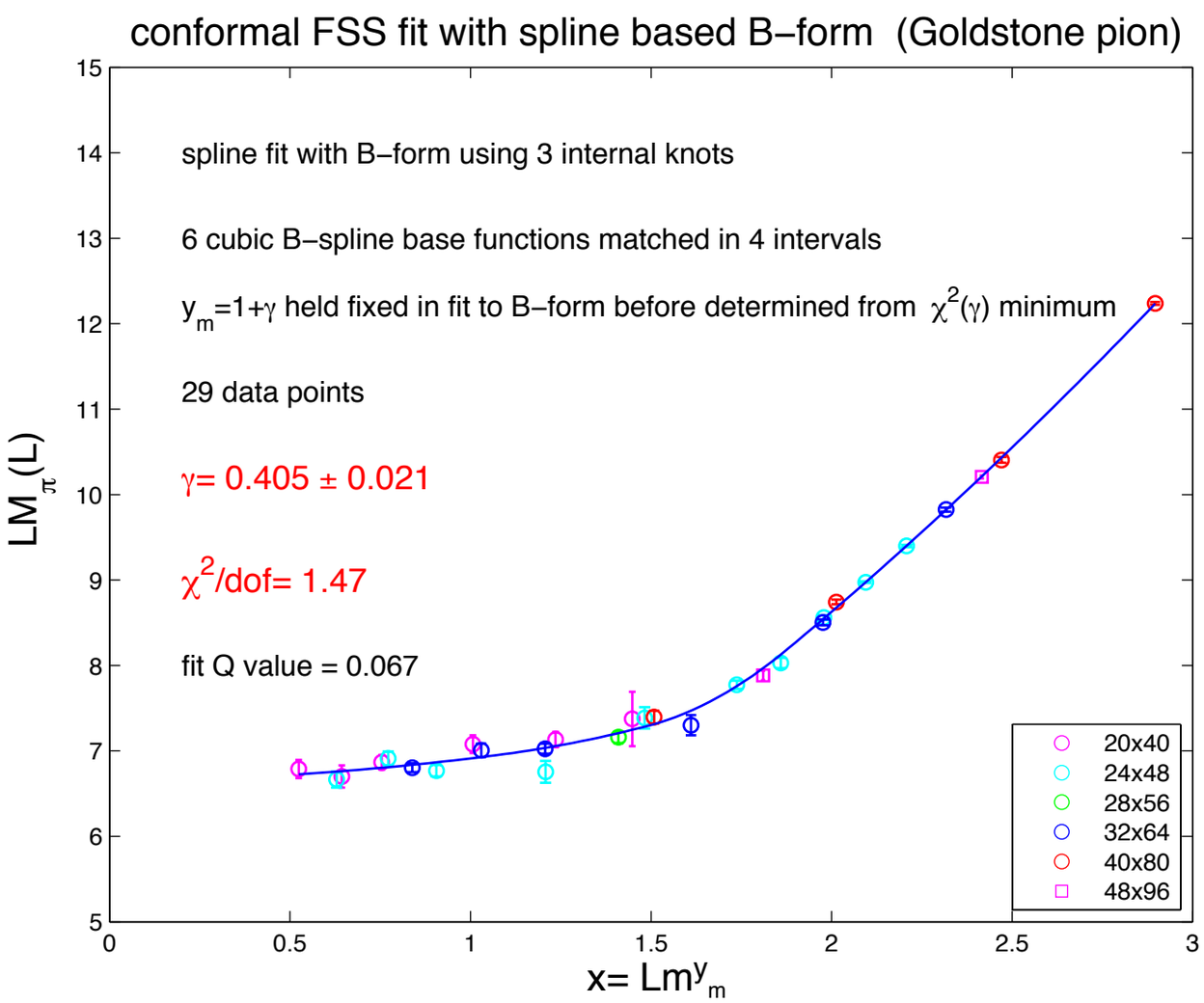

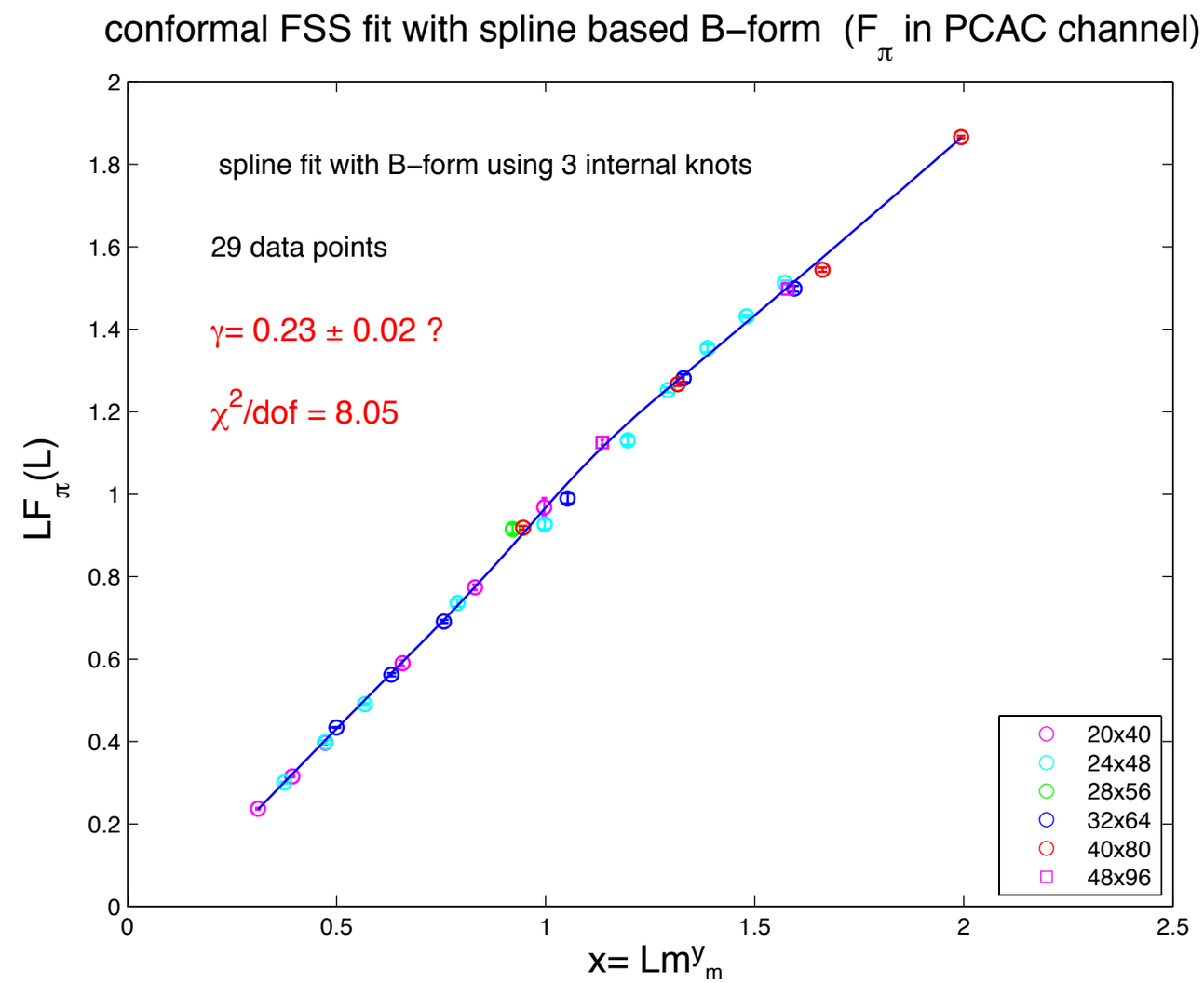

is this glass half full or half empty?

can chiral symmetry breaking fake scaling form?

Deceptions of χSB FSS behavior:

large volume
hadrons point-like

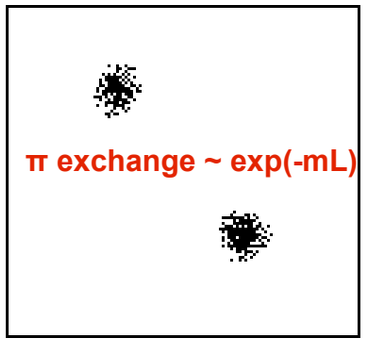

squeezed wavefunction

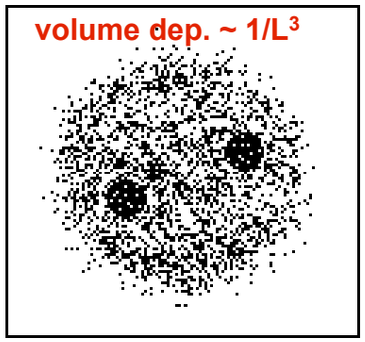

crossover to femto world

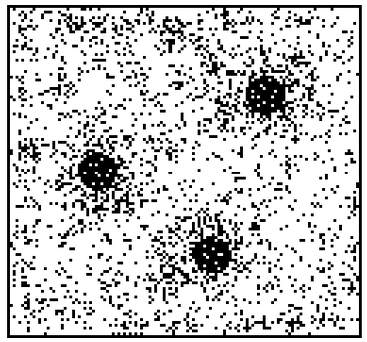

$$\hat{V}(\vec{k}) = \frac{F(\vec{k})^2}{\vec{k}^2 + m^2}$$ extended hadron with form factor

hadron with form-factor

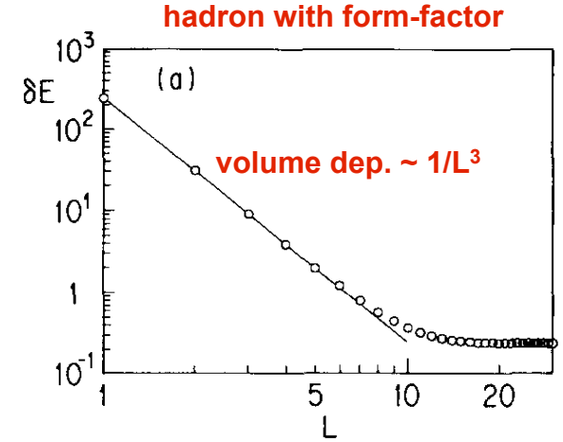

$$F(k) = \frac{1}{1 + c \cdot \vec{k}^2}$$

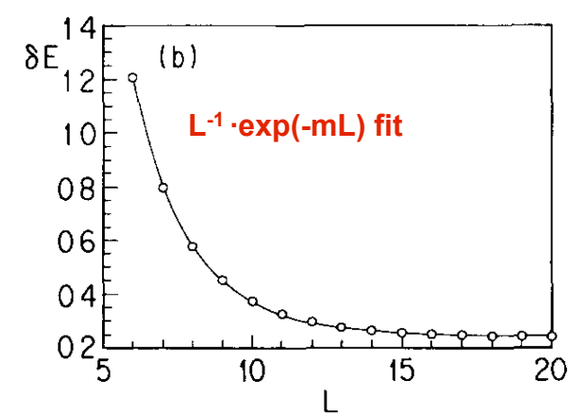

$$F(k) = \frac{1}{1 + c \cdot \vec{k}^2}$$

$$\delta E = \sum_{\vec{n}} V(\vec{n}L)$$ hadrom self energy from interaction with images

Text

$$\delta E = \frac{1}{L^3} \sum_{\vec{n}} \hat{V}(\vec{n}\frac{2\pi}{L})$$ Poisson resummation, $\hat{V}(\vec{k})$ is the Fourier transform

$$\hat{V}(\vec{k}) = \frac{1}{\vec{k}^2 + m^2} \quad \Rightarrow \quad V(r) = \frac{e^{-mr}}{r}$$ for large r in point-like approximation

$$\delta E \approx V(0) + 6V(L) \qquad \delta E \approx \frac{e^{-mL}}{L}$$ point-like interaction for large L (non-relativistic)

Lüscher made it relativistic using field theory

Leutwyler put in the chiral vertices, hence the $\tilde{g}(mL)$ form in chiral PT

the size where the 1/L³ correction to the masses disappears and the exponential behavior sets in depends on the behavior of the hadron form factor

the characteristic inverse power vs. exponential behavior can frustrate at limited lattice sizes the analysis of chiral vs. conformal hypotheses

the size where the 1/L³ correction to the masses disappears and the exponential behavior sets in depends on the behavior of the hadron form factor

Nf=12 SU(3) fundamental rep summary:

- We run in the weak coupling phase

- At fixed coupling and very small fermion mass we see confining potential and finite temp χSB transition

- The effective anomalous dimension γ is not consistent across channels can be explaind by scaling violation effects or underestimated errors?

- We run in the weak coupling phase

- At fixed coupling and very small fermion mass we see confining potential and finite temp χSB transition

- The effective anomalous dimension γ is not consistent across channels can be explaind by scaling violation effects or underestimated errors?

- Running coupling methods like TPL and SF have problems to control systematics

no comment on MCRG

- We run in the weak coupling phase

- At fixed coupling and very small fermion mass we see confining potential and finite temp χSB transition

- The effective anomalous dimension γ is not consistent across channels can be explaind by scaling violation effects or underestimated errors?

- Running coupling methods like TPL and SF have problems to control systematics

  no comment on MCRG

Running coupling problems in TPL and SF schemes:

- We run in the weak coupling phase

- At fixed coupling and very small fermion mass we see confining potential and finite temp χSB transition

- The effective anomalous dimension γ is not consistent across channels can be explaind by scaling violation effects or underestimated errors?

- Running coupling methods like TPL and SF have problems to control systematics

no comment on MCRG

Running coupling problems in TPL and SF schemes:

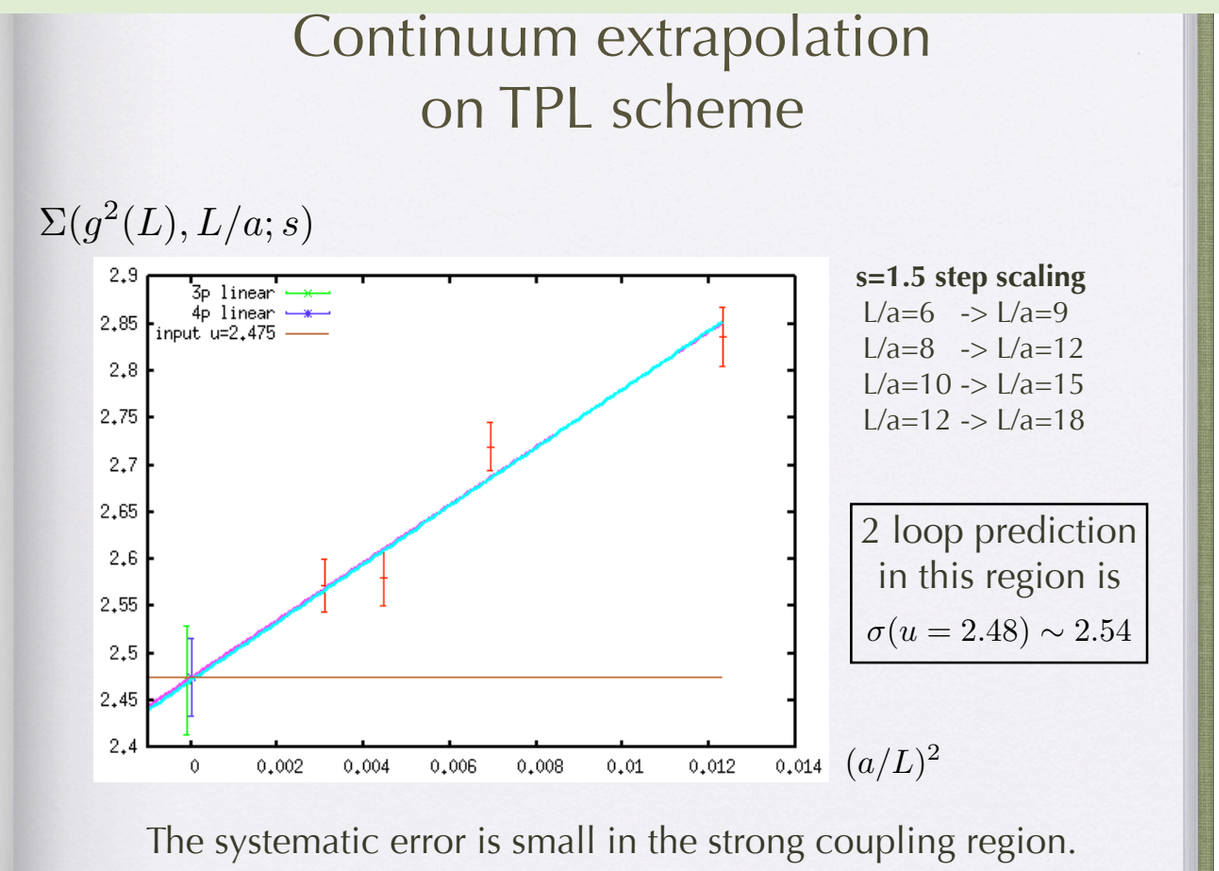

- We run in the weak coupling phase

- At fixed coupling and very small fermion mass we see confining potential and finite temp χSB transition

- The effective anomalous dimension γ is not consistent across channels can be explaind by scaling violation effects or underestimated errors?

- Running coupling methods like TPL and SF have problems to control systematics

no comment on MCRG

Running coupling problems in TPL and SF schemes:

Continuum extrapolation on TPL scheme

$\Sigma(g^2(L), L/a; s)$

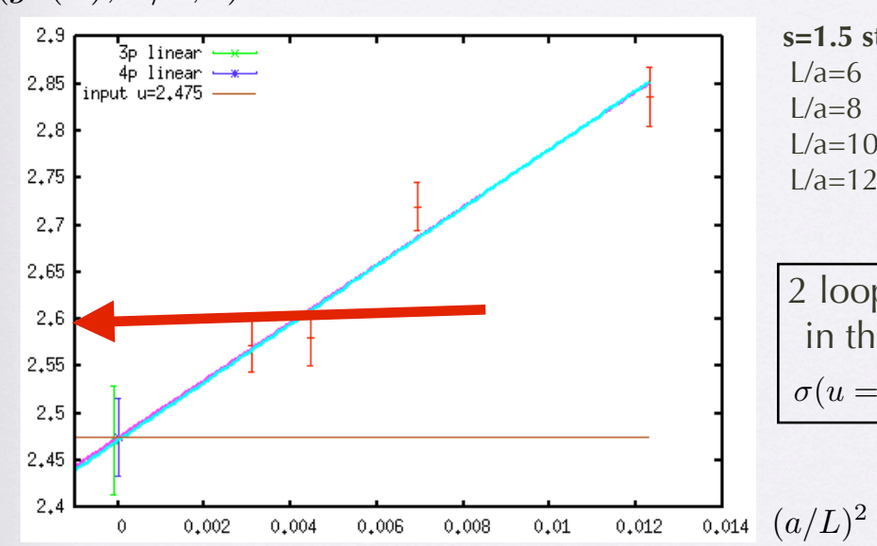

s=1.5 step scaling
L/a=6 -> L/a=9
L/a=8 -> L/a=12
L/a=10 -> L/a=15
L/a=12 -> L/a=18

2 loop prediction in this region is $\sigma(u = 2.48) \sim 2.54$

The systematic error is small in the strong coupling region.

- We run in the weak coupling phase

- At fixed coupling and very small fermion mass we see confining potential and finite temp χSB transition

- The effective anomalous dimension γ is not consistent across channels can be explaind by scaling violation effects or underestimated errors?

- Running coupling methods like TPL and SF have problems to control systematics

no comment on MCRG

Running coupling problems in TPL and SF schemes:

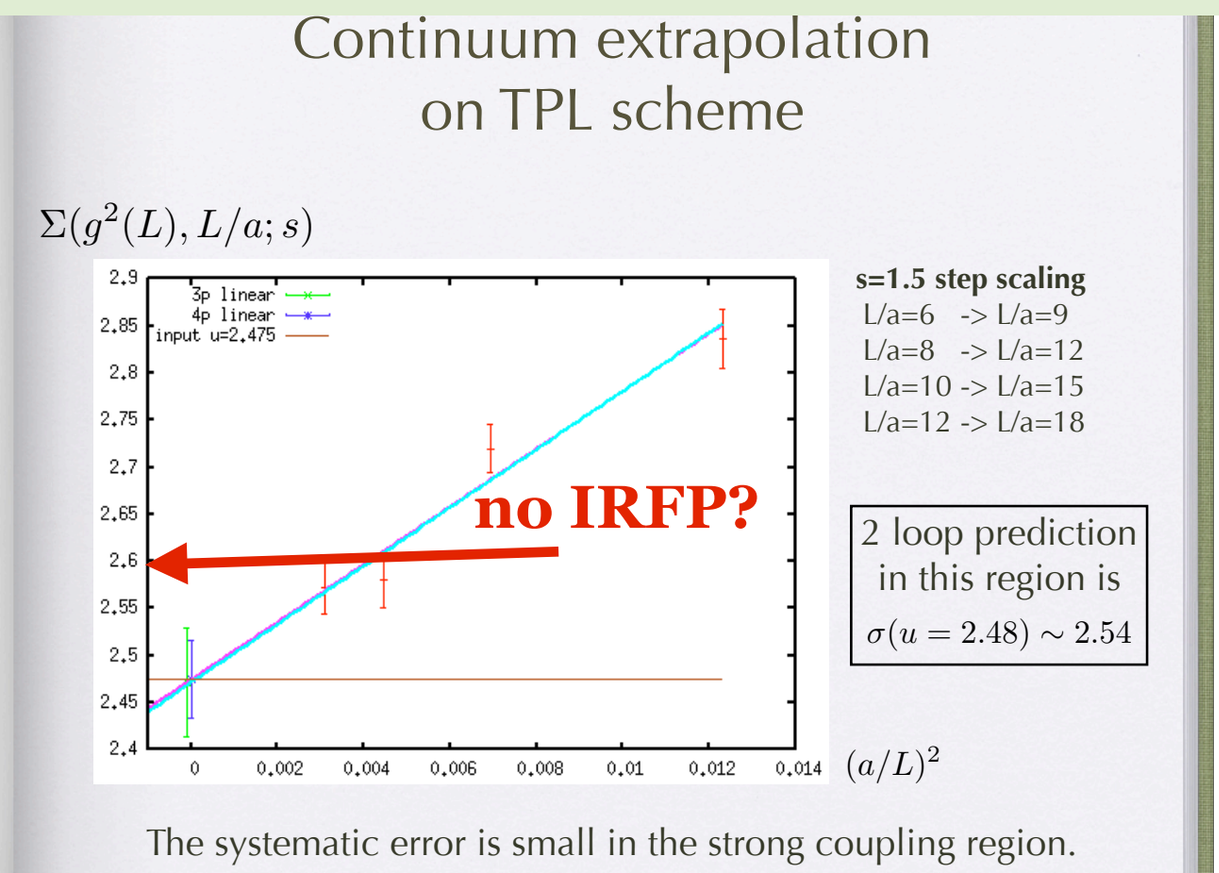

- We run in the weak coupling phase

- At fixed coupling and very small fermion mass we see confining potential and finite temp χSB transition

- The effective anomalous dimension γ is not consistent across channels can be explaind by scaling violation effects or underestimated errors?

- Running coupling methods like TPL and SF have problems to control systematics
  no comment on MCRG

- We are working on two new running coupling methods with massless fermions using moments of current correlators and wilson flows both are g(L)

- Difficult decision on the Nf=12 model: we would probably prefer to put all the resources into the sextet model without the community controversies at Nf=12

- But sextet project benefitted directly from what we have learned from Nf=12

backup slides

conformal scaling and scaling violations

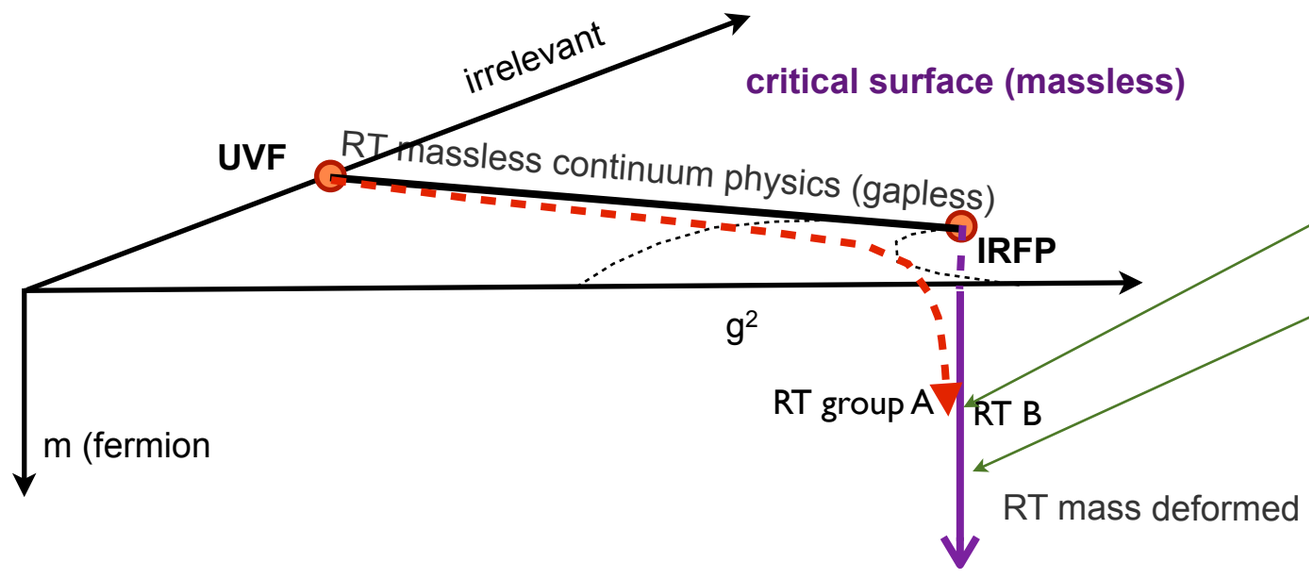

if model had conformal IRFP

two interchangeable RT descriptions?

continuum mass deformed conformal theory is on RT coming out of IRFP

I worked out as an example all the details of 3D scalar theory (Ising model) with IRFP

textbook material

Del Debbio and collaborators
early conform apps

free energy on RT:

$$f(u_1,u_2,\ldots) = g(u_1,u_2,\ldots) \;+\; b^{-d} f_s(b^{y_1}u_1, b^{y_2}u_2\ldots)$$

analytic singular

$y_1 > 0$ only relevant exponent in our case
$u_1 = t \sim m$ identified, $y_1 = y_m$ in Technicolor notation

y_2 controls scaling violations, leading correction term

analytic function which can have terms like $\sim m^k$ are typically sub-leading

Fisher and Brezin worked out most of what we know!

RG scaling of 2-point function:

$$G^{(2)}(r,m,u_2,\ldots) = b^{-2d} G(r/b, b^{y_m} m, b^{y_2} u_2,\ldots)$$

from $G^{(2)}(r,m,u_2,\ldots) \sim e^{-Mr}$ asymptotics with $M \sim m^{1/y_m}$ scaling follows

leading correction to the scaling term should be $\sim m^{\omega}$ where $\omega = \beta'(g^*)$

analysis would change with second relevant operator at IRFP!

- analytic terms exists, but no reason to be leading conformal scaling correction

- correlators of composite operators require inhomogeneous RG!

similarly, in conformal finite size scaling analysis:

$$\xi / L = f_1(x) + L^{-\omega} f_2(x) \;\text{ with }\; x = L m^{1/y_m}$$

→ This directly transcribes to hadron masses and F_π

correlation length measured in L units

finite size scaling correction terms require very accurate data

Strategy I: L=∞ extrapolation first and then scaling test in m

Chiral hypothesis (in)complete analysis on both sides **Conformal hypothesis**

chiral logs not reached yet!
(N_f=8, or N_f=12) N_f=2 sextet easier reach

$$(M_\pi^2)_{NLO} = (M_\pi^2)_{LO} + (\delta M_\pi^2)_{1-loop} + (\delta M_\pi^2)_{m^2} + (\delta M_\pi^2)_{a^2 m} + (\delta M_\pi^2)_{a^4}$$

$\sim m^2$ $\sim a^2 m$ $\sim a^4$

kept cutoff term in B see LO a^2 term

$$(M_\pi^2)_{LO} = 2B \cdot m + a^2 \Delta_B$$

would require more data

$$(\delta M_\pi^2)_{1-loop} = [(M_\pi^2)_{LO} + a^2]^2 \ln(M_\pi^2)_{LO}$$

$$M_\pi^2 = c_1 m + c_2 m^2 \ + \text{logs}$$

fitted function for all Goldstones

$$M_{nuc} = c_0 + c_1 m \ + \ \text{logs}$$

nucleon states, rho, a1, higgs, ...

$$(F_\pi)_{LO} = F, \quad (\delta F_\pi)_{1-loop} = [(M_\pi^2)_{LO} + a^2] \ln(M_\pi^2)_{LO}$$

chiral log regime was not reached in fermion mass range

$$(\delta F_\pi)_{m^2} \sim m, \quad (\delta F_\pi)_{a^2 m} = a^2$$

kept cutoff term in F

$$F_\pi = F + c_1 m + \text{logs}$$

fitted function

$$\langle \bar\psi \psi \rangle = \langle \bar\psi \psi \rangle_0 + c_1 m + c_2 m^2 + \text{logs}$$

chiral condensate

$$M_\pi = c_\pi \cdot m^{1/y_m}, \quad y_m = 1 + \gamma$$

leading conformal scaling
functional form for all hadron masses

$$F_\pi = c_F \cdot m^{1/y_m}, \quad y_m = 1 + \gamma$$

same critical exponent

$$\langle \bar\psi \psi \rangle = c_\gamma \cdot m^{(3-\gamma)/y_m} + c_1 m$$

Del Debbio and Zwicky

Asymptotic infinite volume limit has not been reached yet in important candidate models for conformal window

infinite volume conformal scaling violation analysis ?

conformal finite size scaling analysis and its scaling violations ?

Recent progress in calculating B_K using staggered fermions

Weonjong Lee

Lattice Gauge Theory Research Center
Department of Physics and Astronomy
Seoul National University

BNL Workshop, 05/15/2012

SWME Collaboration
Staggered ε'/ε Project
1998 — Present

SWME Collaboration

- Seoul National University (SNU):
  Prof. Weonjong Lee
  Jon Bailey and Nigel Cundy (Research Assistant Prof's)
  10 graduate students.
- Brookhaven National Laboratory (BNL):
  Dr. Chulwoo Jung.
  Dr. Hyung-Jin Kim (Postdoc).
- University of Washington, Seattle (UW):
  Prof. Stephen R. Sharpe.
- KISTI: Dr. Taegil Bae (Postdoc).
- University of Arizona: Dr. Jongjeong Kim (Postdoc).

Indirect CP Violation and B_K

ε and $\hat{B}_K$

- $\varepsilon = (2.228 \pm 0.011) \times 10^{-3} \times e^{i\pi/4}$ in experiment.

ε and $\hat{B}_K$

- $\varepsilon = (2.228 \pm 0.011) \times 10^{-3} \times e^{i\pi/4}$ in experiment.
- Relation between ε and $\hat{B}_K$ in standard model.

$$
\begin{aligned}
\varepsilon &= \exp(i\phi_\varepsilon)\ \sqrt{2}\sin(\phi_\varepsilon)\ C_\varepsilon\ \mathrm{Im}\lambda_t\ X\ \hat{B}_K + \xi \\
X &= \mathrm{Re}\lambda_c[\eta_1 S_0(x_c) - \eta_3 S_3(x_c, x_t)] - \mathrm{Re}\lambda_t \eta_2 S_0(x_t) \\
\lambda_i &= V_{is}^* V_{id}, \qquad x_i = m_i^2/M_W^2, \qquad C_\varepsilon = \frac{G_F^2 F_K^2 m_K M_W^2}{6\sqrt{2}\pi^2 \Delta M_K} \\
\xi &= \exp(i\phi_\varepsilon)\sin(\phi_\varepsilon)\frac{\mathrm{Im}A_0}{\mathrm{Re}A_0}
\end{aligned}
$$

ε and $\hat{B}_K$

- $\varepsilon = (2.228 \pm 0.011) \times 10^{-3} \times e^{i\pi/4}$ in experiment.
- Relation between ε and $\hat{B}_K$ in standard model.

$$\begin{aligned}
\varepsilon &= \exp(i\phi_\varepsilon)\ \sqrt{2}\sin(\phi_\varepsilon)\ C_\varepsilon\ \mathrm{Im}\lambda_t\ X\ \hat{B}_K + \xi \\
X &= \mathrm{Re}\lambda_c[\eta_1 S_0(x_c) - \eta_3 S_3(x_c, x_t)] - \mathrm{Re}\lambda_t \eta_2 S_0(x_t) \\
\lambda_i &= V_{is}^* V_{id}, \qquad x_i = m_i^2/M_W^2, \qquad C_\varepsilon = \frac{G_F^2 F_K^2 m_K M_W^2}{6\sqrt{2}\pi^2 \Delta M_K} \\
\xi &= \exp(i\phi_\varepsilon)\sin(\phi_\varepsilon)\frac{\mathrm{Im}A_0}{\mathrm{Re}A_0}
\end{aligned}$$

- Definition of B_K in standard model.

$$\begin{aligned}
B_K &= \frac{\langle \bar{K}_0|[\bar{s}\gamma_\mu(1-\gamma_5)d][\bar{s}\gamma_\mu(1-\gamma_5)d]|K_0\rangle}{\frac{8}{3}\langle \bar{K}_0|\bar{s}\gamma_\mu\gamma_5 d|0\rangle\langle 0|\bar{s}\gamma_\mu\gamma_5 d|K_0\rangle} \\
\hat{B}_K &= C(\mu)B_K(\mu), \qquad C(\mu) = \alpha_s(\mu)^{-\frac{\gamma_0}{2b_0}}[1 + \alpha_s(\mu)J_3]
\end{aligned}$$

B_K on the lattice

B_K definition in standard model

$$
\begin{aligned}
B_K &= \frac{\langle \bar{K}_0 | [\bar{s}\gamma_\mu(1-\gamma_5)d][\bar{s}\gamma_\mu(1-\gamma_5)d] | K_0 \rangle}{\frac{8}{3}\langle \bar{K}_0 | \bar{s}\gamma_\mu\gamma_5 d | 0 \rangle \langle 0 | \bar{s}\gamma_\mu\gamma_5 d | K_0 \rangle} \\
\hat{B}_K &= C(\mu) B_K(\mu), \\
C(\mu) &= \alpha_s(\mu)^{-\frac{\gamma_0}{2b_0}} [1 + \alpha_s(\mu) J_3]
\end{aligned}
$$

What do we calculate on the lattice?

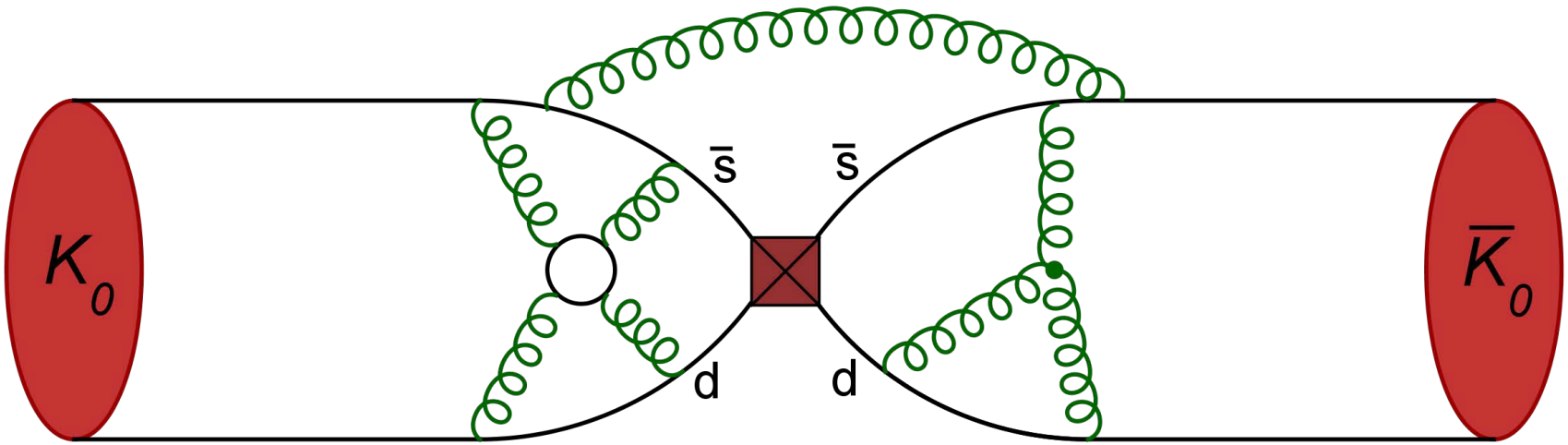

Data Analysis for B_K

Data for B_K with $am_d = am_s = 0.025$ $(20^3 \times 64)$

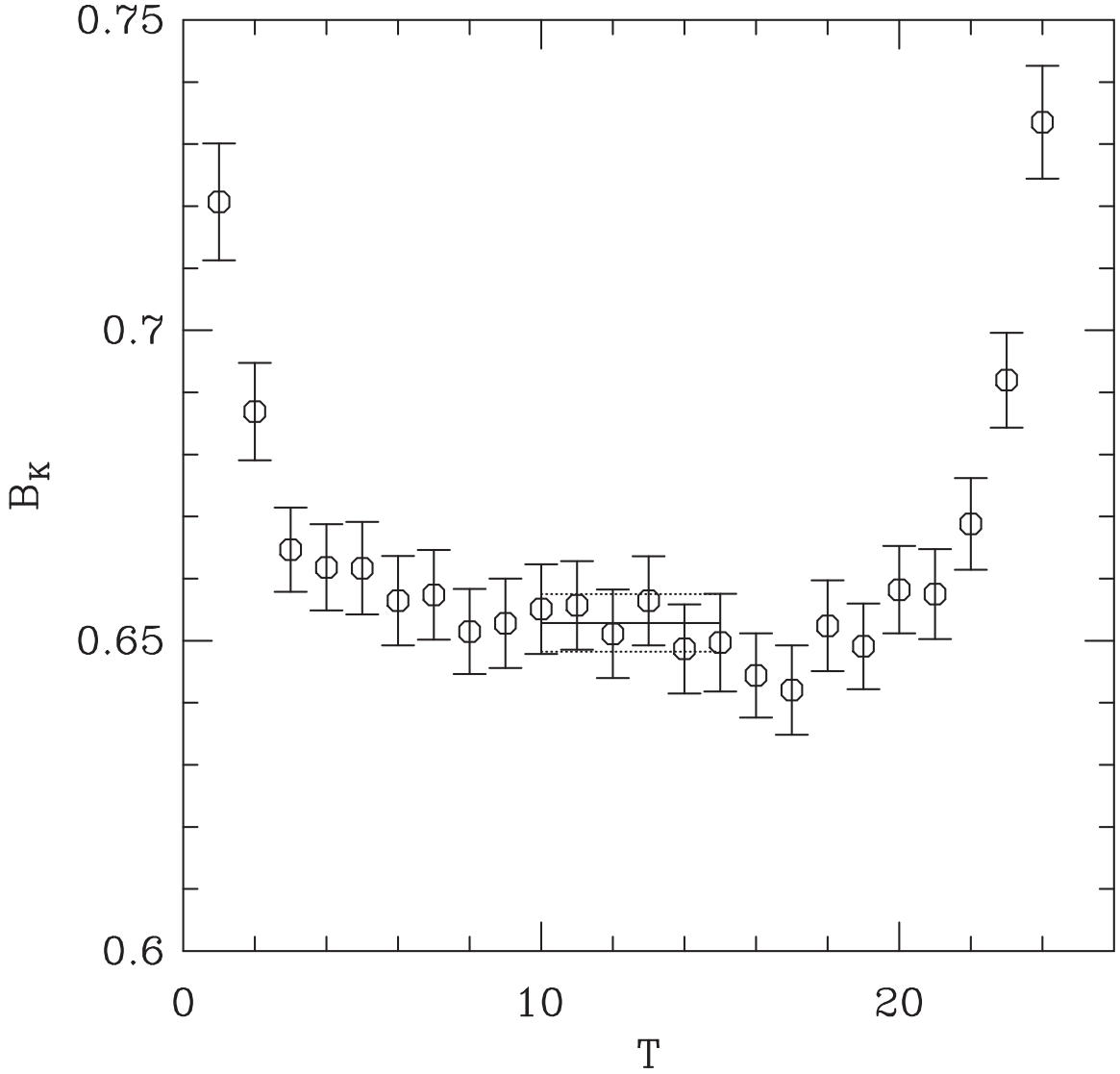

B_K in $N_f = 2 + 1$ QCD

a (fm)	am_l/am_s	geometry	ens×meas	round	production
0.12	0.03/0.05	$20^3 \times 64$	564×9	2nd	done (SNU)
0.12	0.02/0.05	$20^3 \times 64$	486×9	2nd	done (SNU)
0.12	0.01/0.05	$20^3 \times 64$	671×9	2nd	done (SNU)
0.12	0.01/0.05	$28^3 \times 64$	274×8	2nd	done (BNL)
0.12	0.007/0.05	$20^3 \times 64$	651×10	2nd	done (SNU)
0.12	0.005/0.05	$24^3 \times 64$	509×9	2nd	done (SNU)
0.09 (F1)	0.0062/0.031	$28^3 \times 96$	995×9	2nd	done (SNU)
0.09	0.0031/0.031	$40^3 \times 96$	805×1	2nd	SNU(*)
0.06	0.0036/0.018	$48^3 \times 144$	744×2	2nd	SNU/JLAB(
0.06	0.0025/0.018	$56^3 \times 144$	700×1	1st	KISTI(*)
0.06	0.0018/0.018	$64^3 \times 144$	$700 \times -$	–	–
0.045 (U1)	0.0030/0.015	$64^3 \times 192$	705×1	2nd	SNU(*)

SU(2) SChPT Fitting for B_K

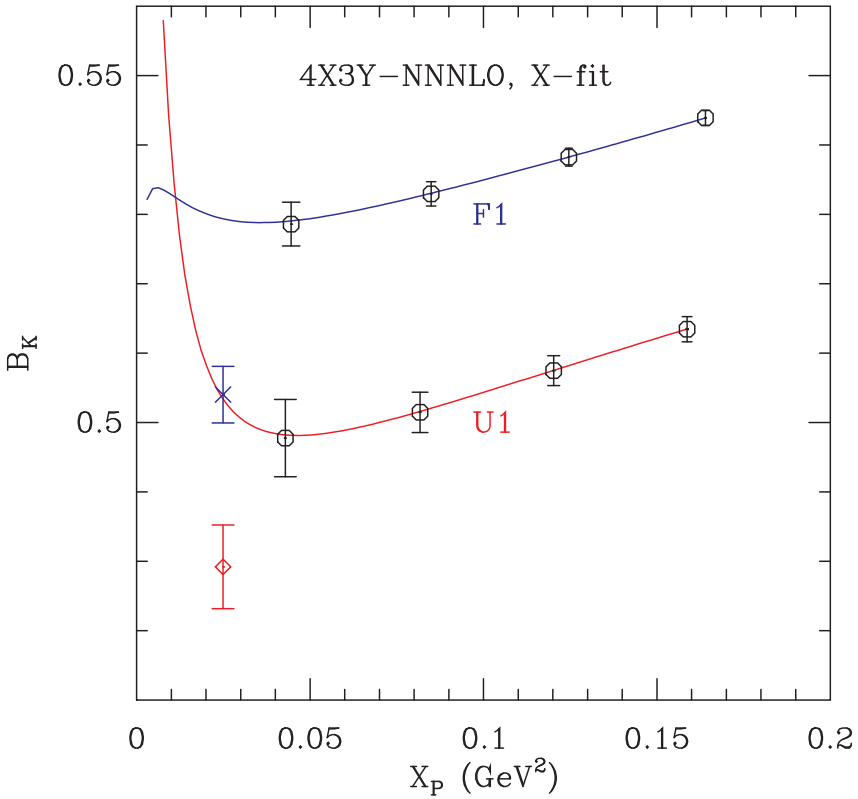

(a) X-fit

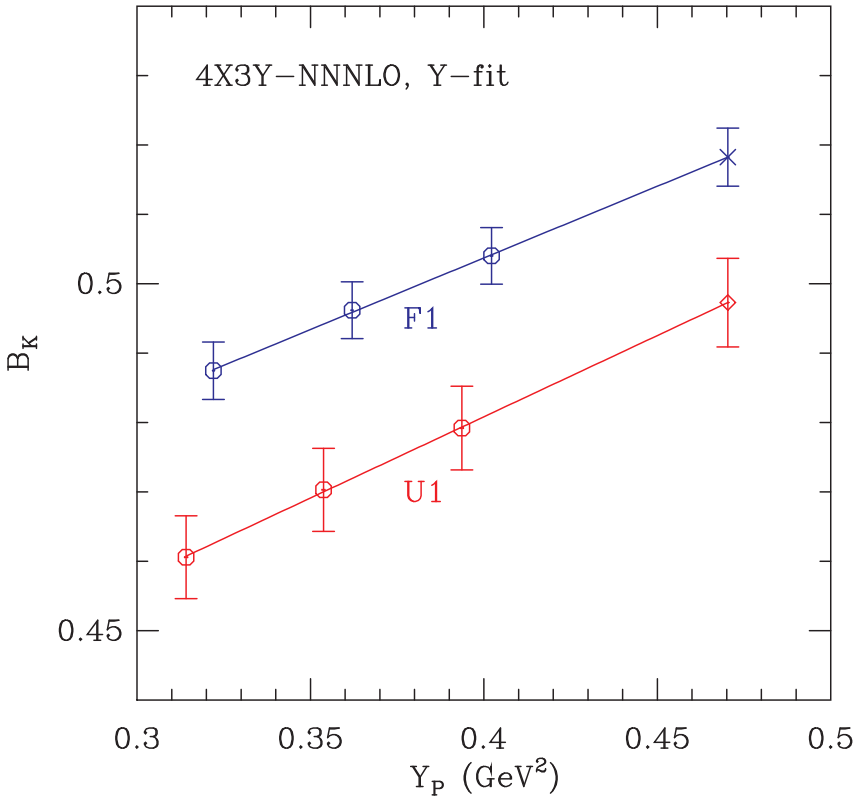

(b) Y-fit

- Fit type = SU(2) SχPT, 4X3Y, NNNLO, Bayesian, FV

B_K vs. a^2: Discretization Error

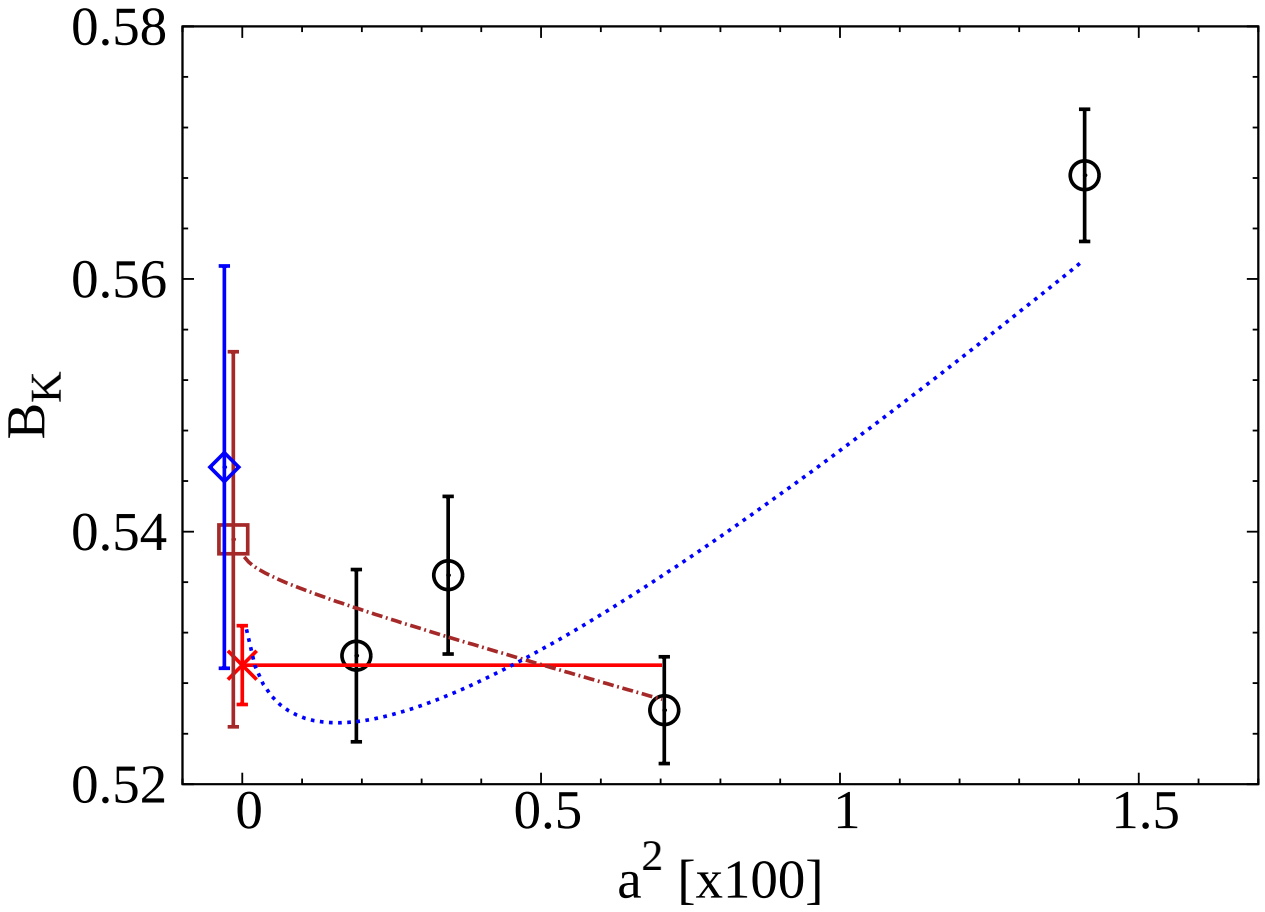

- Fit type = SU(2) SChPT; `const`, `3pt:g4-a2g2-a4`, `4pt:g4-a2g2-a4` fits

Error Budget of B_K [SU(2)-SChPT, 4X3Y, NNNLO]

cause	error (%)	memo
statistics	0.59	4X3Y-NNNLO-BAYES + `const`
matching factor	4.4	$\Delta B_K^{(2)}$ (U1)
discretization	1.9	diff. of `const` and constrained fits
X-fits	0.33	varying Bayesian priors (S1)
Y-fits	0.07	diff. of linear and quadratic (C3)
am_l extrap	1.5	diff. of (C3) and linear extrap
am_s extrap	1.3	diff. of (C3) and linear extrap
finite volume	0.5	diff. of $V = \infty$ and FV fits
r_1	0.14	r_1 error propagation (C3)
f_π	0.4	132 MeV vs. 124.4 MeV

Current Status of B_K (1)

- Lattice QCD (SWME):

$$B_K(\text{RGI}) = \hat{B}_K = 0.727 \pm 0.004(\text{stat}) \pm 0.038(\text{sys})$$

- Experiments: (most updated version in 2012)

$$B_K(\text{RGI}) = \begin{cases} 1.01 \pm 0.11 & \text{for exclusive } V_{cb} \\ 0.824 \pm 0.060 & \text{for inclusive } V_{cb} \end{cases}$$

- Hence, we observe 2.6σ difference between the SM theory and experiments (exclusive V_{cb}) and 1.6σ difference (inclusive V_{cb}). Is this substantial?

Current Status of B_K (2)

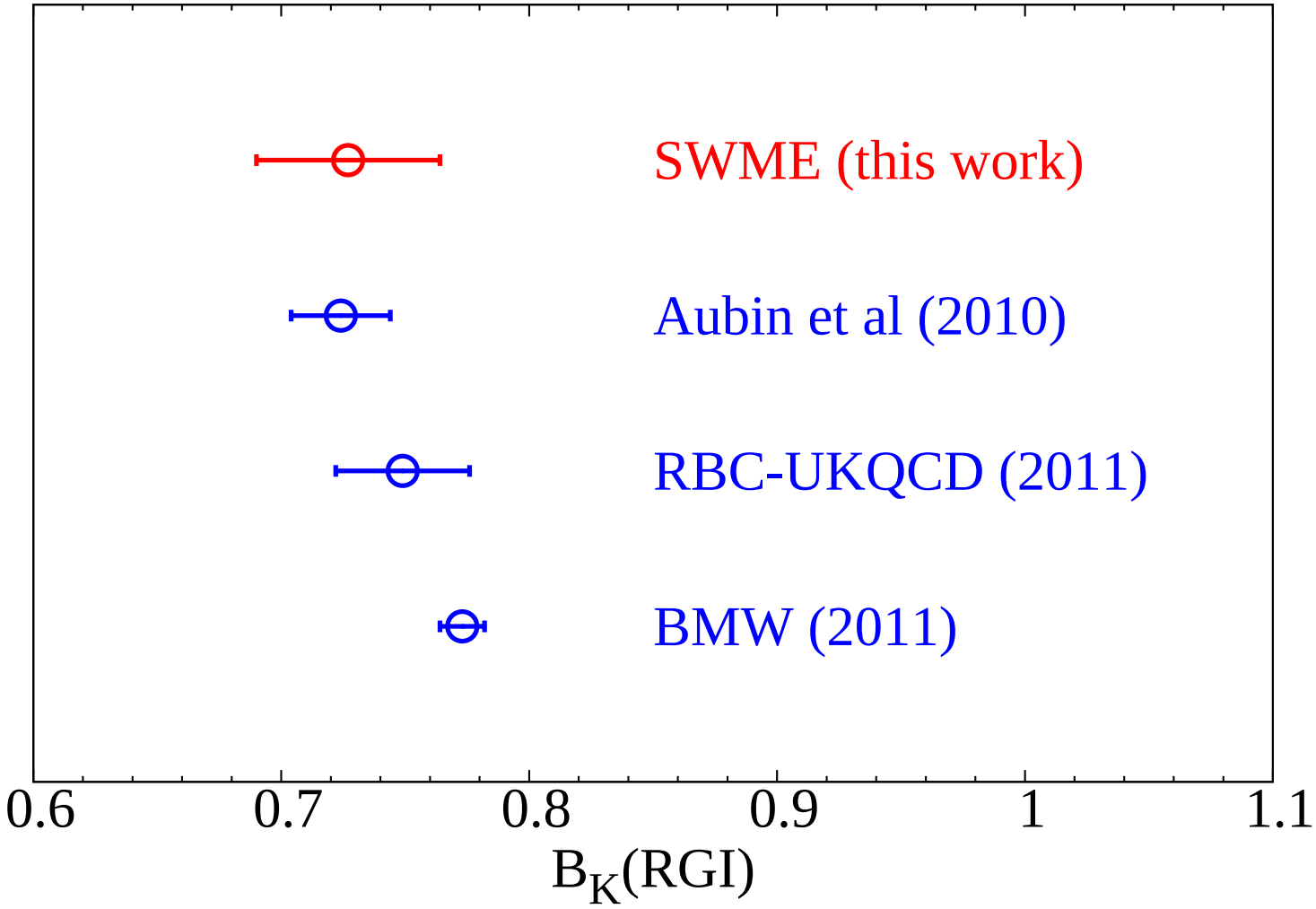

Current Status of B_K (3)

- SWME (Stag):

$$\hat{B}_K = 0.727 \pm 0.004(\text{stat}) \pm 0.038(\text{sys})$$

- Laiho / Van de Water (DWF + Stag):

$$\hat{B}_K = 0.724 \pm 0.008(stat) \pm 0.028(sys)$$

- RBC / UKQCD (DWF):

$$\hat{B}_K = 0.749 \pm 0.007(stat) \pm 0.026(sys)$$

- BMW (Wilson):

$$\hat{B}_K = 0.773 \pm 0.008(stat) \pm 0.009(sys)$$

Preliminary Theoretical Expectation for ε_K

- Inclusive V_{cb}:

$$\varepsilon_K = \begin{cases} 2.07 \pm 0.16 & \text{(Lat Avg)} \\ 1.95 \pm 0.19 & \text{(SWME)} \end{cases}$$

- Exclusive V_{cb}:

$$\varepsilon_K = \begin{cases} 1.66 \pm 0.21 & \text{(Lat Avg)} \\ 1.56 \pm 0.22 & \text{(SWME)} \end{cases}$$

- Experiment:

$$\varepsilon_K = 2.228 \pm 0.011 \quad \text{(PDG)}$$

- We observe about 3.0σ tension in the exclusive V_{cb} channel of ε_K.

Preliminary check for CKM unitarity

- CKM unitarity:

$$[VV^\dagger]_{ct} = 0$$

- Exclusive V_{cb}: Lattice 2012 (Yong-Chull Jang)

$$[VV^\dagger]_{ct} = 0.00153(48) \qquad \text{(preliminary)}$$

- Inclusive V_{cb}: Lattice 2012 (Yong-Chull Jang)

$$[VV^\dagger]_{ct} = 0.00128(47) \sim 0.0084(47) \qquad \text{(preliminary)}$$

- We observe about 3.2σ tension in the exclusive V_{cb} channel of the CKM unitarity.

Preliminary error analysis with **inclusive** V_{cb}

- Lattice 2012: Yong-Chull Jang
- Lat. Avg.:

$$\begin{cases} \bar{\eta} & 27\% \\ \eta_3 & 19\% \\ m_c & 16\% \\ \cdots & \cdots \end{cases}$$

- SWME:

$$\begin{cases} \hat{B}_K & 34\% \\ \bar{\eta} & 18\% \\ \eta_3 & 12\% \\ m_c & 11\% \\ \cdots & \cdots \end{cases}$$

Preliminary error analysis with **exclusive** V_{cb}

- Lattice 2012: Yong-Chull Jang
- Lat. Avg.:

$$\begin{cases} V_{cb} & 58\% \\ \bar{\eta} & 11\% \\ \eta_3 & 9\% \\ m_c & 8\% \\ \cdots & \cdots \end{cases}$$

- SWME:

$$\begin{cases} V_{cb} & 49\% \\ \hat{B}_K & 18\% \\ \bar{\eta} & 9\% \\ \eta_3 & 8\% \\ m_c & 7\% \\ \cdots & \cdots \end{cases}$$

BSM corrections to B_K on the lattice

BSM operators for B_K

- BSM operators:

$$
\begin{aligned}
O_2 &= \bar{s}_a(1-\gamma_5)d_a\bar{s}_b(1-\gamma_5)d_b \\
O_3 &= \bar{s}_a(1-\gamma_5)d_b\bar{s}_b(1-\gamma_5)d_a \\
O_4 &= \bar{s}_a(1-\gamma_5)d_a\bar{s}_b(1+\gamma_5)d_b \\
O_5 &= \bar{s}_a(1-\gamma_5)d_b\bar{s}_b(1+\gamma_5)d_a
\end{aligned}
$$

- B parameters:

$$
B_j(\mu) = \frac{\langle \bar{K}_0 | O_j(\mu) | K_0 \rangle}{N_j \langle \bar{K}_0 | P(\mu) | 0 \rangle \langle 0 | P(\mu) | K_0 \rangle}
$$

What do we calculate on the lattice?

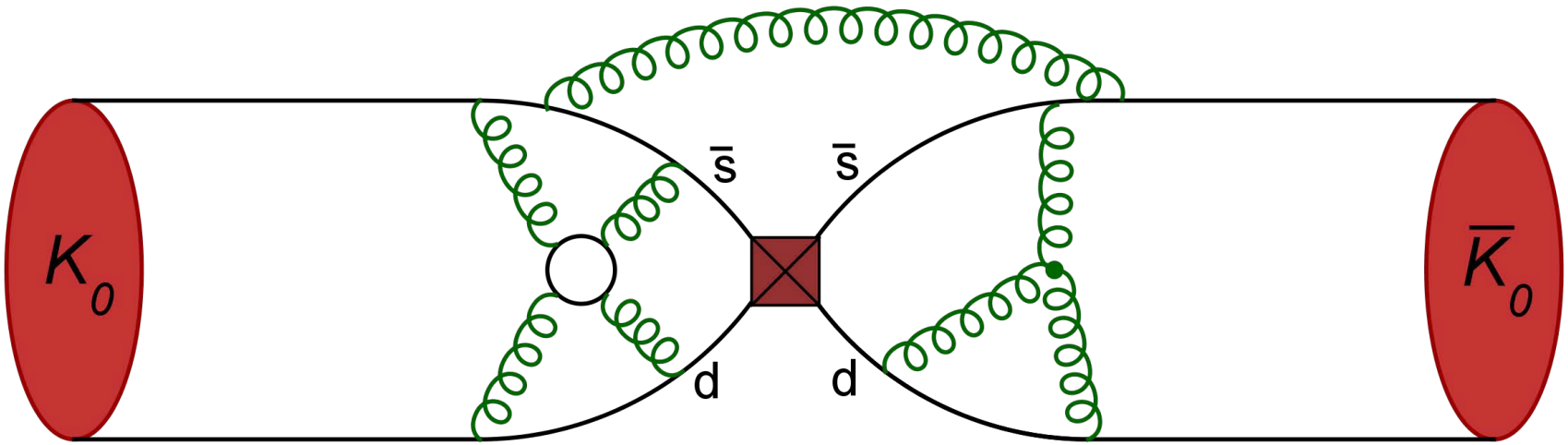

Data Analysis for BSM corrections to B_K

Data analysis for B_2 with $am_d = am_s = 0.025$ $(20^3 \times 64)$

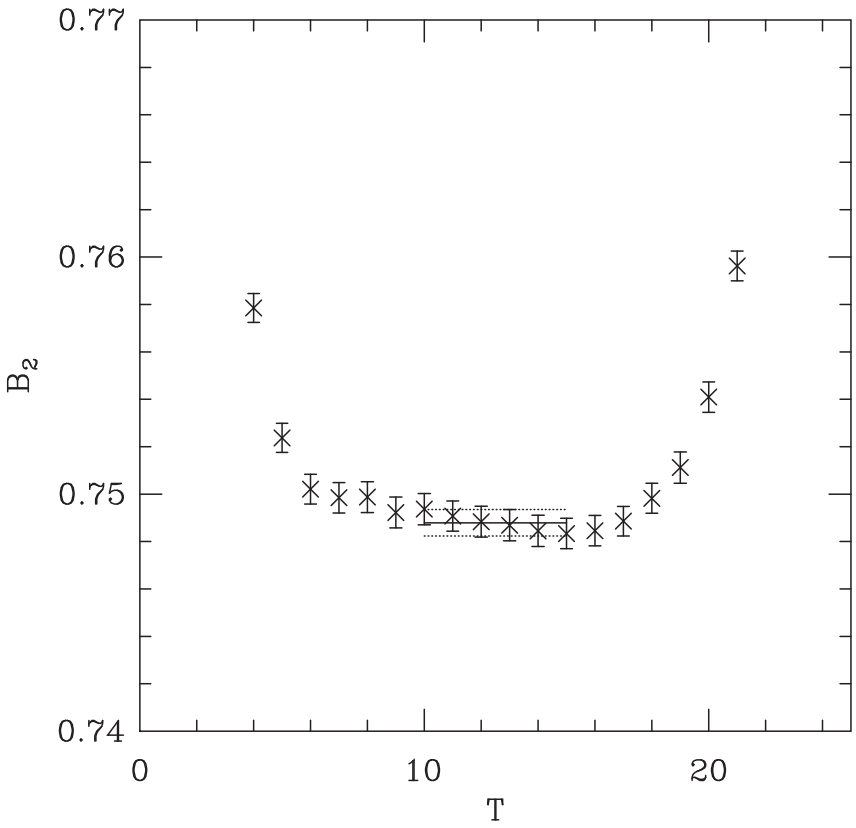

(c) raw data

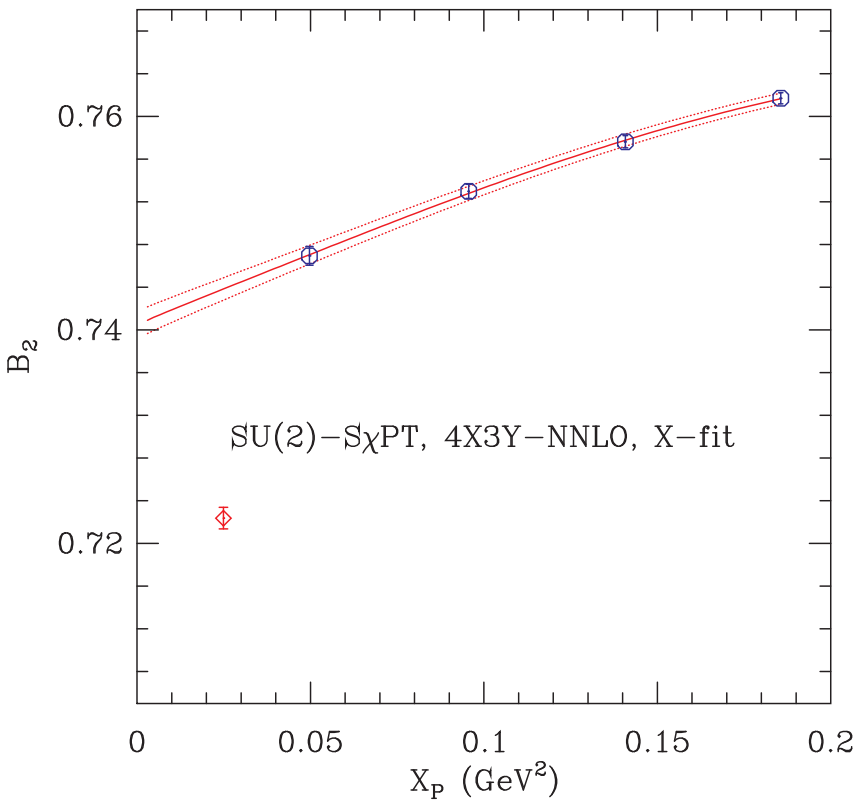

(d) X-fit

Preliminary !!!

Data analysis for B_3 with $am_d = am_s = 0.025$ $(20^3 \times 64)$

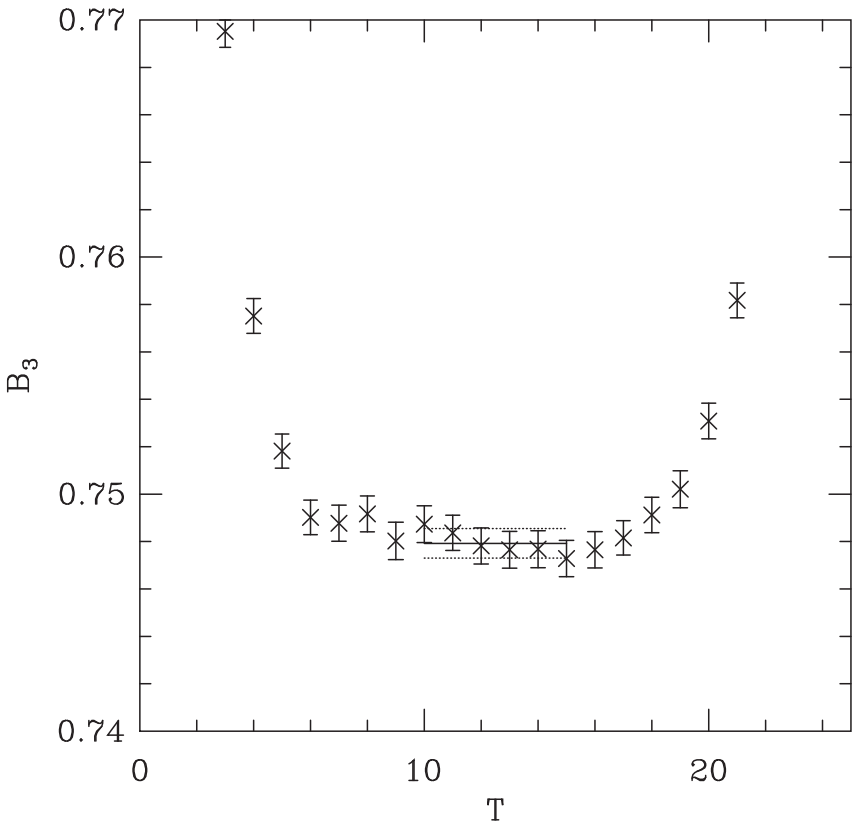

(e) raw data

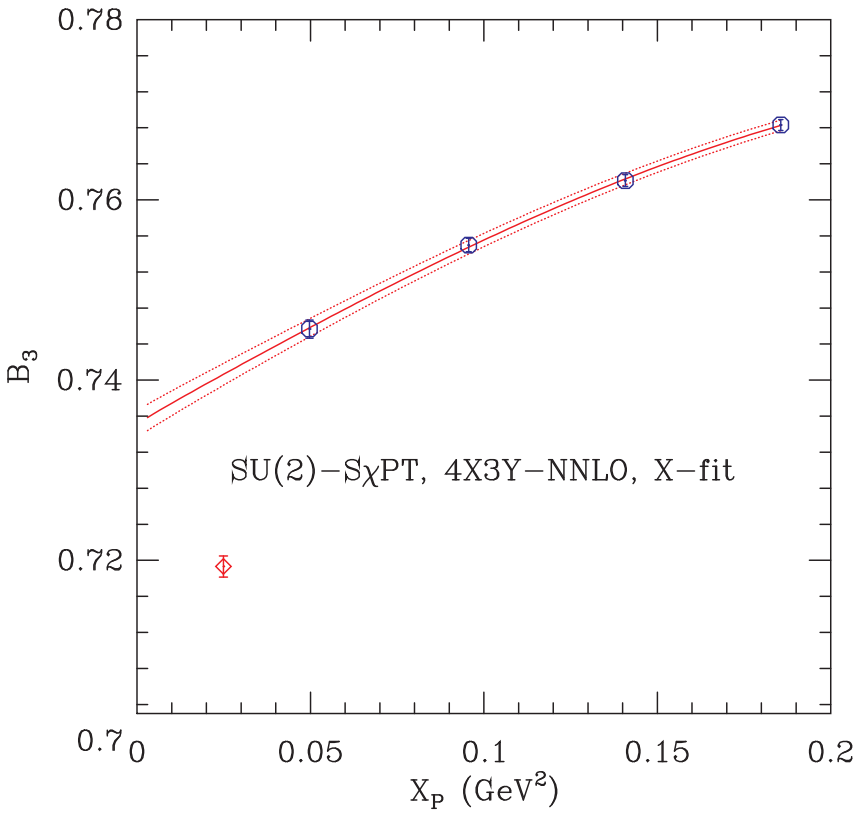

(f) X-fit

Preliminary !!!

Data analysis for B_4 with $am_d = am_s = 0.025$ $(20^3 \times 64)$

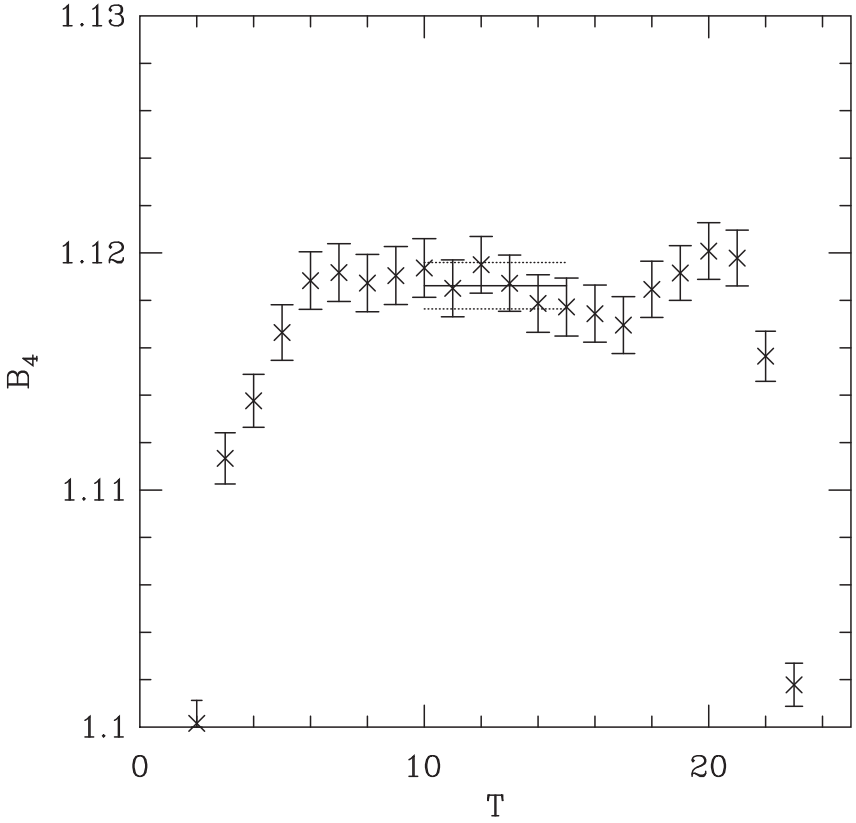

(g) raw data

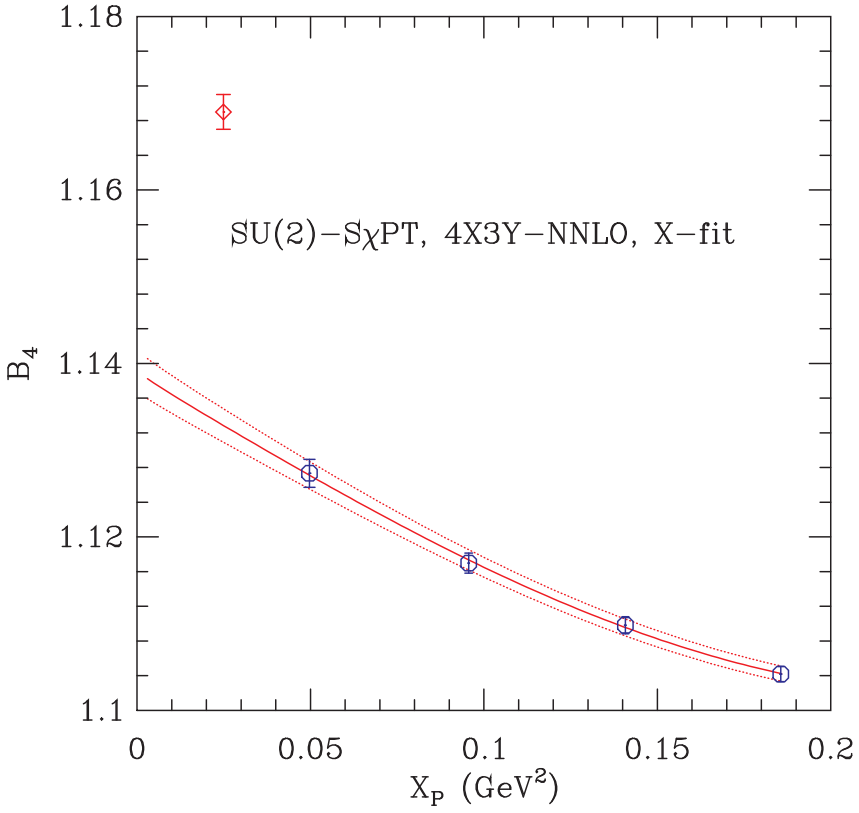

(h) X-fit

Preliminary !!!

Data analysis for B_5 with $am_d = am_s = 0.025$ $(20^3 \times 64)$

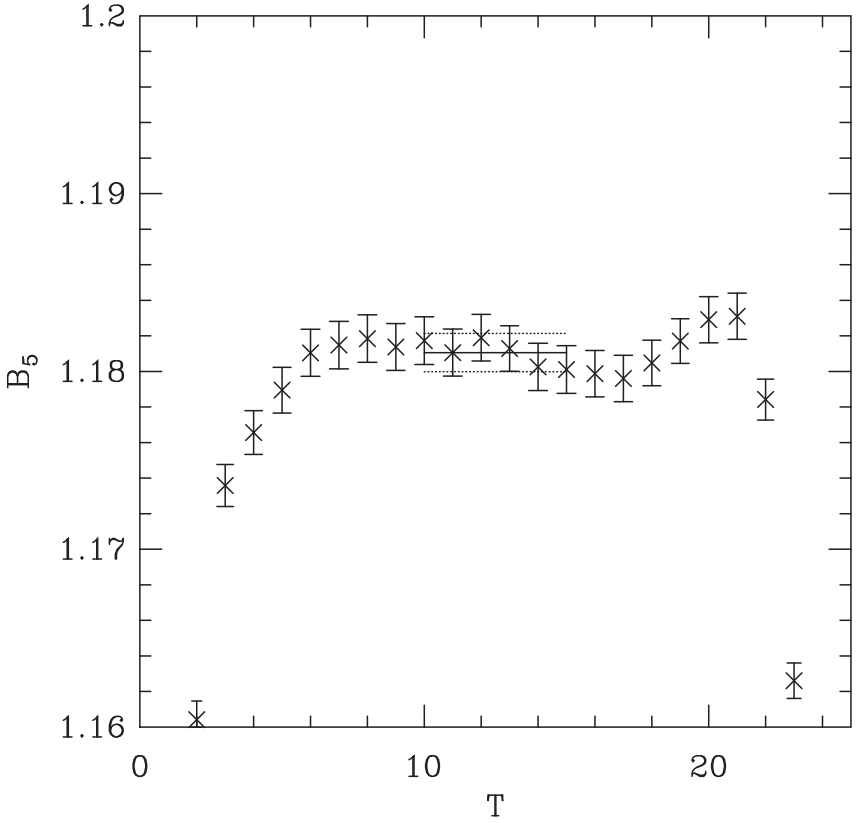

(i) raw data

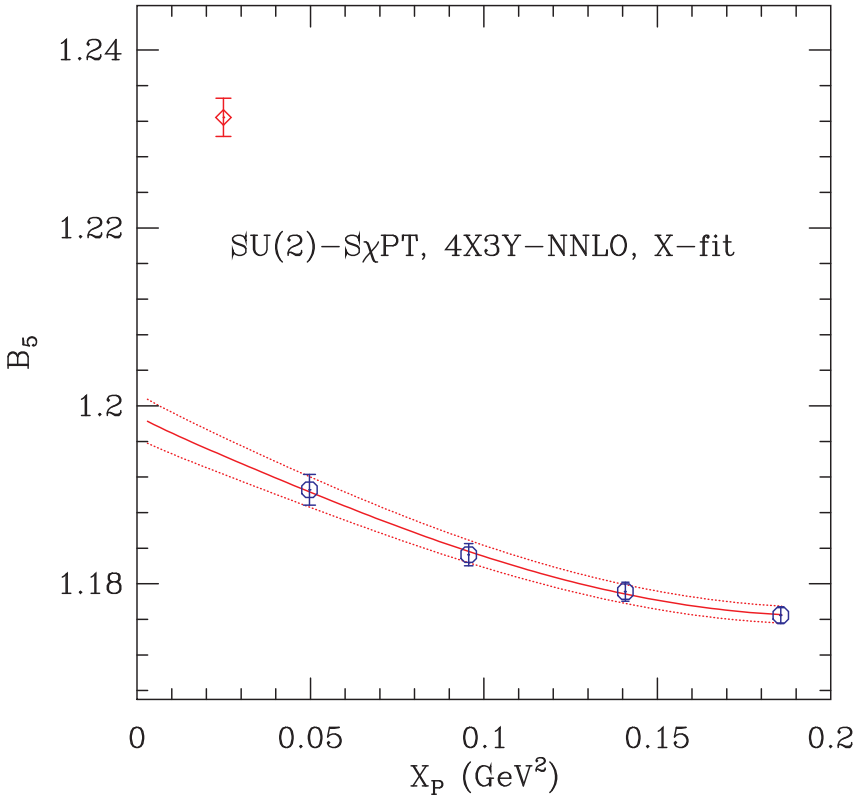

(j) X-fit

Preliminary !!!

Current Status of BSM corrections to B_K

- We are in the middle of data analysis at the tree level. Hence the results are very preliminary.
- We plan to complete the first round data analysis at the one-loop level by Lattice 2012. We will present the preliminary results in Lattice 2012. [Dr. Hyung-Jin Kim]
- We plan to complete the second round data analysis using the NPR matching by the end of 2012.

Summary

- We plan to reduce the overall error of B_K below the 2% level. (at least for SWME). We have to reduce the overall error of exclusive V_{cb} below the 0.5% level.
- How?
  Answer: NPR, or two-loop matching.
- Lattice 2012: Jangho Kim (NPR).
- Lattice 2012: Kwangwoo Kim (two-loop matching ???).

Future Theoretical Perspectives (1)

- Hansen & Sharpe (2012): multiple-channel scattering phase shift formula
- This directly applied to staggered $\pi - \pi$ scattering case: $N = 5$ channels.
- There is a remaining difficulty in the unitarity ansatz of the S-matrix.
- We will overcome this difficulty using the guidance of staggered chiral perturbation theory (SChPT).
- It could be very likely to calculate the $\pi - \pi$ scattering phase shift with the systematic errors under control in near future.
- This will make it possible to calculate the $K \to \pi\pi$ decay amplitude using staggered fermions.

Future Theoretical Perspectives (2)

- We have extended the SChPT calculation to non-Goldstone pion sectors for pion mass and decay constants f_π, f_K.
- We plan to extend the horizon to the mixed action case (HYP stag/asqtad or HYP/HISQ) in 2012.
- We plan to find the best channels to calculate the $\pi - \pi$ scattering phase shift using staggered fermions. The SChPT will be the main tool for this mission.

Lattice study of the phase structure of the strong Yukawa model

arXiv:1111.4544 (with updates)

C.-J. David Lin

National Chiao-Tung University

BNL
14/05/2012

The collaboration

- Germany
  - NIC, DESY Zeuthen and Humboldt University Berlin
    John Bulava (CERN), Philipp Gerhold (→ d-Fine), Karl Jansen, Attila Nagy.
- Japan
  - Kobayashi-Maskawa Institute, Nagoya University
    Kei-Ichi Nagai.
- Taiwan
  - National Chiao-Tung University, Hsinchu
    C.-J.David Lin, Kenji Ogawa.
  - National Taiwan University, Taipei
    George W.-S. Hou, Bastian Knippschild, Brian Smigielski (→ U.S.).

Motivation

Heavy fermions beyond SM3?

- Not much is known for strong (*non-perturbative*) Yukawa theory.
- Heavy extra generation of fermions may
  - enhance CP violation.

    G.W.S. Hou, 2008

  - offer an alternative way to break EW symmetry dynamically and induces bound states to unitarise WW scattering.

    B. Holdom, 2007

  - UV stablise the SM.

    P.Q. Hung, C. Xiong, 2009

Outline

- Goals, general issues and recent developments.
- Simultation setup.
- The phase structure.
- Exploratory numerical studies.
  - VEV.
  - Susceptibility and critical exponents.
  - Binder's cumulant.
- Future plan.

Targets for the bare strong-Yukawa regime

- The nature of the phase transitions.

  $\Rightarrow$ Connection to the continuum world (next slide).

- Possible bound states.

  $\Rightarrow$ Computation of the spectrum.

- Possible new mechanism for dynamical symmetry breaking.

  $\Rightarrow$ Heavy scalar with fermion condensate?

General issues and strategy

- The triviality (Landau-pole) problem.

  $\Rightarrow$ Non-trivial to take the lattice spacing to zero.

- Look for 2nd-order phase transitions via "scanning simulations".

  $\Rightarrow$ $\xi \to \infty$.

- Problem: Finite-volume effects.

  $\Rightarrow$ Phase transitions are washed out.

  $\Rightarrow$ Severe near the critical points since $L = \hat{L}a$.

- Chiral fermions required.

New ingredients in current work

- Previous studies (*circa* 1990):

  Lee, Shigemitsu, Shrock; Bock *et al.*,...

  - Use fermions without exact chiral symmetry.

    $\Rightarrow$ Ambiguity in defining chiral fermions.

  - Small ($\sim 8^3 \times 16$) volumes and no $L \to \infty$ limit taken.

- Current new-generation simulations:
  - Use the overlap fermion (exact chiral symmetry).
  - Several large volumes and $L \to \infty$ limit taken.

    $\Rightarrow$ Test finite-size scaling behaviour.

    $\Rightarrow$ Determine the order of the phase transition.

Reminder: Notaion for scalar field theory

- The discretised Euclidean scalar action ($a = 1$)

$$S_\varphi = -\sum_{x,\mu} \varphi_x^\alpha \varphi_{x+\hat{\mu}}^\alpha + \sum_x \left[\frac{1}{2}(2d + m_0^2)\varphi_x^\alpha \varphi_x^\alpha + \frac{1}{4}\lambda_0 (\varphi_x^\alpha \varphi_x^\alpha)^2 \right].$$

- $\varphi = \sqrt{2\kappa}\phi, \quad m_0^2 = \frac{1-2\hat{\lambda}}{\kappa} - 2d, \quad \lambda_0 = \frac{\hat{\lambda}}{\kappa^2}$

$$S_\phi = -2\kappa \sum_{x,\mu} \phi_x^\alpha \phi_{x+\hat{\mu}}^\alpha + \sum_x \left[\phi_x^\alpha \phi_x^\alpha + \hat{\lambda}(\phi_x^\alpha \phi_x^\alpha - 1)^2 \right],$$

$$Z_\phi = \int \prod_{x,\alpha} d\phi_x^\alpha \, \exp(-S_\phi) = \int \prod_{x,\alpha} d\mu(\phi_x^\alpha) \, \exp\left(2\kappa \sum_{x,\mu} \phi_x^\alpha \phi_{x+\hat{\mu}}^\alpha \right),$$

$$d\mu(\phi_x^\alpha) = d\phi_x^\alpha \, \exp\left[-\phi_x^\alpha \phi_x^\alpha - \hat{\lambda}(\phi_x^\alpha \phi_x^\alpha - 1)^2 \right].$$

- "staggered symmetry": $\kappa \to -\kappa$ and $\phi_x^\alpha \to (-1)^{x_1 + x_2 + \ldots + x_d} \phi_x^\alpha$.

Fermions and the Yukawa couplings

- Use the overlap Dirac operator with exact lattice chiral symmetry.
- The Yukawa terms $S_{HY} = \sum_x y(\bar{t}_x, \bar{b}_x)_L \Phi_x b_{x,R} + y(\bar{t}_x, \bar{b}_x)_L \tilde{\Phi}_x t_{x,R} + \text{h.c.}$.
  - Φ is a complex scalar doublet and $\tilde{\Phi} = i\tau_2 \Phi^*$.
- Results presented in this talk are from $8^3 \times 16$, $12^3 \times 24$ and $16^3 \times 32$.

Phase diagram of the H-Y model (qualitative)

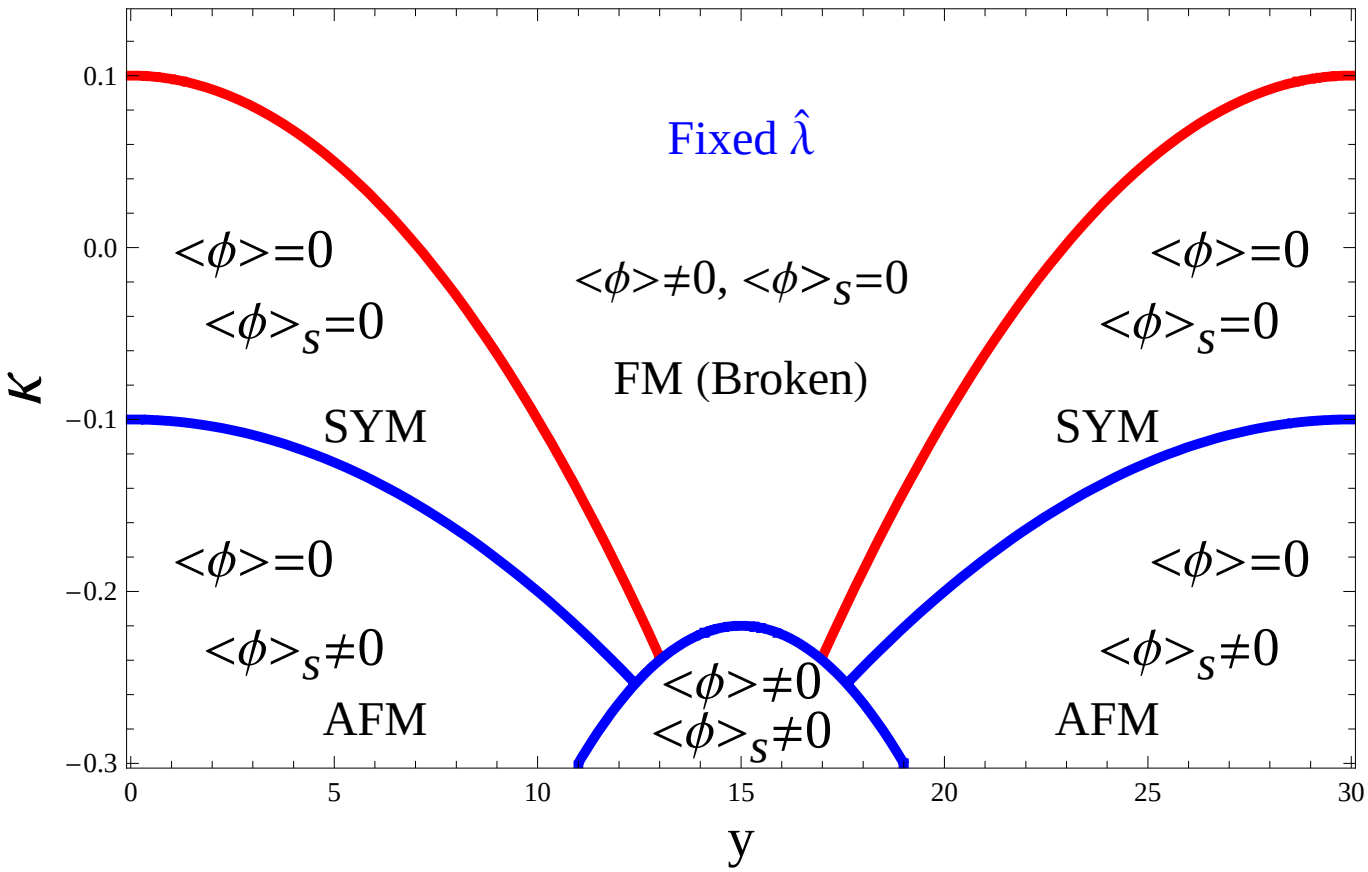

* From earlier work using Wilson fermions.

⇒ Controversy from staggered-fermion calculations.

Evidence of a symmetric phase at large y

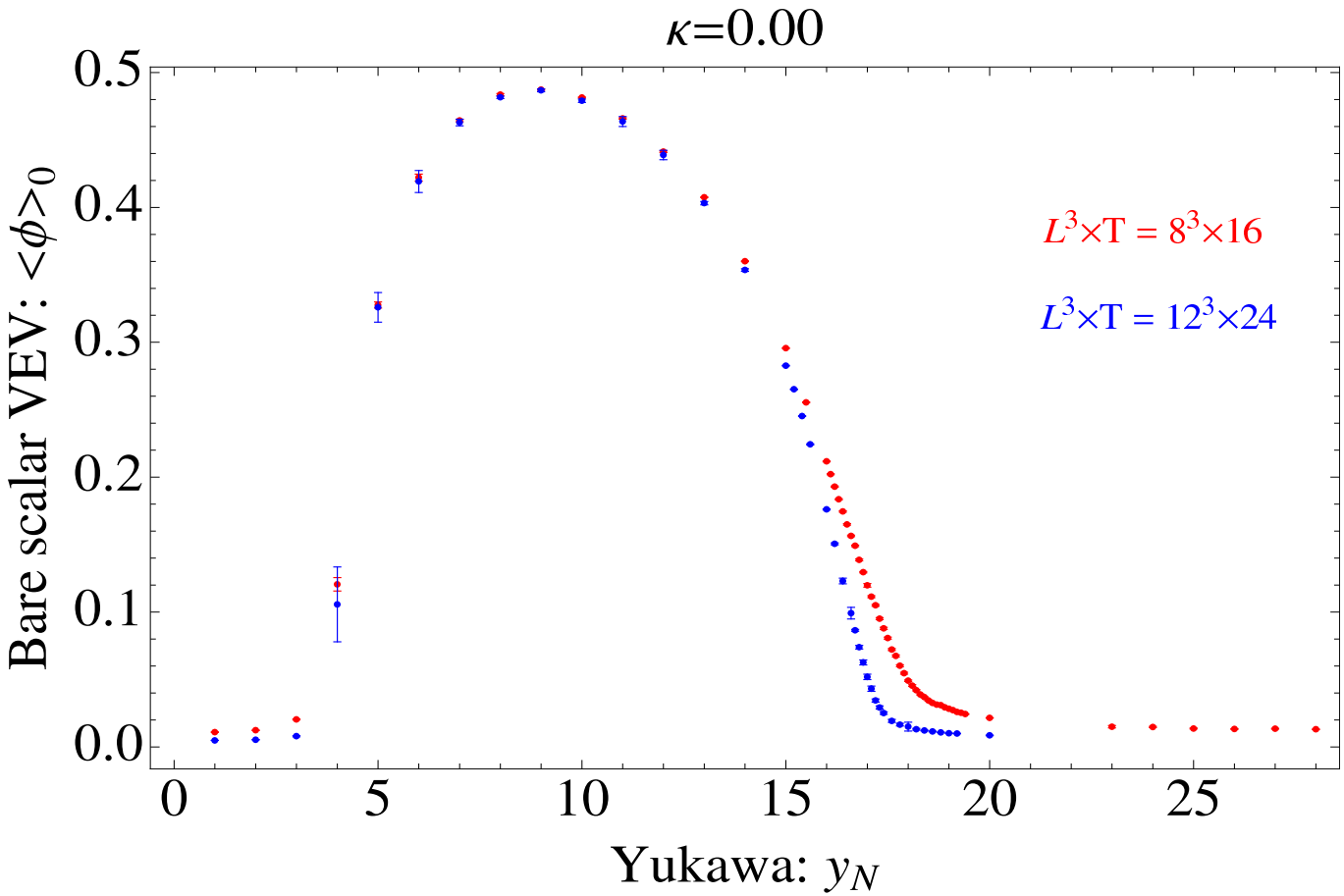

Consistent with recent results in P. Gerhold and K. Jansen, 2007.

The bare scalar vev at large Y

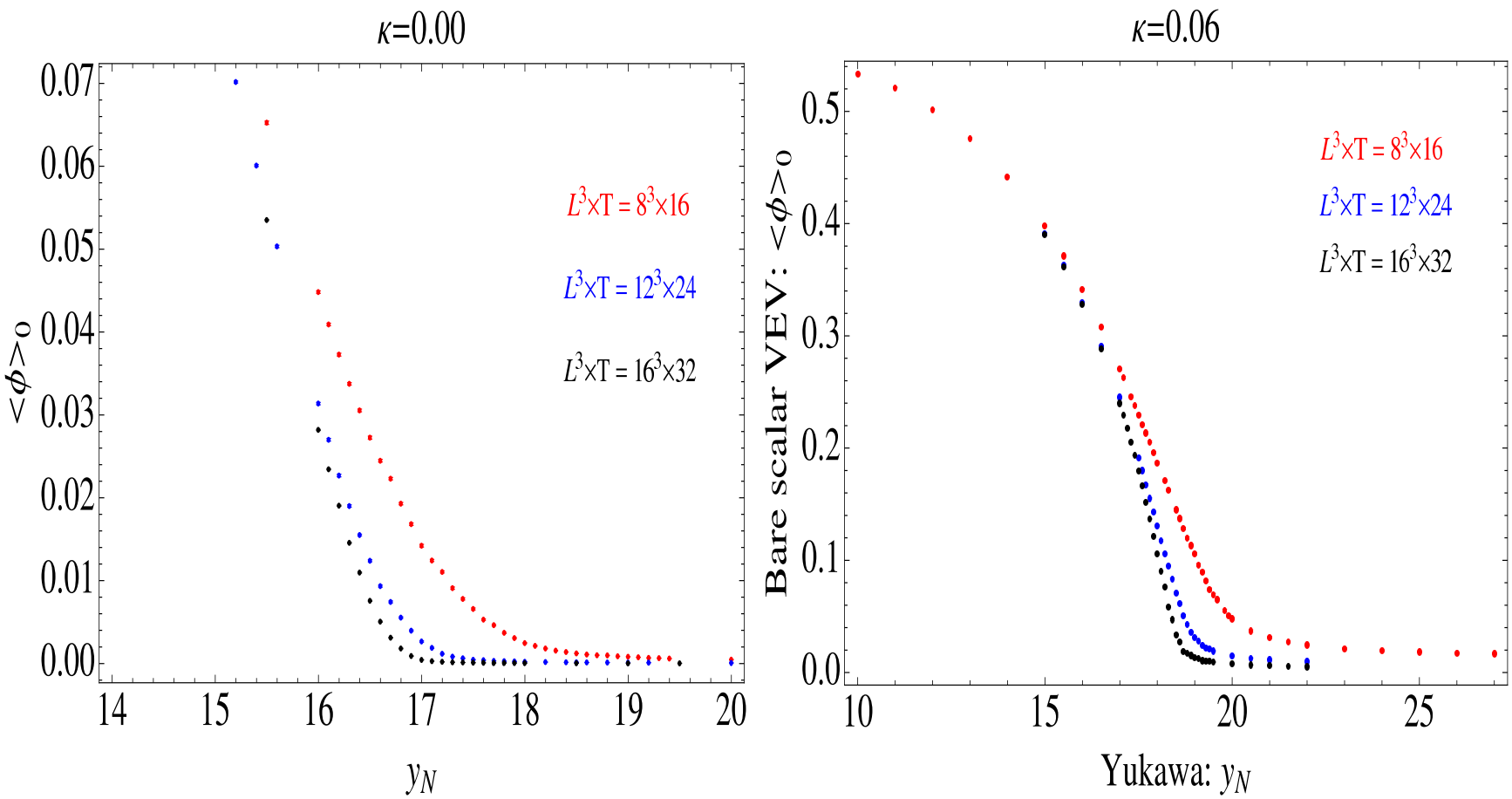

Finite-size scaling of susceptibility

- Susceptibility: $\chi = V_4 \left(\langle \phi^2 \rangle - \langle \phi \rangle \langle \phi \rangle \right)$.
- The scaling behaviour from solving the RGE,
  - Universal function $\chi L_s^{-\gamma/\nu} \sim g(\tilde{t} L_s^{1/\nu})$, where $\tilde{t} = (y/y_{\text{crit}} - 1)$.
  - critical exponents γ and ν.
  - Modelling the scaling violation from

    M. Fisher and M. Barber, 1972

    $\Rightarrow \chi L_s^{-\gamma/\nu} \sim g(t L_s^{1/\nu})$, where $t = (y/(y_{\text{crit}} - A_4/L_s^b) - 1)$.
  - Fit all the data to the (partly empirical) function at fixed κ

    K. Jansen and P. Seuferling, 1990

$$\chi = A_1 \left\{ L_s^{-2/\nu} + A_{2,3} \left(y - y_{\text{crit}} - A_4/L_s^b \right)^2 \right\}^{-\gamma/2}.$$

Finite-size fit of susceptibility

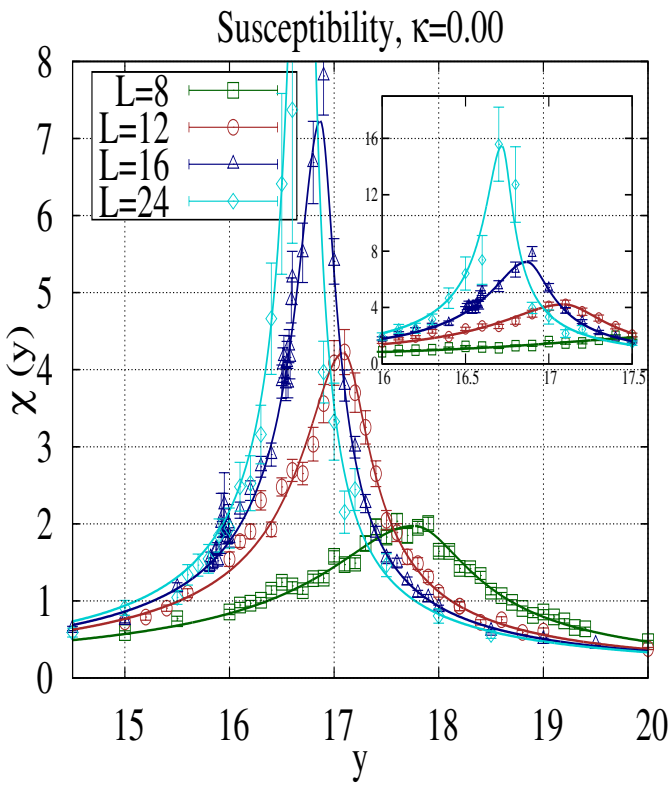

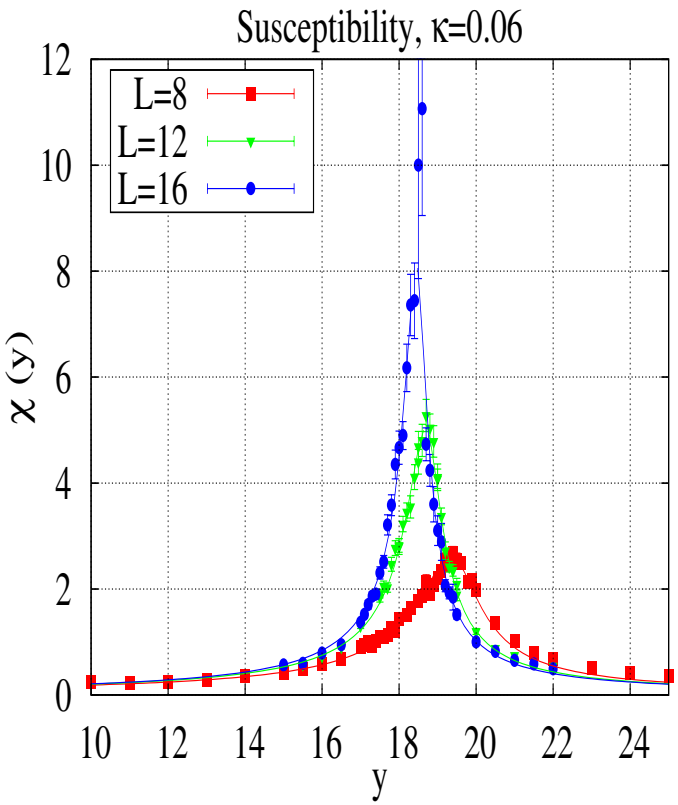

Fit range: $y = 15.0 \sim 20.0$ $y = 14.0 \sim 22.0$

Finite-size scaling of susceptibility

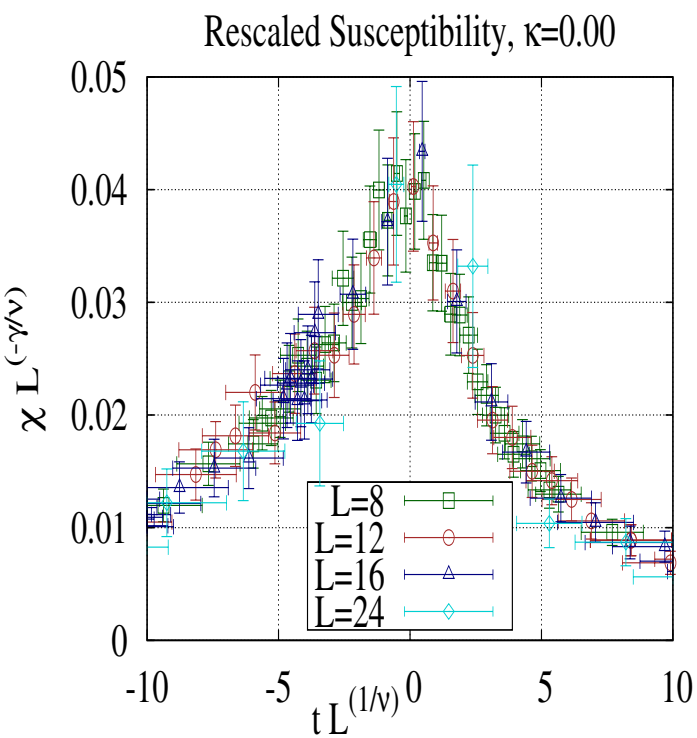

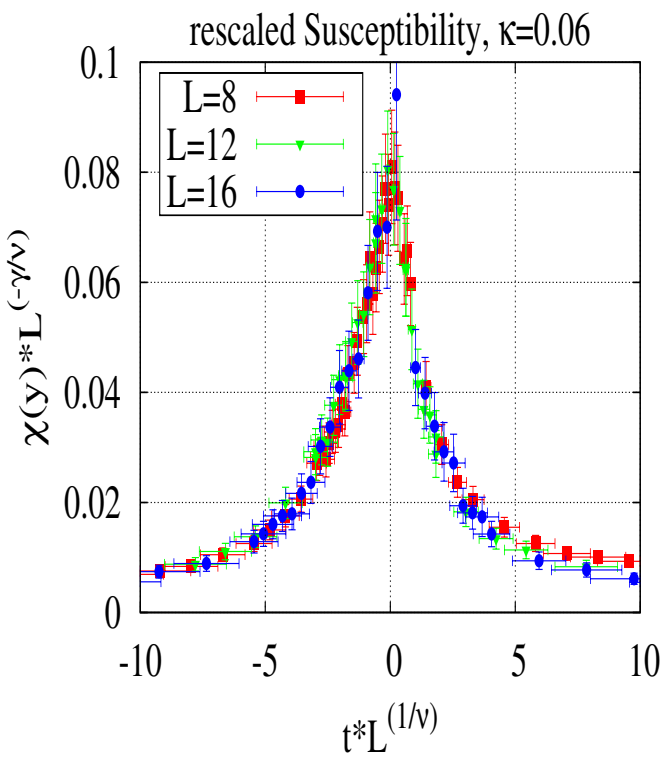

Finite-size scaling of Binder's cumulant

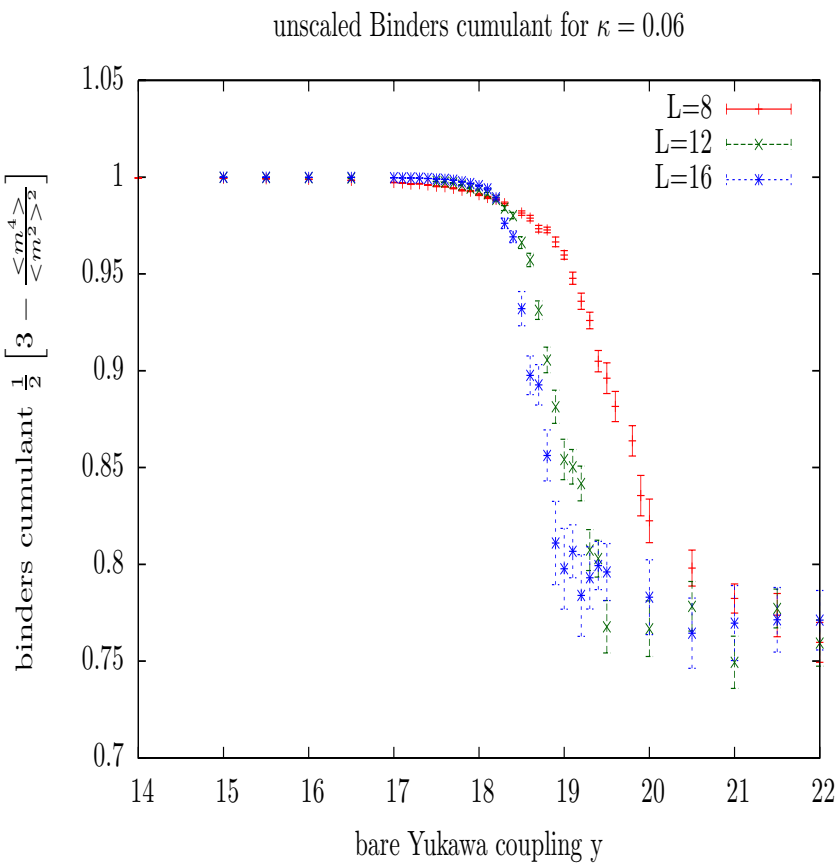

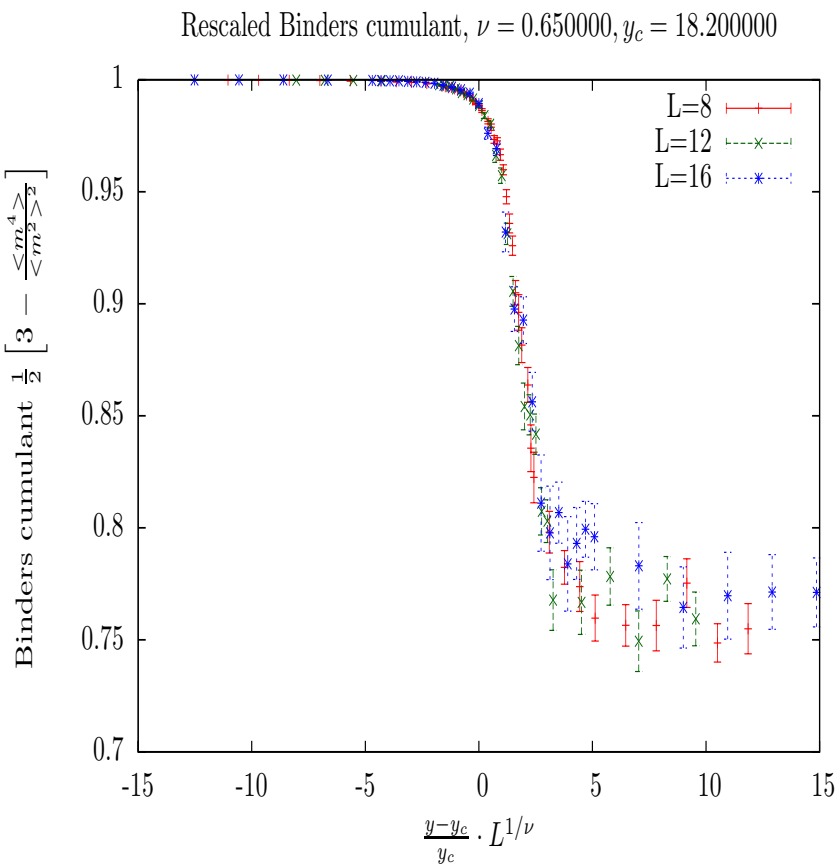

Probing the phase structure using susceptibility

	$\kappa = 0.00$	$\kappa = 0.06$	O(4) scalar model
y_{crit}	16.57 ± 0.06	18.11 ± 0.06	N/A
γ	0.97 ± 0.02	1.08 ± 0.01	1
ν	0.52 ± 0.01	0.66 ± 0.02	0.5
b	2.18 ± 0.09	2.04 ± 0.20	?

- Quoted errors are statistical.
- Estimate systematics by changing the fit range in y.
- Systematic effects
  - y_{crit} is very stable.
  - γ can change by $\sim 2\%$.
  - ν can vary by $\sim 8\%$. $\Rightarrow$ Different from O(4) scalar model?

Outlook

- Improving results by
  - running more at large lattices, $24^3 \times 48$. (finishing soon.)
  - using more sophisticated procedure to investigate the susceptibility.
  - studying the details of the scaling behaviour of Binder's cummulant.

- More information:
  - Compute three renormalised couplings to "trade" with κ, $\hat{\lambda}$ and y.
  - Study the spectrum in the strong Yukawa regime.

A lot more to do and to understand.

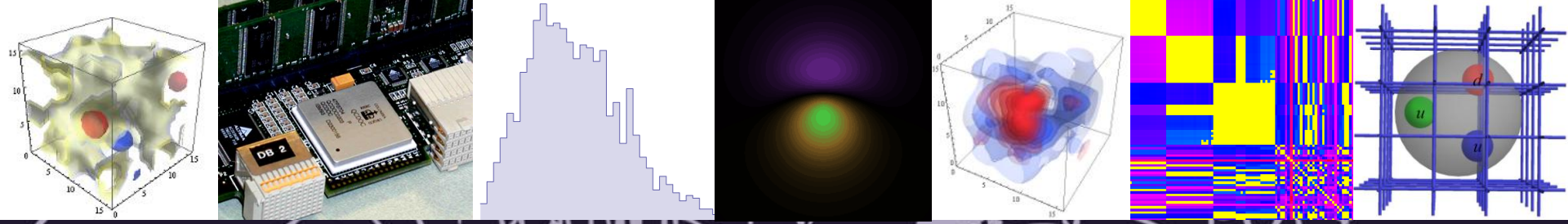

Medium Modification of Pion Structure

Huey-Wen Lin
University of Washington

The Collaboration

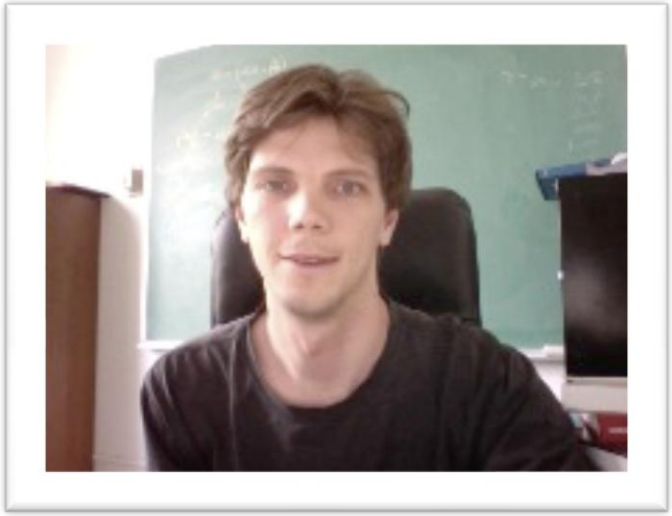

William Detmold
(William & Mary / JLab)

HWL
(U. of Washington)

Hyak @ UW

7n @ JLab

Sporades @ W&M

Hopper @ NERSC

Medium Modification

§ Parton structure function in nuclear medium

- The famous EMC effect
- Significant deviations between heavy nuclei and deuterium
- Many models:
  - pion enhancement
  - nucleon expansion
  - multiquark clusters
  - rescaling
  - shadowing
  - local correlations
  - …

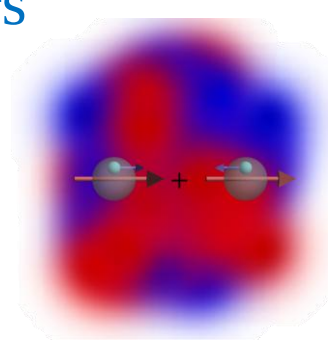

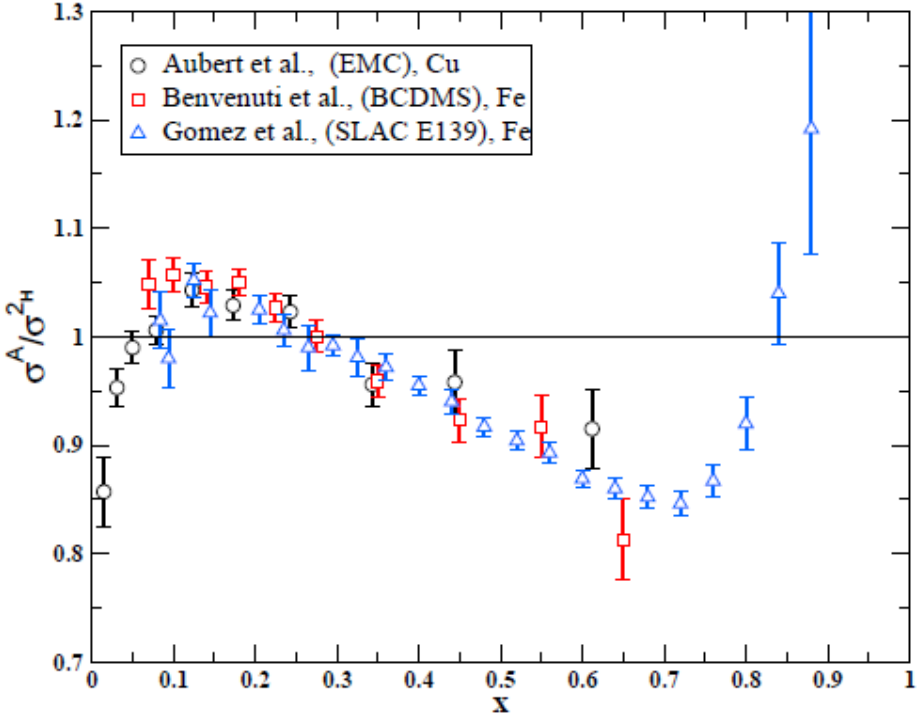

J. J. Aubert et al.
Phys. Lett. 123, 275 (1983)

§ No universal understanding

Medium Modification

§ Not only significant for heavy nuclei,
also important for light-nuclear systems

J. Seely et al., Phys. Rev. Lett. 103, 202301 (2009)

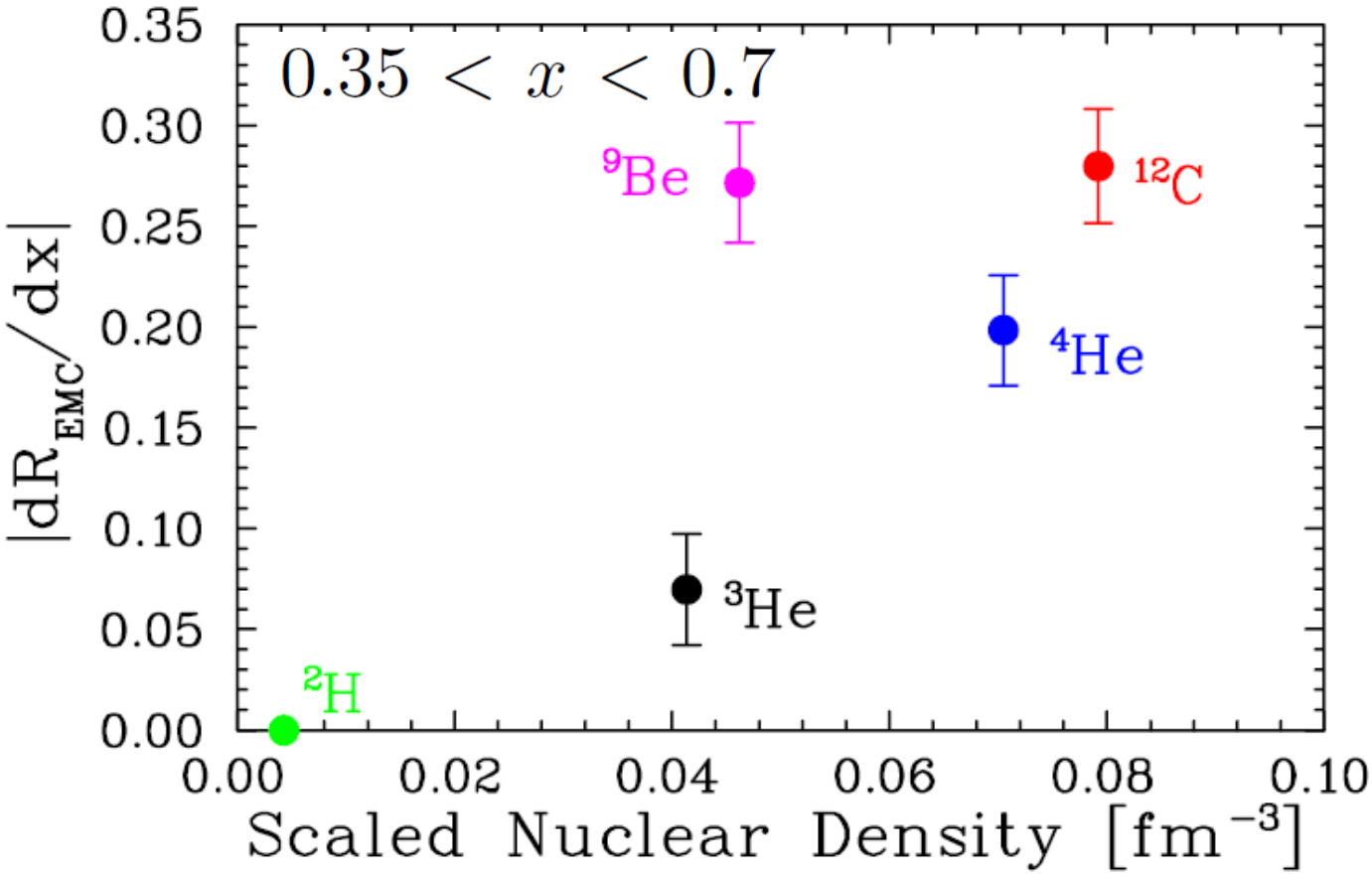

Applications

§ Important for tests of Standard Model

§ For example, NuTeV anomaly

- Weak mixing angle experiment
- 3 sigma away from SM → "NuTeV anomaly"

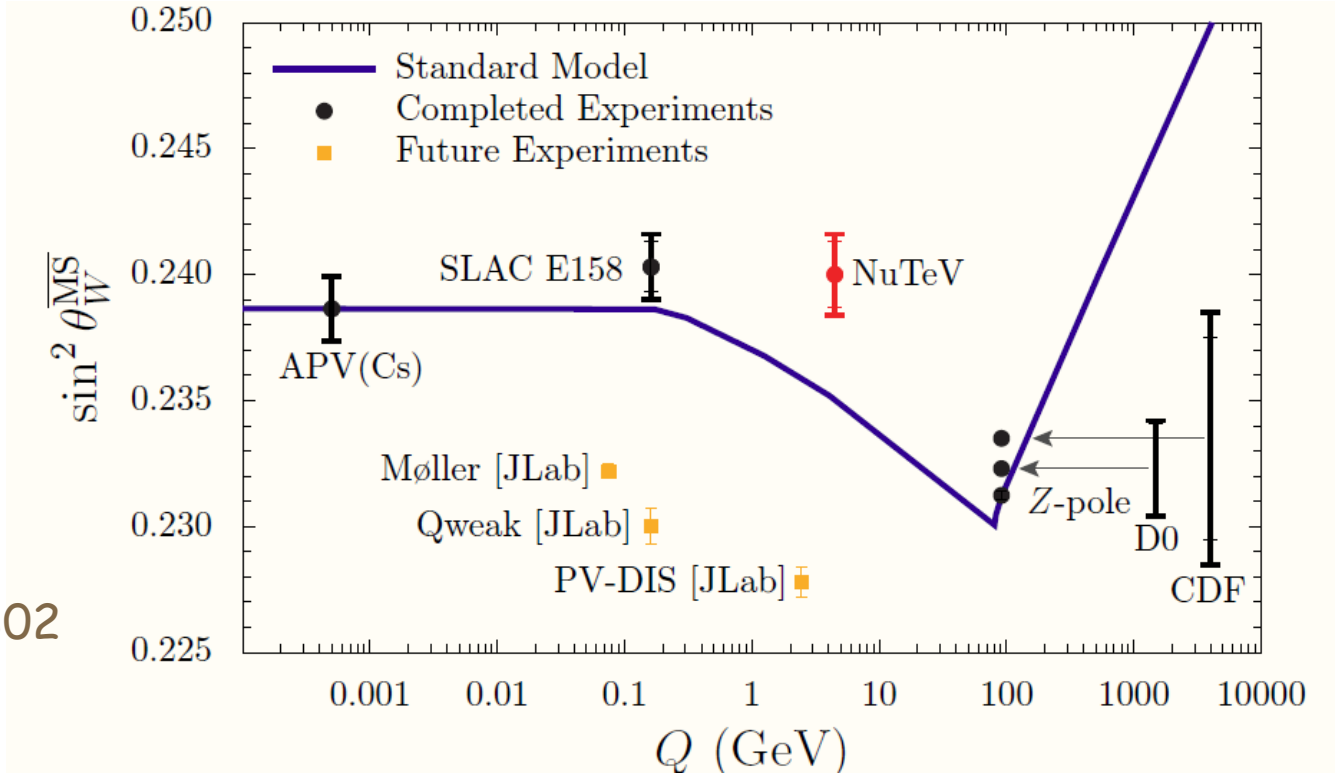

G. P. Zeller et al.
Phys. Rev. Lett. 88, 091802 (2002)

Applications

§ Important for tests of Standard Model

§ For example, NuTeV anomaly

- Weak mixing angle experiment
- 3 sigma away from SM → "NuTeV anomaly"

- Evidence for medium modification?
- Correction looks consistent with SM

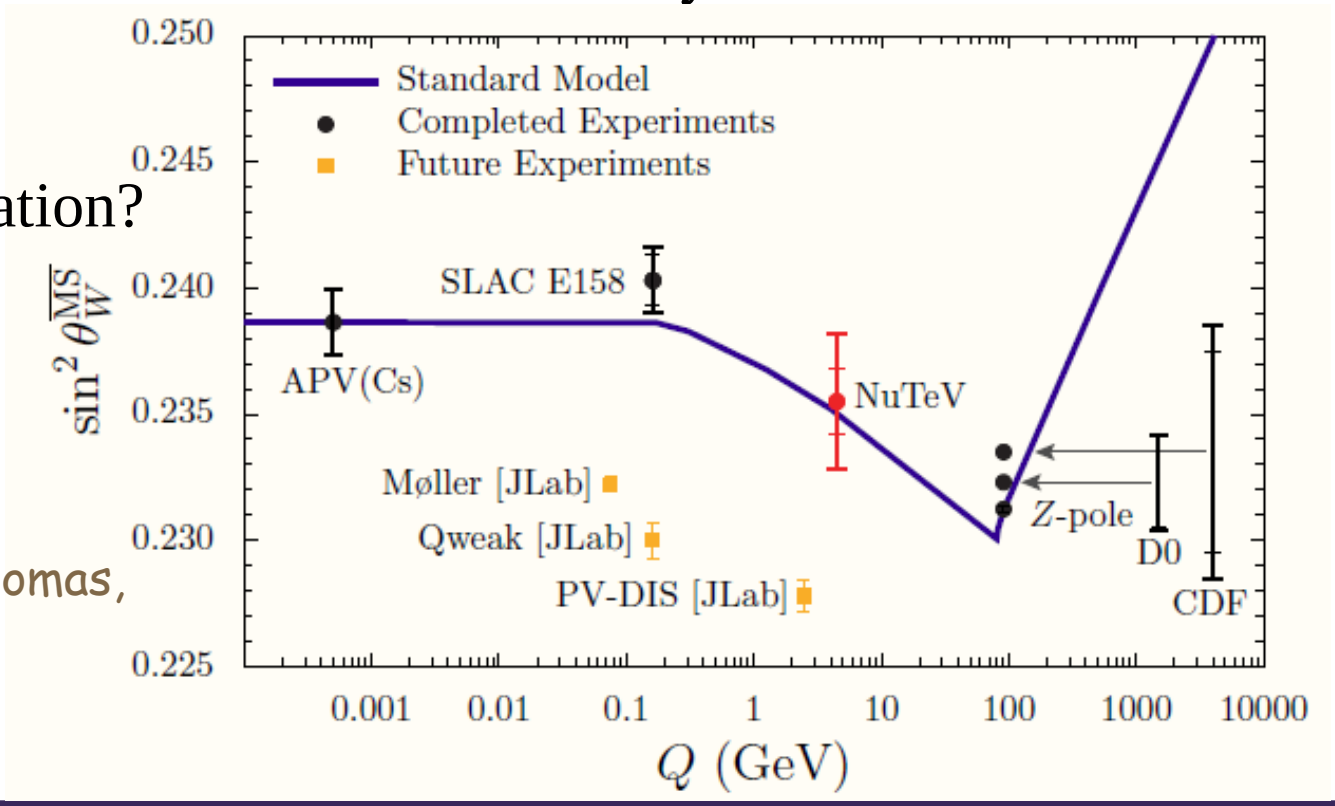

I. Cloët, W. Bentz, A. Thomas, Phys. Lett. B693, 462 (2010)

Medium Modification

§ Interesting physics with multi-baryon systems

- Study with nonzero μ_B
  notorious "sign" problem in Monte Carlo calculation
- Add nucleons to the system
  complicated quark contraction and noise/signal issue

Number of contractions:

$(A+Z)! \times (2A-Z)!$

- Triton: 2880 → 93
- ^{4}He: 518400 → 1107

Signal Quality

- What you want: What you get:

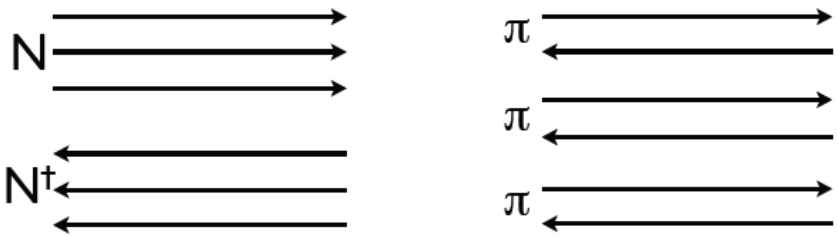

§ Take a step back and look at nonzero-isospin/multi-meson systems

- Many studies: "QCD at Finite Isospin Density", Son & Stephanov
- Gain insight and experience for how to deal with nuclear systems

We do it all the time…

We do it all the time…

We do it all the time…

Multi-Meson System

- § First lattice π-π calculation in ’92
- § Meson number > 2 system is first studied on the lattice

  S. Beane et al., PRL 100: 082004 (2008)
- § Followed by more complicated systems for scattering length and 3-body interactions

  W. Detmold et al., PRD 78: 014507 (2008); W. Detmold et al., PRD 78: 054514 (2008); W. Detmold et al., PRL 102: 032004 (2009); W. Detmold et al., 1103.4362 (2011)
- § Effective theory

  S. Beane, PRD 76: 074507 (2007); W. Detmold et al., PRD 77: 057502 (2008); Smigielski, PRD 79: 054506 (2009)
- § Color-screening effects

  W. Detmold et al., PRL 102: 032004 (2009)
- § Study for $n \geq 13$ system

  W. Detmold et al., PRD 82: 014511 (2010); Z. Shi and W. Detmold, PoS (2011)

Boring Details

§ The tool: Lattice gauge theory

§ The actions

- **Domain-wall fermions on staggered sea**
  - Free forward propagators from LHPC and NPLQCD
  - Chiral symmetry preserved at finite lattice spacing; good for spin physics and weak matrix elements

§ The parameters

Label	a [fm]	$L^3 \times T$	m_π [MeV]	$m_\pi L$	$m_\pi T$	Measurements
F	0.09	$28^3 \times 96$	320	4.1	14.0	432
C1	0.12	$20^3 \times 64$	290	3.7	11.7	1450
C2	0.12	$20^3 \times 64$	350	4.4	14.2	837
C3	0.12	$20^3 \times 64$	490	6.2	19.9	1000

t_{sep} C's ∈ {16, 20, 24, 28, 32}

F's ∈ {24, 32, 48}

π^+ in Medium

§ We calculate

$$C_m(t, \mathbf{p}) = \left\langle 0 \left| \left(\prod_{i=1}^{m} \sum_{\mathbf{x}} e^{i\,\mathbf{p}_i \cdot \mathbf{x}}\, \pi^+(\mathbf{x}, t) \right) (\pi^-(x_0))^m \right| 0 \right\rangle \qquad \mathbf{p} = \sum_{i=1}^{m} \mathbf{p}_i$$

§ Contractions

- Examples from 3-π^+ system

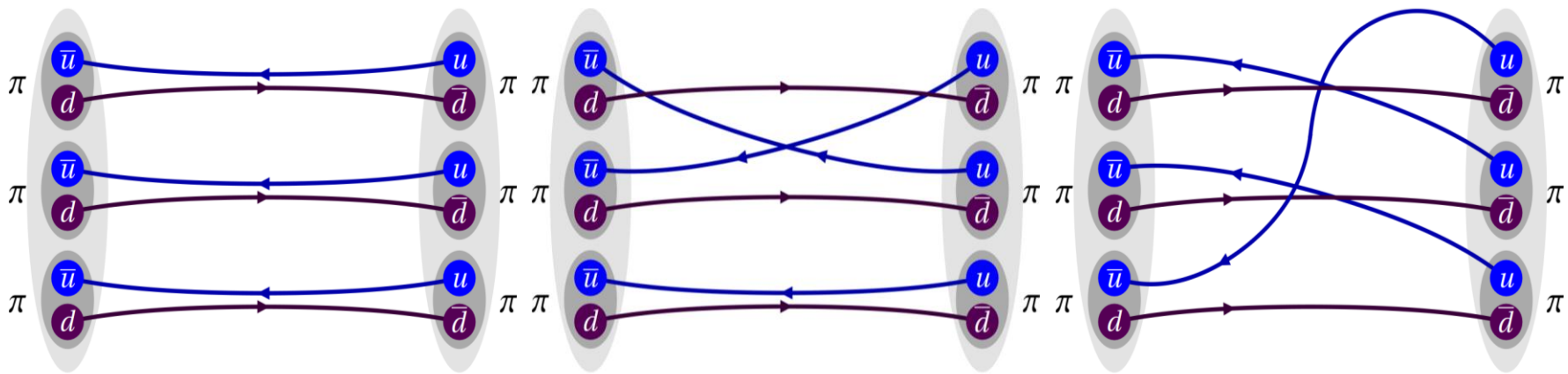

π^+ in Medium

§ We calculate

$$C_m(t, \mathbf{p}) = \left\langle 0 \left| \left(\prod_{i=1}^{m} \sum_{\mathbf{x}} e^{i\,\mathbf{p}_i \cdot \mathbf{x}}\, \pi^+(\mathbf{x}, t) \right) (\pi^-(x_0))^m \right| 0 \right\rangle \qquad \mathbf{p} = \sum_{i=1}^{m} \mathbf{p}_i$$

§ Contractions

- Simplified with recursion relation

W. Detmold et al., Phys.Rev.D82:014511 (2010)

$$C_3(t) = \mathrm{tr}[\Pi]^3 - 3\,\mathrm{tr}[\Pi]\,\mathrm{tr}\left[\Pi^2\right] + 2\,\mathrm{tr}\left[\Pi^3\right]$$

$$\Pi = \sum_{\mathbf{x}} \gamma_5\, S(\mathbf{x}, t; 0)\, \gamma_5\, S^\dagger(\mathbf{x}, t; 0)$$

§ Energy extraction from n-π^+ system

$$C_m(t, \mathbf{0}) \longrightarrow \sum_{\ell=0}^{m} \binom{m}{\ell} Z_m^{(\ell)}\, e^{-E_{m-\ell}\, t}\, e^{-E_\ell (T-t)} + \ldots$$

n-π^+ Energy

§ Can we simplify the analysis?

- Examples from n-π^+ system

Fit 1: $C_m(t, \mathbf{0}) \longrightarrow \sum_{\ell=0}^{m} \binom{m}{\ell} Z_m^{(\ell)} e^{-E_{m-\ell}\, t}\, e^{-E_\ell (T-t)} + \ldots$

Fit 2: $\ell = m$ only (ignore the thermal states)

$a = 0.12$ fm, $M_\pi \approx 490$ MeV

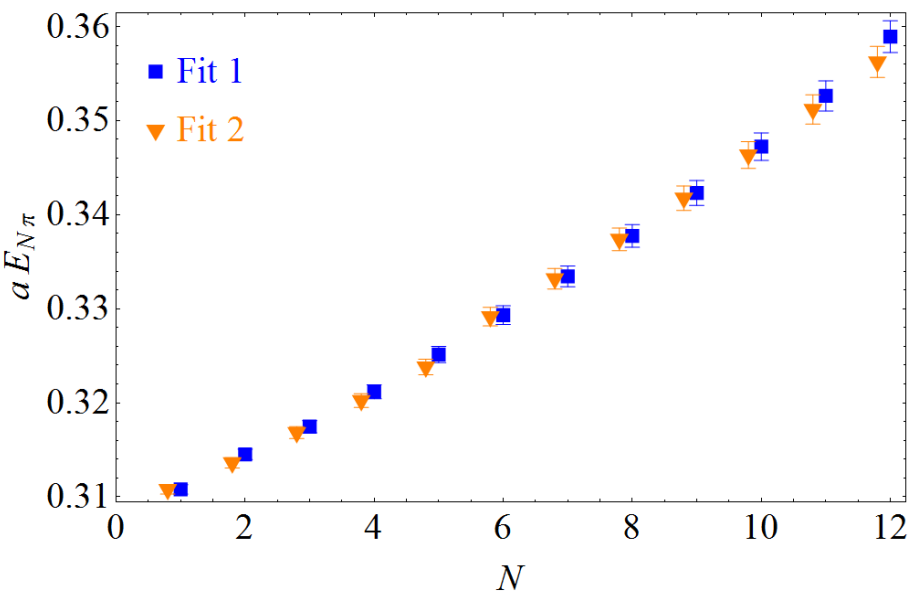

$a = 0.09$ fm, $M_\pi \approx 320$ MeV

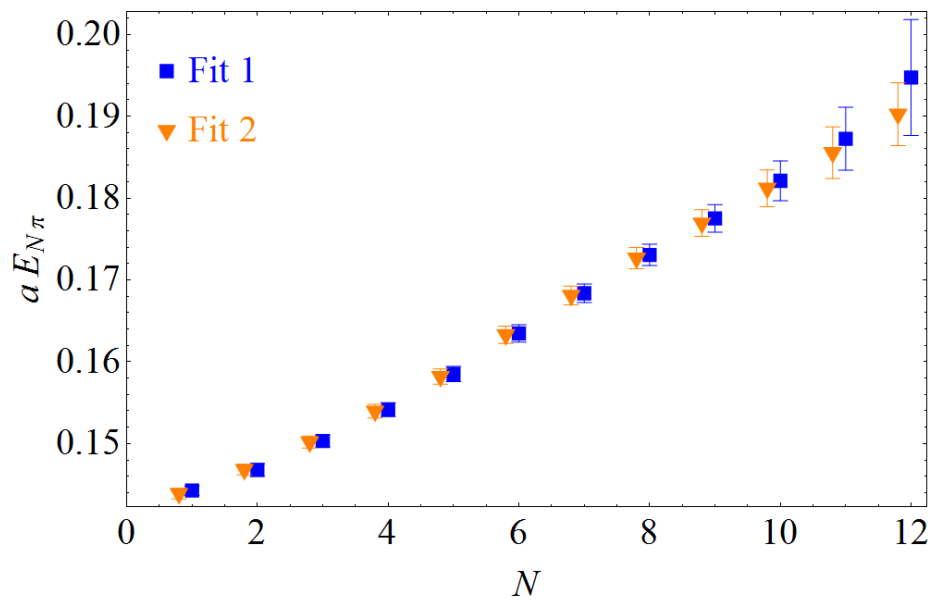

n-π^+ Energy

§ Fitted energies and effective-mass plot

- Examples

$a = 0.09$ fm,
$M_\pi \approx 320$ MeV

$\log(C(t)/C(t+1))$

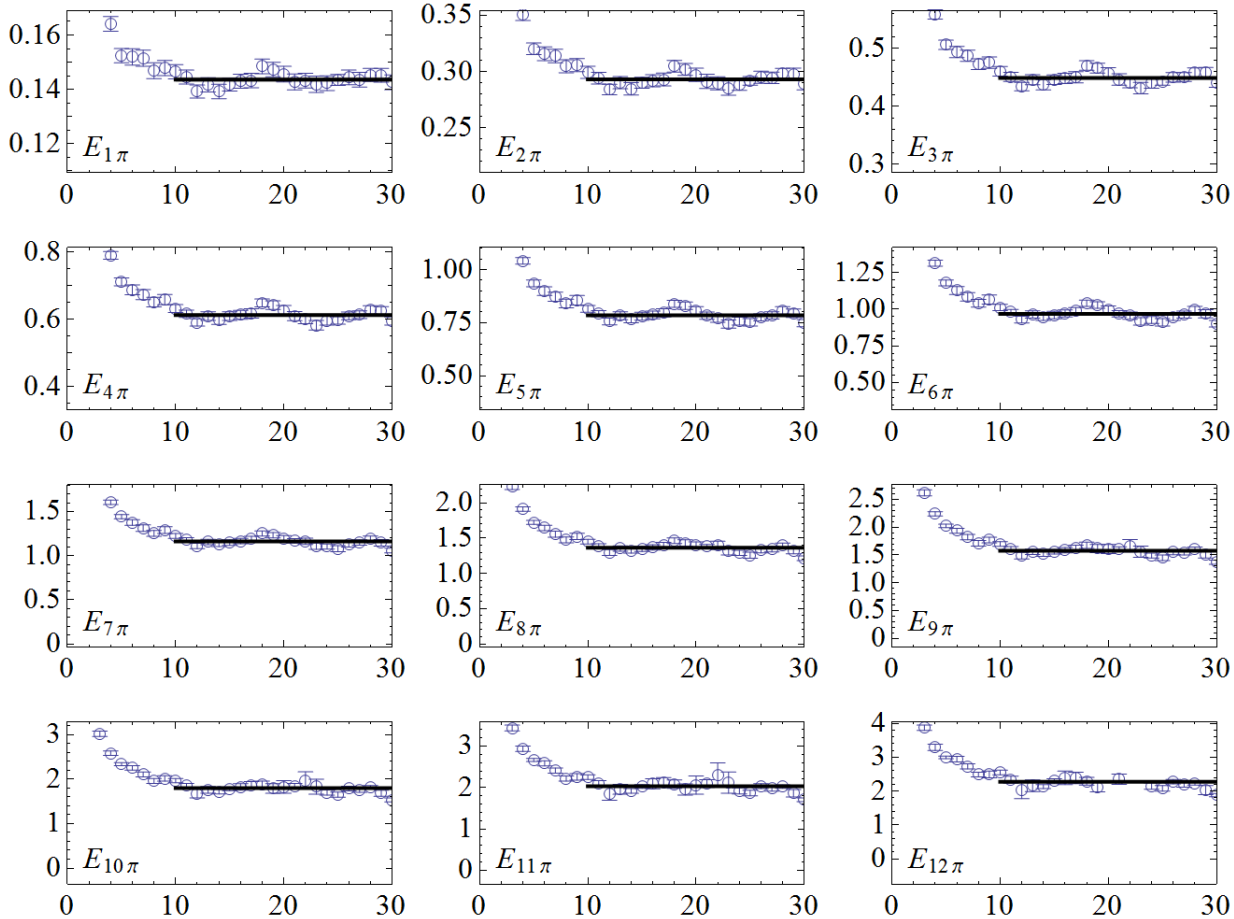

M_π in Medium

§ How pion mass shifts in K^+, π^+ medium

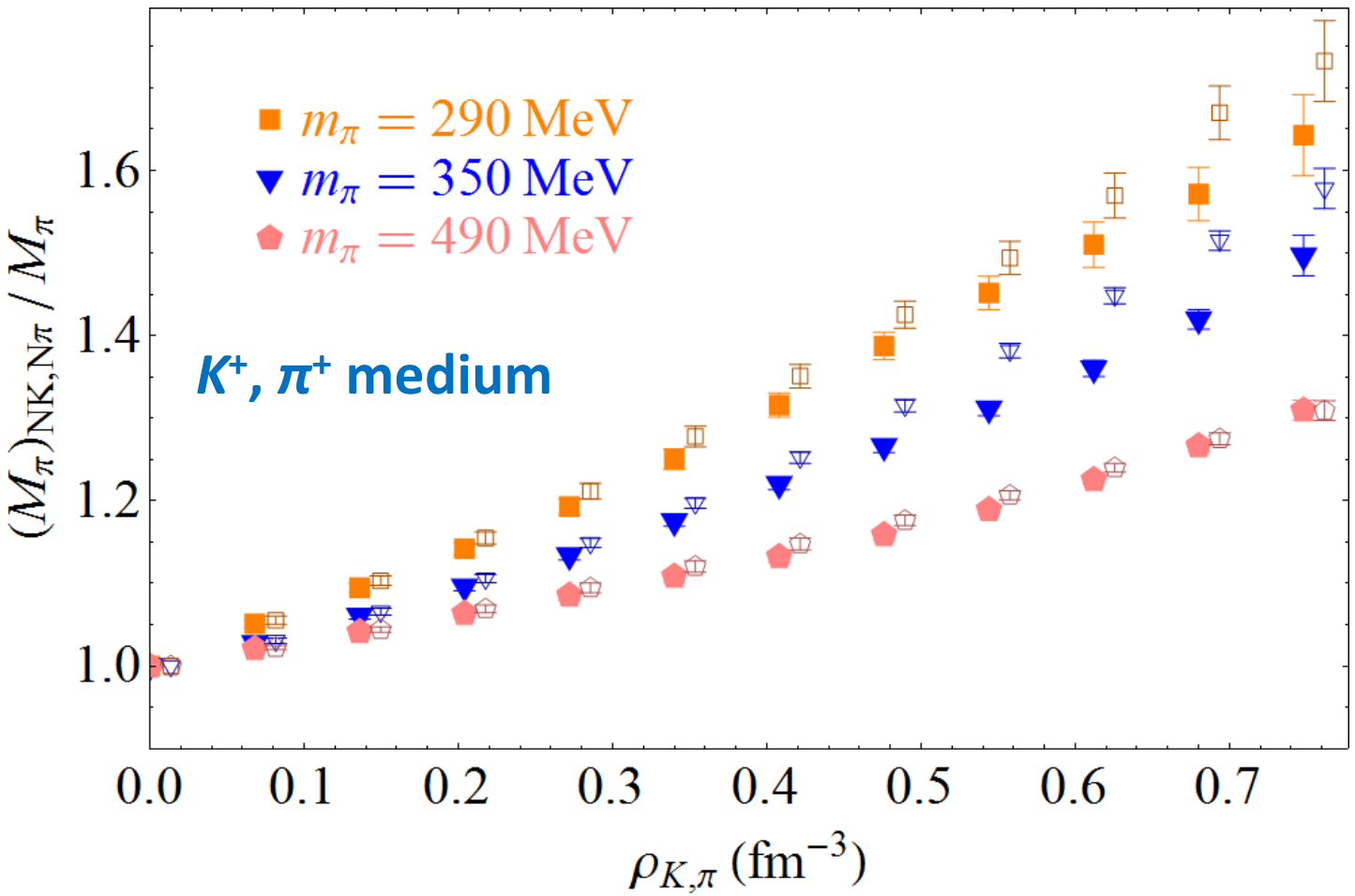

Pion Structure Function

§ We calculate

$$C_m^{(n)}(\tau,\, t,\, \mathbf{p}) = \left\langle 0 \left| \left(\prod_{i=1}^{m} \sum_{\mathbf{x}} e^{i\,\mathbf{p}_i\cdot\mathbf{x}}\, \pi^+(\mathbf{x},\, t) \right) \left(\sum_{\mathbf{y}} \mathcal{O}_{\{\mu_0\,\mu_1\,\ldots\mu_n\}}(\mathbf{y},\, \tau) \right) (\pi^-(x_0))^m \right| 0 \right\rangle$$

where $\mathcal{O}_{\{\mu_0\,\mu_1\,\ldots\mu_n\}} = \left(\frac{i}{2}\right)^n \overline{\psi}\,\gamma_{\mu_0}\,\overleftrightarrow{D}_{\mu_1}\,\ldots\,\overleftrightarrow{D}_{\mu_n}\,\psi - \text{trace}$

§ Contractions

- Examples from 3-π^+ system

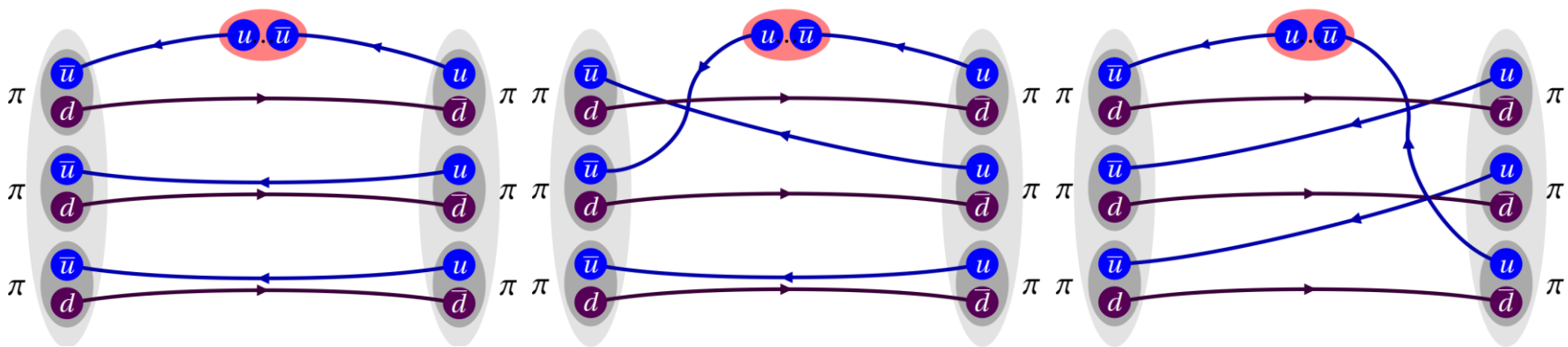

Pion Structure Function

§ We calculate

$$C_m^{(n)}(\tau, t, \mathbf{p}) = \left\langle 0 \left| \left(\prod_{i=1}^{m} \sum_{\mathbf{x}} e^{i\,\mathbf{p}_i\cdot\mathbf{x}}\, \pi^+(\mathbf{x}, t) \right) \left(\sum_{\mathbf{y}} \mathcal{O}_{\{\mu_0\,\mu_1\,\ldots\mu_n\}}(\mathbf{y}, \tau) \right) (\pi^-(x_0))^m \right| 0 \right\rangle$$

where $\mathcal{O}_{\{\mu_0\,\mu_1\,\ldots\mu_n\}} = \left(\frac{i}{2}\right)^n \overline{\psi}\,\gamma_{\mu_0}\,\overleftrightarrow{D}_{\mu_1}\ldots\overleftrightarrow{D}_{\mu_n}\,\psi - \text{trace}$

§ Wick contractions

- Use mixed-meson recursion relations

W. Detmold, B. Smigielski, Phys.Rev.D84:014508 (2011)

$$\Pi = \sum_{\mathbf{x}} \gamma_5\, S(\mathbf{x}, t; 0)\, \gamma_5\, S^\dagger(\mathbf{x}, t; 0)$$

$$\tilde{\Pi} = \sum_{\mathbf{x},\mathbf{y}} \gamma_5\, S(\mathbf{x}, t; \mathbf{y}, \tau)\, \mathcal{O}\, S(y, \tau; 0)\, \gamma_5\, S^\dagger(\mathbf{x}, t; 0)$$

→ Treated as diff. meson spices

Pion Structure Function

§ We calculate

$$C_m^{(n)}(\tau,\, t,\, \mathbf{p}) = \left\langle 0 \,\middle|\, \left(\prod_{i=1}^{m} \sum_{\mathbf{x}} e^{i\,\mathbf{p}_i\cdot\mathbf{x}}\, \pi^+(\mathbf{x},\, t) \right) \left(\sum_{\mathbf{y}} \mathcal{O}_{\{\mu_0\,\mu_1\,\ldots\mu_n\}}(\mathbf{y},\, \tau) \right) (\pi^-(x_0))^m \,\middle|\, 0 \right\rangle$$

where $\mathcal{O}_{\{\mu_0\,\mu_1\,\ldots\mu_n\}} = \left(\frac{i}{2}\right)^n \overline{\psi}\,\gamma_{\mu_0}\,\overleftrightarrow{D}_{\mu_1}\,\ldots\,\overleftrightarrow{D}_{\mu_n}\,\psi - \text{trace}$

§ Wick contractions

- Examples from n-π^+ system

$$C_3^{(n)} = -2\,\mathrm{tr}[\Pi]\,\mathrm{tr}\left[\tilde{\Pi}\,\Pi\right] + 2\,\mathrm{tr}\left[\tilde{\Pi}\,\Pi^2\right] + \mathrm{tr}[\Pi]^2\,\mathrm{tr}[\tilde{\Pi}] - \mathrm{tr}\left[\Pi^2\right]\mathrm{tr}[\tilde{\Pi}]$$

$$\Pi = \sum_{\mathbf{x}} \gamma_5\, S(\mathbf{x},\, t;\, 0)\,\gamma_5\, S^\dagger(\mathbf{x},\, t;\, 0)\ ,\ \tilde{\Pi} = \sum_{\mathbf{x},\mathbf{y}} \gamma_5\, S(\mathbf{x},\, t;\, \mathbf{y},\, \tau)\,\mathcal{O}\, S(y,\, \tau;\, 0)\,\gamma_5\, S^\dagger(\mathbf{x},\, t;\, 0)$$

§ Matrix elements extraction (naively)

$$C_m^{(n)}(\tau,\, t,\, \mathbf{p}) \xrightarrow{t \gg \tau \gg 0} A\, e^{-E_n\, t}\, \langle n\,\pi \,|\, \mathcal{O} \,|\, n\,\pi \rangle + \ldots$$

Pion Momentum Fraction

§ $\langle x\rangle^{\pi,N}/\langle x\rangle^{\pi,0}$ without thermal-state degrees of freedom

$t_{sep} = T/2$

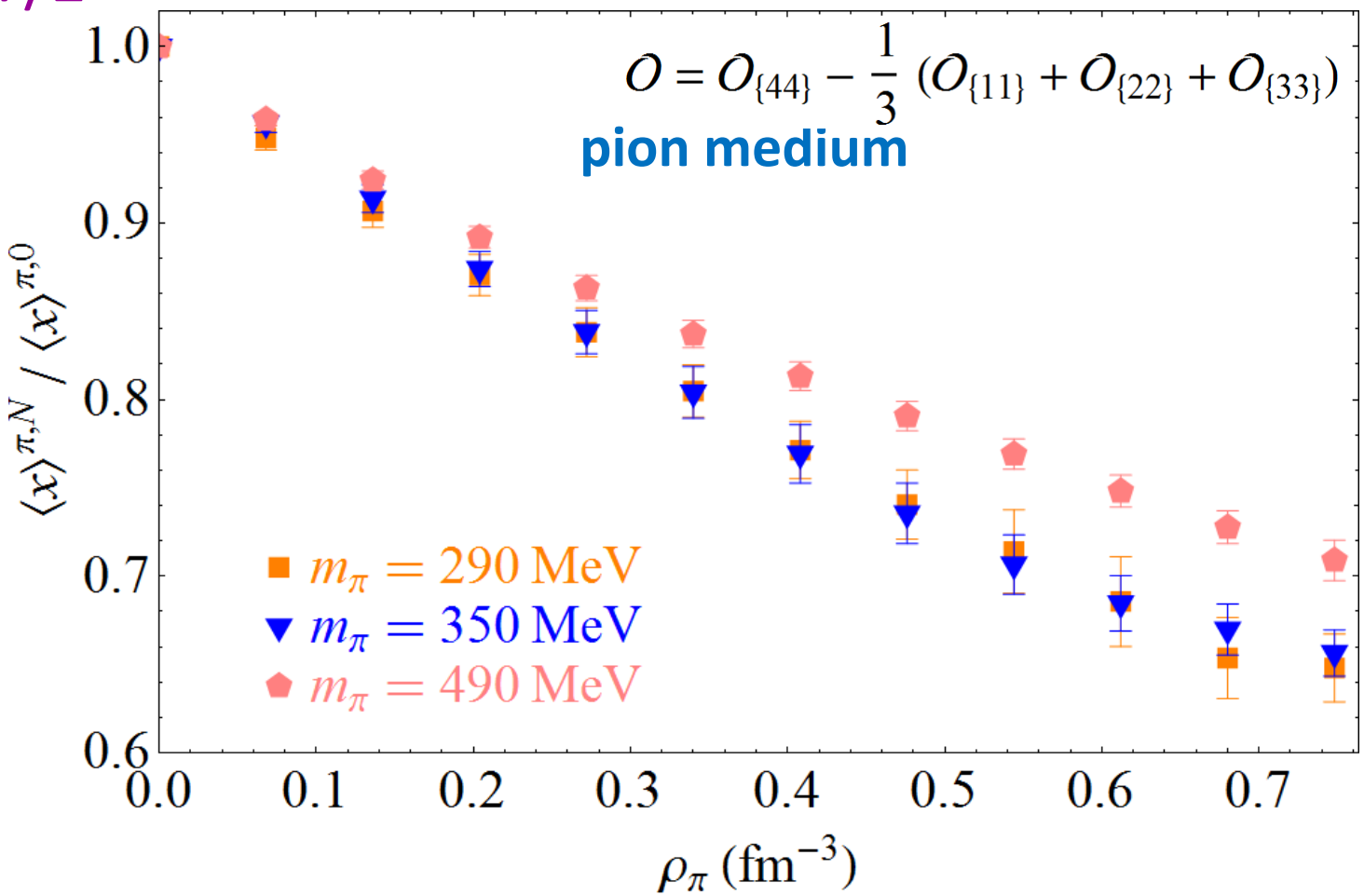

Thermal Contamination

§ Significant for n-π^+ system through amplitudes

§ For example, $a = 0.12$ fm ensemble, $T = 64$

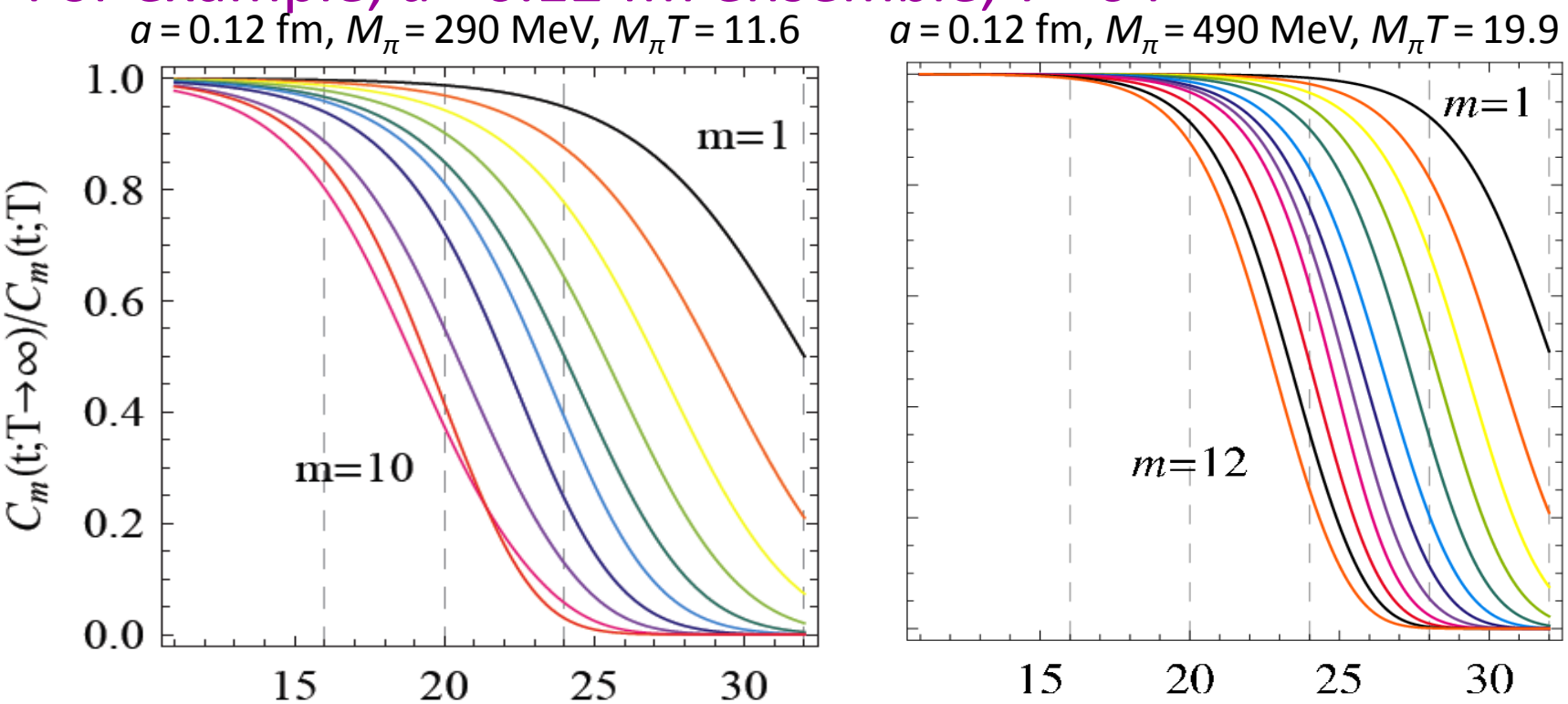

§ Matrix elements extraction for $\boldsymbol{p = 0}$ (in reality)

$$C_m^{(n)}(\tau,\, t,\, 0) \longrightarrow \sum_{\ell=0}^{m} \binom{m}{\ell} Z_m^{(\ell)} \left\langle \mathcal{O}_{m-\ell}^{(n)} \right\rangle e^{-E_{m-\ell}\, t}\, e^{-E_\ell (T-t)} + \ldots$$

Pion Momentum Fraction

§ $\langle x\rangle^{\pi,N}/\langle x\rangle^{\pi,0}$ with thermal-state degrees of freedom

multiple t_{sep} used

$$\mathcal{O} = \mathcal{O}_{\{44\}} - \frac{1}{3}\left(\mathcal{O}_{\{11\}} + \mathcal{O}_{\{22\}} + \mathcal{O}_{\{33\}}\right)$$

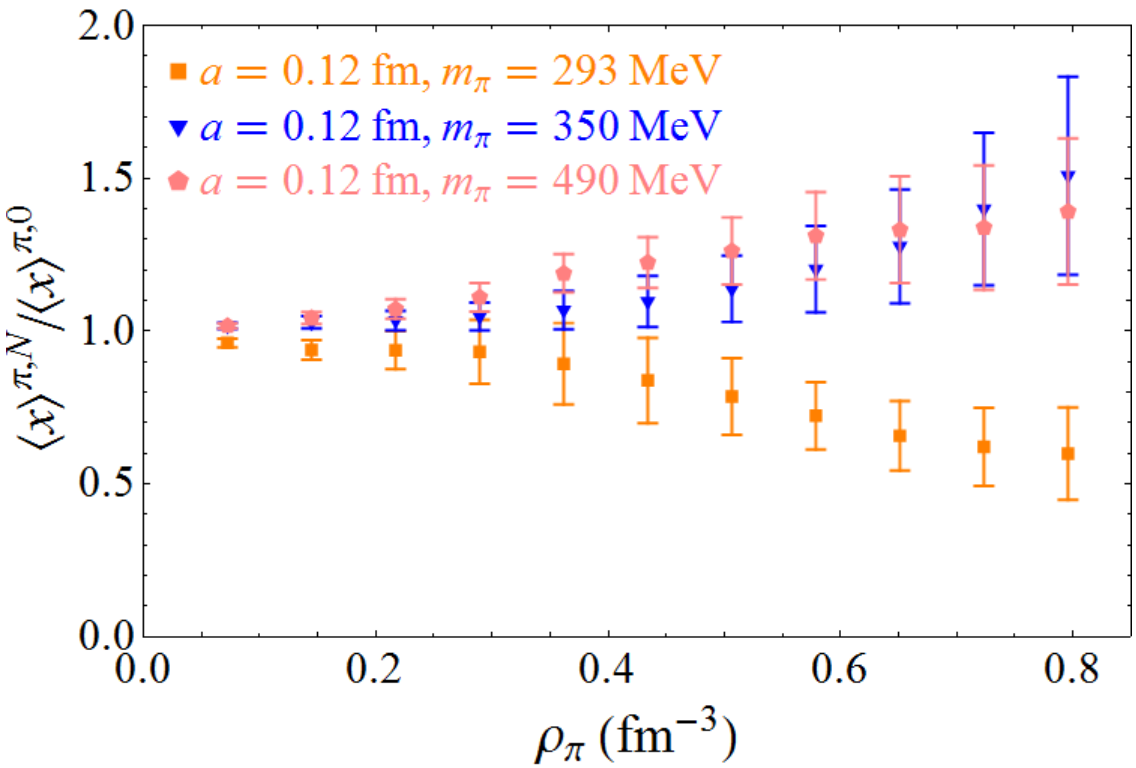

Pion Momentum Fraction

§ $\langle x\rangle^{\pi,N}/\langle x\rangle^{\pi,0}$ with thermal-state degrees of freedom

multiple t_{sep} used

$$\mathcal{O} = \mathcal{O}_{\{44\}} - \frac{1}{3}\left(\mathcal{O}_{\{11\}} + \mathcal{O}_{\{22\}} + \mathcal{O}_{\{33\}}\right)$$

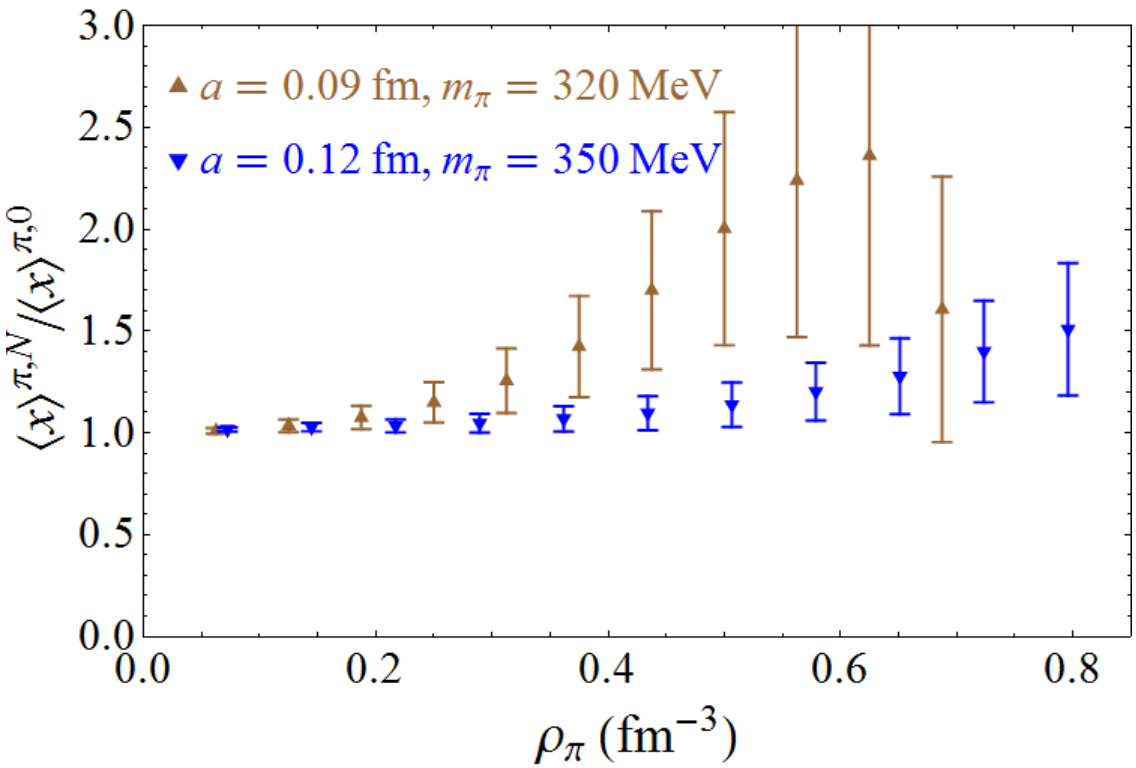

Summary and Outlook

§ First lattice-QCD attempt to measure EMC effects

- Pion momentum fraction in pion medium
- With $m_\pi \approx 290$–490 MeV, 2 lattice spacings

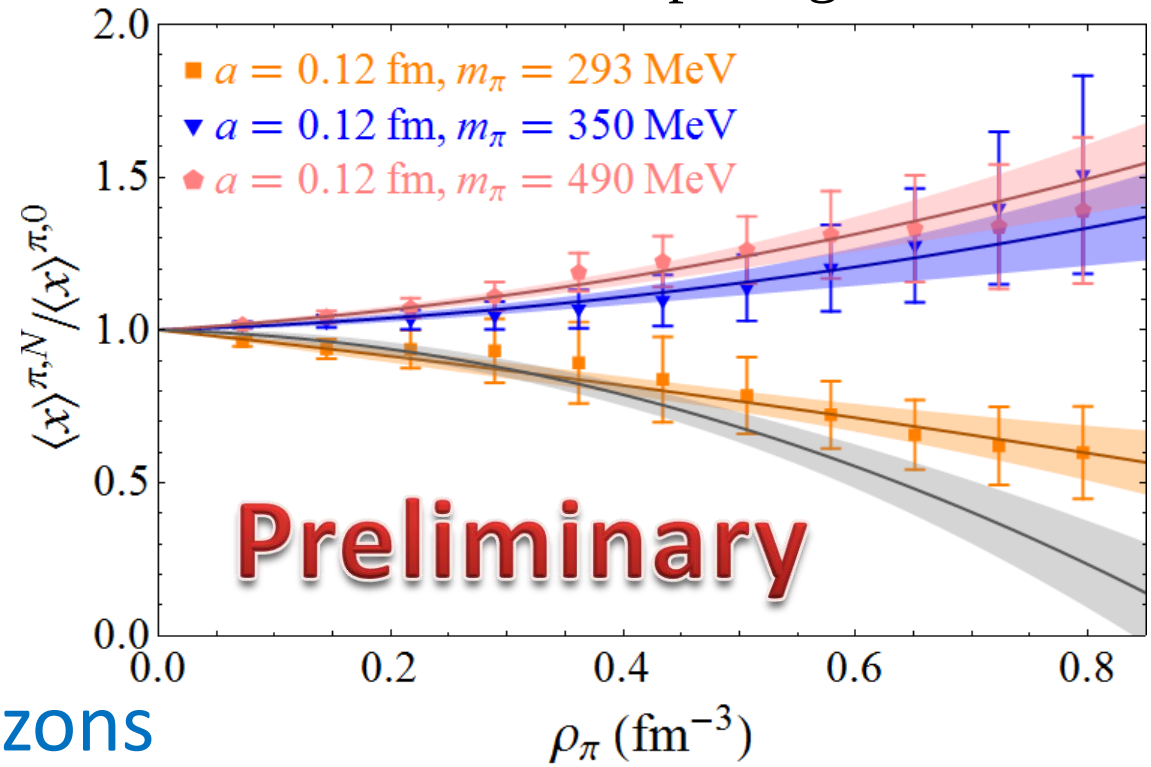

New Horizons

§ Nucleon structure in meson and light-nuclear media

Many-Flavor Domain Wall Fermions and Fixed Topology

Meifeng Lin

Yale

New Horizons for Lattice Computations with Chiral Fermions
BNL, May 14 - 16, 2012

Outline

Motivation

LSD Calculations with Domain Wall Fermions
- Recap: Results for $N_f = 2, 6$
- New: Results for $N_f = 10$

Summary

Motivation

- SU(N) gauge theories with many flavors of fermions may exhibit behaviors that are fundamentally different from QCD.
- Increasing N_f causes the gauge coupling to run slowly, and "walking" may occur, which could lead to some properties desirable for Technicolor model building.
- Specifically, we are interested in
  - enhanced chiral condensate
  - small S parameter
  - new pattern in hadron spectrum
- When $N_f > N_f^c$, the theory becomes conformal, and spectrum vanishes at the chiral limit. Also on our wishlist is to
  - locate N_f^c non-perturbatively

The Lattice Strong Dynamics Collaboration

Tom Appelquist	Yale U.
Ron Babich	NVIDIA
Rich Brower	Boston U.
Michael Buchoff	LLNL
Michael Cheng	Boston U.
Mike Clark	NVIDIA
Saul Cohen	U. Washington
George Fleming	Yale U.
Joe Kiskis	U. of Carlifornia, Davis
Meifeng Lin	Yale U.
Heechang Na	ANL
Ethan Neil	Fermilab
James Osborn	ANL
Claudio Rebbi	Boston U.
David Schaich	Boston U.
Chris Schroeder	LLNL
Sergey Syritsyn	LBL
Joe Wasem	LLNL
Oliver Witzel	Boston U.
Gennady Voronov	Yale U.
Pavlos Vranas	LLNL

Gauge Ensembles

- Fermion action: domain wall fermions.
- Gauge action: Iwasaki.
- Ensemble size: Typically ~ 1200 MD trajectories.

[Cost grows as $N_f^{3/2}$]

N_f	Volume	L_s	β	am_f	am_{res}
2	$32^3 \times 64$	16	2.70	0.005...0.030	2.5×10^{-5}
6	$32^3 \times 64$	16	2.10	0.005...0.030	8.2×10^{-4}
10	$32^3 \times 64$	16	1.95	0.005...0.030	1.7×10^{-3}

- For $N_f = 2$, $aM_V \approx 0.21 \Rightarrow a^{-1} \approx 3.7$ GeV.
- For $N_f = 6$ and 10, match aM_V to within 10% of $N_f = 2$.

Recap: Results for $N_f = 2, 6$

Condensate Enhancement

$$R_m \equiv \frac{M_m^2}{2mF_\pi}_{(N_f=6)} \Big/ \frac{M_m^2}{2mF_\pi}_{(N_f=2)}$$

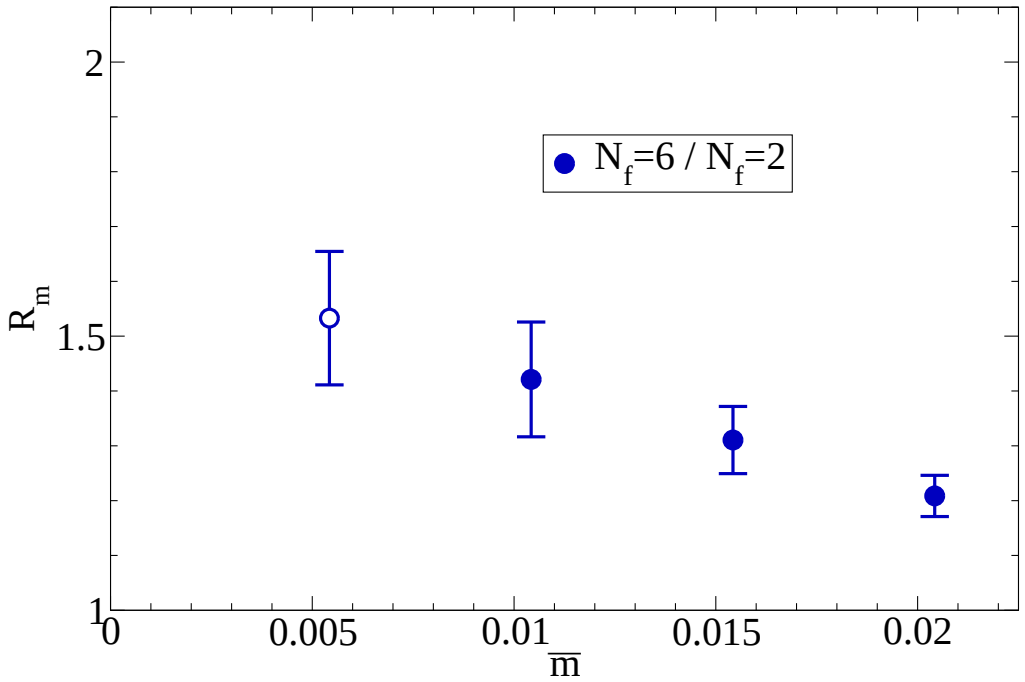

T. Appelquist *et al.* (LSD Collaboration), PRL104:071601,2010

Recap: Results for $N_f = 2, 6$

The S Parameter

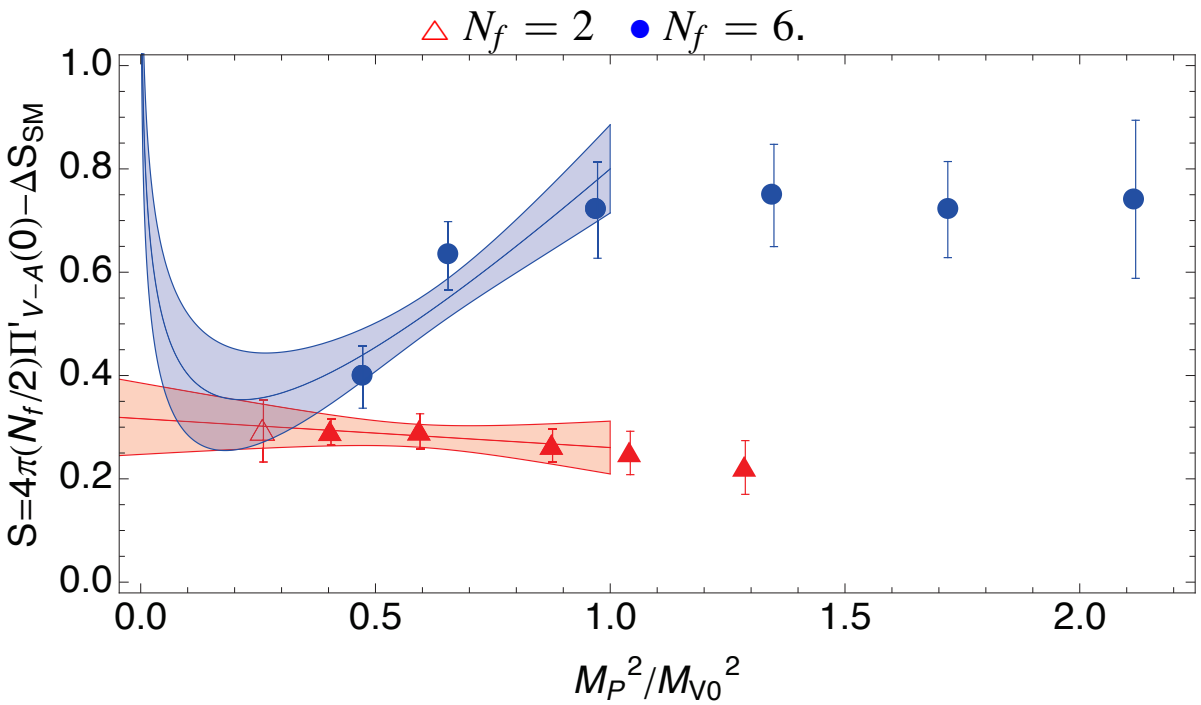

T. Appelquist *et al.* (LSD Collaboration), PRL 106 (2011) 231601

A New Observation for $N_f = 10$

- Two independent ensembles for each quark mass, with ordered and disordered start.
- The ensembles thermalize to different values
- NOT observed for $N_f = 2$ or 6.

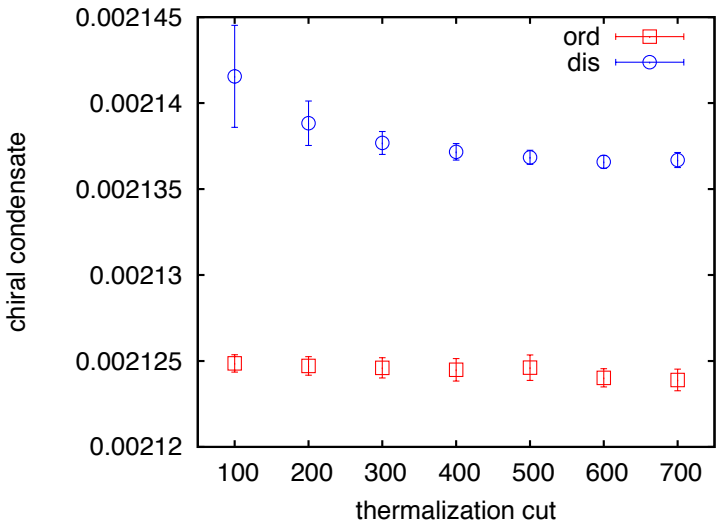

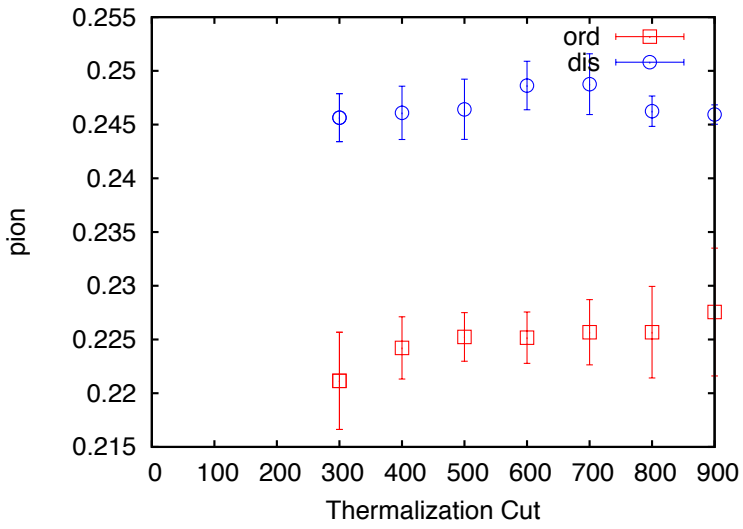

Starting-Config. Dependence

Statistically significant diffference between the ordered-start and disordered-start ensembles are observed for almost all the ensembles.

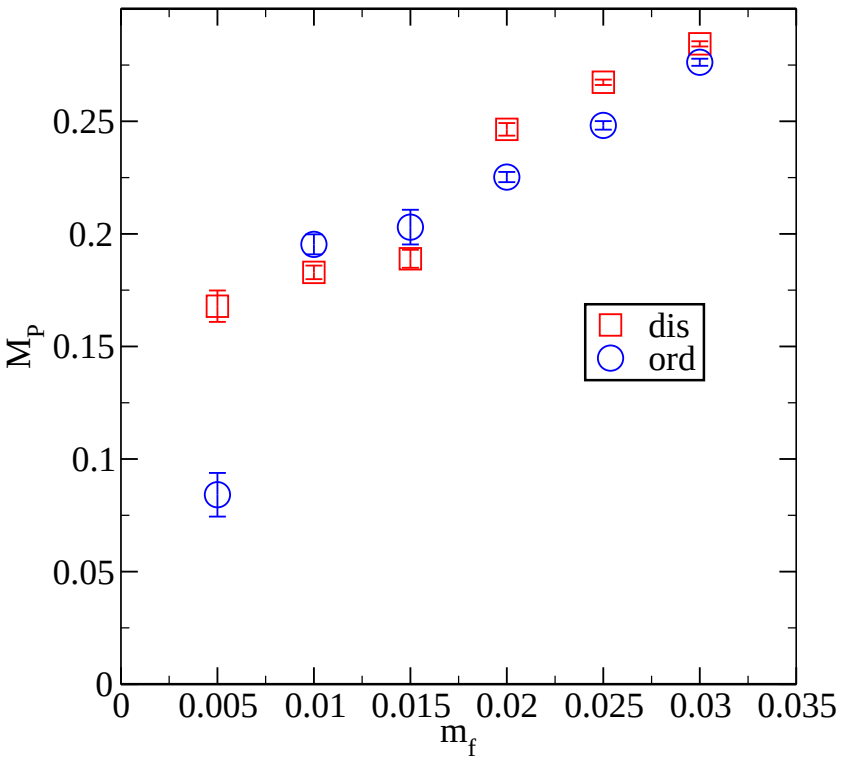

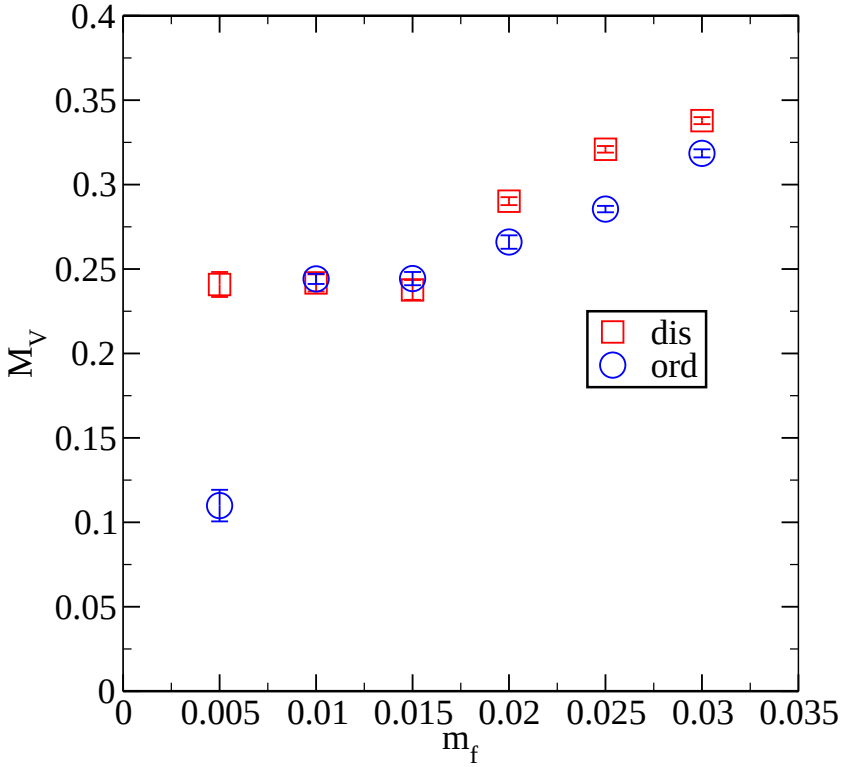

Slowly-moving/Fixed Topology

m_f	start	trajectory range	Q
0.005	O	500 - 1319	0
0.005	D	500 - 919	3
0.010	O	500 - 1373	0
0.010	D	500 - 1259	1
0.015	O	500 - 1204	0
0.015	D	500 - 1450	-1
0.020	O	500 - 1239	0
0.020	D	500 - 1221	12
0.025	O	500 - 1256	0
0.025	D	500 - 609	-19
		610 - 942	-18
		943 - 1095	-17
		1096-1097	-16
		1098 - 1382	-17
		1383 - 1484	-16
0.030	O	500 - 1415	0
0.030	D	500 - 1227	9

Effects of Fixed Topology

- The slight topological tunneling at $m_f = 0.025$ (D) allows us to analyze the data for different topological sectors separately.
- Given the limited number of measurements for each topology, we only block every trajectory, hence the errors will be underestimated.
- Nevertheless, such analysis will give us a crude idea how much the fixed topology may affect our results.

R. Brower, S. Chandrasekharan, John W. Negele, and U.J. Wiese. 2003 has the following formula for the Q-dependence

$$M_Q = M(0) + \frac{1}{2} M^{(2)}(0) \frac{1}{V\chi_t} \left(1 - \frac{Q^2}{V\chi_t}\right) + O\left(\frac{1}{V^3}\right).$$

χ_t is the topological susceptibility, $M^{(2)}(0)$ is the second derivative with respect to θ at $\theta = 0$, and $M(0)$ is the mass at $\theta = 0$ (or equivalently, at non-fixed Q).

Observed Q-Dependence

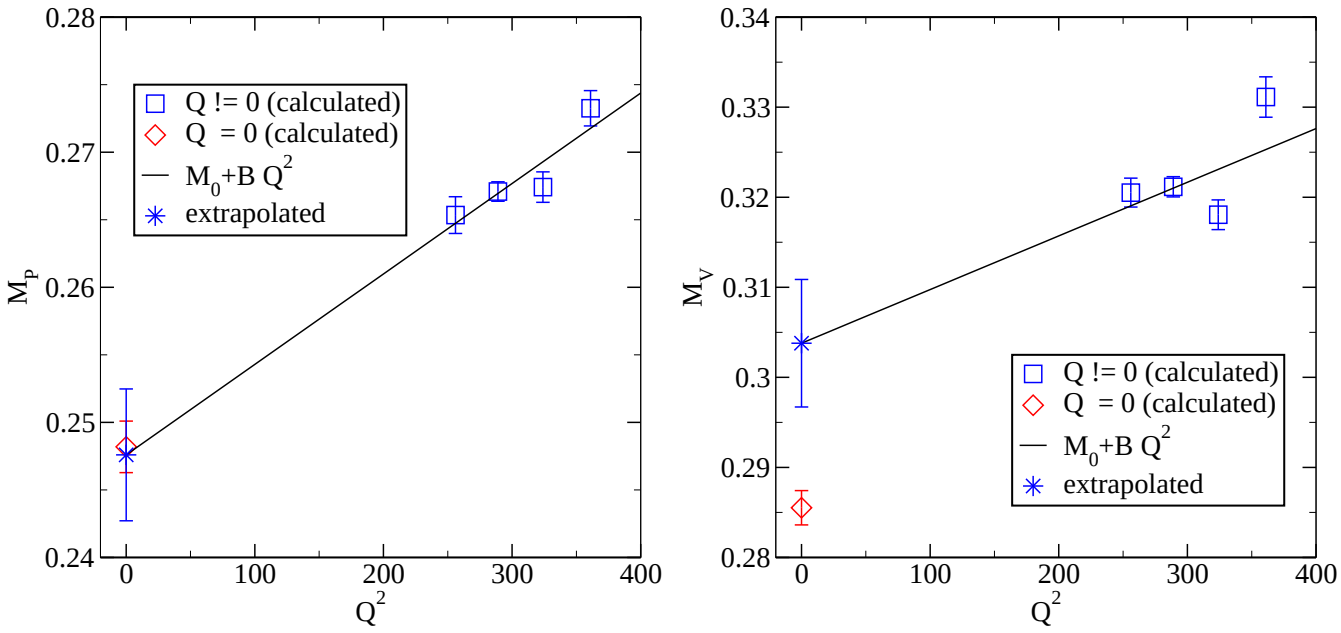

- The discrepancy between ordered and disordered ensembles can be described by the dependence on the fixed topology.
- To get results at $\theta = 0$, we still need to know the topological susceptibility $\rightarrow$ work in progress.
- Large discrepancies $\Rightarrow$ small χ_t? V too small?

Combining Datasets

Lacking the results for the topological susceptibility, can we still combine the two ensembles and obtain some best estimates of the "true" value, $M(0)$?

- From our fits, $M^{(2)}(0)$ is negative, so $M(0)$ is between the results for $Q = 0$ and $Q \neq 0$.
- Take $\overline{M} = (M_0 + M_Q)/2$ as the central value.
- Take the largest relative difference between M_Q and M_0 as systematic error.
- Combine statistical and systematic errors as final error.

Testing Conformality - Qualitatively

In a conformal theory with a small finite mass,

$$M_X = C_X m^{1/(1+\gamma^*)}$$

so the vector-to-pseudoscalar meson mass ratio M_V/M_P should look roughly constant.

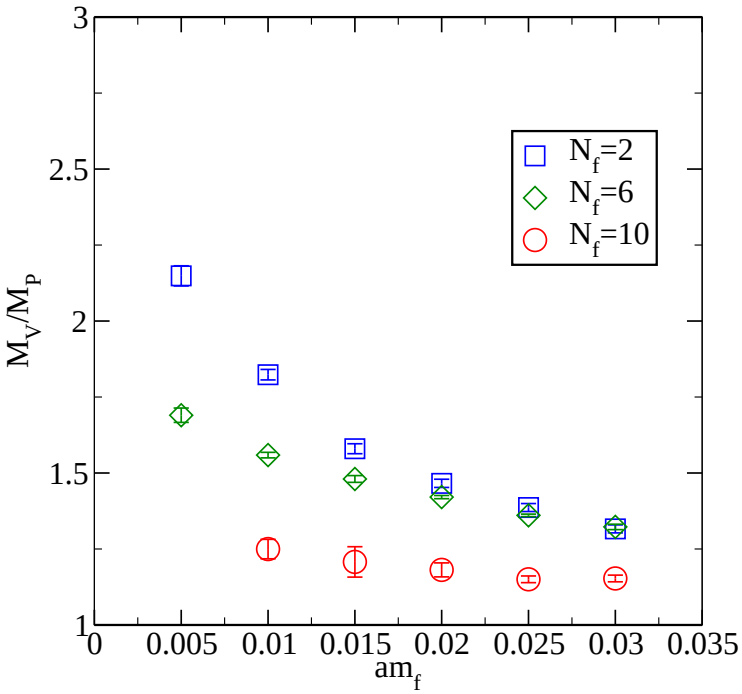

- The $N_f = 2$ data are diverging as $m \to 0$, as expected since $M_P \to 0$.
- Similaryly for $N_f = 6$, though not as fast as $N_f = 2$.
- For $N_f = 10$ the ratios seem to be roughly constant.

New: Results for $N_f = 10$

Testing Conformality - Quantitatively

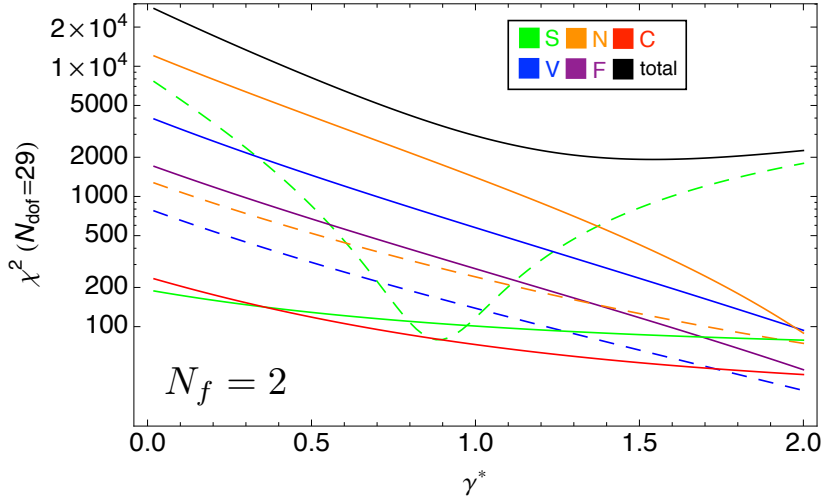

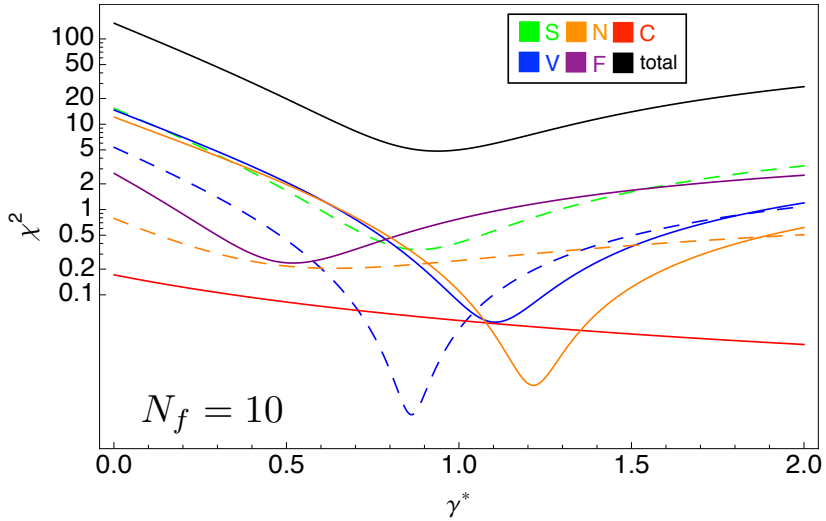

Obs.	$m_f \geq 0.010$	$m_f \geq 0.015$	$m_f \geq 0.020$
$\gamma^\star$	*1.45(15)*	0.94(16)	1.18(44)
[68% CI]	*[0.88,2.47]*	[0.68,1.44]	[1.01,1.69]
C_P	*0.978(9)*	1.44(21)	1.21(42)
C_V	*1.168(10)*	1.70(25)	1.42(49)
C_A	*1.429(13)*	2.14(32)	1.79(63)
C_N	*1.749(16)*	2.53(37)	2.10(73)
$C_{N^\star}$	*2.232(25)*	3.35(56)	2.87(1.02)
C_{FP}	*0.121(12)*	0.190(29)	0.164(57)
χ^2/d.o.f.	*69/31*	14/23	3/15

Finite volume effects may be large for $am_f \leq 0.01$.

Summary

- First SU(3) lattice simulations with $N_f = 6$ and 10 domain wall fermions have been performed.
- Hints of condensate enhancement and reduced S paramter have been seen with $N_f = 6$.
- With increasing N_f, the topology becomes more difficult to evolve. Effects of fixed topology are big for $N_f = 10$.
- Spectrum for $N_f = 10$ is consistent with conformality. But cannot rule out the chirally-broken scenario, as the masses are too heavy to make use of ChPT.

Future Work

- Calculate topological susceptibility at fixed Q for $N_f = 10$.
  S. Aoki *et al.*, 2007, 2008
- Quantative studies of finite volume effects
- Smaller quark masses

Progress with Overlap Fermions

- Overlap on 2+1 flavor DWF configurations with deflation and low-mode sustituion ⟹ quark loops with LMA
- Improvement of nucleon correlator
- Strangeness content in nucleon and other FF
- Glue momentum and angulalr momentum in nucleon
- Roper resonance with wall source

χQCD Collaboration:
A. Alexandru, Y. Chen, M. Deka, T. Doi, S.J. Dong, T. Draper, M. Gong, I. Horvath, B. Joo, F. Lee, A. Li, H.W. Lin, K.F. Liu, N. Mathur, H. Thacker, Y. Yang, J.B. Zhang

http://eagle.phys.gwu.edu/~fxlee/chiQCD.html

New Horizons for Lattice Calculations with Chiral Fermions, BNL, May 14-16, 2012

Overlap on 2+1 Flavor DWF configurations with HYP Smearing

- Mixed action
- For chirally symmetric valence, it is a generalization of partial quenching with one extra low-energy constant in valence-sea mass

$$m^2_{v_1 v_2} = B_{ov}(m_{v_1} + m_{v_2}),$$

$$m^2_{vs} = B_{ov} m_v + B_{dw}(m_s + m_{res}) + a^2 \Delta_{mix},$$

$$m^2_{s_1 s_2} = B_{dw}(m_{s_1} + m_{s_2} + 2m_{res}),$$

$$\Delta_{mix} = 0.030(6)(5)\ \mathrm{GeV}^4$$

M. Lujan et al., 1204.6256

- Mixed action partially quenched chiral PT at NLO

2+1 flavor DWF configurations (RBC-UKQCD)

La ~ 2.8 fm
m_π ~ 330 MeV

24^3 x 32, a =0.115 fm

($O(a^2)$ extrapolation)

La ~ 2.7 fm
m_π ~ 295 MeV

32^3 x 64, a =0.085 fm

DSDR

La ~ 4.5 fm
m_π ~ 180 MeV

32^3 x 64, a =0.12 fm

Some Desirable Features of Overlap

- Calculating eigenmodes is relatively easy

.

- Normality ($D^\dagger D = DD^\dagger$) and GW relation

→ Eigenvalues are on a unit circle and
λ = 0, 2 are chiral modes.
The rest are complex pairs.

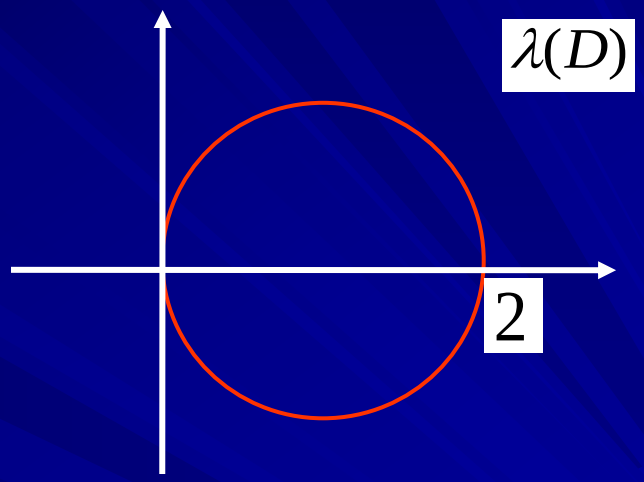

- Normality and $[\gamma_5, D^\dagger D] = 0$

$$\Rightarrow D^\dagger D \varphi_{L,R} = |\lambda|^2 \varphi_{L,R};$$

$$\text{Diagonalize } \langle \varphi_{L,R} | D | \varphi_{L,R} \rangle \Rightarrow D\psi = \lambda\psi$$

Overlap with Deflation (multimass with same eigenvectors)

$$D(m,\rho)X^{H}_{L,R} = \eta_{L,R} - \sum_{i=1}^{n}(1\mp\gamma_5)\,|\,i\rangle\langle i\,|\,\eta_{L,R}\rangle$$

where,

$$D(0,\rho)\,|\,i\rangle = \lambda_i\,|\,i\rangle; \quad D(0,\rho)\gamma_5\,|\,i\rangle = \lambda_i^{*}\gamma_5\,|\,i\rangle$$

Therefore,

$$X^{H}_{L,R} = D^{-1}(m,\rho)\eta_{L,R} - X^{L}_{L,R}$$

where,

$$X^{L}_{L,R} = \sum_{i=1}^{n}\left[\frac{|\,i\rangle\langle i\,|\,\eta_{L,R}\rangle}{\rho\lambda_i + m(1-\lambda_i/2)} \mp \frac{\gamma_5\,|\,i\rangle\langle i\,|\,\eta_{L,R}\rangle}{\rho\lambda_i^{*} + m(1-\lambda_i^{*}/2)}\right]$$

and

$$X = (X^{H}_{L} + X^{H}_{R}) + (X^{L}_{L} + X^{L}_{R})$$ except for the zero modes.

Speedup with deflation and HYP smearing

		16^3 x 32			24^3 x 64			32^3 x 64		
	res	w/o D	D	D+S	w/o D	D	D+S	w/o D	D	D+S
Low mode	10^{-8}	0	200	200	0	200	200	0	400	400
Inner iter	10^{-11}	340	321	108	344	341	107	309	281	101
Outer iter	10^{-8}	627	72	85	2931	147	184	4028	132	156
Speedup				23			51			79
Overhead				5 prop			5 prop			8 prop

$$D(0,\rho) = 1 + \gamma_5 \varepsilon = 1 + \gamma_5 \frac{H_W(\rho)}{\sqrt{H_W{}^2(\rho)}} \approx 1 + \gamma_5 H_W \sum_{i=1}^{n} \frac{b_i}{H_W^2 + c_i}$$

- No critical slowing down
- Multii-mass inversion (30 masses)

A. Li, et al, PRD 82, 114501 (2010)

Z_3 grid (64) source with low-mode substitution

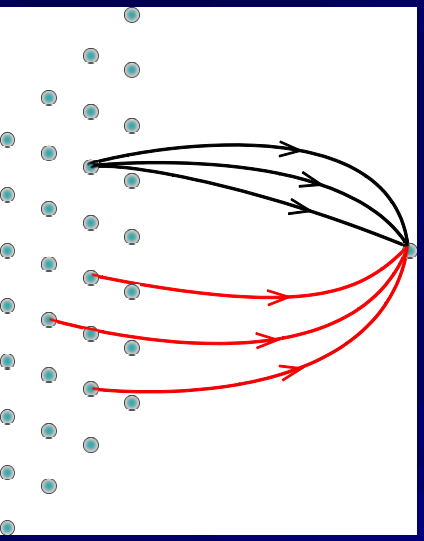

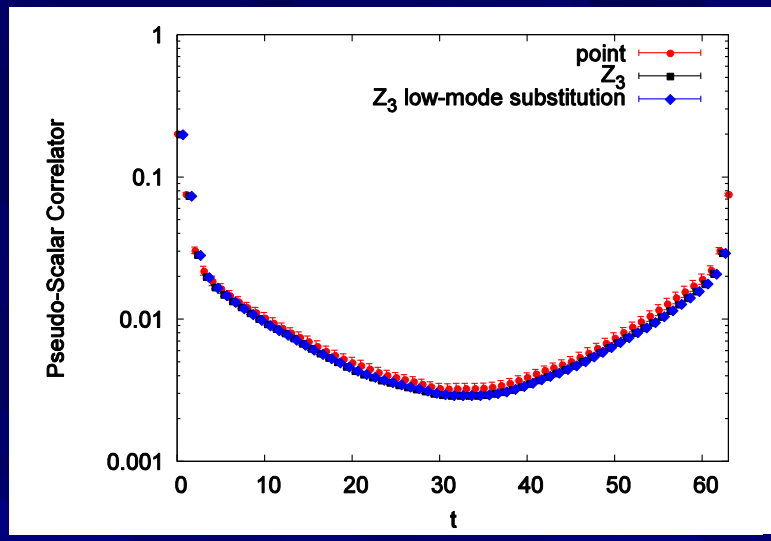

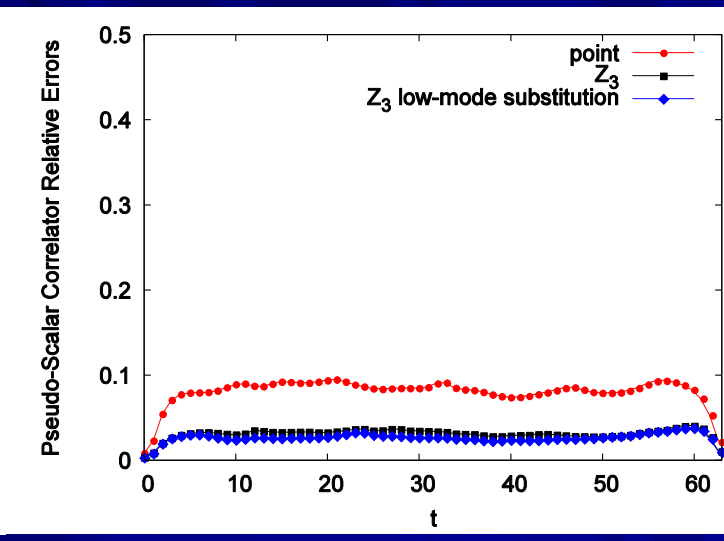

$32^3 \times 64$ lattice, m_l (sea)= 0.004 at $m_\Pi \sim 200$ MeV, 50 conf.

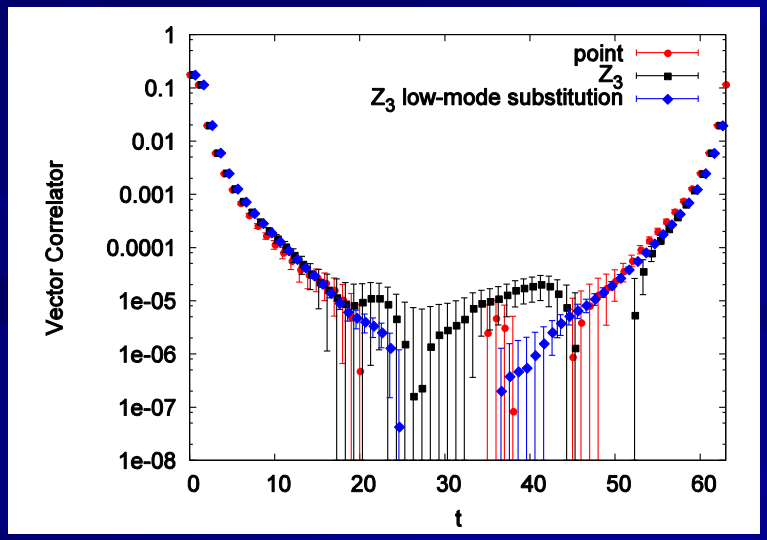

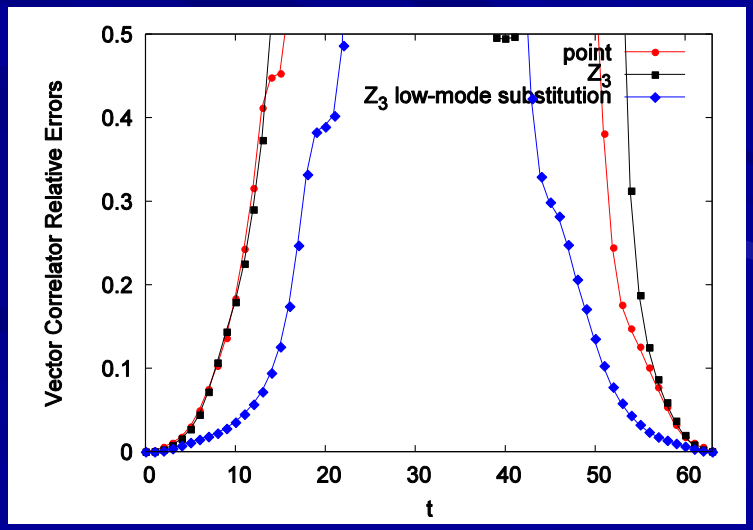

Nucleon with LLL and HLL substitution

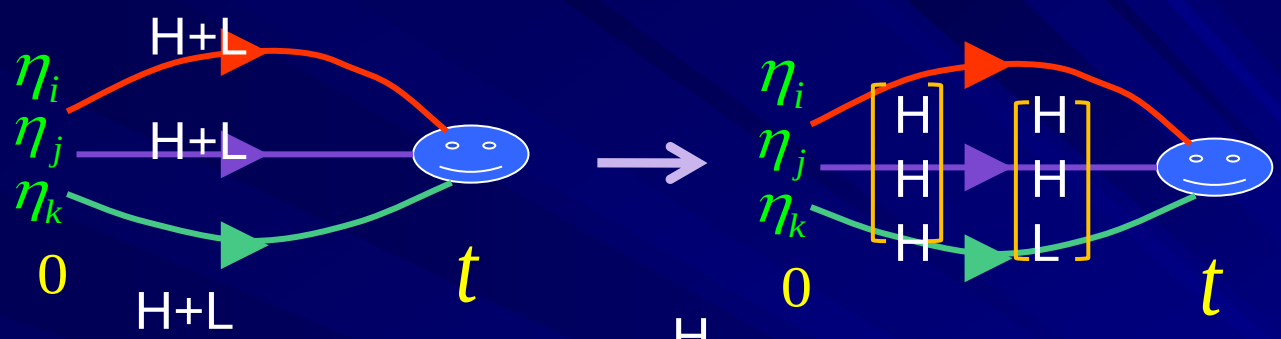

$$\frac{C_N(t)}{\sigma_N(t)} \approx \sqrt{\frac{n}{V_3}}\, e^{-(m_N - 3/2 m_\pi)t}$$

$$\langle \eta_i \eta_j \eta_k \rangle = \delta_{ij}\delta_{jk}$$

$$\langle \eta_i^\dagger \eta_j \rangle = \delta_{ij}$$

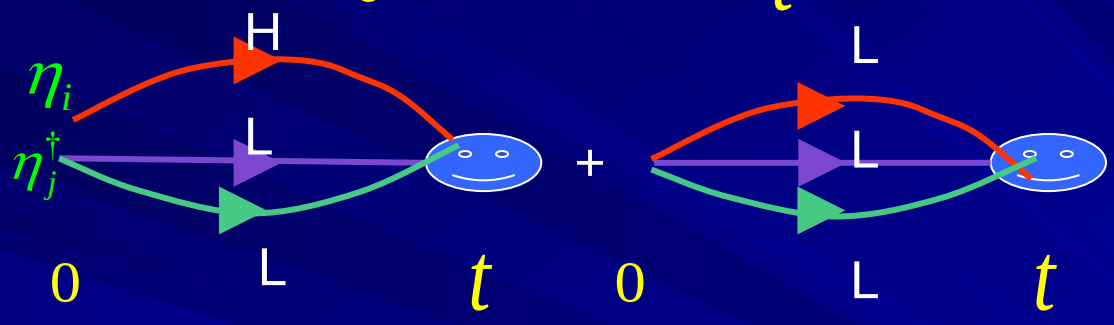

m_π ~ 300 MeV

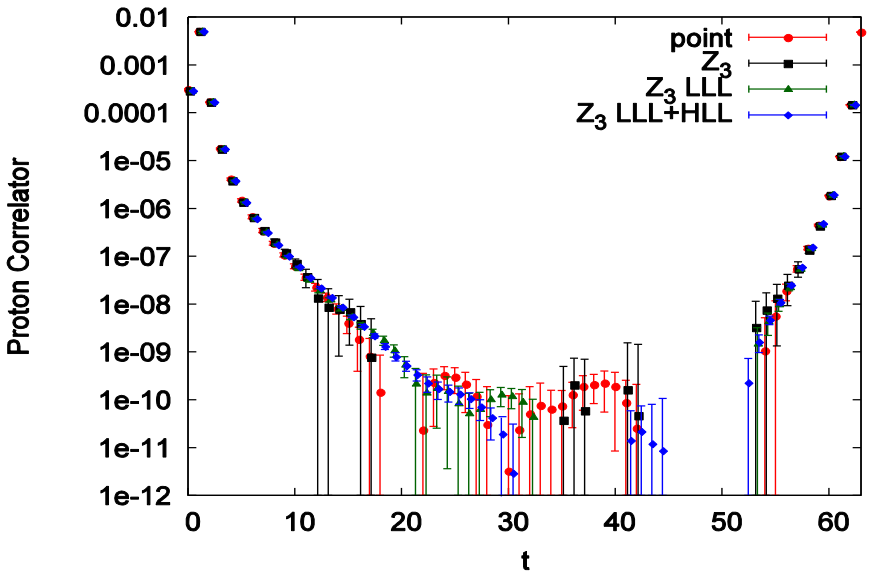

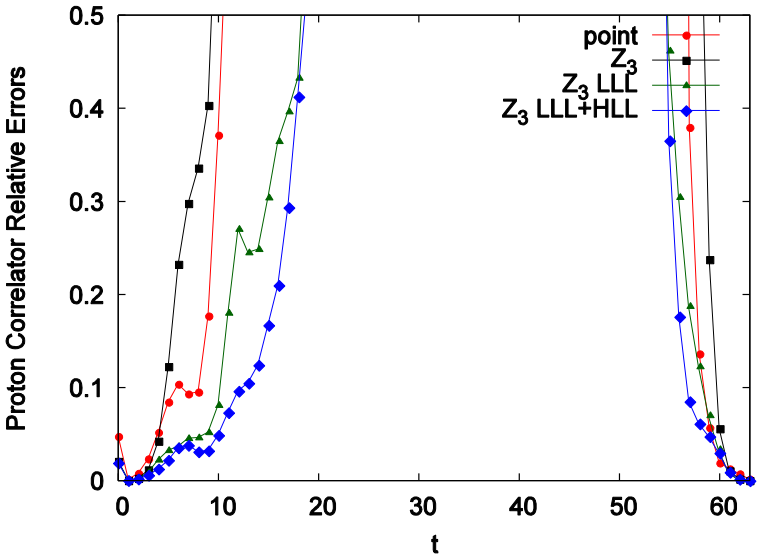

Hadron Structure with Quarks and Glue

- Quark and Glue Momentum and Angular Momentum in the Nucleon

$$(\bar{u}\gamma_\mu D_\nu u + \bar{d}\gamma_\mu D_\nu d)(t)$$

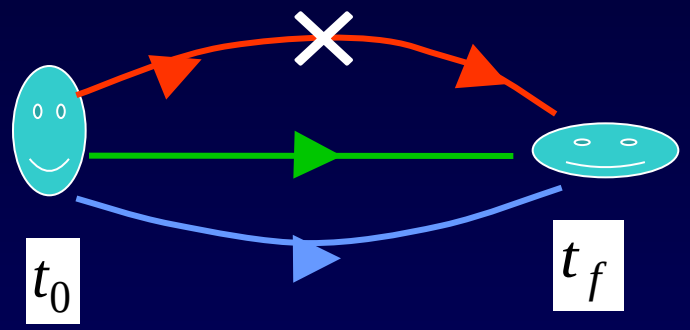

$$\bar{\Psi}\gamma_\mu D_\nu \Psi(t)(u,d,s)$$

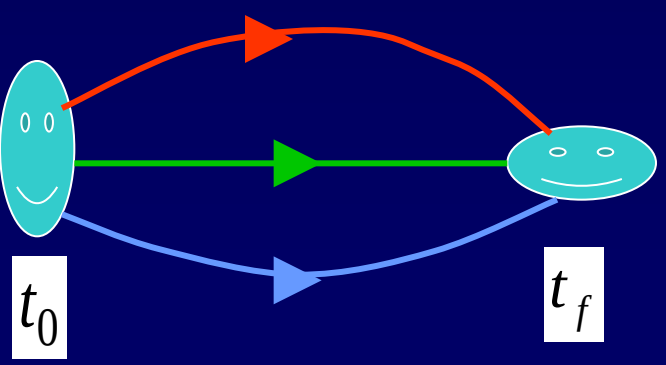

$$F_{\mu\alpha}F_{\nu\alpha} - \frac{1}{4}\delta_{\mu\nu}F^2$$

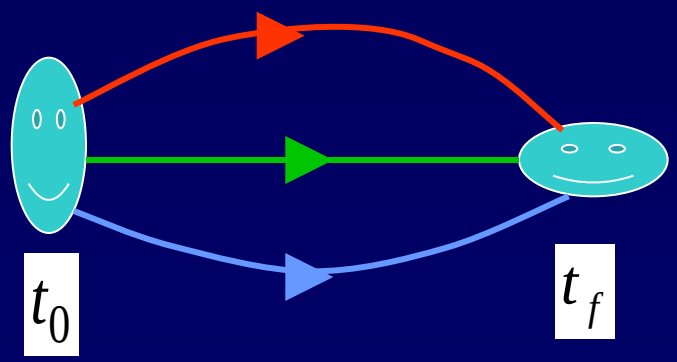

Status of Projects in Progress

- Charmonium and D_s spetra, f_D, f_{Ds}, are under global analysis with three sea masses and two lattice spacings.

- Improvement of nucleon correlator with low-mode substitution

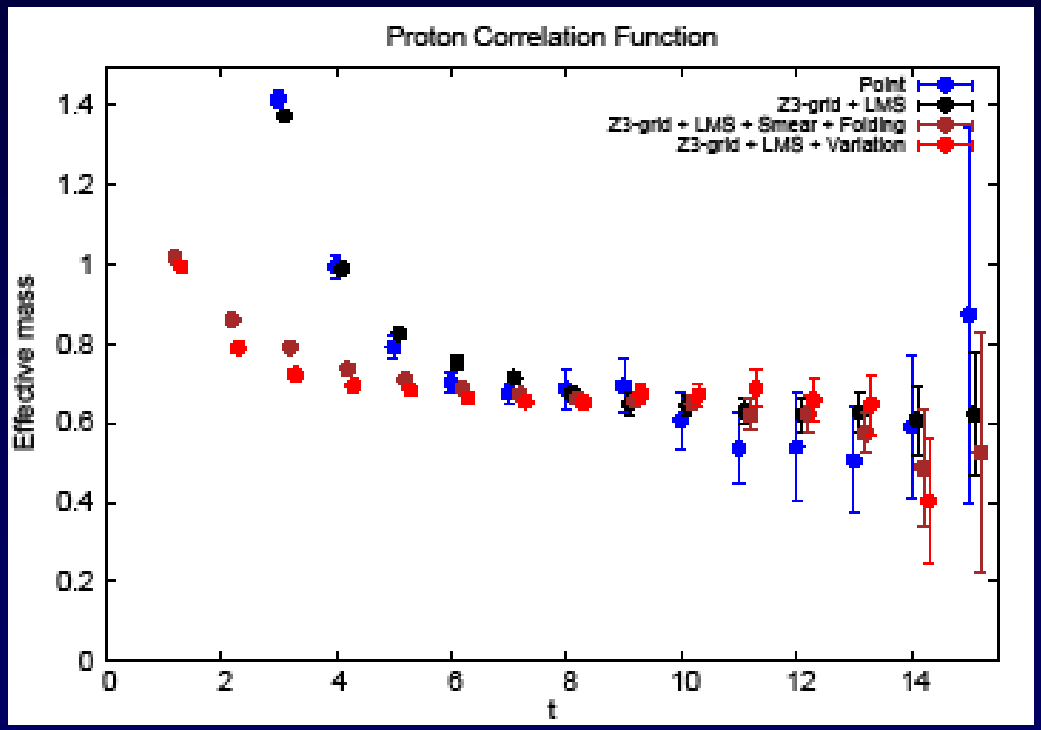

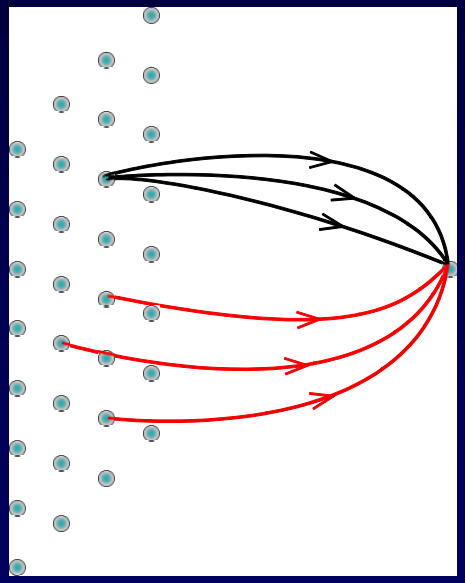

$24^3 \times 64$ lattice with $m_\pi = 331$ MeV, a = 1.73 GeV^{-1}

47 configurations

Point source: $m_N = 1.13(14)$ GeV;

Z_3 grid source: $m_N = 1.08(5)$ GeV;

Z_3 grid smeared source: $m_N = 1.14(2)$ GeV;

Variation: $m_N = 1.16(1)$ GeV

- Quark loop with low-mode averaging and Z_4 noise estimate of high modes with grids and time dilution

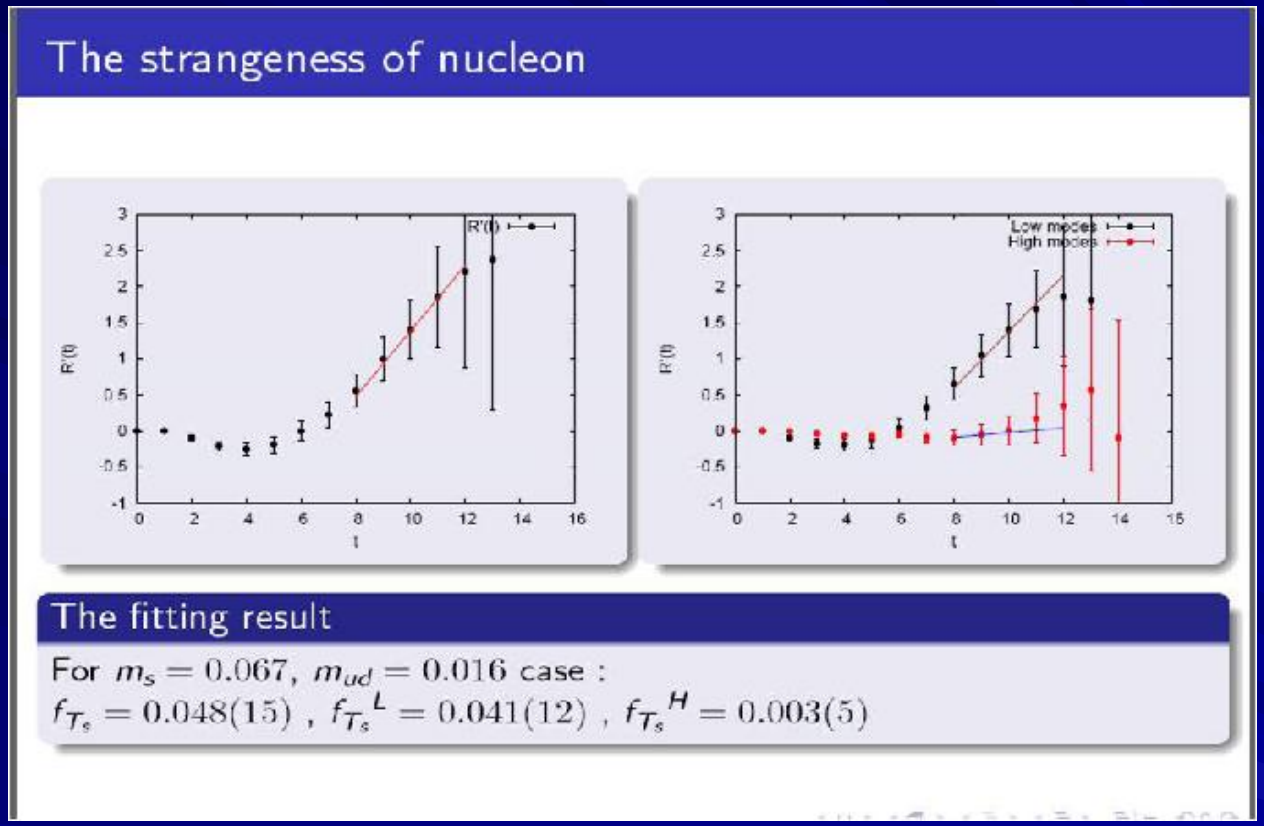

M. Gong
Lattice 2011

$$\text{constant} + m_s < N | \bar{s}s | N > t$$

$24^3 \times 64$, $m_l = 0.005$, $m_s = 0.04$, 50 conf. → 25 - 30% error

$\langle \bar{\Psi}\Psi \rangle$ on different time slices

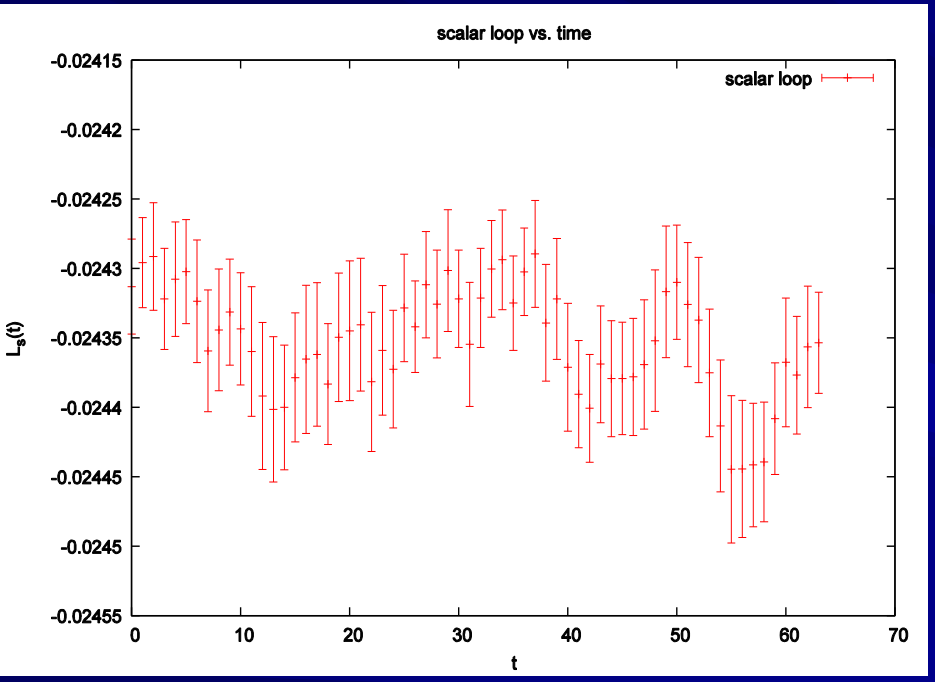

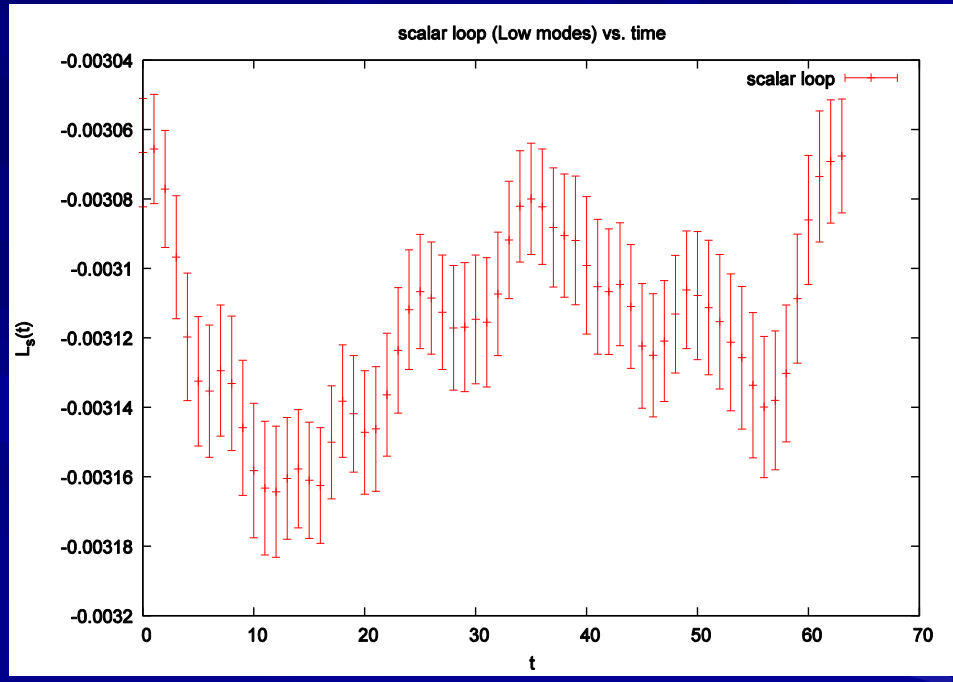

50 configurations: Low+High modes

150 configurations: Low modes only

Momenta and Angular Momenta of Quarks and Glue

- Energy momentum tensor operators decomposed in quark and glue parts gauge invariantly --- Xiangdong Ji (1997)

$$T^q_{\mu\nu} = \frac{i}{4}\left[\bar{\psi}\gamma_\mu \overleftrightarrow{D}_\nu \psi + (\mu \leftrightarrow \nu)\right] \rightarrow \vec{J}_q = \int d^3x \left[\frac{1}{2}\bar{\psi}\vec{\gamma}\gamma_5\psi + \vec{x}\times\bar{\psi}\gamma_4(-i\vec{D})\psi\right]$$

$$T^g_{\mu\nu} = F_{\mu\lambda}F_{\lambda\nu} - \frac{1}{4}\delta_{\mu\nu}F^2 \qquad \rightarrow \vec{J}_g = \int d^3x \left[\vec{x}\times(\vec{E}\times\vec{B})\right]$$

- Nucleon form factors

$$\langle p,s|T_{\mu\nu}|p's'\rangle = \bar{u}(p,s)[T_1(q^2)\gamma_\mu \bar{p}_\nu - T_2(q^2)\bar{p}_\mu \sigma_{\nu\alpha}q_\alpha / 2m$$

$$-iT_3(q^2)(q_\mu q_\nu - \delta_{\mu\nu}q^2)/m + T_4(q^2)\delta_{\mu\nu}m/2]u(p's')$$

- Momentum and Angular Momentum

$$Z_{q,g}T_1(0)_{q,g}\ [\mathrm{OPE}] \rightarrow \langle x\rangle_{q/g}(\mu,\overline{\mathrm{MS}}),\quad Z_{q,g}\left[\frac{T_1(0)+T_2(0)}{2}\right]_{q,g} \rightarrow J_{q/g}(\mu,\overline{\mathrm{MS}})$$

$T_1(q^2)$ and $T_2(q^2)$

- 3-pt to 2-pt function ratios

$$G^{3pt}_{\mu\nu}(\vec{p},t_2;\vec{q},t_1) = \sum_{\vec{x}_1,\vec{x}_2} e^{-i\vec{p}\cdot\vec{x}_2 + i\vec{q}\cdot\vec{x}_1} \left\langle 0 \left| T\left[\chi_N(\vec{x}_2,t_2) T_{\mu\nu} \bar{\chi}_N(0)\right]\right.\right\rangle;$$

$$\mathrm{Tr}\left[\Gamma_m G^{3pt}_{\mu\nu}(\vec{p}=0,t_2;\vec{q},t_1)\right] = W e^{-m(t_2-t_1)} e^{-Et_1}\left[T_1(q^2)+T_2(q^2)\right]$$

- Need both polarized and unpolarized nucleon and different kinematics (p_i, q_j, s) to separate out $T_1(q^2)$, $T_2(q^2)$ and $T_3(q^2)$

Status of Proton Spin

- Quark spin $\Delta\Sigma \sim 20 - 30\%$ of proton spin (DIS, Lattice)
- Quark orbital angular momentum? (lattice calculation (LHPC,QCDSF)→ ~ 0)
- Glue spin $\Delta G/G$ small (COMPASS, STAR) ?
- Glue orbital angular momentum is small (Brodsky and Gardner) ?

→ Dark Spin ?

- Field strength tensor from overlap operator

$$\mathbf{tr}_s \sigma_{\mu\nu} a D_{ov}(x,x) = c^T a^2 F_{\mu\nu} + O(a^3),$$

$$c^T = \rho \int_{-\pi}^{\pi} \frac{d^4k}{(2\pi)^4} \frac{2\left[(\rho + r\sum_\lambda (c_\lambda - 1))c_\mu c_\nu + 2rc_\mu s_\nu^2\right]}{(\sum_\mu s_\mu^2 + [\rho + \sum_\nu (c_\nu - 1)]^2)^{3/2}}$$

where, $r = 1, \quad \rho = 1.368, \quad c^T = 0.11157$

Liu, Alexandru, Horvath – PLB 659, 773 (2007)

- Noise estimation $D_{ov}(x,x) \to \left\langle \eta_x^\dagger (D_{ov}\eta)_x \right\rangle$
  with Z_4 noise with color-spin dilution and some dilution in space-time as well.

- Quark and Glue momenta and angular momenta in the nucleon (quenched approximation)

Disconnected Insertions of T_1 (q^2) and T_2 (q^2) for u/d Quarks

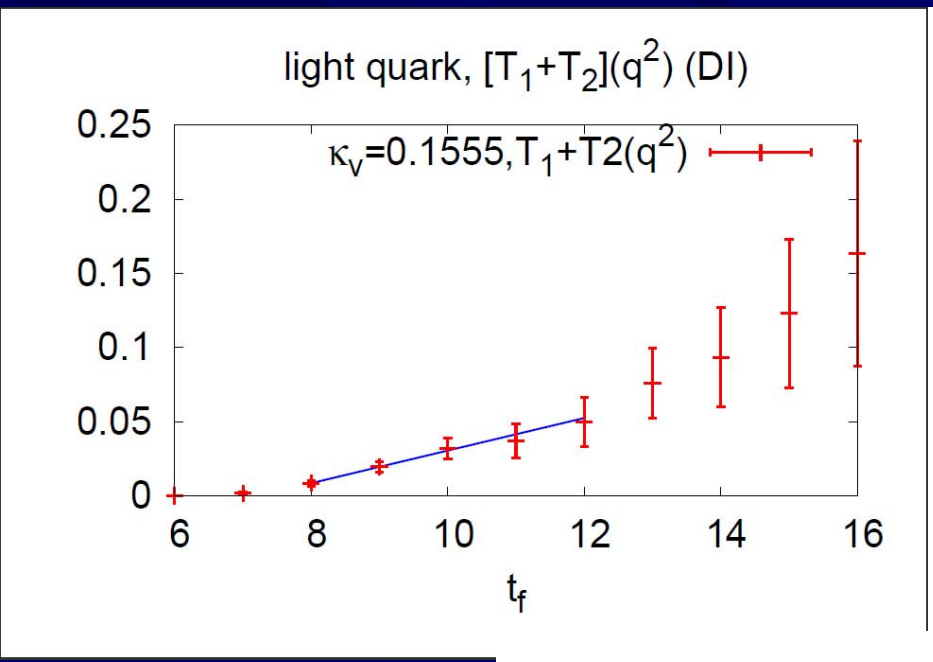

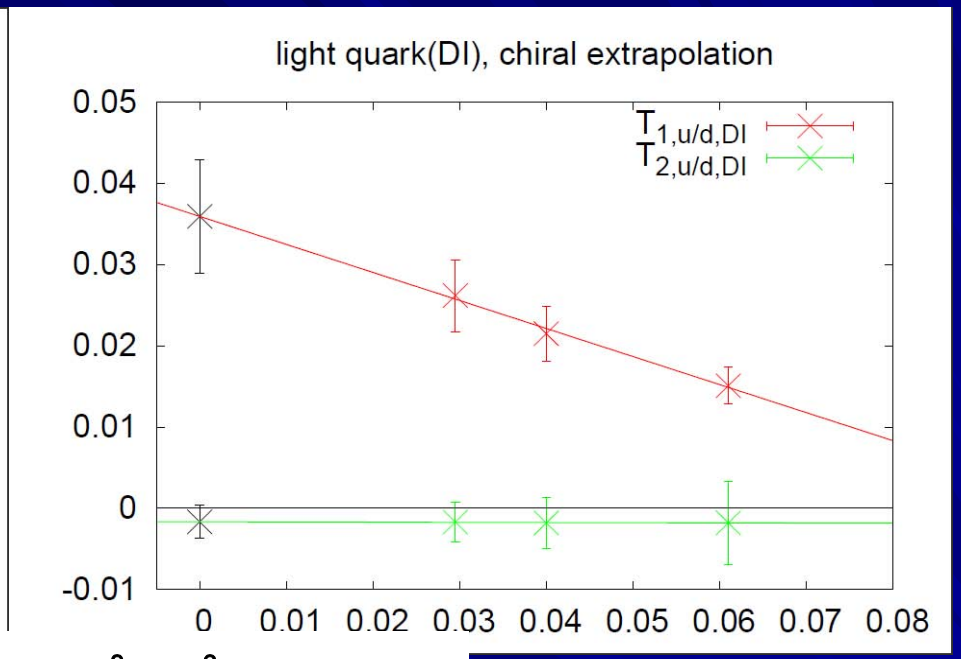

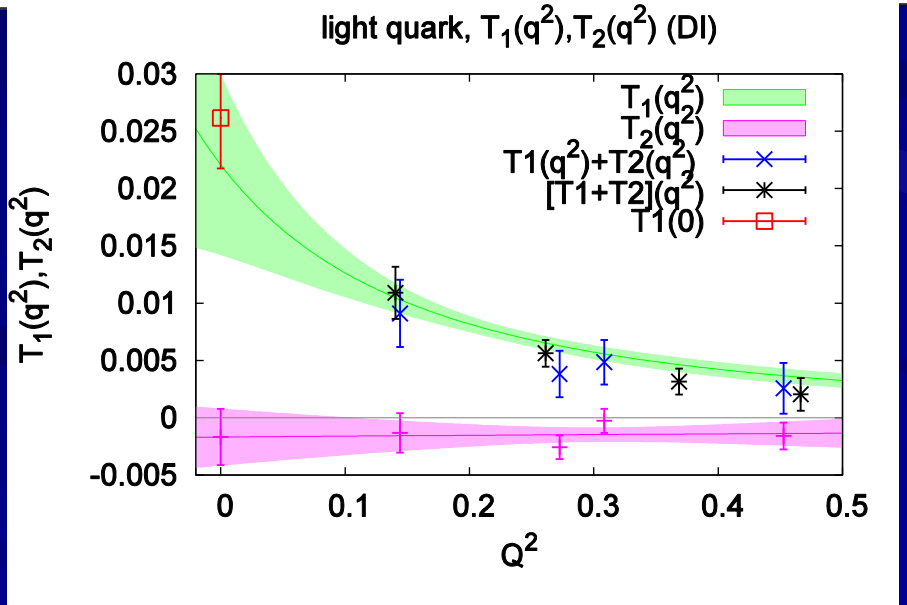

Glue $T_1(q^2)$ and $T_2(q^2)$

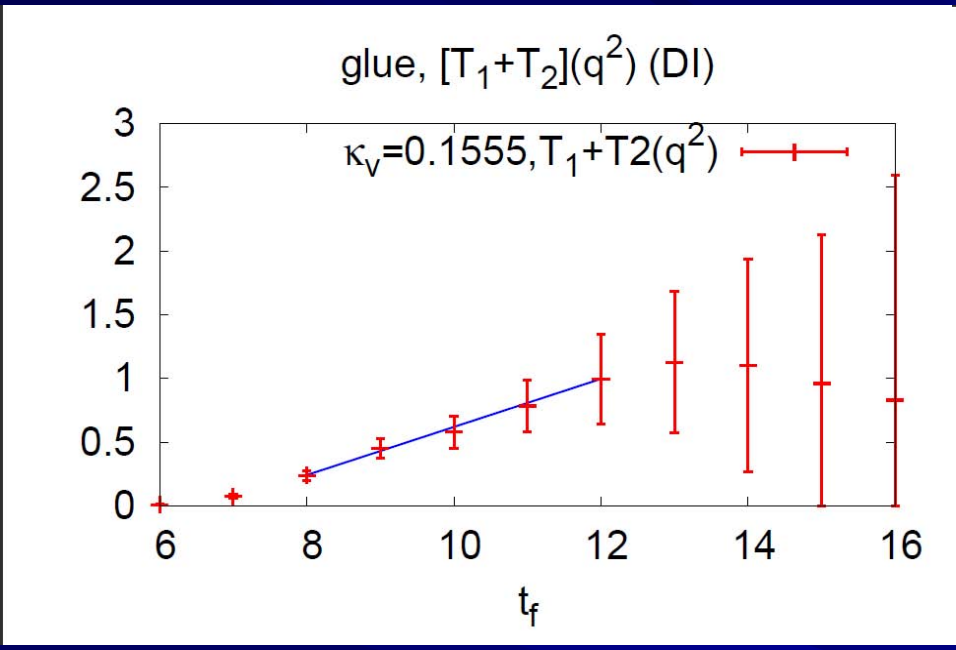

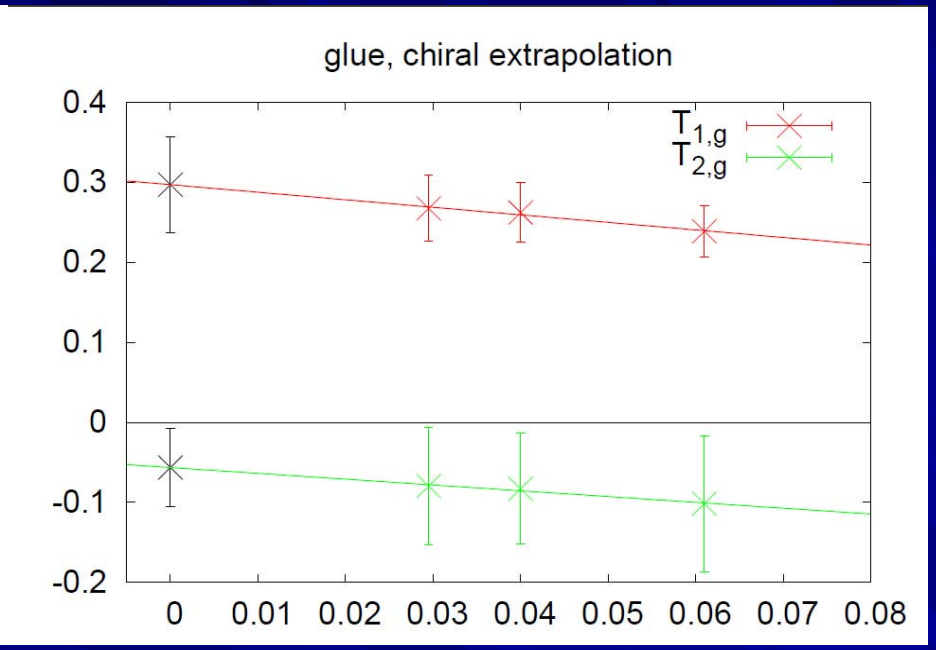

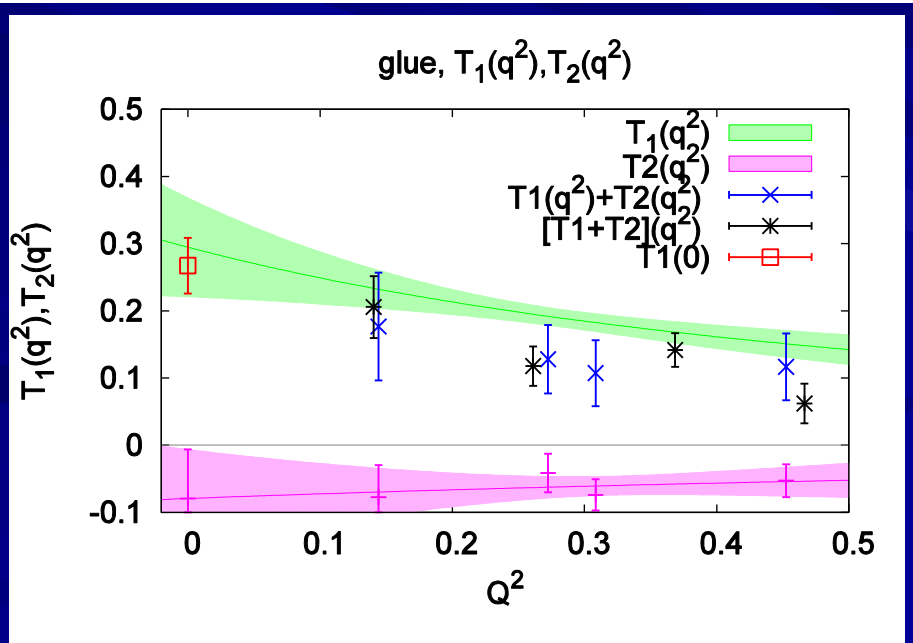

Renormalization and Quark-Glue Mixing

Momentum and Angular Momentum Sum Rules

$$\langle x\rangle_q^R = Z_q \langle x\rangle_q^L, \quad \langle x\rangle_g^R = Z_g \langle x\rangle_g^L,$$

$$J_q^R = Z_q J_q^L, \quad J_g^R = Z_g J_g^L,$$

$$Z_q \langle x\rangle_q^L + Z_g \langle x\rangle_g^L = 1,$$

$$Z_q J_q^L + Z_g J_g^L = \frac{1}{2}$$

$$\Rightarrow \begin{cases} Z_q T_1^q(0) + Z_g T_1^g(0) = 1, \\ Z_q (T_1^q + T_2^q)(0) + Z_g (T_1^g + T_2^g)(0) = 1, \\ Z_q T_2^q(0) + Z_g T_2^g(0) = 0 \end{cases}$$

Matching and Mixing

$$\begin{bmatrix} \langle x\rangle_q^{\overline{MS}}(\mu) \\ \langle x\rangle_g^{\overline{MS}}(\mu) \end{bmatrix} = \begin{bmatrix} C_{qq}(\mu) & C_{qg}(\mu) \\ C_{gq}(\mu) & C_{gg}(\mu) \end{bmatrix} \begin{bmatrix} \langle x\rangle_q^R \\ \langle x\rangle_g^R \end{bmatrix}$$

M. Glatzmaier

Renormalized results: $Z_q = 1.05$, $Z_g = 1.05$

	CI(u)	CI(d)	CI(u+d)	DI(u/d)	DI(s)	Glue
<x>	0.428 (40)	0.156 (20)	0.586 (45)	0.038 (6)	0.024 (6)	0.313 (56)
$T_2(0)$	0.297 (112)	-.218 (80)	0.064 (22)	-0.002 (2)	-.001 (3)	-.059 (52)
2J	0.726 (128)	-.072 (82)	0.651 (51)	0.036 (7)	0.023 (7)	0.254 (76)

$$T_2(0)_{CI} + T_2(0)_{DI} + T_2(0)_g = 0.002(56)$$

S. Brodsky et al. NPB 593, 311(2001) → no anomalous gravitomagnetic moment

E. Leader, arXiv:1109.1230 → transverse angular momentum

Renormalized results:

K.F. Liu et al., 1203.6388

	CI(u)	CI(d)	CI(u+d)	DI(u/d)	DI(s)	Glue
2J	0.726 (128)	-.072 (82)	0.651 (51)	0.036 (7)	0.023 (7)	0.254 (76)
g_A	0.95 (11)	-0.32 (12)	0.65 (8)	-0.12 (1)	-0.12 (1)	
2 L	-0.25 (18)	0.26 (14)	0.00 (10)	0.17 (2)	0.15 (2)	

Quark Spin, Orbital Angular Momentum, and Gule Angular Momentum

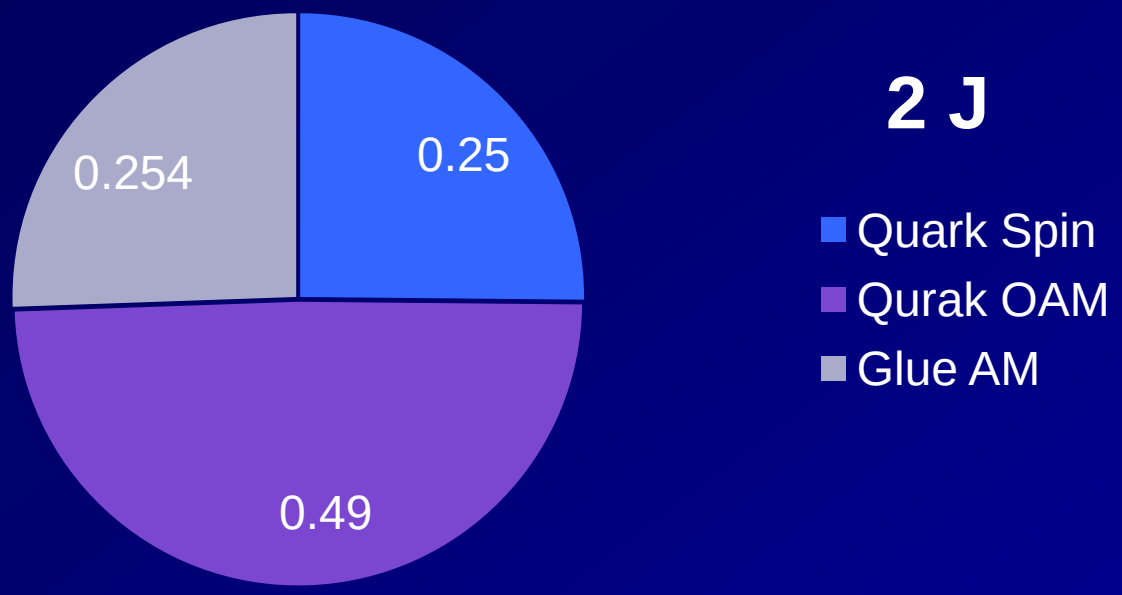

$$\Delta q \approx 0.25;$$

$$2\ L_q \approx 0.49\ (0.0(\mathrm{CI})+0.49(\mathrm{DI}));$$

$$2\ \mathrm{J}_g \approx 0.25$$

Glozman and Riska Challenge Phys. Rep. 268, 263 (1996)

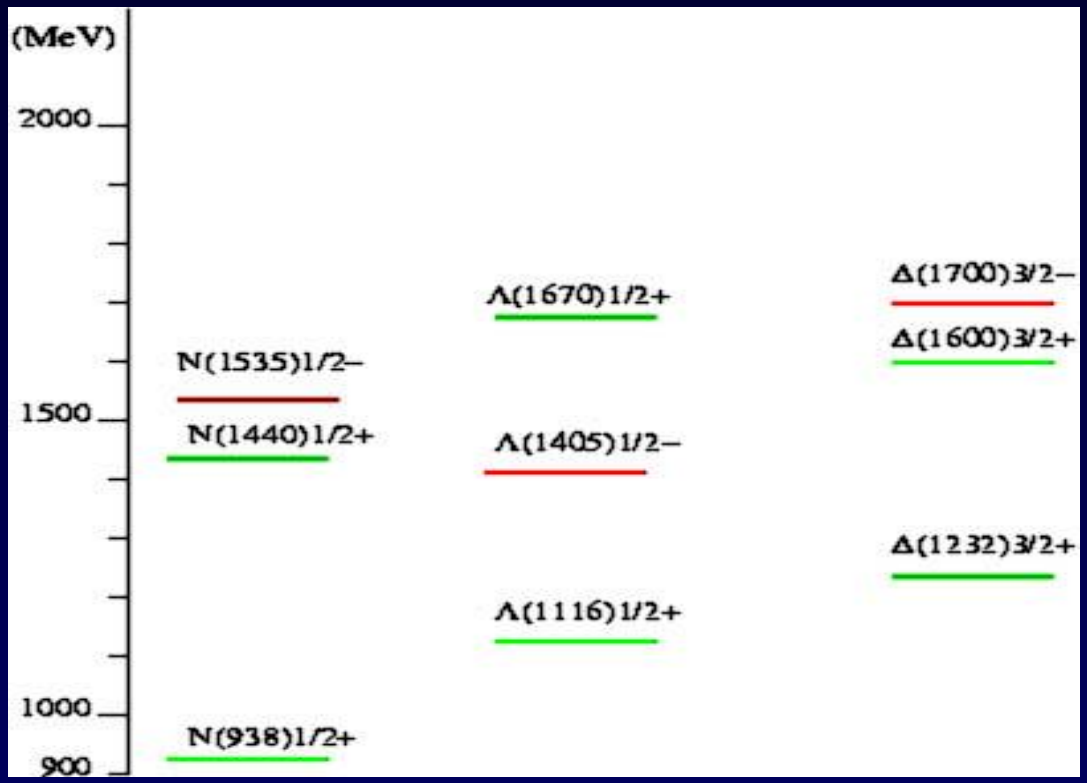

Hyperfine Interaction of Quarks in Baryons

- Color-spin

$$\lambda_1^C \bullet \lambda_2^C \; \vec{\sigma}_1 \bullet \vec{\sigma}_2$$

- One-gluon exchange

- Flavor-spin

$$\lambda_1^F \bullet \lambda_2^F \; \vec{\sigma}_1 \bullet \vec{\sigma}_2$$

- Goldstone boson exchange

Quenched Roper Calculation

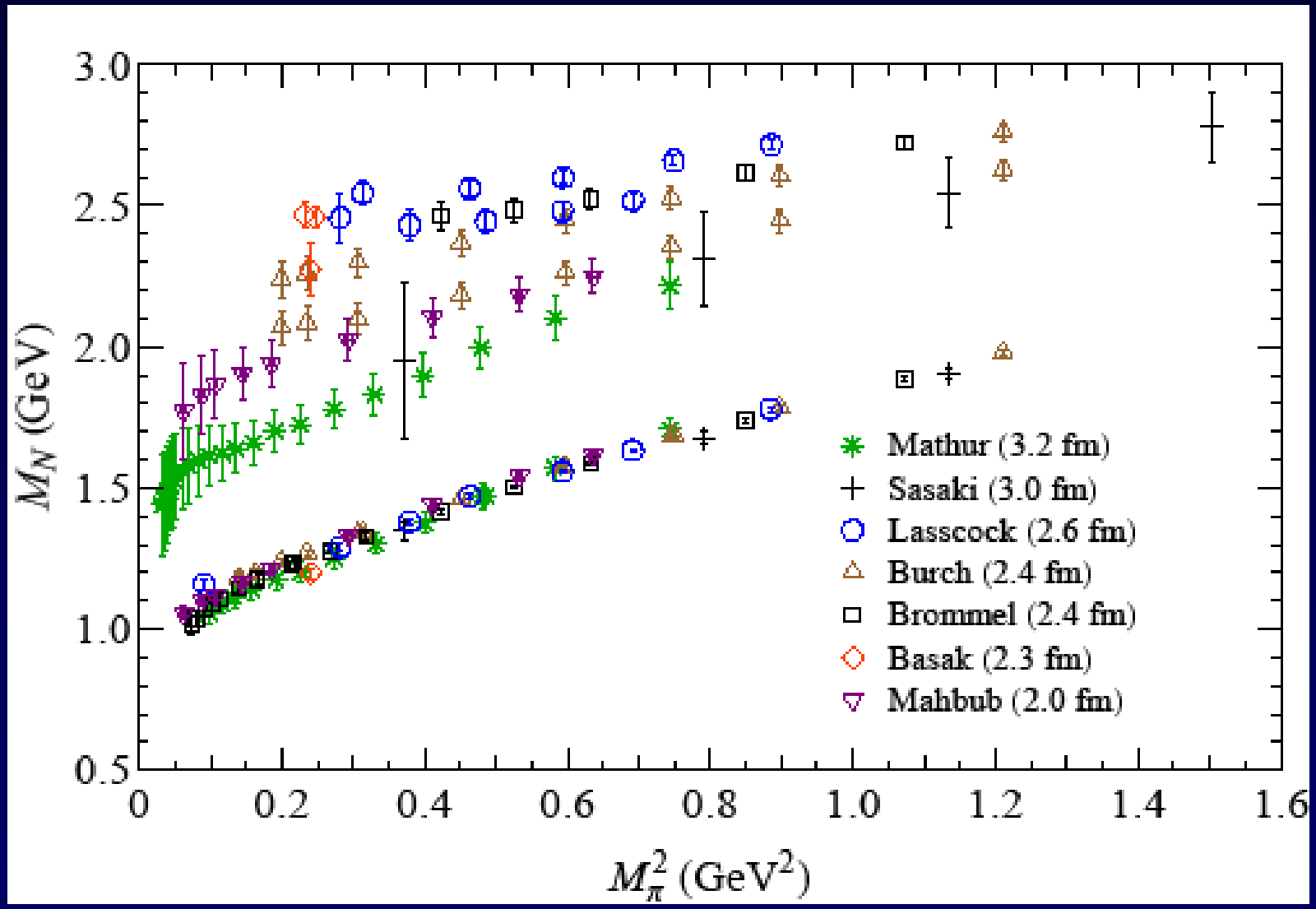

Status of Projects in Progress

- Charmonium and D_S spetra, f_D, f_{Ds}, are under global analysis with three sea masses and two lattice spacings.

- Improvement of nucleon correlator with low-mode substitution

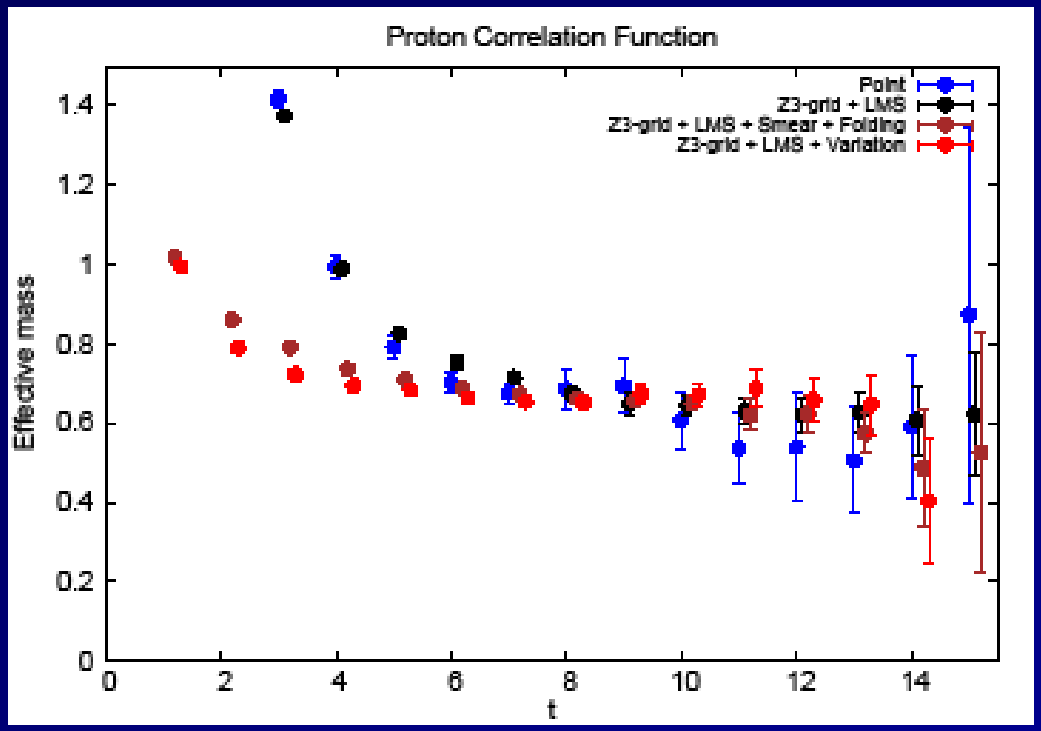

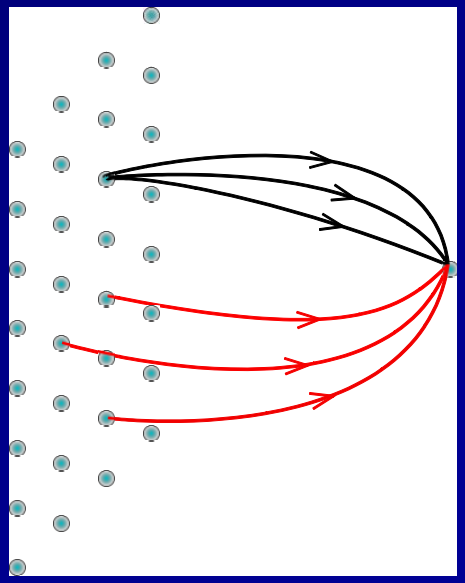

$24^3 \times 64$ lattice with $m_\pi = 331$ MeV, a = 1.73 GeV^{-1}

47 configurations

Point source: $m_N = 1.13(14)$ GeV;

Z_3 grid source: $m_N = 1.08(5)$ GeV;

Z_3 grid smeared source: $m_N = 1.14(2)$ GeV;

Variation: $m_N = 1.16(1)$ GeV

Roper resonance from Coulomb wall source

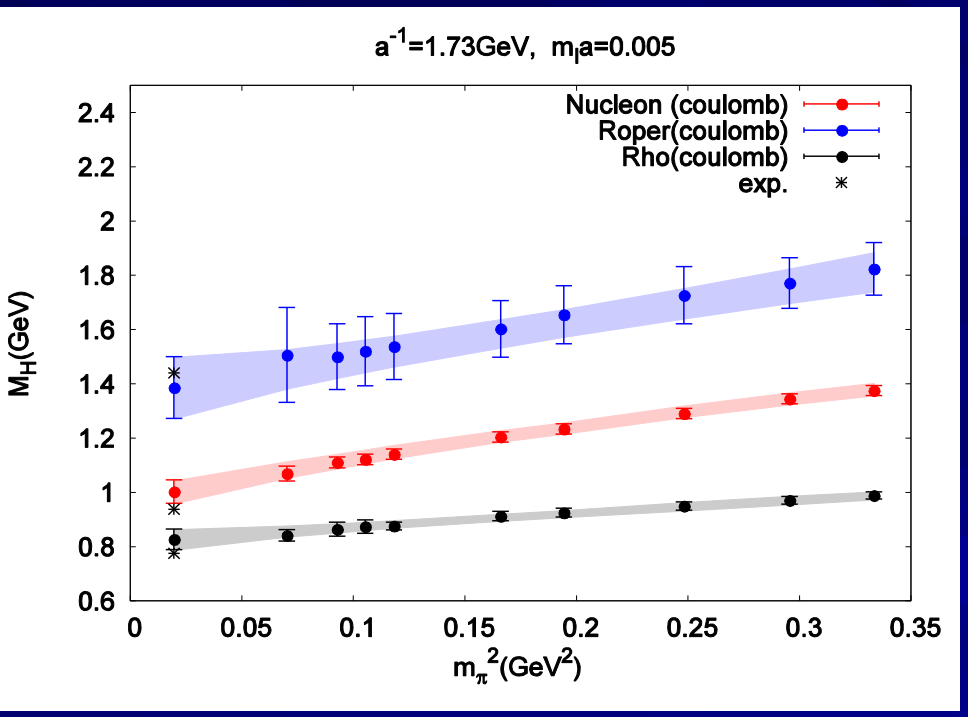

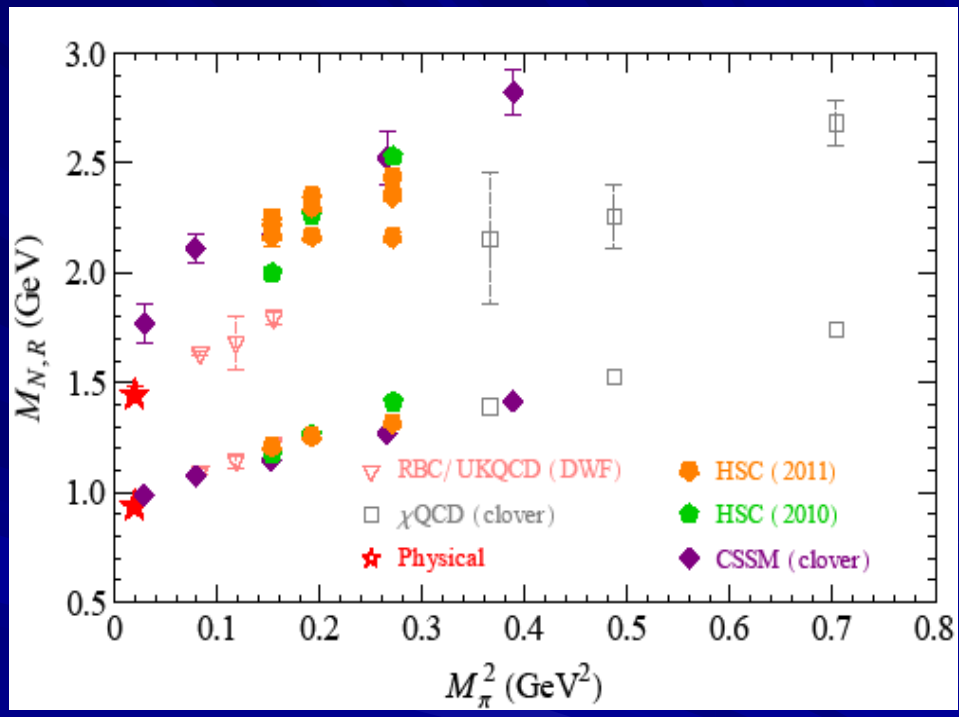

$$m_N = m_0 + c_1 m_\pi^2 + c_2 m_\pi^3 (\text{mixed}) + c_3 m_\pi^4 \ln(m_\pi^2 / \mu^2) + \ldots$$

$24^3 \times 64$ lattice with $m_\pi = 331$ MeV(sea), a = 1.73 GeV^{-1}

Vector meson effective mass from Coulomb wall source

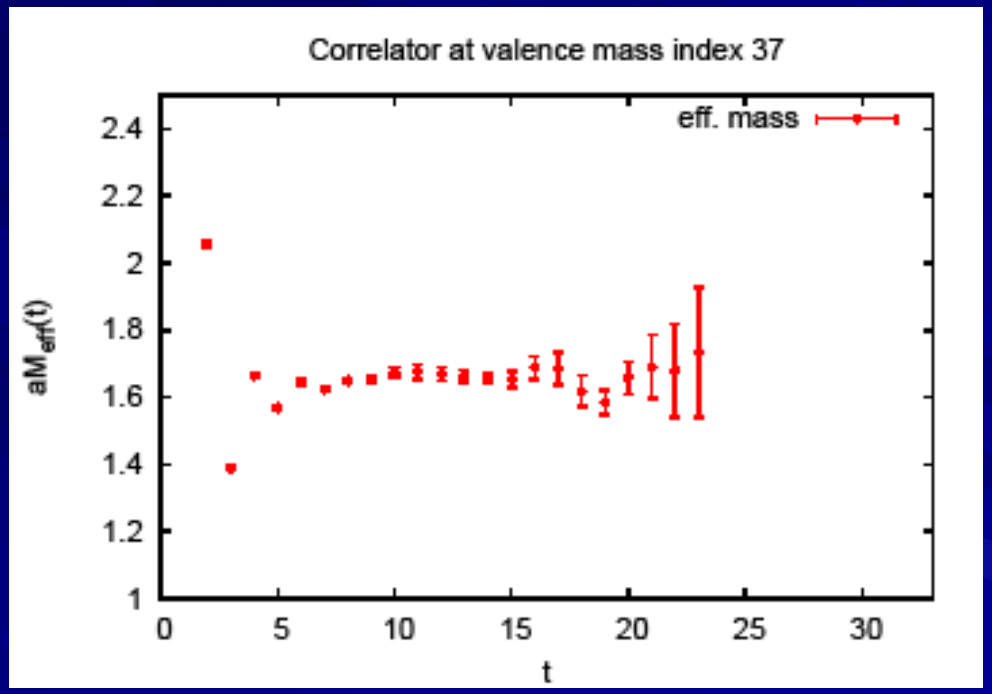

$$C(t) = \sum_n W_n e^{-m_n t} + (-)^t W e^{-Mt}$$

Summary of overlap on DWF config.

- ★ Good: same fermion for charm and light, eigenmodes, inversion with deflation and multimass, correlators with low-mode substitution, quark loop with low-mode averaging, glue field strength tensor.
- ★ Not so good: residual mass, oscillatory behavior at short time slices (DWF sea), not unitary (mixed action), auto-correlation.
- Can and should get better: precise approximation of the matrix sign function, reduced auto-correlation.

Gauge Operators from the Overlap Dirac Operator

- Overlap operator

$$D_{ov} = 1 + \gamma_5 \varepsilon(H); \;\; H = \gamma_5 D_W(m_0)$$

- Index theorem on the lattice (Hasenfratz, Laliena, Niedermayer, Lüscher)

$$\text{index } D_{ov} = -Tr\gamma_5 (1 - \frac{a}{2} D_{ov})$$

- Local version (Kikukawa & Yamada, Adams, Fujikawa, Suzuki)

$$q_L(x) = -tr\gamma_5 (1 - \frac{a}{2} D_{ov}(x,x)) \xrightarrow[a \to 0]{} a^4 q(x) + O(a^6)$$

- Study of topological structure of the vacuum
  - Sub-dimensional long range order of coherent charges (Horvàth et al; Thacker talk in Lattice 2006)
  - Negativity of the local topological charge correlator (Horvàth et al)

Some Desirable Features of Overlap

- Renormalization with chiral Ward identity
  - Light mesons

$$Z_A \partial_\mu A^3_\mu = 2 Z_S^{-1} m Z_P P \Rightarrow \quad f_\pi = \lim_{t \to a} 2m \sqrt{\frac{G_{PP}(\vec{p}=0,t)}{m_\pi^3}}\, e^{m_\pi t/2}$$

  - Heavy-light meson K.F. Liu and S.J. Dong, Int.J.Mod.Phys. A20 (2005) 7241

$$\tilde{Z}_A(m_1,m_2)\partial_\mu A_{\mu 12} = (\tilde{Z}_S^{-1}(m_1)m_1 + \tilde{Z}_S^{-1}(m_2)m_2)\tilde{Z}_P(m_1,m_2)P_{12}$$

    - Gellmann-Oaks-Renner relation

$$\frac{1}{V}\int d^4x \left\langle \pi_{12}^{a\dagger}(x)\pi_{12}^{a}(0)\right\rangle = \frac{-2\left[\left\langle \bar{\Psi}_1\Psi_1\right\rangle + \left\langle \bar{\Psi}_2\Psi_2\right\rangle\right]}{m_1+m_2} \quad \text{(renormalized and unrenormalized)}$$

$$\tilde{Z}_P(m_1,m_2) = \frac{\tilde{Z}_S(m_1)\left\langle \bar{\Psi}_1\Psi_1\right\rangle + \tilde{Z}_S(m_2)\left\langle \bar{\Psi}_2\Psi_2\right\rangle}{\left\langle \bar{\Psi}_1\Psi_1\right\rangle + \left\langle \bar{\Psi}_2\Psi_2\right\rangle}\,\frac{m_1+m_2}{\tilde{Z}_S^{-1}(m_1)m_1 + \tilde{Z}_S^{-1}(m_2)m_2}$$

Decaying Pseudoscalars from DWF LQCD

New Horizons for Lattice Computations with Chiral Fermions
Brookhaven National Laboratory
May 15, 2012

Robert Mawhinney
Columbia University

Generic Process	Examples	Experiment	LQCD calculates
$Kl2$	$K^+ \to \mu^+ \nu_\mu$ $K^+ \to e^+ \nu_e$	f_K	f_K
$Kl3$	$K^+ \to \pi^0\, l^+\, \nu_l$ $K^0 \to \pi^-\, l^+\, \nu_l$	$\lvert V_{us} f^+(0)\rvert^2$	$f^+(0)$
$Kl4$	$K \to \pi\, \pi\, l\, \bar{\nu}_l$		??
$K \to \pi\pi$ (CP conserving)	$K^0 \to \pi^+\, \pi^-$ $K^+ \to \pi^+\, \pi^0$	$\lvert A_0\rvert$ $\lvert A_2\rvert$	$\lvert A_0\rvert\ \lvert A_2\rvert$ (SM_{cpc} inputs)
Δm_K (CP conserving)	$K^0 \leftrightarrow \pi\, \pi \leftrightarrow \overline{K}^0$ (long distance physics) $K^0 \leftrightarrow O_{\Delta S=2} \leftrightarrow \overline{K}^0$ (short distance physics)	Δm_K	Δm_K (SM_{cpc} inputs)
$K^0 \to \pi\ \pi$ (indirect CP violation)	$K_L \to \pi\, \pi$ $\left(K^0 \leftrightarrow \overline{K}^0\right) \to \pi\, \pi$ independent of π π isospin	$\epsilon = \dfrac{\hat{B}_K F_K^2\, \mathrm{SM}}{\Delta m_K}$	$\hat{B}_K$
$K^0 \to \pi\ \pi$ (direct CP violation)	$K_L \to \pi\, \pi$ depends on π π isospin	$\mathrm{Re}(\epsilon'/\epsilon)$ $= f(A_0, A_2, \mathrm{SM})$	$A_0\ \ A_2$ (SM_{cpc} inputs)

SM_{cpc} = Standard Model CP-conserving parameters

RBC/UKQCD 2+1 flavor DWF ensembles

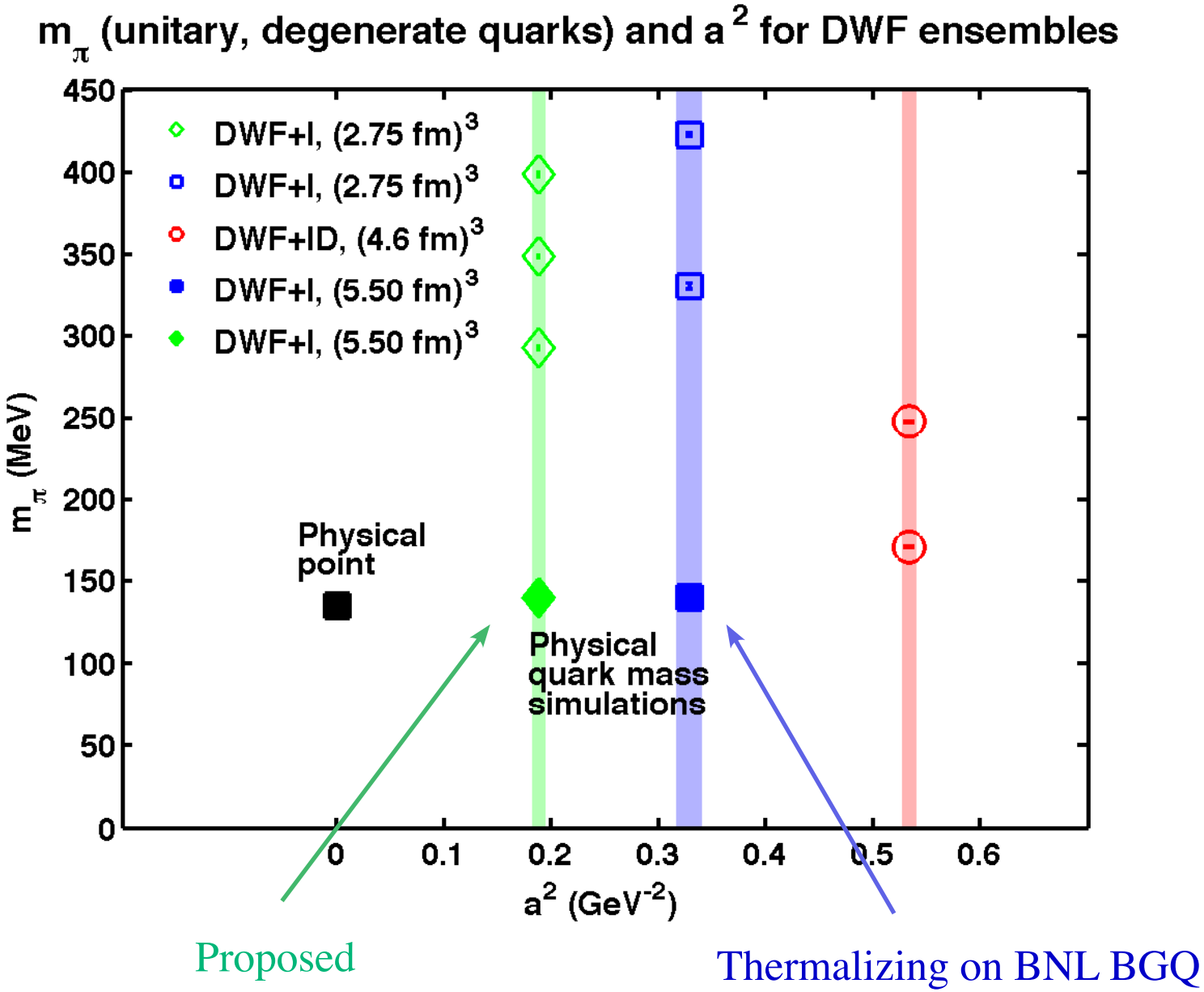

Improving Domain Wall Fermions

- When underlying gauge field changes topology, the DWF modes can extend farther in the fifth dimension
- This gives a non-perturbative contribution to residual chiral symmetry breaking
- Becomes problematic at strong coupling
- Add ratio of determinants of twisted Wilson fermions to suppress these gauge field dislocations
- Tune to minimize residual mass while still preserving toplogical ergodicity

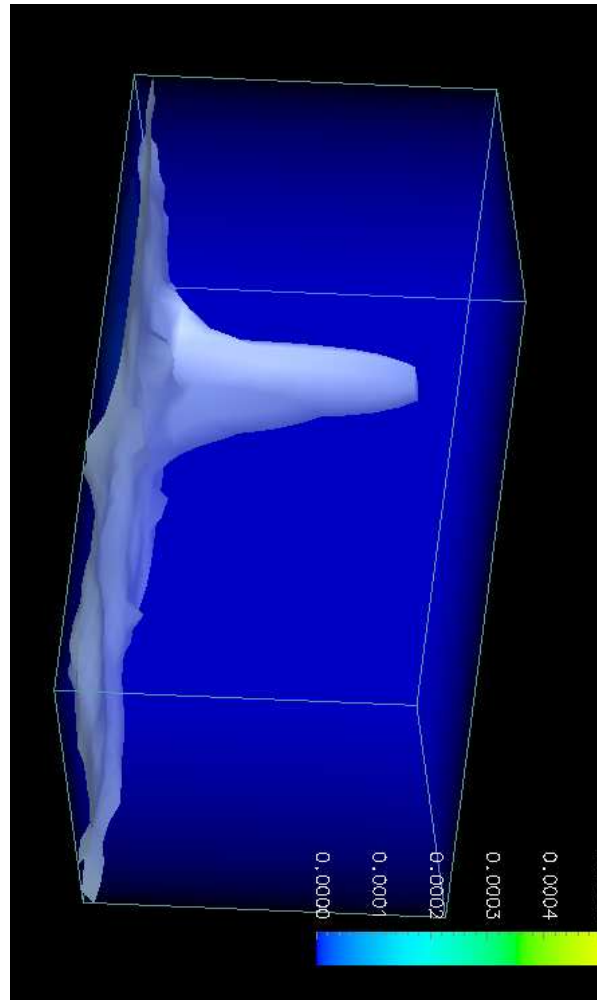

$$\frac{\det\left[D_W(-M+i\varepsilon_f\gamma^5)^\dagger D_W(-M+i\varepsilon_f\gamma^5)\right]}{\det\left[D_W(-M+i\varepsilon_b\gamma^5)^\dagger D_W(-M+i\varepsilon_b\gamma^5)\right]} = \prod_i \frac{\lambda_i^2+\varepsilon_f^2}{\lambda_i^2+\varepsilon_b^2}$$

λ_i are eigenvalues of the Hermitian Wilson operator $\gamma^5 D_W$

Force Gradient Integrator

- Proposed by Clark and Kennedy. Implemented (and simplified) in CPS by Hantao Yin
- For $16^3 \times 32 \times 16$ volumes, no speed-up compared to $O(\delta\tau^2)$ Omelyan

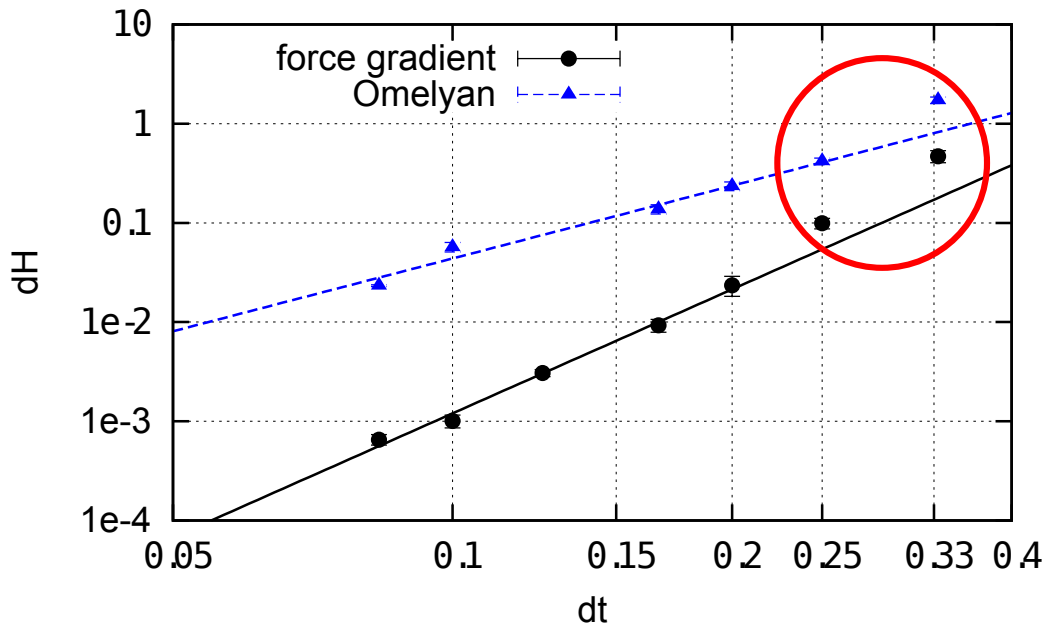

- For larger volumes, where δH grows with volume, force gradient may be helpful
- Tests on $48^3 \times 64 \times 16$ with 220 Mev pions using force gradient and retuning Hasenbush masses, 184 minutes/accepted configuration went down to 108 minutes/accepted configuration.

MADWF Solver

- Other chiral fermion formulations may achieve a smaller m_{res} for smaller L_s
- Mobius is one example: similar to DWF, but same m_{res} for ~ $L_s/2$
- We have many simulations at different lattice spacings to put into our global fits, so not easy to change actions. May also change topological tunneling, ...
- Idea: use Mobius fermions to accelerate the linear solver for DWF

  MADWF = Mobius Accelerated DWF
- Developed and implemented by Hantao Yin
- Gives 2× or more speed-up in quark propagator solves for current measurements.

Direct CG solve			Möbius Accelerated DWF		
operation	Op. count	time(s)	operation	Op. count	time(s)
CG solve(1e-10)	11290*32	2672	initial DWF(1e-2)	16*32	3
			DWF(1e-5)	121*32	28
			Möbius(1e-5)	4447*12	275
			DWF(1e-5)	106*32	25
			DWF(1e-5)	101*32	24
			Möbius(1e-5)	4581*12	284
			DWF(1e-5)	106*32	25
			DWF(1e-5)	102*32	24
			Möbius(1e-5)	4775*12	296
			DWF(1e-5)	106*32	25
			final DWF(1e-10)	517*32	121
total	3.61e5	2672	total	2.03e5	1138

Table 1: Comparison of MADWF CG solver with a regular (zero started) CG solver. $L = 32$, $L' = 12$, with $b = 1.841556$,$c = 0.841556$. Data obtained from a 512 node partition on BG/P, both solve to 1e-10.

Scaling at unphysical light quark mass

Compare

- DWF+I: 1/a = 2.28 GeV
- DWF+I: 1/a = 1.73 GeV

(Phys. Rev. D83 (2011) 074508)

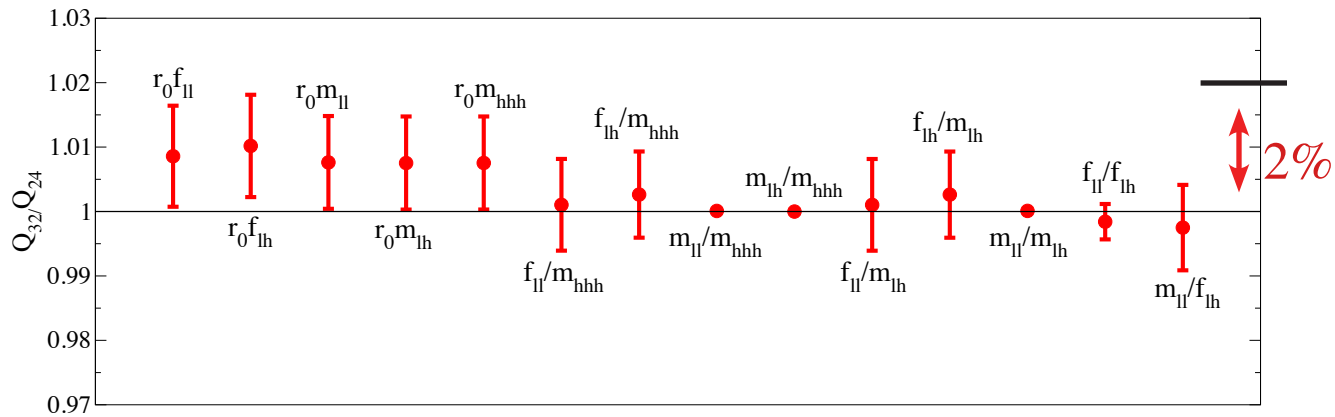

Compare

- DWF+I: 1/a = 2.28 GeV
- DWF+ID: 1/a = 1.37 GeV

(RBC/UKQCD to appear)

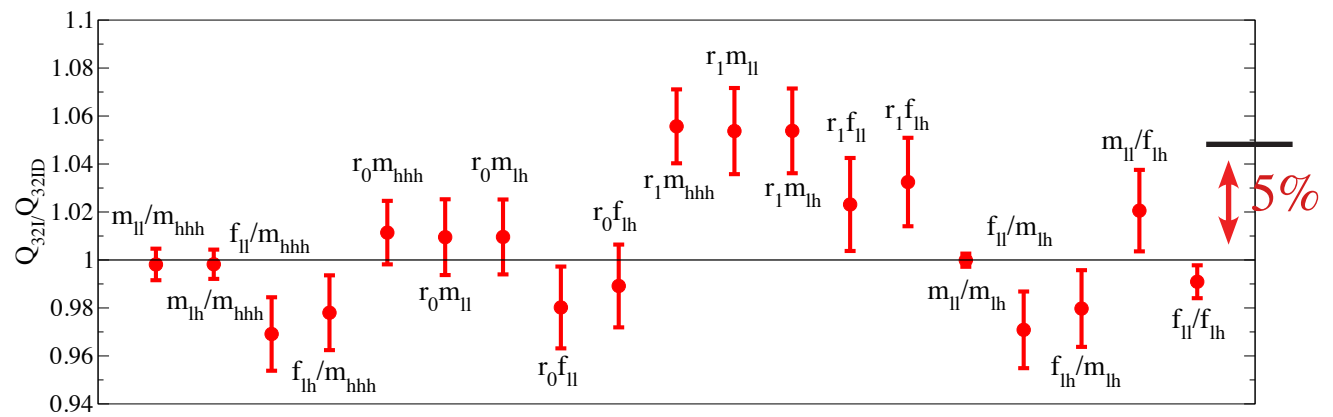

See few percent scaling errors from $1/a = 1.73$ GeV $\to \infty$, with larger $O(5\%)$ errors from 1/a = 1.37 GeV

Parameters in DWF+I and DWF+ID Global Fits

- Simultaneous fit to m_π^2, m_K^2, f_π, f_K, and m_Ω
- m_π, m_K and m_Ω chosen to be quantities without $O(a^2)$ corrections
- Parameters in SU(2) chiral expansion:
  - m_π^2 and f_π: 8 parameters – 2 LO, 4 NLO, $2O(a^2)$
  - m_K^2 and f_K: 6 parameters – 2 LO, 4 NLO, $2O(a^2)$
  - m_Ω: 1 LO, 1 NLO
  - Total: 18 parameters
- Fits also determine
  - 3 lattice spacings
  - 2 ratios of light quark mass renormalization factors
  - 2 ratios of strange quark mass renormalization factors
  - m_s

Global Fits to Multiple Ensembles

- Fit m_π^2, f_π, m_K^2, f_K and m_Ω to an expansion in powers of a^2 and m_l, including SU(2) logs where appropriate. Examples are

$$m_{ll}^2 = \chi_l \left[1 + \boxed{c_B a^2}\right] + \chi_l \cdot \left\{ \frac{16}{f^2}\left((2L_8^{(2)} - L_5^{(2)}) + 2(2L_6^{(2)} - L_4^{(2)})\right)\chi_l + \frac{1}{16\pi^2 f^2}\chi_l \log\frac{\chi_l}{\Lambda_\chi^2} \right\}$$

$$f_{ll} = f\left[1 + \boxed{c_f a^2}\right] + f \cdot \left\{ \frac{8}{f^2}(2L_4^{(2)} + L_5^{(2)})\chi_l - \frac{\chi_l}{8\pi^2 f^2}\log\frac{\chi_l}{\Lambda_\chi^2} \right\}.$$

- Note different $O(a^2)$ coefficients used for DWF+I and DWF+ID
- Fit all partially quenched data, including SU(2) ChPT finite volume corrections in fit
- Reweight data from simulation m_h to self-consistently determined m_s (Jung)
- Interpolate valence propagators to self-consistently determined m_s
- Use m_π m_K and m_Ω set scale.

m_π^2/m_f versus m_f

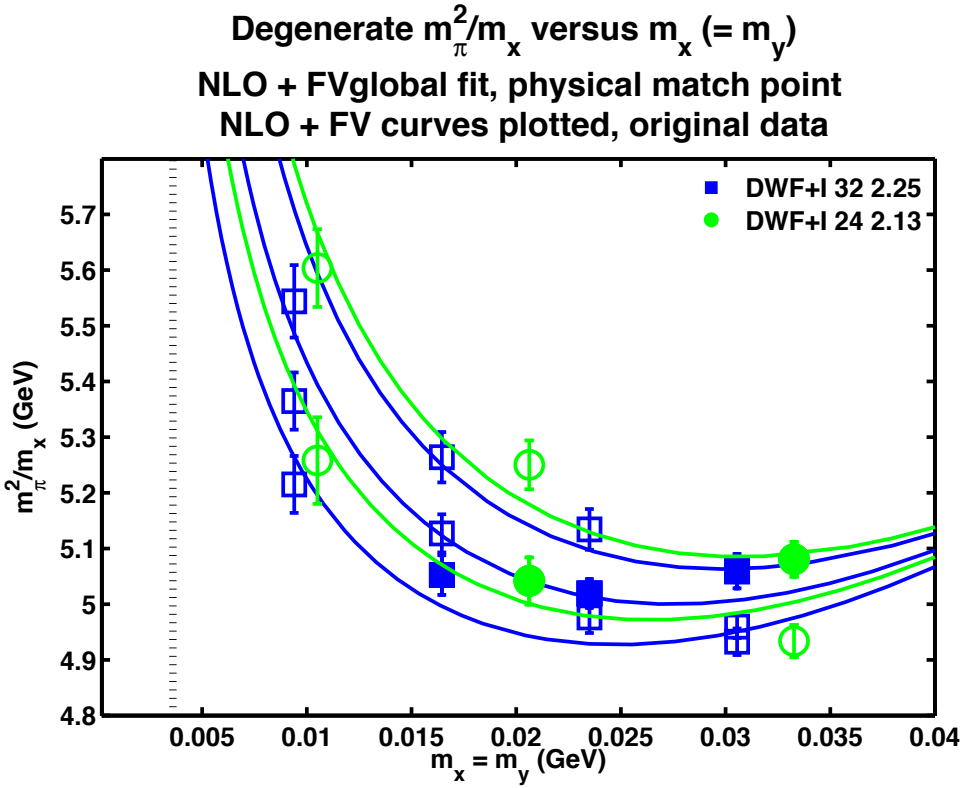

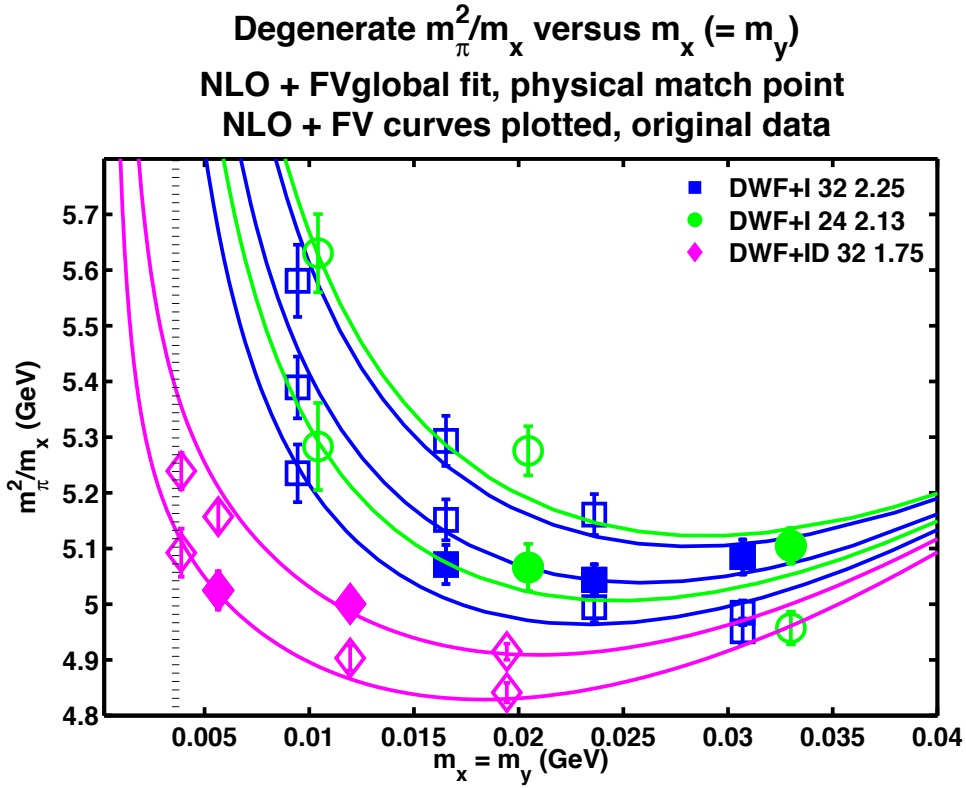

- Early fits from partial DWF+ID dataset
- Data consistent with chiral logarithms

m_π^2/m_f versus m_f

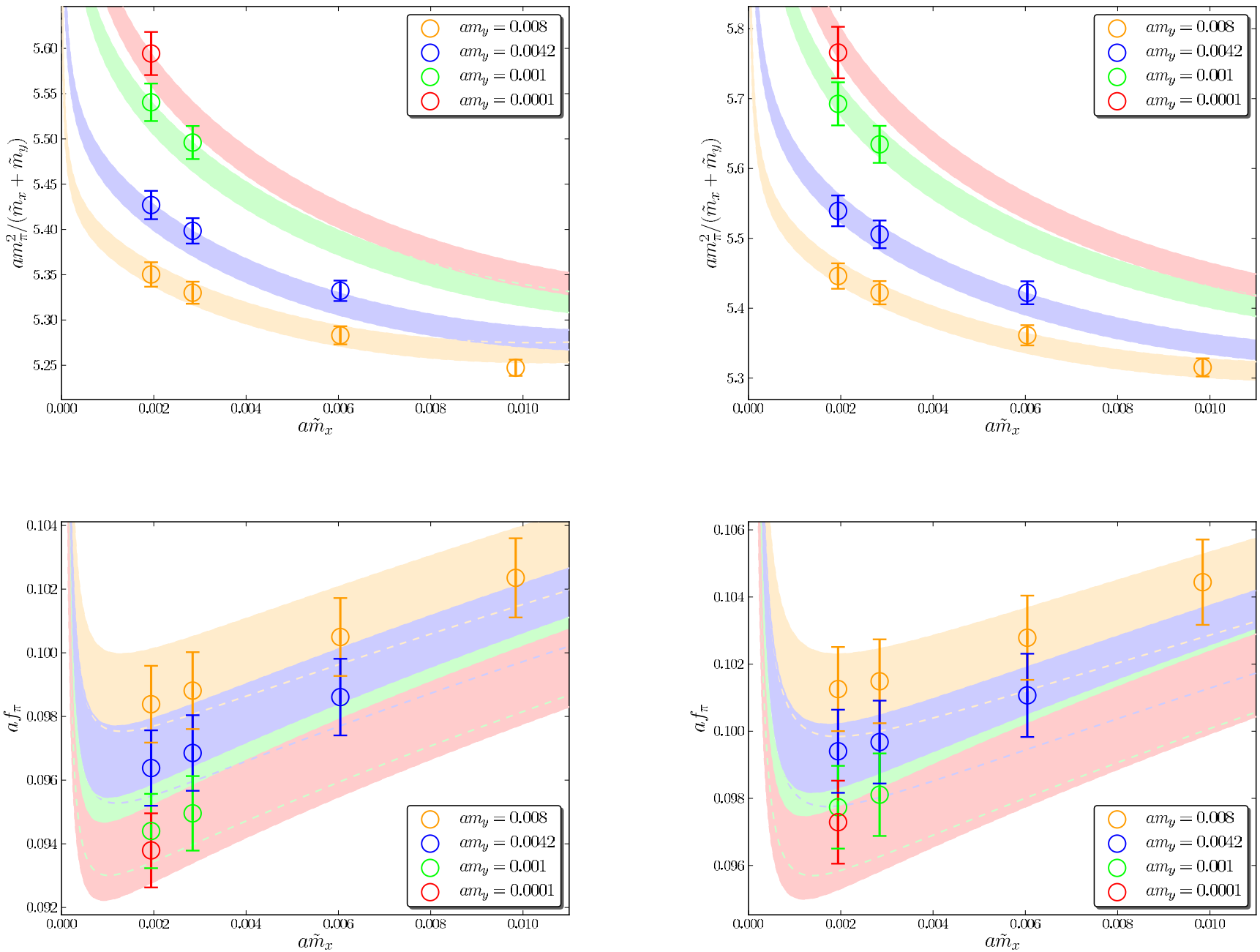

Some physical results

DWF+I	DWF+I and DWF+ID
$f_\pi^{\text{continuum}} = 124(2)(5)\,\text{MeV}$ $f_K^{\text{continuum}} = 149(2)(4)\,\text{MeV}$ $(f_K/f_\pi)^{\text{continuum}} = 1.204(7)(25)\,,$	$f_\pi = 127.1(2.7)(0.7)(2.5)\ \text{MeV},$ $f_K = 152.4(3.0)(0.1)(1.5)\ \text{MeV},$ $f_K/f_\pi = 1.1991(116)(69)(116)\,.$
$m_{ud}^{\overline{\text{MS}}}(2\,\text{GeV}) = (3.59 \pm 0.21)\,\text{MeV}$ $m_s^{\overline{\text{MS}}}(2\,\text{GeV}) = (96.2 \pm 2.7)\,\text{MeV}$ $\dfrac{m_s}{m_{ud}} = 26.8(0.8)_{\text{stat}}(1.1)_{\text{sys}}.$	$m_{u/d}(\overline{\text{MS}}, 3\ \text{GeV}) = 3.05(8)(6)(1)(4)\,\text{MeV},$ $m_s(\overline{\text{MS}}, 3\ \text{GeV}) = 83.6(1.7)(0.7)(0.4)(1.0)\,\text{MeV},$ $\dfrac{m_s}{m_{u/d}} = 27.36(39)(30)(22)(0)$
$B_K(\overline{\text{MS}}, 3\ \text{GeV}) = 0.529(5)(15)(2)(11)$	$B_K(\overline{\text{MS}}, 3\ \text{GeV}) = 0.535(8)(7)(3)(11)$ (stat, chiral, finite V, pert. theory)

Chiral extrapolation errors markedly reduced

Non-perturbative Renormalization

- Many of the quantities discussed in this talk require renormalization
- Needed to match to continuum schemes where low energy effective Hamiltonians are determined to N^nLO and renormalized at some scale μ
- Schrodinger functional and RI-MOM NPR schemes well understood
- RI-MOM is primarily used for kaons - simplicity?
- Recent improvements in RI-MOM
  - * Non-exceptional symmetric momenta - RI-SMOM
  - * Twisted b.c. to allow selection of continuous range of momenta
  - * Volume sources reduce statistical error dramatically
  - * Compute non-perturbative continuum running from fine lattices, use for coarse lattices (Rudy Arthur, Peter, Boyle, PRD 83 (2011) 114511).
  - * Implemented for $K \to \pi\pi$ (N. Garron) for RBC-UKQCD simulations on coarse lattices (1/a = 1.37 GeV).

$$\lim_{a_1 \to 0} \underbrace{\left[Z(\mu_1, a_1) Z^{-1}(\mu_0, a_1) \right]}_{\text{fine lattice}} \times \underbrace{Z(\mu_0, a_0)}_{\text{coarse lattice}} = Z(\mu_1, a_0)$$

Some $K \to \pi\,\pi$ physics

A neutral kaon beam will contain only long-lived K_L far enough from source.
Dominant decay is $K_L \to \pi\,\pi\,\pi$, small phase space gives long lifetime.
Experiments measure decay amplitudes for K_L compared to K_S (2 complex numbers).

$$\eta_{+-} = \frac{A(K_L \to \pi^+\,\pi^-)}{A(K_S \to \pi^+\,\pi^-)} \qquad \eta_{00} = \frac{A(K_L \to \pi^0\,\pi^0)}{A(K_S \to \pi^0\,\pi^0)}$$

If K_L is CP eigenstate, $\eta_{+-} = \eta_{00} = 0$.
Difference in η_{+-} and η_{00} dominantly due to difference in isospin of final state.
Consider amplitudes to decay to states of definite isospin

$$A(K^0 \to \pi\,\pi(I)) = A_I \exp(i\delta_I)$$ (I labels isospin, δ_I is $\pi\pi$ phase shift)

Parameters appearing in description of neutral kaon system

$$\eta_{+-} = \varepsilon + \frac{\varepsilon'}{1+\omega e^{i\theta'}} \approx \varepsilon + \varepsilon' \qquad \eta_{00} = \varepsilon - \frac{2\varepsilon'}{1-\sqrt{2}\,\omega e^{i\theta'}} \approx \varepsilon - 2\varepsilon'$$

$$\varepsilon = \tilde{\varepsilon} + i\left(\frac{\mathrm{Im}(A_0)}{\mathrm{Re}(A_0)}\right) \qquad \varepsilon' = \frac{\omega}{\sqrt{2}}\,e^{i\theta'}\left(\frac{\mathrm{Im}(A_2)}{\mathrm{Re}(A_2)} - \frac{\mathrm{Im}(A_0)}{\mathrm{Re}(A_0)}\right)$$

$$\omega = \frac{\mathrm{Re}(A_2)}{\mathrm{Re}(A_0)} = 0.045 \qquad \theta = \tan^{-1}\left[\frac{2\,\Delta M}{\Gamma_1 - \Gamma_2}\right] = 43.67 \pm 0.14^{\circ}$$

$$\theta' = \delta_2 - \delta_0 + \pi/2 = (43 \pm 6)^{\circ}$$

B_K and corrections to ε

$$\varepsilon = \frac{e^{i\pi/4}}{\sqrt{2}\,\Delta M_K}\left(\mathrm{Im}(M_{12}) + 2\frac{\mathrm{Im}(A_0)}{\mathrm{Re}(A_0)}\,\mathrm{Re}(M_{12})\right)$$

This has been focus, $O(G_F^2)$ contribution from $O^{\Delta S=2}$ operator

$$B_K(\mu) \equiv \frac{\langle \bar{K}^0 | (\bar{s}d)_{V-A} (\bar{s}d)_{V-A} | K^0 \rangle}{\frac{8}{3} f_K^2\, m_K^2}$$

Long distance physics
hep-ph/0201071 (page 58, Nierste)
Buras, Guadagnoli (PRD 78 (2008) 033005
Buras, Guadagnoli, Isidori
(PLB 688 (2010) 309

$$M_{12} = \frac{1}{2m_K}\langle K^0|H^{|\Delta S|=2}|\overline{K}^0\rangle - \boxed{\mathrm{Disp}\,\frac{i}{4m_K}\int \mathrm{d}^4x\,\langle K^0|H^{|\Delta S|=1}(x)\,H^{|\Delta S|=1}(0)|\overline{K}^0\rangle}$$

$$\Gamma_{12} = \mathrm{Abs}\,\frac{i}{2m_K}\int \mathrm{d}^4x\,\langle K^0|H^{|\Delta S|=1}(x)\,H^{|\Delta S|=1}(0)|\overline{K}^0\rangle$$

$$= \boxed{\frac{1}{2m_K}\sum_f (2\pi)^4\delta^4(p_K - p_f)\langle K^0|H^{|\Delta S|=1}|f\rangle\,\langle f|H^{|\Delta S|=1}|\overline{K}^0\rangle} \simeq \frac{1}{2m_K}\,A_0^*\,\overline{A}_0$$

- Norman Christ: measure these by extending Lellouch-Lüscher finite volume methods
- Jianglei Yu: numerical investigation of signal and renormalization for connected graphs

B_K

$$\varepsilon = \frac{e^{i\pi/4}}{\sqrt{2}\,\Delta M_K}\left(\mathrm{Im}(M_{12}) + 2\frac{\mathrm{Im}(A_0)}{\mathrm{Re}(A_0)}\,\mathrm{Re}(M_{12})\right) = \kappa_\varepsilon\,\frac{e^{i\phi_\varepsilon}}{\sqrt{2}}\left[\frac{\mathrm{Im}(M_{12}^{O^{\Delta S=2}})}{\Delta m_K}\right]$$

$$C_\varepsilon = \frac{G_F^2\,F_K^2\,m_K\,M_W^2}{6\sqrt{2}\,\pi^2\,\Delta M_K}$$

$$\lambda_t = V_{ts}^*\,V_{td}$$

Overall $|V_{cb}|^4$

$$\varepsilon_K = \kappa_\varepsilon\,C_\varepsilon\,\hat{B}_K\,\mathrm{Im}(\lambda_t)\,\{\mathrm{Re}(\lambda_c)[\eta_1\,S_0(x_c) - \eta_3\,S_0(x_c,x_t)] - \mathrm{Re}(\lambda_t)\,\eta_2\,S_0(x_t)\}\,e^{i\pi/4}$$

0.94 ± 0.02

Buras,Guadagnoli, Isidori

$$\eta_3^{NLO} \equiv \eta_{ct}^{NLO} \equiv 0.457 \pm 0.073$$

$$\eta_3^{NNLO} \equiv \eta_{ct}^{NNLO} \equiv 0.496 \pm 0.047$$

Brod and Gorbahn, PRD 82 094026 (2010)

3% overall change in ε

$K \to \pi\,\pi$ Decays via Penguins

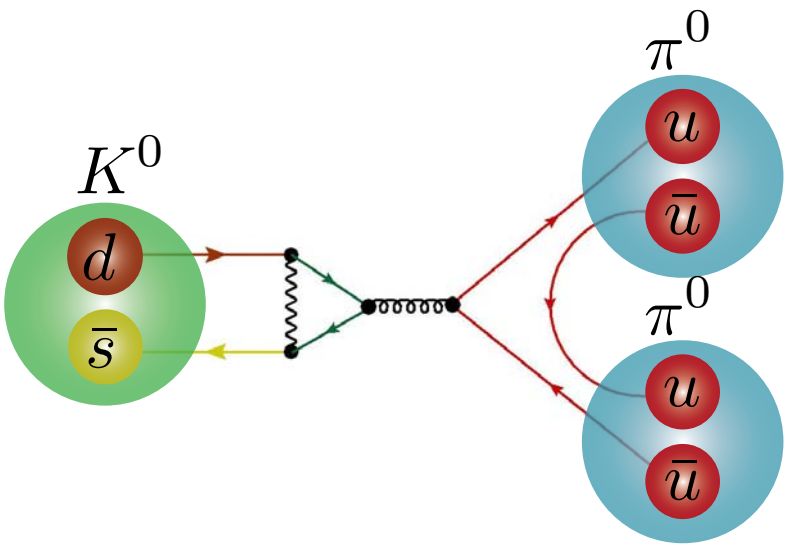

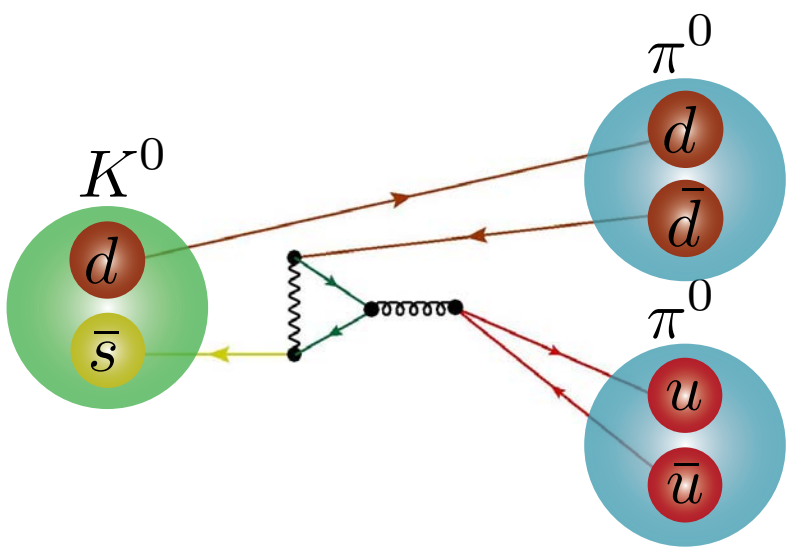

Penguin diagram

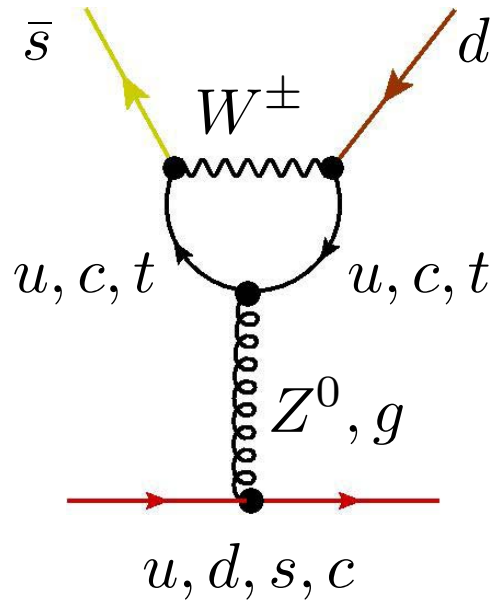

Penguin operators

$$Q_{3,5} = (\bar{s}_\alpha d_\alpha)_{V-A} \sum_{q=u,d,s} (\bar{q}_\beta q_\beta)_{V\mp A}$$

$$Q_{4,6} = (\bar{s}_\alpha d_\beta)_{V-A} \sum_{q=u,d,s} (\bar{q}_\beta q_\alpha)_{V\mp A}$$

$$Q_{7,9} = \frac{3}{2}(\bar{s}_\alpha d_\alpha)_{V-A} \sum_{q=u,d,s} e_q (\bar{q}_\beta q_\beta)_{V\pm A}$$

$$Q_{8,10} = \frac{3}{2}(\bar{s}_\alpha d_\beta)_{V-A} \sum_{q=u,d,s} e_q (\bar{q}_\beta q_\alpha)_{V\pm A}$$

Direct calculations of $K \to \pi\pi$ ΔI = 3/2 amplitudes

- RBC-UKQCD DWF+ID (Iwasaki + DSDR gauge action) ensemble

$$\mathcal{W}(M;\epsilon_f;\epsilon_b) = \frac{\det\left[D_{\mathcal{W}}(-M+i\epsilon_b\gamma^5)^\dagger D_{\mathcal{W}}(-M+i\epsilon_b\gamma^5)\right]}{\det\left[D_{\mathcal{W}}(-M+i\epsilon_f\gamma^5)^\dagger D_{\mathcal{W}}(-M+i\epsilon_f\gamma^5)\right]} = \prod_i \frac{\lambda_i^2+\epsilon_f^2}{\lambda_i^2+\epsilon_b^2}$$

- $m_\pi^{\rm dyn} = 170$ MeV, $32^3 \times 64 \times 16$ lattice volume, $(4.60\ {\rm fm})^3$ physical volume, 1/a = 1.37(2) GeV (a = 0.146(2) fm), $m_{\rm res}^{\overline{MS}}(\mu = 2\ {\rm GeV}) = 3.7$ MeV
- $m_\pi^{\rm PQ} = 142(2)$ MeV, $m_K = 508(9)$ MeV, $\vec{p}_\pi = 199(4)$ MeV
- Physical decays have $m_\pi = 140$ MeV, $m_K = 500$ MeV, $\vec{p}_\pi = 200$ MeV

Single wall source for π's on given lattice
Multiple kaon locations, since inexpensive
Results from 62 configurations

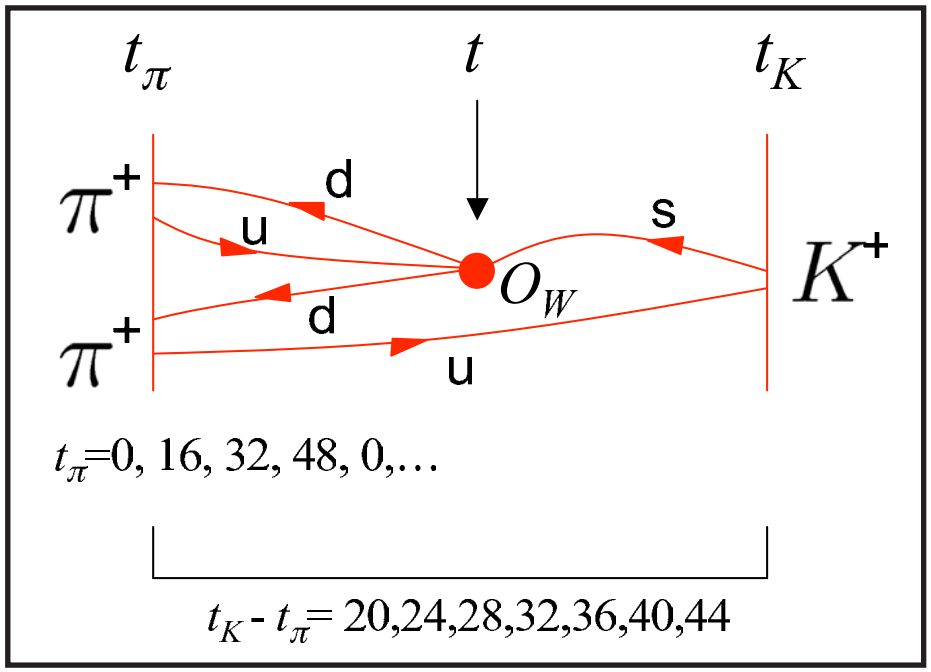

M. Lightman and E. Goode, Lattice 2010
M. Lightman, Columbia PhD thesis, 2011
E. Goode, talk Lattice 2011

Results for $K \to \pi\pi$ ΔI = 3/2 amplitudes

- Simulations also done on quenched lattices, at many kinematic points, which help to estimate errors from extrapolations to physical kinematics on unquenched lattices

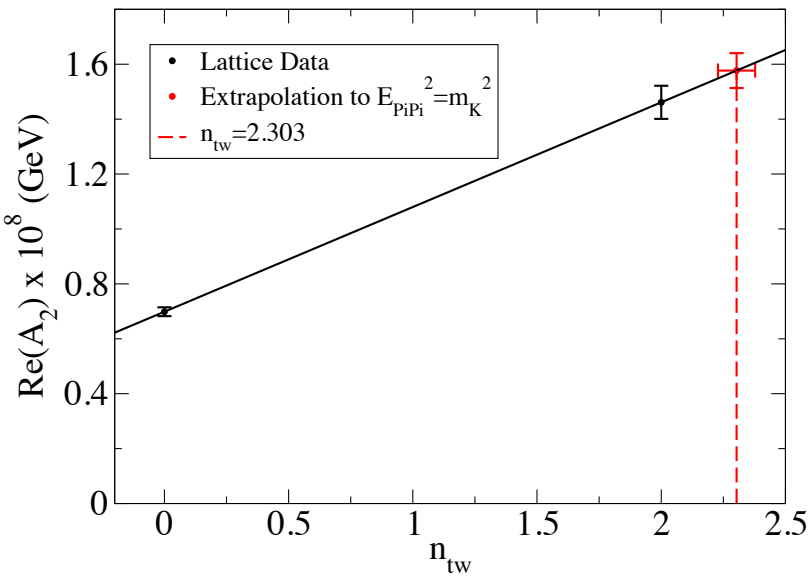

Extrapolation of $Re(A_2)$ to physical kinematics

	$\mathrm{Re}A_2$	$\mathrm{Im}A_2$
lattice artefacts	15%	15%
finite-volume corrections	6.2%	6.8%
partial quenching	3.5%	1.7%
renormalization	1.7%	4.7%
unphysical kinematics	3.0%	0.22%
derivative of the phase shift	0.32%	0.32%
Wilson coefficients	7.1%	8.1%
Total	18%	19%

Error estimates (M. Lightman thesis)

- N. Garron and A. Lytle have NPR results now, using 4 RI-SMOM schemes.
- Reweighting to physical light dynamical mass

$$\mathrm{Re}(A_2) = 1.397(81) \times 10^{-8}\mathrm{GeV} \xrightarrow{\text{reweighting}} 1.46(15) \times 10^{-8}\mathrm{GeV}$$

$$\mathrm{Im}(A_2) = -5.65(31) \times 10^{-13}\mathrm{GeV} \xrightarrow{\text{reweighting}} -5.79(39) \times 10^{-13}\mathrm{GeV}$$

Results for $K \to \pi\pi$ ΔI = 3/2 amplitudes

- 63 configurations analyzed, in ongoing calculation.
- PRL 108 (2012) 141601

$$\mathrm{Re}\, A_2 = (1.436 \pm 0.062_{\mathrm{stat}} \pm 0.258_{\mathrm{syst}})\, 10^{-8}\ \mathrm{GeV}$$
$$\mathrm{Im}\, A_2 = -(6.83 \pm 0.51_{\mathrm{stat}} \pm 1.30_{\mathrm{syst}})\, 10^{-13}\ \mathrm{GeV}.$$

$$\frac{\mathrm{Im} A_2}{\mathrm{Re} A_2} = -4.76(37)_{\mathrm{stat}}(81)_{\mathrm{syst}} \times 10^{-5}$$

$$\mathrm{Re}(A_2) = 1.484 \times 10^{-8}\ \mathrm{GeV}\ \text{(experiment)}$$

Some observations and opinions

- With DWF (or Mobius) plus BGQ, 2+1 flavor simulations with $m_\pi = 140$ MeV are underway
  - * $48^3 \times 96 \times 32$ DWF+I with 1/a = 1.74 GeV gives $(5.5\ \text{fm})^3$ box
    70 time units/BGQ-rack-month -> 500 time units/BGQ-rack-month
  - * $64^3 \times 128 \times 16$ DWF+I with 1/a = 2.28 GeV gives $(5.5\ \text{fm})^3$ box
    2x to 4x harder than 1/a = 1.74 GeV
  - * Many hundreds of configurations with a few BGQ rack-years
  - * Ideal for many physics measurements
- No chiral extrapolations!
  - * Still interesting in their own right, for better determination of LEC's
  - * Might need even lighter pions to know more about convergence of ChPT
  - * Not an issue for real-world QCD physics
- Adding DSDR term gives viable action for finite temperature studies
- We have reached the point where 2+1 flavor QCD with full continuum symmetries, physical pions, physical kaons and large volumes can be done!

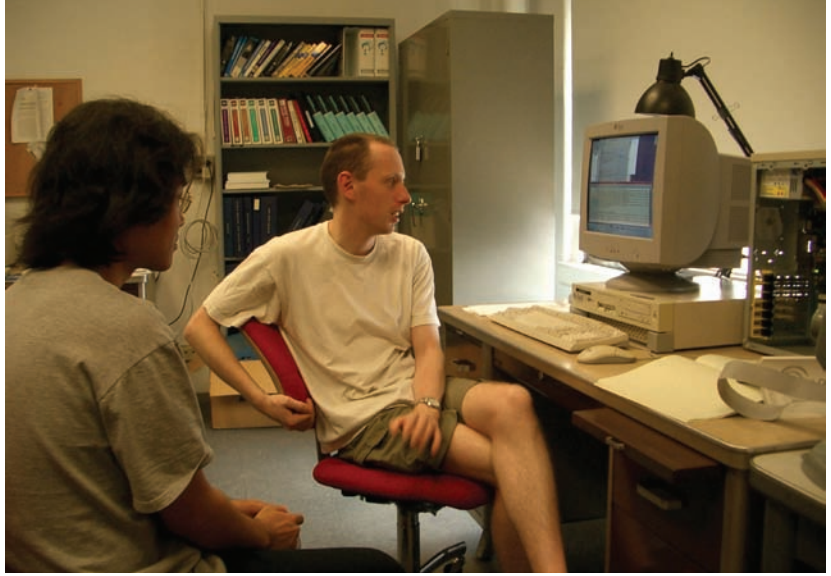

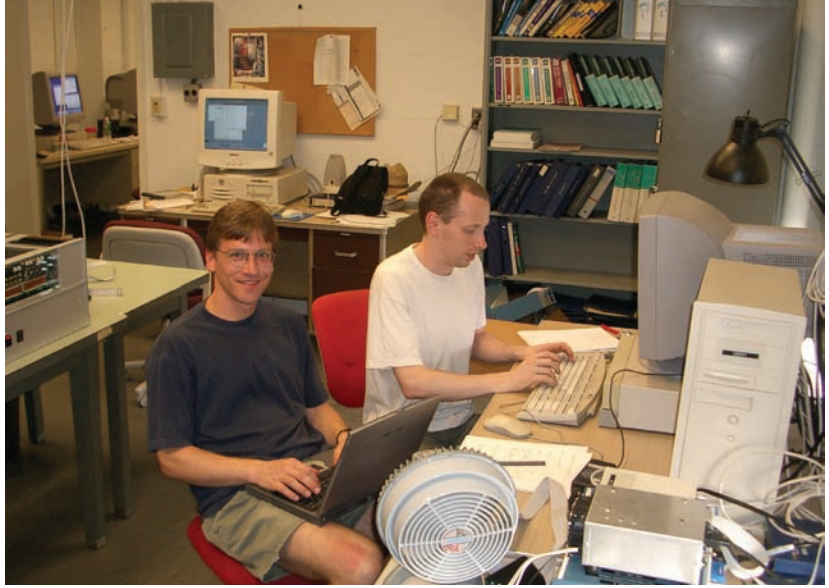

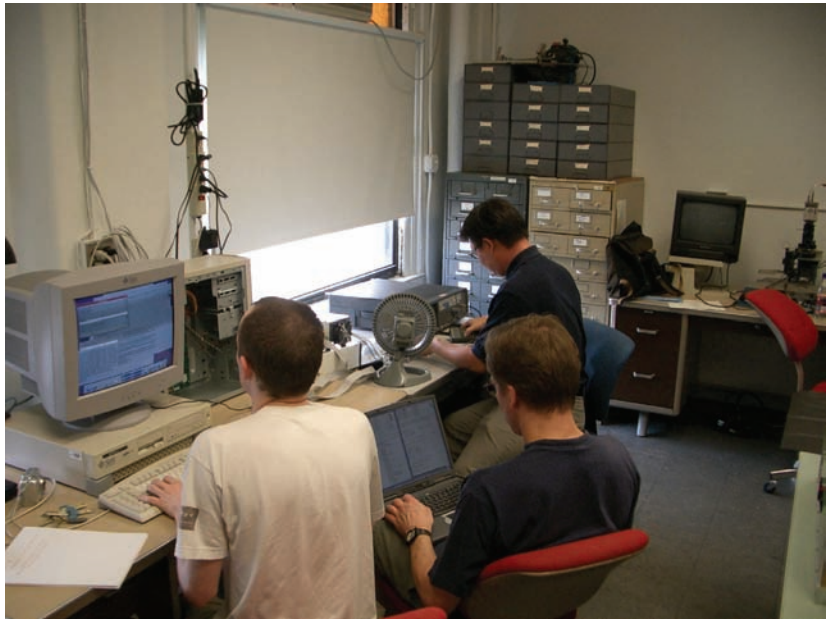

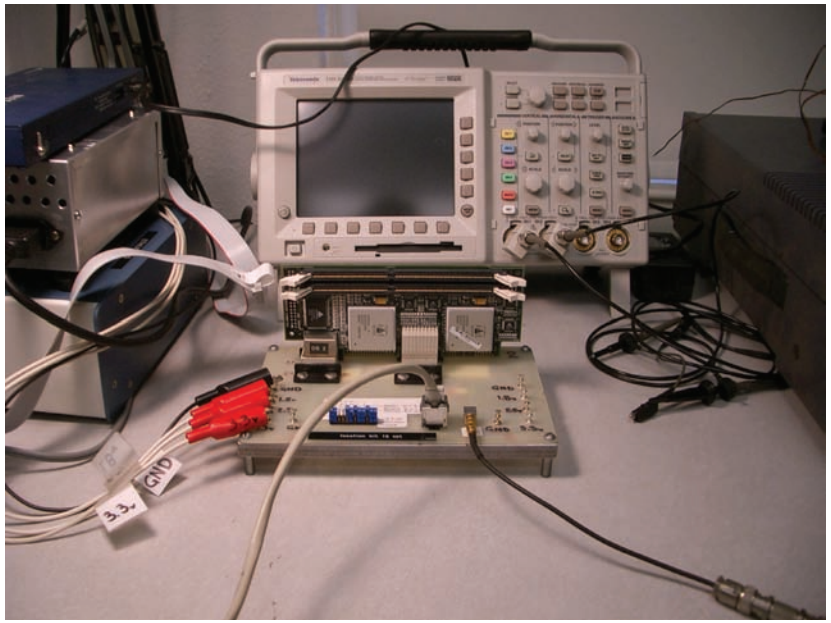
3.3v
GND

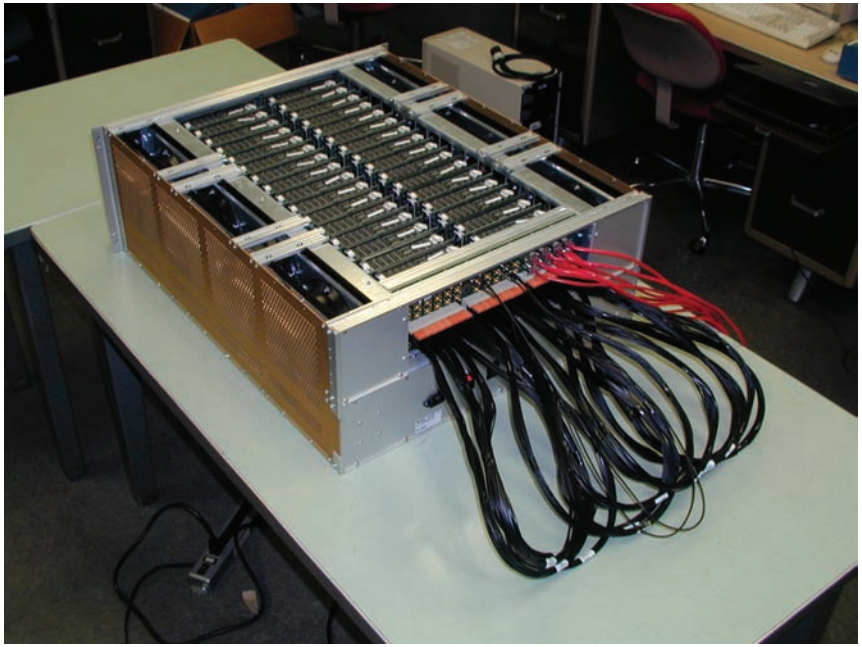

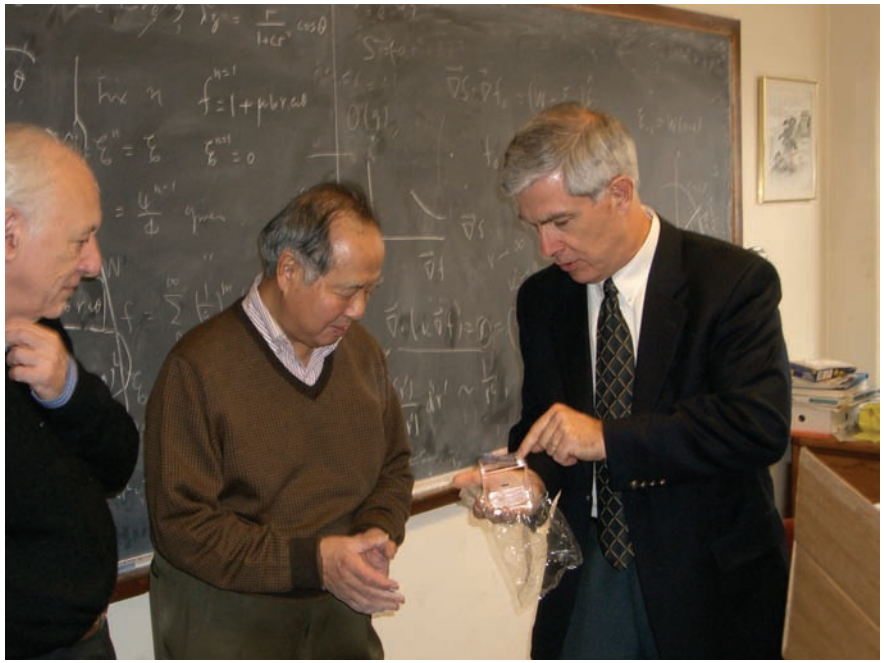

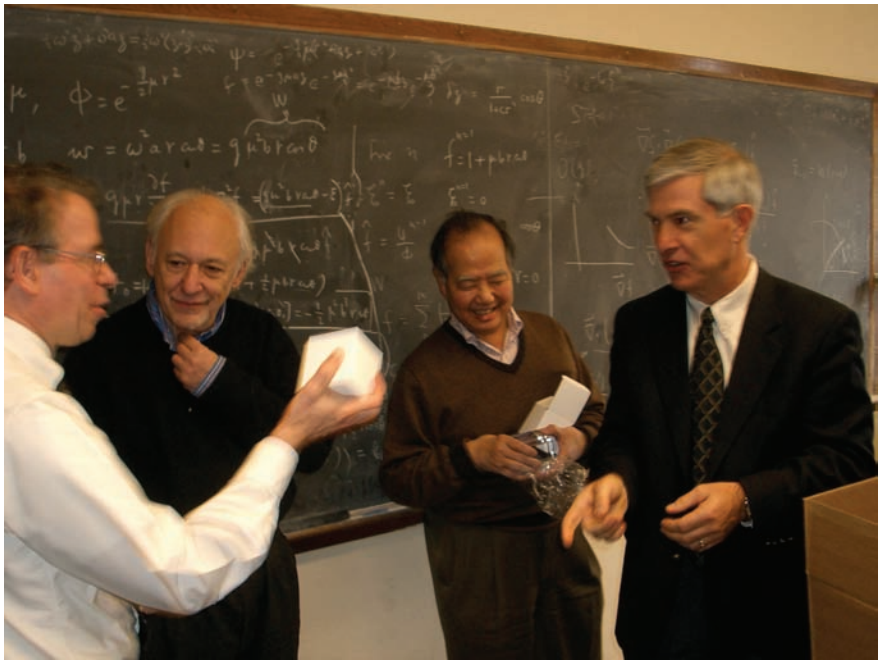

US DOE
RBRC
QCDOC at BNL
20 Teraflops

Shutdown of QCDOC, Sept. 18, 2011

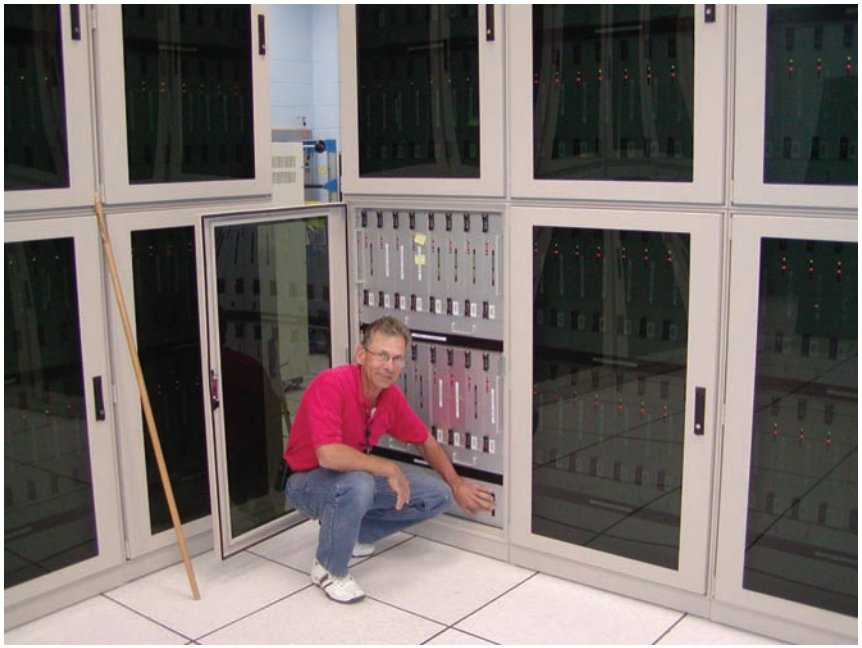

Last days of QCDSP, Nov. 2003

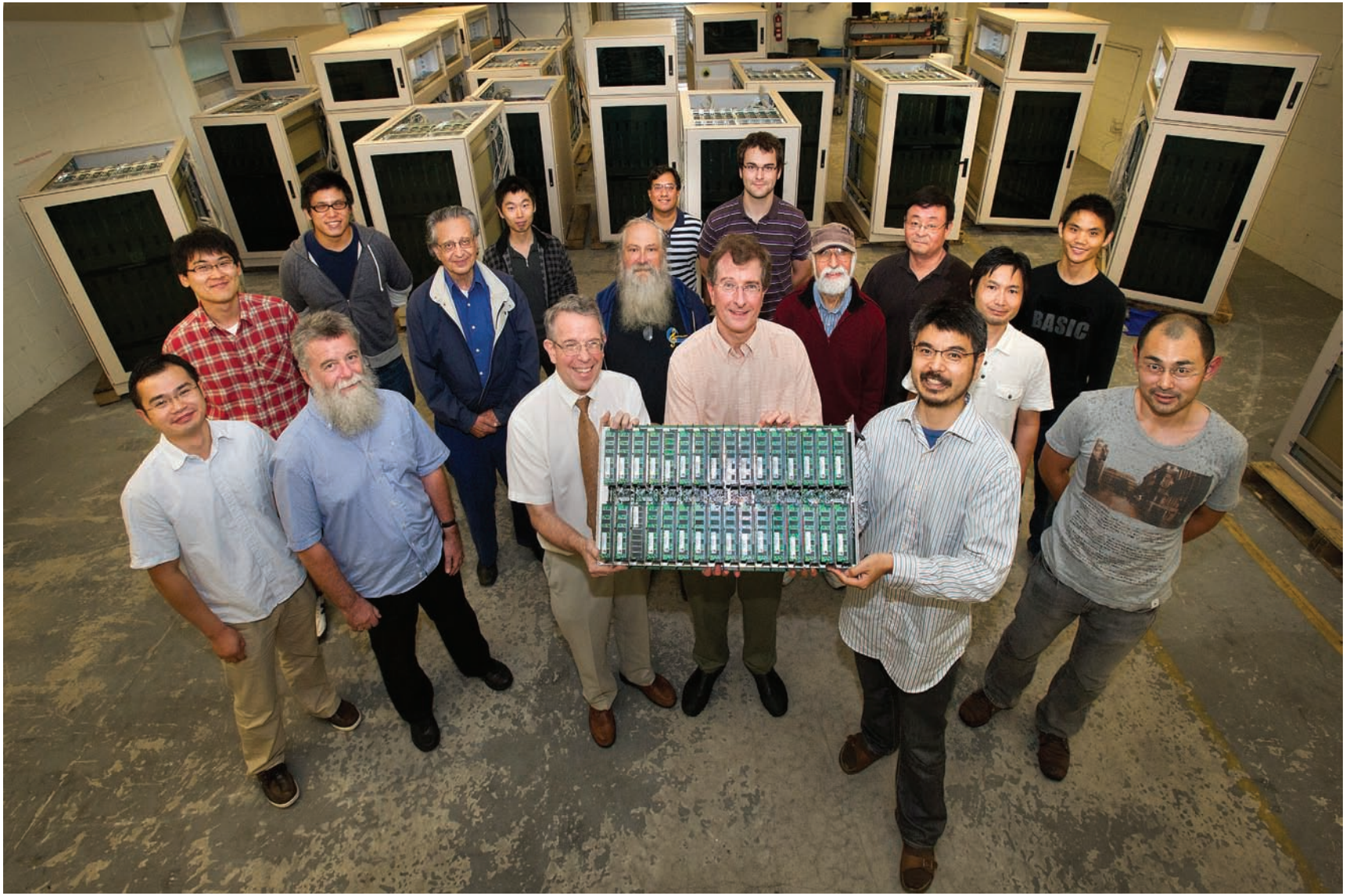
BASIC

BGQ at BNL

- BNL currently has 3+ racks of preproduction BGQ hardware
  - 1 rack is owned by BNL
  - 2 complete racks are owned by the RIKEN-BNL Research Center (RBRC)
  - A fourth partially populated RBRC rack will be used to hold a few small BGQ partitions for code development and testing.

Strong Scaling of BAGEL DWF CG Inverter on 64^4 volume

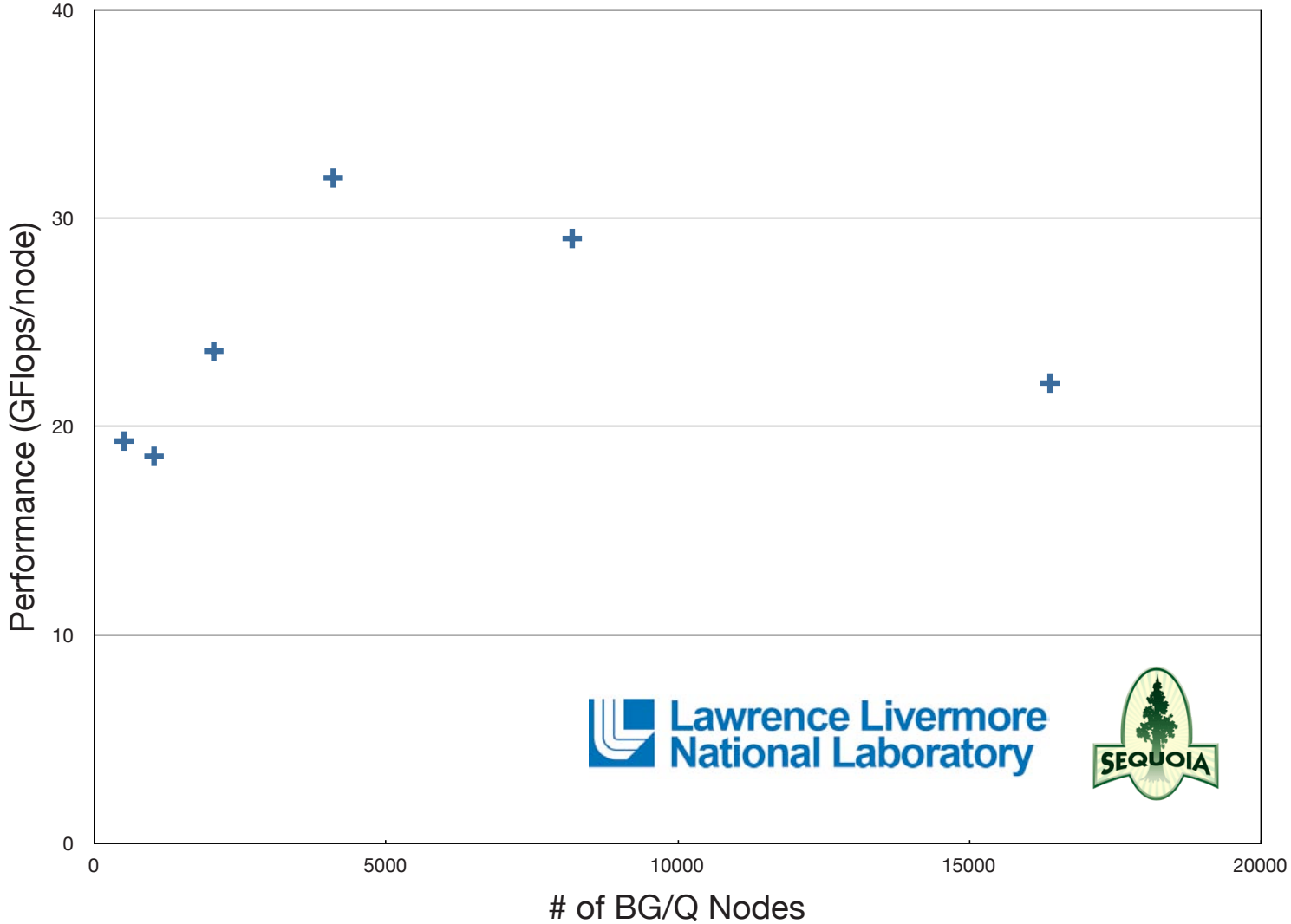

Tests were performed with the STFC funded DiRAC facility at Edinburgh

Weak Scaling for BAGEL DWF CG Inverter

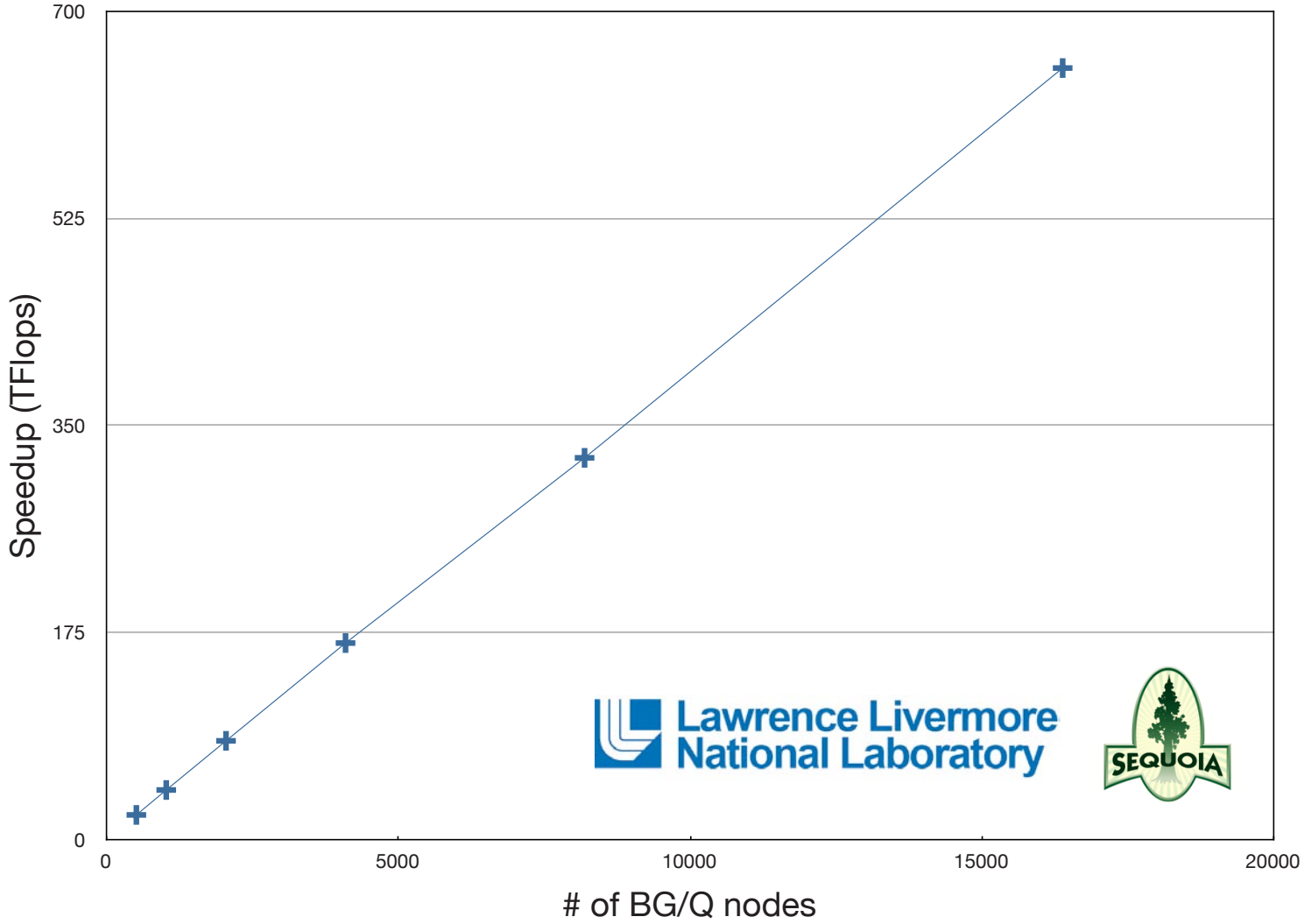

Tests were performed with the STFC funded DiRAC facility at Edinburgh

Axial couplings and strong decay widths of heavy hadrons

Stefan Meinel
The College of William and Mary

In collaboration with **William Detmold** and **C.-J. David Lin**

References:

arXiv:1108.5594 [PRD 84, 094502]
arXiv:1109.2480 [PRL 108, 172003]
arXiv:1203.3378 [to appear in PRD]

New Horizons for Lattice Computations with Chiral Fermions
Brookhaven National Laboratory, May 2012

Heavy-hadron chiral perturbation theory

Effective field theory combining **heavy-quark symmetry** and **chiral symmetry** [M. Wise 1992, T. M. Yan et al. 1992, G. Burdman and J. F. Donoghue 1992, P. Cho 1992]

- pions:

$$\xi = \sqrt{\Sigma} = \exp(i\Phi/f)$$

- heavy-light mesons with $s_l = 1/2$:

$$(P^i) = \begin{pmatrix} B^+ \\ B^0 \end{pmatrix}, \quad (P^{*i})_\mu = \begin{pmatrix} B^{*+} \\ B^{*0} \end{pmatrix}_\mu$$

combined into a single field

$$H^i = \left[-P^i\gamma_5 + P^{*i}_\mu\gamma^\mu\right]\frac{1-\not{v}}{2}$$

Heavy-hadron chiral perturbation theory

- heavy-light baryons with $s_l = 1$:

$$(B^{ij}) = \begin{pmatrix} \Sigma_b^+ & \frac{1}{\sqrt{2}}\Sigma_b^0 \\ \frac{1}{\sqrt{2}}\Sigma_b^0 & \Sigma_b^- \end{pmatrix}, \quad (B^{*ij})_\mu = \begin{pmatrix} \Sigma_b^{*+} & \frac{1}{\sqrt{2}}\Sigma_b^{*0} \\ \frac{1}{\sqrt{2}}\Sigma_b^{*0} & \Sigma_b^{*-} \end{pmatrix}_\mu$$

combined into a single field

$$S_\mu^{ij} = \sqrt{\frac{1}{3}}(\gamma_\mu + v_\mu)\gamma_5 B^{ij} + B_\mu^{*ij}$$

- heavy-light baryons with $s_l = 0$:

$$(T^{ij}) = \frac{1}{\sqrt{2}} \begin{pmatrix} 0 & \Lambda_b \\ -\Lambda_b & 0 \end{pmatrix}$$

Heavy-hadron chiral perturbation theory

At leading order in chiral- and heavy-quark expansion,

$$
\begin{aligned}
\mathcal{L} \;=\; & \frac{f^2}{8}(\partial^\mu \Sigma^\dagger)_{ij}\partial_\mu \Sigma^{ji} - i\mathrm{Tr}\left(\overline{H}_i v\cdot\mathscr{D} H^i\right) - i\overline{S}^\mu_{ij} v\cdot\mathscr{D} S^{ij}_\mu + \Delta \overline{S}^\mu_{ij} S^{ij}_\mu + i\overline{T}_{ij} v\cdot\mathscr{D} T^{ij} \\
& + g_1 \mathrm{Tr}\left(\overline{H}_i (\mathscr{A}^\mu)^i_j \gamma_\mu\gamma_5 H^j\right) \\
& - i g_2 \epsilon_{\mu\nu\sigma\lambda} \overline{S}^\mu_{ki} v^\nu (\mathscr{A}^\sigma)^i_j (S^\lambda)^{jk} \\
& + \sqrt{2} g_3 \left[\overline{S}^\mu_{ki}(\mathscr{A}_\mu)^i_j T^{jk} + \overline{T}_{ki}(\mathscr{A}^\mu)^i_j S^{jk}_\mu\right],
\end{aligned}
$$

where

$$
\mathscr{A}^\mu = \frac{i}{2}\left(\xi^\dagger \partial^\mu \xi - \xi \partial^\mu \xi^\dagger\right) = -\frac{1}{f}\partial^\mu \Phi + \ldots
$$

This gives the vertices

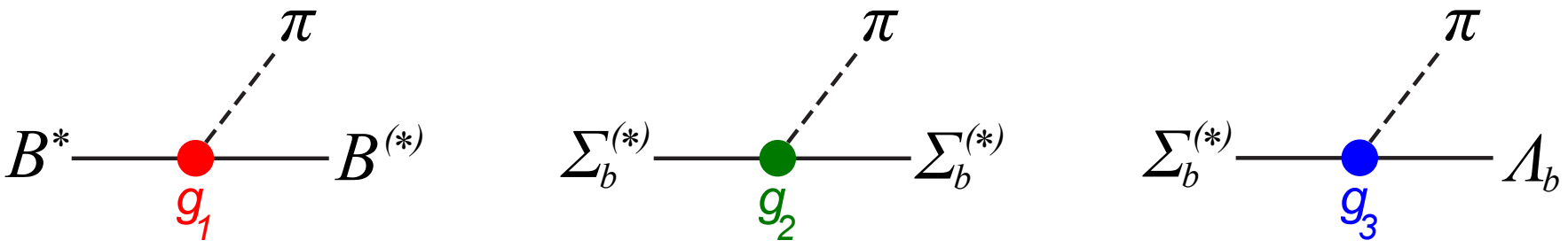

$[g_1 \sim g \sim \hat{g} \sim g_\pi \sim g_{B^* B\pi}]$

Heavy-hadron chiral perturbation theory

Example application 1: strong decay $\Sigma_b \to \Lambda_b \pi$

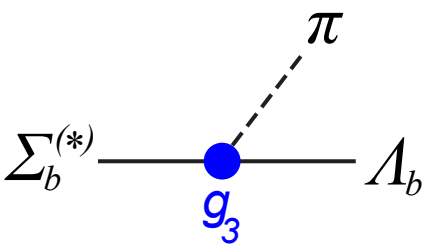

$$\Gamma(\Sigma_b^+ \to \Lambda_b \pi^+)_{\text{LO}} = \frac{g_3^2}{6\pi f^2} |\mathbf{p}_\pi|^3$$

Example application 2: quark-mass dependence of f_B in $SU(2)$ χPT:

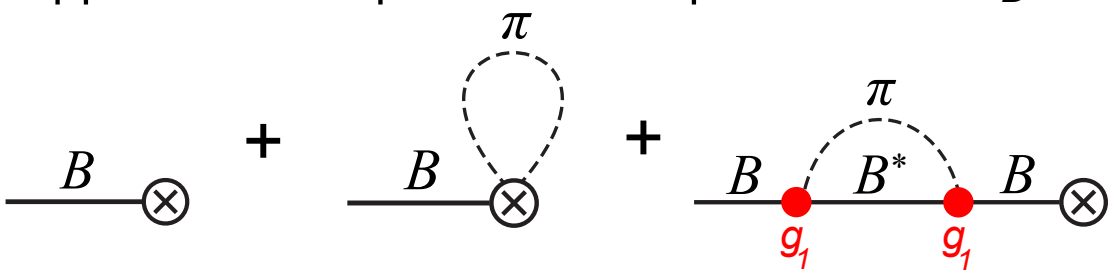

$$f_B = A\left[1 + \frac{3}{4}(1 + 3g_1^2)\frac{m_\pi^2}{(4\pi f)^2}\log\left(\frac{m_\pi^2}{(4\pi f)^2}\right)\right] + B\, m_\pi^2$$

Previous knowledge of g_1, g_2, g_3:

Reference	Method	g_1	g_2	g_3
Yan *et al.*, 1992	Nonrelativistic quark model	1	2	$\sqrt{2}$
Colangelo *et al.*, 1994	Relativistic quark model	$1/3$	...	...
Bećirević, 1999	Quark model with Dirac eq.	0.6 ± 0.1	...	...
Guralnik *et al.*, 1992	Skyrme model	...	1.6	1.3
Colangelo *et al.*, 1994	Sum rules	0.15 - 0.55	...	...
Belyaev *et al.*, 1994	Sum rules	0.32 ± 0.02	...	...
Dosch and Narison, 1995	Sum rules	0.15 ± 0.03	...	...
Colangelo and Fazio, 1997	Sum rules	0.09 - 0.44	...	...
Pirjol and Yan, 1997	Sum rules	...	$< \sqrt{6 - g_3^2}$	$< \sqrt{2}$
Zhu and Dai, 1998	Sum rules	...	$1.56 \pm 0.30 \pm 0.30$	$0.94 \pm 0.06 \pm 0.20$
Cho and Georgi, 1992	$\mathcal{B}[D^* \to D\,\pi, D\,\gamma]$	0.34 ± 0.48	...	...
Arnesen *et al.*, 2005	$\mathcal{B}[D^*_{(s)} \to D_{(s)}\pi, D_{(s)}\gamma]$	0.51	...	...
Li *et al.*, 2010	$d\Gamma[B \to \pi\ell\nu]$	< 0.87	...	...
Cheng, 1997	$\Gamma[\Sigma_c^* \to \Lambda_c\,\pi]$, NRQM	0.70 ± 0.12	1.40 ± 0.24	0.99 ± 0.17
De Divitiis *et al.*, 1998	$n_f = 0$ Lattice QCD	0.42 ± 0.09	...	...
Abada *et al.*, 2004	$n_f = 0$ Lattice QCD	0.48 ± 0.11	...	...
Negishi *et al.*, 2007	$n_f = 0$ Lattice QCD	0.517 ± 0.016	...	...
Ohki *et al.*, 2008	$n_f = 2$ Lattice QCD	0.516 ± 0.052	...	...
Bećirević *et al.*, 2009	$n_f = 2$ Lattice QCD	$0.44 \pm 0.03^{+0.07}_{-0.00}$	...	...
Bulava *et al.*, 2010	$n_f = 2$ Lattice QCD	0.51 ± 0.02	...	...

This work

Complete calculation of g_1, g_2, g_3 from lattice QCD, controlling all systematic uncertainties

- RBC/UKQCD ensembles with 2+1 flavors of domain-wall fermions
- 227 MeV $\leq m_\pi \leq$ 352 MeV (three unitary, three partially quenched)
- $L = 2.7$ fm
- NLO $SU(4|2)$ chiral fits including finite-volume effects
- continuum extrapolation using two lattice spacings $a = 0.112$ fm, $a = 0.085$ fm
- chiral symmetry simplifies nonperturbative renormalization, provides automatic $\mathcal{O}(a)$ improvement

How can we calculate g_1, g_2, g_3 from QCD?

- We compute suitable hadronic observables both in HHχPT and in lattice QCD.
- The expressions derived from HHχPT are then fitted to the lattice data, and in these fits the axial couplings are parameters.
- The simplest quantities that depend on the axial couplings *already at leading order* are the matrix elements of the axial current between single-hadron states.

$$
\begin{aligned}
\langle P^{*d} | A_\mu | P^u \rangle &= -2\,(g_1)_{\text{eff}}\;\varepsilon^*_\mu, \\
\langle S^{dd} | A_\mu | S^{du} \rangle &= -(i/\sqrt{2})\,(g_2)_{\text{eff}}\;v^\sigma\,\epsilon_{\sigma\mu\nu\rho}\,\overline{U}^\nu\,U^\rho, \\
\langle S^{dd} | A_\mu | T^{du} \rangle &= -(g_3)_{\text{eff}}\;\overline{U}_\mu\,\mathcal{U}
\end{aligned}
$$

How can we calculate g_1, g_2, g_3 from QCD?

In $SU(2)$ chiral perturbation theory and for $m_u = m_d$, one finds

$$
\begin{aligned}
(g_1)_{\text{eff}} &= g_1 \left[1 - \frac{2}{f^2} I(m_\pi) + \frac{4 g_1^2}{f^2} H(m_\pi, 0) + \text{analytic terms} \right], \\
(g_2)_{\text{eff}} &= g_2 \left[1 - \frac{2}{f^2} I(m_\pi) + \frac{3 g_2^2}{2 f^2} H(m_\pi, 0) \right. \\
&\qquad \left. + \frac{g_3^2}{f^2} \Big\{ H(m_\pi, -\Delta) - 2K(m_\pi, -\Delta, 0) \Big\} + \text{analytic terms} \right], \\
(g_3)_{\text{eff}} &= g_3 \left[1 - \frac{2}{f^2} I(m_\pi) + \frac{g_2^2}{f^2} \Big\{ -2H(m_\pi, \Delta) + H(m_\pi, 0) \Big\} \right. \\
&\qquad + \frac{g_3^2}{2 f^2} \Big\{ H(m_\pi, -\Delta) + 9H(m_\pi, \Delta) - 2K(m_\pi, \Delta, 0) \Big\} \\
&\qquad \left. + \text{analytic terms} \right]
\end{aligned}
$$

Derived in our paper arXiv:1108.5594, also for $SU(4|2)$, $SU(6|3)$, and in finite volume

Lattice calculation of axial-current matrix elements

Use the interpolating fields

$$
\begin{aligned}
P^i &= (\gamma_5)_{\alpha\beta}\, \overline{Q}_{a\alpha}\, \tilde{q}^i_{a\beta}, \\
P^{*i}_\mu &= (\gamma_\mu)_{\alpha\beta}\, \overline{Q}_{a\alpha}\, \tilde{q}^i_{a\beta}, \\
S^{ij}_{\mu\,\alpha} &= \epsilon_{abc}\, (C\gamma_\mu)_{\beta\gamma}\, \tilde{q}^i_{a\beta}\, \tilde{q}^j_{b\gamma}\, Q_{c\alpha}, \\
T^{ij}_\alpha &= \epsilon_{abc}\, (C\gamma_5)_{\beta\gamma}\, \tilde{q}^i_{a\beta}\, \tilde{q}^j_{b\gamma}\, Q_{c\alpha}, \\
A_\mu &= Z_A\, \overline{d}_{a\alpha}(\gamma_\mu\gamma_5)_{\alpha\beta} u_{a\beta}.
\end{aligned}
$$

Static heavy quark Q: Eichten-Hill action with HYP smearing

Light quarks u, d, s: domain wall action. Nonperturbative Z_A (thanks to chiral symmetry) from RBC/UKQCD [Aoki et al., 2011]

$$
Z_A = \begin{cases} 0.7019(26) & \text{for } a = 0.112 \text{ fm}, \\ 0.7396(17) & \text{for } a = 0.085 \text{ fm} \end{cases}
$$

Three-point correlators

For example

$$\langle S^{dd\,\mu}(\mathbf{x},t)\ \sum_{\mathbf{x}'} A^{\mu}(\mathbf{x}',t')\ \overline{T}_{du}(\mathbf{x},0)\rangle$$

Static heavy quark propagator requires hadron interpolating fields to be at same spatial point $\mathbf{x}$.

We generate pairs of light-quark propagators with sources at $(\mathbf{x},0)$ and $(\mathbf{x},t)$ for multiple values of t.

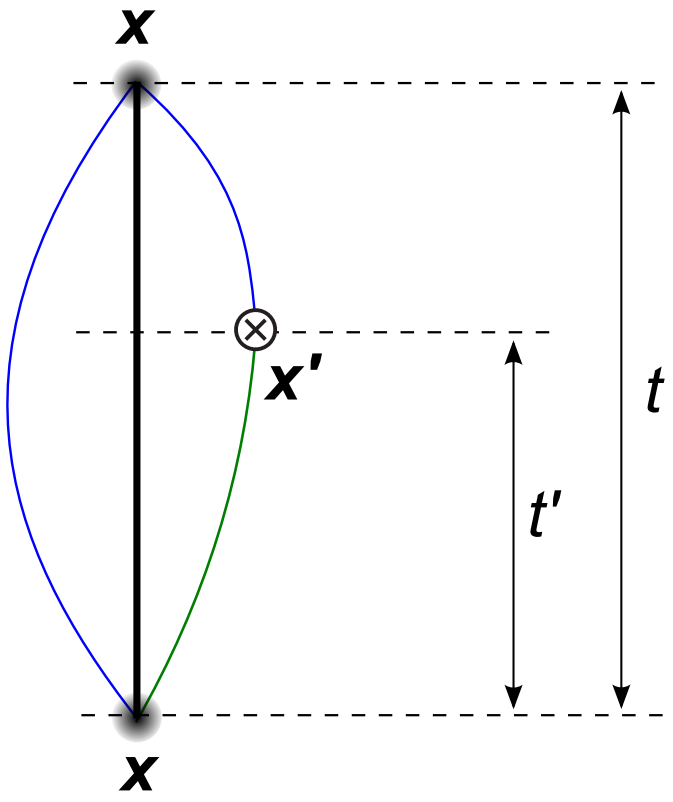

Correlator ratios

Simple ratios for mass-degenerate $P^* \to P$ and $S \to S$ matrix elements

$$R_1(t,\ t') = -\frac{1}{3}\frac{\sum_{\mu=1}^{3}\langle\, P^{*d\,\mu}(t)\, A^{\mu}(t')\, P_u^{\dagger}(0)\,\rangle}{\langle\, P^{u}(t)\, P_u^{\dagger}(0)\,\rangle} \underset{t,t',|t-t'|\to\infty}{\longrightarrow} (g_1)_{\rm eff},$$

$$R_2(t,\ t') = i\,\frac{\sum_{\mu,\nu,\rho=1}^{3}\epsilon_{0\mu\nu\rho}\,\langle\, S^{dd\,\mu}(t)\, A^{\nu}(t')\, \overline{S}^{\rho}_{du}(0)\,\rangle}{\sum_{\mu=1}^{3}\langle\, S^{dd\,\mu}(t)\, \overline{S}^{\mu}_{dd}(0)\,\rangle} \underset{t,t',|t-t'|\to\infty}{\longrightarrow} (g_2)_{\rm eff},$$

Double ratio for $S \to T$ transition matrix element

$$R_3(t,\ t') = \left[\frac{1}{3}\frac{\sum_{\mu,\nu=1}^{3}\langle\, S^{dd\,\mu}(t)\, A^{\mu}(t')\, \overline{T}_{du}(0)\,\rangle\langle\, T^{du}(t)\, A^{\nu\dagger}(t')\, \overline{S}^{\nu}_{dd}(0)\,\rangle}{\sum_{\mu=1}^{3}\langle\, S^{dd\,\mu}(t)\, \overline{S}^{\mu}_{dd}(0)\,\rangle\,\langle\, T^{du}(t)\, \overline{T}_{du}(0)\,\rangle}\right]^{1/2}$$

$$\underset{t,t',|t-t'|\to\infty}{\longrightarrow} (g_3)_{\rm eff}$$

Lattice parameters

RBC/UKQCD ensembles with 2+1 flavors of domain wall fermions

$L^3 \times T$	$m_{u/d}^{(\mathrm{sea})}$	$m_{u/d}^{(\mathrm{val})}$	a (fm)	$m_\pi^{(\mathrm{vs})}$ (MeV)	$m_\pi^{(\mathrm{vv})}$ (MeV)
$24^3 \times 64$	0.005	0.005	0.1119(17)	336(5)	336(5)
$24^3 \times 64$	0.005	0.002	0.1119(17)	304(5)	270(4)
$24^3 \times 64$	0.005	0.001	0.1119(17)	294(5)	245(4)
$32^3 \times 64$	0.006	0.006	0.0848(17)	352(7)	352(7)
$32^3 \times 64$	0.004	0.004	0.0849(12)	295(4)	295(4)
$32^3 \times 64$	0.004	0.002	0.0849(12)	263(4)	227(3)

Examples of ratios

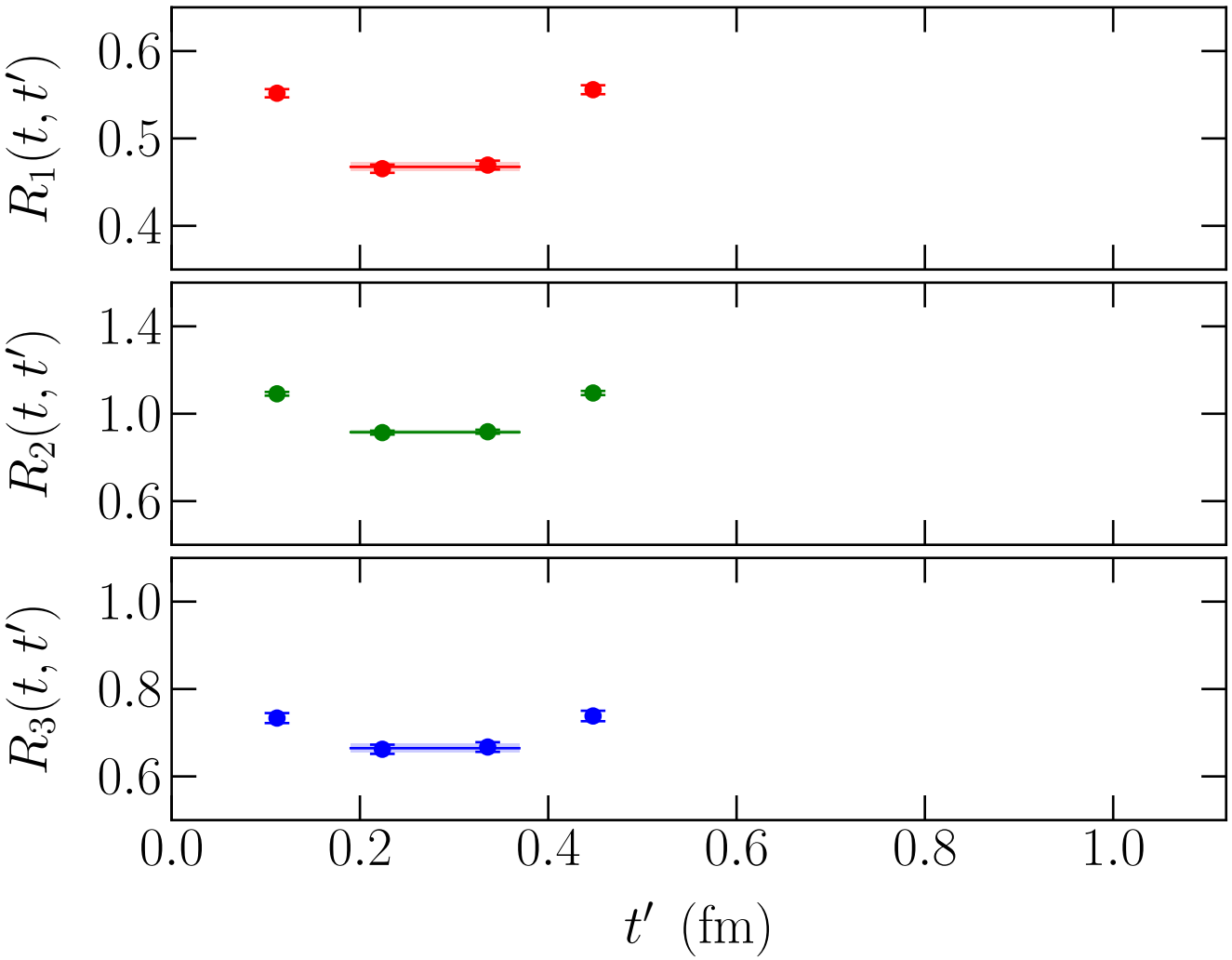

$[a = 0.112 \text{ fm},\ am_{u/d}^{(\text{val})} = 0.002,\ t/a = 5]$

Examples of ratios

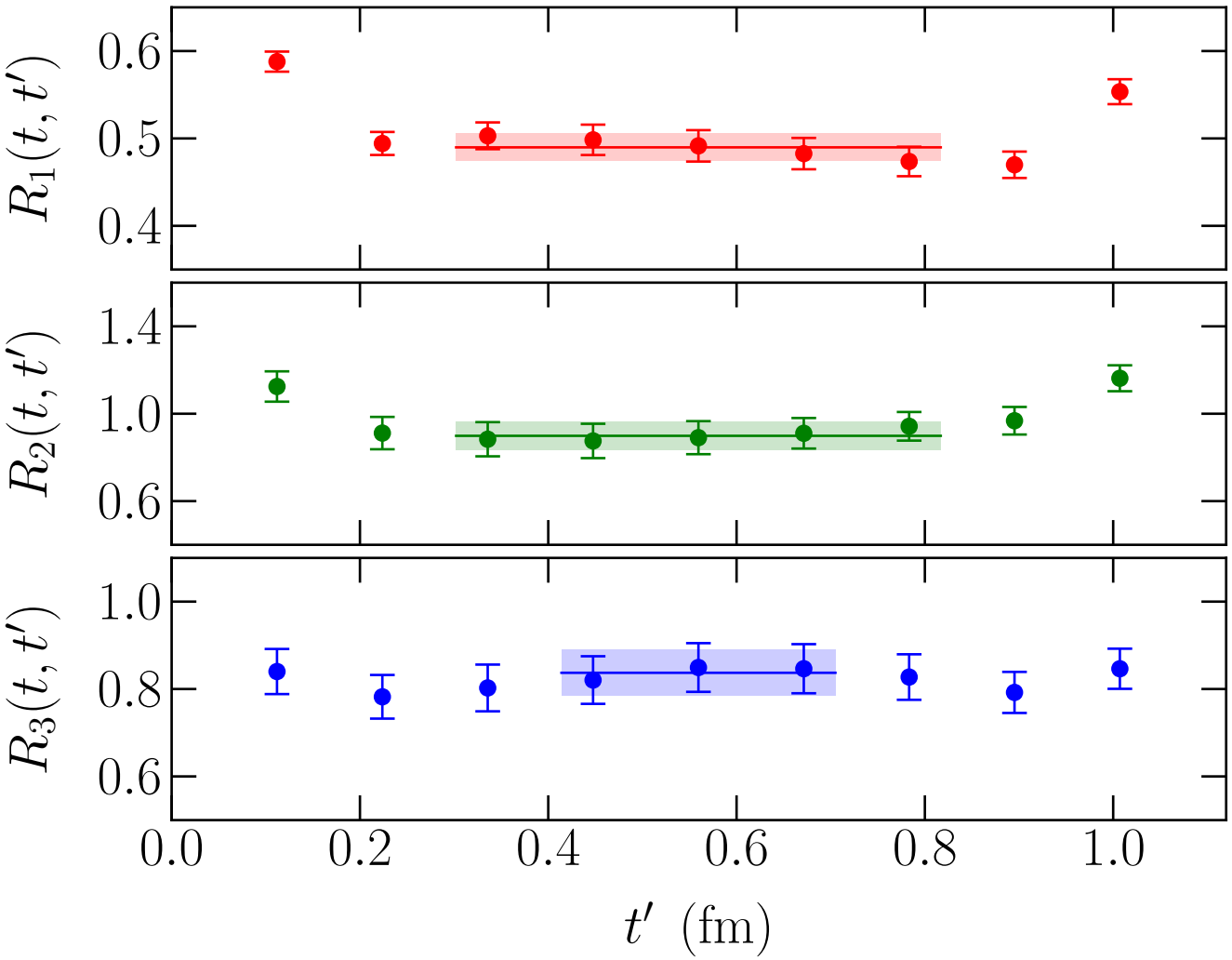

$[a = 0.112 \text{ fm},\ am_{u/d}^{(\text{val})} = 0.002,\ t/a = 10]$

Extrapolation to infinite source-sink separation

Fit t-dependence including first excited-state contamination using

$$R_i(t) = (g_i)_{\text{eff}} - A_i\, e^{-\delta_i\, t}$$

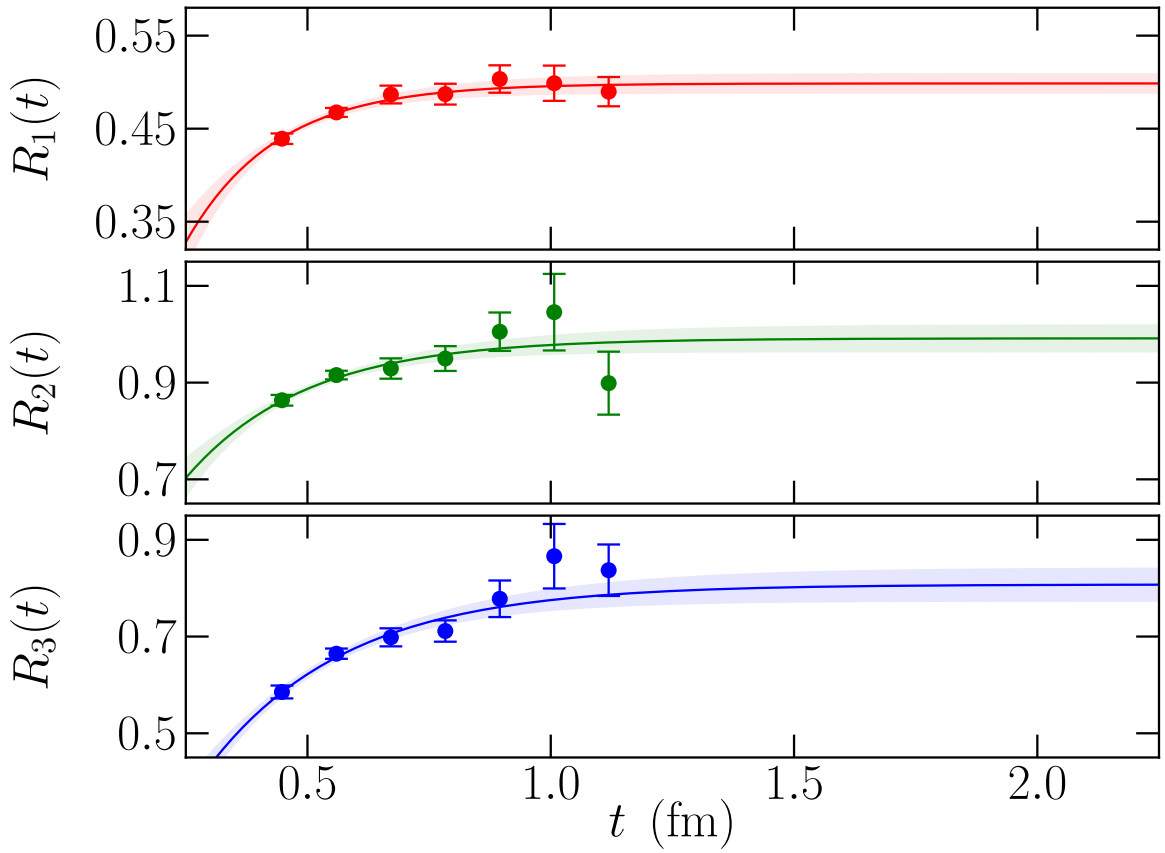

$[a = 0.112 \text{ fm},\ am_{u/d}^{(\text{val})} = 0.002]$

Chiral-continuum fits using $SU(4|2)$ HHχPT

$$(g_1)_{\text{eff}} = g_1 \Big[1 + f_1(g_1, m_\pi^{(\text{vv})}, m_\pi^{(\text{vs})}, L) + d_{1,n_{\text{HYP}}}\, a^2 + c_1^{(\text{vv})}\, [m_\pi^{(\text{vv})}]^2 + c_1^{(\text{vs})}\, [m_\pi^{(\text{vs})}]^2 \Big],$$

$$(g_2)_{\text{eff}} = g_2 \Big[1 + f_2(g_2, g_3, m_\pi^{(\text{vv})}, m_\pi^{(\text{vs})}, \Delta, L) + d_{2,n_{\text{HYP}}}\, a^2 + c_2^{(\text{vv})}\, [m_\pi^{(\text{vv})}]^2 + c_2^{(\text{vs})}\, [m_\pi^{(\text{vs})}]^2 \Big],$$

$$(g_3)_{\text{eff}} = g_3 \Big[1 + f_3(g_2, g_3, m_\pi^{(\text{vv})}, m_\pi^{(\text{vs})}, \Delta, L) + d_{3,n_{\text{HYP}}}\, a^2 + c_3^{(\text{vv})}\, [m_\pi^{(\text{vv})}]^2 + c_3^{(\text{vs})}\, [m_\pi^{(\text{vs})}]^2 \Big]$$

($\Delta = 200$ MeV)

Fits using $SU(4|2)$ HHχPT

Plotted at $L = \infty$, $m_\pi^{(\mathrm{vs})} = m_\pi^{(\mathrm{vv})}$:

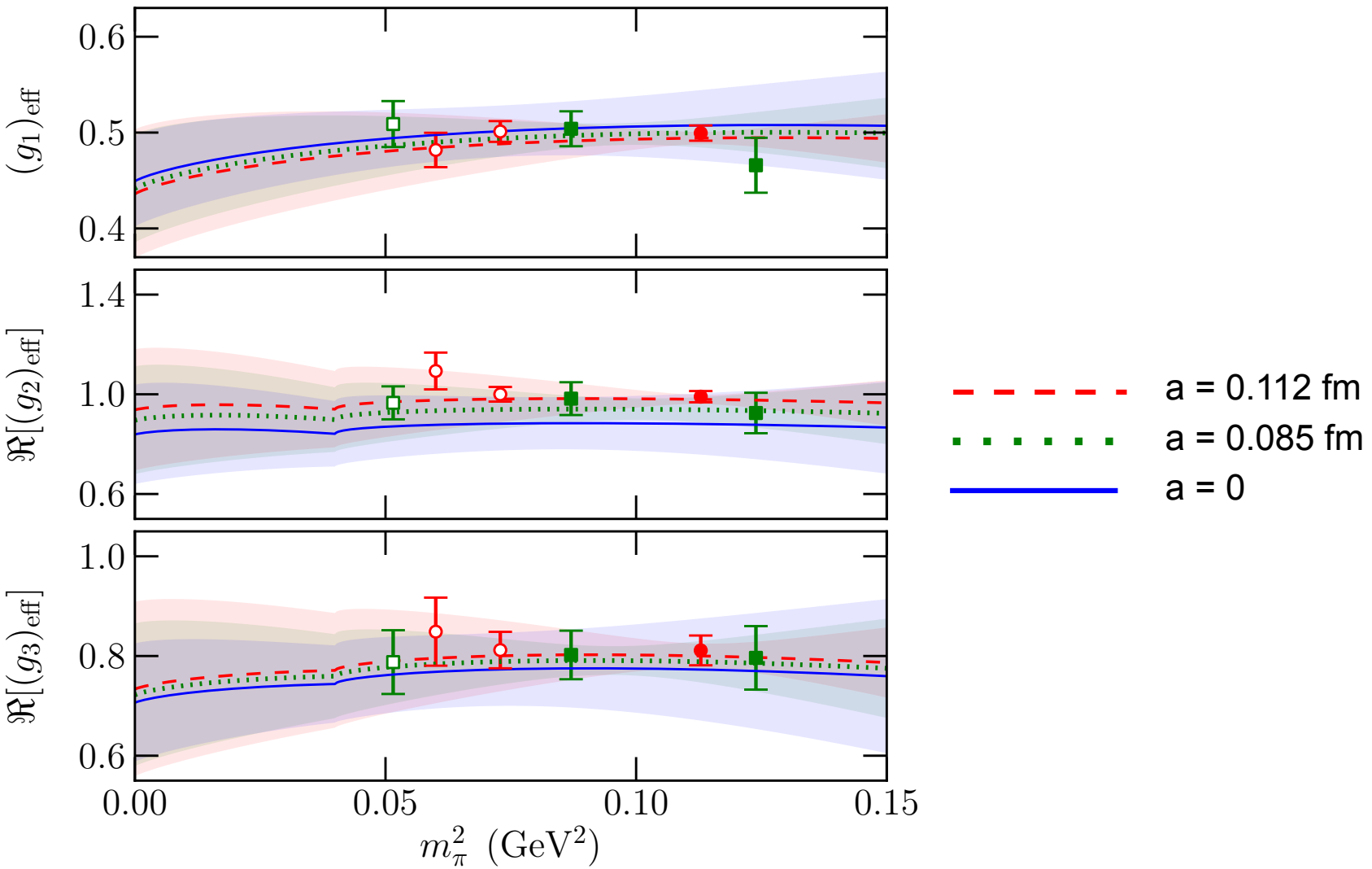

Final results for axial couplings

Final results:

$$
\begin{aligned}
g_1 &= 0.449 \pm 0.047_{\text{stat}} \pm 0.019_{\text{syst}} &&= 0.449 \pm 0.051, \\
g_2 &= 0.84 \pm 0.20_{\text{stat}} \pm 0.04_{\text{syst}} &&= 0.84 \pm 0.20, \\
g_3 &= 0.71 \pm 0.12_{\text{stat}} \pm 0.04_{\text{syst}} &&= 0.71 \pm 0.13.
\end{aligned}
$$

Systematic uncertainties:

Source	g_1	g_2	g_3
NNLO terms in fits of m_π- and a-dep	3.6%	2.8%	3.7%
Higher excited states in fits to $R_i(t)$	1.7%	2.8%	4.9%
Unphysical value of $m_s^{(\text{sea})}$	1.5%	1.5%	1.5%
Total	4.2%	4.3%	6.3%

g_1: comparison with previous lattice results

Reference	n_f, action	$[m_\pi^{(vv)}]^2$ (GeV^2)	g_1
De Divitiis *et al.*, 1998	0, clover	0.58 - 0.81	$0.42 \pm 0.04 \pm 0.08$
Abada *et al.*, 2004	0, clover	0.30 - 0.71	$0.48 \pm 0.03 \pm 0.11$
Negishi *et al.*, 2007	0, clover	0.43 - 0.72	0.517 ± 0.016
Ohki *et al.*, 2008	2, clover	0.24 - 1.2	$0.516 \pm 0.005 \pm 0.033 \pm 0.028$
Bećirević *et al.*, 2009	2, clover	0.16 - 1.2	$0.44 \pm 0.03^{+0.07}_{-0.00}$
Bulava *et al.*, 2010	2, clover	0.063 - 0.49	0.51 ± 0.02
This work	$2+1$, DW	0.052 - 0.12	$0.449 \pm 0.047_{\text{stat}} \pm 0.019_{\text{syst}}$

Note: none of the previous works use correct NLO χPT (linear extrapolation or tadpole missing)

Impact of NLO χPT corrections

In $SU(2)$:

Strong decay: $\mathcal{M}(P^* \to P\,\pi) \propto g_1 \left[1 - 4g_1^2 \frac{m_\pi^2}{(4\pi f_\pi)^2} \log \frac{m_\pi^2}{\mu^2} + \tilde{c}\, m_\pi^2\right]$.

Axial current m. elt.: $(g_1)_{\text{eff}} = g_1 \left[1 - (2 + 4g_1^2) \frac{m_\pi^2}{(4\pi f_\pi)^2} \log \frac{m_\pi^2}{\mu^2} + c\, m_\pi^2\right]$.

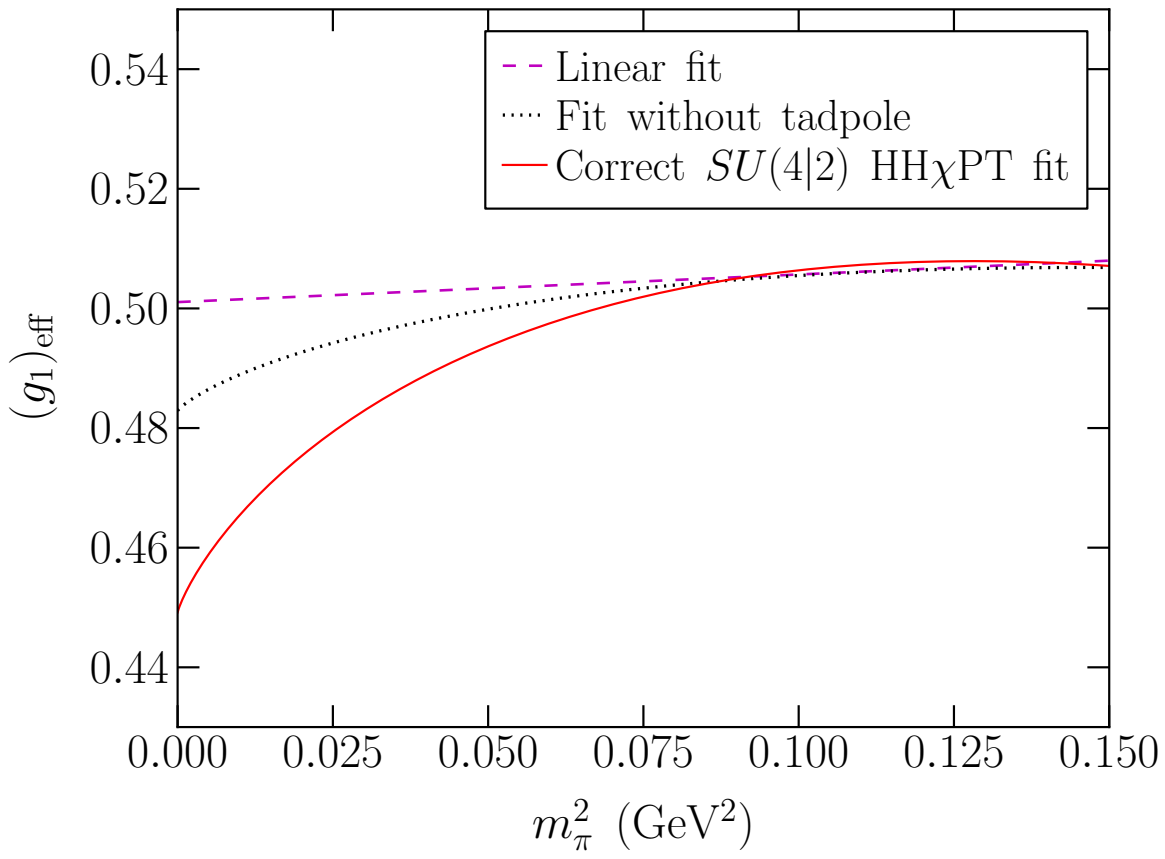

Comparison with other results

Reference	Method	g_1	g_2	g_3
Yan *et al.*, 1992	Nonrelativistic quark model	1	2	$\sqrt{2}$
Colangelo *et al.*, 1994	Relativistic quark model	$1/3$	...	...
Bećirević, 1999	Quark model with Dirac eq.	0.6 ± 0.1	...	...
Guralnik *et al.*, 1992	Skyrme model	...	1.6	1.3
Colangelo *et al.*, 1994	Sum rules	0.15 - 0.55	...	...
Belyaev *et al.*, 1994	Sum rules	0.32 ± 0.02	...	...
Dosch and Narison, 1995	Sum rules	0.15 ± 0.03	...	...
Colangelo and Fazio, 1997	Sum rules	0.09 - 0.44	...	...
Pirjol and Yan, 1997	Sum rules	...	$< \sqrt{6 - g_3^2}$	$< \sqrt{2}$
Zhu and Dai, 1998	Sum rules	...	$1.56 \pm 0.30 \pm 0.30$	$0.94 \pm 0.06 \pm 0.20$
Cho and Georgi, 1992	$\mathcal{B}[D^* \to D\,\pi, D\,\gamma]$	0.34 ± 0.48	...	...
Stewart, 1998	$\mathcal{B}[D^*_{(s)} \to D_{(s)}\pi, D_{(s)}\gamma]$	$0.27^{+0.04+0.05}_{-0.02-0.02}$	...	...
Li *et al.*, 2010	$d\Gamma[B \to \pi\ell\nu]$	< 0.87	...	...
Cheng, 1997	$\Gamma[\Sigma_c^* \to \Lambda_c\,\pi]$, NRQM	0.70 ± 0.12	1.40 ± 0.24	0.99 ± 0.17
This work	Lattice QCD	0.449 ± 0.051	0.84 ± 0.20	0.71 ± 0.13

Our QCD results are MUCH smaller than the quark-model predictions (even for $g_A^{ud} = 0.75$, as needed to get correct nucleon g_A)

Heavy baryon decays

$S \to T$ strong decays: leading-order width

At LO in chiral and heavy quark expansion, HHχPT predicts

$$\Gamma[S \to T\,\pi] = c_{\rm f}^2\,\frac{1}{6\pi f_\pi^2}\,g_3^2\,\frac{M_T}{M_S}\,|\mathbf{p}_\pi|^3$$

where

$$c_{\rm f} = \begin{cases} 1 & \text{for} \quad \Sigma_Q^{(*)} \to \Lambda_Q\,\pi^\pm, \\ 1 & \text{for} \quad \Sigma_Q^{(*)} \to \Lambda_Q\,\pi^0, \\ 1/\sqrt{2} & \text{for} \quad \Xi_Q^{\prime(*)} \to \Xi_Q\,\pi^\pm, \\ 1/2 & \text{for} \quad \Xi_Q^{\prime(*)} \to \Xi_Q\,\pi^0, \end{cases}$$

and

$$|\mathbf{p}_\pi| = \frac{\sqrt{[(M_S - M_T)^2 - m_\pi^2][(M_S + M_T)^2 - m_\pi^2]}}{2M_S}$$

(kinematic factors not expanded in $1/m_Q$ here)

$S \to T$ strong decays: including $1/m_Q$ correction

LO in chiral expansion is precice enough, because physical m_π is so small.

LO in HQ expansion is not good enough. Include generic $1/m_Q$ correction

$$\Gamma[S \to T\,\pi] = c_{\mathrm{f}}^2\,\frac{1}{6\pi f_\pi^2}\left(g_3 + \frac{\kappa_J}{m_Q}\right)^2 \frac{M_T}{M_S}\,|\mathbf{p}_\pi|^3$$

Determine $\kappa_{1/2}$ and $\kappa_{3/2}$ by fitting experimental data for Σ_c^{++}, Σ_c^0 and Σ_c^{*++}, Σ_c^{*0} with g_3 constrained to LQCD value, and $m_Q = \frac{1}{2}M_{J/\psi}$.

$S \to T$ strong decays: including $1/m_Q$ correction

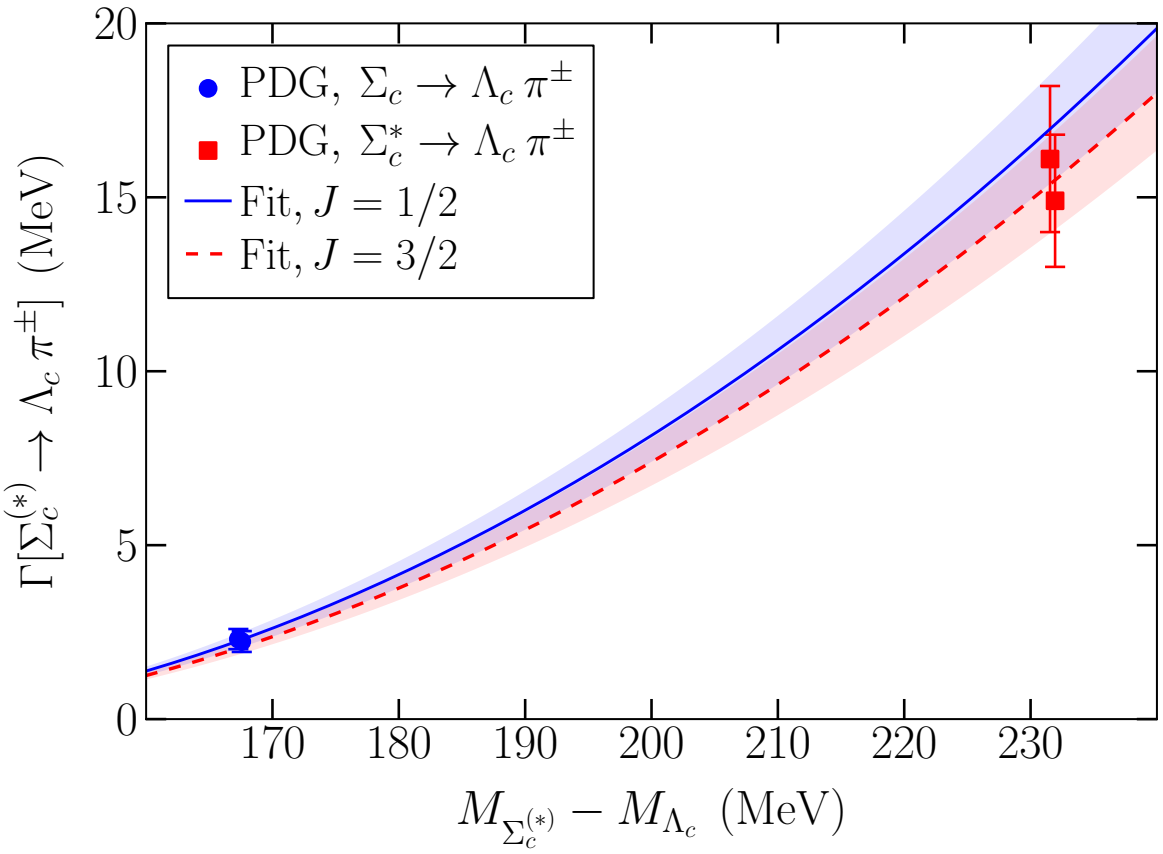

Result:

$$\kappa_{1/2} = 0.55(21)\ \text{GeV}, \quad \text{Cov}(\kappa_{1/2},\, g_3) = -0.025\ \text{GeV},$$
$$\kappa_{3/2} = 0.47(21)\ \text{GeV}, \quad \text{Cov}(\kappa_{3/2},\, g_3) = -0.025\ \text{GeV}.$$

$S \to T$ strong decays: including $1/m_Q$ correction

Effective coupling vs $1/m_Q$:

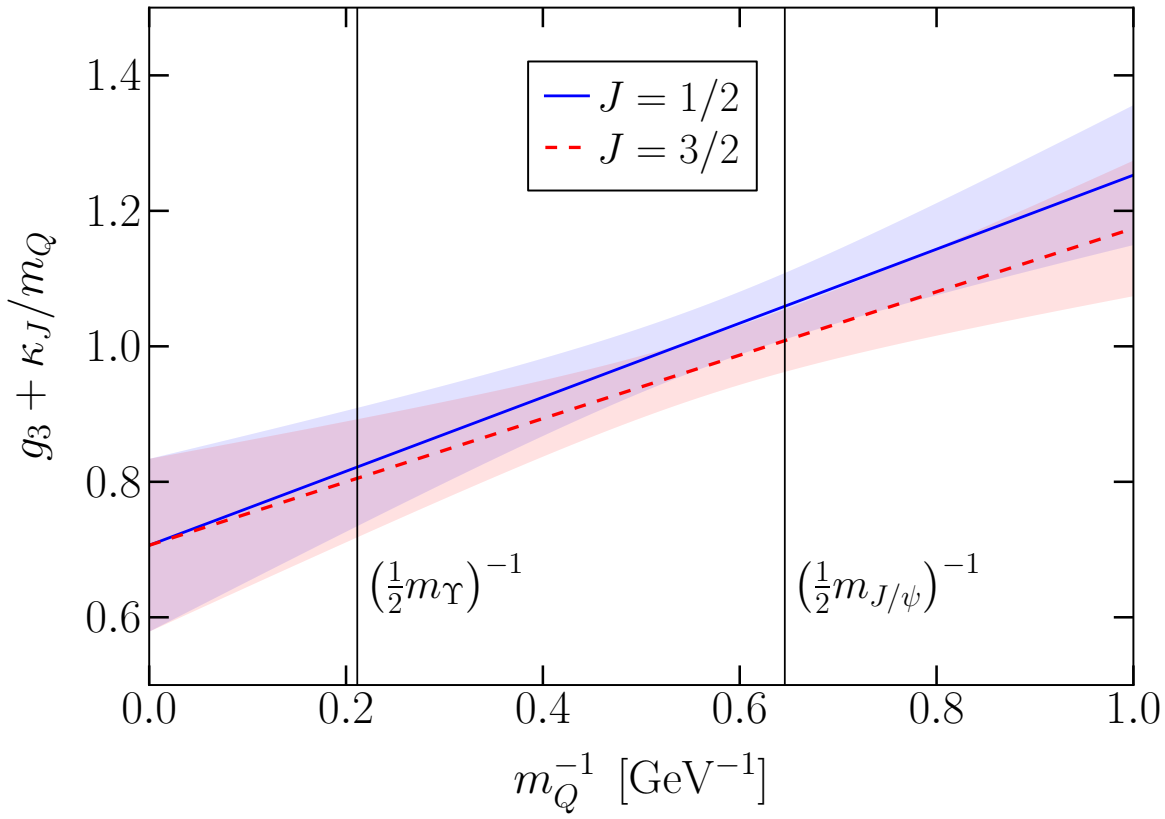

$\to$ Evaluate for $m_Q = \frac{1}{2}M_\Upsilon$ to make predictions for bottom baryons

$S \to T$ strong decays: predictions for bottom baryons

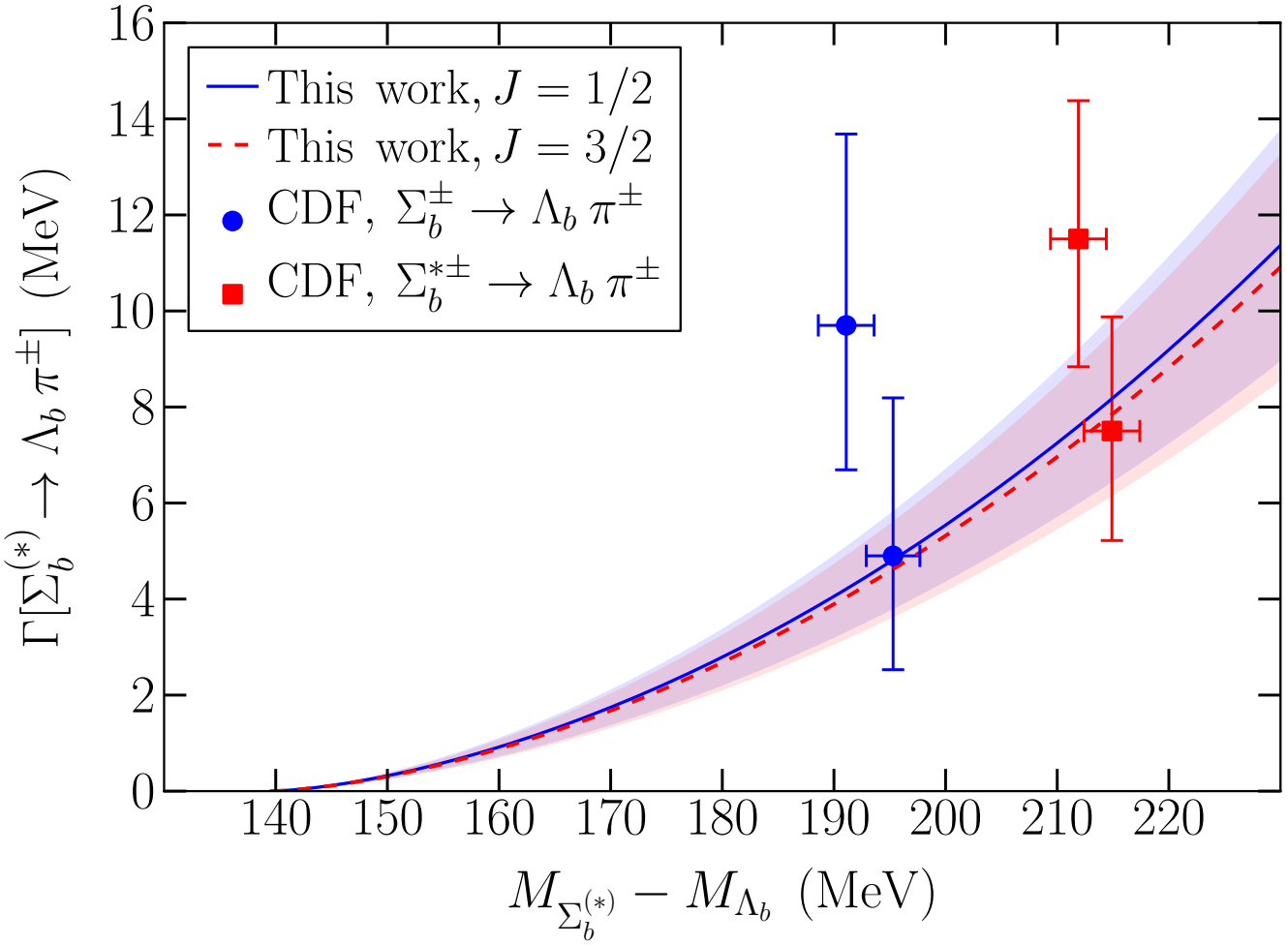

Also: Ξ_b^{*0}, recently discovered by CMS

$\Gamma[\Xi_b^{*0}] = 2.1 \pm 1.7$ MeV (CMS), $\Gamma[\Xi_b^{*0}] = 0.51 \pm 0.26$ MeV (this work)

Conclusions

- First complete lattice QCD determination of heavy-hadron axial couplings, Results are $g_1 = 0.449 \pm 0.051$, $g_2 = 0.84 \pm 0.20$, $g_3 = 0.71 \pm 0.13$
- Systematic uncertainties very small, statistical uncertainties by far dominant
- Chiral expansion of axial-current matrix elements well-behaved here, better than for light baryons
- g_1, g_2, g_3 are much smaller than NRQM prediction, but ratios close to NRQM
- Compare to $g_A \approx 1.26$, $|g_{N\Delta}| \sim 1.6$ and $g_{\Delta\Delta} \sim -1.9$
- $1/m_Q$ corrections in $\Gamma[\Sigma_Q^{(*)} \to \Lambda_Q \pi]$ are significant even for $Q = b$
- Calculated $\Gamma[\Sigma_b^{(*)} \to \Lambda_b \pi]$ widths agree with experiment
- Many future applications (e.g. chiral extrapolations for spectroscopy)

Extra slides

Systematic uncertainties from higher excited states

$$R_i(t) = (g_i)_{\text{eff}} - A_i\, e^{-\delta_i\, t}$$

Fit	$(g_1)_{\text{eff}}$	$\delta(g_1)_{\text{eff}}$	$(g_2)_{\text{eff}}$	$\delta(g_2)_{\text{eff}}$	$(g_3)_{\text{eff}}$	$\delta(g_3)_{\text{eff}}$
Original	0.499(11)	0	0.993(29)	0	0.810(36)	0
$t/a = 4$ removed	0.496(13)	0.0030(76)	0.975(35)	0.016(19)	0.783(43)	0.026(15)
$t/a = 4, 5$ removed	0.494(12)	0.0041(76)	0.984(41)	0.009(26)	0.807(54)	0.003(30)
Second exp. added	0.498(11)	0.0009(77)	0.988(30)	0.005(21)	0.796(40)	0.014(36)

Conservative estimate of uncertainty:

$$\sqrt{[\delta(g_i)_{\text{eff}}]^2 + [\sigma\delta(g_i)_{\text{eff}}]^2}$$

g_1 : 1.7%
g_2 : 2.8%
g_3 : 4.9%

Summation Method

Summed ratio:

$$S_i(t) = a \sum_{t'=0}^{t} R_i(t,\ t')$$

For large t:

$$S_i(t) \to c_i + (g_i)_{\text{eff}}\ t$$

Use slope to extract $(g_i)_{\text{eff}}$:

$$R_i^{\text{sum}}(t) = \frac{\mathrm{d}}{\mathrm{d}t} S_i(t)$$

Expect (if off-diagonal excited state contrib $\neq 0$):

$$\begin{aligned} R_i(t) - (g_i)_{\text{eff}} &= O(e^{-\frac{1}{2}\delta_i\ t}), \\ R_i^{\text{sum}}(t) - (g_i)_{\text{eff}} &= O(t\ e^{-\delta_i\ t}) \end{aligned}$$

[Maiani et al 1987, Gusken et al. 1989, Bulava et al. 2011]

Summation Method

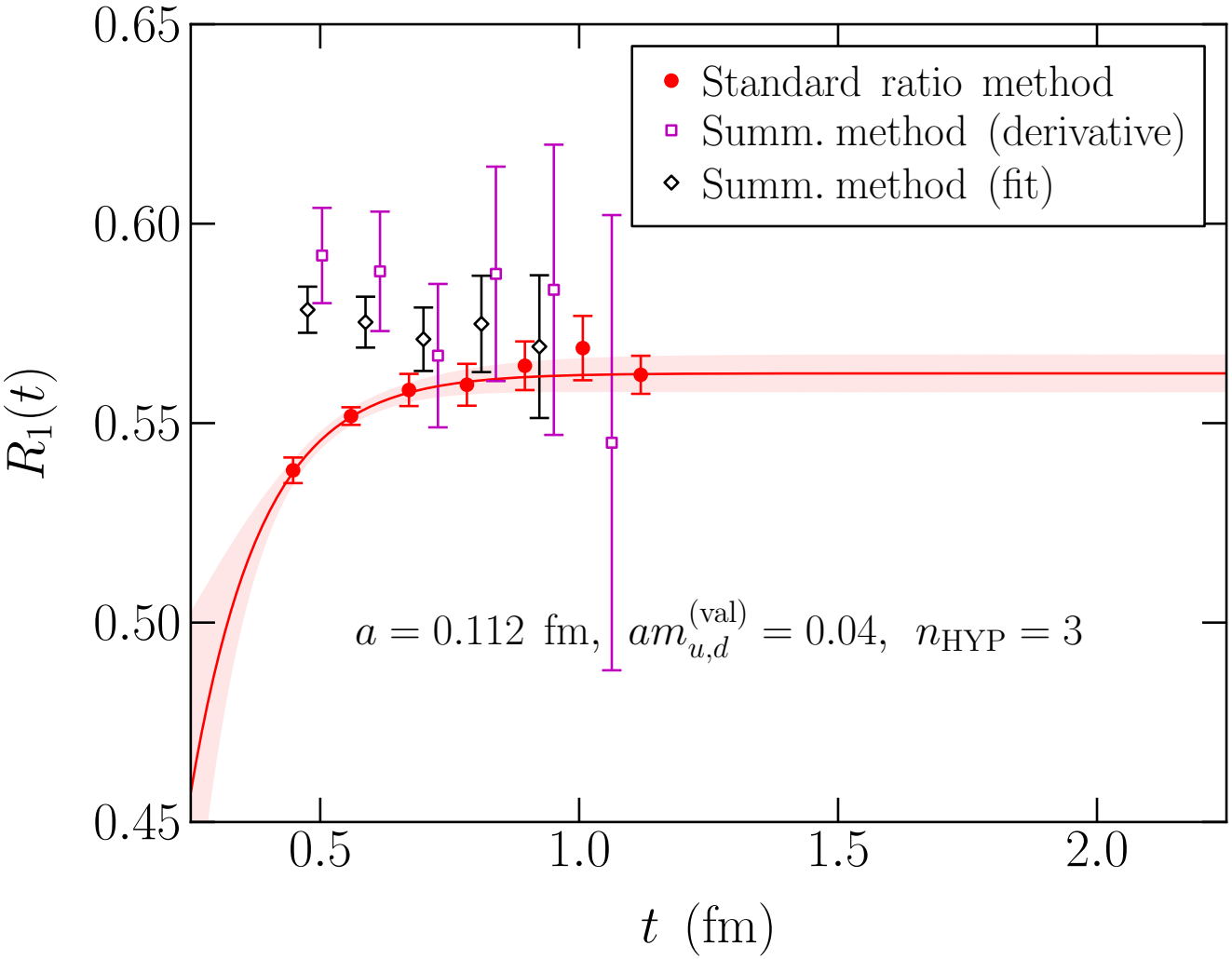

Summation Method

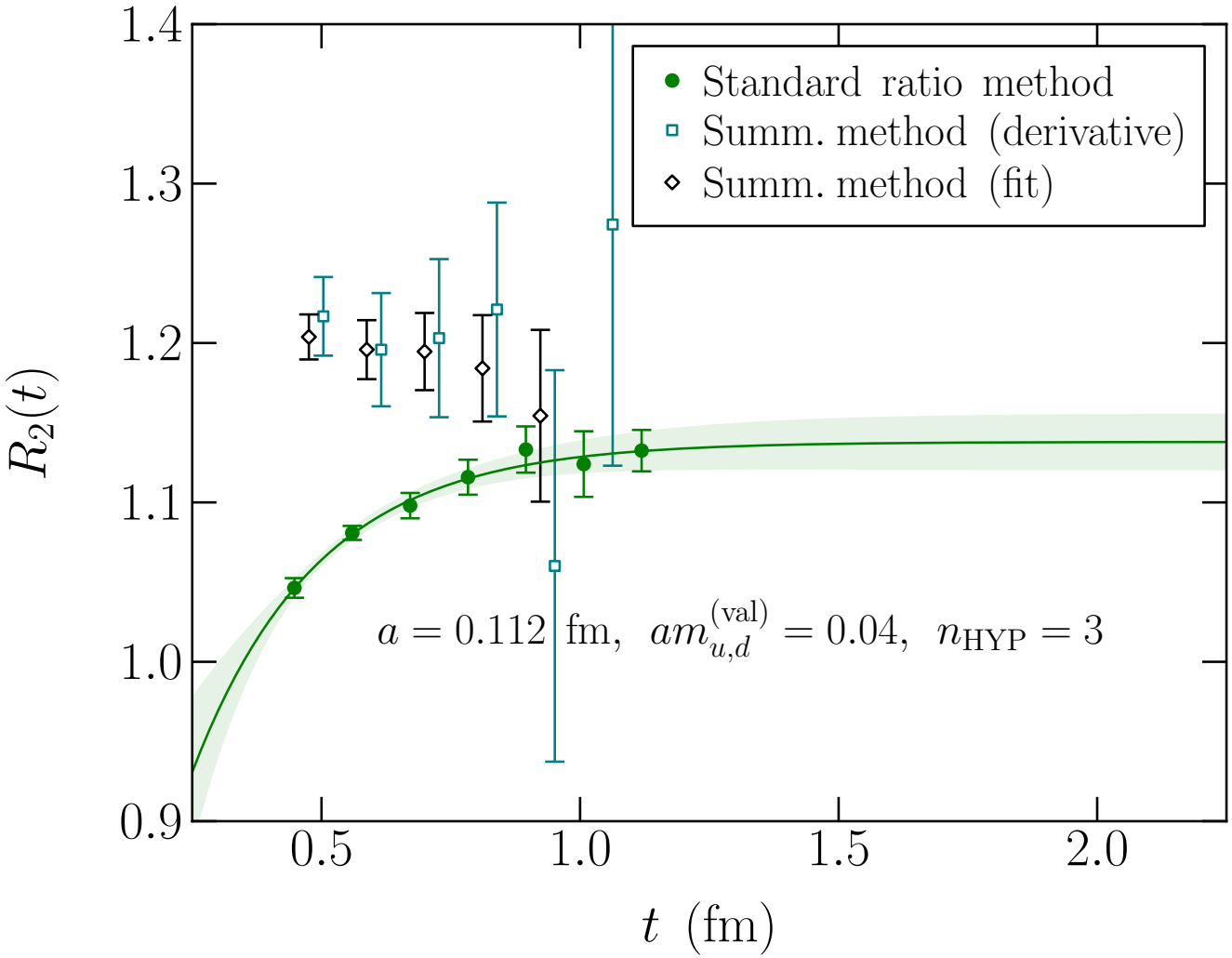

Fits using $SU(4|2)$ HHχPT: estimates of systematic uncertainties

Add higher-order analytic terms.

$$
\begin{aligned}
&(g_i)_{\text{eff}}^{(\text{NLO+HO})}(a, m, n_{\text{HYP}}) \\
&\quad = \quad (g_i)_{\text{eff}}^{(\text{NLO})}(a, m, n_{\text{HYP}}) \\
&\qquad + g_i \Bigg[c_i^{(\text{vv,vv})} \, [m_\pi^{(\text{vv})}]^4 + c_i^{(\text{vs,vs})} \, [m_\pi^{(\text{vs})}]^4 + c_i^{(\text{vv,vs})} \, [m_\pi^{(\text{vv})}]^2 [m_\pi^{(\text{vs})}]^2 \\
&\qquad\qquad + d_{i,\, n_{\text{HYP}}}^{(\text{vv})} \, a^2 \, [m_\pi^{(\text{vv})}]^2 + d_{i,\, n_{\text{HYP}}}^{(\text{vs})} \, a^2 \, [m_\pi^{(\text{vs})}]^2 + h_{i,\, n_{\text{HYP}}} \, a^4 \Bigg]
\end{aligned}
$$

Fits using $SU(4|2)$ HHχPT: estimates of systematic uncertainties

Constrain with Gaussian priors. In terms of the natural scales,

$$
\begin{aligned}
c_i^{(\mathrm{vv,vv})} &= 0 \pm w/\Lambda_\chi^4, \\
c_i^{(\mathrm{vs,vs})} &= 0 \pm w/\Lambda_\chi^4, \\
c_i^{(\mathrm{vv,vs})} &= 0 \pm w/\Lambda_\chi^4, \\
d_{i,\, n_{\mathrm{HYP}}}^{(\mathrm{vv})} &= 0 \pm w\, \Lambda_{\mathrm{QCD}}^2/\Lambda_\chi^2, \\
d_{i,\, n_{\mathrm{HYP}}}^{(\mathrm{vs})} &= 0 \pm w\, \Lambda_{\mathrm{QCD}}^2/\Lambda_\chi^2, \\
h_{i,\, n_{\mathrm{HYP}}} &= 0 \pm w\, \Lambda_{\mathrm{QCD}}^4.
\end{aligned}
$$

w is the width

Fits using $SU(4|2)$ HHχPT: estimates of systematic uncertainties

w	g_1	$\delta\sigma(g_1)$	g_2	$\delta\sigma(g_2)$	g_3	$\delta\sigma(g_3)$
0	0.449(47)	0	0.84(20)	0	0.71(12)	0
1	0.449(47)	0.0020	0.84(20)	0.0023	0.71(12)	0.0045
5	0.452(48)	0.0089	0.84(20)	0.014	0.70(12)	0.017
10	0.455(50)	0.016	0.84(20)	0.024	0.70(12)	0.026
50	0.464(72)	0.054	0.82(22)	0.099	0.68(15)	0.094
100	0.452(94)	0.082	0.78(26)	0.17	0.63(21)	0.17

Conservative estimate: with $w = 10$, use

$$\delta\sigma(g_i) = \sqrt{\sigma^2(g_i)^{(\mathrm{NLO+HO})} - \sigma^2(g_i)^{(\mathrm{NLO})}}$$

g_1 : 3.6%
g_2 : 2.8%
g_3 : 3.7%

Fits using $SU(4|2)$ HHχPT: finite-volume corrections

$m_\pi^{(\mathrm{vs})}$ (MeV)	$m_\pi^{(\mathrm{vv})}$ (MeV)	$\frac{(g_1)_{\mathrm{eff}}^{(\infty)}-(g_1)_{\mathrm{eff}}^{(L)}}{(g_1)_{\mathrm{eff}}^{(\infty)}}$	$\frac{(g_2)_{\mathrm{eff}}^{(\infty)}-(g_2)_{\mathrm{eff}}^{(L)}}{(g_2)_{\mathrm{eff}}^{(\infty)}}$	$\frac{(g_3)_{\mathrm{eff}}^{(\infty)}-(g_3)_{\mathrm{eff}}^{(L)}}{(g_3)_{\mathrm{eff}}^{(\infty)}}$
294	245	0.0057	0.015	0.0074
304	270	0.0040	0.0070	0.0027
336	336	0.0016	0.00037	−0.00079
263	227	0.0072	0.028	0.013
295	295	0.0031	0.00027	−0.0012
352	352	0.0013	0.00033	−0.00071

New fermion discretizations and their applications

Tatsuhiro MISUMI (*BNL*)

In collaborations with M.Creutz(*BNL*), T.Kimura(*RIKEN*), A.Ohnishi(*YITP),*
S. Sharpe (*Washington*), S. Aoki(*Tsukuba*)

05/14/2012 NHCF workshop@BNL

Table of contents

1. Flavored mass 2-flavor QCD

2. Central branch Many-flavor QCD

3. Flavored chemical potential Finite (T, μ) QCD

Naive

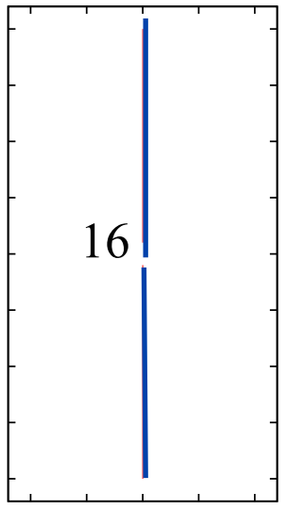

$$\sum_{\mu} C_\mu$$

$$C_\mu = (T_{+\mu} + T_{-\mu})/2$$
$$T_{\pm\mu}\psi_n = U_{n,\pm\mu}\psi_{n\pm\mu}$$

U(4)×U(4)

Wilson

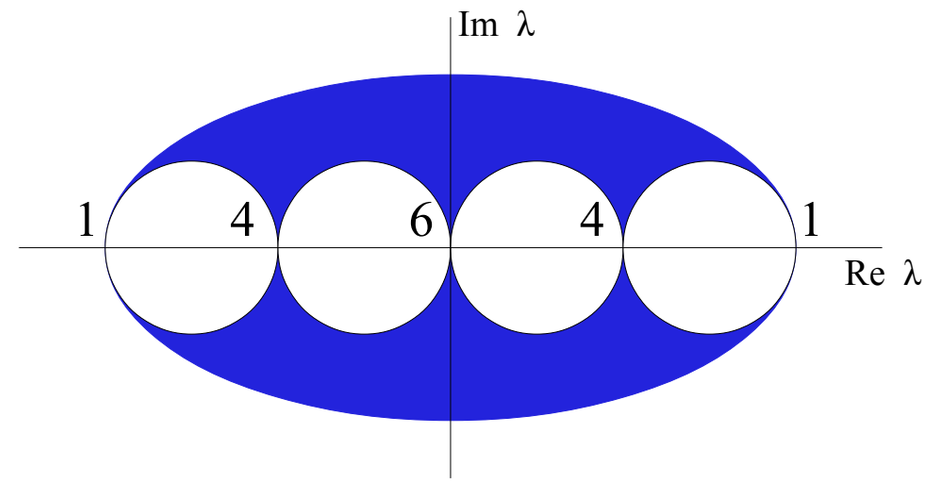

Naive

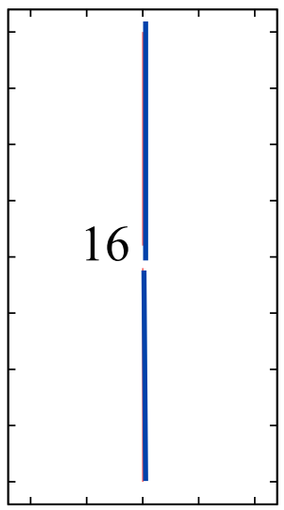

$$\sum_{\mu} C_\mu$$

$$C_\mu = (T_{+\mu} + T_{-\mu})/2$$
$$T_{\pm\mu}\psi_n = U_{n,\pm\mu}\psi_{n\pm\mu}$$

Wilson

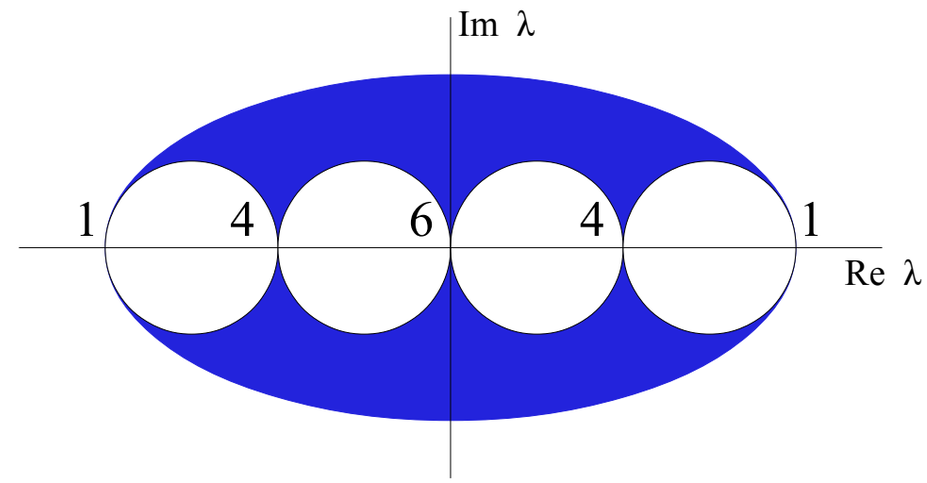

U(4)×U(4)

$$\Gamma_X^{(+)} \in \left\{ \mathbf{1}_4\,,\ (-1)^{n_1+\ldots+n_4}\gamma_5\,,\ (-1)^{\check{n}_\mu}\gamma_\mu\,,\ (-1)^{n_\mu} i\gamma_\mu\gamma_5\,,\ (-1)^{n_{\mu,\nu}}\frac{[\gamma_\mu\,,\gamma_\nu]}{2} \right\}$$
$$\Gamma_X^{(-)} \in \left\{ (-1)^{n_1+\ldots+n_4}\mathbf{1}_4\,,\ \gamma_5\,,\ (-1)^{n_\mu}\gamma_\mu\,,\ (-1)^{\check{n}_\mu}\gamma_\mu\gamma_5\,,\ (-1)^{\check{n}_{\mu,\nu}}\frac{[\gamma_\mu\,,\gamma_\nu]}{2} \right\}$$

$$\psi_n \to \psi_n' = \exp\left[\mathrm{i}\sum_X \left(\theta_X^{(+)}\Gamma_X^{(+)} + \theta_X^{(-)}\Gamma_X^{(-)}\right)\right]\psi_n\,, \qquad \bar{\psi}_n \to \bar{\psi}_n' = \bar{\psi}_n \exp\left[\mathrm{i}\sum_X \left(-\theta_X^{(+)}\Gamma_X^{(+)} + \theta_X^{(-)}\Gamma_X^{(-)}\right)\right]$$

Naive

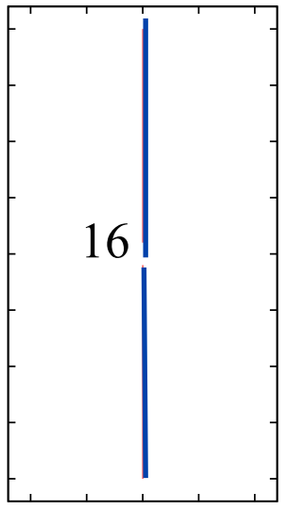

$$\sum_{\mu} C_\mu$$

$$C_\mu = (T_{+\mu} + T_{-\mu})/2$$
$$T_{\pm\mu}\psi_n = U_{n,\pm\mu}\psi_{n\pm\mu}$$

Wilson

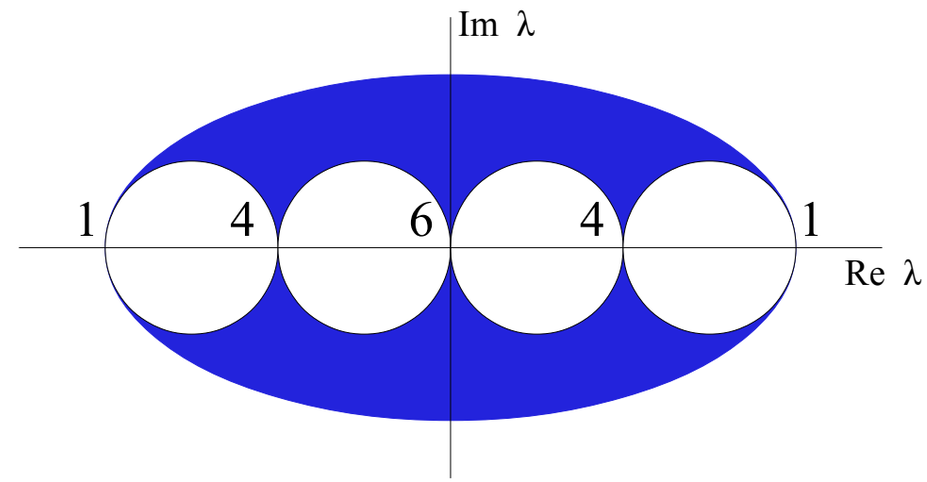

U(4)×U(4) → U(1)

$$\Gamma_X^{(+)} \in \left\{ \mathbf{1}_4 , \right\}$$
$$\Gamma_X^{(-)} \in \left\{ \right\}$$

Naive

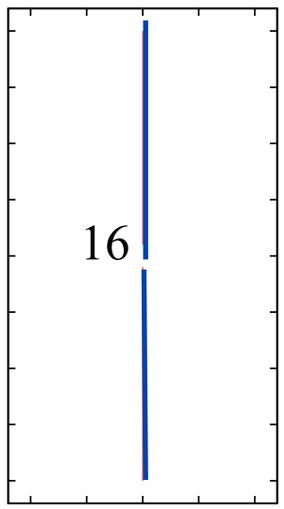

$$\sum_{sym.} C_1 C_2 C_3 C_4$$

$$C_\mu = (T_{+\mu} + T_{-\mu})/2$$
$$T_{\pm\mu}\psi_n = U_{n,\pm\mu}\psi_{n\pm\mu}$$

Wilson'

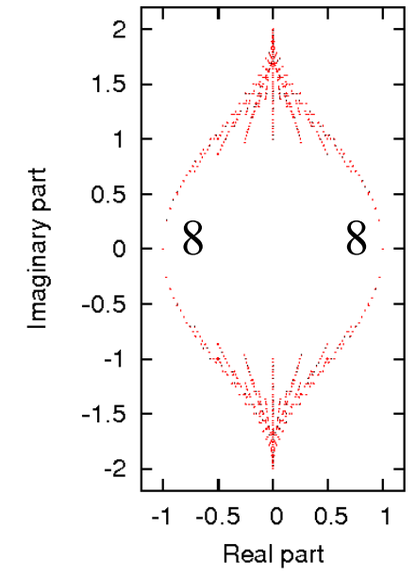

Creutz, Kimura, Misumi(2010)

U(4)×U(4) → U(2)×U(2) Lehner, Misumi(2012)

$$\Gamma_X^{(+)} \in \left\{ \mathbf{1}_4\,,\ (-1)^{n_1+\ldots+n_4}\gamma_5\,,\ (-1)^{n_{\mu,\nu}}\frac{[\gamma_\mu\,,\gamma_\nu]}{2} \right\}$$

$$\Gamma_X^{(-)} \in \left\{ \qquad \right\}$$

1. Flavored mass

Creutz, Kimura, Misumi(2010)

$$M_{\rm V} = \sum_{\mu} C_{\mu},$$ *Vector (1-link)*

$$M_{\rm T} = \sum_{perm.} \sum_{sym.} C_{\mu} C_{\nu},$$ *Tensor (2-link)*

$$M_{\rm A} = \sum_{perm.} \sum_{sym.} \prod_{\nu} C_{\nu},$$ *Axial-V (3-link)*

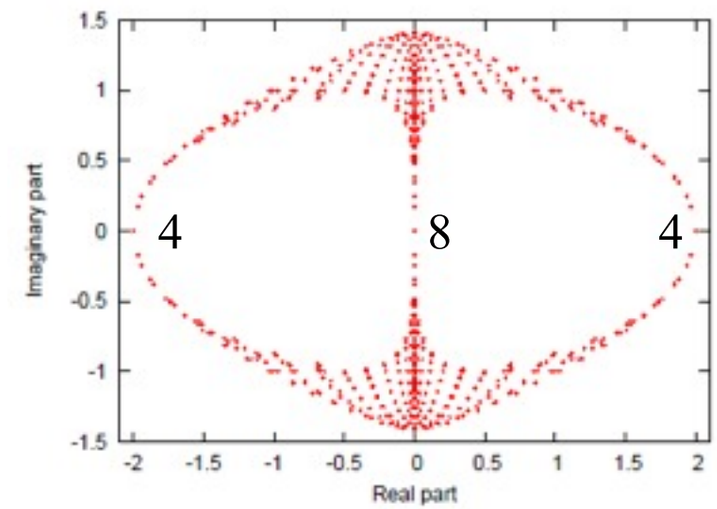

$$M_{\rm P} = \sum_{sym.} \prod_{\mu=1}^{4} C_{\mu},$$ *Pseudo-S (4-link)*

- *gamma-5 hermiticity*
- *2nd derivative terms* $\sum_n \bar{\psi}_n (M_P - 1)\psi_n \;\rightarrow\; -a \int d^4x \bar{\psi}(x) D_\mu^2 \psi(x) + O(a^2)$
- *Cousins of Wilson fermion*

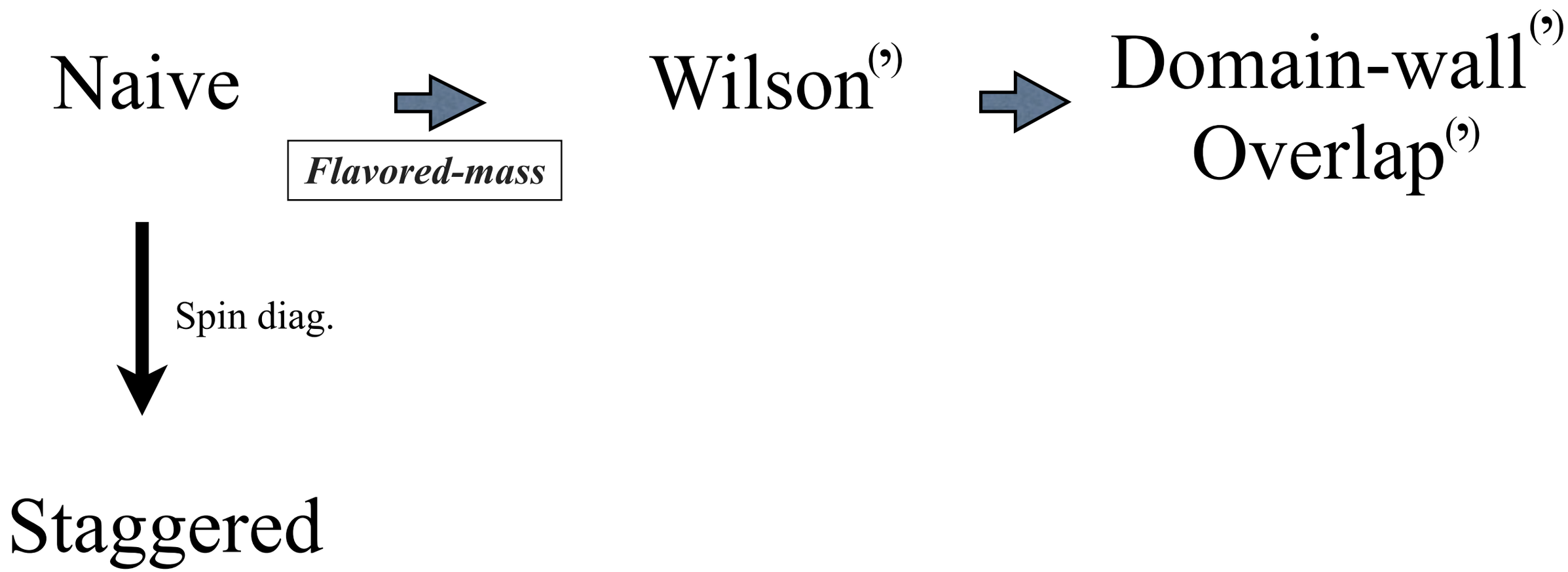
Naive
Flavored-mass
Wilson(')
Domain-wall(')
Overlap(')
Spin diag.
Staggered

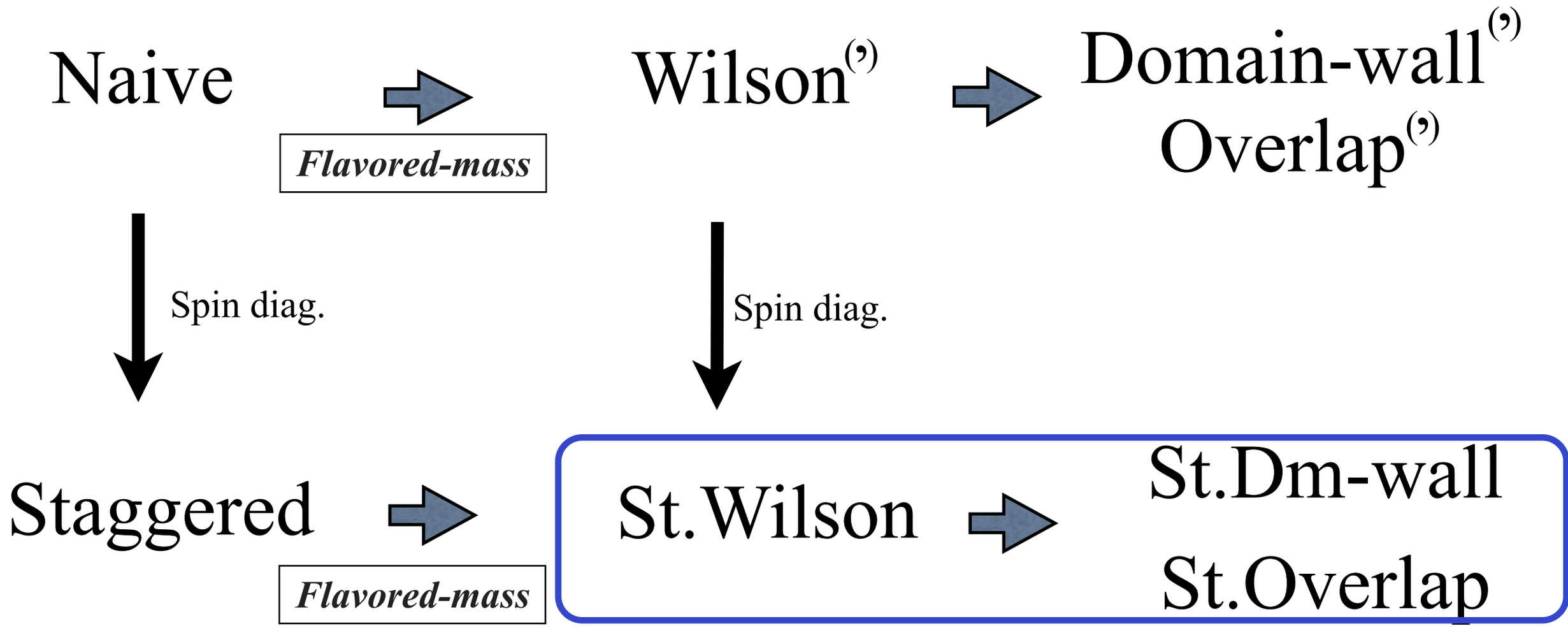
Naive
Flavored-mass
Wilson(')
Domain-wall(')
Overlap(')
Spin diag.
Spin diag.
Staggered
Flavored-mass
St.Wilson
St.Dm-wall
St.Overlap

◆Staggered-Wilson

$$\bar{\psi}_x C_1 C_2 C_3 C_4 \psi_x \xrightarrow[\text{spin diag.}]{} \pm\bar{\chi}_x(\epsilon\eta_1\eta_2\eta_3\eta_4 C_1 C_2 C_3 C_4)\chi_x$$

Staggered flavored-mass

Golterman, Smit (1984) Adams(2009)

$M_{\rm P}$

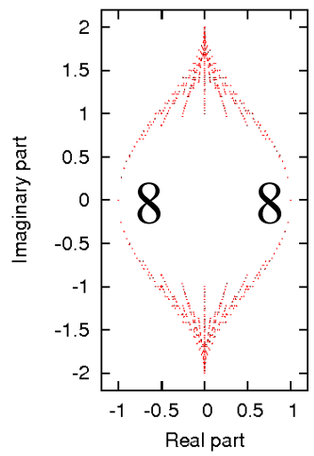

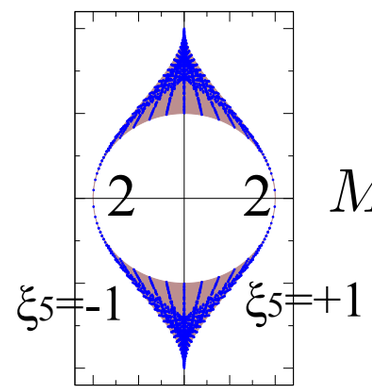

$M_{\mathcal{A}} \sim (\mathbf{1} \otimes \xi_5)$

- With mass shift

  ξ_5=-1 → physical sector : ℓ

  ξ_5=+1 → decoupled sector : h

- Index theorem Adams (09), Creutz,Kimura,Misumi(10), Follana, et.al.(11)
- Aoki phase Creutz, Kimura Misumi (11)

Spectral flow

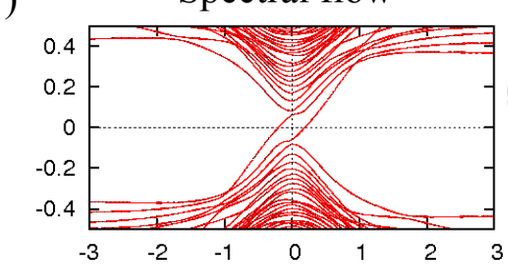

Aoki phase

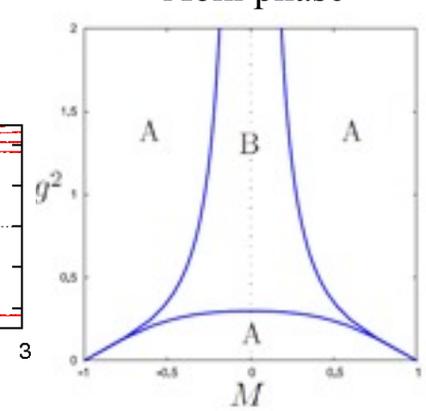

§ Potential advantages of $\eta_\mu D_\mu + r(1 + M_{\mathcal{A}})$

- could reduce numerical costs in 2-flavor overlap de Forcrand, Kurkela, Panero(2012)
- could reduce influence of taste-breaking for 2-flavor Sharpe (2012)

→ Look into symmetries and pion spectrum !

§ Staggered sym.

$\{C_0,\, \Xi_\mu,\, I_s,\, R_{\mu\nu}\} \;\times\; \{U^\epsilon(1)\}_{m=0} \Rightarrow \{C_0, \Xi_j, I_s, R_{ij}\}$

Transfer-matrix sym.

⇒ classify 15 pseudoscalar operators Golterman (1986)

$\mathbf{1} \;:\; \xi_4,\, \xi_{45},\, \xi_5,$

$\mathbf{3} \;:\; \xi_i,\, \xi_{i5},\, \xi_{ij}\, \xi_{i4}$

7 irreps

cf.) ChPT by Lee, Sharpe (1999)

4 irreps of SO(4) upto $O(a^4),\, O(a^2 m)\;\; O(a^2 p^2)$

$\mathbf{1} \;:\; \xi_5,$

$\mathbf{4} \;:\; \xi_\mu,\, \xi_{\mu 5},$

$\mathbf{6} \;:\; \xi_{\mu\nu}.$

§ Staggered-Wilson

$\boxed{\{C_0, \Xi'_\mu, R_{\mu\nu}\}} \Rightarrow \{C_0, \Xi'_j, R_{ij}\}$ Transfer-matrix sym.

$C \quad P \quad SW_4$

Irreps mix in ξ_5 pairs

Physical sector

$\mathbf{1} \;\&\; \xi_5 \longrightarrow \bar{\ell}\ell,\; \bar{h}h \longrightarrow \boxed{\bar{\ell}(\gamma_5 \otimes \mathbf{1})\ell}\;\; \eta'$

⇒ $\xi_4 \;\&\; \xi_{45} \longrightarrow \bar{\ell}h\;,\; \bar{h}\ell$

$\xi_{i4} \;\&\; \xi_{i45} \longrightarrow \bar{\ell}\sigma_j\ell\;,\; \bar{h}\sigma_j h \longrightarrow \boxed{\bar{\ell}(\gamma_5 \otimes \sigma_i)\ell}\;\; \pi_0,\, \pi_\pm$ States in 3d irrep

$\xi_i \;\&\; \xi_{i5} \longrightarrow \bar{\ell}\sigma_j h\;,\; \bar{h}\sigma_j\ell$

Sharpe (2012)

Discrete symmetries seem sufficient for degenerate pion triplet!

cf.) ChPT → SU(2) restoration upto $O(a^4),\, O(a^2 m)\; O(a^2 p^2)$

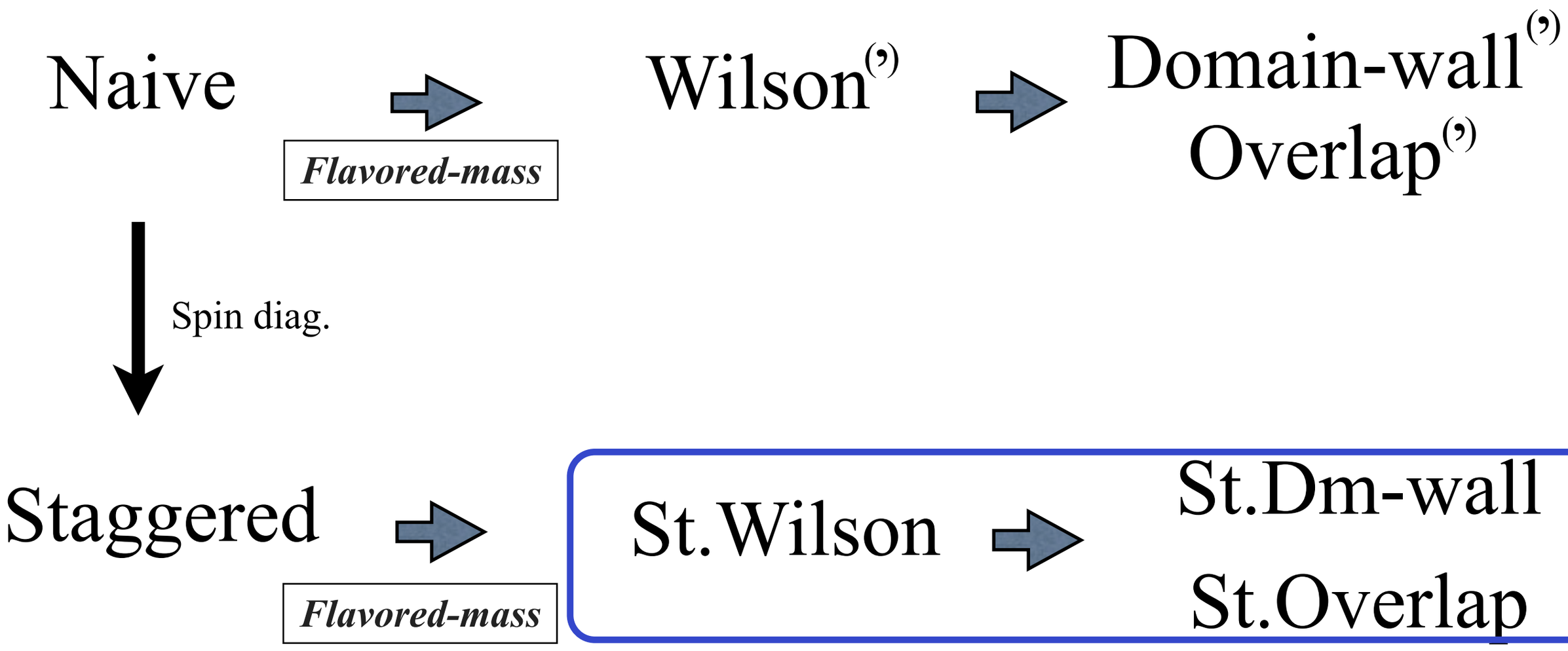
Naive
Flavored-mass
Wilson(')
Domain-wall(')
Overlap(')
Spin diag.
Staggered
Flavored-mass
St.Wilson
St.Dm-wall
St.Overlap

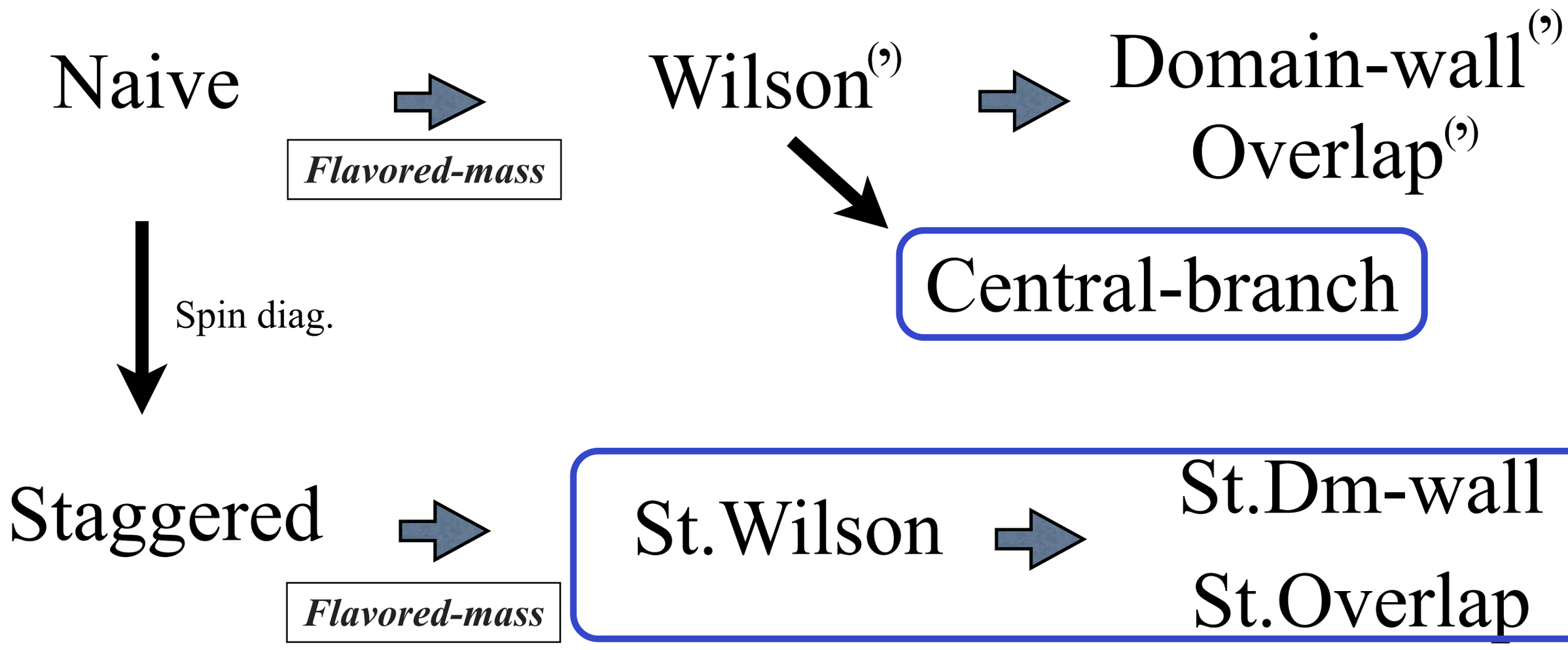
Naive
Flavored-mass
Wilson(')
Domain-wall(')
Overlap(')
Central-branch
Spin diag.
Staggered
Flavored-mass
St.Wilson
St.Dm-wall
St.Overlap

2. Central-branch

Creutz, Kimura, Misumi (2011)
Kimura, Komatsu, Misumi, Noumi, Torii, Aoki (2012)

- Wilson w/o onsite term $M_W \equiv m + 4r = 0$

$$S = \frac{1}{2}\sum_{x,\mu} \bar{\psi}_x [\gamma_\mu(\psi_{x+\mu} - \psi_{x-\mu}) - (\psi_{x+\mu} + \psi_{x-\mu})]$$

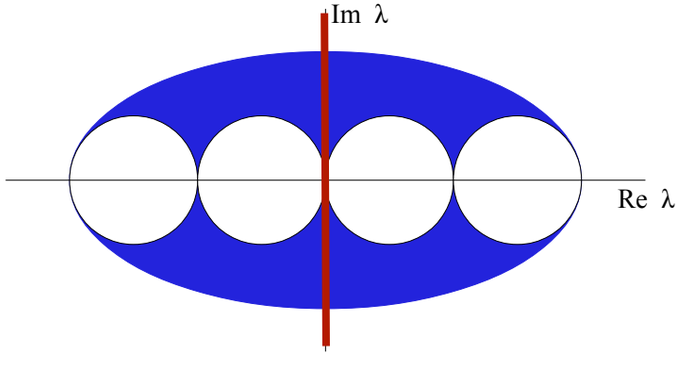

⇒ Another U(1) !

$$\psi_x \;\to\; e^{i\theta(-1)^{x_1+x_2+x_3+x_4}}, \quad \bar{\psi}_x \;\to\; \bar{\psi}_x e^{i\theta(-1)^{x_1+x_2+x_3+x_4}}$$

$$\Gamma_X^{(+)} \;\in\; \left\{ \mathbf{1}_4\,,\; (-1)^{n_1+\ldots+n_4}\gamma_5\,,\; (-1)^{\check{n}_\mu}\gamma_\mu\,,\; (-1)^{n_\mu} i\gamma_\mu\gamma_5\,,\; (-1)^{n_{\mu,\nu}}\frac{[\gamma_\mu\,,\gamma_\nu]}{2} \right\}$$

$$\Gamma_X^{(-)} \;\in\; \left\{ (-1)^{n_1+\ldots+n_4}\mathbf{1}_4\,,\; \gamma_5\,,\; (-1)^{n_\mu}\gamma_\mu\,,\; (-1)^{\check{n}_\mu}\gamma_\mu\gamma_5\,,\; (-1)^{\check{n}_{\mu,\nu}}\frac{[\gamma_\mu\,,\gamma_\nu]}{2} \right\}$$

2. Central-branch

Creutz, Kimura, Misumi (2011)
Kimura, Komatsu, Misumi, Noumi, Torii, Aoki (2012)

- Wilson w/o onsite term $M_W \equiv m + 4r = 0$

$$S = \frac{1}{2}\sum_{x,\mu} \bar{\psi}_x [\gamma_\mu(\psi_{x+\mu} - \psi_{x-\mu}) - (\psi_{x+\mu} + \psi_{x-\mu})]$$

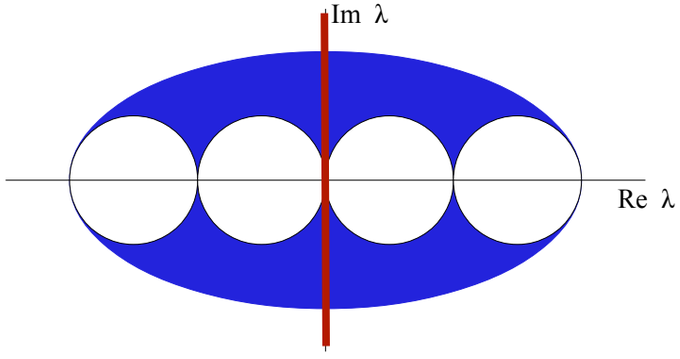

⇨ Another U(1) !

$$\psi_x \;\to\; e^{i\theta(-1)^{x_1+x_2+x_3+x_4}}, \quad \bar{\psi}_x \;\to\; \bar{\psi}_x e^{i\theta(-1)^{x_1+x_2+x_3+x_4}}$$

$$\Gamma_X^{(+)} \in \left\{ \mathbf{1}_4 , \right\}$$

$$\Gamma_X^{(-)} \in \left\{ \underline{(-1)^{n_1+\ldots+n_4}\mathbf{1}_4} , \right\}$$

Prohibits additive mass renormalization !
SSB gives NG boson !

◆ Strong-coupling QCD

$$\cosh(m_{SPA}) = 1 + \frac{2M_W^2(16 + M_W^2)}{16 - 15M_W^2}$$

NG boson associated with SSB of U(1)

- Pion (eta) condensate $\langle\bar{\psi}\gamma_5\psi\rangle \neq 0$
- No chiral condensate $\langle\bar{\psi}\psi\rangle = 0$

$$\bar{\psi}\psi \overset{?}{\leftrightarrow} \bar{\psi}\gamma_5\psi$$

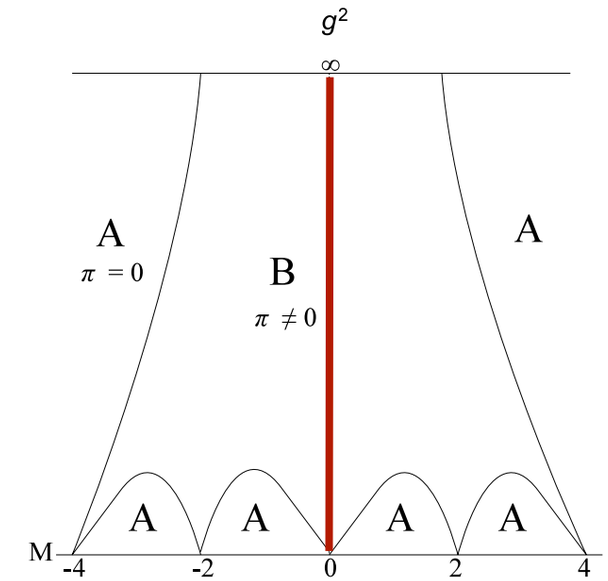

Aoki phase

§ Advantages

- No additive mass renormalization (no fine-tuning)
- SSB of U(1) and massless NG boson

$\bar{\psi}\psi \leftrightarrow \bar{\psi}\gamma_5\psi$ *change of mass base*

6-flavor massless QCD

§ Potential drawbacks

- sign problem
- U(1) problem
- Quark mass

⇒ Twisted-mass works ?

→ *12-flavor massless QCD*

New possibility of many-flavor lattice QCD !

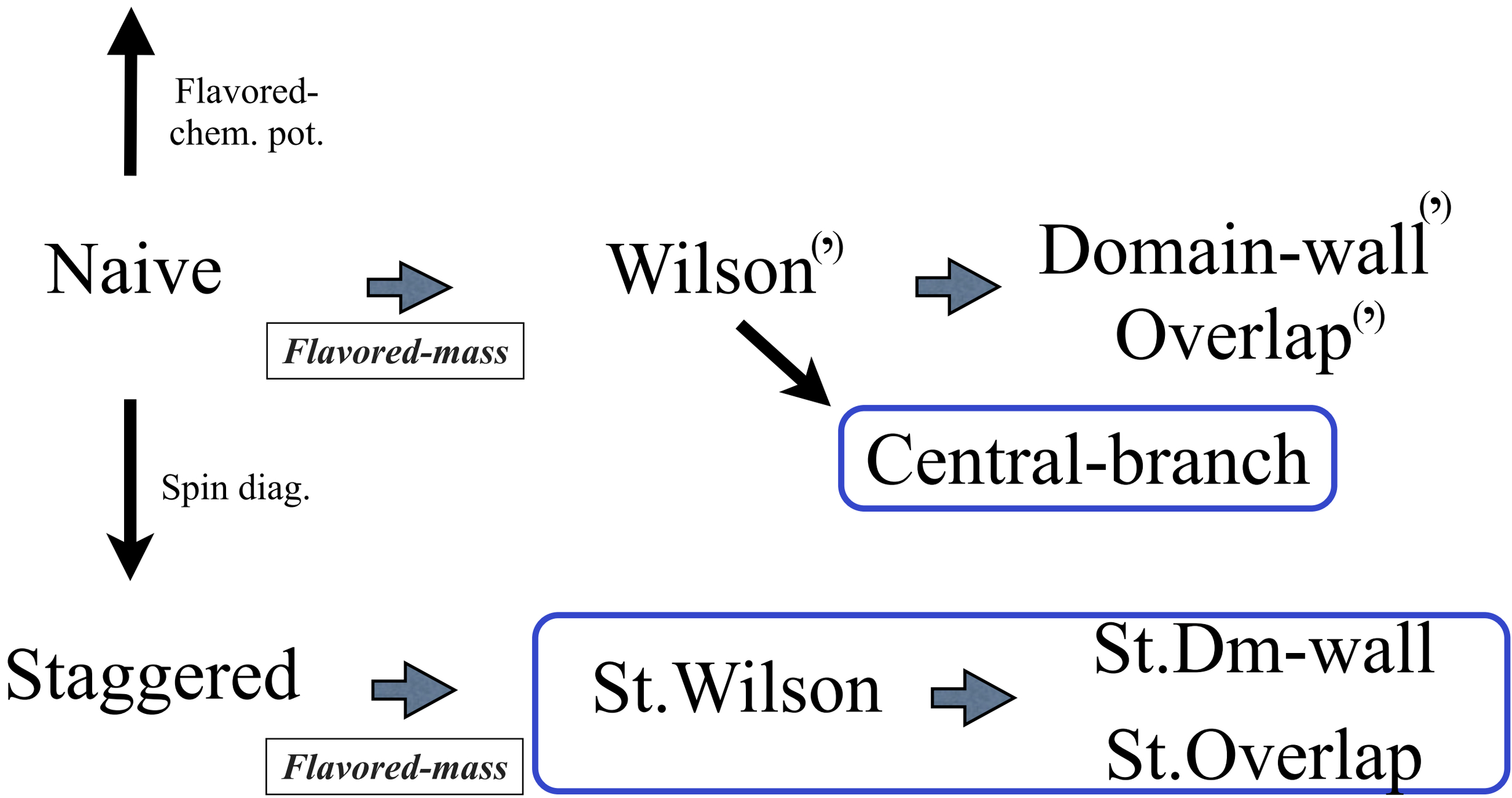
Flavored-
chem. pot.
Naive
Flavored-mass
Wilson(')
Domain-wall(')
Overlap(')
Central-branch
Spin diag.
Staggered
Flavored-mass
St.Wilson
St.Dm-wall
St.Overlap

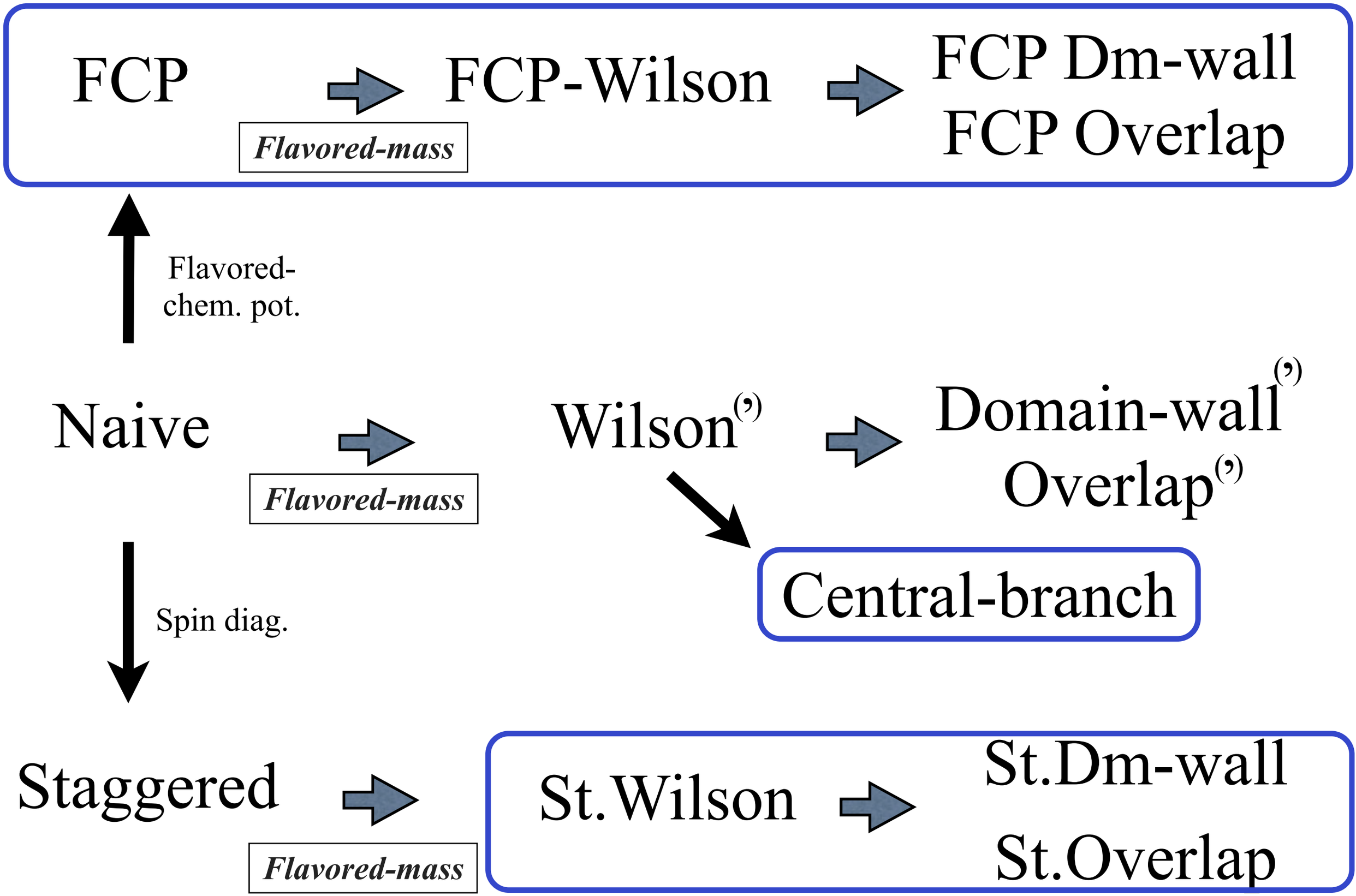
FCP
Flavored-mass
FCP-Wilson
FCP Dm-wall
FCP Overlap
Flavored-
chem. pot.
Naive
Flavored-mass
Wilson(')
Domain-wall(')
Overlap(')
Central-branch
Spin diag.
Staggered
Flavored-mass
St.Wilson
St.Dm-wall
St.Overlap

3. Flavored chemical potential Misumi (2012)

Wilson

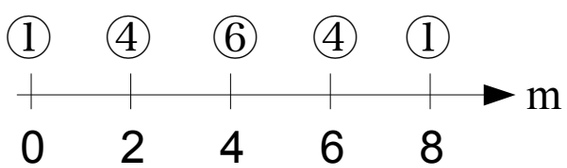

$$\sum_{\mu}(1-\cos p_\mu)$$

Flavored chemical-pot.

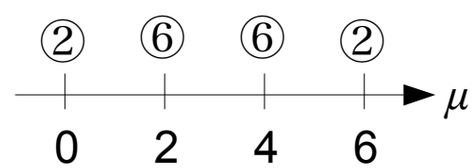

$$\text{(i)}\ \gamma_4 \sum_{j=1}^{3}(1-\cos p_j)$$

- Real type → Sign problem
- Imaginary type → No sign problem

"*Minimal-doubling*" Karsten(81)Wilczek(87)Creutz, Borici(07)Creutz&Misumi(10)

cf.)Bedaque, Buchoff, Tiburzi, Walker-Loud(08)

Finite-mass system(Wil) ⇆ Finite-density system(FCP)

◆ Advantage

- U(1) chiral symmetry
- 2 flavor possible

(1) $U(1)_V \times \underline{U(1)_A}$
(2) P
(3) CT
(4) Cubic symmetry

◆ Drawbacks

- O(1/a) chemical potential renormalization
- Tuning a parameter even for finite-μ QCD

Aoki phase-like structure

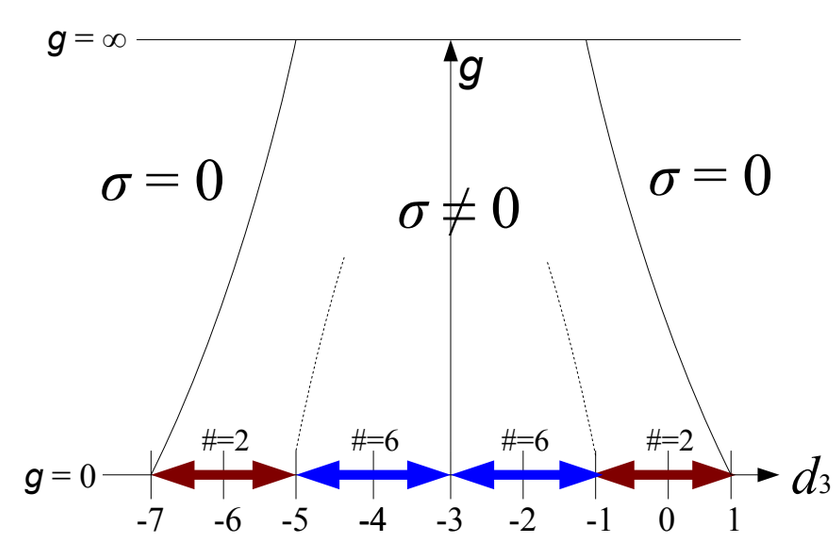

Creutz & Misumi(2012)

◆ Finite (T, μ) QCD with FCP

Misumi, Kimura, Ohnishi (2012)

$$S_{\rm md} = \sum_x \left[\frac{1}{2}\sum_{j=1}^{3} \bar{\psi}_x \gamma_j \left(U_{x,x+j}\psi_{x+j} - U_{x,x-j}\psi_{x-j} \right) + \frac{1}{2}\bar{\psi}_x \gamma_4 \left(e^{\mu} U_{x,x+4}\psi_{x+4} - e^{-\mu} U_{x,x-4}\psi_{x-4} \right) \right.$$
$$\left. + \frac{i}{2}\sum_{j=1}^{3} \underline{\bar{\psi}_x \gamma_4 \left(2\psi_x - U_{x,x+j}\psi_{x+j} - U_{x,x-j}\psi_{x-j} \right)} + i d_3 \bar{\psi}_x \gamma_4 \psi_x \right]$$

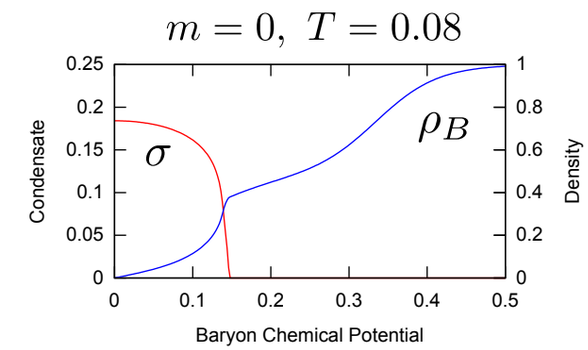

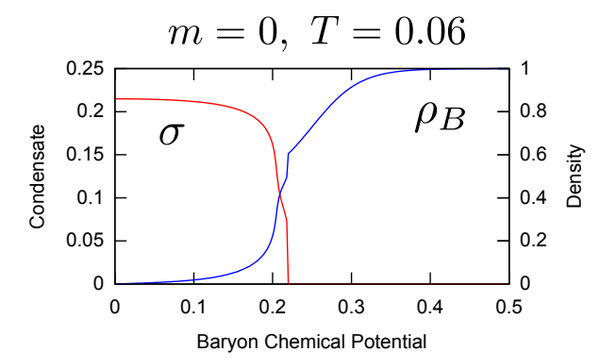

§ Strong-coupling study

Effective potential of σ as a function of T, μ and d3

$$\mathcal{F}_{\rm eff}(\sigma; m, T, \mu, d_3) = \frac{9}{2}\sigma^2 - \frac{3}{2}\log\left(1 + (d_3+3)^2\right) - \max\left\{ 3\ \mathrm{arcsinh}\left(\frac{3\sqrt{2}\sigma}{2\sqrt{1+(d_3+3)^2}} \right), \mu_B \right\}.$$

⇒ Chiral phase structure

- 1st and 2nd phase transition (m=0)
- 1st, critical point and crossover (m≠0)

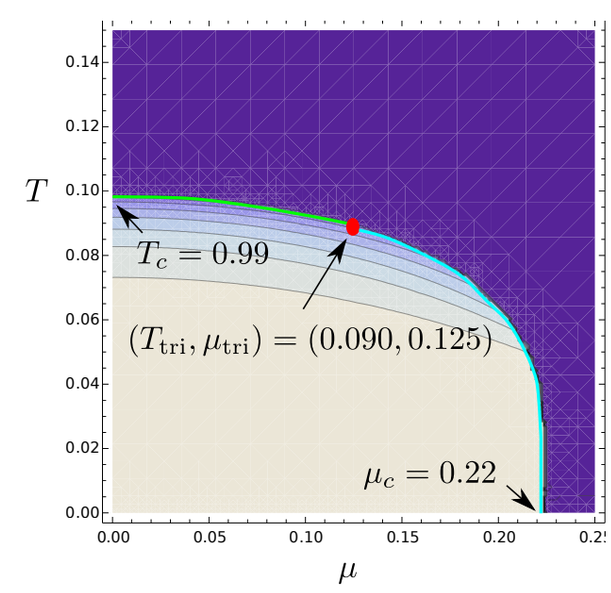

New possibility of (T,μ) lattice QCD !

4. Summary

1. Flavored-mass terms give us new types of Wilson and overlap fermions.

2. Staggered-Wilson can be an alternative Wilson and overlap for 2-flavor QCD (3 degenerate pion spectrum)

3. Central-branch fermion is a new possibility of use of Wilson for many-flavor QCD without fine-tuning of parameters.

4. Flavored-chemical-potential fermion would be useful for finite-temperature & density lattice QCD.

Back-up slides

Adams-type flavored mass

$$\bar{\psi}_x \psi_{x+\hat{1}+\hat{2}+\hat{3}+\hat{4}} = \bar{\chi}_x \gamma_4^{x_4} \gamma_3^{x_3} \gamma_2^{x_2} \gamma_1^{x_1} \gamma_1^{x_1+1} \gamma_2^{x_2+1} \gamma_3^{x_3+1} \gamma_4^{x_4+1} \chi_{x+\hat{1}+\hat{2}+\hat{3}+\hat{4}}$$
$$= (-1)^{x_2+x_4} \bar{\chi}_x \gamma_5 \chi_{x+\hat{1}+\hat{2}+\hat{3}+\hat{4}} \qquad (\gamma_5 \ \text{diagonalized})$$
$$\to \pm \bar{\chi}_x \epsilon \eta_1 \eta_2 \eta_3 \eta_4 \chi_{x+\hat{1}+\hat{2}+\hat{3}+\hat{4}}$$

Hoelbling-type flavored mass

Hoelbling (2010), de Forcrand (2010)

- *spin diagonalization*

$$\bar{\psi}_x \psi_{x+\hat{1}+\hat{2}} + \bar{\psi}_x \psi_{x+\hat{3}+\hat{4}} = (-1)^{x_2} \bar{\chi}_x \gamma_1 \gamma_2 \chi_{x+\hat{1}+\hat{2}} + (-1)^{x_4} \bar{\chi}_x \gamma_3 \gamma_4 \chi_{x+\hat{3}+\hat{4}}$$
$$\to \pm \bar{\chi}_x i\epsilon_{12} \eta_1 \eta_2 \chi_{x+\hat{1}+\hat{2}} \pm \bar{\chi}_x i\epsilon_{34} \eta_3 \eta_4 \chi_{x+\hat{3}+\hat{4}}$$

※ two terms simultaneously diagonalizable : $[\sigma_{12}, \sigma_{34}] = 0$

(4,8,4)

$M_{\mathrm{T}}^{(i)}$

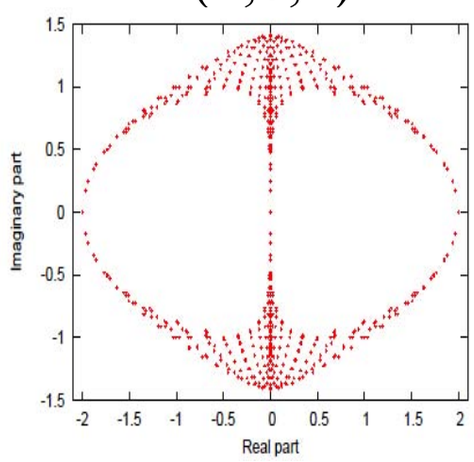

→

(1,2,1)

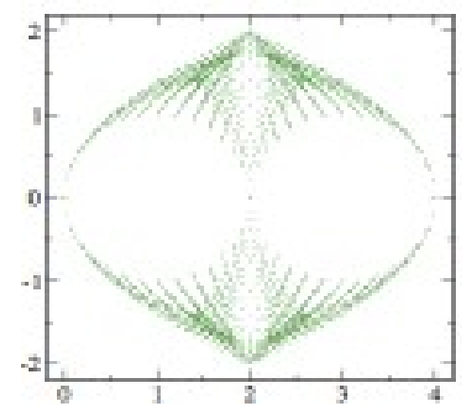

M_H

Hoelbling, PLB696, 422(2011) [1009.5362].

- ***Shift symmetry*** $\longrightarrow$ broken to *2-link shift for S_A*
  broken to *4-link shift for S_H*

$$\mathcal{S}_\rho : \ \chi_x \to \zeta_\rho(x)\chi_{x+\hat{\rho}}, \quad \bar{\chi}_x \to \zeta_\rho(x)\bar{\chi}_{x+\hat{\rho}}, \quad U_{\mu,x} \to U_{\mu,x+\hat{\rho}} \qquad \mathcal{S}_\mu : \ \phi(p) \ \to \ \exp(ip_\mu)\Xi_\mu\,\phi(p)$$

- ***Axis reversal*** $\longrightarrow$ broken to *shifted axis reversal*

$$\mathcal{I}_\rho : \ \chi_x \to (-1)^{x_\rho}\chi_{Ix}, \quad \bar{\chi}_x \to (-1)^{x_\rho}\bar{\chi}_{Ix}, \quad U_{\mu,x} \to U_{\mu,Ix} \qquad \mathcal{I}_\rho : \phi(p) \ \to \ \Gamma_\rho\Gamma_5\Xi_\rho\Xi_5\,\phi(Ip)$$

- ***Rotation*** $\longrightarrow$ remain *in S_A*
  broken to *subgroup in S_H*

$$\mathcal{R}_{\rho\sigma} : \ \chi_x \to S_R(R^{-1}x)\chi_{R^{-1}x}, \quad \bar{\chi}_x \to S_R(R^{-1}x)\bar{\chi}_{R^{-1}x}, \quad U_{\mu,x} \to U_{\mu,Rx} \qquad \mathcal{R}_{\rho\sigma} : \ \phi(p) \ \to \ \exp(\frac{\pi}{4}\Gamma_\rho\Gamma_\sigma)\exp(\frac{\pi}{4}\Xi_\rho\Xi_\sigma)\,\phi(R^{-1}p)$$

- ***Conjugation*** $\longrightarrow$ remain *in S_A*
  broken *in S_H*

$$\mathcal{C} : \ \chi_x \to \epsilon_x\bar{\chi}_x^T, \ \bar{\chi}_x \to -\epsilon_x\bar{\chi}_x^T, \ U_{\mu,x} \to U_{\mu,x}^* \qquad \mathcal{C} : \ \phi(p) \ \to \ \bar{\phi}(-p)^T$$

Axis and Rotation $\quad \to \quad (\Gamma_4 \rtimes SW_{4,\mathrm{diag}})$

Details of StWil symmetries

$$\{\Xi_\mu, I_s, R_{\mu\nu}\} \;\rightarrow\; \Gamma_4 \rtimes SW_4$$

$$\{\Xi'_\mu, R_{\mu\nu}\} \;\rightarrow\; \Gamma_3 \rtimes SW_4$$

Physical-sector symmetry

$$\Xi'_j \Xi'_4 R^2_{j4} = \Xi_j \Xi_4 \sim (1 \otimes \sigma_j)$$

$$\Xi'_4 R^2_{34} R^2_{12} = \Xi_4 I_s \sim (\gamma_4 \otimes \mathbf{1})$$

$$C_0 \Xi'_2 \Xi'_4 R^2_{24} \sim C$$

Details of timeslice symmetries

Enlarged staggered sym : $\{C_0, \Xi_\mu, I_s, R_{\mu\nu}, T_\mu^{1/2}\}$ $\qquad \Xi_\mu^2 = 1$

$$\longrightarrow \; T_\mu^{1/2} \rtimes [\{C_0, \Xi_\mu\} \rtimes \{R_{\mu\nu}, I_s\}] = (\otimes_j Z_{N_\mu}) \rtimes [\Gamma_{4,1} \rtimes W_4]$$

Timeslice sym : $\quad T_\mu^{1/2} \rtimes [\{C_0, \Xi_\mu\} \rtimes \{R_{ij}, I_s\}] = (\otimes_j Z_{N_j}) \rtimes [\Gamma_{4,1} \rtimes W_3]$

Relevant group at rest

$$\begin{aligned}
\Gamma_{4,1} \rtimes W_3 &\sim [\{R_{ij}, \Xi_{ij}\} \times \{C_0, \Xi_4, \Xi_{123}, I_s\}]/Z_2 \\
&= [\{R_{ij}, \tilde{R}_{4i} \equiv \epsilon_{ijk} R_{jk} \Xi_{kj}\} \times \{C_0, \Xi_4, \Xi_{123}, C_0 \Xi_4 I_s\}]/Z_2 \\
&= [SW_4 \times \Gamma_{2,2}]/Z_2
\end{aligned}$$

Staggered-Wilson

$\{C_0, \Xi'_\mu, R_{\mu\nu}, T_\mu'^{1/2}\}$

$$\begin{aligned}
&\sim [\{R_{ij}, \Xi'_{ij}\} \times \{C_0, \Xi'_4, \Xi'_{123}, I_s\}]/Z_2 \\
&= [\{R_{ij}, \tilde{R}_{4i} \equiv \epsilon_{ijk} R_{jk} \Xi'_{kj}\} \times \{C_0, \Xi_4, \Xi_{123}]/Z_2 \\
&= [SW_4 \times \Gamma_{1,2}]/Z_2
\end{aligned}$$

Dim3, 4 : $\bar{Q}(1 \otimes \xi_F)Q \quad \bar{Q}(\gamma_\mu \otimes \xi_F)D_\mu Q$ for $\xi_F = 1$ or ξ_5 ⇒ $\bar{\ell}\gamma_\mu D_\mu \ell, \quad \bar{\ell}\ell$

Dim5 O(a): $\bar{Q}(i\sigma_{\mu\nu}F_{\mu\nu} \otimes \xi_F)Q$ for $\xi_F = 1$ or ξ_5 ⇒ $\bar{\ell} i\sigma_{\mu\nu}F_{\mu\nu}\ell$

No unphysical term nor taste-breaking term up to O(a)

Dim6 O(a^2) : 2 types of four-fermi operators $\mathcal{L}_6^{FF(A)}$ and $\mathcal{L}_6^{FF(B)}$

In $\mathcal{L}_6^{FF(A)}$ the spin and flavor independently forms scalar

⇒ 25 operators with ξ_5 pair → 50 operators

SA, SV, AS, VS, PV, PA, VP, AP, TV, TA, VT, AT, AA, PP , SP, PS, ST, PT, TS, TP, VV, AA, VA, AV, TT

→ No taste-breaking. No derivative terms. Contributes to potential $\mathcal{V}_6^{FF(A)}$

In $\mathcal{L}_6^{FF(B)}$ the spin and flavor are not independent

⇒ 10 operators with ξ_5 pair → 20 operators

TV, TA, VT, AT, VV, AA, VA, AV, TT+, TT-

→ Taste-breaking. Derivative terms. No contribution to potential $\mathcal{V}_6^{FF(B)}$

No taste-breaking in ChPT potential upto O(a^2): SU(2)

◆ Central cusps for other flavored masses

progress in NTFL workshop (2012)

- For other naive flavored mass terms

  M_A : U(1) restored

  $M_T^{(i)}$: U(2) restored

  M_P : U(2)×U(2) restored

- For staggered flavored mass terms

  $M_{\mathcal{A}}$: $C_T\Xi$, $C_T I$ restoed

  $M_{\mathcal{H}}$: C_T restored

$$\mathcal{C}: \ \chi_x \to \bar{\chi}_x^T, \quad \bar{\chi}_x \to \chi_x^T, \quad U_{\mu,x} \to U_{\mu,x}^*$$

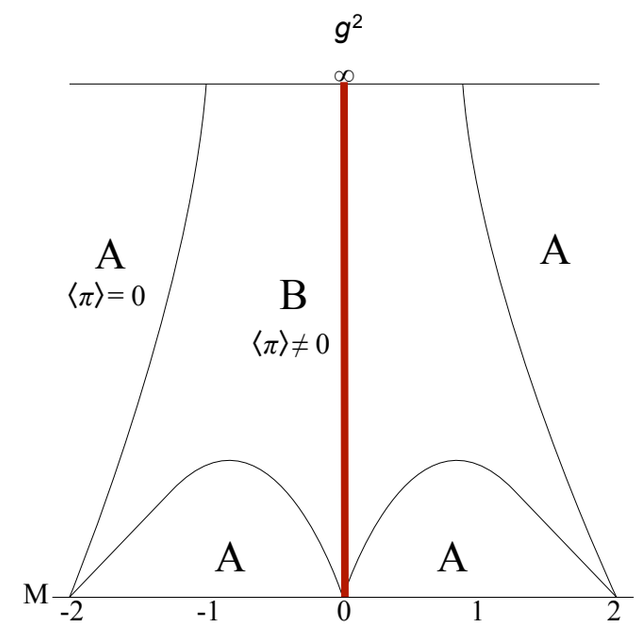

	C'_T	Ξ_μ	I_μ	$C'_T\Xi_\mu$	$C'_T I_\mu$	$\Xi_\mu I_\mu$
S_{st}	○	○	○	○	○	○
$S_{\mathcal{A}}$	×	×	×	○	○	○
$S_{\mathcal{H}}$	○	×	×	×	×	○
S_m	×	○	○	×	×	○

3.2 Strong coupling analysis

Now we employ the strong coupling analysis to show that there appears an NG boson associated with the $\mathrm{U}(1)_V^-$ symmetry breaking in the presence of the pion condensate. An effective action for mesons in the strong coupling limit [42, 9, 10] can be written in general as

$$S_{\rm eff}(M) = N_c \sum_n \left[\sum_\mu \mathrm{Tr}\, f(\Lambda_{n,\mu}) + \mathrm{tr}\, \hat{M} M(n) - \mathrm{tr}\, \log M(n) \right] , \tag{23}$$

$$\Lambda_{n,\mu} = \frac{V_{n,\mu}\bar{V}_{n,\mu}}{N_c^2}, \quad M(n)^{\alpha\beta} = \frac{\sum_a \bar{\psi}_n^{a,\alpha}\psi_n^{a,\beta}}{N_c} ,$$

where N_c is the number of colors, Tr (tr) means a trace over color(spinor) index, and $M(n)$ is a meson field. The explicit form of the function f is determined by performing a one-link integral of the gauge field. More explicitly we can write

$$V_{n,\mu}^{ab} = \bar{\psi}_n^b P_\mu^- \psi_{n+\hat{\mu}}^a , \quad \bar{V}_{n,\mu}^{ab} = -\bar{\psi}_{n+\hat{\mu}}^b P_\mu^+ \psi_n^a , \tag{24}$$

$$\mathrm{Tr}\, f(\Lambda_{n,\mu}) = -\mathrm{tr}\, f\left(-M(n)(P_\mu^+)^{\mathrm{T}} M(n+\hat{\mu})(P_\mu^-)^{\mathrm{T}}\right) , \tag{25}$$

where 4×4 matrices $P_\mu^\pm$ are specified later. In the large N_c limit, it is known that $f(x)$ can be analytically evaluated as

$$f(x) = \sqrt{1+4x} - 1 - \ln \frac{1+\sqrt{1+4x}}{2} = x + O(x^2) . \tag{26}$$

However, in the following part of this paper, we will approximate $f(x)$ as $f(x) = x$ unless otherwise stated because qualitative features such as an appearance of NG bosons remain unchanged by this approximation.

To calculate meson masses we expand the meson field as[5]

$$M(n) = M_0^{\mathrm{T}} + \sum_X \pi^X(n)\Gamma_X^{\mathrm{T}} , \quad X \in \{S, P, V_\alpha, A_\alpha, T_{\alpha\beta}\} , \tag{27}$$

where M_0 is the vacuum expectation value (VEV) of $M(n)$, and

$$\Gamma_S = \frac{\mathbf{1}_4}{2},\ \Gamma_P = \frac{\gamma_5}{2},\ \Gamma_{V_\alpha} = \frac{\gamma_\alpha}{2},\ \Gamma_{A_\alpha} = \frac{\mathrm{i}\gamma_5\gamma_\alpha}{2},\ \Gamma_{T_{\alpha\beta}} = \frac{\gamma_\alpha\gamma_\beta}{2\mathrm{i}}\ (\alpha<\beta). \tag{28}$$

Then the effective action at the second order of π^X is given by

$$\begin{aligned} S_{\rm eff}^{(2)} &= N_c \sum_n \left[\frac{1}{2}\mathrm{tr}\,(M_0^{-1}\Gamma_X M_0^{-1}\Gamma_Y)\,\pi^X(n)\pi^Y(n) + \sum_\mu \mathrm{tr}\,(\Gamma_X P_\mu^- \Gamma_Y P_\mu^+)\pi^X(n)\pi^Y(n+\hat{\mu}) \right] \\ &= N_c \int \frac{d^4p}{(2\pi)^4} \pi^X(-p) D_{XY}(p) \pi^Y(p) , \end{aligned} \tag{29}$$

where

$$D_{XY}(p) = \frac{1}{2}\big(\widetilde{D}_{XY}(p) + \widetilde{D}_{YX}(-p)\big), \tag{30}$$

$$\widetilde{D}_{XY}(p) = \frac{1}{2}\mathrm{tr}\,(M_0^{-1}\Gamma_X M_0^{-1}\Gamma_Y) + \sum_\mu \mathrm{tr}\,(\Gamma_X P_\mu^- \Gamma_Y P_\mu^+) e^{\mathrm{i}p_\mu}. \tag{31}$$

In the case of the Wilson fermion, $\hat{M} = (m+4r)\mathbf{1}_4 \equiv M_W \mathbf{1}_4$ and $P_\mu^\pm = \dfrac{\gamma_\mu \pm r}{2}$. By taking $M_0 = \sigma\mathbf{1}_4 + \mathrm{i}\pi\gamma_5$, we have

$$\begin{cases} \sigma = \dfrac{-M_W \pm \sqrt{M_W^2 + 8(1-r^2)}}{4(1-r^2)}, \quad \pi = 0 , & M_W^2 \geq M_c^2 \\ \sigma = \dfrac{M_W}{4r^2} , \quad \pi^2 = \dfrac{1}{16r^4(1+r^2)}(8r^4 - M_W^2(1+r^2)) , & M_W^2 < M_c^2 \end{cases} \tag{32}$$

where $M_c^2 = \dfrac{8r^4}{1+r^2}$.

As discussed in the previous subsection, at $M_W = 0$ we have an additional U(1) symmetry, $\mathrm{U}(1)_V^-$. Since this parameter regime resides in the parity broken phase, in which $\pi^2 \neq 0$ and $M_W^2 < M_c^2$, $\mathrm{U}(1)_V^-$ is spontaneously broken by the VEV of π in this case.

To compute the meson mass, we hereafter take $r^2 = 1$ for simplicity. Because $D(p)$ is block-diagonal, we concentrate on its submatrix $D_{XY}(p)$ with $X, Y \in \{S, P, A_\alpha\}$. Then, by setting $p = (\pi, \pi, \pi, \pi + \mathrm{i}m_{SPA})$, we find that the S-P-A_α sector mass m_{SPA} is given by

$$\cosh(m_{SPA}) = 1 + \frac{20M_W^2}{6 - 7M_W^2}. \tag{33}$$

Note that since the transformation (22) involves the site-dependent quantity $(-1)^{n_1+\cdots+n_4}$, it is natural to expand the momentum p around (π, π, π, π). Eq. (33) tells us that the meson becomes a massless NG boson at $M_W = 0$ as expected. If we use the exact form of $f(x)$ in the large N_c limit, we then obtain

$$\cosh(m_{SPA}) = 1 + \frac{2M_W^2(16 + M_W^2)}{16 - 15M_W^2}, \tag{34}$$

which again shows that a massless NG boson appears at $M_W = 0$.

A. Effective potential

We first need to derive effective potential of meson fields including scalar one σ from (4) in the strong-coupling limit ($g^2 \to \infty$). We here consider general color number as N_c for $SU(N_c)$ gauge group and general space-time dimensions as $D+1$. For the purpose we perform the 1-link integral for the gauge field in the D-dimensional spatial part, and introduce auxiliary fields to eliminate the 4-point interaction as

$$\begin{aligned}
&\int \mathcal{D}U_1 \cdots \mathcal{D}U_D \, \exp\left[-\sum_x \sum_{j=1}^{D} \left(\bar{\psi}_x P_j^+ U_j(x) \psi_{x+\hat{j}} - \bar{\psi}_{x+\hat{j}} P_j^- U_j^\dagger(x) \psi_x \right) \right] \\
&\qquad = \exp\left[N_c \sum_x \left(\sum_{j=1}^{D} \mathrm{tr}\, \mathcal{M}(\mathrm{x}) (P_\mathrm{j}^+)^\mathrm{T} \mathcal{M}(\mathrm{x}+\hat{\mathrm{j}}) (P_\mathrm{j}^-)^\mathrm{T} \right) + \mathcal{O}(1/\sqrt{D}) \right] \\
&\qquad = \int \mathcal{D}\sigma \mathcal{D}\pi_4 \, \exp\left[-N_c \sum_x \left(D\left((1+r^2)\sigma^2 + (1-r^2)\pi_4^2 \right) \right.\right. \\
&\qquad\qquad \left.\left. - \frac{D}{2} \mathrm{tr}\left(\sqrt{1+\mathrm{r}^2}\sigma - \mathrm{i}\sqrt{1-\mathrm{r}^2}\pi_4\gamma_4 \right) \mathcal{M}(\mathrm{x}) \right) \right],
\end{aligned} \tag{5}$$

with

$$P_\mu^\pm = \begin{cases} (\gamma_\mu \pm ir\gamma_4)/2 & (\mu \neq 4) \\ \gamma_4/2 & (\mu = 4) \end{cases} \tag{6}$$

where we introduce the mesonic field as

$$\mathcal{M}^{\alpha\beta}(x) = \frac{1}{N_c} \delta_{ab} \bar{\psi}_x^{a,\alpha} \psi_x^{b,\beta}. \tag{7}$$

We note that two auxiliary fields σ and π_4 are required to get rid of four-fermi interactions in this case because of the Karsten-Wilczek term. π_4 condensate can be a signal of nonzero effective imaginary chemical potential, and we will discuss on this later. We also note that

we dropped next-leading order of $O(1/\sqrt{D})$ expansions in (5), which corresponds to large D limit. We now have an intermediate form of the effective action from (4),

$$S_{\rm eff} = \sum_x \left[\frac{1}{2}\left(\bar{\psi}_x e^{\mu} U_4(x)\gamma_4\psi_{x+\hat{4}} - \bar{\psi}_{x+\hat{4}} e^{-\mu} U_4^\dagger(x)\gamma_4\psi_x\right) + \bar{\psi}_x\left(m\mathbf{1} + i(d_3+Dr)\gamma_4\right)\psi_x \right.$$
$$\left. + N_c D\left((1+r^2)\sigma^2 + (1-r^2)\pi_4^2\right) + \frac{N_c}{2} D\,\mathrm{tr}\left(\sqrt{1+\mathrm{r}^2}\sigma - \mathrm{i}\sqrt{1-\mathrm{r}^2}\pi_4\gamma_4\right)\mathcal{M}(\mathrm{x})\right]. \tag{8}$$

We here defined complex chemical potential as $\mu \equiv \mu_{\rm Re} + i\mu_{\rm Im}$. We make fourier transformation of the temporal direction ($\mu = 4$) by introducing Matsubara modes as,

$$\psi_{\tau,\vec{x}} = \frac{1}{\sqrt{N_\tau}}\sum_{n=1}^{N_\tau} e^{ik_n\tau}\tilde{\psi}_{n,\vec{x}}, \qquad \bar{\psi}_{\tau,\vec{x}} = \frac{1}{\sqrt{N_\tau}}\sum_{n=1}^{N_\tau} e^{-ik_n\tau}\tilde{\bar{\psi}}_{n,\vec{x}}, \qquad k_n = \frac{2\pi}{N_\tau}\left(n - \frac{1}{2}\right). \tag{9}$$

We here take Polyakov gauge and the link variable in the temporal direction is given by,

$$U_4(\vec{x}) = \begin{pmatrix} e^{i\phi_1(\vec{x})/N_\tau} & & & \\ & e^{i\phi_2(\vec{x})/N_\tau} & & \\ & & \ddots & \\ & & & e^{i\phi_{N_c}(\vec{x})/N_\tau} \end{pmatrix}, \qquad \sum_{a=1}^{N_c}\phi_a(\vec{x}) = 0. \tag{10}$$

with ϕ_a defined as components of gauge fields. It enables us to calculate fermionic determinant analytically as,

$$\begin{aligned}
\det D &= \prod_{\vec{x}}\prod_{a=1}^{N_c}\prod_{n=1}^{N_\tau}\det\left[\left(m + \frac{D}{2}\sqrt{1+r^2}\sigma\right)\mathbf{1} + i\gamma_4\left(\sin\bar{k}_n^{(a)} + d_3 + Dr - \frac{D}{2}\sqrt{1-r^2}\pi_4\right)\right] \\
&\equiv \prod_{\vec{x}}\prod_{a=1}^{N_c}\prod_{n=1}^{N_\tau}\det\left[B + i\gamma_4 A\sin\tilde{k}_n^{(a)}\right] \\
&= \prod_{\vec{x}}\prod_{a=1}^{N_c}\prod_{n=1}^{N_\tau}\left(A^2\sin^2\tilde{k}_n^{(a)} + B^2\right)^2 \\
&= \prod_{\vec{x}} A^{4N_cN_\tau}\prod_{a=1}^{N_c}\left(2\cosh N_\tau E + 2\cos\left(\phi_a - iN_\tau\mu\right)\right)^4,
\end{aligned} \tag{11}$$

where we define

$$A^2 = 1 + \left(d_3 + Dr - \frac{D}{2}\sqrt{1-r^2}\pi_4\right)^2, \qquad B = m + \frac{D}{2}\sqrt{1+r^2}\sigma, \tag{12}$$

$$E = \mathrm{arcsinh}\left(\frac{B}{A}\right) = \log\left[\frac{B}{A} + \sqrt{1+\left(\frac{B}{A}\right)^2}\right], \tag{13}$$

with $\bar{k}_n^{(a)} = k_n + \phi_a/N_\tau - i\mu$. By integrating the temporal gauge field ϕ_a we derive

$$\int \mathcal{D}U_4 \prod_{\vec{x}} A^{4N_cN_\tau}\prod_{a=1}^{N_c}\left(2\cosh N_\tau E + 2\cos\left(\phi_a - iN_\tau\mu\right)\right)^4 = \prod_{\vec{x}}\left[\sum_{n\in Z}\det\left(Q_{n+i-j}\right)_{1\le i,j\le N_c}\right], \tag{14}$$

$$Q_n = \int_{-\pi}^{\pi}\frac{d\phi}{2\pi}\left(2\cosh N_\tau E + 2\cos\theta\right)^4 e^{-in\phi}, \qquad \theta = \phi - iN_\tau\mu. \tag{15}$$

For $N_c = 3$ these Q_n are explicitly given as

$$\begin{aligned}
Q_0 &= 2(8\cosh^4 N_\tau E + 24\cosh^2 N_\tau E + 3) \\
Q_{\pm1} &= 8\cosh N_\tau E(4\cosh^2 N_\tau E + 3)e^{\pm N_\tau\mu} \\
Q_{\pm2} &= 4(6\cosh^2 N_\tau E + 1)e^{\pm 2N_\tau\mu} \\
Q_{\pm3} &= 8\cosh N_\tau E\, e^{\pm 3N_\tau\mu} \\
Q_{\pm4} &= e^{\pm 4N_\tau\mu} \\
Q_{|n|\ge5} &= 0
\end{aligned} \tag{16}$$

As a result, the effective free energy is given by

$$\begin{aligned}
\mathcal{F}_{\rm eff}(\sigma,\pi_4;m,T,\mu,d_3) &= \frac{N_cD}{4}\left((1+r^2)\sigma^2 + (1-r^2)\pi_4^2\right) - N_c\log A \\
&\quad - \frac{T}{4}\log\left(\sum_{n\in Z}\det\left(Q_{n+i-j}\right)_{1\le i,j\le N_c}\right).
\end{aligned} \tag{17}$$

Here we redefine the free energy $4\mathcal{F}_{\rm eff} \to \mathcal{F}_{\rm eff}$. The calculation of the determinant part for $N_c = 3$ is moved to Appendix A 2. We here show only the result as

$$\begin{aligned}
&\sum_{n\in Z}\det\left(Q_{n+i-j}\right)_{1\le i,j\le N_c} \\
&= 8\left(1 + 12\cosh^2\frac{E}{T} + 8\cosh^4\frac{E}{T}\right)\left(15 - 60\cosh^2\frac{E}{T} + 160\cosh^4\frac{E}{T} - 32\cosh^6\frac{E}{T} + 64\cosh^8\frac{E}{T}\right) \\
&\quad + 64\cosh\frac{\mu_B}{T}\cosh\frac{E}{T}\left(-15 + 40\cosh^2\frac{E}{T} + 96\cosh^4\frac{E}{T} + 320\cosh^8\frac{E}{T}\right) \\
&\quad + 80\cosh\frac{2\mu_B}{T}\left(1 + 6\cosh^2\frac{E}{T} + 24\cosh^4\frac{E}{T} + 80\cosh^6\frac{E}{T}\right) \\
&\quad + 80\cosh\frac{3\mu_B}{T}\cosh\frac{E}{T}\left(-1 + \cosh^2\frac{E}{T}\right) + 2\cosh\frac{4\mu_B}{T}.
\end{aligned} \tag{18}$$

with

$$\mu_B = 3\mu. \tag{19}$$

Thermodynamics with Domain Wall Fermions and anomaly in hot QCD

Swagato Mukherjee

BROOKHAVEN NATIONAL LABORATORY

May 2012, BNL

Chiral transition in QCD

$$SU_L(2) \otimes SU_R(2) \otimes U_A(1) \otimes U_B(1)$$

axial anomaly

$$\psi : e^{-i\alpha\gamma_5}\,\psi$$

$$SU_L(2) \otimes SU_R(2) \otimes U_B(1)$$

χSM breaking

$$\psi : e^{-i\alpha\gamma_5\tau_i}\,\psi$$

restores at high T

$$SU_v(2) \otimes U_B(1)$$

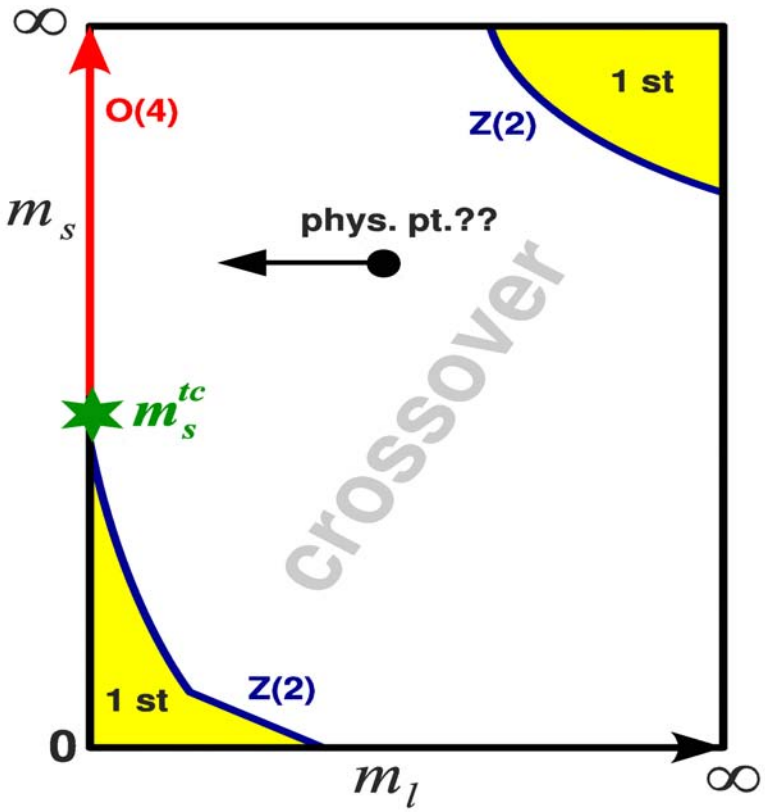

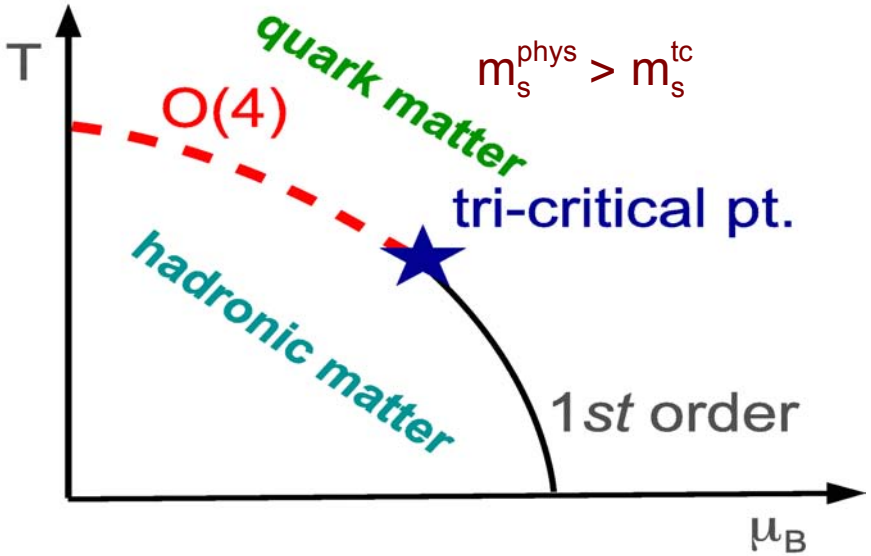

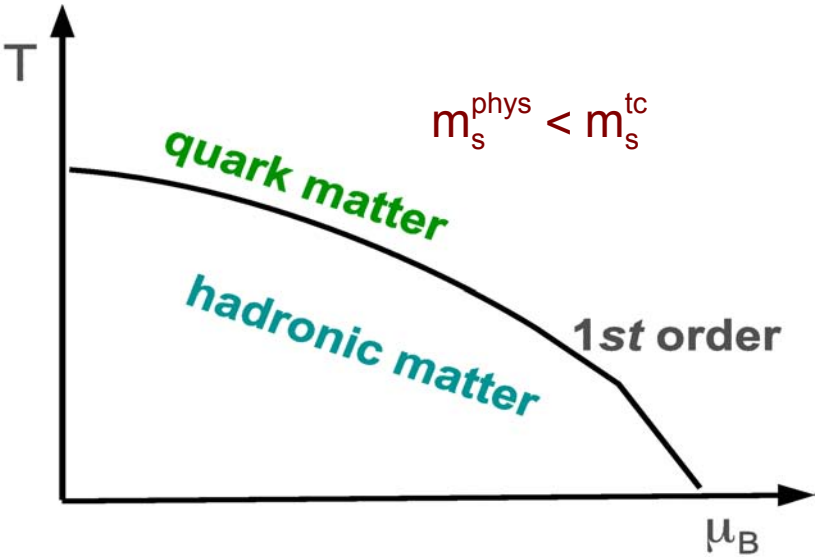

Chiral transition in QCD

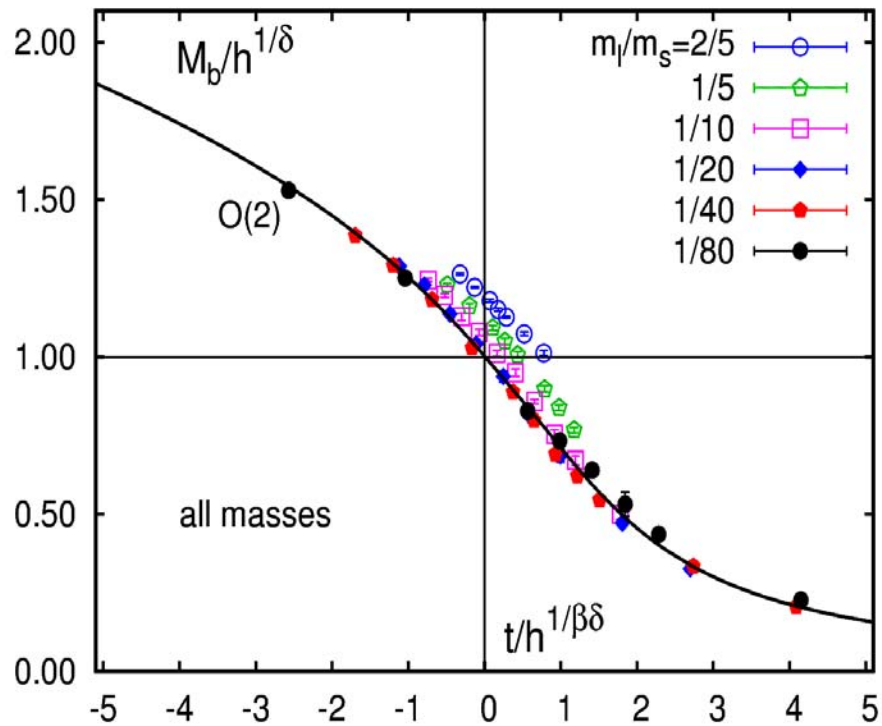

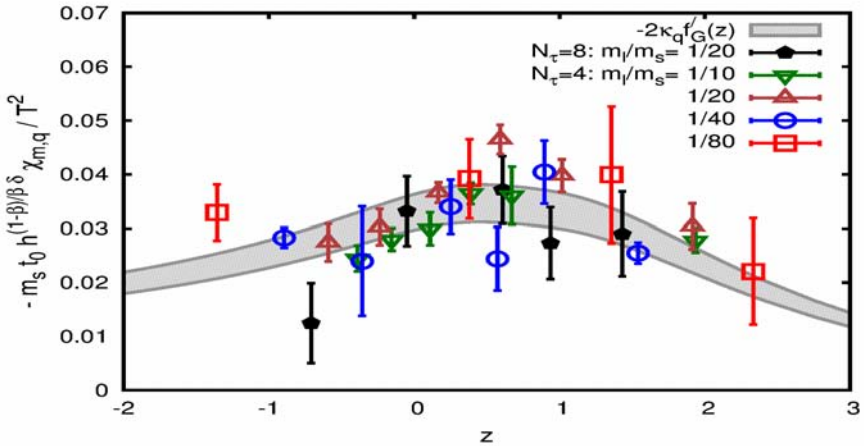

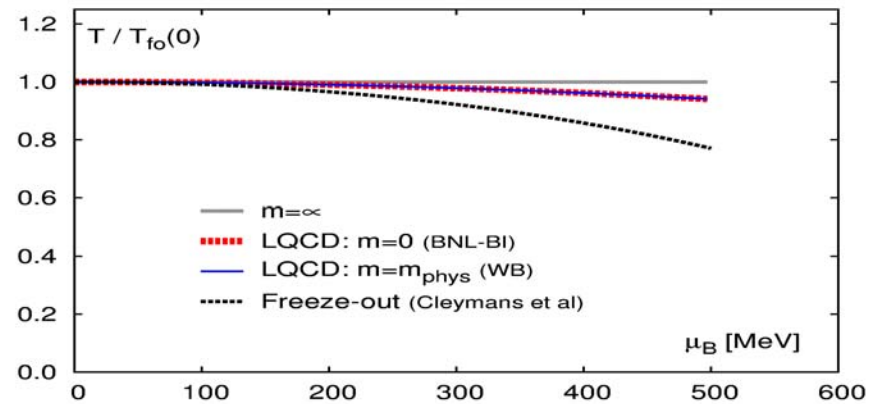

BNL-BI: Phys Rev D80, 094505 (2009)

BNL-BI, Phys Rev D83, 014504 (2011)

staggered fermions: intertwined chiral & continuum limit

$a \neq 0$, $m \rightarrow 0$: O(2), instead of continuum O(4)

need exact chiral symmetry for $a \neq 0$

chiral fermions: Domain Wall Fermions

Thermodynamics with DWF: problem and progress

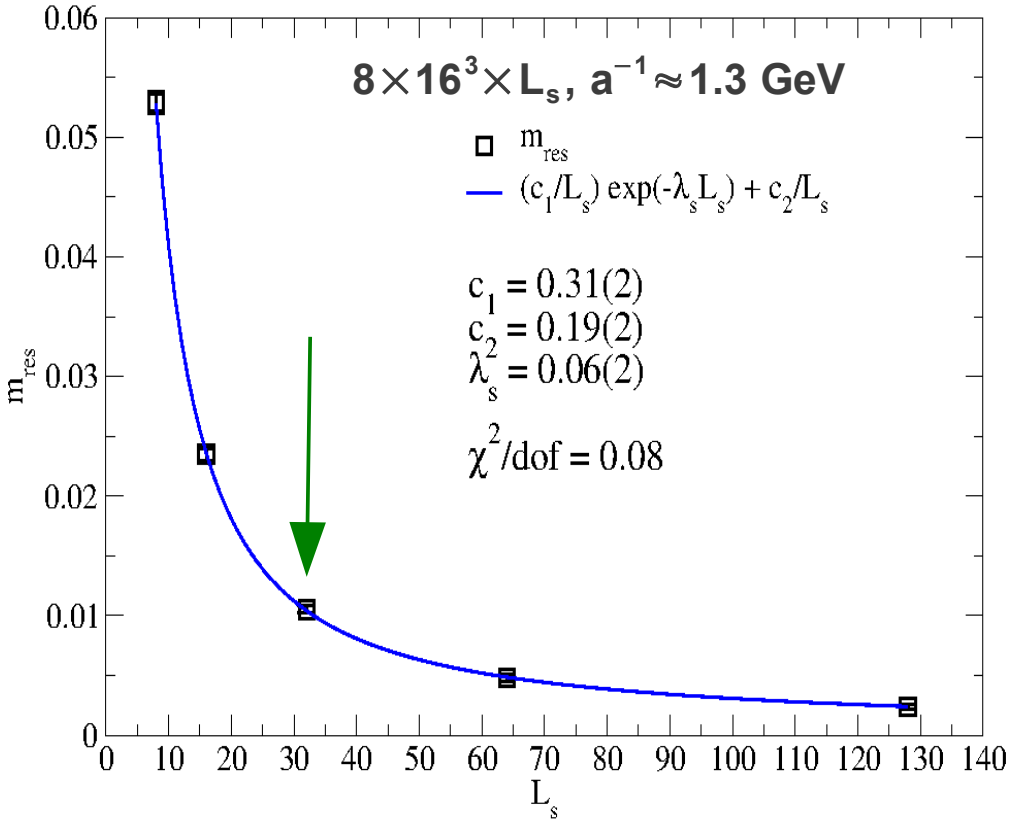

RBC-LLNL: PRD 81, 054510 (2010)

✓ coarse lattice spacings: $m_{res} \sim 1/L_s$

instead of: $m_{res} \sim e^{-\#L_s}$

m_{res} : residual quark mass

L_s: extent of 5th direction

large residual mass

Thermodynamics with DWF: problem and progress

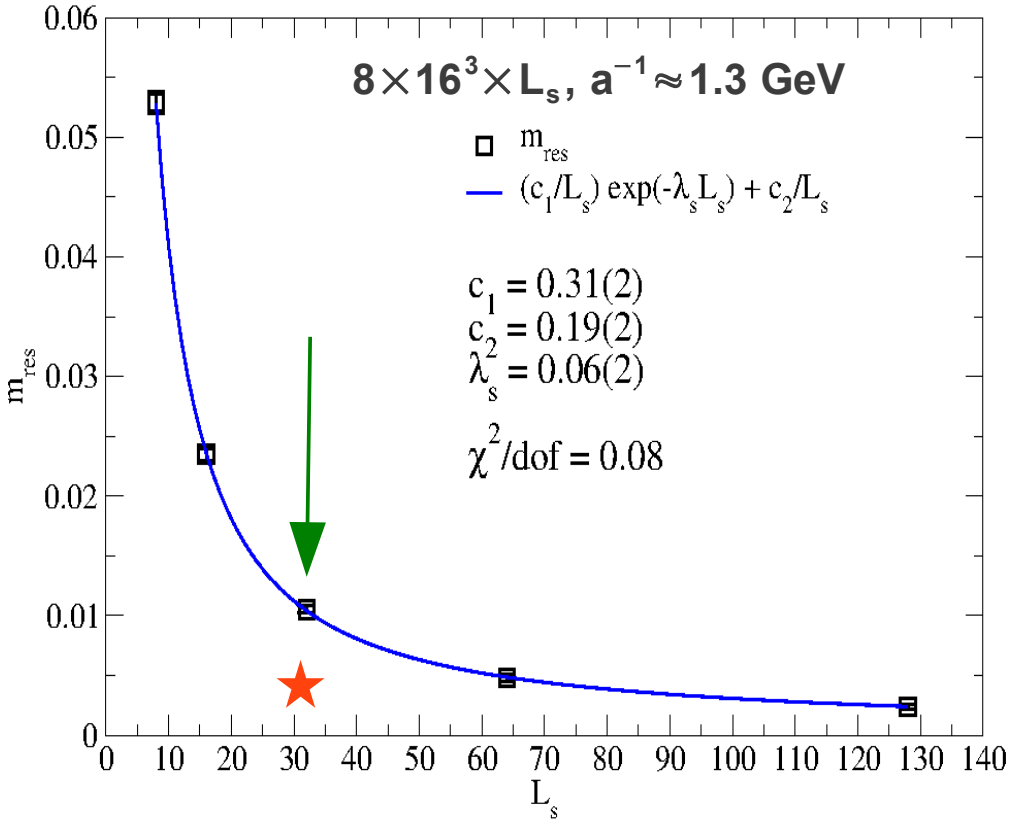

RBC-LLNL: PRD 81, 054510 (2010)

small residual mass for coarser lattices and moderate extent of the *5th* direction

✓ coarse lattice spacings: $m_{res} \sim 1/L_s$

instead of: $m_{res} \sim e^{-\#L_s}$

m_{res} : residual quark mass

L_s: extent of 5th direction

large residual mass

★ DSDR

Dislocation Suppressing Determinant Ratio

$$\frac{\det\left[D_W^\dagger(-M_5+i\epsilon_f\gamma_5)D_W(-M_5+i\epsilon_f\gamma_5)\right]}{\det\left[D_W^\dagger(-M_5+i\epsilon_b\gamma_5)D_W(-M_5+i\epsilon_b\gamma_5)\right]}$$

suppresses gauge field dislocations, but ensures topological tunneling, minimally affects the UV modes

① HotQCD: $8\times16^3\times32(48)$, $m_\pi = 200$ MeV, $m_K = $ phys., $T = 135-200$ MeV

② RBC-LLNL: $8\times32^3\times32(48)$

Chiral crossover with DWF

$$\begin{array}{ccccc}
\chi_{5,con} & \pi : \bar{q}\gamma_5 \frac{\tau}{2} q & \xleftrightarrow{SU(2)_L \times SU(2)_R} & \sigma : \bar{q}q & \chi_{con} + \chi_{disc} \\
 & \updownarrow U(1)_A & & \updownarrow U(1)_A & \\
\chi_{con} & \delta : \bar{q}\frac{\tau}{2} q & \xleftrightarrow[SU(2)_L \times SU(2)_R]{} & \eta : \bar{q}\gamma_5 q & \chi_{5,con} - \chi_{5,disc}
\end{array}$$

susceptibilities: $\chi_i = \sum_{\mathbf{x}} C_i(\mathbf{x})$

χSM $\Rightarrow$ $\chi_\pi = \chi_\sigma$

$\chi_{disc} = \chi_{5,\,disc}$

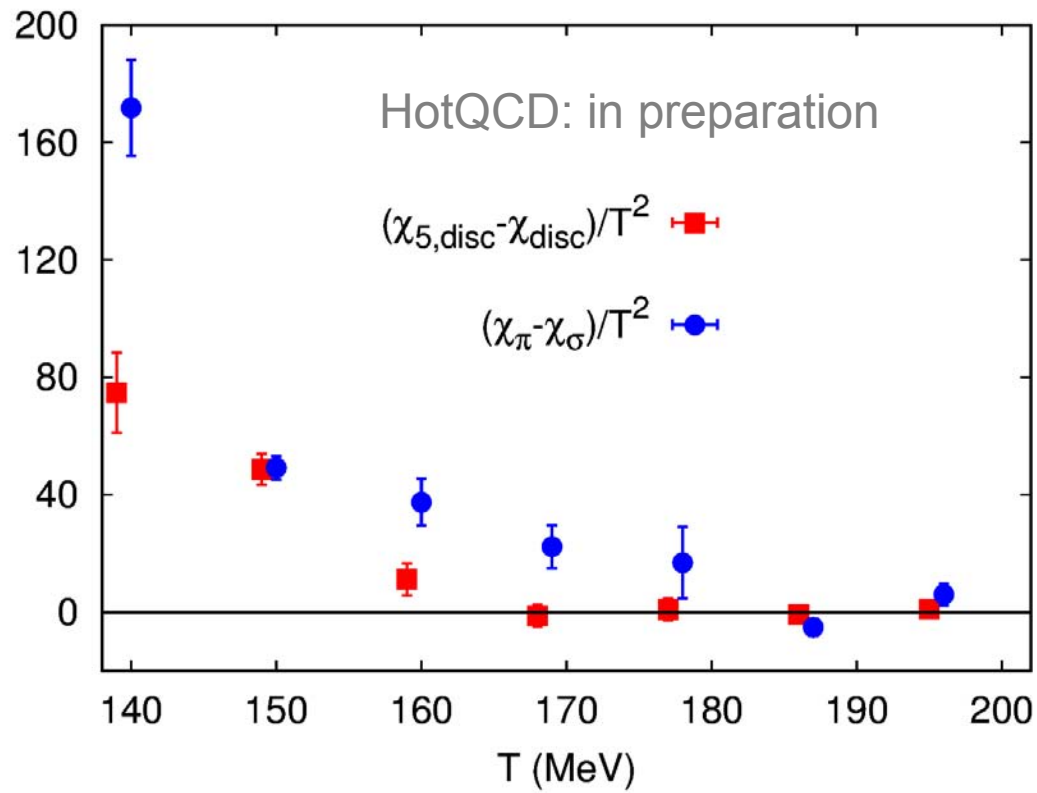

Chiral crossover with DWF

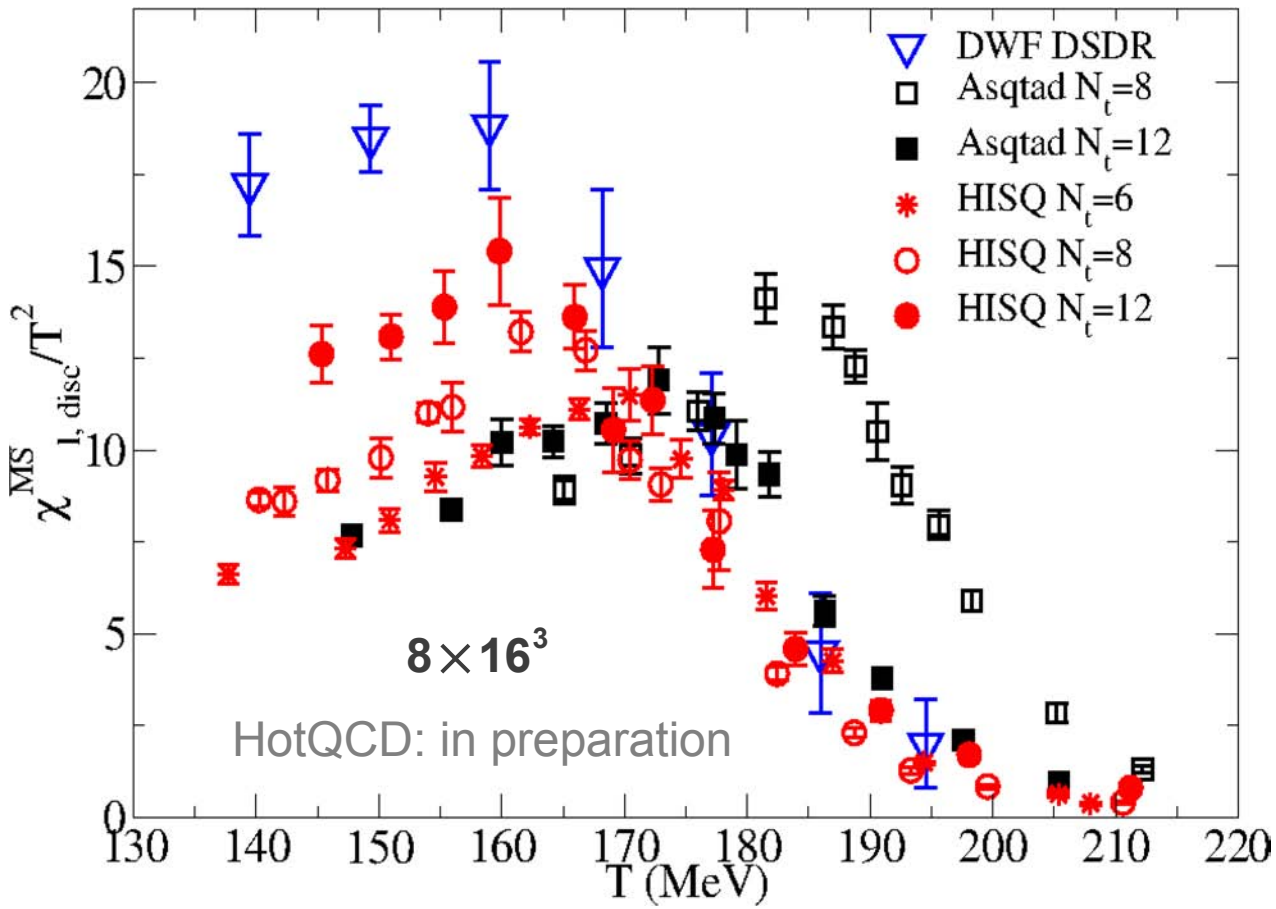

disconnected chiral susceptibility

re-normalized at scale 2 GeV in $\overline{MS}$ scheme

Chiral crossover with DWF

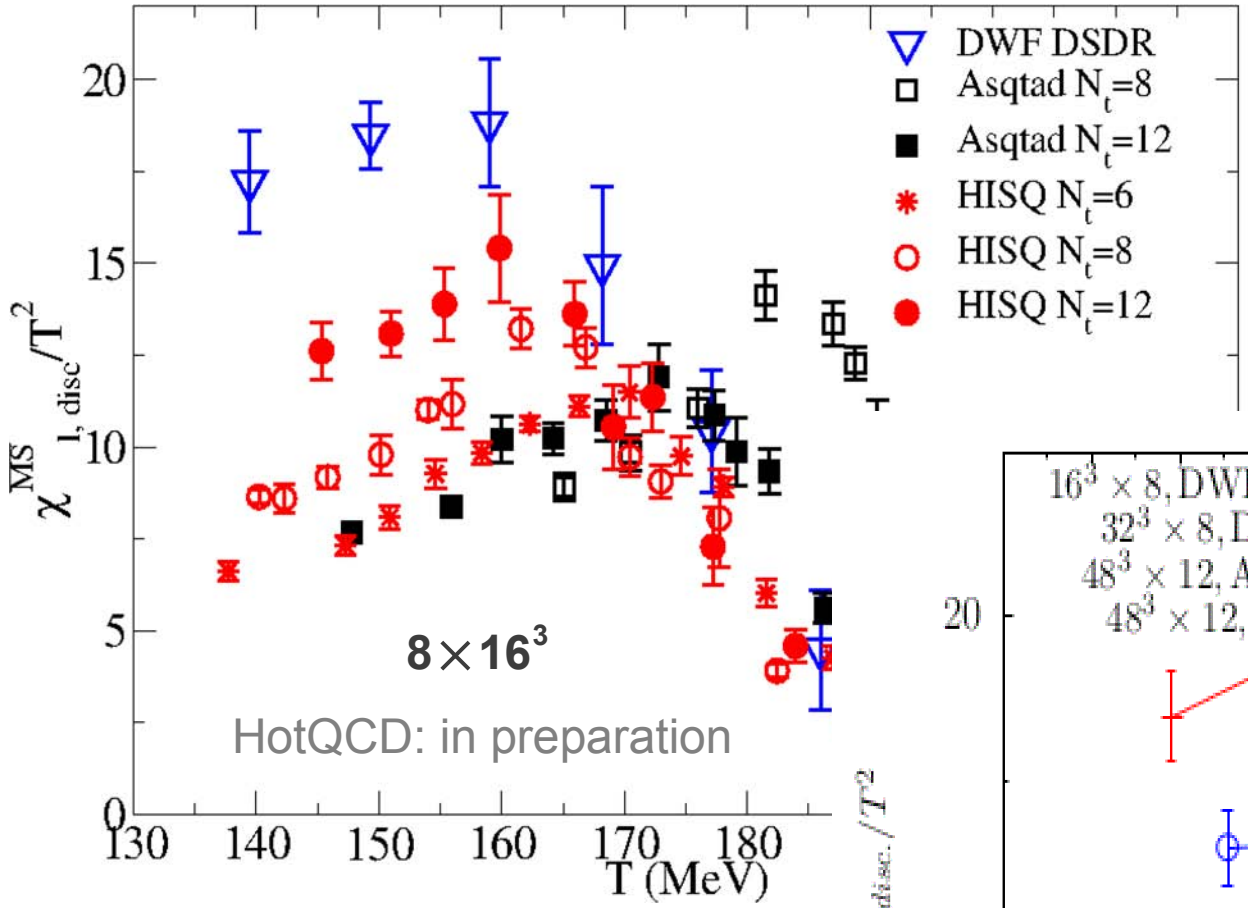

disconnected chiral susceptibility

re-normalized at scale 2 GeV in $\overline{\text{MS}}$ scheme

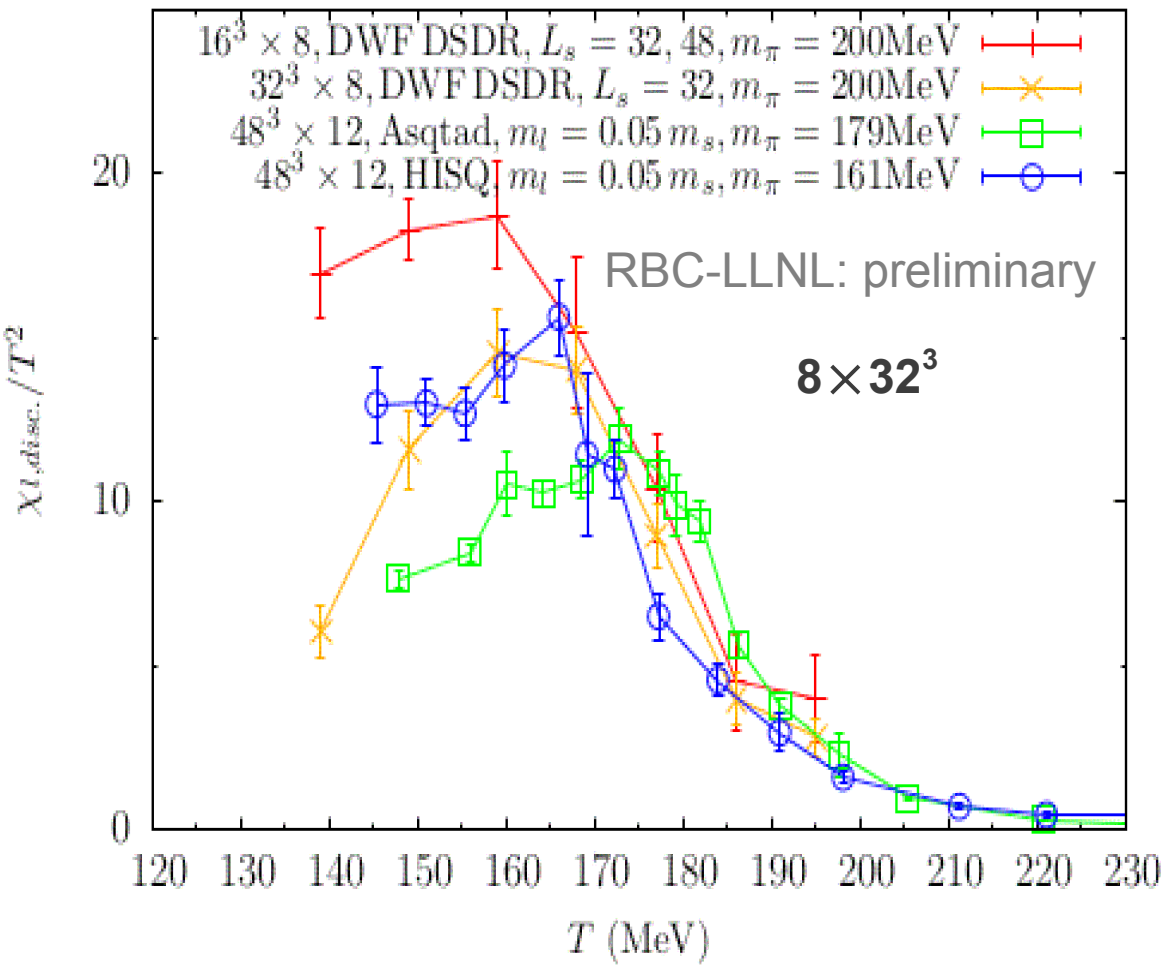

$T_c = 155-165$ MeV

Axial anomaly in hot QCD

- ✓ vacuum: non-zero $\langle \bar{\psi}\psi \rangle$ breaks $U_A(1)$

- ✓ $T > T_c^{\chi}$: $U_A(1)$ is broken due to presence of topologically non-trivial configurations (*e.g.* instantons)

complex non-perturbative mechanism for axial symmetry breaking ?

- ✓ high T: exponential suppression of instanton density due to screening chromo-electric fields leads to exponentially small $U_A(1)$ breaking, dilute instanton gas approximation

Axial anomaly in hot QCD

$T > T_c$, $m_l \to 0$

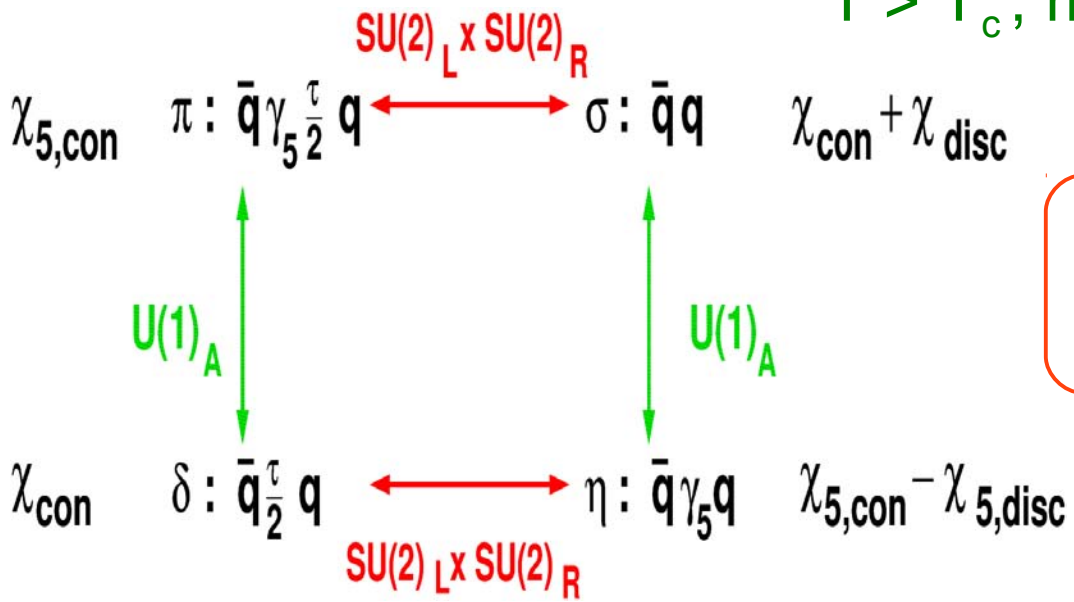

$$\chi_\pi - \chi_\delta = \chi_{disc} = \chi_{5,disc} = \frac{\chi_{top}}{m_l^2}$$

Axial anomaly in hot QCD

$T > T_c$, $m_l \to 0$

$\chi_{5,con}$ $\pi : \bar{q}\gamma_5 \frac{\tau}{2} q$ $\xleftrightarrow{SU(2)_L \times SU(2)_R}$ $\sigma : \bar{q}q$ $\chi_{con} + \chi_{disc}$

$U(1)_A$ $\updownarrow$ $\uparrow$ $U(1)_A$

χ_{con} $\delta : \bar{q}$

$$\chi_\pi - \chi_\delta = \chi_{disc} = \chi_{5,disc} = \frac{\chi_{top}}{m_l^2}$$

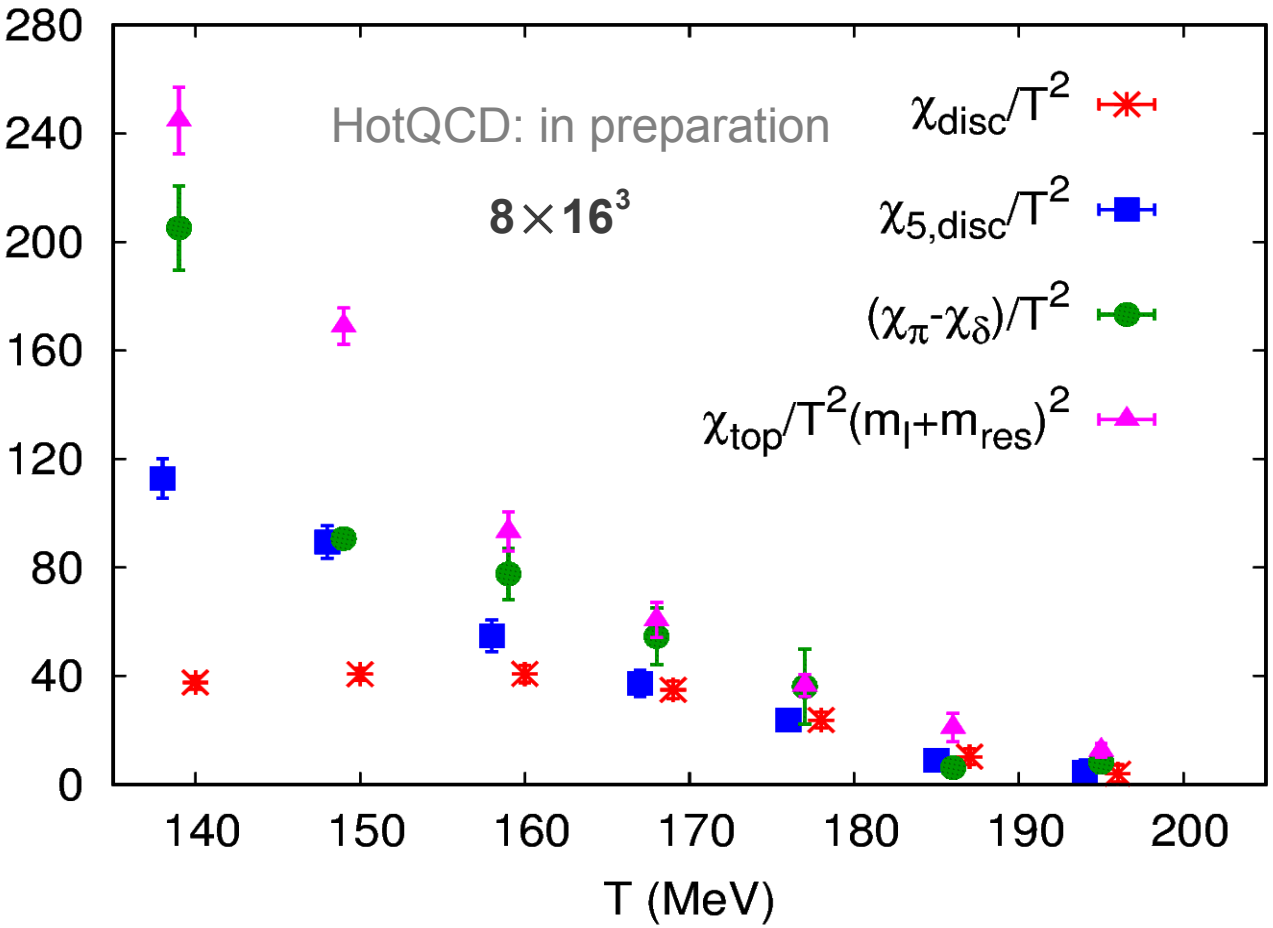

Axial anomaly in hot QCD & the Dirac spectrum

χSM: $\langle \bar{\psi}\psi \rangle = \int_0^\infty d\lambda \, \frac{2 m_l \rho(\lambda)}{m_l^2 + \lambda^2}$

$U_A(1)$: $\chi_\pi - \chi_\delta = \int_0^\infty d\lambda \, \frac{4 m_l^2 \rho(\lambda)}{\left(m_l^2 + \lambda^2\right)^2}$

Banks-Casher: $\lim_{m_l \to 0} \langle \bar{\psi}\psi \rangle = \pi \rho(0)$

a gap in the Dirac spectrum for $T > T_c$

χSM: $\langle \bar{\psi}\psi \rangle = 0$

$U_A(1)$: $\chi_\pi - \chi_\delta = 0$?!

one obvious resolution: dilute instanton gas approximation

$$\rho(\lambda) \sim m_l^2 \delta(\lambda)$$

Axial anomaly in hot QCD & the Dirac spectrum

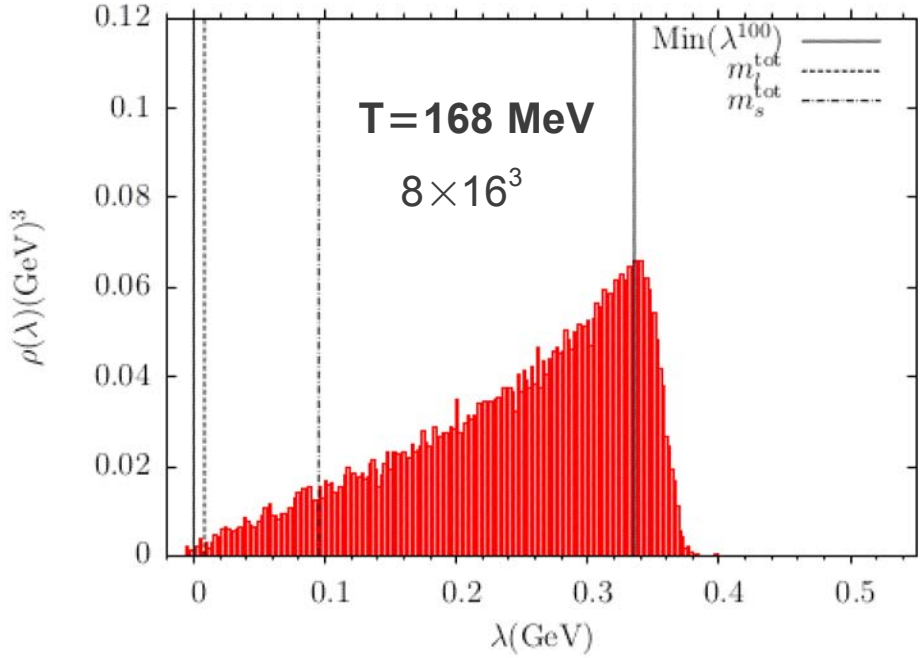

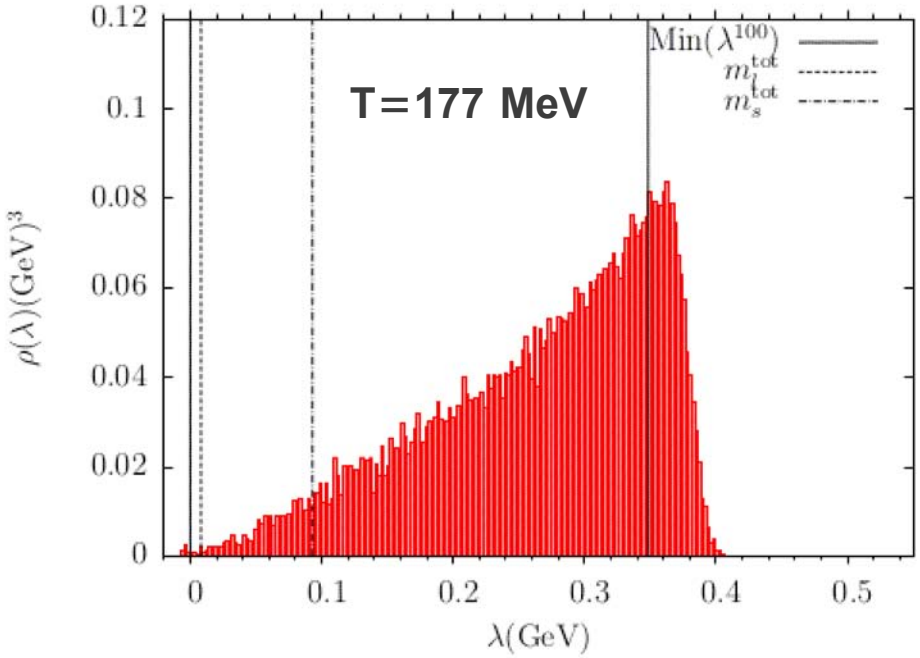

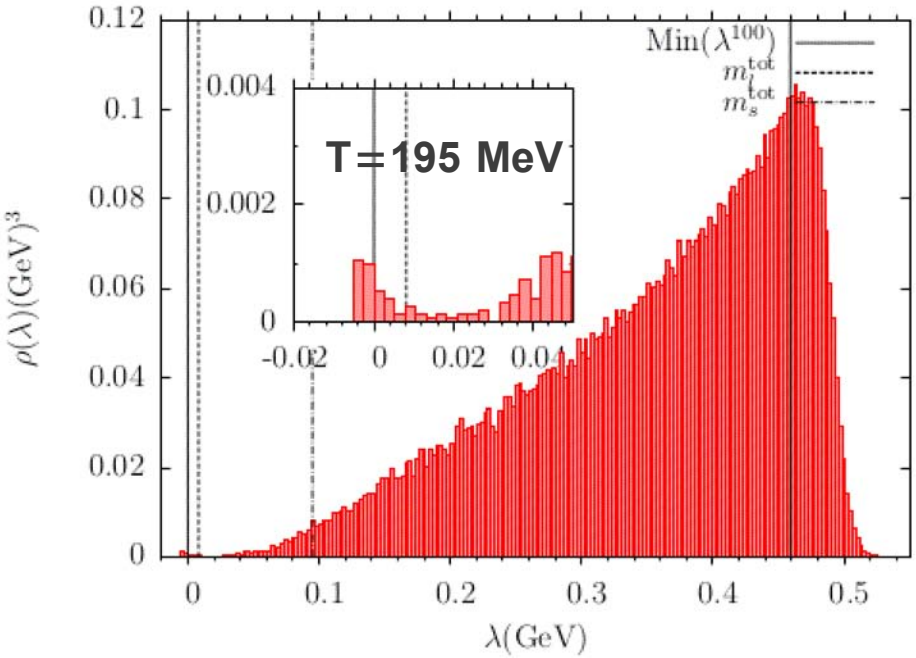

no clear evidence of a gap

or $m_l^2 \delta(\lambda)$ behavior in $\rho(\lambda)$

visible finite-volume and cut-off effects

HotQCD: in preparation

Axial anomaly in hot QCD & the Dirac spectrum

(simple) mechanisms for axial anomaly
in the chirally symmetric phase ??

$m_l \to 0$:

$$\langle \bar{\psi}\psi \rangle = \int_0^\infty d\lambda \, \frac{2 m_l \rho(\lambda)}{m_l^2 + \lambda^2} = 0$$

$$\chi_\pi - \chi_\delta = \int_0^\infty d\lambda \, \frac{4 m_l^2 \rho(\lambda)}{\left(m_l^2 + \lambda^2\right)^2} \neq 0$$

$$\chi_\pi = \langle \bar{\psi}\psi \rangle / m_l = \text{finite}$$

$$\chi_{disc} = \int_0^\infty d\lambda \, \frac{2 m_l \left(d\rho(\lambda)/dm_l\right)}{m_l^2 + \lambda^2} = \chi_\pi - \chi_\delta$$

$$\chi_\delta = \int_0^\infty d\lambda \, 2\rho(\lambda) \frac{d}{dm_l}\left[\frac{2 m_l}{m_l^2 + \lambda^2}\right] = \text{finite}$$

$\lambda \to 0$:

✓ $\rho(\lambda) \sim m_l^2 \delta(\lambda)$

✗ $\rho(\lambda) \sim \lambda$

✓ $\rho(\lambda) \sim m_l$

need to confirm using
chiral / domain wall fermions

requires many quark masses
and larger volumes

Summary

- ✓ chiral fermions are essential for deeper insight into the nature of the QCD chiral transition
- ✓ chiral fermions are required to understand the mechanism of the axial anomaly in QCD
- ✓ RBC-LLNL + HotQCD have started serious efforts to address these questions using Domain Wall Fermions
- ✓ immense technical progress for DWF thermo
- ✓ more physics results coming soon ...

Large N gauge theories with adjoint fermions

Rajamani Narayanan
Florida International University

work done in collaboration with Ari Hietanen

arXiv:0911.2449, arXiv:1011.2150, arXiv:1204.0331

New Horizons for Lattice Computations with Chiral Fermions
14-16 May 2012, Brookhaven National Laboratory

The single site model

Gauge action: $S_g = -12bNP; \quad P = \frac{1}{12}\sum_{\mu\neq\nu=1}^{4} \mathrm{Tr}\left[U_\mu U_\nu U_\mu^\dagger U_\nu^\dagger\right]$

Fermion action:

$$S_f = -f \ln\det H_o(\mu)$$

$$H_o(\mu) = \frac{1}{2}\left[(1+\mu)\,\gamma_5 + (1-\mu)\,\epsilon(H)\right]$$

H is the massive Hermitian Wilson Dirac operator

$b = \frac{1}{g^2 N}$ is the inverse lattice 't Hooft coupling

μ is the fermion mass f is the number of Dirac flavors

We can ignore gauge field topology in the large N limit and assume all gauge fields are in the zero topological sector

Due to the chiral symmetry obeyed by the overlap-Dirac operator, the eigenvalues of $H_o(0)$ come in doubly degenerate positive-negative pairs.

The determinant is positive definite and we can set f to any real value

Weak Coupling Perturbation Theory

Polyakov loop eigenvalues

$$D_\mu^{ij} = e^{i\theta_\mu^i}\delta_{ij}$$

Perturbation

$$U_\mu = e^{ia_\mu} D_\mu e^{-ia_\mu}$$

Leading order result

$$S_g = \sum_{i\neq j} \ln\left[\sum_\mu \sin^2\frac{1}{2}\left(\theta_\mu^i - \theta_\mu^j\right)\right]$$

$$S_f = -2f\sum_{i,j}\ln\left[\frac{1+\mu^2}{2} + \frac{1-\mu^2}{2}\frac{2\sum_\mu \sin^2\frac{\theta_\mu^i-\theta_\mu^j}{2} - m}{\sqrt{\left(2\sum_\mu \sin^2\frac{\theta_\mu^i-\theta_\mu^j}{2} - m\right)^2 + \sum_\mu \sin^2\left(\theta_\mu^i - \theta_\mu^j\right)}}\right]$$

If all $\theta_\mu^i = 0$ then $S_g \to -\infty$

But, if μ=0 then $S_f \to \infty$

Single site Polyakov loop eigenvalues and momenta on the infinite lattice

At lowest order in weak coupling perturbation theory
adjoint fermions on a single site lattice see momentum modes

$$e^{i(\theta^i_\mu - \theta^j_\mu)} \quad 1 \leq i,j \leq N$$

The $N^2 - 1$ angles, $\theta^i_\mu - \theta^j_\mu$, approach a continuum of momenta, p_μ, as N approaches infinity

We want the measure to be $\int \prod_\mu dp_\mu$ in order to reproduce correct infinite volume perturbation theory

Why do we need overlap fermions on a single site lattice?

<u>Naive fermions</u>

$$S_g = \sum_{i \neq j} \ln \left[\sum_\mu \sin^2 \frac{1}{2} \left(\theta^i_\mu - \theta^j_\mu \right) \right] \qquad S_f = -2f \sum_{i,j} \ln \left[\mu^2 + \sum_\mu \sin^2 \left(\theta^i_\mu - \theta^j_\mu \right) \right]$$

Momenta, $p_\mu \in [\frac{\pi}{2}, \pi]$, will spoil the uniform measure in the large N limit.

Massless overlap fermions

$$S_f = -2f \sum_{i \neq j} \ln \left[\frac{1}{2} + \frac{1}{2} \frac{2 \sum_\mu \sin^2 \frac{\theta_\mu^i - \theta_\mu^j}{2} - m}{\sqrt{\left(2 \sum_\mu \sin^2 \frac{\theta_\mu^i - \theta_\mu^j}{2} - m\right)^2 + \sum_\mu \sin^2 \left(\theta_\mu^i - \theta_\mu^j\right)}} \right]$$

Unlike naive fermions, momenta $p_\mu \in [0, \frac{\pi}{2}]$ and $p_\mu \in [\frac{\pi}{2}, \pi]$ are not identified

We need $m > 2 \sum_\mu \sin^2 \frac{\theta_\mu^i - \theta_\mu^j}{2}$ for the mode corresponding to that momentum to be massless

$m \to \infty$ is the naive fermion limit and so we cannot make it too large

Making it too small will restrict the region inside the Brillouin zone, $p_\mu \in [-\pi, \pi]$

where we have massless fermions and therefore the correct momentum measure

Correlated versus uncorrelated momenta

<u>Correlated momenta</u> $\theta_\mu^j = \frac{2\pi j}{N} \quad j = 1 \cdots, N$ in all four directions S_c : action

<u>Uncorrelated momenta</u> $\theta_\mu^j = \frac{2\pi \pi_j^\mu}{N} \quad \pi^\mu$ is a permutation of $j = 1 \cdots, N$ S_u : action

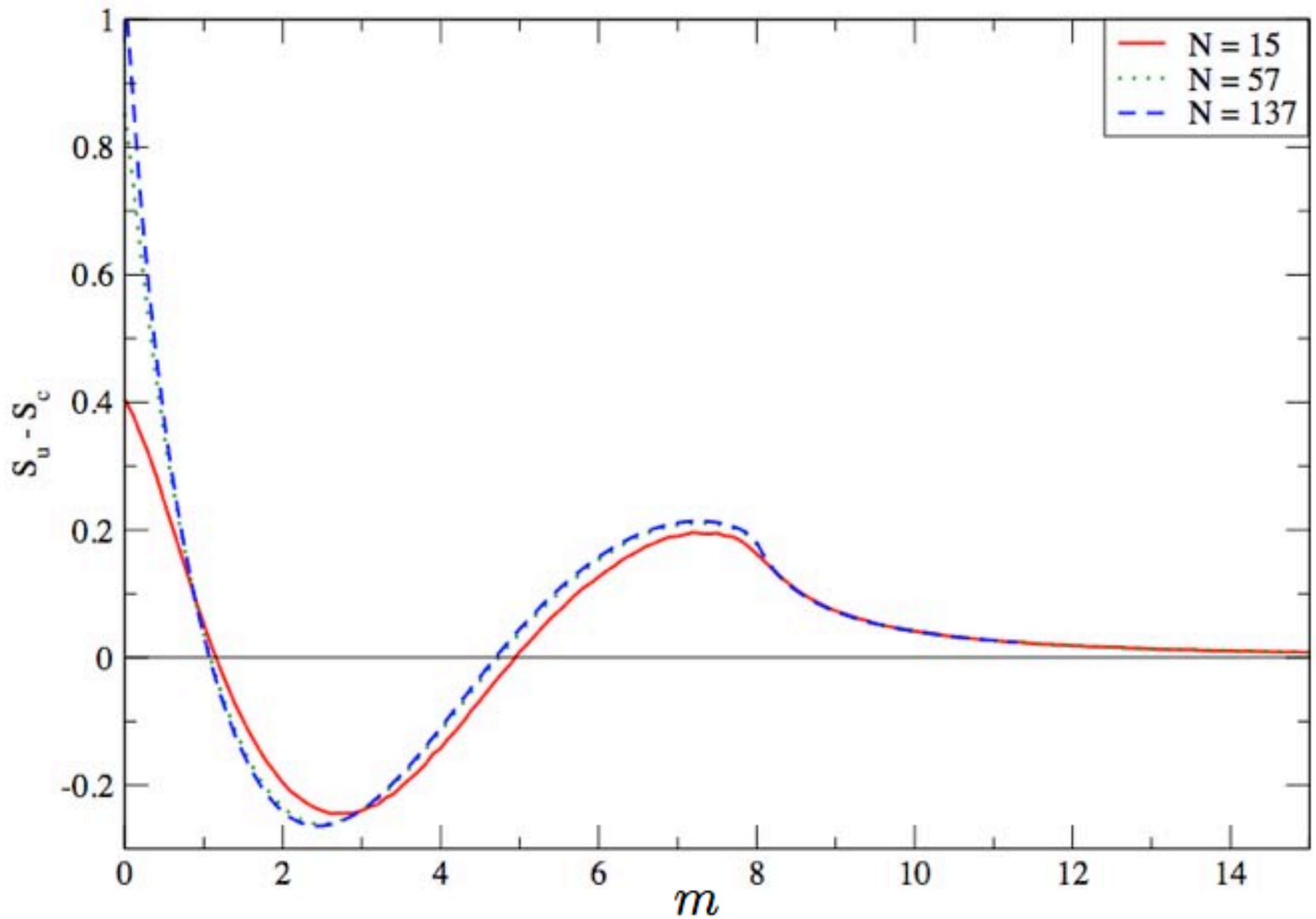

$m \in [3.5, 4.5]$ is a good choice

Distribution of Polyakov loop eigenvalues

$$P_\mu = \frac{1}{2}\left(1 - \frac{1}{N^2}|\mathrm{Tr}U_\mu|^2\right) = \frac{1}{N^2}\sum_{i,j}\sin^2\frac{1}{2}\left(\theta_\mu^i - \theta_\mu^j\right)$$

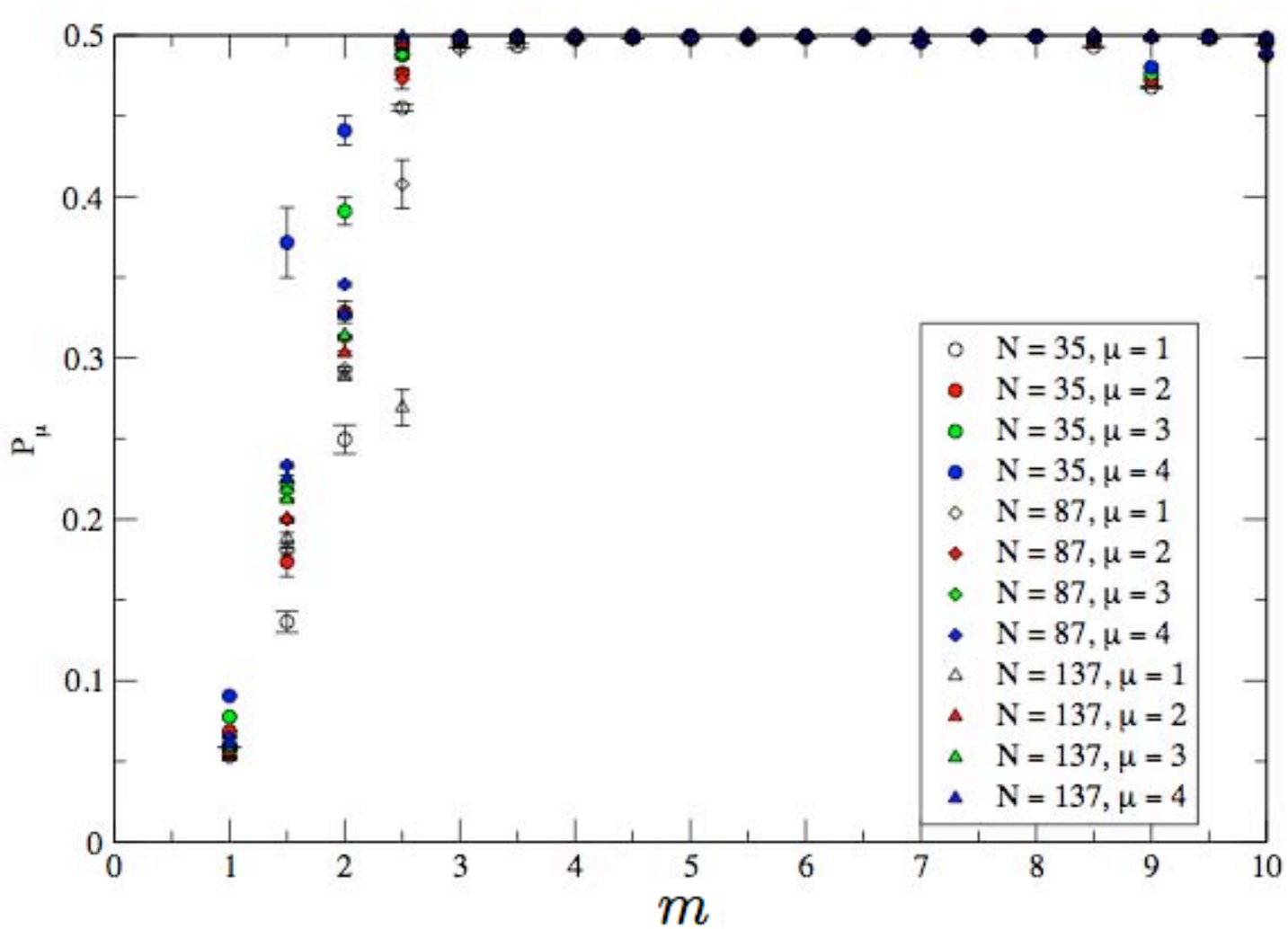

A numerical proposal

- Use Hybrid Monte Carlo Algorithm with Pseudo-fermions.
  - Works for integer number of Dirac flavors.
- A direct fermion HMC algorithm for non-integer Dirac flavors.
- Pick N and b such that we are in the large N limit for that b.
  - We expect N to increase as b increases.
- Pick a quantity to set the scale.
  - Lowest positive eigenvalue of the overlap Dirac operator.
  - Strong to weak coupling transition.
- Find the region of b where we observe scaling.
- Measure physically interesting quantities.

We will report on progress toward this goal by showing some results with

$$b = \frac{1}{\lambda} = \frac{1}{g^2 N} = \frac{\beta}{2N^2}$$

single Dirac flavor
massless fermions
N=18
b from 0.32 to 0.70

$$b = 0.35$$

$$\beta = 2.8, N = 2$$

$$\beta = 6.3, N = 3$$

beta function

Let t = ln a(b) be a logarithmic scale where a(b) could be the square root of the string tension at the lattice coupling, b.

beta function: $\beta(b) = \frac{db(t)}{dt}$

Perturbation theory: $\beta(b) = -b_0 - \frac{b_1}{b} + \cdots$

$$b_0 = \frac{11 - 4f}{24\pi^2}; \quad b_1 = \frac{17 - 16f}{192\pi^4}$$

Higher order coefficients depend on the choice of a(b) and the form of the lattice action

The perturbative beta function has a zero at $b_*(f) = -\frac{b_1}{b_0} = \frac{1}{8\pi^2}\frac{16f - 17}{11 - 4f}.$ if $\frac{11}{4} > f > \frac{17}{16}$

If f is close to 11/4, the zero occurs at very weak coupling and we can expect the zero in perturbation theory to remain essentially unaltered.

If f is close to 17/16, the zero occurs at very strong coupling and it is quite possible that it depends on the choice of a(b) and the form of the lattice action

Since a zero of the beta function could be an infra-red or ultra-violet fixed point, we need to study the behavior of the coupling close to this zero in order to see if we can define a continuum theory at the location of this zero.

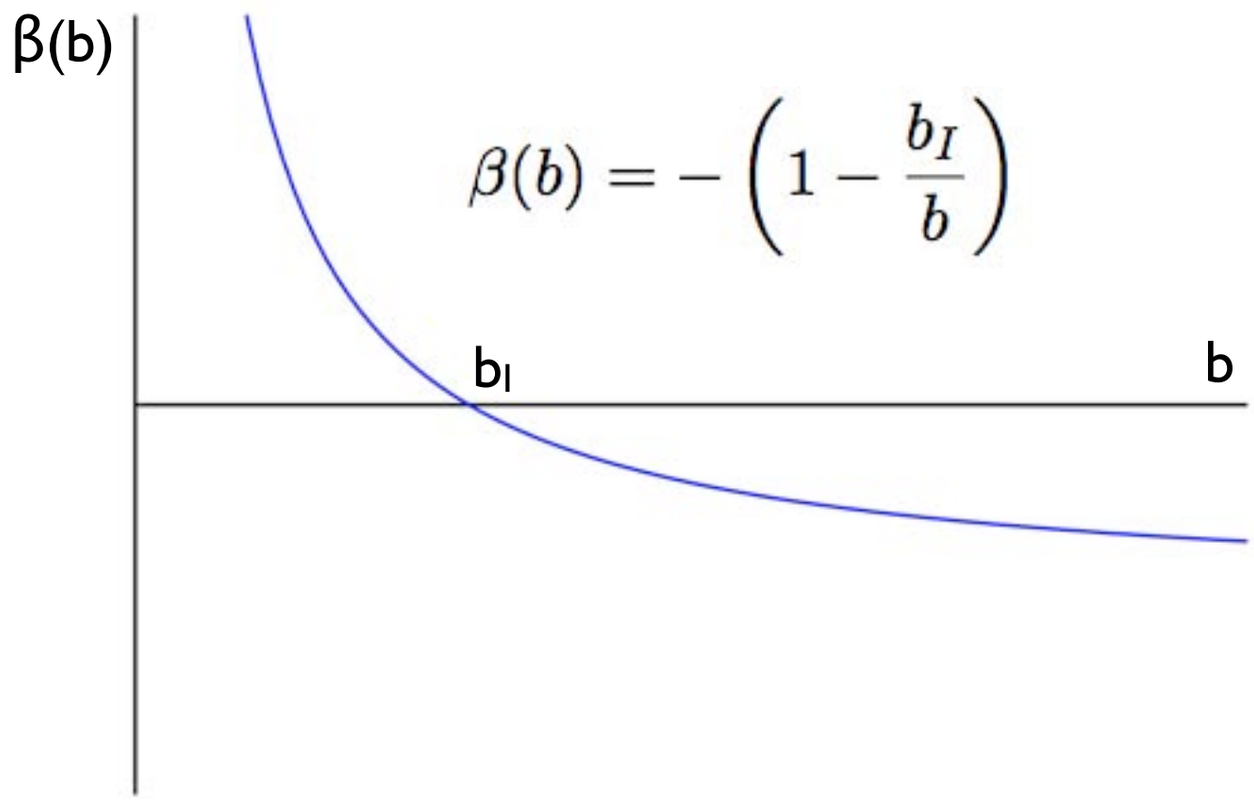
β(b)
$\beta(b) = -\left(1 - \frac{b_I}{b}\right)$
b_I
b

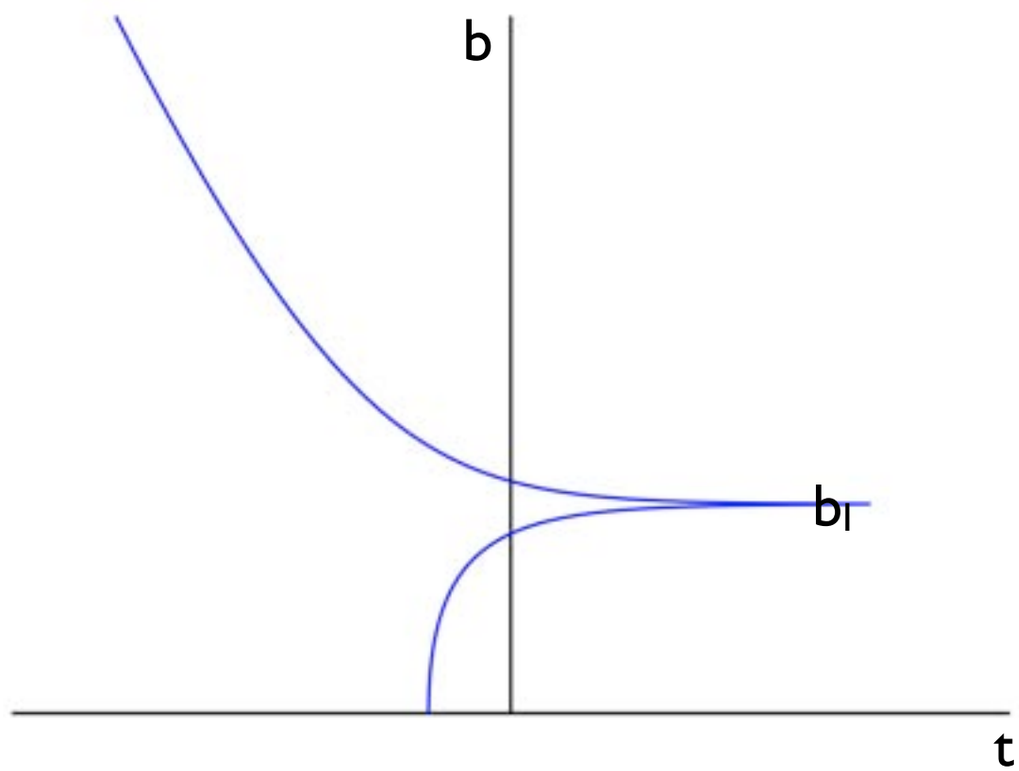
b
b_I
t

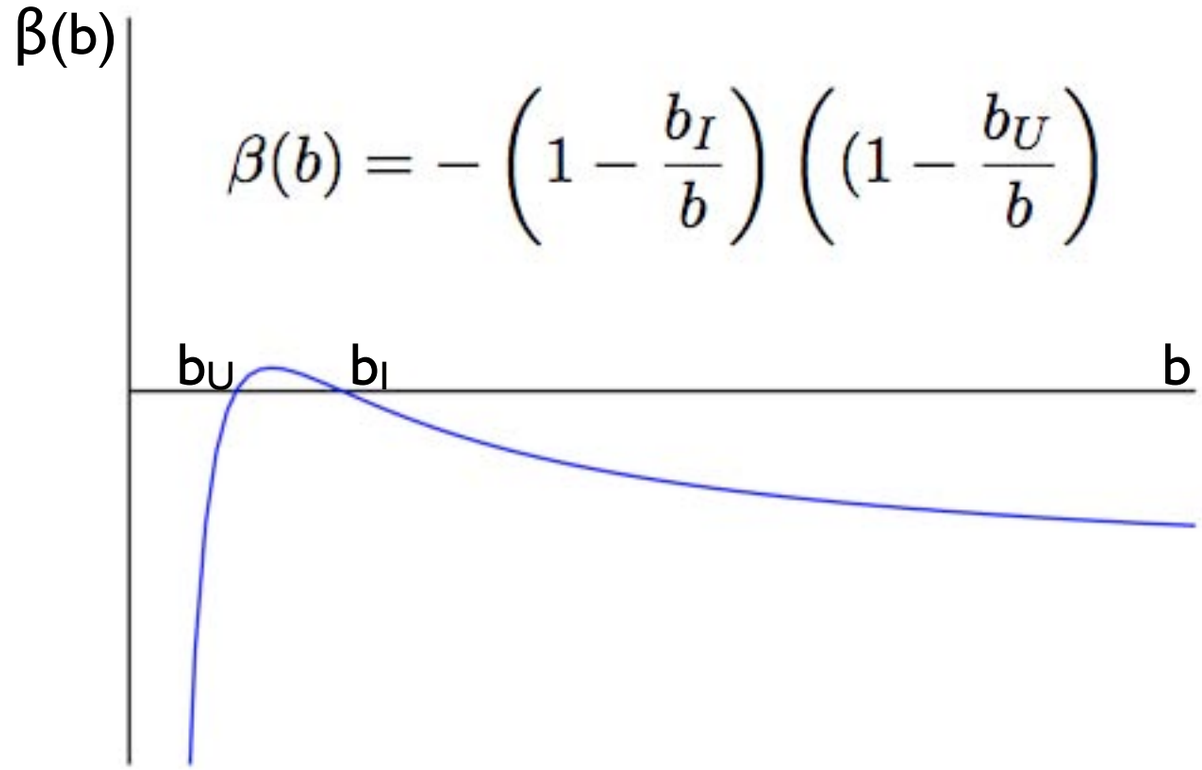
β(b)
$\beta(b) = -\left(1 - \frac{b_I}{b}\right)\left((1 - \frac{b_U}{b}\right)$
bU
bI
b

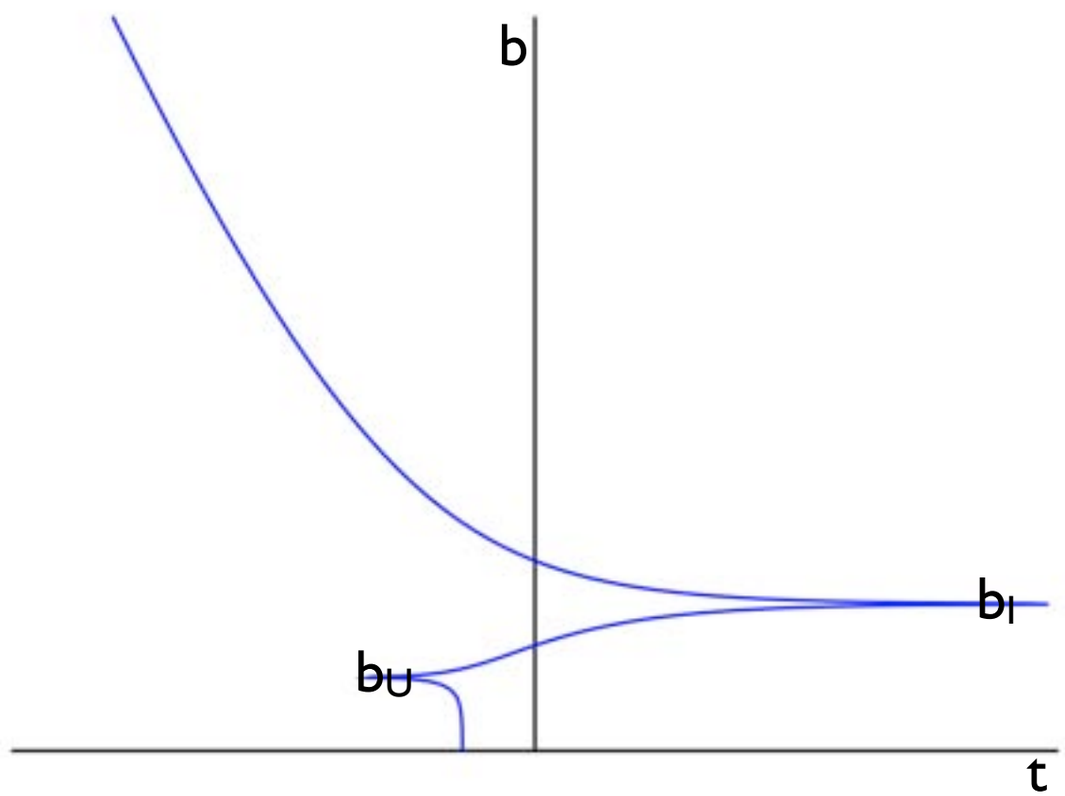
b
bI
bU
t

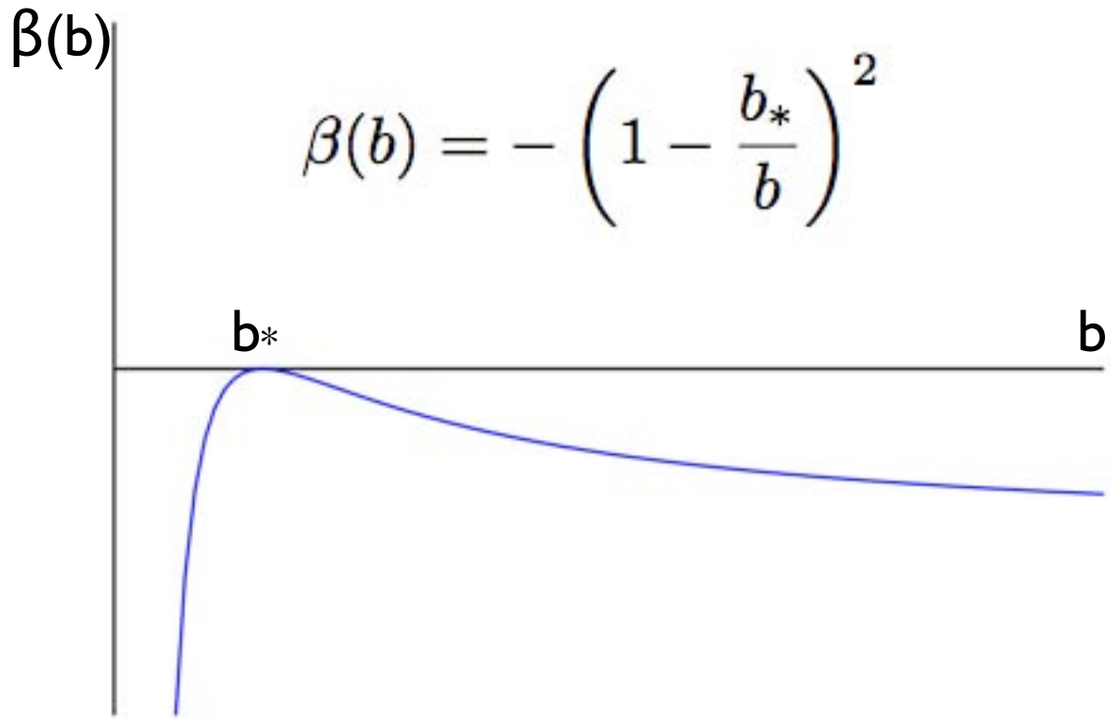
β(b)
$\beta(b) = -\left(1 - \frac{b_*}{b}\right)^2$
b*
b

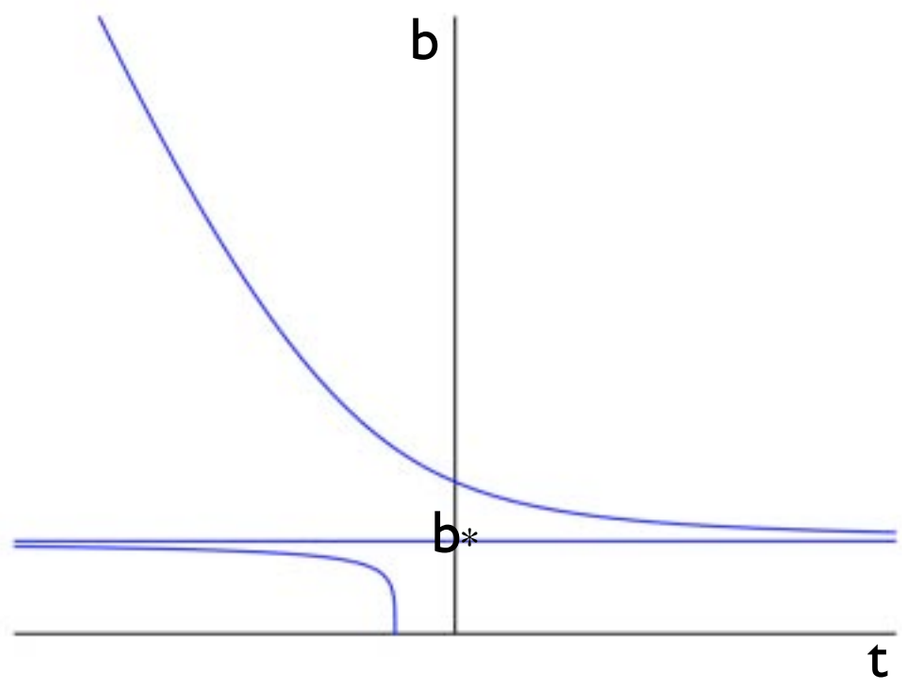
b
b*
t

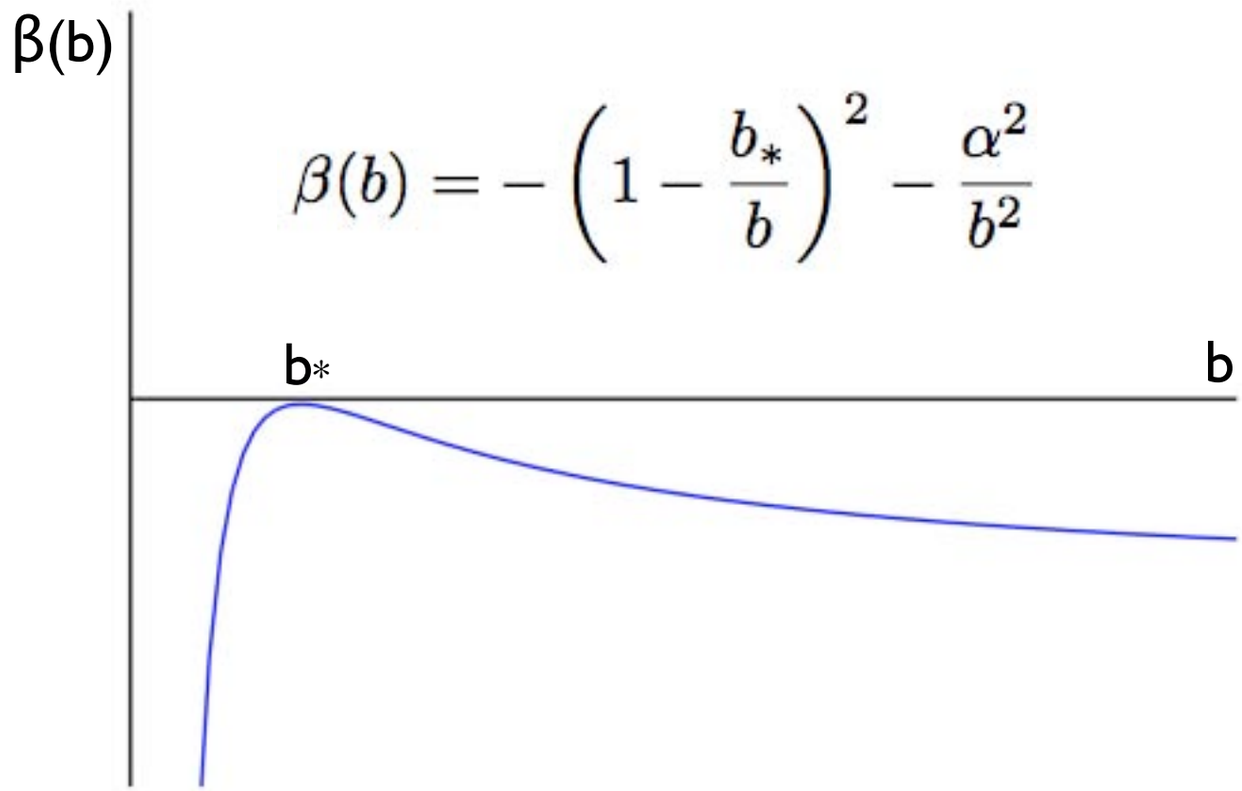
β(b)
$\beta(b) = -\left(1 - \frac{b_*}{b}\right)^2 - \frac{\alpha^2}{b^2}$
b*
b

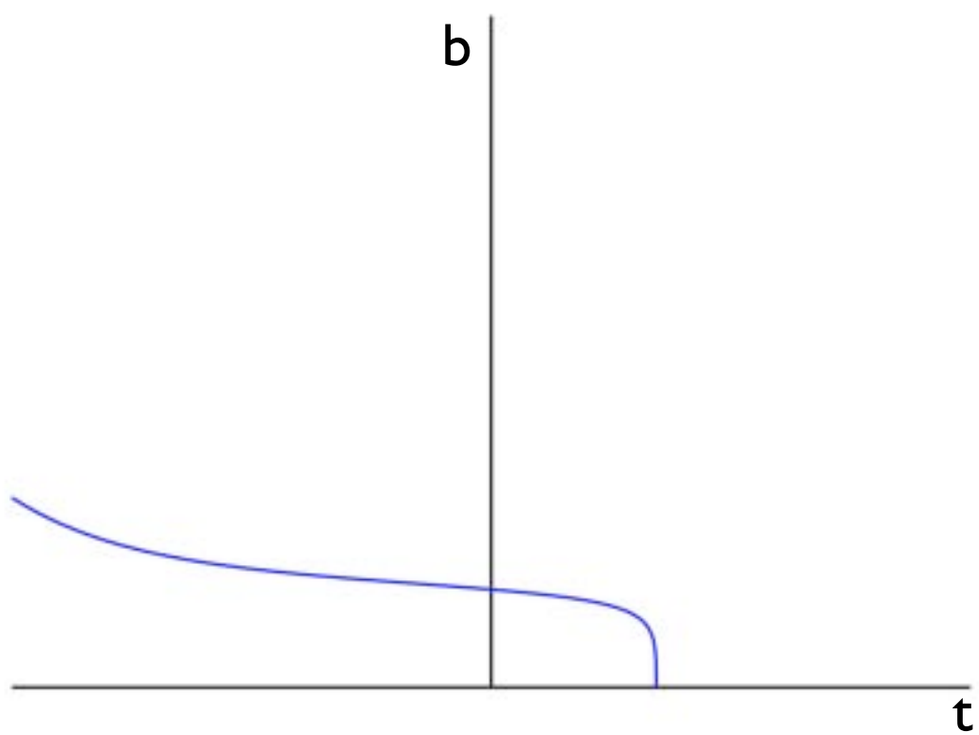
b
t

$$\beta(b) = \begin{cases} -\left|1 - \frac{b_*}{b}\right|^{p_+} & \text{for } b > b_* \\ -a_- \left|1 - \frac{b_*}{b}\right|^{p_-} & \text{for } b < b_* \end{cases}$$

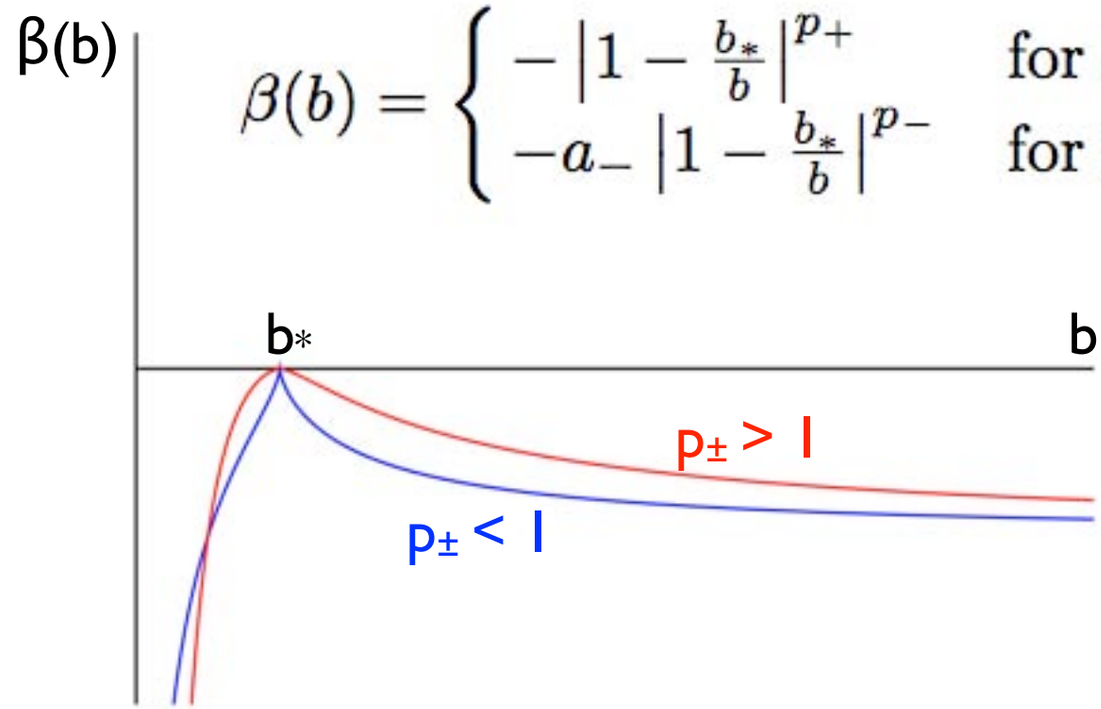

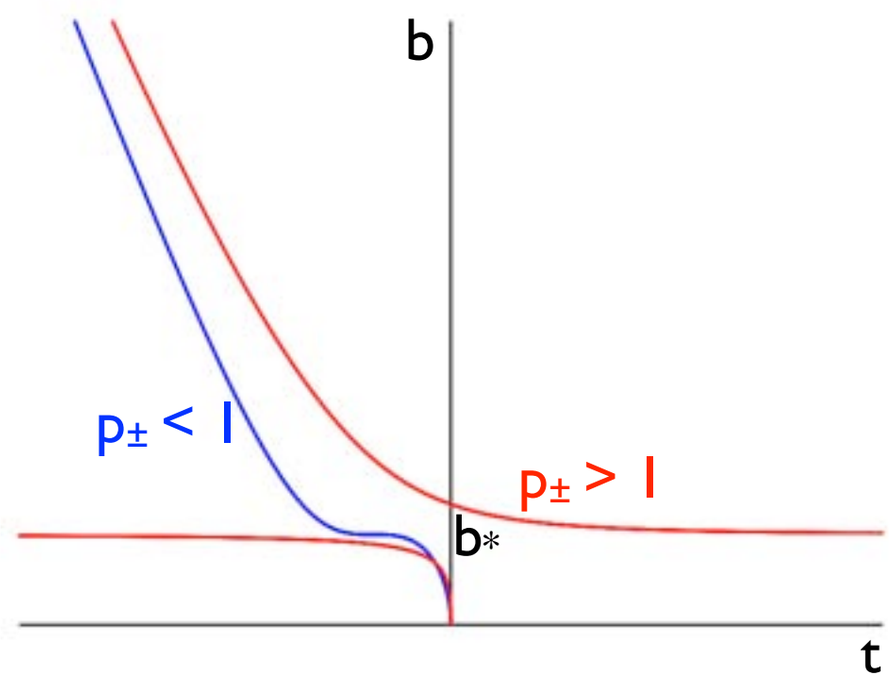

Folded Wilson loop operators

An LXL Wilson loop operator is given by $W(L) = U_\mu^L U_\nu^L U_\mu^{\dagger L} U_\nu^{\dagger L}$

Eigenvalues of this operator are gauge invariant and lie on a unit circle in the complex plane

All eigenvalues will be close to +1 if the loop is small and there will be gap around -1

Eigenvalues will be distributed over the full unit circle for large loops

There is a critical size, $L_c(b,N)$, where the gap will close

We can define $a(b) = \dfrac{1}{L_c(b,N)}$ as a scale

Eigenvalues of the Hermitian massless overlap Dirac operator

$\pm \lambda_k \quad 0 < \lambda_k < 1,\ k = 1, \cdots, N^2 - 1 \text{ with } \lambda_k < \lambda_{k+1}$

We can define $\lambda(b) = \langle \lambda_1 \rangle$ as another scale

If chiral symmetry is broken, we expect the ratios $r_k = \left\langle \dfrac{\lambda_1}{\lambda_k} \right\rangle$ to be independent of coupling for small k at finite N

Average value of the plaquette

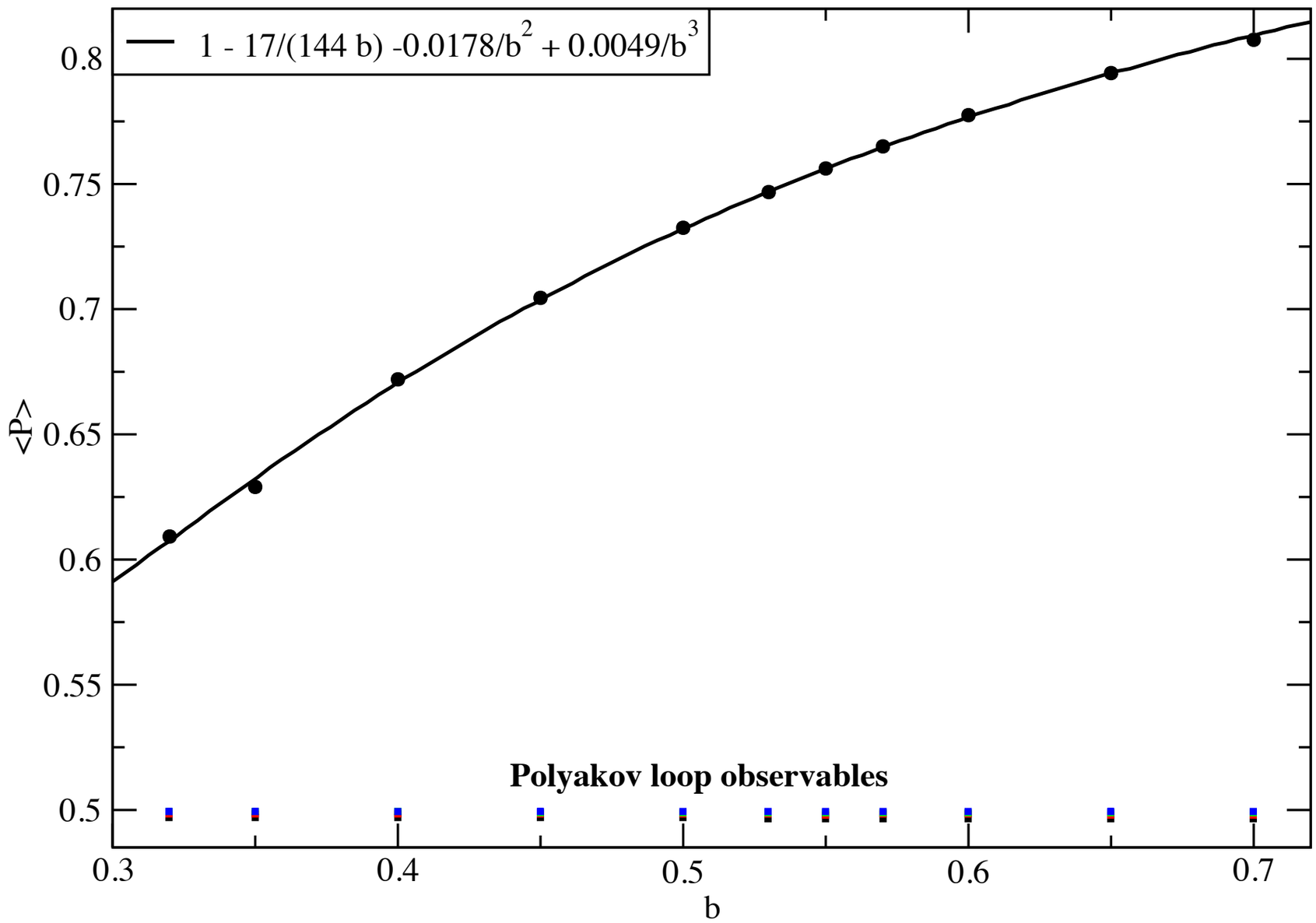

Polyakov loop observables show that we are in the continuum phase

Running of the scale obtained from the folded Wilson loop operator

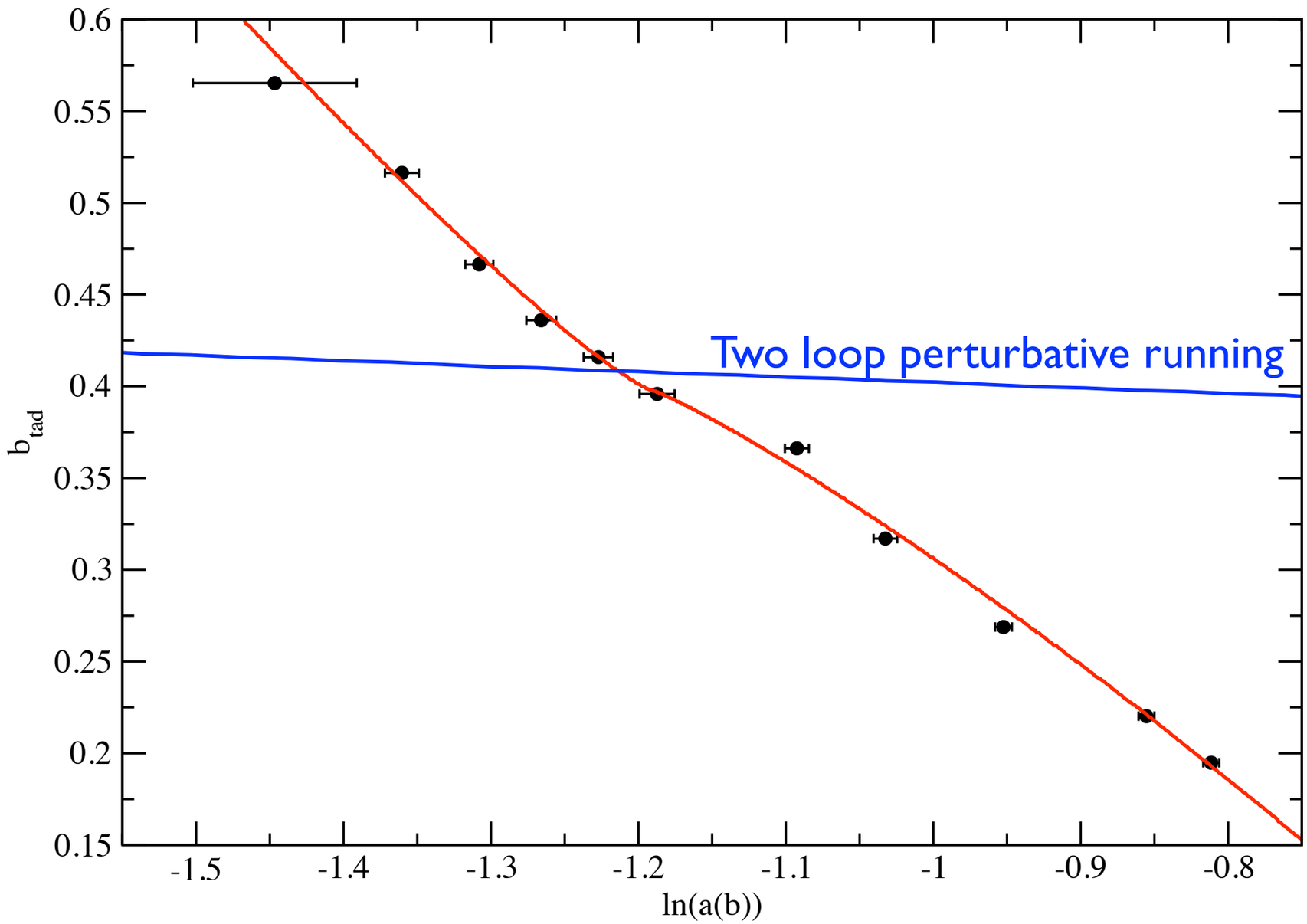

Distribution of the Wilson loop operator eigenvalues at , above and below criticality

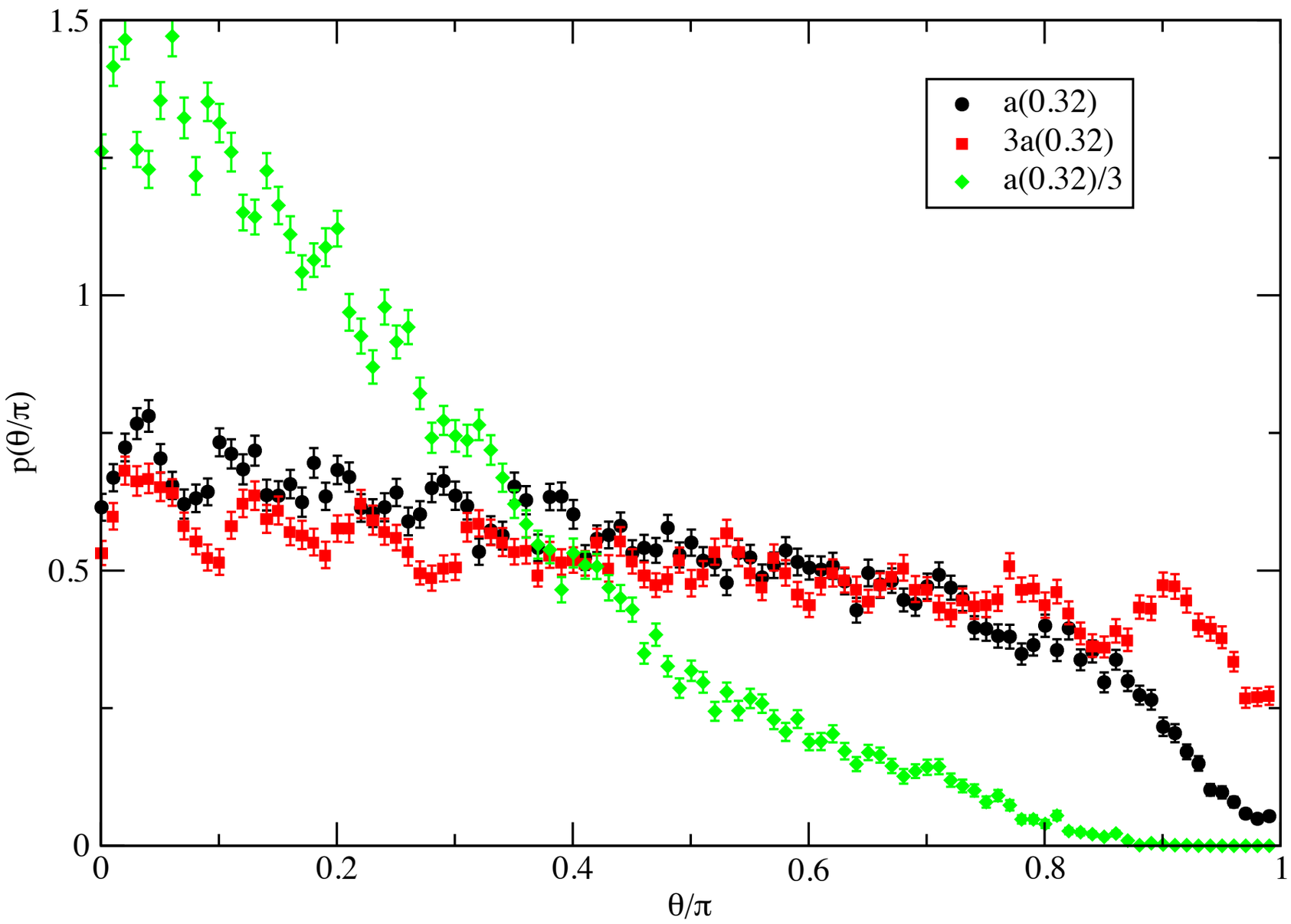

Running of the scale obtained from the lowest positive eigenvalue of the Dirac operator

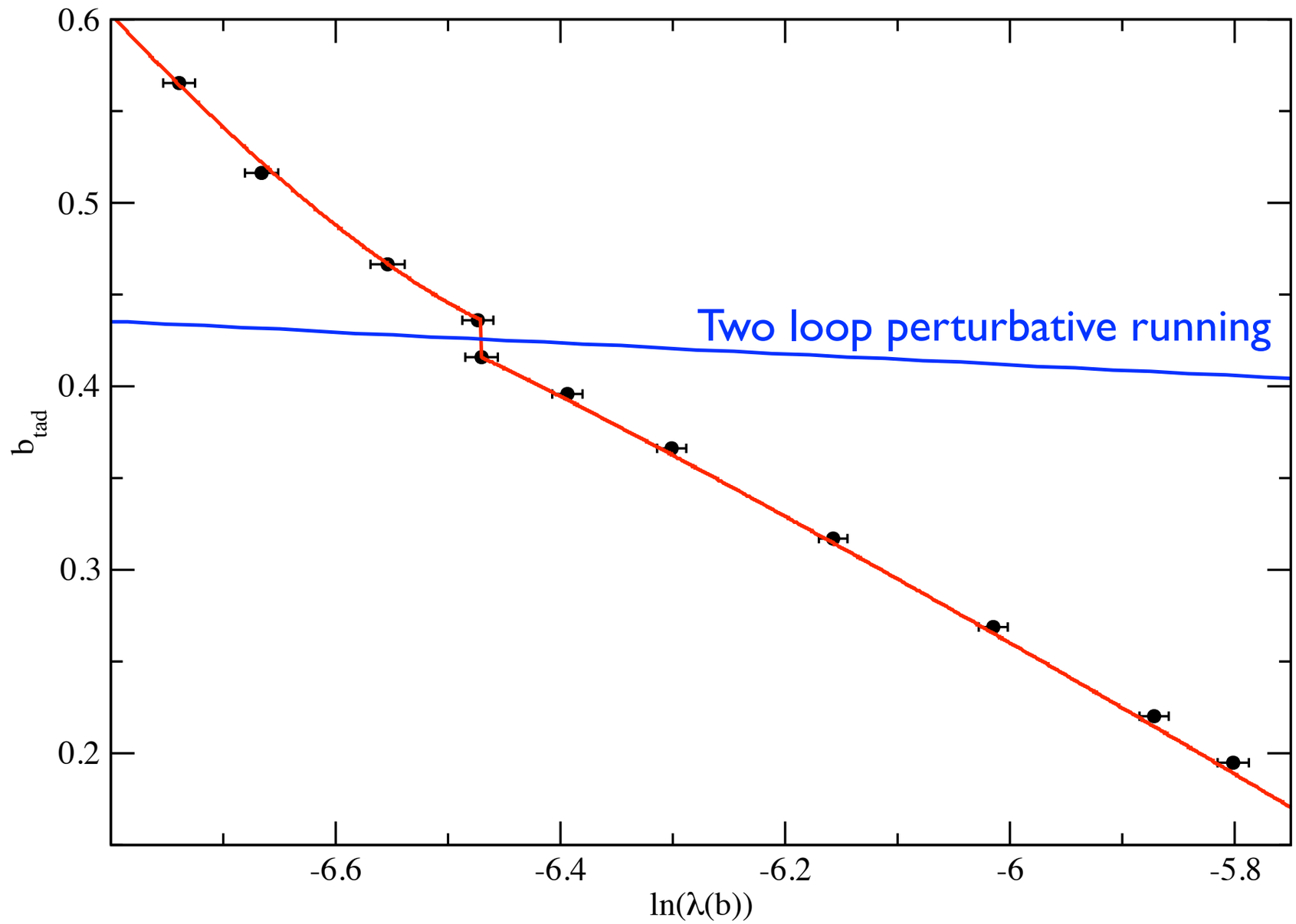

Full distribution of the eigenvalues of the overlap Dirac operator at three different couplings

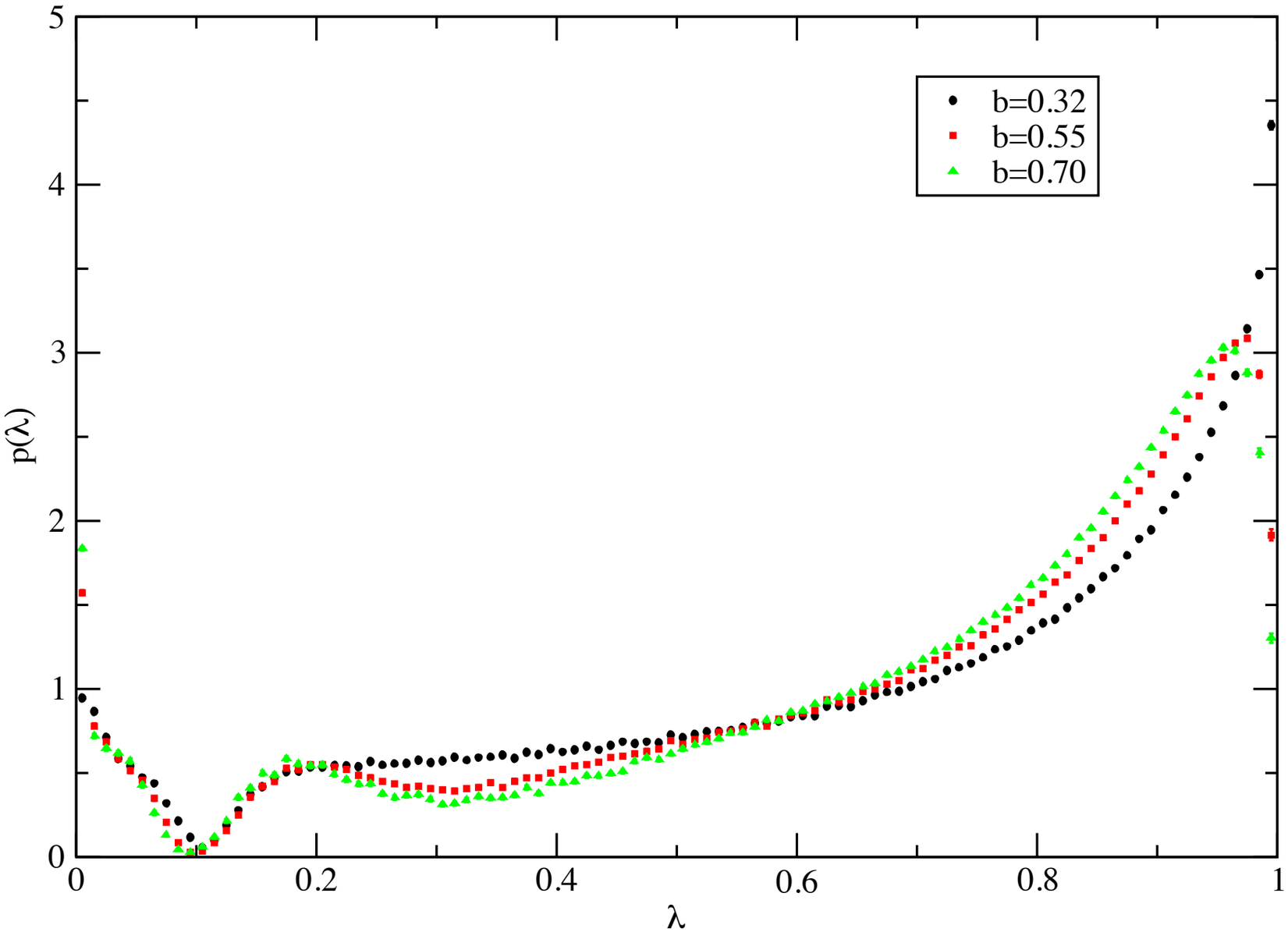

Ratios of the eigenvalues of the overlap Dirac operator

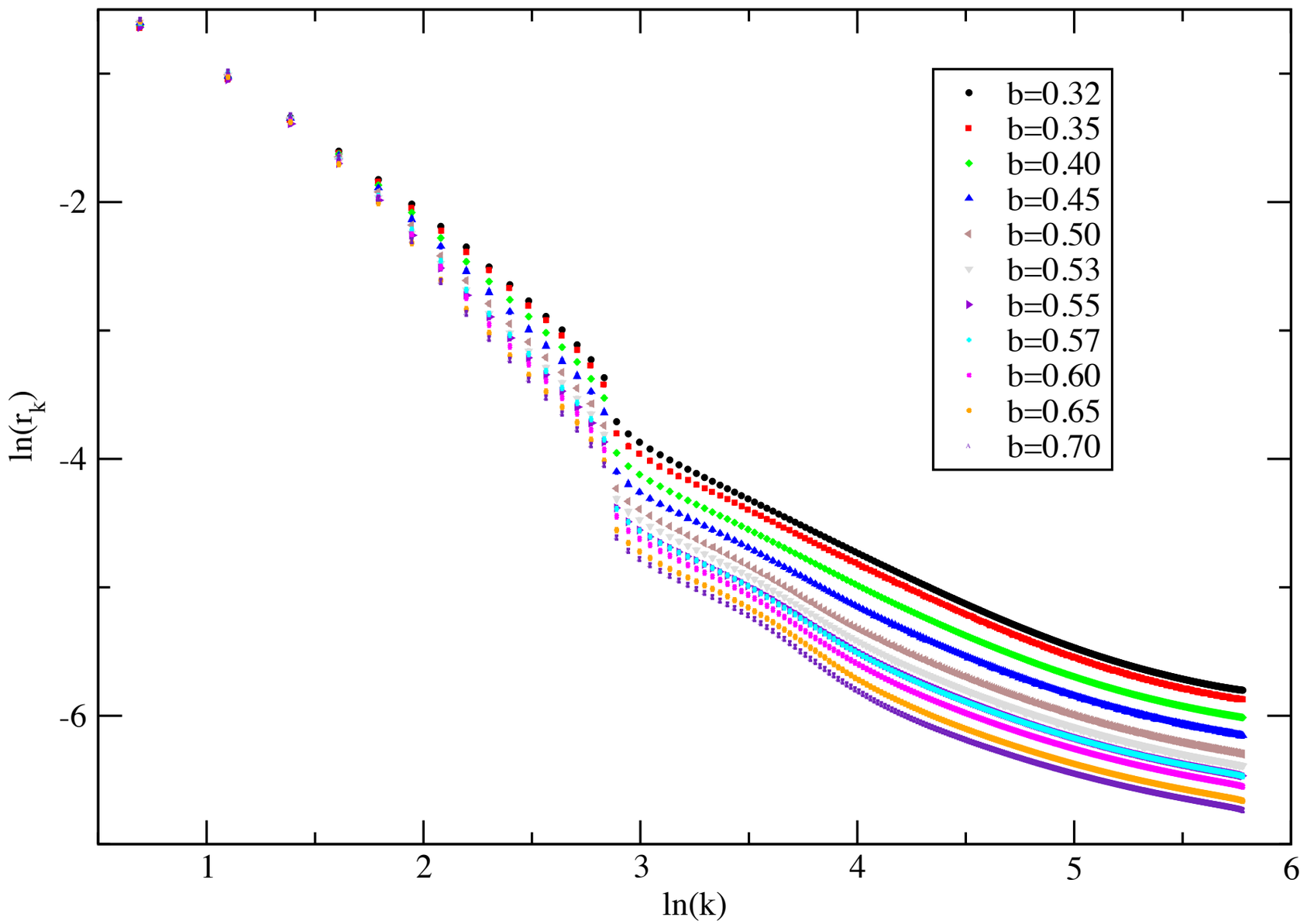

Results for the f=1 massless theory

using a(b) as the scale

$$\beta(b_{\rm tad}) = \begin{cases} -\left|1 - \frac{0.398}{b_{\rm tad}}\right|^{0.16} & \text{for } b_{\rm tad} > 0.398 \\ -0.64\left|1 - \frac{0.398}{b_{\rm tad}}\right|^{0.12} & \text{for } b_{\rm tad} < 0.398 \end{cases}$$

using λ(b) as the scale

$$\beta(b_{\rm tad}) = \begin{cases} -\left|1 - \frac{0.419}{b_{\rm tad}}\right|^{0.37} & \text{for } b_{\rm tad} > 0.419 \\ -0.36\left|1 - \frac{0.419}{b_{\rm tad}}\right|^{0.05} & \text{for } b_{\rm tad} < 0.419 \end{cases}$$

Combining the two results, we say that $b_* = 0.408(11)$ is a location of non-analyticity

All powers are less than unity and so we cannot define a continuum theory at b_* for the f=1 theory

Conclusions

- We can use matrix model in the large N limit to numerically study gauge theories coupled to adjoint fermions.
- We can look at conformal and near-conformal theories by extending f, the number of fermion flavors, to take on any real value.
- One can use exact HMC algorithm (compute the fermion force exactly) or use pseudo-fermion HMC algorithm.
- The beta function is expected to show non-analytical behavior at the infra-red/ultra-violet fixed point.
- It is possible to add a mass term and study the theory.

Lattice Radial Quantization.

Richard Brower, George Fleming and
Herbert Neuberger (speaker)

Department of Physics
Rutgers University
Piscataway, NJ08854

New Horizons for Lattice Gauge Theory Computations,
Brookhaven National Laboratory, May 14-16, 2012, NY

Abstract

We regularize conformal field theories in radial quantization using lattice techniques. Only angular separations matter. Scale is logarithmically discretized in equal intervals. As an application, we set out to compute the critical exponent η for the 3D Ising model and present some preliminary results.

Outline

Beautiful theories

Conformal theories

Foliations

The icosahedral Transfer matrix

Spectrum

Regularization

Velocity of light renormalization

Preliminary numerical results

Outline

Beautiful theories

Conformal theories

Foliations

The icosahedral Transfer matrix

Spectrum

Regularization

Velocity of light renormalization

Preliminary numerical results

Being a snob

"Beauty" $= \frac{\text{nr. of nontrivial results}}{\text{nr. of free continuos parameters}}$. To be worthwhile of our time, a beautiful theory ought to be relevant to Nature. Such beautiful theories never are exactly soluble, nor are they completely perturbative. The top examples for particle physicists are

- The most relevant beautiful particle theory is QCD with a moderate number of massless quarks.
- The most beautiful unparticle theory is $SU(N)$ gauge theory with massless fermionic matter in the conformal window. Maybe it is relevant to Nature.

QCD is essentially a single scale theory, and lattice techniques work and are in principle exact. Walking technicolor type of theories are harder because they have too wide a range of scales for an ordinary lattice approach. One can make progress however by considering their conformal cousins. Of primary importance are the anomalous dimensions of some composite scaling fields in the IR.

Outline

Beautiful theories

Conformal theories

Foliations

The icosahedral Transfer matrix

Spectrum

Regularization

Velocity of light renormalization

Preliminary numerical results

Main point and application

In a conformal theory there is no scale and only angles matter. Rather than uniformly discretizing scales one should uniformly discretize their logarithm as per AMR logic. Simulating a conformal theory by uniformly discretizing scales might be impractical. What to do in the “almost conformal” case is another topic.
There is no point in further generalities. I’ll focus on the critical 3D Ising model because one can simulate it very efficiently using cluster algorithms. The objective would be to exploit it being a CFT in order to extract the anomalous dimension of the magnetization operator. Our numerical results are preliminary.

Outline

Beautiful theories

Conformal theories

Foliations

The icosahedral Transfer matrix

Spectrum

Regularization

Velocity of light renormalization

Preliminary numerical results

Radial quantization and its cousins

In radial quantization one views R^3 as a sequence of 2D concentric spherical shells whose radial density is uniform in the logarithm of the radius measured from the common center. The coordinates on the shells are angles. By a conformal transformation flat R^3 gets mapped into an infinite cylinder raised on top of a 2D sphere. One quantizes by defining a transfer matrix along the cylinder. The logarithm of the eigenvalues of this transfer matrix provide the spectrum of dimensions of all operators.
We could foliate R^3 in other ways. We choose to foliate it into concentric 2D icosahedral shells, again at uniform density in the logarithm of the distance from the common center. The shells have 20 flat equilateral triangular faces and 12 corners. One can define now an icosahedral transfer matrix.

Outline

Beautiful theories

Conformal theories

Foliations

The icosahedral Transfer matrix

Spectrum

Regularization

Velocity of light renormalization

Preliminary numerical results

Spectrum and states

The icosahedral transfer matrix T has the same spectrum as the radial one: it consists of the exponent of all the eigenvalues of the dilatation operator in the Wilson-Fisher CFT.
The eigenstates of T are different from the radial case. Most spectral regularities would seem accidental because the $SO(3)$ invariance is hidden. Regularities reflecting the discrete symmetry group $\mathbf{I}$ of the icosahedron remain evident. A multiplet of angular momentum l under $SO(3)$ would transform irreducibly under $\mathbf{I}$ if $l = 0, 1, 2$ because the icosahedron has 3-fold and 5-fold symmetry axes. The remaining 2 irreps of $\mathbf{I}$ appear in the decomposition of $l = 3$; their degeneracy would seem accidental if we did not know about the hidden $SO(3)$.
Let $M(x)$ be the exact scaling field corresponding to the highest eigenvalue of T in the Z_2-odd sector. One can construct out of it 5 orthogonal multiplets transforming irreducibly under $\mathbf{I}$ in representations subduced from the $l = 1, 2, 3$ irreps of $SO(3)$.

Outline

Beautiful theories

Conformal theories

Foliations

The icosahedral Transfer matrix

Spectrum

Regularization

Velocity of light renormalization

Preliminary numerical results

Descendants

Let m_0 be the dimension of $M(x)$ and m_l the dimensions of the descendants constructed from $M(x)$ for $l = 0, 1, 2$. One has

$$m_l = m_0 + l$$

At this point we went beyond just using scaling, which reflects only dilatation invariance. The integer spacing is a consequences of full conformal invariance. Our regularization preserves (if present in the continuum) the crucial discrete inversion transformation which extends the symmetry in the flat case to the full conformal group.

Outline

Beautiful theories

Conformal theories

Foliations

The icosahedral Transfer matrix

Spectrum

Regularization

Velocity of light renormalization

Preliminary numerical results

The lattice

Each equilateral triangle is replaced by a fine triangular mesh defined by adding $s-1$ extra points at equal distance on each icosahedral edge. The total number of sites per shell is $10s^2+2$. Our UV cutoff Λ will be $\propto s$ for large s because the size of a shell is some fixed number in terms of angular extent. The UV cutoff is dimensionless in radial quantization.
On each site we place an Ising spin. To all intra- and inter- links connecting sites i and j we attach the standard weight

$$e^{b\sigma_i\sigma_j}$$

$b>0$ is the Ising coupling and needs to be tuned to b_c to get into the domain of attraction of the Wilson Fisher fixed point. The SW cluster update algorithm only needs the abstract graph of the structure in order to proceed.

Outline

Beautiful theories

Conformal theories

Foliations

The icosahedral Transfer matrix

Spectrum

Regularization

Velocity of light renormalization

Preliminary numerical results

Fixing homogeneity

Except at the corners, the shells are locally a flat triangular lattice. Neighboring shells are connected chain like. There is local regularity, but the approximate local discrete rotational invariance around a vertex does no mix in-shell with intra-shell directions.

For a given s, the eigenvalues corresponding to m_l are μ_l and the near shell separation is $\Delta\tau = 1$. The continuum shell separation is Δt. We define κ so that $m_l = \kappa\mu_l\Lambda$. Then, $t = \frac{\tau}{\Lambda}$ to ensure $m_l t = \kappa\mu_l\tau$.

We can extract $\kappa\Lambda$ from

$$\mu_l' - \mu_l = \frac{l' - l}{\kappa\Lambda}$$

Then we can extract m_0 from $m_0 = \kappa\Lambda\mu_0$. The anomalous dimension of $M(x)$, η is defined by

$$m_0 = \frac{1+\eta}{2}$$

Outline

Beautiful theories

Conformal theories

Foliations

The icosahedral Transfer matrix

Spectrum

Regularization

Velocity of light renormalization

Preliminary numerical results

The refinement level is s and the number of shells is $16s$; at $b = b_c$, $\kappa\Lambda \propto s$ must hold to leading order in s. $b = 0.16107$.

b	s	$\frac{\mu_2-\mu_1}{\mu_1-\mu_0}$	$\frac{s}{\kappa\Lambda}$	η
0.16107	6	0.966(5)	0.724(2)	0.084(2)
0.16107	7	0.966(5)	0.728(1)	0.066(2)
0.16107	8	0.958(2)	0.7288(2)	0.052(1)
0.16107	9	0.954(2)	0.7311(2)	0.036(1)
0.16107	10	0.957(2)	0.7298(2)	0.044(1)
0.16107	11	0.961(2)	0.7267(2)	0.064(1)
0.16107	12	0.973(2)	0.7181(2)	0.123(1)

Previous simulations, using cubic shells and a different approach, gave, after extrapolation to infinite cutoff, $\eta = 0.002 \pm 0.010$; the expected value is $\eta \approx 0.036$.
Maybe we found the correct value of η at $s = 9$ not by accident.

“Masses” or more correctly dimensions

We probably are not at $b = b_c(\infty)$. Something is happening at $s = 9$. Maybe we are in the would-be Z_2 broken side of $b_c(\infty)$. Maybe periodic boundary conditions are better. So far, our analysis has been rough.

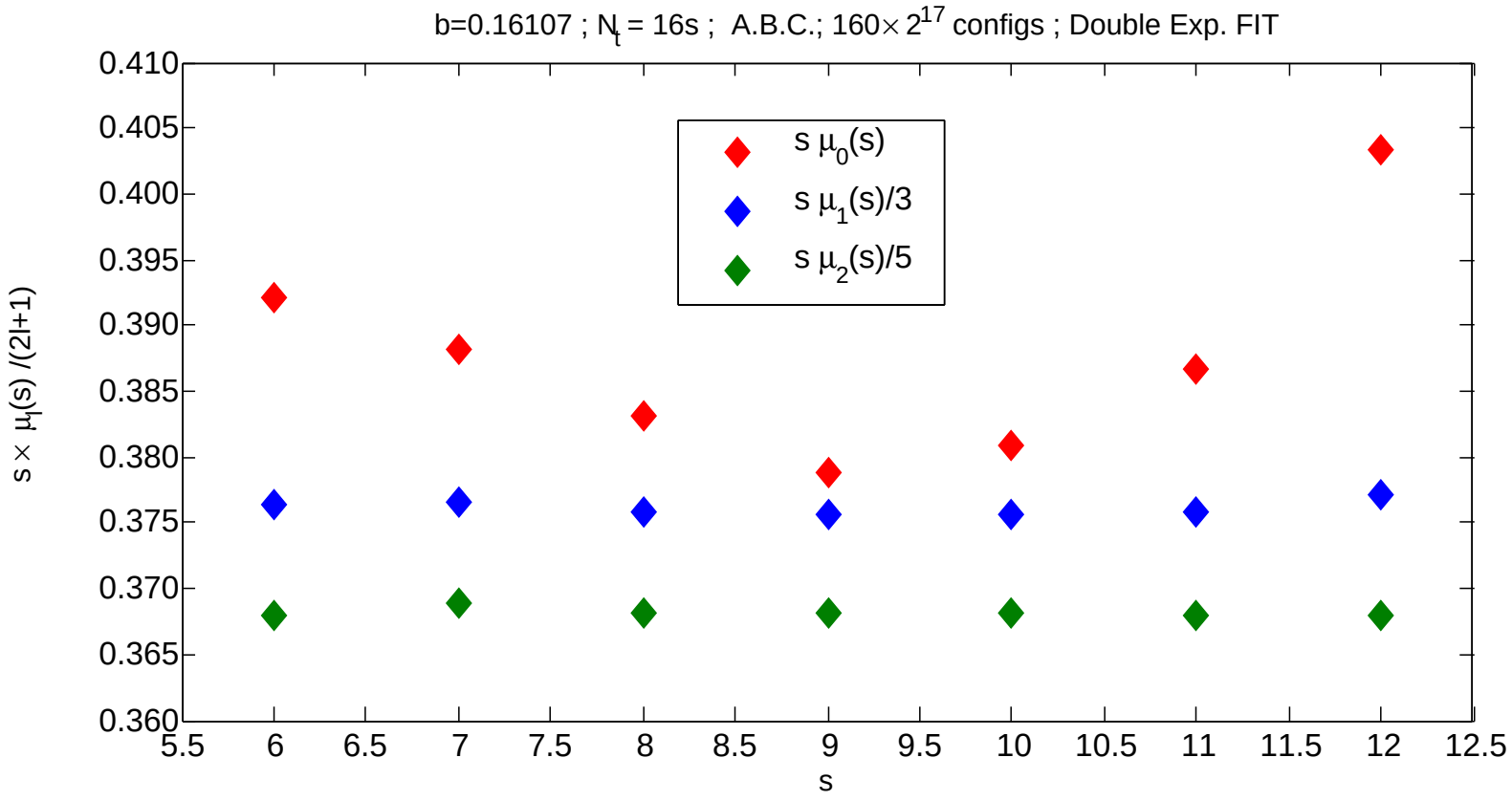

LATTICE QCD FOR NUCLEAR PHYSICS

Kostas Orginos

Jefferson Lab
Thomas Jefferson National Accelerator Facility

NPLQCD Collaboration

Silas R. Beane
New Hampshire

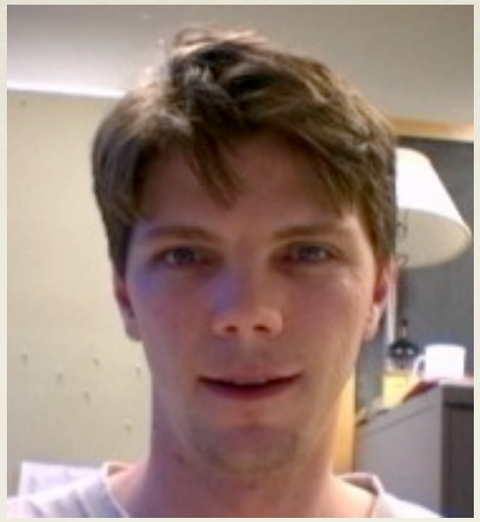

William Detmold
William & Mary

Huey-Wen Lin
U of Washington

Tom Luu
Livermore

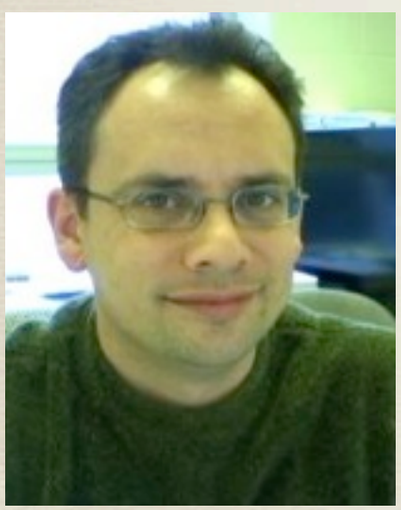

Kostas Orginos
William & Mary

Assumpta Parreño
Barcelona

Martin J. Savage
U of Washington

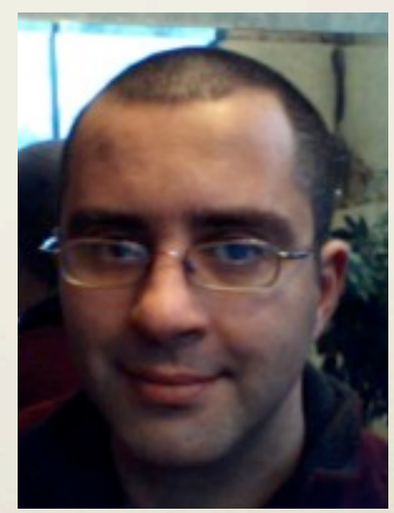

Aaron Torok
Indiana

André Walker-Loud
William & Mary

Emmanuel Chang

Hadron Interactions

Goals:

- Challenge: Compute properties of nuclei from QCD
  - Spectrum and structure
- Confirm well know experimental observation for two nucleon systems
- Explore the largely unknown territory of hyper-nuclear physics
- Provide input for the equation of state for nuclear matter in neutron stars
- Provide input for understanding the properties of multi-baryon systems

Jefferson Lab

FAIR

J-PARC

KEK
HIGH ENERGY ACCELERATOR RESEARCH ORGANIZATION

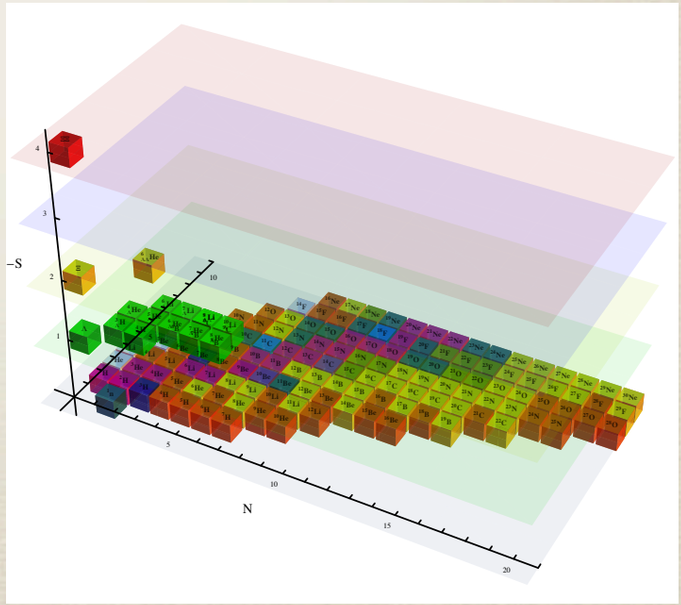

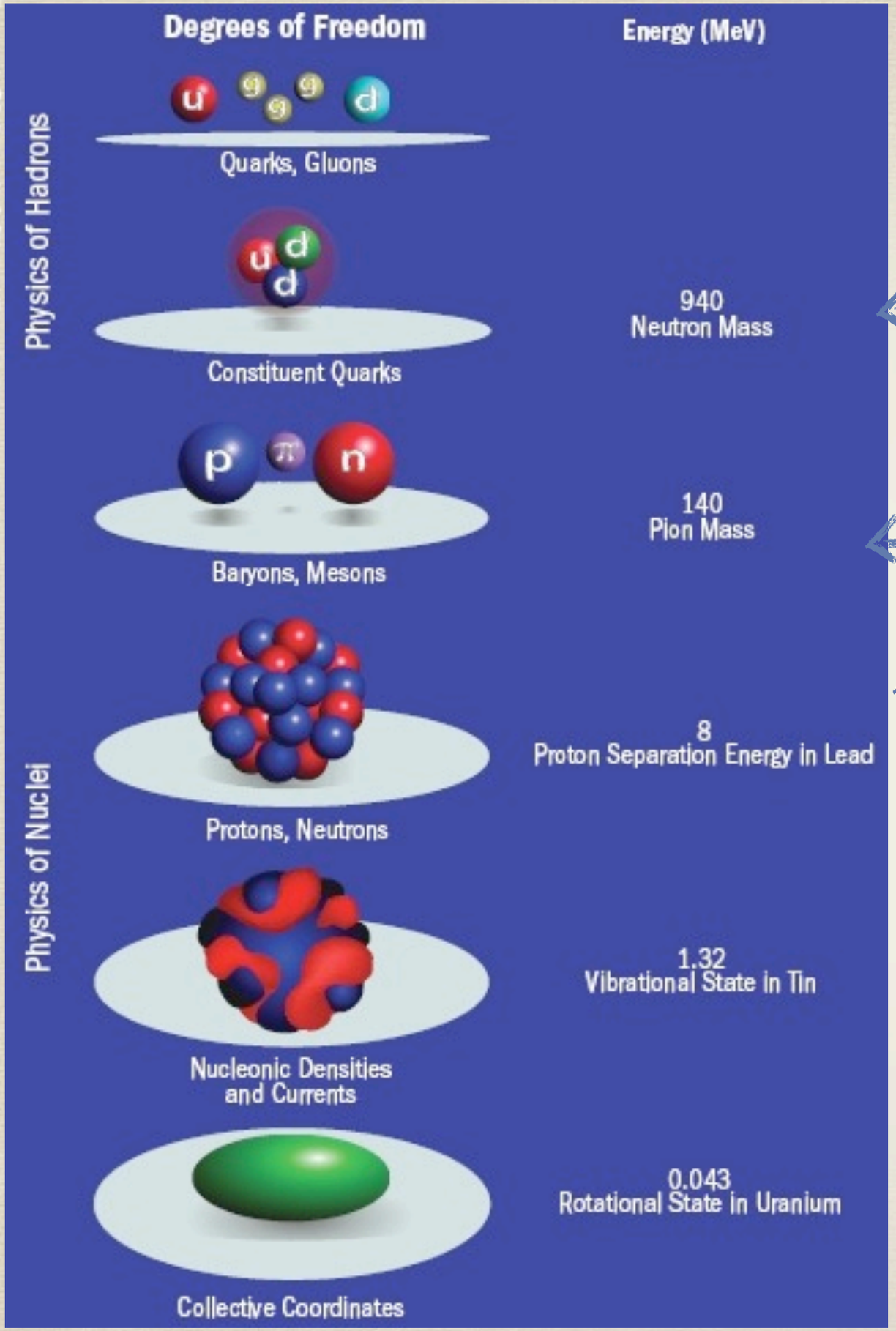

QCD

Hadron structure and spectrum

Hadronic Interactions

Nuclear physics

Figure by W. Nazarewicz

What does it take?

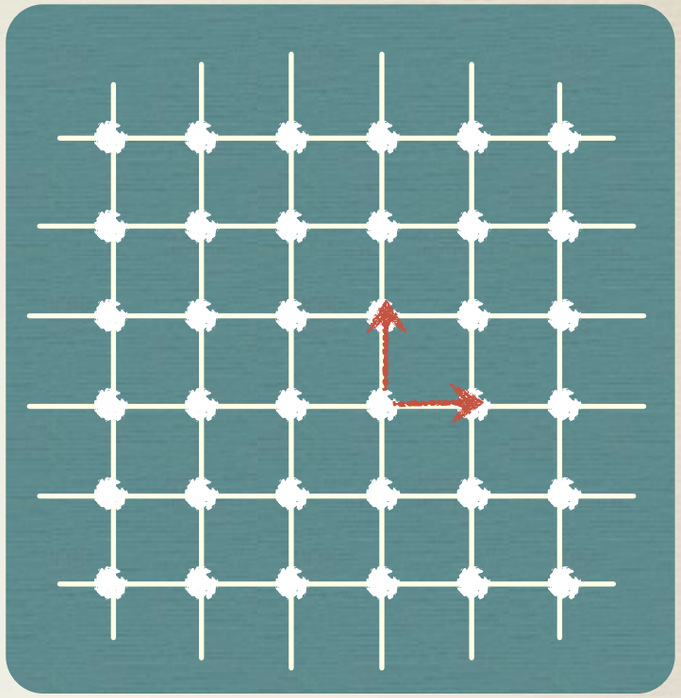

- Hadronic Scale: 1fm ~ 1×10^{-13} cm
- Lattice spacing << 1fm
  - take a=0.1fm
- Lattice size La >> 1fm
  - take La = 3fm
- Lattice 32^4
- Gauge degrees of freedom: $8 \times 4 \times 32^4 = 3.4 \times 10^7$

color

dimensions

sites

The pion mass is an additional small scale

$\sim 1/m_\pi \sim 1.4$fm

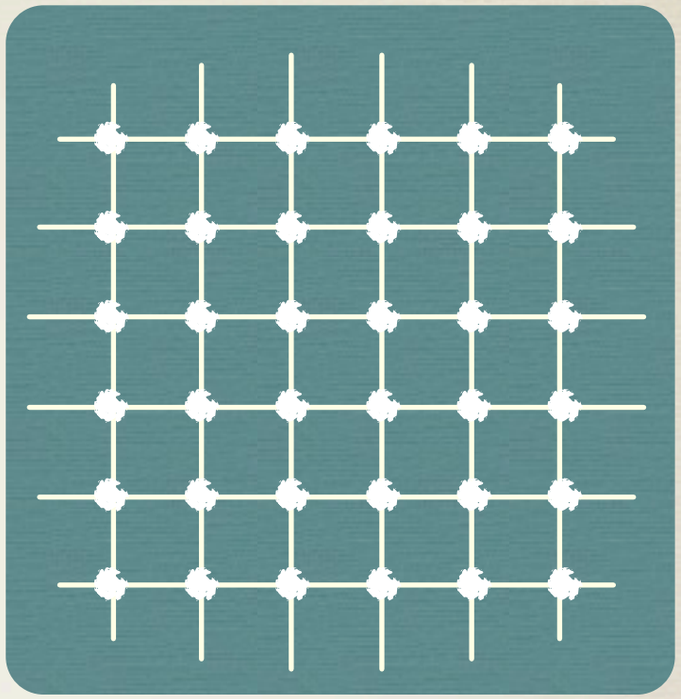

Volume corrections $\sim e^{-m_\pi L}$

6 -7 fm boxes might be needed at the physical point

Smaller scale: Binding momentum of the deuteron ~ 40MeV

Nuclear energy level splittings are a few MeV

Box sizes of about 10fm will be needed

Scattering on the Lattice

Luscher Comm. Math. Phys 105, 153 '86

Elastic scattering amplitude (s-wave):

$A(p) =$ 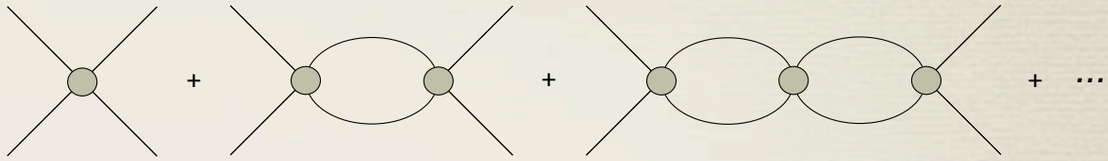

$$A(p) = \frac{4\pi}{m}\frac{1}{p\cot\delta - ip}$$

At finite volume one can show:

$$E_n = 2\sqrt{p_n^2 + m^2}$$

$$p\cot\delta(p) = \frac{1}{\pi L}\,\mathbf{S}\left(\frac{p^2L^2}{4\pi^2}\right) \qquad \mathbf{S}(\eta) \equiv \sum_{\mathbf{j}}^{|\mathbf{j}|<\Lambda}\frac{1}{|\mathbf{j}|^2-\eta} - 4\pi\Lambda$$

Small p:

$$p\cot\delta(p) = \frac{1}{a} + \frac{1}{2}rp^2 + \ldots.$$

a is the scattering length

Bound States

Luscher Comm. Math. Phys 104, 177 '86

$$E_b = \sqrt{p^2 + m_1^2} + \sqrt{p^2 + m_2^2} - m_1 - m_2 \qquad p^2 < 0$$

$$E_b \approx \frac{p^2}{2\mu} = -\frac{\kappa^2}{2\mu} \qquad \kappa = |p|$$

κ is the "binding momentum" and μ the reduced mass

Finite volume corrections:

$$\Delta E_b = -3|A|^2 \frac{e^{-\kappa L}}{\mu L} + \mathcal{O}\left(e^{-\sqrt{2}\kappa L}\right)$$

cubic group irrep: A_1^+

Two Nucleon spectrum

free nucleons

free 2 particle spectrum

M_n

3fm box

24^3 lattice

anisotropy factor 3.5

$M_\pi = 390$ MeV

Signal to Noise ratio for correlation functions

$$C(t) = \langle N(t)\bar{N}(0)\rangle \sim Ee^{-M_N t}$$

$$var(C(t)) = \langle N\bar{N}(t)N\bar{N}(0)\rangle \sim Ae^{-2M_N t} + Be^{-3m_\pi t}$$

$$StoN = \frac{C(t)}{\sqrt{var(C(t))}} =\sim Ae^{-(M_N - 3/2m_\pi)t}$$

* The signal to noise ratio drops exponentially with time
* The signal to noise ratio drops exponentially with decreasing pion mass
* For two nucleons: StoN(2N) = StoN(1N)^2

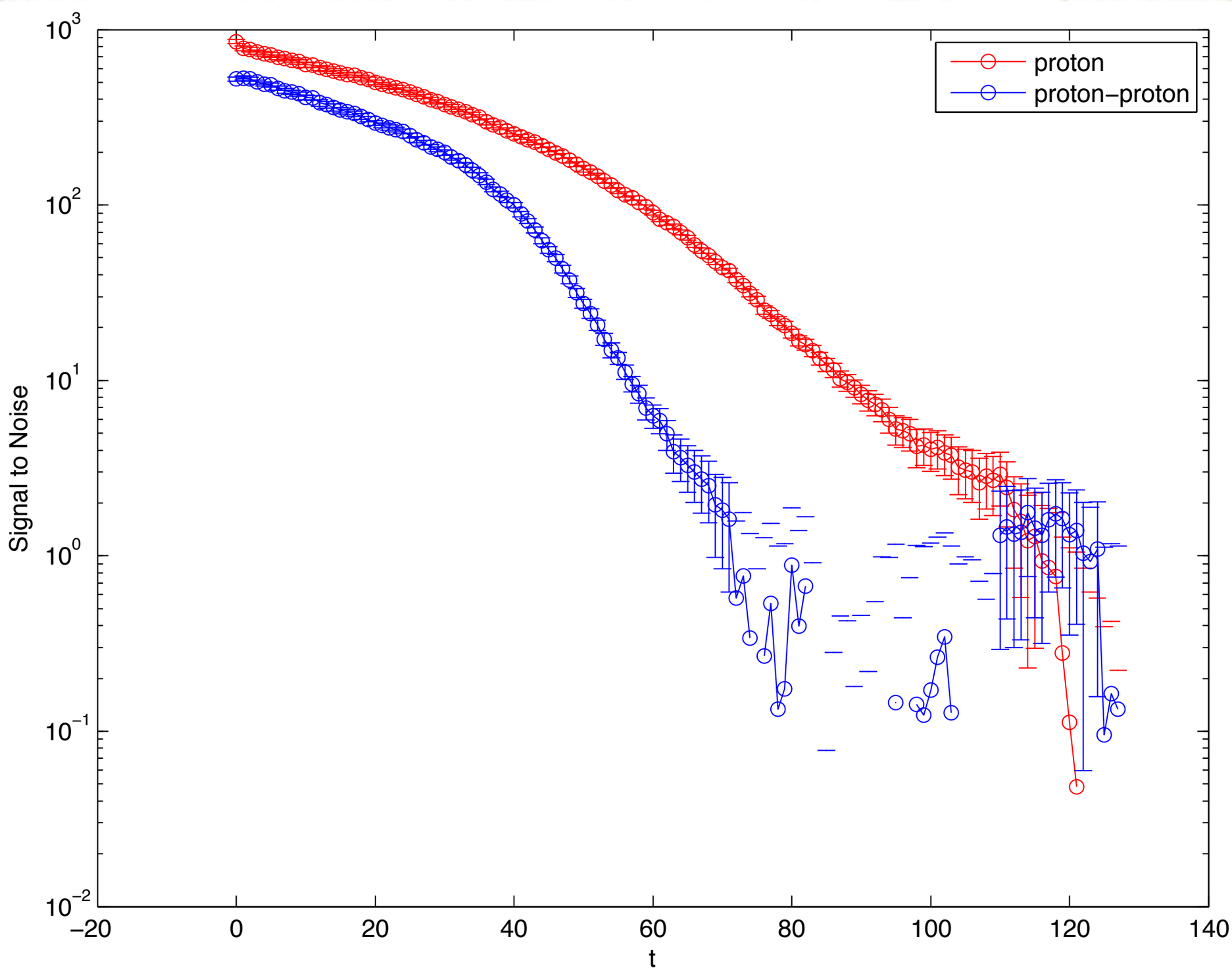

Signal to Noise

$32^3 \times 256$
M_π=390MeV

anisotropy factor 3.5

NPLQCD data

We need to fit for several low lying states for reliable estimation of the ground state of the two particle system in a finite box.

Use “variational methods”

We need very high statistics to be able to resolve excited state contamination

We need to fit for several low lying states for reliable estimation of the ground state of the two particle system in a finite box.

Use “variational methods”

We need very high statistics to be able to resolve excited state contamination

We really need better algorithms to deal with an exponentially hard problem

1. Hyperon-Hyperon Interactions

2. Hyperon-Nucleon Interactions

H-dibaryon

R. L. Jaffe, Phys. Rev. Lett. 38, 195 (1977)

$S=-2$,
$B=2$,
$J^P=0^+$

* Proposed by R. Jaffe 1977
  * Perturbative color-spin interactions are attractive for (uuddss)
  * Diquark picture of scalar diquarks (ud)(ds)(su)
* Experimental searches of the H have not found it
  * BNL RHIC (+model): Excludes the region [-95, 0] MeV

    A. L. Trattner, PhD Thesis, LBL, UMI-32-54109 (2006).
  * KEK: Resonance near threshold

    C. J. Yoon et al., Phys. Rev. C 75, 022201 (2007).
* Several Lattice QCD calculations have been addressing the existence of a bound H

Lattice QCD

* P. B. Mackenzie and H. B. Thacker, Phys. Rev. Lett. 55,2539 (1985)
  * Did not find it
* Y. Iwasaki, T. Yoshie and Y. Tsuboi, Phys. Rev. Lett. 60, 1371 (1988)
  * Found it
* A. Pochinsky, J. W. Negele and B. Scarlet, Nucl. Phys. Proc. Suppl. 73, 255 (1999)
  * Concluded H is not bound in the infinite volume limit
* I. Wetzorke and F. Karsch Nucl. Phys. Proc. Suppl. 119, 287 (2003)
  * Concluded the H is not bound

Lattice QCD

* NLPQCD Phys.Rev.Lett.106.162001 2011
* HALQCD Phys.Rev.Lett.106.162002 2011
* Luo, Loan and Liu arXiv:1106.1945
  * Anisotropic Clover (quenched)
  * Multiple lattice spacings and volumes
  * Result: B_H = 70(11)(15)MeV

NPLQCD: lattice set up

* Anisotropic 2+1 clover fermion lattices
  * a ~ 0.125fm (anisotropy of ~ 3.5)
  * pion mass ~ 390 MeV
  * Volumes 16^3 x 128, 20^3 x 128, 24^3 x 128, 32^3 x 256
  * Smeared source - 3 sink interpolating fields
* Interpolating fields have the structure of s-wave Λ-Λ system
  * I=0, S=-2, A_1 , positive parity

Hadron Spectrum/JLAB

largest box 4fm

NPLQCD methods

* Compute the ground state energy using Euclidian correlators
  * Use a single source operator with three sinks operator (varied smearing)
* "Diagonalize" the correlators to isolate the ground state
  * Matrix Prony and Multi-exponential fits
* Extract the binding momentum
* Extrapolate to infinite volume using multiple volumes
* Use very high statistics $O(500K)$ correlation functions

NPLQCD

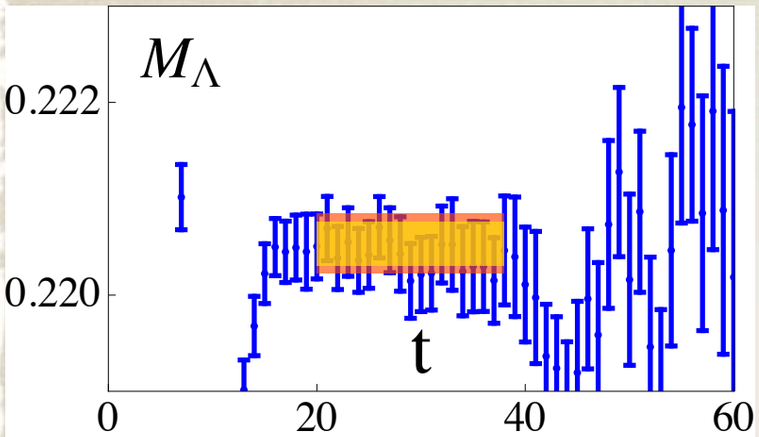

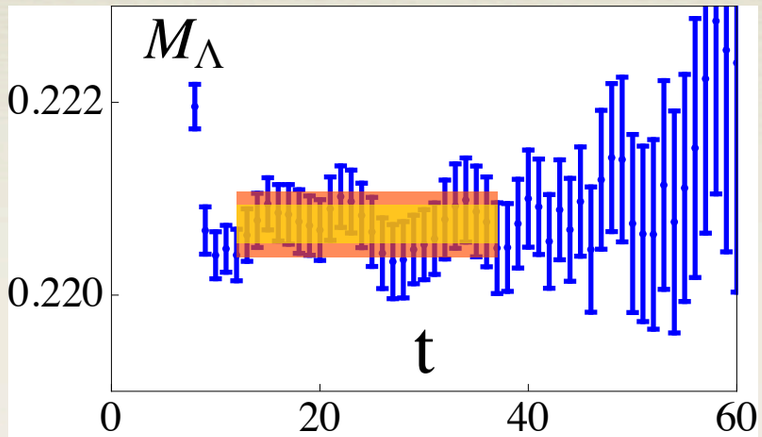

ΛΛ Energy

$$E_{\Lambda\Lambda} = 2\sqrt{p^2 + m_\Lambda^2}$$

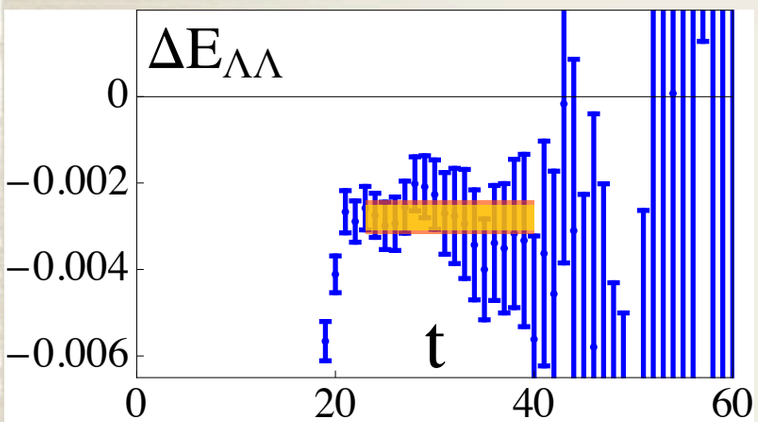

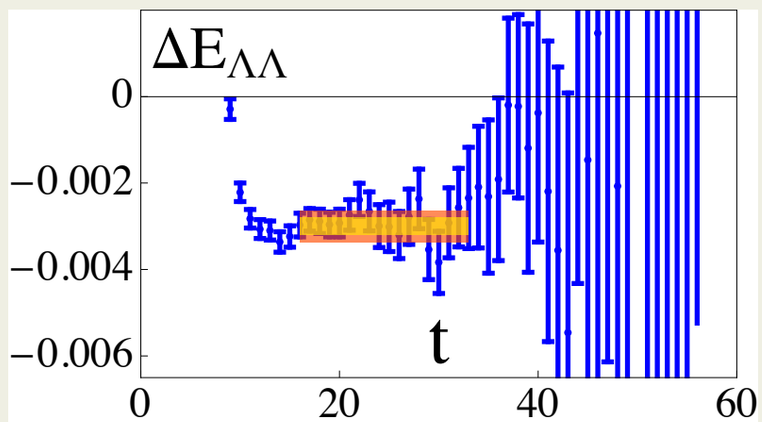

binding momentum

$$\kappa = |p|$$

$$\kappa = \gamma + \frac{g_1}{L}\left(e^{-\gamma L} + \sqrt{2}e^{-\sqrt{2}\gamma L}\right)$$

$$B_H = \frac{\gamma^2}{m_\Lambda}$$

NPLQCD: H-dibaryon

$B_H = 16.6 \pm 2.1 \pm 4.6$ MeV

statistical systematic

$M_\pi = 390$ MeV
2+1 Clover anisotropic fermions

NPLQCD: arXiv:1012.3812

Phys. Rev. Lett. **106**, 162001
(Published April 20, 2011)

NPLQCD: H-dibaryon

B_H= 16.6 ± 2.1 ± 4.6 MeV

statistical systematic

M_π=390MeV
2+1 Clover anisotropic fermions

NPLQCD: arXiv:1012.3812

Phys. Rev. Lett. **106**, 162001
(Published April 20, 2011)

Continuum limit?

Physical pion mass?

Isospin breaking?

Electromagnetism?

NPLQCD: H-dibaryon

$B_H = 16.6 \pm 2.1 \pm 4.6$ MeV

statistical systematic

$M_\pi = 390$MeV
2+1 Clover anisotropic fermions

NPLQCD: arXiv:1012.3812

Phys. Rev. Lett. **106**, 162001
(Published April 20, 2011)

Continuum limit?

Physical pion mass?

Isospin breaking?

Electromagnetism?

Chiral extrapolation

P. Shanahan et.al. arXiv:1106.2851

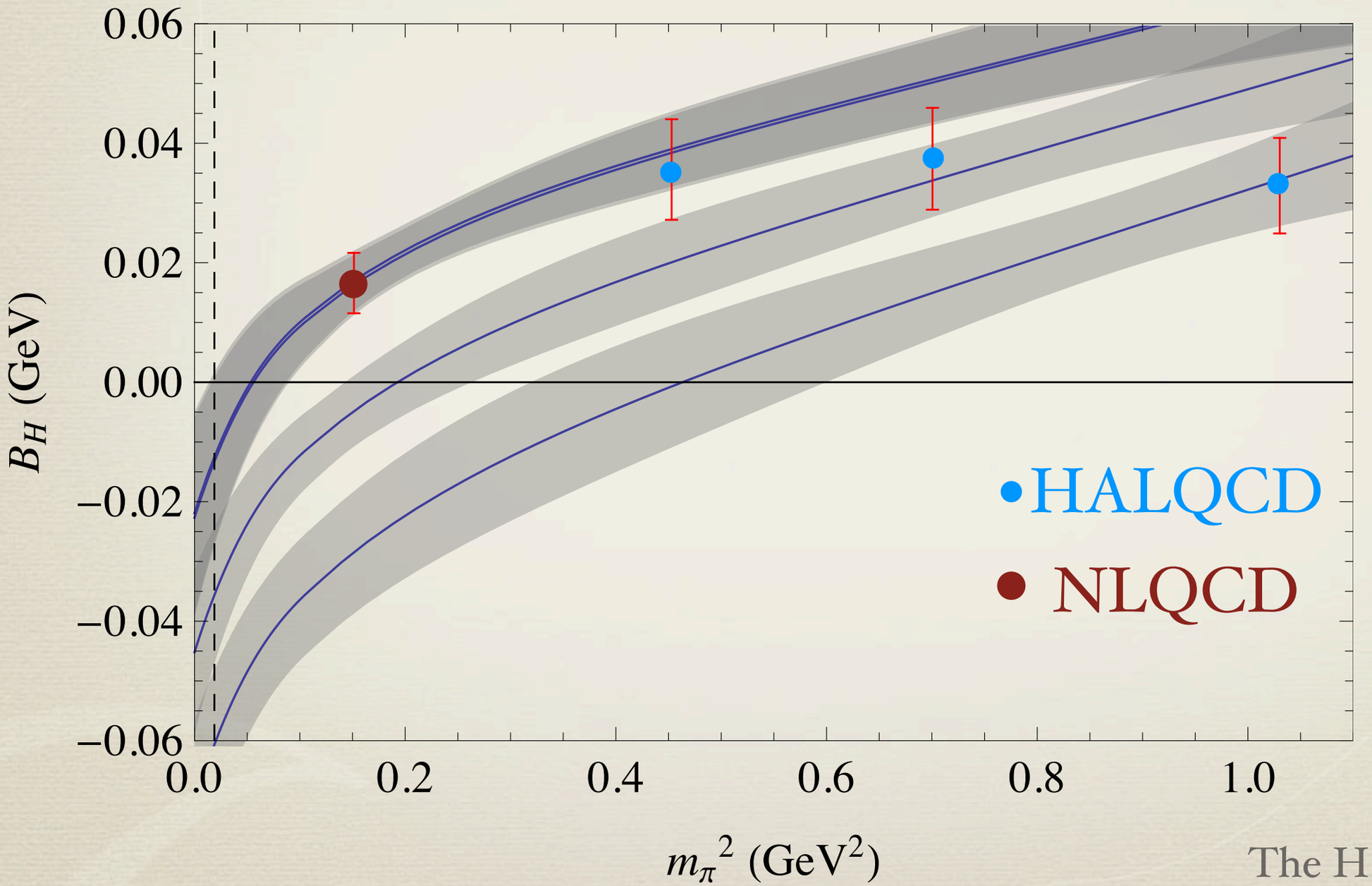

The H may not be bound

Chiral extrapolation

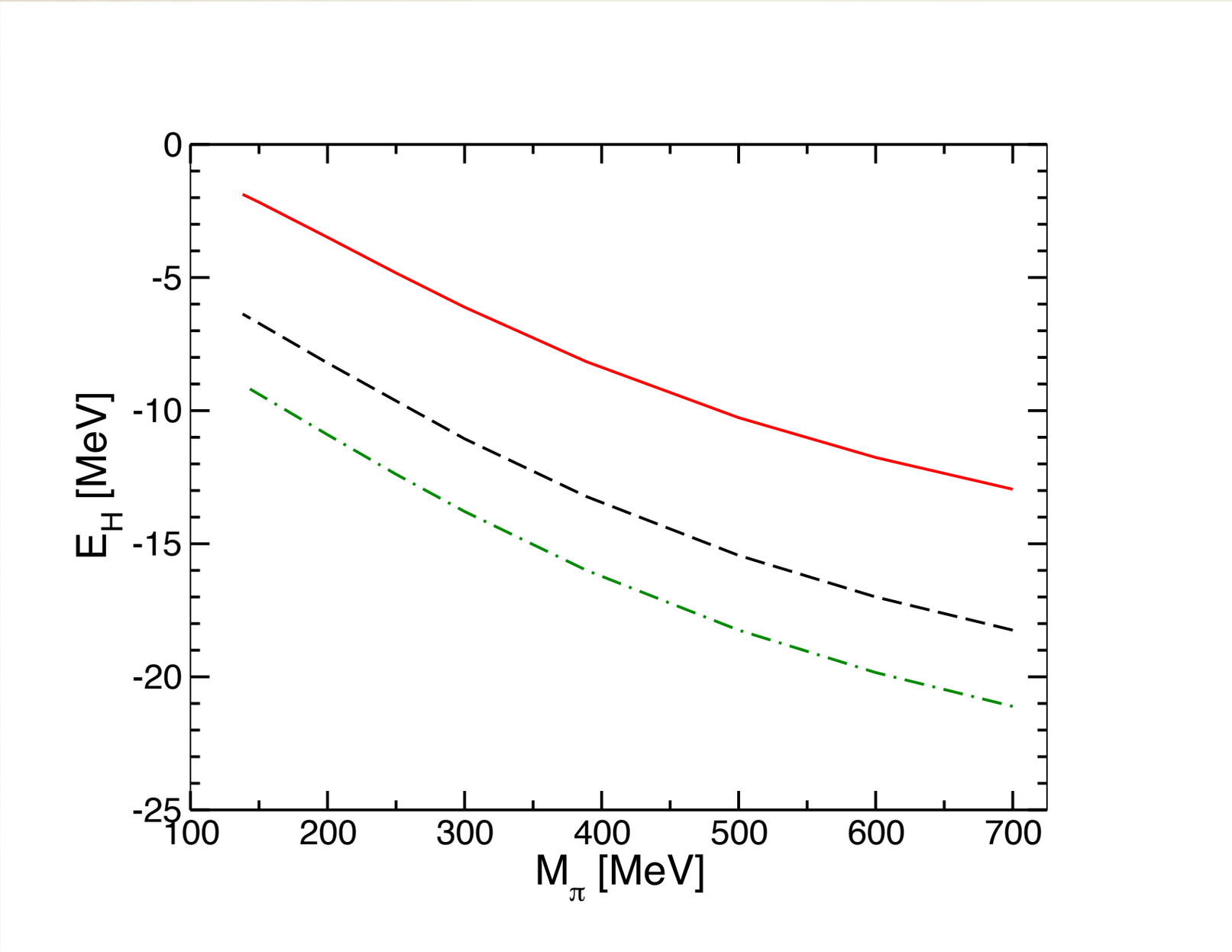

J. Haidenbauer, Ulf-G. Meisner
arXiv:1109.3590

H-dibaryon: Towards the physical point

[S. Beane et.al. arXiv:1103.2821 Mod. Phys. Lett. A26: 2587, 2011]

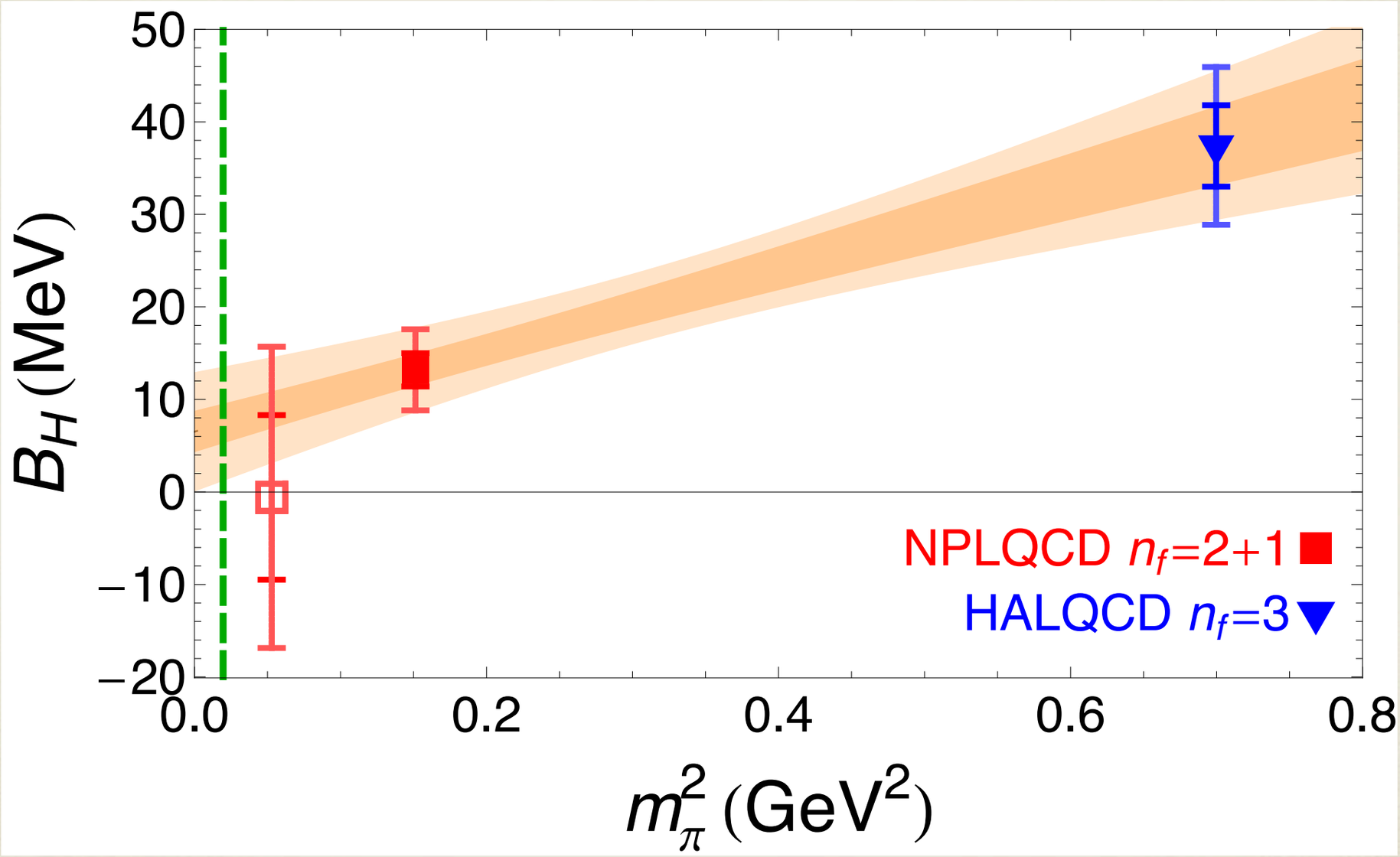

HALQCD:Phys.Rev.Lett.106:162002,2011

H-dibaryon:

Is bound at heavy quark masses. May be unbound at the physical point

NPLQCD

H-dibaryon: Towards the physical point

[S. Beane et.al. arXiv:1103.2821 Mod. Phys. Lett. A26: 2587, 2011]

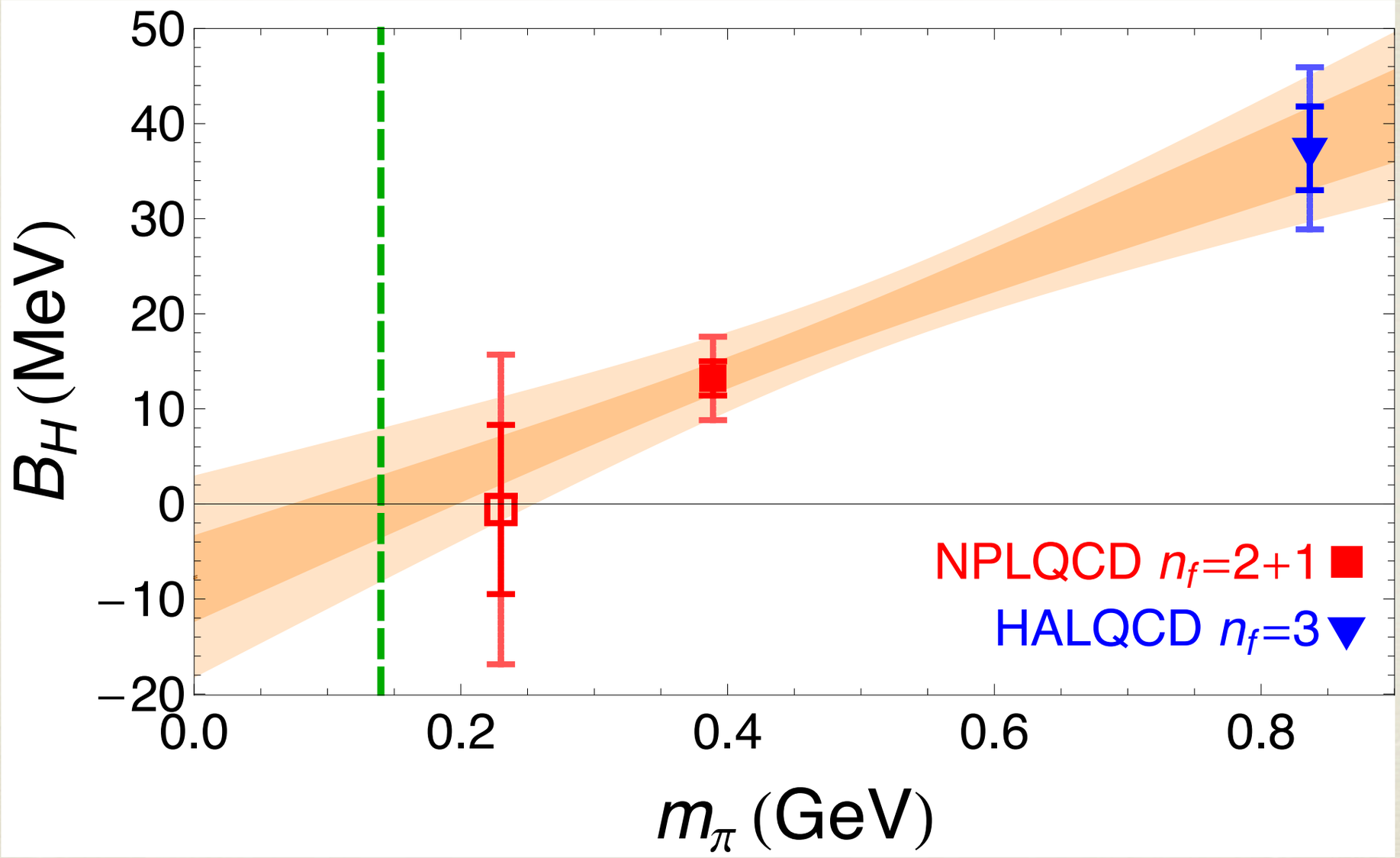

HALQCD:Phys.Rev.Lett.106:162002,2011

H-dibaryon:

Is bound at heavy quark masses. May be unbound at the physical point

NPLQCD

Two baryon bound states

[S. Beane et.al. arXiv:1108.2889 submitted to Phys.Rev.D]

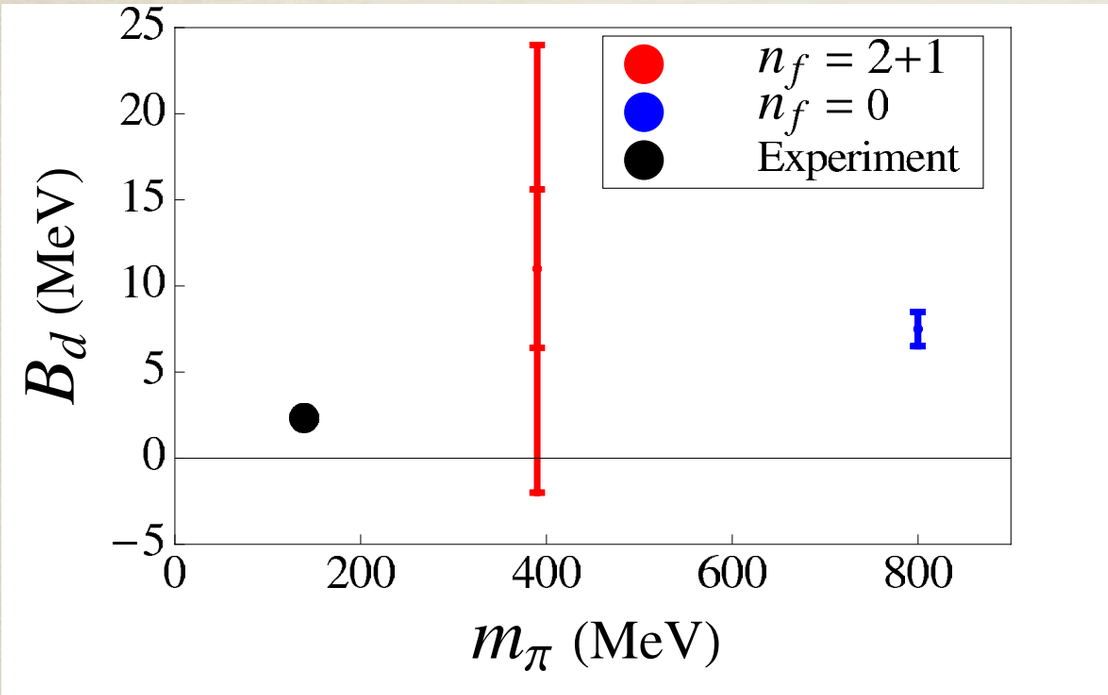

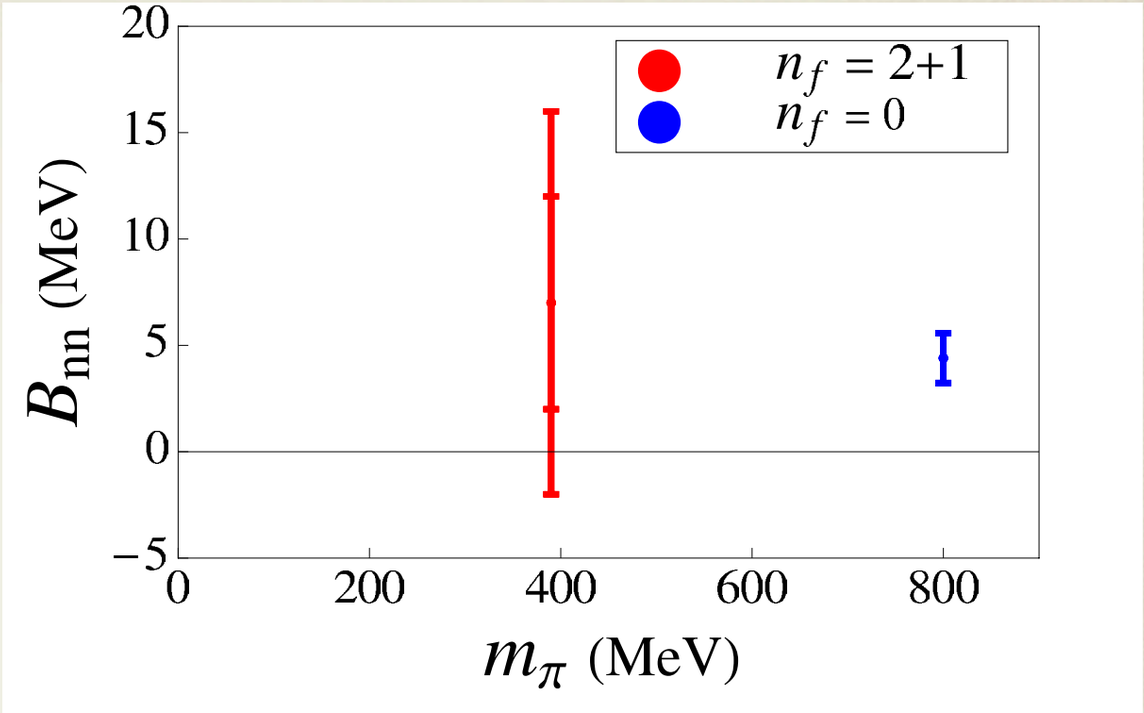

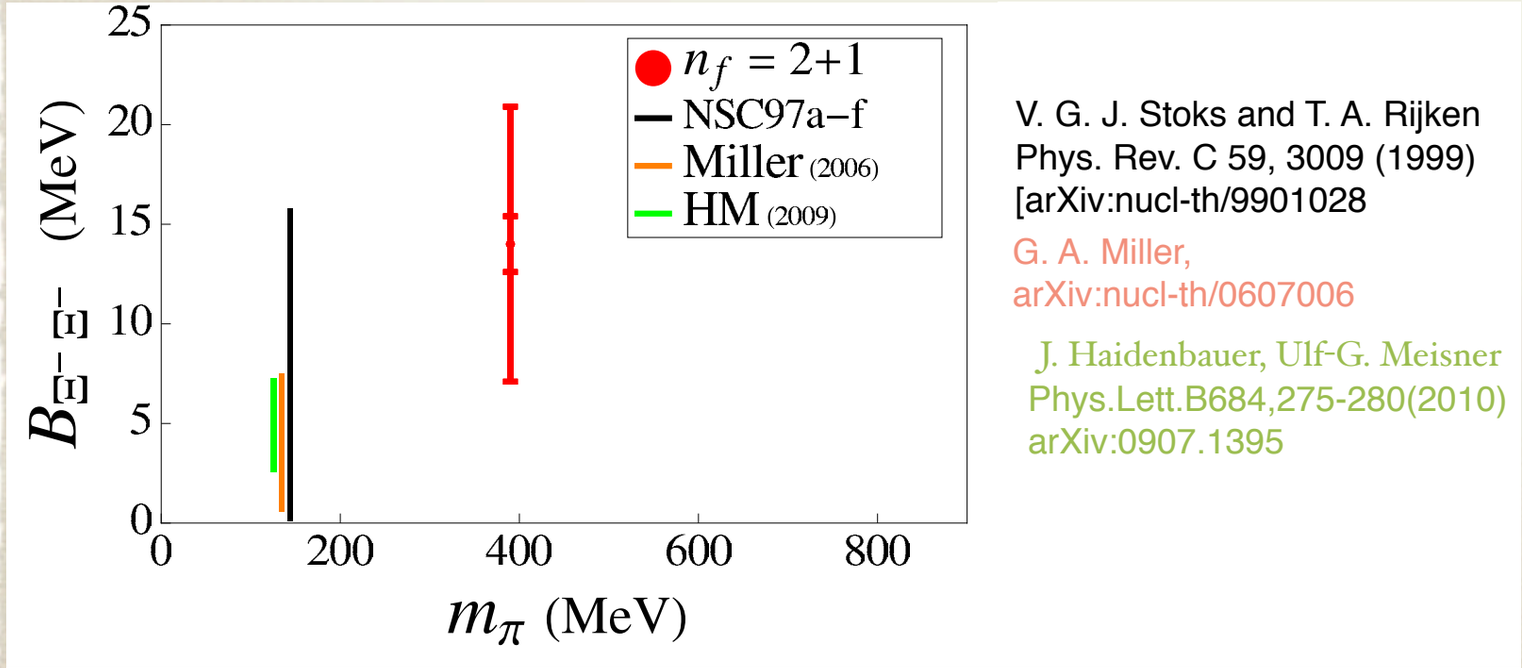

V. G. J. Stoks and T. A. Rijken
Phys. Rev. C 59, 3009 (1999)
[arXiv:nucl-th/9901028

G. A. Miller,
arXiv:nucl-th/0607006

J. Haidenbauer, Ulf-G. Meisner
Phys.Lett.B684,275-280(2010)
arXiv:0907.1395

n_f=0:
Yamazaki, Kuramashi, Ukawa
Phys.Rev. D84 (2011) 054506
arXiv: 1105.1418

gauge fields 2+1 flavors (JLab)
anisotropic clover m_π~ 390MeV

NPLQCD

Hyperon-Nucleon interactions

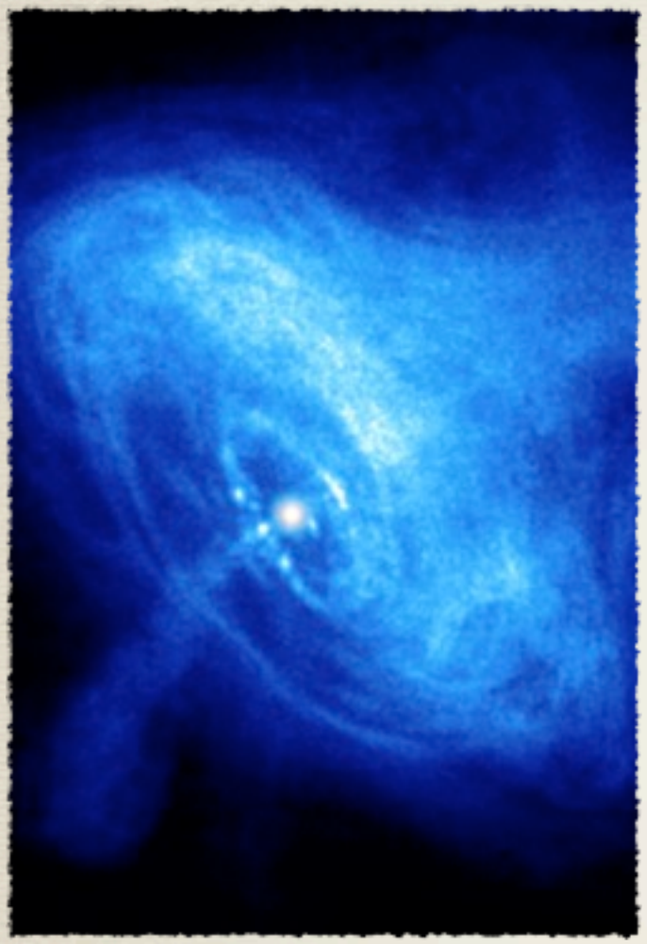

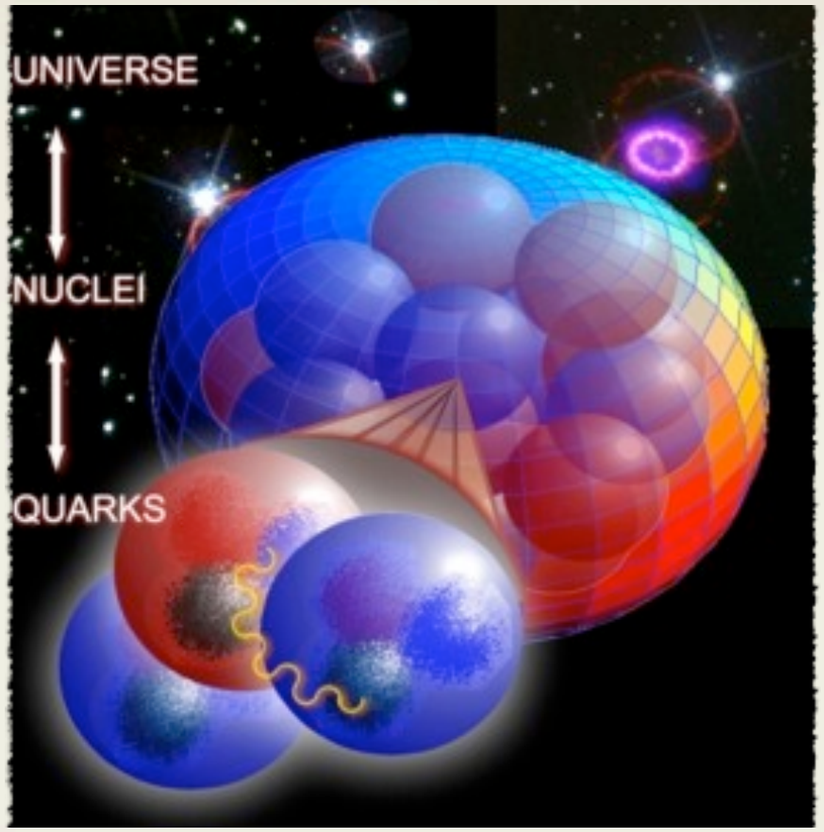

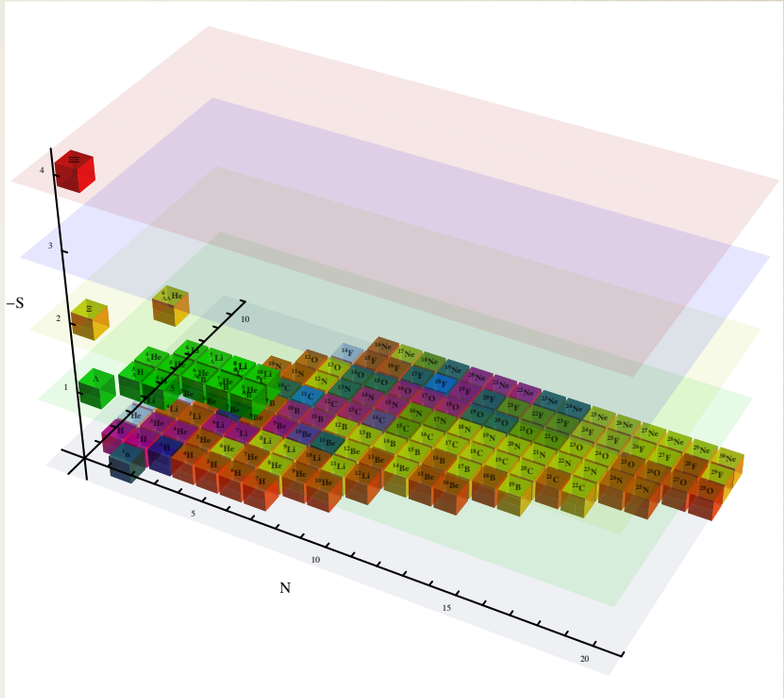

equation of state for nuclear matter in neutron stars

hyper-nuclear physics

$n\Sigma^-$ interactions

$24^3 \times 128$

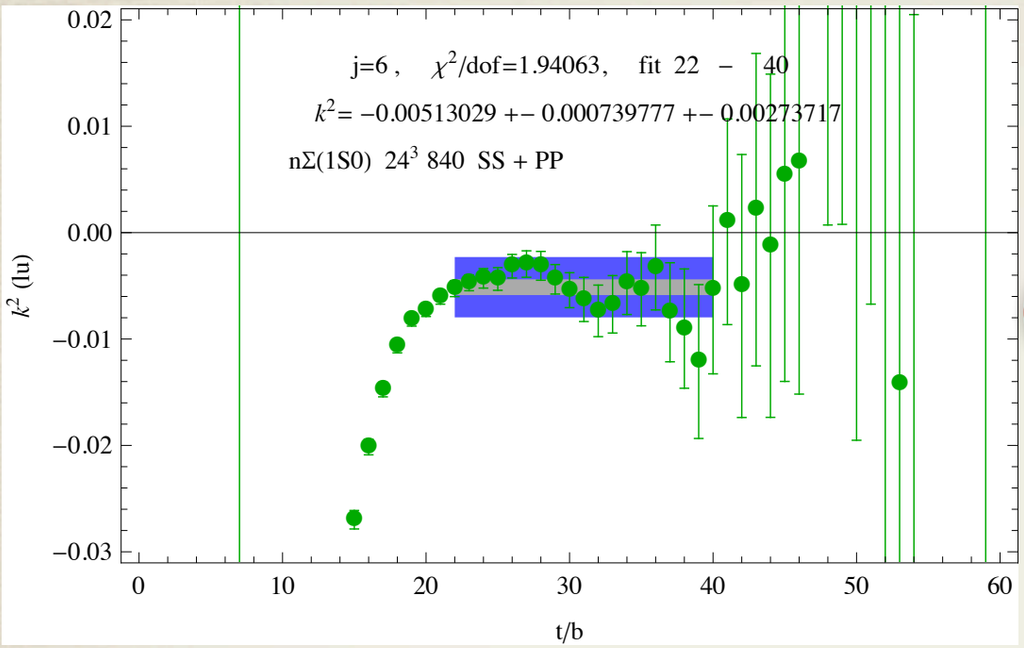

$(^1S_0)$

$32^3 \times 256$

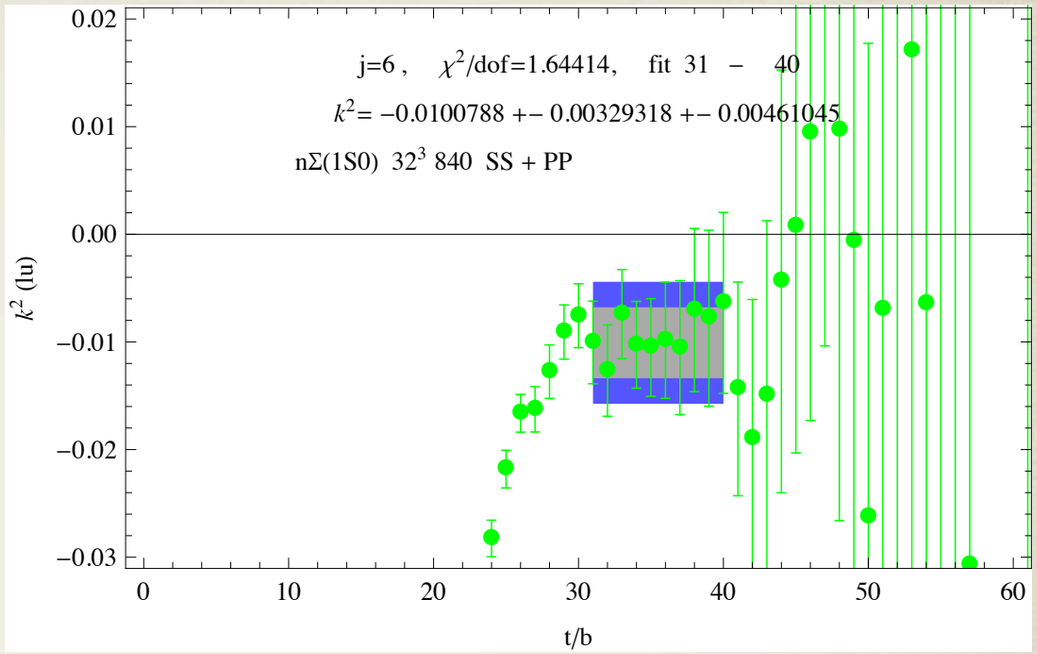

Finite volume scaling: $\kappa = \gamma + \frac{g_1}{L}\left(e^{-\gamma L} + \sqrt{2}e^{-\sqrt{2}\gamma L}\right)$

$$B_{n\Sigma} = \frac{\gamma^2}{2\mu_{n\Sigma}} = 25 \pm 9.3 \pm 11 \text{ MeV}$$

constrain LO YN EFT

gauge fields: 2+1 flavors (JLab), anisotropic clover $m_\pi \sim 390$MeV

NPLQCD

Hyperon-Nucleon

[S. Beane et.al. arXiv:1204.3606 submitted to Phys. Rev. Lett.]

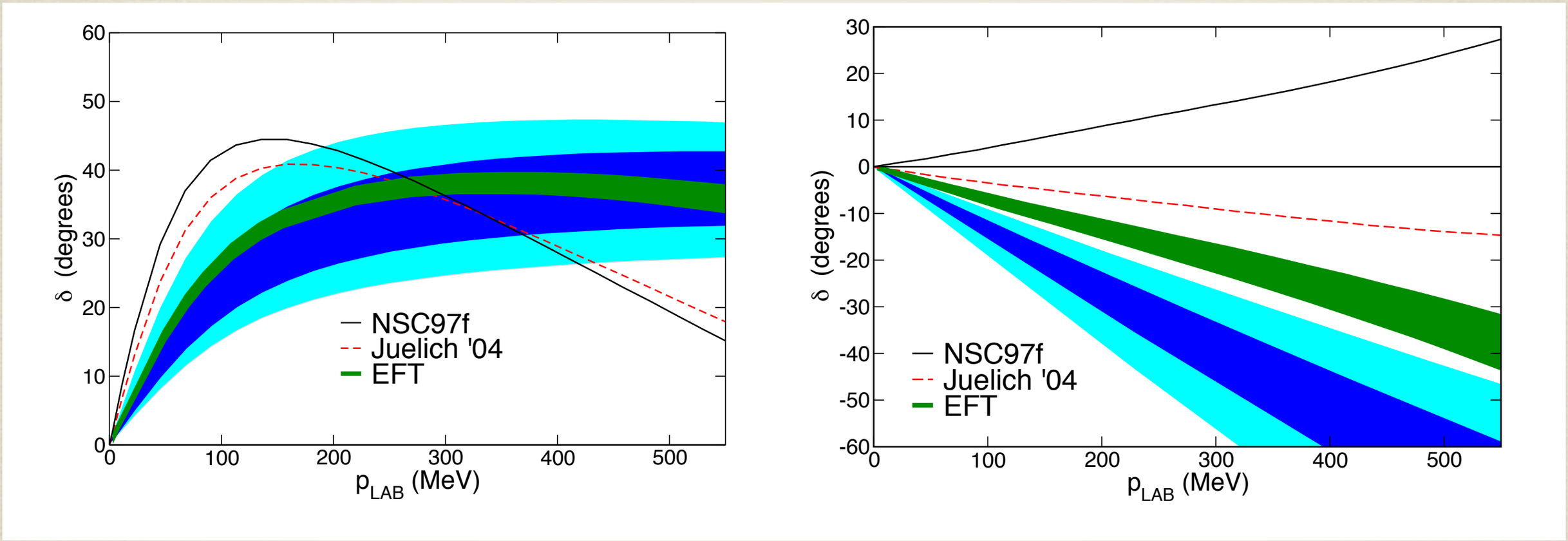

n-Σ spin singlet

n-Σ spin triplet

gauge fields 2+1 flavors (JLab)
anisotropic clover
m_π~ 390MeV

NPLQCD

Conclusions

- Observables related to Hadronic interactions are now being computed
  - Meson-Meson sector: Precision results already exist
  - Progress in the Baryon sector
  - Calculation of deuteron and He binding energy on the way

Yamazaki, Kuramashi, Ukawa (PACS-CS)
Phys.Rev.D81:111504 (2010)
Phys.Rev.D84:054506 (2011)

- Petaflop computing is here
  - Significant aid in achieving precision in the baryon sector
  - Will take us a long way in understanding how the nuclear force emerges from QCD

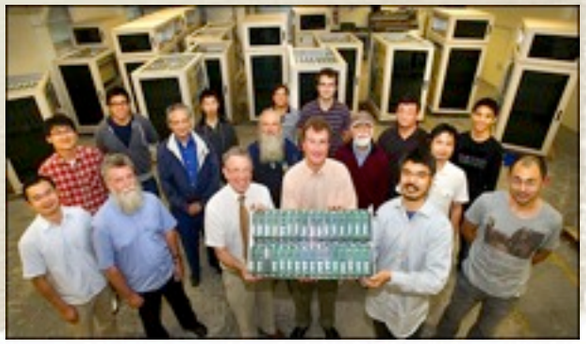

Conclusions

* Observables related to Hadronic interactions are now being computed
  * Meson-Meson sector: Precision results already exist
  * Progress in
  * Calculation way
* Petaflop comp amashi, Ukawa (PACS-CS) .D81:111504 (2010) .D84:054506 (2011)
  * Significant or
  * Will take us a long way in understanding how the nuclear force emerges from QCD

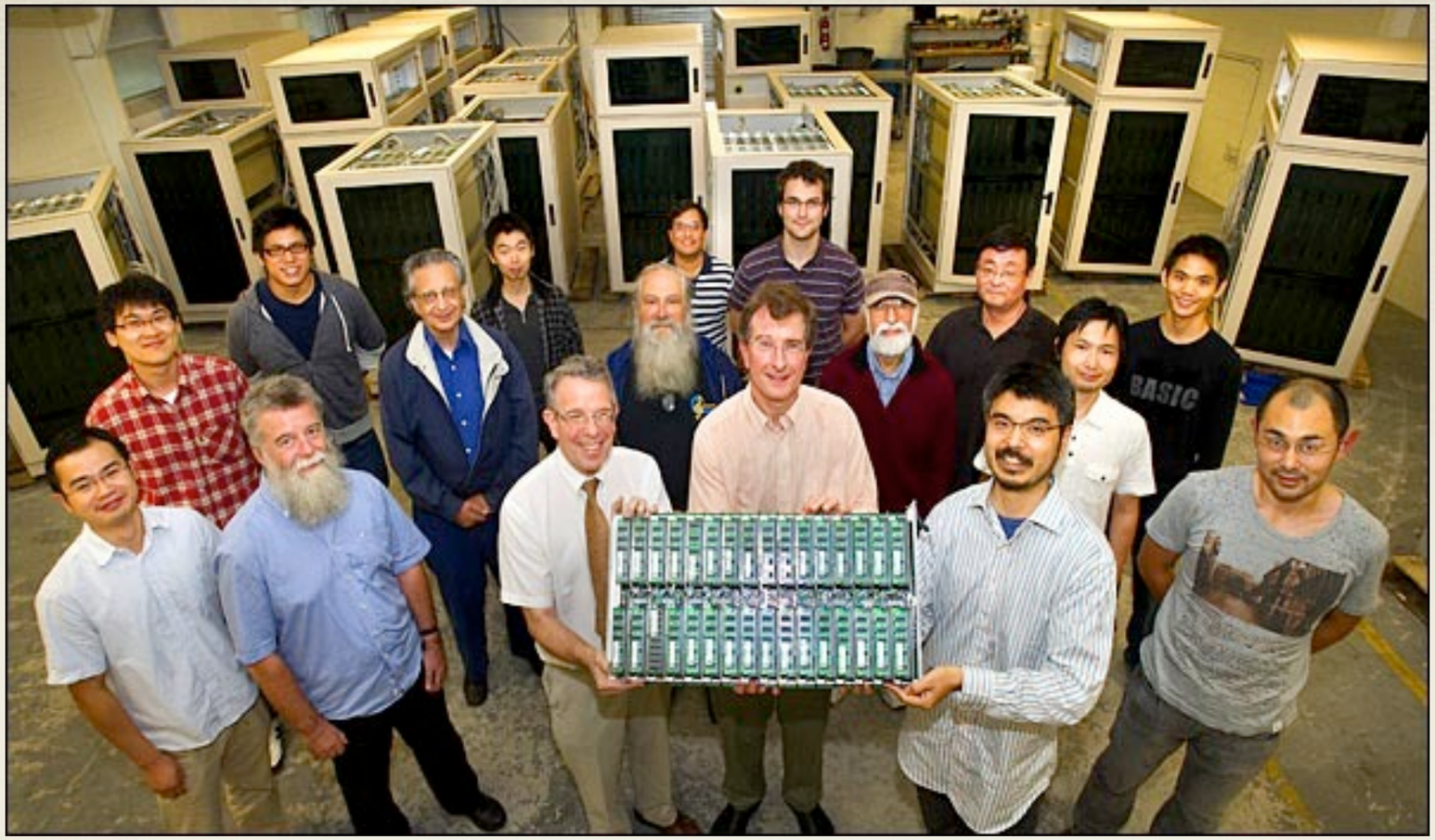
BASIC

QCDCQ
DCDCD
QCDCQ

The anomaly triangle and muon $g-2$

SANTI PERIS (SFSU and UAB)

2-loop EW contribution to $g-2$

Kukhto et al. '92
SP, Perrottet, de Rafael '95
Czarnecki, Krause, Marciano '95, '96
Knecht, SP, Perrottet, de Rafael '02
Czarnecki, Marciano,Vainshtein '03

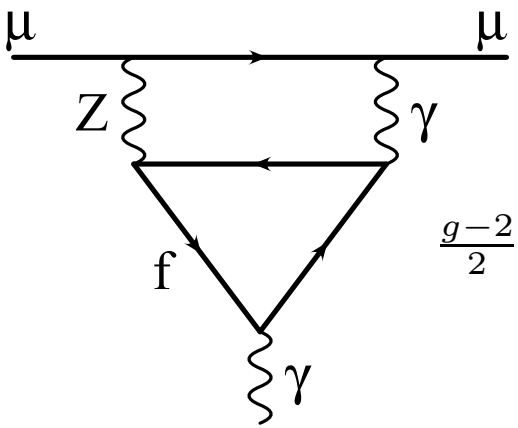

$$\frac{g-2}{2} \propto \frac{\alpha}{\pi}\frac{G_\mu}{8\pi^2}\frac{m_\mu^2}{\sqrt{2}} \int_{m_\mu^2}^{\infty} dQ^2 \underbrace{\left[w_L(Q^2) + \frac{M_Z^2}{M_Z^2+Q^2}\, w_T(Q^2) \right]}_{w_L=2\ w_T=2\frac{N_c}{Q^2}\quad (one-loop,\ m_f=0)}$$

$$\frac{g-2}{2}\Big|_{e,u,d} \sim 2\times 10^{-11}$$

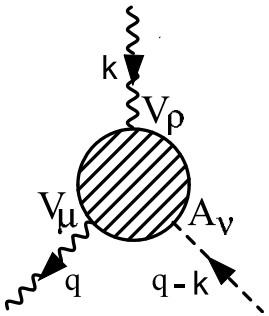

$Q^2 = -q^2$, "Gluon-irreducible" triangle

$$W_{\mu\nu\rho}(q,k) = T_f^{(3)} Q_f^2 \Big[w_L(Q^2)\, q_\nu\, \epsilon_{\mu\rho\alpha\beta} q^\alpha\, k^\beta + w_T(Q^2)\, k^\sigma \left(q^2 \epsilon_{\mu\nu\rho\sigma} + q_\nu \epsilon_{\mu\rho\lambda\sigma} q^\lambda + q_\mu \epsilon_{\rho\nu\lambda\sigma} q^\lambda \right) \Big] + \mathcal{O}(k^2)$$

- $w_L(Q^2)$ related to the chiral anomaly $\Longrightarrow \sum_{\nu,e,u,d} w_L = 0$.
- $w_T(Q^2)$ not but...

Theorem

Vainshtein '02

Knecht, SP, Perrottet, de Rafael, '03

In the <u>massless limit</u>, to all orders in α_s:

$$\boxed{w_L(Q^2) = 2\, w_T(Q^2)}$$

and, since anomaly does not get renormalized: $w_L = 2\frac{N_c}{Q^2}$ (Adler,Bardeen '69; Witten '83)

$\Rightarrow$ neither does $2w_T = 2\frac{N_c}{Q^2}$, <u>to all orders in α_s</u>.

Using $L_\mu^{(3)} = \sum_{\ell=\nu,e} \overline{\ell_L}\gamma_\mu T^{(3)}\ell_L + \sum_{q=u,d} \overline{q_L}\gamma_\mu T^{(3)} q_L$, etc...in $SU(2)_L \times U(1)_Y$:

$$Q^2\left[w_L(Q^2) - 2w_T(Q^2)\right] \propto \int d^4x d^4y\, e^{iqx}\,(y-x)_\lambda \epsilon^{\mu\nu\rho\lambda} \underbrace{\left\langle T\left\{L_\mu^{(3)}(x) V_\nu^{(Y)}(y) R_\rho^{(Y)}(0)\right\}\right\rangle}_{\not\ni \mathbb{1}_L \otimes \mathbb{1}_R}$$

- i.e., $w_L - 2w_T$ has no pert. contributions in α_s, it is like, e.g., $\langle LR\rangle = \langle VV - AA\rangle$.

Non-perturbative effects

1) Adler-Bardeen-Witten : $w_L(Q^2) = 2\frac{N_c}{Q^2}$ (exact for all Q !)

2) However, for $w_T(Q^2)$:

- Large Q^2:

$$2w_T(Q^2) \approx 2\frac{N_c}{Q^2}\left(1 + \underline{NO\ \ \alpha_s}\right) + (const.)\ \alpha_s\ \chi\frac{\langle\overline{\psi}\psi\rangle^2}{Q^6} + \mathcal{O}(1/Q^8)$$

Magnetic susceptibility, $\chi = \frac{\Pi_{VT}(0)}{\langle\overline{\psi}\psi\rangle}$, very poorly known.

- Small Q^2:

$$2w_T(Q^2) \approx (const.)\ C_{22}^{(p^6)} + \mathcal{O}(Q^2) \quad , \quad C_{22}^{(p^6)} \sim 1/M_{Hadron}^2 \quad \text{(unknown)}$$

Chiral Pert. Theory, $\mathcal{L}_{eff}$ (parity-odd):

$$\mathcal{L}_{\mathcal{O}(p^6)} = C_{22}^{(p^6)}\ \epsilon_{\mu\nu\alpha\beta}\ \underbrace{\mathrm{Tr}\left(u^\mu\left\{\nabla_\gamma f_+^{\gamma\nu}, f_+^{\alpha\beta}\right\}\right)}_{\pi,\eta,\ldots} + \ldots \qquad (SU_{N_F} \times SU_{N_F} \to SU_{N_F})$$

Conjectures

- Conjecture 1: $w_L(Q^2) - 2\, w_T(Q^2) = -2\, \frac{N_c}{f_\pi^2}\, \Pi_{LR}(Q^2)$ (Son-Yamamoto '10)

in wide class of "AdS/QCD" models (chiral limit, $N_c \to \infty$)
(not without caveats, e.g. OPE is exponential; mismatch in pert. theory if treated as a WI)
(Knecht, SP, de Rafael '11)

Chiral log's respect this relation. (Gorsky, Kopnin,Krikun, Vainshtein '12)

Test: $C_{22}^{(p^6)}(\mu) = -\frac{N_c}{32\pi^2 f_\pi^2}\, L_{10}^{(p^4)}(\mu)$??

If true at one $\mu \Rightarrow$ true at all μ

- Conjecture 2: $\chi = -\frac{N_c}{4\pi^2 f_\pi^2} \sim -9\ \mathrm{GeV}^{-2}$ (Magnetic susceptibility) ??

(Vainshtein '02):

Other results: $\chi \sim -3\ \mathrm{GeV}^{-2}$, sum rules, VMD, (Ioffe, Fadin, Lipatov '10; Balitsky et al. '85; Belyaev et al. '84; Ball et al. '02)

Another Perturbative Surprise

Up to now, special kinematic configuration in $\langle VVA \rangle$.

Jegerlehner,Tarasov '06

However, it has been found at two loops <u>for all momenta</u> that :

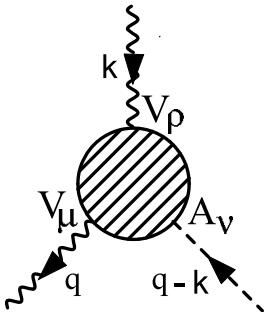

$$W_{\mu\nu\rho}(q,k) \quad = \quad W_{\mu\nu\rho}(q,k)|_{one-loop}\,(1+\underbrace{\mathcal{O}(\alpha_s)}_{=0\ !!})$$

i.e., no renormalization, not just for the anomaly, but for the <u>whole</u> triangle !

Given the non-trivial momentum dependence,

can this be just a coincidence ?

could this be true to all orders in α_s ?

Summary

- VVA is a very interesting theoretical laboratory for QCD
- Most results obtained in chiral limit: can lattice help/check ?
- The LbL $\longleftrightarrow \langle VVA \rangle$ connection:

(Melnikov, Vainshtein '04; Prades, de Rafael, Vainshtein '09)

$k_1 \approx k_2 \gg k_3$

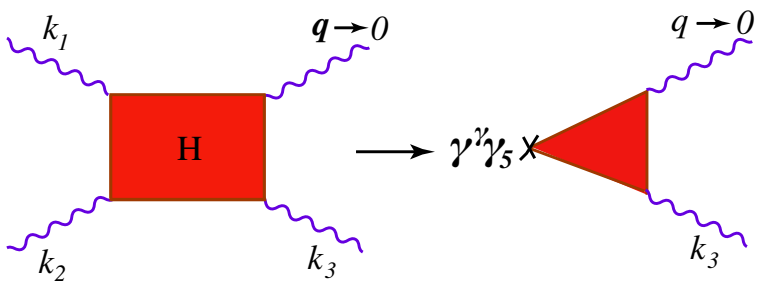

The new Fermilab muon (g-2) experiment: A challenge for experiment and theory

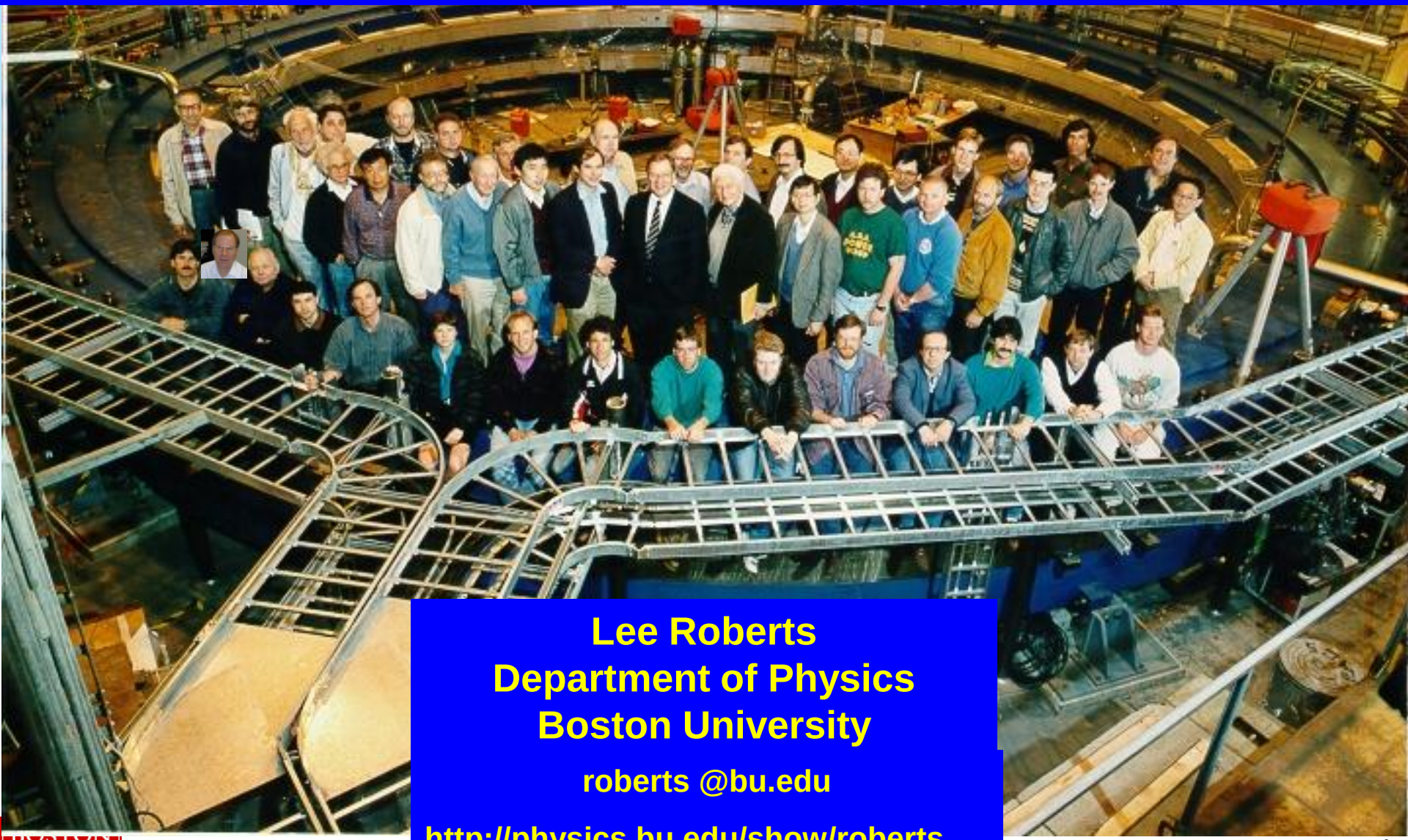

Lee Roberts
Department of Physics
Boston University

roberts @bu.edu

http://physics.bu.edu/show/roberts

BOSTON UNIVERSITY

Last year's good news: the lattice can do it!

PRL 107, 081802 (2011) PHYSICAL REVIEW LETTERS week ending 19 AUGUST 2011

Two-Flavor QCD Correction to Lepton Magnetic Moments at Leading Order in the Electromagnetic Coupling

Xu Feng,[1,2,*] Karl Jansen,[1] Marcus Petschlies,[3] and Dru B. Renner[1,†]

[1]*NIC, DESY, Platanenallee 6, D-15738 Zeuthen, Germany*

[2]*Universität Münster, Institut für Theoretische Physik, Wilhelm-Klemm-Strasse 9, D-48149, Germany*

[3]*Institut für Physik, Humboldt-Universität zu Berlin, D-12489, Berlin, Germany*

(Received 28 March 2011; published 17 August 2011)

We present a reliable nonperturbative calculation of the QCD correction, at leading order in the electromagnetic coupling, to the anomalous magnetic moment of the electron, muon, and tau leptons using two-flavor lattice QCD. We use multiple lattice spacings, multiple volumes, and a broad range of quark masses to control the continuum, infinite-volume, and chiral limits. We examine the impact of the commonly ignored disconnected diagrams and introduce a modification to the previously used method that results in a well-controlled lattice calculation. We obtain $1.513(43) \times 10^{-12}$, $5.72(16) \times 10^{-8}$, and $2.650(54) \times 10^{-6}$ for the leading-order two-flavor QCD correction to the anomalous magnetic moment of the electron, muon, and tau, respectively, each accurate to better than 3%.

DOI: 10.1103/PhysRevLett.107.081802 PACS numbers: 13.40.Em, 12.38.Gc, 14.60.Ef

In the beginning there was Dirac

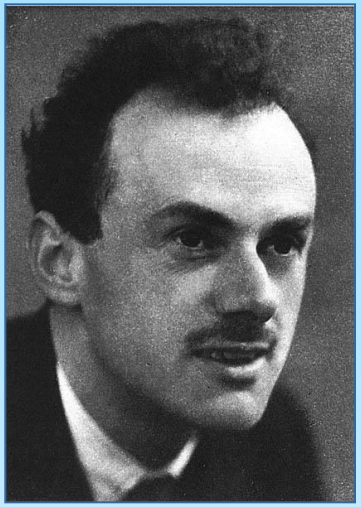

$$i(\partial_\mu - ieA_\mu(x))\gamma^\mu\psi(x) = m\psi(x)$$

predicted electron magnetic moment

$$\vec{\mu} = g\left(\frac{Qe}{2m}\right)\vec{s}, \quad e > 0$$

$$g \equiv 2$$

However, experimentally g > 2; need to add a Pauli term

$$\frac{Qe}{4m}a\bar{\psi}(x)F_{\mu\nu}(x)\sigma^{\mu\nu}\psi(x)$$

dimension 5 operator

(only from loops)

where a is the anomaly,

$$g = 2(1+a) \qquad a = \frac{(g-2)}{2}$$

In the QED, a becomes an expansion in (α/π) from loops

$$a = \sum_{j=1} C_j \left(\frac{\alpha}{\pi}\right)^j$$

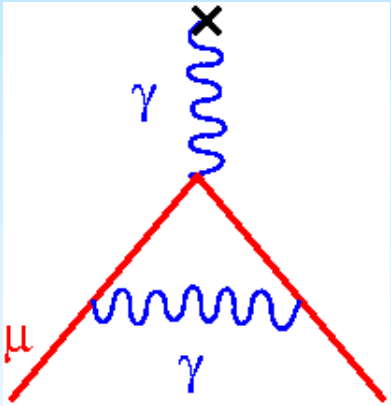

New Physics contribution to a at some scale Λ

$$a(NewPhysics) = C\left(\frac{m}{\Lambda}\right)^2$$

where C could be $\mathcal{O}(1)$, **or**

$\mathcal{O}(\alpha)$ **in weak coupling loop scenarios**

Magnetic and Electric Dipole Interactions

$$\Gamma_\beta = eF_1\bar{\psi}_R\gamma_\beta\psi_R + \frac{ie}{2m}F_2\bar{\psi}_R\sigma_{\beta\delta}q^\delta\psi_L + HC$$

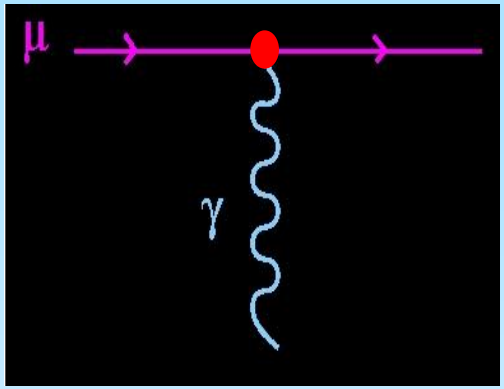

- Muon Magnetic Dipole Momoment a_μ chiral changing

$$\bar{u}_\mu[eF_1(q^2)\gamma_\beta + \frac{ie}{2m_\mu}F_2(q^2)\sigma_{\beta\delta}q^\delta]u_\mu$$

$$F_1(0) = 1 \quad F_2(0) = a_\mu$$

- Muon EDM

$$\bar{u}_\mu\left[\frac{ie}{2m_\mu}F_2(q^2) - F_3(q^2)\gamma_5\right]\sigma_{\beta\delta}q^\delta u_\mu$$

$$F_2(0) = a_\mu \quad F_3(0) = d_\mu;\ \text{EDM}$$

The SM Value for a_μ from $e^+e^- \rightarrow$ *hadrons* (Updated 6/09)

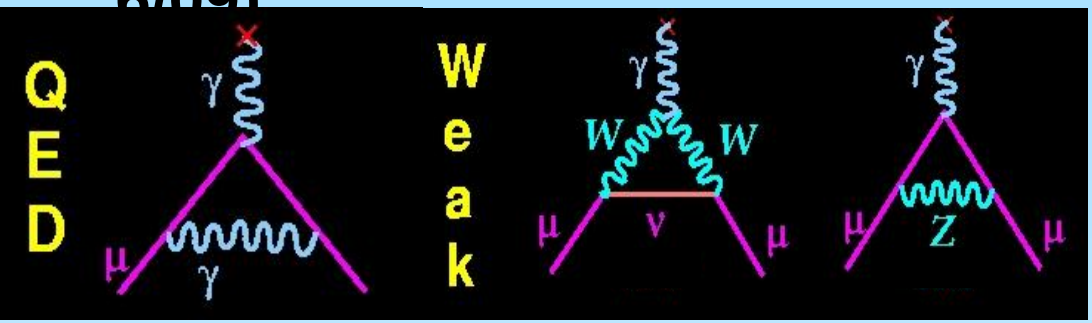

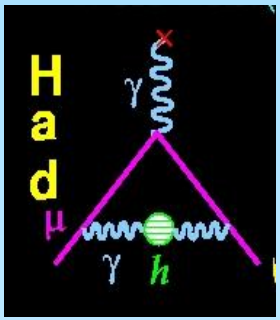

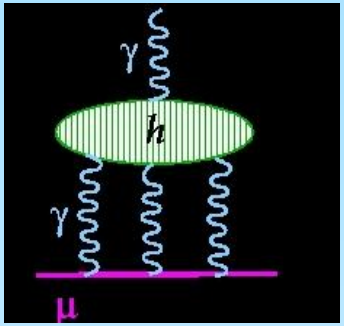

well known | **significant work ongoing**

- Lowest order hadronic from data and a dispersion relation
  - More data to come
- KLOE setting up to measure $\gamma^*\gamma^* \rightarrow \pi\,\pi$ to determine the amplitudes and remove some of the theoretical uncertainty on the HLBL

a_μ^{had}(LO) Analyticity + Optical Theorem

$$a_\mu(\text{had}) = \left(\frac{\alpha m_\mu}{3\pi}\right)^2 \int_{4m_\pi^2}^{\infty} \frac{ds}{s^2} K(s) \left(\frac{\sigma(e^+e^- \to \text{hadrons})}{\sigma(e^+e^- \to \mu^+\mu^-)}\right)$$

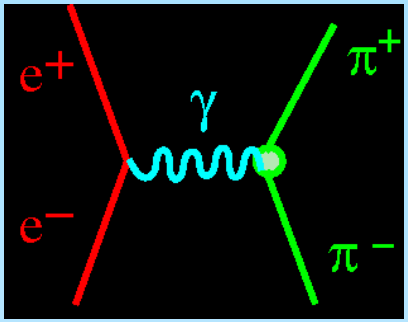

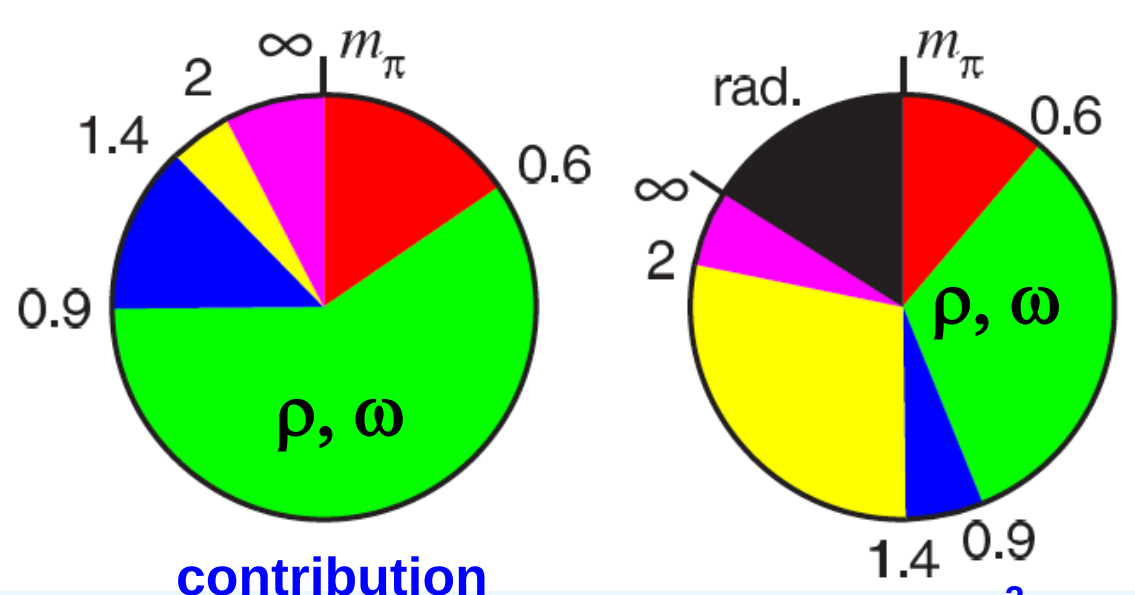

contribution **error²**

(from T. Teubner)

(w/o BaBar)

- Future efforts will reduce errors
  - CMD3 at VEPP2000, up to 2.0 GeV (next 5 years)
  - perhaps Belle

Measured Cross section for $e^+e^- \to \pi^+\pi^-$

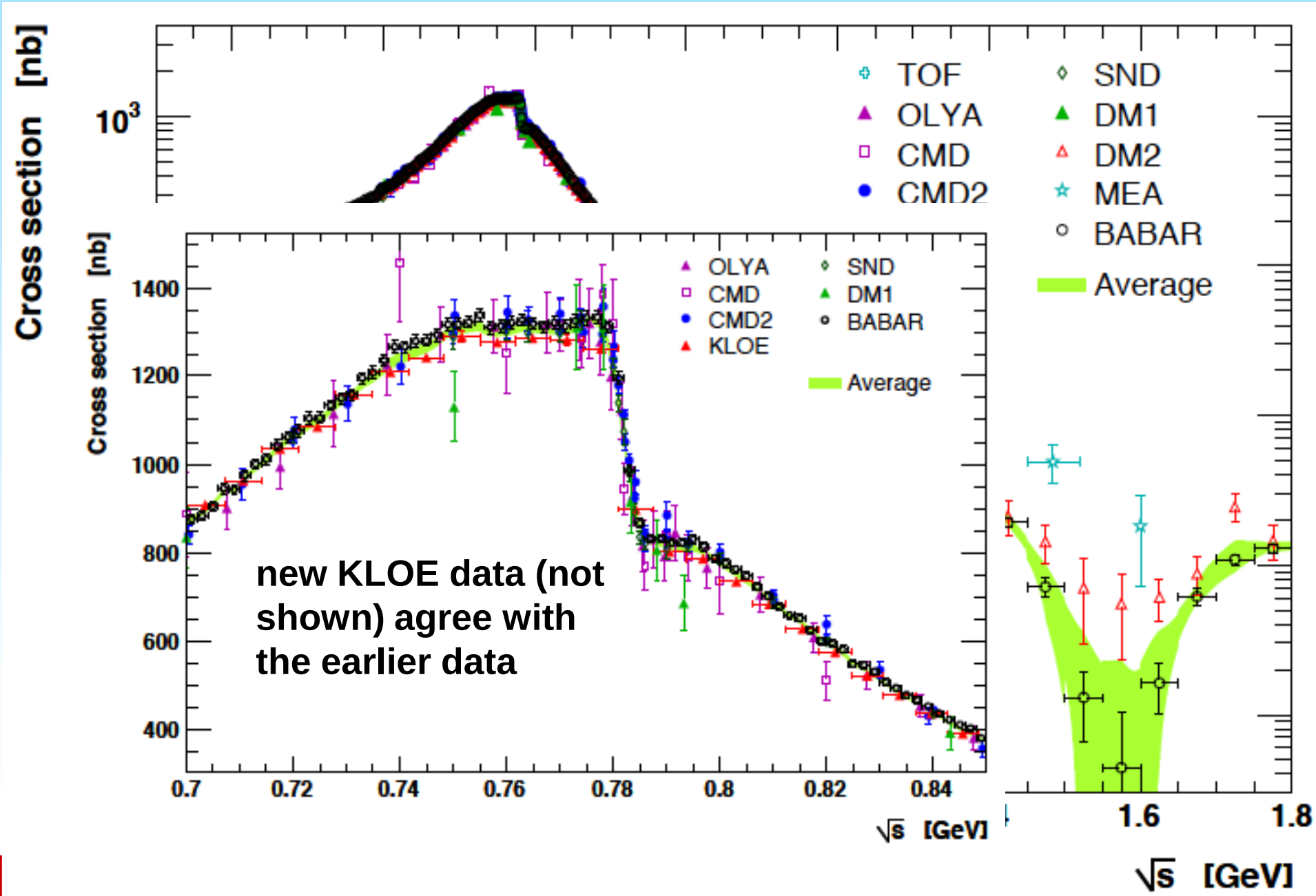

new KLOE data (not shown) agree with the earlier data

The SM Value for a_μ from $e^+e^- \to$ *hadrons* (Updated 9/09)

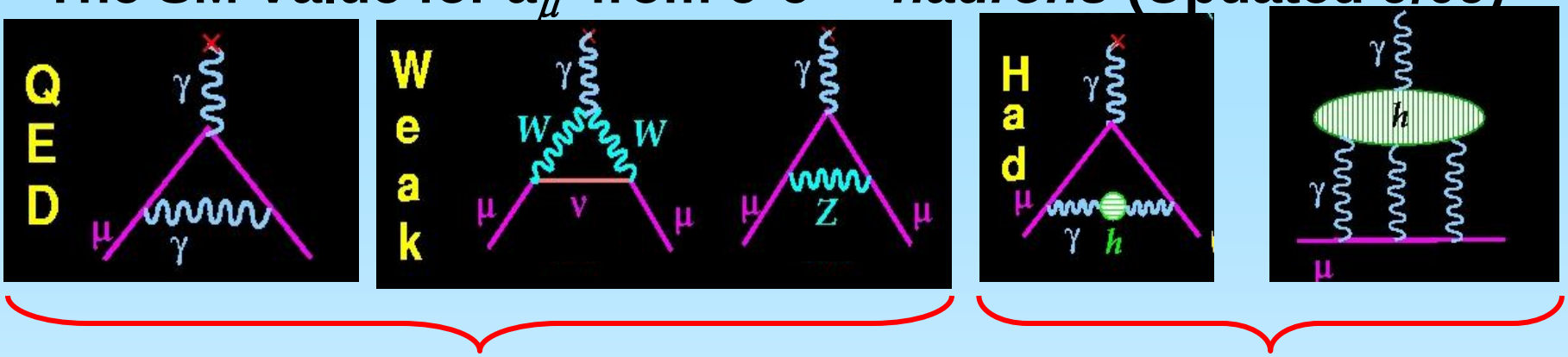

well known

significant work ongoing

		Value ($\times 10^{-11}$) units
QED ($\gamma + \ell$)		$116\,584\,718.09 \pm 0.14 \pm 0.04_\alpha$
HVP(lo)	w. BaBar, no KLOE LA	$6\,923 \pm 42$
HVP(ho)		-97.9 ± 0.9
EW		$154 \pm 1 \pm 2$
Total SM		$116\,591\,802 \pm 42_{\text{H-LO}} \pm 26_{\text{H-HO}} \pm 2_{\text{other}}\ (\pm 49_{\text{tot}})$

$\sigma_{\text{exp}} = \pm 63$

Davier et al, Eur. Phys. J. C (2011) 71:1515

I will return the the theory issue soon, but first a word about the experimental value

- I'll give the cartoon version of the experiment for theorists

We measure the difference frequency between the spin and momentum precession

$$\omega_a = \omega_S - \omega_C = \left(\frac{g-2}{2}\right)\frac{QeB}{m}B \Rightarrow \langle B \rangle_{\mu-\text{dist}}$$

With an electric quadrupole field for vertical focusing

without vertical focussing

$$\vec{\omega}_a = -\frac{Qe}{m}\left[a_\mu \vec{B} - \left(a_\mu - \frac{1}{\gamma^2 - 1}\right)\frac{\vec{\beta} \times \vec{E}}{c}\right]$$

0

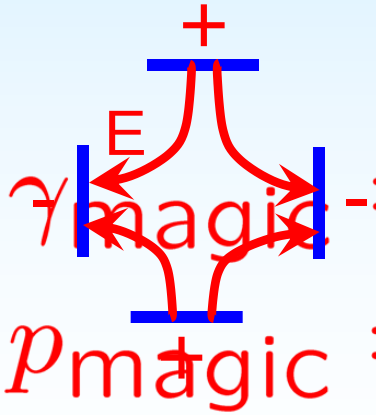

$\gamma_{\text{magic}} = 29.3$

$p_{\text{magic}} = 3.09$ GeV/c

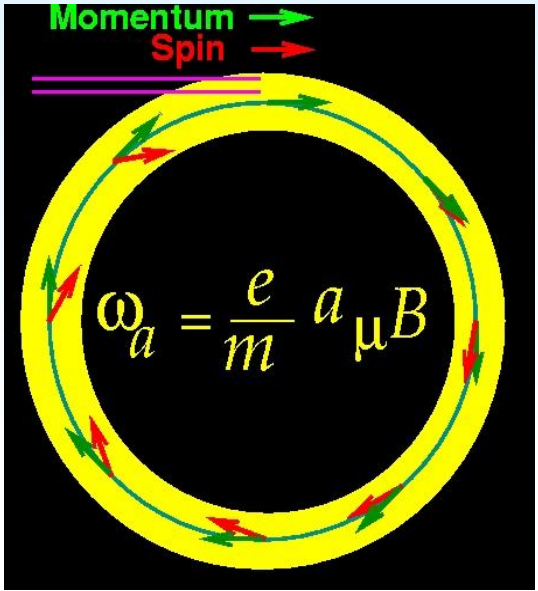

Experimental Technique

25ns bunch of
5 X 10^{12} protons
from AGS

$x_c \approx 77$ mm

$\beta \approx 10$ mrad

$B \cdot dl \approx 0.1$ Tm

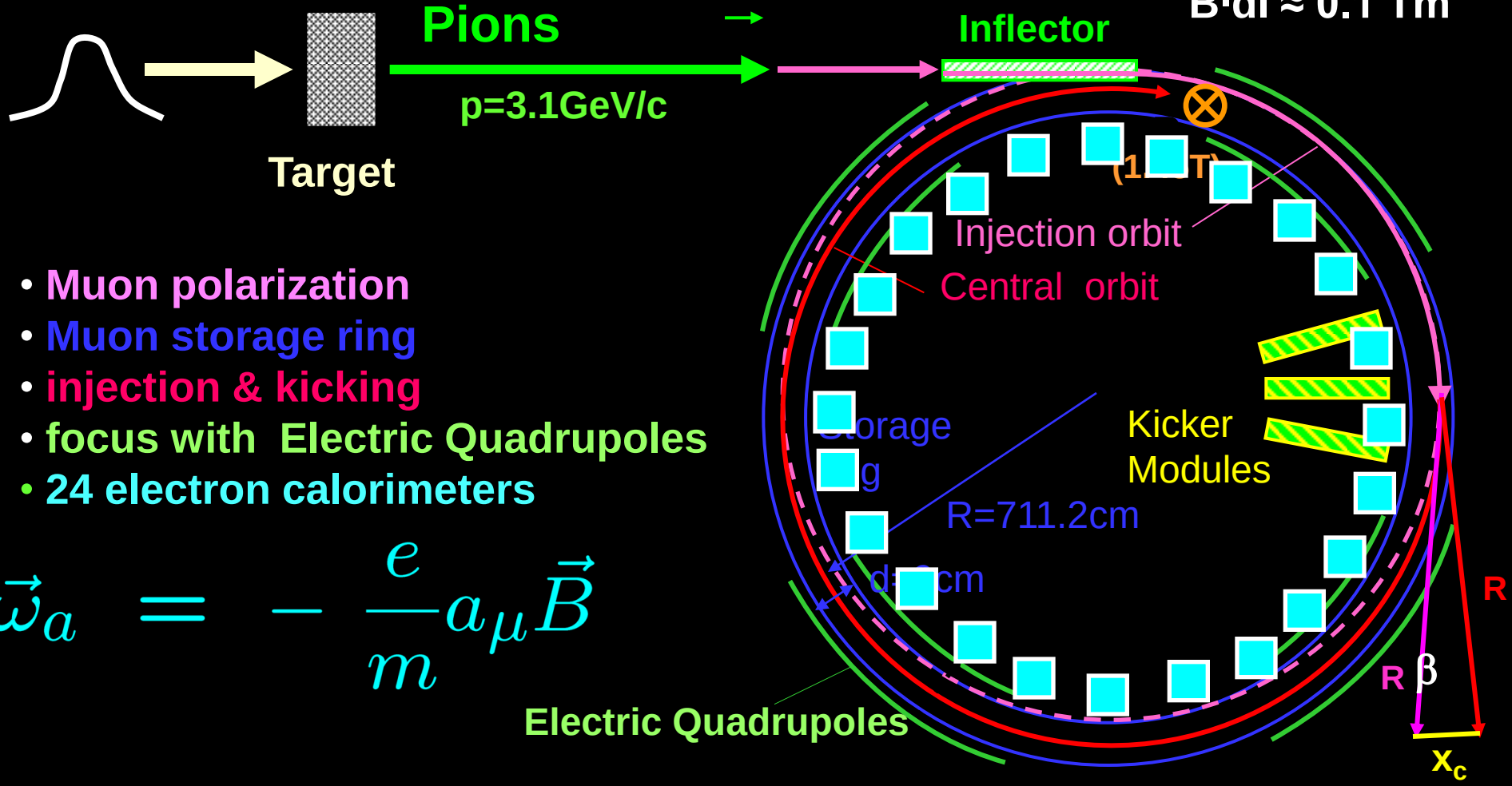

- Muon polarization
- Muon storage ring
- injection & kicking
- focus with Electric Quadrupoles
- 24 electron calorimeters

$$\vec{\omega}_a = -\frac{e}{m} a_\mu \vec{B}$$

e PRL **100,** 120801 (2008

μ PRL, **92, 161802** (2004)

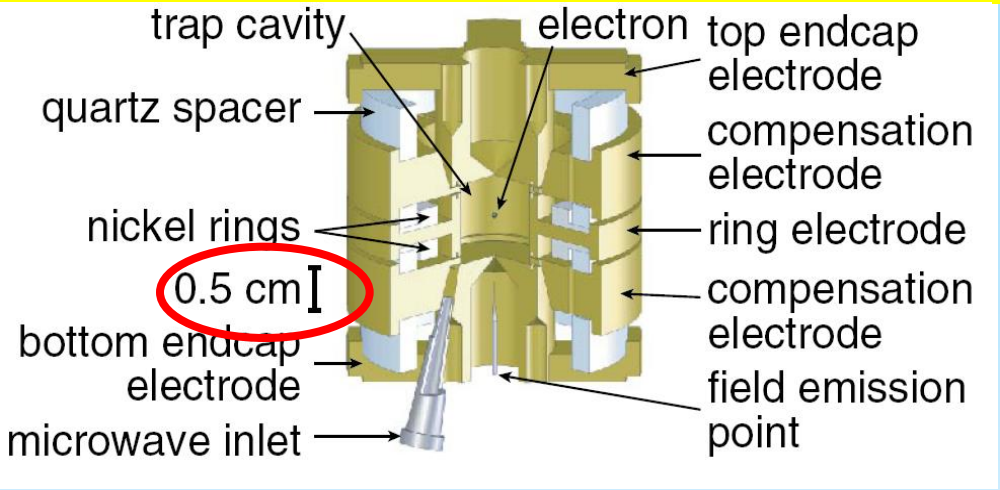

$$a_\mu = (116\,592\,089 \pm 63) \times 10^{-11} (0.54\ \text{ppm})$$

$$a_e = (115\,965\,218\,073 \pm 28) \times 10^{-14}\ (0.24\ \text{ppb})$$

muon more sensitive to heavier physics by

$$\sim \left(\frac{m_\mu}{m_e}\right)^2 \simeq 42,000$$

and interpretation of the electron anomaly limited by precision of independent measurements of α, ~4.5 ppb.

To determine a_μ we measure two numbers:

The muon spin frequency: ω_a

$$\omega_a = a\frac{eB}{mc}$$

The magnetic field normalized to the Larmor frequency of the free proton: ω_p

$$a_\mu = \frac{\frac{\omega_a}{\omega_p}}{\frac{\mu_\mu}{\mu_p} - \frac{\omega_a}{\omega_p}}$$

To measure ω_a, we used Pb-scintillating fiber calorimeters.

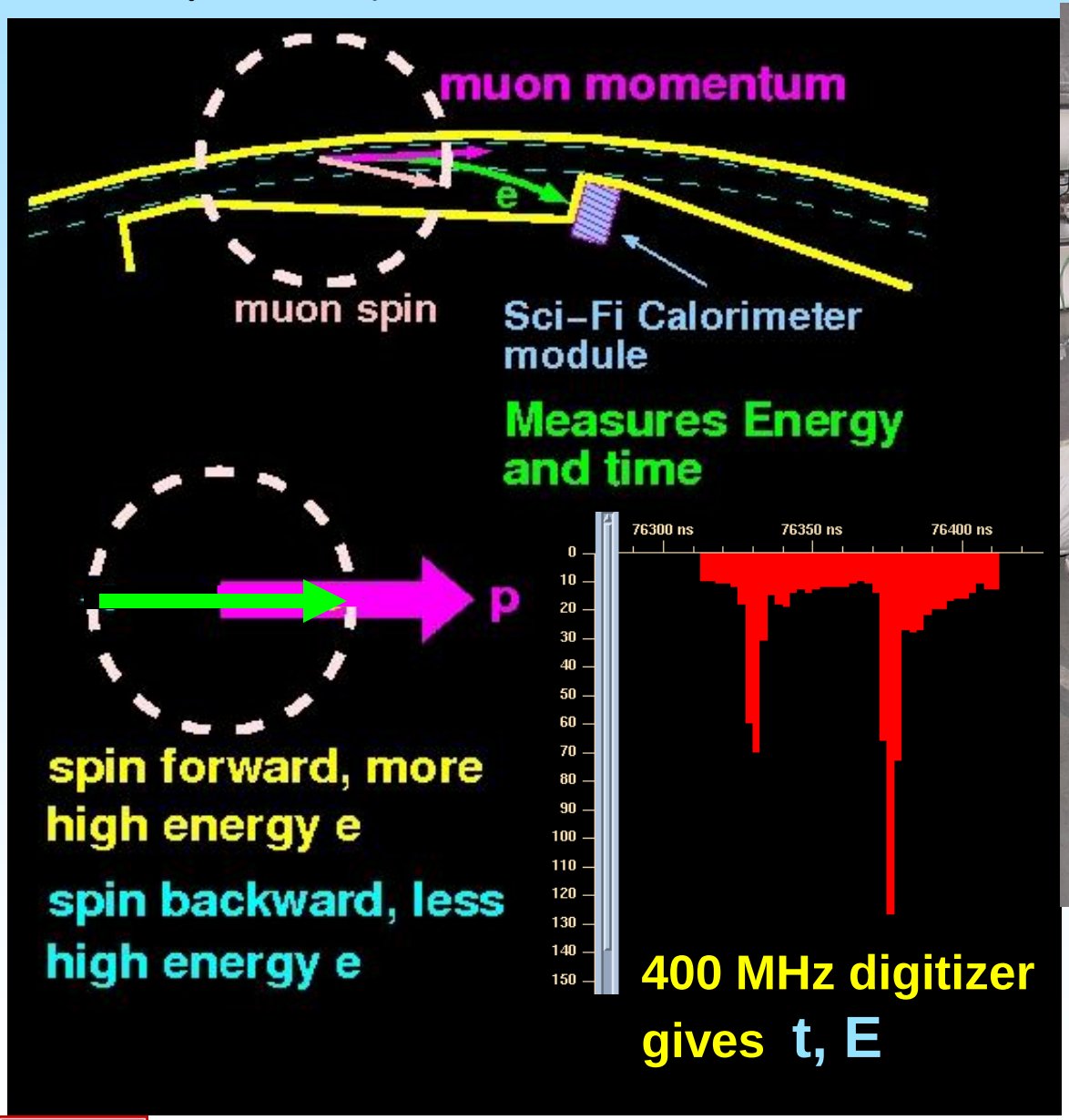

Count number of e^- with $E_e \geq 1.8$ GeV

Arrival time spectrum

$$f(t) \simeq N_0 e^{-\lambda t}[1 + A\cos\omega_a t + \phi)]$$

$$4 \times 10^9\ e^-,\ E_{e^-} \geq 1.8\ \text{GeV}$$

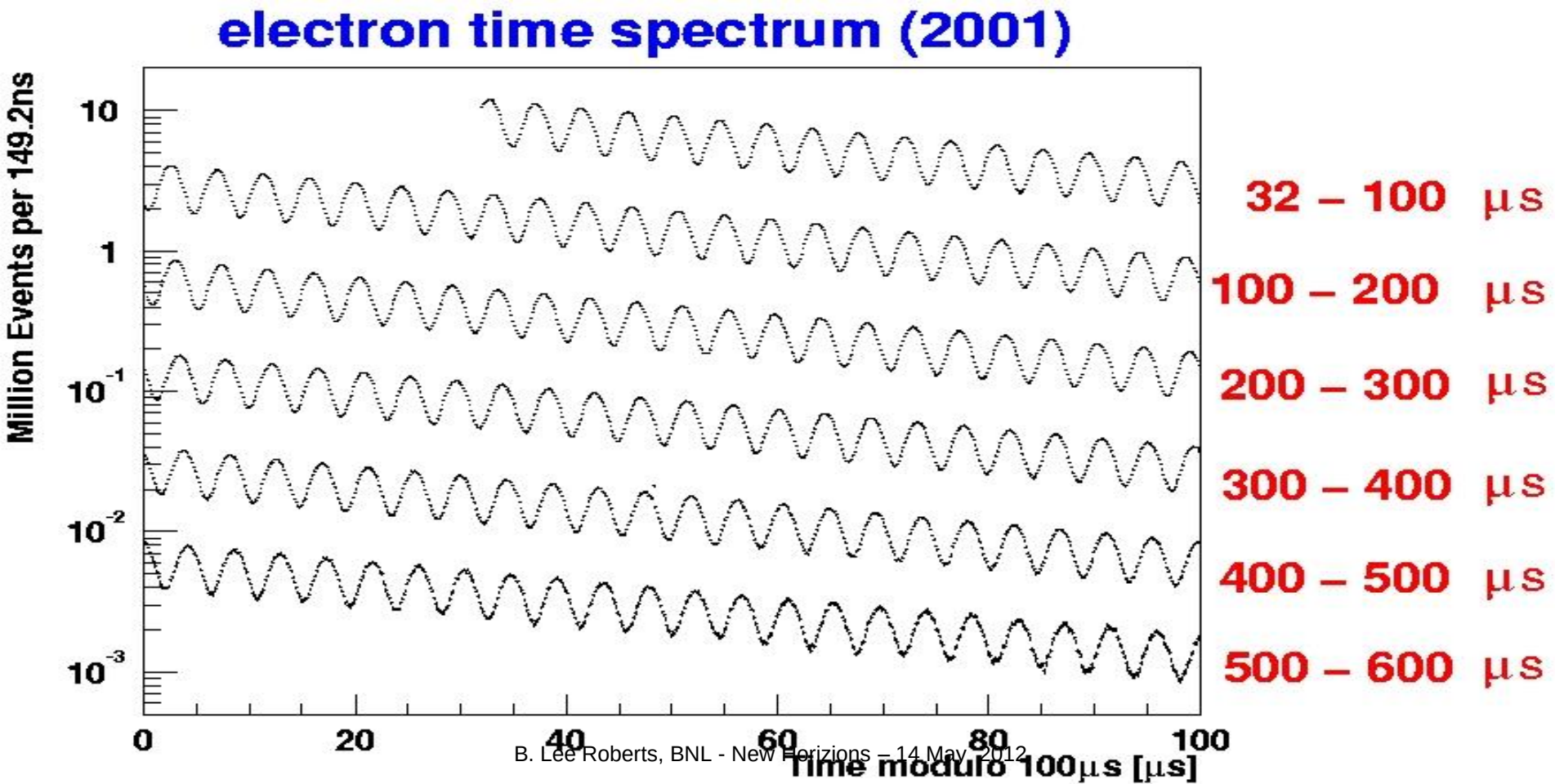

The magnetic field is measured and controlled using pulsed NMR and the free-induction decay.

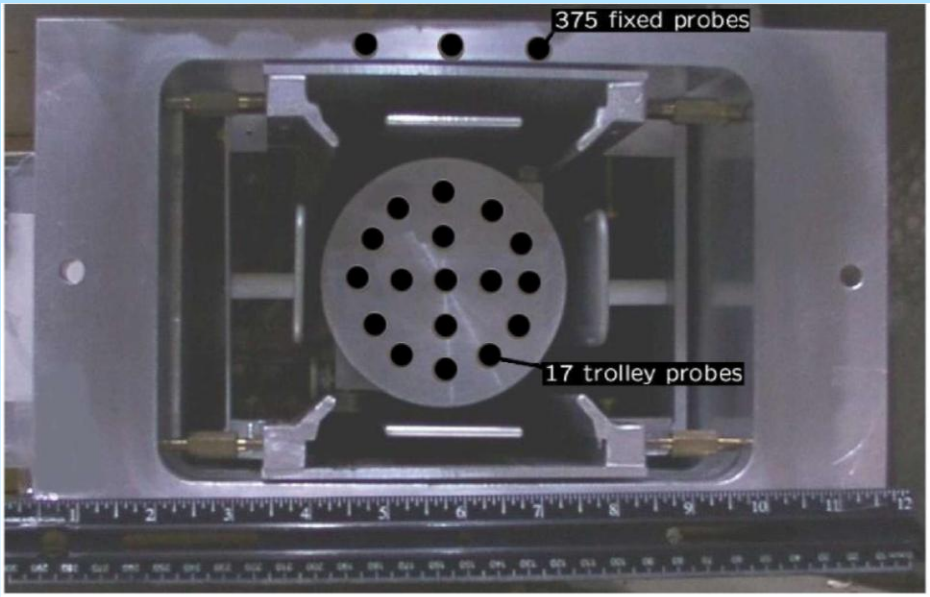

- Calibration to a spherical water sample that ties the field to the Larmor frequency of the free proton ω_p.
- We measure ω_a and ω_p

$$a_\mu = \frac{\dfrac{\omega_a}{\omega_p}}{\dfrac{\mu_\mu}{\mu_p} - \dfrac{\omega_a}{\omega_p}}$$

Free induction decay signals:

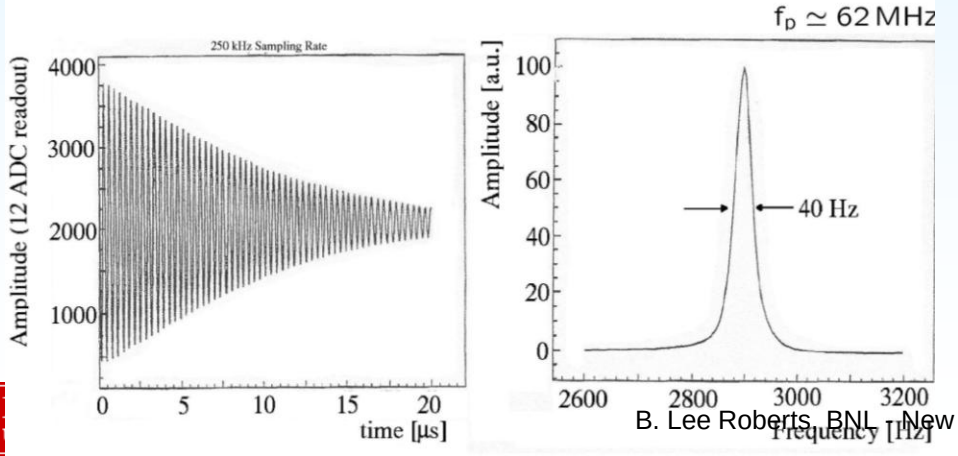

E821 achieved ± 0.54 ppm. The e^+e^- based theory is at the ~0.4 ppm level. Difference is >3σ

SM: Davier et al, , Eur. Phys. J. C (2011) 71:1515

Hagiwara, et al., J.Phys. G **38** (2011) 085003

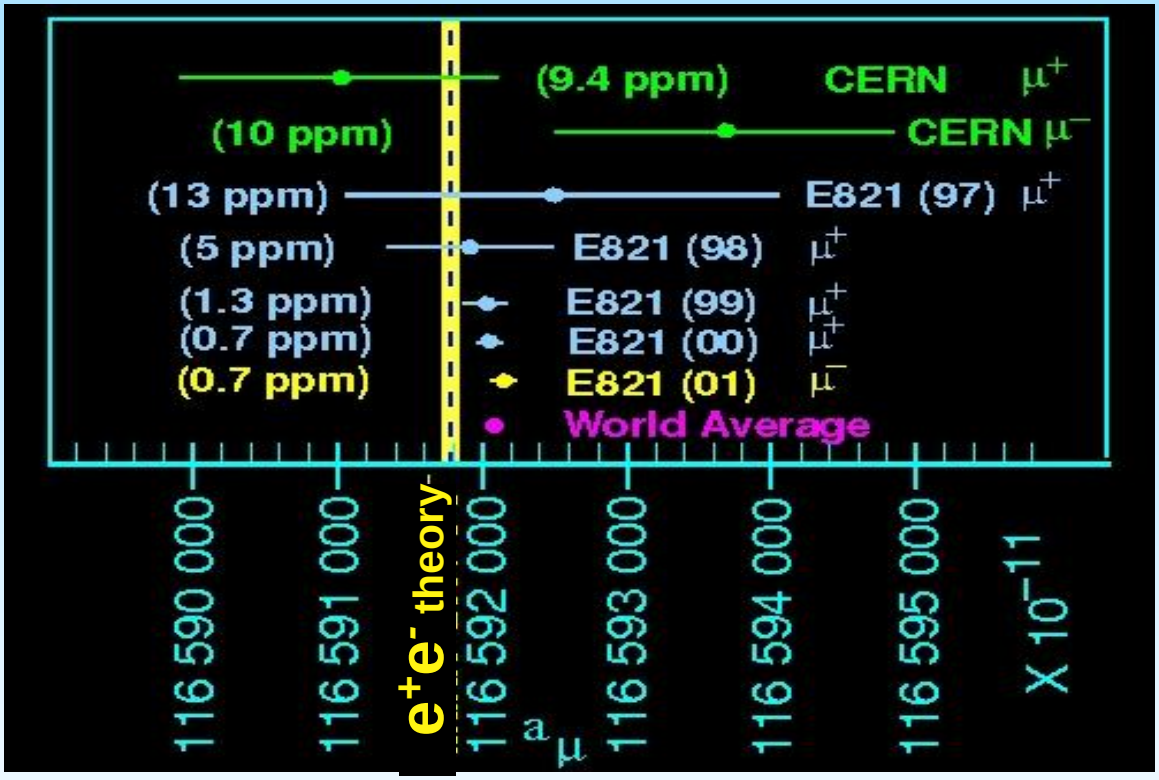

$$a_\mu^{SM} = 116\,591\,802(49) \times 10^{-11} \ (0.42\,\text{ppm})$$

$$a_\mu^{exp} = 116\,592\,089(63) \times 10^{-11} \ (0.54\,\text{ppm})$$

$$\Delta a_\mu \equiv a_\mu^{exp} - a_\mu^{SM} = (287 \pm 80) \times 10^{-11}$$

$$a_\mu^{EW} = 154(1)(2) \times 10^{-11}$$

Muon g-2 is a powerful discriminator between models; chiral-changing, flavor and CP conserving interaction.

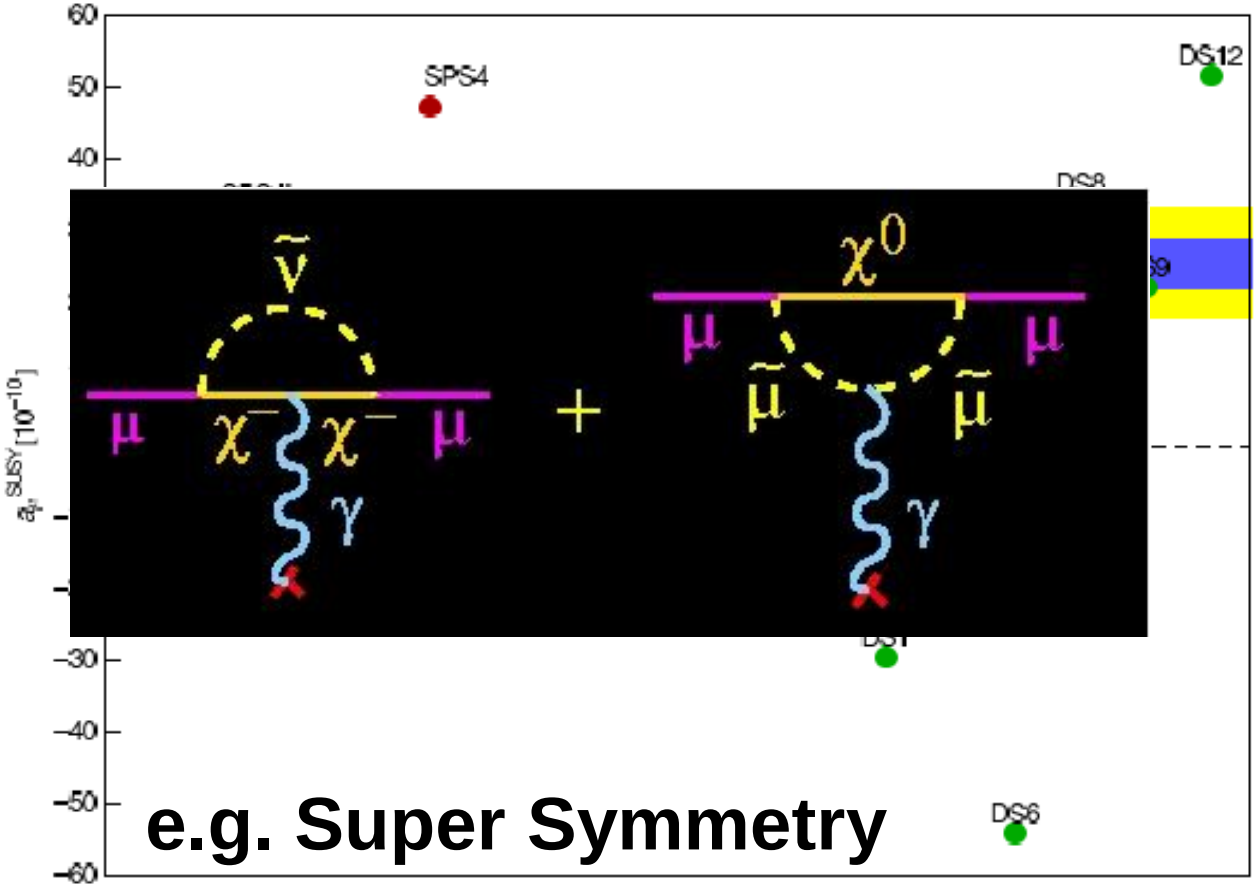

tan *b* sensitivity

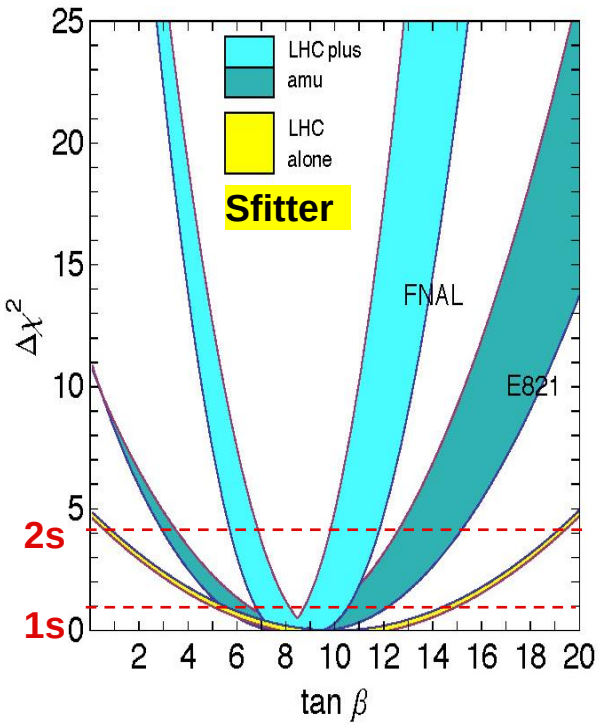

SPS1a; LHC 100 fb-1 at 14 TeV

Snowmass points and slopes (SUSY)

from D. Stöckinger

LHC Inverse Problem (300fb^{-1})

can't be distinguished at LHC [Sfitter: Adam, Kneur, Lafaye, Plehn, Rauch, Zerwas '10]

Other Models

- Technicolor
  - small Δa_μ
- Littlest Higgs with T-parity
  - small Δa_μ
- Universal Extra Dimensions
  - small Δa_μ
- Randall Sundrum
  - could accommodate large Δa_μ

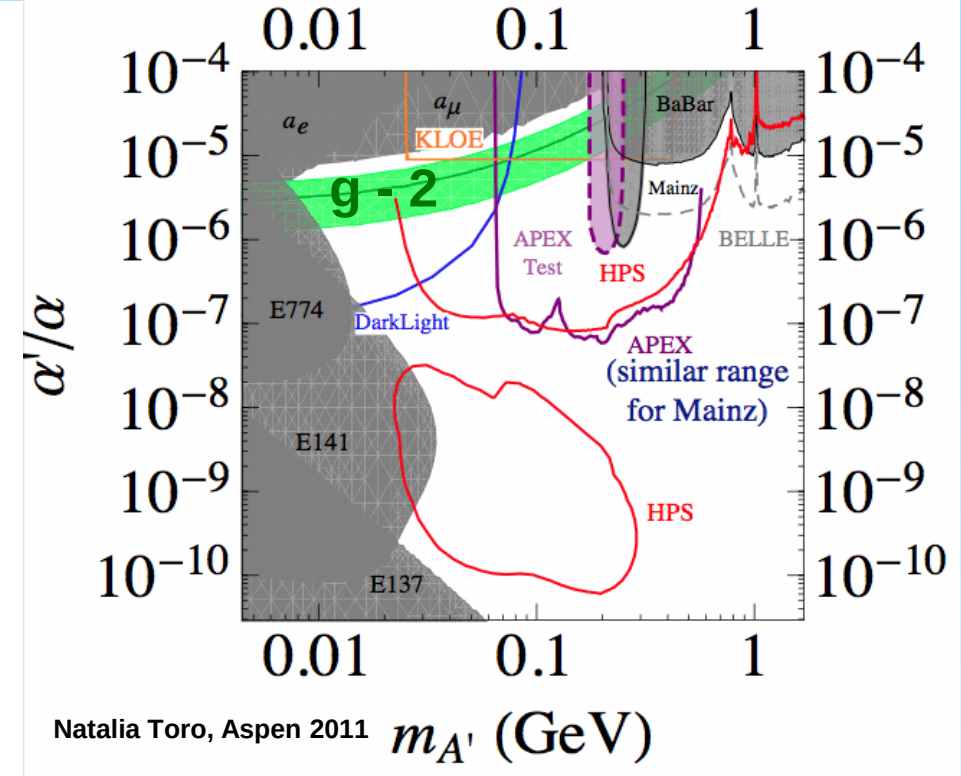

Natalia Toro, Aspen 2011

- Two Higgs doublets, shadow Higgs
  - small Δa_μ
- Additional light bosons that can affect EM interactions (difficult to study at LHC)
  - secluded U(1),etc., could have significant Δa_μ

How to clarify this 3.3 – 3.6 σ situation?

Good question!

B.

3.3 – 3.6 σ: Theory & Experiment must do better

- Experiment: E989 at Fermilab ≥ X4 better
  - move the storage ring to Fermilab
  - use the p-bar debuncher (now called the delivery ring) as a long decay line.

Fermilab Muon Campus

Fermilab Muon Beam

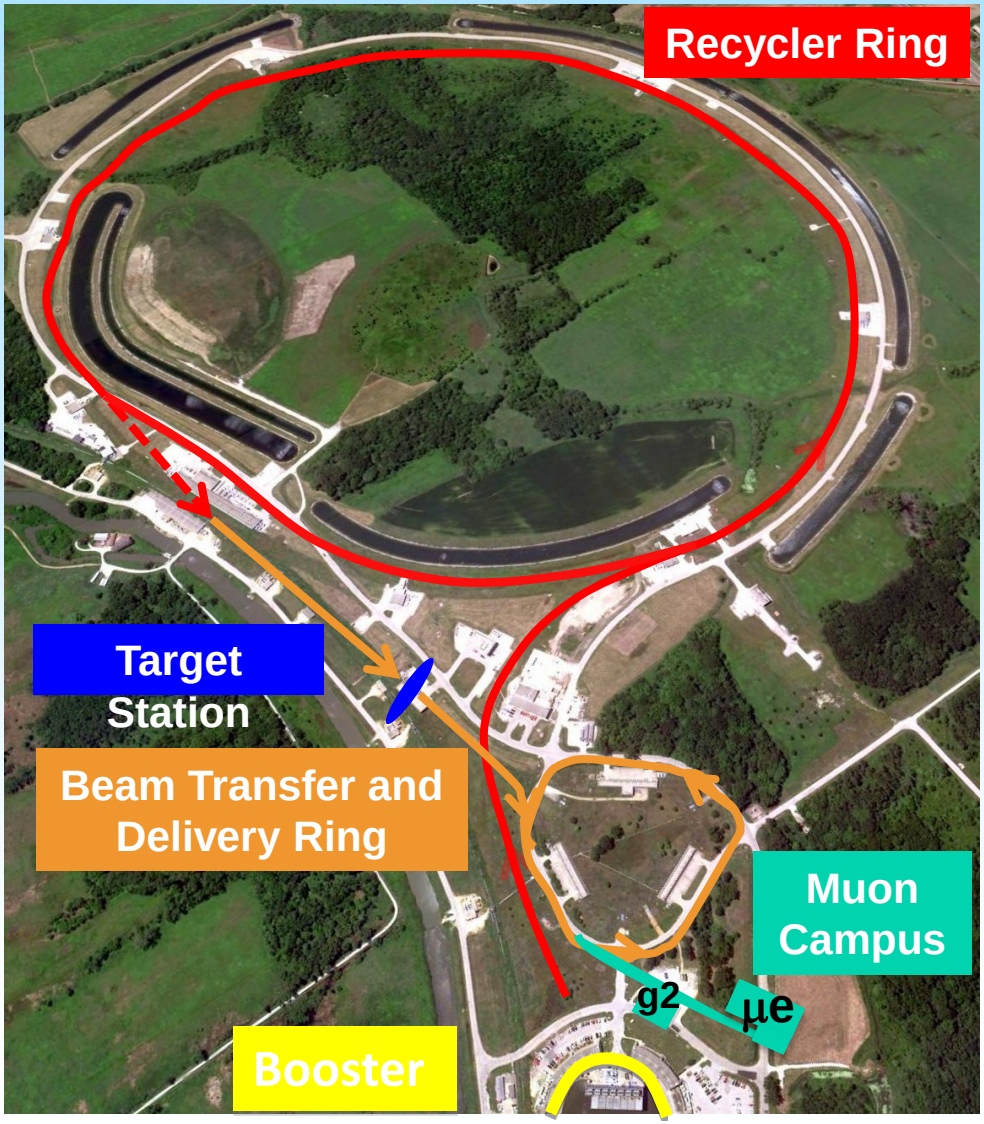

Polarized muons delivered and stored in the ring at the magic momentum, 3.094 GeV/c

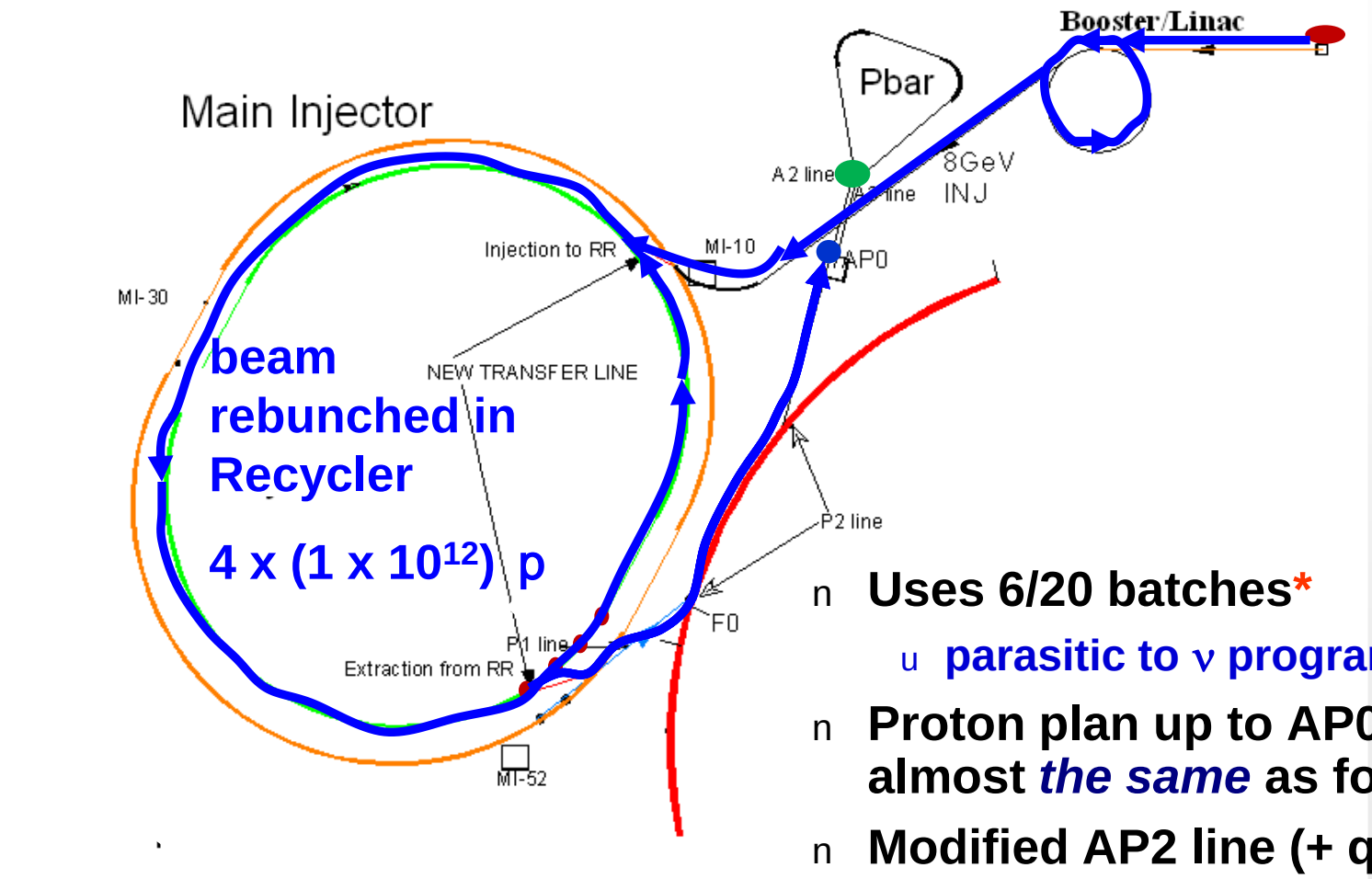

- Uses 6/20 batches*
  - parasitic to ν program
- Proton plan up to AP0 target is almost *the same* as for Mu2e
- Modified AP2 line (+ quads)
- New beam stub into ring

*Can use all 20 if MI program is off

Theory: It's the hadronic contribution

$\sigma_{H\text{-}LO} = 42$ $\sigma_{H\text{-}LBL} = 26$ $\sigma_{Tot} = 49$

Dispersion relation and data?

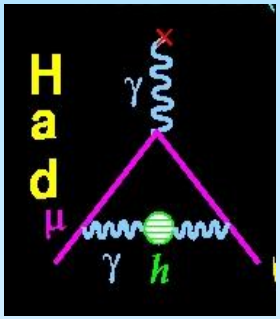

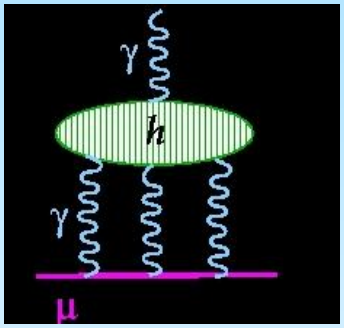

Models Are data relevant?

- The lowest-order hadronic comes from e^+e^- data and a dispersion relation
  - can't they just take more data?
- It's not so simple because of the τ-decay data

So what's the problem

- It looks like data can determine the lowest-order hadronic just fine

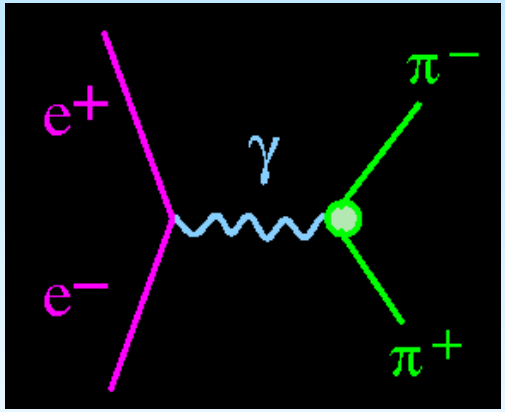

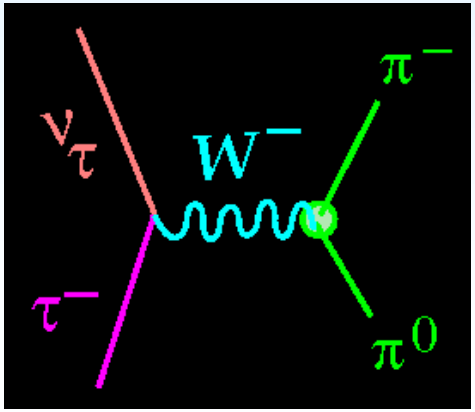

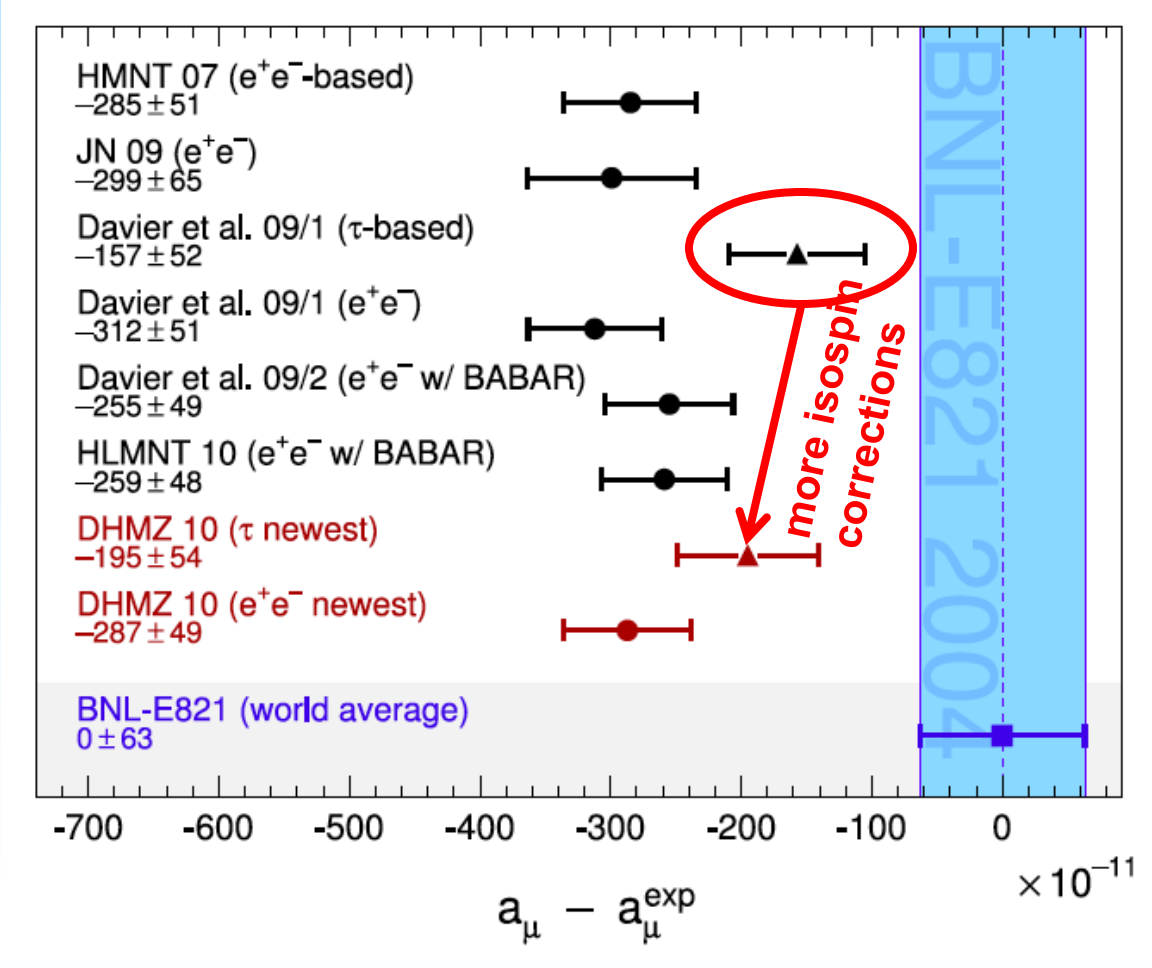

Clarifying the τ problem for H-LO

- It is claimed that if ρ-γ mixing is correctly included the τ-e^+e^- difference goes away.
- What's the path forward
  - More e^+e^- data?

–The Lattice!

- The lattice can make an important contribution in the determination of the lowest-order hadronic contribution

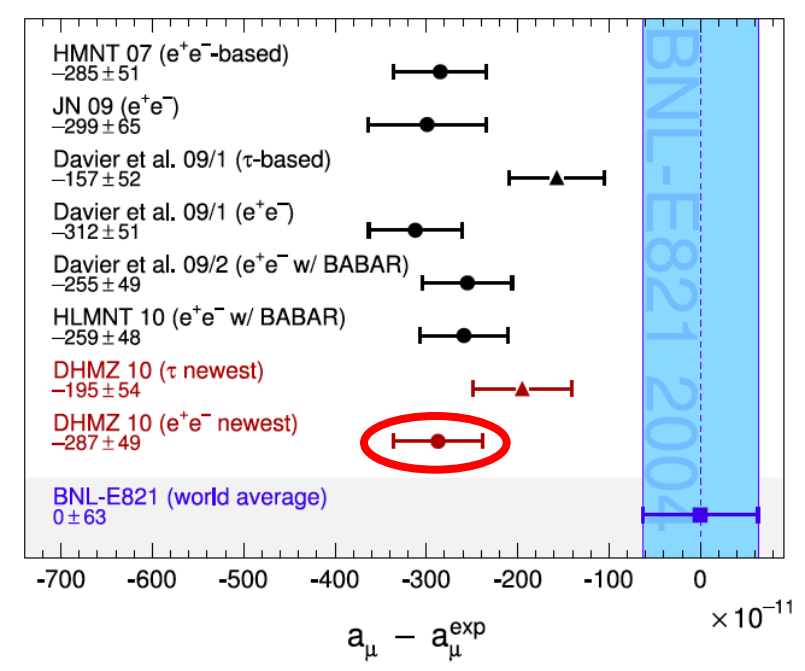

- The proof of principle was published last year

Even more urgent: Hadronic light-by-light

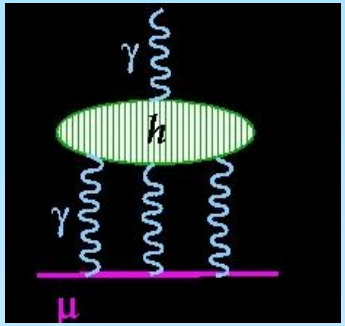

$$a_\mu^{(\mathrm{HLbyL})} = (105 \pm 26) \times 10^{-11}$$

- Model calculation
  - (Prades, de Rafael, Vainshtein compilation)

- Here the lattice can make an extremely important calculation.
  - even 10 to 20% would be fabulous

Summary and Conclusions

- Fermilab E989 will improve g-2 by at least X4
- Additional data for the dispersion relation will be taken at CMD3 (Novosibirsk), BESS3, and Super Belle.
- The Lattice has the opportunity to play an important role in the confrontation between the Standard Model and experiment
  - lowest-order hadronic
  - hadronic light-by-light
- It's an opportunity to make a huge impact in the search for physics beyond the standard model.

Prospects for the computation of rare kaon-decay amplitudes

Chris Sachrajda
(based on discussions with P.Boyle, E.Goode, P.Kassel and A.Lytle)

School of Physics and Astronomy
University of Southampton
Southampton SO17 1BJ
UK

(RBC-UKQCD)

New Horizons for Lattice Computations with Chiral Fermions
Brookhaven National Laboratory, 14 – 16 May 2012

UNIVERSITY OF Southampton
School of Physics and Astronomy

Motivation and Introduction

- Lattice simulations are contributing to a wide variety of fundamental issues in particle physics and increasingly to nuclear physics.
- For me personally, a major motivation is the important complementarity of high-energy experiments (most notably the LHC) and precision flavour physics in discovering and unraveling the next layer of fundamental physics.
  - If, as expected/hoped the LHC experiments discover new elementary particles, then precision flavour physics will be necessary to understand the underlying framework.
  - The discovery potential of precision flavour physics should also not be underestimated. (In principle, the reach is about two-orders of magnitude deeper than the LHC!)
  - Precision flavour physics requires control of hadronic effects for which lattice QCD simulations are essential.
- For many years we have been calculating matrix elements of the forms:

$$\begin{aligned} \langle 0 \,|\, O(0) \,|\, h \rangle &\quad \rightarrow \quad f_P\,, \text{ for example} \\ \langle h_2 \,|\, O(0) \,|\, h_1 \rangle &\quad \rightarrow \quad B_P, \text{ semileptonic form factors}, \cdots . \end{aligned}$$

$\Rightarrow$ unitarity triangle tests of the SM, determination of CKM matrix elements etc.

Extending the reach of Lattice Simulations

- Recent RBC-UKQCD extensions to the above include the evaluation of $K \to \pi\pi$ decay amplitudes. arXiv:1106.2714, arXiv:1111.1699
- More recently we have began to consider long-distance contributions to physical quantities. These are not given in terms of matrix elements of local operators, but require the evaluation for example of:

$$\int d^4x \int d^4y \, \langle h_2 | T\{O_1(x)\, O_2(y)\} | h_1 \rangle \, .$$

- The most advanced of our projects is on the evaluation of long-distance contributions to the $K_L - K_S$ mass difference.

Jianglei Yu, arXiv:1111.6953; paper in preparation.

$$\int d^4x \int d^4y \, \langle \bar{K}^0 | T\{H_W(x)\, H_W(y)\} | K^0 \rangle \, .$$

- Here instead, I will present some preliminary thoughts about the rare kaon decays $K \to \pi\nu\bar{\nu}$ and $K \to \pi\ell^+\ell^-$:

$$\int d^4x\, e^{-iq\cdot x} \int d^4y \, \langle \pi | T\{J^\mu(x)\, H_W(y)\} | K^0 \rangle \, .$$

- Up to now, the main theoretical tool for these processes has been Chiral Perturbation Theory with its many limitations and uncertainties.

Example: $K_L \to \pi^0 \ell^+ \ell^-$

F.Mescia, C,Smith, S.Trine hep-ph/0606081

- Rare kaon decays which are dominated by short-distance FCNC processes, $K \to \nu\bar{\nu}$ in particular, provide a potentially valuable window on new physics at high-energy scales.
- The decays $K_L \to \pi^0 e^+ e^-$ and $K_L \to \pi^0 \mu^+ \mu^-$ are also considered promising because the long-distance effects are reasonably under control using ChPT.
  - They are sensitive to different combinations of short-distance FCNC effects and hence in principle provide additional discrimination to the neutrino modes.
  - A challenge for the lattice community is therefore either to calculate the long-distance effects reliably or at least to determine the Low Energy Constants of ChPT.

$K_L \to \pi^0 \ell^+ \ell^-$ cont.

There are three main contributions to the amplitude:

1. Short distance contributions: F.Mescia, C,Smith, S.Trine hep-ph/0606081

$$H_{\rm eff} = -\frac{G_F \alpha}{\sqrt{2}} V_{ts}^* V_{td} \{ y_{7V} (\bar{s}\gamma_\mu d)(\bar{\ell}\gamma^\mu \ell) + y_{7A} (\bar{s}\gamma_\mu d)(\bar{\ell}\gamma^\mu \gamma_5 \ell) \} + \text{h.c.}$$

   - Direct CP-violating contribution.
   - In BSM theories other effective interactions are possible.

2. Long-distance indirect CP-violating contribution

$$A_{ICPV}(K_L \to \pi^0 \ell^+ \ell^-) = \varepsilon A(K_1 \to \pi^0 \ell^+ \ell^-) .$$

3. The two-photon CP-conserving contribution $K_L \to \pi^0 (\gamma^* \gamma^* \to \ell^+ \ell^-)$.

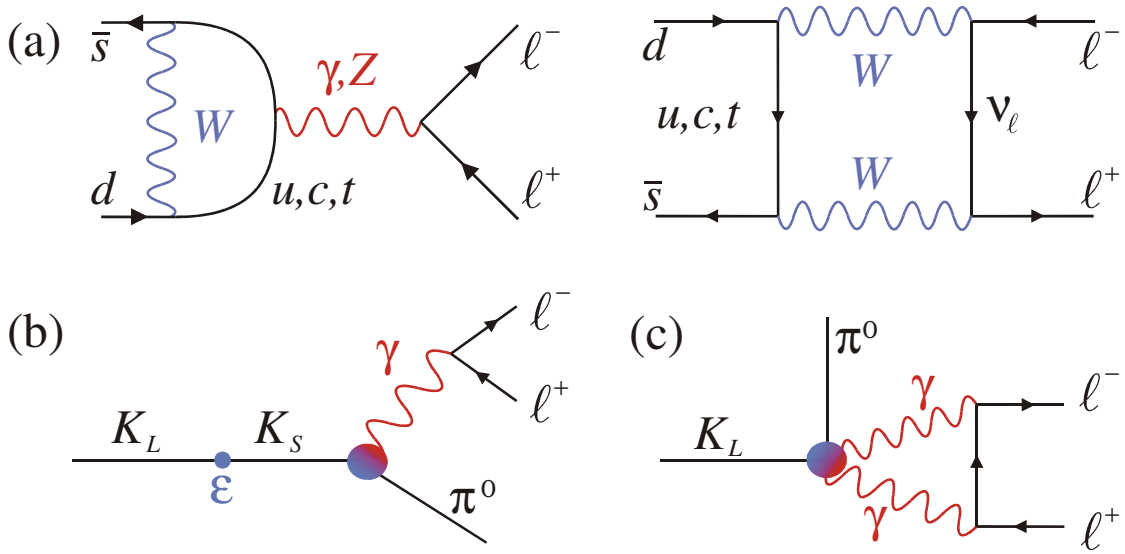

$K_L \to \pi^0 \ell^+ \ell^-$ cont.

- The current phenomenological status for the SM predictions is nicely summarised by: V.Cirigliano et al., arXiv1107.6001

$$\mathrm{Br}(K_L \to \pi^0 e^+ e^-)_{\mathrm{CPV}} = 10^{-12} \times \left\{ 15.7|a_S|^2 \pm 6.2|a_S| \left(\frac{\mathrm{Im}\,\lambda_t}{10^{-4}}\right) + 2.4 \left(\frac{\mathrm{Im}\,\lambda_t}{10^{-4}}\right)^2 \right\}$$

$$\mathrm{Br}(K_L \to \pi^0 \mu^+ \mu^-)_{\mathrm{CPV}} = 10^{-12} \times \left\{ 3.7|a_S|^2 \pm 1.6|a_S| \left(\frac{\mathrm{Im}\,\lambda_t}{10^{-4}}\right) + 1.0 \left(\frac{\mathrm{Im}\,\lambda_t}{10^{-4}}\right)^2 \right\}$$

  - $\lambda_t = V_{td} V_{ts}^*$ and $\mathrm{Im}\,\lambda_t \simeq 1.35 \times 10^{-4}$.
  - $|a_S|$, the amplitude for $K_S \to \pi^0 \ell^+ \ell^-$ at $q^2 = 0$ as defined below, is expected to be $O(1)$ but the sign of a_S is unknown. $|a_S| = 1.06^{+0.26}_{-0.21}$.
  - For $\ell = e$ the two-photon contribution is negligible.
  - Taking the positive sign (?) the prediction is

$$\begin{aligned} \mathrm{Br}(K_L \to \pi^0 e^+ e^-)_{\mathrm{CPV}} &= (3.1 \pm 0.9) \times 10^{-11} \\ \mathrm{Br}(K_L \to \pi^0 \mu^+ \mu^-)_{\mathrm{CPV}} &= (1.4 \pm 0.5) \times 10^{-11} \\ \mathrm{Br}(K_L \to \pi^0 \mu^+ \mu^-)_{\mathrm{CPC}} &= (5.2 \pm 1.6) \times 10^{-12}. \end{aligned}$$

  - The current experimental limits (KTeV) are:

$$\mathrm{Br}(K_L \to \pi^0 e^+ e^-) < 2.8 \times 10^{-10} \quad \text{and} \quad \mathrm{Br}(K_L \to \pi^0 \mu^+ \mu^-) < 3.8 \times 10^{-10}.$$

CPC Decays: $K_S \to \pi^0 \ell^+ \ell^-$ and $K^+ \to \pi^+ \ell^+ \ell^-$

G.Isidori, G.Martinelli and P.Turchetti, hep-lat/0506026

- We now turn to the CPC decays $K_S \to \pi^0 \ell^+ \ell^-$ and $K^+ \to \pi^+ \ell^+ \ell^-$ and consider

$$T_i^\mu = \int d^4x\, e^{-iq\cdot x} \langle \pi(p) \,|\, \mathrm{T}\{ J^\mu_{\mathrm{em}}(x)\, Q_i(0) \} \,|\, K(k) \rangle \,,$$

where Q_i is an operator from the effective Hamiltonian.

- Gauge invariance implies that

$$T_i^\mu = \frac{\omega_i(q^2)}{(4\pi)^2} \left\{ q^2 (p+k)^\mu - (m_K^2 - m_\pi^2)\, q^\mu \right\} .$$

- Within ChPT the Low energy constants a_+ and a_S are defined by

$$a = \frac{1}{\sqrt{2}} V_{us}^* V_{ud} \left\{ C_1 \omega_1(0) + C_2 \omega_2(0) + \frac{2N}{\sin^2\theta_W} f_+(0) C_{7V} \right\}$$

where $Q_{1,2}$ are the two current-current GIM subtracted operators and the C_i are the Wilson coefficients. (C_{7V} is proportional to y_{7V} above).

G.Ambosio, G.Ecker, G.Isidori and J.Portoles, hep-ph/9808289

- Phenomenological values: $a_+ = -0.578 \pm 0.016$ and $|a_S| = 1.06^{+0.26}_{-0.21}$.

Can we do better in lattice simulations?

The fiducial volume

- Ideas developed (or being developed) from our ΔM_K project.
- How do you prepare the states $h_{1,2}$ in

$$\int d^4x \int d^4y \, \langle h_2 | T\{O_1(x)\, O_2(y)\} | h_1 \rangle \,,$$

when the time of the operators is integrated.

- The practical solution is to integrate over a large subinterval in time $t_A \leq t_{x,y} \leq t_B$, but to create h_1 and to annihilate h_2 well outside of this region:

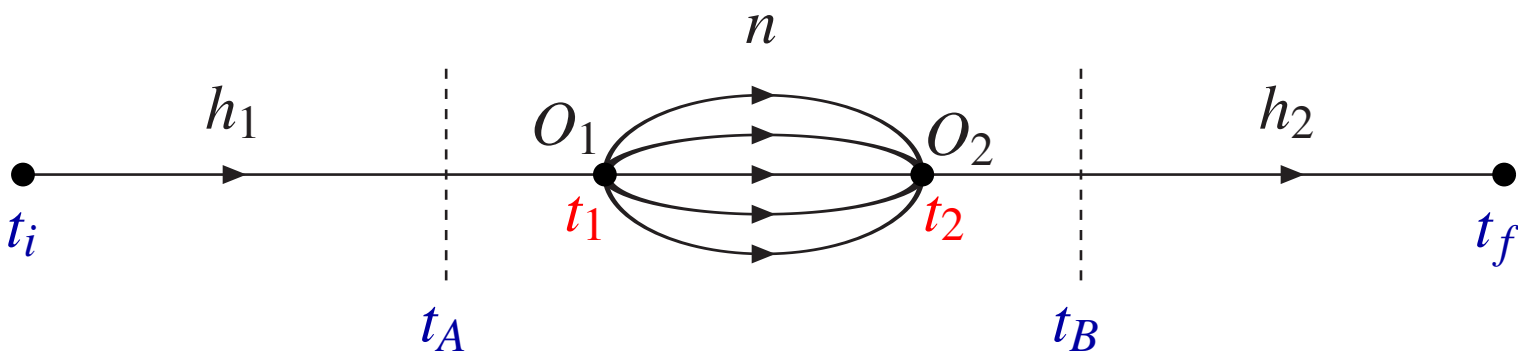

- This is the natural modification of standard field theory for which the asymptotic states are prepared at $t \to \pm\infty$ and then the operators are integrated over all time.
- This approach has been successfully implemented in the ΔM_K project.

N.Christ arXiv:1012.6034; Jianglei Yu arXiv:1111.6953; paper in preparation

Minkowski and Euclidean Correlation Functions

- The generic non-local matrix elements which we wish to evaluate is

$$
\begin{aligned}
X &\equiv \int_{-\infty}^{\infty} dt_x\, d^3x\, \langle \pi(p)\,|\,\mathrm{T}\,[\,J(0)\,H(x)\,]\,|K\rangle \\
&= i\sum_n \frac{\langle \pi(p)\,|\,J(0)\,|n\rangle\,\langle n\,|H(0)\,|\,K\rangle}{m_K - E_n + i\varepsilon} - i\sum_{n_s} \frac{\langle \pi(p)\,|\,H(0)\,|n_s\rangle\,\langle n_s\,|J(0)\,|\,K\rangle}{E_{n_s} - E_\pi + i\varepsilon}\,,
\end{aligned}
$$

  - $\{|n\rangle\}$ and $\{|n_s\rangle\}$ represent complete sets of non-strange and strange sets.
- In Euclidean space we envisage calculating correlation functions of the form

$$
C \equiv \int_{-T_a}^{T_b} dt_x\, \langle \phi_\pi(\vec{p}, t_\pi)\,\mathrm{T}\,[\,J(0)\,H(t_x)\,]\,\phi_K^\dagger(t_K)\,\rangle \equiv \sqrt{Z_K}\,\frac{e^{-m_K|t_K|}}{2m_K}\,X_E\,\sqrt{Z_\pi}\,\frac{e^{-E_\pi t_\pi}}{2E_\pi}\,,
$$

where

$$
\begin{aligned}
X_{E_-} &= -\sum_n \frac{\langle \pi(p)\,|\,J(0)\,|n\rangle\,\langle n\,|H(0)\,|\,K\rangle}{m_K - E_n}\left(1 - e^{(m_K - E_n)T_a}\right) \quad \text{and} \\
X_{E_+} &= \sum_{n_s} \frac{\langle \pi(p)\,|\,H(0)\,|n_s\rangle\,\langle n_s\,|J(0)\,|\,K\rangle}{E_{n_s} - E_\pi}\left(1 - e^{-(E_{n_s} - E_\pi)T_b}\right).
\end{aligned}
$$

Removing the single-pion intermediate state

- Chiral ward identities imply that we can add a term proportional to the scalar density $\bar{s}d$ to the Hamiltonian without changing physical results. We can therefore subtract the single pion intermediate state by imposing $\langle\pi|H+c_S\,\bar{s}d|K\rangle=0$.
- It is instructive to see how this works in the present case at lowest order in chiral perturbation theory. The scalar density in the effective theory can be written as

$$S^{sd}=\mathrm{Tr}\left[\lambda^{sd}\left(\Sigma+\Sigma^\dagger\right)\right]\quad\text{where}\quad\lambda^{sd}=\begin{pmatrix}0&0&0\\0&0&0\\0&1&0\end{pmatrix}.$$

- The em current is of the form

$$J^\mu=i\frac{f^2}{4}\,\mathrm{Tr}\left[Q\left(\Sigma\partial^\mu\Sigma^\dagger+\Sigma\partial^\mu\Sigma\right)\right]$$

- The c_S term leads to additional diagrams:

which are proportional to

$$\frac{(p_\pi+p_K)^\mu}{p_K^2-m_\pi^2}+\frac{(p_\pi+p_K)^\mu}{p_\pi^2-m_K^2}.$$

On shell, when $p_K^2=m_K^2$ and $p_\pi^2=m_\pi^2$, the sum of the two terms indeed gives zero.

Rescattering effects in the computation of ΔM_K

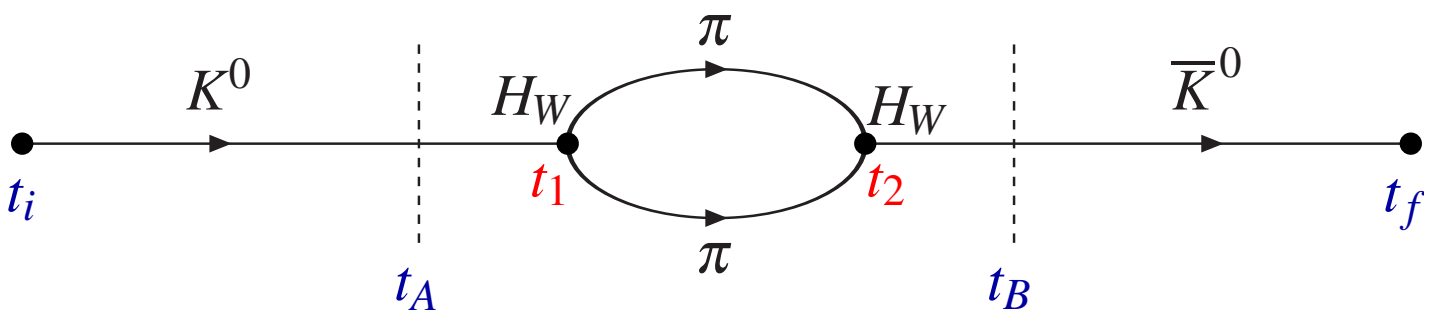

- In the ΔM_K computation, there is, of course, a two-pion intermediate state and we have had to control the corresponding finite-volume effects.
- This has been done on the assumption that the dominant intermediate states below m_K are the two-pion states.

Rescattering Effects in rare kaon decays

- We have seen that we can remove the single pion intermediate state.
- Which intermediate states contribute?
  - Are there any states below M_K?
  - We can control q^2 and stay below the two-pion threshold.

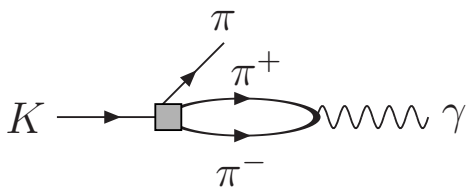

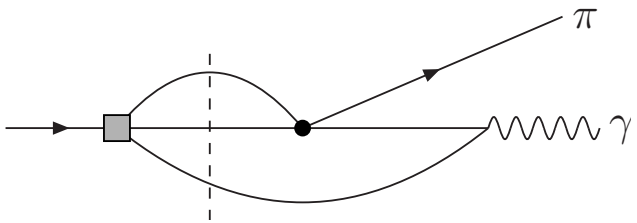

  - Are there two-pion intermediate states as a result of the Wess-Zumino term?
  - Do we need to consider three-pion intermediate states?
  - Answers to the above questions will affect what the finite-volume corrections are?
  - The ChPT-based phemomenology community neglect such possibilities.

All to be investigated further!

- It looks as though the FV corrections are much simpler than for ΔM_K and may be exponentially small?

UNIVERSITY OF Southampton
School of Physics and Astronomy

$$T_i^\mu = \int d^4x\, e^{-iq\cdot x} \langle \pi(p) | \mathrm{T}\{J^\mu(x)\, Q_i(0)\} | K(k) \rangle ,$$

- Each of the two local Q_i operators can be normalized in the standard way and J can be normalized.
- Calculation of long-distance effects $\Rightarrow$ must treat additional divergences as $x \to 0$.

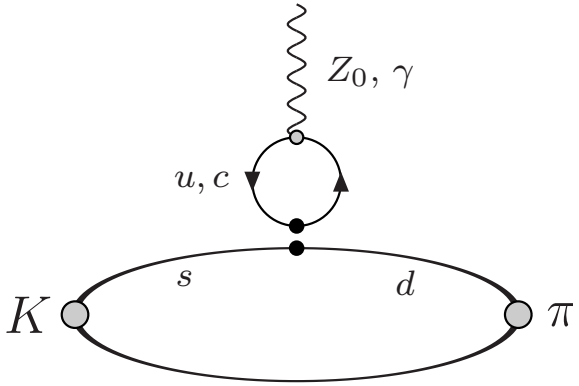

- Quadratic divergence is absent by gauge invariance $\Rightarrow$ Logarithmic divergence.
  - Checked explicitly for Wilson and Clover at one-loop order.

    G.Isidori, G.Martinelli and P.Turchetti, hep-lat/0506026
  - Absence of power divergences does not require GIM.
  - Logarithmic divergence cancelled by GIM.
  - For DWF the same applies for the axial current.
- Control of short-distance effects also appears to be much simpler than for ΔM_K.

To be investigated further!

Lots of diagrams to evaluate!

- Sample diagrams:

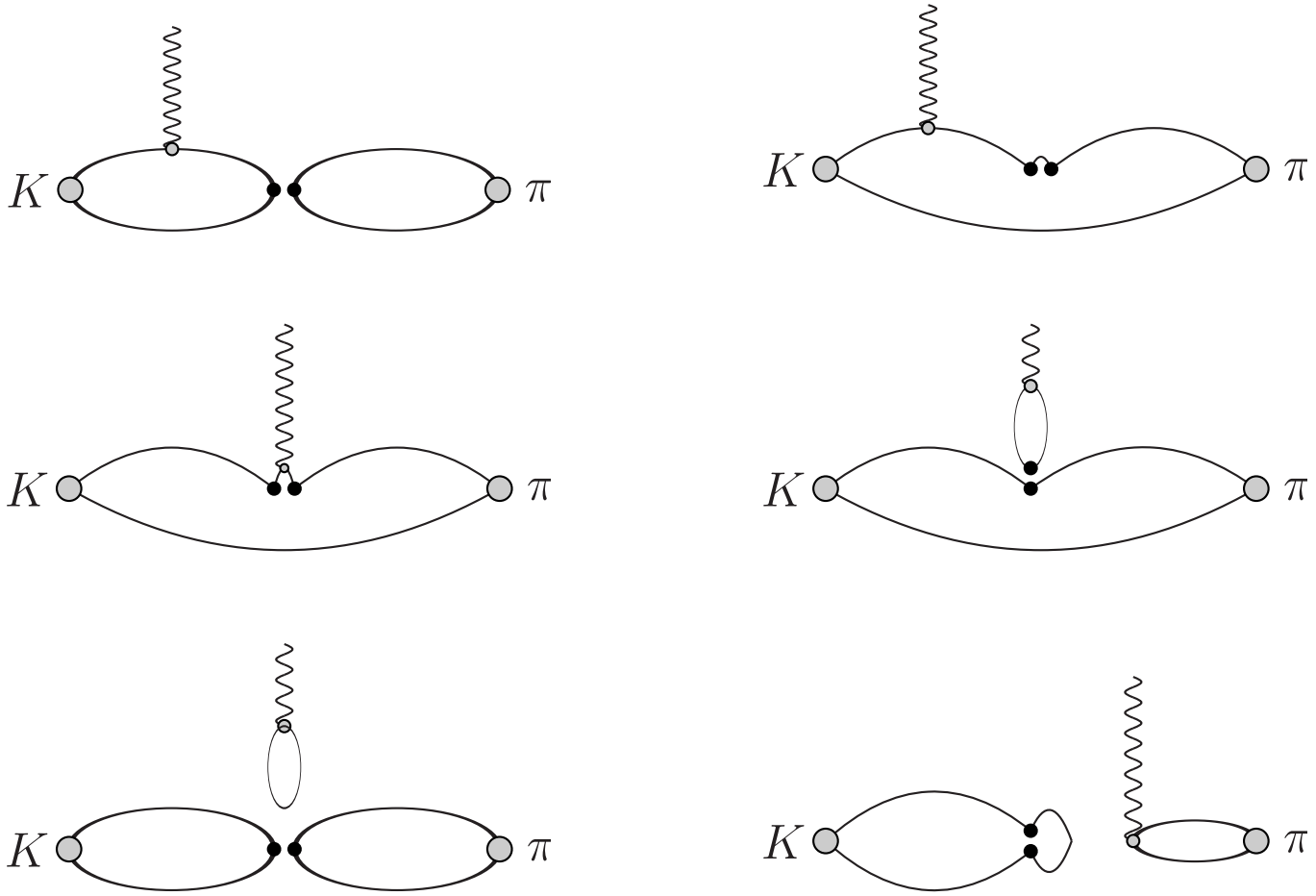

+ lots more

- The last two diagrams are examples of *disconnected* diagrams.

Summary and Conclusions

- Our community must continue to strive to
  1. improve the precision of computations of quantities we know well how to compute;
  2. extend the range of quantities which can be computed.

  This is necessary of precision flavour physics is to play a complementary rôle to large $p_\perp$ experiments in exploring the limits of the standard model and unravelling the basic framework of new physics.
- I have reviewed one such possible future extension, that of the calculation of long-distance physics in rare kaon decays.
  - There are many similarities to our calculation of the long-distance contributions to ΔM_K which is further advanced.
  - Although much still remains to be done, the theoretical background appears to be simpler than for ΔM_K (both finite-volume effects and short distance subtractions).
  - The calculations will rely on progress in the computation of disconnected diagrams.
- There are many important rare B-decays which should be studied but
- I still don't know how to tackle nonleptonic B decays, even in principle.

Physics Prospects and Status of SuperKEKB/Belle II

Outline

- **Introduction**
- **KEKB and Belle**
- **Physics Achievement and Prospects**
- **SuperKEKB and Belle II**

- Physics at Super B Factory [arXiv:1002.5012]
- SuperB Progress Report [arXiv:1008.1541]

KEK *Y.Sakai*
High Energy Accelerator Reseach Organization

SuperKEKB project

Upgrade of KEKB/Belle

	KEKB		SuperKEKB
Luminosity :	2.1×10^{34}	$\rightarrow$	8×10^{35} (x 40)
Total Data:	1 ab^{-1}	$\rightarrow$	>50 ab^{-1} (x50)
Detector :	Belle	$\rightarrow$	Belle II

KEK
High Energy Accelerator Reseach Organization

High Energy Physics

PARTICLE PHYSICS

Mainly using particle Accelerators

Goal :

Ultimate nature of Matter

Fundamental law
Elementary particle
Interactions, Symmetries

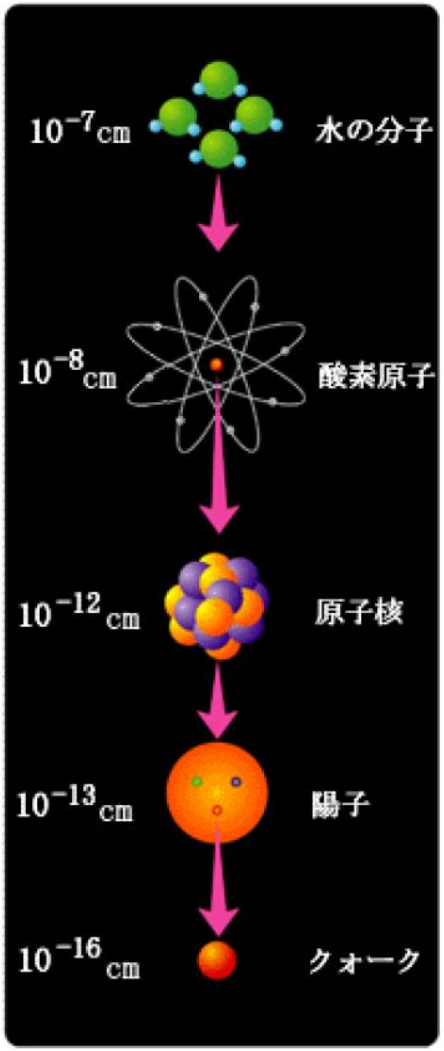

Particle Physics & Universe

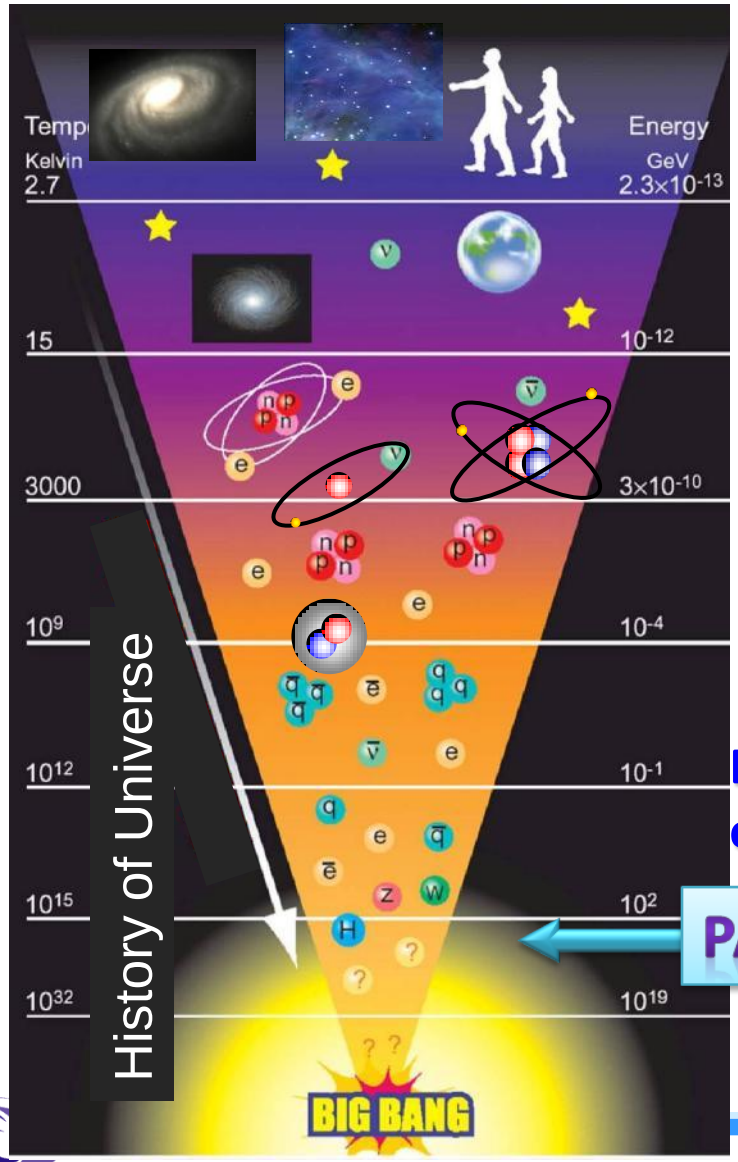

Key to
understand both

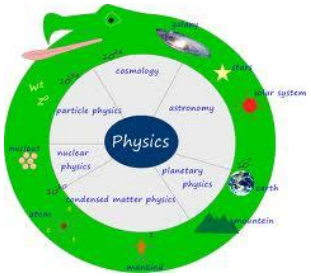

Early history of the Universe

PARTICLE PHYSICS

Ultimate nature of matter

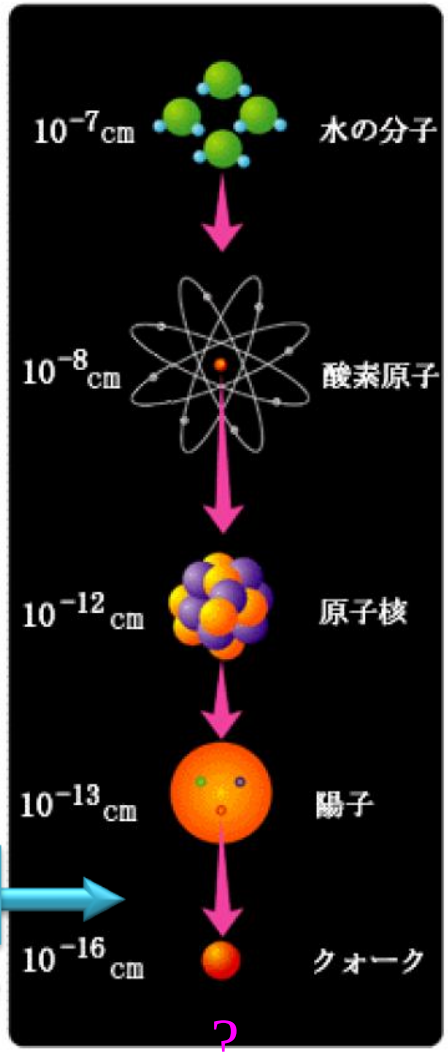

"Standard Model"

Elementary Particles in SM

Quark

Lepton

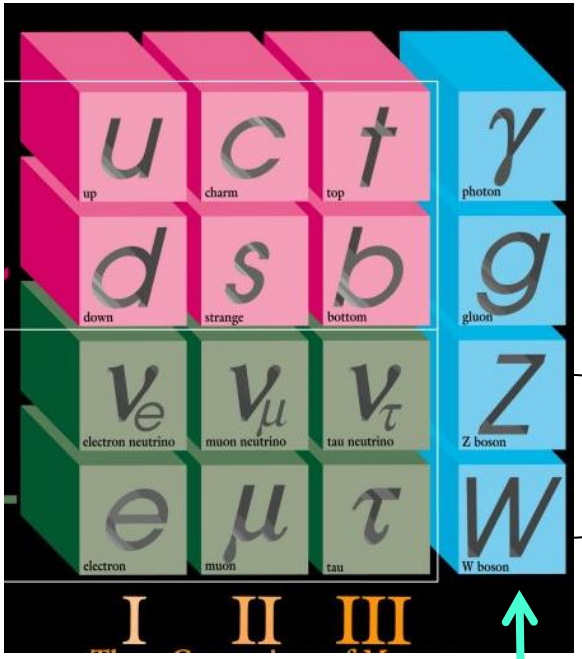

EM

Strong

Weak

3 Generations

Matter
(Fermions)

Force
(Bosons)

+ Anti-particles

1897 Discovery of
electron ~

Latest
"missing piece"

❖ CP Violation
Kobayashi-Maskawa
(→ B-Factory)

❖ Higgs (→ LHC)

⇩

Search for New Physics

Goal/Milestones of B-factory

Step1

Discovery of CPV in B decays

2001 summer !

Step2

Precise test of KM and SM

Step3

Search for NP

(SUSY, Extra-dim…)

Hints of NP

Establish procedures

SuperB-factory

~50 times more data
(higher luminosity)

CP Violation

Difference between particle & anti-particle
(matter & anti-matter)

Universe: almost "matter" only (no anti-matter)

Big-Bang → N(particles) = N(anti-particles)

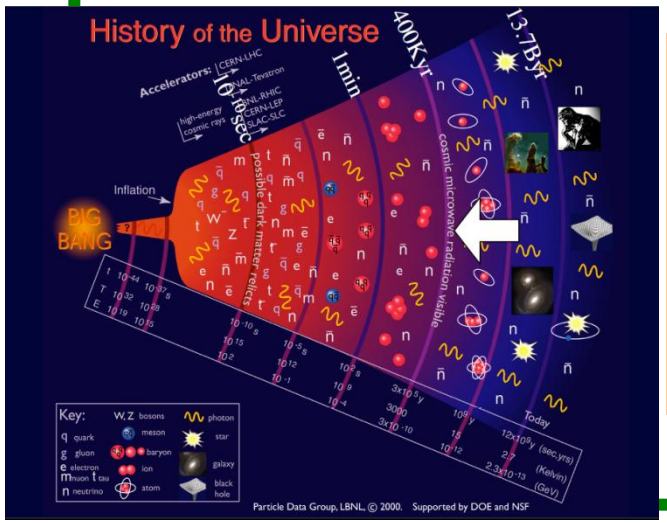

Sakhalov's 3 conditions (1967):

1. baryon number violation
2. **CP violation**
3. existence of non-equiblium

CPV is a key for Existence of Universe & us !

Andrei Sakharov (1921-1989)

Kobayashi-Maskawa (1 9 7 3

Mechanism of CPV

Weak interaction

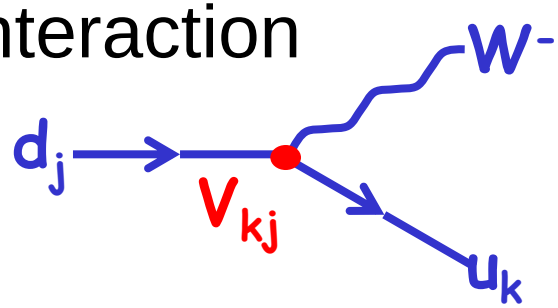

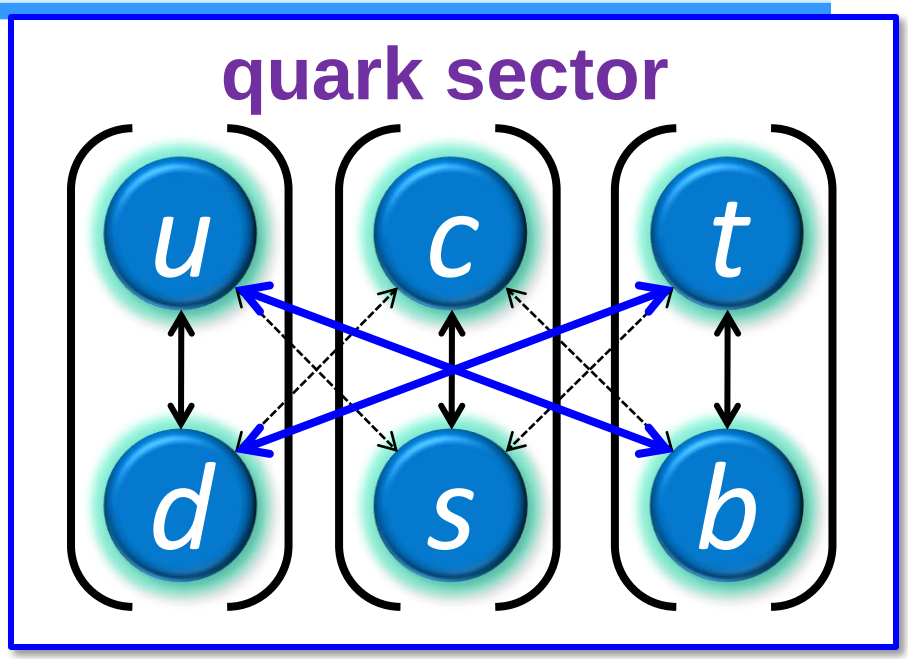

CKM Matrix

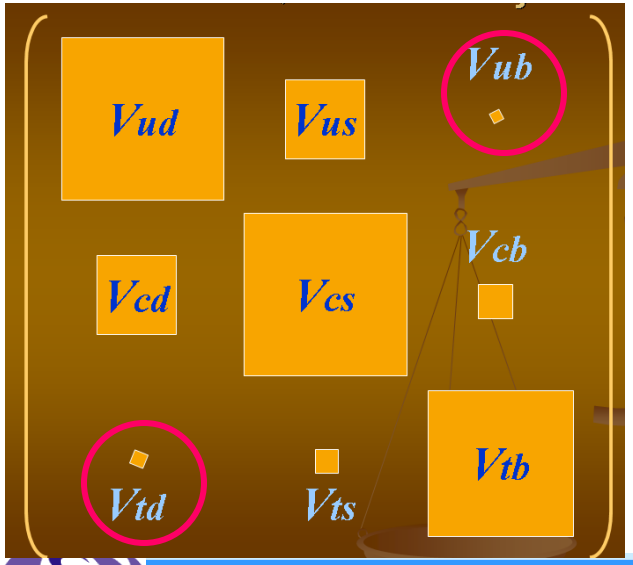

Irreducible
Complex Phase

(3 Generation)

C P V

(Unitarity Triangle)

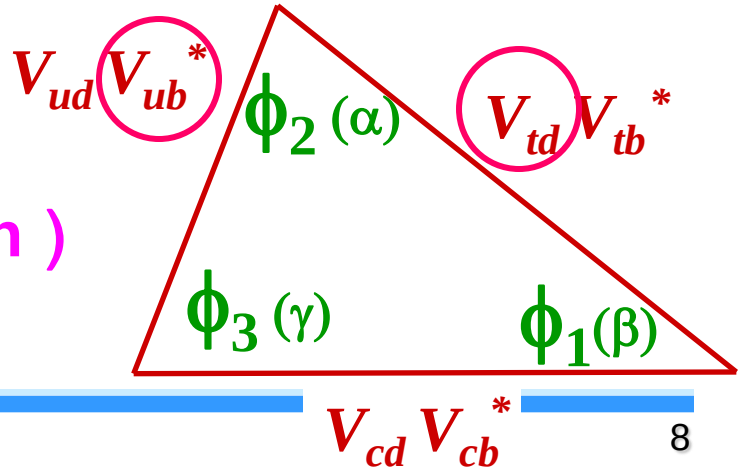

KEKB accelerator

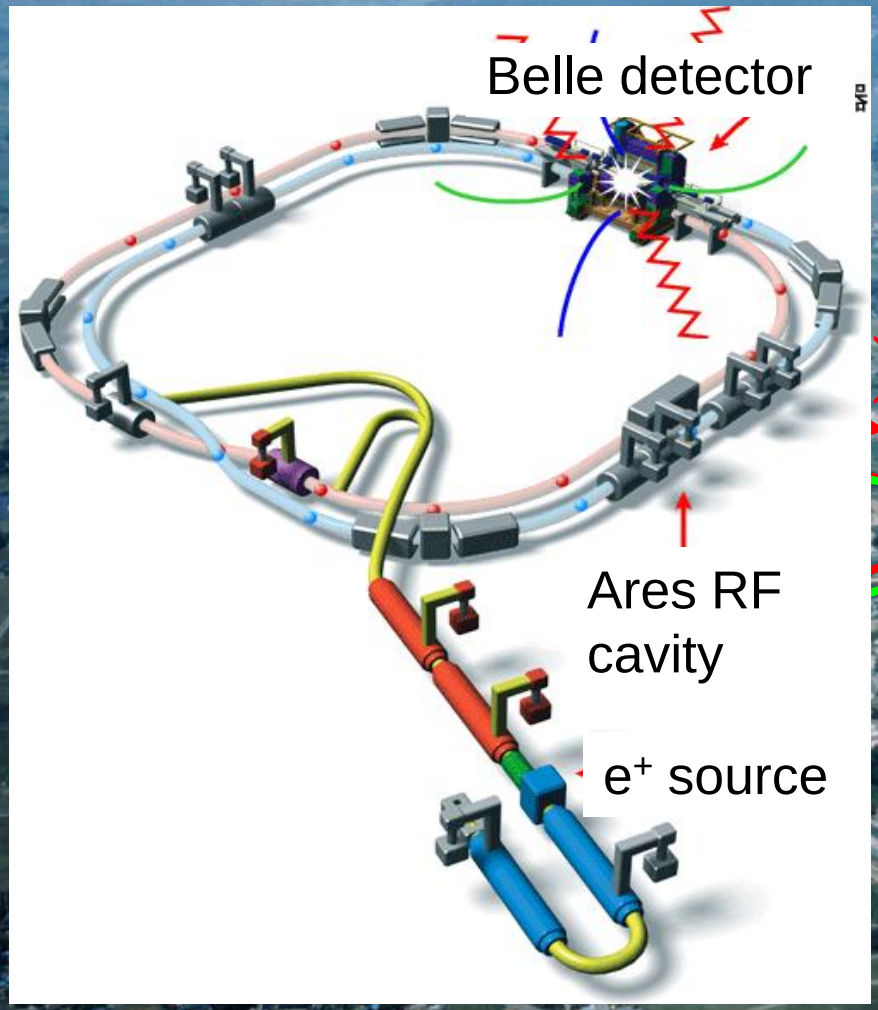

- Asymmetric energy collider (8 GeV e- x 3.5 GeV e+)
- Finite angle beam crossing (22mrad)

Luminosity

2.11×10^{34} cm^{-2}s^{-1} !

Produces 2M $B\bar{B}$/year

World Highest Lum. !

2009 June17

KEKB Peak Luminosity

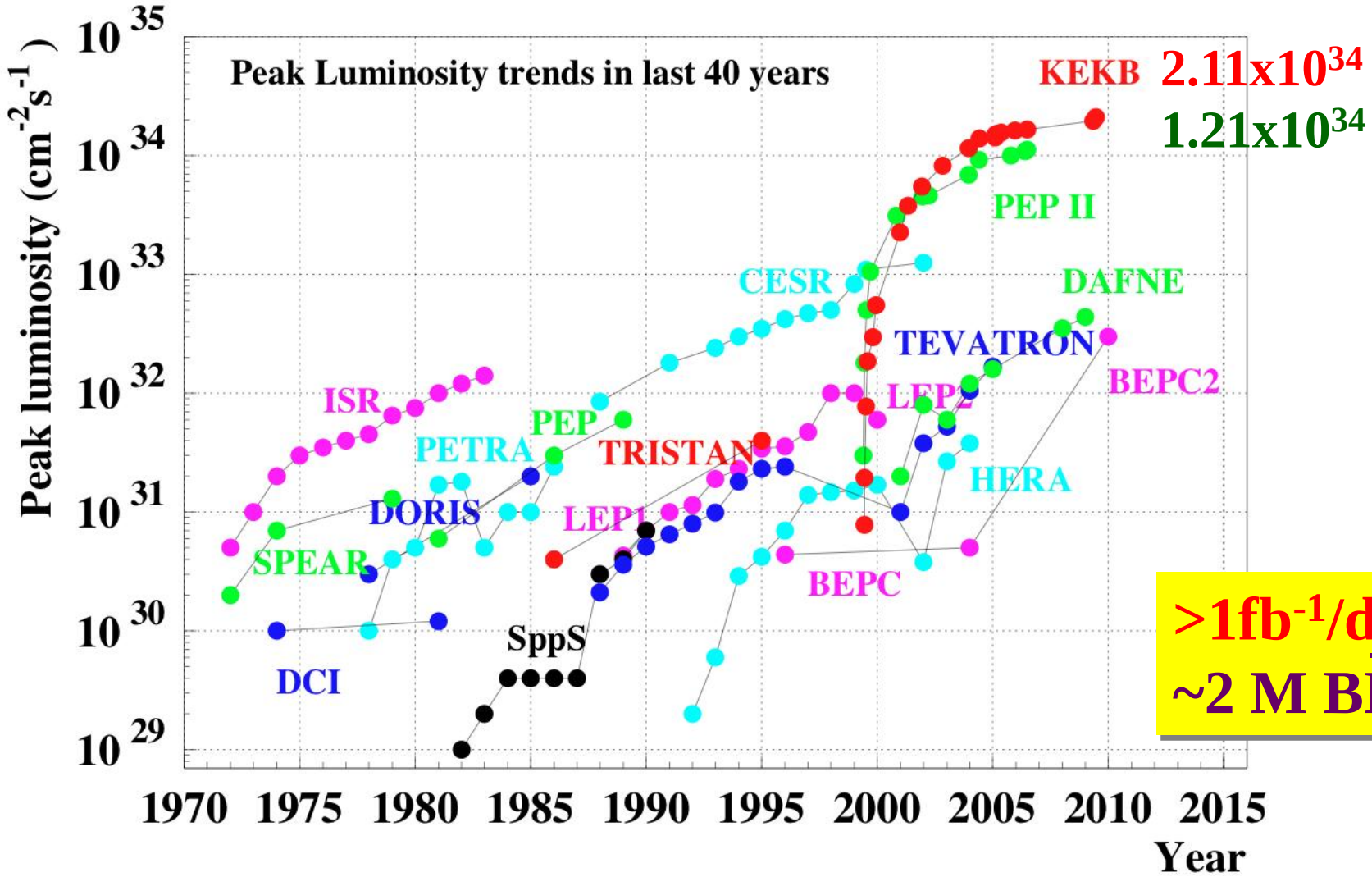

>1fb^{-1}/day
~2 M $B\bar{B}$

Data at KEKB/Belle

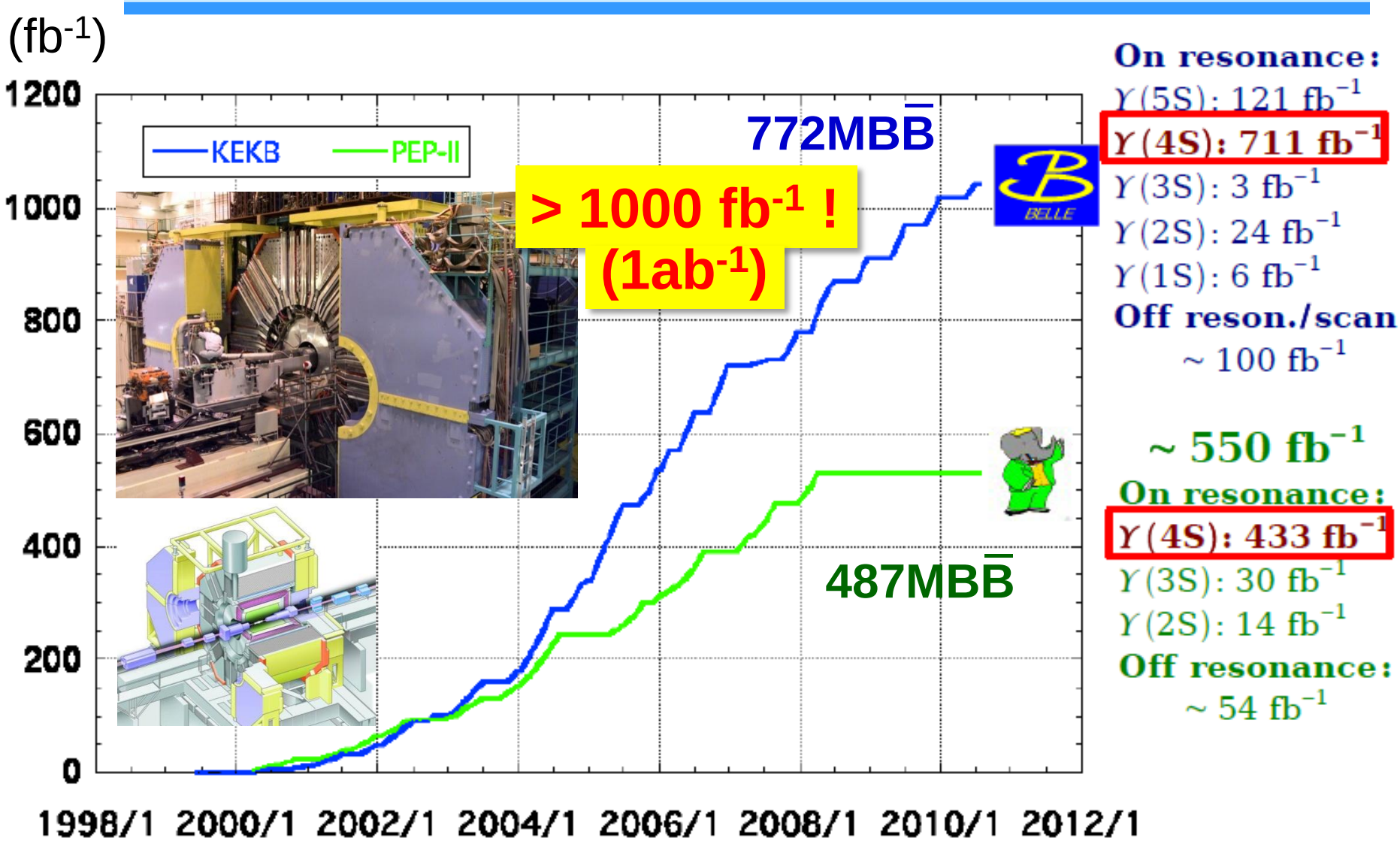

CPV in B^0 decays

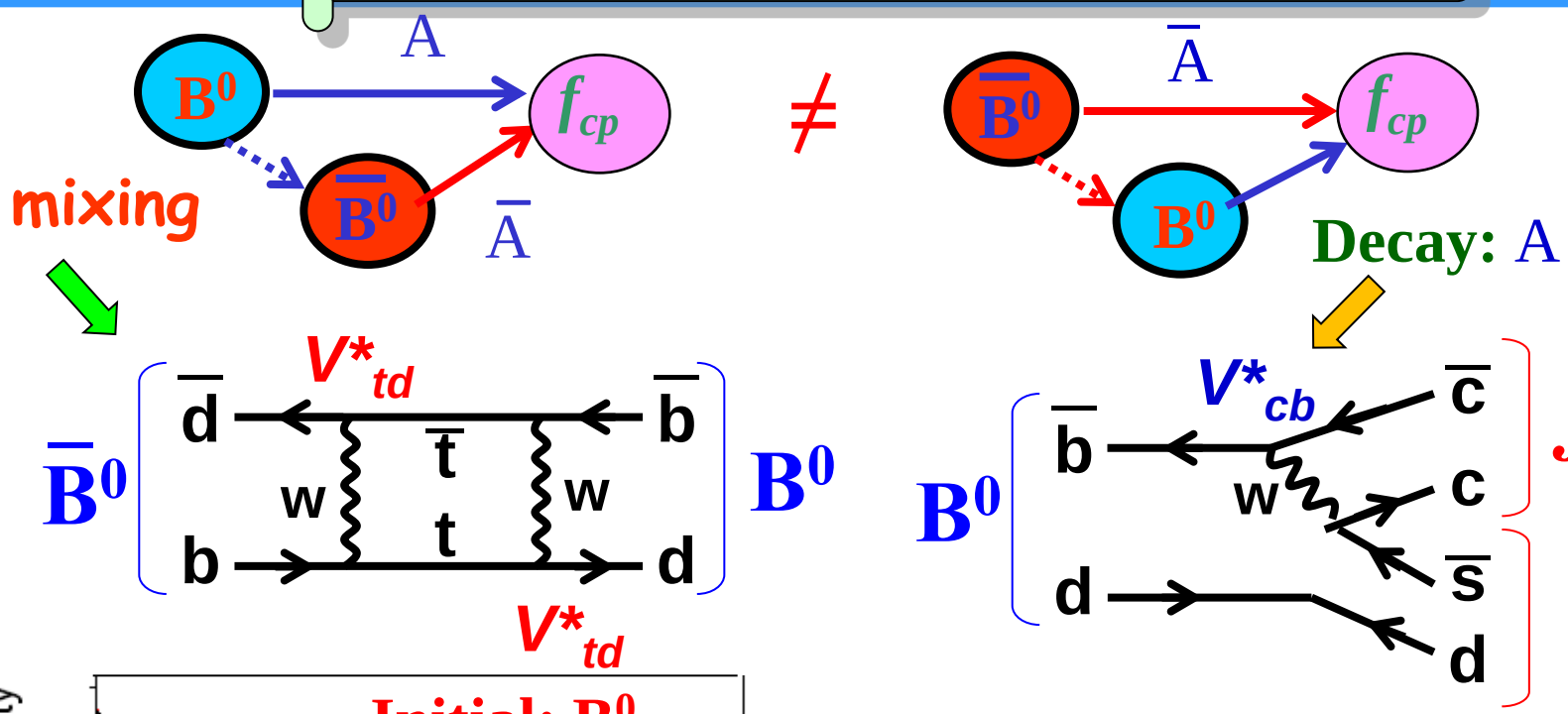

Sanda
Bigi
Carter

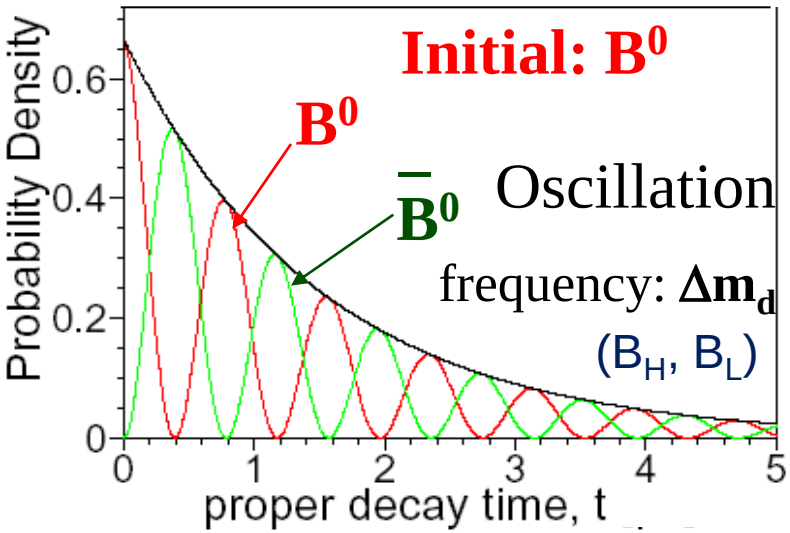

Interference

Direct decay
Mixing + Decay

} **Weak Phase difference**

Decay-time dependent CPV

CPV in B^0 decays

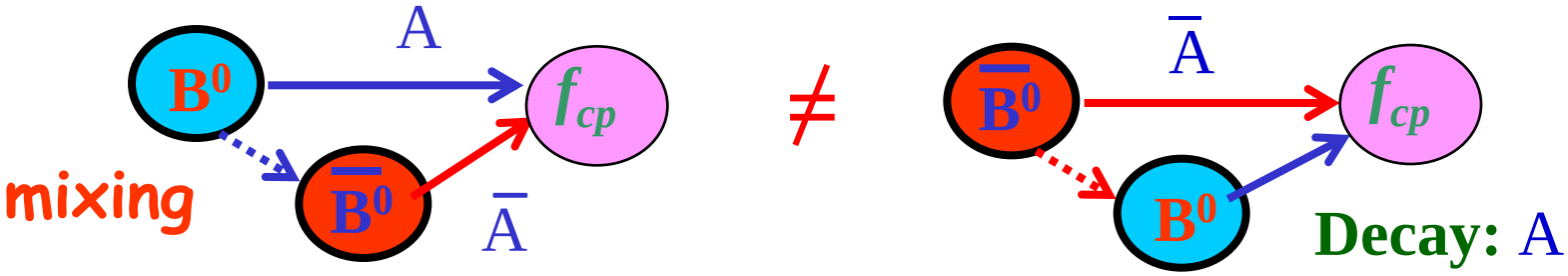

Sanda
Bigi
Carter

$$A_{CP} \equiv \frac{\Gamma(\overline{B}^0 \to f_{CP}\,;\,\Delta t\,) - \Gamma(B^0 \to f_{CP}\,;\,\Delta t\,)}{\Gamma(\overline{B}^0 \to f_{CP}\,;\,\Delta t\,) + \Gamma(B^0 \to f_{CP}\,;\,\Delta t\,)}$$

$$= -\eta_f \sin 2\phi_1 \sin(\Delta m_d \Delta t)$$

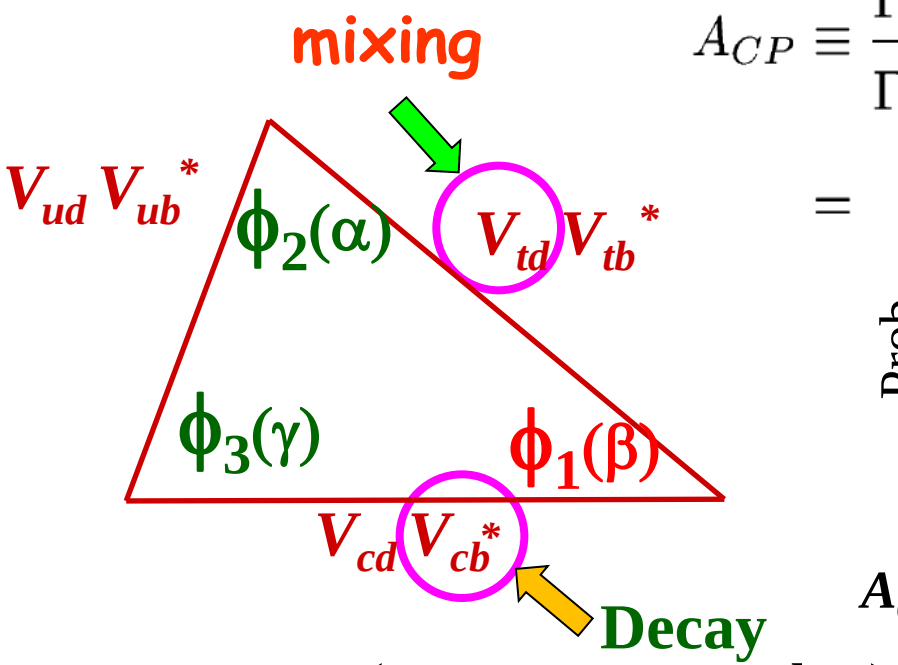

(η_f : CP eigenvalue)

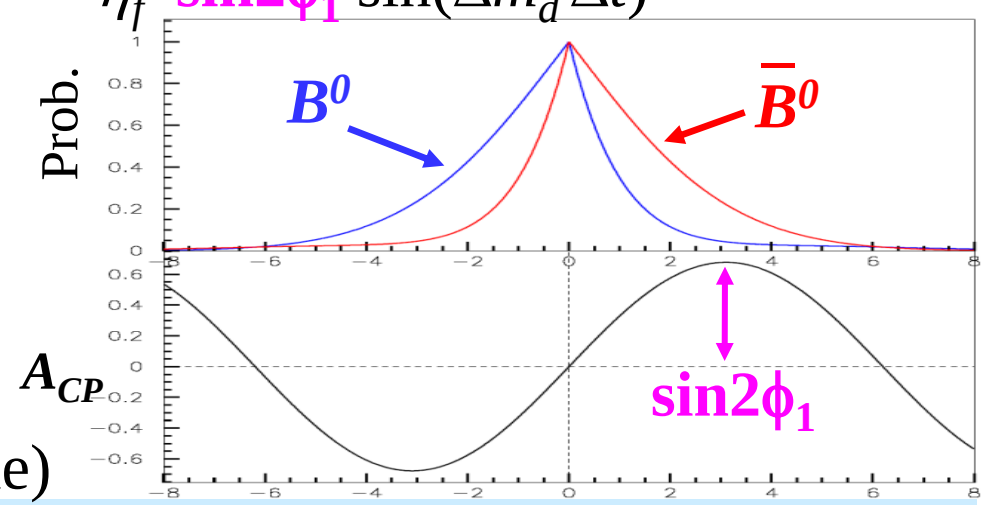

Δt (decay time)[ps]

Time-dep CPV Measurement

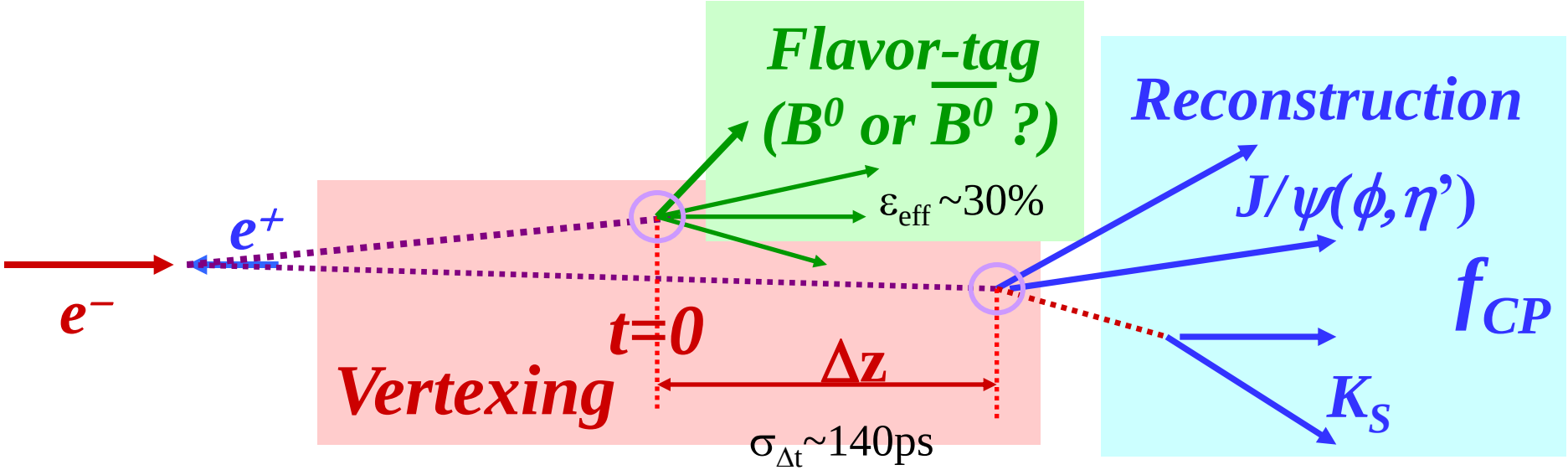

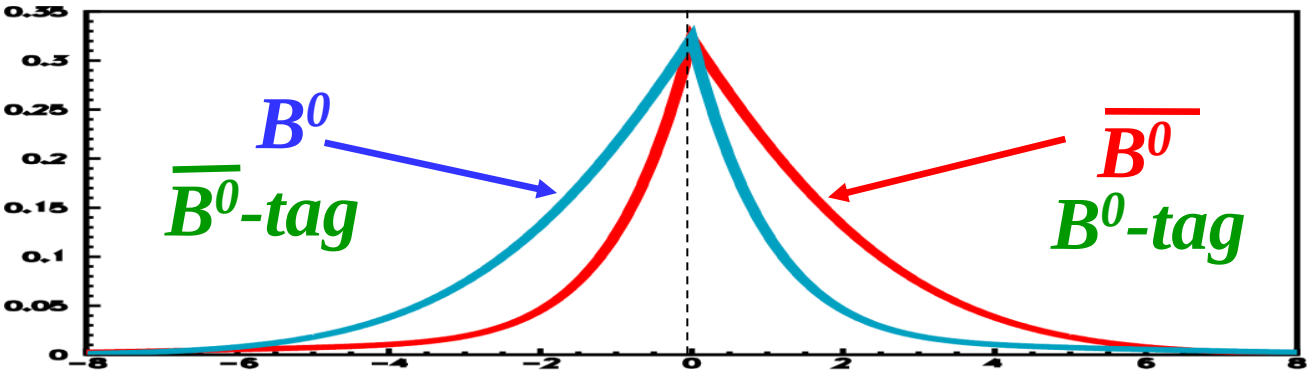

fit → **Extract CPV**

$$\Delta t \approx \Delta z / c\beta\gamma$$

$\beta\gamma$=0.425 (KEKB)
0.56 (PEP-II)

same analysis method applied for all modes

Discovery of CPV in B decays

$$B^0 \to J/\psi K^0$$

2001(31M $\bar{B}B$) **Discovery!**

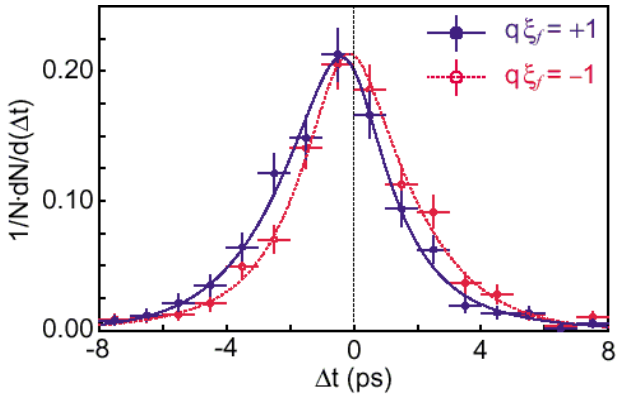

$$A_{CP}(\Delta t) = \frac{\Gamma(\bar{B}^0 \to f_{CP}) - \Gamma(B^0 \to f_{CP})}{\Gamma(\bar{B}^0 \to f_{CP}) + \Gamma(B^0 \to f_{CP})}$$
$$= -\xi_f \sin 2\phi_1 \sin \Delta m \Delta t$$

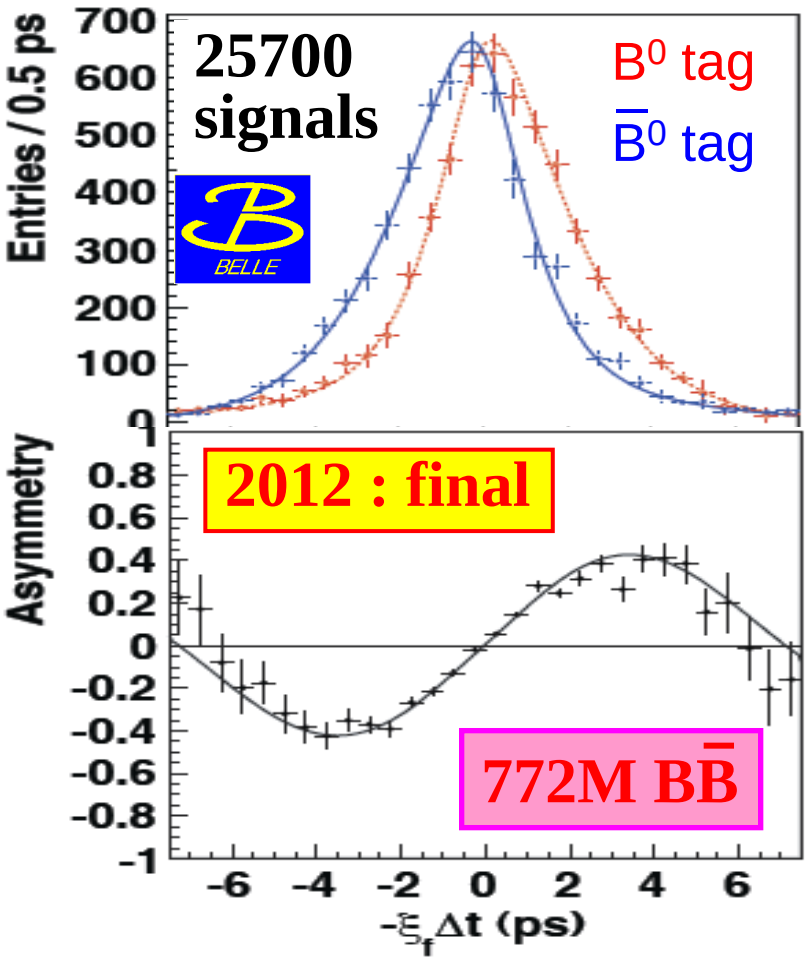

Precise Measurement [PRL 108, 171802]

$\sin 2\phi_1$= 0.667 ±0.023 (stat) ±0.012 (syst)

Complete Test of KM & SM

Measurements of CKM

Determination of UT

LQCD: important roles

$B \to \pi\pi$, $\rho\pi$, $\rho\rho$

$b \to u\, l^- \nu$

$B \to \pi/\rho\, l\, \nu$

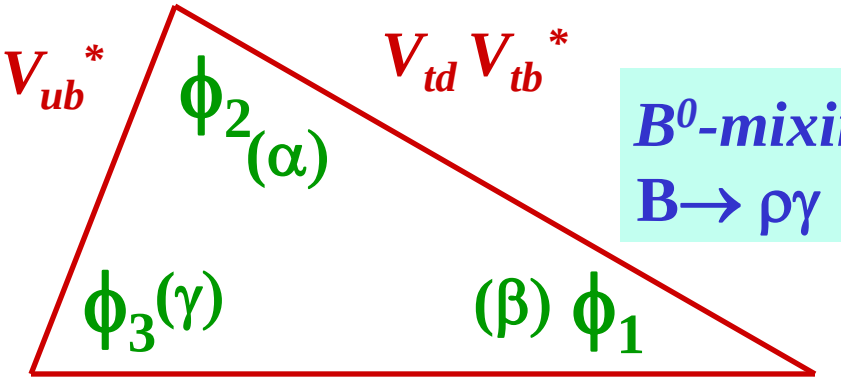

B^0-mixing (Δm_d)

$B \to \rho\gamma$

$B^- \to D_{com} K^-$

$B^0 \to D^{(*)+} \pi^-$

$b \to c\, l^- \nu$

$B \to D^{(*)} l\, \nu$

$B^0 \to (cc) K^{(*)0}$

$B^0 \to D^{*+} D^{(*)-} (K)$

Over constraint !

B experiments can provide all measurements !

Verification of KM for CPV

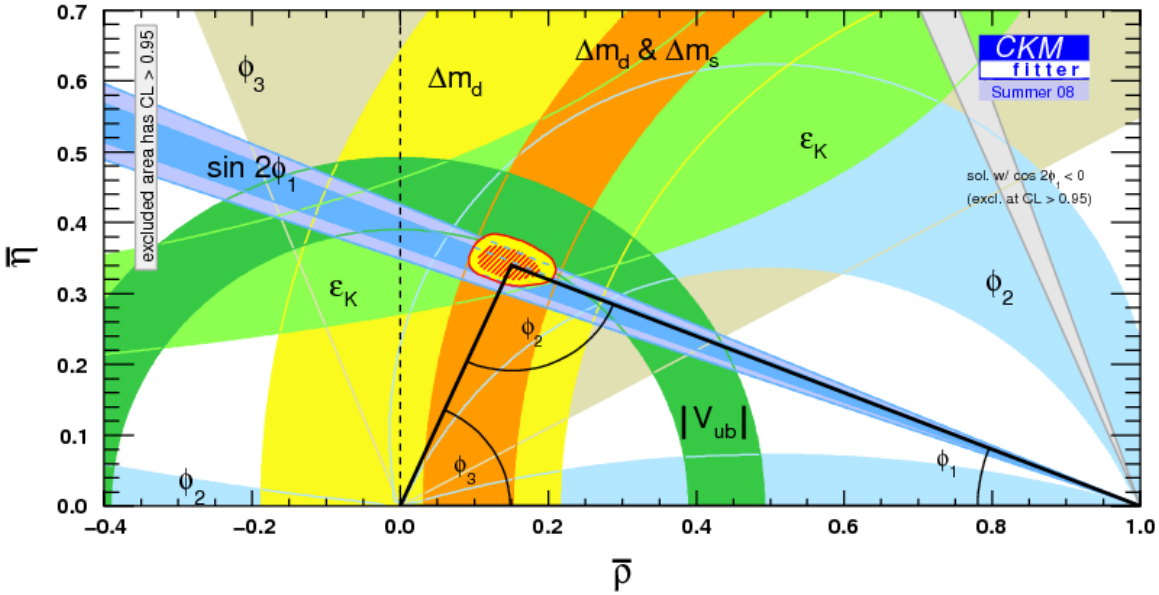

All consistent

CPV:
caused by a single phase of CKM matrix

Verified by B-factory experiments

2008 Physics Nobel Prize

Next Challenge

In spite of Great Success of SM, there must be
New Physics beyond SM at High Energy scale
(SM is valid effective theory at current E-scale)

Observed CPV in SM is not enough to explain matter dominance of Universe [>O(10^{10})] !

New Source of CPV should exists (beyond SM)

One of Next important goals of Flavor Physics

⇔ **Energy Frontier**

Note) NP effects appear in Flavor Physics in various way !

Search for New Physics

CPV in B provide Powerful tool for Search NP (**New Phase**)
[$b \to sqq$ tCPV]

Rare B decays excellent opportunities for NP search

Loop diagram Penguins [$b \to s(d)\,\gamma$, $b \to s(d)\,l^+l^-$]

Key

Decays involving τ (↔ $H^\pm$)

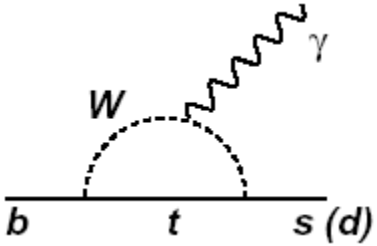

$A_{NP} \sim A_{SM}$ (small/forbidden)

τ Decays (Lepton Flavor Violation = NP) : B-factory = τ-factory

KEKB

Establish analyses
Hint of NP

SuperKEKB

Energy Frontier vs Flavor Physics

Direct Production by High Energy Coll.

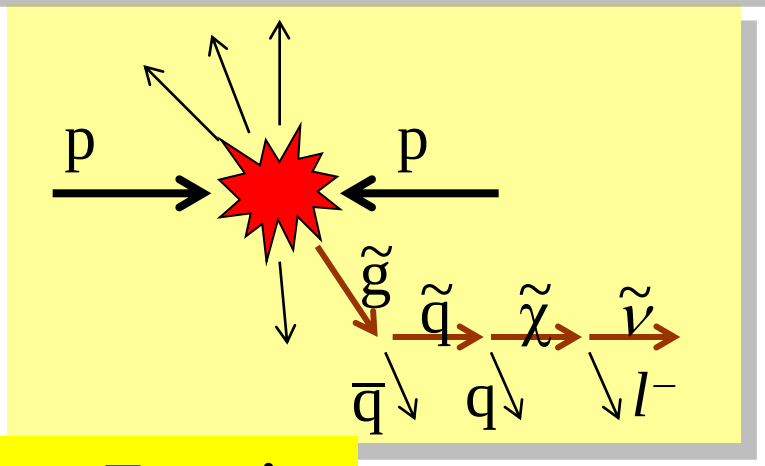

Energy Frontier

Virtual Production via Quantum Eff.

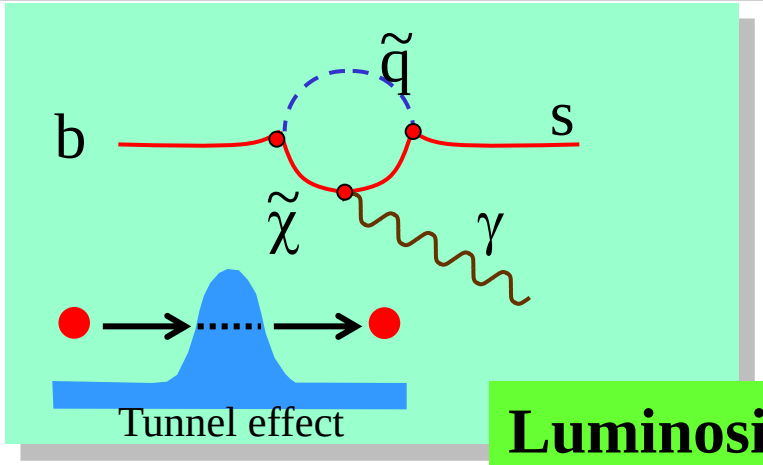

Luminosity Frontier

Diagonal terms

Off-diagonal terms

$$\left(m^2_{\tilde{q}}\right)_{ij} = \begin{pmatrix} m^2_{11} & m^2_{12} & m^2_{13} \\ m^2_{21} & m^2_{22} & m^2_{23} \\ m^2_{31} & m^2_{32} & m^2_{33} \end{pmatrix}$$

Higher Energy Scale
Can be searched
(even if LHC finds
no New Physics)

LHC vs SuperKEKB

Illustrative reach of NP searches

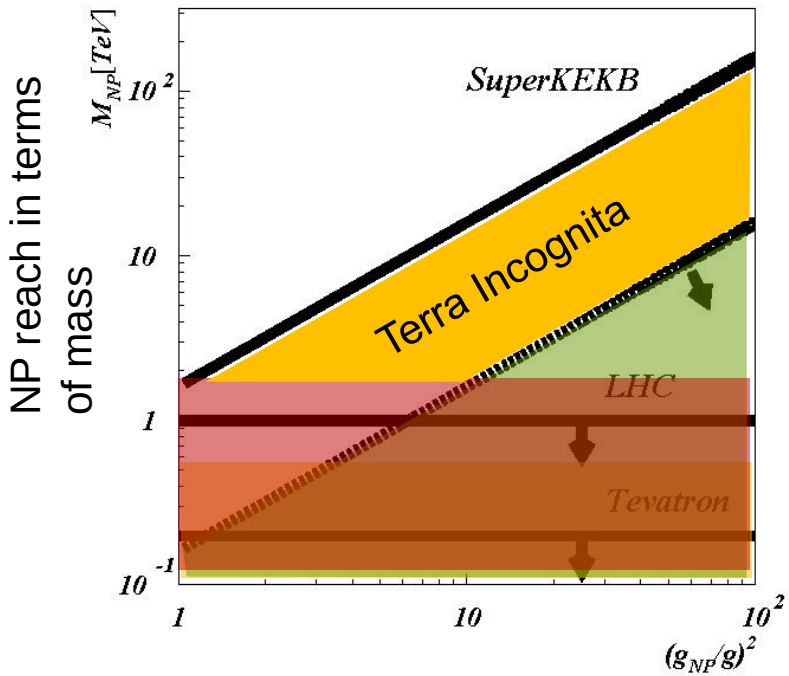

LHCb vs SuperKEKB

LHCb is producing nice Flavor Physics results

- SuperKEKB: can do Missing-E, Inclusive Neutrals
- Single measurement only Confirmation is important

[similar in LQCD]

Hints/Sensitive to NP

CPV in b → s Penguin ?

A(B → Kπ) Puzzle

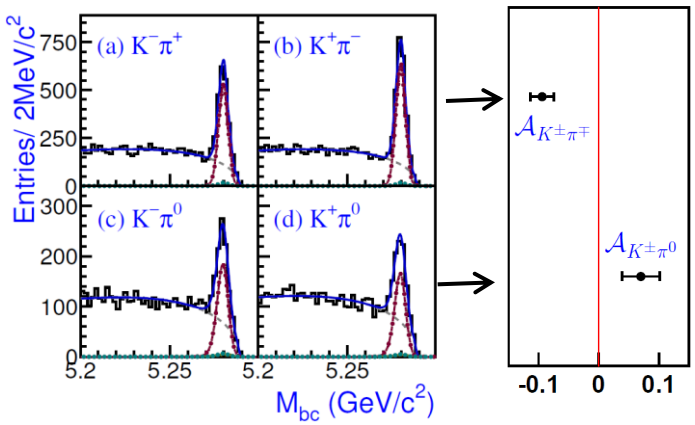

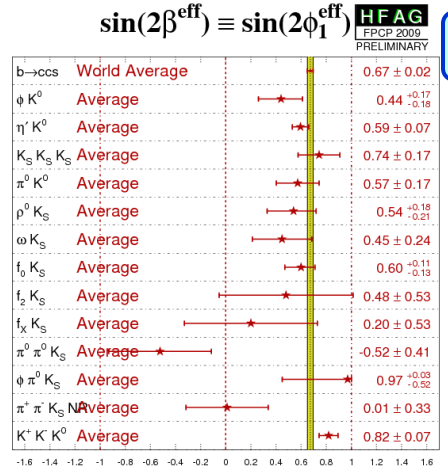

Forwad-Backword Asy,.B → K*ℓ⁺ℓ⁻

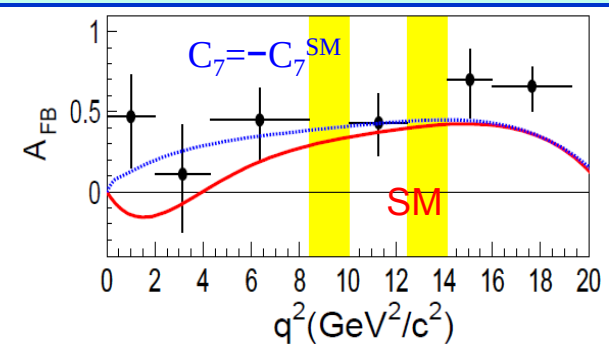

Large D⁰-mixing

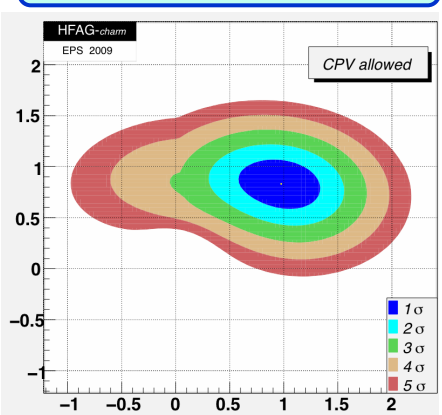

CKM Unitarity Triangle

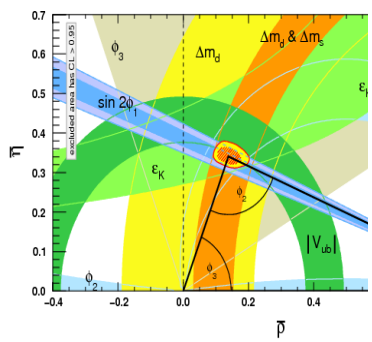

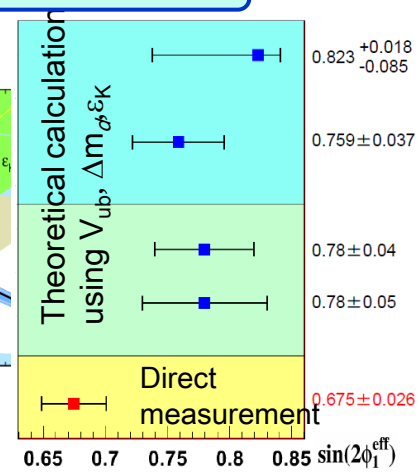

$f_L(B \to VV) \neq 1$

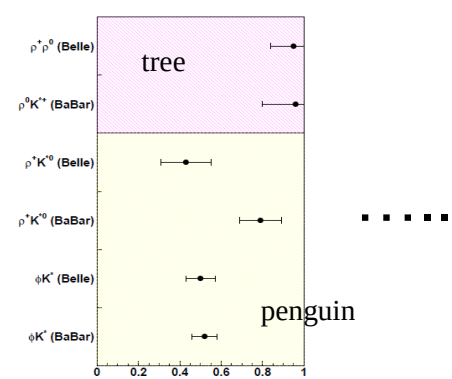

NP search : Precise CKM

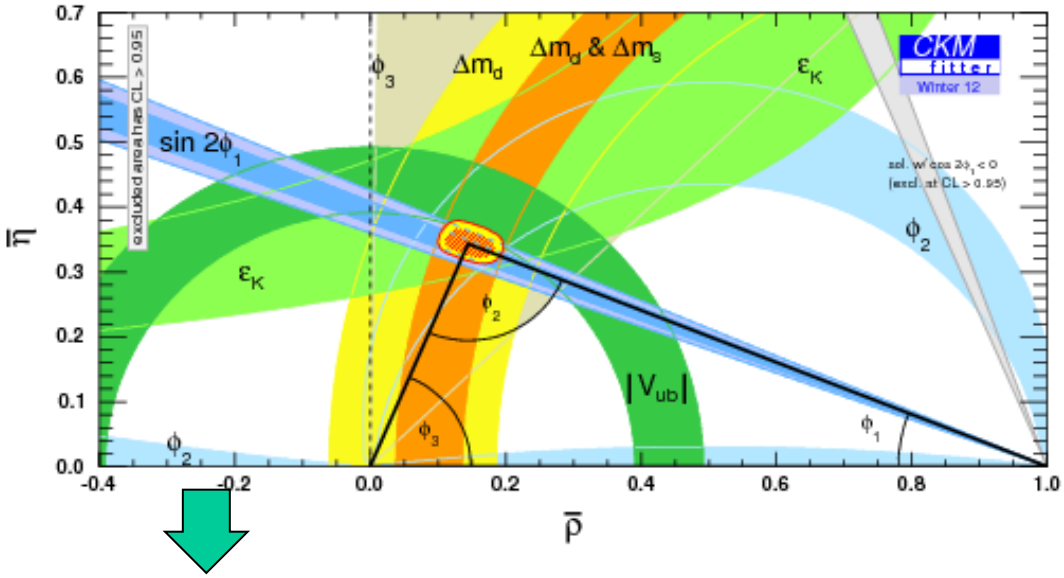

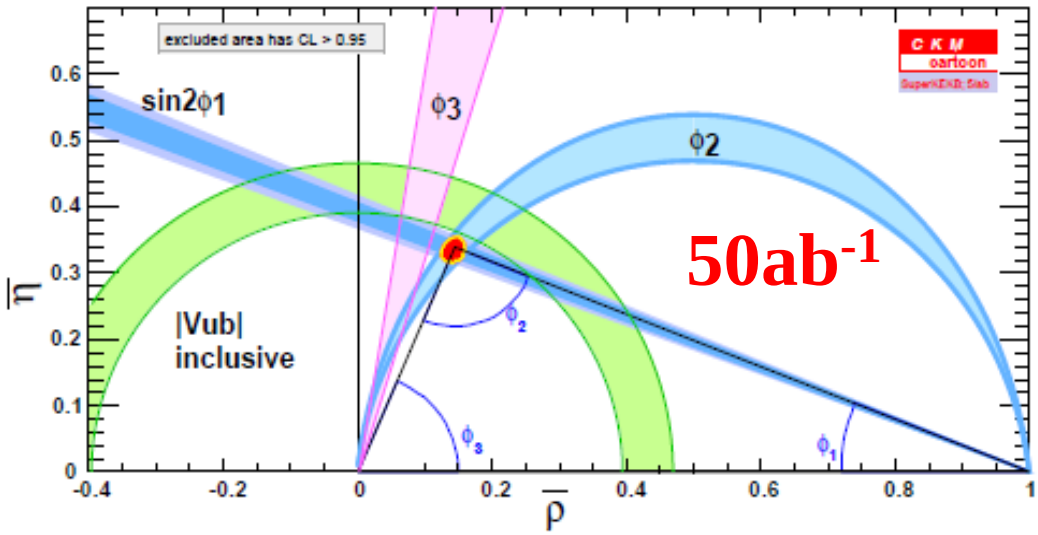

Still ~10% room for NP

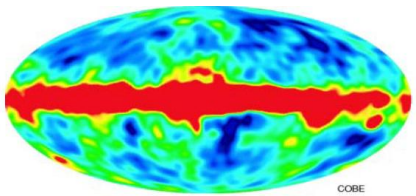

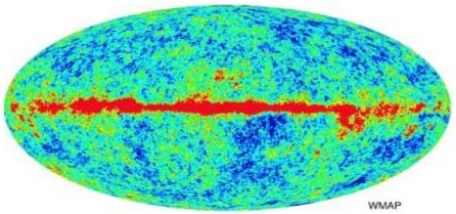

New Source of CPV: $b \to s q\bar{q}$

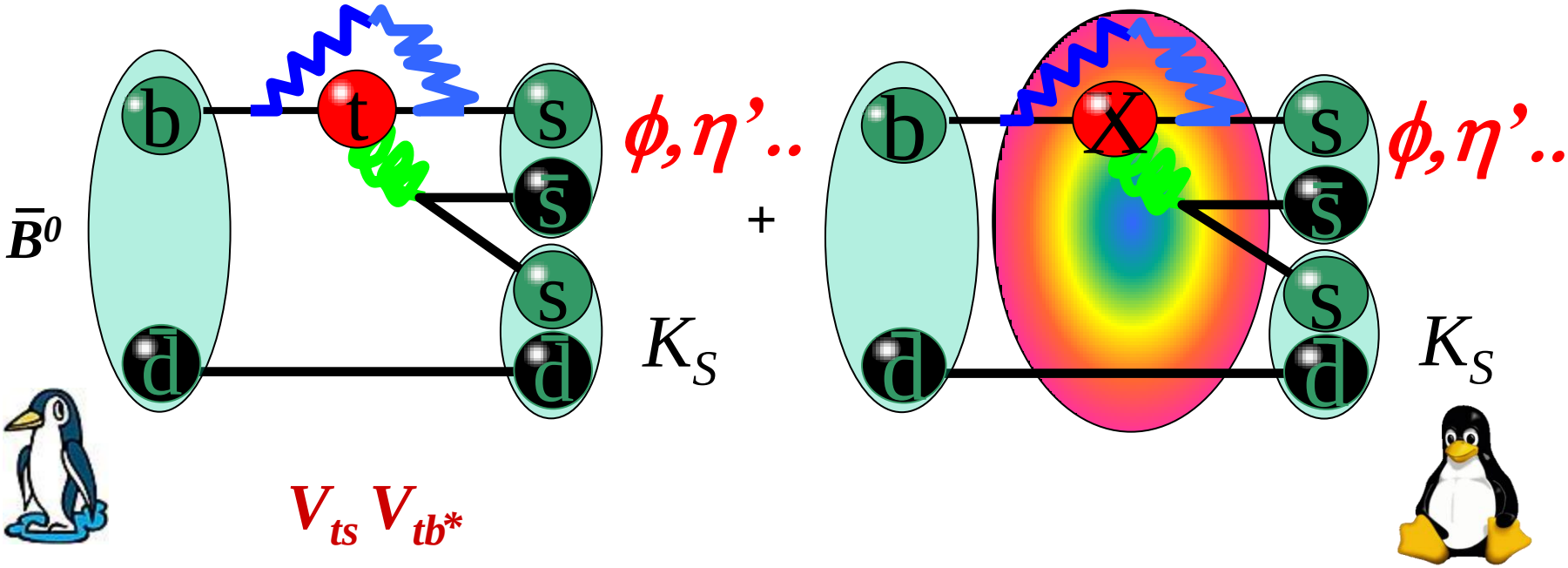

SM: b→s Penguin phase = ($c\bar{c}$) K^0	**+ New Physics with New Phase**
	$S_{bs} \neq S_{bc}$, A_{DCP} can $\neq 0$

"b → $c\bar{c}$s: sin2ϕ_1" (SM reference) ➡ deviation

Summary of New CPV search

$B^0 \rightarrow J/\psi K^0$

Reference point of SM

No clear deviation seen in all modes (1~2σ)

New CPV effect can be seen with much larger data

Super B-factory

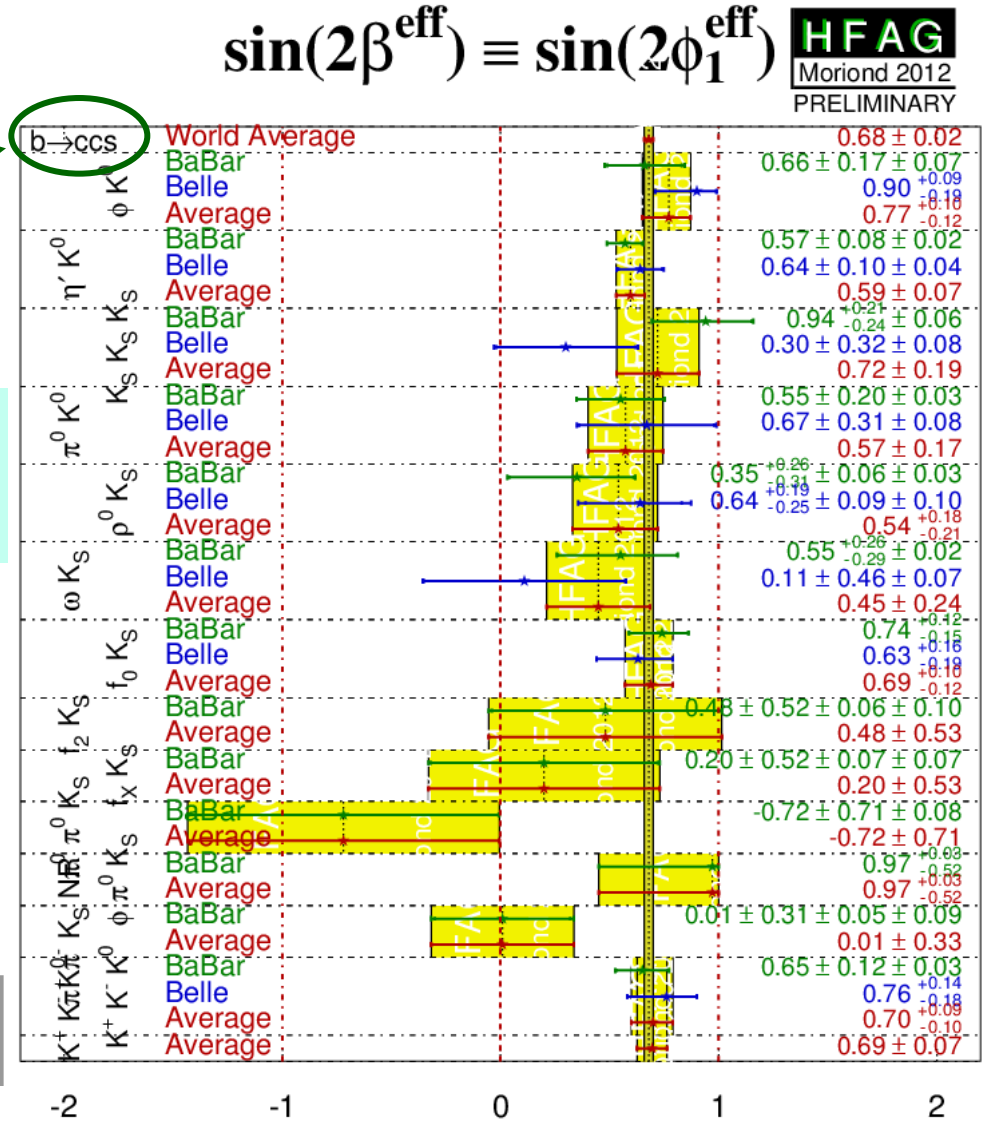

SuperKEKB prospect

$B \to \phi K^0$ at 50/ab with ~2010 WA values

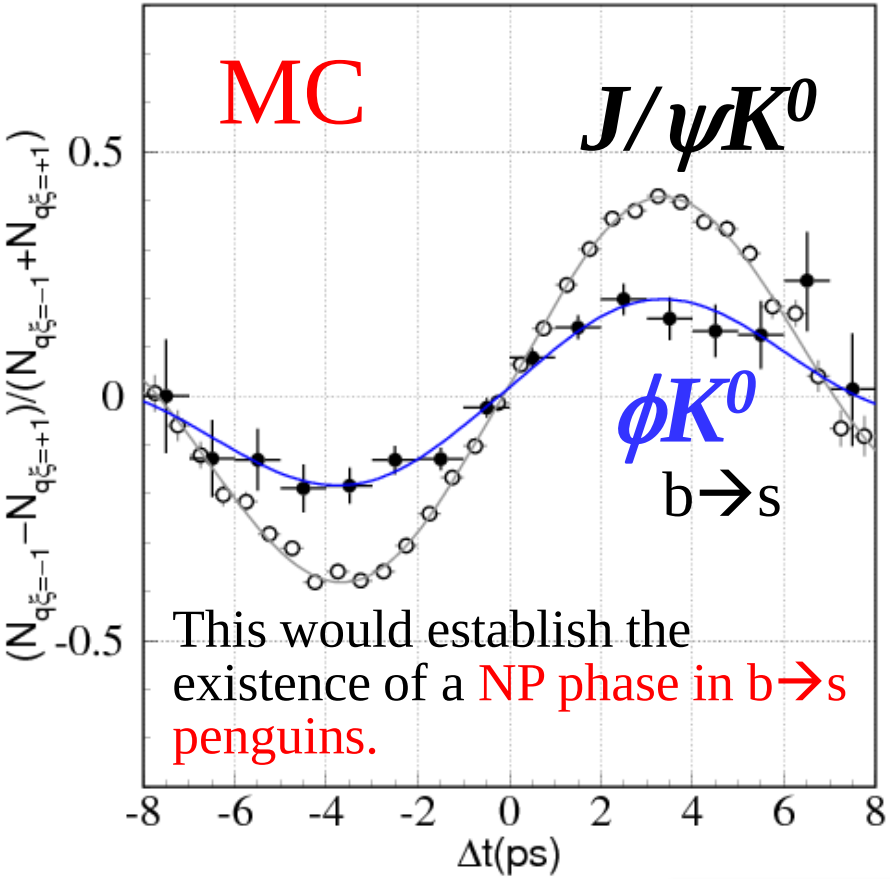

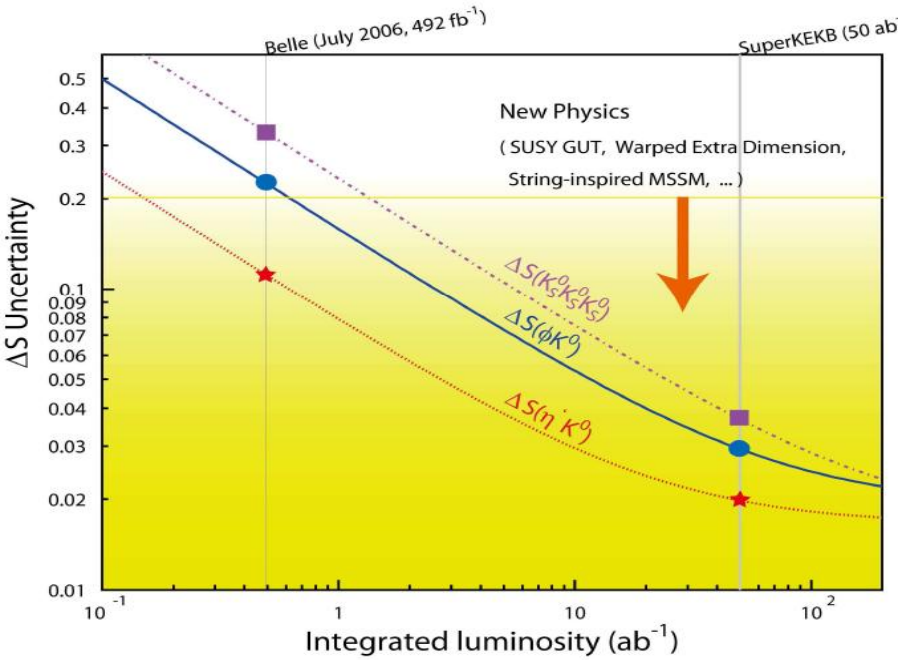

Prospect $\delta(S_{b\to s}) \sim 0.012$ @ 50ab^{-1}

Charged Higgs Hunting

B-Factory:

Variety of Modes sensitive to Charged Higgs

Some are only possible at B-Factory

Inclusive b → s γ

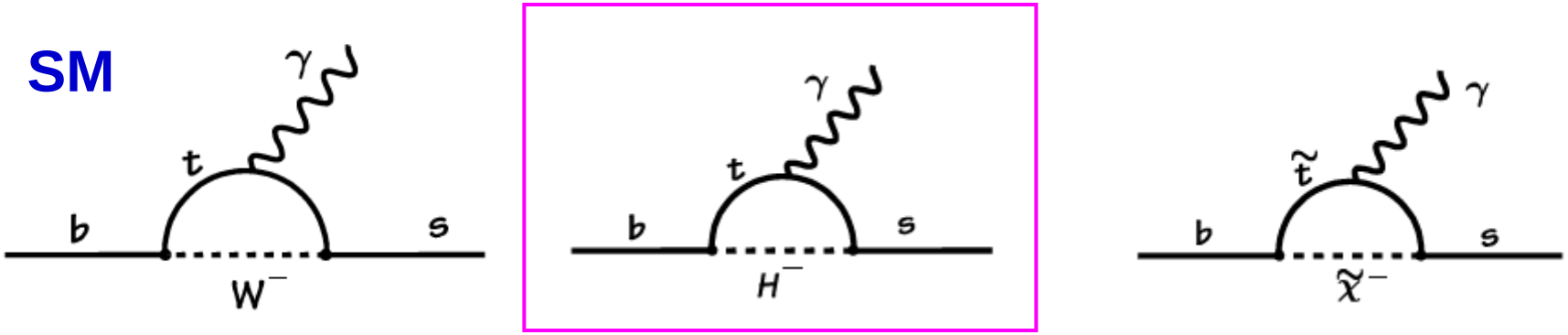

Fully Inclusive measurement

657M $B\bar{B}$

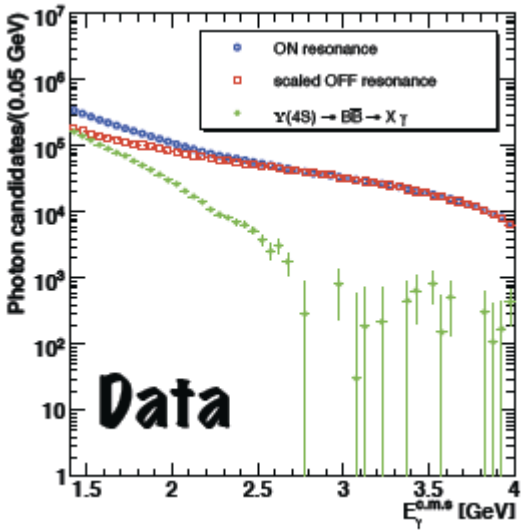

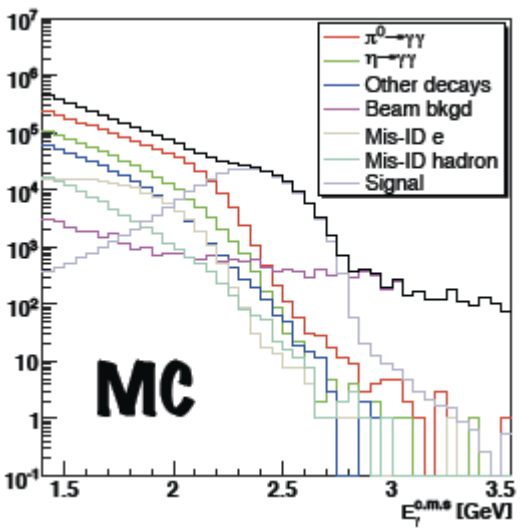

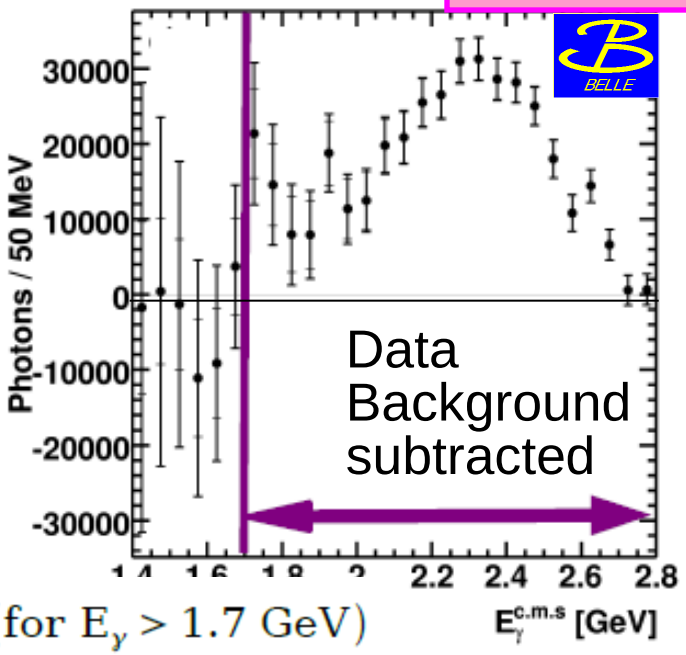

$B(B \to X_s \gamma) = (3.45 \pm 0.15 \pm 0.40) \times 10^{-4}$ (for $E_\gamma > 1.7$ GeV)

Most precise measurement of $B(B \to X_s \gamma)$ (lowest E_γ threshold)

$b \to s\gamma$ Summary

HFAG 2010: $B(B \to X_s \gamma) = (3.55 \pm 0.26) \times 10^{-4}$ (for $E_\gamma > 1.6$ GeV)

vs

SM: $B(B \to X_s \gamma) = (3.15 \pm 0.23) \times 10^{-4}$ (for $E_\gamma > 1.6$ GeV)

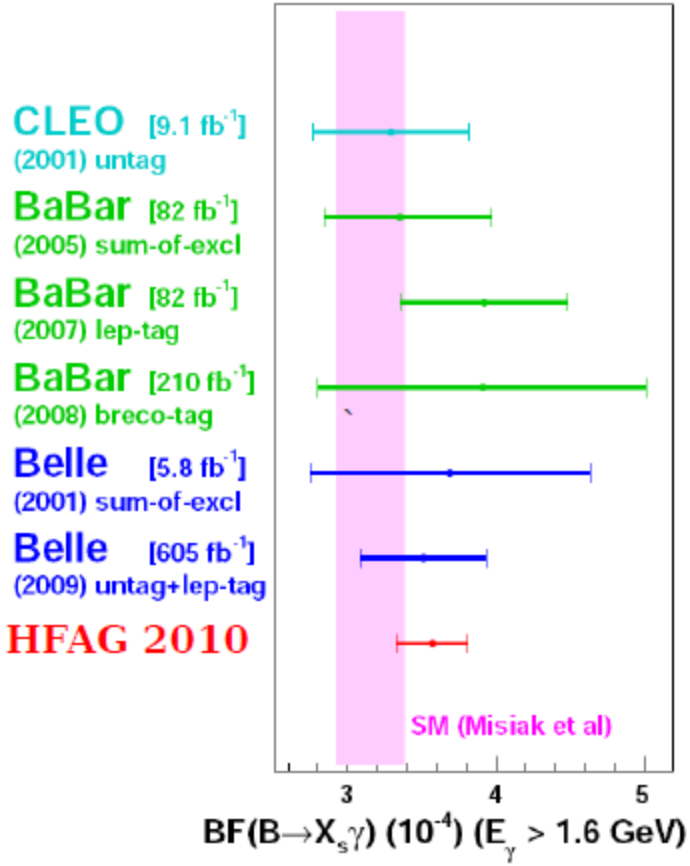

Charged Higgs bound (2HDM TypeII)
$M_{H^+} > 300$ GeV

M. Misiak et al., PRL98, 022002 (2007)

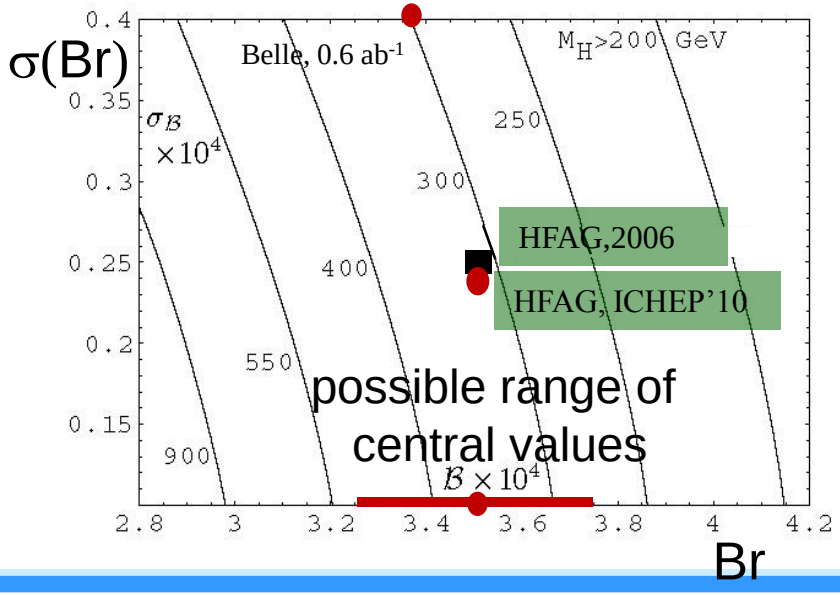

H^+ Search: $B^+ \rightarrow \tau^+ \upsilon_\tau$

(Decays with *Large* Missing Energy)

Sensitivity to new physics from charged Higgs

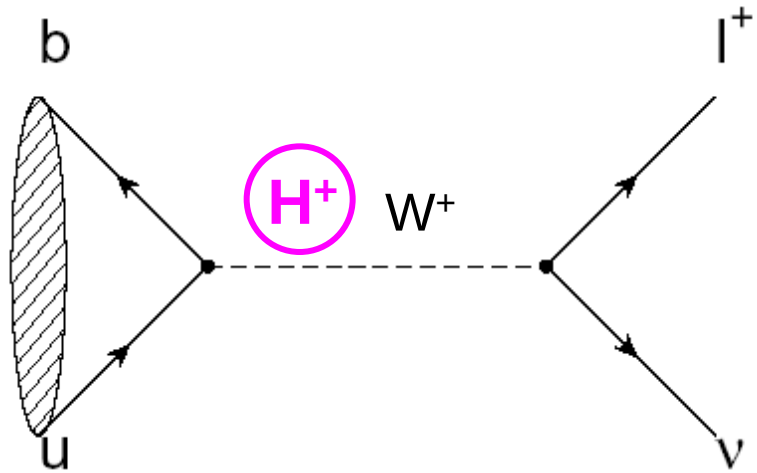

SM:

$$\mathcal{B}(B^+ \to \tau^+ \nu_\tau) = \frac{G_F^2 m_B}{8\pi} m_\tau^2 \left(1 - \frac{m_\tau^2}{m_B^2}\right)^2 f_B^2 |V_{ub}|^2 \tau_B$$

The B meson decay constant

LQCD

$|V_{ub}|$: from indep. measurements.

$B \to \tau\nu$: Experimental Challenge

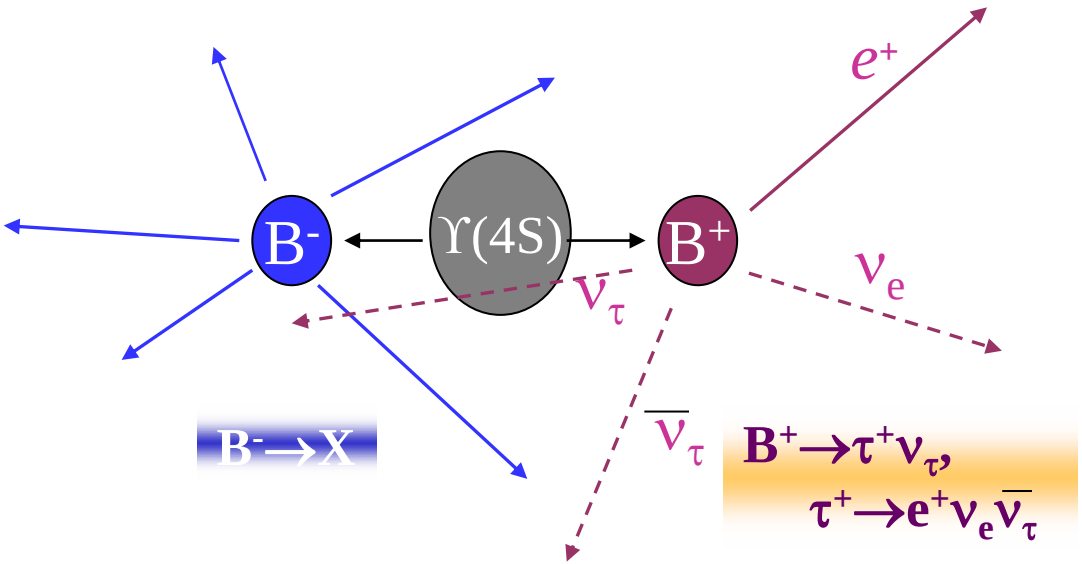

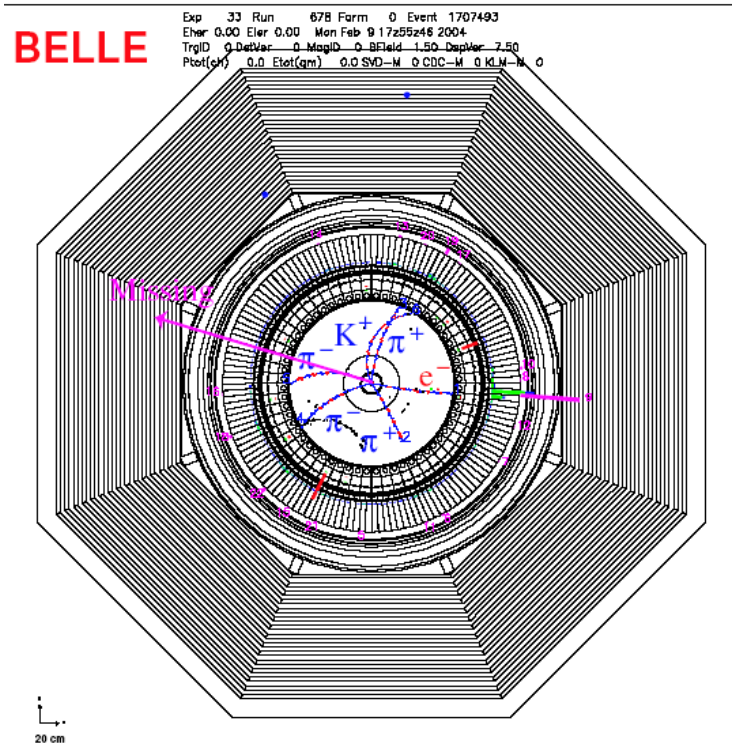

Always ≥ 2 neutrinos appear in B → τ ν decay

Signature : 1 track +invisible

Experimental Challenge !

$B \to \tau\nu$: Experimental Challenge

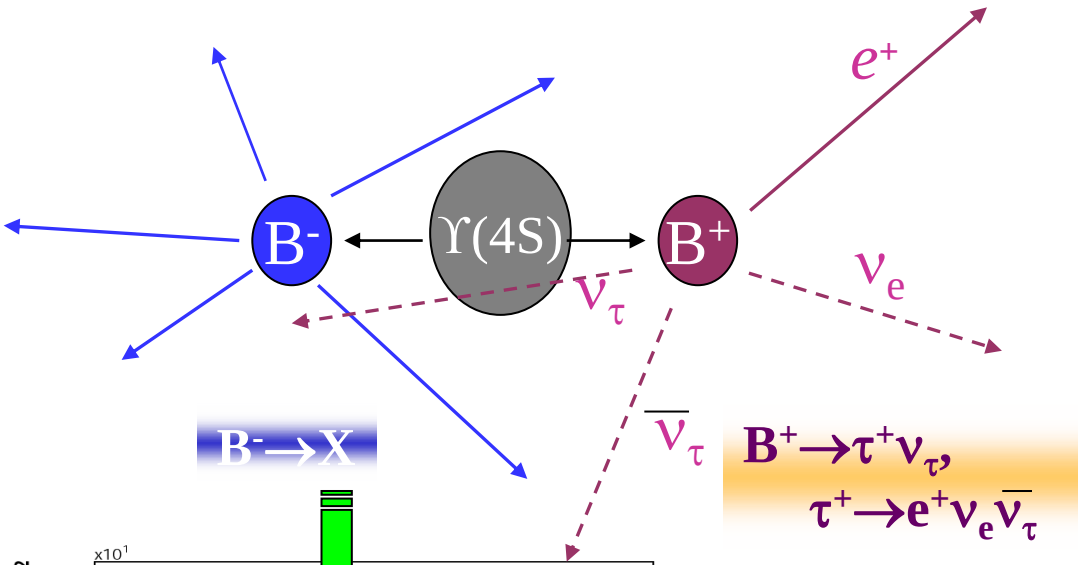

$B^+ \to \tau^+ \nu_\tau$,
$\tau^+ \to e^+ \nu_e \bar{\nu}_\tau$

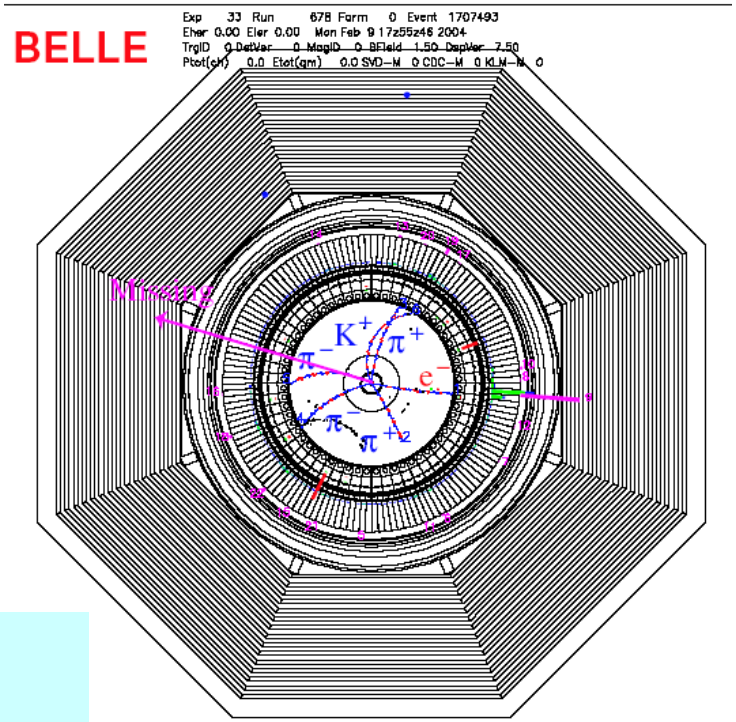

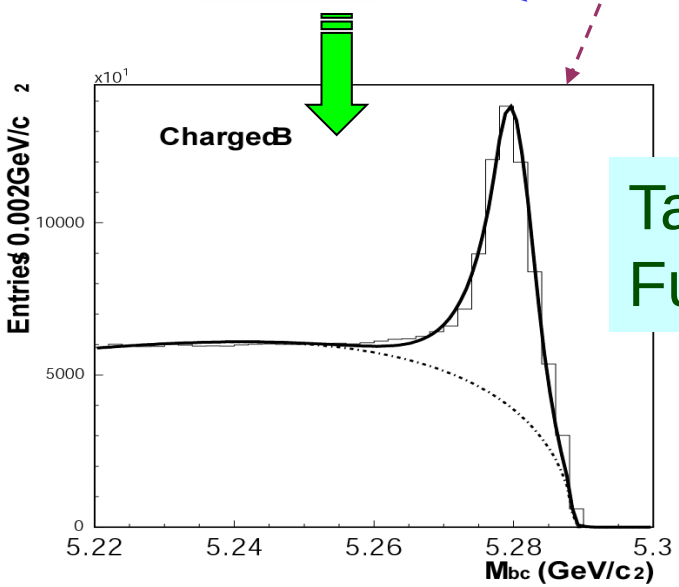

Tag-side:
Full reconstruction

$$B^+ \to \bar{D}^{(*)0} + \pi^+ / \rho^+ / a_1^+ / D_S^{(*)+}$$
$$\hookrightarrow \bar{D}^0\pi^0 / \bar{D}^0\gamma \qquad \hookrightarrow D_s^+\gamma$$

Also for
$B \to D^{(*)}\tau\nu$
$B \to K\nu\bar{\nu}$

Can be measured only by B-Factory !

B–>τν Results

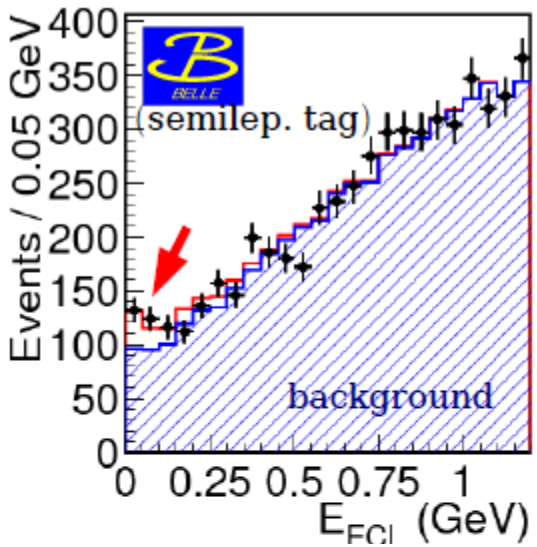
Events / 0.05 GeV
(semilep. tag)
background
E_{ECL} (GeV)

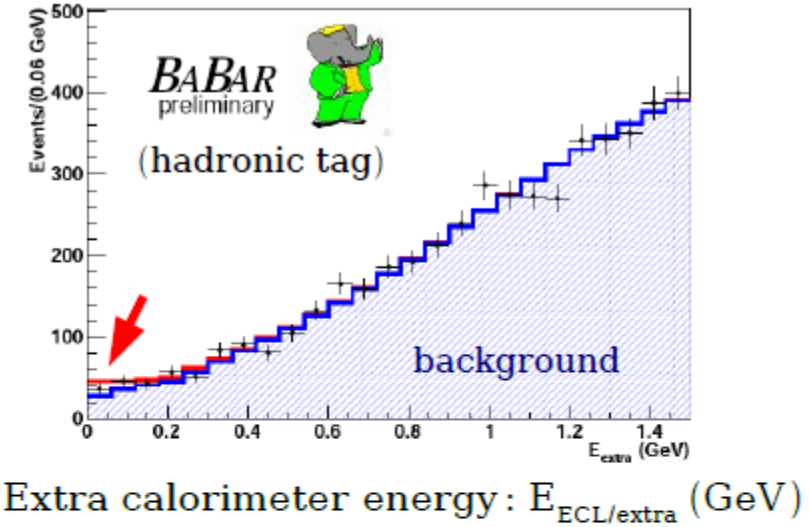
Events/(0.06 GeV)
BABAR
preliminary
(hadronic tag)
background
E_{extra} (GeV)
Extra calorimeter energy : $E_{ECL/extra}$ (GeV)

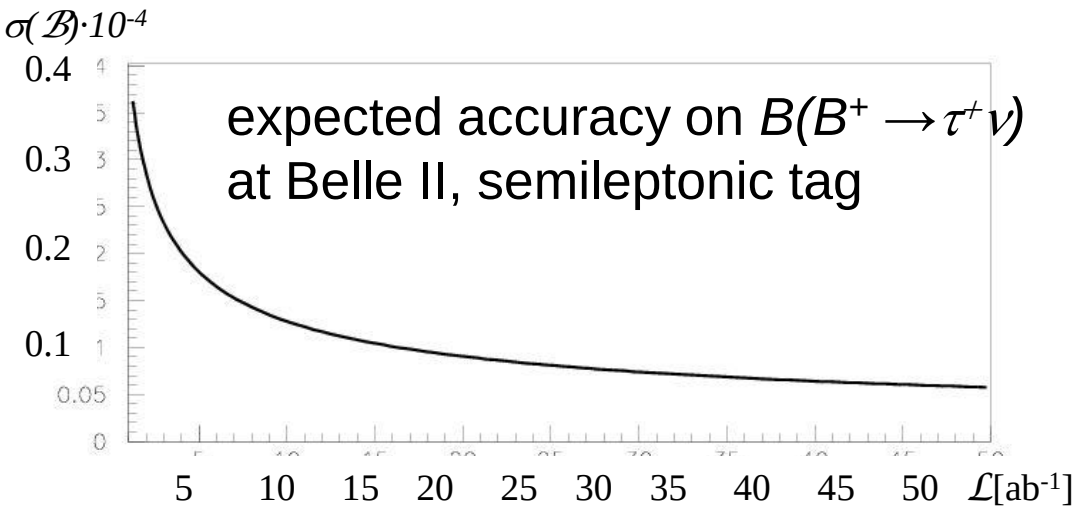
$\sigma(\mathcal{B})\cdot 10^{-4}$
expected accuracy on $B(B^+ \to \tau^+ \nu)$
at Belle II, semileptonic tag
$\mathcal{L}$[ab^{-1}]

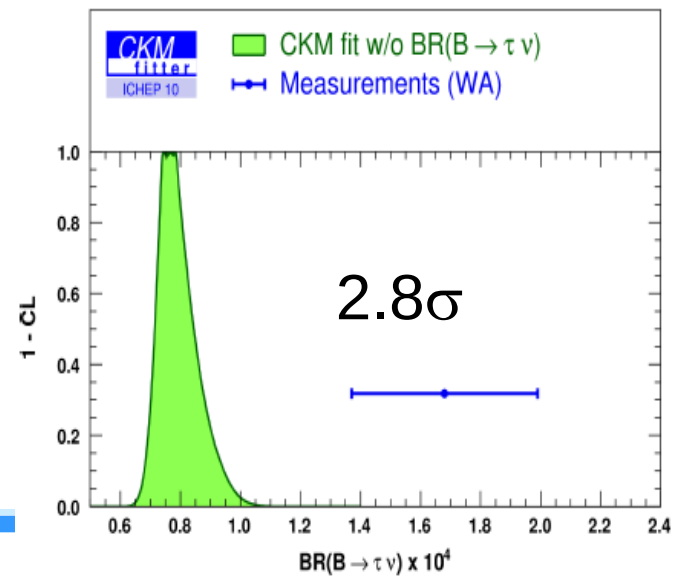
CKM fitter
ICHEP 10
CKM fit w/o BR(B → τ ν)
Measurements (WA)
2.8σ
1 - CL
BR(B → τ ν) x 10^4

$B \to D^{(*)}\tau\nu$

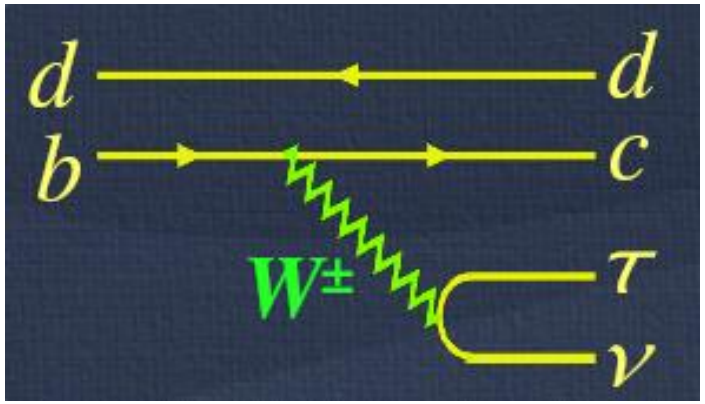

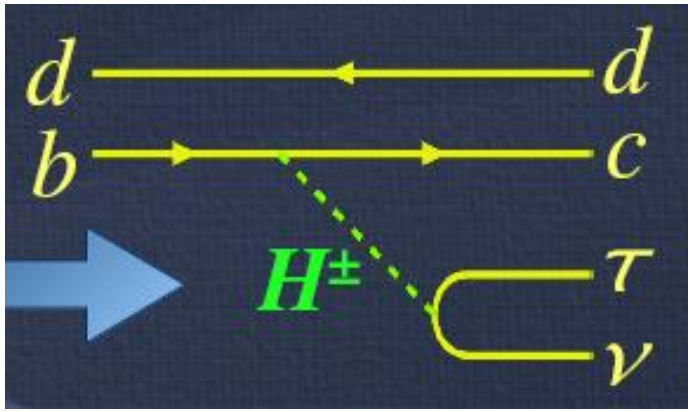

- $B \to D^* \tau\nu$: Lepton (τ) polarization info.

  Expected $\mathcal{B} \sim 1.4\%$ in SM (large) [e.g. D.S.Hwang EPJ C14,271(2000)]

  But, large background ($D^{*(**)}l\nu$, D^*X)

➢ **Always involve ≥ 2 ν (Missing E):**

$B \to D^{(*)}\tau\nu$ Results

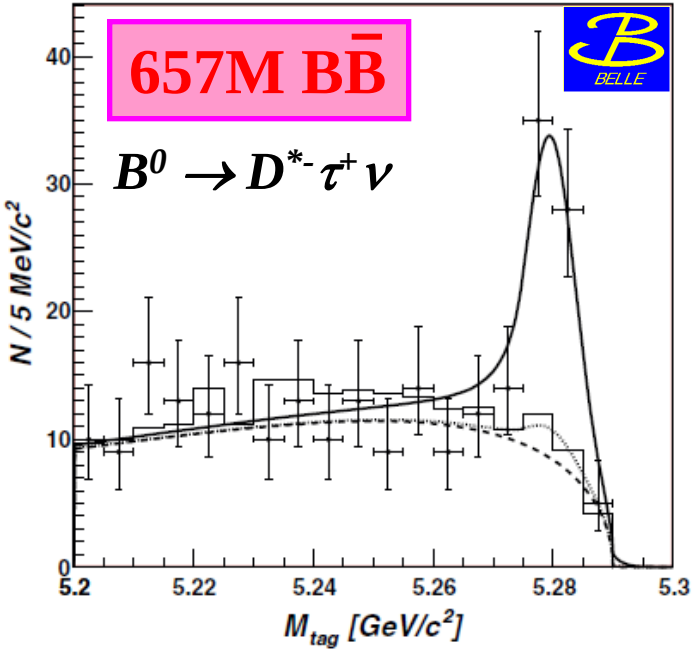

[PRL 99, 191807(2007)]

First Observation !

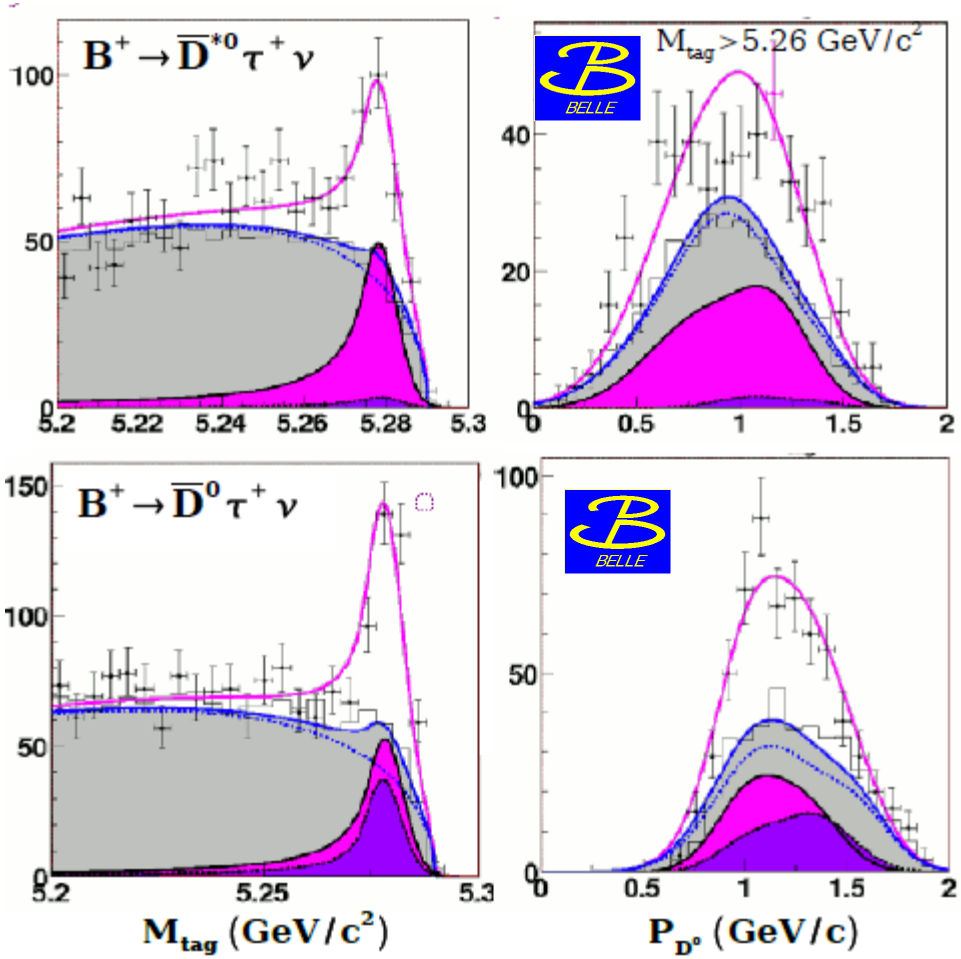

[PRD 82, 0720005(2010)]

$B \to D^{(*)}\tau\nu$ Summary

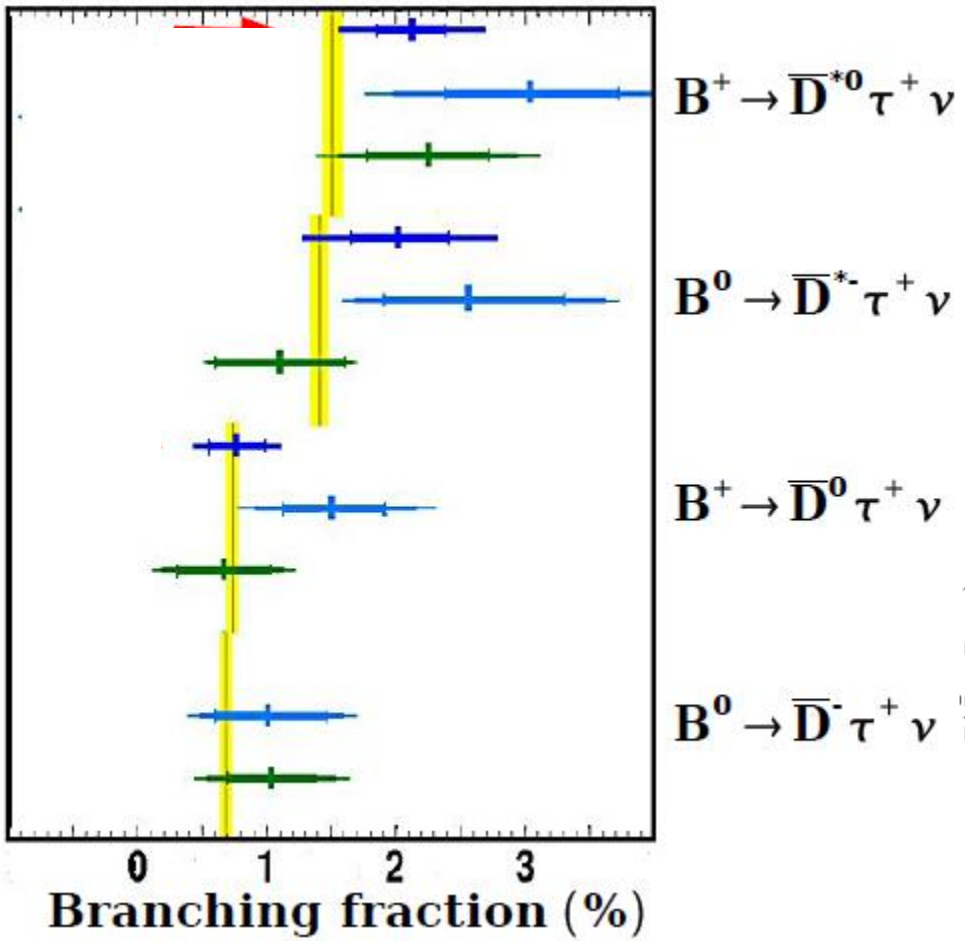

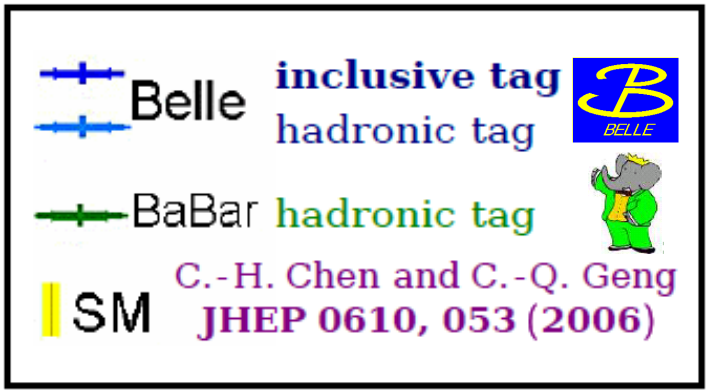

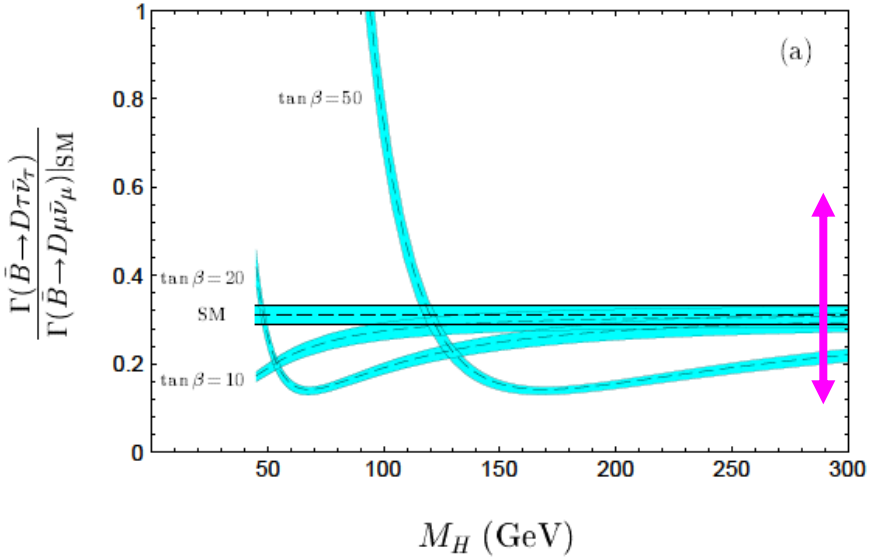

[M.Tanaka Z.Phys. C67,321(1995)]

Constraints on charged Higgs

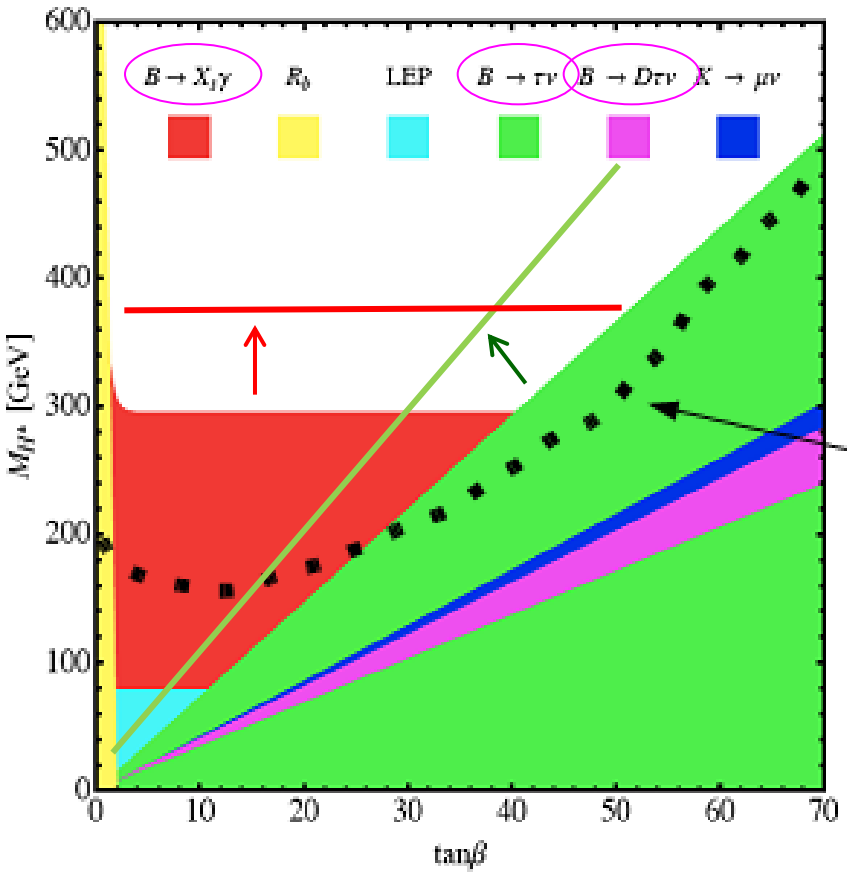

Current flavour constraints are already very competitive with LHC expected direct search sensitivity for charged Higgs

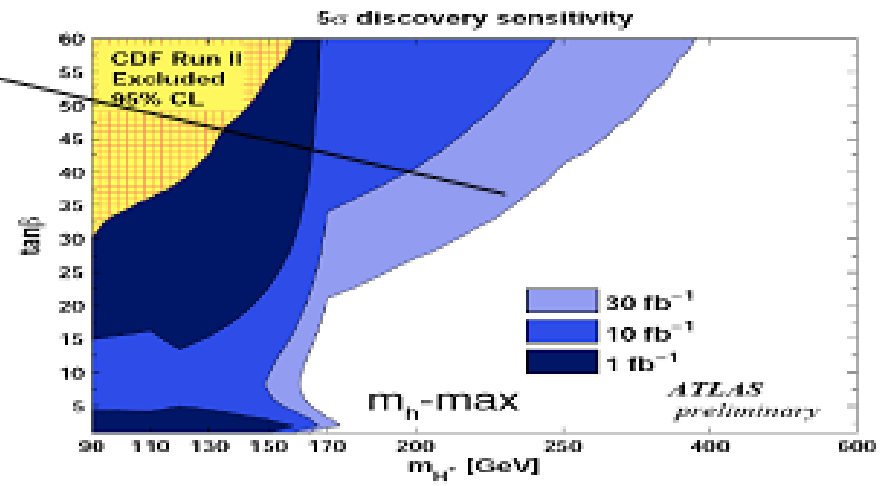

U. Haisch, hep-ph/0805.2141; ATLAS curve added by *Steve Robertson*

Also see (MSSM),D. Eriksson,F.Mahmoudi and 0.Stal

New Physics Prospects

Complemantarity

Super B factory

LHCb

K experiments

→ theory uncertainty matches the expected exp. precision

→ theory uncertainty will match the expected exp. precision with expected progress in LQCD

G. Isidori et al., Ann.Rev.Nucl.Part.Sci. 60, 355 (2010)

Observable	SM prediction	Theory error	Present result	Future error	Future Facility
$\lvert V_{us}\rvert$ $[K \to \pi\ell\nu]$	input	$0.5\% \to 0.1\%_{\rm Latt}$	0.2246 ± 0.0012	0.1%	K factory
$\lvert V_{cb}\rvert$ $[B \to X_c\ell\nu]$	input	1%	$(41.54 \pm 0.73) \times 10^{-3}$	1%	Super-B
$\lvert V_{ub}\rvert$ $[B \to \pi\ell\nu]$	input	$10\% \to 5\%_{\rm Latt}$	$(3.38 \pm 0.36) \times 10^{-3}$	4%	Super-B
γ $[B \to DK]$	input	$< 1^\circ$	$(70^{+27}_{-30})^\circ$	3°	LHCb
$S_{B_d \to \psi K}$	$\sin(2\beta)$	$\lesssim 0.01$	0.671 ± 0.023	0.01	LHCb
$S_{B_s \to \psi\phi}$	0.036	$\lesssim 0.01$	$0.81^{+0.12}_{-0.32}$	0.01	LHCb
$S_{B_d \to \phi K}$	$\sin(2\beta)$	$\lesssim 0.05$	0.44 ± 0.18	0.1	LHCb
$S_{B_s \to \phi\phi}$	0.036	$\lesssim 0.05$	—	0.05	LHCb
$S_{B_d \to K^*\gamma}$	few $\times$ 0.01	0.01	-0.16 ± 0.22	0.03	Super-B
$S_{B_s \to \phi\gamma}$	few $\times$ 0.01	0.01	—	0.05	LHCb
$A^d_{\rm SL}$	-5×10^{-4}	10^{-4}	$-(5.8 \pm 3.4) \times 10^{-3}$	10^{-3}	LHCb
$A^s_{\rm SL}$	2×10^{-5}	$< 10^{-5}$	$(1.6 \pm 8.5) \times 10^{-3}$	10^{-3}	LHCb
$A_{CP}(b \to s\gamma)$	< 0.01	< 0.01	-0.012 ± 0.028	0.005	Super-B
$\mathcal{B}(B \to \tau\nu)$	1×10^{-4}	$20\% \to 5\%_{\rm Latt}$	$(1.73 \pm 0.35) \times 10^{-4}$	5%	Super-B
$\mathcal{B}(B \to \mu\nu)$	4×10^{-7}	$20\% \to 5\%_{\rm Latt}$	$< 1.3 \times 10^{-6}$	6%	Super-B
$\mathcal{B}(B_s \to \mu^+\mu^-)$	3×10^{-9}	$20\% \to 5\%_{\rm Latt}$	$< 5 \times 10^{-8}$	10%	LHCb
$\mathcal{B}(B_d \to \mu^+\mu^-)$	1×10^{-10}	$20\% \to 5\%_{\rm Latt}$	$< 1.5 \times 10^{-8}$	[?]	LHCb
$A_{\rm FB}(B \to K^*\mu^+\mu^-)_{q^2_0}$	0	0.05	(0.2 ± 0.2)	0.05	LHCb
$B \to K\nu\bar\nu$	4×10^{-6}	$20\% \to 10\%_{\rm Latt}$	$< 1.4 \times 10^{-5}$	20%	Super-B
$\lvert q/p\rvert_{D-\rm mixing}$	1	$< 10^{-3}$	$(0.86^{+0.18}_{-0.15})$	0.03	Super-B
ϕ_D	0	$< 10^{-3}$	$(9.6^{+8.3}_{-9.5})^\circ$	2°	Super-B
$\mathcal{B}(K^+ \to \pi^+\nu\bar\nu)$	8.5×10^{-11}	8%	$(1.73^{+1.15}_{-1.05}) \times 10^{-10}$	10%	K factory
$\mathcal{B}(K_L \to \pi^0\nu\bar\nu)$	2.6×10^{-11}	10%	$< 2.6 \times 10^{-8}$	[?]	K factory
$R^{(e/\mu)}(K \to \pi\ell\nu)$	2.477×10^{-5}	0.04%	$(2.498 \pm 0.014) \times 10^{-5}$	0.1%	K factory
$\mathcal{B}(t \to cZ,\gamma)$	$\mathcal{O}(10^{-13})$	$\mathcal{O}(10^{-13})$	$< 0.6 \times 10^{-2}$	$\mathcal{O}(10^{-5})$	LHC ($100\,{\rm fb}^{-1}$)

$B(B \to X_s\gamma)$	6%	Super-B
$B(B \to X_d\gamma)$	20%	Super-B
$S(B \to \rho\gamma)$	0.15	Super-B
$B(\tau \to \mu\gamma)$	$3 \cdot 10^{-9}$	Super-B (90% U.L.)
$B(B^+ \to D\tau\nu)$	3%	Super-B
$B(B_s \to \gamma\gamma)$	$0.25 \cdot 10^{-6}$	Super-B (5 ab^{-1})
$\sin^2\theta_W$ @ $\Upsilon(4S)$	$3 \cdot 10^{-4}$	Super-B

Identification of NP type

➡ Identify by the pattern of deviations from SM

SUSY models →

Measurements ↓	mSU GRA	MSSM+ν_R degenerate	MSSM+ν_R non-degenerate	SU(5)+ν_R degenerate	SU(5)+ν_R non-degenerate	U(2) FS	···
$A_{CP}(s\gamma)$						✓	
$S(K^*\gamma)$				✓	✓	✓	
$S(\rho\gamma)$				✓	✓	✓	
$S(\phi K_S)$				✓	✓	✓	
$S(B_s \to J/\psi\ \phi)$				✓	✓	✓	
$\mu \to e\gamma$		✓		✓	✓	?	
$\tau \to \mu\gamma$		✓	✓	✓	✓	?	
$\tau \to e\gamma$			✓		✓	?	
⋮							

✓: deviation from SM

[based on T.Goto et.al. PRD77, 095010(2008)]

Physics at Super B-factory

is "DNA chip of New Physics"

+ LHC,…

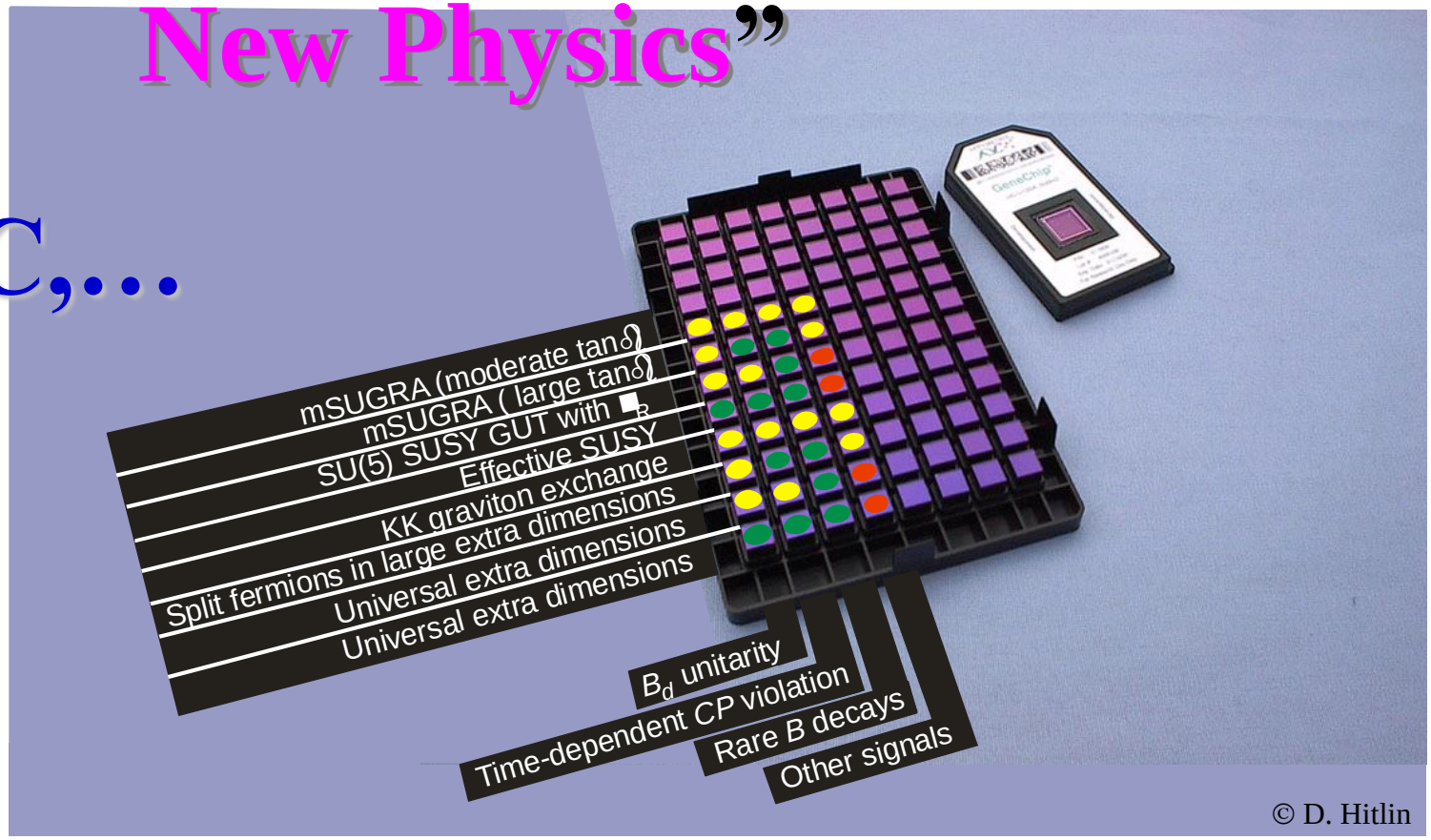

© D. Hitlin

New Hadron Structures: QCD

Another Layer of "New" Physics

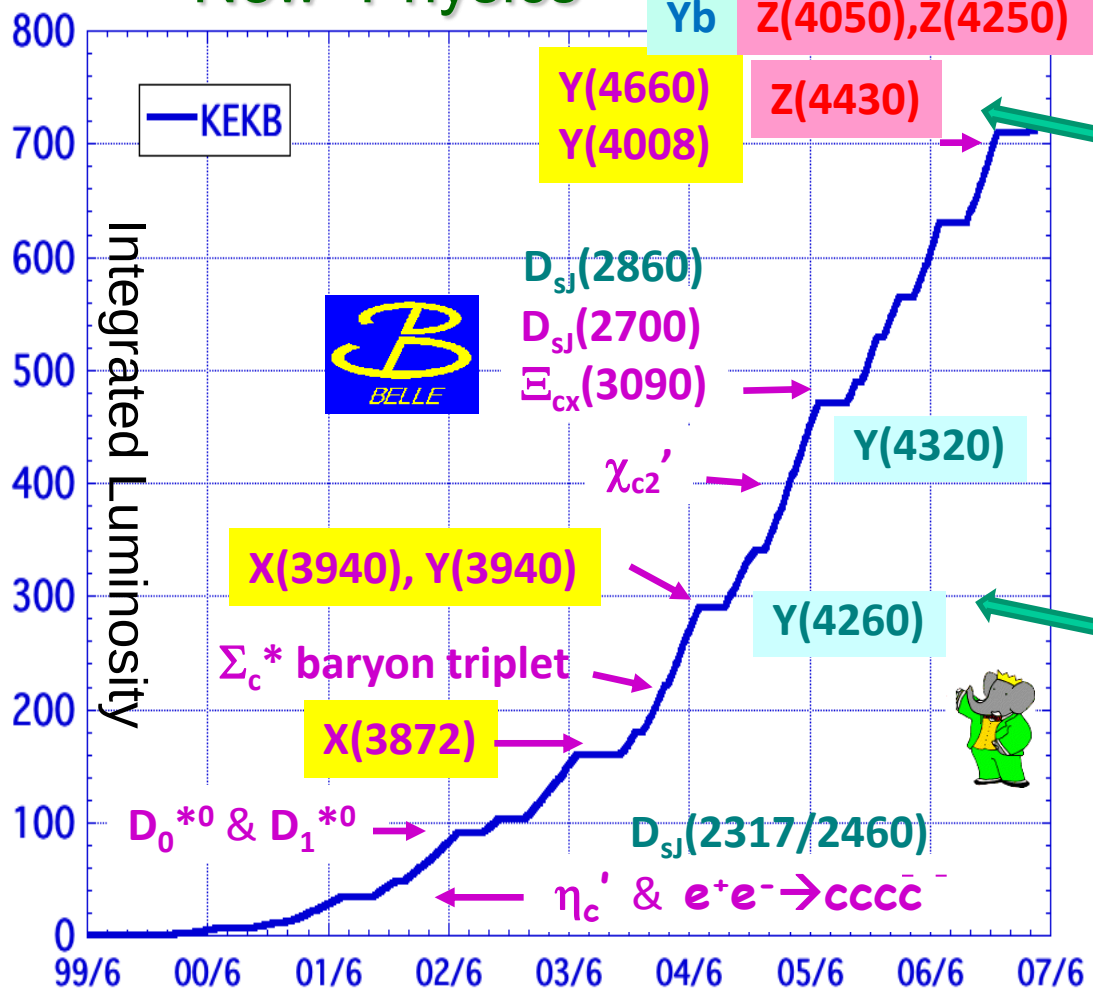

"Exotic Hadrons"

Charged

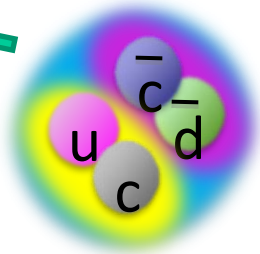

Tetraquark

Neutral

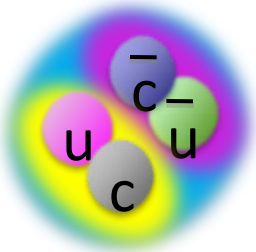

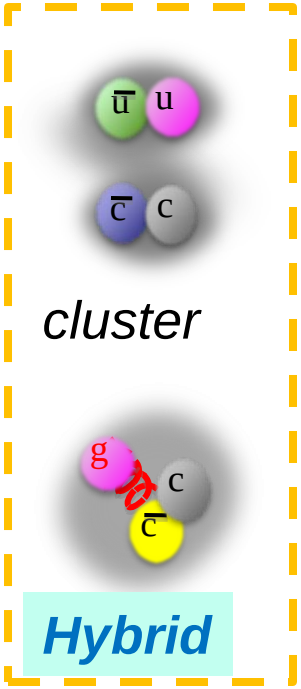

LQCD: important roles

SuperKEKB

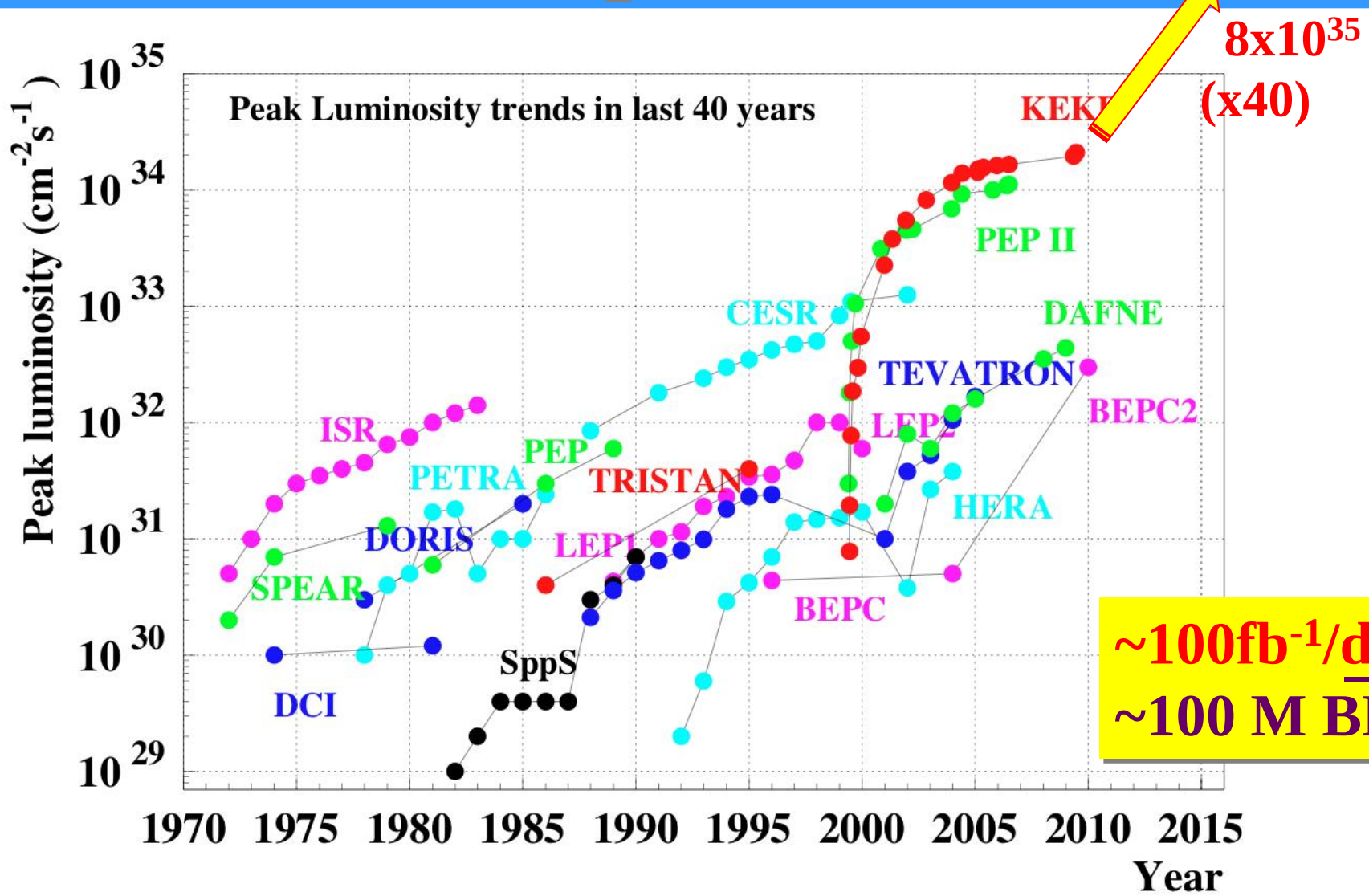
Peak Luminosity trends in last 40 years
Peak luminosity (cm^{-2}s^{-1})
10^{35}
10^{34}
10^{33}
10^{32}
10^{31}
10^{30}
10^{29}
1970 1975 1980 1985 1990 1995 2000 2005 2010 2015
Year
KEKB
PEP II
CESR
DAFNE
TEVATRON
BEPC2
LEP2
ISR
PEP
PETRA
TRISTAN
HERA
DORIS
LEP1
SPEAR
BEPC
SppS
DCI
8×10^{35}
(x40)
~100fb^{-1}/day
~100 M $B\bar{B}$

To High Luminosity

Lorentz factor

$$L = \frac{\gamma_\pm}{2er_e}\left(1+\frac{\sigma_y^*}{\sigma_x^*}\right)\frac{I_\pm \xi_{\pm y}}{\beta_y^*}\left(\frac{R_L}{R_y}\right)$$

Classical electron radius

Beam size ratio

Geometrical reduction factors due to crossing angle and hour-glass effect

- **Increase beam current, I** — **x 2**
- **Larger beam-beam par, ξ_y** — **~ same**
- **Smaller β^*_y** — **<1/20** **+low emmittance** (long bunch)

Nano-beam approach

Nano-Beam Scheme

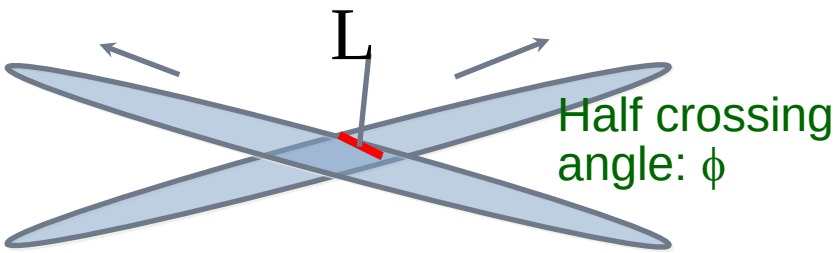

Hourglass condition:

$\beta_y^* >\sim L=\sigma_x/\phi$

present KEKB (w/o crab)

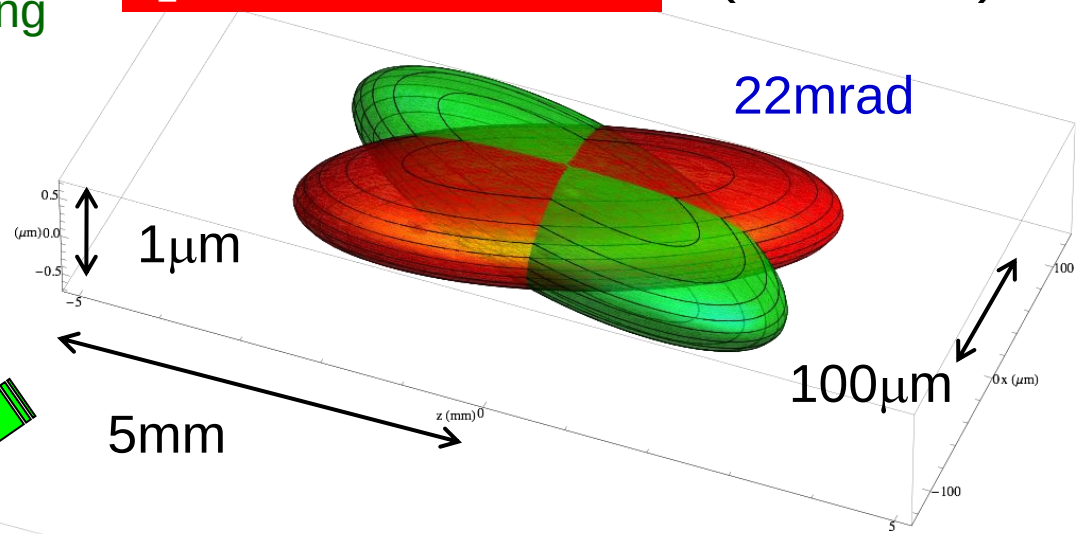

SuperKEKB

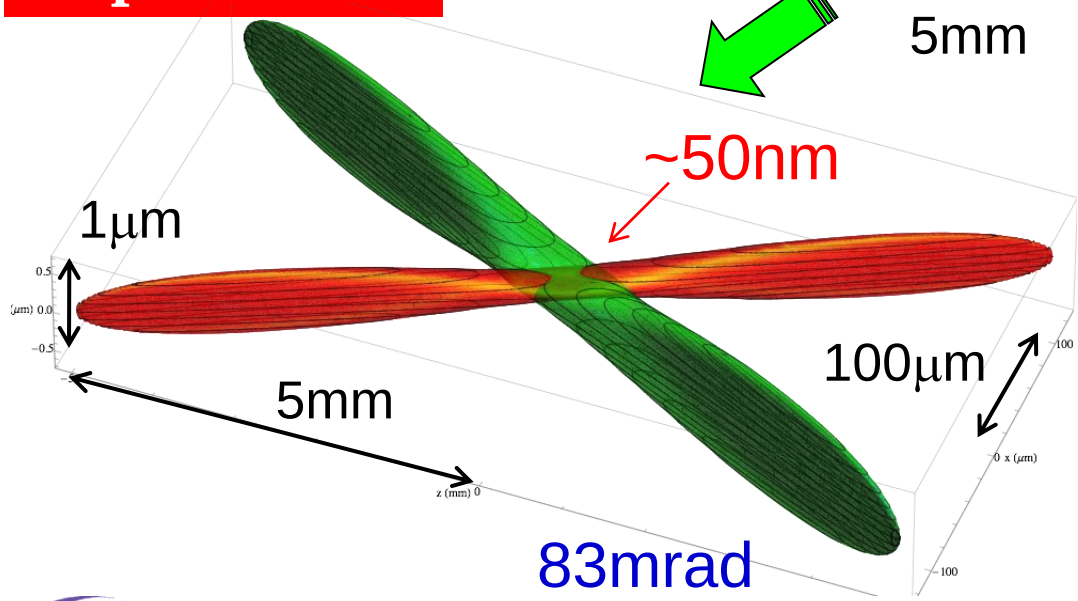

$$L=\frac{\gamma_\pm}{2er_e}\left(1+\frac{\sigma_y^*}{\sigma_x^*}\right)\frac{I_\pm\xi_{\pm y}}{\beta_y^*}\left(\frac{R_L}{R_y}\right)$$

$$L=\frac{N_+N_-f}{4\pi\sigma_x^*\sigma_y^*}R_L$$

SuperKEKB

Replace short dipoles with longer ones (LER)

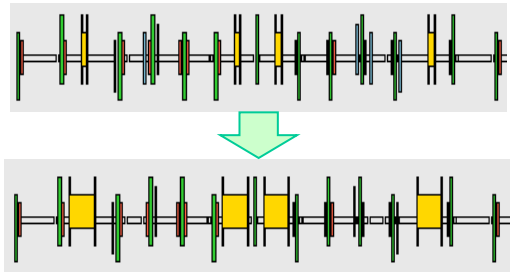

Redesign the lattices of HER & LER to squeeze the emittance

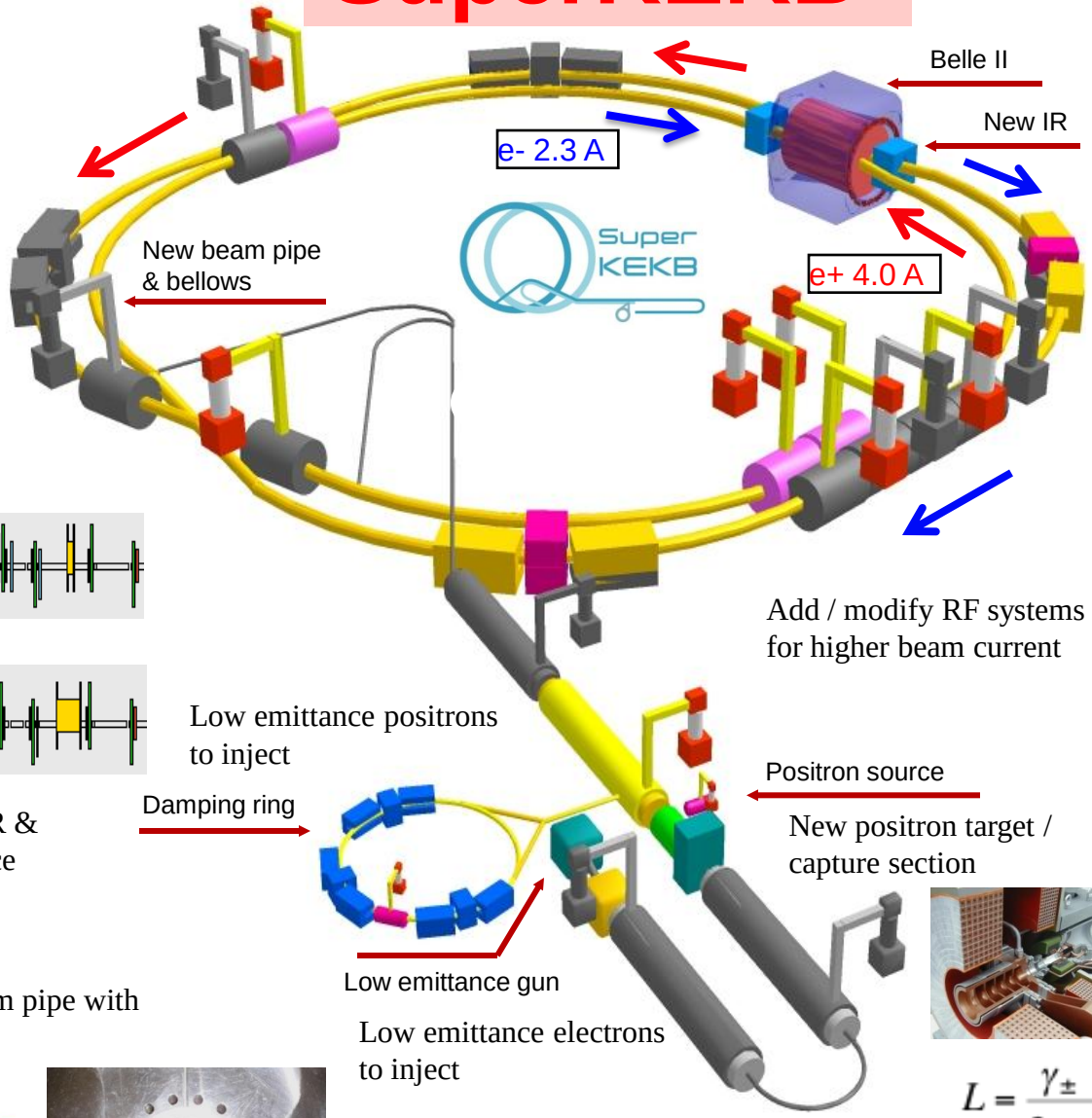

Colliding bunches

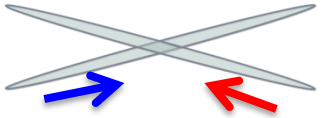

New superconducting /permanent final focusing quads near the IP

Add / modify RF systems for higher beam current

Low emittance positrons to inject

New positron target / capture section

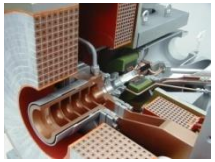

Low emittance electrons to inject

TiN-coated beam pipe with antechambers

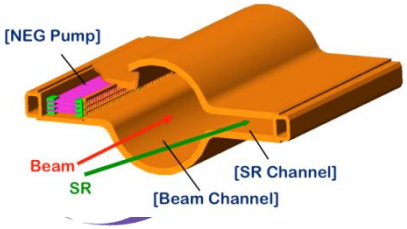

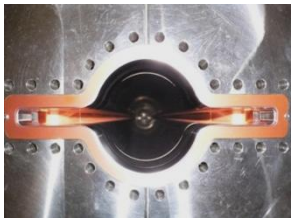

$$L = \frac{\gamma_\pm}{2er_e}\left(1+\frac{\sigma_y^*}{\sigma_x^*}\right)\frac{I_\pm \xi_{\pm y}}{\beta_y^*}\left(\frac{R_L}{R_y}\right)$$

$L = 8 \cdot 10^{35}\ s^{-1} cm^{-2}$

x 40 Gain in Luminosity

IR Design

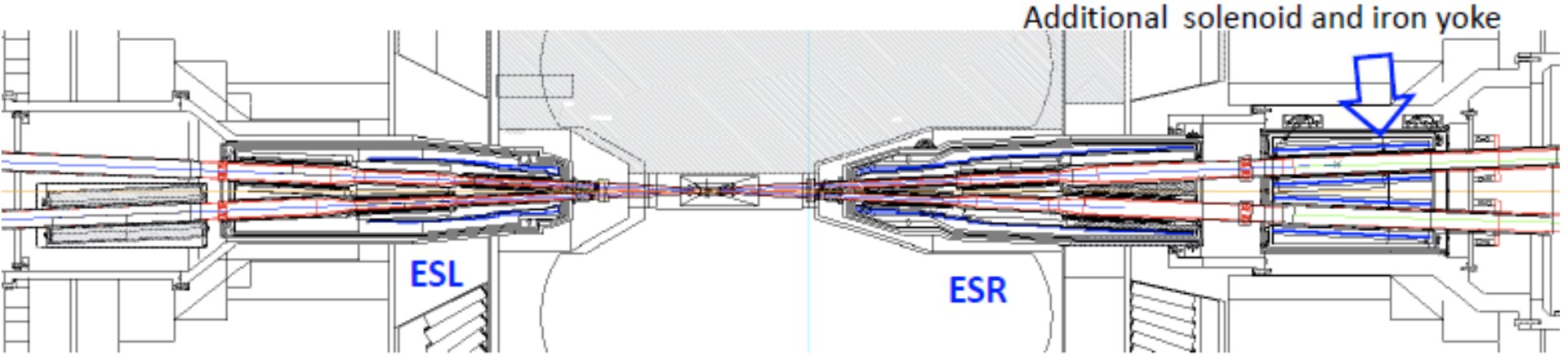

IR is one of crucial items of SuperKEKB

QCS and Compensation Solenoids ⟵ collaboration KEK/BNL

Beam Focusing, Orbit Stability

Background to detector

Luminosity Prospects

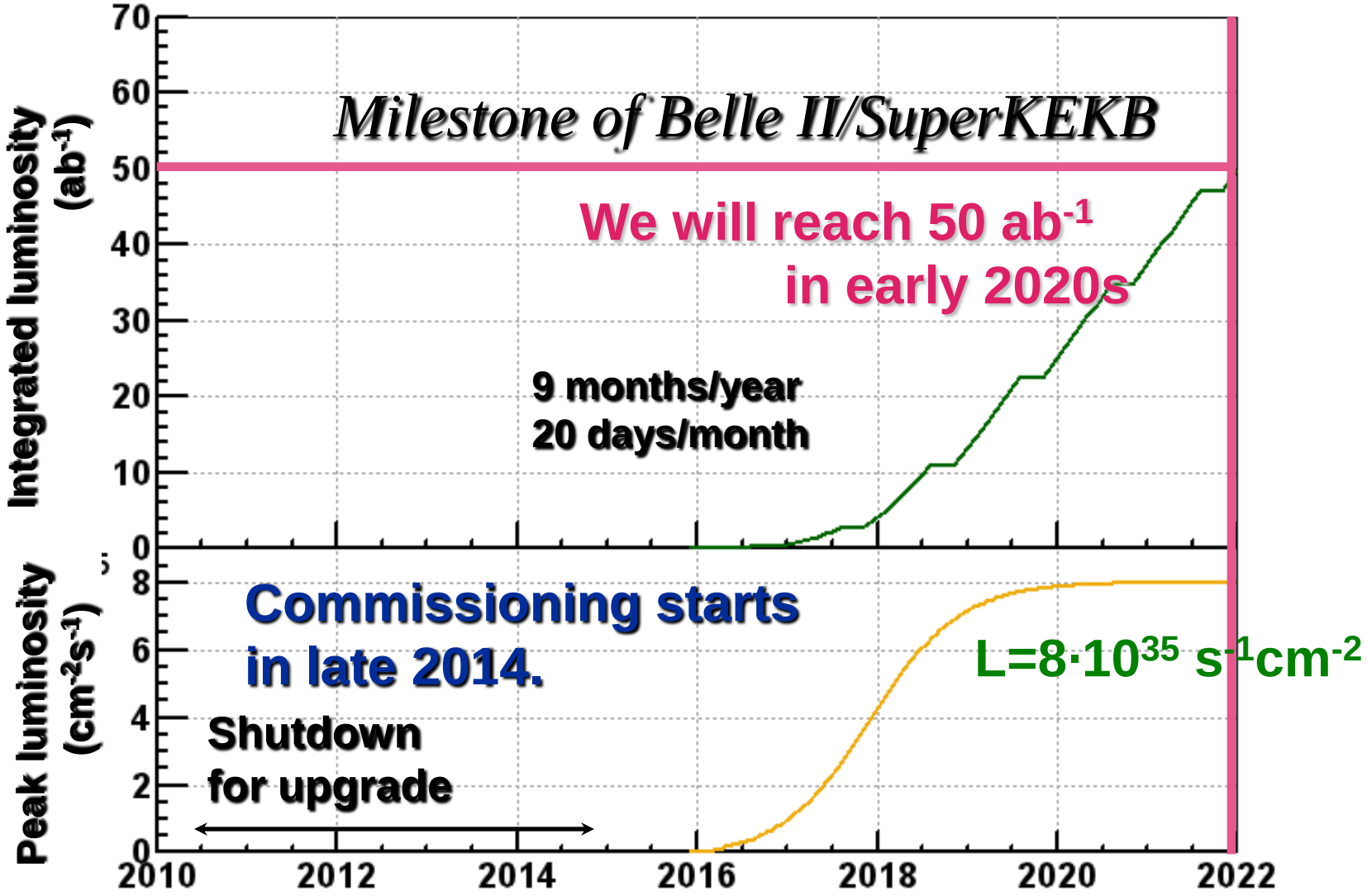

SuperKEKB 開始記念式
SuperKEKB Groundbreaking Ceremony
高エネルギー加速器研究機構 2011. 11. 18

SuperKEKB Project
x40
SuperKEKB

Construction work going

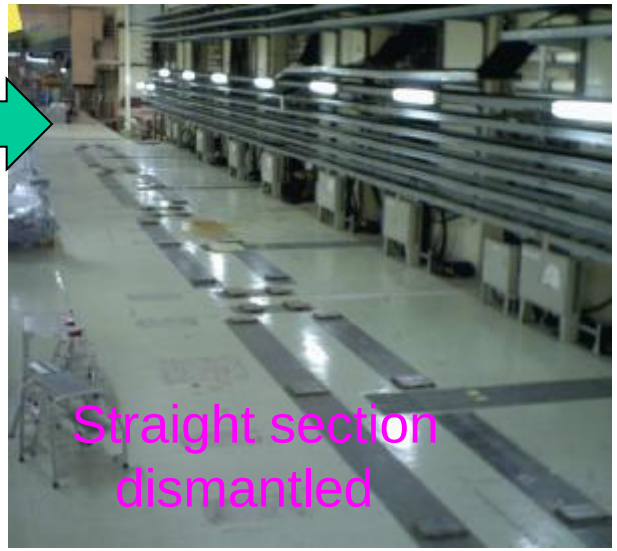

New LER Dipole

Field measurement set up

Relocate ARES cavities

Beam pipe @BINP

Belle II Collaboration

2004.06 **SuperKEKB LoI**

2008.01 **KEK Roadmap**

2008.03 **1st Proto collaboration meeting**

2008.10 **Detector study report**

2008.12 **New collaboration, Belle-II, started**

~400 collaborators from 57 institutions in 13 countries

Peter Krizan (Ljubljana) elected as the first spokesperson

~2012.03 **Series of open collaboration meetings**

International Collaboration

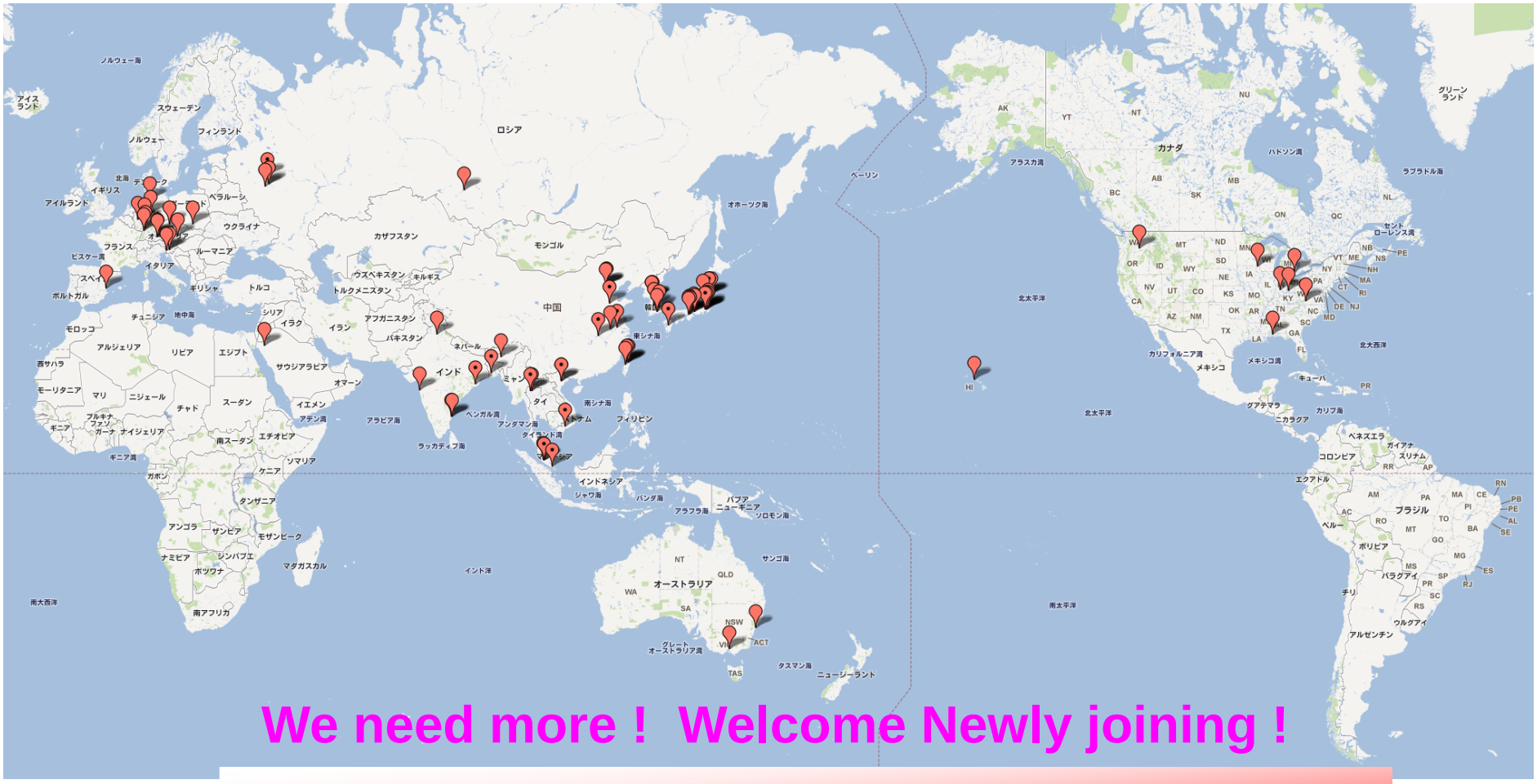

19 countries, 65 institutes, ~400 collaborators

Belle II Detector

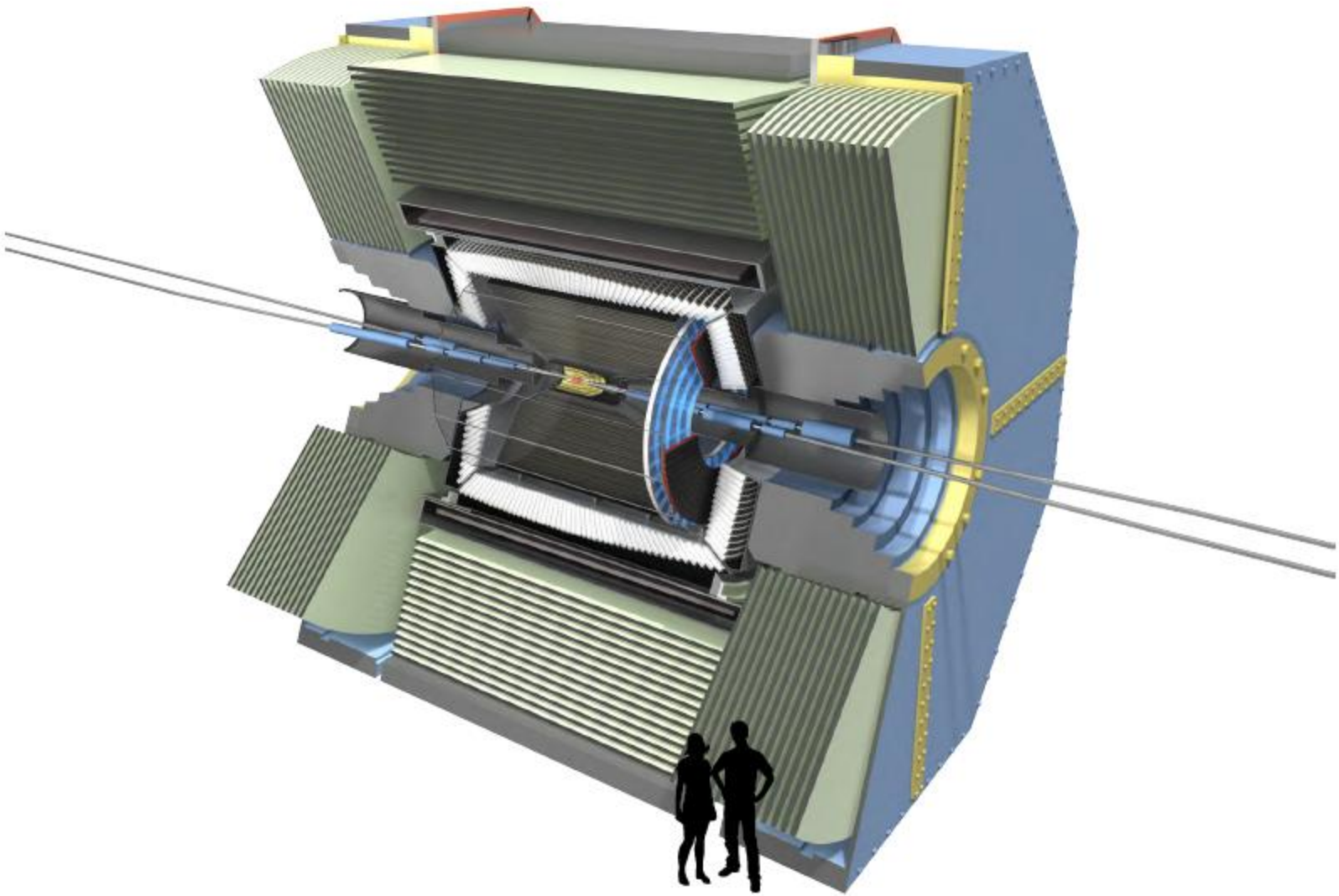

Belle → Belle II

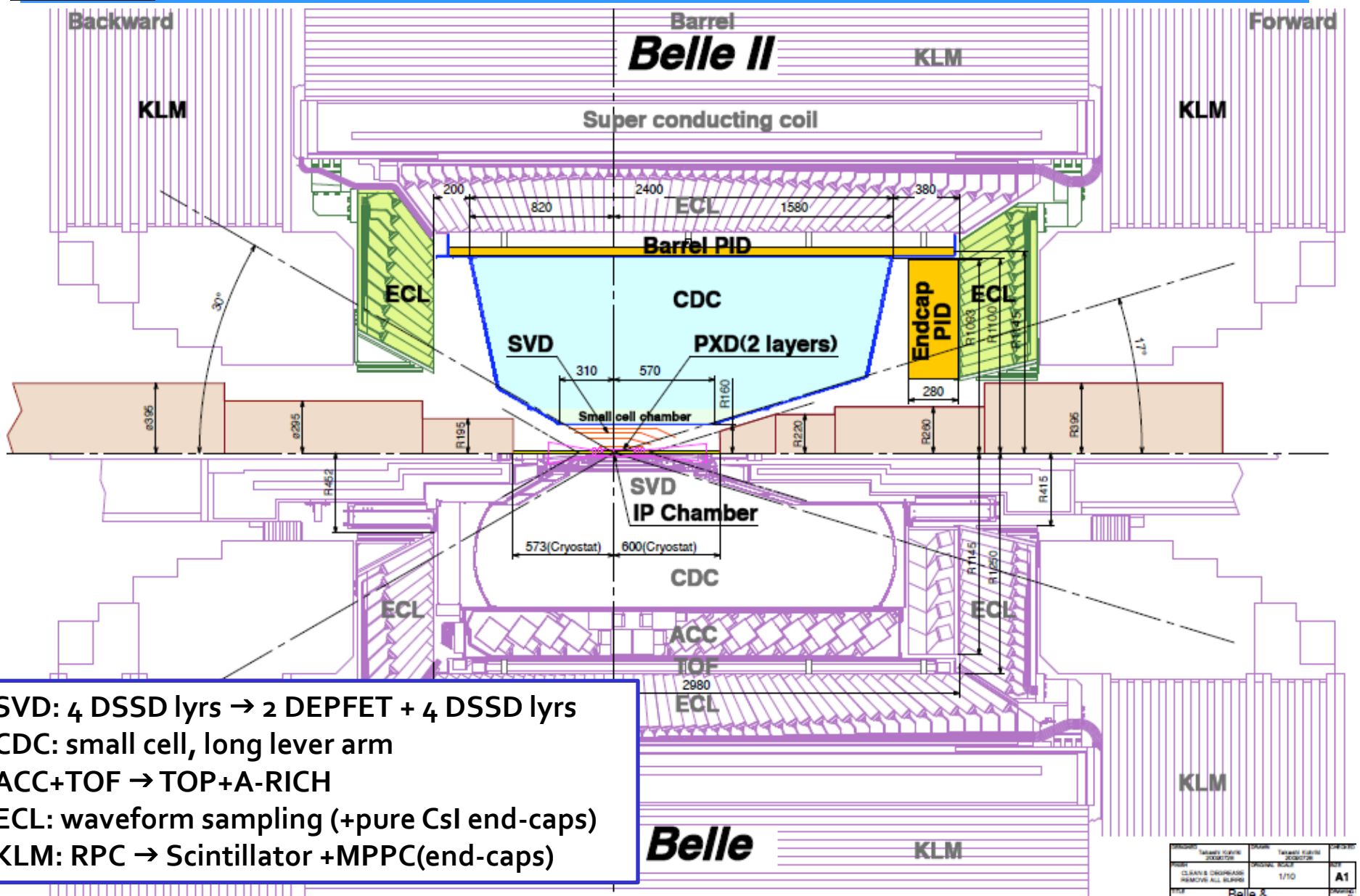

SVD: 4 DSSD lyrs → 2 DEPFET + 4 DSSD lyrs
CDC: small cell, long lever arm
ACC+TOF → TOP+A-RICH
ECL: waveform sampling (+pure CsI end-caps)
KLM: RPC → Scintillator +MPPC(end-caps)

Vertex detectors PXD/SVD

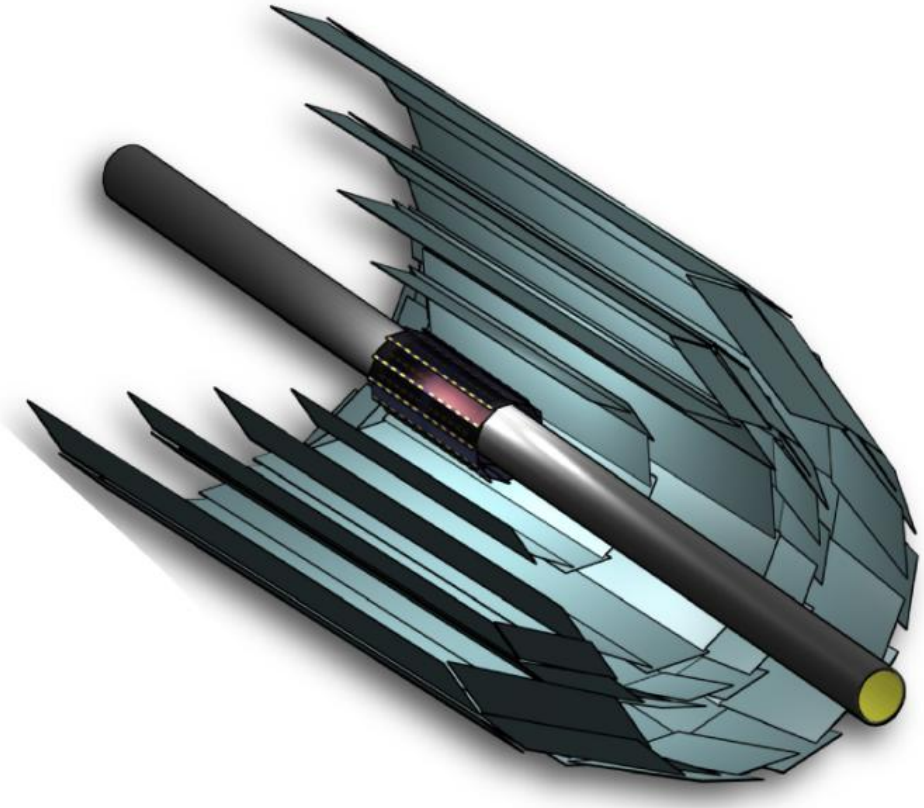

Beam Pipe	**r = 10mm**
DEPFET	
Layer 1	**r = 14mm**
Layer 2	**r = 22mm**
DSSD	
Layer 3	**r = 38mm**
Layer 4	**r = 80mm**
Layer 5	**r = 105mm**
Layer 6	**r = 130mm**

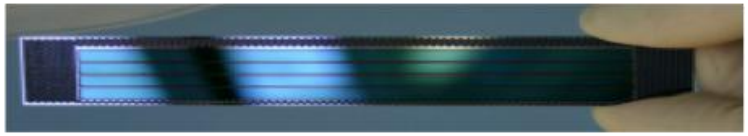

Expected performance

$$\sigma = a + \frac{b}{p\beta\sin^{\nu}\theta}$$

Significant improvement in IP resolution!

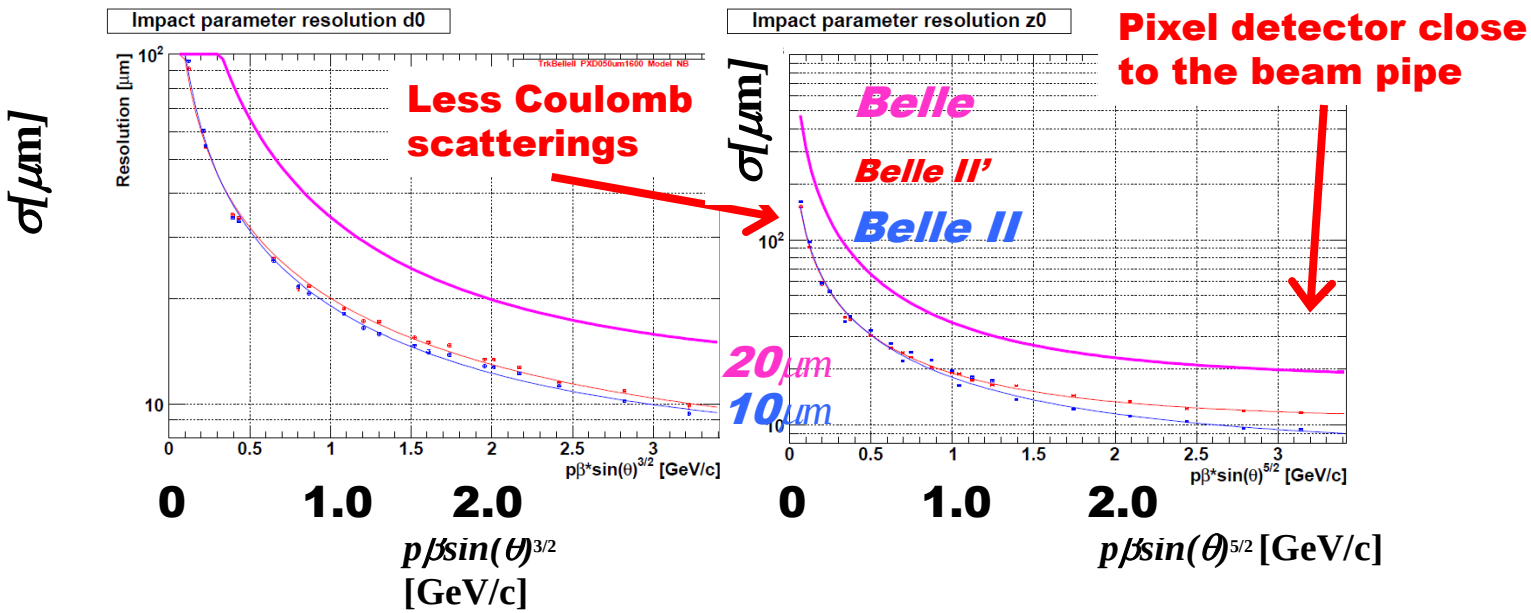

Significant improvement in $\delta S(K_S\pi^0\gamma)$

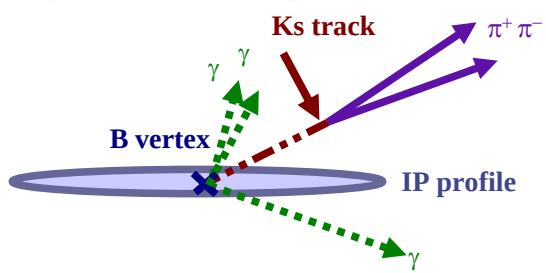

B decay point reconstruction with K_S trajectory

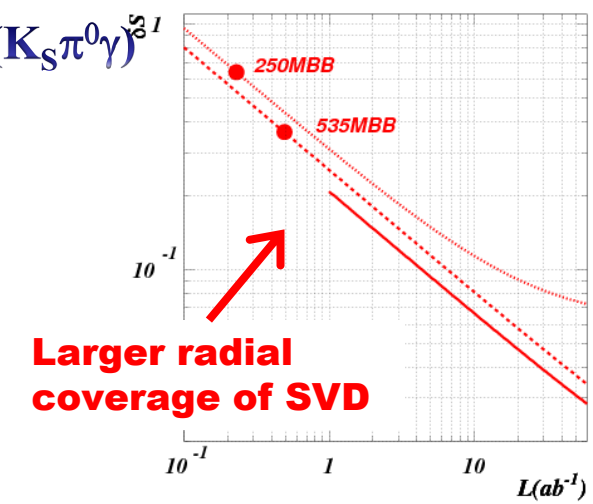

CDC

Belle

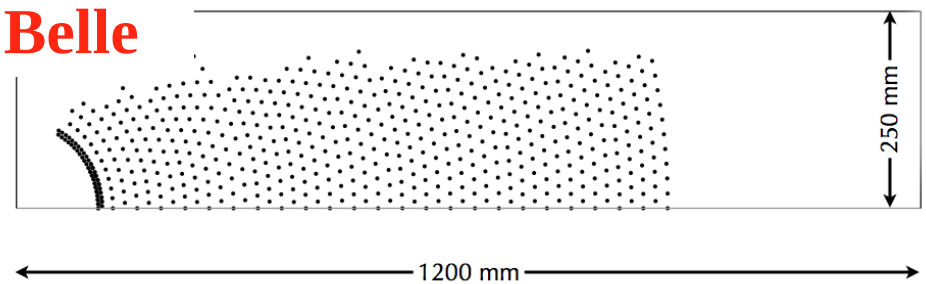

Belle II

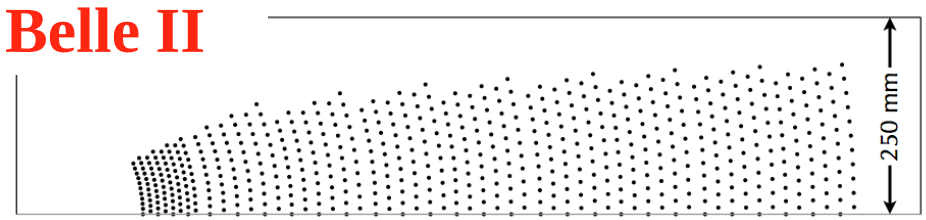

longer lever arm

improve resolution of momentum and dE/dx

$$\sigma_{P_t}/P_t = 0.19P_t \oplus 0.30/\beta$$
$$\sigma_{P_t}/P_t = 0.11P_t \oplus 0.30/\beta$$

new readout system

dead time 1-2μs → 200ns

small cell

smaller hit rate for each wire

shorter maximum drift time

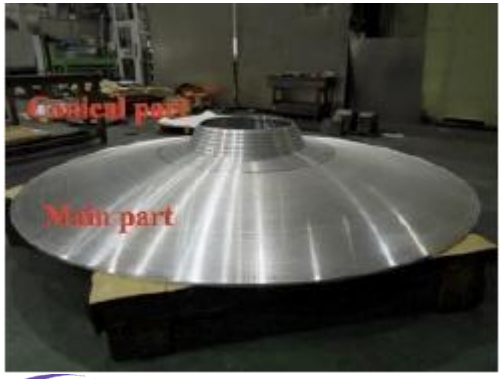

	Belle	Belle II
radius of inner most sense wire	88	168
radius of outer most sense wire	863	1111.4
Number of layers	50	56
Number of total sense wire	8400	14336
Gas	He:C_2H_6	He:C_2H_6
sense/field wire	W(Φ30μm)/Al(Φ120μm)	W(Φ30μm)/Al(Φ120μm)

Particle ID

Barrel PID: Time of Propagation Counter (TOP)

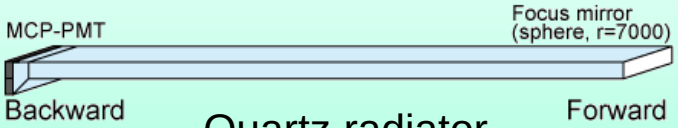

Quartz radiator

Focusing mirror

Small expansion block

Hamamatsu MCP-PMT (measure t, x and y)

Endcap PID: Aerogel RICH(ARICH)

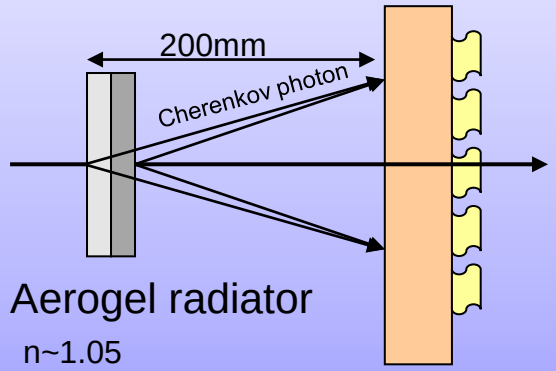

Aerogel radiator

n~1.05

Hamamatsu HAPD
+ new ASIC

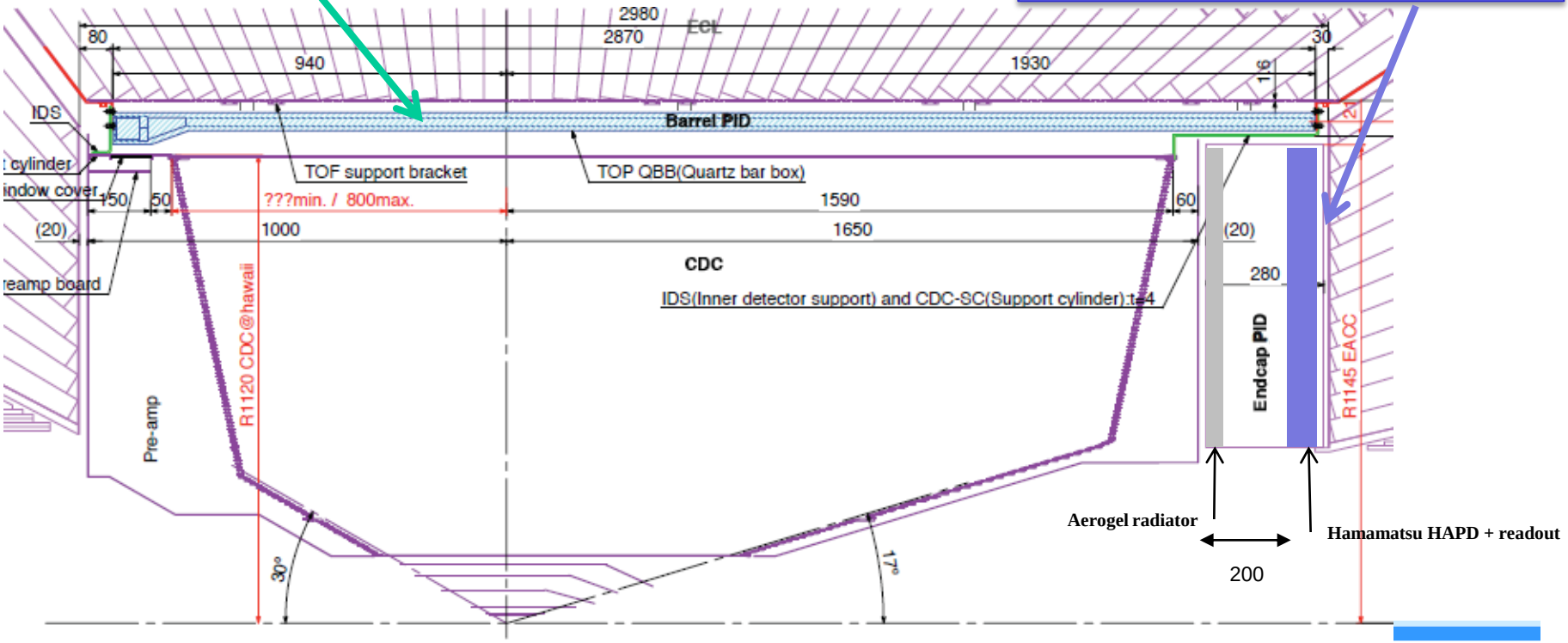

TOP counter

- Quartz radiator
  - 2.6m^{L} x 45cm^{W} x 2cm^{T}
  - Excellent surface accuracy
- MCP-PMT
  - Hamamatsu 16ch MCP-PMT
    - Good TTS (<35ps) & enough lifetime
    - Multialkali photo-cathode → SBA

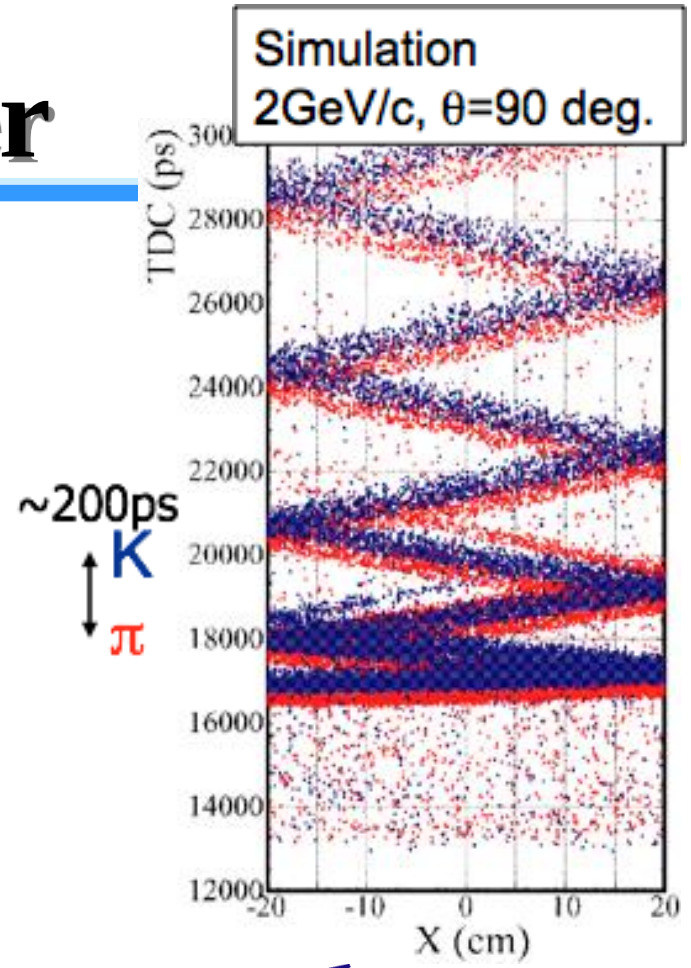

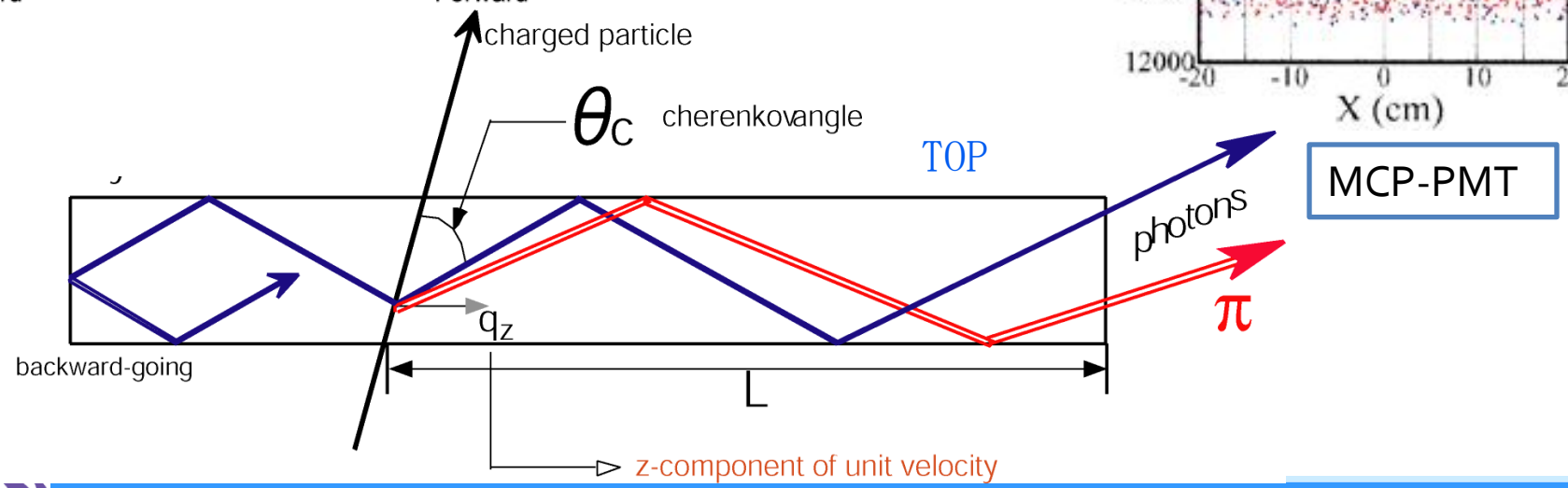

TOF ~ 1.2m

KLM

- Endcap & Barrel 2 lyrs
  - RPC → Scintillator+MPPC
  - (7-10)x40mm^2 scintillator strip+WLS
  - 14 layers Superlayer (X,Y)
  - MPPC from HPK
    - same design as T2K

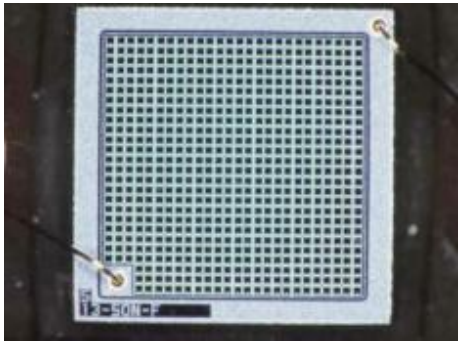

MPPC: Hamamatsu
1.3×1.3 mm 667 pixels
(used in T2K ND)

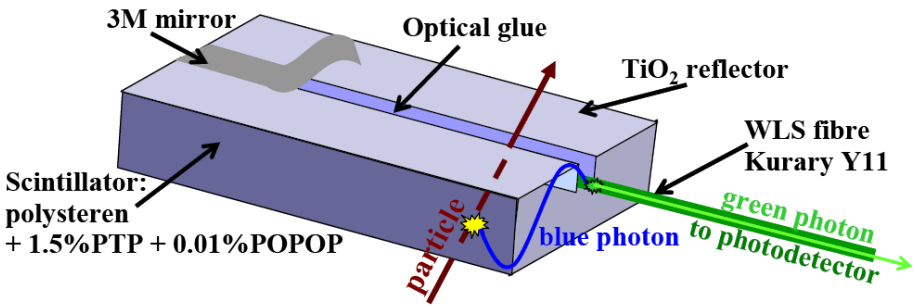

Mechanical Mockup

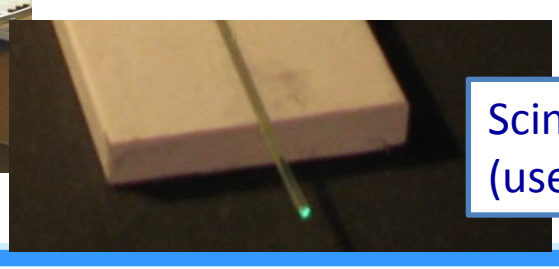

Scintillator bar: Vladimir (Russia)
(used in T2K ND)

Summary

Step1

Discovery of CPV in B decays

2001 summer !

Step2

Precise test of KM and SM

Step3

Search for NP

(SUSY, Extra-dim…)

Hints of NP

Establish procedures

LHC: New particle, masses

SuperKEKB: couplings

Understand NP→ ***need Both***

SuperB-factory

~50 ab^{-1} data (L ~10^{36}cm^{-2}s^{-1})

Summary

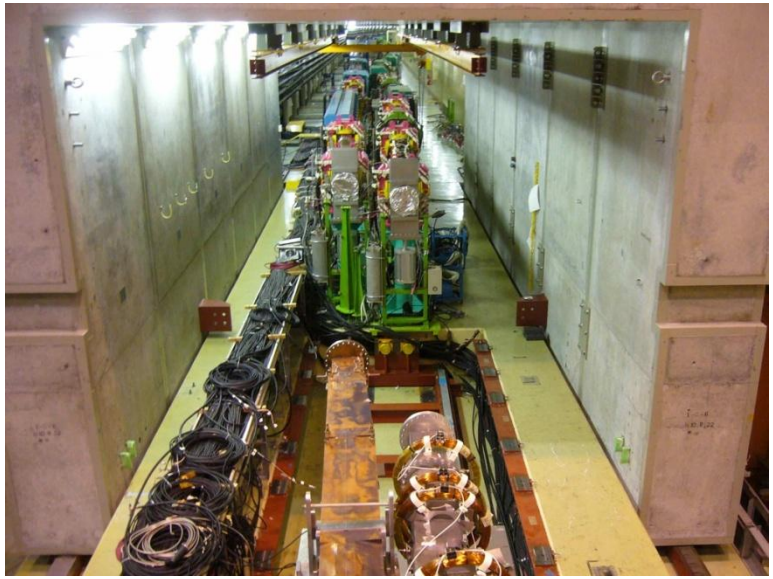

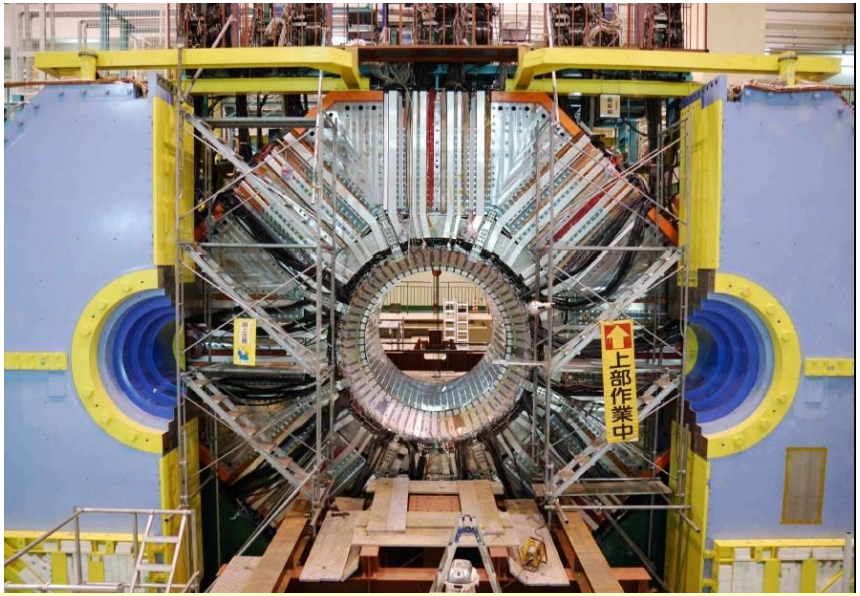

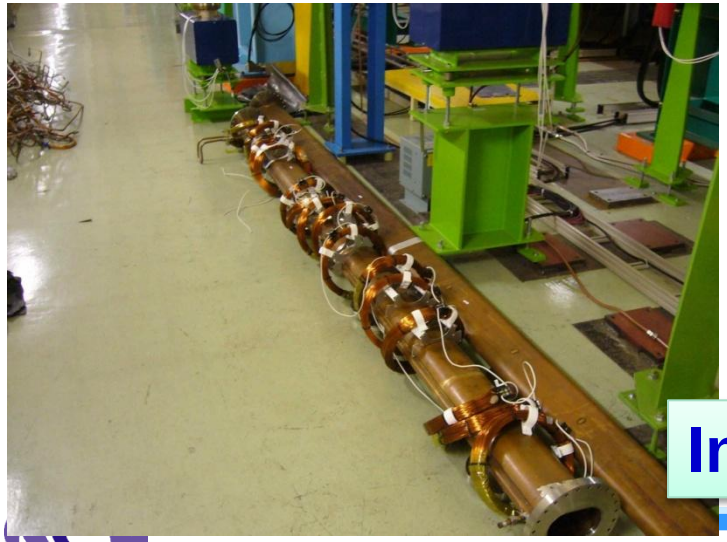

KEKB accelerator and Belle detector have been disassembled

SuperKEKB
Upgrade is on going !

International Collaboration is crucial !

Machine Parameters

2011/July/20	LER	HER	unit	
E	4.000	7.007	GeV	
I	3.6	2.6	A	
Number of bunches	2,500			
Bunch Current	1.44	1.04	mA	
Circumference	3,016.315		m	
$\varepsilon_x/\varepsilon_y$	3.2(1.9)/8.64(2.8)	4.6(4.4)/11.5(1.5)	nm/pm	0:zero current
Coupling	0.27	0.28		includes beam-beam
β_x^*/β_y^*	32/0.27	25/0.30	mm	
Crossing angle	83		mrad	
α_p	3.25×10^{-4}	4.55×10^{-4}		
σ_δ	$8.08(7.73)\times10^{-4}$	$6.37(6.31)\times10^{-4}$		0:zero current
V_c	9.4	15.0	MV	
σ_z	6.0(5.0)	5(4.9)	mm	0:zero current
ν_s	−0.0247	−0.0280		
ν_x/ν_y	44.53/44.57	45.53/43.57		
U_0	1.87	2.43	MeV	
$\tau_{x,y}/\tau_s$	43.1/21.6	58.0/29.0	msec	
ξ_x/ξ_y	0.0028/0.0881	0.0012/0.0807		
Luminosity	8×10^{35}		$cm^{-2}s^{-1}$	

Construction Schedule

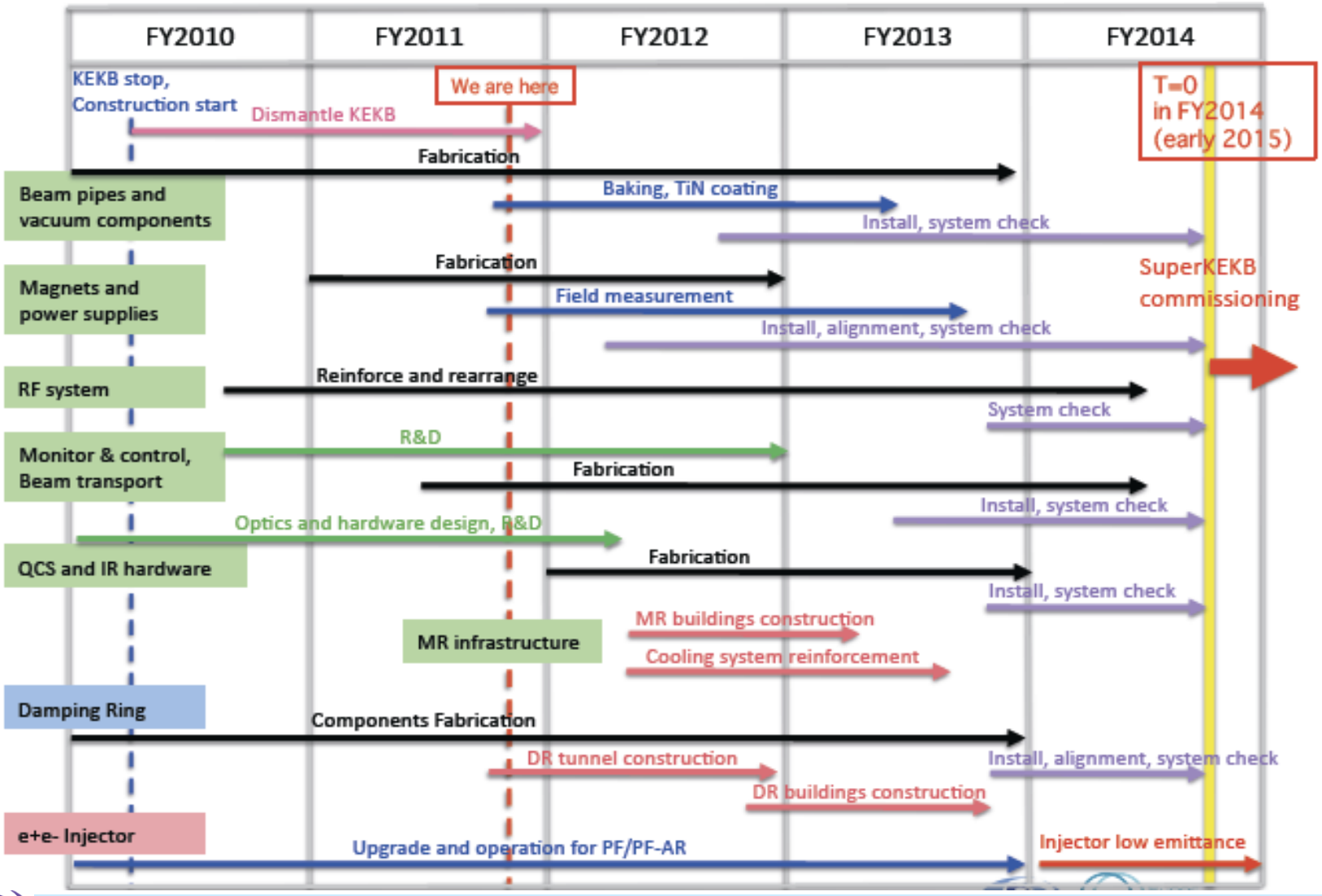

Kobayashi-Maskawa: CPV

CPV: due to **a complex phase** in the quark mixing matrix

CKM matrix

$$\begin{pmatrix} d' \\ s' \\ b' \end{pmatrix} = \begin{pmatrix} V_{ud} & V_{us} & V_{ub} \\ V_{cd} & V_{cs} & V_{cb} \\ V_{td} & V_{ts} & V_{tb} \end{pmatrix} \begin{pmatrix} d \\ s \\ b \end{pmatrix}$$

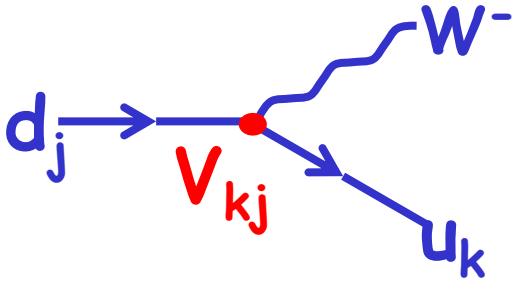

Wolfenstein representation

$$\begin{pmatrix} 1-\lambda^2/2 & \lambda & A\lambda^3(\rho - i\eta) \\ -\lambda & 1-\lambda^2/2 & A\lambda^2 \\ A\lambda^3(1-\rho-i\eta) & -A\lambda^2 & 1 \end{pmatrix}$$

Unitarity triangle

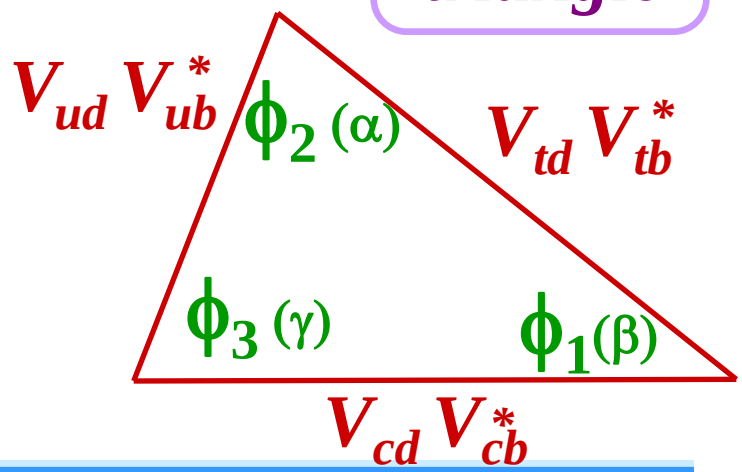

DAQ & Trigger

KEK, IHEP, Korea

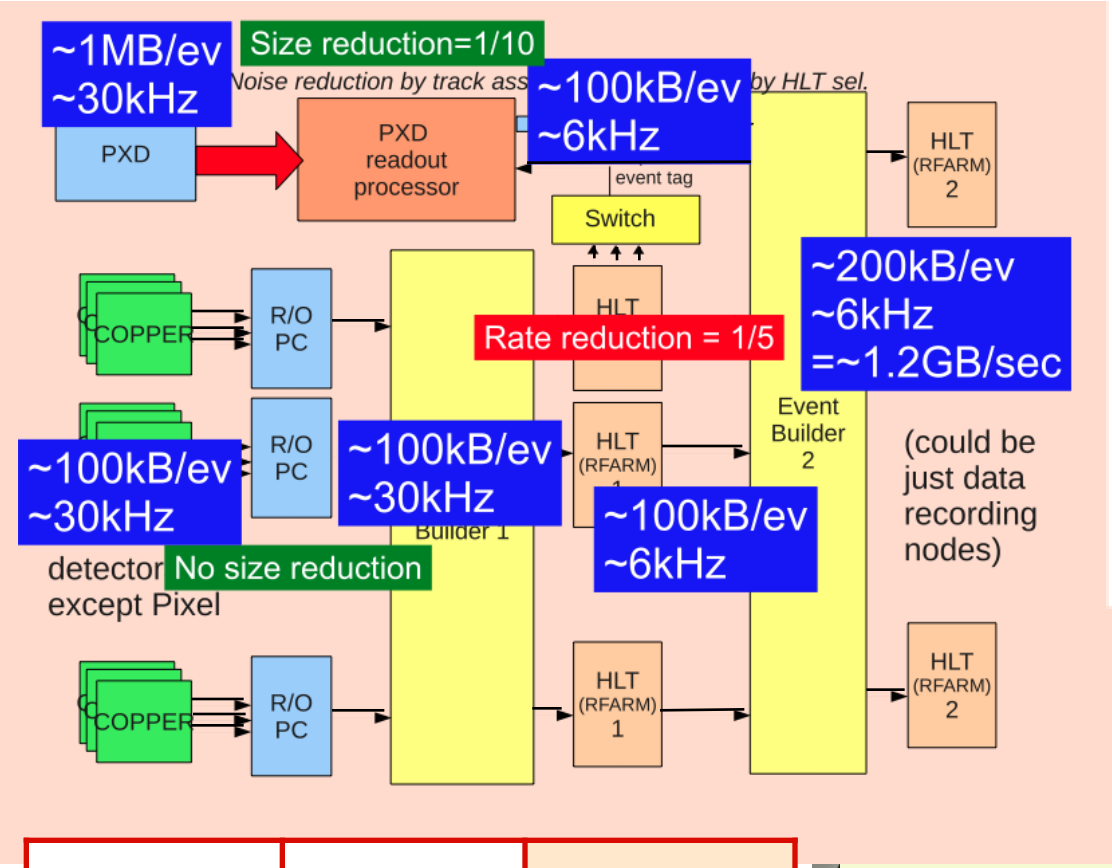

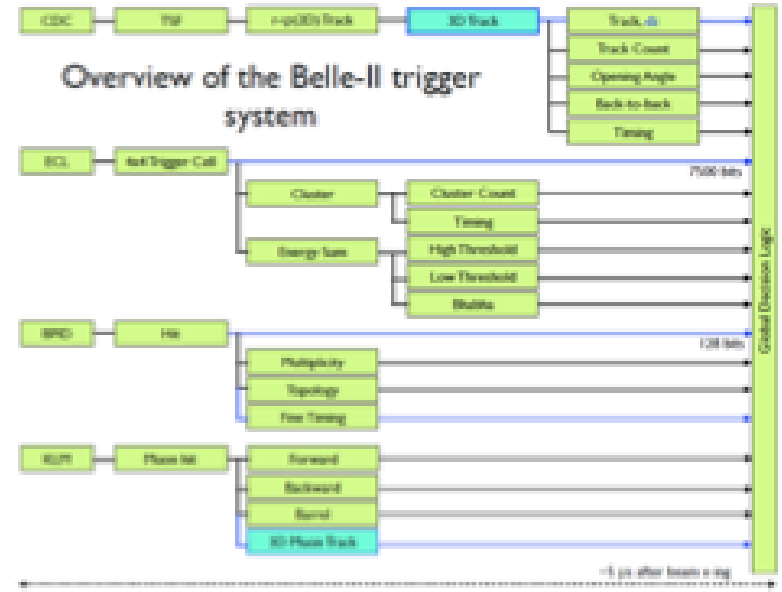

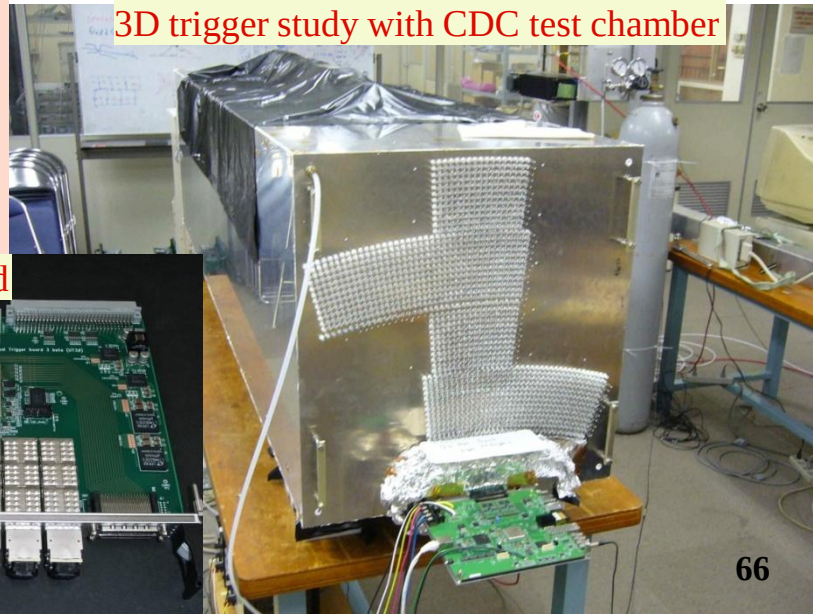

	Belle	Belle II
Trigger rate	500Hz	30kHz
Event size	40kB	300kB(max)

Computing

	HLT rate	event size
Belle II	3.6kHz	300kB
ATLAS	0.2kHz	1.6MB

~same amount of Accumulated data

Belle : Centralised computing → Belle II : Distributed computing

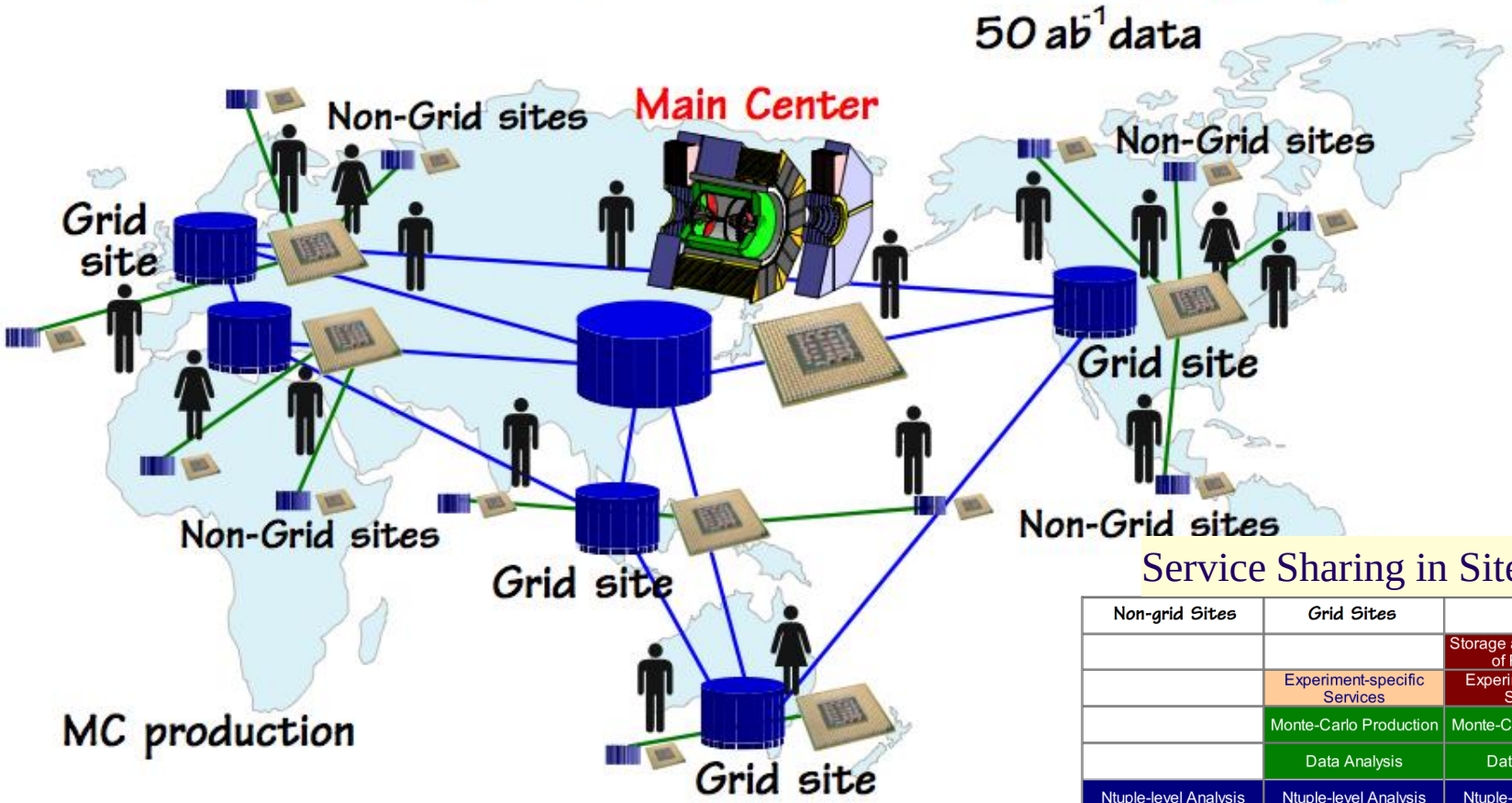

Service Sharing in Sites

Non-grid Sites	Grid Sites	KEK	
		Storage and Processing of Raw Data	Main Center
	Experiment-specific Services	Experiment-specific Services	
	Monte-Carlo Production	Monte-Carlo Production	Grid Resource
	Data Analysis	Data Analysis	
Ntuple-level Analysis	Ntuple-level Analysis	Ntuple-level Analysis	Local Resource
User Interface	User Interface	User Interface	

Physics at B factory

- **B physics (~1.1nb)**
  - CP violation & CKM
  - Rare decays

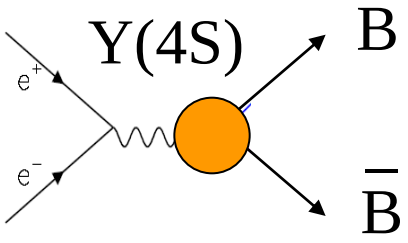

- **Charm physics (~1.3 nb)**

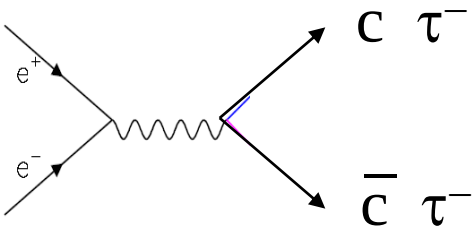

- **τ physics (~0.9nb)**

- **two-photon processes**

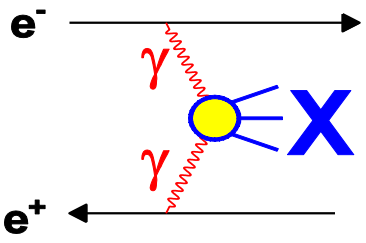

- **New Resonance**
  - ordinary & exotics

Variety of Physics !

Complement/Cooperative with τ/Charm factory !

Physics Prospects: τ/charm

Also, Super-Factory for **τ/charm** !

τ LFV decays

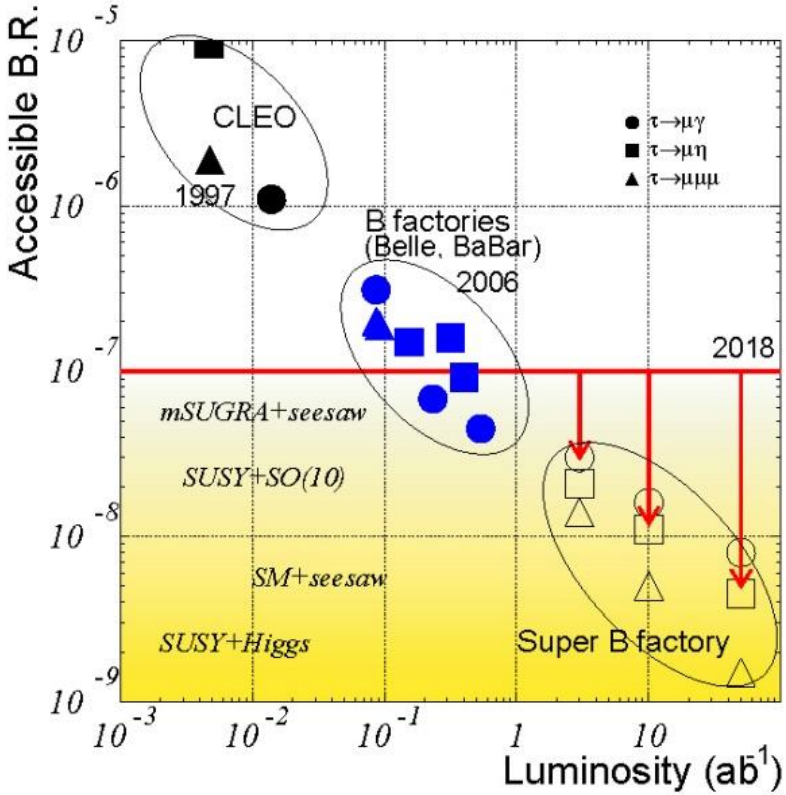

D^0-mixing

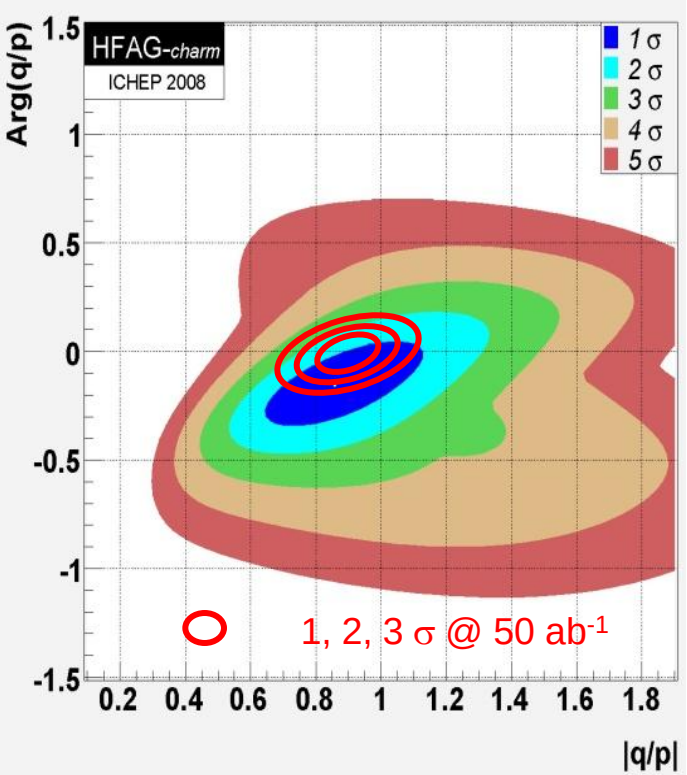

LFV, CPV in D/τ : Clear New Physics !

Lattice QCD with open boundary conditions

Stefan Schaefer

CERN

May 14, 2012

Based on work done in collaboration with Martin Lüscher

Problem

Rising cost as $a \to 0$

- Need more points for fixed volume $L =$const $\to N = L^4 a^{-4}$.
- Monte Carlo time scales as a^{-2}.
- Topological sectors emerge $\to$ simulation gets stuck

Solutions

- Fix topological sector.
  - Loss of unitarity.
  - Deal with $1/V$ corrections.
- Open the lattice.

Scaling in pure gauge theory

- Topological charge shows dramatic slow down: periodic b.c.
- Pure gauge theory

SOMMER, VIROTTA, ST.S'10

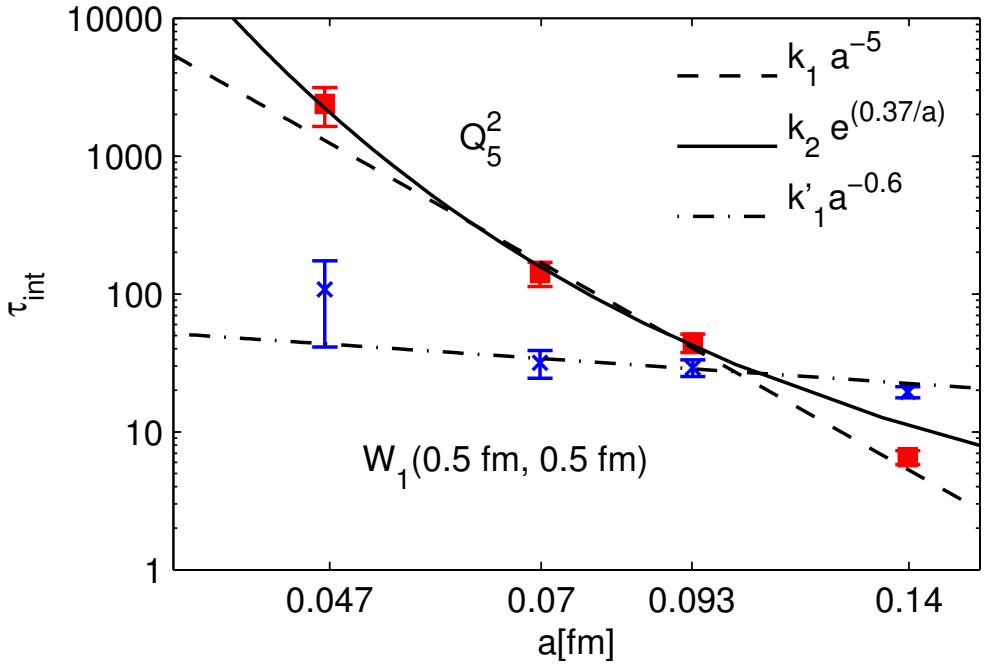

Topological Charge

Slowing down

- Topological sectors emerge in continuum limit.
- Simulation gets stuck.

Fermions

- Some folklore that fermions solve the problem.
- Distribution of Q gets narrower at light quark mass.
- Different effective gluonic action
  $\rightarrow$ influences coefficient.
- Slow topology observed, e.g., by MILC, ALPHA.

Open boundary conditions

Proposed solution

- open boundary condition in time direction
  $\rightarrow$ same transfer matrix, same particle spectrum
- periodic boundary condition in spatial directions
  $\rightarrow$ momentum projection possible

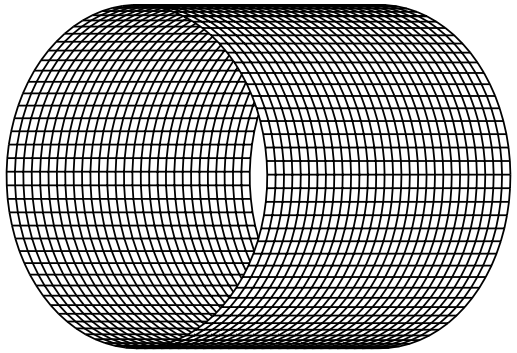

Open boundary conditions

- Periodic boundary conditions in space.
- Neumann boundary conditions in time.

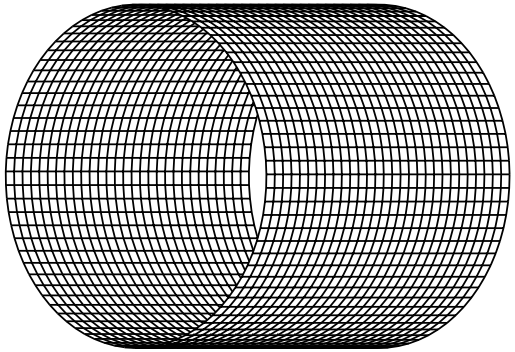

- Gauge fields

$$F_{0k}|_{x_0=0} = F_{0k}|_{x_0=T} = 0, \quad k = 1, 2, 3$$

- Fermion fields

$$P_+\psi(x)|_{x_0=0} = P_-\psi(x)|_{x_0=T} = 0 \qquad P_\pm = \frac{1}{2}(1 \pm \gamma_0)$$

$$\bar{\psi}(x)P_-|_{x_0=0} = \bar{\psi}(x)P_+|_{x_0=T} = 0$$

On shell improvement

Boundary terms

Gauge action

$$\delta S_{G,b} = \frac{1}{2g_0^2}(c_G - 1)\sum_{p_s} \mathrm{tr}(1 - U(p_s))$$

Fermion action

$$\delta S_{F,b} = a^3(c_F - 1)\sum_{\vec{x}} \left(\bar{\psi}(x)\psi(x)|_{x_0=a} + \bar{\psi}(x)\psi(x)|_{x_0=T-a}\right)$$

- Very similar to Schrödinger functional.
- If one stays clear of boundaries, might not be needed.

Pure gauge theory: $\tau_{\rm int}$ vs a^{-2}

M. LÜSCHER, ST.S, JHEP 1107 (2011) 036

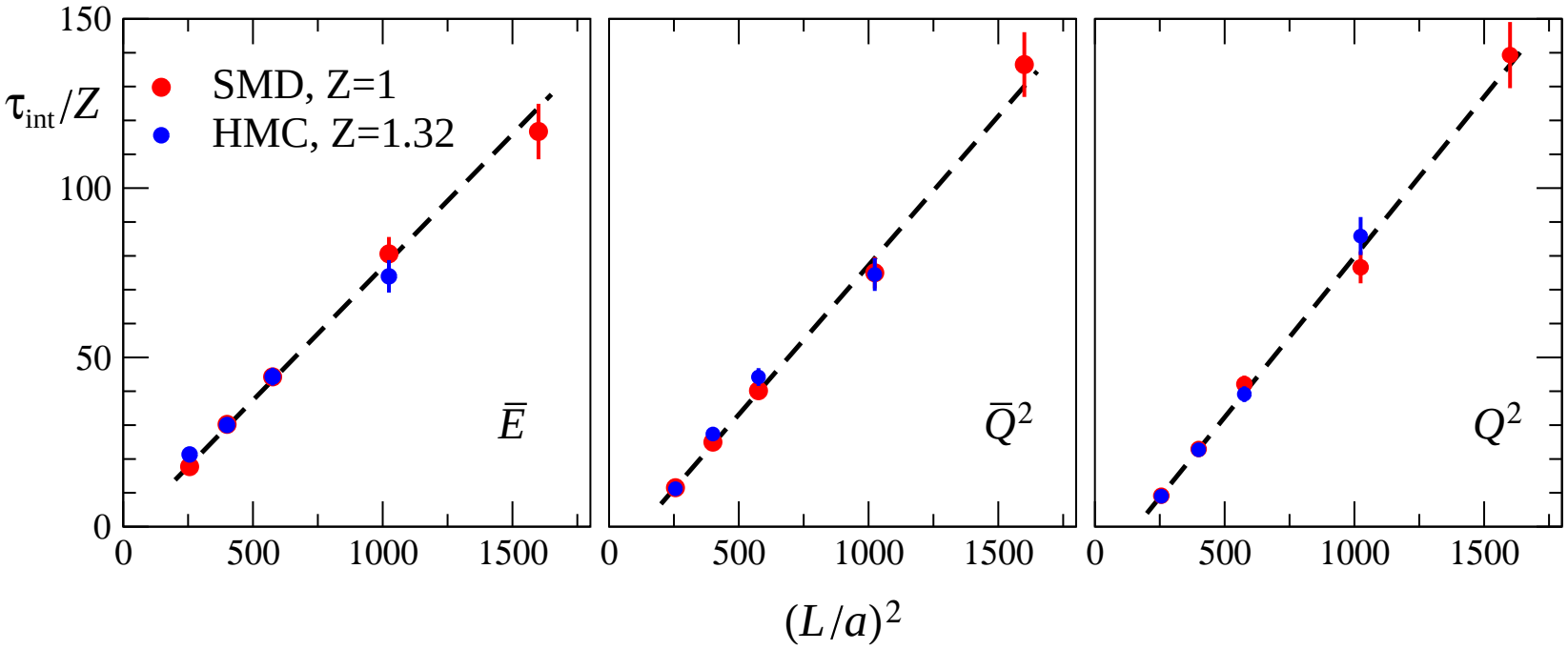

- L =const
- scaling linear in a^{-2}.
- no effect of sector forming visible.

Pure gauge theory: Periodic vs Open boundaries

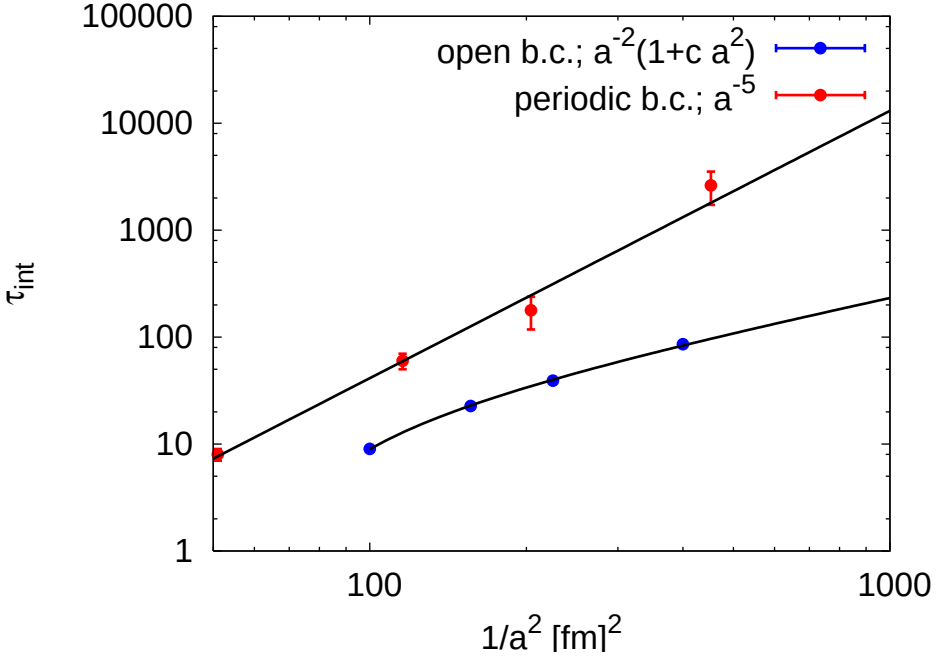

- Open boundary conditions solve problem.
- Scaling of the topological charge same as other observables.
- Already at typical a sizable improvement.

Large T

Finite volume

- For $T \to \infty$ the effect of the b.c. vanishes.
- But also the effect on observables vanishes as V^{-1}.

Dependence on T

- Width of distribution of Q is $\propto \sqrt{TL^3}$.
- Change of charge through boundary $\propto \sqrt{L^3}$.
  $\to$ expect $\tau_{\mathrm{int}} \propto T$, for random walk
- For each T, there is an a from which the boundary tunneling dominates over the bulk tunneling.

Analysis

- Physics in the center as with period. bound. cond.
- Boundary effects decay with lightest state of vaccuum quantum numbers. $\rightarrow 2\pi$
- How is the effect in actual simulations?

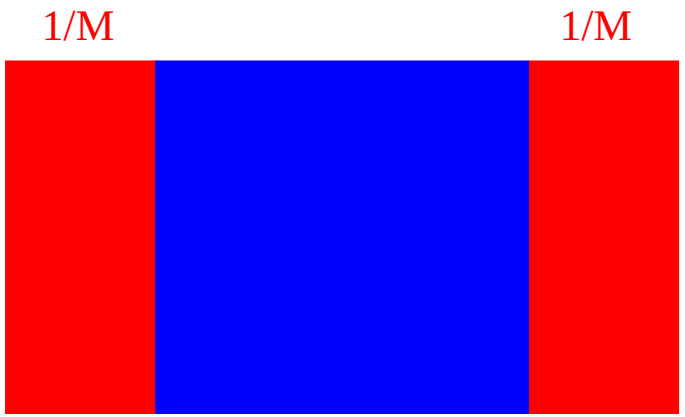

Setup

Action

- $N_\mathrm{f} = 2 + 1$ NP improved Wilson fermions
- Iwasaki gauge action
- 64×32^3 lattice with $a = 0.09$fm
- studied extensively by PACS-CS
- $m_\pi = 200$MeV; $m_\pi L = 3$

Reweighting

- Simulate fermion action with spectral gap.
- Include reweighting factor in measurement.
- Stabil simulation, no ergodicity problems.

Yang-Mills action density

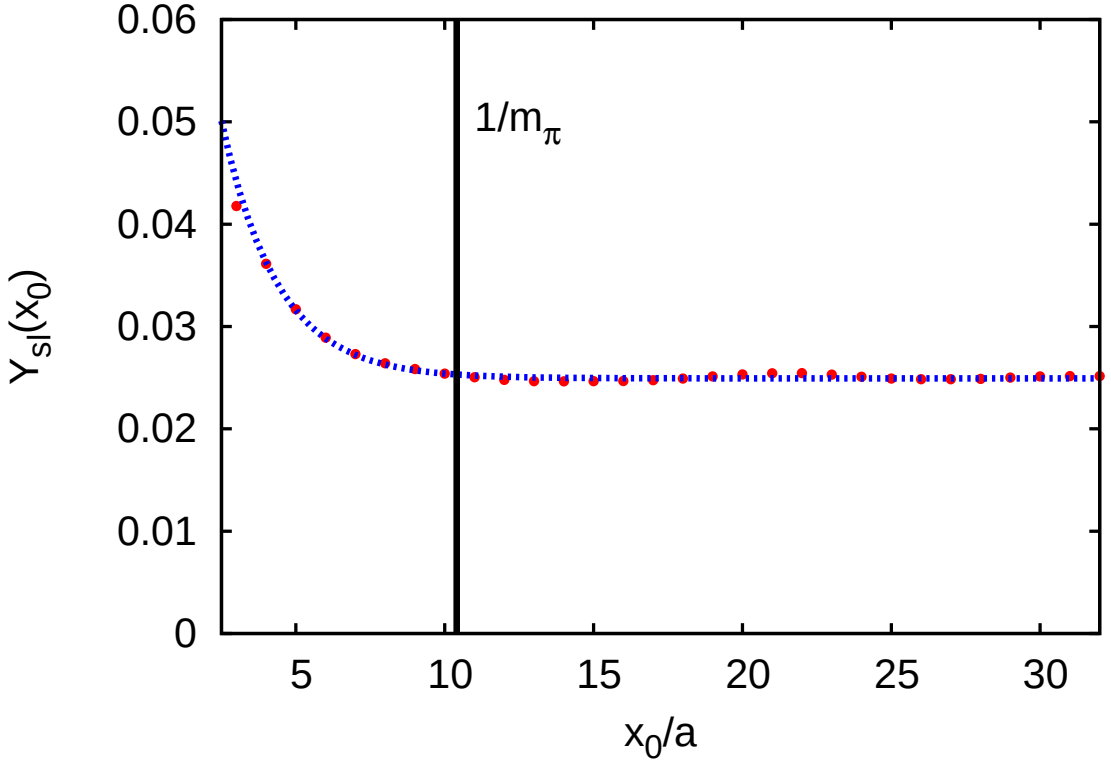

- Gauge action density from smoothed links.
- Boundary effects decay with mass ≈ 1GeV.
- $m_\pi \approx 200$MeV.

Boundary conditions

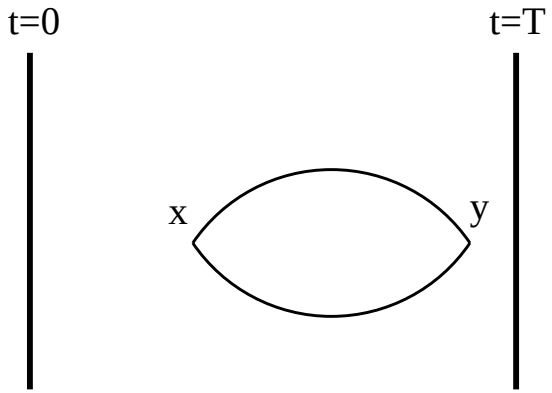

$$C(x_0, y_0) = \sum_{\mathbf{x},\mathbf{y}} \langle P(x_0, \mathbf{x}) P(y_0, \mathbf{y}) \rangle$$

- Source point y, zero momentum projection
- With periodic bc get $\cosh(m(x_0 - y_0))$ behavior

Open boundary conditions

Dirichlet boundary condtions for hadron propagator

$$C(x, y) \propto \sinh(m(T - x_0)) \qquad \text{for} \quad x_0 > y_0$$

Pseudoscalar Correlator

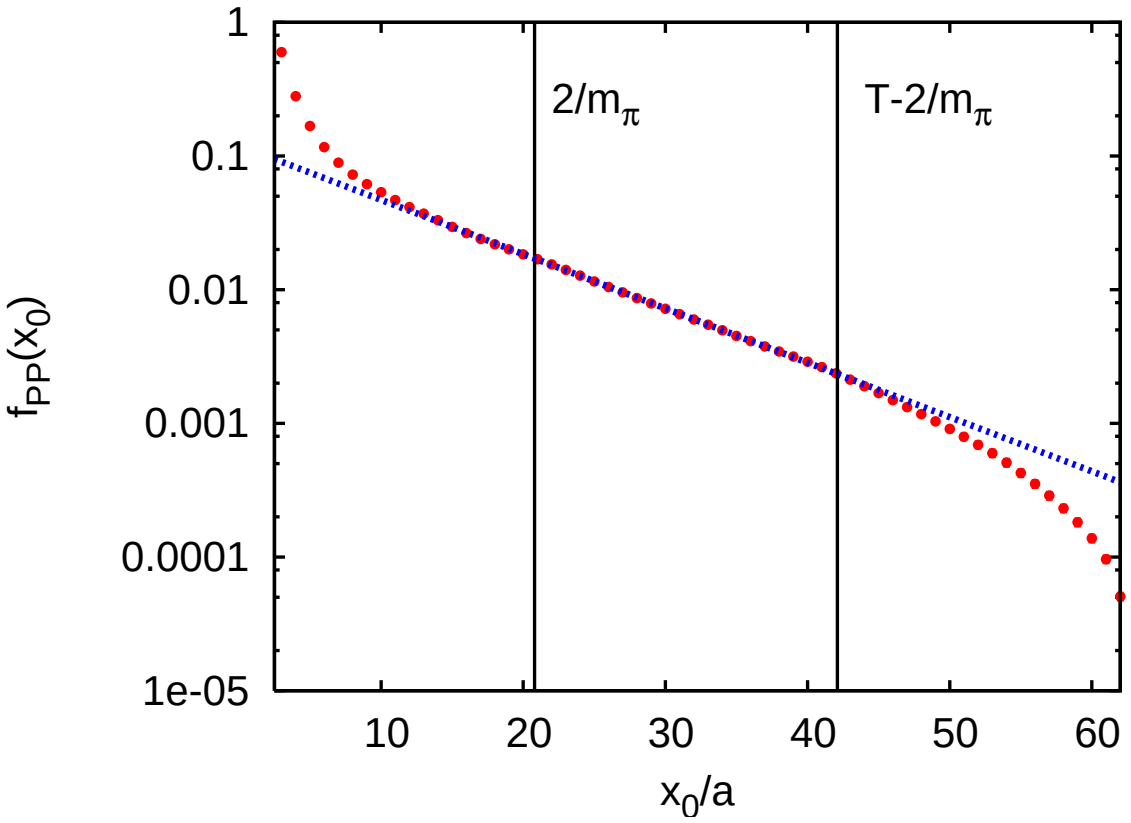

- source at $y_0/a = 1$
- exponential fall-off $2/m_\pi$ away from source/boundary

Pseudoscalar Correlator: effective mass

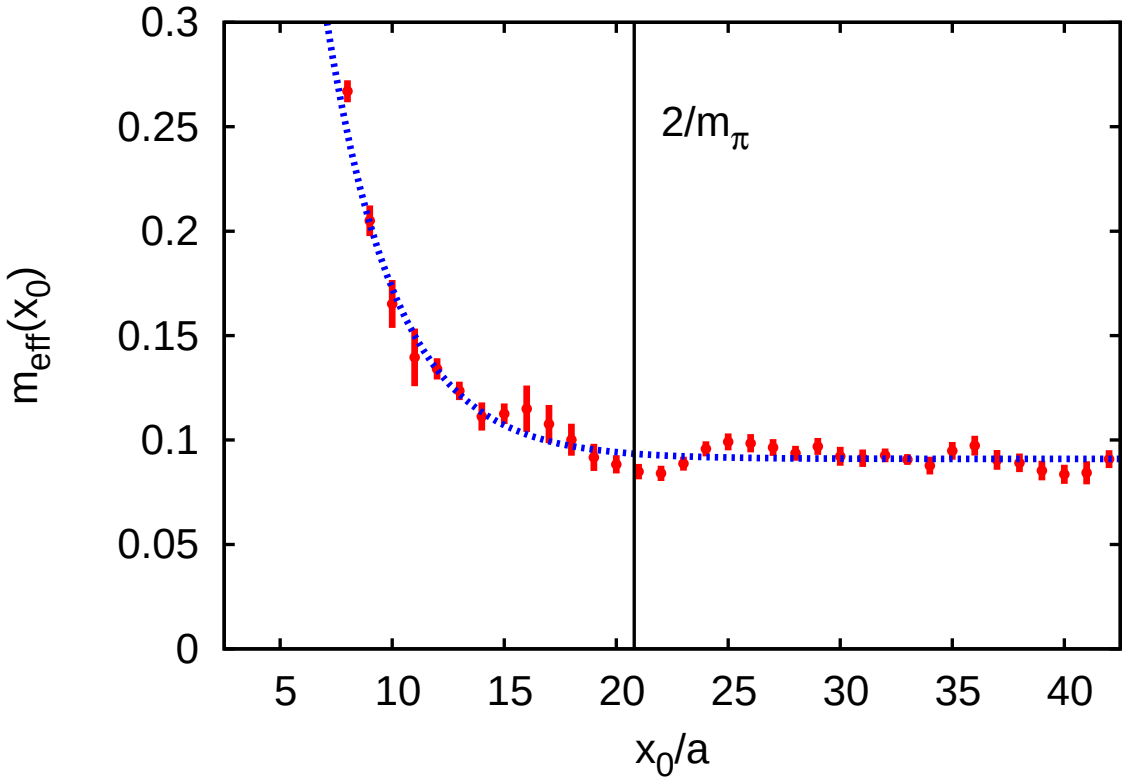

- Mass agrees with PACS-CS (interpolated) value

Effect of the position of the source

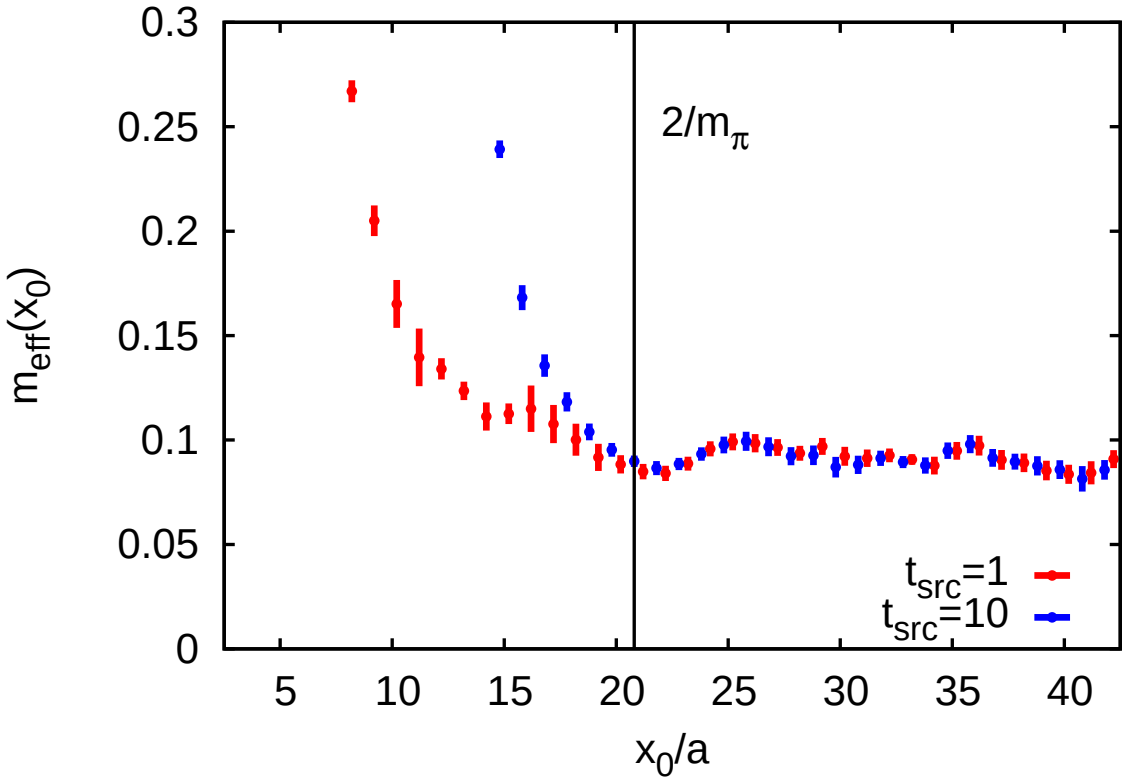

- Source on boundary couples strongy to excited states
- Plateau starts about at same time slice.

Conclusions

- Simulations with reduced rate of tunneling cannot produce accurate results.
- Open boundary conditions **in time** solve the problem of frozen topology.
- Fermion simulations without particular problems.
- Measurements $2/m_\pi$ from boundary.
- Reweighting makes Wilson simulations safe.

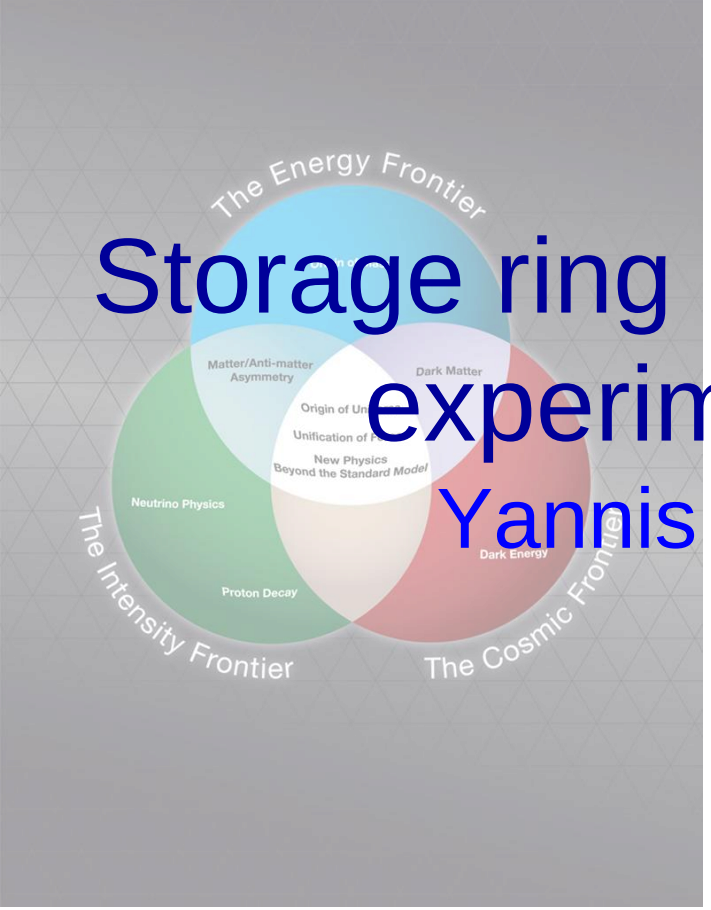

Storage ring Electric Dipole Moment experiment for the proton

Yannis K. Semertzidis, BNL

✓Goal: 10^{-29} e□cm; Probe New Physics ~10^3 TeV

✓Systematics best in an all-electric ring and counter-rotating (CR) beams.

Why is there so much matter after the Big Bang;

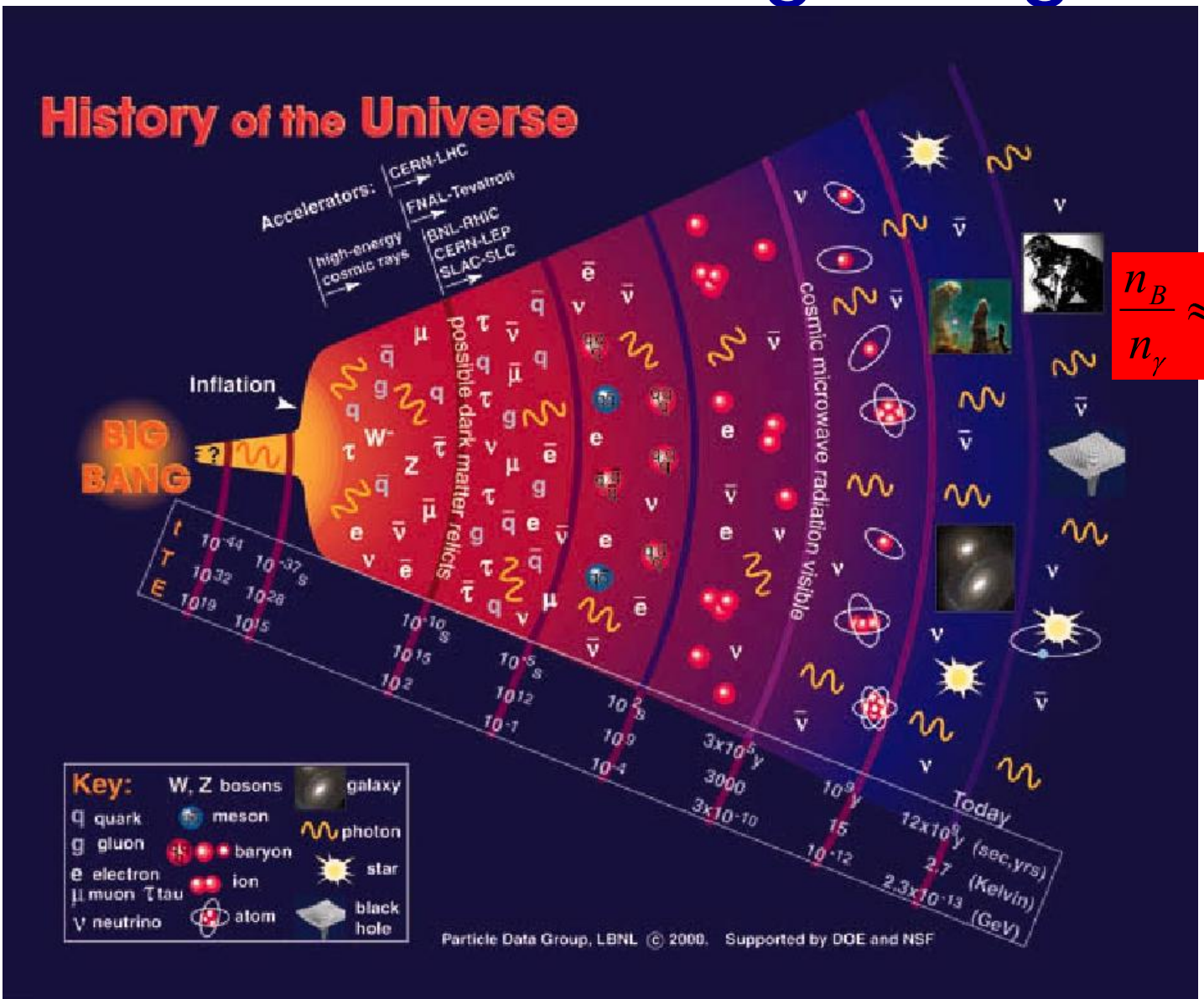

We see:

$$\frac{n_B}{n_\gamma} \approx (6.08 \pm 0.14) \times 10^{-10}$$

From the SM:

$$\frac{n_B}{n_\gamma} = \frac{n_{\bar{B}}}{n_\gamma} \approx 10^{-18}$$

Spin is the only vector defining a direction of a “fundamental” particle with spin

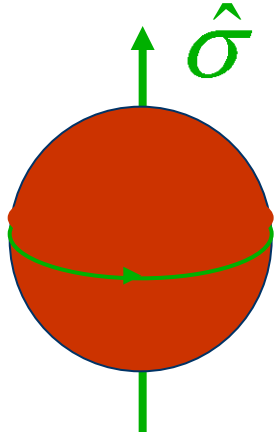

$\vec{d} = 0$

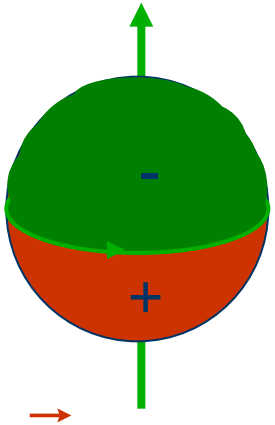

$\vec{d} = d\hat{\sigma}$

Electric Dipole Moment: two possibilities

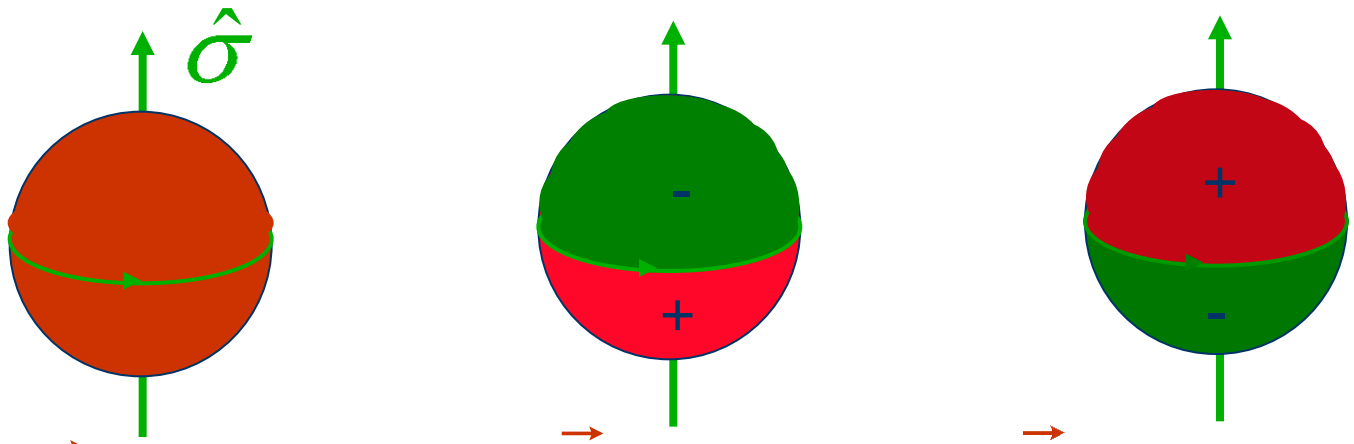

$\vec{d} = 0$ $\quad$ $\vec{d} = d\hat{\sigma}$ $\quad$ $\vec{d} = -d\hat{\sigma}$

If we discover that the proton

- Has a non-zero EDM value, i.e. prefers only one of the two possible states:

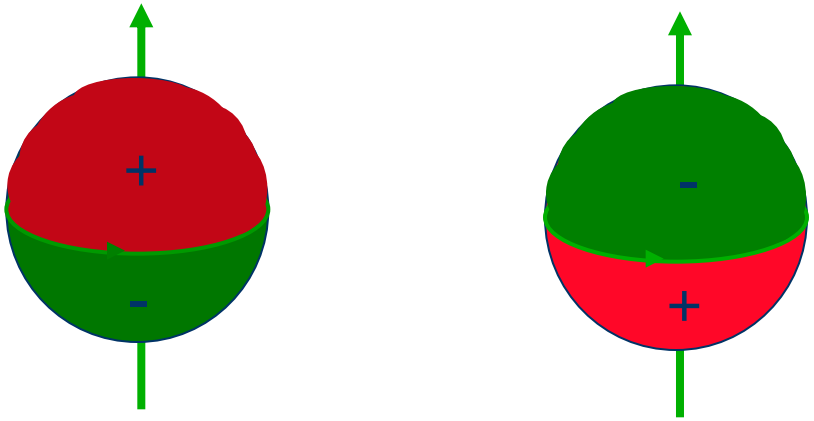

- Then P and T symmetries are violated and through CPT, CP-symmetry is also violated.
- CP-violation is one of three necessary conditions to obtain a matter dominated universe starting from a symmetric one…

Purcell and Ramsey:

"The question of the possible existence of an electric dipole moment of a nucleus or of an elementary particle…becomes a purely <u>experimental</u> matter"

Phys. Rev. 78 (1950)

Short History of EDM

- 1950's neutron EDM experiment started to search for parity violation (Ramsey and Purcell).
- After P-violation → EDMs require both P,T-Violation
- 1960's EDM searches in atomic systems
- 1970's Indirect Storage Ring EDM method from the CERN muon g-2 exp.
- 1980's Theory studies on systems (molecules) w/ large enhancement factors
- 1990's First exp. attempts w/ molecules. Dedicated Storage Ring EDM method developed
- 2000's Proposal for sensitive dEDM exp. developed.
- 2010's Proposal for sensitive pEDM exp. developed.

- Muon g-2: Precision physics in a Storage Ring

- Statistics limited… to improve sensitivity by a factor of 4 at Fermilab

Muon g-2: 4 Billion e^+ with E>2GeV

$$dN/dt = N_0 e^{-\frac{t}{\tau}} \left[1 + A\cos\left(\omega_a t + \phi_a\right) \right]$$

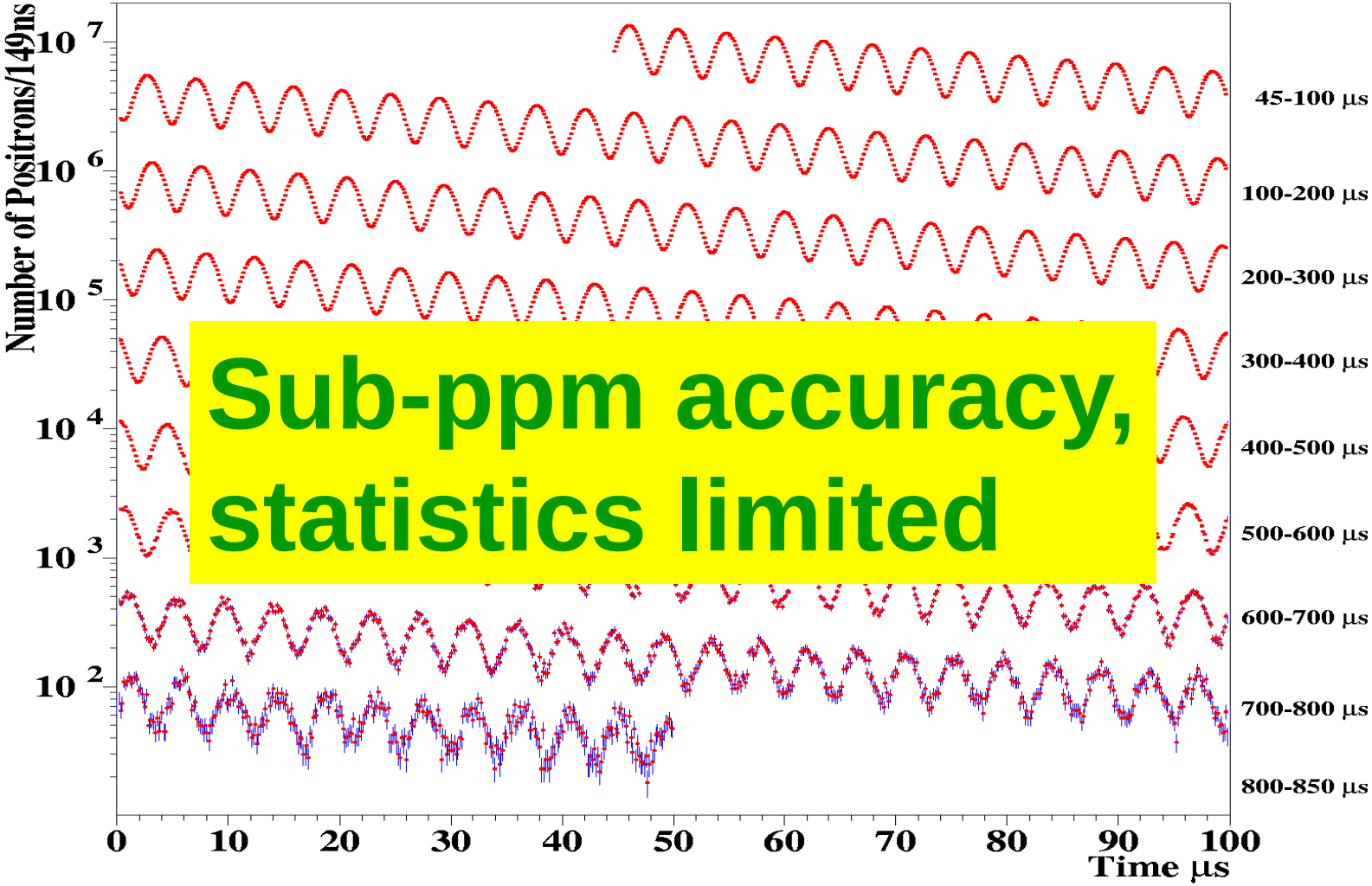

Sub-ppm accuracy, statistics limited

Breakthrough concept: Freezing the horizontal spin precession due to E-field

$$\vec{\omega}_a = \frac{e}{m}\left\{ a\vec{B} + \left[a - \left(\frac{m}{p}\right)^2 \right] \frac{\vec{\beta} \times \vec{E}}{c} \right\}$$

Muon g-2 focusing is electric: The spin precession due to E-field is zero at "magic" momentum (3.1GeV/c for muons, 0.7 GeV/c for protons,…)

$$p = \frac{m}{\sqrt{a}}, \text{ with } a = \frac{g-2}{2}$$

The "magic" momentum concept was used in the muon g-2 experiments at CERN, BNL, and …next at FNAL.

The proton EDM uses an ALL-ELECTRIC ring: spin is aligned with the momentum vector

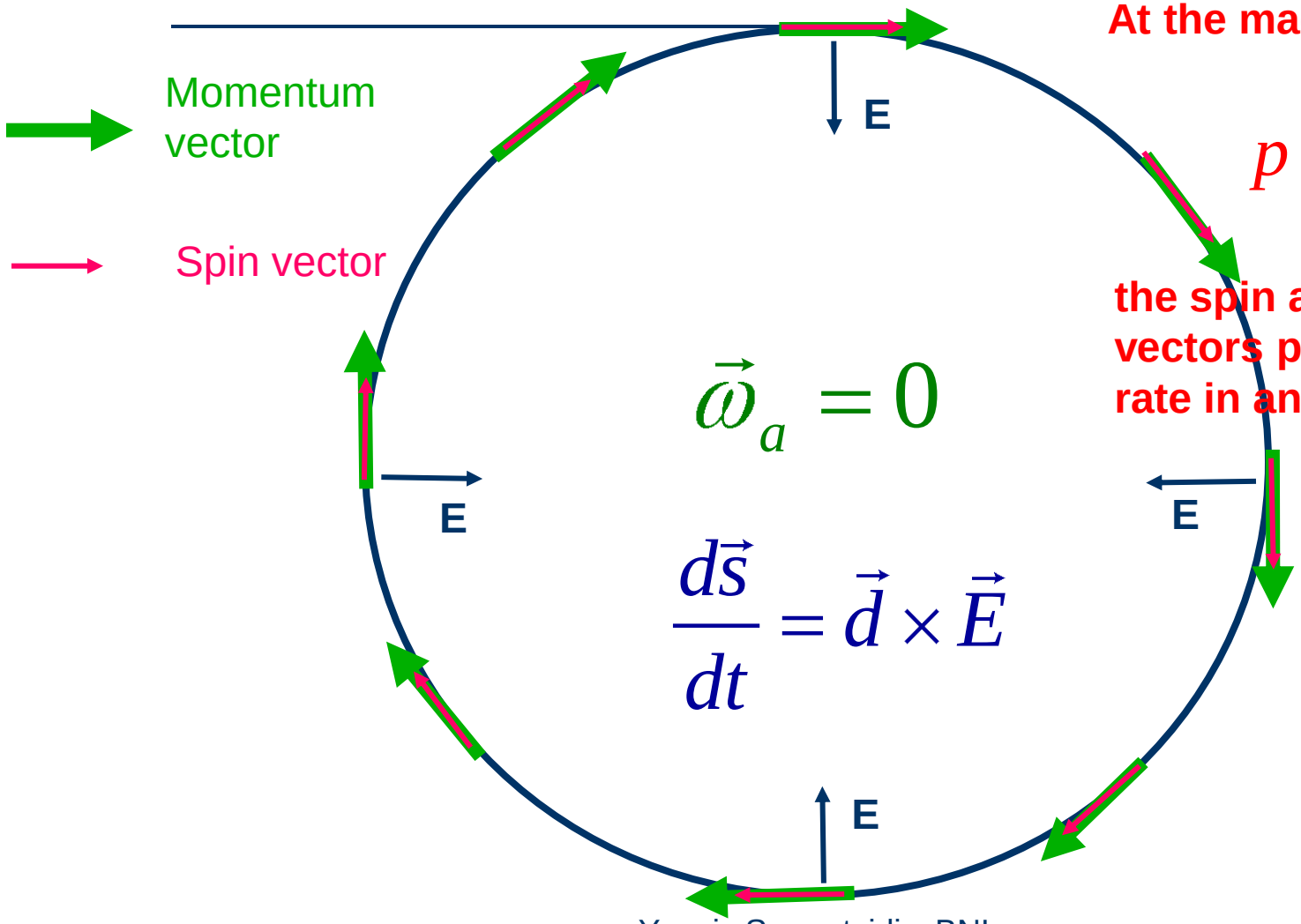

At the magic momentum

$$p = \frac{m}{\sqrt{a}}$$

the spin and momentum vectors precess at same rate in an E-field

$$\vec{\omega}_a = 0$$

$$\frac{d\vec{s}}{dt} = \vec{d} \times \vec{E}$$

Is the polarimeter analyzing power good at P_{magic}? YES!

Analyzing power can be further optimized

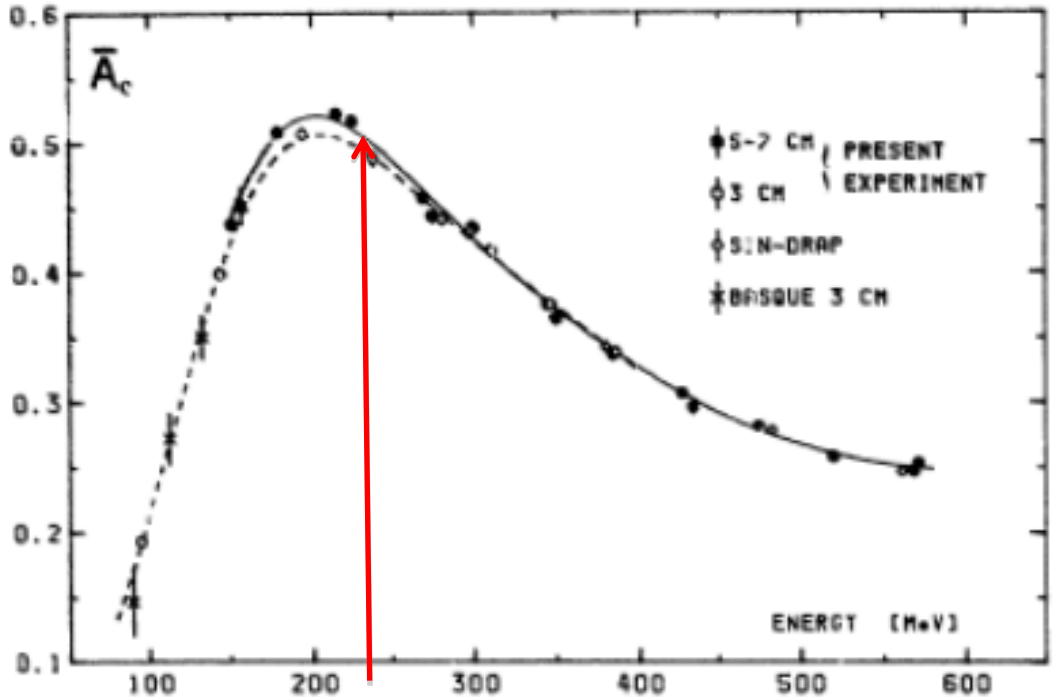

Fig. 4. Angle-averaged effective analyzing power. Curves show our fits. Points are the data included in the fits. Errors are statistical only

Fig.4. The angle averaged effective analyzing power as a function of the proton kinetic energy. The magic momentum of 0.7GeV/c corresponds to 232MeV.

The proton EDM ring

As shown on the March 2011 review with limited straight-section length

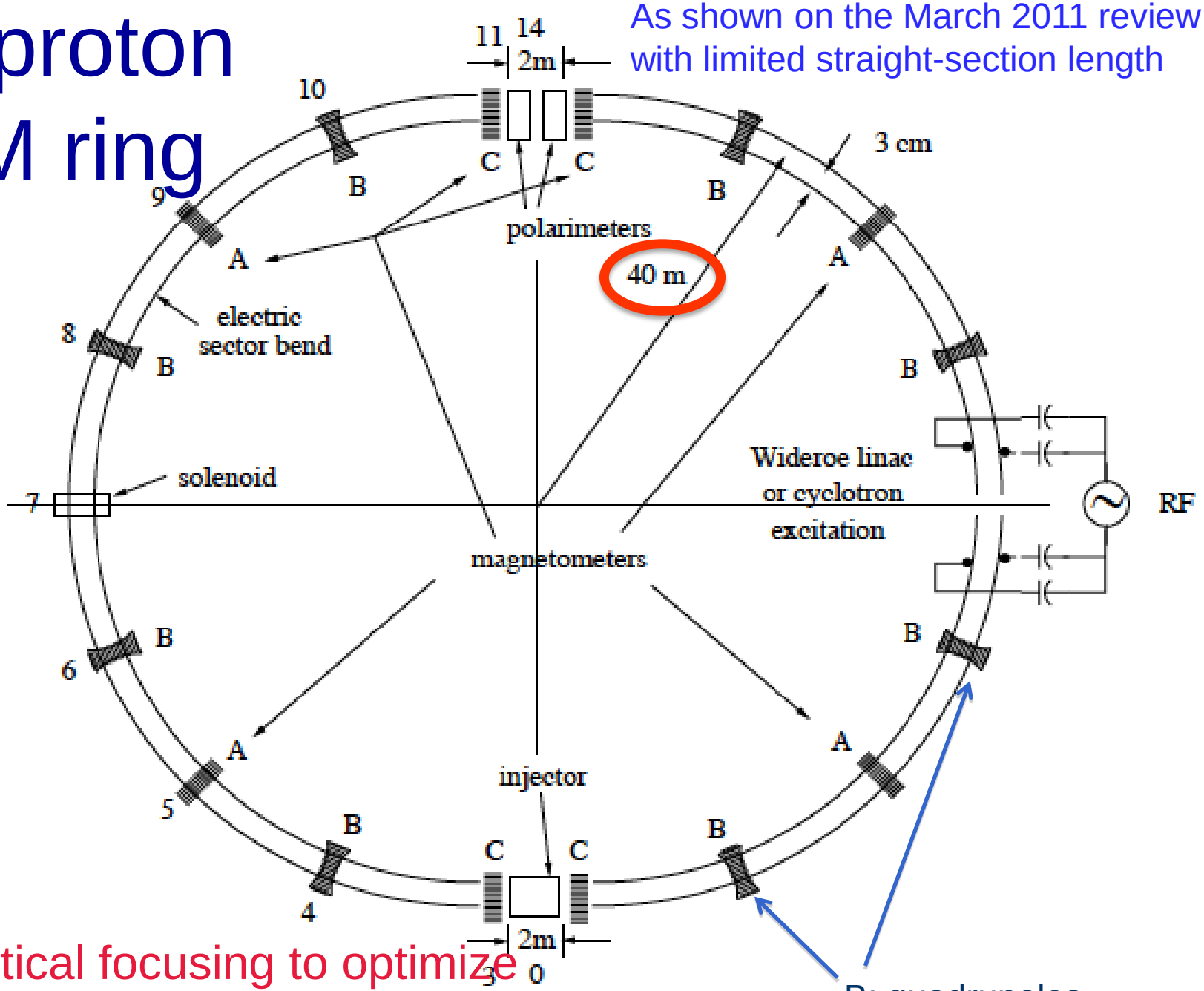

Weak vertical focusing to optimize SCT and BPM operation

B: quadrupoles

Important Stages in an EDM Experiment

1. Polarize: state preparation, intensity of beams

2. Interact with an E-field: the higher the better

3. Analyze: high efficiency analyzer

4. Scientific Interpretation of Result! Easier for the simpler systems (theory; lattice?)

The grand issues in the proton EDM experiment

1. BPM magnetometers (need to demonstrate in a storage ring environment)
2. Polarimeter development: high efficiency, small systematic errors
3. Spin Coherence Time (SCT): study at COSY/simulations; Simulations for an all-electric ring: SCT and systematic error studies
4. Electric field development for large surface area plates

Clock-wise (CW) & Counter-Clock-wise Storage

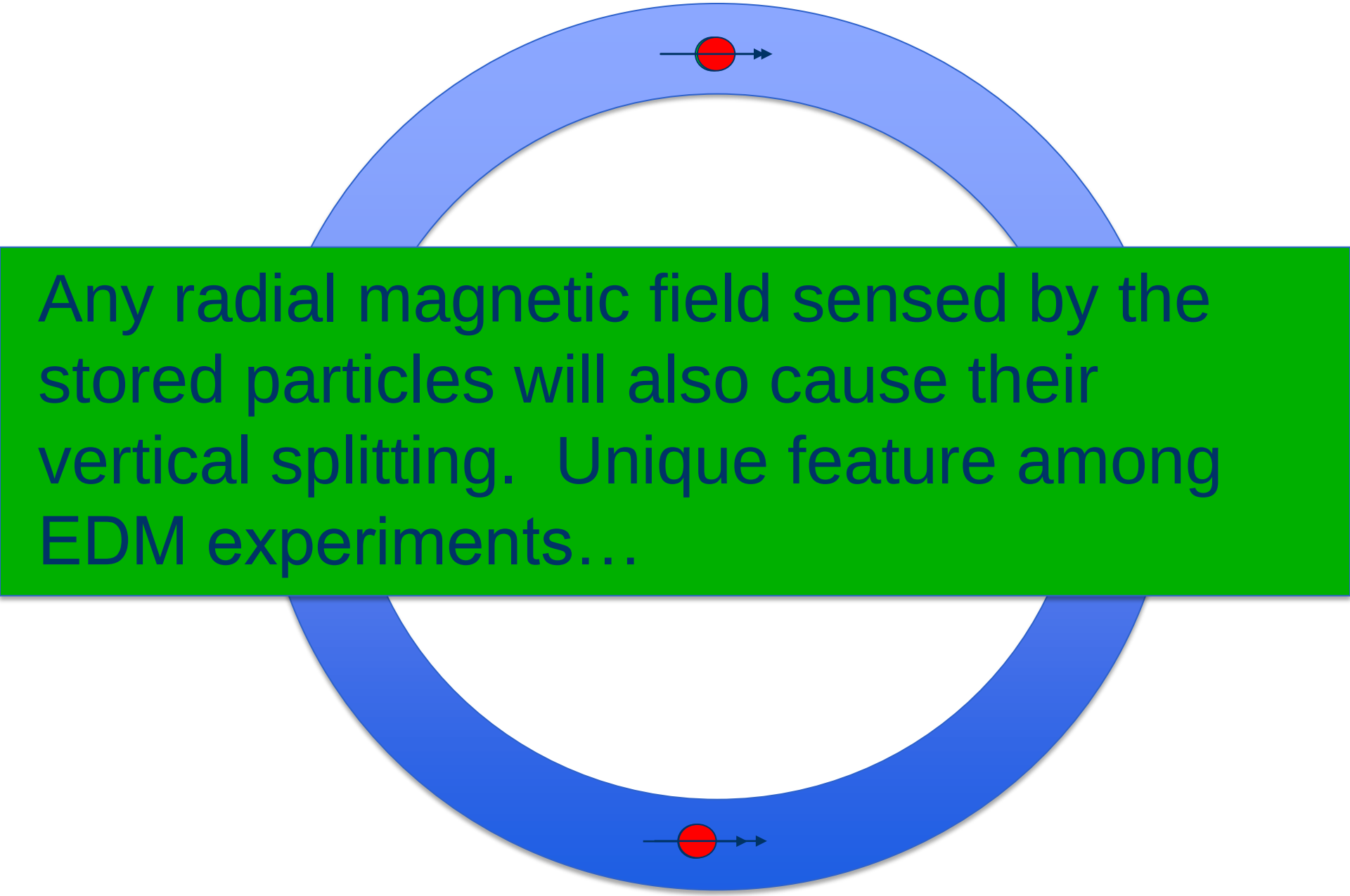

Any radial magnetic field sensed by the stored particles will also cause their vertical splitting. Unique feature among EDM experiments…

1. Beam Position Monitors

- Technology of choice: Low T_c SQUIDS, signal at 10^2-10^4Hz (10% vertical tune modulation)
- R&D sequence: (First funding from US-Japan)

1. Operate SQUIDS in a magnetically shielded area-reproduce current state of art
2. Operate in RHIC at an IP (evaluate noise in an accelerator environment);
3. Operate in E-field string test

2. Polarimeter Development

- Polarimeter tests with runs at COSY (Germany) demonstrated < 1ppm level systematic errors: N. Brantjes et al., NIM A **664**, 49, (2012)

- Technologies under investigation:

1. Micro-Megas/Greece: high rate, pointing capabilities, part of R&D for ATLAS upgrade
2. MRPC/Italy: high energy resolution, high rate capability, part of ALICE development

3. Spin Coherence Time: need >10^2 s

- Not all particles have same deviation from magic momentum, or same horizontal and vertical divergence (all second order effects)

- They cause a spread in the g-2 frequencies:

$$d\omega_a = a\vartheta_x^2 + b\vartheta_y^2 + c\left(\frac{dP}{P}\right)^2$$

- Present design parameters allow for 10^3 s. Cooling/mixing during storage could prolong SCT (upgrade option?).

SCT Development

- We have a SCT working solution (precision tracking and analytically-work in progress).
- Tests with polarized deuterons and protons at COSY to benchmark software
- Test runs at COSY are very encouraging.
- Bonus: Electric ring with weak vertical focusing →SCT is long enough for 10^3s storage

4. Electric Field Development

- ✓ Reproduce Cornell/JLAB results of stainless steel plates treated with high pressure water rinsing (part of ILC/ERL development work)

Recent Progress from ILC/ERL R&D (~5mm gap tests) Cornell/JLab

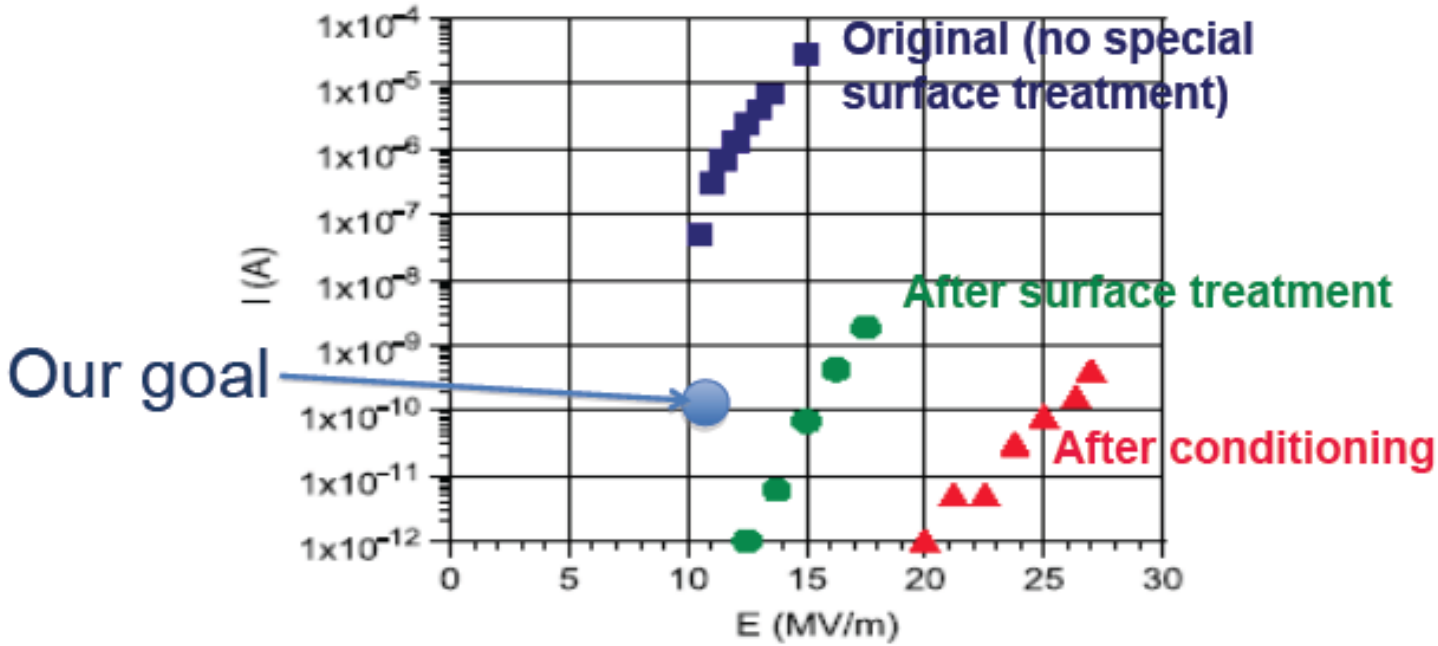

Large Scale Electrodes, New: pEDM electrodes with HPWR

Parameter	Tevatron pbar-p Separators	BNL K-pi Separators	pEDM
Length	2.6m	4.5m	3m
Gap	5cm	10cm	3cm
Height	0.2m	0.4m	0.2m
Number	24	2	10^2
Max. HV	±180KV	±200KV	±150KV

E-field plate module: Similar to the (26) FNAL Tevatron ES-separators

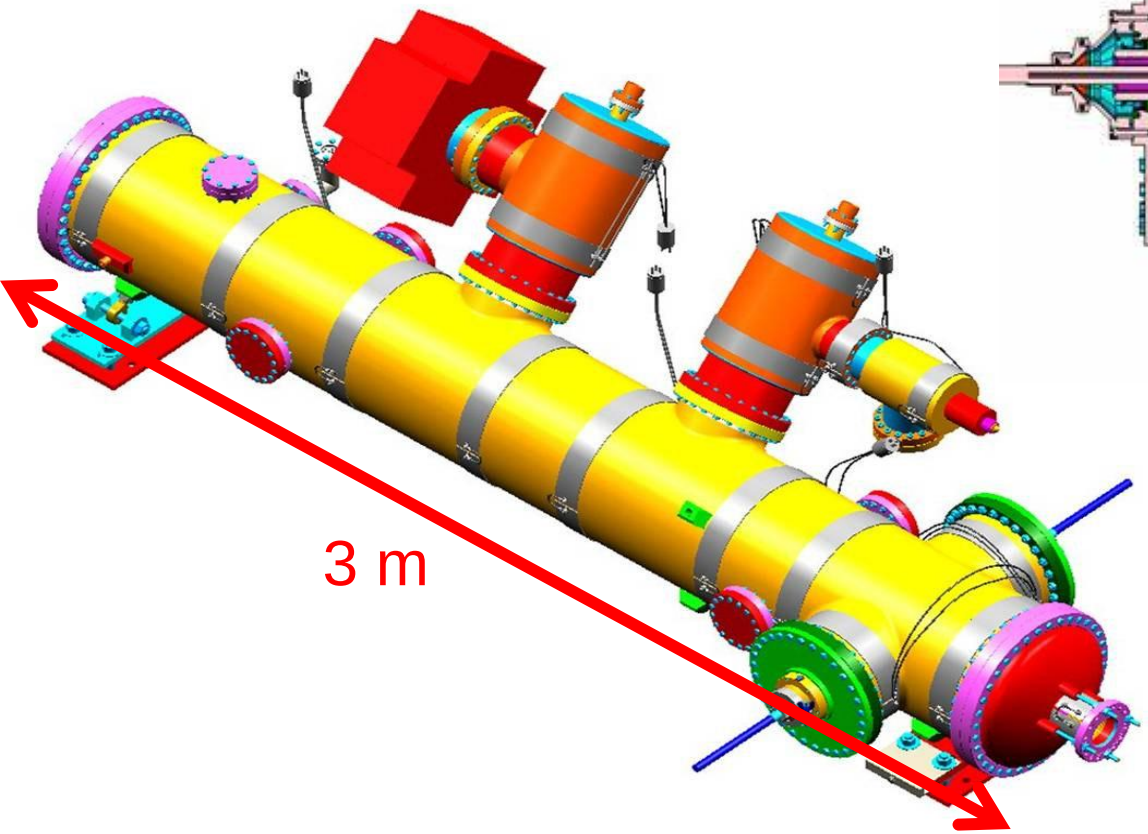

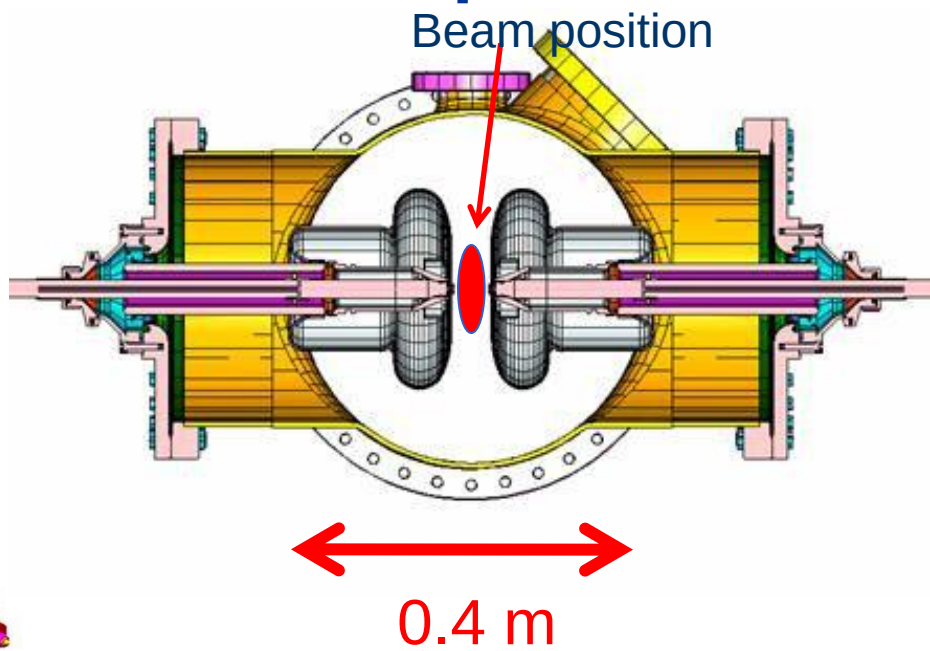

E-field plate module: Similar to the (26) FNAL Tevatron ES-separators

position

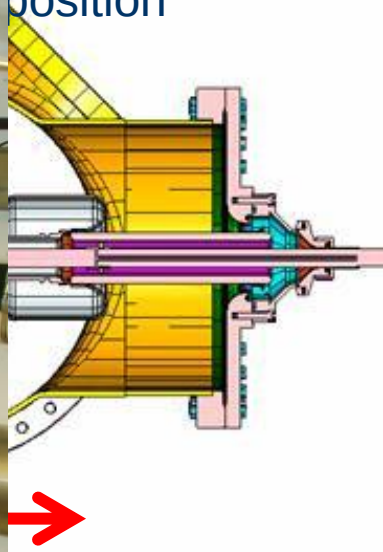

The miracles that make the pEDM

1. Magic momentum (MM): high intensity charged beam in an all-electric storage ring
2. High analyzing power: A>50% at the MM
3. Weak vertical focusing in an all-electric ring: SCT allows for 10^3s beneficial storage; prospects for much longer SCT with mixing (cooling and heating)

4. The beam vertical position tells the average radial B-field; the main systematic error source

Technically driven pEDM timeline

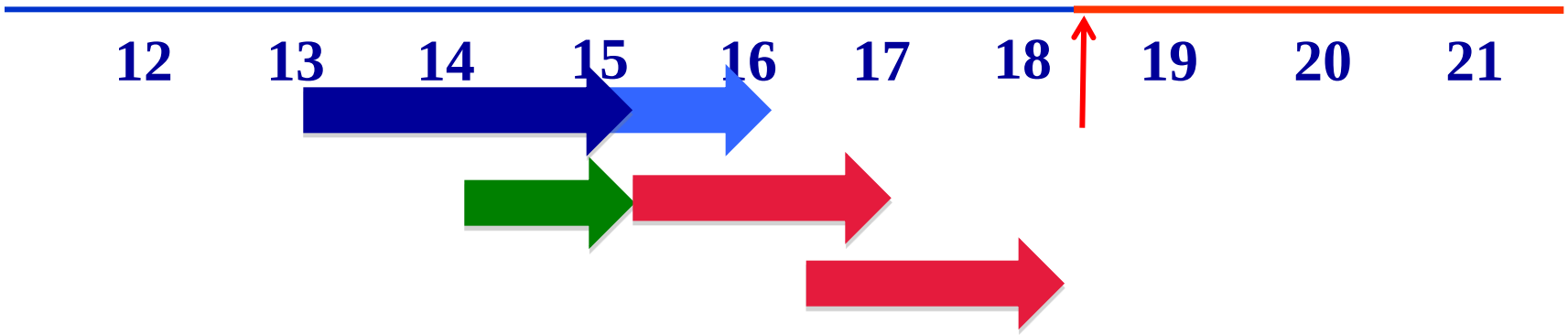

- Two years R&D
- One year final ring design
- Two years ring/beam-line construction
- Two years installation
- One year “string test”

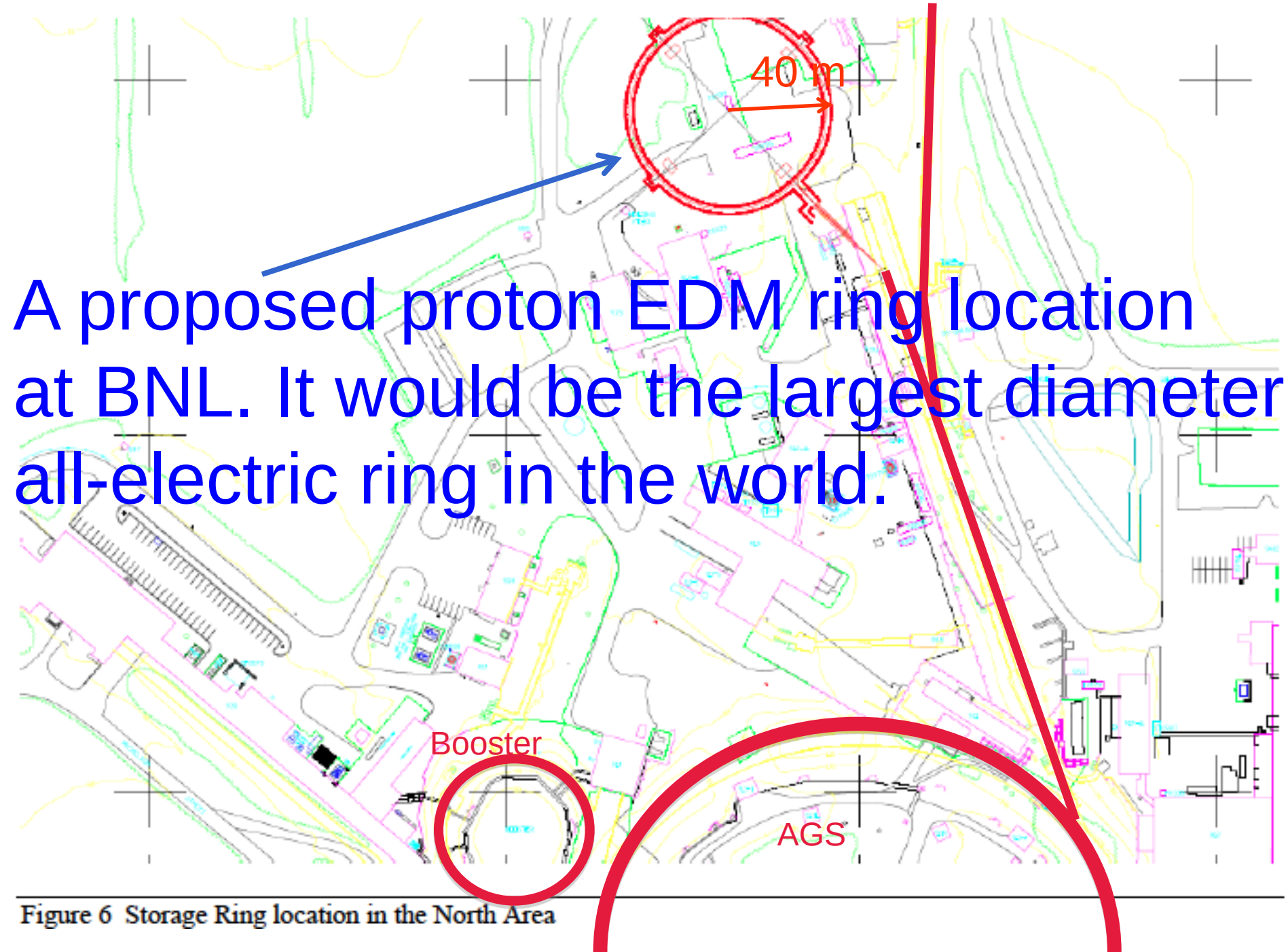

A proposed proton EDM ring location at BNL. It would be the largest diameter all-electric ring in the world.

Figure 6 Storage Ring location in the North Area

Total cost: exp + ring + beamline for two different ring locations @ BNL

System	Experiment w/ indirects	Conventional plus beamline w/ indirects	Total
pEDM at ATR	**$25.6M**	**$20M**	**$45.6M**
pEDM at SEB	**$25.6M**	**$14M**	**$39.6M**

System	Experiment w/ 55% contingency	Conv. & Beamline w/ contingency	Total
pEDM at ATR	$39.5M	$29.2M	**$68.7M**
pEDM at SEB	$39.5M	$22.6M	**$62.1M**

EDM ring

EDM ring+tunnel and beam line

Storage Ring EDM Collaboration

>20 Institutions
>80 Collaborators

- Aristotle University of Thessaloniki, Thessaloniki/Greece
- Research Inst. for Nuclear Problems, Belarusian State University, Minsk/Belarus
- Brookhaven National Laboratory, Upton, NY/USA
- Budker Institute for Nuclear Physics, Novosibirsk/Russia
- Royal Holloway, University of London, Egham, Surrey, UK
- Cornell University, Ithaca, NY/USA
- Institut für Kernphysik and Jülich Centre for Hadron Physics Forschungszentrum Jülich, Jülich/Germany
- Institute of Nuclear Physics Demokritos, Athens/Greece
- University and INFN Ferrara, Ferrara/Italy
- Laboratori Nazionali di Frascati dell'INFN, Frascati/Italy
- Joint Institute for Nuclear Research, Dubna/Russia
- Indiana University, Indiana/USA
- Istanbul Technical University, Istanbul/Turkey
- University of Massachusetts, Amherst, Massachusetts/USA
- Michigan State University, East Lansing, Minnesota/USA
- Dipartimento do Fisica, Universita' "Tor Vergata" and Sezione INFN, Rome/Italy
- University of Patras, Patras/Greece
- CEA, Saclay, Paris/France
- KEK, High Energy Accel. Res. Organization, Tsukuba, Ibaraki 305-0801, Japan
- University of Virginia, Virginia/USA

http://www.bnl.gov/edm

Sensitivity to Rule on Several New Models

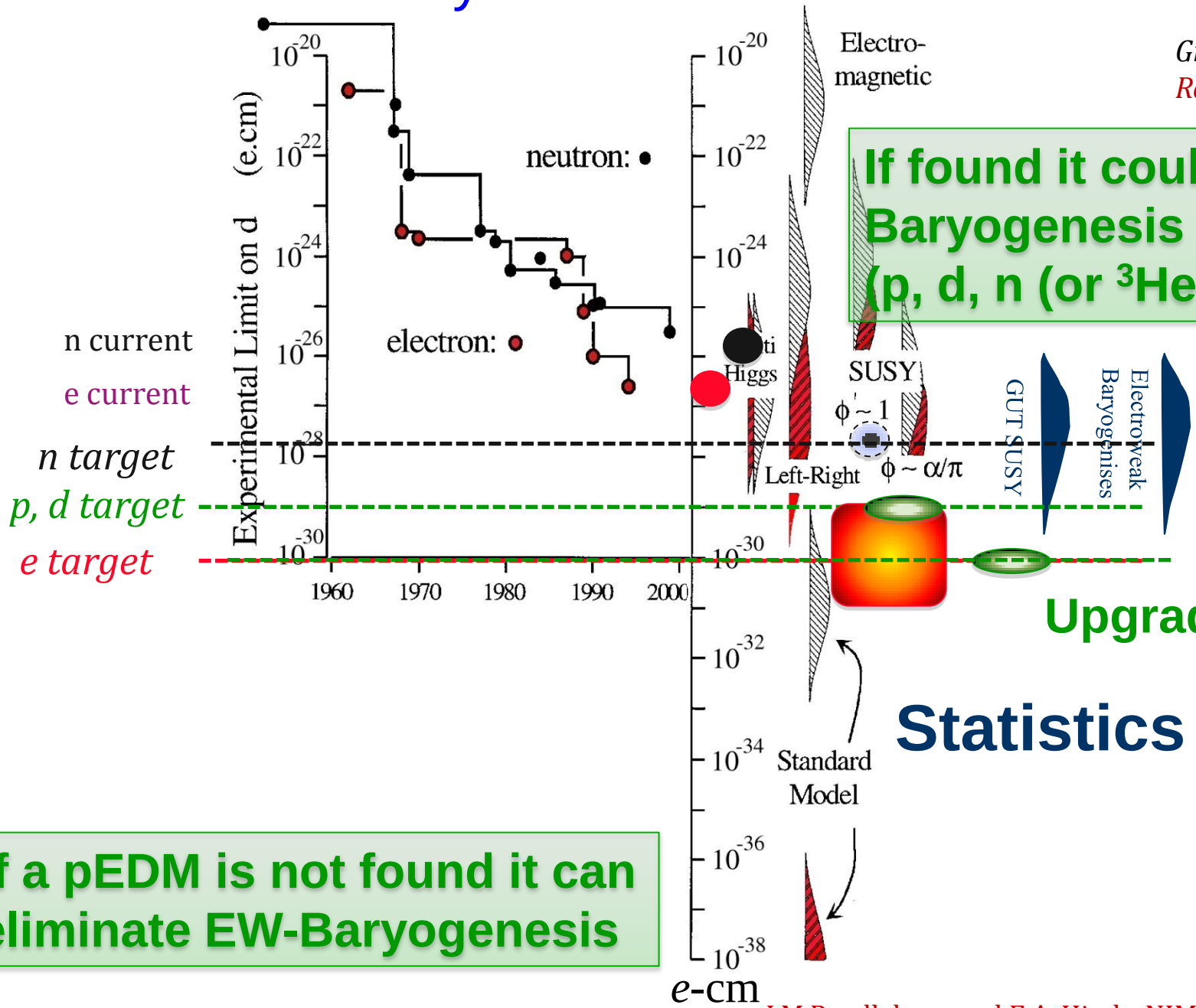

If found it could explain Baryogenesis (p, d, n (or ^{3}He))

Upgrade?

Statistics limited

If a pEDM is not found it can eliminate EW-Baryogenesis

J.M.Pendlebury and E.A. Hinds, NIMA 440 (2000) 471

EDMs of hadronic systems are mainly sensitive to

- Theta-QCD (part of the SM)

- CP-violating sources beyond the SM

Alternative simple systems are needed to be able to differentiate the CP-violating source (e.g. neutron, proton, deuteron,…).

pEDM at 10^{-29}e•cm is > an order of magnitude more sens. than the best current nEDM plans

Measure all three: proton, deuteron and neutron EDMs to determine CPV source

Super-Symmetry (SUSY) model predictions:

$$d_n \simeq 1.4(d_d - 0.25 d_u) + 0.83e(d_u^c + d_d^c) - 0.27e(d_u^c - d_d^c)$$

Theoretical estimation on the lattice?

$$d_N^{I=1} \simeq 0.87(d_u - d_d) + 0.27e(d_u^c - d_d^c)$$

$$d_N^{I=0} \simeq 0.5(d_u + d_d) + 0.83e(d_u^c + d_d^c)$$

$$d_N^{I=1} = (d_p - d_n)/2$$

$$d_N^{I=0} = (d_p + d_n)/2$$

Physics reach of magic pEDM (Marciano)

- Currently: $\bar{\theta} \leq 10^{-10}$, Sensitivity with pEDM: $\bar{\theta} < 0.3 \times 10^{-13}$

- **Sensitivity to new contact interaction: 3000 TeV**

- **Sensitivity to SUSY-type new Physics:**

$$pEDM \approx 10^{-24}\,\mathrm{e}\cdot\mathrm{cm} \times \sin\delta \times \left(\frac{1\mathrm{TeV}}{M_{\mathrm{SUSY}}}\right)^2$$

The proton EDM at 10^{-29}e·cm has a reach of >300TeV or, if new physics exists at the LHC scale, $\delta < 10^{-7}$-10^{-6} rad CP-violating phase; an unprecedented sensitivity level.

The deuteron EDM sensitivity is similar.

The current status

- Have developed R&D plans (need $1M/year for two years) for

  1) BPM magnetometers, 2) SCT tests at COSY, 3) E-field development, and 4) Polarimeter prototype

- We had two successful technical reviews: Dec 2009, and March 2011.
- Sent a proposal to DOE NP for a proton EDM experiment at BNL: November 2011

Other possible places?

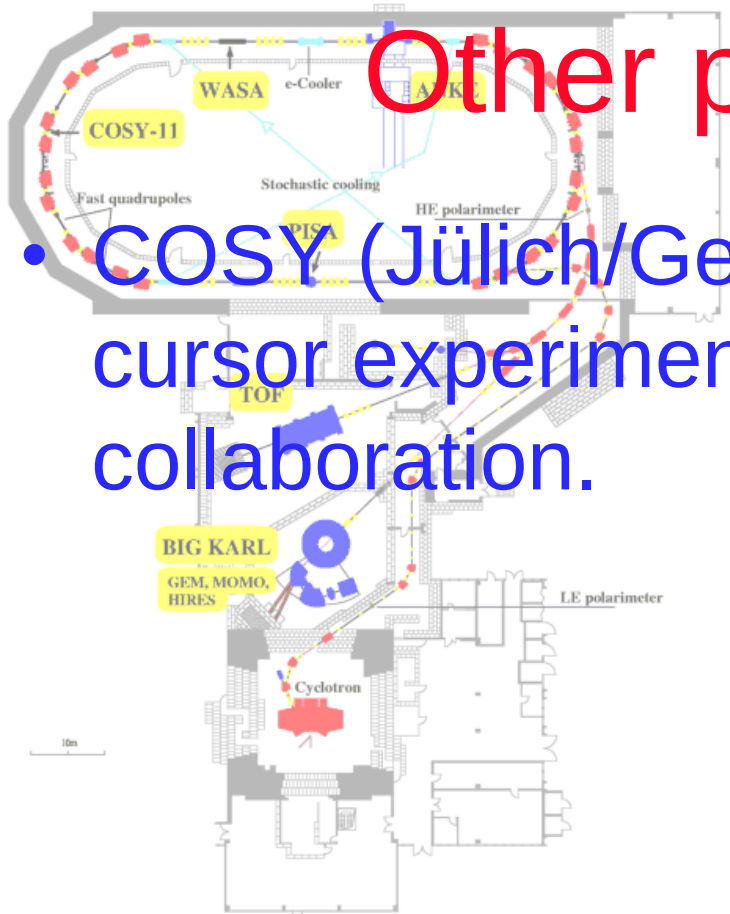

- COSY (Jülich/Germany); proposal for a pre-cursor experiment; we have a common R&D collaboration.

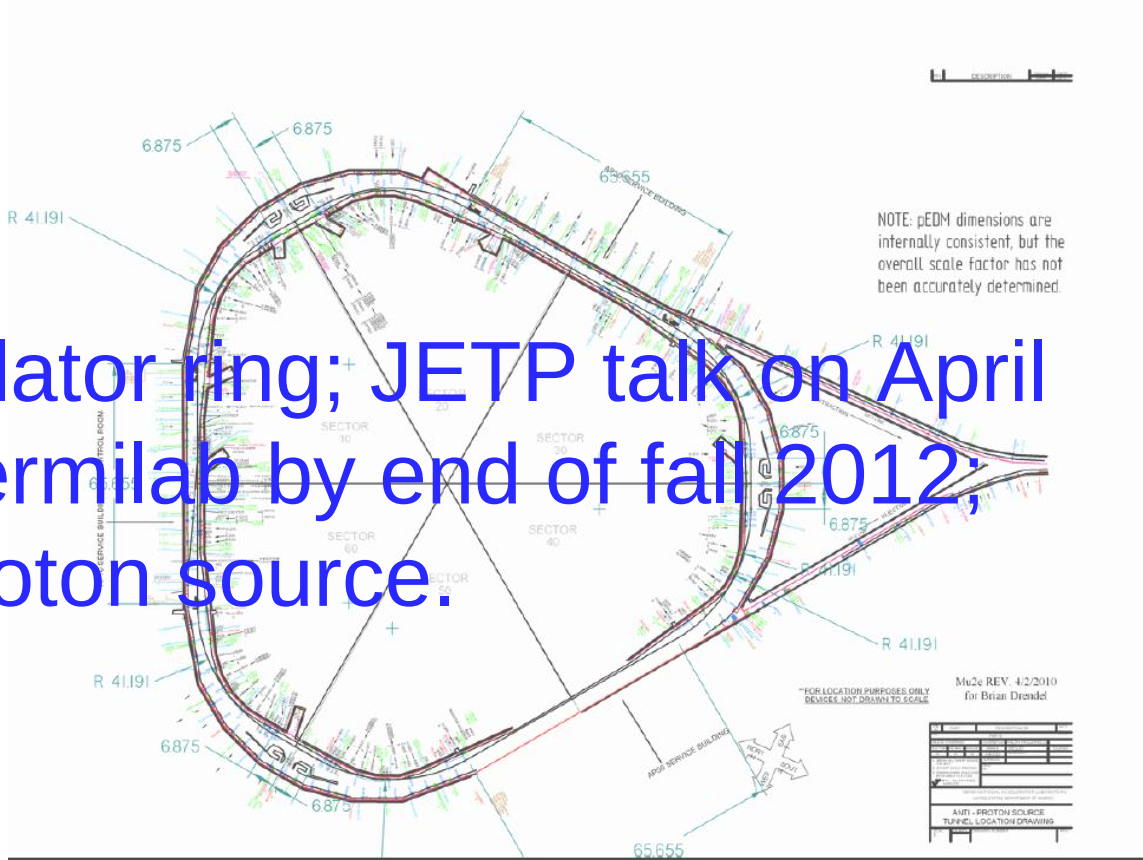

- Fermilab, accumulator ring; JETP talk on April 20; Proposal to Fermilab by end of fall 2012; Need polarized proton source.

Common R&D with COSY

EDM at Storage Rings

JÜLICH FORSCHUNGSZENTRUM

International srEDM Network

Institutional (MoU) and Personal (Spokespersons ...) Cooperation

srEDM Collaboration (BNL)	srEDM Collaboration (FZJ)

Common R & D

RHIC	EDM-at-COSY
Beam Position Monitors	Polarimetry
(...)	Spin Coherence Time
	Cooling
Spin Tracking	(...)

Slide by H. Stroeher, Director of IKP II

	Study Group
DOE-Proposal	Precursor; Ring Design
CD0, 1, ...	HGF Application(s)

Summary

- ✓ Proton EDM physics is a must do, > order of magnitude improvement over the neutron EDM
- ✓ E-field issues well understood
- ✓ Working EDM lattice with long SCT and large enough acceptance (~10^{-29}e•cm/year)
- ✓ Polarimeter work
- ▪ Planning BPM-prototype demonstration including tests at RHIC
- ▪ Old accumulator ring could house the proton EDM ring at Fermilab; BNL: new tunnel needed
- ✓ At COSY a pre-cursor proposal to PAC

Extra slides

Physics strength comparison (Marciano)

System	Current limit [e·cm]	Future goal	Neutron equivalent
Neutron	$<1.6\times10^{-26}$	$\sim10^{-28}$	10^{-28}
^{199}Hg atom	$<3\times10^{-29}$	$<10^{-29}$	10^{-25}-10^{-26}
^{129}Xe atom	$<6\times10^{-27}$	$\sim10^{-29}$-10^{-31}	10^{-25}-10^{-27}
Deuteron nucleus		$\sim10^{-29}$	3×10^{-29}-5×10^{-31}
Proton nucleus	$<7\times10^{-25}$	$\sim10^{-29}$	10^{-29}

M. Conte

$$\gamma_{\rm m} = \sqrt{1 + \frac{1}{a}} = 1.248$$

where $a = 1.793$ is the proton anomaly. Consequently we have:

$$\begin{aligned}
\beta_{\rm m} &= 0.598 \\
p_{\rm m} &= \frac{mc}{\sqrt{a}} = 0.701 \text{ GeV/c} \\
U_{\rm m} &= \gamma_{\rm m}\, mc^2 = 1.171 \text{ GeV} \\
W_{\rm m} &= U_{\rm m} - mc^2 = 0.233 \text{ GeV} \\
m &= \text{proton mass} = 0.938 \text{ GeV/c}^2
\end{aligned}$$

and

$$B_{\rm eq} = \frac{E_{\rm rad}}{\beta c}, \quad \text{for} \quad E_{\rm rad} = 1.5 \times 10^7 \text{ Vm}^{-1} = 150 \text{ kV/cm}$$

or

$$B_{\rm eq} = 8.37 \times 10^{-2} \text{ Tesla, which yields a bending radius } \rho = \frac{p}{eB_{\rm eq}} = 28 \text{ m}$$

$$\boxed{\nu_{\rm H}^2 = 2 - \beta_0^2 = 1 + \frac{1}{\gamma_0^2}}$$

Why does the world need a Storage Ring EDM experiment at the 10^{-29} e-cm level ?

1. The proton, deuteron and neutron combined can pin-down the CP-violating source should a non-zero EDM value is discovered. Critical: they can differentiate between a theta-QCD source and beyond the SM.
2. The proton and deuteron provide a path to the next order of sensitivity.

Why Storage Ring EDMs?

- Storage rings offer a unique setting for a sensitive electric dipole moment (EDM) probe of charged particles. A number of simple systems can be probed with high accuracy: p, d, ^{3}He,…
- The mechanical (centrifugal) force balances the strong radial E-fields.
- Pencil-like, high intensity/high polarization beams of protons and deuterons have been around for decades.
- Ready for prime time.

Beam parameters

C.R. proton beams	0.7 GeV/c	≥80% polariz.; ↑	~4×10^{10} protons/store
~10^2 m base length	Repetition period: 20 minutes	Beam energy: ~1J	Average beam power: ~1mW
Beam emittance: 95%, norm.	Horizontal: 2 mm-mrad	Vertical: 6 mm-mrad	$(dp/p)_{rms}$~ 2×10^{-4}

- CW & CCW injections: Average emittance parameters: same to ~10% at injection.

Fermi would need to get into polarized beams physics

Proton EDM R&D cost: $2M

- BPM development & testing over two years: $0.6M
- E-field prototype development & testing: 1.8 years: $0.4M
- SCT tests at COSY, 2 years: $0.4M
- Polarimeter prototype, 2 years: $0.6M

Polarimeter rates:

- Beam intensity with 2×10^{10} pol. protons/ ~10^3s and a detection efficiency of 1% → 200KHz for ~3000cm^2 area, or ~100Hz/cm^2 on average but much higher at small radius. Design: ~1KHz/pad.

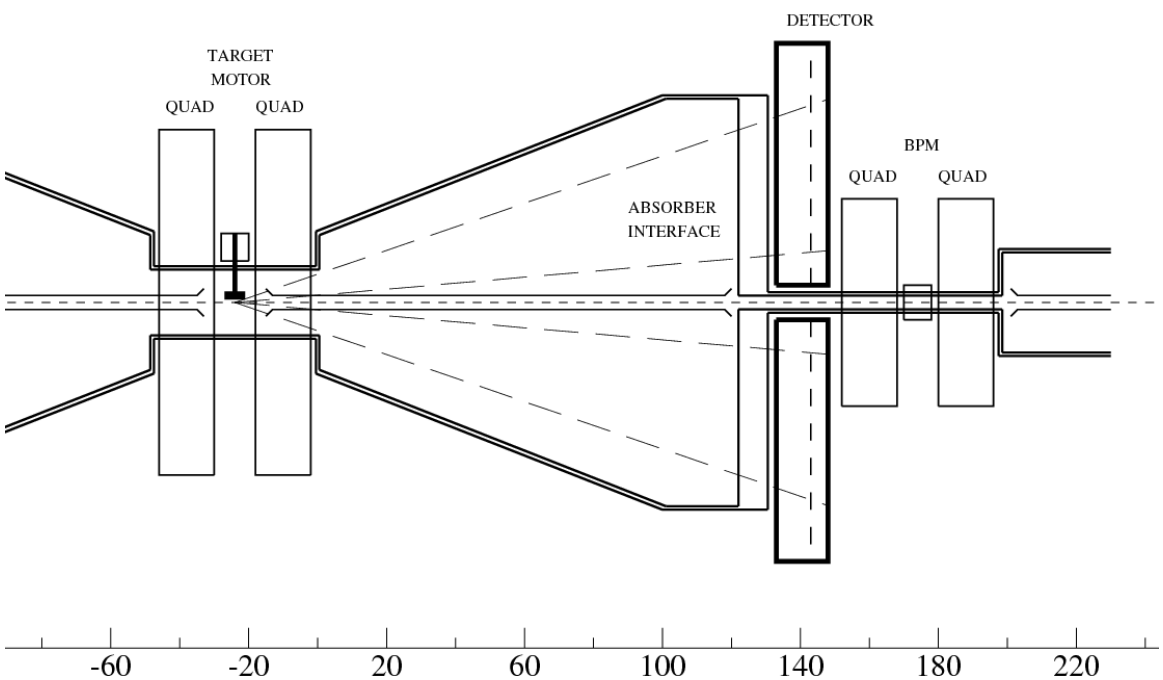

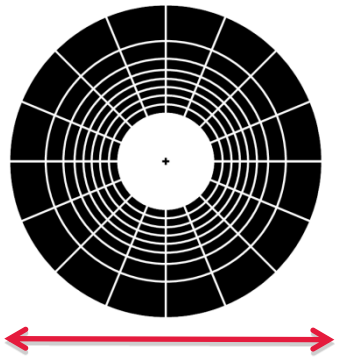

The Electric Dipole Moment precesses in an Electric field

The EDM vector *d* is along the particle spin direction

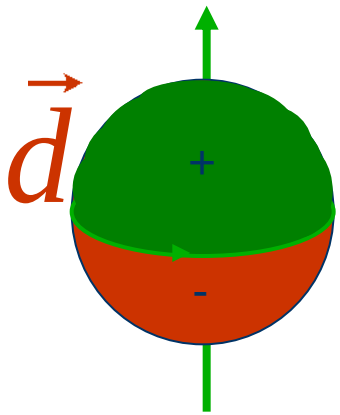

$$\frac{d\vec{s}}{dt} = \vec{d} \times \vec{E}$$

Parameters of current lattice

Table 2. The table of parameters for the proton EDM ring is shown here. The lattice has been estimated using the exact electric field and not an effective dipole magnetic field.

Parameter	Value	Comment
Proton Momentum	0.7007405 GeV/c	Kinetic energy: 232.8 MeV, $\beta = 0.59838$, $\gamma = 1.2481$
Ring bending radius	40 m	
Total length of straight sections	11.6 m	If more straight section length is needed the ring bending radius has to increase proportionally.
Radial E-field strength	10.5 MV/m	For plate separation of 3 cm the voltage on the plates is about ±160 KV.
Number of sections	16	The E-field plates within a section are ~16m long each. They can be segmented into 5 pieces, 3.14 m long each.
Radial E-field dependence at y=0	$R^{0.2}$	The E-field is slightly increased at larger radius.
Total length of orbit	263 m	
Horizontal tune	1.3	
Vertical tune	0.2-0.1	To be modulated by ~10% around 0.1
$\beta_{x,max}$	28 m	Horizontal aperture: 3 cm
$\beta_{y,max}$	240 m	Vertical aperture: 8 cm
Cyclotron frequency	0.6839 MHz	
$f_{rf} = 135 \times 0.6839$ MHz	90 MHz	Total RF voltage: 5 KV for synchrotron tune of 0.01
Slip factor	0.45	Sign is – (TBC)

The EDM signal: early to late change

- Comparing the (left-right)/(left+right) counts vs. time we monitor the vertical component of spin

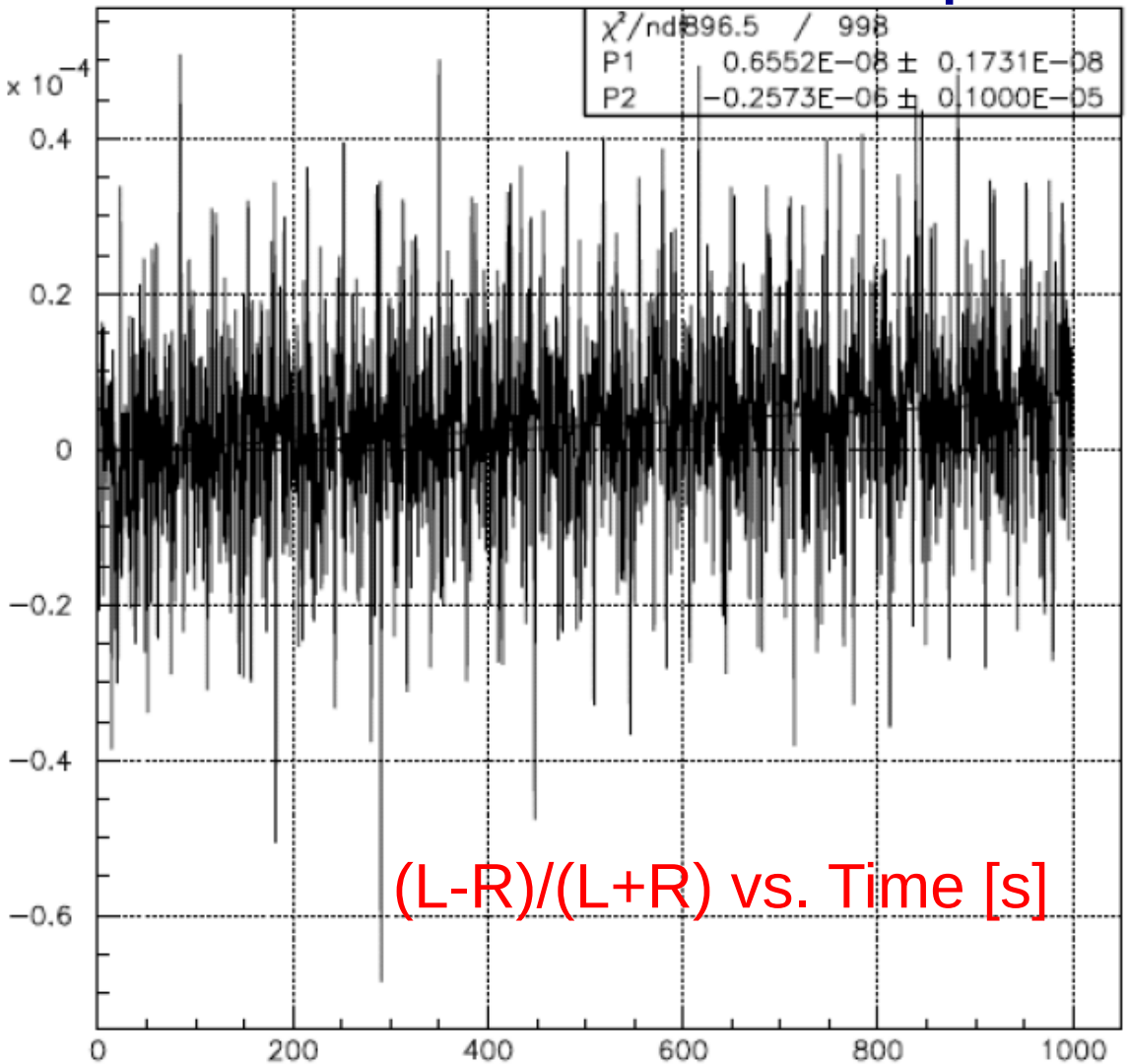

M.C. data

MINOS Tidal Data

Difference in two sensors 90 meters apart

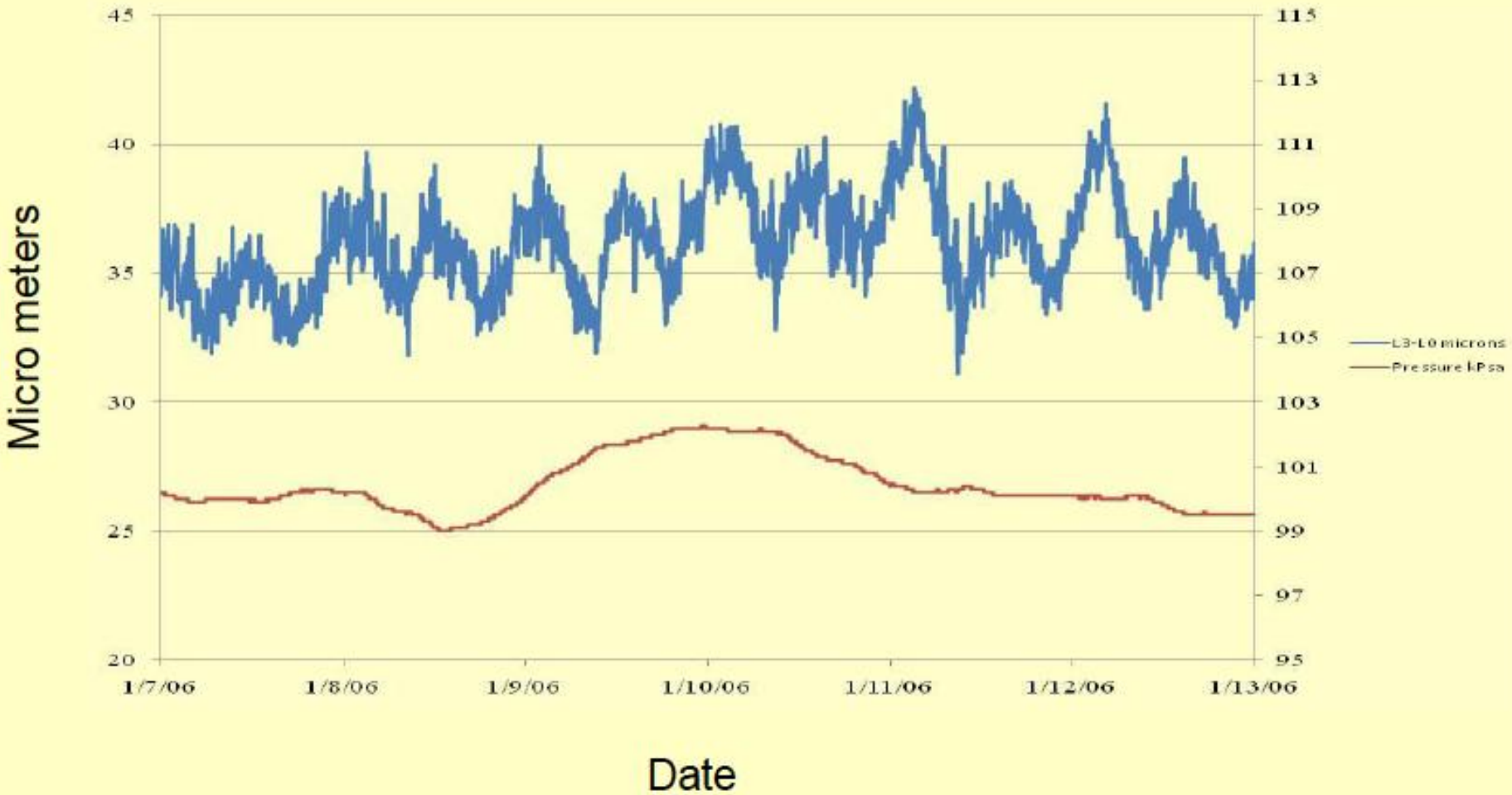

J T Volk Fermilab Dec 2008

Why COSY?

- Scale like EDM ring
- Polarized P/D beams
- Electron cooling
- Outside user program
- Available equipment

History

- Proposal in 2007
- Visit SPIN@COSY run
- Three polarimeter runs:
  - June 2008 – initial tests
  - September 2008 – trial data
  - June 2009 – final long run (paper in preparation)
- Polarization lifetime runs:
  - January 2011 – initial tests

Prior work at KVI, Groningen
- d=C data, 2004 + 2005
- Systematic errors, 2007

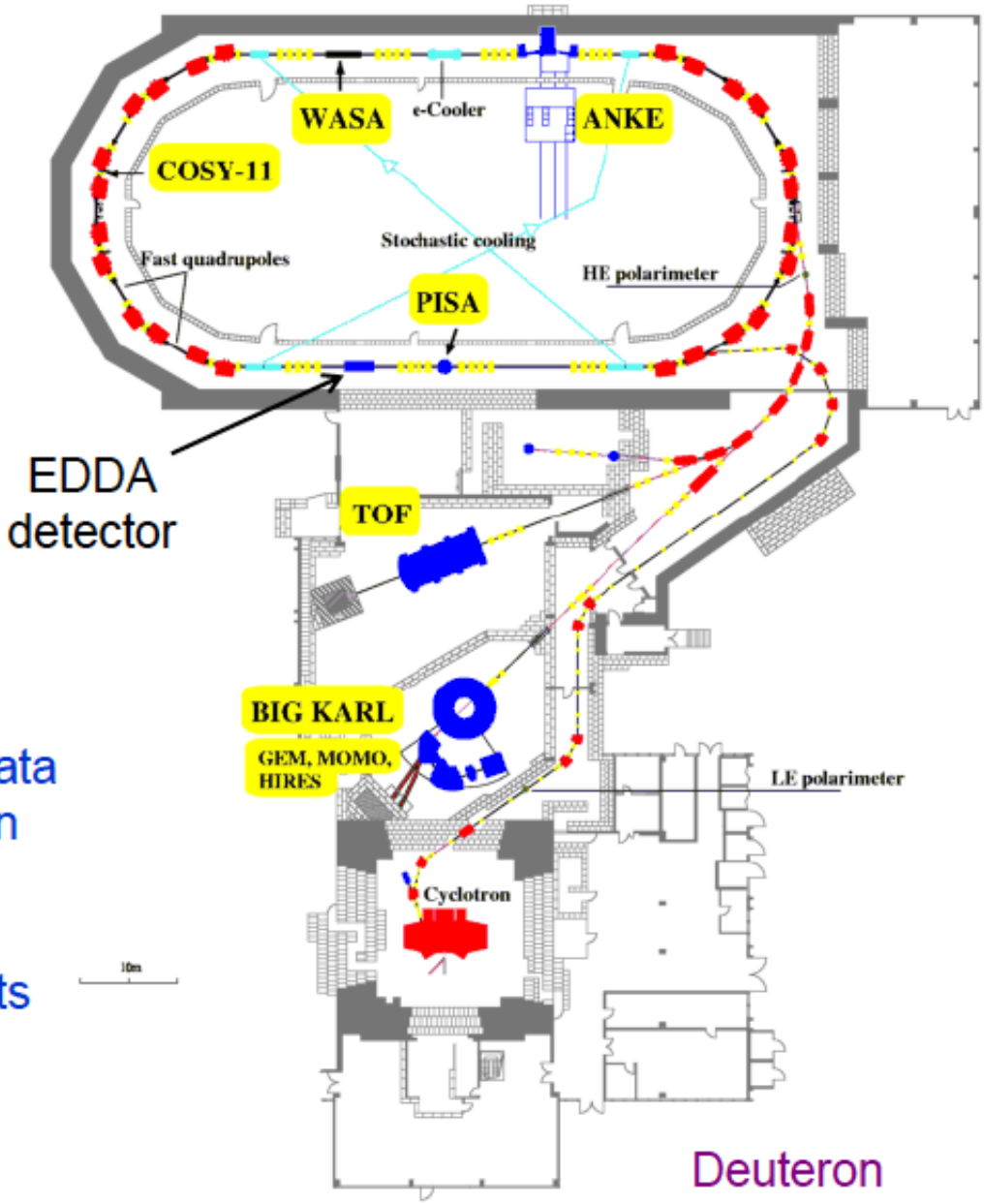

Deuteron beam

How to Scale HPWR to 3cm gap?

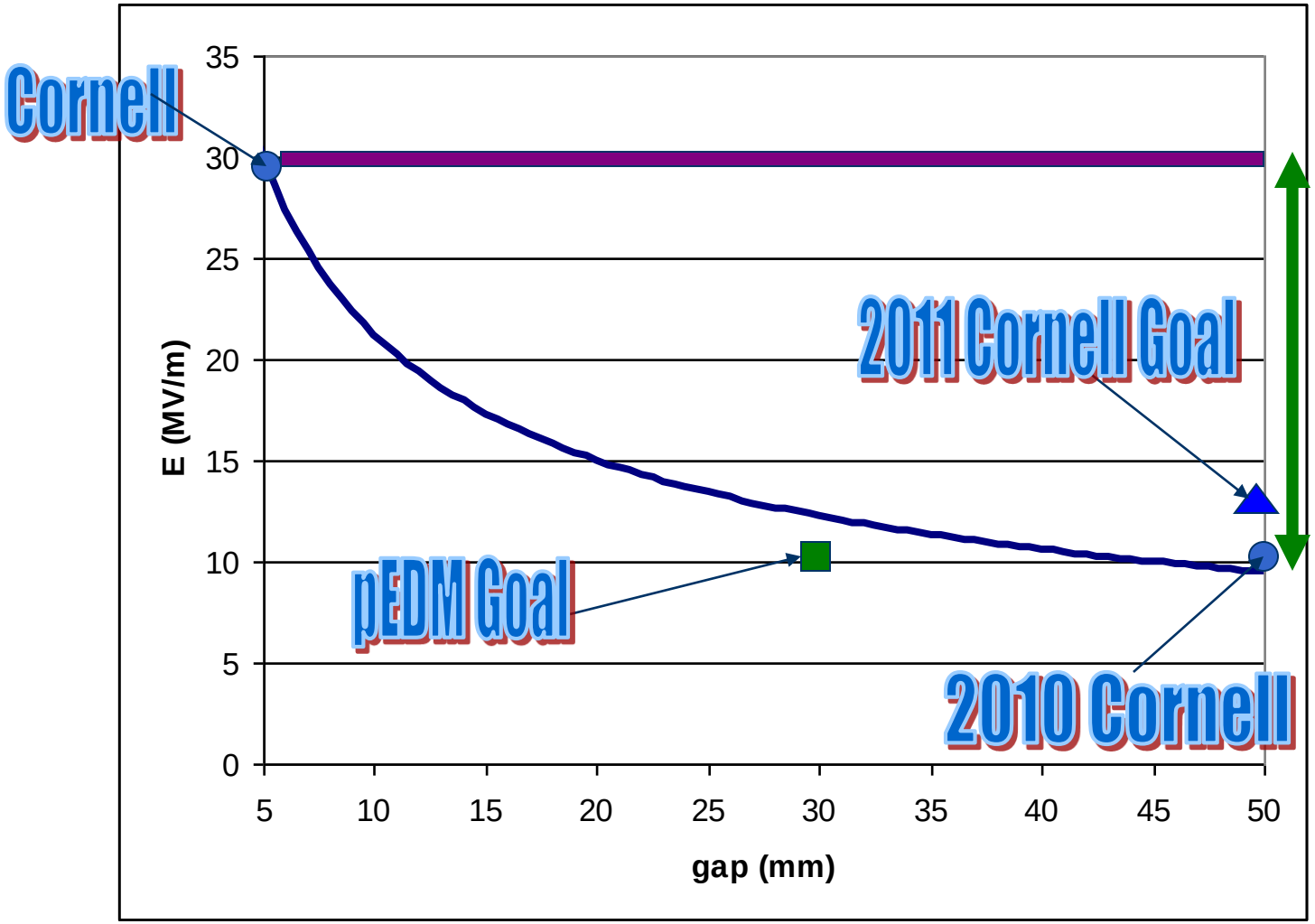

Detector systems: alternatives to scintillators

A

Multi-resistive plate chambers(Italy)

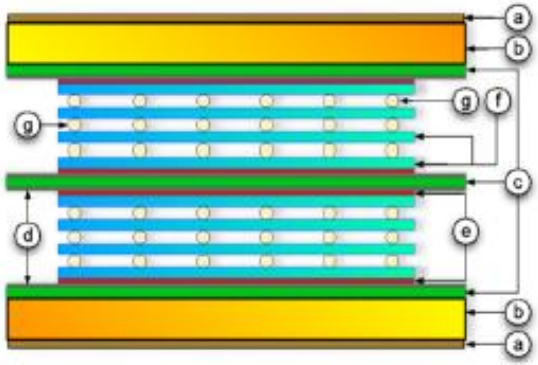

pickup electrodes (green) also shown in photograph

The 20cm x 50cm prototype

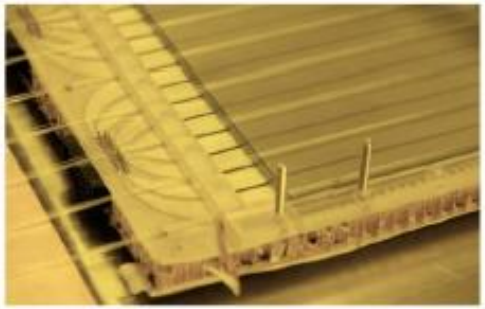

B

Micro-megas avalanche detection system Greece)

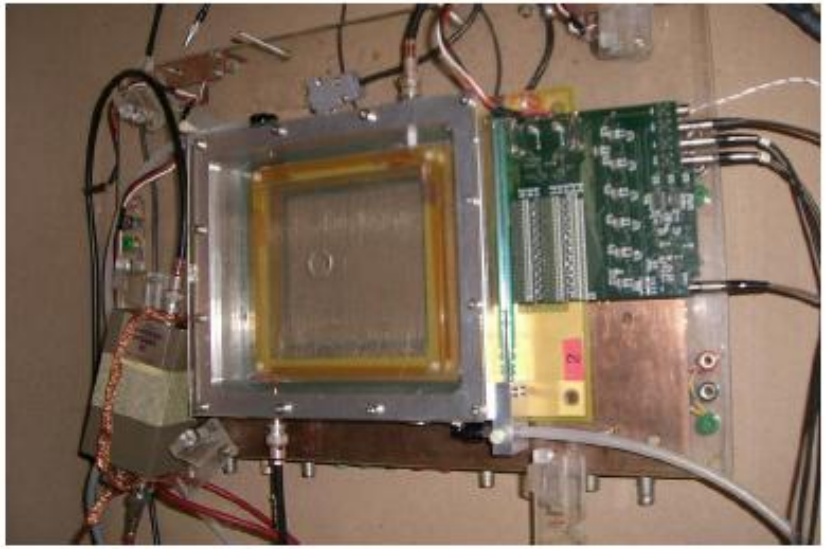

C

Gas electron multiplier (GEM) system

In-beam tests are needed (COSY) to provide sample data sets.

Gas cluster ion beam surface treatment: getting rid of ~μm level asperities

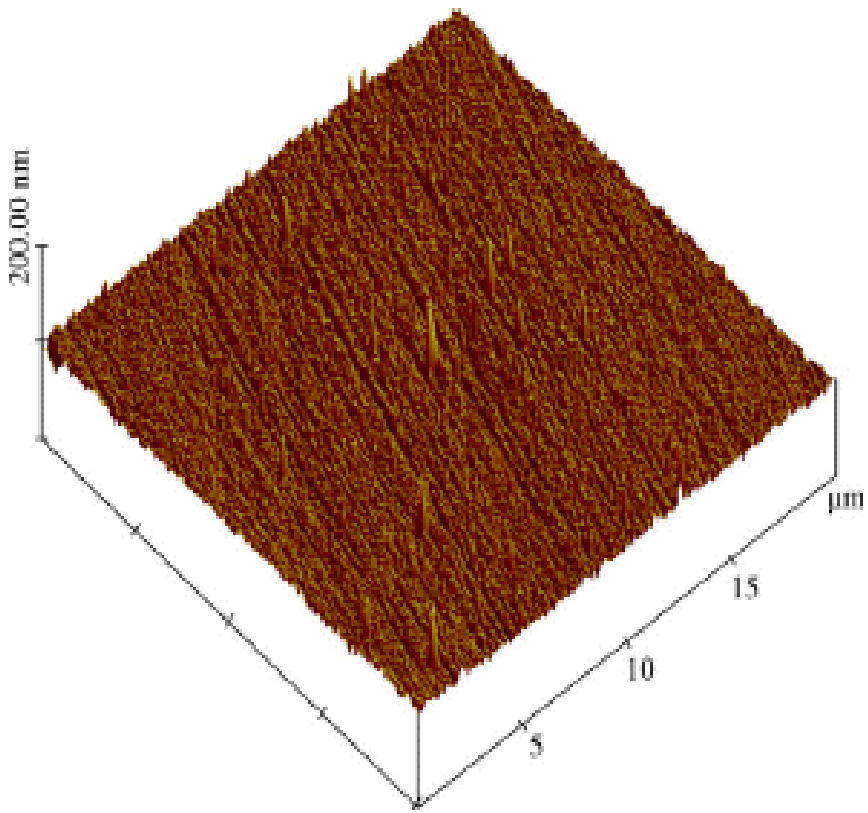

Fig. 1. AFM image (20 × 20 μm) of highly polished stainless steel electrode material before GCIB treatment showing asperities and scratch marks from polishing. The vertical scale is 120 nm/division.

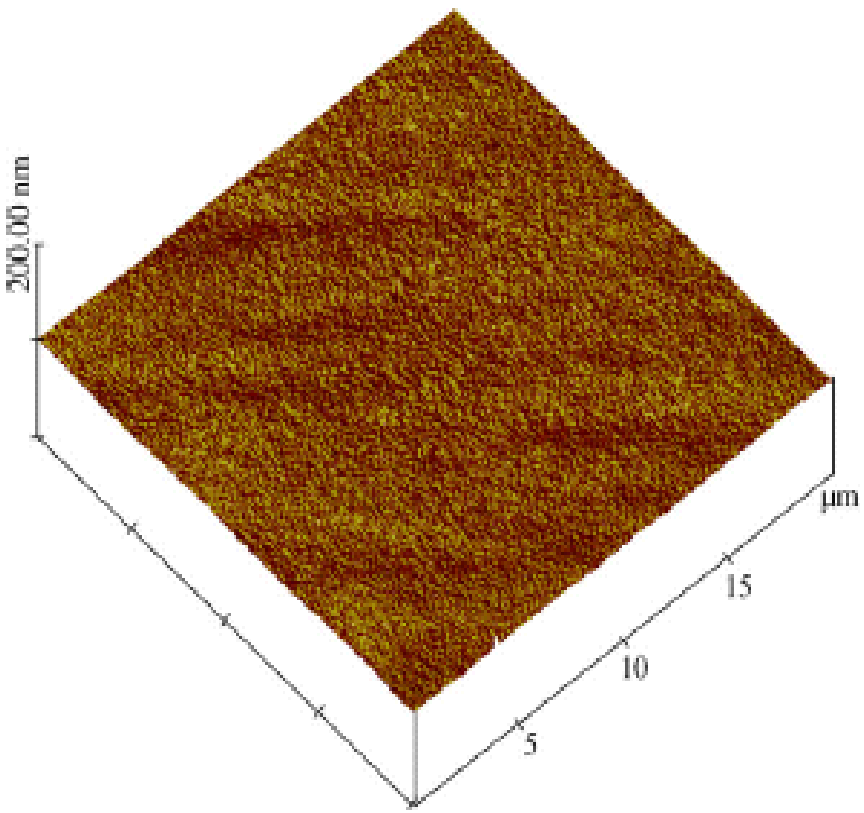

Fig. 2. AFM image (20 × 20 μm) of highly polished stainless steel electrode material after GCIB treatment. The vertical scale is 120 nm/division.

Electropolishing Process Verses Mechanical Polishing

Roughness: 4 - 40 microinches
(depends from abrasive grit number)

Mechanical polishing is an operation designed to prepare a metal surface for electropolishing or to satisfy non-critical surface roughness requirements. Mechanical polishing reduces all surface ridges, microprotrusions, pits and discrepancies to provide a homogeneous appearance and roughness.

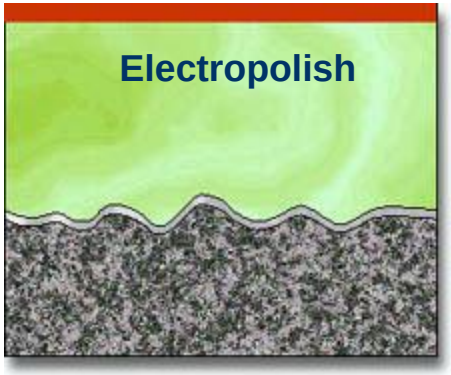

Roughness: 2 - 5 microinches

Electropolishing (used since early 1950's) is the electrochemical removal of microscopic irregularities or diminution scratches, burns and unwanted harp edges from metal surfaces. Typical material removal is .0001"- .0004" per surface.

Smoothness of the metal surface is one of the primary and most advantageous effects of electropolishing.

<u>Electropolishing should improve separator performance.</u>

High Voltage Electrical Breakdown in Vacuum

It is generally agreed that a vacuum breakdown is a vapor arc, taking place in material evaporated from the electrodes. Evidence is the observation of localized light during breakdown and electrode material transferred across the gap.

- ## Electron field emission mechanism for initiating the breakdown

  According with this model, electrons are assumed to be field emitted from the tip of microprotrusion at an isolated site on the surface of broad-area cathode. Question: where is the metal vapor produced at the anode or cathode?

  Is it enough power to vaporize anode material by field emitted electrons bombarded anode or positive ions produced at the anode lead to rupture of the cathode or that resistive heating on the cathode causes them to melt and ultimately to vaporize. This mechanism dominates at gaps less than 2 mm.

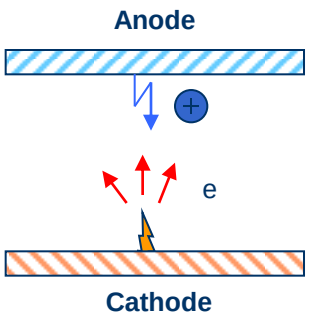

- ## Microparticle or "clump" model

  Clump of loosely adhesive material is drawn across the gap by the electric field so as to strike the opposite electrode with enough energy to produce high local temperature in the electrode or clump material with melting and vaporizing.

  Pre-operational electrode surface will be characterized by having a finite number of microscopic particles. These will originate from various stages of mechanical polishing, and may be in the form of either impurity particle of polishing material or dust particles. Another source of microparticles are those originated from thermal instabilities at either the cathode or anode "hot" spot. For uniform gaps the breakdown voltage should vary as the square root of the gap spacing. The model is dominating at large gaps.

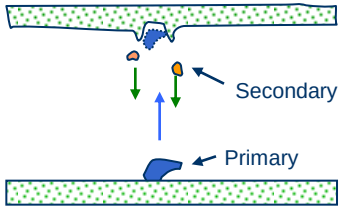

- ## Ion exchange mechanism

  This mechanism is assumed to be initiated by say random positive ion created in the gap that is then accelerated by the field to generate further negative ions on impact with cathode, which subsequently generate more positive ions on impact with the anode etc. Thus, if the ion multiplication factor > 1, the process will develop in the breakdown mode. It is very sensitive to chemicals contaminations.

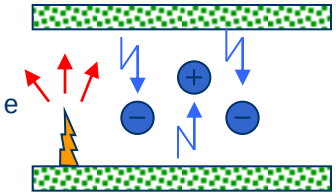

The breakdown consists of many complicated and complex phenomena with no single process involved.

When $P=P_{magic}$ the spin follows the momentum

No matter what the E-field value is the spin follows the momentum vector creating an ideal Dirac-like particle (g=2)

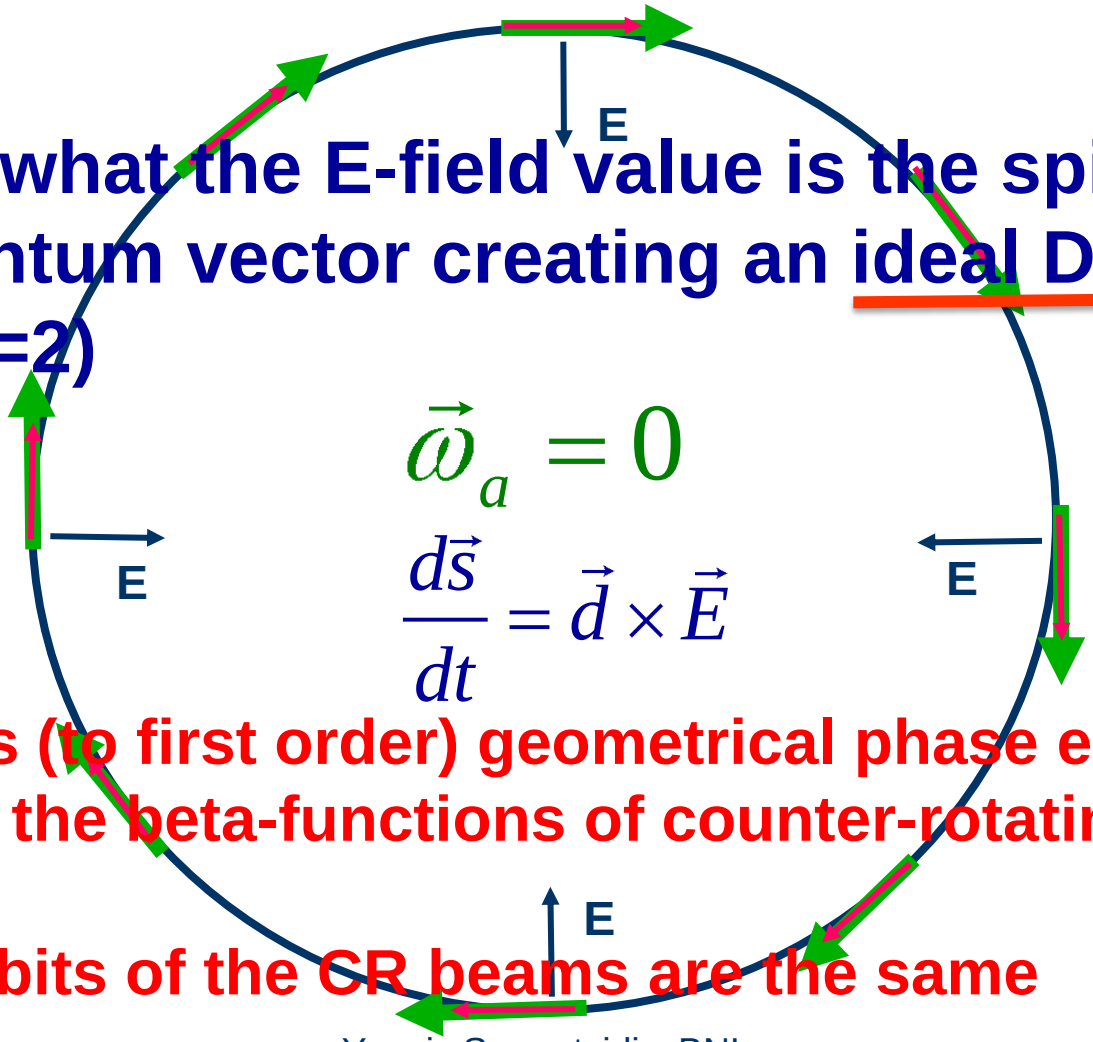

$$\vec{\omega}_a = 0$$

$$\frac{d\vec{s}}{dt} = \vec{d} \times \vec{E}$$

1. **Eliminates (to first order) geometrical phase effect**
2. **Equalizes the beta-functions of counter-rotating (CR) beams**
3. **Closed orbits of the CR beams are the same**

Proton Statistical Error (230MeV):

$$\sigma_d = \frac{2\hbar}{E_R P A \sqrt{N_c f \tau_p T_{tot}}}$$

τ_p : 10^3s Polarization Lifetime (Spin Coherence Time)

A : 0.6 Left/right asymmetry observed by the polarimeter

P : 0.8 Beam polarization

N_c : 4×10^{10}p/cycle Total number of stored particles per cycle

T_{Tot}: 10^7s Total running time per year

f : 0.5% Useful event rate fraction (efficiency for EDM)

E_R : 10.5 MV/m Radial electric field strength (95% azim. cov.)

$$\sigma_d = 1.6\times10^{-29}\,\mathrm{e\cdot cm/year}\ \text{for uniform counting rate and}$$

$$\sigma_d = 1.1\times10^{-29}\,\mathrm{e\cdot cm/year}\ \text{for variable counting rate}$$

Physics/effort comparison

- Physics reach ~10^3 TeV, similar to mu2e (MECO) experiment at FNAL; moreover, it can explain BAU (EW-Baryogenesis)
- SUSY-like new physics at LHC scale, it probes CP-violating phases to sub micro-radian level, complementary to LHC (plus fine-tuned SUSY)
- At 10^{-29}e·cm it's > an order of magnitude better than the best neutron EDM plans anywhere. Statistically superior to neutron EDM exps.
- Method can be applied to proton, deuteron, and ^{3}He to unravel the underlying physics. More than other methods can do.

SU(N) gauge theories with symmetric-rep fermions

Yigal Shamir [⋆]

with

Tom DeGrand [◇] and Ben Svetitsky [⋆]

Part I. $SU(N)$, $N = 2, 3, 4$, with $N_f = 2$ two-index sym rep Dirac fermions:
"continuum" issues; physics results

Part II: Fat (nHYP) links and what they do for us
$\Rightarrow$ It's a good idea to try DWF with fat links

[⋆] Tel Aviv University
[◇] Boulder, CO

Walking [extended] Technicolor

- Confinement & Chiral symmetry breaking are lost for $N_f > N_{\text{critical}}$
- "Walking" theories are found just below the conformal window
- Condensate enhancement needed $\Leftrightarrow$ mass anomalous dimension $\gamma \approx 1$
- Natural candidates: $N_f = 2$ higher-irrep fermions [Sannino *et al.*]

Schrödinger functional

- Induce background field thru boundary conditions in L^4 box
- Measure $1/g^2(L)$ from response to small change in boundary conditions
- Extract mass anomalous dimension γ from scaling of pseudoscalar renormalization constant Z_P, on the same lattices

Life inside (or near) the conformal window

Two-loop beta function, SU(2) with $N_f = 2$ of:

adjoint

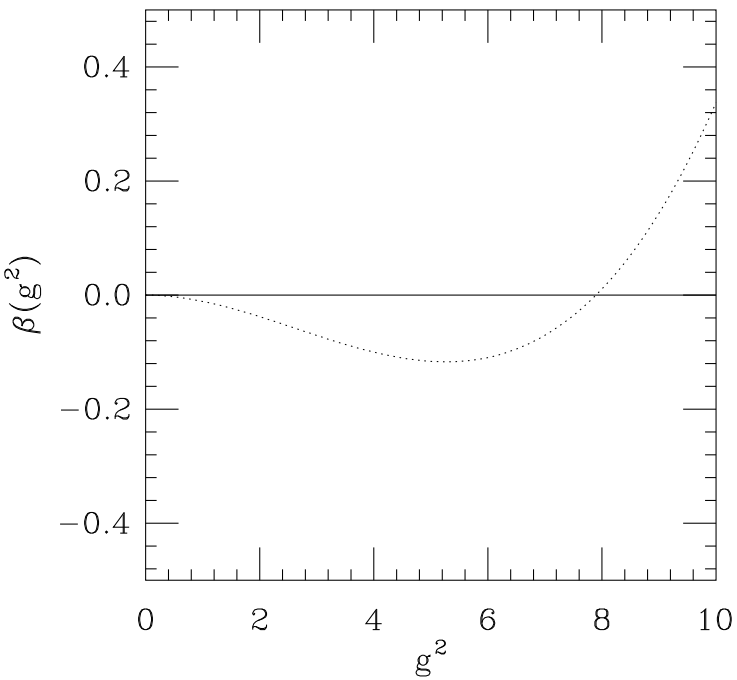

fundamental

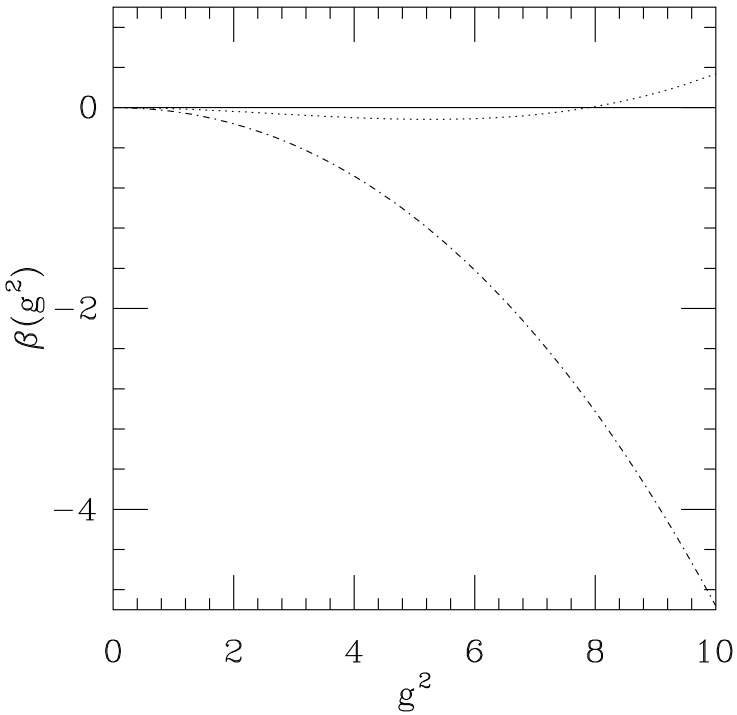

⇒ Strategy of ALPHA developed for QCD; performs poorly here

Nearly constant beta function

define: $$\tilde{\beta}(1/g^2) \equiv \frac{d(1/g^2)}{d\log(L)} = 2\beta(g^2)/g^4$$

- Solution: $1/g^2 \simeq a + b\log(L)$
- Exact at one loop
- Treat dataset at each bare β as separate fitting problem
- slope = beta fn.
- Systematics: add $\log^2$ term, or remove smallest volume
- Slope changes sign $\Longrightarrow$ IRFP!

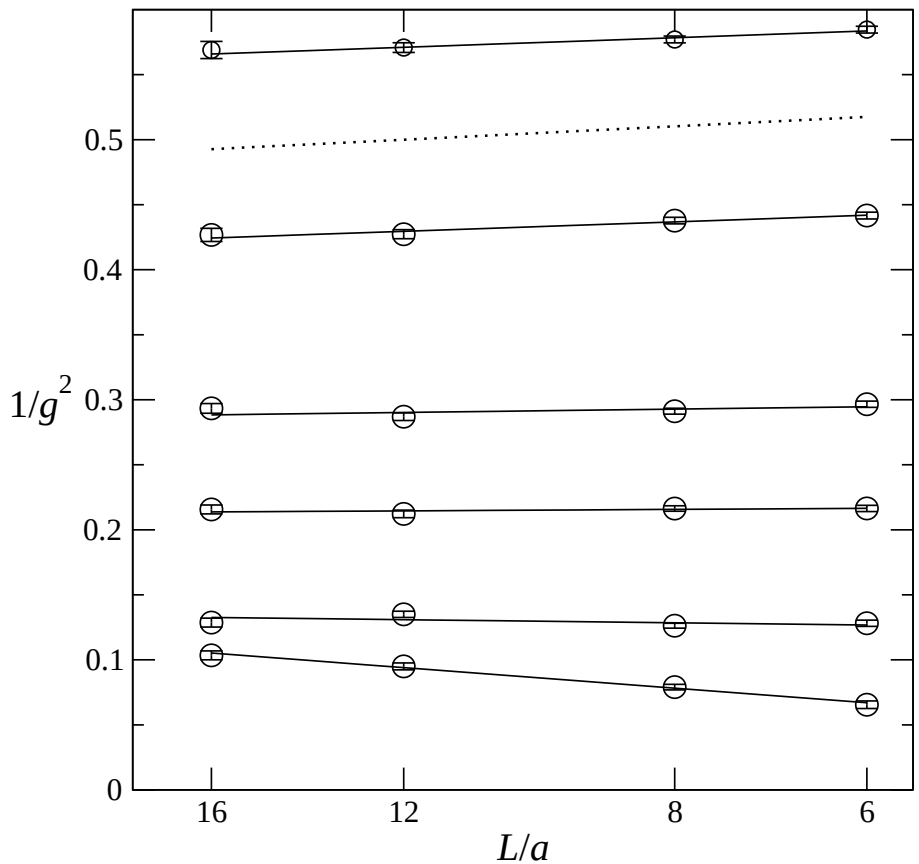

SU(2)/adjoint

Fitting $1/g^2$: $x = L/8$, Black: $L = 6,8,12,16$, Red: $L = 8,12,16$

$a + b\log(x)$

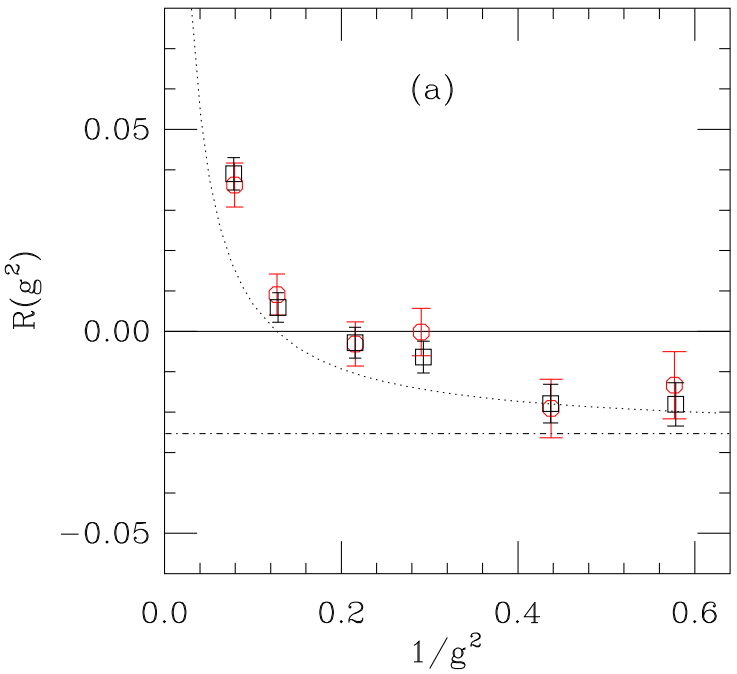

$a + b\log(x) + c\log^2(x)$

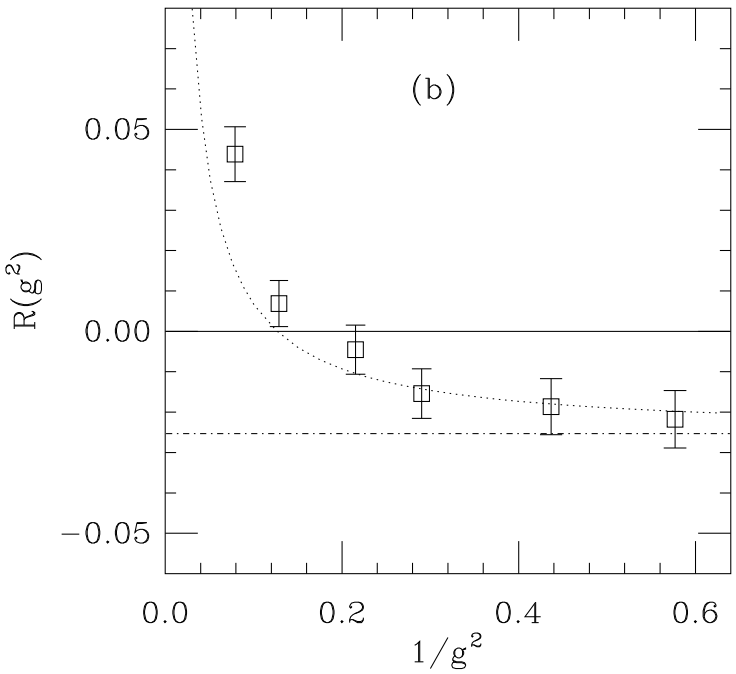

$$1/g_*^2 = 0.20(4)(3)$$

SU(2)/adjoint, SU(3)/sextet, SU(4)/decuplet

- Qualitatively agrees with $\beta^{[\text{2-loop}]}$
- Actual $\beta > \beta^{[\text{2-loop}]}$
- With increasing N_c, IRFP moves to stronger coupling, or disappears
- Consistent with no IRFP of $\beta^{[\text{2-loop}]}$ for $N_c \to \infty$ limit
- Can one use SU(4)/decuplet for walking technicolor?

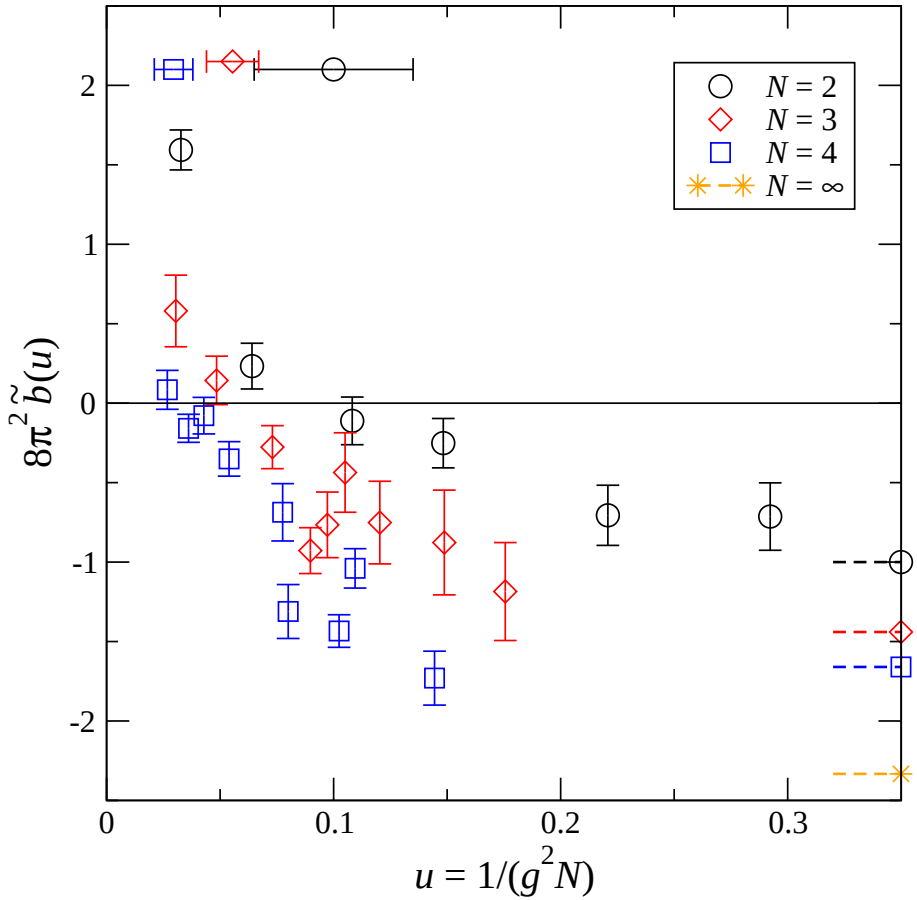

Mass anomalous dimension

- Dashed line:
  one-loop for $N_c \to \infty$
- Remarkable universality
- Saturation: $\gamma \lesssim 0.45$
- Missed by analytic calculations!
- No good for walking technicolor

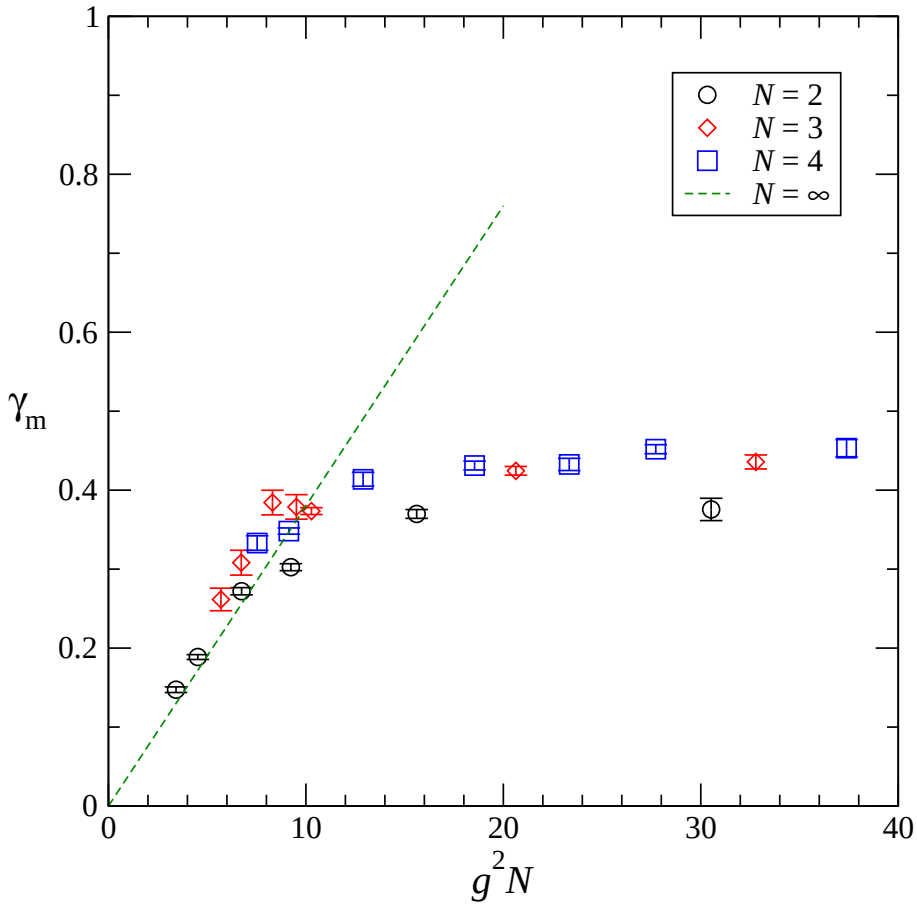

Part II. What nHYP links do for us

- Results from SU(3)/sextet

	β	$g^2_{SF}(L=6)$	κ_c	m_c	M
thin	6.0	~ 2	0.1610	-0.89	1.9
fat	5.8	1.9	0.1283	-0.10	1.1

Critical hopping parameter $\kappa_c = 1/(8 + 2m_c)$

Optimal Domain-Wall height $M = 1 + |m_c|$ (to be explained later on)

- Similar improvement for optimal clover coefficient
  (big enough that we've decided to set $c_{SW} = 1$)

- Fat links allow us to probe much larger $g^2(L)$

DWF primer

- 5-d Wilson fermions, supercritical (negative bare mass), with chiral 4-d fields located near the boundaries $s = 0$ and $s = L$
- Effective 4-dim operator: $D_{\text{eff}}(L) = 1 + \gamma_5 \tanh\big((L/2)a_5 H\big)$
- For $L \to \infty$ it becomes a GW operator: $D_{\text{eff}}(\infty) = 1 + \gamma_5 H/\sqrt{H^2}$
- DWF transfer matrix: $T = \exp(-a_5 H) = 1 - a_5 H_W + \cdots$ where $H_W = \gamma_5 D_W$ is the 4-d hermitian Wilson operator
- Penetration into the 5-d bulk from near-unity eigenvalues of T, hence from near-zero eigenvalues of H_W
- PCAC: $\partial_\mu A_\mu = 2m_q J_5 + 2m_{\text{res}}\big(J_5 + \text{[more] lattice artifacts}\big)$
- Need $m_{\text{res}} \sim 10^{-3}$ (or smaller). Want L to be small.

spectrum of D_W in complex plane

- Optimal DW height = center of leftmost "void"
- Fat links tame the Wilson spectrum: $m_c(\text{fat}) \ll m_c(\text{thin})$
- Expect many more ev's inside the thin-links "void": $m_{\text{res}}(\text{fat}) \ll m_{\text{res}}(\text{thin})$

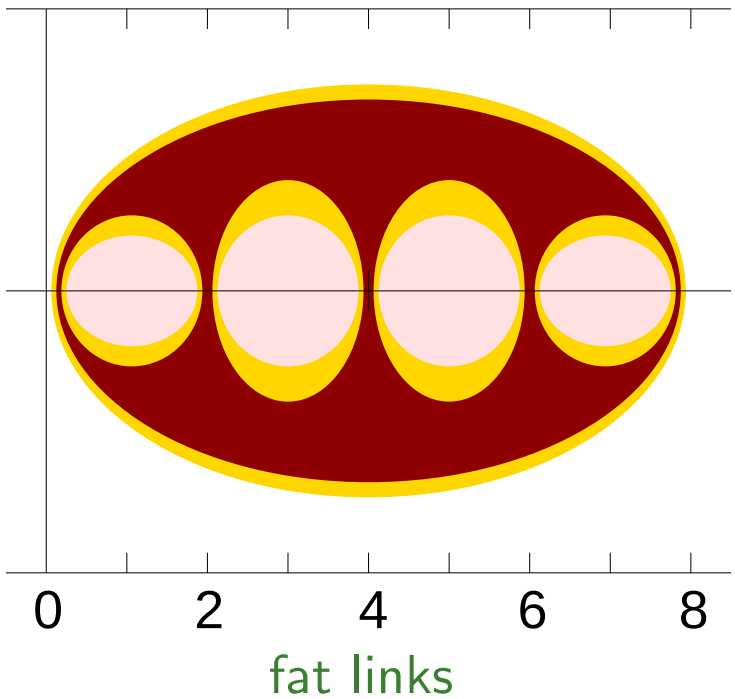

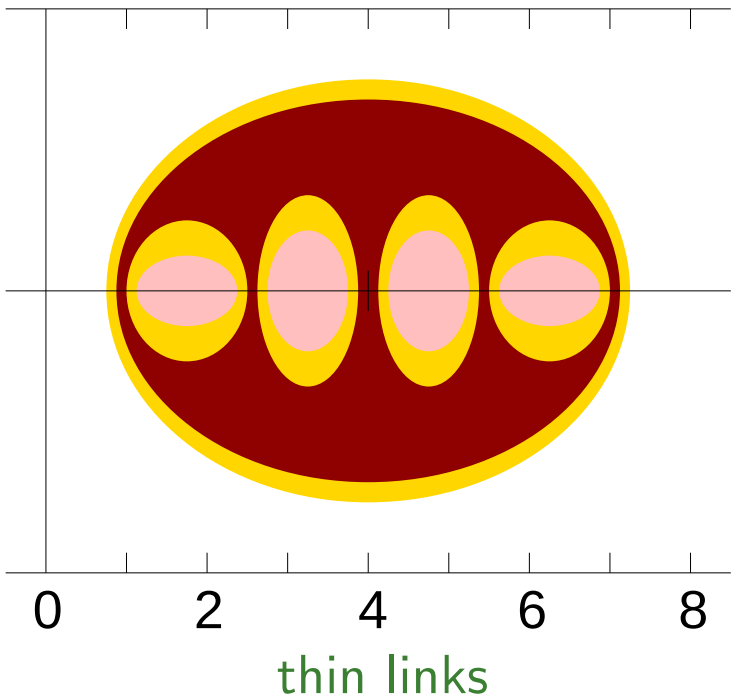

Fat links and DWF

- DWF on staggered MILC lattices: [LHP Collaboration, . . .]
  thin: m_{res} "too big to measure"
  fat: $m_{\text{res}} \sim 10^{-3}$

- Locality
  – It's true that D_W is less local with fat links
  – nHYP links only mildly nonlocal: [Hasenfratz, Hoffmann & Schaefer]
    Smeared link depends only on thin links that share a hypercube with it

- GW operators are never ultra-local

- Relevant notion: exponential localization of $D_{\text{eff}}(L)$.
  – Depending on suppression of near-zero eigenmodes,
    in principle $D_{\text{eff}}(L)$ might be <u>more</u> local with fat links!

Summary

- $SU(N), \quad N = 2, 3, 4,$ with $N_f = 2$ two-index sym rep Dirac fermions are no good for walking technicolor
  because mass anomalous dimension saturates at $\gamma \lesssim 0.45$

- While several nice tricks are already being used to bring down m_{res} [improved gauge action, Dislocations Suppressing Determinant Ratio], and to speed up the inversion [Möbius], it's a good idea to
  try DWF with fat links

Walking (extended) Technicolor

For acceptable flavor physics, candidate theories should have:

- Chiral symmetry breaking
- Small S-parameter
- Avoid massless GBs (except those eaten by $W^{\pm}$ and Z)
- Condensate enhancement

$\Rightarrow$ need mass anomalous dimension $\gamma \approx 1$

$\Rightarrow$ this is expected for nearly conformal ("walking") theories

$\Rightarrow$ Natural candidates: $N_f = 2$ higher-irrep fermions [Sannino *et al.*]

Schrödinger functional

- Prescribe gauge field $A_k(L,\eta)$ on time boundaries: $t=0$ and $t=L$

$\Rightarrow$ induce background color-electric field in the bulk

$$\begin{aligned}\Gamma(L,\eta) \equiv -\log(Z) &= \text{tree-level} + \text{one-loop} + \cdots \\ &= \left(\frac{1}{g_0^2(a)} + \frac{b_1}{32\pi^2}\log(L/a) + \cdots\right) S_{cl}(\eta) \\ &= \frac{1}{g^2(L)}\, S_{cl}(\eta)\end{aligned}$$

- Obtain $1/g^2(L)$ from variation w.r.t. η, which is an observable

- Extract mass anomalous dimension γ from scaling of pseudoscalar renormalization constant Z_P, on the same lattices

Soft gauge action

- Soft action: $S_{\rm gauge} = \beta \sum U_{\rm plaq}(\text{thin links}) + \tilde{\beta} \sum U_{\rm plaq}(\text{fat links})$
- Pushes 1st-order bulk transition back into stronger bare coupling
- SU(3)/sextet:
  - thin links: transition at $g^2_{SF} \approx 2.5$, lattice artifacts for $g^2_{SF} \gtrsim 2.0$
  - fat links, $\tilde{\beta} = 0$: transition at $g^2_{SF} \approx 5.0$, lattice artifacts for $g^2_{SF} \gtrsim 3.5$
  - fat links, $\tilde{\beta} = 0.5$: up to $g^2_{SF} \approx 11$ before running out of steam
- Stabilize nHYP reunitarization step:

$$V_\mu = \Omega_\mu \left(\Omega_\mu^\dagger \Omega_\mu\right)^{-1/2} \qquad \Rightarrow \qquad V_\mu = \Omega_\mu \left(\Omega_\mu^\dagger \Omega_\mu + \epsilon\right)^{-1/2}$$

We use $\epsilon = 10^{-6}$

Soft gauge action: weak-coupling universality

bare coupling: $$\frac{1}{g_0^2} = \frac{\beta}{N} T(f) + \frac{\tilde{\beta}}{d_R} T(R),$$

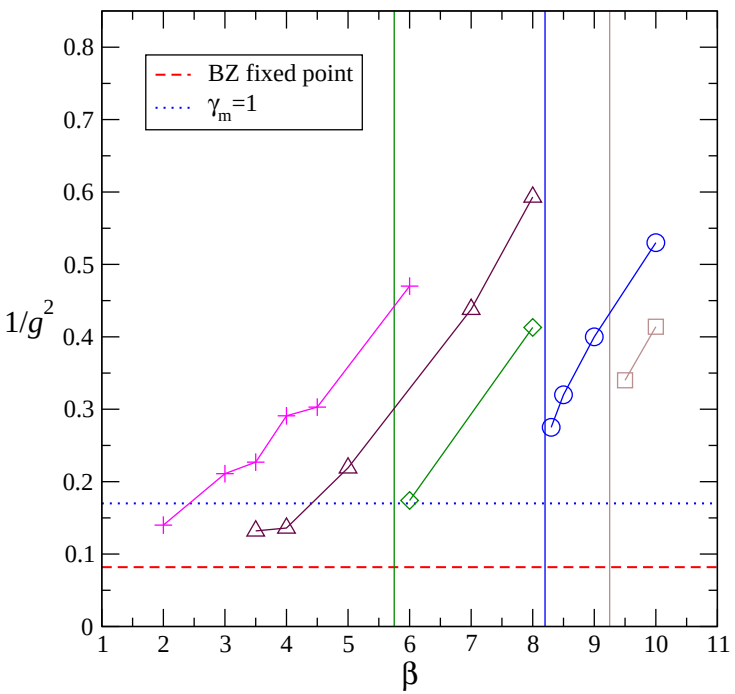

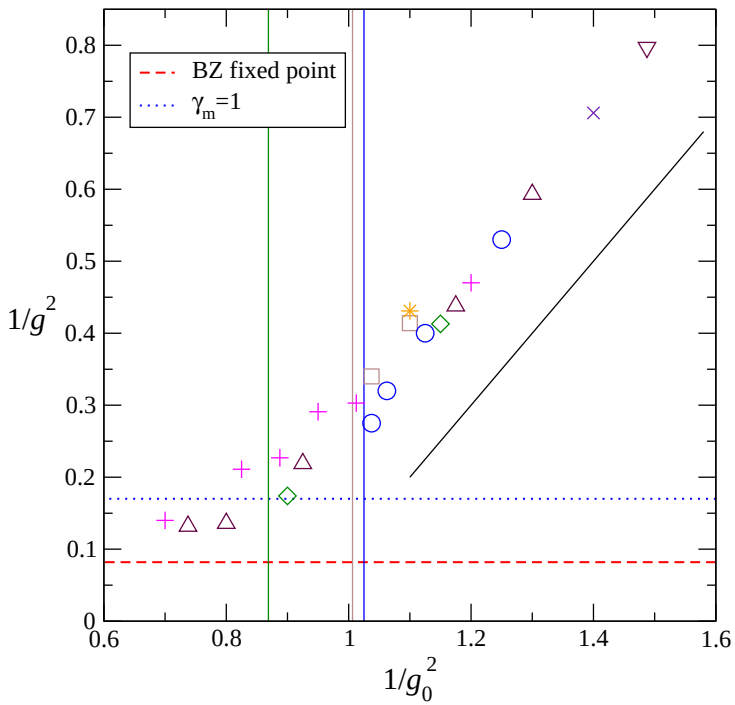

SU(4), Right to left: $\tilde{\beta} = -0.5,\ 0.0,\ 0.5,\ 1.0,\ 1.5$

Soft gauge action: κ_c

- Perturbation theory:
  κ_c increases with $\tilde{\beta}$ at fixed $1/g_0^2$
- Beyond $8/g_0^2 \approx 9$ trend reverses

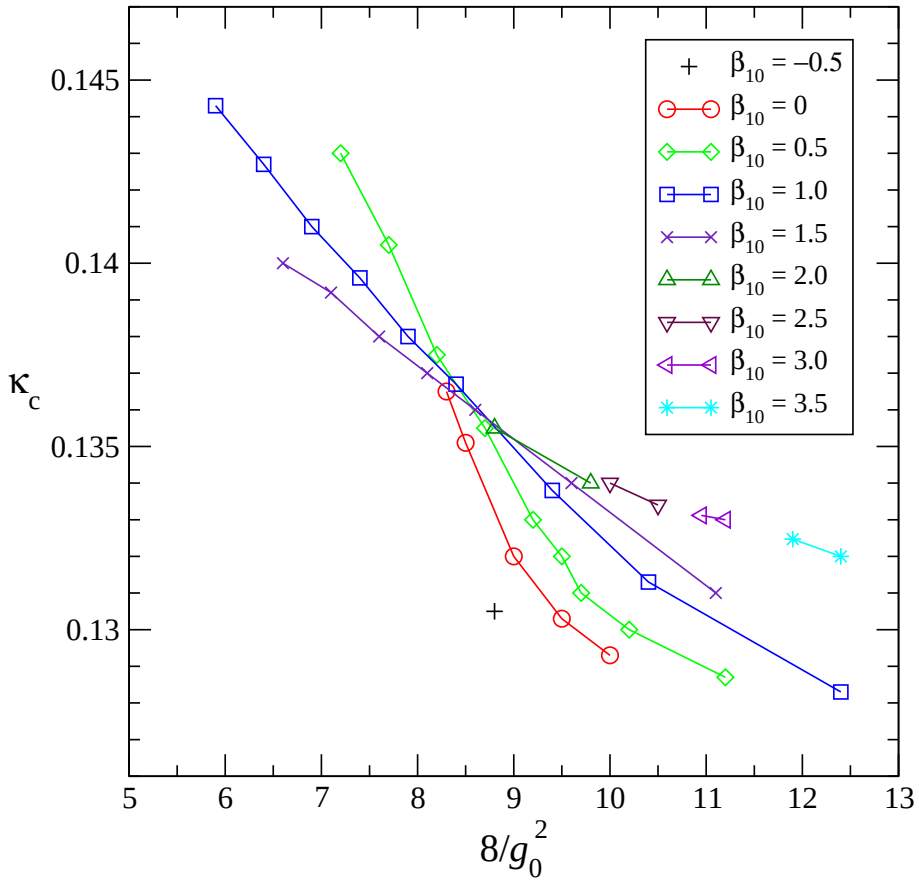

Effects of the bulk transition, SU(3)

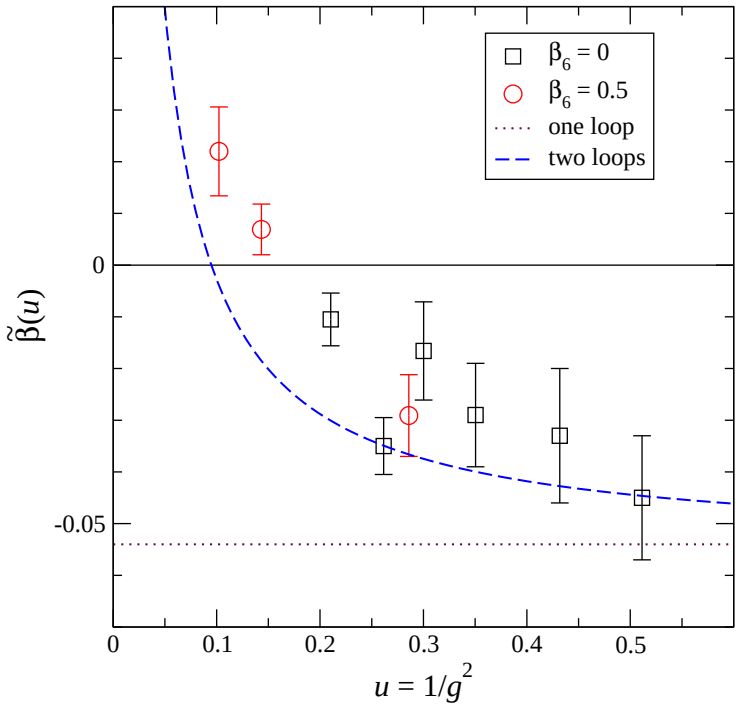

SF coupling: agreement

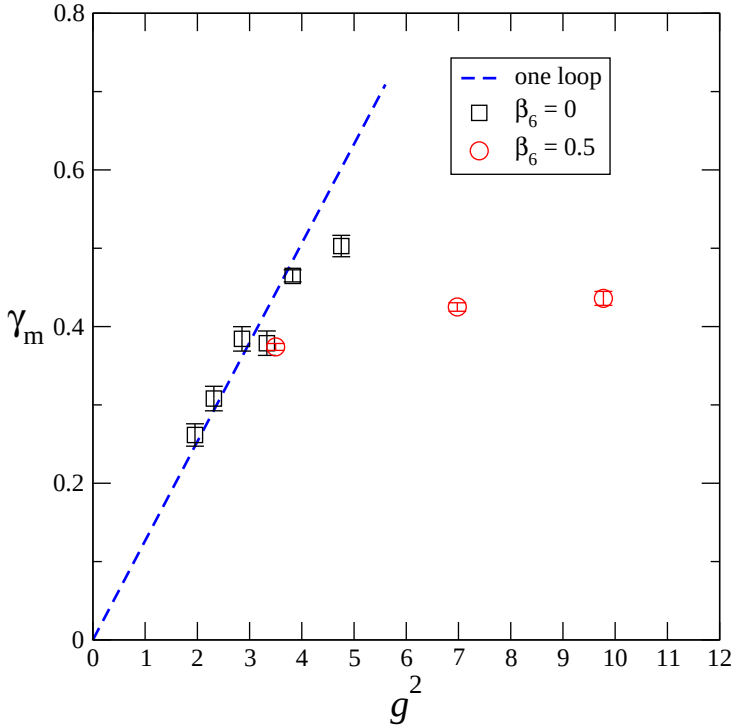

Mass anomalous dimension: discrepancy – due to proximity of bulk transition for $\tilde{\beta} = 0$

Nucleon EDM from Lattice QCD

Eigo Shintani (RIKEN-BNL)
for RBC/UKQCD collaboration

New Horizons for Lattice Computations with Chiral Fermions, May 16 2012

CP symmetry breaking in the SM

- EW
  - It has been known the CP violation occurs by the phase of CKM matrix
  - K, D, B meson decay via direct and indirect CP violation
  - Contribution to EDM is very tiny, $\Rightarrow d_N^{\mathrm{KM}} \simeq 10^{-30\sim-33}\,\mathrm{e}\cdot\mathrm{cm}$

    6-orders magnitude below the exp. upper limit: $|d_N^{\mathrm{exp}}| < 2.9\times 10^{-26}\,\mathrm{e}\cdot\mathrm{cm}$
- QCD
  - θ term in the QCD Lagrangian:

$$\mathcal{L}_\theta = \bar{\theta}\frac{1}{64\pi^2}\int d^4x G\widetilde{G}, \quad \bar{\theta} = \theta + \arg\det M$$

    renormalizable and CP-violation comes due to topological charge density.
  - EDM experiment provides very strong constraint on $\bar{\theta} < 10^{-9}$

    $\Rightarrow$ θ and $\arg\det$ M need to be unnaturally canceled ! (strong CP problem)

CP symmetry breaking beyond the SM

- Possible higher dimension operators
  - Effective Hamiltonian with higher dimension than 4

$$H_{\not{CP}} = \sum_k C_k(\mu)\,\mathcal{O}_k$$

$$\begin{aligned}
\mathcal{O}_{\rm qEDM} &= \bar{q}(\sigma\cdot F)\gamma_5 q && \text{: Quark-photon}\\
\mathcal{O}_{\rm cEDM} &= \bar{q}(\sigma\cdot G)\gamma_5 q && \text{: Quark-gluon}\\
\mathcal{O}_{\rm Weinberg} &= GG\widetilde{G} && \text{: Pure gluonic}\\
&\vdots
\end{aligned}$$

SUSY model

$$d_N \sim d_d^{\rm cEDM} \sim -\frac{\alpha m_d \tan\beta}{64\pi^3 m_A^2}\sum_{q=t,b}\xi_q Q_q^2 F$$

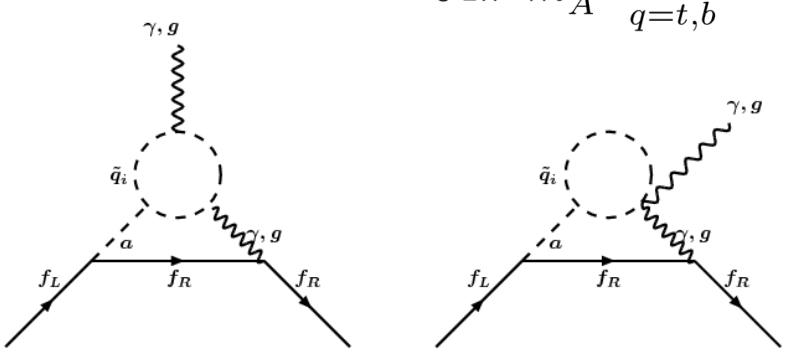

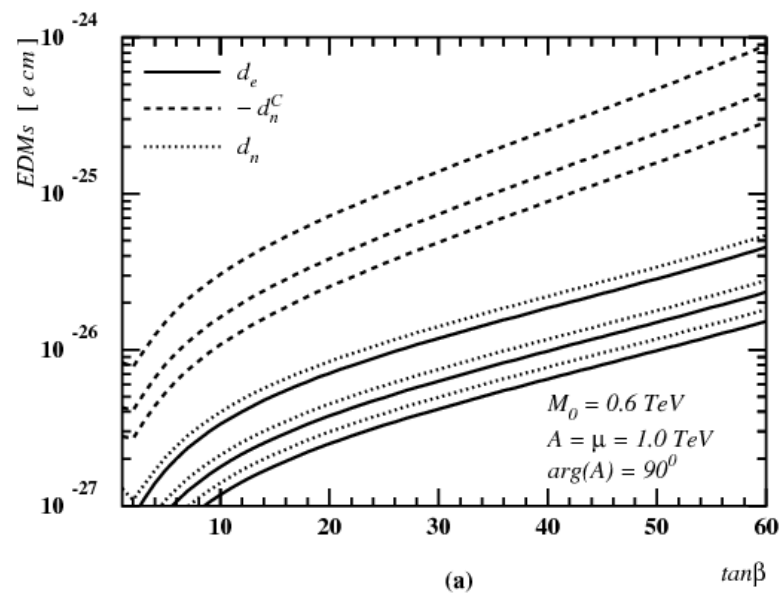

Chang, et al. (99), Ibrahim and Nath (08)

Constraint on nEDM

- The present and future experiment is close to "exclude" of MSSM
  pEDM experiment @ BNL,
  nEDM experiment @ J-PARC, …
  ⇒ reaching a sensitivity of 10^{-29} e・cm !
- Current theoretical bound is based on quark model.
- Non-perturbative computation is necessary to draw more reliable conclusion.

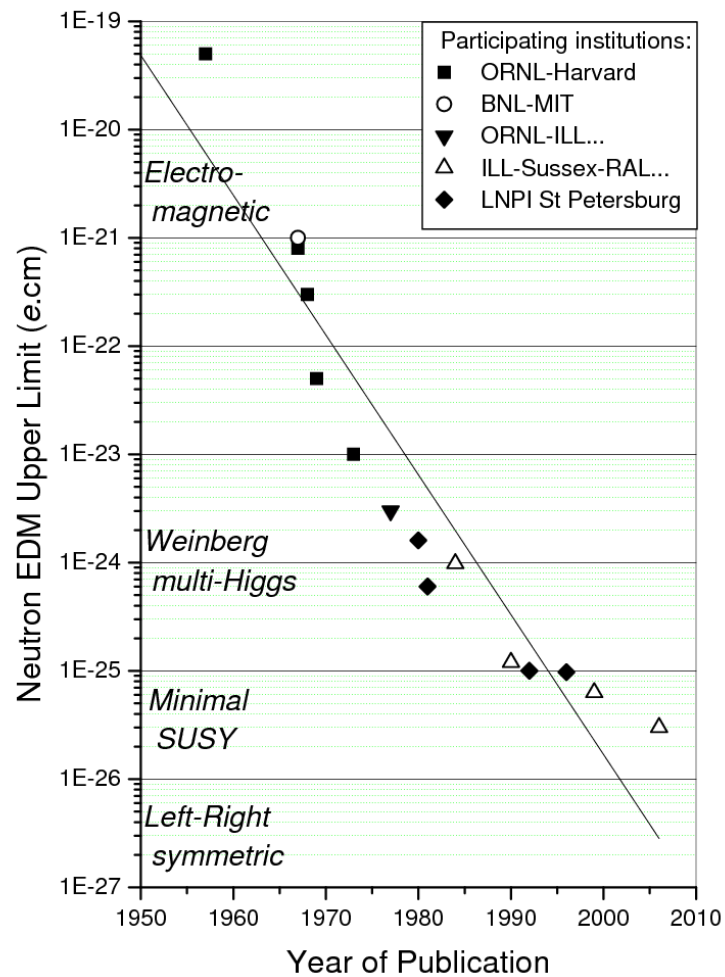

Harris, 0709.3100

What lattice QCD can do for nEDM

- In principle
  - Direct estimate of neutron and proton EDM from θ term, higher dim. $\not{C}\not{P}$ operators
  - Matrix elements of higher dimension operators

    $\langle N|\bar{q}\gamma_5\sigma\cdot Fq|N\rangle,\ \langle N|\bar{q}\gamma_5\sigma\cdot Gq|N\rangle, \langle N|GG\tilde{G}|N\rangle, \cdots$
- In practice there are some difficulties
  - Statistical error

    Source of CP violation comes from gauge background (topological charge, sea quark) which is intrinsically noisy.

    Disconnected diagram is necessary because of flavor singlet contraction.
  - Systematic error

    Volume effect may be significant.

    Chiral behavior is important, $d_N \sim O(m)$?

Possible lattice methods

- Spectrum method

  Aoki-Gocksch(89), ES et al. CP-PACS(06, 07)

  - Spin splitting of nucleon energy in external electric field and θ term, which is given by 2-pt function: $m_{\uparrow} - m_{\downarrow} = 2d_N\theta E$
  - Computational cost is cheap, and directly obtain EDM.
- Form factor

  ES et al. CP-PACS(05), RBC(06)

$$\langle n(P_1)|J_\mu^{\rm EM}|n(P_2)\rangle_\theta = \bar{u}_N^\theta \Big[\underbrace{\frac{F_3^\theta(Q^2)}{2m_N}\gamma_5\sigma_{\mu\nu}Q_\nu}_{\text{P,T-odd}} + \underbrace{F_1\gamma_\mu + \frac{F_2}{2m_N}\sigma_{\mu\nu}Q_\nu}_{\text{P,T-even}} + \cdots \Big] u_N^\theta$$

  - F_3 in $Q^2 \to 0$ provides d_N
  - Subtraction to contribution of CP-odd phase in n propagator.
- Imaginary θ
  - Generate new configurations with imaginary θ term, which may enhance signal.

    Izubuchi (07), Horsley et al. (08)

Spectrum method

ES et al. (06, 07)

- Ratio of spin up and down

$$R_3 = \frac{\langle N(t)\bar{N}(0)\rangle^{\rm up}_{\theta,E}}{\langle N(t)\bar{N}(0)\rangle^{\rm down}_{\theta,E}} \simeq 1 + d_N E\theta t$$

Linear response, gradient is a signal of EDM.

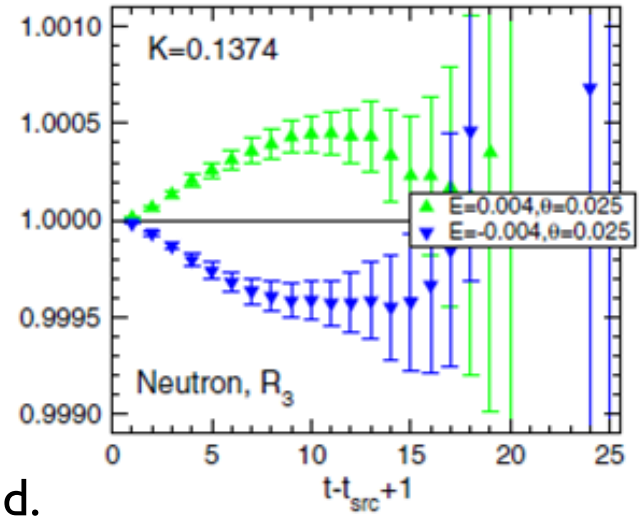

- Remarks
  - Reweighting works well for small real θ
  - Temporal periodicity is broken by electric field.

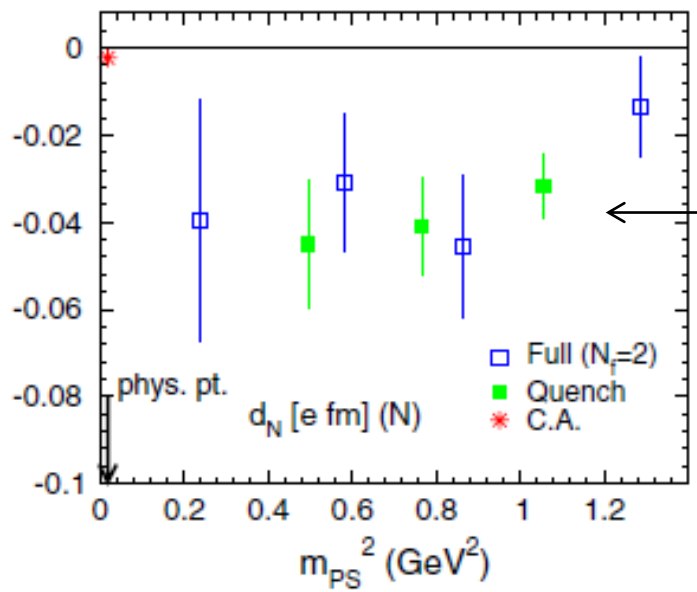

Full QCD with clover fermion:

- There seems to be no significant difference between quench and full QCD.
- Statistical error is still large.

- Finite size effect from breaking of temporal periodicity is also significant

Form factor method

ES(08)

- F_3 signal

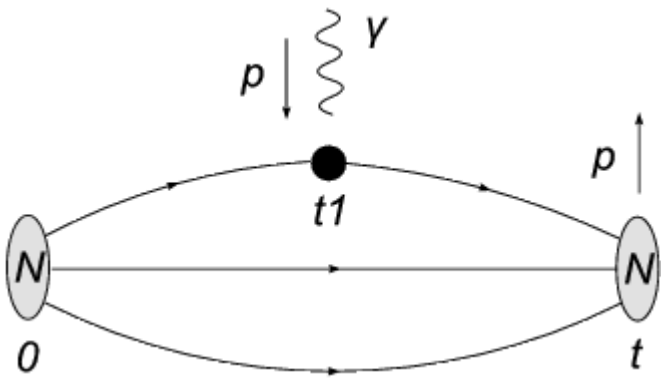

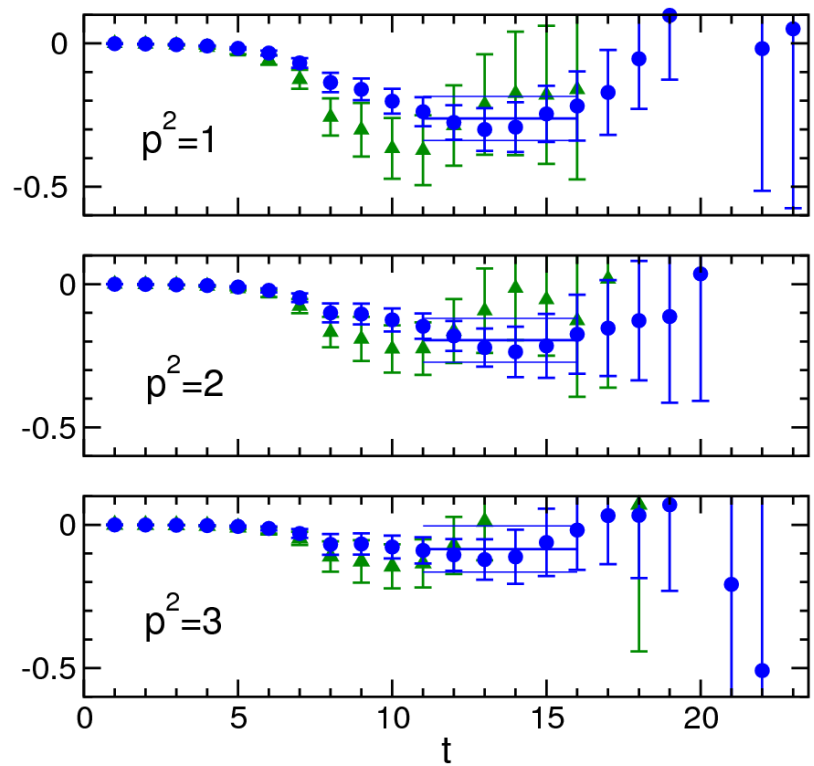

- Nf=2 clover fermion
- Sequential source for V current

Imaginary θ

Izubuchi(07), Horsley et al. (08)

- Analytically continued to pure imaginary, $\theta \to i\theta^I$

$$\langle O e^{i\theta Q} \rangle \to \langle O e^{-\theta^I Q} \rangle$$

  - There is no sign problem, expect better signal.
  - Generate the QCD ensemble with θ^I: distribution of topological charge is shifted by θ^I

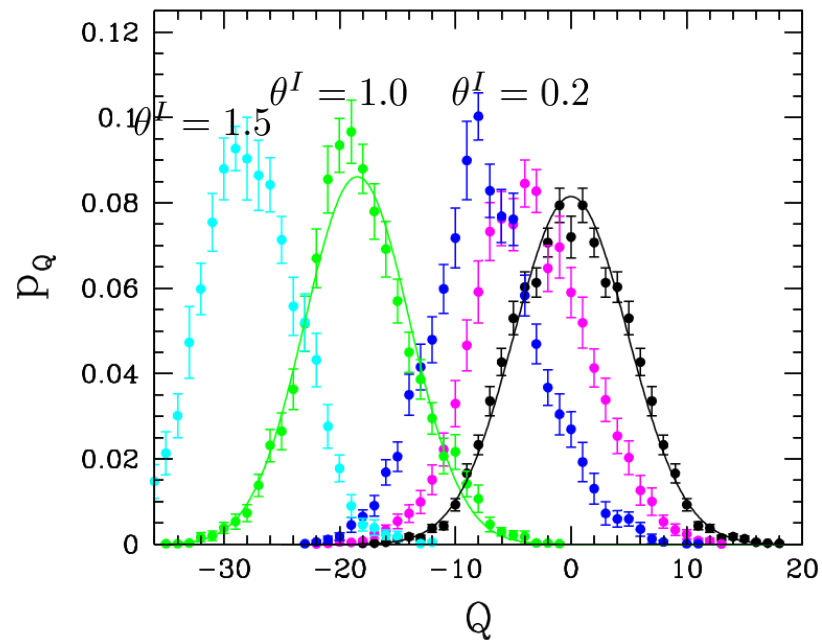

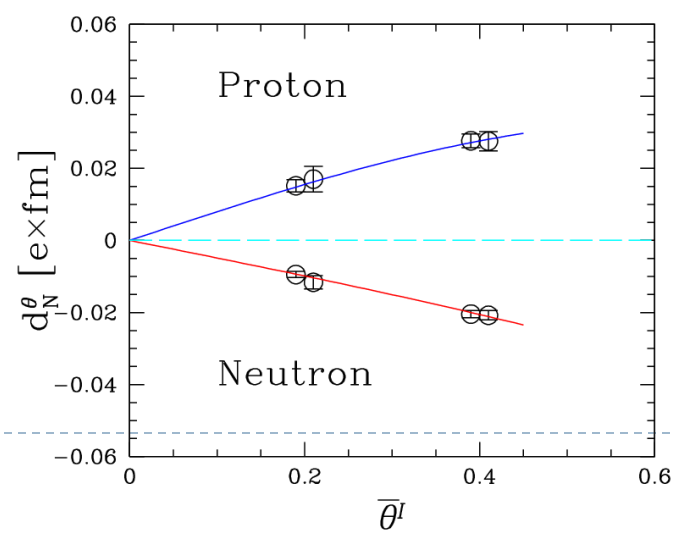

Full QCD with clover fermion

- EDM is given by the slope.
- Clear signal, but systematic error due to chiral symmetry breaking of clover fermion has not been taken into account.

Comparison of results

- Full QCD
  - Lattice results are consistent within 1σ.
  - An order of magnitude larger than the results of current algebra.
  - N_f = 2+1 DWF configs. (RBC/UKQCD) are available for near physical pion mass.
  - Large statistical error is still problem. (O(100) measurements is not enough)

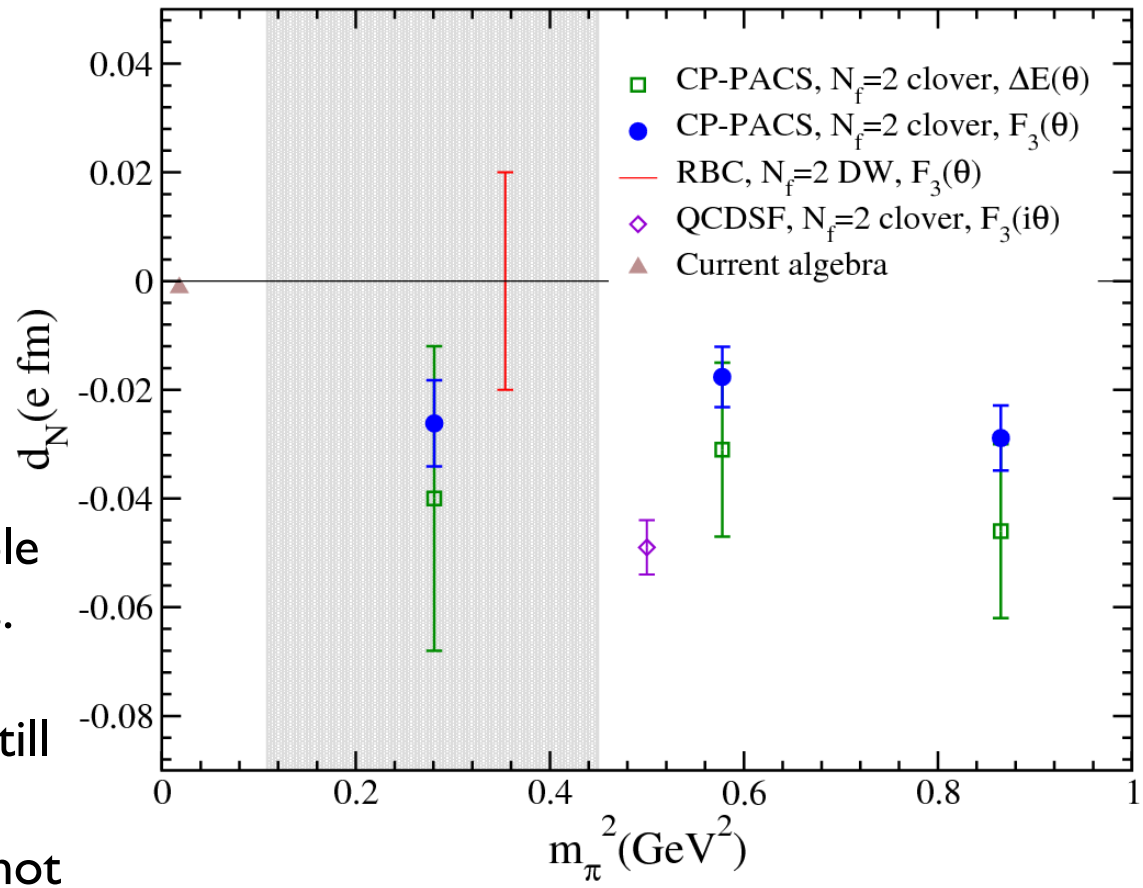

Error reduction techniques

RBC in prep.

- Covariant approximation averaging (CAA)
  - For original observables O, (unbiased) improved estimator

$$\mathcal{O}^{(\mathrm{imp})} = \mathcal{O}^{(\mathrm{rest})} + \frac{1}{N_G}\sum_{g\in G}\mathcal{O}^{(\mathrm{appx}),g}, \quad \mathcal{O}^{(\mathrm{rest})} = \mathcal{O} - \mathcal{O}^{(\mathrm{appx})}$$

which satisfies <O> = <O^{imp}> if approximation is covariant under lattice symmetry g, and error becomes $\boxed{\mathrm{err}^{\mathrm{imp}} \simeq \mathrm{err}/\sqrt{N_G}}$

  - Ideal approximation

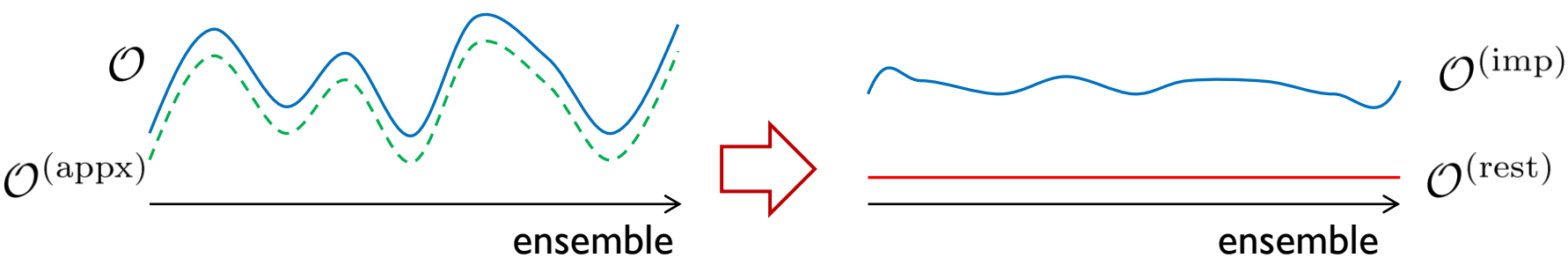

- Ignoring the error from O$^{(\mathrm{rest})}$
- There may be many candidates of O$^{(\mathrm{appx})}$ e.g. LMA, heavy mass, …
- The cost of approximated observable need to be smaller than the original.

Examples of CAA

- Lowmode averaging (LMA)

Guisti et al.(04), Neff et al.(01), DeGrand et al. (04)

  - Using lowlying eigenmode of Dirac operator to approximate propagator:

$$\mathcal{O}^{(\mathrm{appx})} = \sum_{\lambda}^{N_\lambda} \mathcal{O}_\lambda^{\mathrm{low}}$$

where N_λ is number of lowmode computed by Lanczos.

Except for computational cost of eigenmode, Cost(LMA) $\simeq$ 0, but approximation is only lowmode part (long distance contribution).

- All-mode averaging (AMA)
  - Using sloppy CG (loose stopping condition),

$$\mathcal{O}^{(\mathrm{appx})} = \mathcal{O}^{\mathrm{sloppy}}$$

If stopping cond. is 0.003, Cost(AMA) $\simeq$ Cost(CG)/50(without deflation).

Approximation becomes better than LMA for other than lowmode dominanted observables (nucleon, finite momentum hadron, …).

Examples of Covariant Approximations

- All Mode Averaging
  AMA
  Sloppy CG or Polynomial approximations

$$\mathcal{O}^{(\mathrm{appx})} = \mathcal{O}[S_l],$$

$$S_l = \sum_\lambda v_\lambda f(\lambda) v_\lambda^\dagger,$$

$$f(\lambda) = \begin{cases} \frac{1}{\lambda}, & |\lambda| < \lambda_{\mathrm{cut}} \\ P_n(\lambda) & |\lambda| > \lambda_{\mathrm{cut}} \end{cases}$$

$$P_n(\lambda) \approx \frac{1}{\lambda}$$

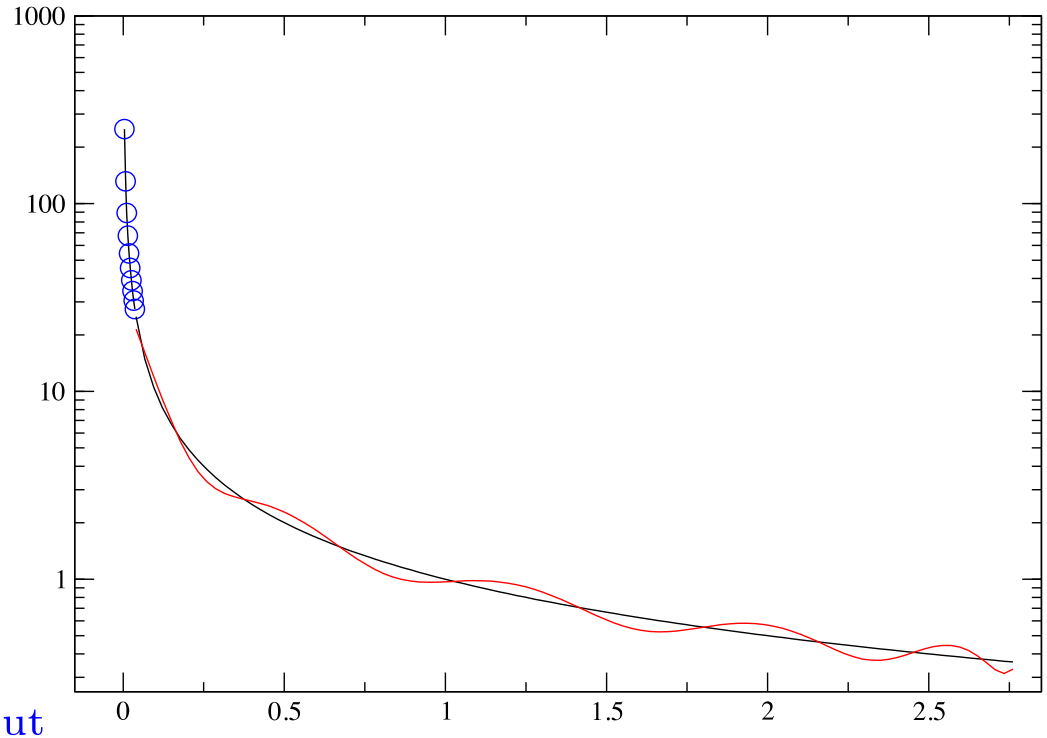

accuracy control :

- low mode part : # of eig-mode
- mid-high mode : degree of poly.

Comparison between LMA/AMA

RBC in prep.

- Preliminary result
  - 8 configs, Gaussian smearing, $N_G = 2^3 \times 4 = 32$ sources, $24^3 64 \times 16$ DWF

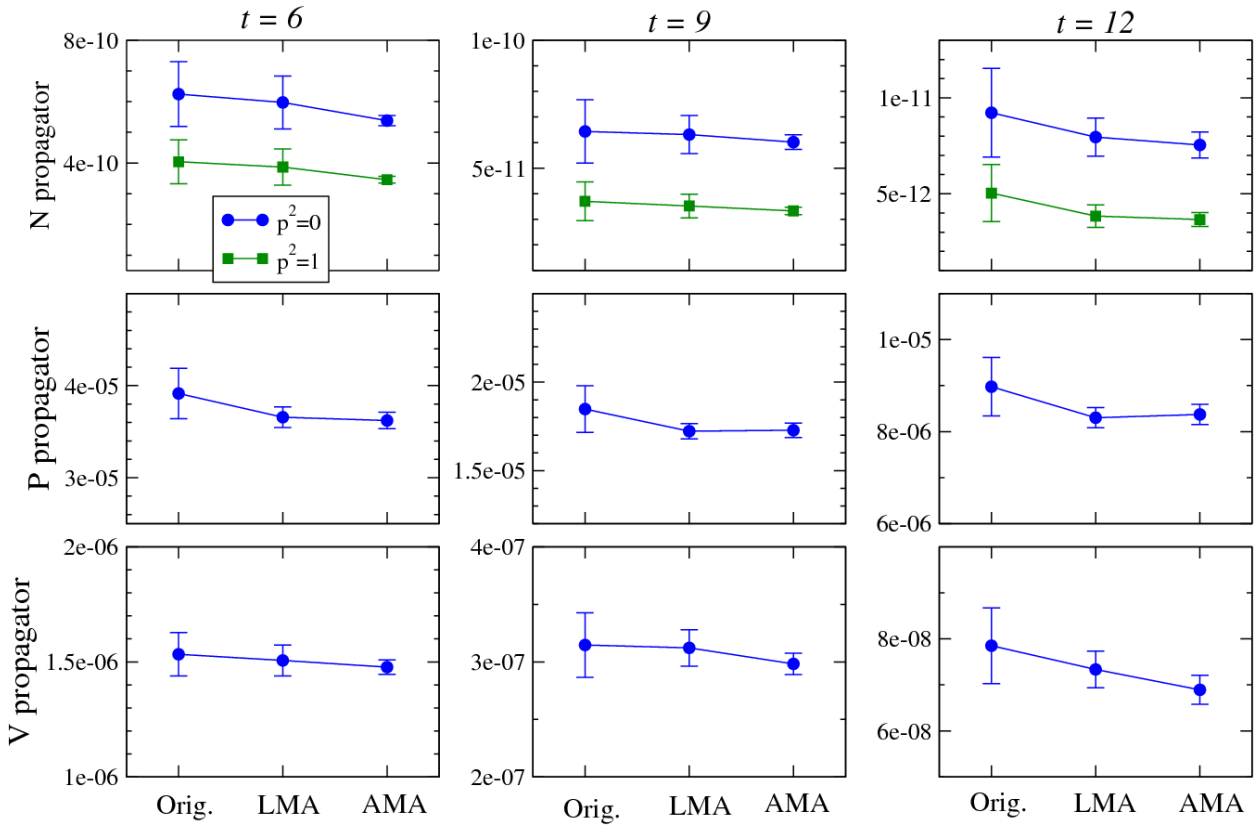

- t = 6:
  Error in AMA is actually reduced by factor 5 compared with orig. and LMA.

- t = 12
  Error in AMA/LMA is reduced by factor 3--4 compared with original.

Comparison between LMA/AMA

- Very preliminary

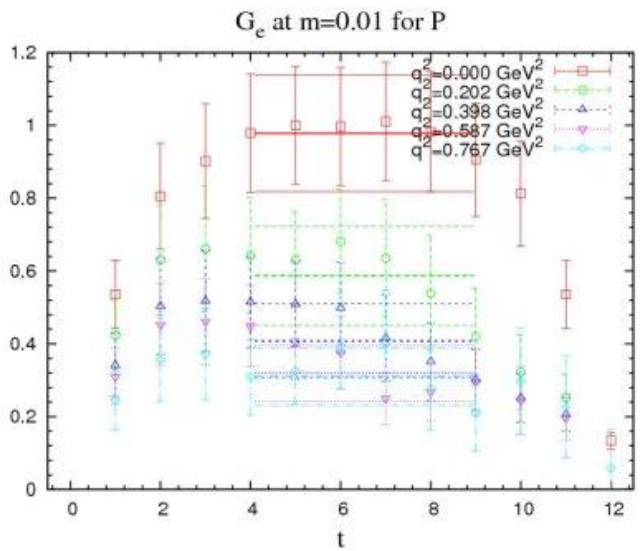

Proton Ge (Original)

Proton Ge (LMA)

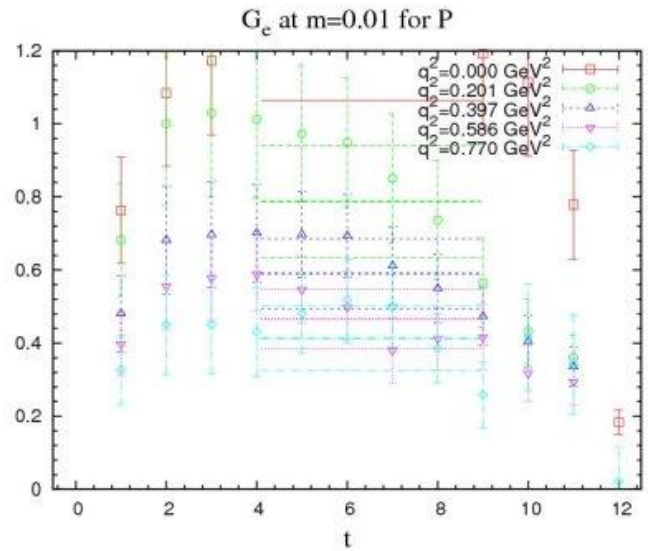

Proton Ge (AMA)

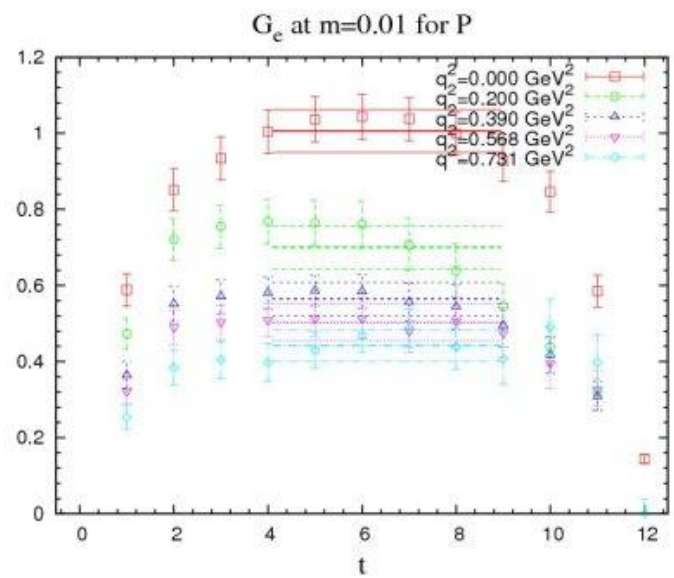

Conclusion and future work

- Nucleon EDM in lattice QCD
  - Large statistical error is problem.
  - LMA/AMA may work well.
  - Aim for less than 10% statistical error.
  - Systematic study of finite size effect, chiral behavior, …
  - Other source $\not{CP}$ effect

Thank you.

Backup

Electric dipole moment (EDM)

- P(arity), T(ime reversal)[=CP] symmetry breaking

EDM:

$$\vec{D} = d\vec{S}, \quad \Delta H = \vec{D} \cdot \vec{E}$$

under discrete symmetries, spin and E have different behavior

$$\begin{aligned} \mathrm{P}: &\quad \vec{E} \to -\vec{E} \quad \vec{S} \to \vec{S} \\ \mathrm{T}: &\quad \vec{E} \to \vec{E} \quad \vec{S} \to -\vec{S} \end{aligned}$$

If $d \neq 0$,

$$\mathrm{P}, \mathrm{T} : \Delta H \to -\Delta H$$

Non-vanishing EDM is a signal of the P, CP violation.

- In EW P, CP violation following Kobayashi-Maskawa mechanism.
- In QCD, it is natural to exist but there has been no signal the breaking would be also.

Strong CP problem ?

- Possible solution
  - Massless quark

    One of the quark flavor is massless ($m_u = 0$ or $m_d = 0$),

    i.e. $\arg\det M \propto m_u m_d m_s/(m_u+m_d+m_s) = 0$

    This has been refused by spectrum study in lattice QCD+QED.

  - Axion model
    - Pecci-Quinn (additional chiral) symmetry is spontaneously broken.

      Axion of (in-)visible model has been almost excluded by cosmology.

  - Spontaneous breaking

CP symmetry breaking in the SM

- Contribution to EDM from weak interaction is very small
  - Vanishing 1-loop (no Im part), 2-loop diagram
  - Three-loop order(short) and pion loop correction (long):

Short distance

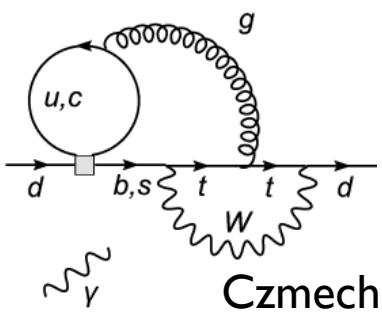

Czmechi, Krause (1997)

Long distance

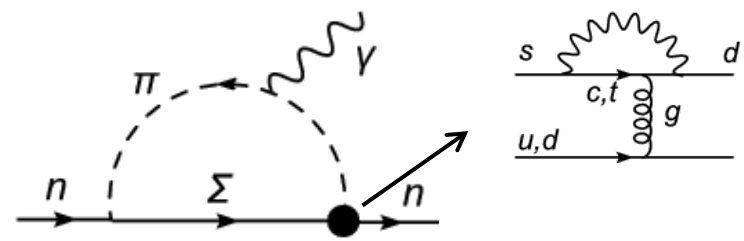

Khriplovich, Zhitnitsky (1982)

$$d_N^{\mathrm{KM\,short}} \sim \mathcal{O}(\alpha_s G^2) \sim -10^{-34}\,\mathrm{e\cdot cm} \qquad d_N^{\mathrm{KM\,long}} \sim 10^{-30\sim-33}\,\mathrm{e\cdot cm}$$

$$\Rightarrow d_N^{\mathrm{KM}} = d_N^{\mathrm{KM\,short}} + d_N^{\mathrm{KM\,long}} \simeq 10^{-30\sim-33}\,\mathrm{e\cdot cm}$$

which is the 6-order magnitude below the exp. upper limit: $|d_N^{\mathrm{exp}}| < 2.9\times 10^{-26}\,\mathrm{e\cdot cm}$

Spectrum method

Aoki-Gocksch(89), ES(06,07), Horsley(07), QCD-SF(08)

- Energy difference between nucleon spin
  - Energy eigenvalue if θ exist in the background

$$\mathcal{E}_{+S_3}(\vec{E}) - \mathcal{E}_{-S_3}(\vec{E}) = 2d_N\bar{\theta}S_3E_3 + \mathcal{O}(E^2, \bar{\theta}^2, E\bar{\theta})$$

in the case of $\vec{E}(t) = (0, 0, E_3)$

  - 2-pt function provides EDM as exponents

$$\langle N(t)\bar{N}(0)\rangle_{\theta,E}^{\text{upper}} \simeq Z(1 + A_N(E^2)\theta E_3)\exp(-m_N t - d_N\theta E_3 t/2)$$

$$\langle N(t)\bar{N}(0)\rangle_{\theta,E}^{\text{lower}} \simeq Z(1 - A_N(E^2)\theta E_3)\exp(-m_N t + d_N\theta E_3 t/2)$$

d_N is given by fitting with the above asymptotic function.

  - Two reweighting method

$$\langle N\bar{N}\rangle_{\theta,E} = \langle N\bar{N}(Ue^{q_e E})e^{i\theta Q}\rangle$$ Eucleadian E, real θ

$$= \langle N\bar{N}(Ue^{iq_e E})e^{\theta m_q\bar{q}\gamma_5 q}\rangle$$ Minkowski E, imaginay θ

Form factor

ES(05, 08)

- Matrix element

$$\langle n(P_1)|J_\mu^{\rm EM}|n(P_2)\rangle_\theta = \bar{u}_N^\theta \Big[\underbrace{\frac{F_3^\theta(Q^2)}{2m_N}\gamma_5\sigma_{\mu\nu}Q_\nu}_{\text{P,T-odd}} + \underbrace{F_1\gamma_\mu + \frac{F_2}{2m_N}\sigma_{\mu\nu}Q_\nu}_{\text{P,T-even}} + \cdots \Big] u_N^\theta$$

  - F_3 in $Q^2 \to 0$ is equivalent to d_N
  - Expansion of 3pt func. at $O(\theta)$ into different CP-odd sources:

$$\langle N(t)J_\mu^{\rm EM}(t_1)\bar{N}(0)Q\rangle$$
$$= \Big[u_N \otimes \bar{u}_N \frac{F_3}{2m_N} Q_\nu\sigma_{\mu\nu}\gamma_5 u_N \otimes \bar{u}_N$$
$$+ u^{\theta^1} \otimes \bar{u}_N^{\theta^1}\Big(F_1\gamma_\mu + \frac{F_2}{2m_N}Q_\nu\sigma_{\mu\nu}\Big) u_N \otimes \bar{u}_N$$
$$+ u_N \otimes \bar{u}_N\Big(F_1\gamma_\mu + \frac{F_2}{2m_N}Q_\nu\sigma_{\mu\nu}\Big) u^{\theta^1} \otimes \bar{u}_N^{\theta^1}\Big] e^{-E_N(P_1)t_1 - E_N(P_2)(t-t_1)}$$

Subtraction of CP-odd phase in n propagator (2nd and 3rd terms) is essential.

Error reduction technique

- Statistical error

$$\mathrm{err} \simeq C/\sqrt{N_{\mathrm{mes}}}$$

  - In order to reduce error,

    do more N_{mes} independent measurements.

    change to C of observables with small fluctuation.

  - Due to limited gauge ensembles, usually covariant observables under lattice symmetry O^g are regarded as independent measurements:

$$\langle O \rangle = \langle O^g \rangle$$

    e.g. g : lattice rotation, translation, …

  - Problem is computational cost.

Lattice QCD's works

- One of the most successful non-perturbative calculation in the particle physics.
  - Reproduce the hadron spectrum using a few input parameters.

    BMW, PACS-CS, …
  - Monte-Carlo simulation is powerful tool.
  - Precision of lattice computations are getting better year by year thanks to development of algorithm (improved HMC, CAA) and machine (GPGPU, Blue Gene, Kei, …).
  - Flexible methodology to apply other physics concerned with strong interaction (e.g. many flavor, Graphene, …)

B-physics with domain-wall light quarks and relativistic heavy quarks

Oliver Witzel
Center for Computational Science

BOSTON UNIVERSITY

BNL, May 15, 2012

Phenomenological Importance

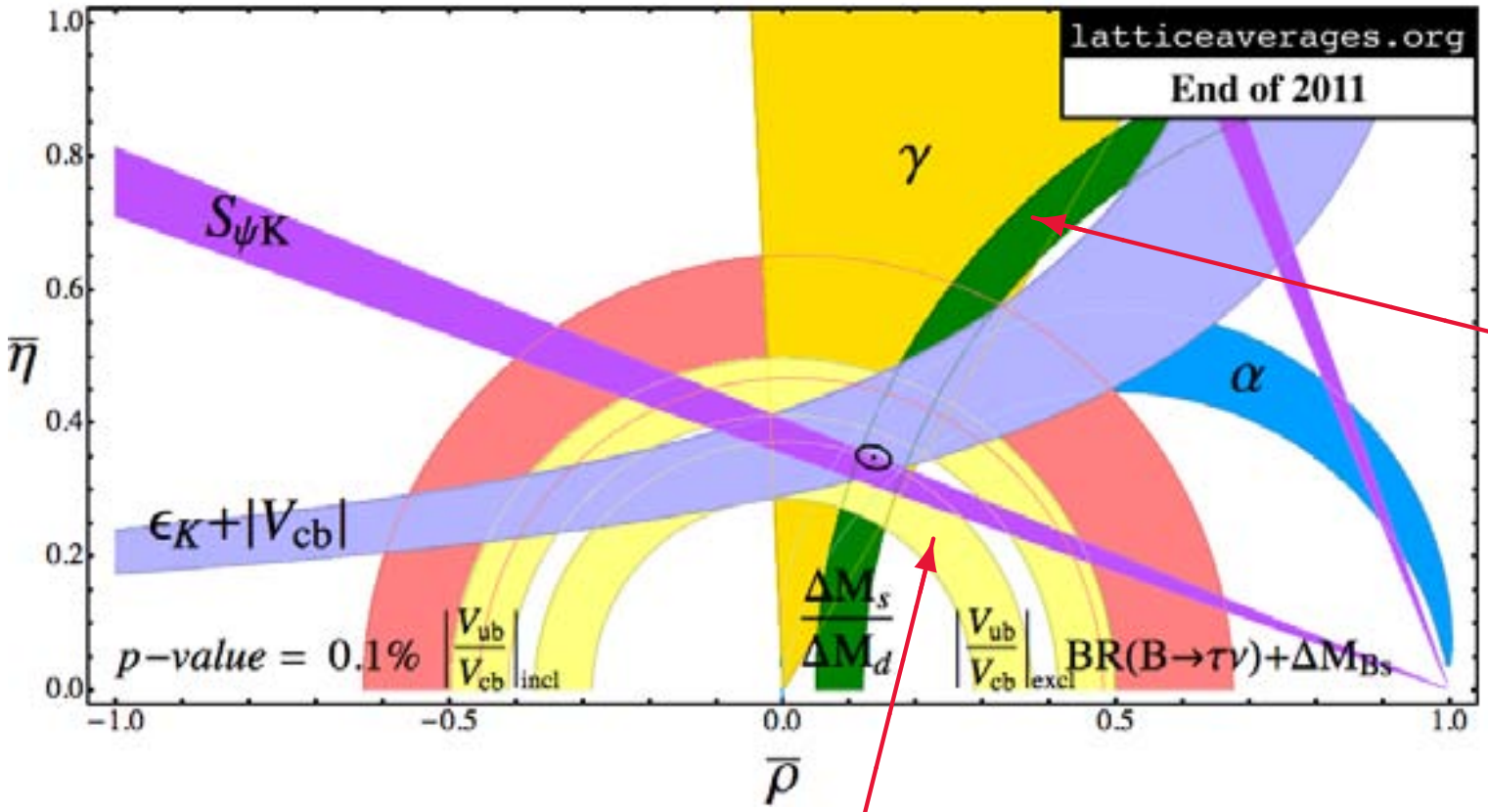

B^0–$\overline{B^0}$ mixing

$B \to \pi \ell \nu$ form factor

B^0–$\overline{B^0}$ Mixing

- Allows us to determine the CKM matrix elements
- Dominant contribution in SM: box diagram with top quarks

$$\left.\begin{array}{l} |V_{td}^* V_{tb}| \text{ for } B_d\text{−mixing} \\ |V_{ts}^* V_{tb}| \text{ for } B_s\text{−mixing} \end{array}\right\} \Delta M_q = \frac{G_F^2 m_W^2}{6\pi^2} \eta_B S_0 M_{B_q} f_{B_q}^2 B_{B_q} |V_{tq}^* V_{tb}|^2$$

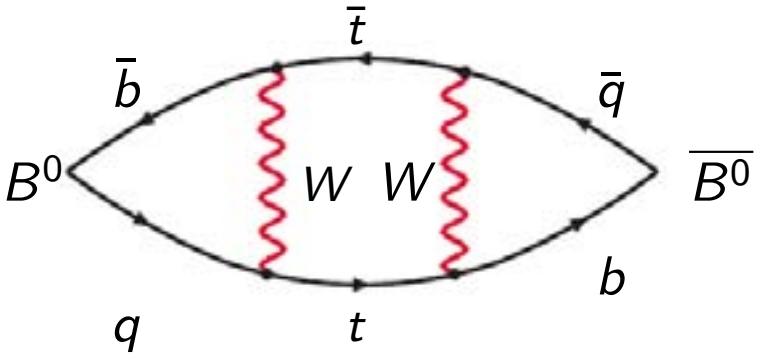

- Nonperturbative contribution: $f_q^2 B_{Bq}$
- Define the $SU(3)$ breaking ratio $\xi^2 = f_{B_s}^2 B_{B_s} / f_{B_d}^2 B_{B_d}$
- CKM matrix elements are extracted by

$$\frac{\Delta M_s}{\Delta M_d} = \frac{M_{B_s}}{M_{B_d}} \xi^2 \frac{|V_{ts}|^2}{|V_{td}|^2}$$

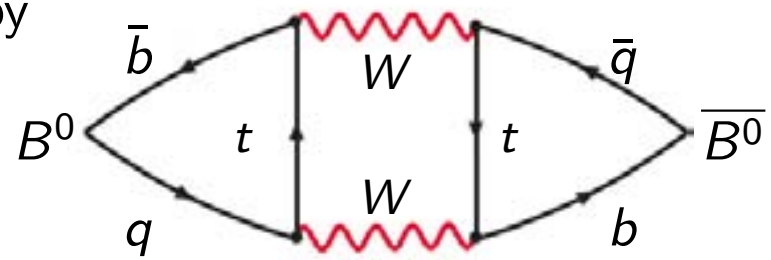

- Experimental error of ΔM_q is better than a percent; lattice uncertainty for ξ is about 3%

$B \to \pi l \nu$ form factor

- Allows to determine the CKM matrix element V_{ub} from the experimental branching ratio

$$\frac{d\Gamma(B \to \pi l \nu)}{dq^2} = \frac{G_F^2 |V_{ub}|^2}{192\pi^3 M_B^3} \left[(M_B^2 + M_\pi^2 - q^2)^2 - 4M_B^2 M_\pi^2\right]^{3/2} |f_+(q^2)|^2$$

- Tension between exclusive determination and inclusive determinations of V_{ub} is greater than 3σ

Possible Deviations from the Standard Model

[Lunghi and Soni 2010/11]

- Experimental value for $\sin(2\beta)$ is 3.3σ lower than SM expectation
- Measured value for $\mathrm{BR}(B \to \pi l \nu)$ is 2.8σ lower than predicted
- Most likely source of deviation in $B_{d(s)}$ mixing and $\sin(2\beta)$; less likely in $B \to \tau\nu$

[Laiho, Lunghi and Van de Water 2012, http://www.latticeaverages.org]

- Scenario in which new physics is in $B \to \tau\nu$ decay and/or in B_d-mixing preferred
- If tension is taken at face value, points to physics at a few-GeV mass scale

See also: http://ckmfitter.in2p3.fr, http://utfit.roma1.infn.it

2+1 Flavor Lattice Calculations of f_{B_s}, f_B, f_{B_s}/f_B, ξ, V_{ub}

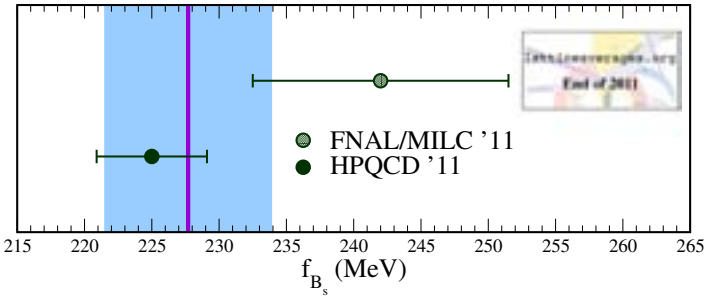

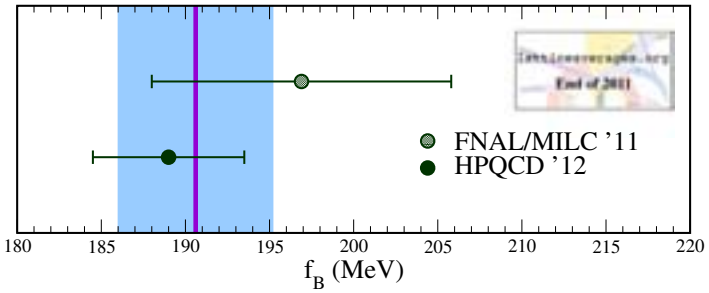

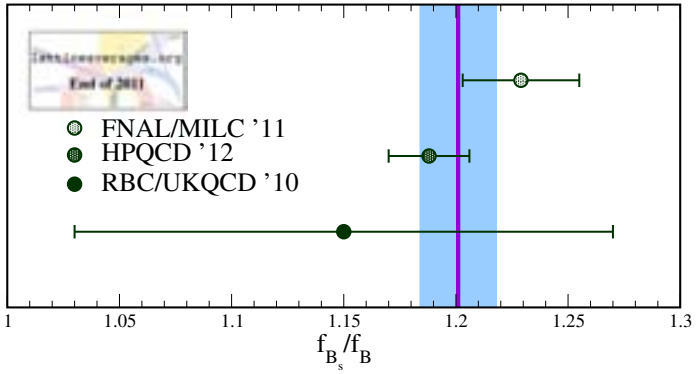

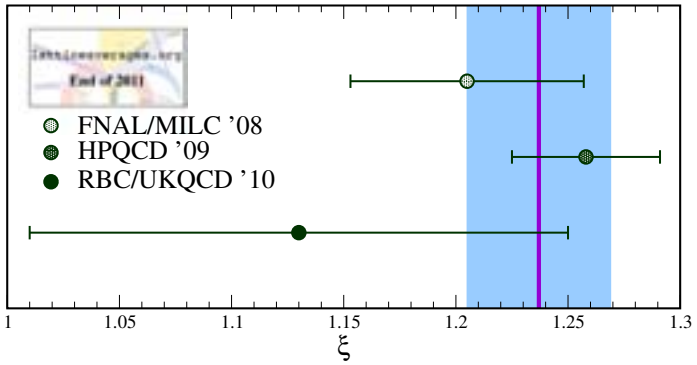

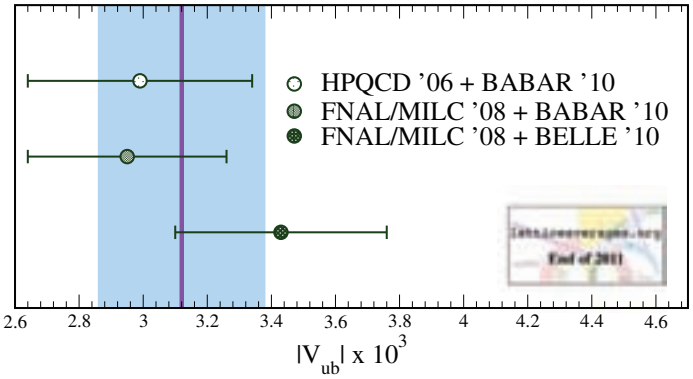

- HPQCD and FNAL-MILC result both based on the asqtad-improved staggered ensembles generated by MILC

Our Project

- Use domain-wall light quarks and nonperturbatively tuned relativistic b-quarks to compute at few-percent precision
  - B^0–$\overline{B^0}$ mixing
  - Decay constants f_B and f_{B_s}
  - $B \to \pi \ell \nu$ form factor
- Tune RHQ parameters using bottom-strange states and high statistics
  - Improve upon exploratory studies and verify made assumptions
  - Validate tuning procedure by computing $b\bar{b}$ masses and splittings
- Derive lattice perturbation theory for matching lattice results to continuum 1-loop in tadpole-improve lattice perturbation
  - Improve matching using a mostly-nonperturbative scheme for f_B, f_{B_s} and $B \to \pi \ell \nu$

2+1 Flavor Domain-Wall Gauge Field Configurations

- Domain-wall fermions for the light quarks (u, d, s) [Kaplan 1992, Shamir 1993]
- Iwasaki gauge action [Iwasaki 1983]
- Configurations generated by RBC and UKQCD collaborations [C. Allton et al. 2008], [Y. Aoki et al. 2010]

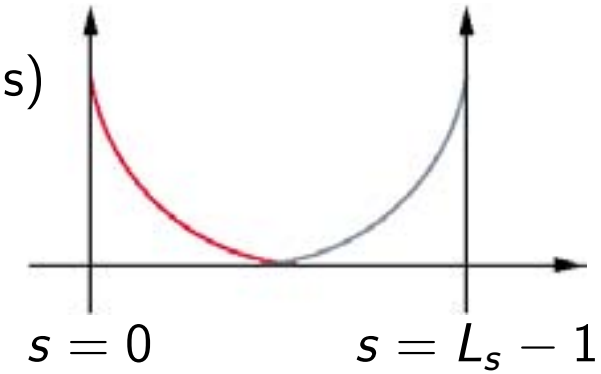

L	a(fm)	m_l	m_s	m_π(MeV)	approx. # configs.	# time sources
24	≈ 0.11	0.005	0.040	331	1636	1
24	≈ 0.11	0.010	0.040	419	1419	1
32	≈ 0.08	0.004	0.030	307	628	2
32	≈ 0.08	0.006	0.030	366	889	2
32	≈ 0.08	0.008	0.030	418	544	2

Relativistic Heavy Quark Action for the b-Quarks

- Relativistic Heavy Quark action developed by Christ, Li, and Lin for the b-quarks in 2-point and 3-point correlation functions

  [Christ, Li, Lin 2007; Lin and Christ 2007]

- Builds upon Fermilab approach [El Khadra, Kronfeld, Mackenzie 1997] by tuning all parameters of the clover action non-perturbatively; close relation to the Tsukuba formulation [Aoki, Kuramashi, Tominaga 2003]

- Heavy quark mass is treated to all orders in $(m_b a)^n$
- Expand in powers of the spatial momentum through $O(\vec{p}a)$
  - Resulting errors will be of $O(\vec{p}^2 a^2)$
  - Allows computation of heavy-light quantities with discretization errors of the same size as in light-light quantities
- Applies for all values of the quark mass
- Has a smooth continuum limit

Tuning the Parameters of the RHQ Action

$$S = \sum_{n,n'} \bar{\Psi}_n \left\{ m_0 + \gamma_0 D_0 - \frac{a D_0^2}{2} + \zeta \left[\vec{\gamma} \cdot \vec{D} - \frac{a \left(\vec{D}\right)^2}{2} \right] - a \sum_{\mu\nu} \frac{i c_P}{4} \sigma_{\mu\nu} F_{\mu\nu} \right\}_{n,n'} \Psi_{n'}$$

- Start from an educated guess for $m_0 a$, c_P, and ζ

$$\begin{bmatrix} m_0 a \\ c_P \\ \zeta \end{bmatrix} \pm \begin{bmatrix} \sigma_{m_0 a} \\ 0 \\ 0 \end{bmatrix}, \begin{bmatrix} 0 \\ \sigma_{c_P} \\ 0 \end{bmatrix}, \begin{bmatrix} 0 \\ 0 \\ \sigma_\zeta \end{bmatrix}$$

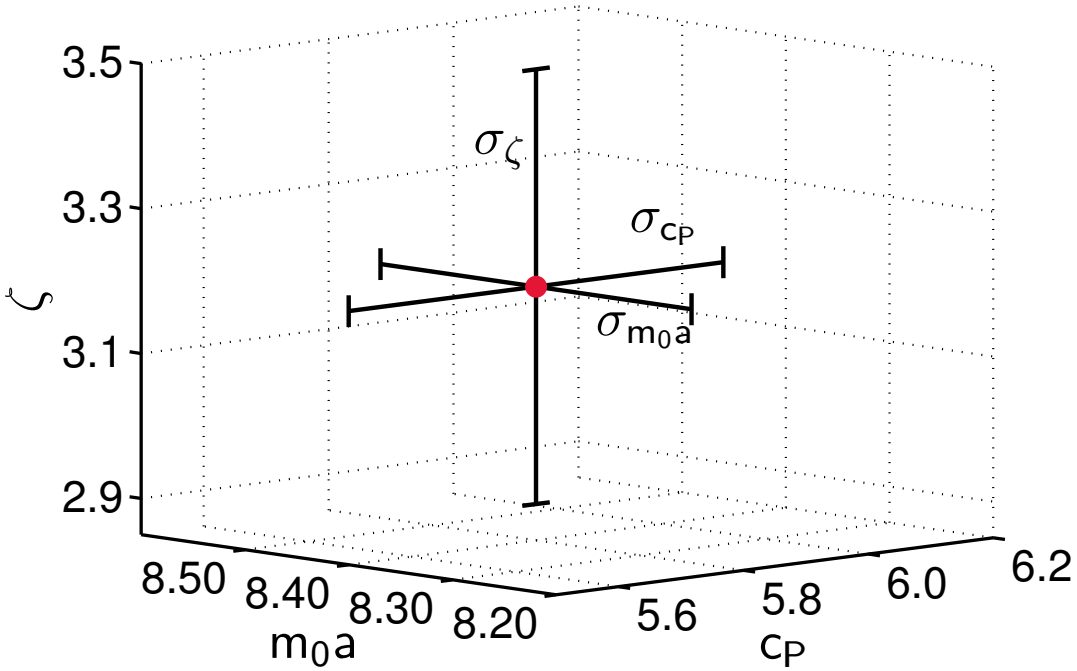

- Compute for all seven parameter sets

spin-averaged mass	$\overline{M} = (M_{B_s} + 3M_{B_s^*})/4$	$\rightarrow$	5403.1(1.1) MeV
hyperfine-splitting	$\Delta_M = (M_{B_s^*} - M_{B_s})$	$\rightarrow$	49.0(1.5) MeV
ratio	$\frac{M_1}{M_2} = M_{\text{rest}}/M_{\text{kinetic}}$	$\rightarrow$	1

- Assuming linearity

$$Y_r = \begin{bmatrix} \overline{M} \\ \Delta_M \\ \frac{M_1}{M_2} \end{bmatrix}_r = J^{(3\times 3)} \begin{bmatrix} m_0 a \\ c_P \\ \zeta \end{bmatrix}_r + A^{(3\times 1)} \qquad (r = 1, \ldots, 7)$$

and defining

$$J = \left[\frac{Y_3 - Y_2}{2\sigma_{m_0 a}}, \frac{Y_5 - Y_4}{2\sigma_{c_P}}, \frac{Y_7 - Y_6}{2\sigma_\zeta} \right] \qquad A = \begin{bmatrix} \overline{M} \\ \Delta_M \\ \frac{M_1}{M_2} \end{bmatrix}_1 - J \times \begin{bmatrix} m_0 a \\ c_P \\ \zeta \end{bmatrix}_1$$

- We extract the RHQ parameters and iterate until result is inside uncertainties

$$\begin{bmatrix} m_0 a \\ c_P \\ \zeta \end{bmatrix}^{\text{RHQ}} = J^{-1} \times \left(\begin{bmatrix} \overline{M} \\ \Delta_M \\ \frac{M_1}{M_2} \end{bmatrix}^{\text{PDG}} - A \right)$$

Nonperturbatively Tuned Parameters of the RHQ Action (preliminary)

m^l_{sea}	$m_0 a$	c_P	ζ
0.005	8.43(7)	5.7(2)	3.11(9)
0.010	8.47(9)	5.8(2)	3.1(2)
average	8.45(6)	5.8(1)	3.10(7)

m^l_{sea}	$m_0 a$	c_P	ζ
0.004	4.07(6)	3.7(1)	1.86(8)
0.006	3.97(5)	3.5(1)	1.94(6)
0.008	3.95(6)	3.6(1)	1.99(8)
average	3.99(3)	3.57(7)	1.93(4)

Preliminary Predictions for the Heavy-Heavy States

- RHQ action describes heavy-light as well as heavy-heavy mesons
- Tuning the parameters in the B_s system we can predict bottomonium states and mass splittings

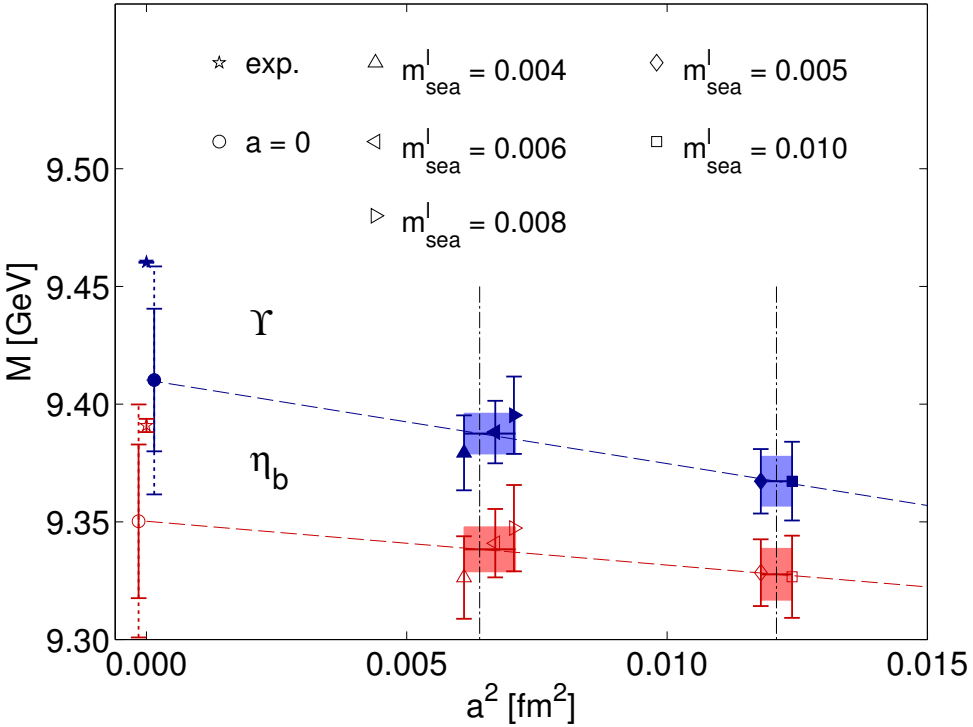

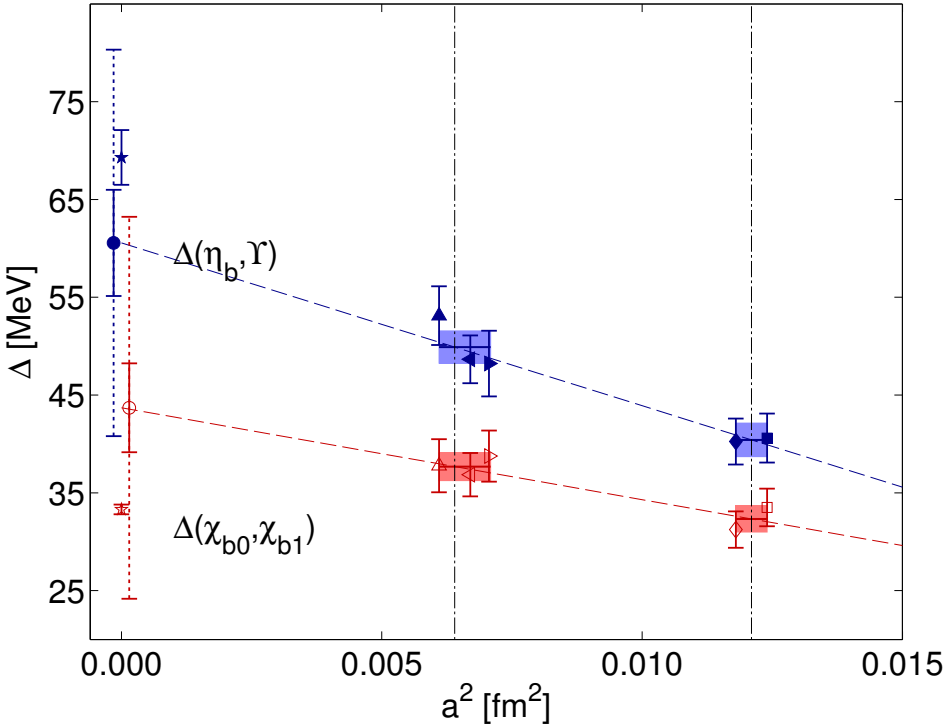

$\eta_b = 9350(33)(37)$ MeV

$\Upsilon = 9410(30)(38)$ MeV

$\Delta(\eta_b, \Upsilon) = 60(05)(20)$ MeV

$\Delta(\chi_{b0}, \chi_{b1}) = 44(05)(19)$ MeV

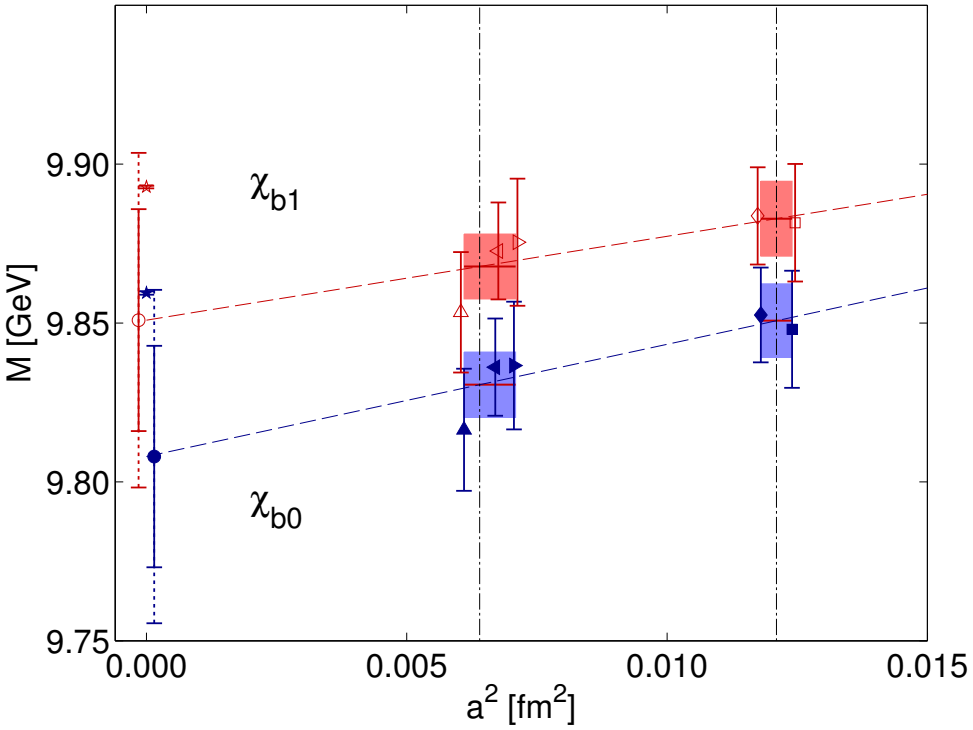

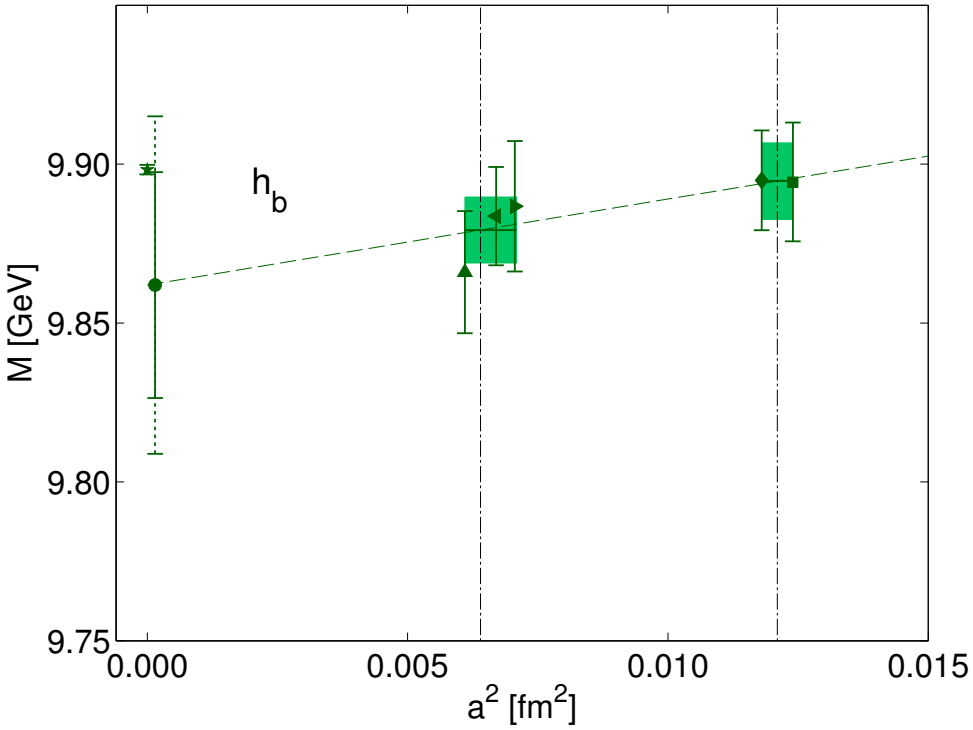

$\chi_{b0} = 9808(35)(39)$ MeV

$\chi_{b1} = 9851(35)(39)$ MeV

$h_b = 9862(36)(39)$ MeV

- Publication on tuning and bottomonium spectroscopy to appear soon

RHQ Lattice Perturbation Theory [C. Lehner]

Motivation

- Knowing the RHQ parameters nonperturbatively we can compare the outcome with lattice perturbation theory
- Helps to build confidence that lattice perturbation theory is working also in cases where we do not have fully non-perturbative matching (e.g. decay constants, form factors)

Method

- Computation at 1-loop order
- Mean field improved
- Use nonperturbative inputs for $\langle P \rangle$, $\langle R \rangle$, $\langle L \rangle$ and $m_0 a$
- Predict: c_P and ζ
- Naive $\alpha_S^2 \sim 5\%$ power-counting estimate

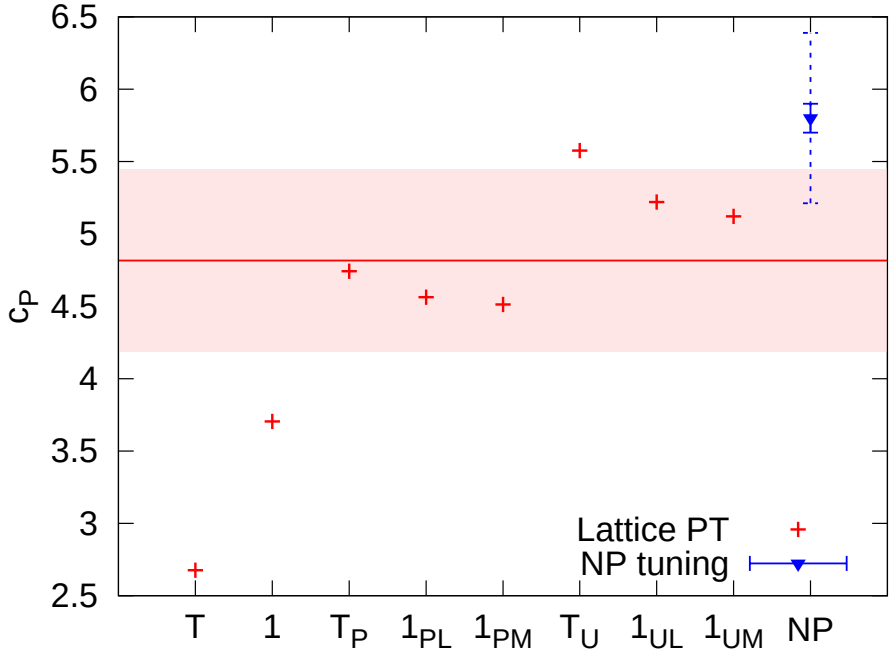

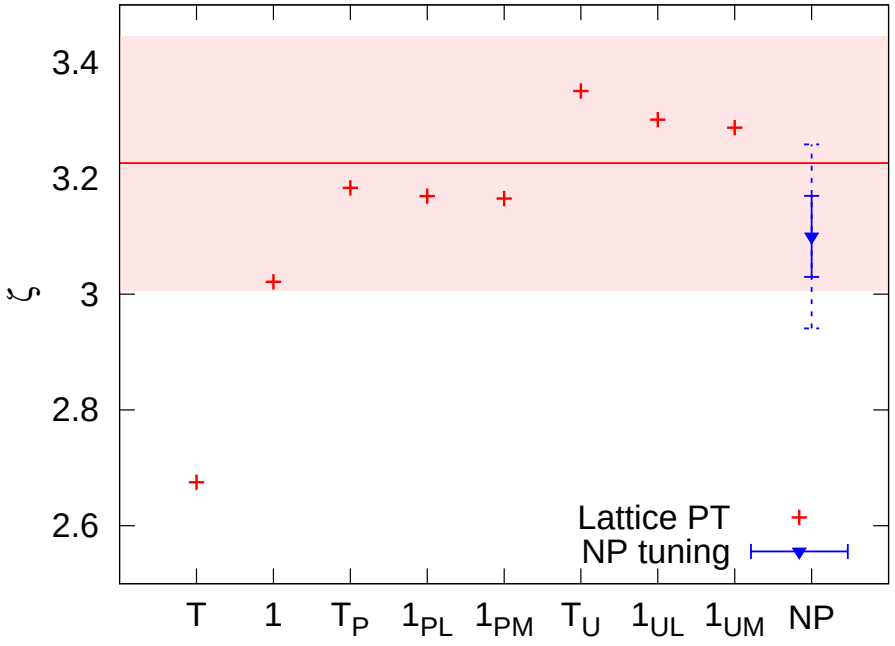

- Central values: average of one-loop mean-field improved values computed with u_0 obtained from the plaquette and from the spatial Landau link
- Error on perturbative c_P: difference between mean field methods dominates
- Error on perturbative ζ: naive power-counting dominates
- Nonperturbative values include systematic errors from discretization errors in quantities used for tuning
- Agreement within errors $\Rightarrow$ MF-improved LPT can be trusted in situations for which NP matching factors are not available

$B^0 - \overline{B^0}$ Mixing Matrix Element Calculation

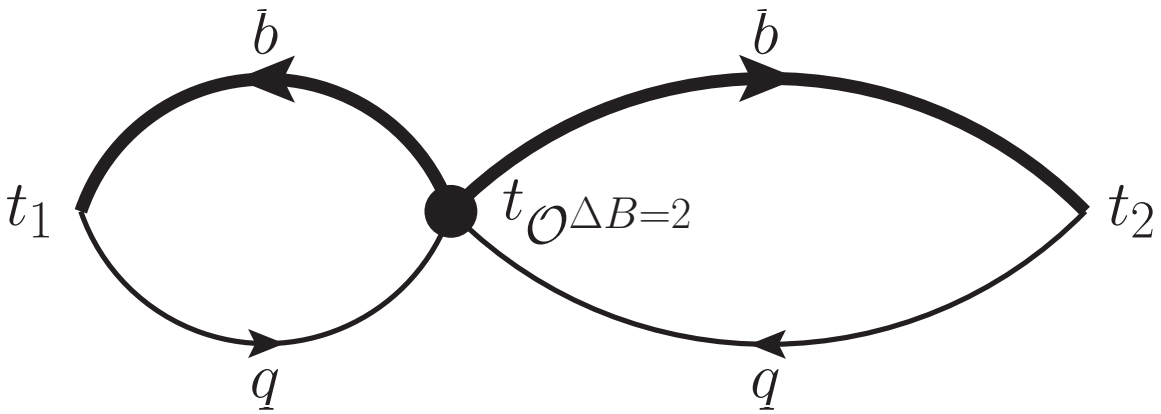

- Location of four-quark operator is fixed
- Location of B-mesons is varied over all possible time slices
- Need: one point-source light quark and one point-source heavy quark originating from operator location
- Propagators can be used for B- and $\overline{B}$-meson
- Project out zero-momentum component using a Gaussian sink
- Optimize Gaussian wavefunction to minimize excited-state contamination in B-meson 2-point correlation function

Preliminary B- and B^*-meson mass

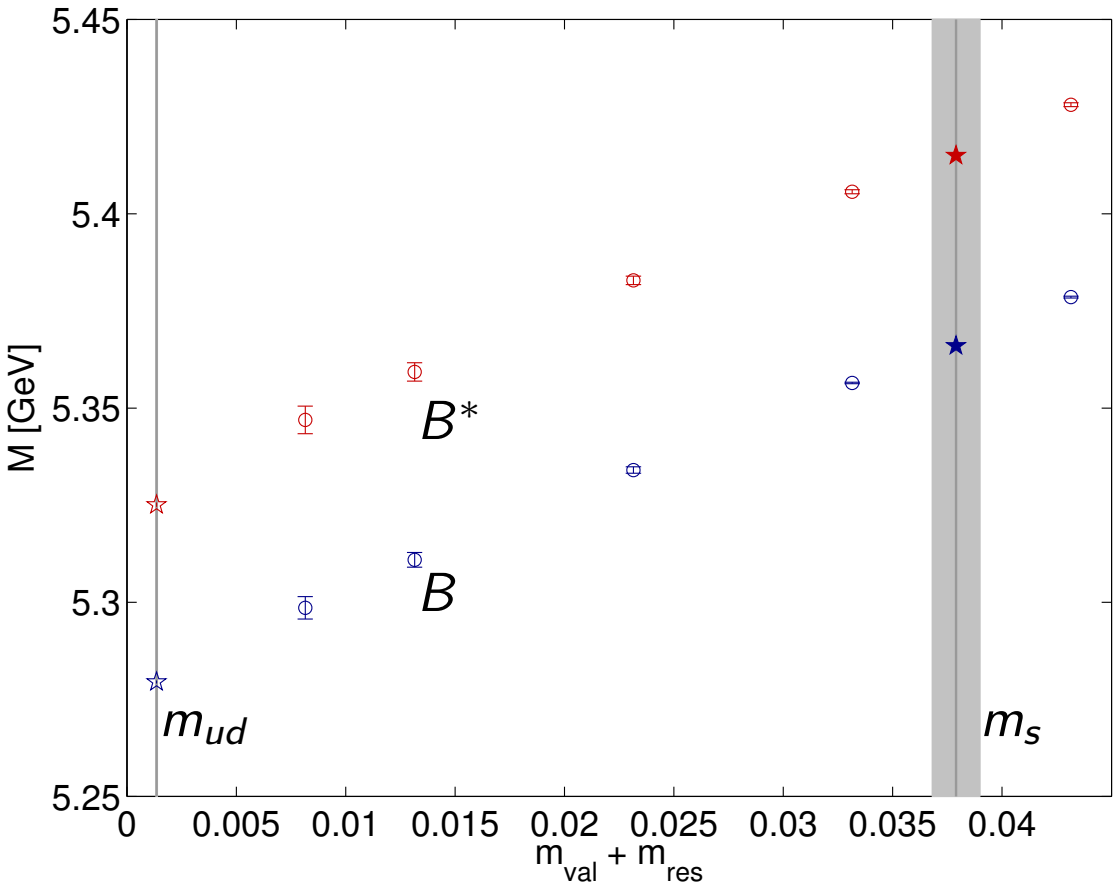

- $L = 24$, $m^l_{\text{sea}} = 0.005$, $N = 1636$, only statistical uncertainty

Mostly Nonperturbative Renormalization

For f_B, f_{B_s} and $B \to \pi$ we plan to compute mostly non-perturbative renormalization factors á la [El Khadra et al. 2001]

$$\varrho^{bl} = \frac{Z_V^{bl}}{\sqrt{Z_V^{bb} Z_V^{ll}}}$$

- Compute Z_V^{ll} and Z_V^{bb} non-perturbatively and only ϱ^{bl} perturbatively
- Enhanced convergence of perturbative serious of ϱ^{bl} w.r.t. Z_V^{bl} because tadpole diagrams cancel in the ratio
- Bulk of the renormalization is due to flavor conserving factor $\sqrt{Z_V^{ll} Z_V^{bb}} \sim 3$
- ϱ^{bl} is expected to be of $\mathcal{O}(1)$; receiving only small corrections
- For domain-wall fermions $Z_A = Z_V + \mathcal{O}(m_{\text{res}})$ i.e. we know Z_V^{ll} [Y. Aoki et al. 2011]
- Mostly nonperturbative renormalization not yet computed for B^0–$\overline{B^0}$ mixing

B-meson Decay Constant Calculation

- Re-use: point-source light quark and generate Gaussian smeared-source heavy quark
- Final result will use mostly nonperturbative renormalization

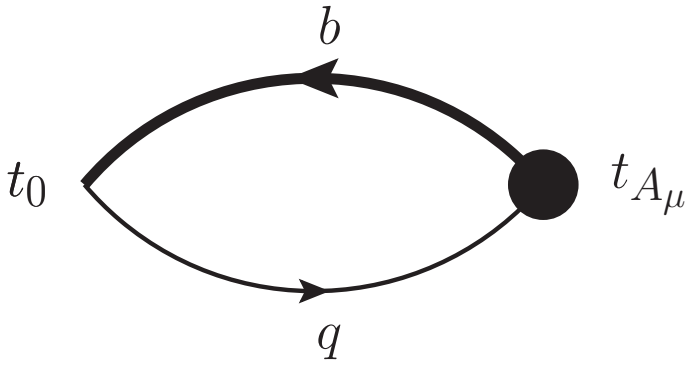

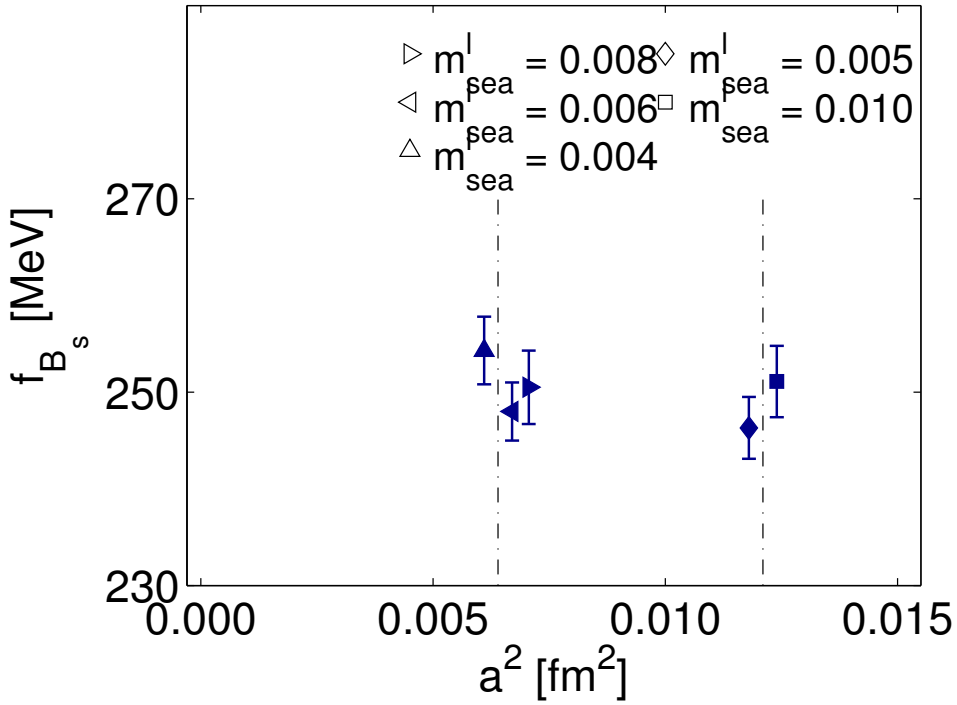

- Very preliminary result for f_{B_s}
- Renormalization and matching to be improved:
  nonperturbative Z_V^{ll}
  perturbative Z_V^{bb}
  (tree level, 20% error)
  $\varrho_{bl} = 1$
- Axial current tree-level $O(a)$ improved
- Small scaling violations

$B \to \pi l \nu$ form factor [T. Kawanai]

- Compute matrix element of the $b \to u$ vector current between B-meson and pion
- Fix location of pion at t_0 and B meson at $T - t_{\text{sink}} - t_0$
- Vary operator location t_{V_μ} in that range
- B-meson is at rest, inject momentum on pion side
- Using partially quenched daughter quark-masses should help to better resolve quark-mass dependence and pion-energy dependence

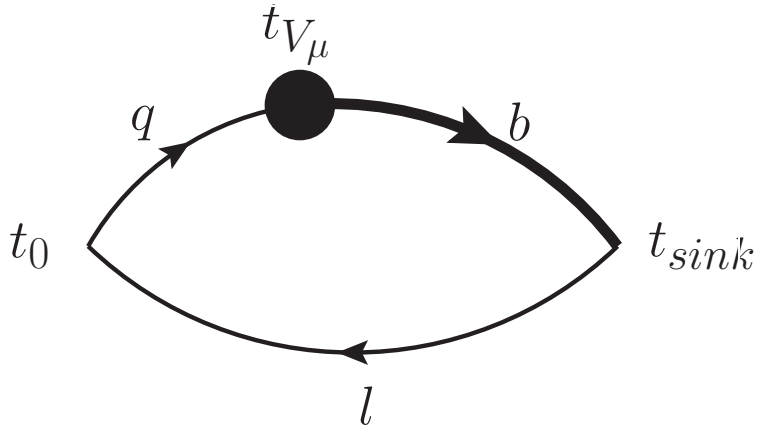

Conclusion

- We have completed tuning the parameters of the RHQ action for b-quarks, and find good agreement between our predictions for bottomonium masses and fine splittings with experiment.
- Given this success, we are now using this method for B-meson quantities such as decay constants and form factors, and expect to obtain errors competitive with other groups.
- The RHQ action can also be used for charm quarks, and Hao Peng is currently performing the necessary parameter tuning.
- We should have results for decay constants, mixing parameters, and form factors within the next year, and maybe sooner!

Exploring Many Flavor QCD with Wilson Fermion

N. Yamada (KEK/GUAS)

based on collaboration with

M. Hayakawa (Nagoya), K.-I. Ishikawa (Hiroshima),
Y. Iwasaki (KEK/Tsukuba), Y. Osaki(Hiroshima),
S. Takeda (Kanazawa), S. Uno(Nagoya), T. Yoshie (Tsukuba)

New Horizons for Lattice Computations With Chiral Fermions@BNL 2012/05/16

Conformal Window

Phase of a theory with N_F degenerate massless flavors at T=0

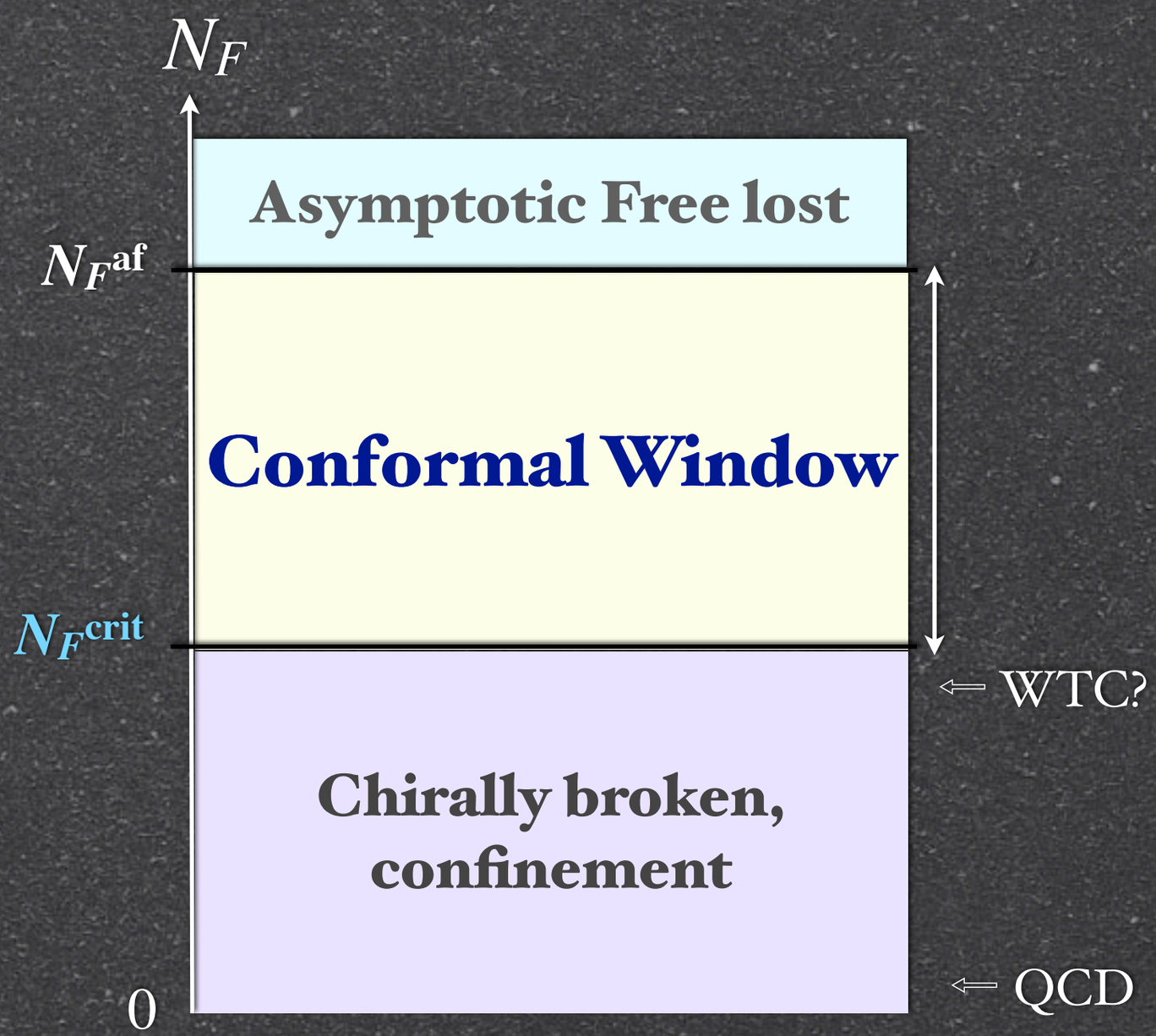

Phase diagram@T=0

Conformal Window:
$N_F^{crit} < N_F < N_F^{af}$

Viable Technicolor model (e.g. WTC) is expected to exist in vicinity of N_F^{crit}.

First task : Identifying N_F^{crit}

We take Wilson fermion.

Disadvantages:

✓O(a) scaling violation

✓Fine-tuning,

✓...

Advantages:

✓Simple, tractable and well understood

✓Able to study arbitrary N_F without any subtlety

✓Independent check to KS (or other) results

Contents

There are several approaches to identify N_F^{crit}.
Focusing on SU(3) gauge theory, we are performing the following studies:

1. Running coupling and anomalous dimension in 10-flavor QCD. IRFP?

2. Finite temperature study of Many Flavor QCD ($N_F = 6$ - 10)
   - Strategy
   - Future prospect

$\alpha(\mu)$ and γ_m in 10-flavor QCD

M. Hayakawa, K.-I. Ishikawa, Y. Osaki, S. Takeda, S. Uno, NY

$g_{SF}^2(\mu)$ in 10-flavor QCD

Hayakawa, Ishikawa, Osaki, Takeda, Uno, NY, PRD(2011) and work in progress

$$B^{\rm SF}(u,s) = \frac{1}{g^2_{\rm SF}(u,s)} - \frac{1}{u}$$

Preliminary

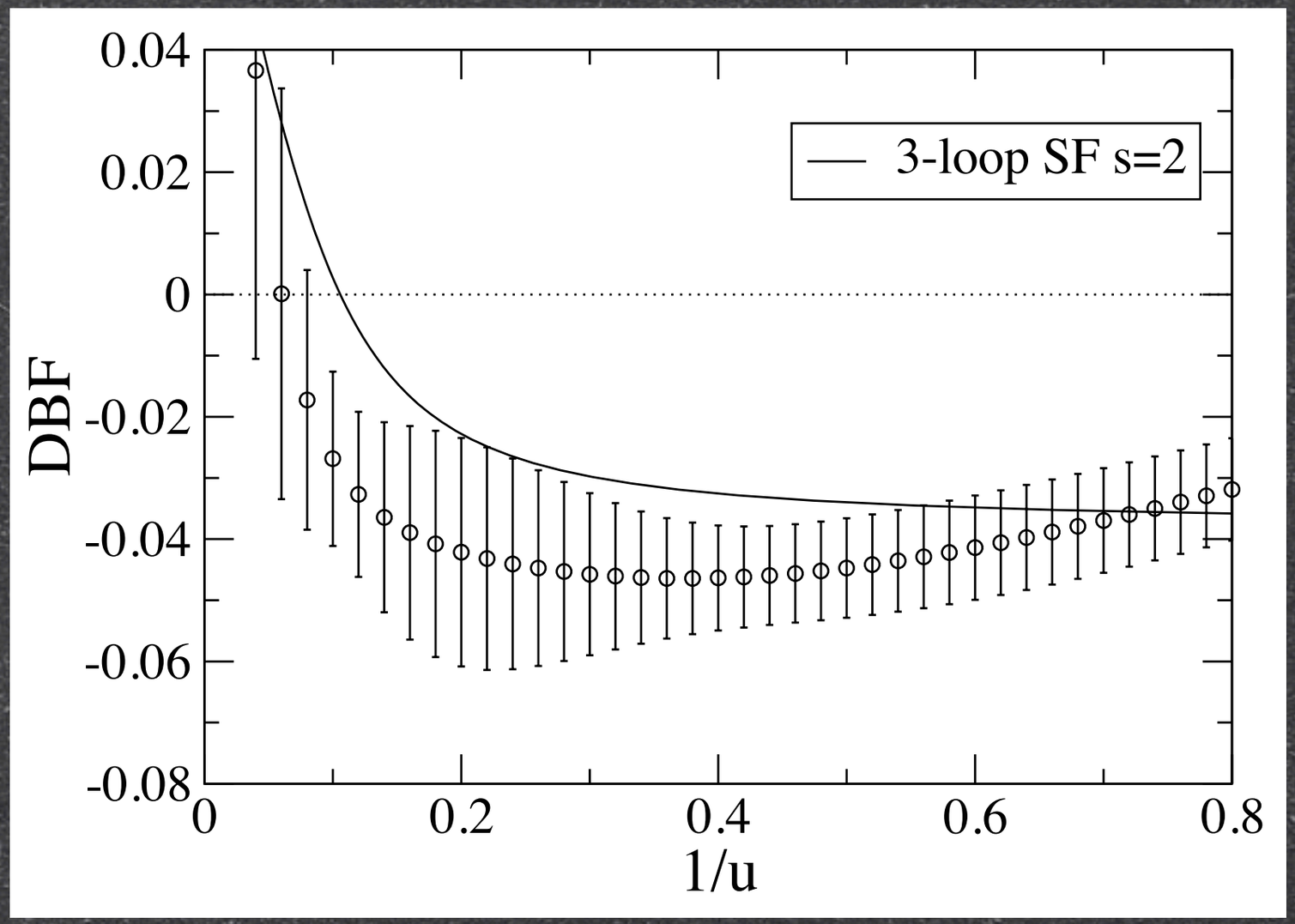

DBF=0 ⇒ IRFP

$g^2_{FP} \geq 12$

Continuum extrapolation with two data points.

In order to have more confidence, large V calculation is on-going.

$g_{SF}^2(\mu)$ in 10-flavor QCD

Hayakawa, Ishikawa, Osaki, Takeda, Uno, NY, PRD(2011) and work in progress

Preliminary

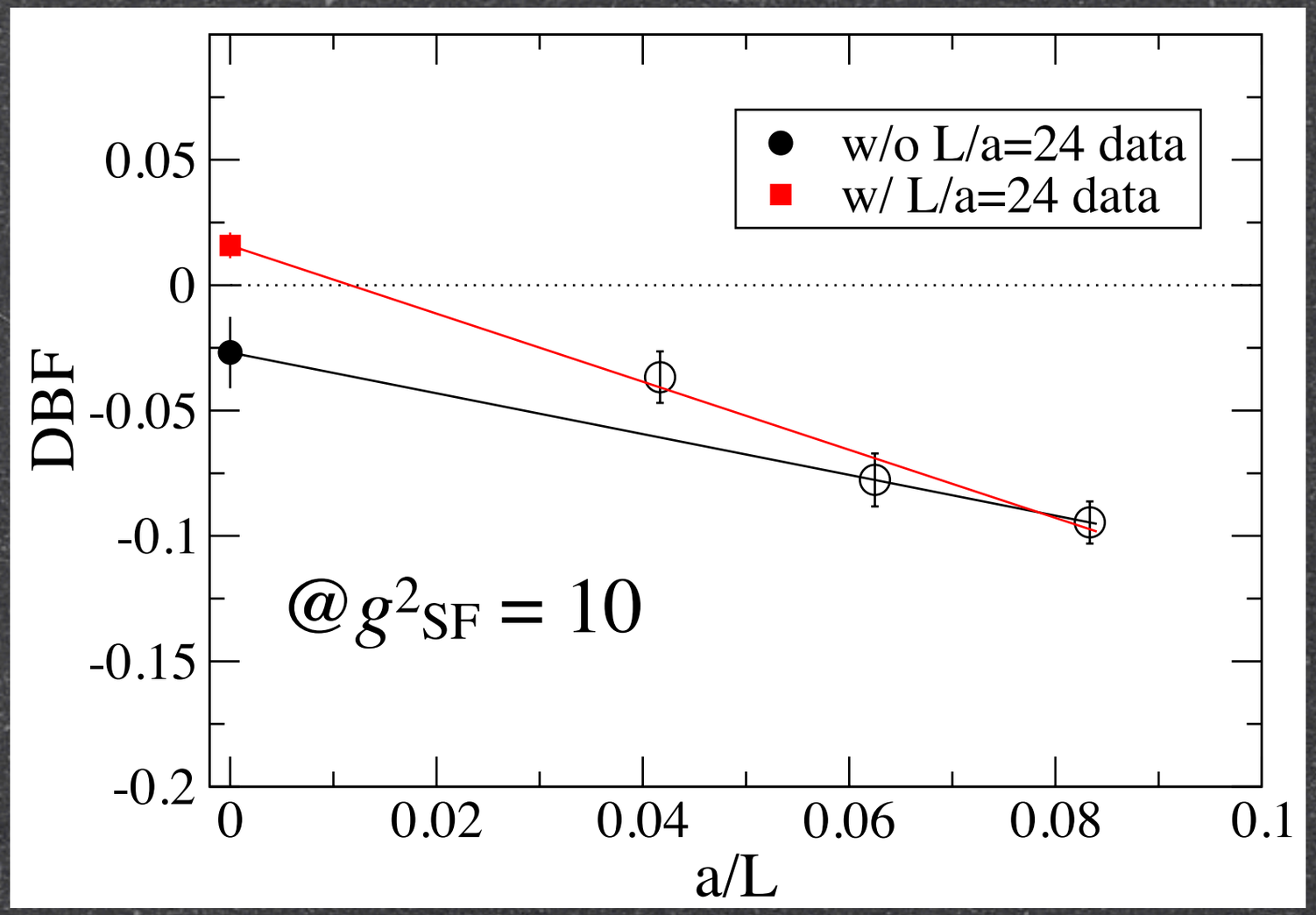

Adding large V data, the continuum limit shits upward.

$g^2_{FP} \geq 12 \Rightarrow g^2_{FP} \sim 10$

⬇

More confident on IRFP

γ_m of 10-flavor QCD

Hayakawa, Ishikawa, Osaki, Takeda, Uno, N.Y., work in progress

Preliminary

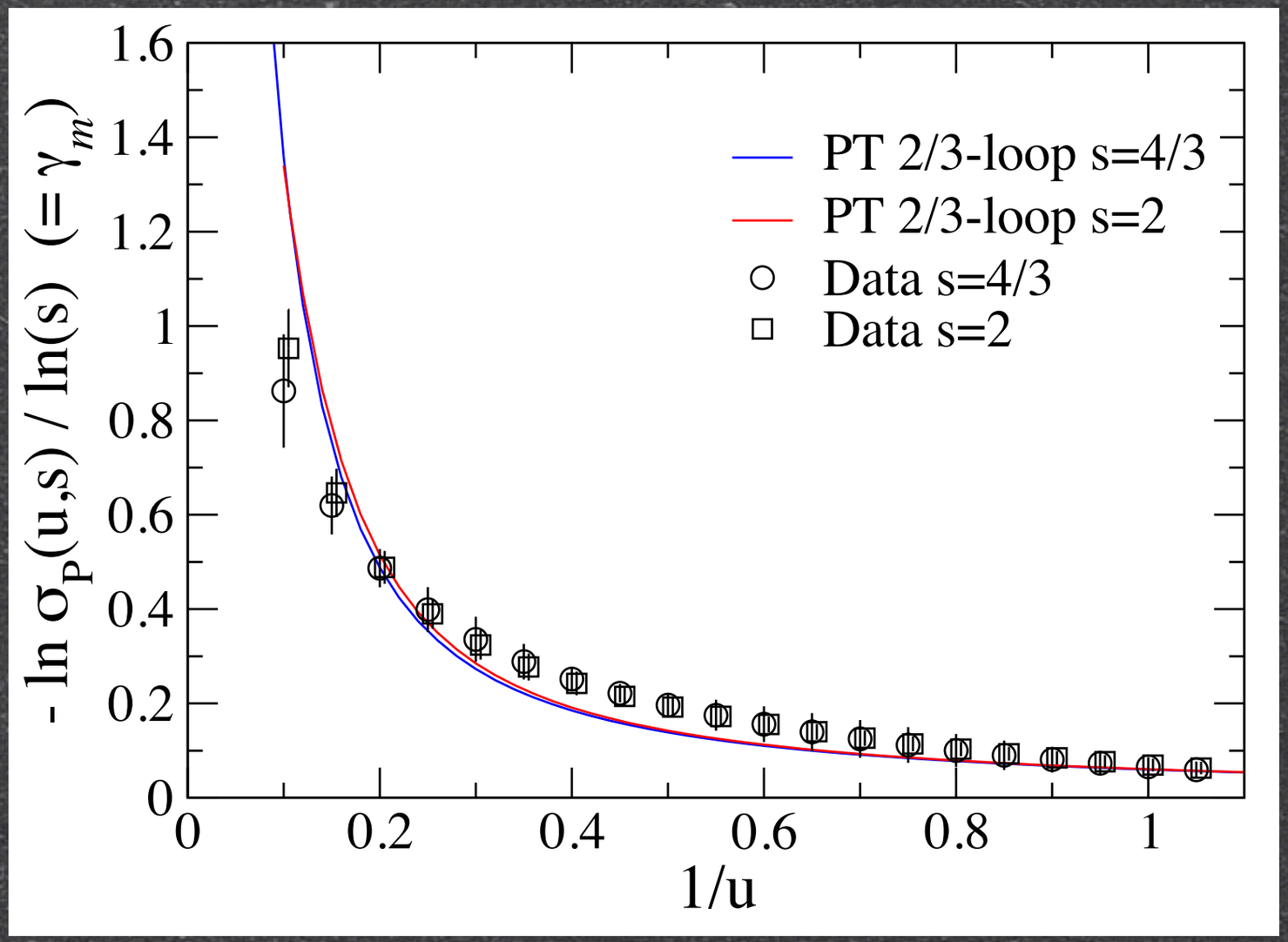

Two different step scaling factors give consistent result.

Assuming $g_{FP}^2 \sim 10$, $\gamma_m \sim 1$!

10-flavor QCD appears to be in CW ($N_F^{crit} < 10$) and have $\gamma_m \sim O(1)$.

Finite temperature study of Many Flavor QCD

WMF Collaboration: **M. Hayakawa, K.-I. Ishikawa, Y. Iwasaki, S. Takeda, T. Yoshie, NY**

Phase diagram of Wilson fermion for $N_F < N_F^{crit}$ Iwasaki et al. (91,04)

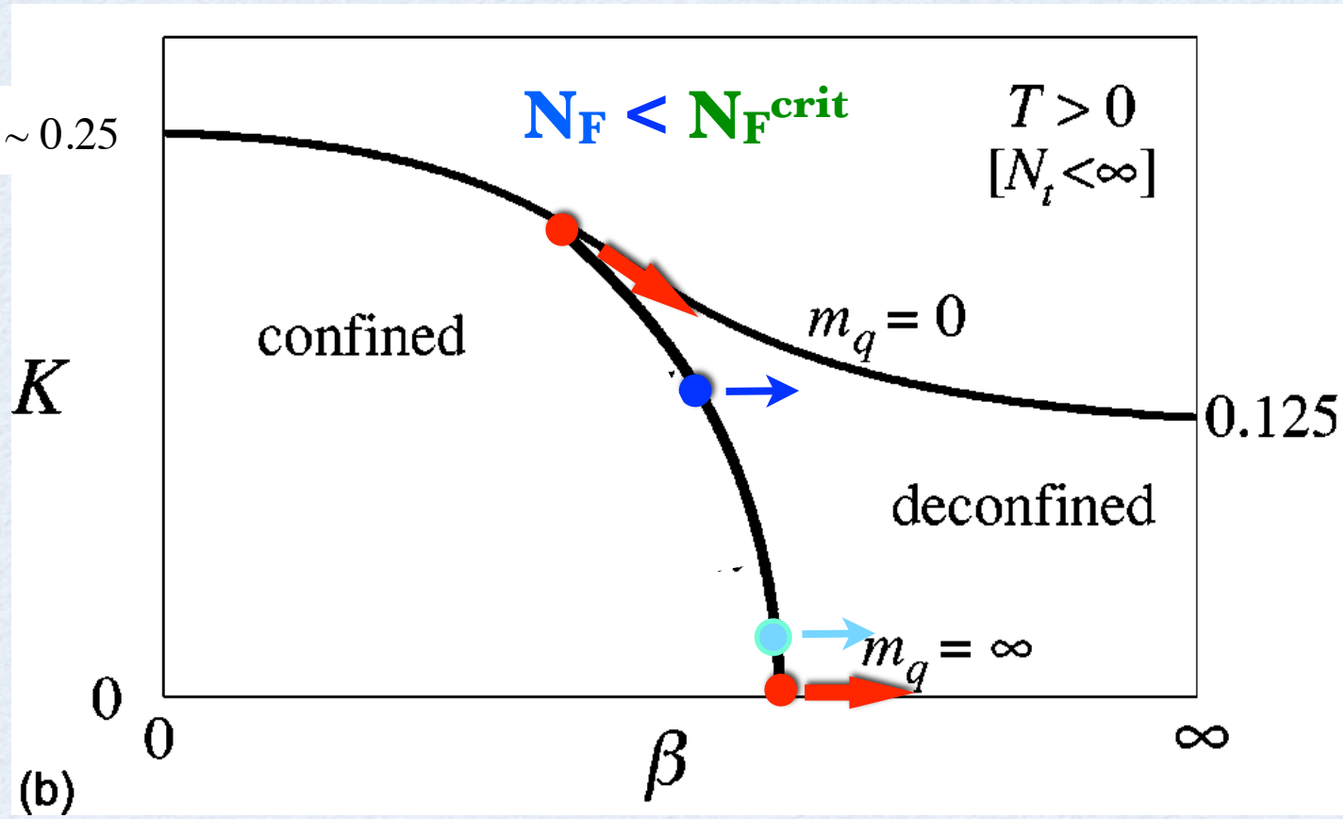

If the theory is confining, the transition line move to the right as T decreases (or V increases).

Phase diagram of Wilson fermion for $N_F < N_F^{crit}$ Iwasaki et al. (91,04)

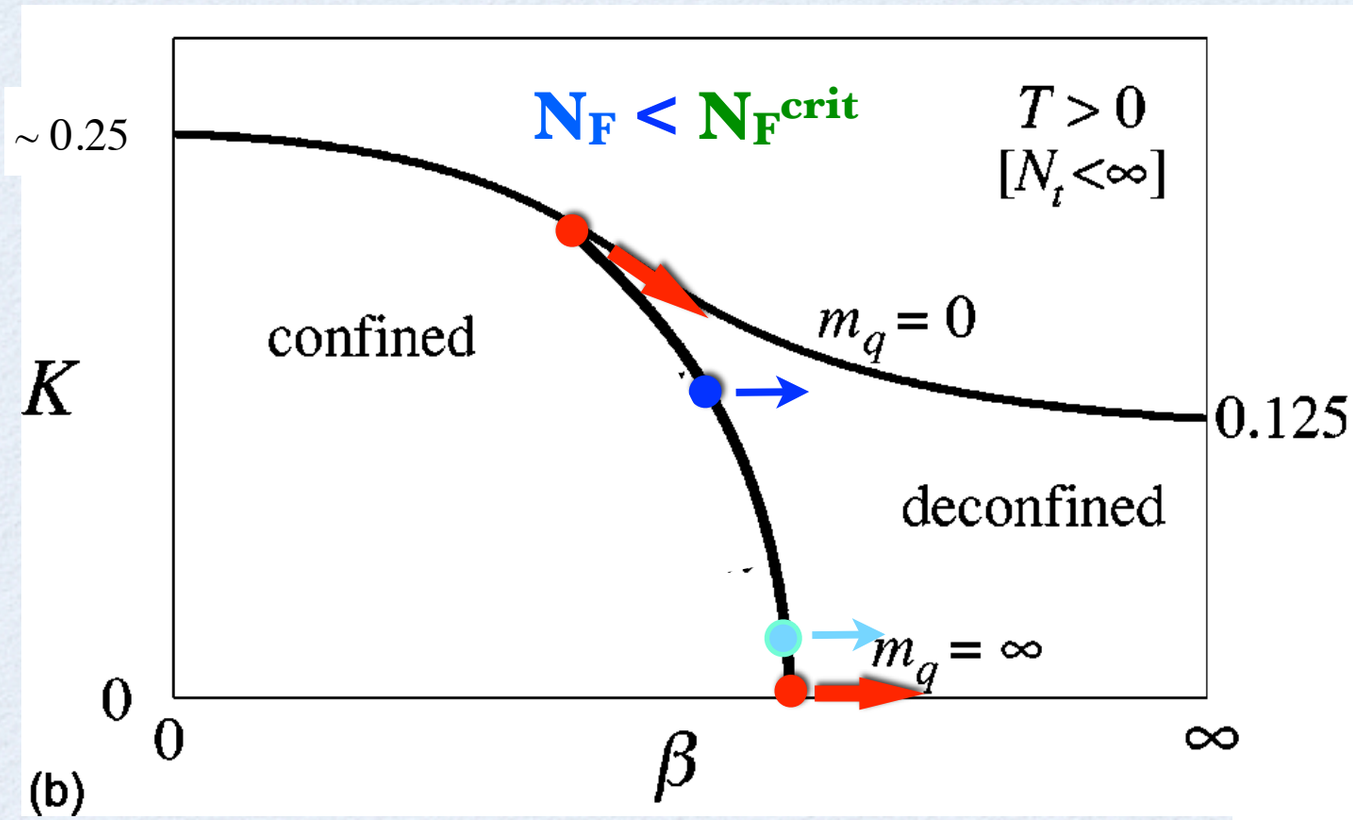

If the theory is confining, the transition line move to the right as T decreases (or V increases).

Eventually, the whole region is covered by confining phase.

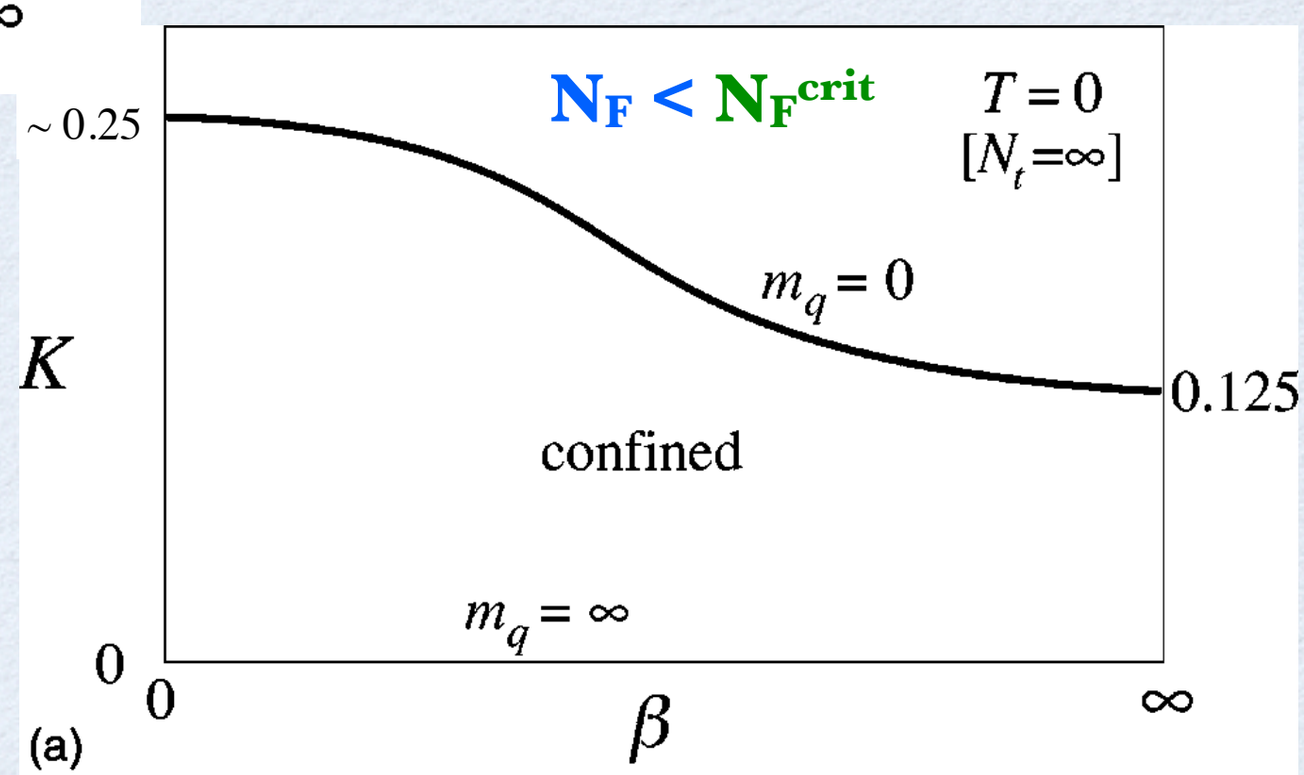

Phase diagram of Wilson fermion with $N_F^{crit} < N_F < N_F^{af}$ (speculation)

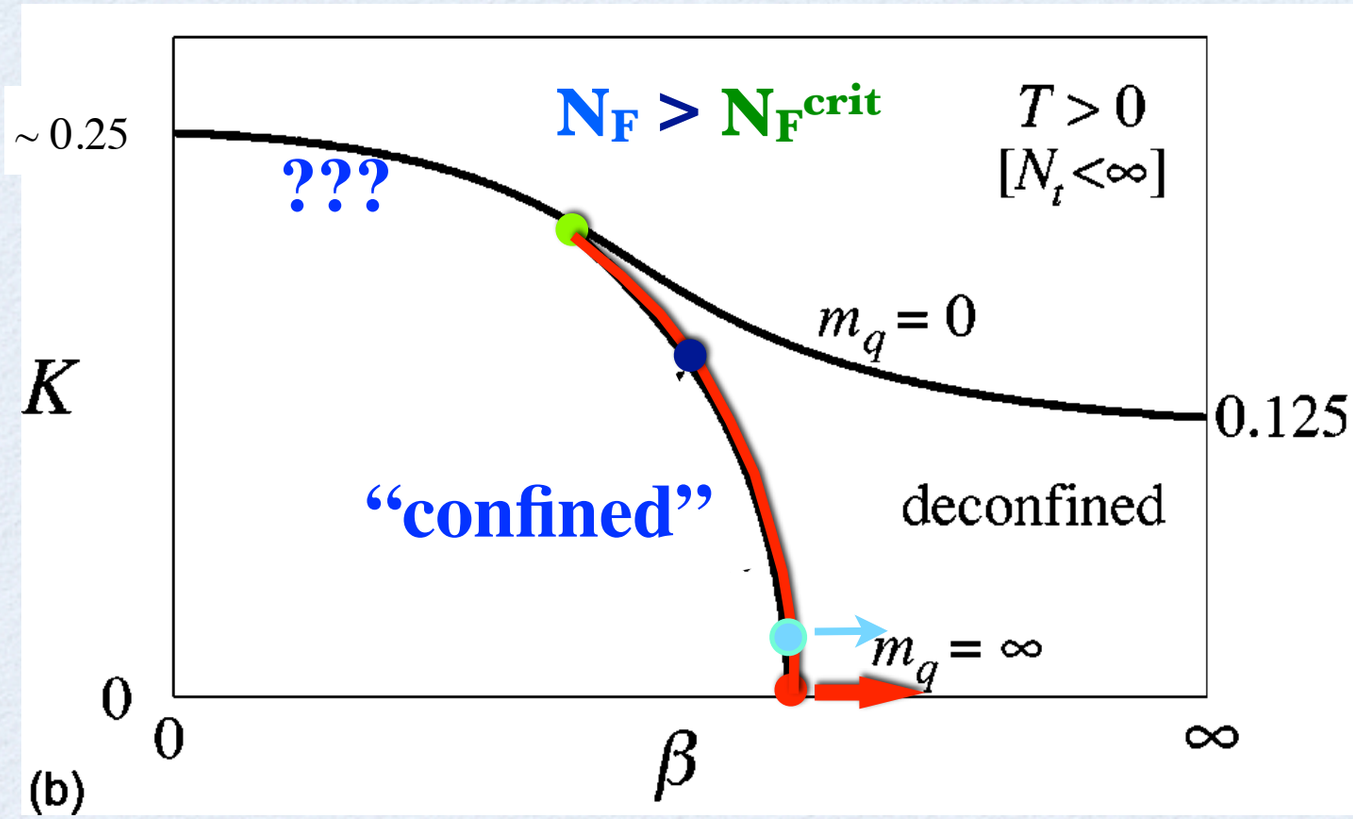

The one end of the transition line at $m_q=\infty$ moves to the right with V as before, while the other end at $m_q=0$ won't.

Phase diagram of Wilson fermion with $N_F^{crit} < N_F < N_F^{af}$ (speculation)

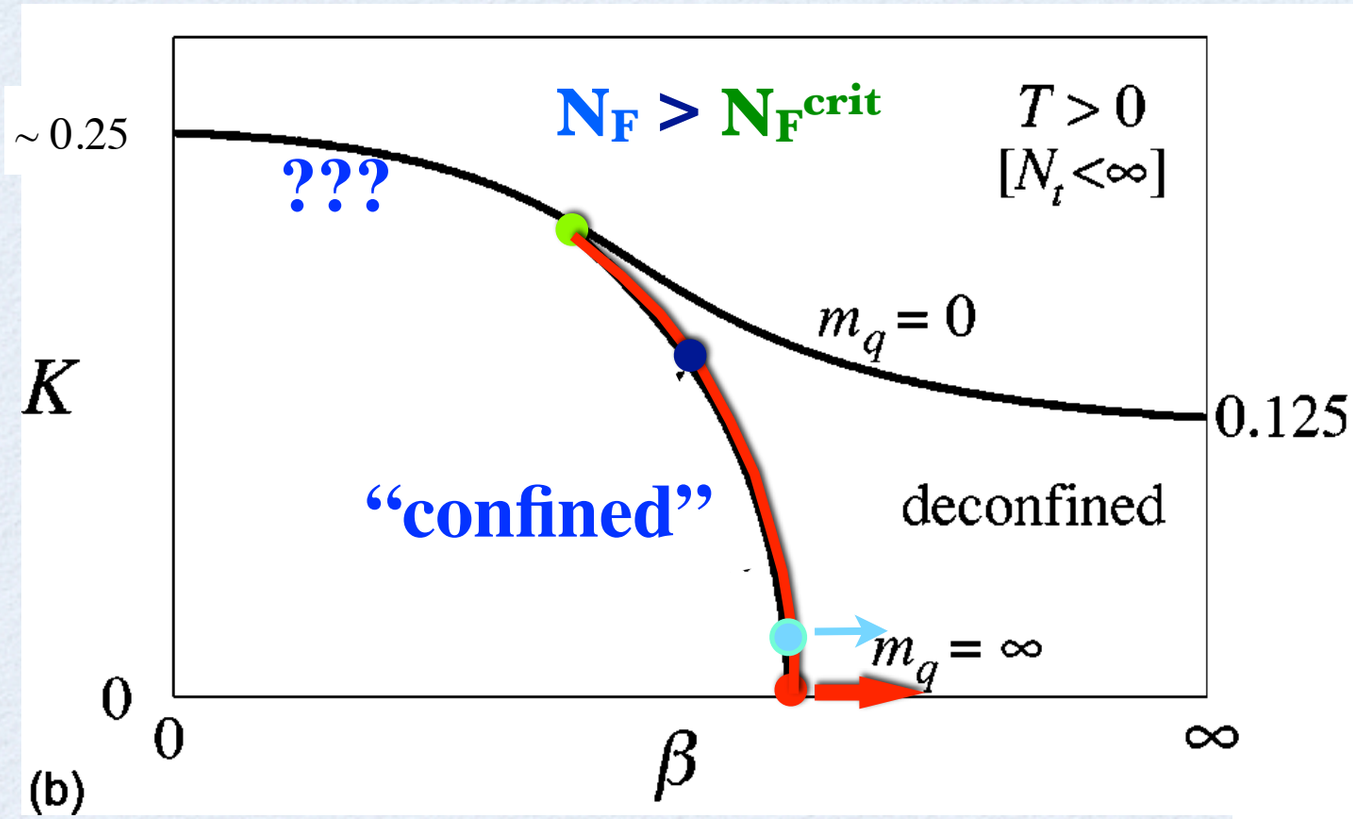

The one end of the transition line at $m_q=\infty$ moves to the right with V as before, while the other end at $m_q=0$ won't.

In the large V limit, the relevant region is covered by "confined" phase except for the chiral limit

In **"confined"**, Λ_{TC} depends on m_q and vanishes in the chiral limit

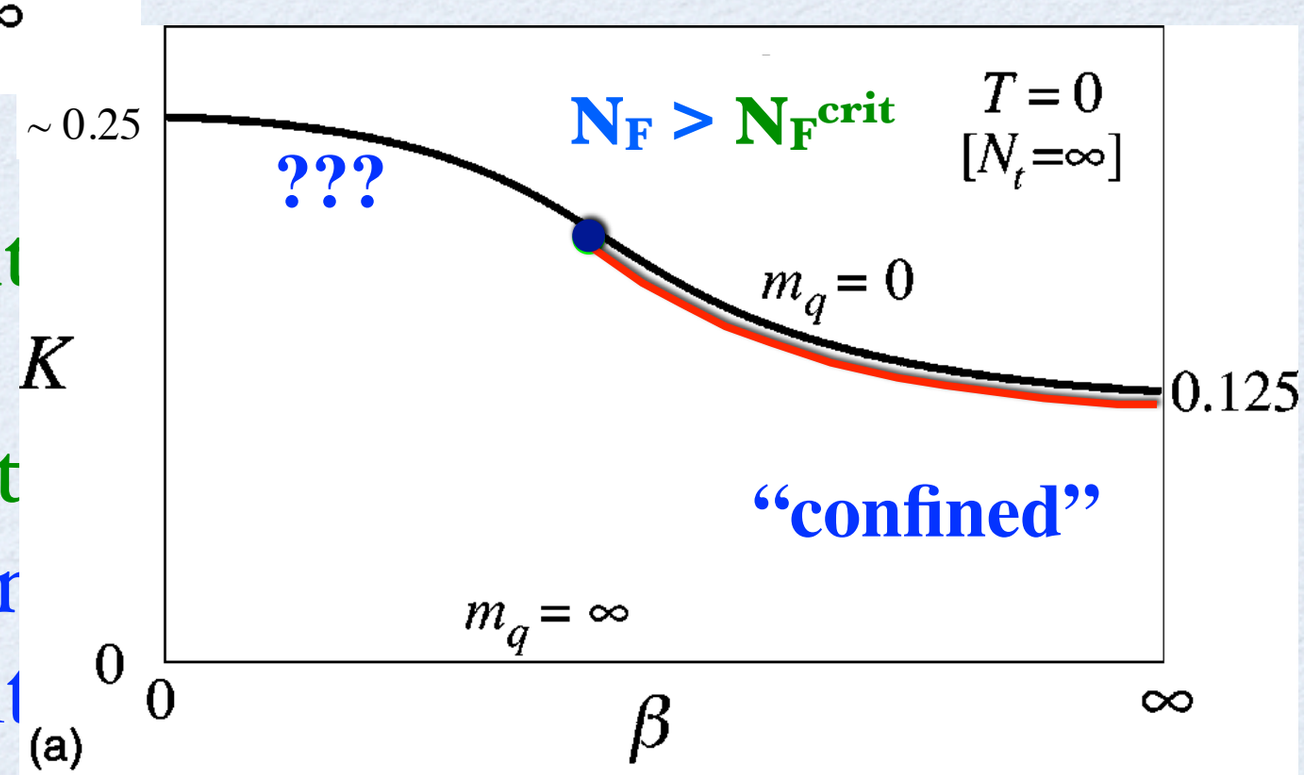

General Strategy

- ✓ Find **the critical endpoint around m_q=0**.
- ✓ Keep monitoring it while changing V to see whether it moves to the right with N_T or V.
- ✓ If the endpoint moves to the right as in QCD, the theory is outside of Conformal Window.

This work (N_F=10)

m_Q and β dependence of Polyakov loop@N_F=10

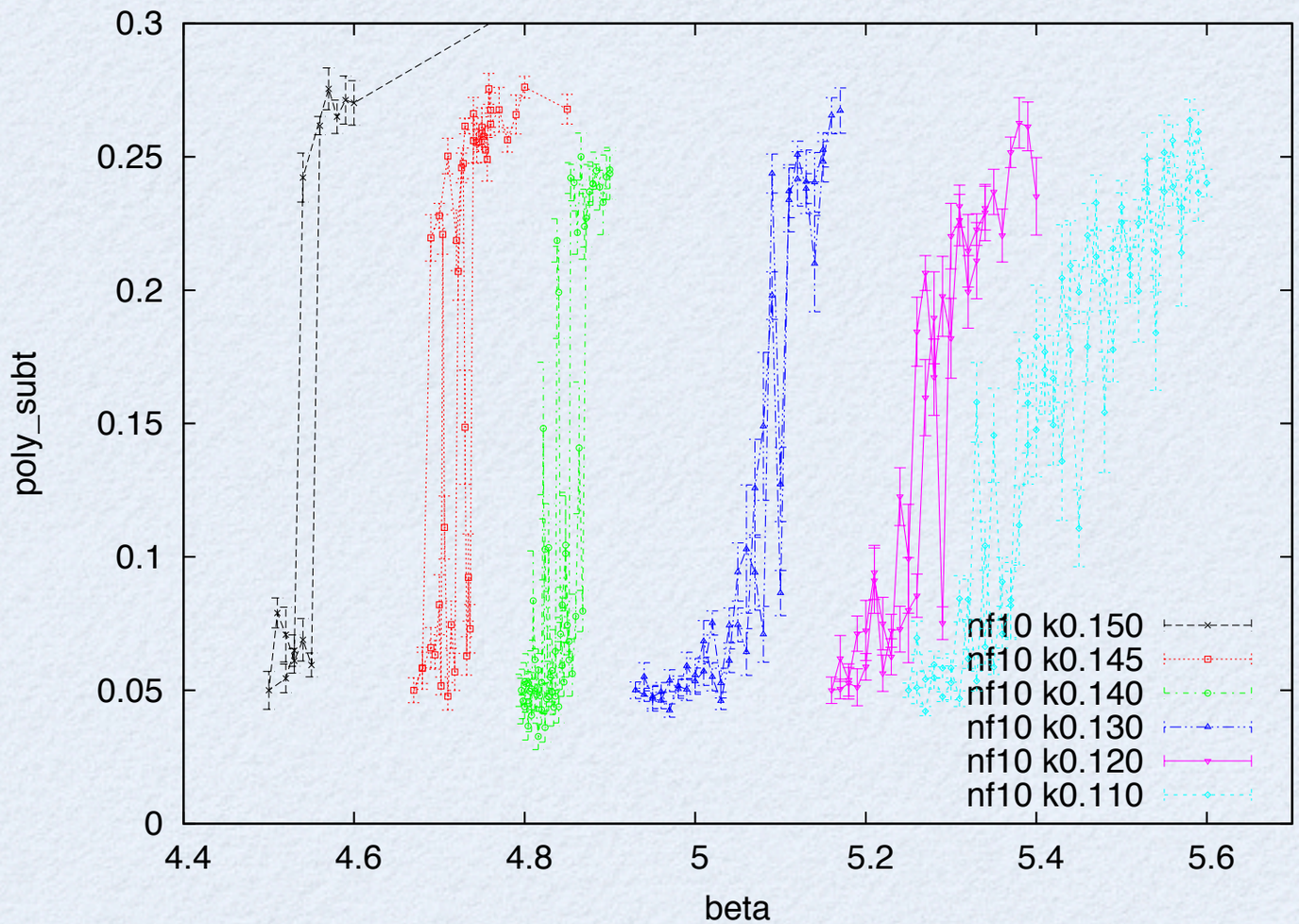

This work using Wilson Fermion on V=4^3x4.

1st oder weakens as going to small kappa.

Previous Results (N_F=10)

Fukugita, Ohta, Ukawa (88)

m_Q and β dependence of Polyakov loop@N_F =10

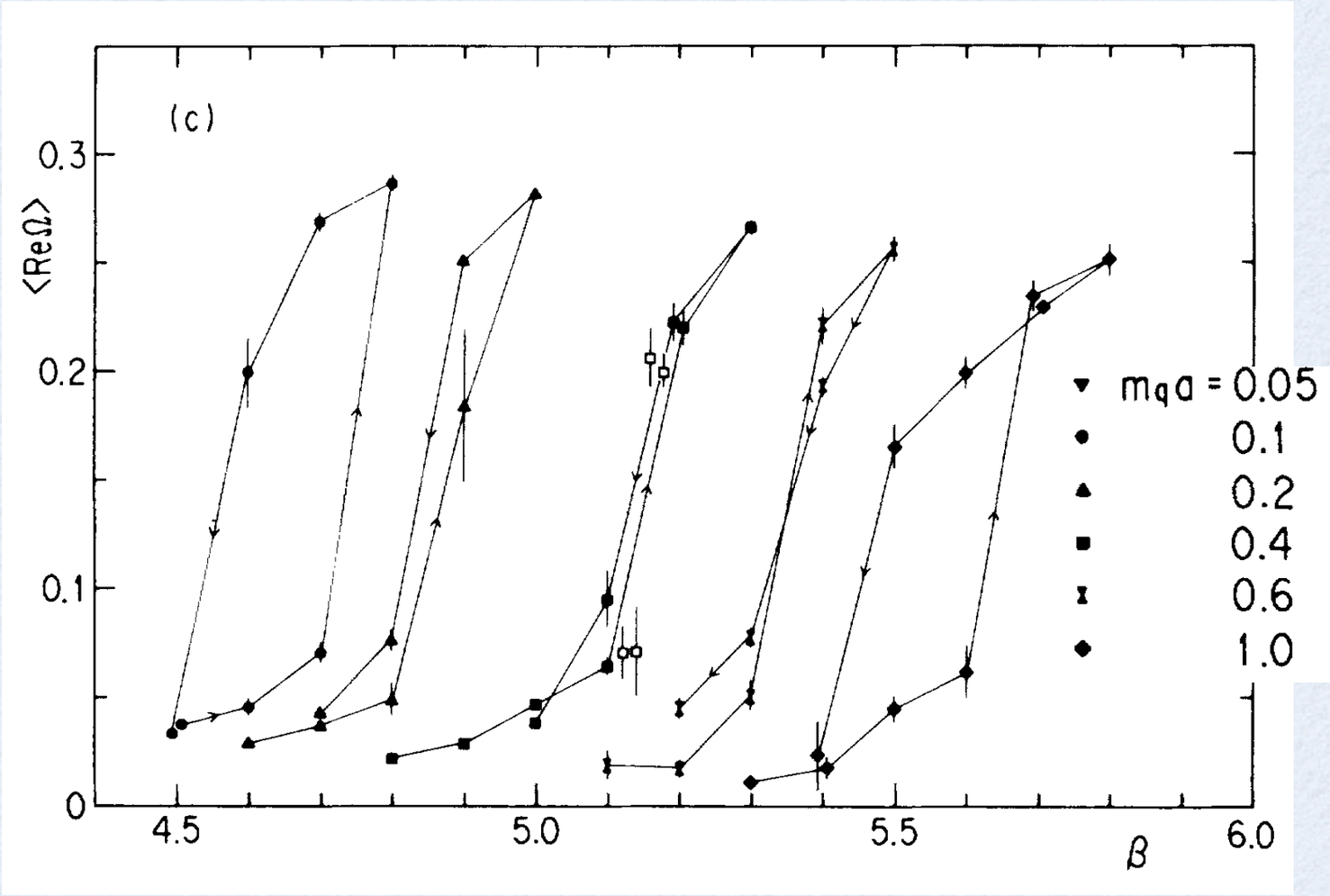

KS, V=8^3x4.

Observation:

Transitions are 1st order over the entire range of fermion mass at N_F=10. No end point.

$V=8^3x8$, $N_F=6\text{-}10$

Preliminary Results for $N_F=6, 7, 8, 10$

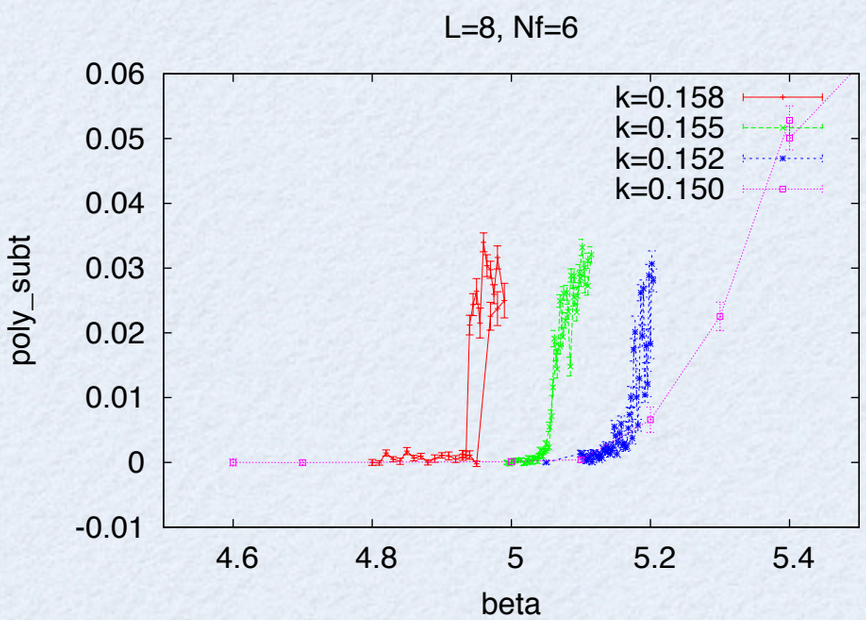

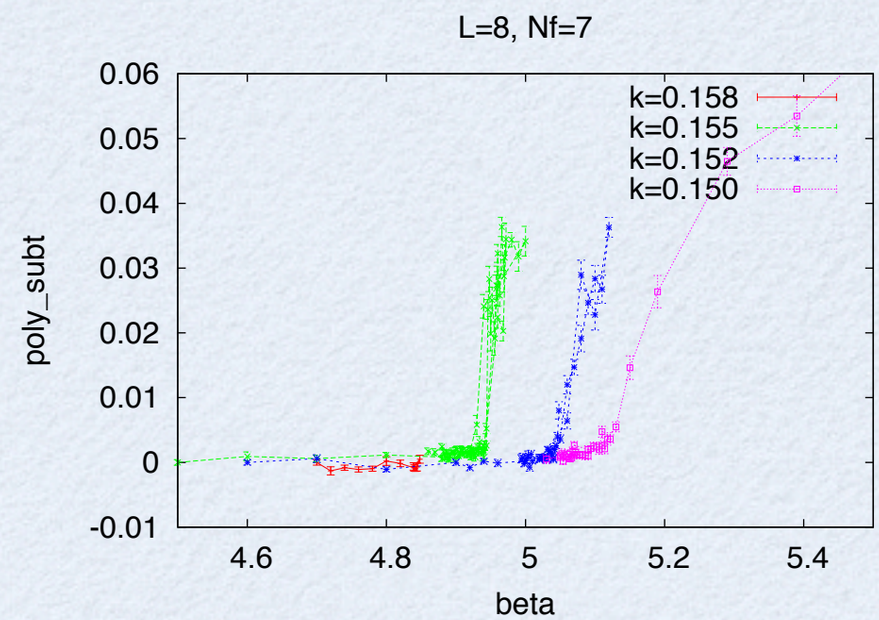

1st order at large kappa weakens as going to small kappa.

Calc. on $V=16^4$ is on going.

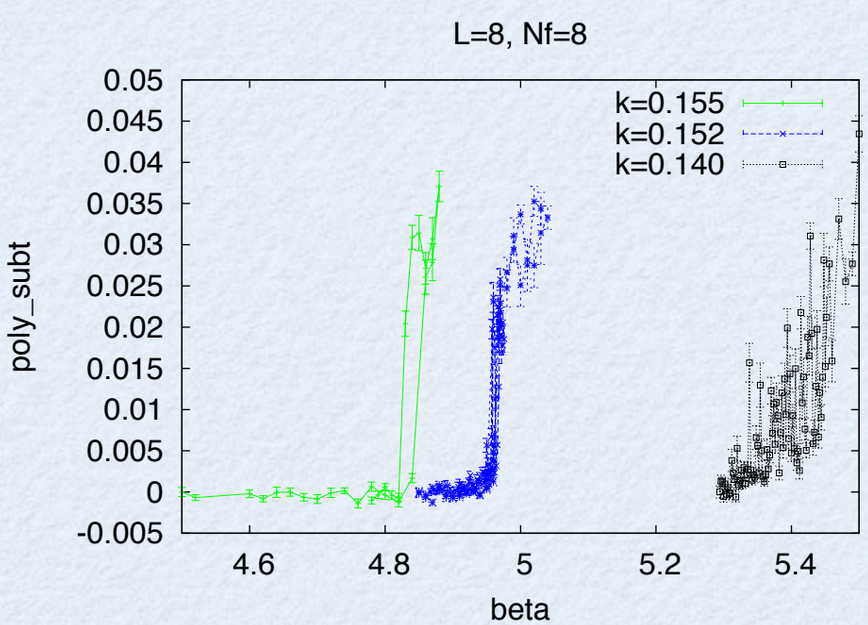

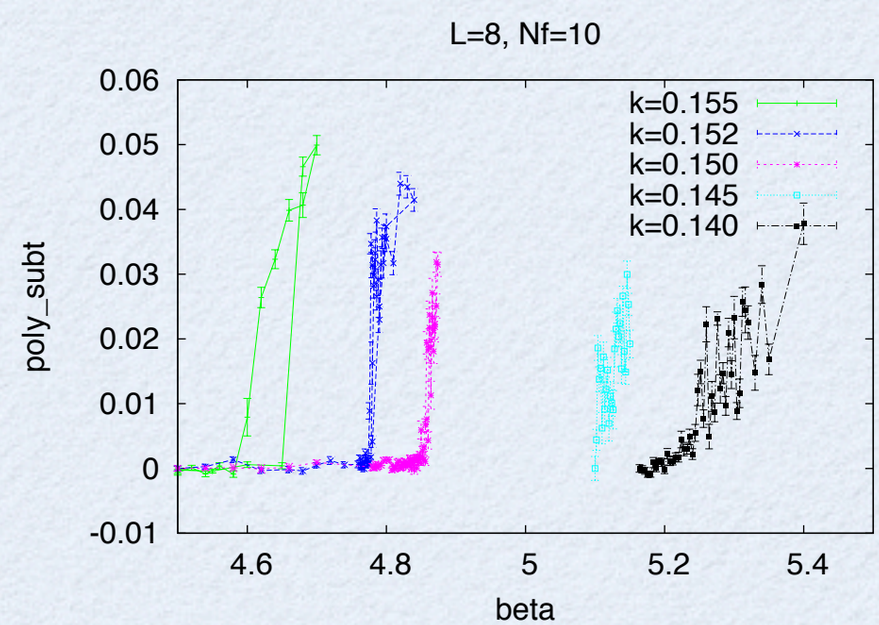

(Far) Future plan

(strongly depends on what LHC@CERN observes.)

- ✓ In realistic TC model, only two of N_F flavors must be exact massless while the other N_F-2 flavors shouldn't be so.
- ✓ Go to 2 + (N_F-2) QCD
- ✓ Nice to discuss such a theory on the basis of Columbia plot

Columbia plot

Brown, Butler, Chen, Christ, Dong, Schaffer, Unger, and Vaccarino (90),
N.H. Christ, Z. Dong (92) and N.H. Christ(92)

Kanaya, Lattice 2010

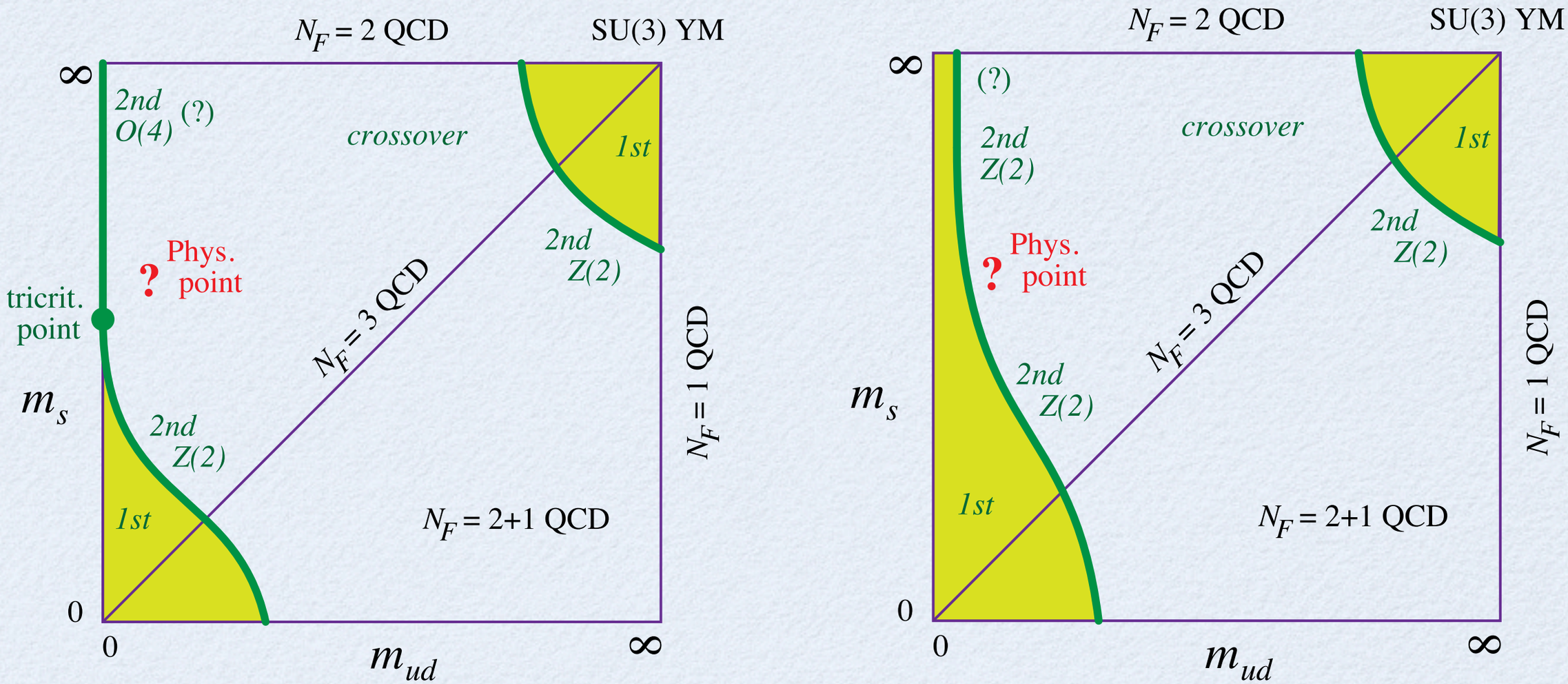

Recent lattice results seems to favor the left.

How does this plot for many flavor QCD look like?

$N_F = 4$ ($< N_F^{crit}$)

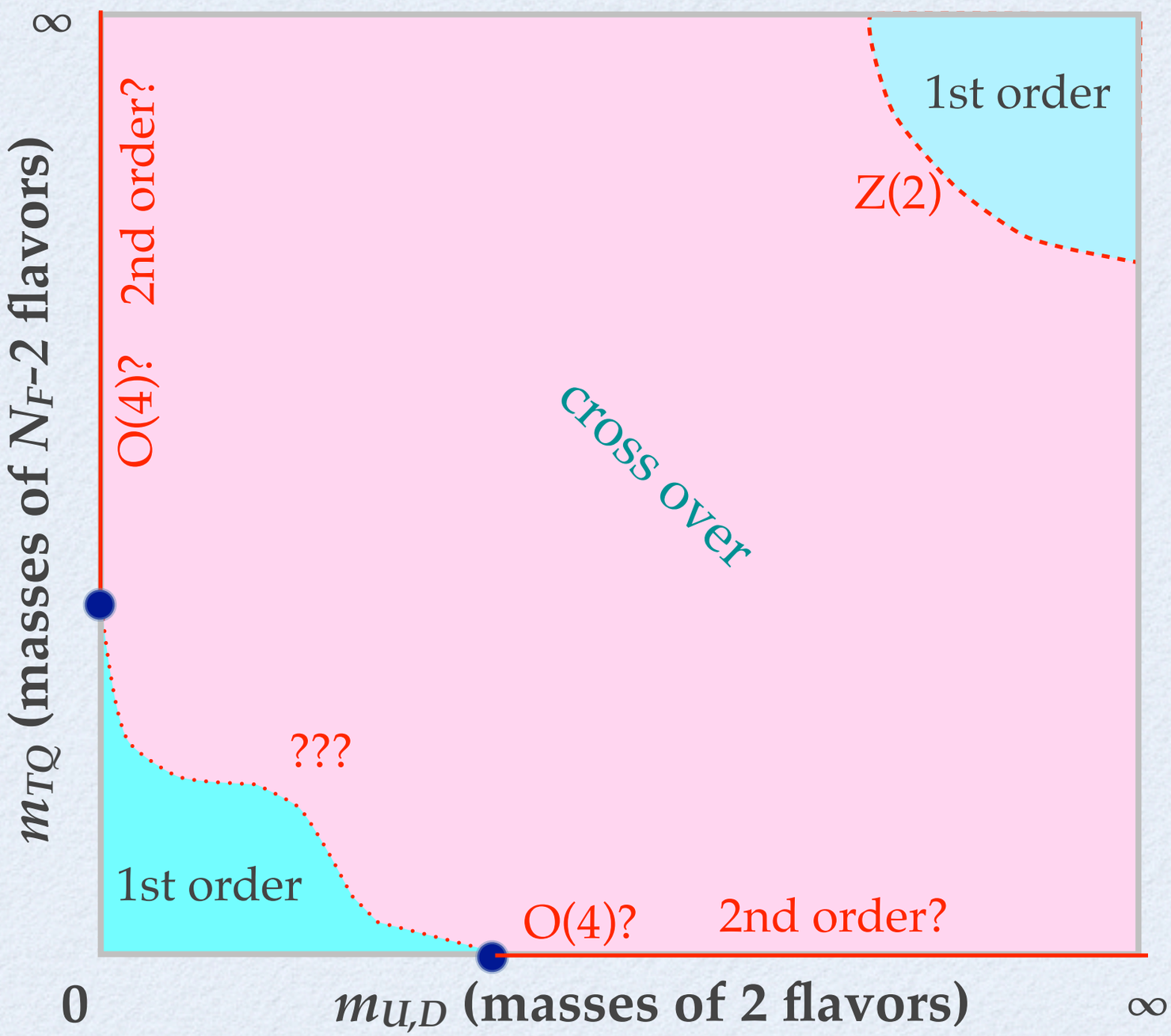

$N_F^{crit} > 4$ is assumed.

Symmetric phase diagram

Probably running is not slow enough.

Less interesting.

$5 \leqq N_F < N_F^{crit}$

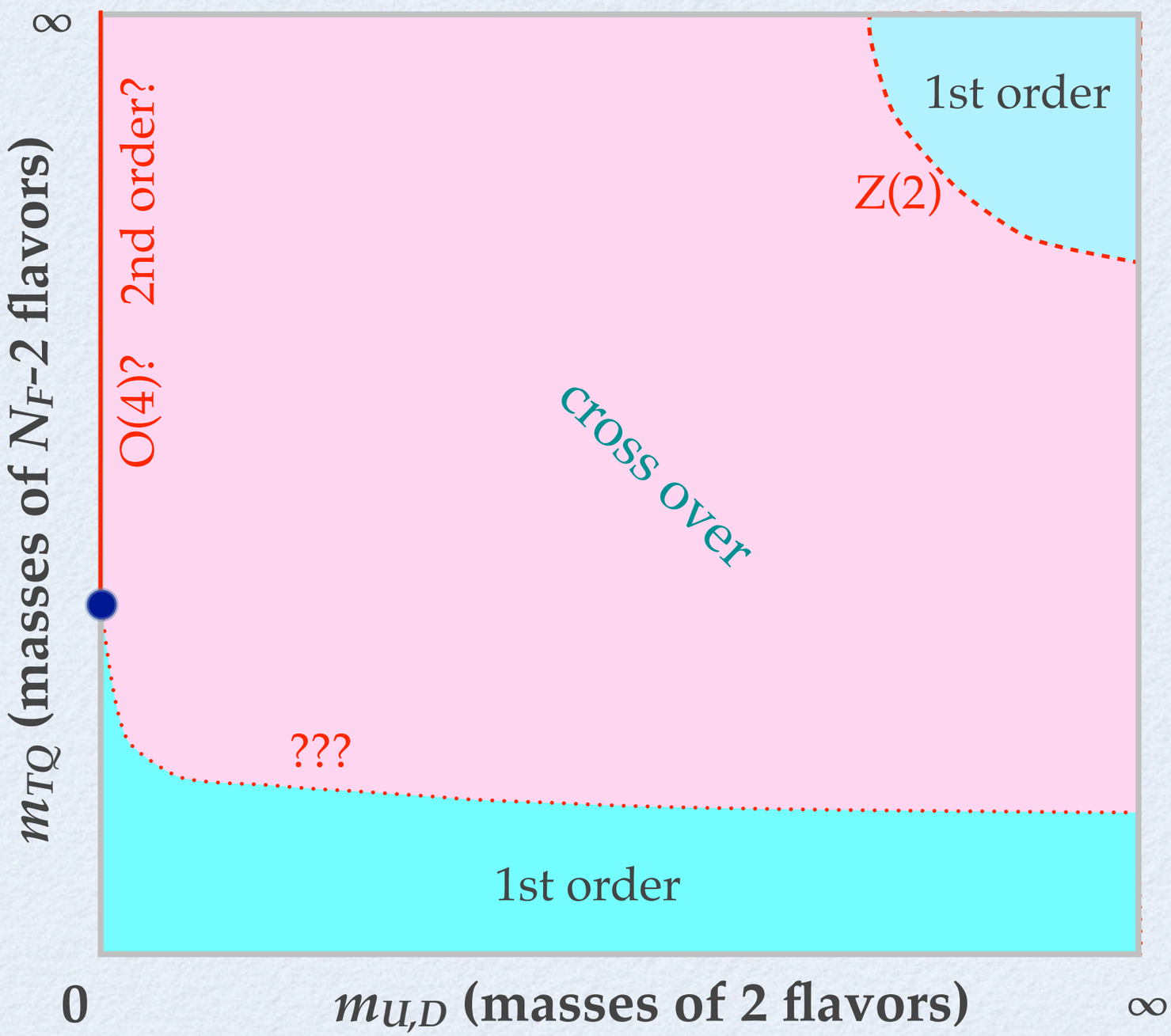

$N_F^{crit} > 5$ is assumed.

1st order persists to $m_{U,D} = \infty$ for small m_{TQ}.

Slow running and large γ_m may be expected at some N_F.

$5 \leqq N_F < N_F^{crit}$

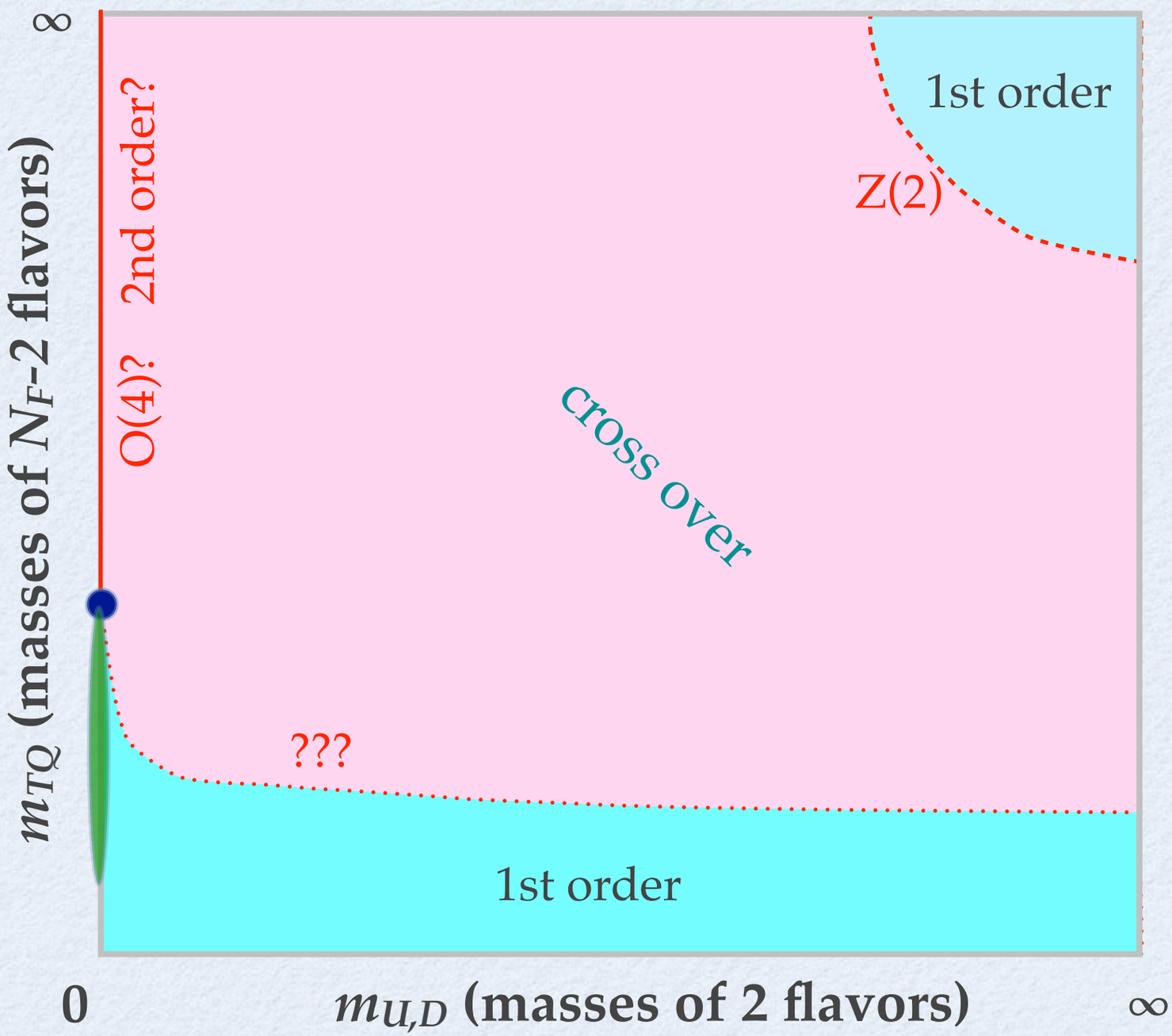

$N_F^{crit} > 5$ is assumed.

1st order persists to $m_{U,D} = \infty$ for small m_{TQ}.

Slow running and large γ_m may be expected at some N_F.

Furthermore,

- 1st order P.T. is attractive because of baryongenesis.

Appelquist, Schwetz and Selipsky, PRD52, 4741 (1995).
Kikukawa, Kohda and Yasuda, PRD77 (2008) 015014

Phenomenologically interesting!

$N_F - 2 < N_F^{crit} < N_F$ (Speculation)

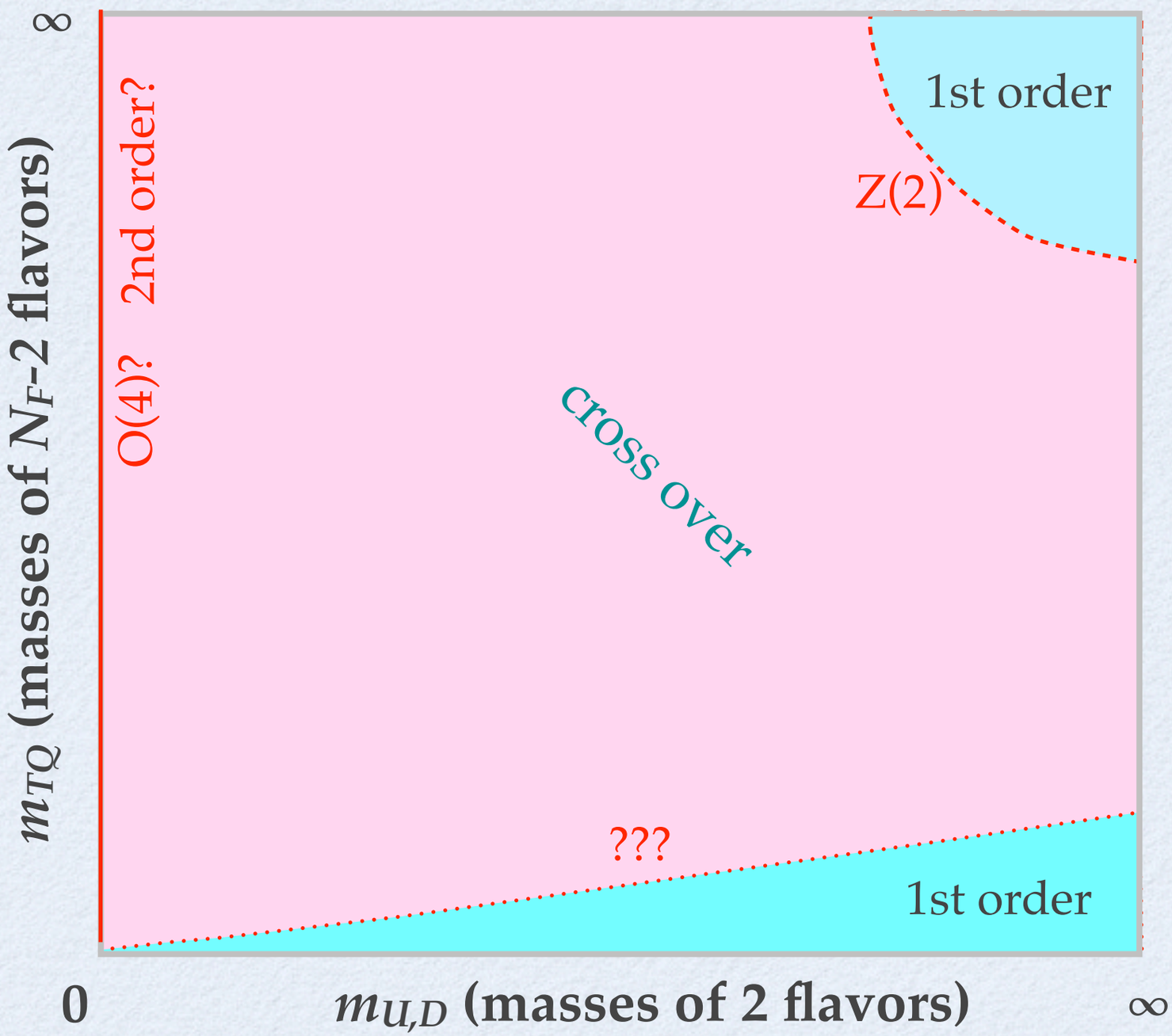

If this is the case,

EW Baryongenesis within TC seems to difficult.

$N_F^{crit} < N_F - 2 < N_F$ (Speculation)

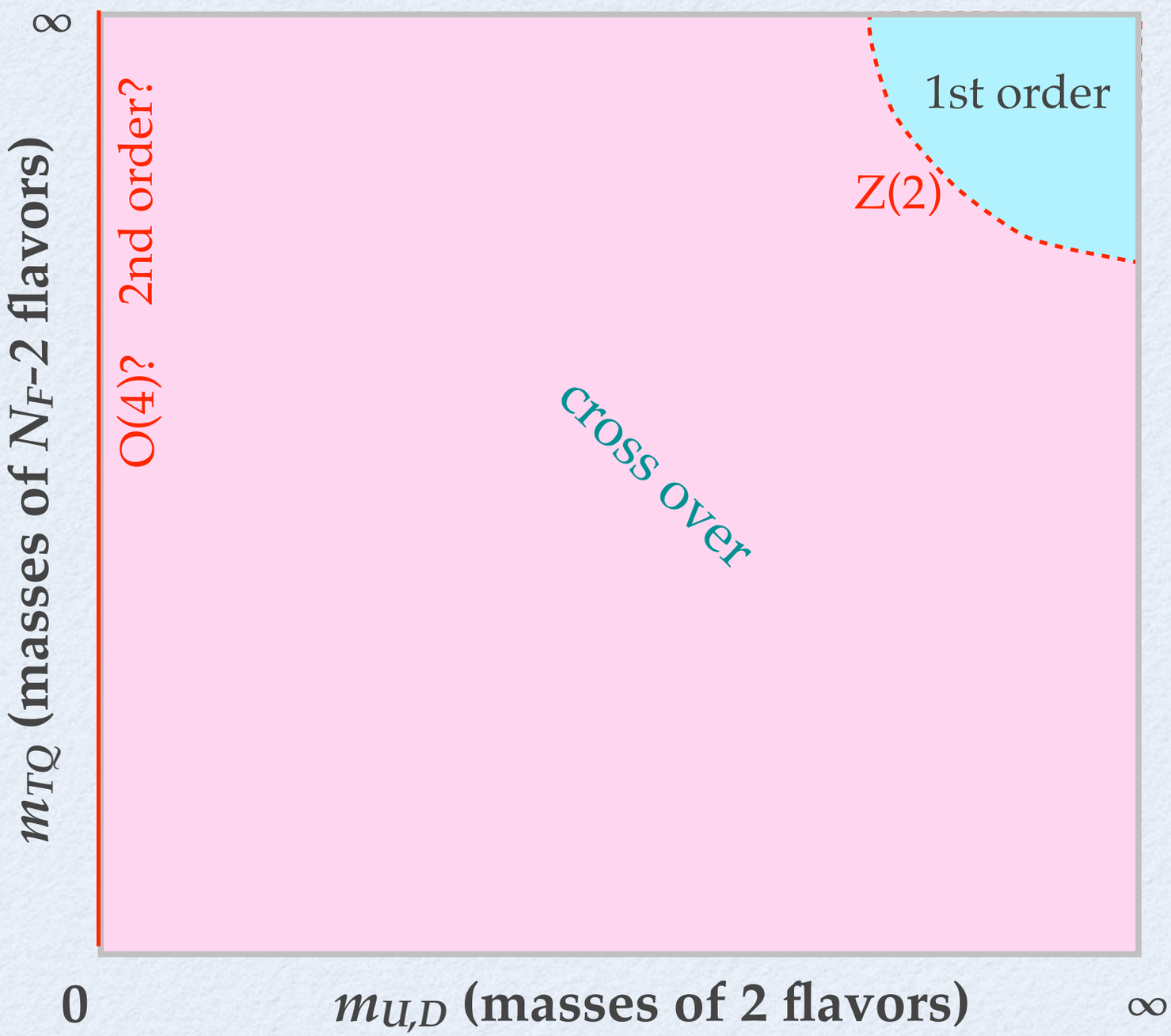

If this is the case, not interesting.

Summary

- ✓ Important to have several complementary approaches in the search for Conformal Window.
- ✓ We employ Wilson fermion to study the properties of Many Flavor QCD.
- ✓ Important to know Wilson Phase diagram when interpreting spectroscopy results.
- ✓ Establishing Columbia plot for Many Flavor QCD clarifies phenomenologically interesting region.

Finite Volume effect

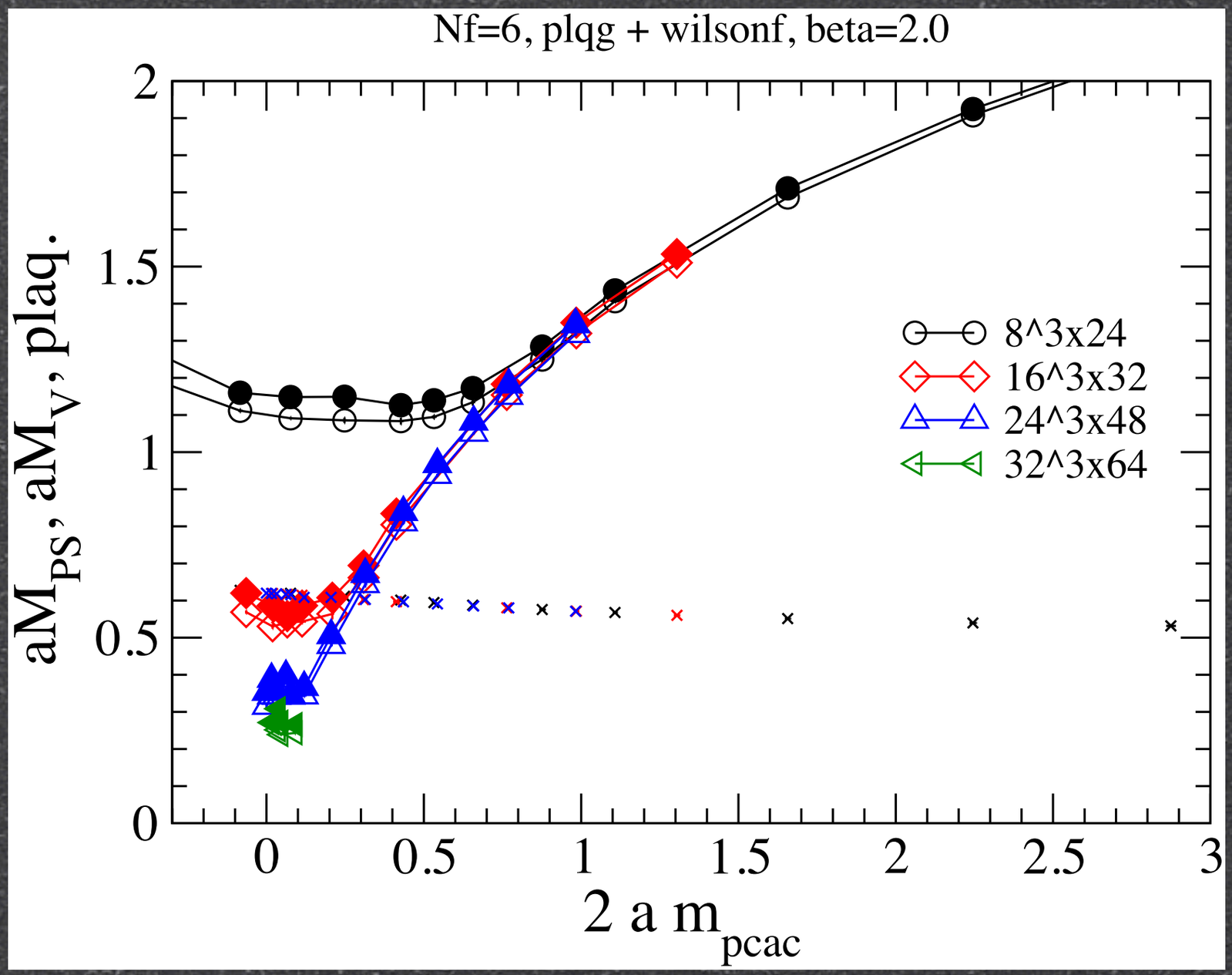

- Finite volume effect is significant.
- Masses are bounded from below.
- Minimum decreases as volume → large.

Expected behavior in Conformal Window

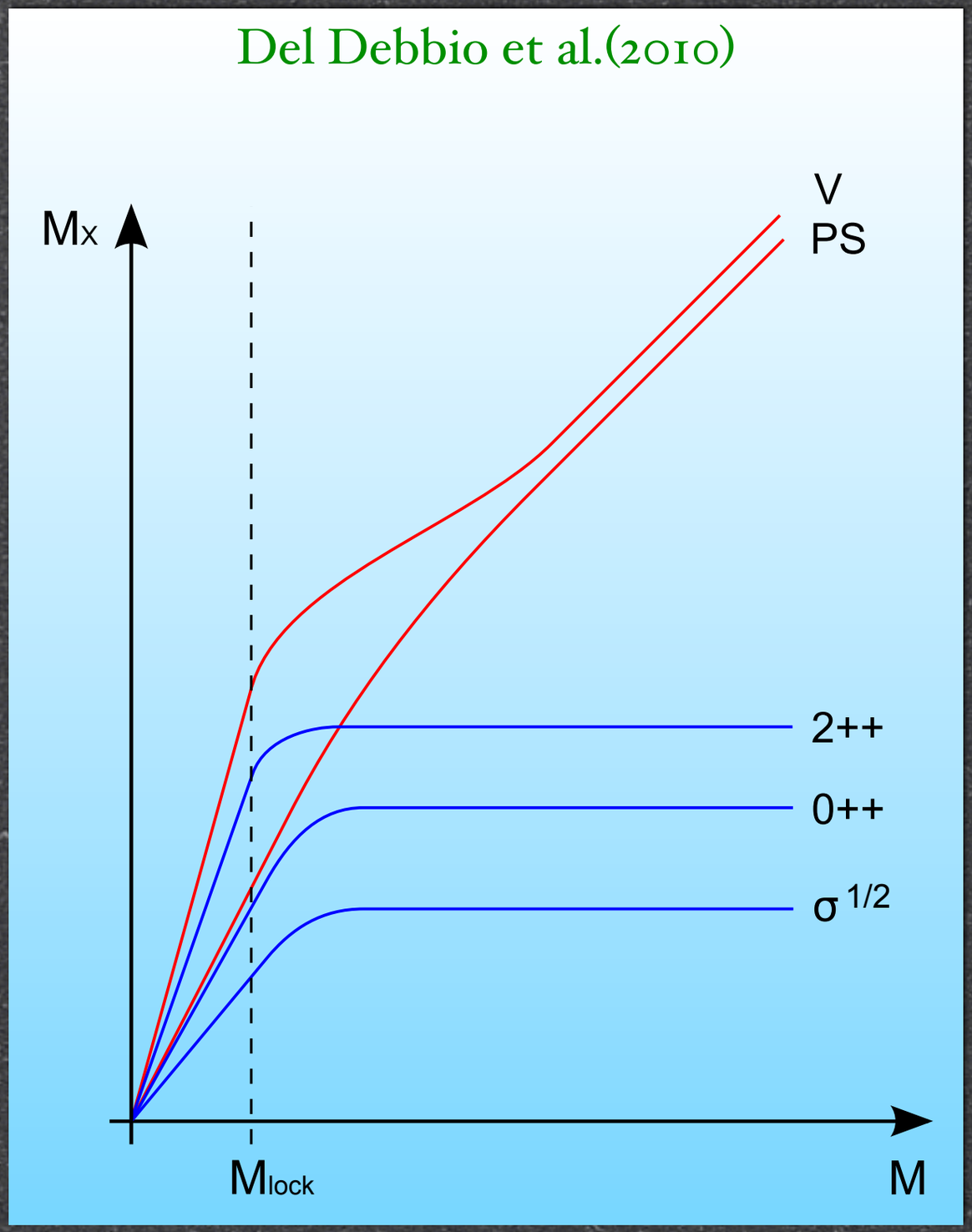

- Static limit = Quench
- In the massless limit, everything becomes massless.
- Dynamical scale (e.g. Λ_{QCD} in QCD) also vanishes there in contrast to QCD.
- Therefore, mass dependence of gluonic quantities is the key.

M_H and σ

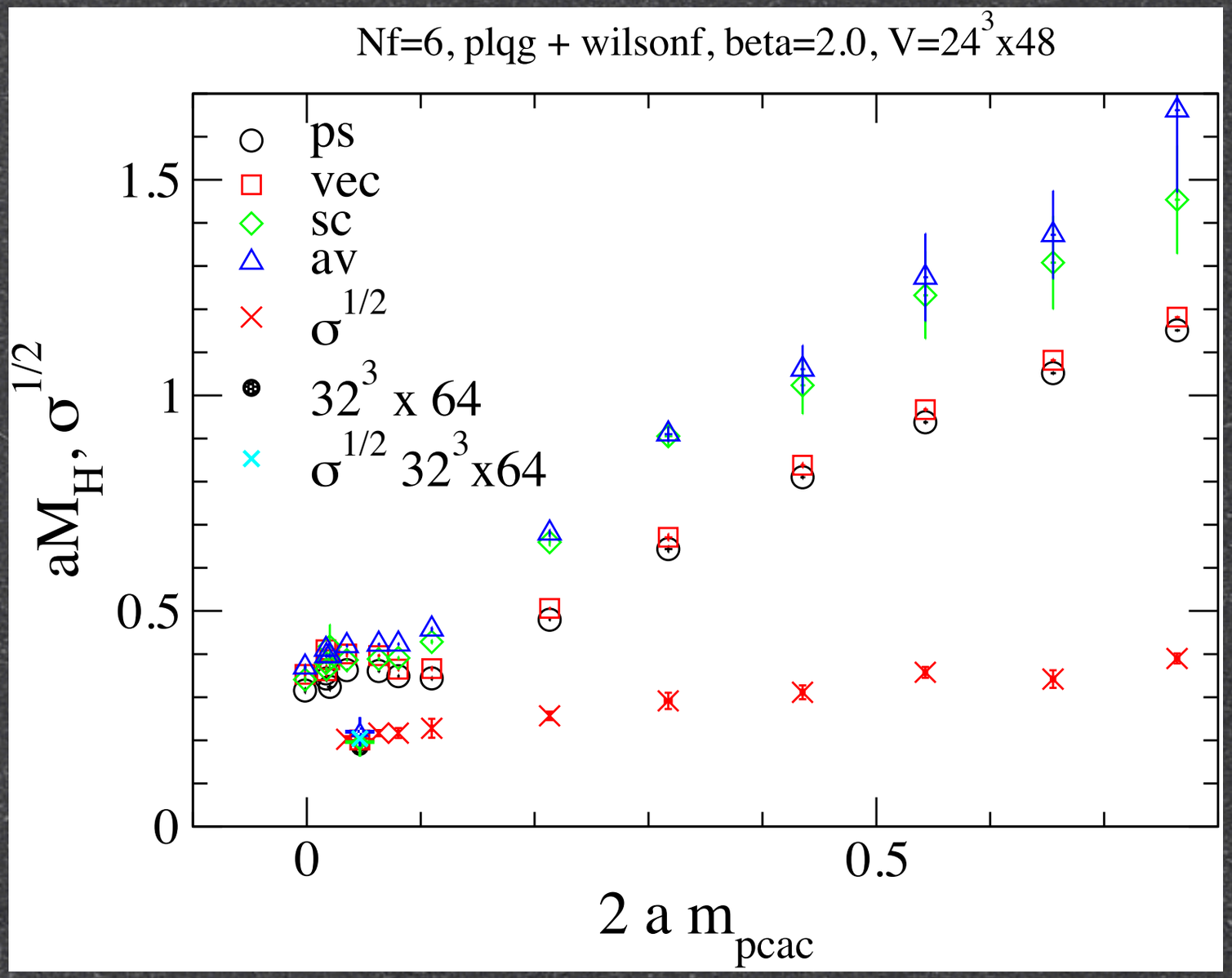

- $M_P \approx M_V$ and $M_S \approx M_{AV}$ are typical pattern in the presence of heavy quark symmetry.
- $\sigma^{1/2}$ is smaller than M_H in most region.
- At $V=32^3 \times 64$, $\sigma^{1/2} \approx M_H$
- FVE is small for $\sigma^{1/2}$.
- $\sigma^{1/2}$ seems to remain finite in the chiral limit.
- Confinement?

Light nuclei from quenched lattice QCD

Takeshi Yamazaki

Kobayashi-Maskawa Institute for the Origin of Particles and the Universe

Nagoya University

Y. Kuramashi and A. Ukawa for PACS-CS Collaboration

PRD81:111504(R)(2010); PRD84:054506(2011)

New Horizons for Lattice Computations with Chiral Fermions

@ BNL May 14–16 2012

Outline

1. Introduction
2. Simulation parameters
3. Results
    1. 3- and 4-nucleon channels
    2. NN channels
4. Preliminary results of $N_f = 2 + 1$
5. Summary and future work

1. Introduction

Strong interaction

$$\text{Bind} \begin{cases} \text{protons and neutrons} & \rightarrow \quad \text{nuclei} \\ \text{quarks and gluons} & \rightarrow \quad \text{protons and neutrons} \end{cases}$$

Spectrum of nuclei

success of Shell model since 1949: Jensen and Mayer

degrees of freedom of protons and neutrons

Spectrum of proton and neutron (nucleons)

success of non-perturbative calculation of QCD

such as lattice QCD

degrees of freedom of quarks and gluons

$$\underbrace{\text{quarks and gluons} \rightarrow \overbrace{\text{protons and neutrons}}^{\text{Shell model}}}_{\text{(lattice) QCD}} \rightarrow \text{nuclei}$$

1. Introduction

Strong interaction

$$\text{Bind} \begin{cases} \text{protons and neutrons} \rightarrow \text{nuclei} \\ \text{quarks and gluons} \rightarrow \text{protons and neutrons} \end{cases}$$

Spectrum of nuclei

success of Shell model since 1949: Jensen and Mayer

degrees of freedom of protons and neutrons

Spectrum of proton and neutron (nucleons)

success of non-perturbative calculation of QCD

such as lattice QCD

degrees of freedom of quarks and gluons

Motivation: Understand property of nuclei from (lattice) QCD

$$\underbrace{\text{quarks and gluons} \rightarrow \overbrace{\text{protons and neutrons} \rightarrow \text{nuclei}}^{\text{Shell model}}}_{\text{(lattice) QCD}}$$

1. Introduction

Motivation :

Understand property and structure of nuclei from QCD

If we can study nuclei from QCD, we may be able to

1. reproduce spectrum of nuclei
2. predict property of nuclei hard to calculate or observe

such as neutron rich nuclei

So far only few works for multi-baryon bound states
Before studying such difficult problems, we should check

$\rightarrow$ Can we calculate known binding energy in a-few-nucleon systems?

Multi-baryon bound state from lattice QCD

Not observed before '09 (except H-dibaryon '88 Iwasaki *et al.*)

Recent studies of lattice QCD for bound state of multi-baryon systems

1. 3- and 4-nucleon systems
   '10 PACS-CS $N_f = 0$ $m_\pi = 0.8$ GeV PRD81:111504(R)(2010)
2. H dibaryon in ΛΛ system (S=−2, I=0)
   '11 NPLQCD $N_f = 2 + 1$ $m_\pi = 0.39$ GeV
   '11 HALQCD $N_f = 3$ $m_\pi = 0.67$–1.02 GeV
   '11 Luo et al. $N_f = 0$ $m_\pi = 0.5$–1.3 GeV
3. NN systems
   '11 PACS-CS $N_f = 0$ $m_\pi = 0.8$ GeV PRD84:054506(2011)
   '12 NPLQCD $N_f = 2 + 1$ $m_\pi = 0.39$ GeV
4. ΞΞ system
   '12 NPLQCD $N_f = 2 + 1$ $m_\pi = 0.39$ GeV

presented in this talk

Other studies: 2- and 3-nucleon forces HALQCD, ΩΩ channel Buchoff *et al.*

Problems of multi-nucleon bound state

Traditional calculation method of 0th state energy

Example: ^{4}He channel ($J^P = 0^+, I = 0$)

$$\begin{aligned} C_4(t) &= \langle 0|O_{^4\mathrm{He}}(t)\overline{O}_{^4\mathrm{He}}(0)|0\rangle \\ &= \sum_n \langle 0|O_{^4\mathrm{He}}|n\rangle\langle n|\overline{O}_{^4\mathrm{He}}|0\rangle e^{-E_n t} \xrightarrow[t\gg 1]{} A_0\, e^{-E_0 t} \end{aligned}$$

1. Statistical error
   → Unphysically heavy quark mass + large # of measurements
2. Calculation cost
   → Reduce calculation costs with several methods

   Multi-meson systems: '10 Detmold and Savage
   Multi-baryon systems: '12 Doi and Endres
3. Identification of bound state in finite volume
   → Volume dependence of energy shift of 0th state

2. Simulation parameters

Quenched Iwasaki gauge action at $\beta = 2.416$

$a^{-1} = 1.54$ GeV with $r_0 = 0.49$ fm

Tad-pole improved Wilson fermion action

$m_\pi = 0.8$ GeV and $m_N = 1.62$ GeV

reduce large statistical fluctuation

Finite volume dependence of 0th state

(^{4}He, ^{3}He, $^3S_1$ and $^1S_0$ channels)

- Three volumes: $L = 3.1, 6.1, 12.3$ fm

L	L [fm]	N_{conf}	N_{meas}
24	3.1	2500	2
48	6.1	400	12
96	12.3	200	12

- Two smearing sources: for consistency check

Simulations:

PACS-CS, T2K-Tsukuba at Univ. of Tsukuba, HA8000 at Univ. of Tokyo

4. Results

Effective energy of ^{4}He channel at $L = 48$ $E_0 = \log\left(\frac{C_{\mathrm{He}}(t)}{C_{\mathrm{He}}(t+1)}\right)$

and $\Delta E_L = \log\left(\frac{R_{^4\mathrm{He}}(t)}{R_{^4\mathrm{He}}(t+1)}\right)$ with $R_{^4\mathrm{He}}(t) = \frac{C_{^4\mathrm{He}}(t)}{(C_N(t))^4}$

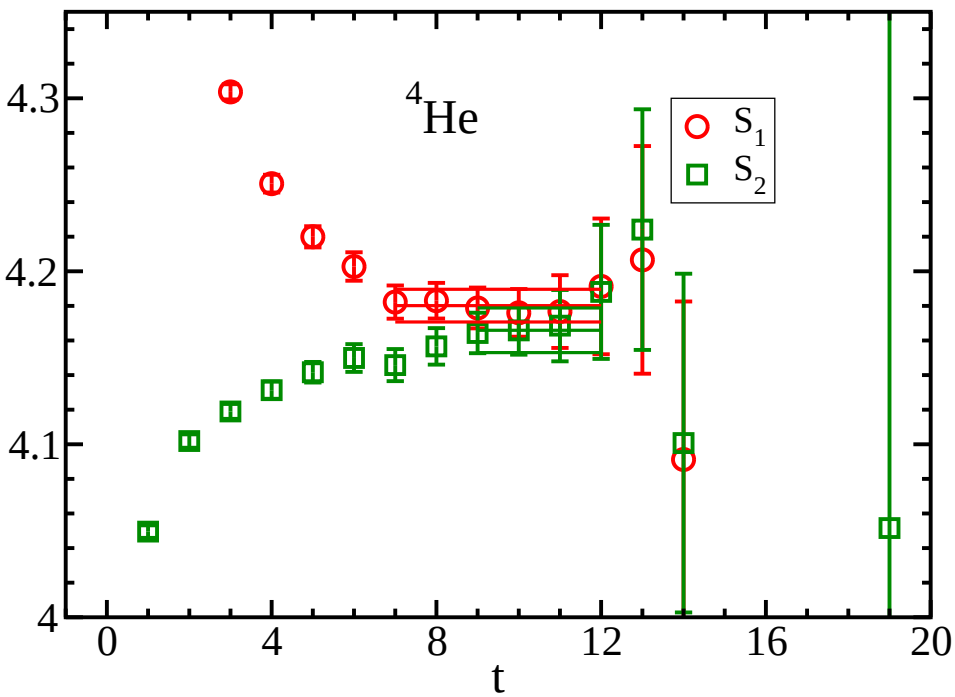

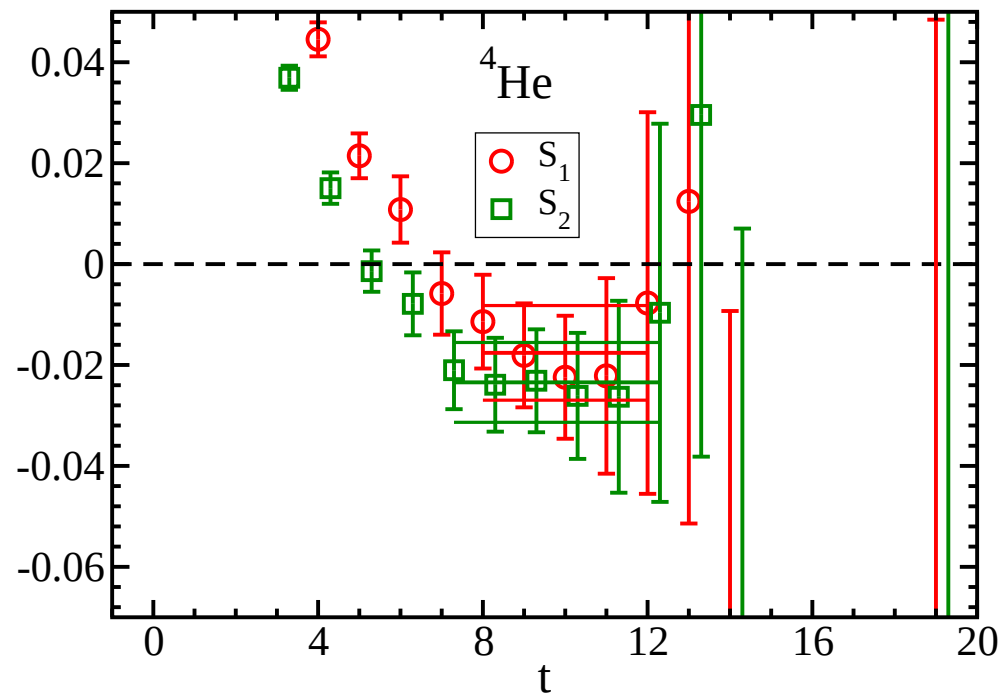

- Clear signal in $t < 12$, but larger error in $t \geq 12$
- consistent plateaus in $8 \lesssim t \leq 12$

3. Results

3- and 4-nucleon channels $\Delta E_L = E_0 - N_N m_N$

PACS-CS Collaboration, PRD81:111504(R)(2010)

Identification of bound state from volume dependence of ΔE

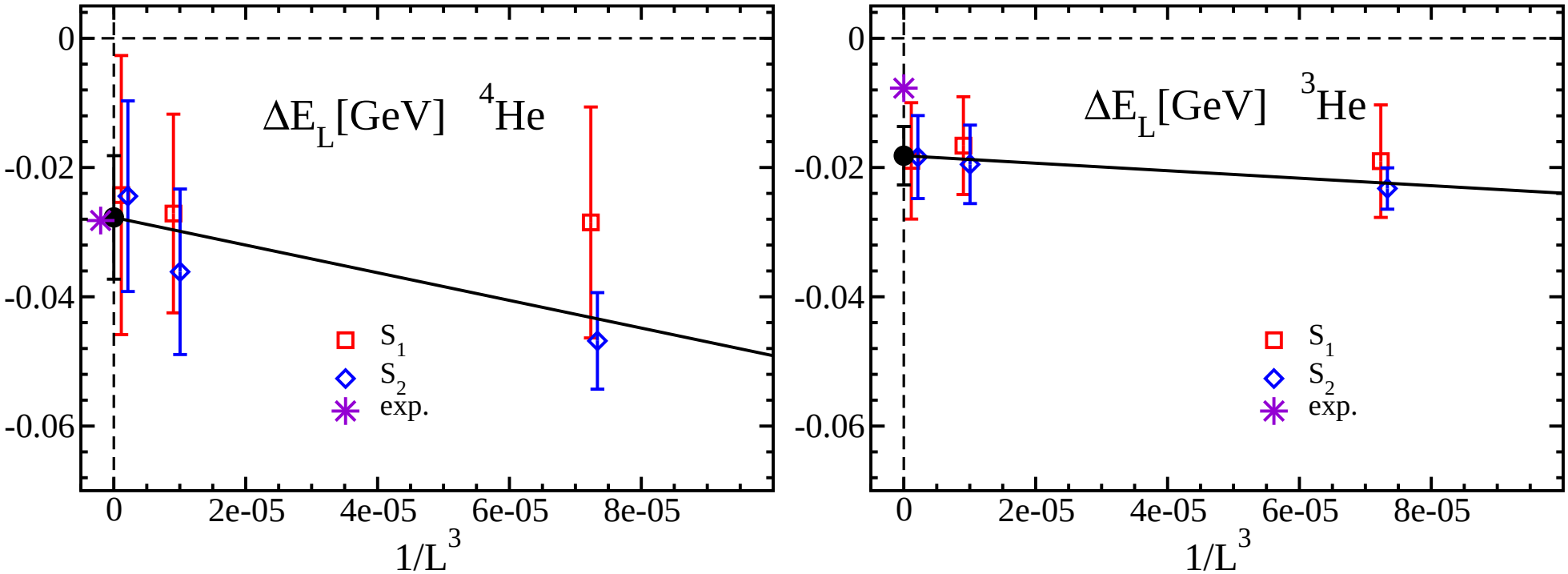

- $\Delta E_L < 0$ in three volumes $\Leftarrow$ statistically independent ensembles
- Small volume dependence
- Infinite volume limit with $\Delta E_L = -\Delta E_{\text{bind}} + C/L^3$

3. Results

3- and 4-nucleon channels $\Delta E_L = E_0 - N_N m_N$

PACS-CS Collaboration, PRD81:111504(R)(2010)

Identification of bound state from volume dependence of ΔE

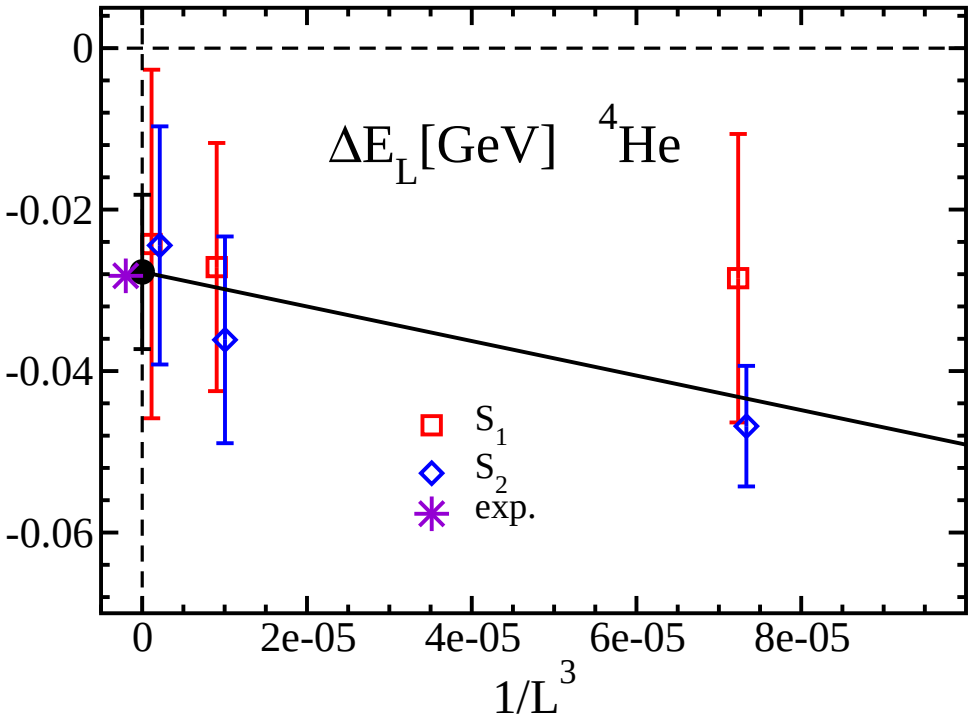

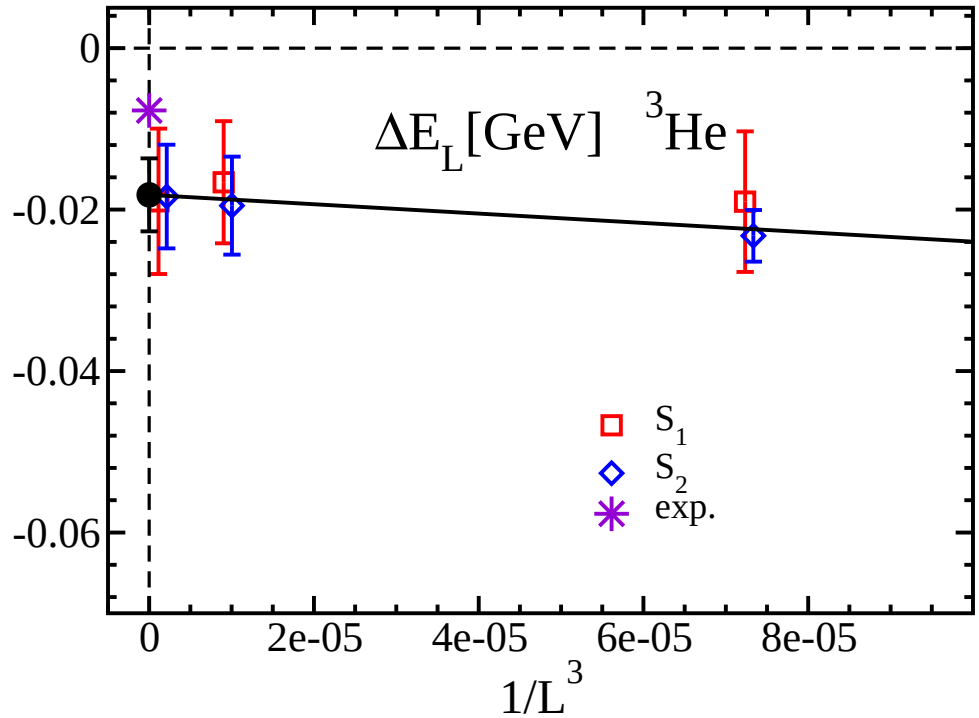

$\Delta E_{^4\mathrm{He}} = 27.7(7.8)(5.5)$ MeV $\qquad$ $\Delta E_{^3\mathrm{He}} = 18.2(3.5)(2.9)$ MeV

1. Observe bound state in both channels
2. Same order of ΔE to experiment

However, large systematic errors, e.g., $m_\pi = 0.8$ GeV

3. Results

NN ($^3S_1$ and $^1S_0$) channels $\Delta E_L = E_0 - 2m_N$

PACS-CS Collaboration, PRD84:054506(2011)

Identification of bound state from volume dependence of ΔE

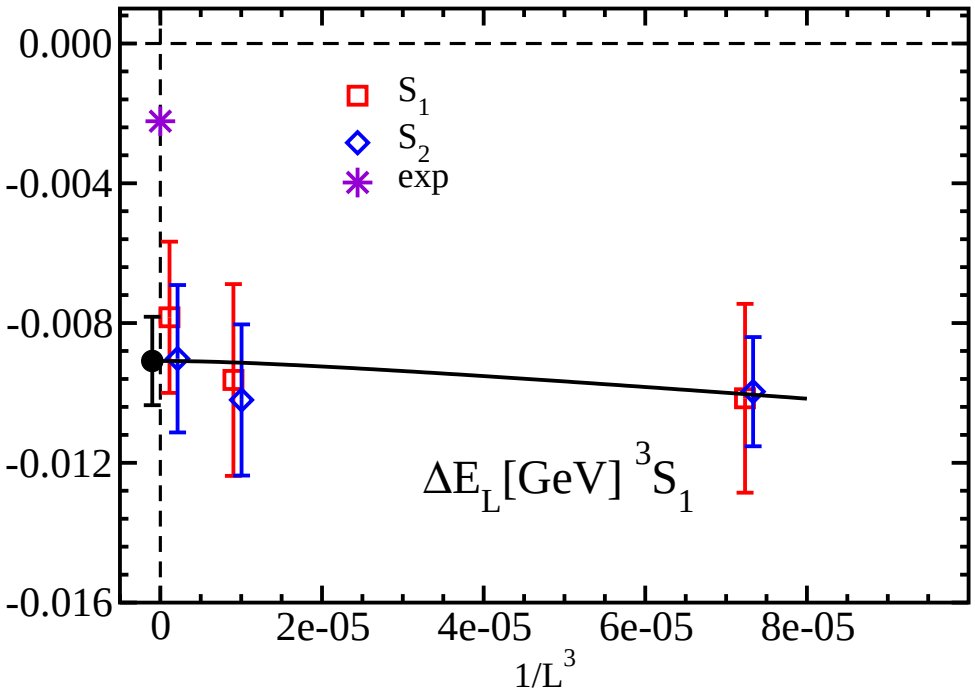

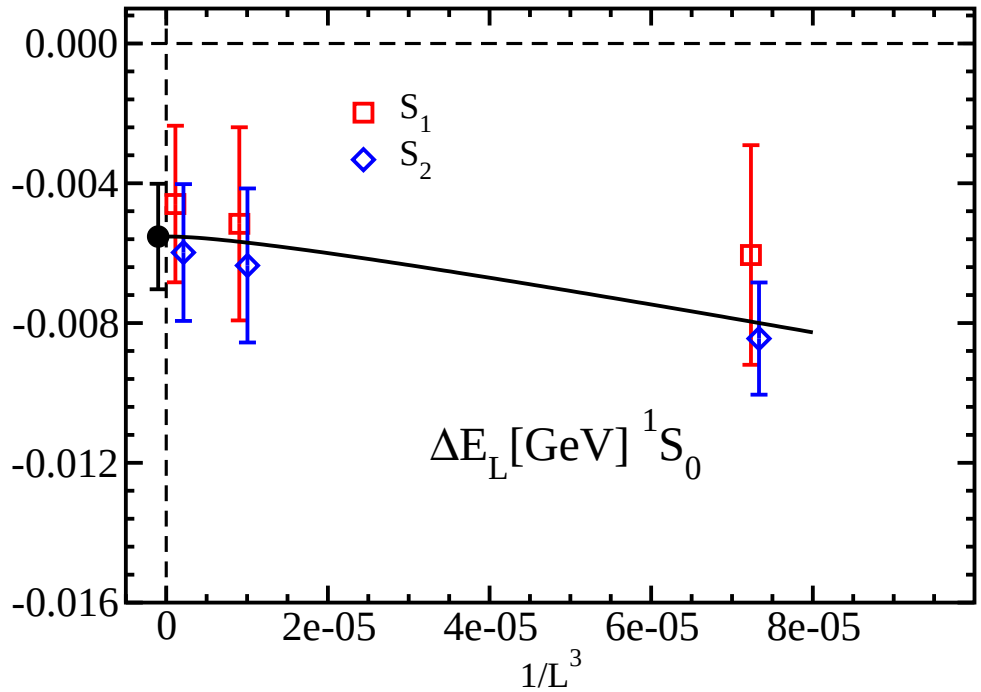

$\Delta E_L < 0$ in three volumes

Infinite volume extrapolation

'04 Beane *et al.*, '06 Sasaki & TY

$$\Delta E_L = -\frac{\gamma^2}{m_N}\left\{1 + \frac{C_\gamma}{\gamma L}\sum_{\vec{n}}{}' \frac{\exp(-\gamma L\sqrt{\vec{n}^2})}{\sqrt{\vec{n}^2}}\right\},\ \Delta E_{\text{bind}} = \frac{\gamma^2}{m_N}$$

based on Lüscher's finite volume formula

3. Results

NN ($^3S_1$ and $^1S_0$) channels $\Delta E_L = E_0 - 2m_N$

PACS-CS Collaboration, PRD84:054506(2011)

Identification of bound state from volume dependence of ΔE

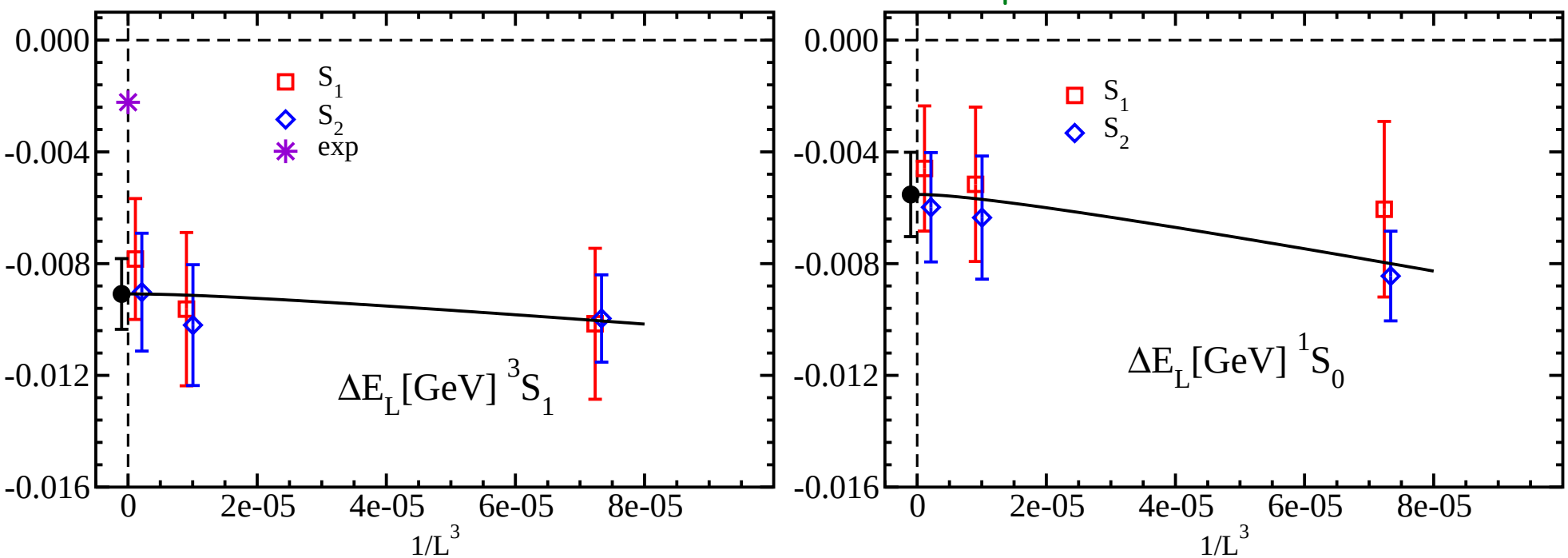

Bound state in both channels ← different from experiment

$\Delta E_{^3S_1} = 9.1(1.1)(0.5)$ MeV $\qquad$ $\Delta E_{^1S_0} = 5.5(1.1)(1.0)$ MeV

Probably bound states in $N_f = 2+1$ $m_\pi = 0.39$ GeV ('12 NPLQCD)

might be caused by heavy quark mass in calculation

4. Preliminary results of $N_f = 2 + 1$

Reduce systematic errors

Quark mass dependence of ΔE and a_0

Bound state in $^1S_0$ vanishes as quark mass decreases?

Heavy quark mass

$m_\pi = 0.8$ GeV

Quenched effect

Finite lattice spacing

$a^{-1} = 1.54$ GeV

4. Preliminary results of $N_f = 2 + 1$

Reduce systematic errors

Quark mass dependence of ΔE and a_0

Bound state in $^1S_0$ vanishes as quark mass decreases?

Heavy quark mass

$m_\pi = 0.8$ GeV $\rightarrow$ 0.5 (and 0.7) GeV

Quenched effect

$N_f = 2 + 1$ QCD

Finite lattice spacing

$a^{-1} = 1.54$ GeV $\rightarrow a^{-1} \sim 2$ GeV

Calculation of NN, ^{3}He, ^{4}He channels

4. Preliminary results of $N_f = 2 + 1$

Simulation parameters

- Iwasaki gauge action at $\beta = 1.90$

$$a^{-1} = 2.194 \text{ GeV with } m_\Omega$$

- Non-perturbative improved Wilson fermion action

$$m_\pi = 0.5 \text{ GeV and } m_N = 1.3 \text{ GeV}$$

$$m_s \sim \text{physical strange mass}$$

Finite volume dependence of 0th state

Four volumes: $L = 2.9, 3.6, 4.3, 5.8$ fm

Measurements: $\sim$ 200 confs $\times$ $O(100)$/per conf

Simulations:

PACS-CS, T2K-Tsukuba, HA-PACS at Univ. of Tsukuba, HA8000 at Univ. of Tokyo and K at AICS

4. Preliminary results of $N_f = 2 + 1$

3- and 4-nucleon channels

Identification of bound state from volume dependence of ΔE

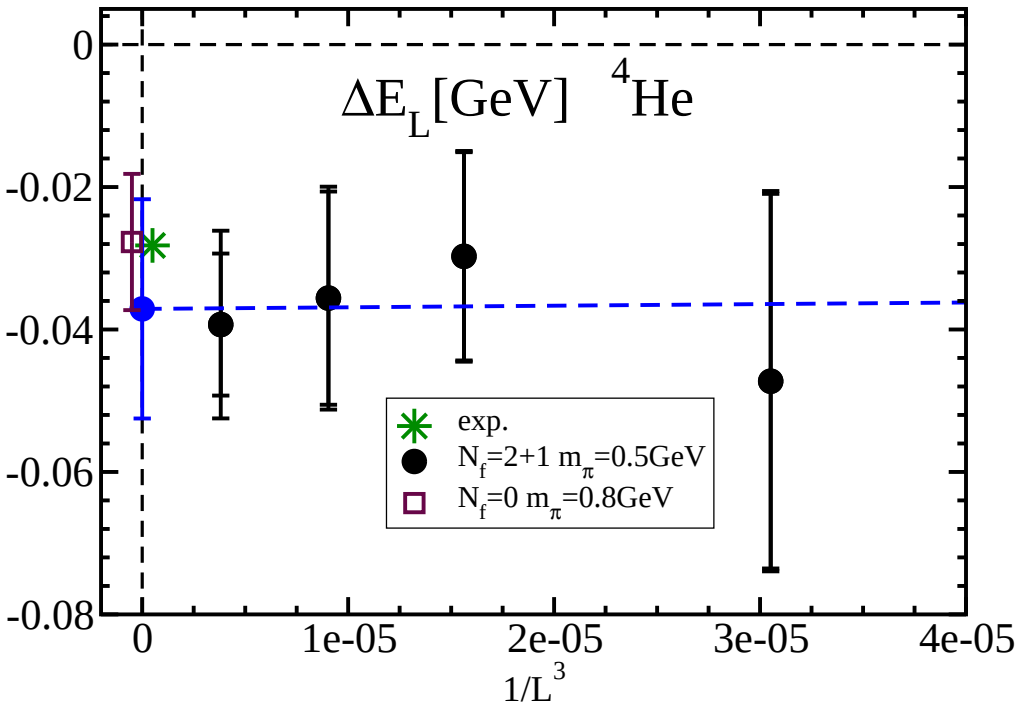

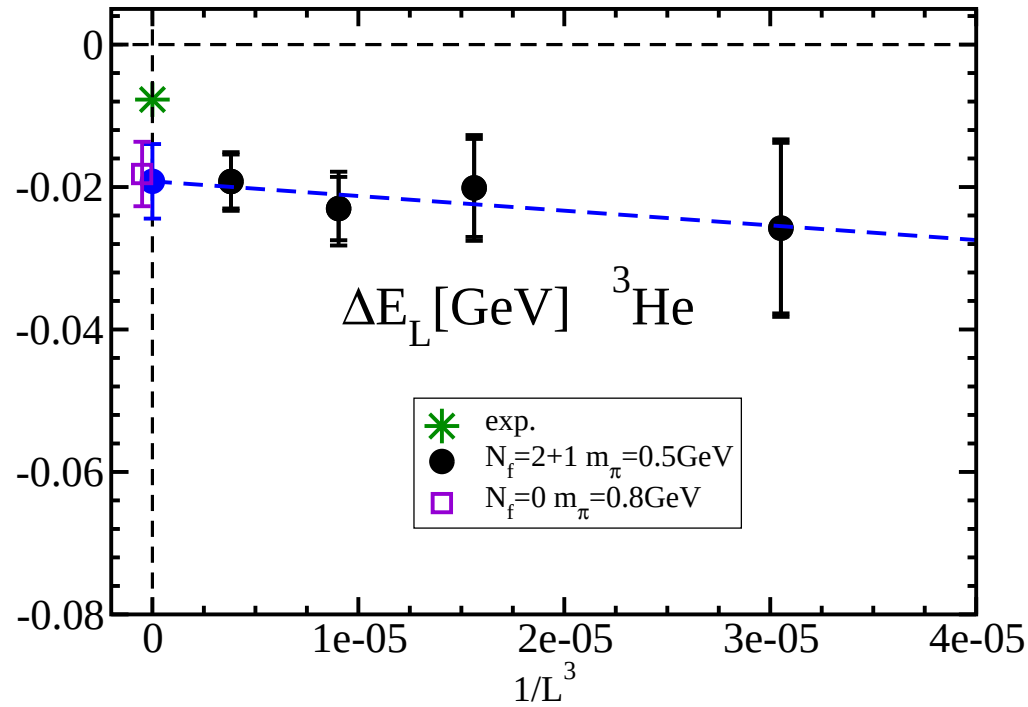

Similar results to $N_f = 0$ $m_\pi = 0.8$ GeV

4. Preliminary results of $N_f = 2 + 1$

NN ($^3S_1$ and $^1S_0$) channels

Identification of bound state from volume dependence of ΔE

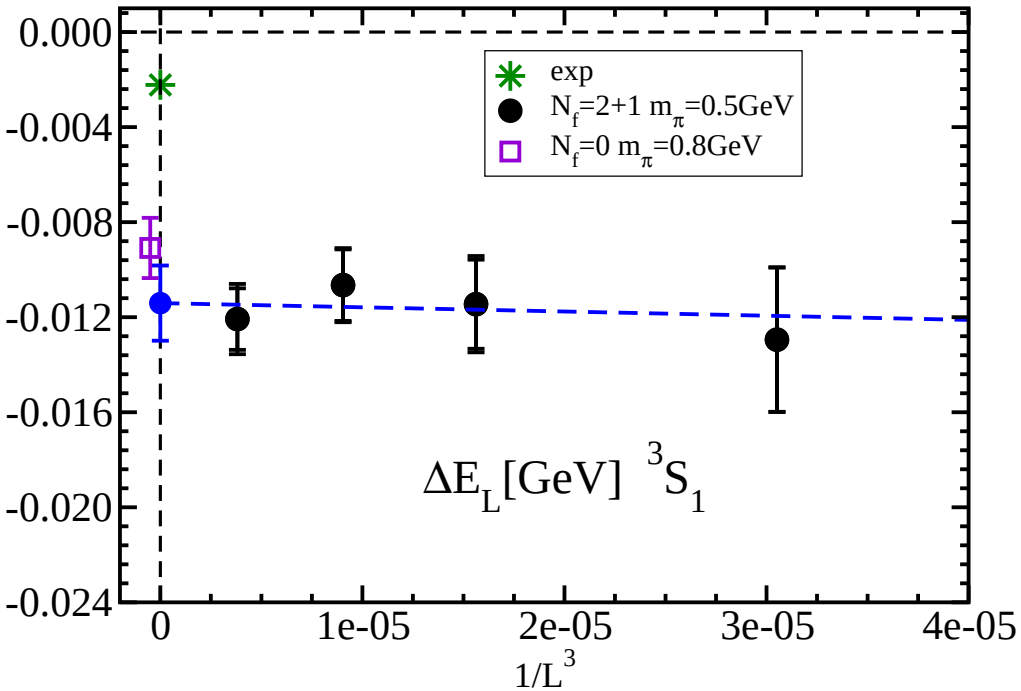

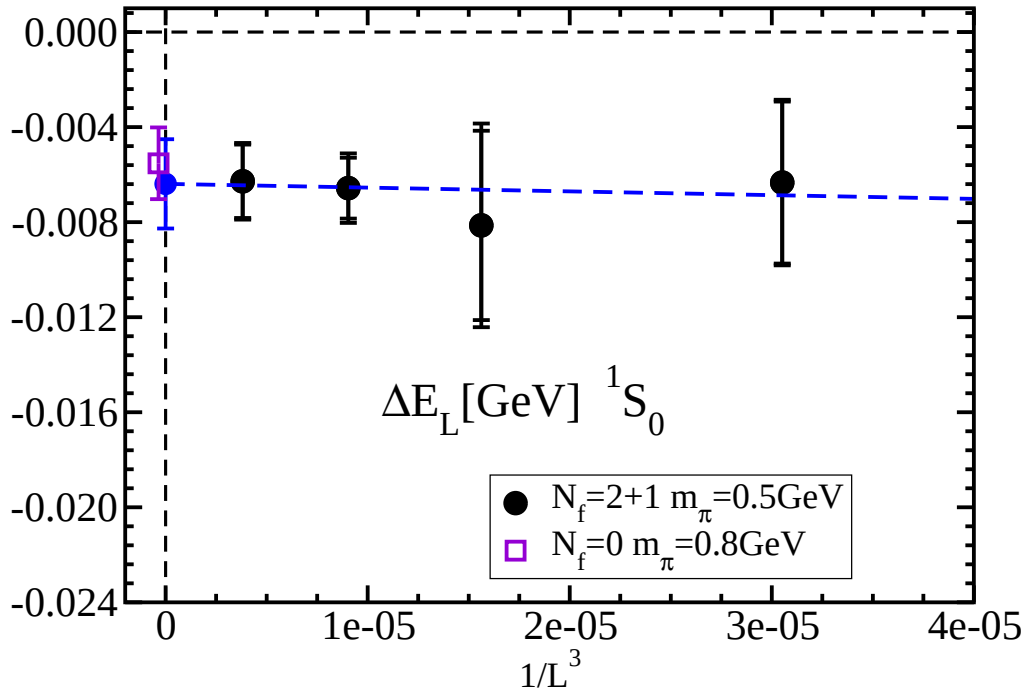

Similar results to $N_f = 0$ $m_\pi = 0.8$ GeV

4. Preliminary results of $N_f = 2 + 1$

NN ($^3S_1$ and $^1S_0$) channels

Current status of ΔE

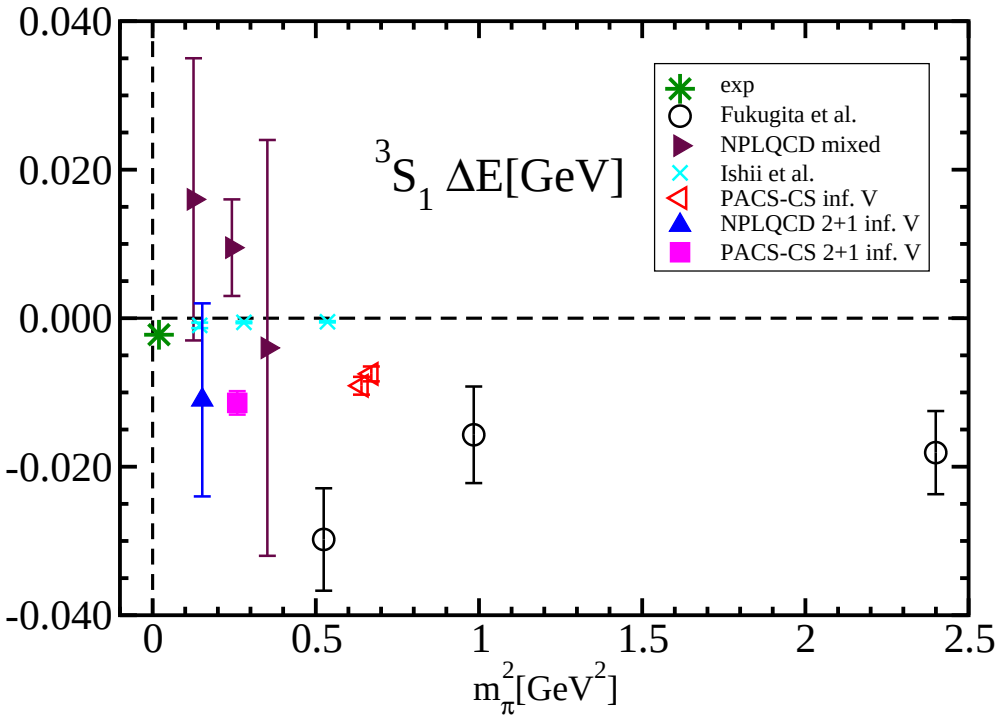

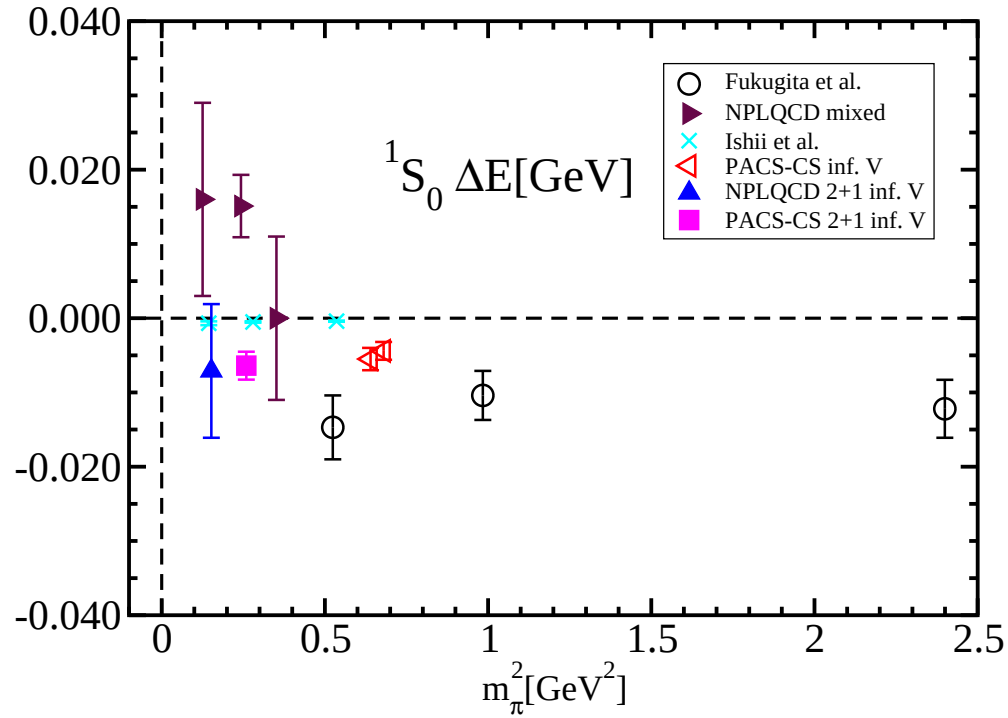

filled(open) symbols: $N_f = 2 + 1$(quenched) results

Roughly consistent with other results

Still quark mass might be heavy

Need further lighter quark mass for clear quark dependence

5. Summary and future work

Exploratory study of light nuclei in quenched lattice QCD

- Unphysically heavy quark mass
- Volume dependence of energy shift of ground state

1. $\Delta E \neq 0$ of 0th state in infinite volume limit

(2. Expected properties of 1st excited state in NN)

$\rightarrow$ bound state in ^{4}He, ^{3}He, ^{3}S$_1$ and ^{1}S$_0$ at $m_\pi = 0.8$ GeV

Larger ΔE than experiment

Bound state in ^{1}S$_0$ not observed in experiment

probably observed $N_f = 2 + 1$ at $m_\pi = 0.39$ GeV ('12 NPLQCD)

Need to reduce systematic errors

5. Summary and future work

$N_f = 2 + 1$ calculation is on-going at $m_\pi = 0.5$ GeV

Similar result to quenched case

$\rightarrow$ bound state in ^{4}He, ^{3}He, ^{3}S$_1$ and ^{1}S$_0$ at $m_\pi = 0.5$ GeV

Need further lighter quark mass calculation

Back up

Very preliminary $N_f = 2 + 1$ results at $m_\pi = 0.7$ GeV

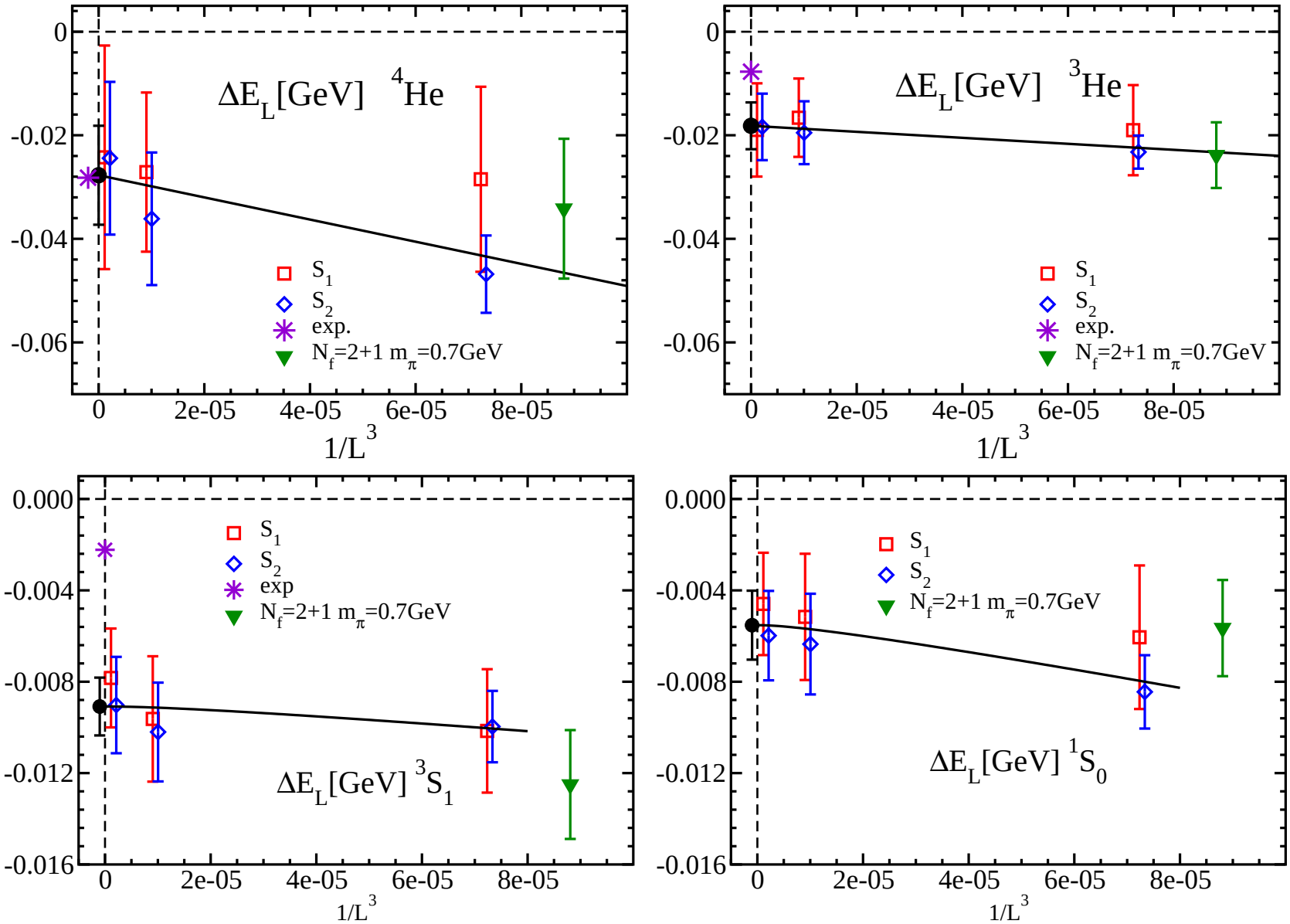

Larger volumes at $m_\pi = 0.5$ and 0.7 GeV underway

Example of large quark mass dependence

rms radii from form factors F_1 and F_2

'09 RBC + UKQCD

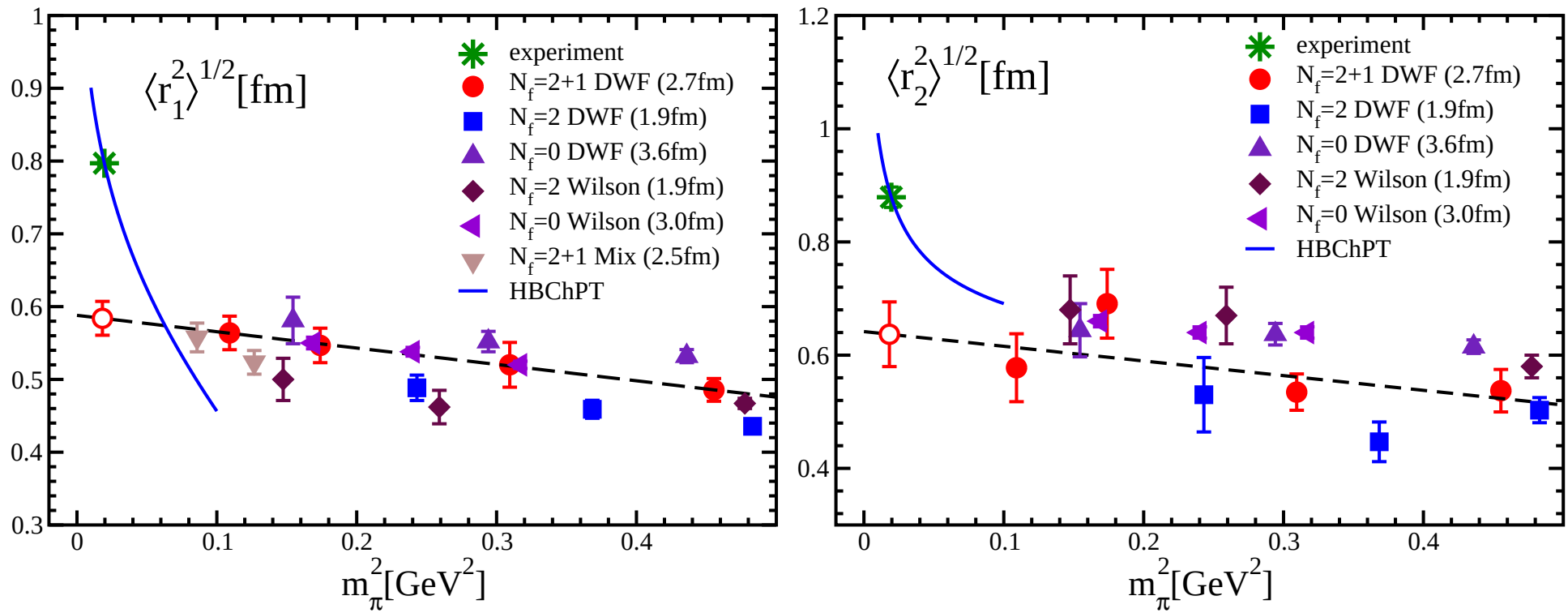

Effective energy shift $\Delta E_L = E_{\mathrm{NN}} - 2m_N$ of $^3\mathrm{S}_1$ at $L = 24$ and $L = 96$

$$\Delta E_L(t) = \log\left(\frac{R(t)}{R(t+1)}\right), \quad R(t) = \frac{C_{\mathrm{NN}}(t)}{(C_N(t))^2}$$

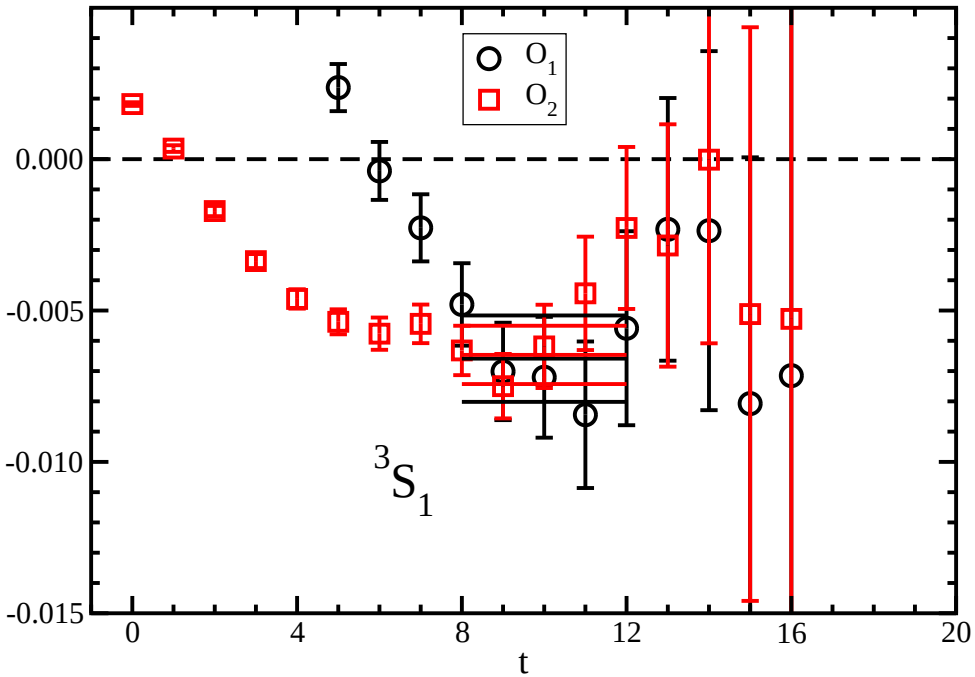

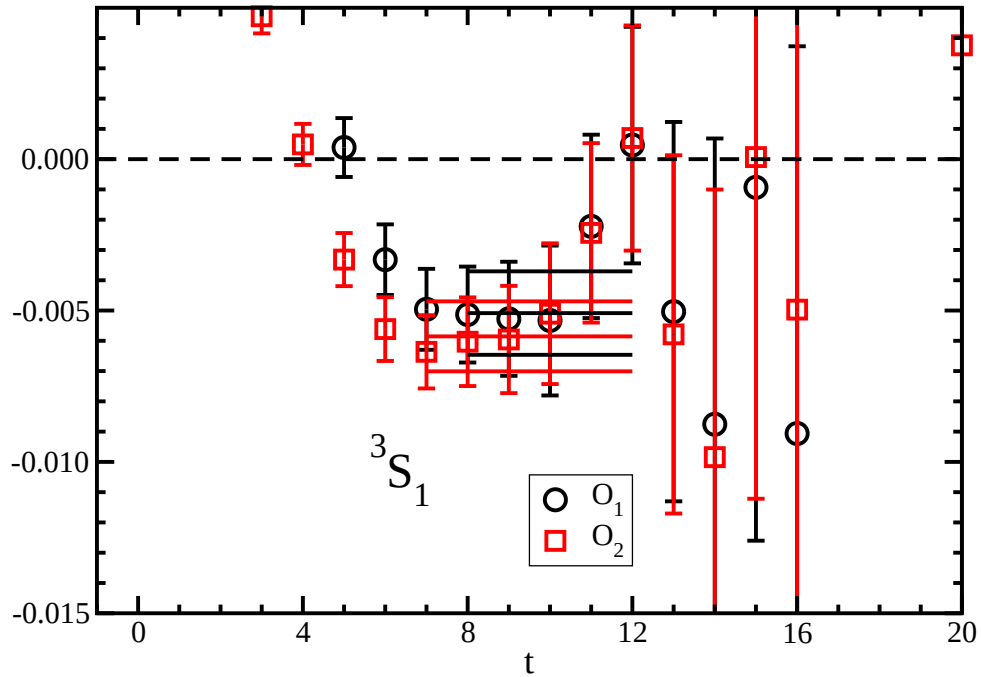

Smearing functions of sink operator at $L = 32$ and $L = 48$

$$N(\mathbf{x})W_{q^2}(|\mathbf{x}-\mathbf{y}|)N(\mathbf{y})$$

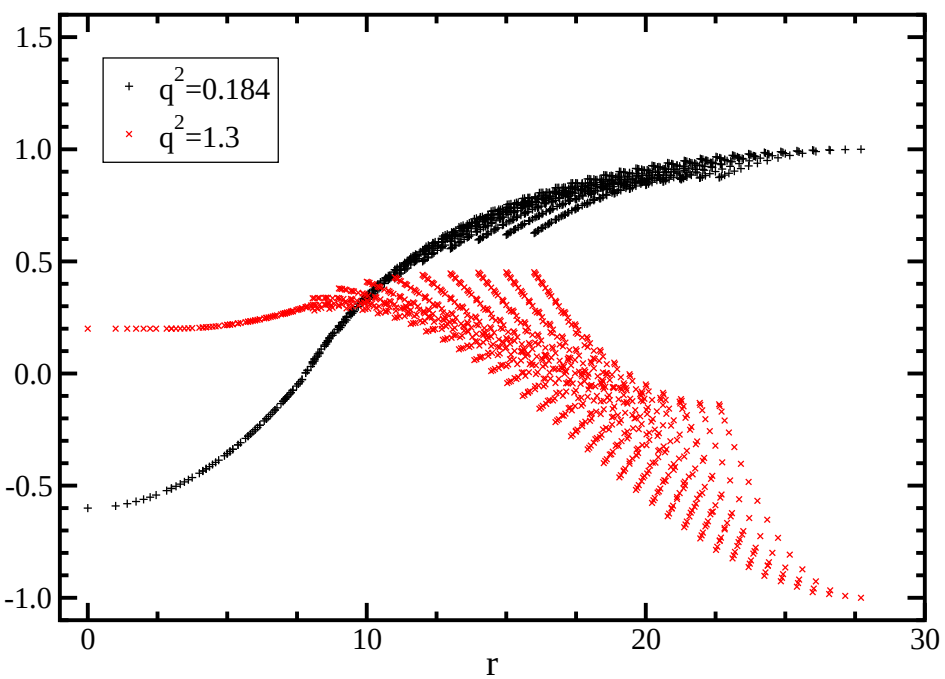

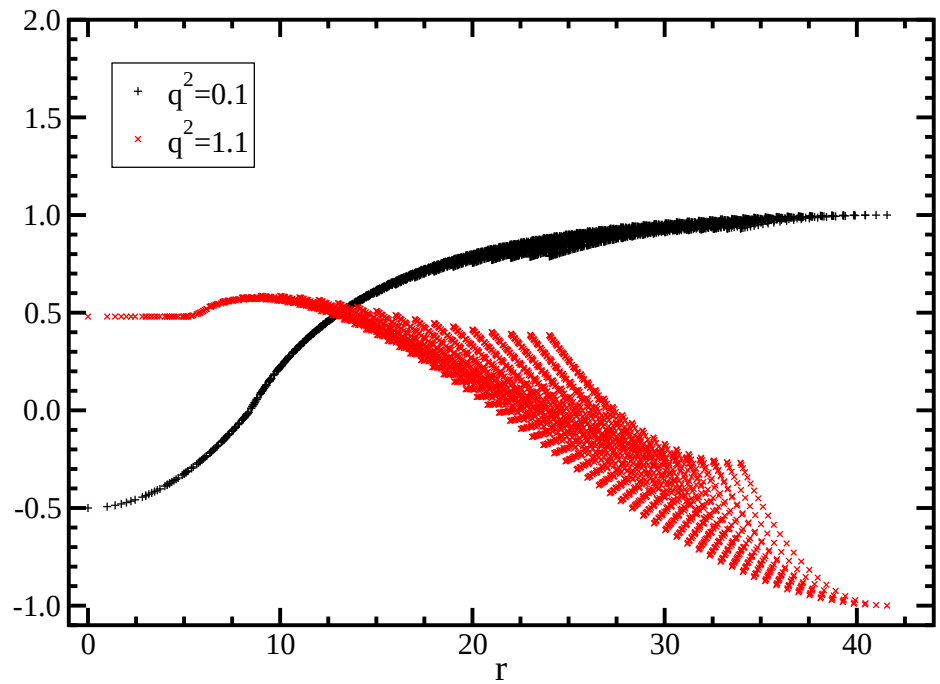

Effective nucleon mass at $L = 48$

$$M_N(t) = \log\left(\frac{C_N(t)}{C_N(t+1)}\right)$$

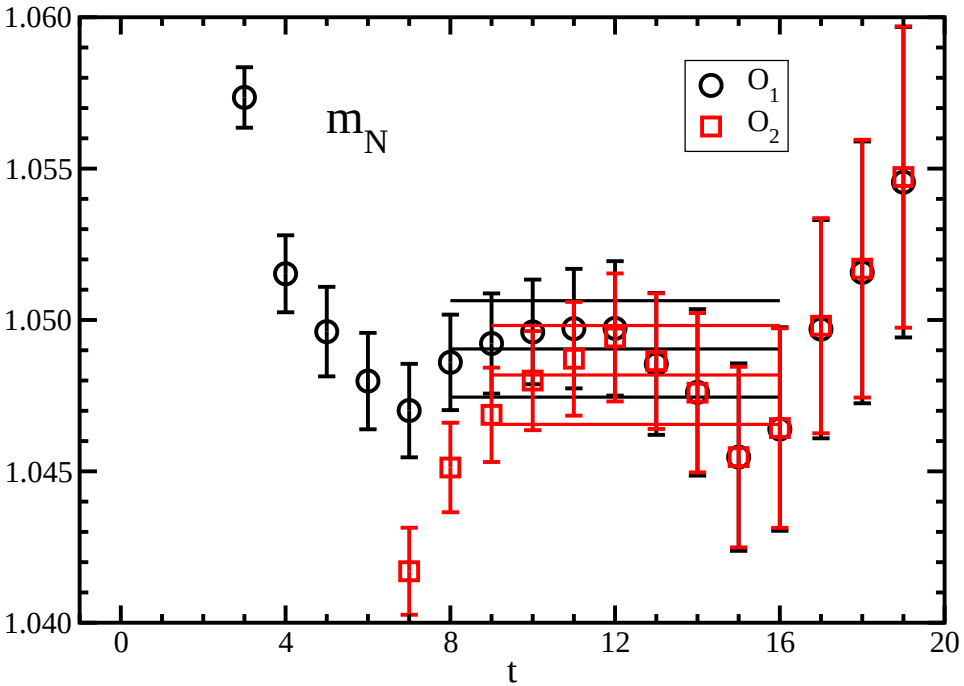

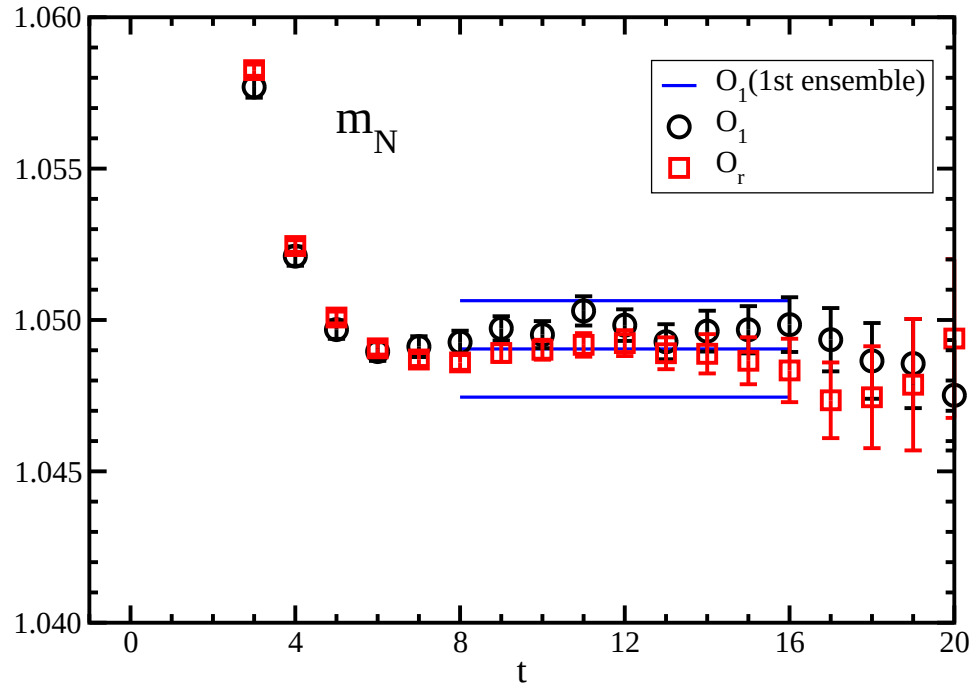

Effective energy before and after diagonalization $L = 48$

$$E_{ij}(t) = \log\left(\frac{G_{ij}(t)}{G_{ij}(t+1)}\right)$$

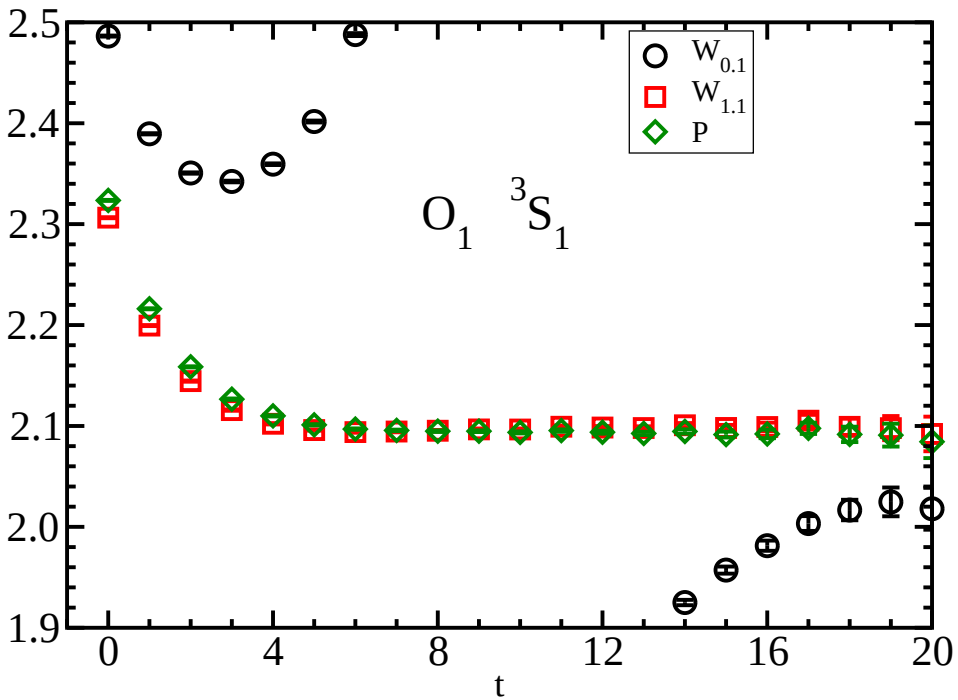

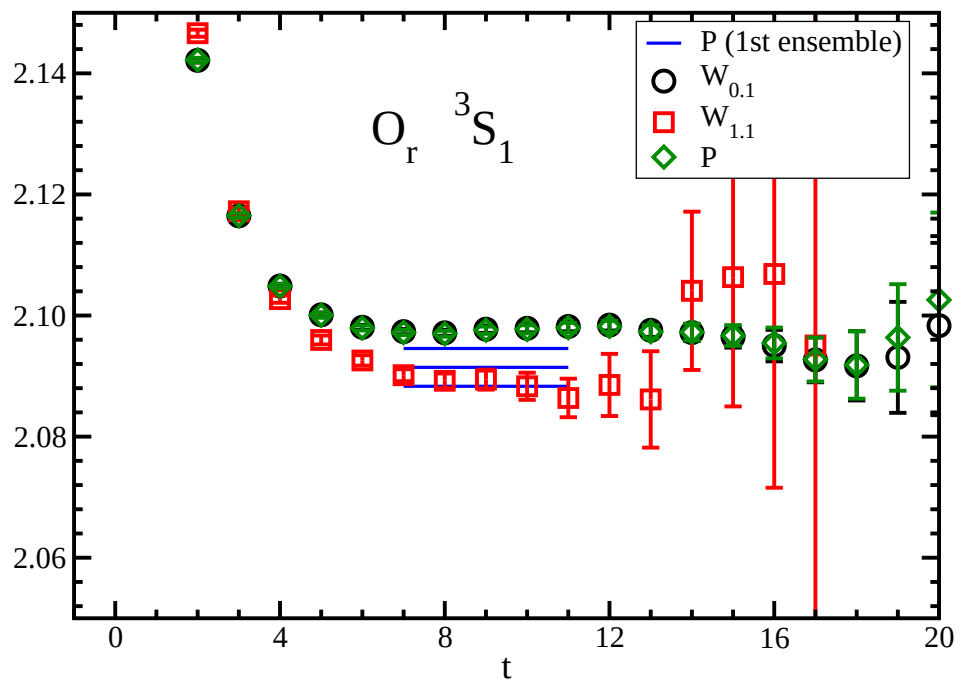

Effective energy before and after diagonalization $L = 32$

$$E_{ij}(t) = \log\left(\frac{G_{ij}(t)}{G_{ij}(t+1)}\right)$$

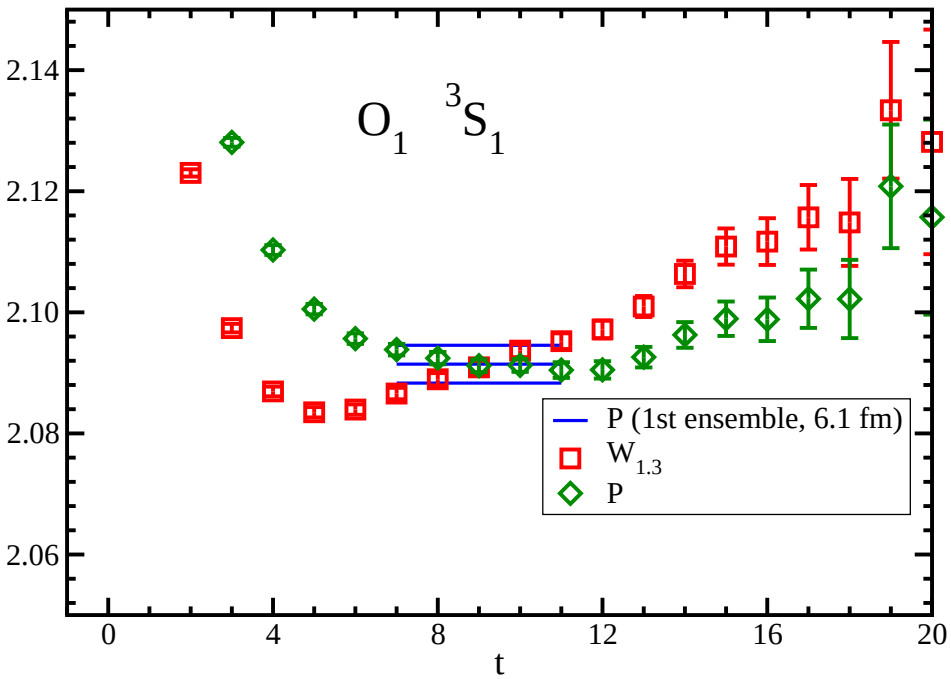

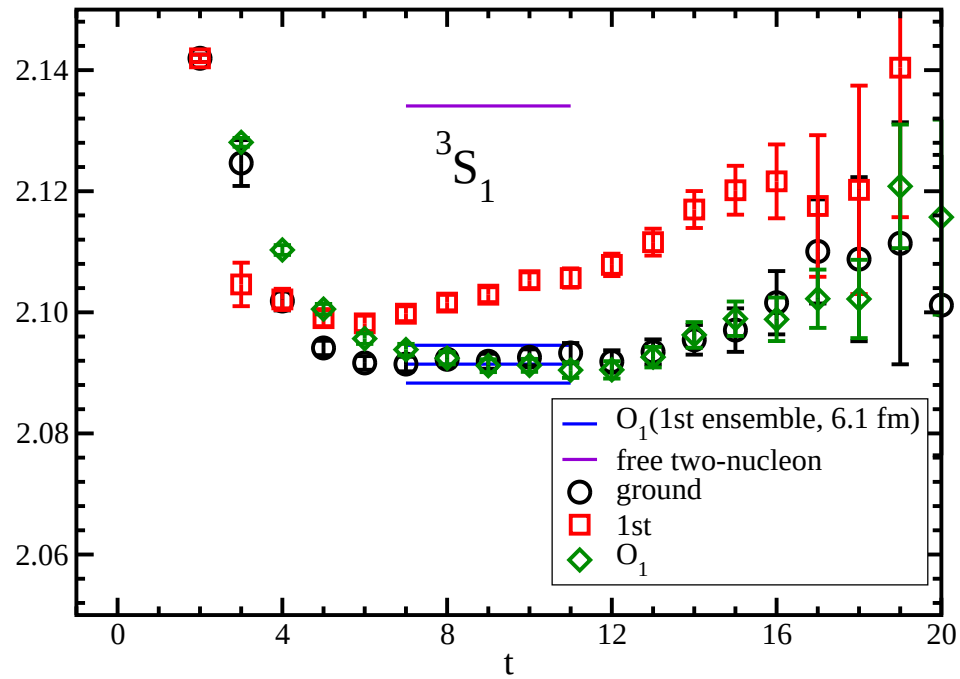

Effective energy shift $\Delta\overline{E}_{L,\alpha} = \overline{E}_\alpha - 2m_N$

for ground and 1st excited states of $^3S_1$ at $L = 48$

$$\Delta\overline{E}_{L,\alpha}(t) = \log\left(\frac{\overline{R}_\alpha(t)}{\overline{R}_\alpha(t+1)}\right), \quad \overline{R}_\alpha(t) = \frac{\lambda_\alpha(t)}{(C_N(t))^2}$$

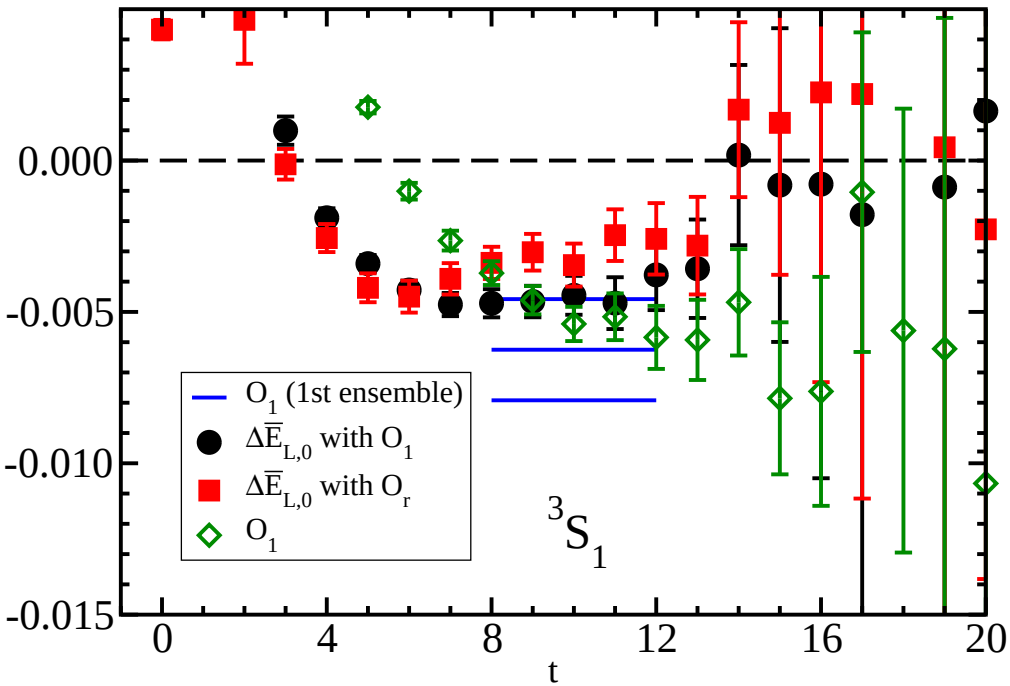

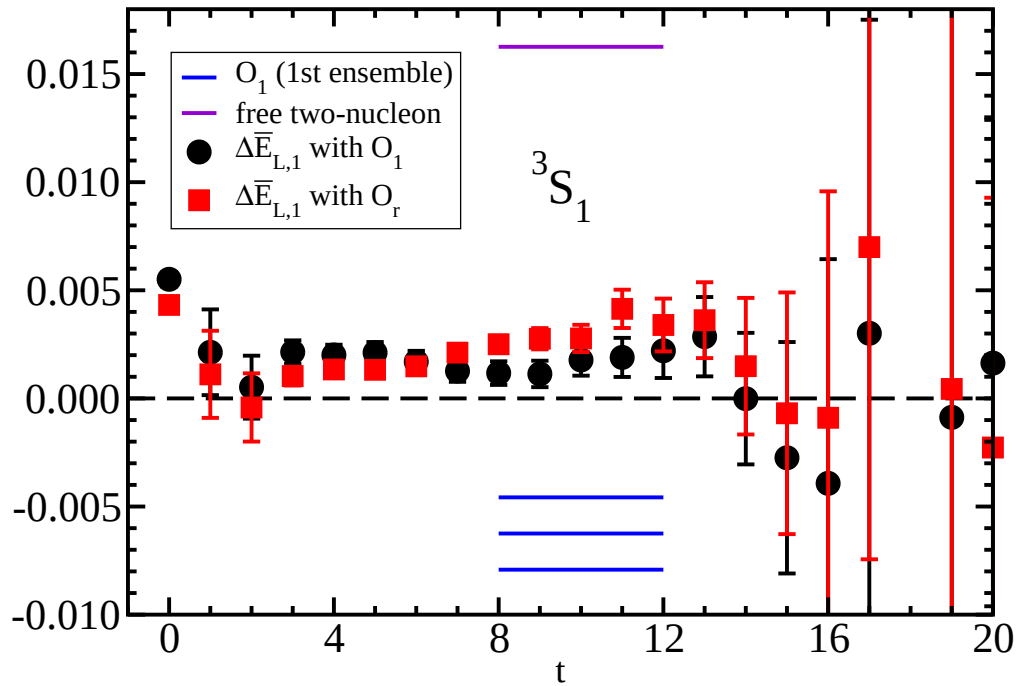

Effective energy shift $\Delta\overline{E}_{L,\alpha} = \overline{E}_\alpha - 2m_N$

for ground and 1st excited states of $^1S_0$ at $L = 48$

$$\Delta\overline{E}_{L,\alpha}(t) = \log\left(\frac{\overline{R}_\alpha(t)}{\overline{R}_\alpha(t+1)}\right), \quad \overline{R}_\alpha(t) = \frac{\lambda_\alpha(t)}{(C_N(t))^2}$$

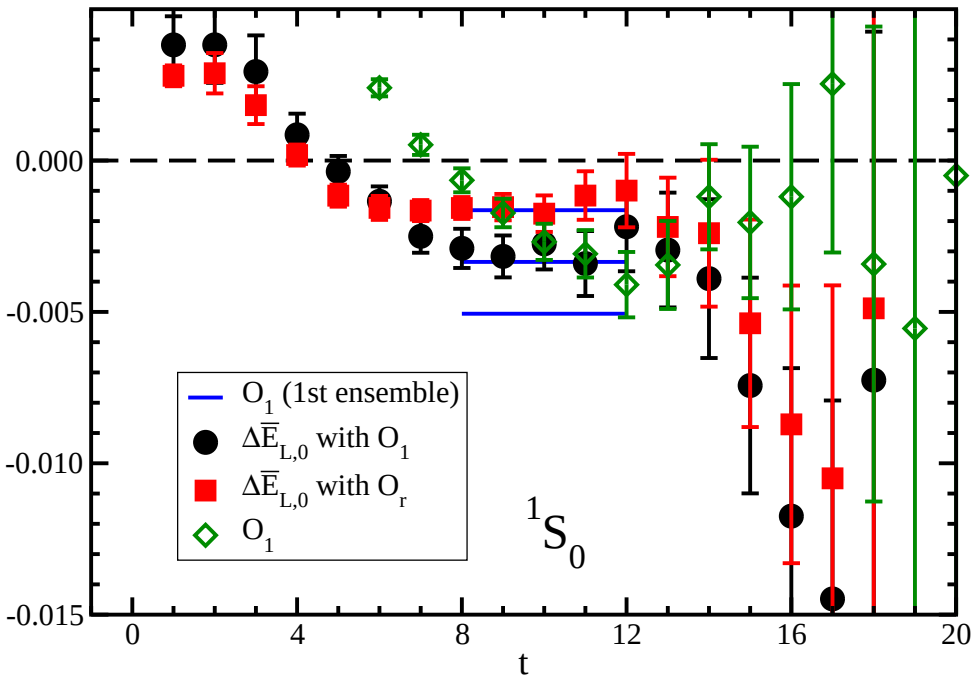

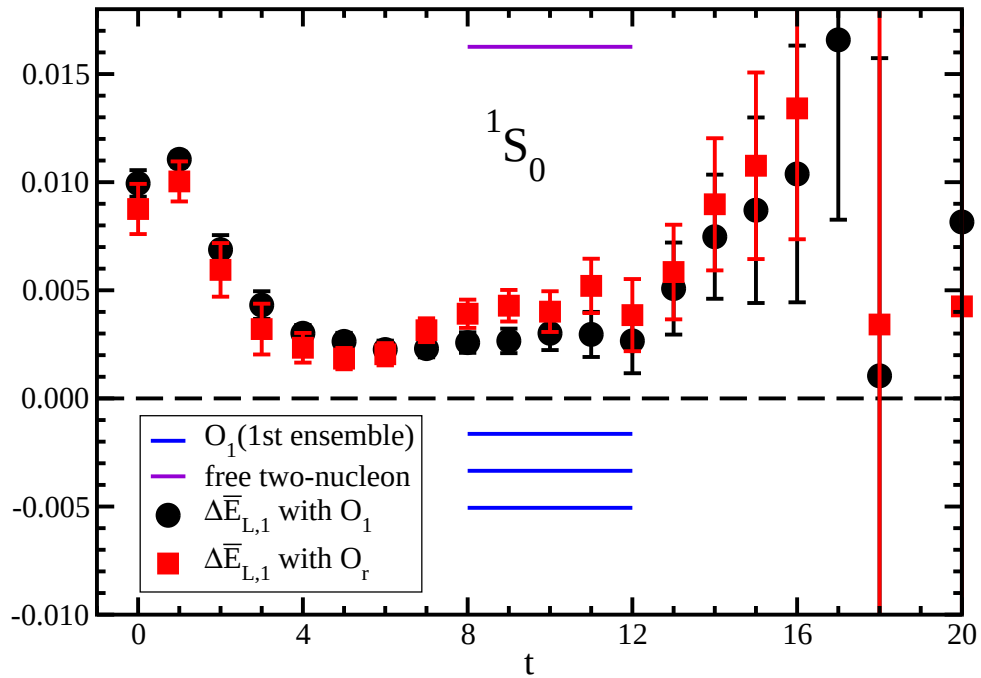

3. Results (cont'd)

2. Two-state analysis

Volume dependence of ΔE_L and $\Delta \overline{E}_{L,0}$

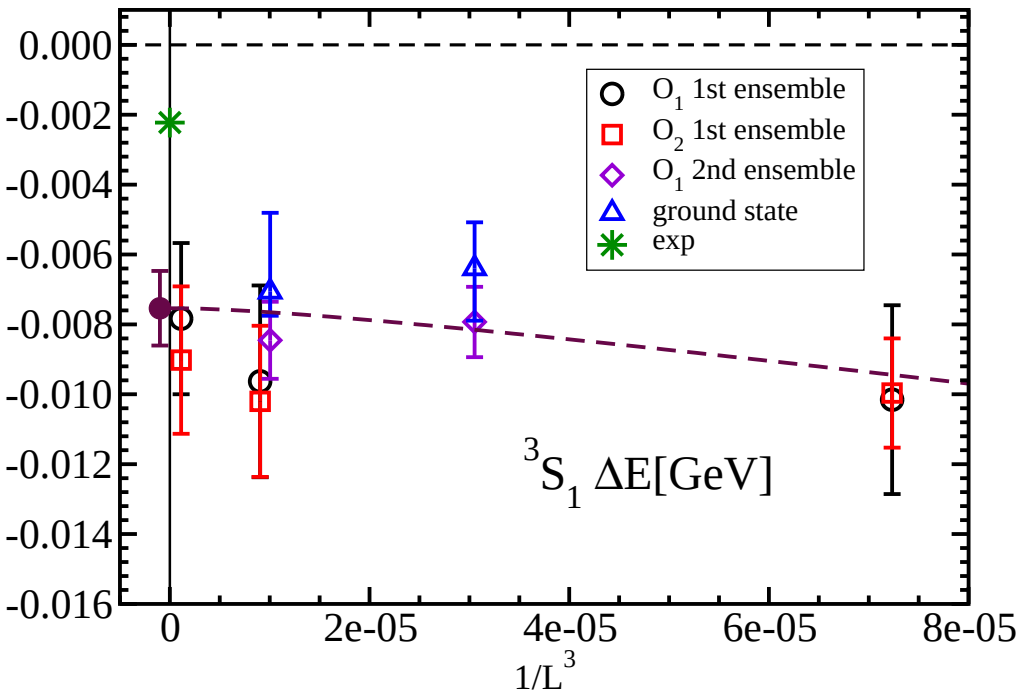

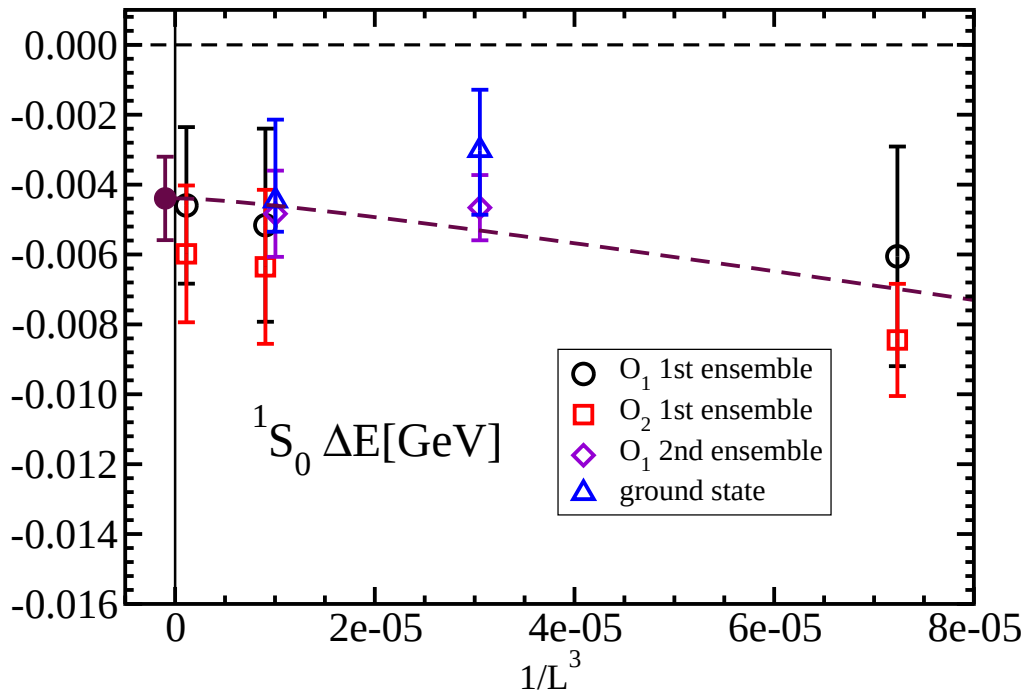

$\Delta E_{^3S_1} = 7.5(0.5)(0.9)$ MeV $\qquad$ $\Delta E_{^1S_0} = 4.4(0.6)(1.0)$ MeV

$^3S_1$: almost four times larger than experimental values

$^1S_0$: bound state exists different from experiment

mainly caused by heavy quark mass in calculation, probably

Future work quark mass dependence

Assume: our results smoothly continue to physical one

Quark mass $\searrow$

$^3S_1$: $\Delta E \searrow$ and $|a_0| \nearrow$

$^1S_0$: $\Delta E \searrow$ and $|a_0| \nearrow$

$\rightarrow$ bound state vanishes, $|a_0| = \infty$ and $\mathrm{sign}(a_0) = +$

$\rightarrow a_0 \searrow$

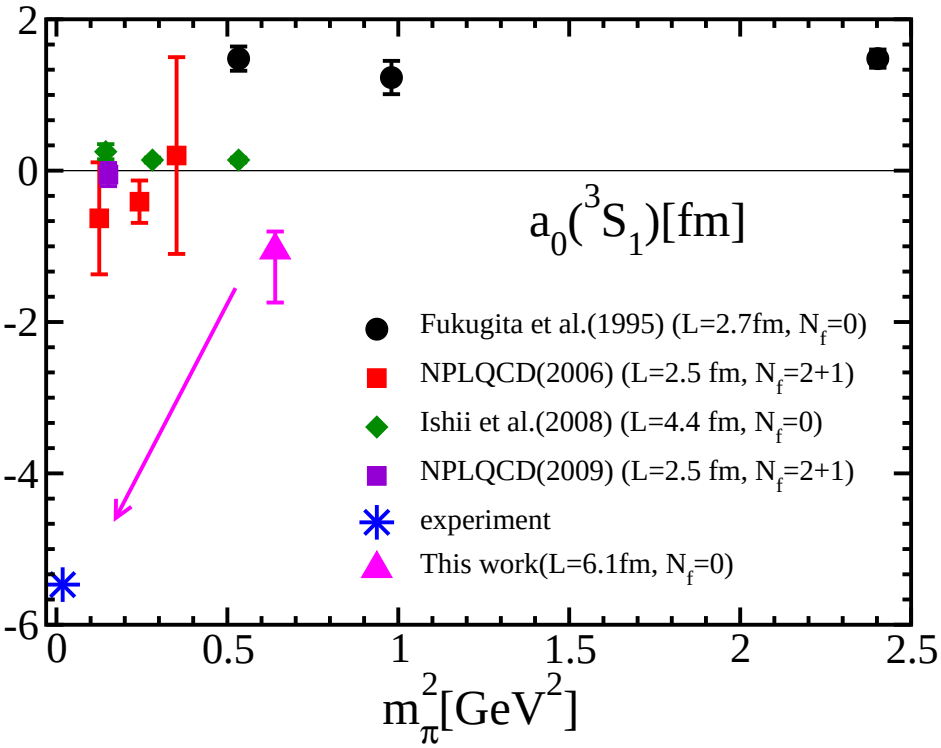

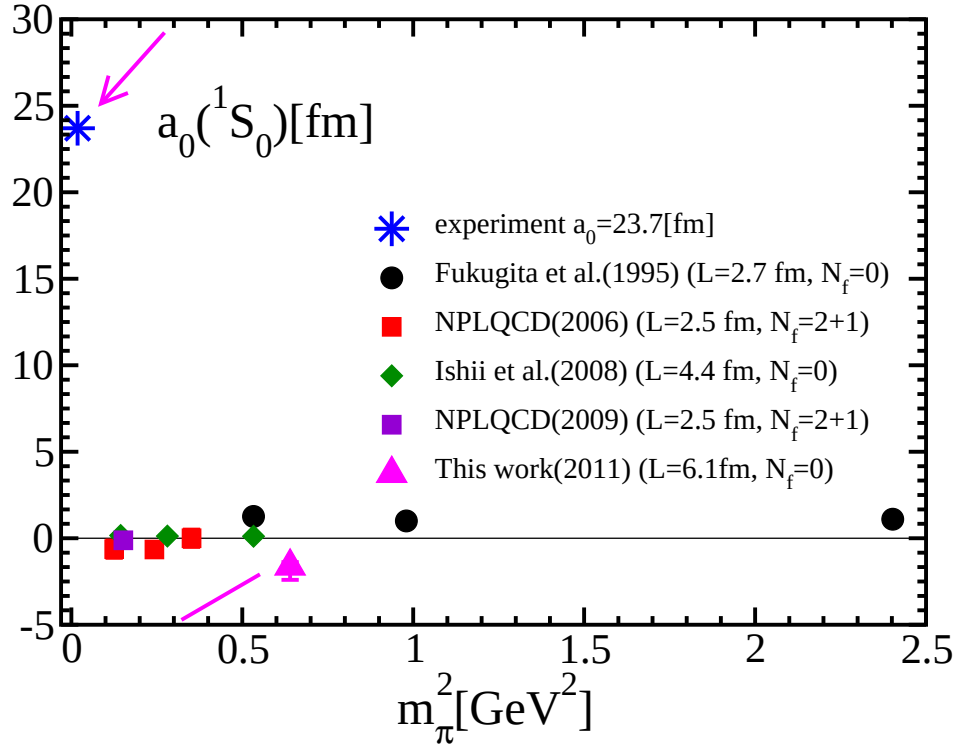

Certainly need to study quark mass dependence

3. Simulation parameters

- Quenched Iwasaki gauge action at $\beta = 2.416$

  $a^{-1} = 1.54$ GeV with $r_0 = 0.49$ fm
- Tad-pole improved Wilson fermion action

  $m_\pi = 0.8$ GeV and $m_N = 1.62$ GeV

  reduce large statistical fluctuation

1. Single state analysis

- Three volumes

L	L [fm]	N_{conf}	N_{meas}
24	3.1	2500	2
48	6.1	400	12
96	12.3	200	12

- Exponential smearing sources $q(\vec{x}) = A\ \exp(-B|\vec{x}|)$

  O_1 O_2

  $(A, B) = (0.5, 0.5),\ (0.5,\ 0.1)$ for $L = 24$

  $(A, B) = (0.5, 0.5),\ (1.0,\ 0.4)$ for $L = 48, 96$
- quark operator with non-relativistic projection in nucleon operator

3. Simulation parameters

2. Two-state analysis with 2×2 diagonalization

- Two volumes

L	L [fm]	N_{conf}	N_{meas}	N_r	q_1^2	q_2^2
32	4.1	300	192	40	0.184	1.3
48	6.1	300	144	32	0.1	1.1

- Exponential smearing sources $q(\vec{x}) = A \exp(-B|\vec{x}|)$

  O_1: $(A, B) = (0.5, 0.5)$

  O_r: spread random source with $(A, B) = (0.5, 0.5)$

- Two Wavefunction smearing sinks $N(\mathbf{x}) W_{q^2}(|\mathbf{x} - \mathbf{y}|) N(\mathbf{y})$

  $W_{q^2}(|\mathbf{r}|)$: Based on solution of 3-dimension Helmholtz equation

  parameters: q^2 and overall normalization

- quark operator with non-relativistic projection in nucleon operator

Simulations:

PACS-CS, T2K-Tsukuba at Univ. of Tsukuba

HA8000 at Univ. of Tokyo

4. Results

1. Single state analysis

Effective two-nucleon energy at $L = 6.1$ fm

$$E_{\mathrm{NN}}(t) = \log\left(\frac{C_{\mathrm{NN}}(t)}{C_{\mathrm{NN}}(t+1)}\right)$$

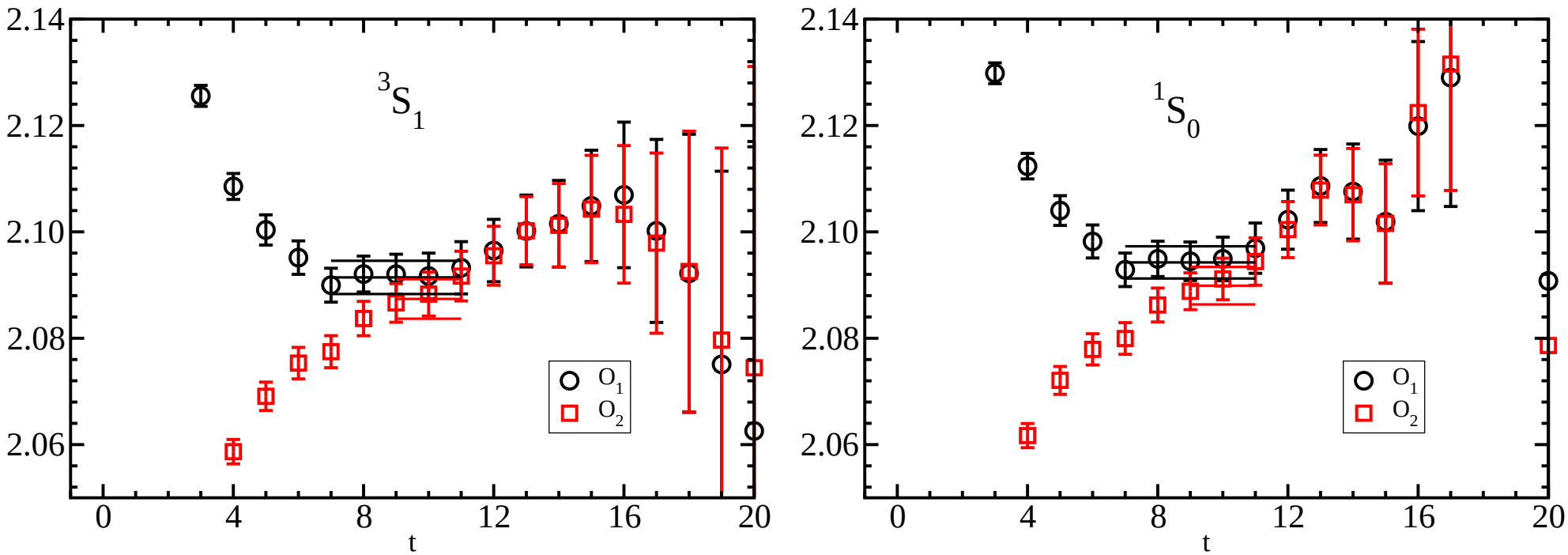

- Clear signal in $t < 12$, but larger error in $t \geq 11$
- consistent plateaus in $8 \lesssim t \leq 11$

2. Two-state analysis

Effective two-nucleon energy after diagonalization at $L = 6.1$ fm

$$\overline{E}_\alpha(t) = \log\left(\frac{\lambda_\alpha(t)}{\lambda_\alpha(t+1)}\right), \quad \text{Diag}\left[G^{-1}(t_0)G(t)\right] = \lambda(t) \text{ with } t_0 = 6$$

$$G_{ij}(t) = \langle 0|O_i(t)O_j(0)|0\rangle$$

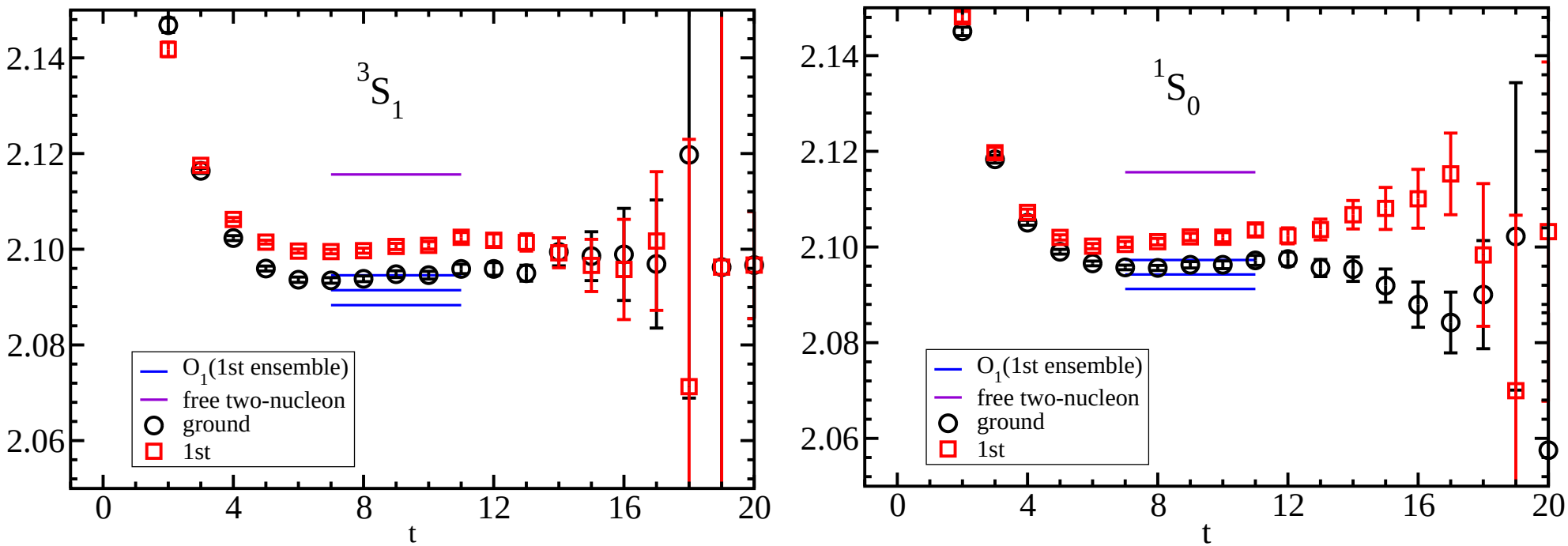

- Close two states, but clearly split
- ground state agree with one in single state analysis
- 1st excited state below free state $2\sqrt{M_N^2 + (2\pi/L)^2}$

4. Results

1. Single state analysis

Effective energy shift $\Delta E_L = E_{\mathrm{NN}} - 2m_N$ at $L = 6.1$ fm

$$\Delta E_L = \log\left(\frac{R(t)}{R(t+1)}\right), \quad R(t) = \frac{C_{\mathrm{NN}}(t)}{(C_N(t))^2}$$

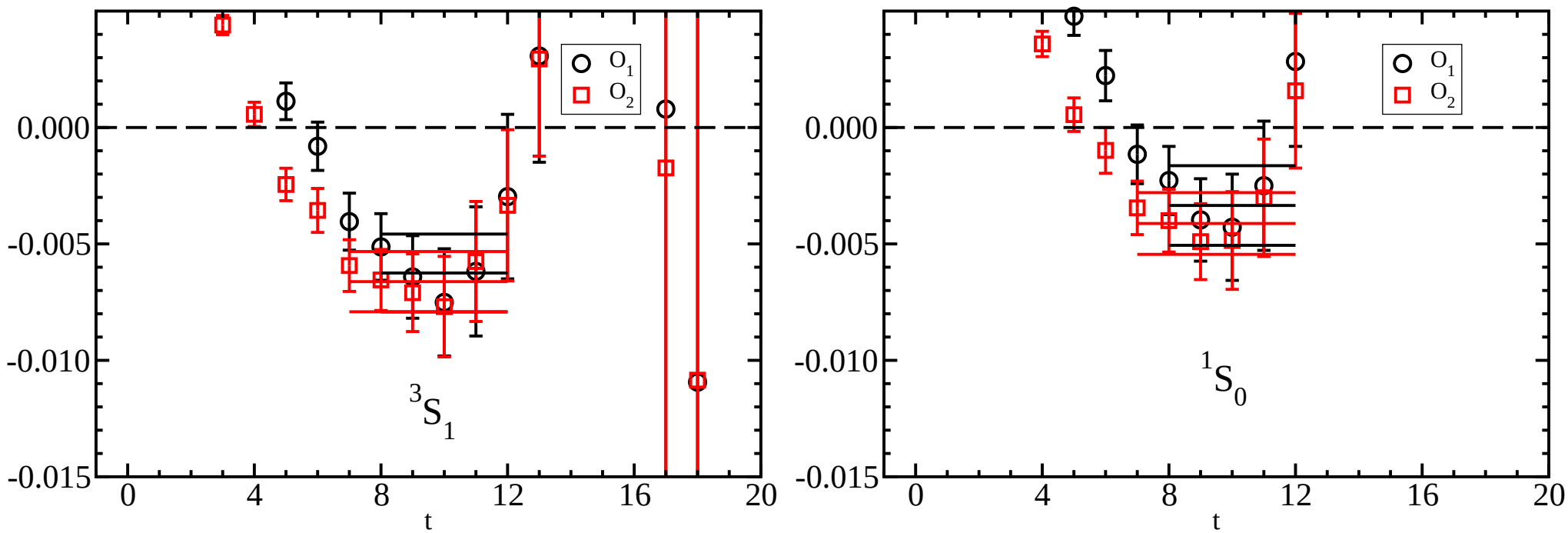

- $\Delta E_L < 0$ in $8 \lesssim t \leq 11$
- consistent plateaus in $8 \lesssim t \leq 11$

Existence of bound state for a_0

System	w/ bound state	w/o bound state
0th	bound state	scattering state
1st	scattering state	scattering state
a_0	< 0 from 1st	> 0 from 0th

Bound state exists $\rightarrow$ a_0 never obtained from 0th state

by Lüscher's finite volume method

$$\Delta E_L = E^0_{NN} - 2m_N = -\frac{4\pi a_0}{m_N L^3} + \cdots$$ ('86, '91 Lüsher)

Need to check existence of bound state to calculate a_0

Two properties in w/ bound state system

1. 0th state energy
2. a_0 (1st state energy)

2. 1st excited state energy

Effective energy shift for ground and 1st excited states at $L = 6.1$ fm

$$\text{Diag}\left[G^{-1}(t_0)G(t)\right] = \lambda(t) \text{ with } G_{ij}(t) = \langle 0|O_i(t)O_j(0)|0\rangle$$

$$\Delta\overline{E}_{L,\alpha} = E_\alpha - 2m_N = \log\left(\frac{\overline{R}_\alpha(t)}{\overline{R}_\alpha(t+1)}\right), \quad \overline{R}_\alpha(t) = \frac{\lambda_\alpha(t)}{(C_N(t))^2}$$

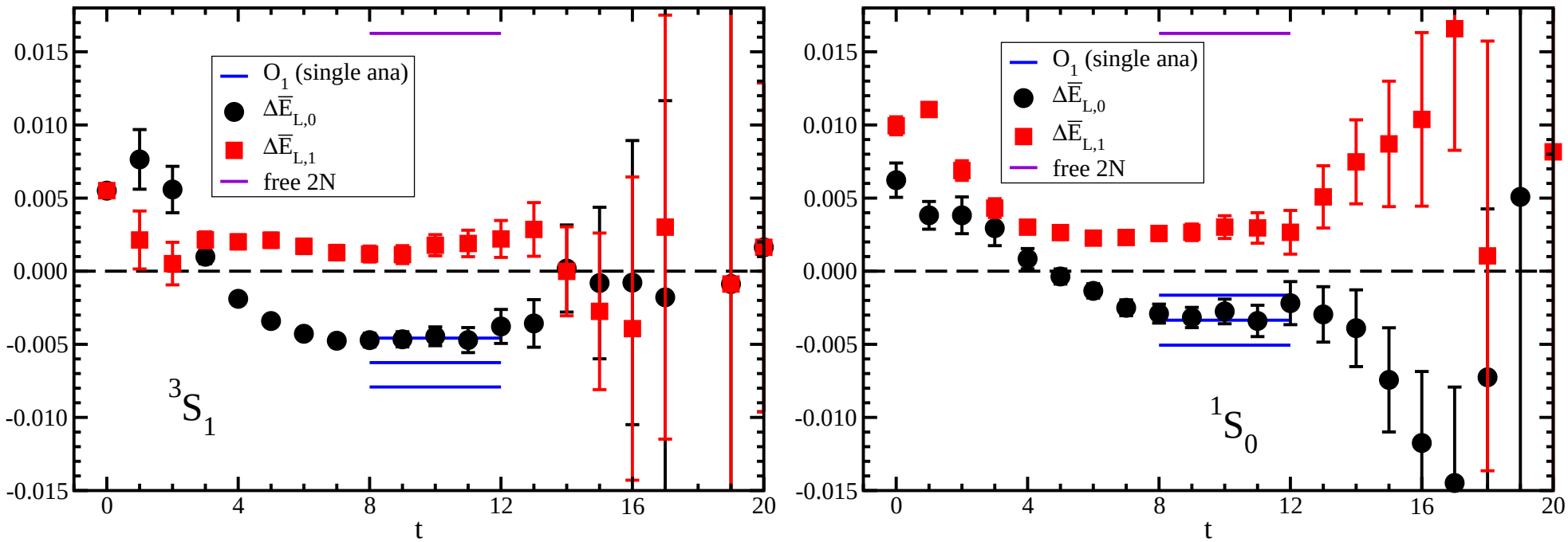

- $\Delta\overline{E}_{L,0} < 0$ and consistent with ΔE_L
- small, but $\Delta\overline{E}_{L,1} > 0$ as expected

Exploratory study of three- and four-nucleon systems

PACS-CS Collaboration, PRD81:111504(R)(2010)

Traditional method for example ^{4}He channel

$$\langle 0|O_{^4\mathrm{He}}(t)O^\dagger_{^4\mathrm{He}}(0)|0\rangle = \sum_n \langle 0|O_{^4\mathrm{He}}|n\rangle\langle n|O^\dagger_{^4\mathrm{He}}|0\rangle e^{-E_n t} \xrightarrow[t\gg 1]{} A_0\, e^{-E_0 t}$$

Difficulties for multi-nucleon calculation

1. Statistical error

Statistical error $\propto \exp\left(N_N\left[m_N - \frac{3}{2}m_\pi\right]t\right)$

2. Calculation cost

Wick contraction for ^{4}He $= p^2n^2 = (udu)^2(dud)^2$: 518400

3. Identification of bound state on finite volume

Finite volume effect in energy E_0

Exploratory study of three- and four-nucleon systems

PACS-CS Collaboration, PRD81:111504(R)(2010)

Traditional method for example ^{4}He channel

$$\langle 0|O_{^4\mathrm{He}}(t)O^\dagger_{^4\mathrm{He}}(0)|0\rangle = \sum_n \langle 0|O_{^4\mathrm{He}}|n\rangle\langle n|O^\dagger_{^4\mathrm{He}}|0\rangle e^{-E_n t} \xrightarrow[t\gg 1]{} A_0\, e^{-E_0 t}$$

Difficulties for multi-nucleon calculation

1. Statistical error

Statistical error $\propto \exp\left(N_N\left[m_N - \frac{3}{2}m_\pi\right]t\right)$

$\rightarrow$ heavy quark mass corresponding to $m_\pi = 0.8$ GeV

c.f. physical pion mass $m_\pi = 0.135$ GeV

2. Calculation cost

Wick contraction for ^{4}He $= p^2n^2 = (udu)^2(dud)^2$: 518400

$\rightarrow$ 1107 using symmetries

$p \leftrightarrow p$, $n \leftrightarrow n$, $p \leftrightarrow n$, $u(d) \leftrightarrow u(d)$ in $p(n)$

3. Identification of bound state on finite volume

Finite volume effect in energy E_0

$\rightarrow$ Finite volume dependence of $\Delta E = E_0 - N_N m_N$

1. Introduction

Hadron spectrum from $N_f = 2 + 1$ QCD

'09 PACS-CS Collaboration

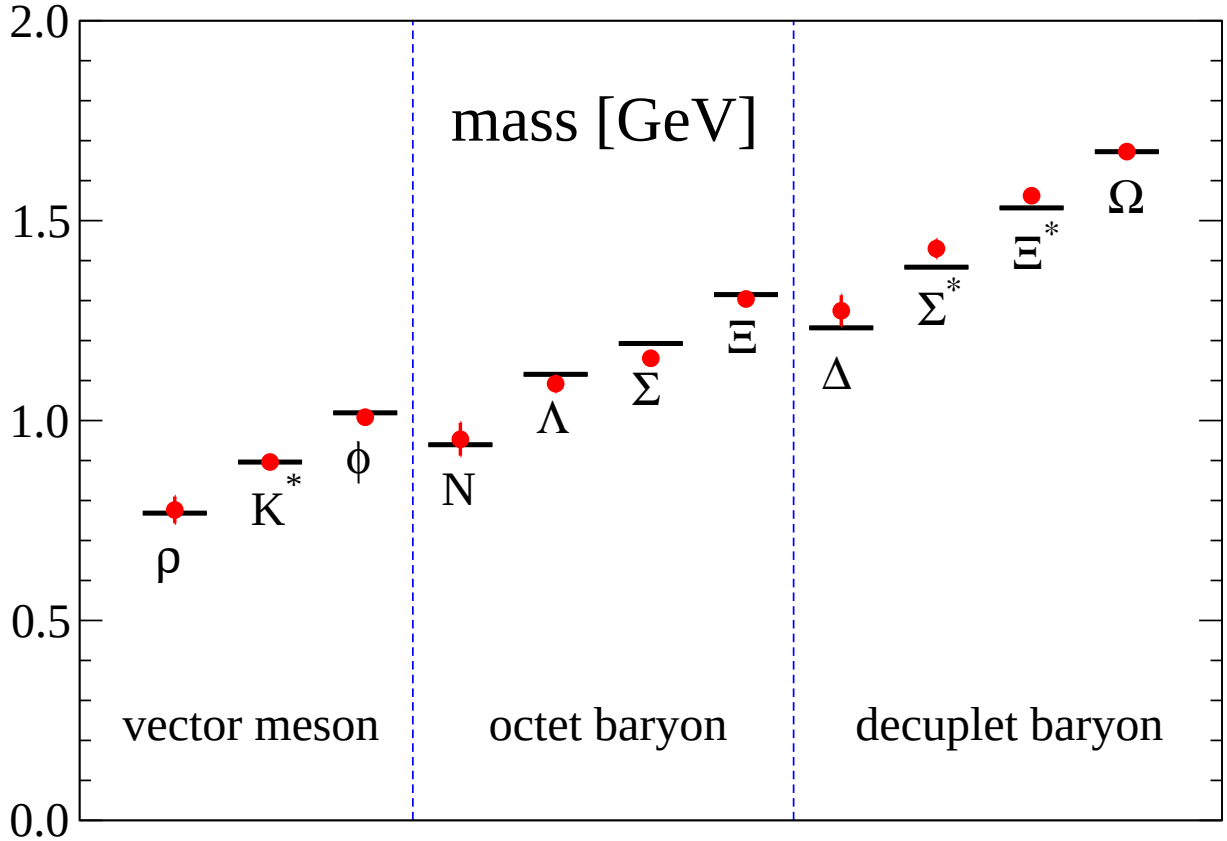

Input: m_π, m_K and m_Ω

Multi-baryon system from lattice QCD at '09

1. $\Lambda\Lambda$ system (Quenched QCD)

'85 Mackenzie & Thacker
'88 Iwasaki *et al.*
'99 Pochinsky *et al.*
'00 Wetzorke *et al.*
'02 Wetzorke & Karsch
'09 NPLQCD ($N_f = 2 + 1$)

H dibaryon: unbound

2. NN system $^3S_1$ and $^1S_0$

'95 Fukugita *et al.* : Quenched QCD

'06 NPLQCD : $N_f = 2 + 1$ QCD

'08 Ishii *et al.* : Quenched and $N_f = 2 + 1$ QCD

'09 NPLQCD : $N_f = 2 + 1$ QCD

Deuteron: unbound due to $m_\pi \gtrsim 0.3$ GeV

3. NNN system

'09 NPLQCD : $N_f = 2 + 1$ QCD

Triton: likely unbound

1. Statistical error

$$C_4(t) = \langle 0|O_{^4\mathrm{He}}(t)\overline{O}_{^4\mathrm{He}}|0\rangle \xrightarrow[t\gg 1]{} A_0\, e^{-E_0 t}$$

Rough estimate of noise-to-signal ratio for N_N-nucleon channel

$$\frac{\delta C_{N_N}(t)}{C_{N_N}(t)} \propto \frac{1}{\sqrt{N_{\mathrm{meas}}}} \exp\left(N_N\left[m_N - \frac{3}{2}m_\pi\right]t\right)$$

m_π: proportional to (quark mass)$^{1/2}$

$$\begin{array}{ccc} \text{quark mass} & \to & \text{small} \\ N_N & \to & \text{large} \\ N_{\mathrm{meas}} & \to & \text{small} \end{array} \Rightarrow \frac{\delta C_{N_N}(t)}{C_{N_N}(t)} \to \text{large} \Rightarrow \frac{\delta E_0}{E_0} \to \text{large}$$

Avoid large statistical fluctuation

- unphysically heavy quark mass $m_\pi = 0.8$ GeV and $m_N = 1.62$ GeV
- larger number of measurements than typical calculation

Lighter quark mass

$\to$ new method or much larger number of measurements

2. Calculation cost

$C_4(t) = \langle 0|O_{^4\mathrm{He}}(t)\overline{O}_{^4\mathrm{He}}(0)|0\rangle$ with $O_{^4\mathrm{He}} = p^2n^2 = [udu]^2[dud]^2$

Number of Wick contraction $N_u! \times N_d! = (2N_p + N_n)! \times (2N_n + N_p)!$

^{4}He: $6! \times 6! = 518400$

^{3}He: $5! \times 4! = 2880$

NN: $4! \times 2! = 48$

but contain identical contractions

Summation of $\sim$ (color and dirac)^{2N_N} in each contraction

Reduction of contractions

- Symmetries
  - $p \leftrightarrow p$, $n \leftrightarrow n$ in ^{4}He operator
  - Isospin all $p \leftrightarrow$ all n
- Calculate two contractions simultaneously
  - $u \leftrightarrow u$ in p or $d \leftrightarrow d$ in n

2. Calculation cost (cont'd)

$C_4(t) = \langle 0|O_{^4\mathrm{He}}(t)\overline{O}_{^4\mathrm{He}}(0)|0\rangle$ with $O_{^4\mathrm{He}} = p^2n^2 = [udu]^2[dud]^2$

Number of Wick contraction $N_u! \times N_d! = (2N_p + N_n)! \times (2N_n + N_p)!$

^{4}He: $6! \times 6! = 518400 \longrightarrow 1107$

^{3}He: $5! \times 4! = 2880 \longrightarrow 93$

Summation of $\sim$ (color and dirac)^{2N_N} in each contraction

Further reduction: avoid same calculations of dirac and color indices

Block of three quark propagators B_3

zero momentum nucleon operator in sink time slice

Blocks of two B_3

1, 2, 3 dirac contractions carried out

Multi-meson systems : '10 Detmold and Savage

Recursion relations: $R_{n+1} = \langle R_n \rangle \cdot R_1 - nR_n \cdot R_1$

Multi-baryon systems : '12 Doi and Endres

Unified contraction algorithm

3. Identification of bound state in finite volume

$$C_4(t) = \langle 0|O_{^4\mathrm{He}}(t)\overline{O}_{^4\mathrm{He}}|0\rangle \xrightarrow[t\gg 1]{} A_0\, e^{-E_0 t}$$

Observed state is whether bound state or not?

Example) Two-particle system

observe small $\Delta E = E - 2m < 0$ at single L

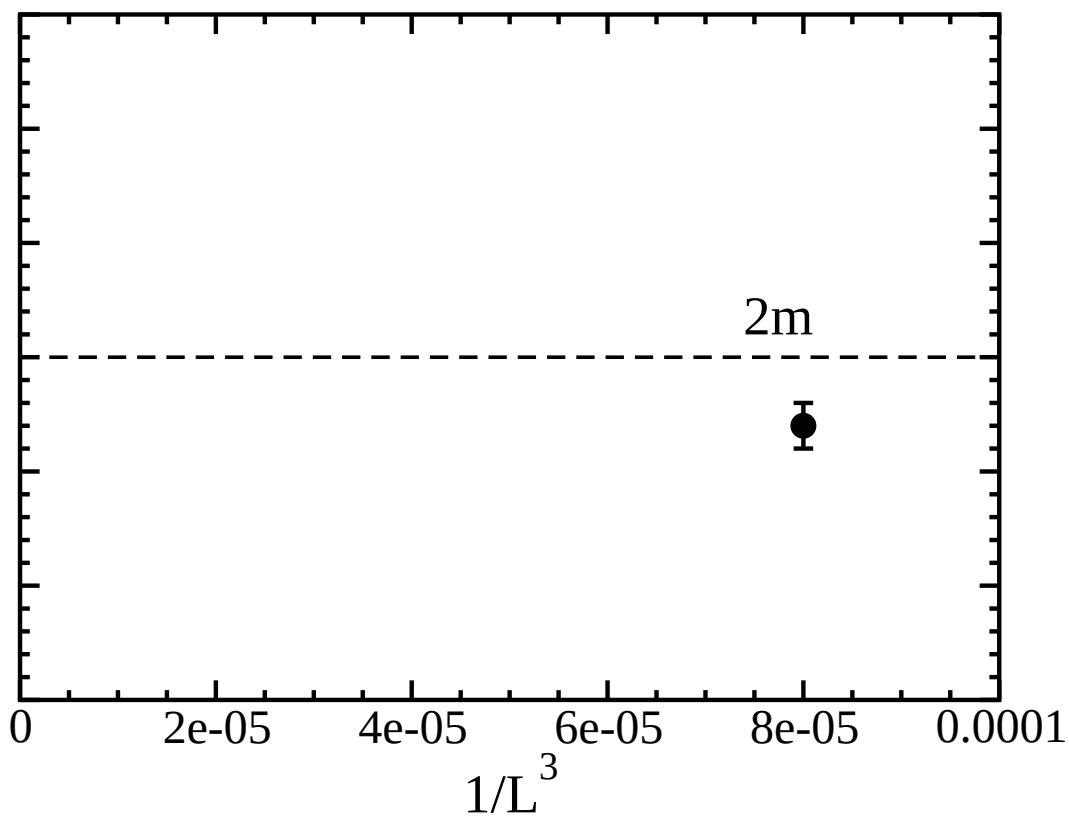

3. Identification of bound state in finite volume (cont'd)

Example) Two-particle system

observe small $\Delta E = E - 2m < 0$ at single L

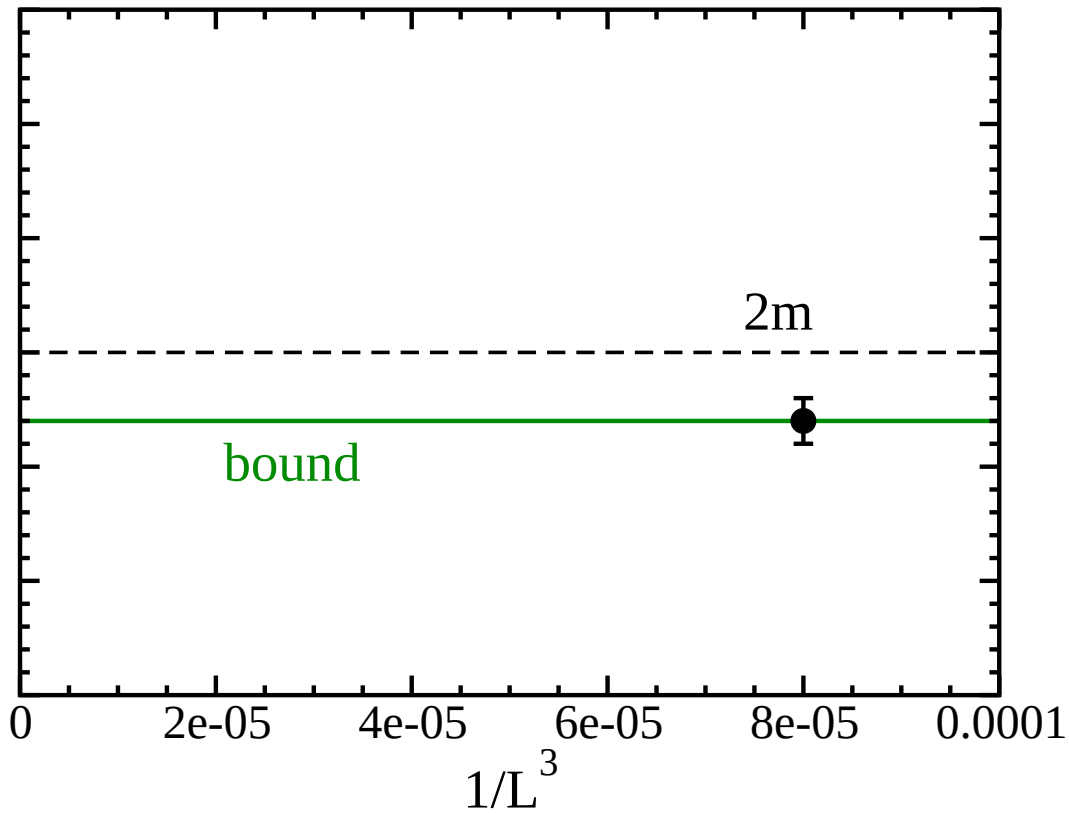

Bound state : $\Delta E = -\Delta E_{\text{bind}} + O(\mathrm{e}^{-\gamma L}) < 0$

Beane *et al.*, PLB585:106(2004), Sasaki & TY, PRD74:114507(2006)

3. Identification of bound state in finite volume (cont'd)

Example) Two-particle system

observe small $\Delta E = E - 2m < 0$ at single L

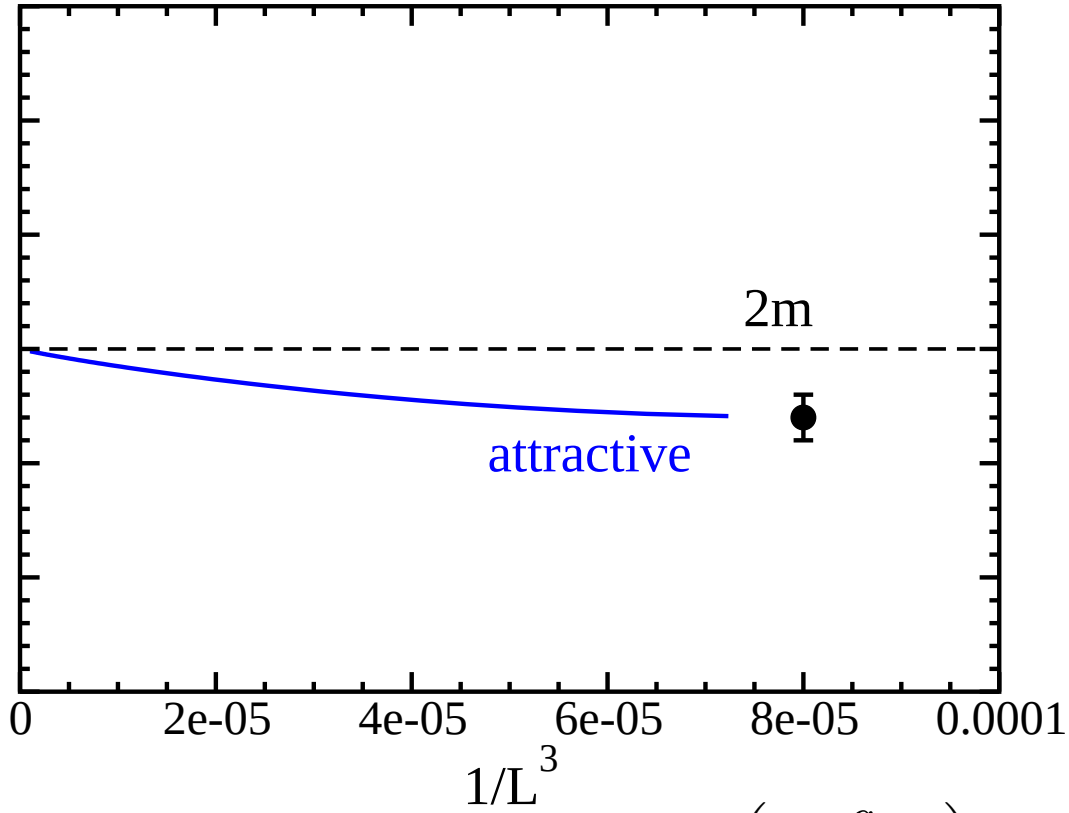

Attractive scattering state : $\Delta E = O\left(-\frac{a_0}{ML^3}\right) < 0 \quad (a_0 > 0)$

Lüscher, CMP105:153(1986), NPB354:531(1991)

c.f.) N-particle scattering state : $\Delta E = E_{\text{scat}} - Nm = O\left(-\frac{{}_N C_2\, a_0}{ML^3}\right)$

Beane *et al.*, PRD76:074507(2007)

3. Identification of bound state in finite volume (cont'd)

Example) Two-particle system

observe small $\Delta E = E - 2m < 0$ at single L

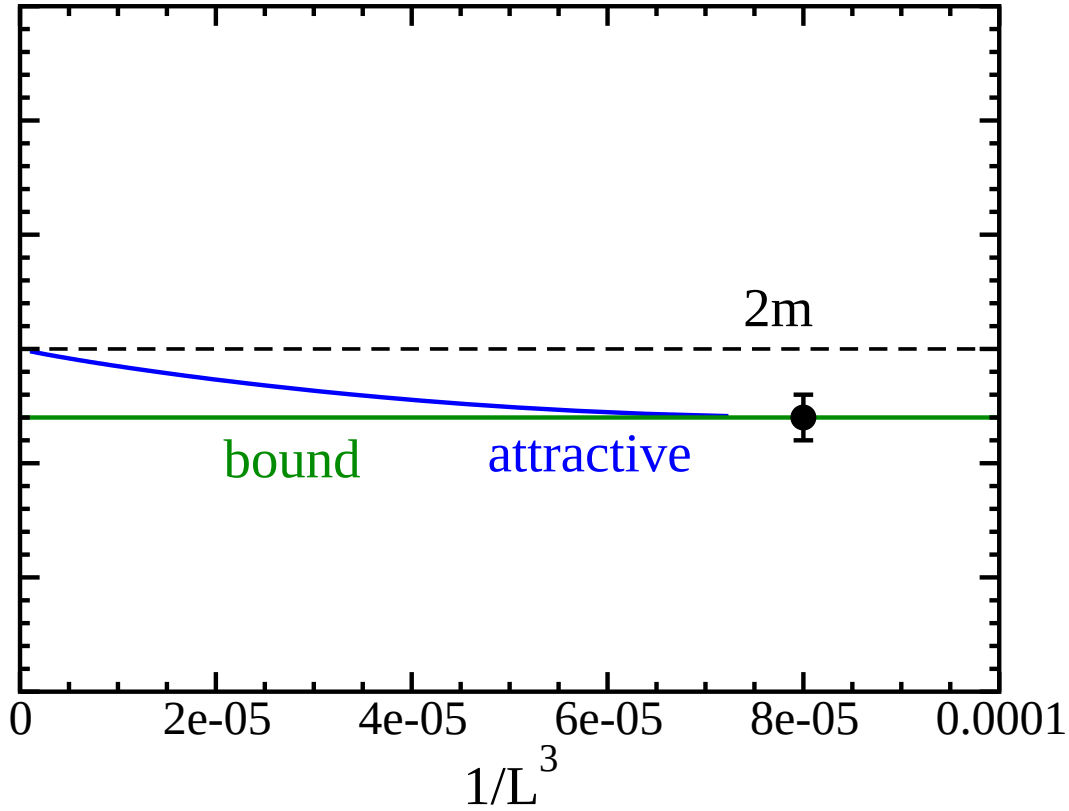

Hard to distinguish at single L

Bound state and Attractive scattering state

3. Identification of bound state in finite volume (cont'd)

Example) Two-particle system

observe small $\Delta E = E - 2m < 0$ at several L

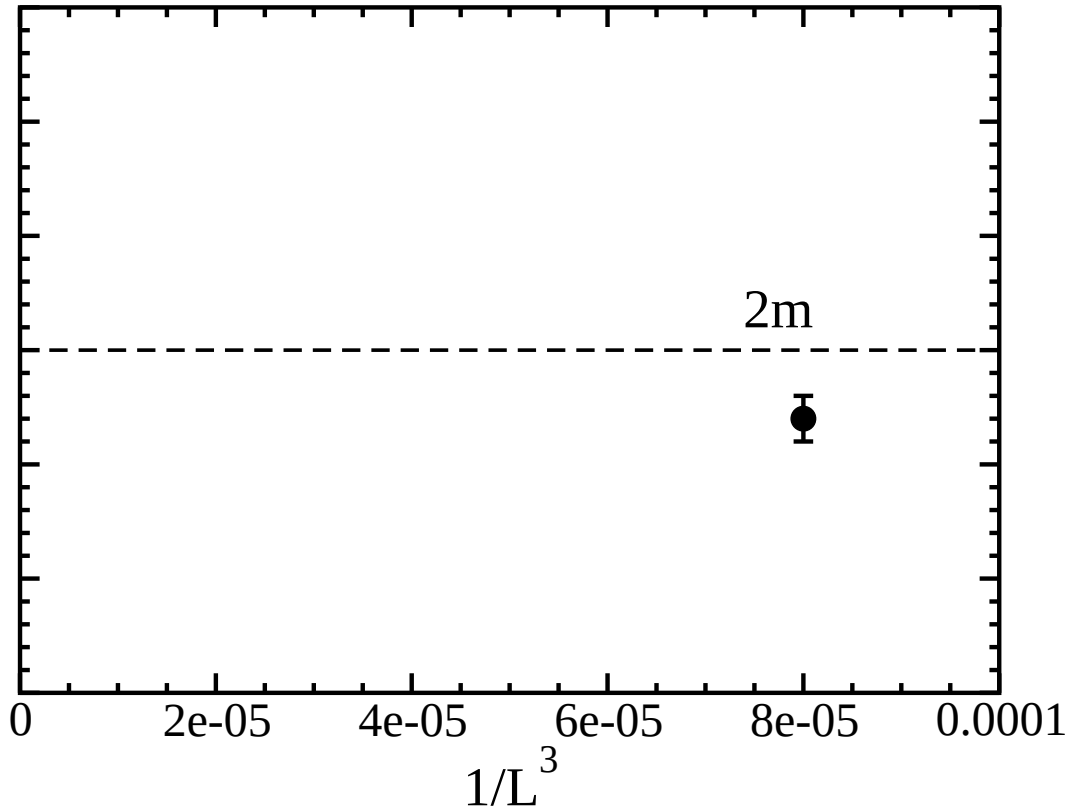

3. Identification of bound state in finite volume (cont'd)

Example) Two-particle system

observe small $\Delta E = E - 2m < 0$ at several L

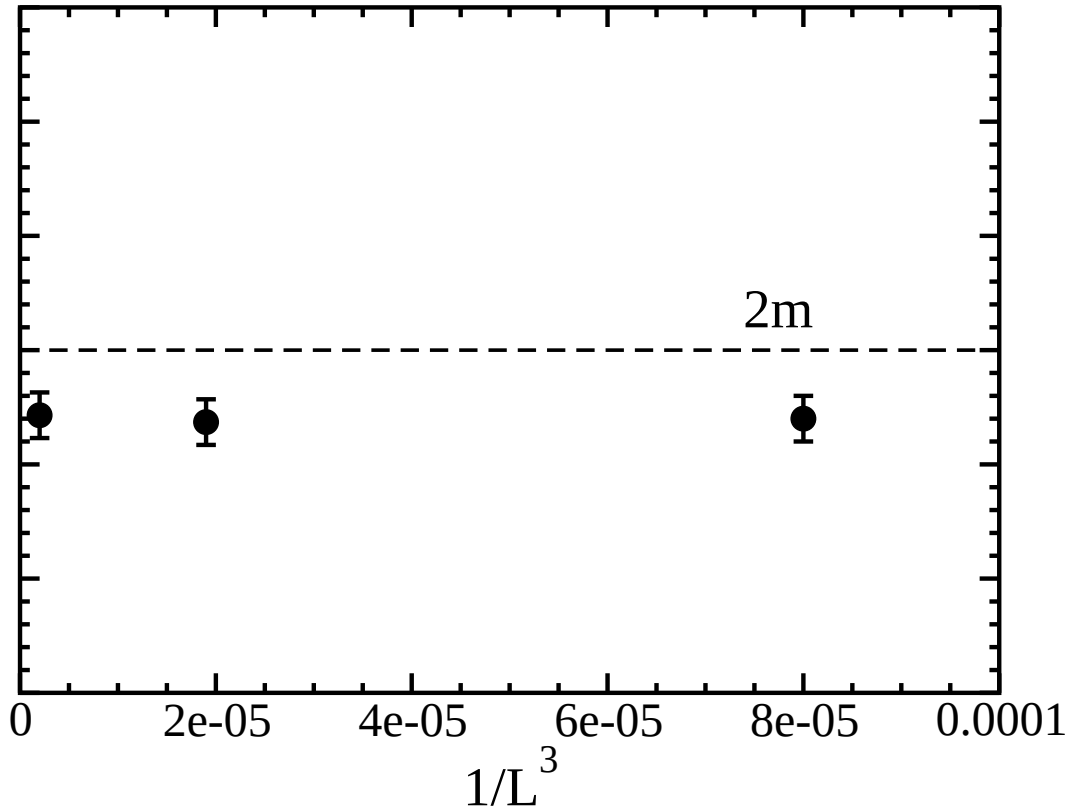

3. Identification of bound state in finite volume (cont'd)

Example) Two-particle system

observe small $\Delta E = E - 2m < 0$ at several L

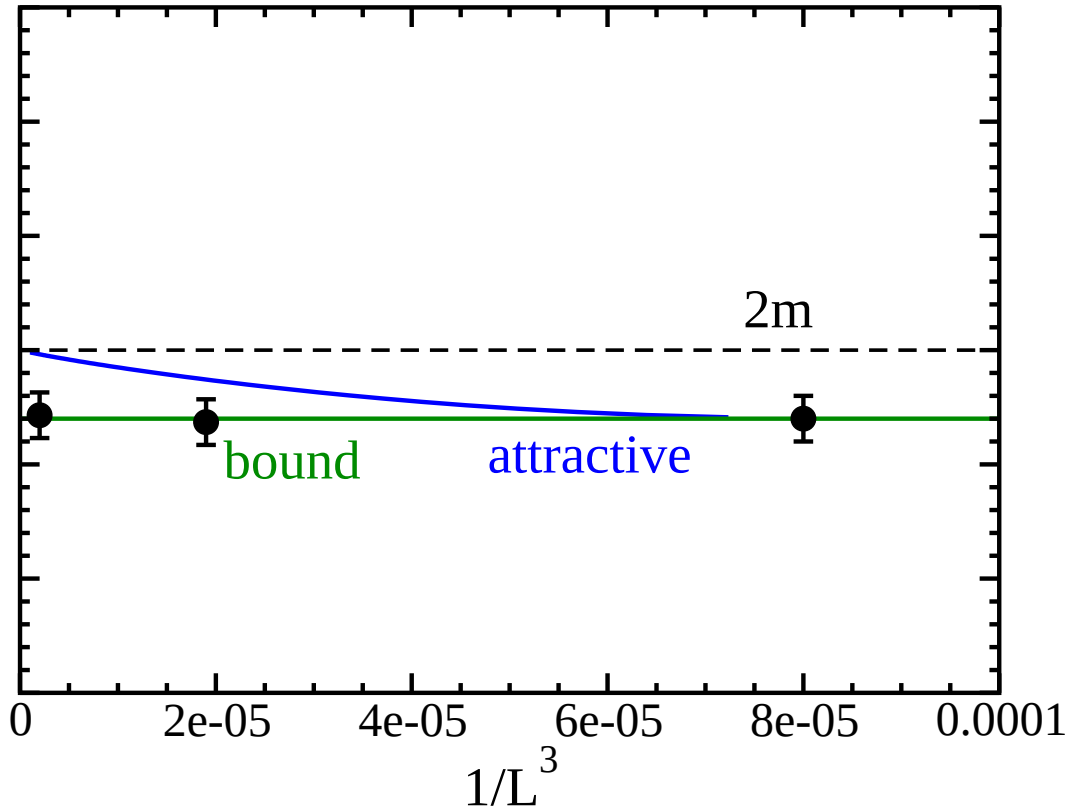

Identify bound state from volume dependence of ΔE

observe constant in infinite volume limit with $L = 3.1, 6.1, 12.3$ fm

Other methods: spectral weight: Mathur *et al.*, PRD70:074508(2004)

anti-periodic boundary.: Ishii *et al.*, PRD71:034001(2005)

2. Problems of multi-nucleon bound state

NN channels

1. Statistical error

   Not so severer than 3- and 4-nucleon channels

$$\frac{\delta C_{N_N}(t)}{C_{N_N}(t)} \propto \frac{1}{\sqrt{N_{\text{meas}}}} \exp\left(N_N \left[m_N - \frac{3}{2} m_\pi\right] t\right)$$

2. Calculation cost

   Not so severer than 3- and 4-nucleon channels

   # of contraction < 10 after reduction

3. Identification of bound state in finite volume

   Similar to 3- and 4-nucleon channels

Bound state in simplest multi-nucleon system, NN system?

Scattering length a_0 in NN system at '09

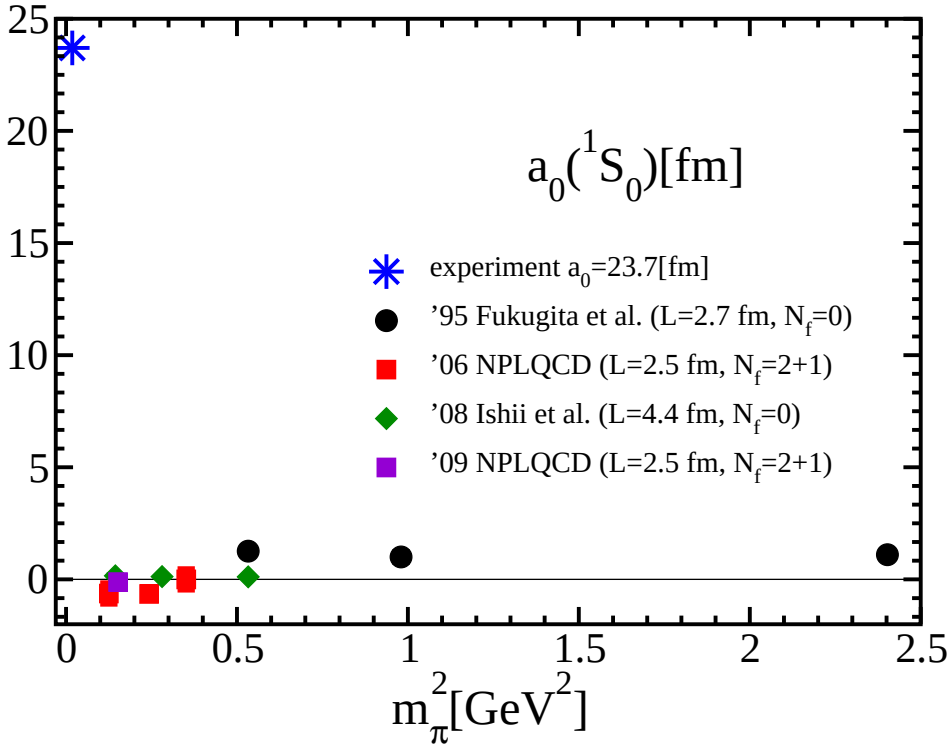

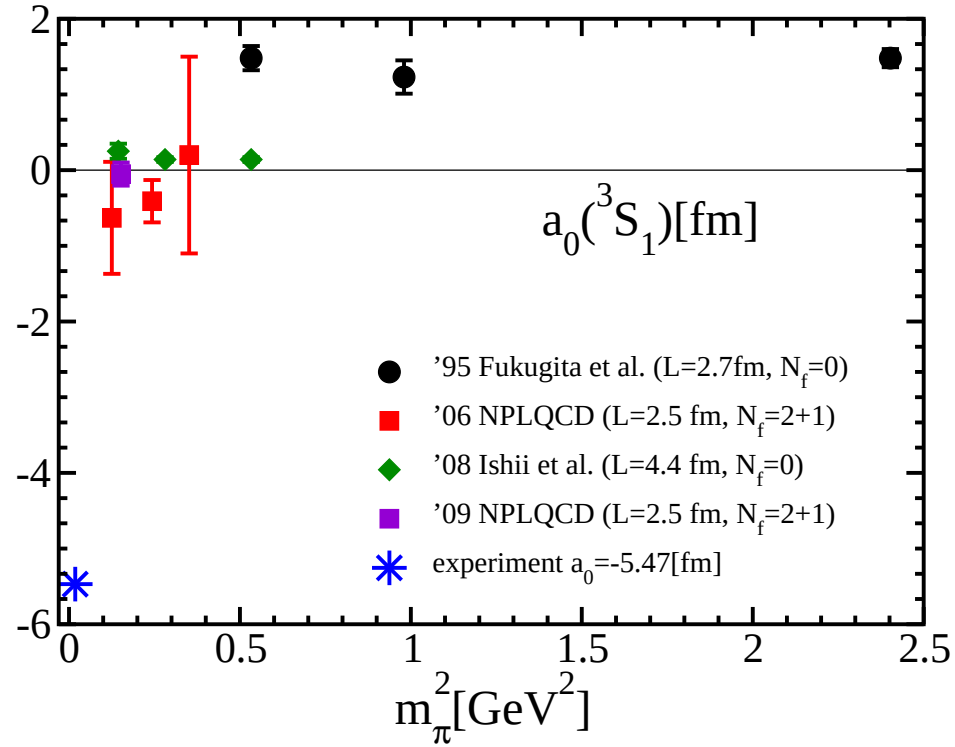

a_0: Far from experiments due to $m_\pi \gtrsim 0.3$ GeV

Assumption: Deuteron in $^3S_1$ channel unbound due to $m_\pi \gtrsim 0.3$ GeV

Aim of this work: check assumption by simpler method

c.f. using nuclear force '09 HALQCD

Existence of bound state for a_0

System	w/ bound state	w/o bound state
0th	bound state	scattering state
1st	scattering state	scattering state
a_0	< 0 from 1st	> 0 from 0th

Bound state exists $\rightarrow$ a_0 never obtained from 0th state

by Lüscher's finite volume method

$$\Delta E_L = E^0_{NN} - 2M = -\frac{4\pi a_0}{ML^3} + \cdots$$ ('86, '91 Lüsher)

Need to check existence of bound state to calculate a_0

Two methods

1. Volume dependence of 0th state
2. Properties of 1st state energy

Properties of 1st excited state energy in finite volume

'06 Sasaki & TY

bound state exists $\rightarrow$ 1st excited state = scattering state with $a_0 < 0$

$\rightarrow \Delta E_{L,1} > 0$ at finite L

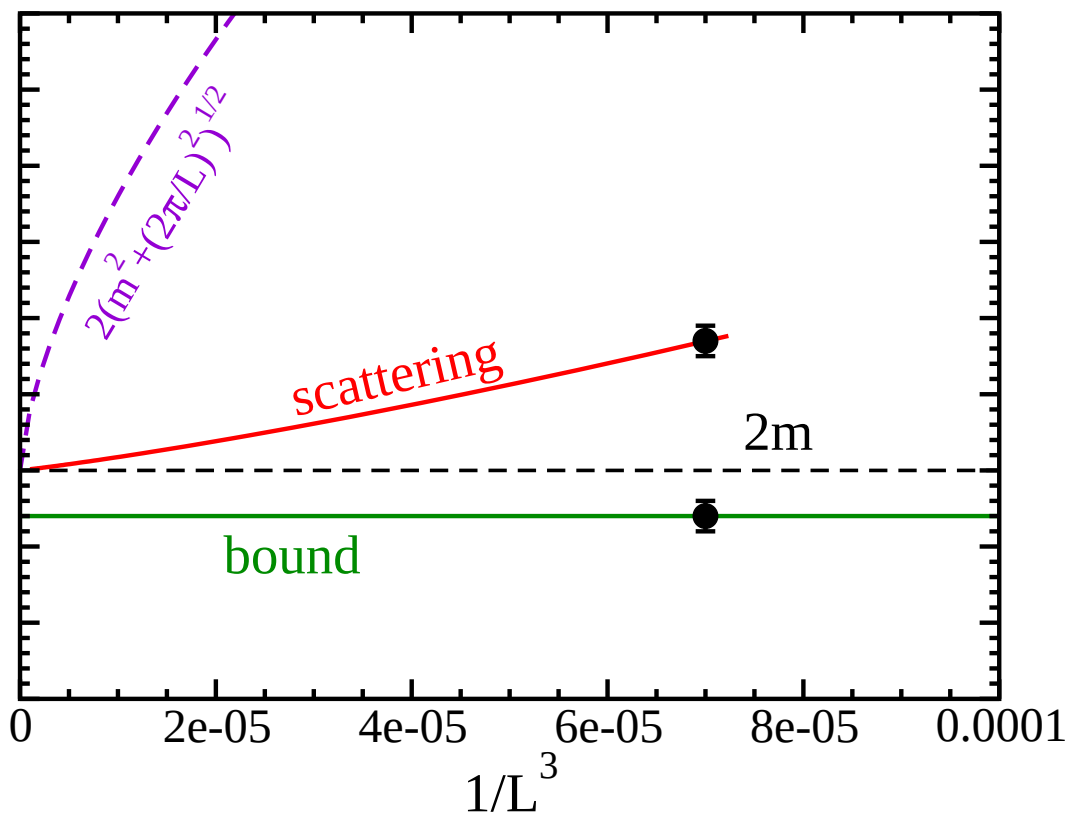

Scattering state : $\Delta E_L = O\left(-\frac{a_0}{mL^3}\right) > 0 \quad (a_0 < 0)$ '86, '91 Lüscher

1st excited state $\leftarrow$ diagonalization method '90 Lüscher & Wolff

4. Results

NN ($^3S_1$ and $^1S_0$) channels $\Delta E_{L,1} = E_1 - 2m_N$

PACS-CS Collaboration, PRD84:054506(2011)

Volume dependence of $\Delta E_{L,1}$

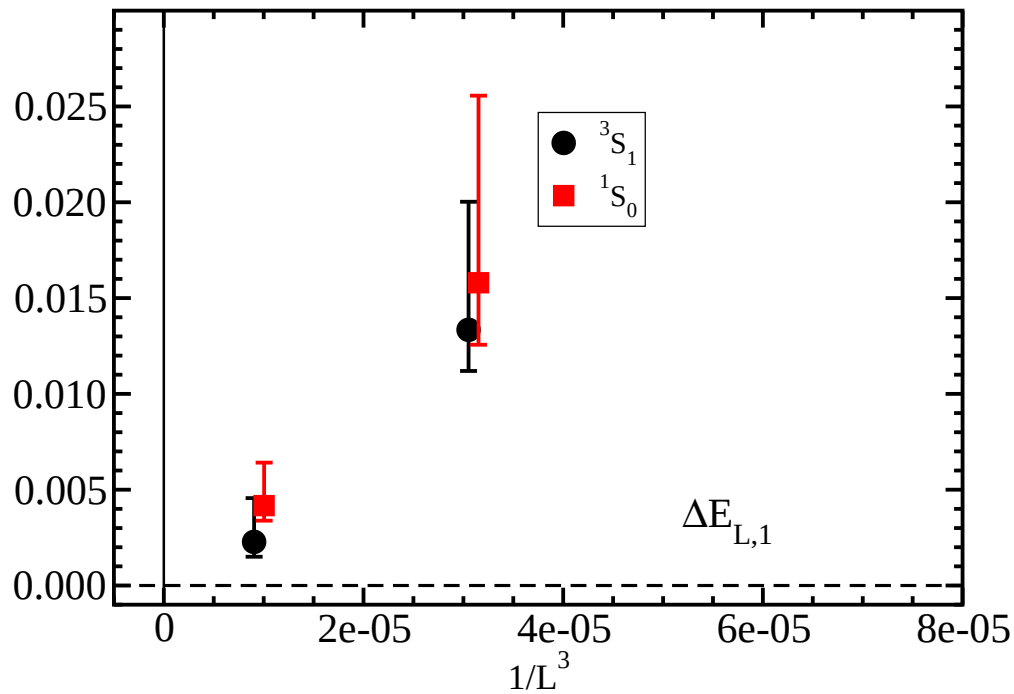

$\Delta E_{L,1} > 0$ and $1/L^3$ tendency

Scattering length a_0 fm

L[fm]	$^3S_1$
3.1	$-1.5(0.2)\left(^{+0.2}_{-1.4}\right)$
6.1	$-1.05(24)\left(^{+0.05}_{-0.65}\right)$
L[fm]	$^1S_0$
3.1	$-1.8(0.3)\left(^{+0.4}_{-12.9}\right)$
6.1	$-1.62(24)\left(^{+0.01}_{-0.75}\right)$

Observe expected properties of 1st excited state

Computing the K_L - K_S mass difference in Lattice QCD

Jianglei Yu

RBC and UKQCD Collaborations

May 15 2012, BNL

Outline

- Introduction
- Summary of the method
- Setup of the calculation
- Short distance effect
- Long distance effect
- Mass difference
- Conclusion and future plans

Introduction

- $K^0 - \bar{K}^0$ mixing :

  $\Delta M_K = 3.4583(6) \times 10^{-12}$ Mev

- Perturbative calculation can explain 70% of the mass difference
- Long distance effect

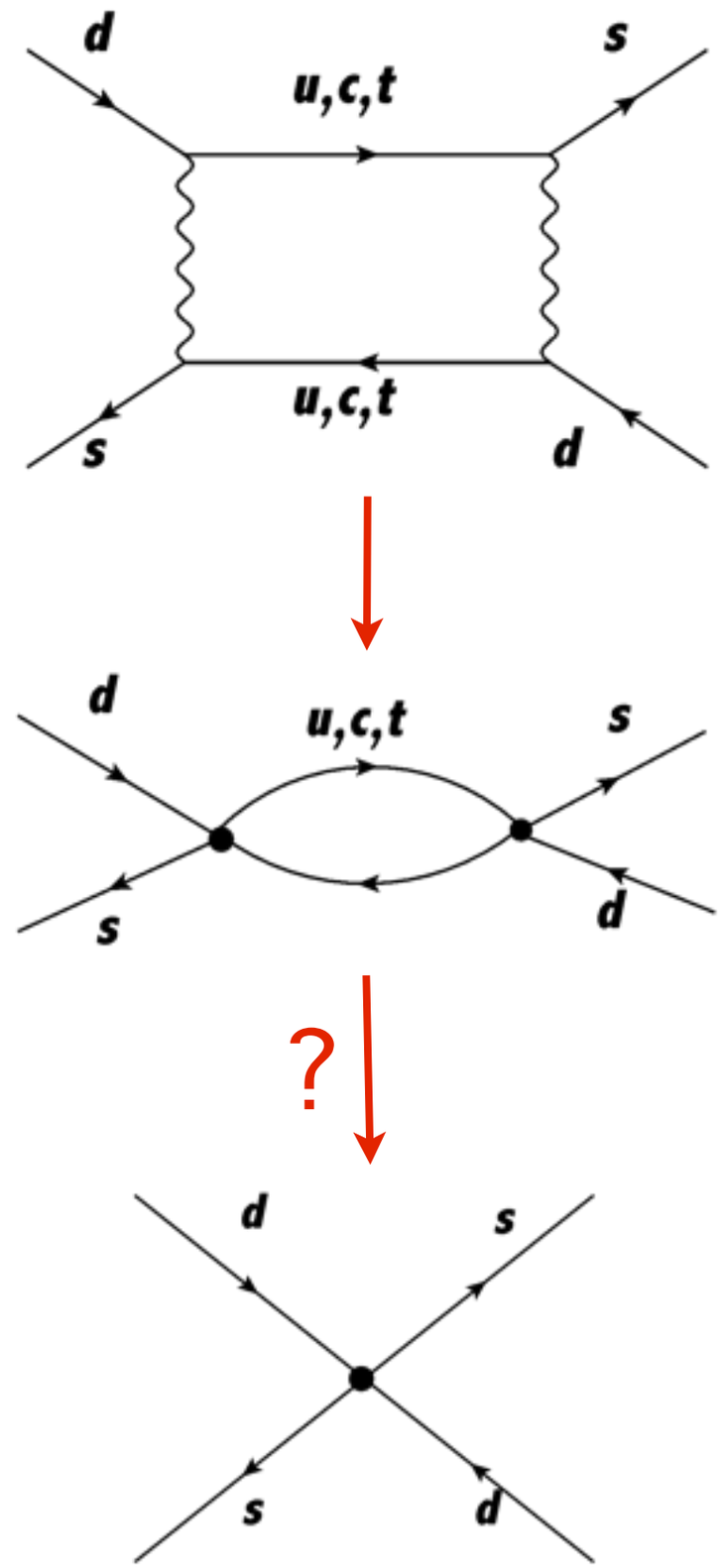

Directly evaluate second order weak process on a Lattice

Summary of the method

Neglect CP violation, K_L-K_S mass difference is given by :

$$\Delta M_K = 2\mathscr{P}\int dE_n \frac{\langle \overline{K}^0 | H_W | n \rangle \langle n | H_W | K^0 \rangle}{M_K - E_n}$$

Two parts to calculate ΔM_K :

✓ Evaluate lattice four point function

- Correct finite volume effect

Principal part should be taken when dealing with $M_K = E_n$ singularity

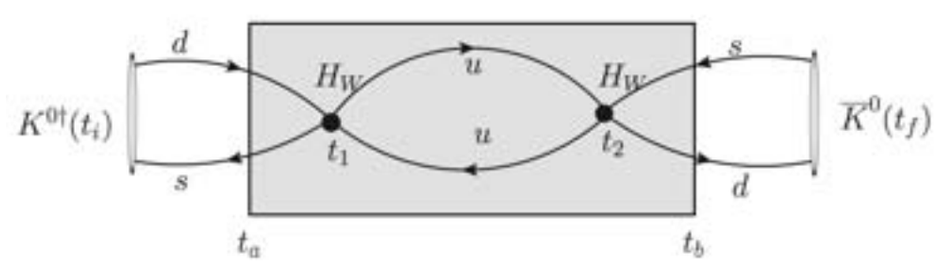

Lattice four point function

Four point correlator :

$$G(t_f, t_1, t_2, t_i) = \langle \overline{K^0}(t_f) H_W(t_2) H_W(t_1) K^{0\dagger}(t_i) \rangle$$

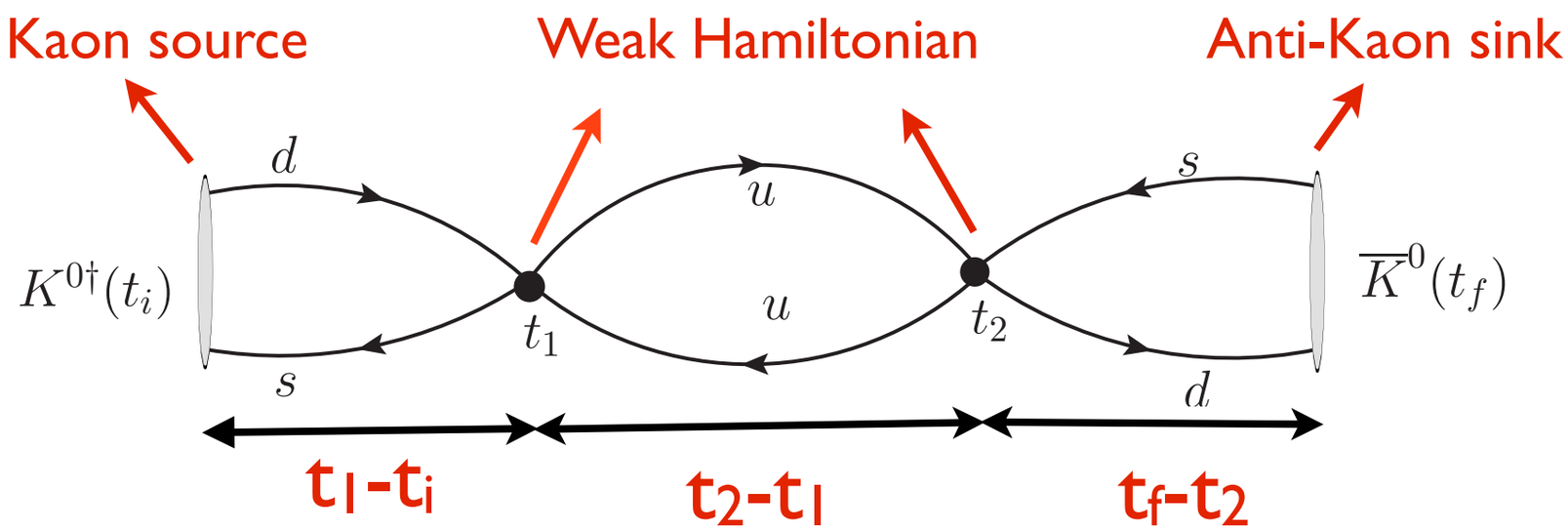

- t_1-t_i and t_f-t_2 should be sufficiently large to get a kaon
- Fix t_i and t_f, correlator depends only on t_2-t_1
- Refer to this quantity as unintegrated correlator

Integrated Correlator

Integrate the unintegrated correlator over a time interval :

$$\mathscr{A} = \frac{1}{2} \sum_{t_1=t_a}^{t_b} \sum_{t_2=t_a}^{t_b} \langle \overline{K^0}(t_f) H_W(t_2) H_W(t_1) K^{0\dagger}(t_i) \rangle$$

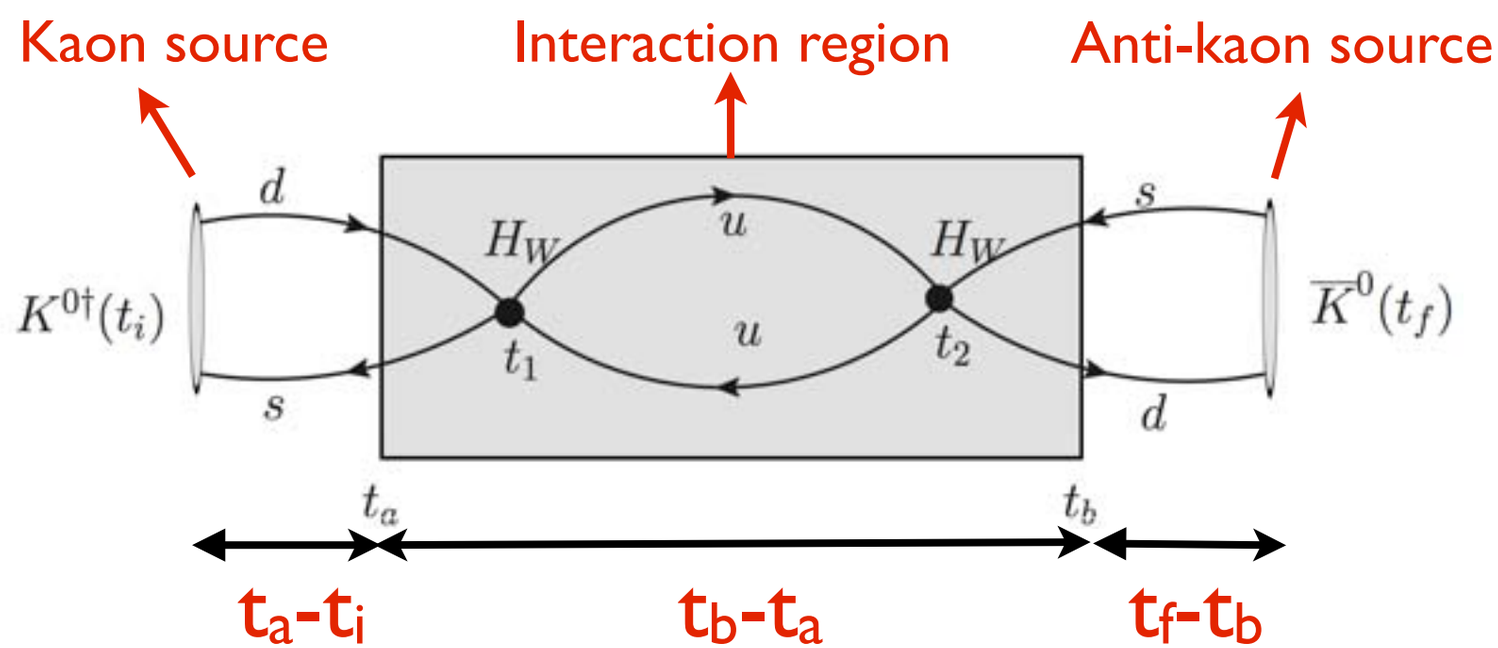

- t_f-t_b and t_a-t_i should be sufficiently large to get a kaon
- Fix t_i and t_f , correlator depends only on t_b-t_a
- Refer to this quantity as integrated correlator

After inserting a sum over intermediate states one obtains :

$$\mathscr{A} = N_K^2 e^{-M_K(t_f-t_i)} \left\{ \sum_{n\neq n_0} \frac{\langle \overline{K}^0 | H_W | n \rangle \langle n | H_W | K^0 \rangle}{M_K - E_n} \left(-T - \frac{1}{M_K - E_n} + \frac{e^{(M_K-E_n)T}}{M_K - E_n} \right) + \frac{1}{2} \langle \overline{K}^0 | H_W | n_0 \rangle \langle n_0 | H_W | K^0 \rangle T^2 \right\}$$

1 2 3,4

5

T = t_b-t_a+1 is the integration range, the terms in correlator fall into five categories:

1. Linear term, the coefficient gives finite volume approximation to ΔM_K
2. Constant term, which is trival
3. Exponential decreasing term, come from states $E_n > M_K$
4. Exponential increasing term, come from states $E_n < M_K$
5. Quadratic term, come from state $E_n = M_K$

Subtract from correlator

Correct finite volume effect

Finite Volume :

- ΔM_K is given by finite volume sum
- Tune lattice so $E_{\pi\pi} = M_K$
- Use degenerate perturbation theory, relate $E_{\pi\pi}$ with ΔM_K

Infinite volume :

- ΔM_K is given by infinite volume integral
- π-π phase shift relate to ΔM_K through kaon pole

Luscher condition:

$$\phi(E) + \delta_0(E) + \delta_W(E) = n\pi$$

Result for ΔM_K

Leading order term

- Tune volume so $M_K = E_{\pi\pi}$
- Remove $\pi\pi$ state

Add back finite volume correction

$$\Delta M_K = 2 \sum_{n \neq n_0} \frac{\langle \overline{K}^0 | H_W | n \rangle \langle n | H_W | K^0 \rangle}{M_K - E_n} - \frac{\partial^2 (\phi + \delta_0)/\partial E^2}{2 \partial (\phi + \delta_0)/\partial E} |\langle n_0 | H_W | K_S \rangle|^2 - \frac{\partial}{\partial E} |\langle n_0 | H_W | K_S \rangle|^2$$

The finite volume correction is not done in this calculation

Setup of the calculation

Lattice ensemble :

- $16^3 \times 32 \times 16$, 2+1 flavor DWF
- Inverse lattice spacing 1.73(3) Gev
- M_π = 421 Mev, M_K = 559Mev
- 800 configurations, each separated by 10 time units

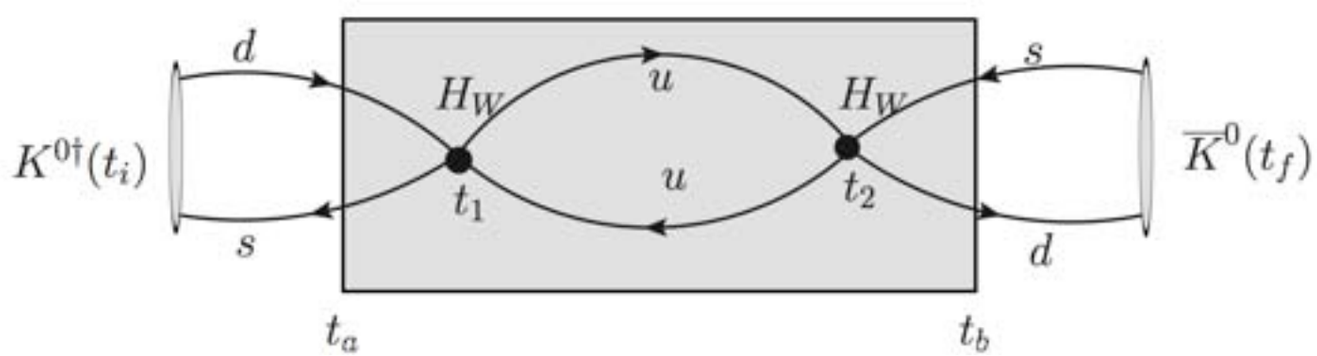

- Kaon wall sources at t_i = 0 at t_f = 27
- Weak Hamiltonian act between t_a=4 and t_b=23

Effective weak Hamiltonian

The ΔS=1 effective weak Hamiltonian in a 4 flavor theory :

$$H_W = \frac{G_F}{\sqrt{2}} \sum_{q,q'=u,c} V_{qd} V^*_{q's} (C_1 Q_1^{qq'} + C_2 Q_2^{qq'})$$

Here we only include current-current operators :

$$Q_1^{qq'} = (\bar{s}_i d_i)_{V-A} (\bar{q}_j q'_j)_{V-A}$$
$$Q_2^{qq'} = (\bar{s}_i d_j)_{V-A} (\bar{q}_j q'_i)_{V-A}$$

All the penguin operators are neglected, since they are highly suppressed because of GIM cancellation

Type 1 diagrams

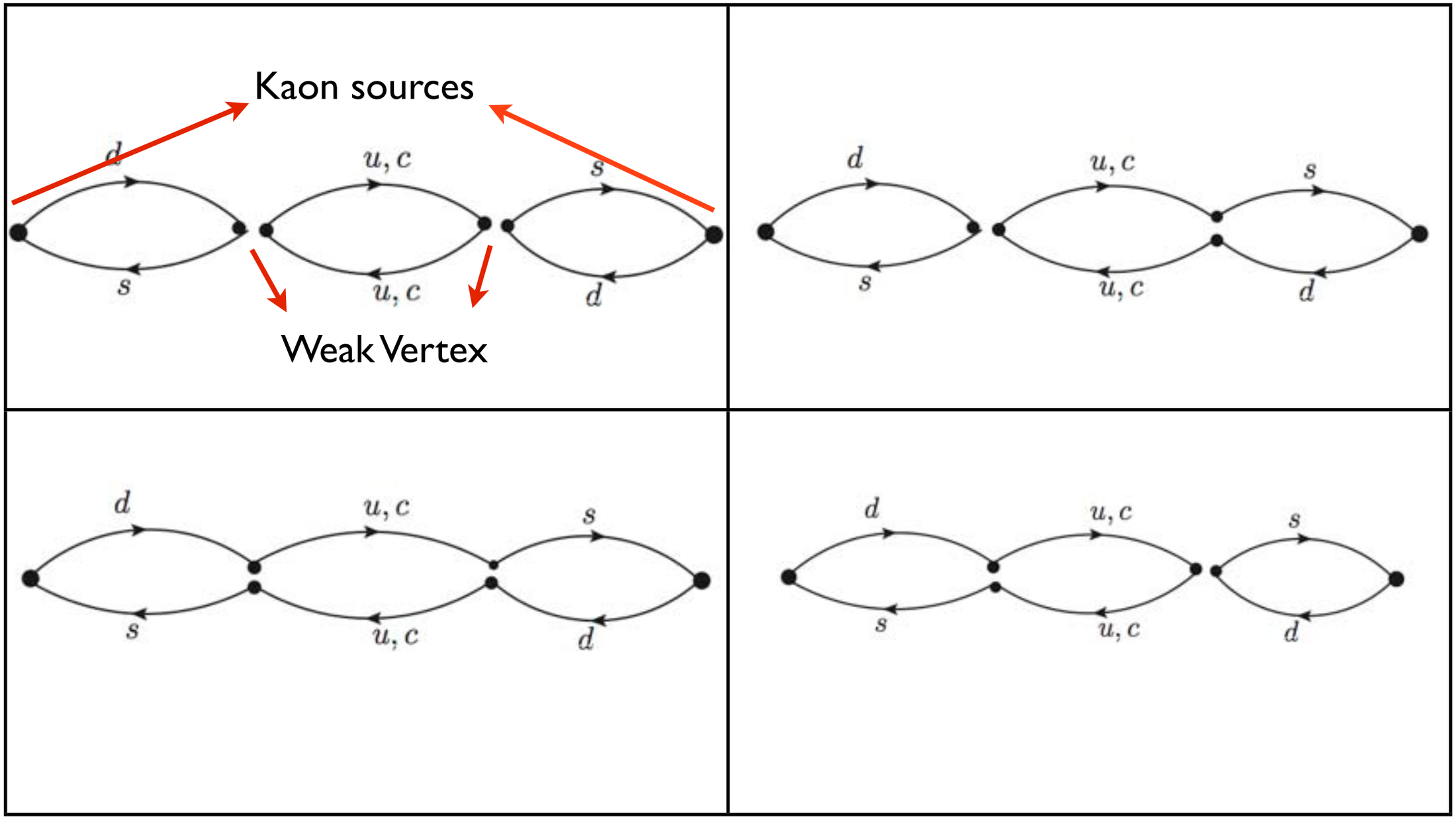

Type 2 diagrams

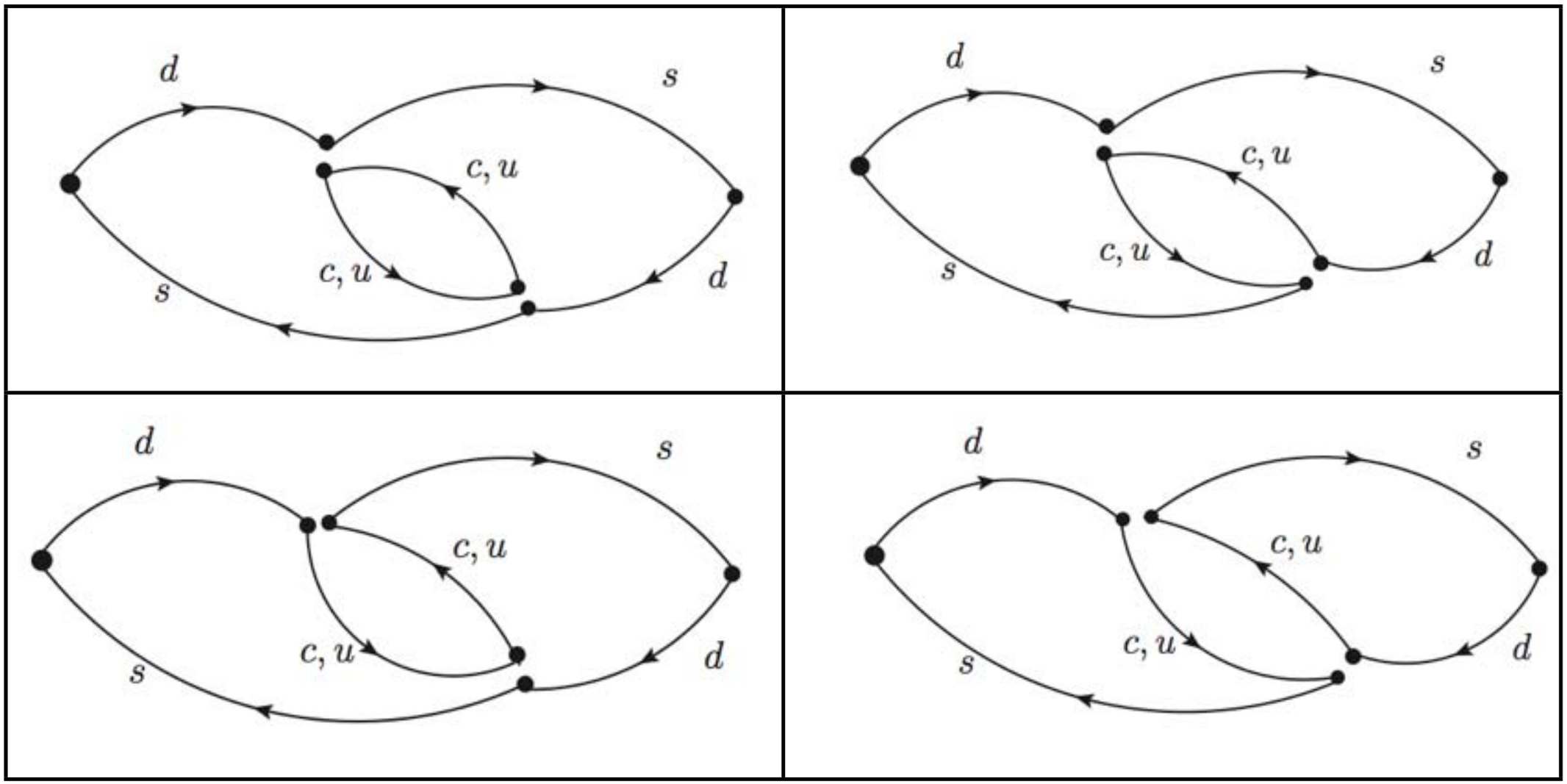

Type 3 digrams, not calculated

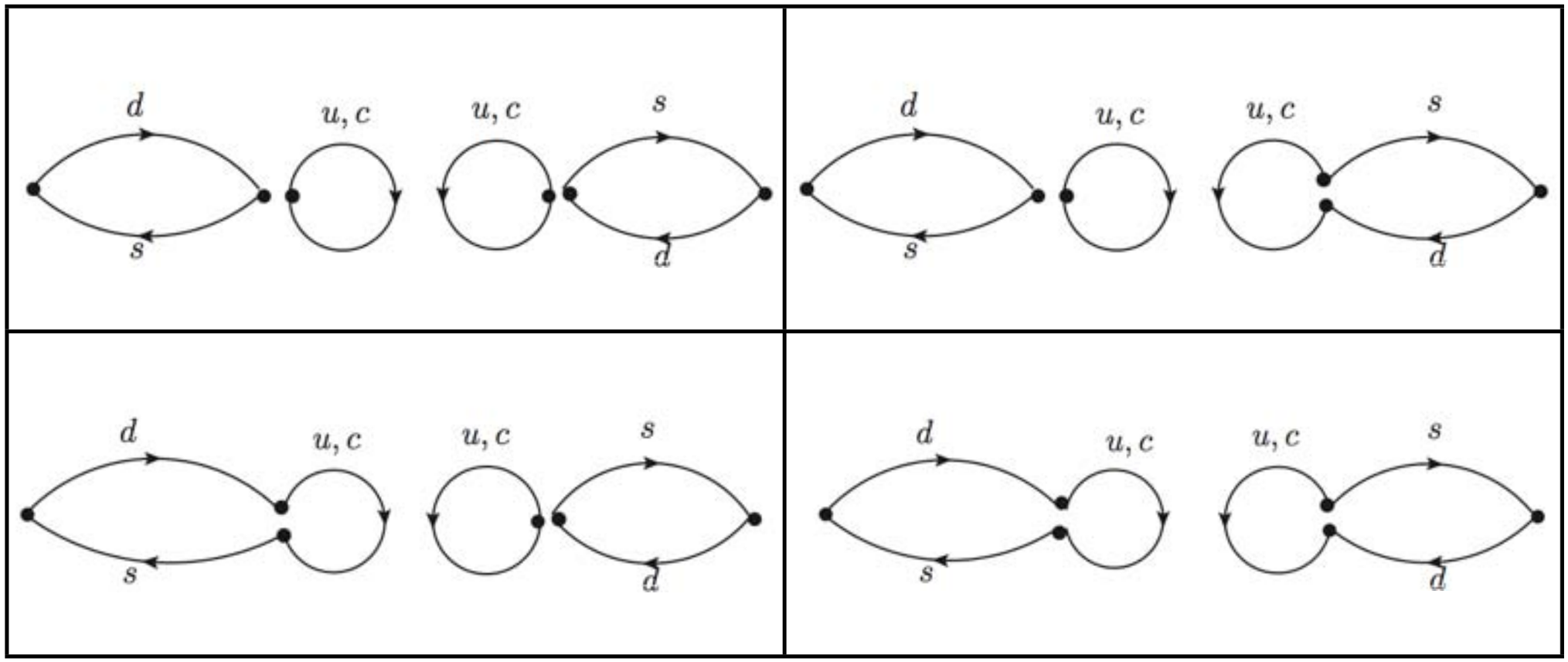

Type 4 diagrams, not calculated

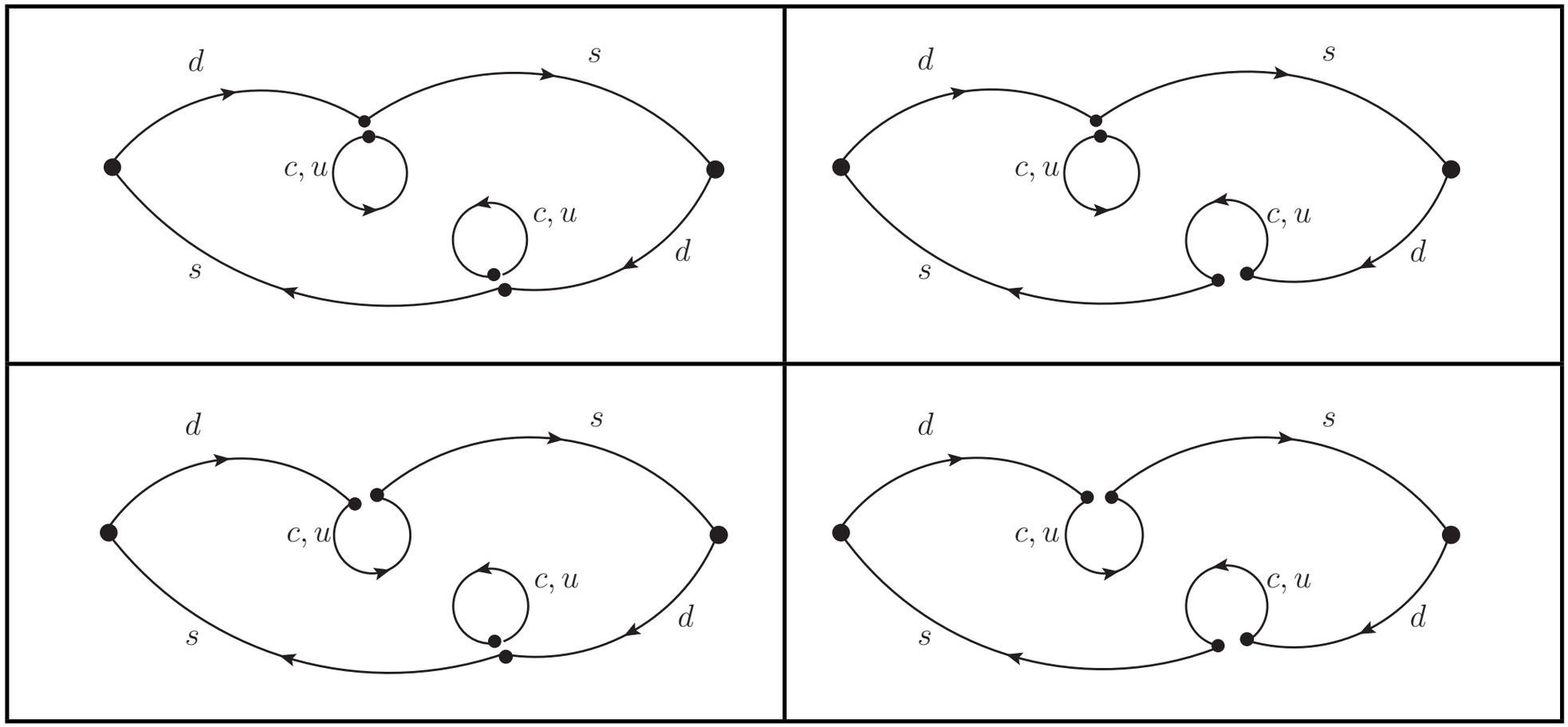

π^0 intermediate state

π^0 intermediate state contributes an exponentially increasing term in the integrated correlator, which must be identified and removed. In this non unitary calculation, π^0 and η have same mass, since only up quark can appear in our intermediate state,we define $\pi^0 = i\bar{u}\gamma_5 u$, calculate following diagrams to compute kaon to pion decay amplitude :

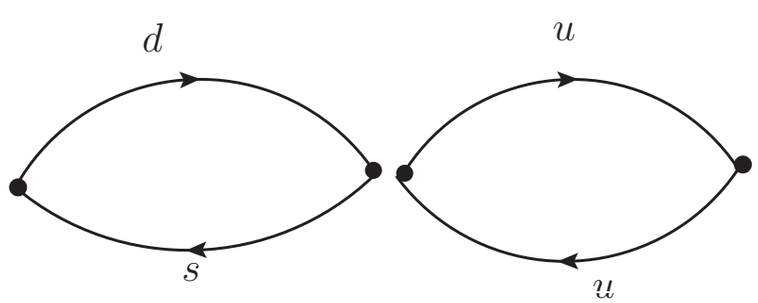

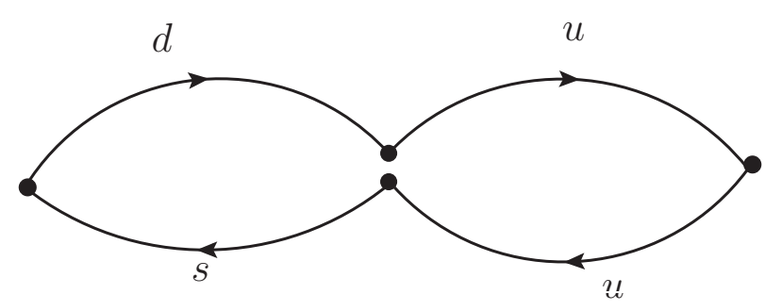

Result without GIM cancellation

- Both operators are Q_1
- Without GIM, there will be divergent short distance effect
- The dependence of correlator on time is almost linear imply that largest contribution comes from short distance

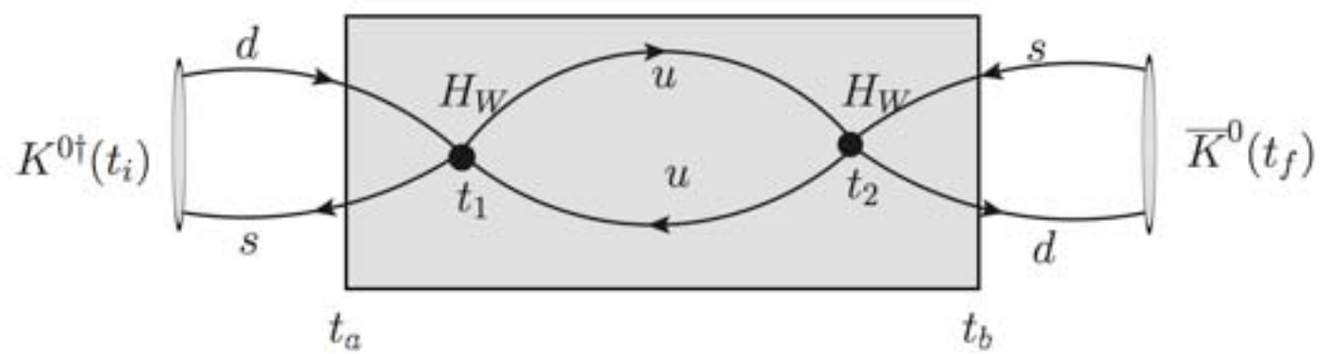

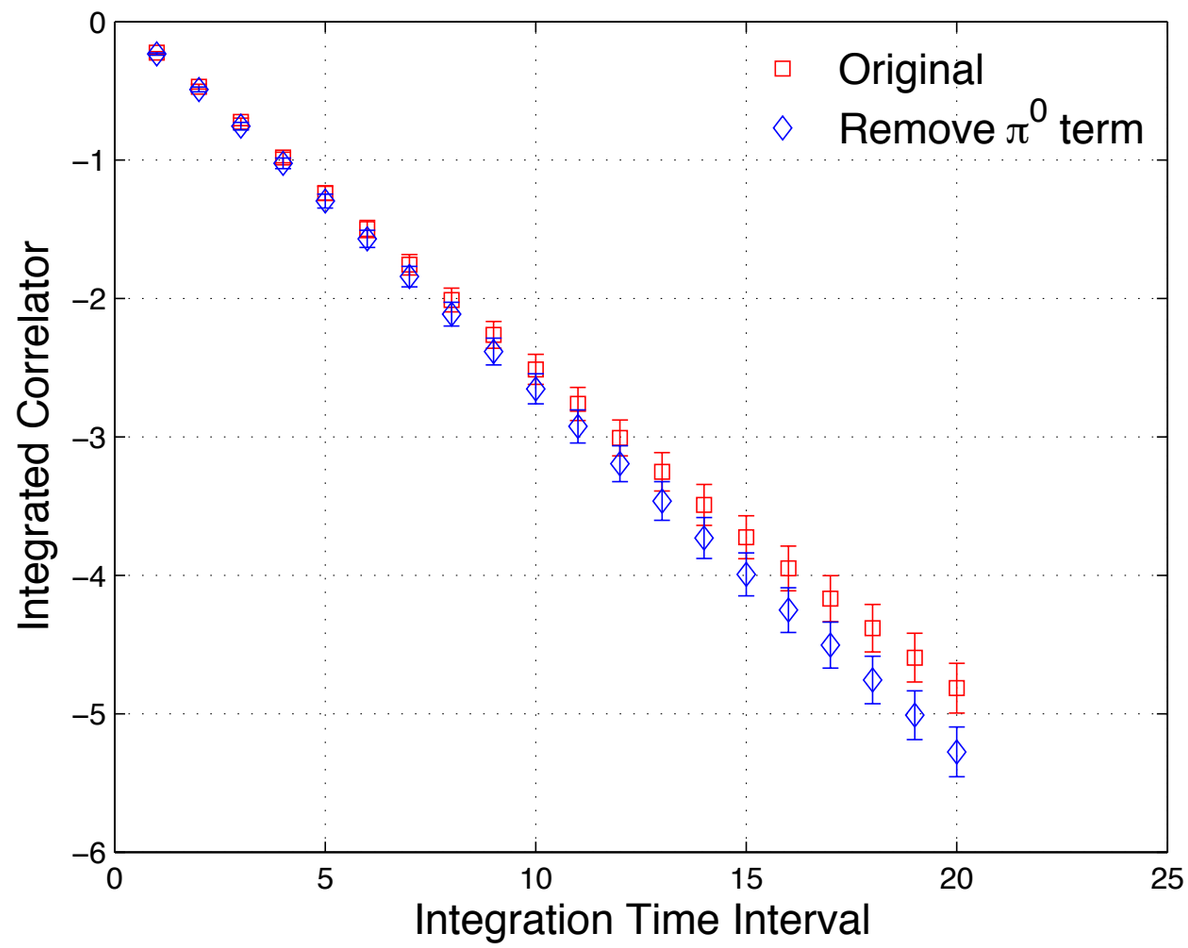

Artificial cutoff

We can impose an artificial cutoff, require $|x_2 - x_1| \geq r$ while doing integral :

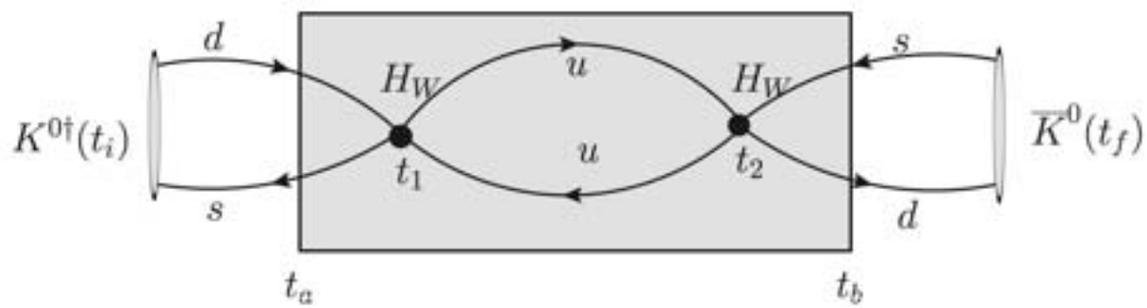

No cutoff

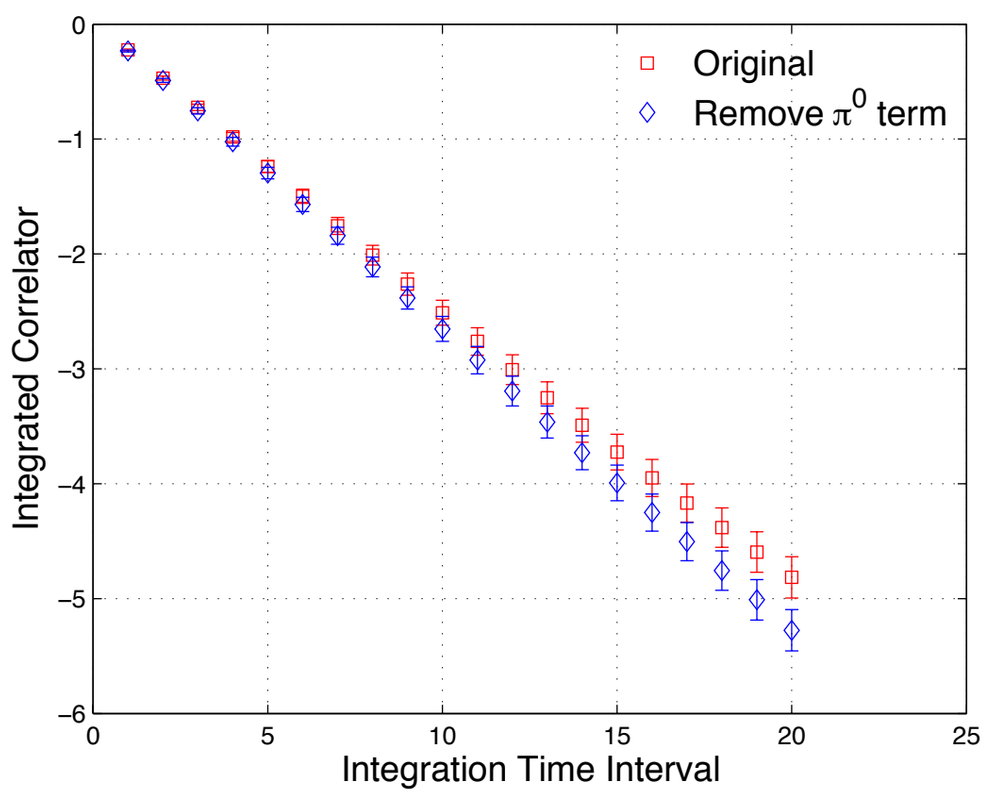

Cutoff = 5

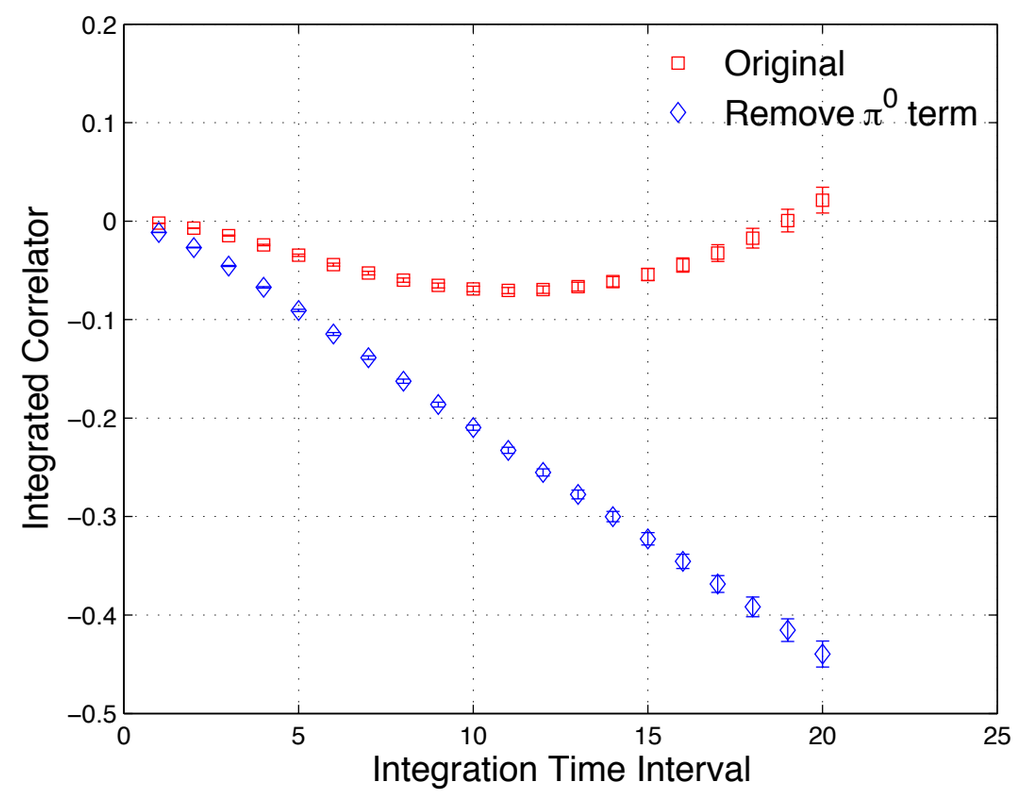

Quadratic divergence

Mass difference is given by the slope of integrated correlator plot while the integration range is large enough.

$$\Delta M_K(R) = \frac{a}{R^2} + b$$

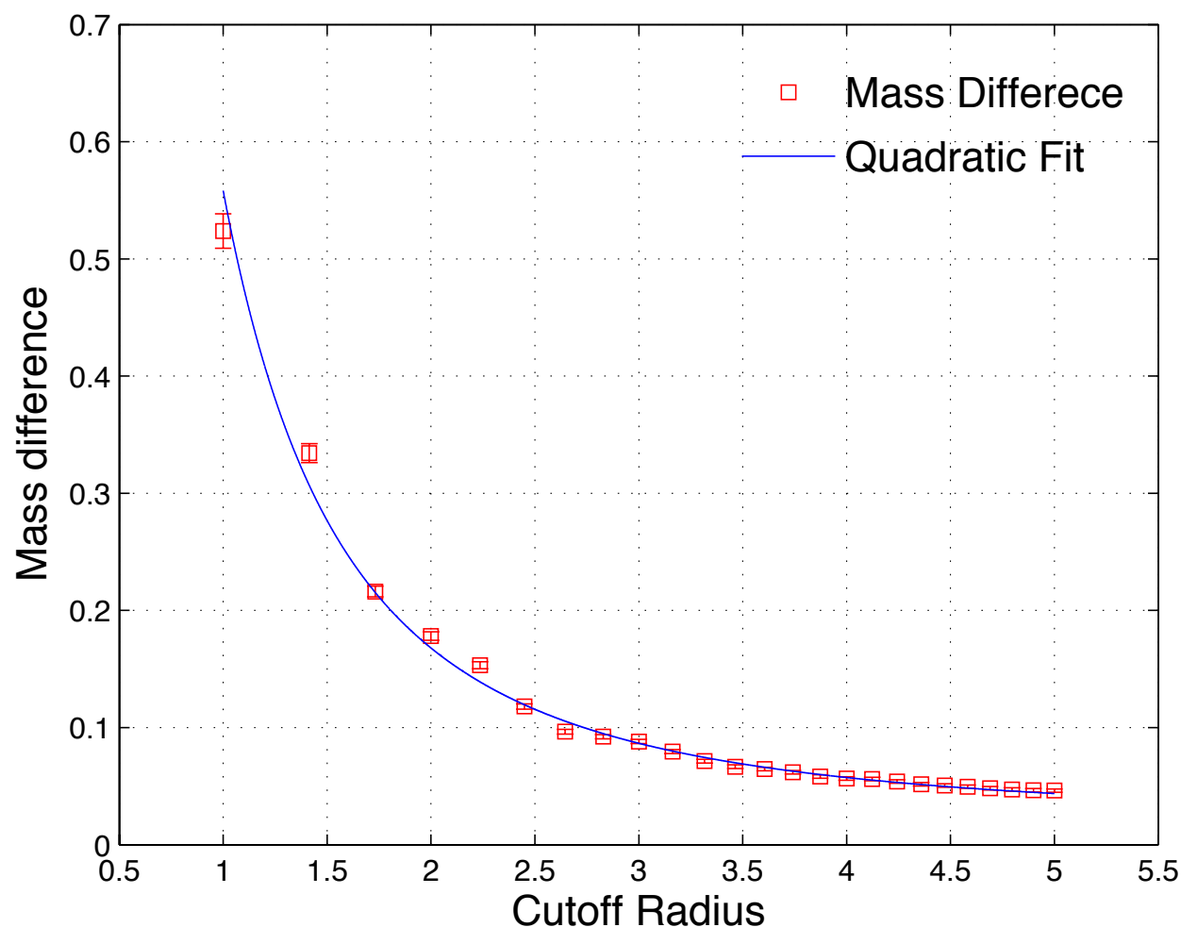

GIM remove the divergence in short distance :

No charm quark

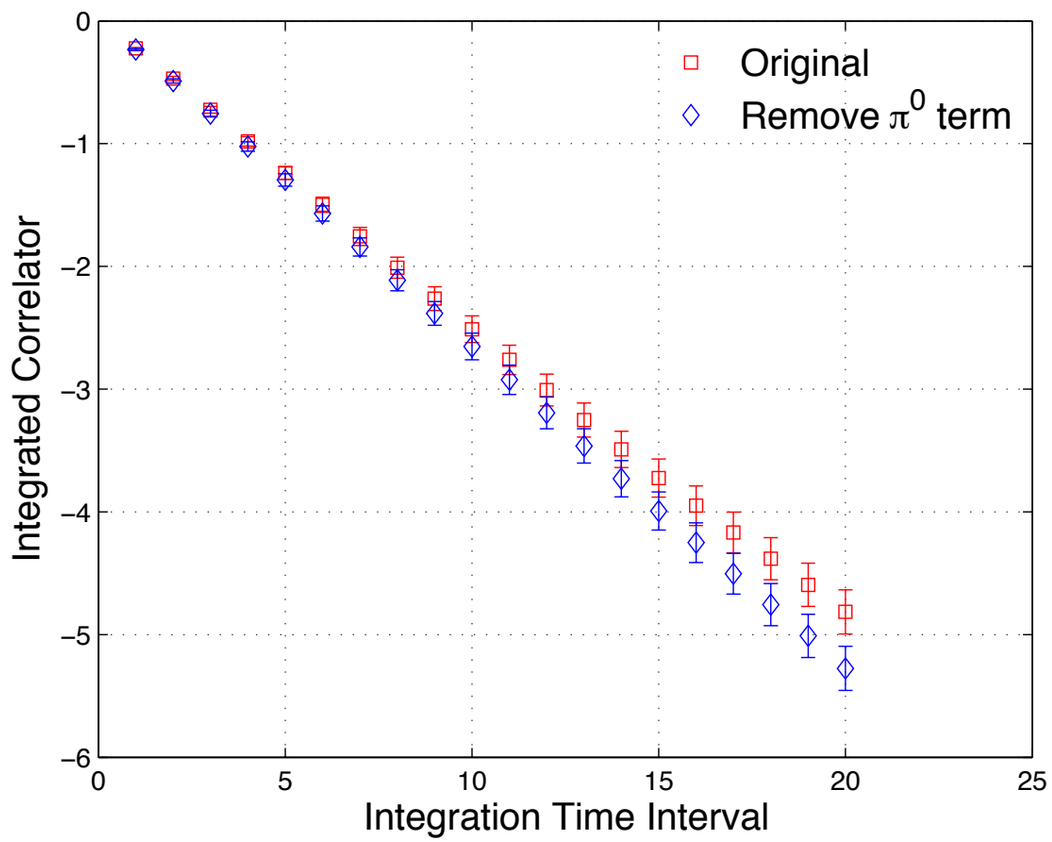

1 Gev charm quark

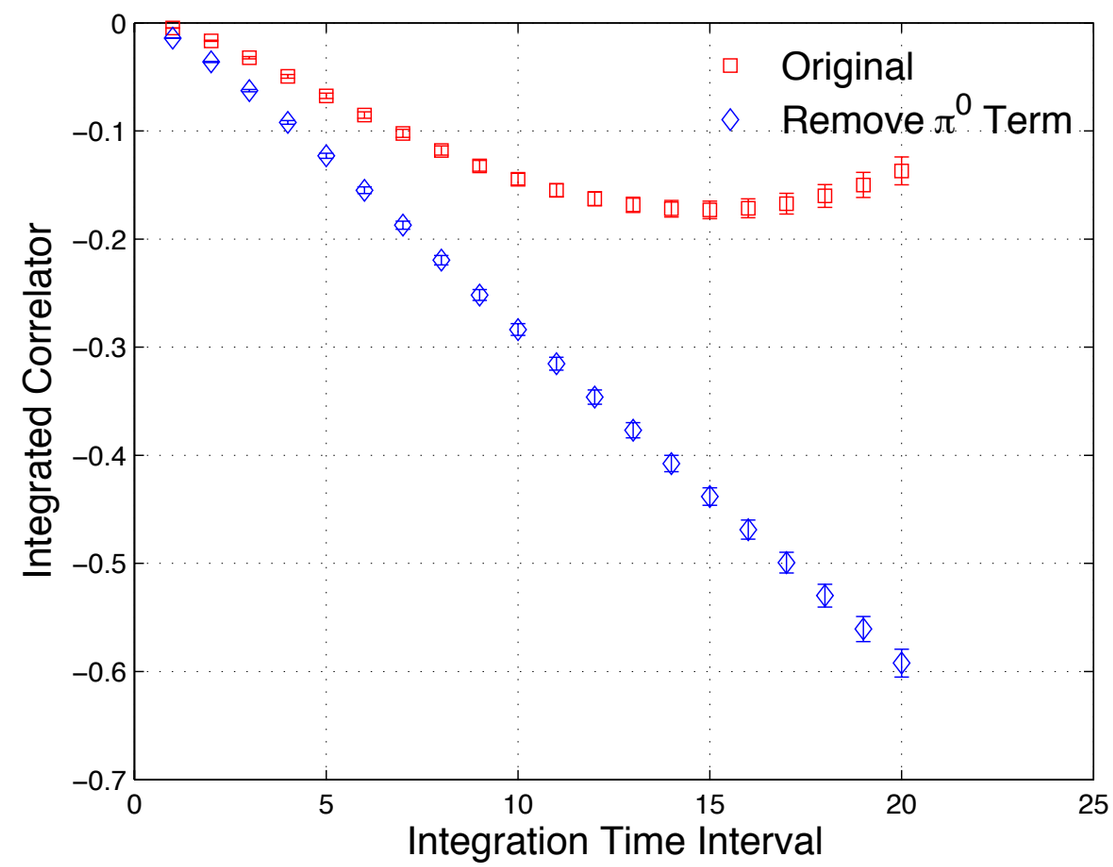

Quadratic Fit :

$$\Delta M_K(m_c) = a\ m_c^2 + b$$

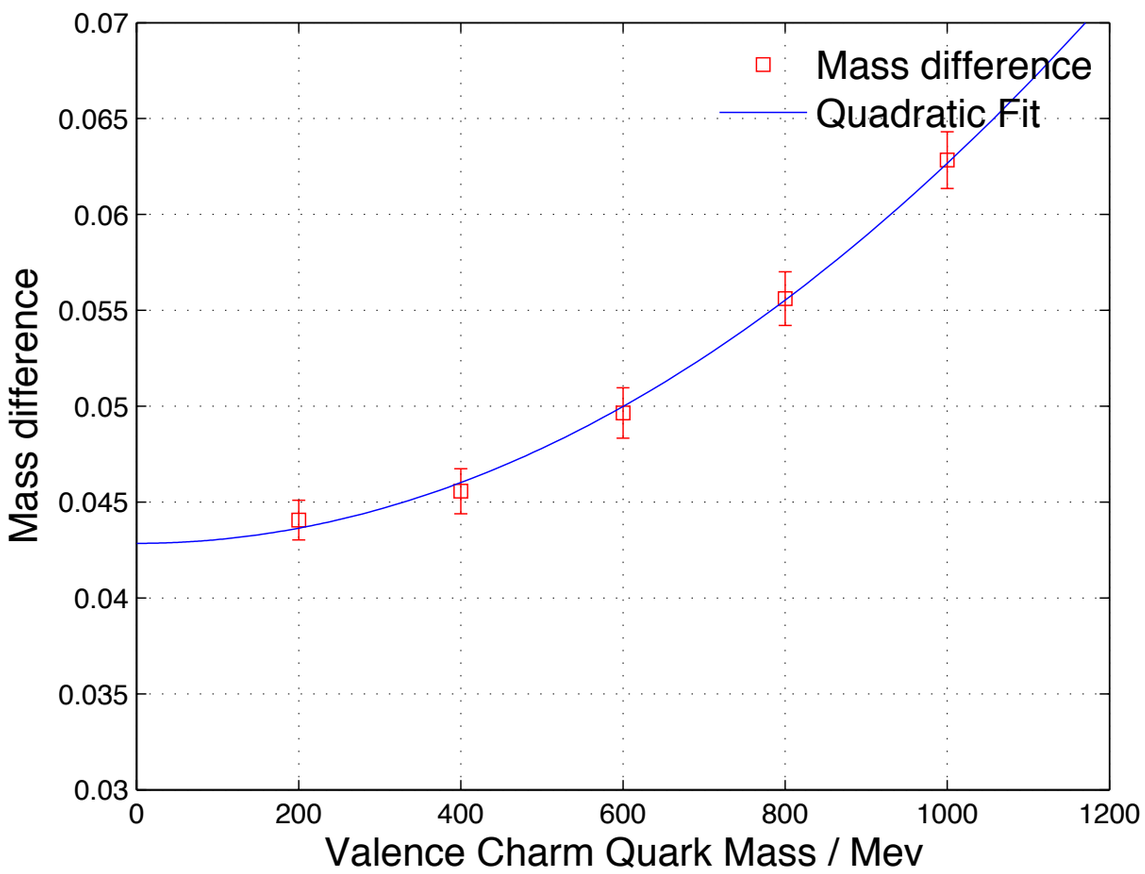

Is 1 Gev charm too heavy ?
Quadratic dependence on m_c will be cutoff buy lattice spacing if charm is too heavy.
The fitting result suggest we haven't reach that region

Long distance effect

Investigate unintegrated correlator :

$$G(T;t_i,t_f) = N_K^2 e^{-M_K(t_f-t_i)} \sum_n \langle \overline{K^0}|H_W|n\rangle\langle n|H_W|K^0\rangle e^{-(E_n-M_K)T}$$

Here T is the time separation between to weak Hamiltonian

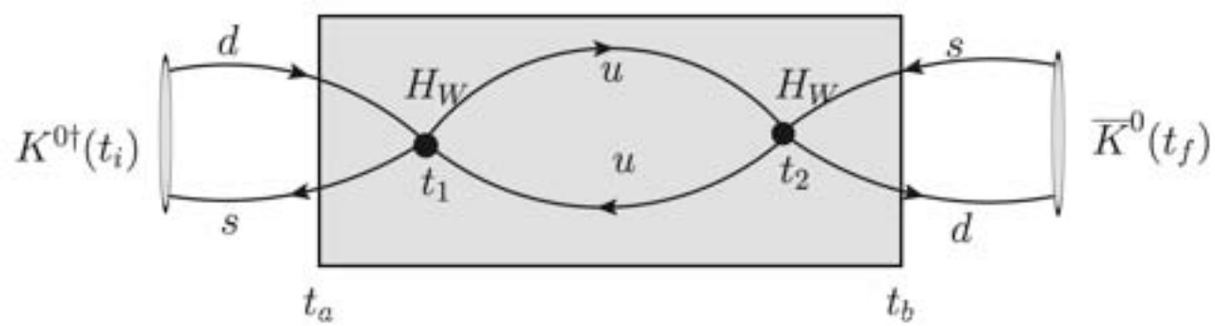

- Separate the Hamiltonian into two parity channel :
  - Parity conserving channel, long distance effect dominate by π^0 intermediate state
  - Parity violating channel, long distance effect dominate by $\pi\pi$ intermediate state
- Use various kaon masses

Parity conserving channel

In long distance, correlator dominate by π^0 term :

$$G(T;t_i,t_f) = N_K^2 e^{-M_K(t_f-t_i)} \langle \overline{K^0}|H_W|\pi^0\rangle\langle\pi^0|H_W|K^0\rangle e^{-(E_\pi - M_K)T}$$

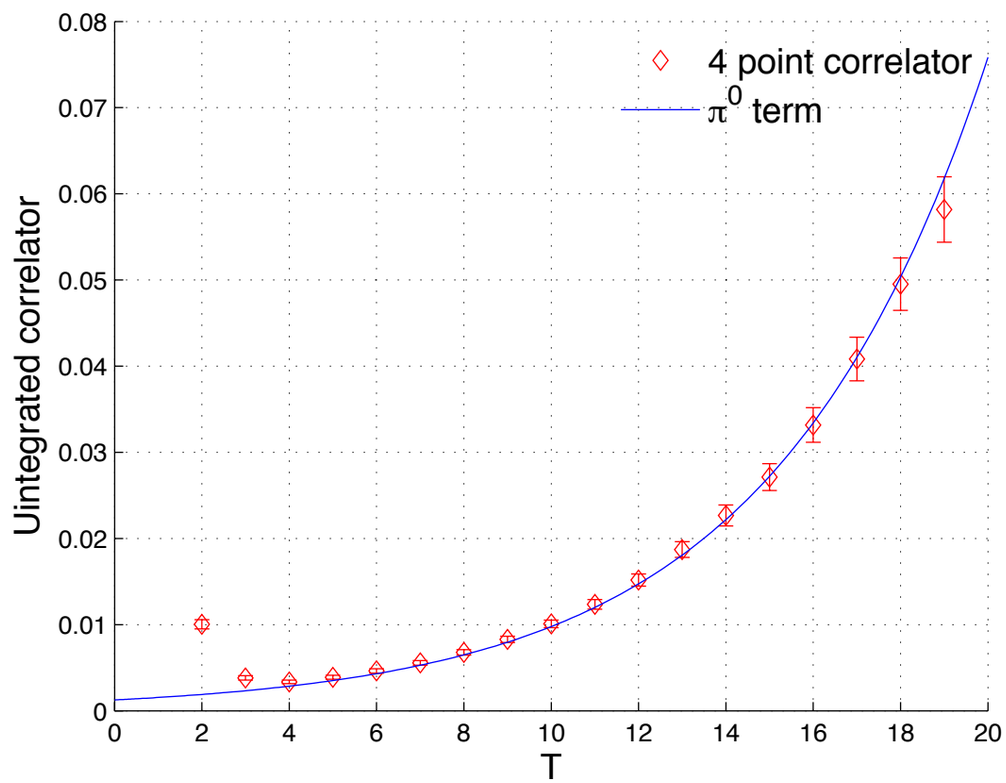

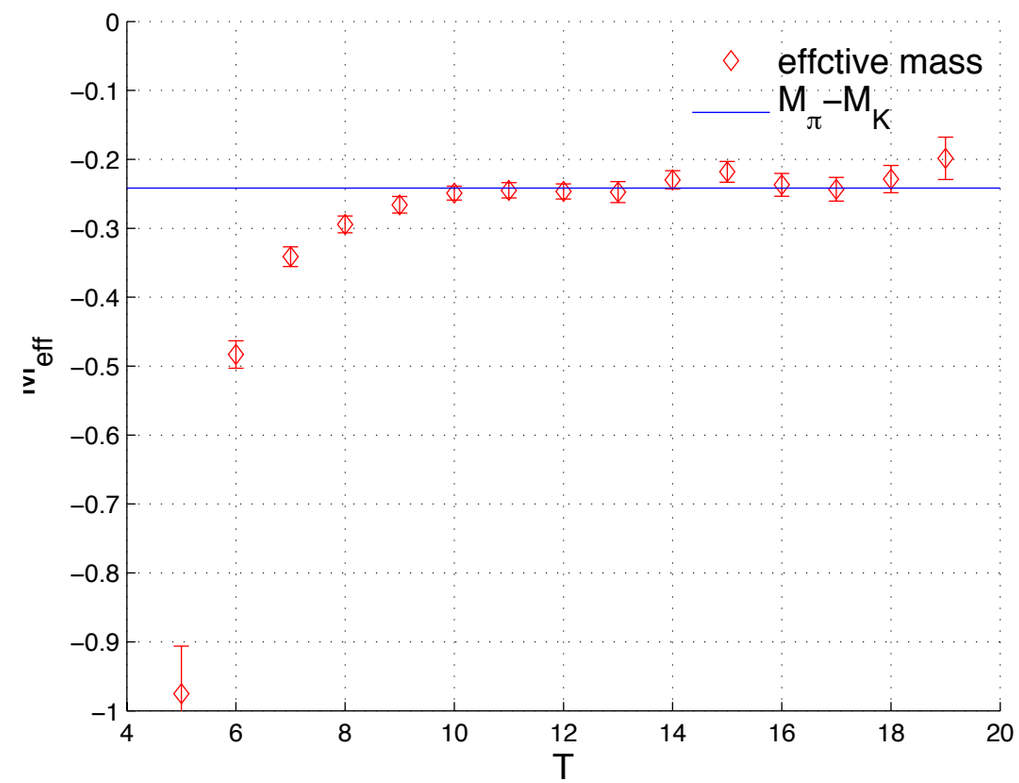

Parity conserving channel

- Points are the fitting results from unintegrated correlators at various kaon masses
- Horizontal line is the "exact" pion mass given by two point correlator calculation

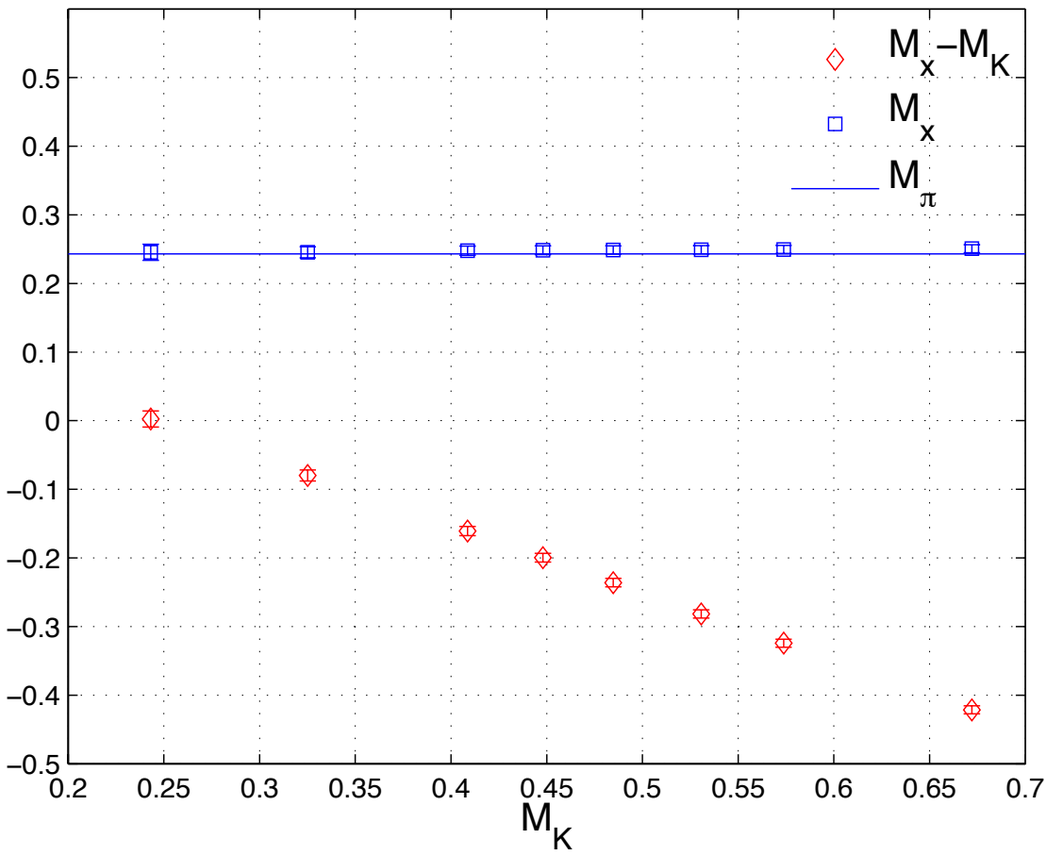

Parity violating channel

In long distance, correlator dominate by ππ term :

$$G(T;t_i,t_f) = N_K^2 e^{-M_K(t_f-t_i)} \langle \overline{K^0}|H_W|\pi\pi\rangle\langle\pi\pi|H_W|K^0\rangle e^{-(E_{\pi\pi}-M_K)T}$$

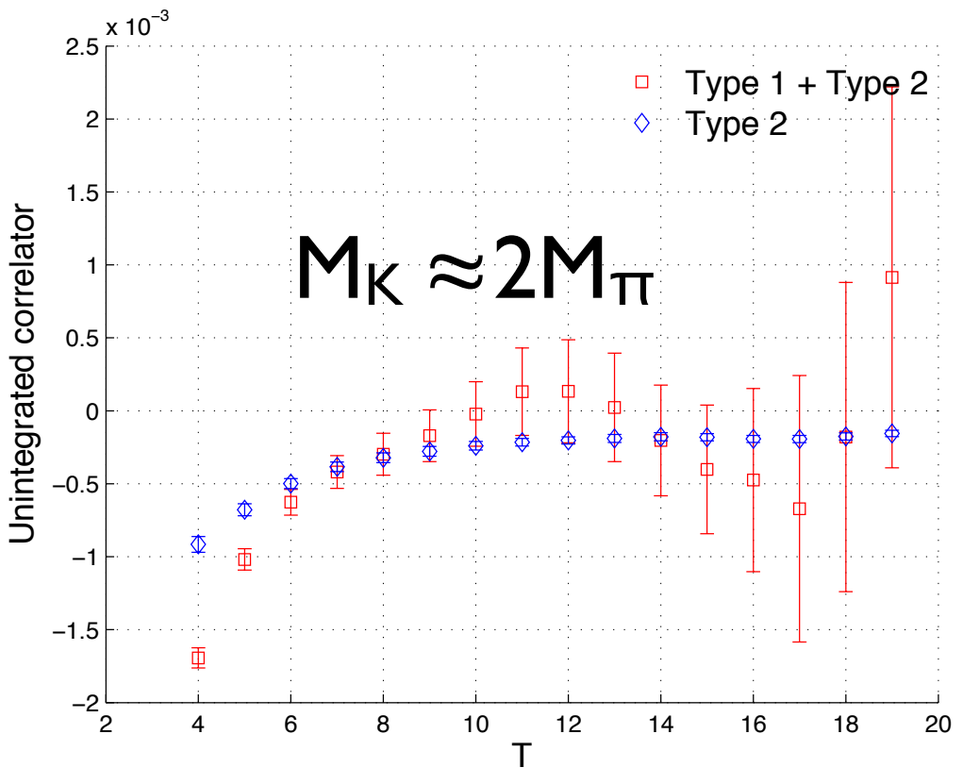

We expect to see plateau at long distance :

- No signal at long distance
- Good signal from type 2 diagrams only

Parity violating channel

Type 1

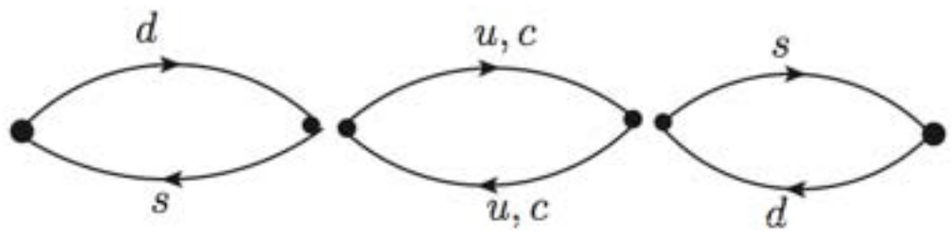

Type 2

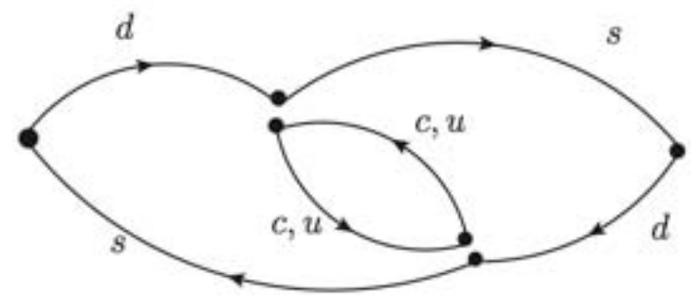

Noise behave like π ,exponentially increasing noise to signal ratio

The signal from type 2 contractions don't have such noise

Parity violating channel

- Points are the fitting results from unintegrated correlators at various kaon masses, type 2 contractions only
- Horizontal line is the "exact" 2 pion mass given by two point correlator calculation

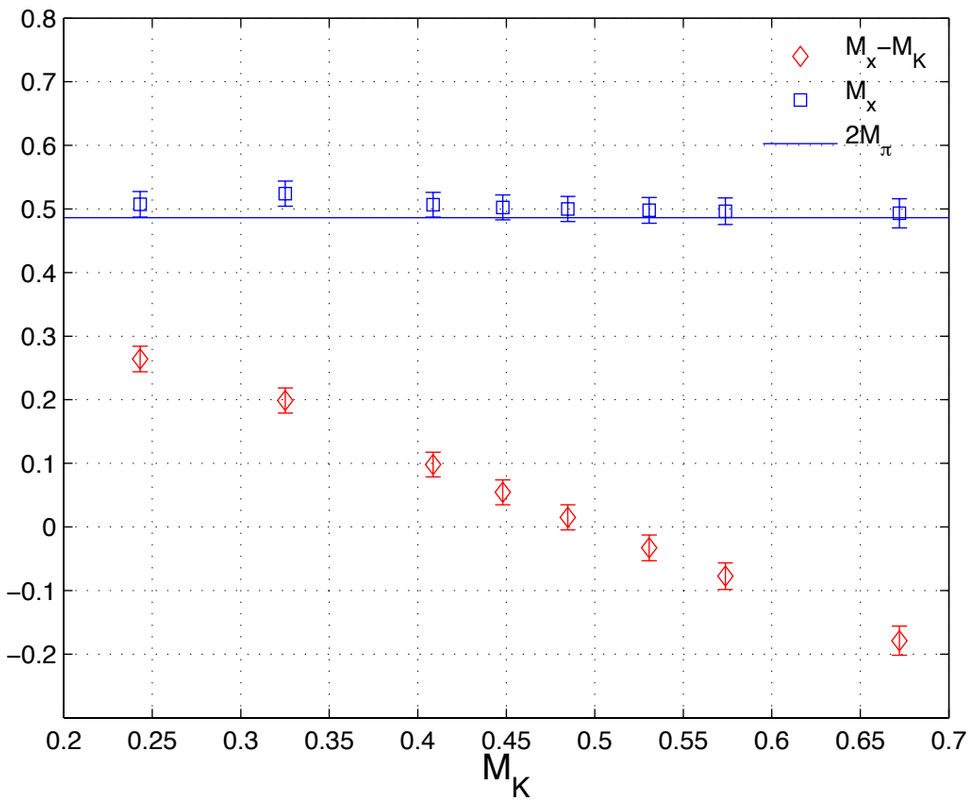

Mass difference

M_π = 421 Mev
M_c = 1 Gev

- Only included statistical error
- Finite volume effect not corrected

$$\Delta M_K^{exp} = 3.483(6) \times 10^{-12} \text{ Mev}$$

M_K (Mev)	ΔM_K^{11}	ΔM_K^{12}	ΔM_K^{22}	ΔM_K ($\times 10^{-12}$ Mev)
563	6.38(14)	-2.64(14)	1.47(8)	5.52(24)
707	8.90(21)	-2.96(23)	2.10(12)	7.38(37)
775	10.63(27)	-3.18(30)	2.48(15)	8.61(49)
839	12.56(34)	-3.62(40)	2.89(20)	9.93(65)

$\approx 2M_\pi$

Conclusions and future plans

- Lattice calculation of ΔM_K is possible :
  - ✓ Use GIM to remove divergence in short distance
  - ✓ Remove π exponentially term
  - Use on-shell $K \to \pi\pi$ kinematics, remove quadratic term from integrated correlator
  - Add finite volume correction term
- Include type 3 and type 4 diagrams in future
- Use Low mode averaging or A2A to collect statistics more efficiently

Operator mixing and renormalization

Three group of operators :

$$\tilde{Q}_1 = (\bar{s}_i d_i)_{V-A}(\bar{u}_j u_j)_{V-A} - (\bar{s}_i d_i)_{V-A}(\bar{c}_j c_j)_{V-A}$$
$$\tilde{Q}_2 = (\bar{s}_i d_j)_{V-A}(\bar{u}_j u_i)_{V-A} - (\bar{s}_i d_j)_{V-A}(\bar{c}_j c_i)_{V-A}$$
$$Q_1^{cu} = (\bar{s}_i d_i)_{V-A}(\bar{c}_j u_j)_{V-A}$$
$$Q_2^{cu} = (\bar{s}_i d_j)_{V-A}(\bar{c}_j u_i)_{V-A}$$
$$Q_1^{uc} = (\bar{s}_i d_i)_{V-A}(\bar{u}_j c_j)_{V-A}$$
$$Q_2^{uc} = (\bar{s}_i d_j)_{V-A}(\bar{u}_j c_i)_{V-A}$$

Equivalent basis :

$$Q_+^X = Q_1^X + Q_2^X \qquad (84,1)$$
$$Q_-^X = Q_1^X - Q_2^X \qquad (27,1)$$

X= ~, cu, uc SU(4)×SU(4)

- Operators will not mix with penguin
- Renormalization for three groups of operators should be identical

Correct finite volume effect

- Singular energy denominator $1/(M_K - E_n)$ will introduce uncontrolled errors
- Use generalized Lellouch-Lucsher method :
  - Tune lattice so $E_{\pi\pi} = M_K$
  - Finite volume $E_{\pi\pi}$ depend on finite volume sum
  - Infinite volume π-π resonant phase shift δ_W depend on infinite volume integral
  - Luscher condition relate them :

$$\phi(E) + \delta_0(E) + \delta_W(E) = n\pi$$

Finite volume energy

- Let $|n_0\rangle$ be the π-π state degenerate with kaon
- Second order perturbation theory

$$\begin{pmatrix} M_K + \sum_{n \neq n_0} \frac{|\langle n|H_W|K\rangle|^2}{M_K - E_n} & \langle K|H_W|n_0\rangle \\ \langle n_0|H_W|K\rangle & E_{n_0} + \sum_{n \neq K} \frac{|\langle n|H_W|n_0\rangle|^2}{E_{n_0} - E_n} \end{pmatrix}$$

- π-π state energy is given by :

$$E_\pm = M_K \pm \langle K|H_W|n_0\rangle + \frac{1}{2}\left\{ \sum_{n \neq n_0} \frac{|\langle n|H_W|K\rangle|^2}{M_K - E_n} + \sum_{n \neq K} \frac{|\langle n|H_W|n_0\rangle|^2}{E_{n_0} - E_n} \right\}$$

Infinite volume scattering

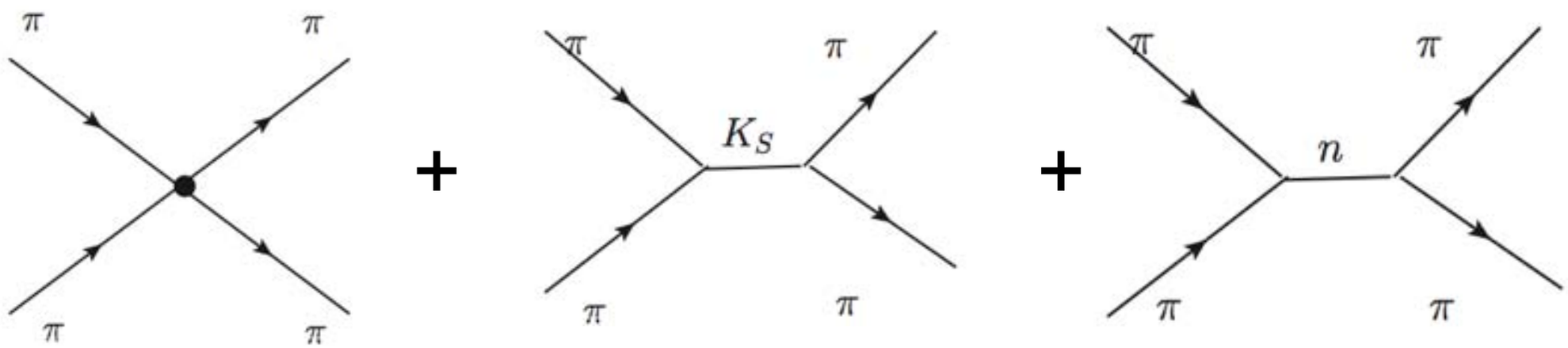

Strong interaction Kaon pole Weak interaction

Total phase shift is given by :

$$\delta(E) = \delta_0(E) + arctan(\frac{\Gamma(E)/2}{M_K + \Delta M_K - E}) - \pi \sum_{n \neq K} \frac{\langle n|H_W|\pi\pi\rangle|^2}{E - E_n}$$

Require that :

$$\delta(E_\pm) + \phi(E_\pm) = n\pi$$

Form factors for $B \to K l^+ l^-$ semileptonic decay from three-flavor lattice QCD

Ran Zhou

Indiana University

(In collaboration with FNAL/MILC)

New Horizons for Lattice Computations with Chiral Fermions,
BNL, NY

05/15/2012

Motivations and theoretical background

$B \to Kll$ semileptonic decay occurs through Penguin diagram ($b \to sll$).

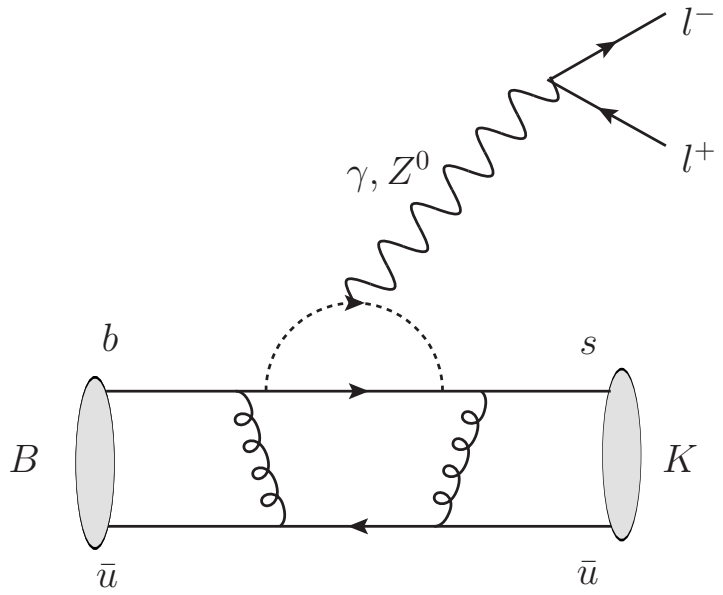

- Standard Model (SM) contributes via FCNC (suppressed)
- Suitable process to detect physics BSM
- Studied by many experiment groups (BABAR, Belle, CDF, LHCb etc.)

Example of observable in $B \to Kll$ process

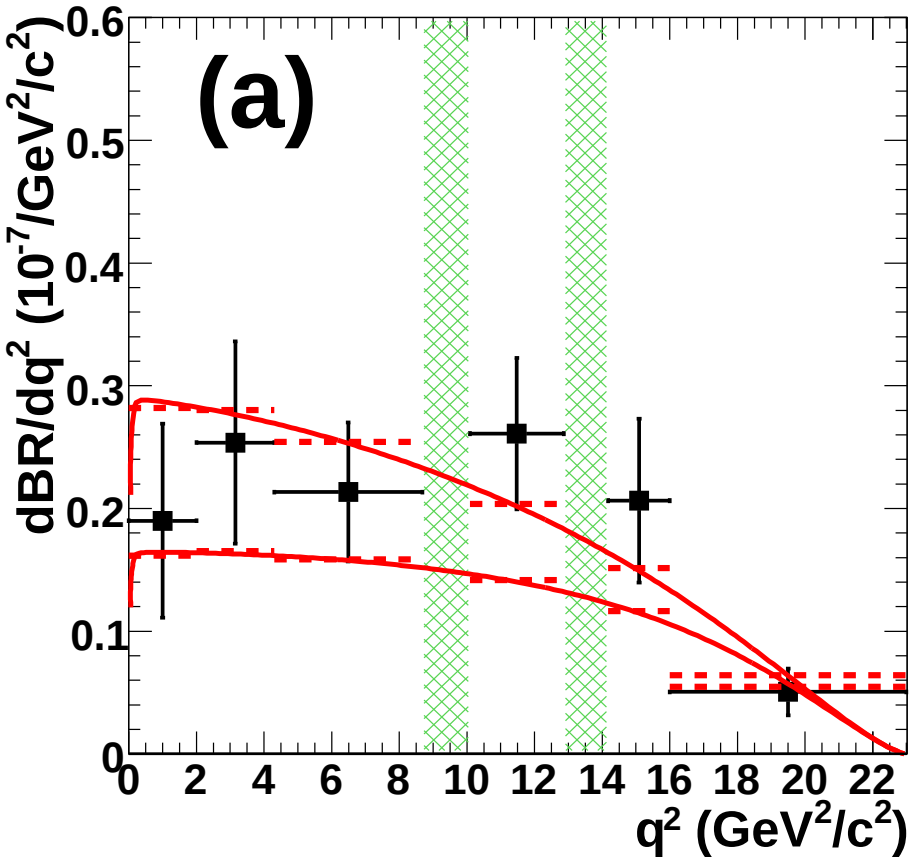

- $B^+ \to K^+\mu^+\mu^-$ differential branching ratio from CDF 2011
- Uncertainties in form factors are crucial to theoretical predictions(Red lines).
- High intensity front experiment(LHCb, SuperB) will come to with more accurate result.

Studies of $B \to Kll$ form factors from lattice QCD

Quenched lattice QCD:

- A. Al-Haydari et al. (QCDSF) Eur. Phys. J. A 43, 107120 (2010)
- D. Becirevic et al. Nucl. Phys. B 769, 31 (2007)
- L. Del Debbio et al. Phys. Lett. B 416, 392 (1998)
- A. Abada et al. Phys. Lett. B 365, 275 (1996)

Recent studies on dynamical Nf=2+1 flavors ensembles:

- FNAL/MILC.($B \to Kll$) hep-lat/1111.0981
- Cambridge group.($B \to K/K^* ll$) hep-ph/1101.2726

Lattice ensembles used in $B \to Kll$ work

$a^{-1}(fm)$	size	am_l/am_s	$N_{\rm meas}$
0.12	$20^3 \times 64$	0.02/0.05	2052
0.12	$20^3 \times 64$	0.01/0.05	2259
0.12	$20^3 \times 64$	0.007/0.05	2110
0.12	$20^3 \times 64$	0.005/0.05	2099
0.09	$28^3 \times 96$	0.0124/0.031	1996
0.09	$28^3 \times 96$	0.0062/0.031	1931
0.09	$32^3 \times 96$	0.00465/0.031	984
0.09	$40^3 \times 96$	0.0031/0.031	1015
0.09	$64^3 \times 96$	0.00155/0.031	791
0.06	$48^3 \times 144$	0.0036/0.018	673
0.06	$64^3 \times 144$	0.0018/0.018	827

Table: Ensembles of QCD gauge field configurations used in the current B2K analysis. Four sources($0, \frac{N_t}{4}, \frac{N_t}{2}, \frac{3N_t}{4}$) are used for all measurements

Form factors in $B \to Kll$ semileptonic decays

- Two matrix elements are needed in $B \to Kll$ work:

$\langle B(p)|\bar{b}\gamma^\mu s|K(k)\rangle$, $\langle B(p)|\bar{s}\sigma^{\mu\nu} b|K(k)\rangle$

$$\langle B(p)|\bar{b}\gamma^\mu s|K(k)\rangle = f_+(p^\mu + k^\mu - \frac{m_B^2 - m_K^2}{q^2}q^\mu) + f_0\frac{m_B^2 - m_K^2}{q^2}q^\mu$$

$$= \sqrt{2m_B}\left[f_\parallel \frac{p^\mu}{m_B} + f_\perp p_\perp^\mu\right]$$

$$\begin{cases} f_\parallel(E_K) = \dfrac{\langle B(p)|\bar{b}\gamma^0 s|K(k)\rangle}{\sqrt{2m_B}} \\ f_\perp(E_K) = \dfrac{\langle B(p)|\bar{b}\gamma^i s|K(k)\rangle}{2\sqrt{m_B}}\dfrac{1}{p_i} \end{cases}$$

$$\begin{cases} f_0(E_K) = \dfrac{2m_B}{m_B^2 - m_K^2}\left[(m_B - E_K)f_\parallel(E_K) + (E_K^2 - m_K^2)f_\perp(E_K)\right] \\ f_+(E_K) = \dfrac{1}{\sqrt{2m_B}}\left[f_\parallel(E_K) + (m_B - E_K)f_\perp(E_K)\right] \end{cases}$$

Form factors in $B \to Kll$ semileptonic decays

Semileptonic $B \to K$ transition from tensor current:

$$q_\nu \langle K(k)|\bar{s}\sigma^{\mu\nu}b|B(p)\rangle = \frac{i f_T}{m_B + m_K}\left[q^2(p^\mu + k^\mu) - (m_B^2 - m_K^2)q^\mu\right]$$

Solve for f_T:

$$f_T = \frac{m_B + m_K}{\sqrt{2m_B}} \frac{\langle K(k)|ib\sigma^{0i}s|B(p)\rangle}{\sqrt{2m_B}k^i}$$

$B_x \to P_{xy} ll$ semileptonic decays in NLO SChPT

$$f_{\parallel} = \frac{C_0}{f}(1 + \text{logs} + C_1 m_x + C_2 m_y + C_3 E + C_4 E^2 + C_4 a^2)$$

$$f_{\perp} = \frac{C_0}{f}\left[\frac{g}{E + \Delta_B^* + D}\right] + \frac{(C_0/f)g}{E + \Delta_B^*}(\text{logs} + C_1 m_x + C_2 m_y + C_3 E + C_4 E^2 + C_5 a^2)$$

where $\Delta_B^* = m_{B_s^*} - m_B$, D and logs are chiral log terms.

- We use SU(2) chiral logs in the chiral fit.
- The same formula are used for f_T and $f_{\perp}$.

$f_{\|}$, $f_{\perp}$ and f_T chiral-continuum extrapolations

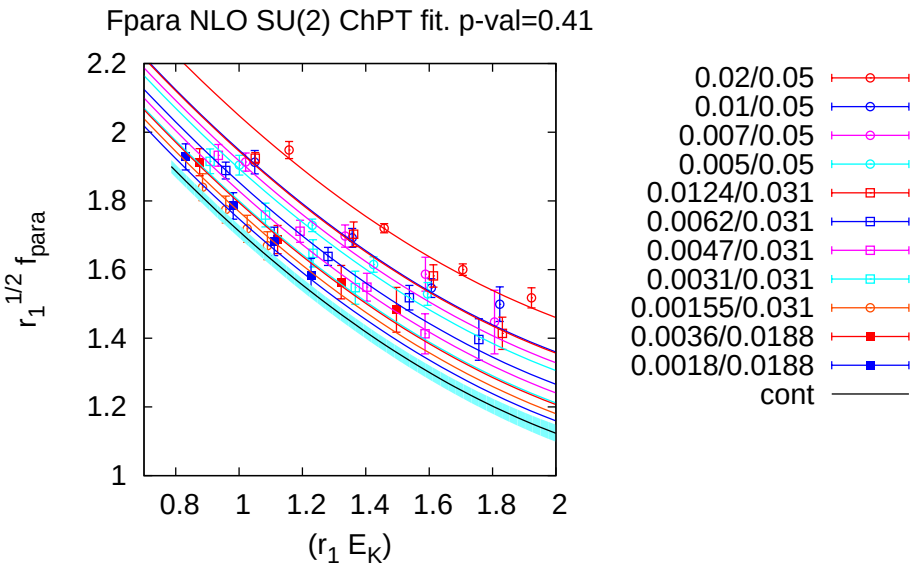

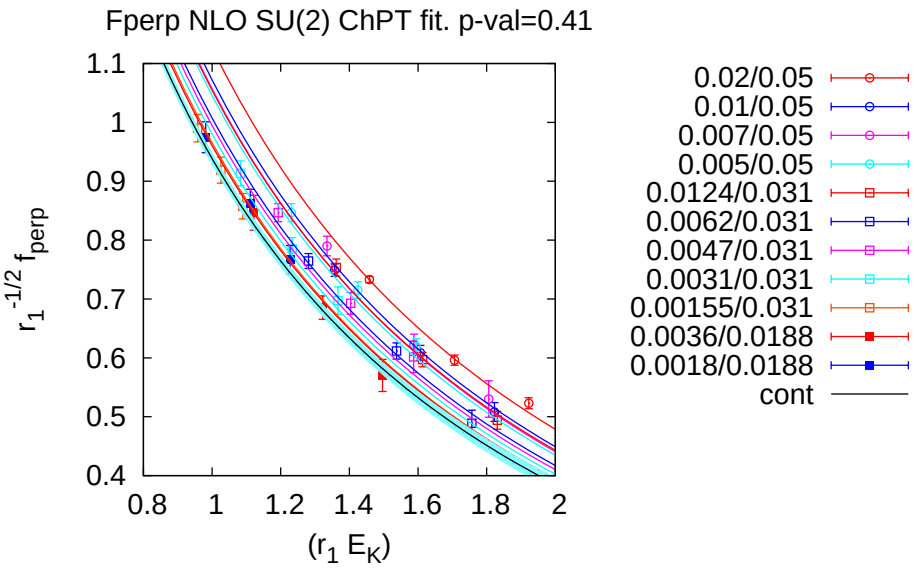

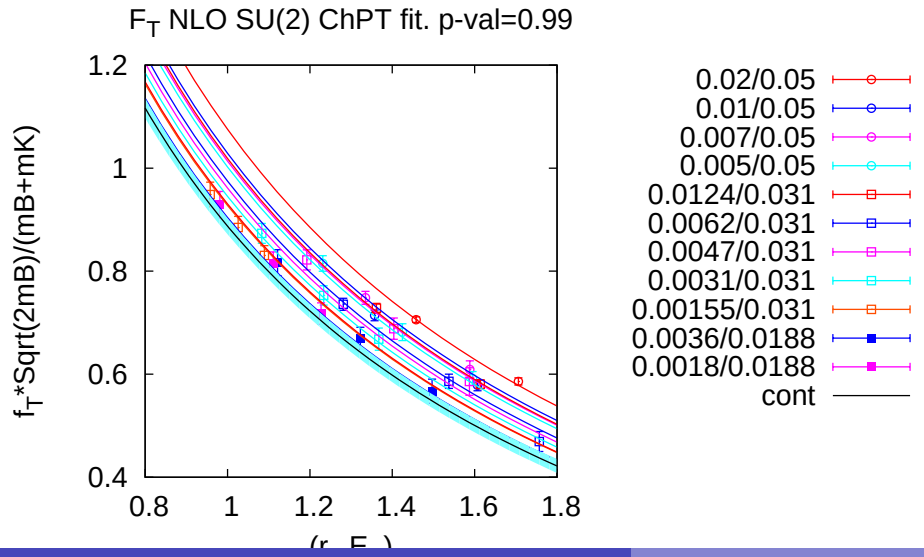

- Chiral-Continuum extrapolations give FFs at small E_K. (large q^2)
- $q^2 = (p_B - p_K)^2 = m_B^2 + m_K^2 - 2m_B E_K$
- z-expansion is a model independent extrapolation method to small q^2.

z-expansion on $B \to Kll$ form factors

- z-expansion maps q^2 to z by:

$$z(q^2, t_0) = \frac{\sqrt{t_+ - q^2} - \sqrt{t_- - t_0}}{\sqrt{t_+ - q^2} + \sqrt{t_- - t_0}}, \qquad t_\pm = (m_B \pm m_K)^2$$

- Choose $t_0 = t_+(1 - \sqrt{1 - \frac{t_-}{t_+}}) \to z \in (-0.15, 0.15)$ for $B \to Kll$, corresponding $q^2 \in (0, 23)$.
- Expand form factors as a function of z.

$$f(q^2) = \frac{1}{B(z)\phi(z)} \sum_{k=0}^{\infty} a_k z^k,$$

where $B(z) = z(q^2, m_R^2)$ and $\phi(z)$ is selected such that $\sum_{k=0}^{\infty} a_k^2 \leq 1$

z-expansion on $B \to Kll$ form factors

$$f(q^2) = \frac{1}{B(z)\phi(z)} \sum_{k=0}^{\infty} a_k z^k,$$

Numerical recipe for z-expansion:

- Fit $f(q^2)B(z)\phi(z)$ as a polynomial of z in the range of $z \in (-0.15, 0)$
- Extrapolate z-expansion fit to $z = 0.15$
- Convert variable z back to q^2

Now, we extend lattice measured form factors from $q^2 \in (15, 23) GeV^2$ to whole q^2 range.

z-expansion on $B \to Kll$ form factors

z-expansion on $B \to Kll$ form factors. (Statistical error only.)

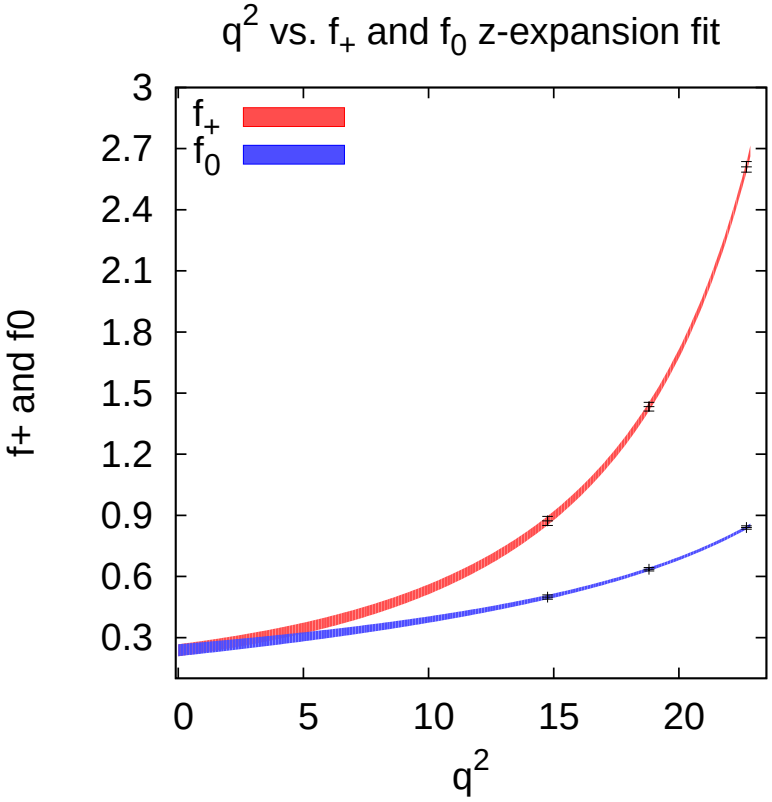

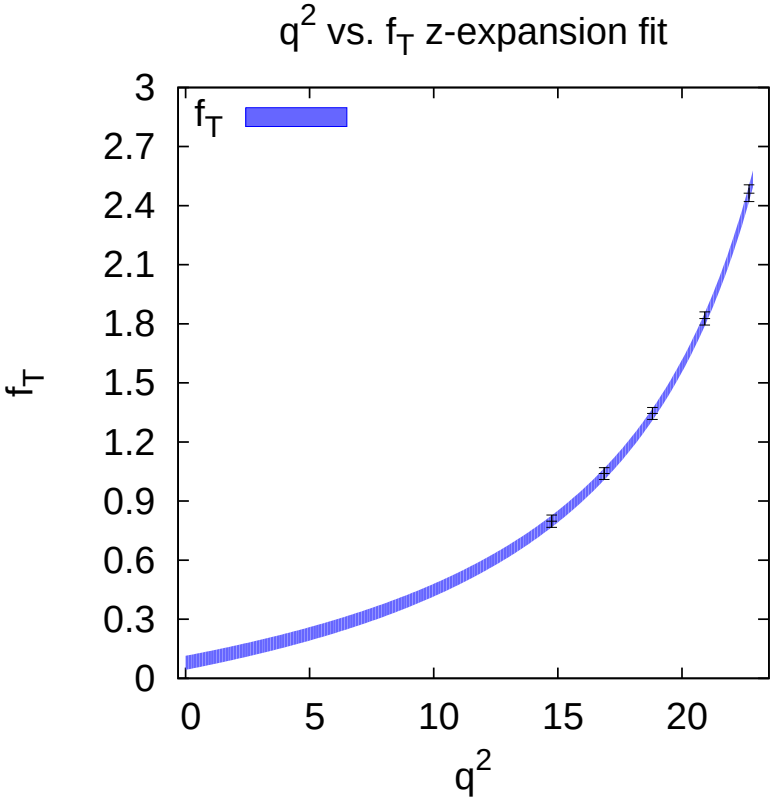

kinematic constraint, $f_+(q^2 = 0) = f_0(q^2 = 0)$, is applied in z-expansion fit.

z-expansion on $B \to Kll$ form factors

z-expansion on $B \to Kll$ form factors. (Statistical and systematic error.)

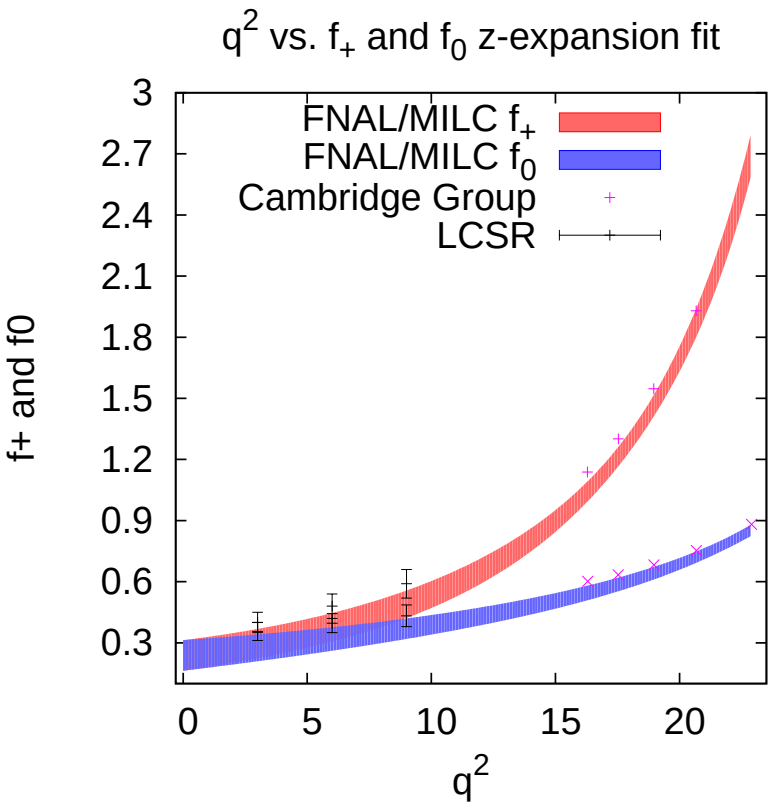

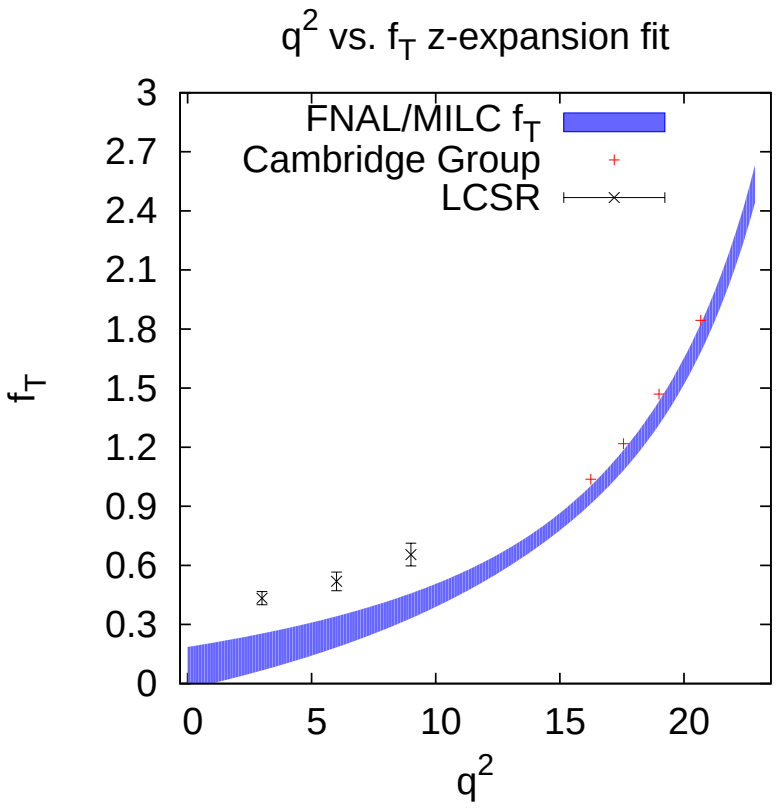

Systematic error budget

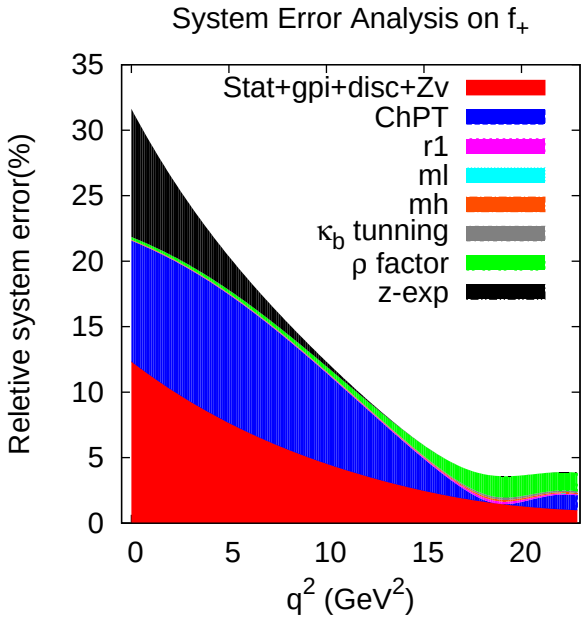

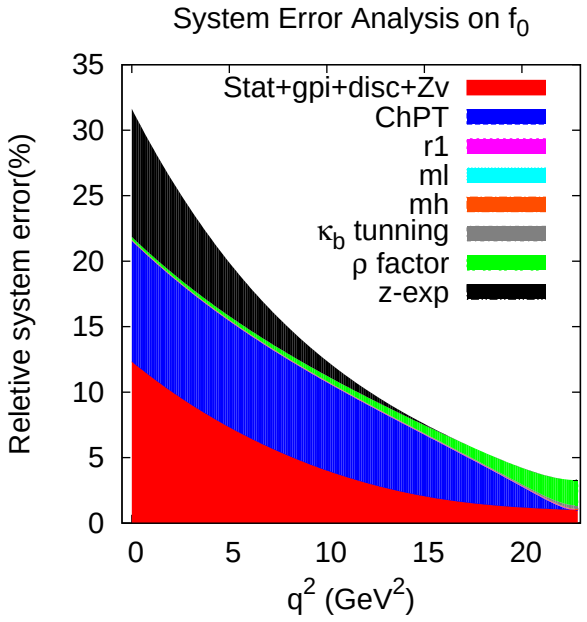

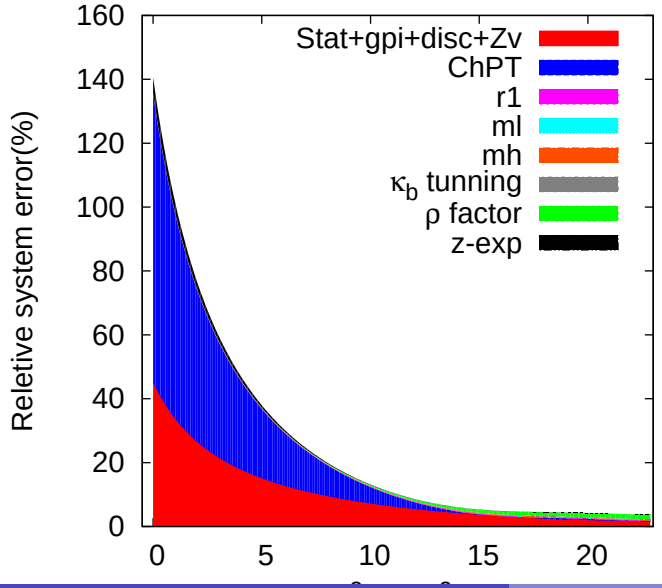

- Renormalization error could be smaller in the final result.
- ChPT error is important.
- Direct measurement of form factors at small q^2 is valuable.

Future work

- Study possible impact from the accurate form factors
- Consider to measure form factors at smaller quark masses and lower q^2.
- Consider form factors in $B \to K^* ll$ semileptonic decay

Backup slides

$f_{\parallel}$ SU(3) chiral log:

$$\frac{1}{(4\pi f)^2}\Bigg\{\frac{1}{16}\sum_{\Xi}\Bigg[\frac{2-3g_\pi^2}{2}I_1(m_{K,\Xi})-3g_\pi^2 I_1(m_{\pi,\Xi})+\frac{1}{2}I_1(m_{S,\Xi})$$

$$+2I_2(m_{K,\Xi},E)+I_2(m_{S,\Xi},E)\Bigg]$$

$$-\frac{1}{2}I_1(m_{S,I})+\frac{3g_\pi^2}{4}I_1(m_{\pi,I})+\frac{8-3g_\pi^2}{12}I_1(m_{\eta,I})+I_2(m_{\eta,I},E)-I_2(m_{S,I},E)$$

$$+a^2\delta_V'\Bigg[\frac{I_1(m_{\eta',V})-I_1(m_{\eta,V})+I_2(m_{\eta',V},E)-I_2(m_{\eta,V},E)}{m_{\eta',V}^2-m_{\eta,V}^2}$$

$$-\sum_{j\in\{S,\eta,\eta'\}}R_j^{[3,1]}\left(\{m_{S,V},m_{\eta,V},m_{\eta',V}\};\{m_{\pi,V}\}\right)\left(\frac{1}{2}I_1(m_{j,V})+I_2(m_{j,V},E)\right)$$

$$+\frac{3g_\pi^2}{2}\sum_{j\in\{\pi,\eta,\eta'\}}R_j^{[3,1]}\left(\{m_{\pi,V},m_{\eta,V},m_{\eta',V}\};\{m_{S,V}\}\right)I_1(m_{j,V})\Bigg]$$

$$+[V\to A]\Bigg\}$$

Backup slides

$f_{\|}$ SU(2) chiral log:

$$\begin{aligned}\mathrm{logs}^{B\to K} &= \frac{1}{(4\pi f)^2}\left\{\frac{1}{16}\sum_{\Xi}\left[-3g_\pi^2 I_1(m_{\pi,\Xi})\right] + \frac{3g_\pi^2}{4} I_1(m_{\pi,I}) \right. \\ &\left. + \frac{3g_\pi^2}{2}\left[2I_1(m_{\pi,V}) - 2I_1(m_{\eta,V})\right] + [V\to A]\right\}\end{aligned}$$

New Horizons for Lattice Computations with Chiral Fermions

Hamilton Seminar Room
Chemistry Department, Bldg. 555

May 14 - 16, 2012

Monday, May 14, 2012

Chair: Taku Izubuchi

08:00 - 08:25		**Registration / Coffee / Light Snacks**
08:25 - 08:40	SAMIOS, Nick et al.	Welcome
08:40 - 09:20	ROBERTS, Lee	The New Muon g-2 Experiment at Fermilab: A Challenge for Theorists and Experimentalists
09:20 - 09:40	GOLTERMAN, Maarten	On the Hadronic Vacuum Polarization Contribution to g-2
09:40 - 10:00	PERIS, Santiago	The Anomaly Triangle and g-2
10:00 - 10:20	FENG, Xu	The Two-Photon Decay of Neutral Pion from Lattice QCD
10:20 - 10:50		**Coffee Break**

Chair: Norman Christ

10:50 - 11:20	AOKI, Sinya	Chiral Symmetry Restoration and Eigenvalue Density of Dirac Operator at Finite Temperature
11:20 - 11:40	COSSU, Guido	The Axial Symmetry at Finite Temperature in Lattice QCD with Overlap Fermions
11:40 - 12:00	MUKHERJEE, Swagato	Thermodynamics with Domain Wall Fermions and Anomaly in Hot QCD
12:00 - 12:30	GIUSTI, Leonardo	Thermodynamic Potentials from Shifted Boundary Conditions
12:30 - 14:00		**Lunch Break**

Chair: Yasumichi Aoki

14:00 - 14:30	FODOR, Zoltan	High-precision Scale Setting in Lattice QCD
14:30 - 15:00	SHAMIR, Yigal	SU(N) Gauge Theories with Symmetric-representation Fermions
15:00 - 15:30	LIN, C.-J. David	Lattice Study of the Phase Structure of the Strong-Yukawa Model
15:30 - 16:00	KUTI, Julius	The Composite Higgs Mechanism and the Conformal Window
16:00 - 16:30		**Coffee Break**

Chair: Artan Borici

16:30 - 17:00	NARAYANAN, Rajamani	Large N Gauge Theories with Adjoint Fermions
17:00 - 17:20	SCHAEFER, Stefan	Lattice QCD with Open Boundary Conditions
17:20 - 17:40	MISUMI, Tatsuhiro	New Fermion Discretizations and their Application
17:40 - 18:00	CREUTZ, Michael	On Quark Masses

19:00 - 20:00 ..... **Reception / Light Meal** (Berkner Hall Lobby)

Back to Contents

Tuesday, May 15, 2012

Chair: Stefan Schaefer

08:00 - 08:30		**Coffee / Light Snacks**
08:30 - 09:00	BROWER, Richard	Prospects of Multi-grid and Domain Decomposition Dirac Solvers on GPU
09:00 - 09:20	COHEN, Saul	Multigrid Acceleration for Domain-Wall Fermion Inversion
09:20 - 09:40	KIM, Hyung-Jin	Recent Progress in Multi GPU Conjugate Gradient Convertor with Staggered Fermion
09:40 - 10:10	ORGINOS, Kostas	Lattice Gauge Theory and Applications to Nuclear Physics
10:10 - 10:40		**Coffee Break / Group Photo**

Chair: Shoji Hashimoto

10:40 - 11:10	BERNARD, Claude	Status and Prospects for Some MILC and Fermilab/MILC Projects
11:10 - 11:40	LEE, Weonjong	Recent Progress in Calculating B_K using Staggered Fermions
11:40 - 12:10	MAWHINNEY, Robert	Decaying Pseudoscalars from DWF LQCD
12:10 - 12:40	YU, Jianglei	Computing the K_L – K_S Mass Difference in Lattice QCD
12:40 - 14:20		**Lunch Break**

Chair: Ruth Van de Water

14:20 - 14:50	SACHRAJDA, Christopher	Prospects for the Computation of Rare Kaon Decay Amplitudes
14:50 - 15:10	KANEKO, Takashi	Kaon Semileptonic Decays in QCD with Exact Chiral Symmetry
15:10 - 15:30		**Coffee Break**

Chair: Taku Izubuchi

15:30 - 16:30	SAKAI, Yoshihide	Physics Prospects and Status of SuperKEKB/Belle II
16:30 - 16:40		**Break**

Chair: Jonathan Flynn

16:40 - 17:00	KELLY, Christopher	Progress Towards Delta I=1/2 K to pi pi Decays with G-parity Boundary Conditions
17:00 - 17:20	WITZEL, Oliver	B-physics with Domain-wall Light and Relativistic Heavy Quarks
17:20 - 17:40	AUBIN, Christopher	An Approach to Non-leptonic B-decays on the Lattice
17:40 - 18:00	ZHOU, Ran	B to Kll and B K\gamma Decay Form Factors from Three-flavor Lattice QCD

19:00 - 20:30 **Workshop Dinner (Brookhaven Center, South Room)**

Back to Contents

Wednesday, May 16, 2012

Chair: Tom Blum

08:00 - 08:30		**Coffee / Light Snacks**
08:30 - 09:10	SEMERTZIDIS, Yannis	Storage Ring Electric Dipole Moment Experiment for the Proton
09:10 - 09:30	SHINTANI, Eigo	Nucleon EDM from Lattice QCD
09:30 - 09:50	LIN, Huey-Wen	Medium-Modification Effects on Pion Structure
09:50 - 10:10	MEINEL, Stefan	Axial Couplings and Strong Decay Widths of Heavy Hadrons
10:10 - 10:40		**Coffee Break**

Chair: Michael Creutz

10:40 - 11:00	DOI, Takumi	Exploring Three-Nucleon Forces in Lattice QCD
11:00 - 11:20	YAMAZAKI, Takeshi	Light Nuclei from Quenched Lattice QCD
11:20 - 11:50	LIU, Keh-Fei	Progress with Overlap Fermions
11:50 - 12:20	NEUBERGER, Herbert	Lattice Radial Quantization
12:20 - 13:50		**Lunch Break**

Chair: Hideo Matsufuru

13:50 - 14:20	JANSEN, Karl	Status of Four Flavor Simulations using Maximally Twisted Mass Fermions
14:20 - 14:50	KURAMASHI, Yoshinobu	1+1+1 Flavor QCD+QED Simulation at the Physical Point
14:50 - 15:20	CHIU, Ting-Wai	Optimal Domain-Wall Fermions
15:20 - 15:40	BORICI, Artan	Chiral Fermions via Energy Level Splitting
15:40 - 16:10		**Coffee Break**

Chair: Maarten Golterman

16:10 - 16:40	HASENFRATZ, Anna	A Novel Phase with Many Flavors of Staggered Fermions
16:40 - 17:00	AOKI, Yasumichi	Exploring for Technicolor from QCD
17:00 - 17:20	LIN, Meifeng	Many-flavor Domain Wall Fermions and Fixed Topology
17:20 - 17:40	YAMADA, Norikazu	Exploring Many Flavor QCD with Wilson Fermion
17:40 - 18:00	JIN, Xiao-Yong	Exploring the Phases of QCD with Many Flavors
18:00 - 18:02	ISHIKAWA, Tomomi	**Closing**

Back to Contents

New Horizons for Lattice Computations with Chiral Fermions

Registered Participants

Name	Affiliation	E-Mail Address
Sinya Aoki	University of Tskuba	saoki@het.ph.tsukuba.ac.jp
Yasumichi Aoki	KMI, Nagoya University	yaoki@kmi.nagoya-u.ac.jp
Rudy Arthur	University of Edinburgh	R.Arthur@sms.ed.ac.uk
Christopher Aubin	Fordham University	caubin@fordham.edu
Claude Bernard	Washington University, St. Louis	cb@wustl.edu
Tom Blum	University of CT	tblum@phys.uconn.edu
Artan Borici	University of Tirana	borici@proteus.al
Peter Boyle	University of Edinburgh	paboyle@ph.ed.ac.uk
Richard Brower	Boston University	brower@bu.edu
Ting-Wai Chiu	National Taiwan University	twchiu@phys.ntu.edu.tw
Norman Christ	Columbia University	nhc@phys.columbia.edu
Saul Cohen	University of Washington	sdcohen@uw.edu
Guido Cossu	KEK High Energy Phy Res Center	neo.cossu@gmail.com
Michael Creutz	BNL	mike@latticeguy.net
Takumi Doi	RIKEN	doi@ribf.riken.jp
Robert Edwards	JLab	edwards@jlab.org
Xu Feng	KEK	pkufengxu@gmail.com
Zoltan Fodor	University of Wuppertal	fodor@bodri.elte.hu
Jonathan Flynn	University of Southampton	j.m.flynn@soton.ac.uk
Leonardo Giusti	University of Milano-Bicocca	Leonardo.Giusti@cern.ch
Maarten Golterman	San Francisco State University	maarten@stars.sfsu.edu
Anna Hasenfratz	University of Colorado	anna@eotvos.colorado.edu
Shoji Hashimoto	KEK	shoji.hashimoto@kek.jp
Urs Heller	American Physical Society	heller@aps.org
Tomomi Ishikawa	RBRC	tomomi@quark.phy.bnl.gov
Taku Izubuchi	RBRC & BNL	izubuchi@bnl.gov
Karl Jansen	NIC, DESY	karl.jansen@desy.de
Xiao-Yong Jin	RIKEN AICS	xjin@riken.jp
Chulwoo Jung	BNL	chulwoo@bnl.gov
Takashi Kaneko	KEK	takashi.kaneko@kek.jp
Christopher Kelly	Columbia University	giltirn@gmail.com
Hyung-Jin Kim	BNL	windy510@gmail.com
Yoshinobu Kuramashi	University of Tsukuba	kuramasi@het.ph.tsukuba.ac.jp
Julius Kuti	U.C. San Diego	jkuti@ucsd.edu
Weonjong Lee	Seoul National University	wlee@snu.ac.kr
Christoph Lehner	RBRC	clehner@bnl.gov
Matthew Lightman	Washington University	mlightman@physics.wustl.edu
C.-J. David Lin	National Chiao-Tung University	dlin1971@gmail.com
Huey-Wen Lin	University of Washington	hwlin@phys.washington.edu
Meifeng Lin	Yale University	meifeng.lin@yale.edu
Zhongjie Lin	Columbia University	jasper@phys.columbia.edu
Keh-Fei Liu	University of Kentucky	liu@pa.uky.edu
Andrew Lytle	University of Southampton	atlytle@gmail.com
Paul Mackenzie	FermiLab	mackenzie@fnal.gov
Hideo Matsufuru	KEK	hideo.matsufuru@kek.jp
Robert Mawhinney	Columbia University	rdm@physics.columbia.edu

Back to Contents

New Horizons for Lattice Computations with Chiral Fermions

Registered Participants

Name	Affiliation	E-Mail Address
Stefan Meinel	College of William and Mary	smeinel@wm.edu
Tatsuhiro Misumi	BNL	tatsuhiromisumi@gmail.com
Swagato Mukherjee	BNL	swagato@bnl.gov
Rajamani Narayanan	Florida International University	rajamani.narayanan@fiu.edu
Herbert Neuberger	Rutgers University	NEUBERG@PHYSICS.RUTGERS.EDU
Junichi Noaki	KEK	noaki@post.kek.jp
Shigemi Ohta	KEK & RBRC	shigemi.ohta@kek.jp
Kostas Orginos	College of William and Mary	kostas@wm.edu
Santiago Peris	SFSU/UAB	peris@ifae.es
Frank Quarant	BNL	quarant@bnl.gov
David Richards	JLab	dgr@jlab.org
Bradley Roberts	Boston University	roberts@bu.edu
Christopher Sachrajda	University of Southampton	cts@soton.ac.uk
Yoshihide Sakai	KEK	Yoshihide.Sakai@kek.jp
Stefan Schaefer	CERN	stefan.schaefer@cern.ch
Yannis Semertzidis	BNL	yannis@bnl.gov
Yigal Shamir	Tel Aviv University	shamir@post.tau.ac.il
Eigo Shintani	RBRC	shintani@riken.jp
Amarjit Soni	BNL	adlersoni@gmail.com
Ruth Van de Water	BNL	ruthv@bnl.gov
Chip Watson	Thomas Jefferson Nat'l Accelerator Facility	watson@jlab.org
Oliver Witzel	Boston University	owitzel@bu.edu
Norikazu Yamada	KEK	norikazu.yamada@kek.jp
Takeshi Yamazaki	KMI, Nagoya Univ	yamazaki@kmi.nagoya-u.ac.jp
Hantao Yin	Columbia University	yinnht@phys.columbia.edu
Jianglei Yu	Columbia University	physhark@gmail.com
Daiqian Zhang	Columbia University	dz2203@columbia.edu
Ran Zhou	Indiana University	ZHOURAN123@GMAIL.COM

Back to Contents

RBRC Workshop Proceedings

Volume 108 – Hyperon-Hyperon Interactions and Searches for Exotic Di-Hyperons in Nuclear Collisions, February 29 – March 2, 2012 – BNL-97035-2012
Volume 107 – Future Directions in High Energy QCD, October 20-22, 2011 – BNL-98119-2011
Volume 106 – Fluctuations, Correlations and RHIC Low Energy Runs, October 3-5, 2011 – BNL-96514-2011
Volume 105 – Opportunities for Polarized He-3 in RHIC and EIC, September 28-30, 2011 – BNL-96418-2011
Volume 104 – Brookhaven Summer Program on Quarkonium Production in Elementary and Heavy Ion Collisions, June 6-18, 2011 – BNL-96171-2011
Volume 103 – Opportunities for Drell-Yan Physics at RHIC, May 11-13, 2011 – BNL-95236-2011-2011
Volume 102 – Initial State Fluctuations and Final-State Particle Correlations, February 2-4, 2011 – BNL-94704-2011
Volume 101 – RBRC Scientific Review Committee Meeting, October 27-29, 2010 – BNL-94589-2011
Volume 100 – Summer Program on Nucleon Spin Physics, July 14-27, 2010 – BNL-96163-2011
Volume 99 – The Physics of W and Z Bosons, June 24-25, 2010 – BNL-94287-2010
Volume 98 – Saturation, the Color Glass Condensate and the Glasma: What Have we Learned from RHIC? – May 10-12, 2010 – BNL-94271-2010
Volume 97 – RBRC Scientific Review Committee Meeting, October 21-22, 2009 – BNL-90674-2009
Volume 96 – P- and CP-Odd Effects in Hot and Dense Matter, April 26-30, 2010 – BNL-94237-2010
Volume 95 – Progress in High-pT Physics at RHIC, March 17-19, 2010 – BNL-94214-2010
Volume 94 – Summer Program on Nucleon Spin Physics at LBL, June 1-12, 2009
Volume 93 – PHENIX Spinfest School 2009 at BNL - July 1-31, 2009. BNL-90343-2009
Link: PHENIXSpinfestSchool2009@BNL
Volume 92 – PKU-RBRC Workshop on Transverse Spin Physics, June 30 - July 4, 2008, Beijing, China – BNL-81685-2008
Volume 91 – RBRC Scientific Review Committee Meeting, November 17-18, 2008 – BNL-81556-2008
Volume 90 – PHENIX Spinfest School 2008 at BNL, August 4-8, 2008 – BNL-81478-2008
Volume 89 – Understanding QGP through Spectral Functions and Euclidean Correlators, April 23-25, 2008 – BNL-81318-2008
Volume 88 – Hydrodynamics in Heavy Ion Collisions and QCD Equation of State, April 21-22, 2008 – BNL-81307-2008
Volume 87 – RBRC Scientific Review Committee Meeting, November 5-6, 2007 – BNL-79570-2007
Volume 86 – Global Analysis of Polarized Parton Distributions in the RHIC Era, October 8, 2007 – BNL-79457-2007
Volume 85 – Parity-Violating Spin Asymmetries at RHIC-BNL, April 26-27, 2007 – BNL-79146-2007
Volume 84 – Domain Wall Fermions at Ten Years, March 15-17, 2007 – BNL 77857-2007
Volume 83 – QCD in Extreme Conditions, July 31 - August 2, 2006 – BNL-76933-2006
Volume 82 – RHIC Physics in the Context of the Standard Model, June 18-23, 2006 – BNL-76863-2006
Volume 81 – Parton Orbital Angular Momentum (Joint RBRC/University of New Mexico Workshop) February 24-26, 2006 – BNL-75937-2006
Volume 80 – Can We Discover the QCD Critical Point at RHIC?, March 9-10, 2006 – BNL-75692-2006
Volume 79 – Strangeness in Collisions, February 16-17, 2006 – BNL-79763-2008
Volume 78 – Heavy Flavor Productions and Hot/Dense Quark Matter, December 12-14, 2005 – BNL-76915-2006
Volume 77 – RBRC Scientific Review Committee Meeting, October 10-12, 2005 – BNL-52649-2005
Volume 76 – Odderon Searches at RHIC, September 27-29, 2005 – BNL-75092-2005
Volume 75 – Single Spin Asymmetries, June 1-3, 2005 – BNL-74717-2005
Volume 74 – RBRC QCDOC Computer Dedication and Symposium on RBRC QCDOC, May 26, 2005 – BNL-74813-2005
Volume 73 – Jet Correlations at RHIC, March 10-11, 2005 – BNL-73910-2005
Volume 72 – RHIC Spin Collaboration Meetings XXXI (January 14, 2005), XXXII (February 10, 2005), XXXIII (March 11, 2005) – BNL-73866-2005
Volume 71 – Classical and Quantum Aspects of the Color Glass Condensate – BNL-73793-2005
Volume 70 – Strongly Coupled Plasmas: Electromagnetic, Nuclear & Atomic – BNL-73867-2005
Volume 69 – RBRC Scientific Review Committee – BNL-73546-2004
Volume 68 – Workshop on the Physics Programme of the RBRC and UKQCD QCDOC Machines – BNL-73604-2004
Volume 67 – High Performance Computing with BlueGene/L and QCDOC Architectures
Volume 66 – RHIC Spin Collaboration Meeting XXIX, October 8-9, 2004, Torino Italy – BNL-73534-2004
Volume 65 – RHIC Spin Collaboration Meetings XXVII (July 22, 2004), XXVIII (September 2, 2004), XXX (December 6, 2004) – BNL-73506-2004
Volume 64 – Theory Summer Program on RHIC Physics – BNL-73263-2004

Back to Contents

Volume 63 – RHIC Spin Collaboration Meetings XXIV (May 21, 2004), XXV (May 27, 2004), XXVI (June 1, 2004) – BNL-72397-2004
Volume 62 – New Discoveries at RHIC, May 14-15, 2004 – BNL- 72391-2004
Volume 61 – RIKEN-TODAI Mini Workshop on "Topics in Hadron Physics at RHIC", March 23-24, 2004 – BNL-72336-2004
Volume 60 – Lattice QCD at Finite Temperature and Density – BNL–72083-2004
Volume 59 – RHIC Spin Collaboration Meeting XXI (January 22, 2004), XXII (February 27, 2004), XXIII (March 19, 2004)– BNL-72382-2004
Volume 58 – RHIC Spin Collaboration Meeting XX – BNL-71900-2004
Volume 57 – High pt Physics at RHIC, December 2-6, 2003 – BNL-72069-2004
Volume 56 – RBRC Scientific Review Committee Meeting – BNL-71899-2003
Volume 55 – Collective Flow and QGP Properties – BNL-71898-2003
Volume 54 – RHIC Spin Collaboration Meetings XVII, XVIII, XIX – BNL-71751-2003
Volume 53 – Theory Studies for Polarized pp Scattering – BNL-71747-2003
Volume 52 – RIKEN School on QCD "Topics on the Proton" – BNL-71694-2003
Volume 51 – RHIC Spin Collaboration Meetings XV, XVI – BNL-71539-2003
Volume 50 – High Performance Computing with QCDOC and BlueGene – BNL-71147-2003
Volume 49 – RBRC Scientific Review Committee Meeting – BNL-52679
Volume 48 – RHIC Spin Collaboration Meeting XIV – BNL-71300-2003
Volume 47 – RHIC Spin Collaboration Meetings XII, XIII – BNL-71118-2003
Volume 46 – Large-Scale Computations in Nuclear Physics using the QCDOC – BNL-52678
Volume 45 – Summer Program: Current and Future Directions at RHIC – BNL-71035
Volume 44 – RHIC Spin Collaboration Meetings VIII, IX, X, XI – BNL-71117-2003
Volume 43 – RIKEN Winter School – Quark-Gluon Structure of the Nucleon and QCD – BNL-52672
Volume 42 – Baryon Dynamics at RHIC – BNL-52669
Volume 41 – Hadron Structure from Lattice QCD – BNL-52674
Volume 40 – Theory Studies for RHIC-Spin – BNL-52662
Volume 39 – RHIC Spin Collaboration Meeting VII – BNL-52659
Volume 38 – RBRC Scientific Review Committee Meeting – BNL-52649
Volume 37 – RHIC Spin Collaboration Meeting VI (Part 2) – BNL-52660
Volume 36 – RHIC Spin Collaboration Meeting VI – BNL-52642
Volume 35 – RIKEN Winter School – Quarks, Hadrons and Nuclei – QCD Hard Processes and the Nucleon Spin – BNL-52643
Volume 34 – High Energy QCD: Beyond the Pomeron – BNL-52641
Volume 33 – Spin Physics at RHIC in Year-1 and Beyond – BNL-52635
Volume 32 – RHIC Spin Physics V – BNL-52628
Volume 31 – RHIC Spin Physics III & IV Polarized Partons at High Q^2 Region – BNL-52617
Volume 30 – RBRC Scientific Review Committee Meeting – BNL-52603
Volume 29 – Future Transversity Measurements – BNL-52612
Volume 28 – Equilibrium & Non-Equilibrium Aspects of Hot, Dense QCD – BNL-52613
Volume 27 – Predictions and Uncertainties for RHIC Spin Physics & Event Generator for RHIC Spin Physics III – Towards Precision Spin Physics at RHIC – BNL-52596
Volume 26 – Circum-Pan-Pacific RIKEN Symposium on High Energy Spin Physics – BNL-52588
Volume 25 – RHIC Spin – BNL-52581
Volume 24 – Physics Society of Japan Biannual Meeting Symposium on QCD Physics at RIKEN BNL Research Center – BNL-52578
Volume 23 – Coulomb and Pion-Asymmetry Polarimetry and Hadronic Spin Dependence at RHIC Energies – BNL-52589
Volume 22 – OSCAR II: Predictions for RHIC – BNL-52591
Volume 21 – RBRC Scientific Review Committee Meeting – BNL-52568
Volume 20 – Gauge-Invariant Variables in Gauge Theories – BNL-52590
Volume 19 – Numerical Algorithms at Non-Zero Chemical Potential – BNL-52573
Volume 18 – Event Generator for RHIC Spin Physics – BNL-52571
Volume 17 – Hard Parton Physics in High-Energy Nuclear Collisions – BNL-52574
Volume 16 – RIKEN Winter School - Structure of Hadrons - Introduction to QCD Hard Processes – BNL-52569
Volume 15 – QCD Phase Transitions – BNL-52561
Volume 14 – Quantum Fields In and Out of Equilibrium – BNL-52560
Volume 13 – Physics of the 1 Teraflop RIKEN-BNL-Columbia QCD Project First Anniversary Celebration – BNL-66299
Volume 12 – Quarkonium Production in Relativistic Nuclear Collisions – BNL-52559

Back to Contents

Volume 11 – Event Generator for RHIC Spin Physics – BNL-66116
Volume 10 – Physics of Polarimetry at RHIC – BNL-65926
Volume 9 – High Density Matter in AGS, SPS and RHIC Collisions – BNL-65762
Volume 8 – Fermion Frontiers in Vector Lattice Gauge Theories – BNL-65634
Volume 7 – RHIC Spin Physics – BNL-65615
Volume 6 – Quarks and Gluons in the Nucleon – BNL-65234
Volume 5 – Color Superconductivity, Instantons and Parity (Non?)-Conservation at High Baryon Density – BNL-65105
Volume 4 – Inauguration Ceremony and Non-Equilibrium Many Body Dynamics – BNL-64912
Volume 3 – Hadron Spin-Flip at RHIC Energies – BNL-64724
Volume 2 – Perturbative QCD as a Probe of Hadron Structure – BNL-64723
Volume 1 – Open Standards for Cascade Models for RHIC – BNL-64722

Back to Contents

Li Keran

Nuclei as heavy as bulls
Through collision
Generate new states of matter.
T.D. Lee

©CCASTA

Organizers
Thomas Blum (UConn)
Tomomi Ishikawa (BNL)
Taku Izubuchi, Chair (BNL/RBRC)
Amarjit Soni (BNL)

RIKEN BNL Research Center
Bldg. 510A, Brookhaven National Laboratory
Upton, NY 11973-5000, USA

August 2012